VOLUME 26 / NUMBER 13
JULY 8, 1988
ACC. NOS. N88-20254 TO N88-21115

STAR
AN ABSTRACT JOURNAL

Scientific and Technical Aerospace Reports

PRODUCED BY THE
SCIENTIFIC AND TECHNICAL
INFORMATION
DIVISION

NASA

NATIONAL AERONAUTICS AND SPACE ADMINISTRATION

WHAT YOU CAN DO FOR *STAR*

All users of this abstract service are urged to forward reports to be considered for announcement in *STAR*. This will aid NASA in its efforts to provide the fullest possible coverage of all scientific and technical publications that might support aeronautics and space research and development. If you have prepared relevant reports (other than those that you will transmit to NASA, DoD, or DOE through the usual contract- or grant-reporting channels), please send them for consideration to the NASA Scientific and Technical Information Facility, P.O. Box 8757, B.W.I. Airport, Maryland 21240.

Reprints of journal articles, book chapters, and conference papers are also welcome. These will be considered for announcement in *STAR*'s companion journal, *International Aerospace Abstracts*.

You may specify a particular source to be included in a report announcement if you wish; otherwise the report will be placed on public sale at the National Technical Information Service. Copyrighted publications will be announced but not distributed or sold.

PURCHASE OF *STAR*

The semimonthly issues are available for sale by the Superintendent of Documents, U.S. Government Printing Office, Washington, D.C. 20402.

PUBLISHED BY:

UNITED STATES GOVERNMENT
NATIONAL AERONAUTICS AND SPACE ADMINISTRATION
SCIENTIFIC AND TECHNICAL INFORMATION DIVISION
Scientific and Technical Aerospace Reports, Volume 26, is prepared by the NASA Scientific and Technical Information Facility operated for the National Aeronautics and Space Administration by RMS Associates.

The Administrator of the National Aeronautics and Space Administration has determined that the publication of this periodical is necessary in the transaction of the public business required by law of this Agency. Use of funds for printing this periodical has been approved by the Director of the Office of Management and Budget through March 22, 1989.

US ISSN 0036-8741

INTRODUCTION

Scientific and Technical Aerospace Reports (STAR) is a major component of a comprehensive National Aeronautics and Space Administration information system covering aeronautics, space, and supporting disciplines. *STAR* is issued on the 8th and 23rd of each month and announces current publications of the following types:

- NASA, NASA contractor, and NASA grantee reports
- Reports issued by other U.S. Government Agencies, domestic and foreign institutions, universities, and private firms
- Translations in report form
- NASA-owned patents and patent applications
- Dissertations and theses

Journal, book, and conference literature, cover-to-cover journal translations, and certain foreign dissertations are announced in a companion journal, *International Aerospace Abstracts (IAA)*, available on subscription from the American Institute of Aeronautics and Astronautics, Technical Information Service, 555 West 57th Street, 12th Floor, New York, New York 10019.

SUBJECT SCOPE

Subject scope of *STAR*, and *IAA* includes all aspects of aeronautics and space research and development, supporting basic and applied research, and applications. Aerospace aspects of earth resources, energy development, conservation, oceanography, environmental protection, urban transportation, and other topics of high national priority are also covered.

OTHER NASA PUBLICATIONS

Other NASA publications and information services are described in the publication, *The NASA Scientific and Technical Information System ... and How to Use It*, available without charge from the NASA Scientific and Technical Information Facility, P.O. Box 8757, B.W.I. Airport, Maryland 21240.

HOW TO USE *STAR* SUBJECT CATEGORIES

STAR is categorized by 10 major subject divisions divided into 76 specific subject categories and one general category/division. The major subject divisions are listed in the Table of Contents, together with a note for each that defines its scope and provides any cross-references. For example:

AERONAUTICS

Includes aeronautics (general); aerodynamics; air transportation and safety; aircraft communications and navigation; aircraft design, testing and performance; aircraft instrumentation; aircraft propulsion and power; aircraft stability and control; and research and support facilities (air).

For related information see also *Astronautics*.

Each major division is further divided into as many as nine specific categories, which are identified by category numbers.

Abstracts in *STAR* are grouped by specific category, the categories appearing in sequential order. Category breaks in the abstract section are identified by the category number and title, and a scope note. Cross-references to other categories are provided as appropriate. For example:

02 AERODYNAMICS

Includes aerodynamics of bodies, combinations, wings, rotors, and control surfaces; and internal flow in ducts and turbomachinery.

For related information see also *34 Fluid Mechanics and Heat Transfer.*

CROSS-REFERENCES

Individual *STAR* abstracts are not ordinarily cross-referenced, except for certain conference reports or book translations that have had separate abstracts written for their component papers or chapters. Citations and abstracts of the components follow immediately after those of the parent document. When the subject content of a component differs sufficiently from the general content of the parent, a cross-reference citation also is printed at the end of the category to which it normally would have been assigned if it were independent.

DOCUMENTS ON MICROFICHE

Documents on microfiche(1) are designated by a pound sign (#) following the accession number. The pound sign is used without regard to the source or quality of the microfiche.

AVAILABILITIES

One or more sources from which a document announced in *STAR* is available to the public is given in each citation. The most commonly indicated sources and their acronyms or abbreviations are listed below. If the publication is available from a source other than those listed, the publisher and his address will be displayed on the availability line or in combination with the corporate source line.

Avail: NTIS. Sold by the National Technical Information Service. Prices for hard copy (HC) and microfiche (MF) are indicated by a price code following the letters HC or MF in the *STAR* citation. Current values for the price codes are given in the tables on page vii.

Initially distributed microfiche under the NTIS SRIM (Selected Research in Microfiche) is available at greatly reduced unit prices. For this service and for information concerning subscription to NASA printed reports, consult the NTIS Subscription Section, Springfield, Va. 22161.

NOTE ON ORDERING DOCUMENTS: When ordering NASA publications (those followed by the * symbol), use the N accession number. NASA patent applications (only the specifications are offered) should be ordered by the US-Patent-Appl-SN number. Non-NASA publications (no asterisk) should be ordered by the AD, PB, or other *report number* shown on the last line of the citation, not by the N accession number. It is also advisable to cite the title and other bibliographic identification.

Avail: SOD (or GPO). Sold by the Superintendent of Documents, U.S. Government Printing Office, in hard copy. The current price and order number are given following the availability line. (NTIS will fill microfiche requests, as indicated above, for those documents identified by a # symbol.)

(1) A microfiche is a transparent sheet of film, 105 by 148 mm in size, containing as many as 60 to 98 pages of information reduced to micro images (not to exceed 26:1 reduction).

Avail: BLL (formerly NLL): British Library Lending Division, Boston Spa, Wetherby, Yorkshire, England. Photocopies available from this organization at the price shown. (If none is given, inquiry should be addressed to the BLL.)

Avail: DOE Depository Libraries. Organizations in U.S. cities and abroad that maintain collections of Department of Energy reports, usually in microfiche form, are listed in *Energy Research Abstracts*. Services available from the DOE and its depositories are described in a booklet, *DOE Technical Information Center - Its Functions and Services* (TID-4660), which may be obtained without charge from the DOE Technical Information Center.

Avail: ESDU. Pricing information on specific data, computer programs, and details on ESDU topic categories can be obtained from ESDU International Ltd. Requesters in North America should use the Virginia address while all other requesters should use the London address, both of which are on page vi.

Avail: Fachinformationszentrum, Karlsruhe. Sold by the Fachinformationszentrum Energie, Physik, Mathematik GMBH, Eggenstein Leopoldshafen, Federal Republic of Germany, at the price shown in deutschmarks (DM).

Avail: HMSO. Publications of Her Majesty's Stationery Office are sold in the U.S. by Pendragon House, Inc. (PHI), Redwood City, California. The U.S. price (including a service and mailing charge) is given, or a conversion table may be obtained from PHI.

Avail: NASA Public Document Rooms. Documents so indicated may be examined at or purchased from the National Aeronautics and Space Administration, Public Documents Room (Room 126), 600 Independence Ave., S.W., Washington, D.C. 20546, or public document rooms located at each of the NASA research centers, the NASA Space Technology Laboratories, and the NASA Pasadena Office at the Jet Propulsion Laboratory.

Avail: Univ. Microfilms. Documents so indicated are dissertations selected from *Dissertation Abstracts* and are sold by University Microfilms as xerographic copy (HC) and microfilm. All requests should cite the author and the Order Number as they appear in the citation.

Avail: US Patent and Trademark Office. Sold by Commissioner of Patents and Trademarks, U.S. Patent and Trademark Office, at the standard price of $1.50 each, postage free. (See discussion of NASA patents and patent applications below.)

Avail: (US Sales Only). These foreign documents are available to users within the United States from the National Technical Information Service (NTIS). They are available to users outside the United States through the International Nuclear Information Service (INIS) representative in their country, or by applying directly to the issuing organization.

Avail: USGS. Originals of many reports from the U.S. Geological Survey, which may contain color illustrations, or otherwise may not have the quality of illustrations preserved in the microfiche or facsimile reproduction, may be examined by the public at the libraries of the USGS field offices whose addresses are listed in this Introduction. The libraries may be queried concerning the availability of specific documents and the possible utilization of local copying services, such as color reproduction.

Avail: Issuing Activity, or Corporate Author, or no indication of availability. Inquiries as to the availability of these documents should be addressed to the organization shown in the citation as the corporate author of the document.

NASA PATENTS AND PATENT APPLICATIONS

Patents and patent applications owned by NASA are announced in *STAR* under appropriate subject categories and are referenced in the *STAR* indexes. In the Report/Accession Number Index, patents are indexed by the NASA Case Number (which appears in lieu of the report number in other indexes), the U.S. Patent Number, the U.S. Patent Application Serial Number, and the U.S. Patent Class. Patent applications for which patents have not yet been issued are indexed by the NASA Case Number and the U.S. Patent Application Serial Number.

NASA *patent application specifications* are sold in paper copy by the National Technical Information Service at price code A02. Microfiche are sold at price code A01. The US-Patent-Appl-SN- number should be used in ordering either paper copy or microfiche from NTIS. Printed copies of *patents* (which are not microfiched) are available for purchase at $1.50 per copy from:

Commissioner of Patents and Trademarks
U.S. Patent and Trademark Office
Washington, D.C. 20231

When ordering patents, the U.S. Patent Number should be used, and payment must be remitted in advance, preferably by money order or check payable to the Commissioner of Patents and Trademarks. Prepaid purchase coupons for ordering are also available from the Patent and Trademark Office. The patents and patent applications announced in *STAR* are owned by NASA and are available for royalty-free licensing. Requests for licensing terms and further information should be addressed to:

Associate General Counsel for Intellectual Property/Code GP
National Aeronautics and Space Administration
Washington, D.C. 20546

ELIGIBILITY AND REGISTRATION FOR NASA INFORMATION PRODUCTS AND SERVICES

A variety of services is available to organizations of the following types that have registered with NASA to receive specific services or products:

1. NASA offices, research centers, contractors, subcontractors, grantees, and consultants;
2. Other U.S. Government agencies and their contractors;
3. Libraries in the United States that have arrangements with NASA to maintain collections of NASA documents for public reference;
4. Other organizations in the United States having a need for NASA documents in work related to aeronautics and space research;
5. Organizations abroad that have established reciprocal document exchange arrangements with NASA.

Only the central service points or central points of document acquisition and control within qualified organizations are eligible to register for NASA products and services. Domestic organizations that may be eligible to receive various classes of NASA publications and services should address their requests for registration or for further information to:

NASA Scientific and Technical Information Facility
ATTN: Registration Activity
P.O. Box 8757
B.W.I. Airport, Maryland 21240

Organizations abroad should direct requests to the same address, but to the attention of: International Exchange Program.

AVAILABILITY OF *STAR* ABSTRACTS ON MICROFICHE

Microfiche of the abstract sections of this issue and other issues of *STAR* are available on annual subscription from NTIS as PB88-911300, Attn: Subscriptions, 5285 Port Royal Road, Springfield, Virginia 22161. Annual subscription rates are $70.00 North America; $140.00 foreign. Abstract sections for previous years retroactive to 1964 are available at the current rates. Microfiche for individual *STAR* issue abstract sections are not available.

PUBLIC COLLECTIONS OF NASA DOCUMENTS

DOMESTIC: NASA and NASA-sponsored documents and a large number of aerospace publications are available to the public for reference purposes at the library maintained by the American Institute of Aeronautics and Astronautics, Technical Information Service, 555 West 57th Street, 12th Floor, New York, New York 10019

EUROPEAN: An extensive collection of NASA and NASA-sponsored publications is maintained by the British Library Lending Division, Boston Spa, Wetherby, Yorkshire, England for public access. The British Library Lending Division also has available many of the non-NASA publications cited in *STAR*. European requesters may purchase facsimile copy or microfiche of NASA and NASA-sponsored documents, those identified by both the symbols # and * from ESA - Information Retrieval Service European Space Agency, 8-10 rue Mario-Nikis, 75738 Paris CEDEX 15, France.

FEDERAL DEPOSITORY LIBRARY PROGRAM

In order to provide the general public with greater access to U.S. Government publications, Congress established the Federal Depository Library Program under the Government Printing Office (GPO), with 50 regional depositories responsible for permanent retention of material, inter-library loan, and reference services. At least one copy of nearly every NASA and NASA-sponsored publication, either in printed or microfiche format, is received and retained by the 50 regional depositories. A list of the regional GPO libraries, arranged alphabetically by state, appears on the inside back cover. These libraries are *not* sales outlets. A local library can contact a Regional Depository to help locate specific reports, or direct contact may be made by an individual.

ADDRESSES OF ORGANIZATIONS

American Institute of Aeronautics and Astronautics
Technical Information Service
555 West 57th Street, 12th Floor
New York, New York 10019

British Library Lending Division,
Boston Spa, Wetherby, Yorkshire,
England

Commissioner of Patents and Trademarks
U.S. Patent and Trademark Office
Washington, D.C. 20231

Department of Energy
Technical Information Center
P.O. Box 62
Oak Ridge, Tennessee 37830

ESA-Information Retrieval Service
ESRIN
Via Galileo Galilei
00044 Frascati (Rome) Italy

ESDU International, Ltd.
1495 Chain Bridge Road
McLean, Virginia 22101

ESDU International, Ltd.
251-259 Regent Street
London, W1R 7AD, England

Fachinformationszentrum Energie, Physik, Mathematik GMBH
7514 Eggenstein Leopoldshafen
Federal Republic of Germany

Her Majesty's Stationery Office
P.O. Box 569, S.E. 1
London, England

NASA Scientific and Technical Information Facility
P.O. Box 8757
B.W.I. Airport, Maryland 21240

National Aeronautics and Space Administration
Scientific and Technical Information Division (NTT-1)
Washington, D.C. 20546

National Technical Information Service
5285 Port Royal Road
Springfield, Virginia 22161

Pendragon House, Inc.
899 Broadway Avenue
Redwood City, California 94063

Superintendent of Documents
U.S. Government Printing Office
Washington, D.C. 20402

University Microfilms
A Xerox Company
300 North Zeeb Road
Ann Arbor, Michigan 48106

University Microfilms, Ltd.
Tylers Green
London, England

U.S. Geological Survey Library
National Center - MS 950
12201 Sunrise Valley Drive
Reston, Virginia 22092

U.S. Geological Survey Library
2255 North Gemini Drive
Flagstaff, Arizona 86001

U.S. Geological Survey
345 Middlefield Road
Menlo Park, California 94025

U.S. Geological Survey Library
Box 25046
Denver Federal Center, MS914
Denver, Colorado 80225

NTIS PRICE SCHEDULES

(Effective January 1, 1988)

Schedule A
STANDARD PRICE DOCUMENTS AND MICROFICHE

PRICE CODE	NORTH AMERICAN PRICE	FOREIGN PRICE
A01	$ 6.95	$13.90
A02	9.95	19.90
A03	12.95	25.90
A04-A05	14.95	29.90
A06-A09	19.95	39.90
A10-A13	25.95	51.90
A14-A17	32.95	65.90
A18-A21	38.95	77.90
A22-A25	44.95	89.90
A99	*	*
NO1	49.50	89.90
NO2	48.00	80.00

Schedule E
EXCEPTION PRICE DOCUMENTS AND MICROFICHE

PRICE CODE	NORTH AMERICAN PRICE	FOREIGN PRICE
E01	$ 8.50	17.00
E02	11.00	22.00
E03	12.00	24.00
E04	14.50	29.00
E05	16.50	33.00
E06	19.00	38.00
E07	21.50	43.00
E08	24.00	48.00
E09	26.50	53.00
E10	29.00	58.00
E11	31.50	63.00
E12	34.00	68.00
E13	36.50	73.00
E14	39.50	79.00
E15	43.00	86.00
E16	47.00	94.00
E17	51.00	102.00
E18	55.00	110.00
E19	61.00	122.00
E20	71.00	142.00
E99	*	*

* Contact NTIS for price quote.

IMPORTANT NOTICE

NTIS Shipping and Handling Charges

U.S., Canada, Mexico — ADD $3.00 per TOTAL ORDER

All Other Countries — ADD $4.00 per TOTAL ORDER

Exceptions — Does NOT apply to:

ORDERS REQUESTING NTIS RUSH HANDLING

ORDERS FOR SUBSCRIPTION OR STANDING ORDER PRODUCTS *ONLY*

NOTE: Each additional delivery address on an order requires a separate shipping and handling charge.

VOLUME 26 NUMBER 13 / JULY 8, 1988

TABLE OF CONTENTS

AERONAUTICS

Includes aeronautics (general); aerodynamics; air transportation and safety; aircraft communications and navigation; aircraft design, testing and performance; aircraft instrumentation; aircraft propulsion and power; aircraft stability and control; and research and support facilities (air).

For related information see also *Astronautics.*

01 AERONAUTICS (GENERAL) 1715

02 AERODYNAMICS 1715

Includes aerodynamics of bodies, combinations, wings, rotors, and control surfaces; and internal flow in ducts and turbomachinery.

For related information see also *34 Fluid Mechanics and Heat Transfer*

03 AIR TRANSPORTATION AND SAFETY 1719

Includes passenger and cargo air transport operations; and aircraft accidents.

For related information see also *16 Space Transportation* and *85 Urban Technology and Transportation.*

04 AIRCRAFT COMMUNICATIONS AND NAVIGATION 1720

Includes digital and voice communication with aircraft; air navigation systems (satellite and ground based); and air traffic control.

For related information see also *17 Space Communications, Spacecraft Communications, Command and Tracking* and *32 Communications and Radar.*

05 AIRCRAFT DESIGN, TESTING AND PERFORMANCE 1721

Includes aircraft simulation technology.

For related information see also *18 Spacecraft Design, Testing and Performance* and *39 Structural Mechanics.* For land transportation vehicles see *85 Urban Technology and Transportation.*

06 AIRCRAFT INSTRUMENTATION 1723

Includes cockpit and cabin display devices; and flight instruments.

For related information see also *19 Spacecraft Instrumentation* and *35 Instrumentation and Photography.*

07 AIRCRAFT PROPULSION AND POWER 1723

Includes prime propulsion systems and systems components, e.g., gas turbine engines and compressors; and onboard auxiliary power plants for aircraft.

For related information see also *20 Spacecraft Propulsion and Power, 28 Propellants and Fuels,* and *44 Energy Production and Conversion.*

08 AIRCRAFT STABILITY AND CONTROL 1724

Includes aircraft handling qualities; piloting; flight controls; and autopilots.

For related information see also *05 Aircraft Design, Testing and Performance.*

09 RESEARCH AND SUPPORT FACILITIES (AIR) 1724

Includes airports, hangars and runways; aircraft repair and overhaul facilities; wind tunnels; shock tubes; and aircraft engine test stands.

For related information see also *14 Ground Support Systems and Facilities (Space).*

ASTRONAUTICS

Includes astronautics (general); astrodynamics; ground support systems and facilities (space); launch vehicles and space vehicles; space transportation; space communications, spacecraft communications, command and tracking; spacecraft design, testing and performance; spacecraft instrumentation; and spacecraft propulsion and power.

For related information see also *Aeronautics*

12 ASTRONAUTICS (GENERAL) 1724

For extraterrestrial exploration see *91 Lunar and Planetary Exploration.*

13 ASTRODYNAMICS 1727

Includes powered and free-flight trajectories; and orbital and launching dynamics.

14 GROUND SUPPORT SYSTEMS AND FACILITIES (SPACE) 1728

Includes launch complexes, research and production facilities; ground support equipment, e.g., mobile transporters; and simulators.

For related information see also *09 Research and Support Facilities (Air).*

15 LAUNCH VEHICLES AND SPACE VEHICLES 1728

Includes boosters; operating problems of launch/space vehicle systems; and reusable vehicles.

For related information see also *20 Spacecraft Propulsion and Power.*

16 SPACE TRANSPORTATION 1729

Includes passenger and cargo space transportation, e.g., shuttle operations; and space rescue techniques.

For related information see also *03 Air Transportation and Safety* and *18 Spacecraft Design, Testing and Performance.* For space suits see *54 Man/System Technology and Life Support.*

17 SPACE COMMUNICATIONS, SPACECRAFT COMMUNICATIONS, COMMAND AND TRACKING 1730

Includes telemetry; space communications networks; astronavigation and guidance; and radio blackout.

For related information see also *04 Aircraft Communications and Navigation* and *32 Communications and Radar.*

18 SPACECRAFT DESIGN, TESTING AND PERFORMANCE 1730

Includes satellites; space platforms; space stations; spacecraft systems and components such as thermal and environmental controls; and attitude controls.

For life support systems see *54 Man/System Technology and Life Support.* For related information see also *05 Aircraft Design, Testing and Performance, 39 Structural Mechanics,* and *16 Space Transportation.*

19 SPACECRAFT INSTRUMENTATION N.A.

For related information see also *06 Aircraft Instrumentation* and *35 Instrumentation and Photography.*

20 SPACECRAFT PROPULSION AND POWER 1732

Includes main propulsion systems and components, e.g. rocket engines; and spacecraft auxiliary power sources.

For related information see also *07 Aircraft Propulsion and Power, 28 Propellants and Fuels, 44 Energy Production and Conversion,* and *15 Launch Vehicles and Space Vehicles.*

CHEMISTRY AND MATERIALS

Includes chemistry and materials (general); composite materials; inorganic and physical chemistry; metallic materials; nonmetallic materials; propellants and fuels; and materials processing.

23 CHEMISTRY AND MATERIALS (GENERAL) 1733

24 COMPOSITE MATERIALS 1733

Includes physical, chemical, and mechanical properties of laminates and other composite materials.

For ceramic materials see *27 Nonmetallic Materials.*

25 INORGANIC AND PHYSICAL CHEMISTRY 1736

Includes chemical analysis, e.g., chromatography; combustion theory; electrochemistry; and photochemistry.

For related information see also *77 Thermodynamics and Statistical Physics.*

26 METALLIC MATERIALS 1740

Includes physical, chemical, and mechanical properties of metals, e.g., corrosion; and metallurgy.

27 NONMETALLIC MATERIALS 1746

Includes physical, chemical, and mechanical properties of plastics, elastomers, lubricants, polymers, textiles, adhesives, and ceramic materials.

For composite materials see *24 Composite Materials.*

28 PROPELLANTS AND FUELS 1753

Includes rocket propellants, igniters and oxidizers; their storage and handling procedures; and aircraft fuels.

For related information see also *07 Aircraft Propulsion and Power, 20 Spacecraft Propulsion and Power,* and *44 Energy Production and Conversion.*

29 MATERIALS PROCESSING N.A.

Includes space-based development of products and processes for commercial application.

For biological materials see *55 Space Biology.*

ENGINEERING

Includes engineering (general); communications and radar; electronics and electrical engineering; fluid mechanics and heat transfer; instrumentation and photography; lasers and masers; mechanical engineering; quality assurance and reliability; and structural mechanics.

For related information see also *Physics.*

31 ENGINEERING (GENERAL) 1754

Includes vacuum technology; control engineering; display engineering; cryogenics; and fire prevention.

32 COMMUNICATIONS AND RADAR 1757

Includes radar; land and global communications; communications theory; and optical communications.

For related information see also *04 Aircraft Communications and Navigation* and *17 Space Communications, Spacecraft Communications, Command and Tracking.* For search and rescue see *03 Air Transportation and Safety,* and *16 Space Transportation.*

33 ELECTRONICS AND ELECTRICAL ENGINEERING 1760

Includes test equipment and maintainability; components, e.g., tunnel diodes and transistors; microminiaturization; and integrated circuitry.

For related information see also *60 Computer Operations and Hardware* and *76 Solid-State Physics.*

34 FLUID MECHANICS AND HEAT TRANSFER 1765

Includes boundary layers; hydrodynamics; fluidics; mass transfer and ablation cooling.

For related information see also *02 Aerodynamics* and *77 Thermodynamics and Statistical Physics.*

35 INSTRUMENTATION AND PHOTOGRAPHY 1772

Includes remote sensors; measuring instruments and gages; detectors; cameras and photographic supplies; and holography.

For aerial photography see *43 Earth Resources and Remote Sensing.* For related information see also *06 Aircraft Instrumentation* and *19 Spacecraft Instrumentation.*

36 LASERS AND MASERS 1774

Includes parametric amplifiers.

For related information see also *76 Solid-State Physics.*

37 MECHANICAL ENGINEERING 1778

Includes auxiliary systems (nonpower); machine elements and processes; and mechanical equipment.

38 QUALITY ASSURANCE AND RELIABILITY 1780

Includes product sampling procedures and techniques; and quality control.

39 STRUCTURAL MECHANICS 1780

Includes structural element design and weight analysis; fatigue; and thermal stress.

For applications see *05 Aircraft Design, Testing and Performance* and *18 Spacecraft Design, Testing and Performance.*

GEOSCIENCES

Includes geosciences (general); earth resources and remote sensing; energy production and conversion; environment pollution; geophysics; meteorology and climatology; and oceanography.

For related information see also *Space Sciences.*

42 GEOSCIENCES (GENERAL) 1784

43 EARTH RESOURCES AND REMOTE SENSING 1790

Includes remote sensing of earth resources by aircraft and spacecraft; photogrammetry; and aerial photography.

For instrumentation see *35 Instrumentation and Photography.*

44 ENERGY PRODUCTION AND CONVERSION 1792

Includes specific energy conversion systems, e.g., fuel cells; global sources of energy; geophysical conversion; and windpower.

For related information see also *07 Aircraft Propulsion and Power, 20 Spacecraft Propulsion and Power,* and *28 Propellants and Fuels.*

45 ENVIRONMENT POLLUTION 1796

Includes atmospheric, noise, thermal, and water pollution.

46 GEOPHYSICS 1796

Includes aeronomy; upper and lower atmosphere studies; ionospheric and magnetospheric physics; and geomagnetism.

For space radiation see *93 Space Radiation.*

47 METEOROLOGY AND CLIMATOLOGY 1799

Includes weather forecasting and modification.

48 OCEANOGRAPHY 1802

Includes biological, dynamic, and physical oceanography; and marine resources.

For related information see also *43 Earth Resources and Remote Sensing.*

LIFE SCIENCES

Includes life sciences (general); aerospace medicine; behavioral sciences; man/system technology and life support; and space biology.

51 LIFE SCIENCES (GENERAL) 1808

52 AEROSPACE MEDICINE 1809

Includes physiological factors; biological effects of radiation; and effects of weightlessness on man and animals.

53 BEHAVIORAL SCIENCES 1811

Includes psychological factors; individual and group behavior; crew training and evaluation; and psychiatric research.

54 MAN/SYSTEM TECHNOLOGY AND LIFE SUPPORT 1811

Includes human engineering; biotechnology; and space suits and protective clothing.

For related information see also *16 Space Transportation.*

55 SPACE BIOLOGY N.A.

Includes exobiology; planetary biology; and extraterrestrial life.

MATHEMATICAL AND COMPUTER SCIENCES

Includes mathematical and computer sciences (general); computer operations and hardware; computer programming and software; computer systems; cybernetics; numerical analysis; statistics and probability; systems analysis; and theoretical mathematics.

59 MATHEMATICAL AND COMPUTER SCIENCES (GENERAL) 1813

60 COMPUTER OPERATIONS AND HARDWARE 1813

Includes hardware for computer graphics, firmware, and data processing.

For components see *33 Electronics and Electrical Engineering.*

61 COMPUTER PROGRAMMING AND SOFTWARE 1814

Includes computer programs, routines, algorithms, and specific applications, e.g., CAD/CAM.

62 COMPUTER SYSTEMS 1821

Includes computer networks and special application computer systems.

63 CYBERNETICS 1823

Includes feedback and control theory, artificial intelligence, robotics and expert systems.

For related information see also *54 Man/System Technology and Life Support.*

64 NUMERICAL ANALYSIS 1825

Includes iteration, difference equations, and numerical approximation.

65 STATISTICS AND PROBABILITY 1828

Includes data sampling and smoothing; Monte Carlo method; and stochastic processes.

66 SYSTEMS ANALYSIS 1830

Includes mathematical modeling; network analysis; and operations research.

67 THEORETICAL MATHEMATICS 1831

Includes topology and number theory.

PHYSICS

Includes physics (general); acoustics; atomic and molecular physics; nuclear and high-energy physics; optics; plasma physics; solid-state physics; and thermodynamics and statistical physics.

For related information see also *Engineering.*

70 PHYSICS (GENERAL) 1832

For precision time and time interval (PTTI) see *35 Instrumentation and Photography;* for geophysics, astrophysics or solar physics see *46 Geophysics, 90 Astrophysics,* or *92 Solar Physics.*

71 ACOUSTICS 1833
Includes sound generation, transmission, and attenuation.
For noise pollution see *45 Environment Pollution.*

72 ATOMIC AND MOLECULAR PHYSICS 1835
Includes atomic structure, electron properties, and molecular spectra.

73 NUCLEAR AND HIGH-ENERGY PHYSICS 1838
Includes elementary and nuclear particles; and reactor theory.
For space radiation see *93 Space Radiation.*

74 OPTICS 1839
Includes light phenomena and optical devices.
For lasers see *36 Lasers and Masers.*

75 PLASMA PHYSICS 1841
Includes magnetohydrodynamics and plasma fusion.
For ionospheric plasmas see *46 Geophysics.* For space plasmas see *90 Astrophysics.*

76 SOLID-STATE PHYSICS 1844
Includes superconductivity.
For related information see also *33 Electronics and Electrical Engineering* and *36 Lasers and Masers.*

77 THERMODYNAMICS AND STATISTICAL PHYSICS 1849
Includes quantum mechanics; theoretical physics; and Bose and Fermi statistics.
For related information see also *25 Inorganic and Physical Chemistry* and *34 Fluid Mechanics and Heat Transfer.*

SOCIAL SCIENCES

Includes social sciences (general); administration and management; documentation and information science; economics and cost analysis; law, political science, and space policy; and urban technology and transportation.

80 SOCIAL SCIENCES (GENERAL) N.A.
Includes educational matters.

81 ADMINISTRATION AND MANAGEMENT 1850
Includes management planning and research.

82 DOCUMENTATION AND INFORMATION SCIENCE 1851
Includes information management; information storage and retrieval technology; technical writing; graphic arts; and micrography.
For computer documentation see *61 Computer Programming and Software.*

83 ECONOMICS AND COST ANALYSIS 1851
Includes cost effectiveness studies.

84 LAW, POLITICAL SCIENCE AND SPACE POLICY N.A.
Includes NASA appropriation hearings; aviation law; space law and policy; international law; international cooperation; and patent policy.

85 URBAN TECHNOLOGY AND TRANSPORTATION 1852
Includes applications of space technology to urban problems; technology transfer; technology assessment; and surface and mass transportation.
For related information see *03 Air Transportation and Safety, 16 Space Transportation,* and *44 Energy Production and Conversion.*

SPACE SCIENCES

Includes space sciences (general); astronomy; astrophysics; lunar and planetary exploration; solar physics; and space radiation.
For related information see also *Geosciences.*

88 SPACE SCIENCES (GENERAL) N.A.

89 ASTRONOMY 1852
Includes radio, gamma-ray, and infrared astronomy; and astrometry.

90 ASTROPHYSICS 1853
Includes cosmology; celestial mechanics; space plasmas; and interstellar and interplanetary gases and dust.
For related information see also *75 Plasma Physics.*

91 LUNAR AND PLANETARY EXPLORATION 1855
Includes planetology; and manned and unmanned flights.
For spacecraft design or space stations see *18 Spacecraft Design, Testing and Performance.*

92 SOLAR PHYSICS 1857
Includes solar activity, solar flares, solar radiation and sunspots.
For related information see *93 Space Radiation.*

93 SPACE RADIATION 1858
Includes cosmic radiation; and inner and outer earth's radiation belts.
For biological effects of radiation see *52 Aerospace Medicine.* For theory see *73 Nuclear and High-Energy Physics.*

GENERAL

Includes aeronautical, astronautical, and space science related histories, biographies, and pertinent reports too broad for categorization; histories or broad overviews of NASA programs.

99 GENERAL 1858

Note: N.A. means that no abstracts were assigned to this category for this issue.

SUBJECT INDEX I-1
PERSONAL AUTHOR INDEX I-55
CORPORATE SOURCE INDEX I-63
CONTRACT NUMBER INDEX I-75
REPORT/ACCESSION NUMBER INDEX I-79

TYPICAL CITATION AND ABSTRACT

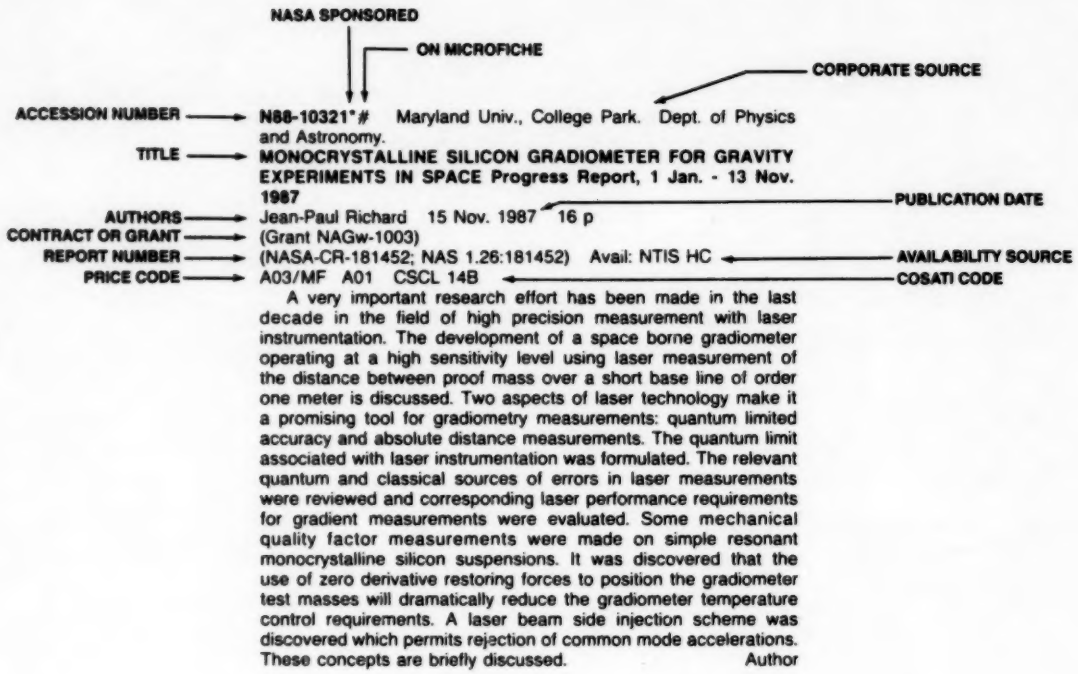
NASA SPONSORED
ON MICROFICHE
CORPORATE SOURCE
ACCESSION NUMBER
N88-10321*# Maryland Univ., College Park. Dept. of Physics and Astronomy.
TITLE
MONOCRYSTALLINE SILICON GRADIOMETER FOR GRAVITY EXPERIMENTS IN SPACE Progress Report, 1 Jan. - 13 Nov. 1987
PUBLICATION DATE
AUTHORS
Jean-Paul Richard 15 Nov. 1987 16 p
CONTRACT OR GRANT
(Grant NAGw-1003)
REPORT NUMBER
(NASA-CR-181452; NAS 1.26:181452) Avail: NTIS HC
AVAILABILITY SOURCE
PRICE CODE
A03/MF A01 CSCL 14B
COSATI CODE
A very important research effort has been made in the last decade in the field of high precision measurement with laser instrumentation. The development of a space borne gradiometer operating at a high sensitivity level using laser measurement of the distance between proof mass over a short base line of order one meter is discussed. Two aspects of laser technology make it a promising tool for gradiometry measurements: quantum limited accuracy and absolute distance measurements. The quantum limit associated with laser instrumentation was formulated. The relevant quantum and classical sources of errors in laser measurements were reviewed and corresponding laser performance requirements for gradient measurements were evaluated. Some mechanical quality factor measurements were made on simple resonant monocrystalline silicon suspensions. It was discovered that the use of zero derivative restoring forces to position the gradiometer test masses will dramatically reduce the gradiometer temperature control requirements. A laser beam side injection scheme was discovered which permits rejection of common mode accelerations. These concepts are briefly discussed. Author

VOLUME 26 NUMBER 13/ JULY 8, 1988

Scientific and Technical Aerospace Reports

A Semimonthly Publication of the National Aeronautics and Space Administration

01 AERONAUTICS (GENERAL)

N88-20254* National Aeronautics and Space Administration, Washington, D.C.
AERONAUTICAL ENGINEERING: A CONTINUING BIBLIOGRAPHY WITH INDEXES (SUPPLEMENT 224)
Mar. 1988 127 p
(NASA-SP-7037(224); NAS 1.21:7037(224)) Avail: NTIS HC A07 CSCL 01B

This bibliography lists 447 reports, articles and other documents introduced into the NASA scientific and technical information system in February, 1988. Author

N88-20255# Rijksluchtvaartdienst, The Hague (Netherlands).
[ACTIVITIES REPORT IN CIVIL AERONAUTICS] Annual Report, 1986 [JAARVERSLAG 1986]
1986 51 p In DUTCH
(ETN-88-91344) Avail: NTIS HC A04/MF A01

Air traffic control, regional airports, air transportation policy, and air traffic safety are discussed. The activities of the civil aeronautics school, the national aeronautics and astronautics museum AVIODOME, and the national aeronautics and astronautics medical center are presented. ESA

02 AERODYNAMICS

Includes aerodynamics of bodies, combinations, wings, rotors, and control surfaces; and internal flow in ducts and turbomachinery.

For related information see also *34 Fluid Mechanics and Heat Transfer.*

N88-20256*# Science Applications International Corp., Princeton, N.J.
FULLY-COUPLED ANALYSIS OF JET MIXING PROBLEMS. THREE-DIMENSIONAL PNS MODEL, SCIP3D Final Report
D. E. Wolf, N. Sinha, and S. M. Dash NASA Apr. 1988 147 p
(Contract NAS1-16535)
(NASA-CR-4139; NAS 1.26:4139; SAIC/PR-TR-67) Avail: NTIS HC A07/MF A01

Numerical procedures formulated for the analysis of 3D jet mixing problems, as incorporated in the computer model, SCIP3D, are described. The overall methodology closely parallels that developed in the earlier 2D axisymmetric jet mixing model, SCIPVIS. SCIP3D integrates the 3D parabolized Navier-Stokes (PNS) jet mixing equations, cast in mapped cartesian or cylindrical coordinates, employing the explicit MacCormack Algorithm. A pressure split variant of this algorithm is employed in subsonic regions with a sublayer approximation utilized for treating the streamwise pressure component. SCIP3D contains both the ks and kW turbulence models, and employs a two component mixture approach to treat jet exhausts of arbitrary composition. Specialized grid procedures are used to adjust the grid growth in accordance with the growth of the jet, including a hybrid cartesian/cylindrical grid procedure for rectangular jets which moves the hybrid coordinate origin towards the flow origin as the jet transitions from a rectangular to circular shape. Numerous calculations are presented for rectangular mixing problems, as well as for a variety of basic unit problems exhibiting overall capabilities of SCIP3D. Author

N88-20257*# National Aeronautics and Space Administration. Ames Research Center, Moffett Field, Calif.
AN EXPERIMENTAL INVESTIGATION OF THE FLAP-LAG-TORSION AEROELASTIC STABILITY OF A SMALL-SCALE HINGELESS HELICOPTER ROTOR IN HOVER
David L. Sharpe Jan. 1986 86 p Prepared in cooperation with Army Aviation Research and Development Command, Moffett Field, Calif.
(NASA-TP-2546; Rept-85142; NAS 1.60:2546; AVSCOM-TR-85-A-9) Avail: NTIS HC A05/MF A01 CSCL 01A

A small scale, 1.92 m diam, torsionally soft, hingeless helicopter rotor was investigated in hover to determine isolated rotor stability characteristics. The two-bladed, untwisted rotor was tested on a rigid test stand at tip speeds up to 101 m/sec. The rotor mode of interest is the lightly damped lead-lag mode. The dimensionless lead-lag frequency of the mode is approximately 1.5 at the highest tip speed. The hub was designed to allow variation in precone, blade droop, pitch control stiffness, and blade pitch angle. Measurements of modal frequency and damping were obtained for several combinations of these hub parameters at several values of rotor speed. Steady blade bending moments were also measured. The lead-lag damping measurements were found to agree well with theoretical predictions for low values of blade pitch angle. The test data confirmed the predicted effects of precone, droop, and pitch control stiffness parameters on lead-lag damping. The correlation between theory and experiment was found to be poor for the mid-to-high range of pitch angles where the theory substantially overpredicted the experimental lead-lag damping. The poor correlation in the mid-to-high blade pitch angle range is attributed to low Reynolds number nonlinear aerodynamics effects not included in the theory. The experimental results also revealed an asymmetry in lead-lag damping between positive and negative thrust conditions. Author

N88-20258# Aeronautical Research Labs., Melbourne (Australia).
AUSTRALIAN AERODYNAMIC DESIGN CODES FOR AERIAL TOW BODIES
N. Matheson 27 Aug. 1987 25 p
(AD-A189048; ARL-AERO-TM-389; DODA-AR-004-553) Avail: NTIS HC A03/MF A01 CSCL 01A

An overview is presented of the design codes developed in Australia that are directly applicable or related to the Aerodynamics of towed bodies. In view of the continuing need for increasingly sophisticated towed targets, often as an alternative to costly subscale targets, a collaborative activity was undertaken to: (1) review the availability and applicability of existing design codes for the free flight phase of deployed aerial tow bodies in the subsonic and supersonic flight regimes; and (2) recommend either an existing design approach or cooperative action to provide a satisfactory capability. In this report, an overview of the design codes developed in Australia that are directly applicable or related to the aerodynamics of towed bodies is presented. GRA

N88-20259# Naval Surface Weapons Center, Dahlgren, Va.
NONAXISYMMETRIC BODY SUPERSONIC, AERODYNAMIC PREDICTION Final Report
Leroy Devan Aug. 1987 93 p
(AD-A189338; NSWC/TR-86-253) Avail: NTIS HC A05/MF A01 CSCL 16B

A supersonic flow computational model was developed for flight vehicles with nonaxisymmetric bodies. The bodies may be pointed, with arbitrary initial cross section, or blunted, with initially circular cross section; the remainder of the body may have an arbitrary cross-sectional variation. A vertical plane of symmetry is assumed except for fin deflections. The body is divided into piecewise continuous sections by planar discontinuities including inlets. All sections, except for the first one, may have fin sets. The fins, up to six per set: (1) are assumed to be aligned with a cylindrical coordinate ray, (2) depart only slightly from the midplane (thin fin approximation), (3) and are symmetric about the midplane. For the low Mach-number range, new research was developed for the inviscid flow regime. The computational model is based on a finite-difference, second-order, linear, potential solution. For pointed bodies, the computation is implicit up to the first planar body discontinuity and an explicit MacCormack scheme thereafter. Blunt body computations: (1) assume an effective origin of disturbances and a modified Newtonian pressure distribution up to a matching or starting plane, and (2) use an explicit solution thereafter. Local jump relations for discontinuities on the body, at fin roots, and fin edges are conservation relations obtained by applying the method of weak solutions to first-and second-order equations. GRA

N88-20260# Naval Postgraduate School, Monterey, Calif.
APPLICATION OF A FLUX VECTOR SPLITTING METHODOLOGY TOWARDS THE SOLUTION OF UNSTEADY TRANSONIC FLOWS, WITH FUTURE EMPHASIS ON THE BLADE FLUTTER PROBLEM Final Report, Aug. 1986 - Aug. 1987
Torsten H. Fransson Jul. 1987 256 p
(AD-A189500; NPS67-87-006) Avail: NTIS HC A12/MF A01 CSCL 20D

This study presents a method, based on the flux vector splitting approach, to the problem of unsteady two dimensional inviscid transonic flows, with emphasis on the numerical determination of the shock position, through nozzles with varying back pressure. The method, governed by Euler equations, is first explained for one and two dimensional steady state applications, and the accuracy of the results is validated by comparison with exact (one dimension and numerical (two dimensions) solutions. The model is then applied to the problem of fluctuating back pressure in quasi one dimensional and two dimensional flows. The one dimensional results are validated by comparison with a small perturbation analytical unsteady solution, whereafter sample cases are performed with the objective to understand fundamental aspects of unsteady flows. It is concluded that both the amplitude and frequency of the imposed fluctuating exit pressure are important parameters for location of the unsteady shock. It is also shown that the average unsteady shock position is not identical with the steady state position, and that the unsteady shock may, under certain circumstances, propagate upstream into the subsonic flow domain. GRA

N88-20261# Air Force Inst. of Tech., Wright-Patterson AFB, Ohio. School of Engineering.
INTERACTION BETWEEN TWO-DIMENSIONAL SONIC JETS AND SUPERSONIC FLOW TO MODEL HEAT ADDITION IN A SUPERSONIC COMBUSTOR M.S. Thesis
John M. Traxler Dec. 1987 113 p
(AD-A189572; AFIT/GA/AA/87D-07) Avail: NTIS HC A06/MF A01 CSCL 21B

Displacement effects of heated addition to a supersonic flow through a simulated combustor were simulated with mass addition. The structure of precombustion shocks was experimentally investigated by an optical and pressure study of two parallel sonic jets expanding into a two-dimensional supersonic test cavity. Base flow and recompression shocks were studied for two test section depths. A test section to add heat to a two dimensional flow was demonstrated. It was determined that the performance of the constant-area test section was dominated by frictional, rather than shock effects. An off-design nozzle, used for preliminary investigation, caused turbulence and high losses in the channel. The structure of the precombustion zone was found to be a base flow problem and was analyzed using a simple one dimensional model. Static pressure measurements on the sidewalls of the test cavity were found to differ from the static pressure in the center of the two dimensional test cavity, due to diffusion of pressure upstream and downstream through the boundary layer. A welding torch was used to inject premixed oxygen and acetylene into the base region on the end of a centerbody between two supersonic nozzles. The flame was successfully ignited and burned continuously in the flowstream. GRA

N88-20262*# National Aeronautics and Space Administration. Lewis Research Center, Cleveland, Ohio.
NUMERICAL SIMULATION OF SUBSONIC AND TRANSONIC PROPELLER FLOW Ph.D. Thesis
Aaron Snyder Apr. 1988 191 p
(NASA-TM-100163; E-3725; NAS 1.15:100163) Avail: NTIS HC A09/MF A01 CSCL 01A

The numerical simulation of 3-D transonic flow about a system of propeller blades is investigated. In particular, it is shown that the use of helical coordinates significantly simplifies the form of the governing equation when the propeller system is assumed to be surrounded by an irrotational flow field of an inviscid fluid. The unsteady small disturbance equation, valid for lightly loaded blades and expressed in helical coordinates, is derived from the general blade-fixed potential equation, given for an arbitrary coordinate system. The use of a coordinate system which inherently adapts to the mean flow results in a disturbance equation requiring relatively few terms to accurately model the physics of the flow. Furthermore, the helical coordinate system presented here is novel in that it is periodic in the circumferential direction while, simultaneously, maintaining orthogonal properties at the mean blade locations. The periodic characteristic allows a complete cascade of blades to be treated, and the orthogonality property affords straightforward treatment of blade boundary conditions. An ADI numerical scheme is used to compute the solution of the steady flow as an asymptotic limit of an unsteady flow. As an example of the method, solutions are presented for subsonic and transonic flow about a 5 percent thick bicircular arc blade of an 8-bladed cascade. Both high and low advance ratio cases are computed and include a lifting as well as nonlifting cases. The nonlifting solutions obtained are compared to solutions from a Euler code. Author

N88-20263*# National Aeronautics and Space Administration. Langley Research Center, Hampton, Va.
APPLICATION OF A NONISENTROPIC FULL POTENTIAL METHOD TO AGARD STANDARD AIRFOILS
Woodrow Whitlow, Jr. Jan. 1988 16 p Presented at the AIAA 26th Aerospace Sciences Meeting, Reno, Nev., 11-14 Jan. 1988 Previously announced in IAA as A88-22535
(NASA-TM-100560; NAS 1.15:100560; AIAA-88-0710) Avail: NTIS HC A03/MF A01 CSCL 01A

An entropy-correction method for the unsteady full potential equation is presented. The unsteady potential equation is modified to model the entropy jumps across shock waves. The conservative form of the modified equation is solved in generalized coordinates using an implicit, approximate factorization method. A flux-biasing differencing method, which generates the proper amounts of artificial viscosity in supersonic regions, is used to discretize the flow equations in space. Calculated results are presented for the NLR 7301, NACA 0012, and NACA 64A010A airfoils. Comparisons of the present method and solutions of the Euler equations are presented for the NLR 7301 airfoil, and comparisons of the present method and experimental data are presented for all three airfoils. The comparisons show that the present method more accurately models solutions of the Euler equations and experiment than does

the isentropic potential formulation. In addition, it is shown that modeling shock-generated entropy extends the range of validity of the full potential method. Author

N88-20264*# National Aeronautics and Space Administration. Langley Research Center, Hampton, Va.
A REVIEW OF TECHNOLOGIES APPLICABLE TO LOW-SPEED FLIGHT OF HIGH-PERFORMANCE AIRCRAFT INVESTIGATED IN THE LANGLEY 14- X 22-FOOT SUBSONIC TUNNEL
John W. Paulson, Jr., P. Frank Quinto, Daniel W. Banks, Guy T. Kemmerly, and Gregory M. Gatlin May 1988 94 p
(NASA-TP-2796; L-16364; NAS 1.60:2796) Avail: NTIS HC A05/MF A01 CSCL 01A

An extensive research program has been underway at the NASA Langley Research Center to define and develop the technologies required for low-speed flight of high-performance aircraft. This 10-year program has placed emphasis on both short takeoff and landing (STOL) and short takeoff and vertical landing (STOVL) operations rather than on regular up and away flight. A series of NASA in-house as well as joint projects have studied various technologies including high lift, vectored thrust, thrust-induced lift, reversed thrust, an alternate method of providing trim and control, and ground effects. These technologies have been investigated on a number of configurations ranging from industry designs for advanced fighter aircraft to generic wing-canard research models. Test conditions have ranged from hover (or static) through transition to wing-borne flight at angles of attack from -5 to 40 deg at representative thrust coefficients. Author

N88-20265# National Aerospace Lab., Amsterdam (Netherlands). Fluid Dynamics Div.
ARSPNSC: A METHOD TO CALCULATE SUBSONIC STEADY AND UNSTEADY POTENTIAL FLOW ABOUT COMPLEX CONFIGURATIONS
M. H. L. Hounjet Dec. 1986 24 p Sponsored in part by the Royal Netherlands Air Force Material Directorate
(NLR-TR-86122-U; ETN-88-91723) Avail: NTIS HC A03/MF A01

A panel method (ARSPSC) for the calculation of steady and time-linearized unsteady subsonic potential flow about complex 2D and 3D configurations is described. The code is an extension of the ARSPNS code for rotating structures in incompressible flow. The ARSPSC method enables the calculation of steady and unsteady incompressible and subsonic potential flow and deals with arbitrary configurations involving lifting and nonlifting components. Lifting components with small thickness may be modeled by a thin lifting surface approximation. The wakes which start at the sharp trailing edges of the lifting components can be modeled in a fairly arbitrary way and are extended towards infinity as planar wakes in the direction of the x-axis. The load integration scheme is as applied in the ARSPNS code, which allows the correct determination of the suction force in a lifting surface approximation and improves the drag prediction in a full body approximation. Applications to a 2D oscillating flat plate, a 2D multicomponent airfoil with oscillating flap, and a 3D fighter-type wing are described. ESA

N88-20266# National Aerospace Lab., Amsterdam (Netherlands). Fluid Dynamics Div.
TESTS ON THE AFWAL 65 DEG DELTA WING AT NLR: A STUDY OF VORTEX FLOW DEVELOPMENT BETWEEN MACH = 0.4 AND 4
S. J. Boersen and A. Elsenaar Sep. 1986 18 p Presented at the Joint International Vortex Flow Symposium, Stockholm, Sweden, 13 Oct. 1986
(NLR-MP-86058-U; B8725238; ETN-88-91731) Avail: NTIS HC A03/MF A01

As a part of a vortex flow experiment, force and pressure measurements were carried out in transonic and supersonic wind tunnels on a 65 deg swept delta wing configuration. Experimental results concern one configuration with a sharp and one with a rounded leading edge, both tested over a range of Mach numbers between 0.4 and 4.0. A classification of the various types of flow as observed in the experiment is given. Typical aspects of the flow are discussed, including conicity, the occurrence of shocks in the flow field, and the effect of the leading edge shape on the separation development and subsequent vortex formation. The data represent an excellent test case for the evaluation and validation of computational methods such as Euler and Navier-Stokes codes. ESA

N88-20267# National Aerospace Lab., Amsterdam (Netherlands). Fluid Dynamics Div.
THE INTERNATIONAL VORTEX FLOW EXPERIMENT: A TEST CASE FOR COMPRESSIBLE EULER CODES
A. Elsenaar 31 Oct. 1986 19 p Presented at the GAMM Workshop on the Numerical Simulation of Compressible Euler Flows, Rocquencourt, France, 10-13 Jun. 1986
(NLR-MP-86076-U; B8725240; ETN-88-91733) Avail: NTIS HC A03/MF A01

As part of a vortex flow experiment, force and pressure measurements were carried out on a 65 deg delta wing configuration in transonic and supersonic wind tunnels. Three test cases were selected. The test cases are all for the configuration with a sharp leading edge without the canard wing. Three flow conditions are to be used for comparison with the results of Euler codes: the model at an angle of attack of 10 deg at free stream Mach numbers of 0.4, 0.85, and 1.2. The following experimental data is available: overall loads (lift, drag and pitching moment); pressure distributions; surface streamlines, obtained from oil flow pictures (note however that they visualize limiting streamlines in the boundary layer and not inviscid streamlines); and flow field surveys by pressure probes. ESA

N88-20268# Deutsche Forschungs- und Versuchsanstalt fuer Luft- und Raumfahrt, Brunswick (West Germany). Abteilung Trans-Ueberschall-Entwurfsverfahren.
ON THE KUTTA CONDITION FOR FLOWS AROUND LIFTING AIRFOILS AND WINGS
Arabindo Das Oct. 1987 88 p
(DFVLR-FB-87-40; ISSN-0171-1342; ETN-88-91923) Avail: NTIS HC A05/MF A01; DFVLR, VB-PL-DO, Postfach 90 60 58, 5000, Cologne, Federal Republic of Germany, 28 deutsche marks

Analyses were performed to examine the flow conditions at the trailing edge of lifting airfoils and wings moving in inviscid medium, and to reveal the significance of the Kutta condition. The analysis includes the origin of dipole and vortex system of lifting surfaces moving in a medium at rest; flow fields of lifting airfoils; flows around edges and wedges in incompressible and compressible medium; and the setting in of the Kutta condition in the numerical methods using Euler equations. In all these cases it is shown that the Kutta condition corresponds to a natural physical process, without resorting to the viscosity of the medium. ESA

N88-20269*# National Aeronautics and Space Administration. Langley Research Center, Hampton, Va.
STEADY AND UNSTEADY TRANSONIC SMALL DISTURBANCE ANALYSIS OF REALISTIC AIRCRAFT CONFIGURATIONS
John T. Batina, David A. Seidel, Robert M. Bennett, Herbert J. Cunningham, and Samuel R. Bland Mar. 1988 33 p Presented at the Transonic Symposium, Hampton, Va., 19-21 Apr. 1988
(NASA-TM-100557; NAS 1.15:100557) Avail: NTIS HC A03/MF A01 CSCL 01A

A transonic unsteady aerodynamic and aeroelasticity code CAP-TSD (Computational Aeroelasticity Program-Transonic Small Disturbance) has been developed for application to realistic aircraft configurations. The code uses a time-accurate approximate factorization (AF) algorithm for solution of the unsteady transonic small-disturbance potential equation. The paper gives an overview of the CAP-TSD code development effort and reports on recent algorithm modifications. The algorithm modifications include: an Engquist-Osher (E-O) type-dependent switch to treat regions of supersonic flow, extension of the E-O switch for second-order spatial accuracy, nonisentropic effects to treat strong-shock cases, nonreflecting far field boundary conditions for unsteady

applications, and several modifications to accelerate convergence to steady state. The modifications have significantly improved the stability of the AF algorithm and hence the reliability of the CAP-TSD code in general. Calculations are also presented from a flutter analysis of a 45-deg sweptback wing which agree well with experimental data. The paper present descriptions of the CAP-TSD code and algorithm details along with results. Author

N88-20270 Cornell Univ., Ithaca, N.Y.
AN L-U IMPLICIT MULTIGRID ALGORITHM TO SOLVE THE EULER EQUATIONS FOR TRANSONIC FLOW IN ROTATING TURBOMACHINERY PASSAGES Ph.D. Thesis
Jeffrey Wayne Yokota [1987] 174 p
Avail: Univ. Microfilms Order No. DA8724164

An LU implicit multigrid scheme was developed for the calculation of three dimensional transonic flow through rotating cascades using the unsteady Euler equations. The Euler equations are the conservation laws that govern the flow of inviscid, compressible fluids and are numerically approximated by a finite volume formulation on a body-fitted mesh. The unsteady Euler equations are solved in an implicit linearized delta form that allows a much larger time step to be taken than is normally permitted by most explicit schemes. The linearized delta form produces a large block banded tridiagonal matrix system that is impractical to solve and therefore an approximate factorization is performed to produce two smaller triangular matrix systems, one upper and one lower. The LU scheme has temporary storage requirements comparable to those of explicit methods and the advantage of requiring only two point-implicit inversions as opposed to the three line-implicit inversions necessary in Alternating Direction Implicit (ADI) factored schemes. The LU scheme is unconditionally stable in all dimensions and is developed within the framework of the multigrid method to accelerate the convergence rate for steady state calculations. Results show the feasibility of using the LU Implicit scheme to solve the three-dimensional unsteady Euler equations and the steady state convergence acceleration achieved when the multigrid method is used. Dissert. Abstr.

N88-20271*# Old Dominion Univ., Norfolk, Va. Dept. of Mechanical Engineering and Mechanics.
COMPUTATIONAL TECHNIQUE FOR COMPRESSIBLE VORTEX FLOWS USING THE INTEGRAL EQUATION SOLUTION Final Report, 31 Jul. 1986
Osama A. Kandil Apr. 1988 3 p
(Grant NAG1-591)
(NASA-CR-182695; NAS 1.26:182695) Avail: NTIS HC A02/MF A01 CSCL 01A

The steady full-potential equation is written in the form of Poisson's equation, and the solution for the velocity field is expressed in terms of an integral equation. The integral solution consists of two surface integrals and one volume integral. The solution is obtained through successive iteration cycles. Each cycle of iteration consists of two sub-cycles, an inner cycle for wake relaxation and an out cycle for the strength of the source distribution integrals representing the flow compressibility. The density gradients in the source distribution is computed by using a type-differencing scheme of the Murman-Cole type. The method is applied to delta wings and the numerical examples show that a curved shock is captured on the wing suction side beneath the leading edge vortex sheet. Recently, a modified version of the scheme was applied to rectangular wings. In this modified scheme, the surface integral terms were computed by using a bilinear distribution of vorticity on triangular vortex panels which represent the wing and its wake. The results were compared with the available experimental data and they are in good agreement. Author

N88-20272*# National Aeronautics and Space Administration, Washington, D.C.
FINITE ELEMENT CALCULATIONS FOR AERODYNAMIC COEFFICIENTS OF A 3-DIMENSIONAL BODY IN SUBSONIC FLOW USING GREEN'S FUNCTION METHOD
Mitsunori Yanagizawa and Kazuo Kikuchi Mar. 1988 46 p Transl. into ENGLISH of report (Tokyo, Japan, National Aerospace Lab.) p 1-28 Original language document was announced as N83-18661 Transl. by Scientific Translation Service, Santa Barbara, Calif.
(Contract NASw-4307)
(NASA-TT-20208; NAS 1.77:20208) Avail: NTIS HC A03/MF A01 CSCL 01A

An accurate method for evaluating the derivatives along circular paths on the surface is proposed. Calculations are made on various practical configurations such as wing-body combinations, tandem wings, wings with dihedral angles at sideslip, ground effects, interference between a sphere and wind tunnel, etc. Comparisons with experiment show good agreement. Author

N88-20273*# Computer Sciences Corp., Hampton, Va. Applied Technology Div.
CODAC (COCKPIT ORIENTED DISPLAY OF AIRCRAFT CONFIGURATIONS) VERSION 1.4 USER'S GUIDE
Bradford D. Bingel, Erma L. Wilson, and Michelle S. Hollis Jan. 1988 65 p
(Contract NAS1-17999)
(NASA-CR-181650; NAS 1.26:181650) Avail: NTIS HC A04/MF A01 CSCL 01A

The Cockpit Oriented Display of Aircraft Configurations (CODAC) package is an interactive FORTRAN 77 graphics program which produces high quality publication grade hidden line images of three dimensional wireframe objects. The term, Cockpit Oriented, is used because CODAC rotates objects relative to the changing aircraft axis system (rather than about a fixed global axis system) and uses the more familiar directions of yaw, roll, and pitch. In addition, CODAC accepts geometry data in a variety of formats (LaWGS, Craidon, Hess, and FVS data check), and automatically selects the appropriate panel driver. Finally, CODAC makes full use of the Precision Visuals' DI-3000 metafile option, allowing users to save, edit, and print images for group presentations or research publications. Author

N88-20274*# Vigyan Research Associates, Inc., Hampton, Va.
THE EFFECT OF STING INTERFERENCE AT LOW SPEEDS ON THE DRAG COEFFICIENT OF AN ELLIPSOIDAL BODY USING A MAGNETIC SUSPENSION AND BALANCE SYSTEM
A. W. Newcomb Feb. 1988 79 p
(Contract NAS1-17919)
(NASA-CR-181611; NAS 1.26:181611) Avail: NTIS HC A05/MF A01 CSCL 01A

A Boltz body of revolution (fineness ratio 7.5:1) was tested in the Southampton University Magnetic Suspension and Balance System. The effects of sting interference on the drag coefficient of the model at zero angle of attack were noted as well as the effects on drag coefficient values at boundary layer trips. The drag coefficient values were compared with other sources and seemed to show agreement. The pressure distribution over the rear of the model with no sting interference was investigated including the use of boundary layer trips. Author

N88-20275# Technische Hogeschool, Eindhoven (Netherlands). Vakgroep Transportfysica.
VERIFICATION OF THE MOMEMTUM THEORY FOR ROTORS USING MEASUREMENTS ON A MODEL HELICOPTER [VERIFICATIE VAN DE IMPULSTHEORIE VOOR ROTOREN MIDDELS METINGEN AAN EEN MODELHELIKOPTER]
H. vanderHoek and L. Pel Feb. 1987 42 p In DUTCH
(R-840-S; ETN-88-91315) Avail: NTIS HC A03/MF A01

Measurements were performed on the rotor of a model helicopter in order to test classical momemtum theory, in the framework of a research project for the improvement of the aerodynamic theory of wind mills. Pressure and velocity measurements were conducted in two planes underneath the rotor. The hot-wire anemometer measurements in the first only provide an angle-averaged picture of the velocity vectors; the total pressure in this plane was determined using a rake. In the second plane the flow velocity was measured with a hot-wire anemometer; the measurements with the total-pressure tube are unreliable. The goal of the measuring campaign is not obtained. ESA

N88-20276# Messerschmitt-Boelkow-Blohm G.m.b.H., Ottobrunn (West Germany). Unternehmensgruppe Hubschrauber und Flugzeuge.
DOCUMENTATION AND INSTALLATION OF THE HYPERSONIC ARBITRARY-BODY COMPUTER PROGRAM (MARK 3 VERSION) OF A.E. GENTRY ON THE IBM COMPUTER SYSTEM [DOKUMENTATION UND INSTALLIERUNG DES HYPERSONIC ARBITRARY-BODY COMPUTER PROGRAM (MARK 3 VERSION) VON A. E. GENTRY AN DER IBM RECHENANLAGE]
Frank A. Haidinger 31 Jul. 1986 195 p In GERMAN
(MBB/LKE-127/S/PUB/256; ETN-88-91437) Copyright Avail: NTIS HC A19/MF A01

The Mark-3 version of the hypersonic arbitrary-body computer program, reprogrammed for the IBM computer system is presented. A complete description of the input and output parameters of the program and examples are given. The theories applied in the program are described. It is shown that the program calculates the global aerodynamic characteristics for arbitrary bodies in an inviscid hypersonic flow with sufficient accuracy. The most important computer programs are enclosed, together with basic explanations and a user manual. ESA

N88-20277# Aeronautical Research Inst. of Sweden, Stockholm. Aerodynamics Dept.
THE CONSTRUCTION OF A THREE-DIMENSIONAL FINITE VOLUME GRID GENERATOR FOR A WING IN A WIND TUNNEL WITH APPLICATION TO NAVIER-STOKES FLOW SOLVERS
Tony Lindeberg 15 Oct. 1987 64 p
(FFA-TN-1987-58; ETN-88-91879) Avail: NTIS HC A04/MF A01

A grid generation method for three-dimensional single block finite volume meshes is presented. A wing in a wind tunnel with application to Navier-Stokes flow solvers serves as a test example. The selected topology of the mesh is of O-O-type, which gives an inherent grid point concentration near the wing surface. The approach is to define a transformation, which maps the region between the wing and the wind tunnel onto a unit cube in a computational space. A surface mesh on the wing as well as a surface mesh on the wind tunnel walls are generated. The three-dimensional grid is then obtained from transfinite interpolation between the two surfaces. A stretching function makes it possible to control the grid spacing near the wing and the wind tunnel wall surfaces in order to resolve the very thin boundary layers which are needed for a Navier-Stokes flow simulation. A simple second order grid smoother is used in the generation of the two surface meshes. ESA

N88-20278*# National Aeronautics and Space Administration, Washington, D.C.
CALCULATION OF THE DISTRIBUTED LOADS ON THE BLADES OF INDIVIDUAL MULTIBLADE PROPELLERS IN AXIAL FLOW USING LINEAR AND NONLINEAR LIFTING SURFACE THEORIES
N. N. Pesetskaya, I. Ya. Timofeev, and S. D. Shipilov May 1988 14 p Transl. into ENGLISH from TsAGI, Uchenye Zapiski (USSR), v. 16, no. 3, 1985 p 122-126 Original language document was announced in IAA as A86-48804 Transl. by Scientific Translation Service, Santa Barbara, Calif.
(Contract NASw-4307)
(NASA-TT-20173; NAS 1.77:20173; ISSN-0321-3429) Avail: NTIS HC A03/MF A01 CSCL 01A

In recent years much attention has been given to the development of methods and programs for the calculation of the aerodynamic characteristics of multiblade, saber-shaped air propellers. Most existing methods are based on the theory of lifting lines. Elsewhere, the theory of a lifting surface is used to calculate screw and lifting propellers. In this work, methods of discrete eddies are described for the calculation of the aerodynamic characteristics of propellers using the linear and nonlinear theories of lifting surfaces. Author

N88-20279*# National Aeronautics and Space Administration. Hugh L. Dryden Flight Research Center, Edwards, Calif.
FLIGHT TESTS OF EXTERNAL MODIFICATIONS USED TO REDUCE BLUNT BASE DRAG
Sheryll Goecke Powers 1988 17 p Proposed for presentation at the AIAA 6th Applied Aerodynamics Conference, Williamsburg, Va., 6-8 Jun. 1988
(NASA-TM-100433; H-1472; NAS 1.15:100433; AIAA-88-2553) Avail: NTIS HC A03/MF A01 CSCL 01A

The effectiveness of a trailing disk (the trapped vortex concept) in reducing the blunt base drag of an 8-in diameter body of revolution was studied from measurements made both in flight and in full-scale wind-tunnel tests. The experiment demonstrated the significant base drag reduction capability of the trailing disk to Mach 0.93. The maximum base drag reduction obtained from a cavity tested on the flight body of revolution was not significant. The effectiveness of a splitter plate and a vented-wall cavity in reducing the base drag of a quasi-two-dimensional fuselage closure was studied from base pressure measurements made in flight. The fuselage closure was between the two engines of the F-111 airplane; therefore, the base pressures were in the presence of jet engine exhaust. For Mach numbers from 1.10 to 1.51, significant base drag reduction was provided by the vented-wall cavity configuration. The splitter plate was not considered effective in reducing base drag at any Mach number tested. Author

N88-20280*# National Aeronautics and Space Administration. Langley Research Center, Hampton, Va.
STATIC PERFORMANCE OF AN AXISYMMETRIC NOZZLE WITH POST-EXIT VANES FOR MULTIAXIS THRUST VECTORING
Bobby L. Berrier and Mary L. Mason May 1988 54 p
(NASA-TP-2800; L-16371; NAS 1.60:2800) Avail: NTIS HC A04/MF A01 CSCL 01A

An investigation was conducted in the static test facility of the Langley 16-Foot Transonic Tunnel to determine the flow-turning capability and the nozzle internal performance of an axisymmetric convergent-divergent nozzle with post-exit vanes installed for multiaxis thrust vectoring. The effects of vane curvature, vane location relative to the nozzle exit, number of vanes, and vane deflection angle were determined. A comparison of the post-exit-vane thrust-vectoring concept with other thrust-vectoring concepts is provided. All tests were conducted with no external flow, and nozzle pressure ratio was varied from 1.6 to 6.0.
Author

N88-20497# Joint Publications Research Service, Arlington, Va.
ADAPTIVE CONTROL OF SCIENTIFIC BALLOON-BORNE GONDOLA ATTITUDE Abstract Only
Yan Yan *In its* JPRS Report: Science and Technology. China 12 Feb. 1988 p 27 Transl. into ENGLISH from Kongjian Kexue Xuebao (Beijing, People's Republic of China), v. 7, no. 4, Oct. 1987 p 262-271 (For primary document see N88-20495 13-31) Avail: NTIS HC A07/MF A01

03 AIR TRANSPORTATION AND SAFETY

Includes passenger and cargo air transport operations; and aircraft accidents.

For related information see also *16 Space Transportation* and *85 Urban Technology and Transportation.*

N88-20281# National Aerospace Lab., Amsterdam (Netherlands). Flight Div.
FLIGHT SIMULATOR EXPERIMENTS CONCERNING TAKE-OFF VISIBILITY MINIMA
M. F. C. vanGool 18 Apr. 1986 40 p Sponsored by the Netherlands Dept. of Civil Aviation
(NLR-TR-86050-U; ETN-88-91719) Avail: NTIS HC A03/MF A01

In two sessions on a Boeing 747 flight simulator, the experimental conditions were defined for an investigation directed

at the minimum required visual reference to control the aircraft after a failure of the most critical engine at an inconvenient moment during the takeoff run. An investigation was carried out involving a large number of Boeing 747 crews, in which a total of 159 aborted takeoffs were performed in low visibility. Pilot comments and ratings as well as measured pilot-aircraft performance data for these takeoffs are presented. It is concluded that aborted takeoffs can be performed safely in night conditions on runways with 15 or 30 m centerline light spacing with an RVR of as low as 150 m, provided the pilot flying keeps looking outside and the pilot not-flying gives speed calls. ESA

N88-20282# National Transportation Safety Board, Washington, D. C.
AIRCRAFT ACCIDENT REPORT: MIDAIR COLLISION OF CESSNA-340A, N8716K, AND NORTH AMERICAN SNJ-4N, N711SQ, ORLANDO, FLORIDA, MAY 1, 1987
16 Feb. 1988 28 p
(PB88-910402; NTSB/AAR-88/02) Avail: NTIS HC A03/MF A01 CSCL 01C

On May 1, 1987, a Cessna-340A and a SNJ-4 collided in midair about 3,000 ft over Orlando, Florida. The Cessna-340A was level at 3,000 ft operating under instrument flight rules on radar vectors to runway 18R at Orlando International Airport. The SNJ-4 was in descent to 1,500 ft and had completed a turn direct to Orlando Executive Airport when the airplanes collided. Both airplanes were in contact with and were being radar vectored by the Orlando approach control. The Cessna pilot, 2 passengers, and the SNJ-4 pilot were killed. Both airplanes were destroyed. The National Transportation Safety Board determines that the probable cause of the accident was the failure of the Orlando West controller to coordinate the handoff of traffic to the Orlando North controller and the failure of the North controller to maintain radar target identification. Contributing to the accident was the limited capability of the radar system to continually track the targets in proximity to one another and the lack of traffic advisories. Also contributing to the accident was the limitation of the see-and-avoid principle in the circumstances of this accident to serve as a means of collision avoidance. Author

04 AIRCRAFT COMMUNICATIONS AND NAVIGATION

Includes digital and voice communication with aircraft; air navigation systems (satellite and ground based); and air traffic control.

For related information see also *17 Space Communications, Spacecraft Communications, Command and Tracking* and *Communications and Radar.*

N88-20283# Carnegie-Mellon Univ., Pittsburgh, Pa. Robotics Inst.
NAVLAB: AN AUTONOMOUS NAVIGATION TESTBED Interim Report
Kevin Dowling, Rob Guzlkowski, Jim Ladd, Henning Pangels, and Jeff Singh Nov. 1987 51 p
(Contract DACA76-86-C-0019)
(AD-A189049; CMU-RI-TR-87-24) Avail: NTIS HC A04/MF A01 CSCL 17G

The NavLab is a testbed for research in outdoor navigation, image understanding, and the role of human interaction with intelligent systems; it accommodates researchers and all computing onboard. The core of the NavLab is the vehicle controller, a multi-processor computer that controls all locomotion, actuation and physical sensing; it interacts with a computer host and and human operator to implement varying degrees of autonomy. The chassis is a modified van with a computer-controllable, hydraulic drivetrain. The NavLab supports a choice of sensing to accommodate many types of navigation research. This technical report details the control computing and physical configuration of the NavLab vehicle. GRA

N88-20284# Federal Aviation Administration, Atlantic City, N.J.
ALASKA LORAN C PROBE TEST RESULTS
Robert Erikson, Jean Evans, Mark Dickinson, Thomas Wisser, and Martin Wortham Sep. 1987 75 p
(AD-A189131; DOT/FAA/CT-TN87/23) Avail: NTIS HC A04/MF A01 CSCL 17G

This report describes a flight test probe into Alaska to determine the extent of usable signals in space from Loran C stations Port Clarence, Narrow Cape, and Tok, Alaska. Flight measurements indicated adequate signal strength exists from the three Loran C stations over the routes flown. Therefore, it is feasible to dual rate Port Clarence as a new secondary in the Gulf of Alaska Loran C chain. Dual rating Port Clarence will increase the area where Loran C navigation is possible by providing proper chain structure. This largely increased area will be located in the middle to southern interior of Alaska. The tests were conducted in the summer of 1985 and in the winter of 1985 and 1986. GRA

N88-20285# Air Force Geophysics Lab., Hanscom AFB, Mass.
LASER GYRO ATTITUDE CONTROL SYSTEM FEASIBILITY Final Report, Oct. 1984 - Mar. 1986
Christopher R. Cassell 24 Apr. 1987 41 p
(AD-A189368; AFGL-TR-87-0137; AFGL-ERP-974) Avail: NTIS HC A03/MF A01 CSCL 17G

This report briefly reviews the principles of optical rate sensors. It then further describes some existing ring laser gyro systems and considers how their utilization would affect performance, cost and reliability of attitude control systems currently used or proposed for use in sounding rocket applications at the Air Force Geophysics Laboratory (AFGL). GRA

N88-20286# Air Force Inst. of Tech., Wright-Patterson AFB, Ohio. School of Engineering.
THE EVALUATION AND SELECTION OF A 5TH GROUND ANTENNA SITE FOR THE GLOBAL POSITIONING SYSTEM M.S. Thesis
Tery L. Donelson 7 Dec. 1987 82 p
(AD-A189495; AFIT/GSO/ENS/87D-4) Avail: NTIS HC A05/MF A01 CSCL 17G

The NAVSTAR Global Positioning System (GPS) is a space based radio navigation system being developed to provide accurate position, velocity and time any place on or near the earth, 24 hours of every day, and under all weather conditions. The GPS performance characteristics provide significant benefits in the areas of spacecraft navigation, satellite delivery, equipment positioning, resource mapping, payload deployment and retrieval, propellant economies, data processing, and mission planning (13:204). GPS is a passive radio system and is comprised of space, control, and user segments. The space segment consists of 18 navigational satellites in six orbital planes, plus three operational spares. The three in-orbit spares will be positioned in such a way as to provide optimum coverage of the continental United States. A satellite failure in one of the three planes containing a spare will result in the spare being moved to a position close to the failed satellite. A failure in one of the other planes will cause satellites in adjacent orbital planes to be moved within their planes to provide the best possible coverage until a new satellite can be launched(6:1). GRA

N88-20287# National Aerospace Lab., Amsterdam (Netherlands). Flight Div.
A METHOD AND MEASURES TO EVALUATE TRACKERS FOR AIR TRAFFIC CONTROL
H. A. P. Blom 7 Jul. 1986 37 p Sponsored by the Netherlands Dept. of Civil Aviation
(NLR-TR-86072-U; ETN-88-91721) Avail: NTIS HC A03/MF A01

The general setup of the evaluation of a radar tracking algorithm in a civil air traffic control (ATC) system is considered from an operational point of view. Present and potential use of trackdate are taken in account. The result is a method to evaluate trackers for ATC on the basis of live-traffic data, assuming that a sufficiently accurate reconstructed trajectory is available. The evaluation starts

with an identification of all moments the pilot or disturbances cause changes in the trajectory and track continuity. The resulting parts of tracks are classified on the basis of this kind of change. For the subclasses quality measures with a distinct operational interpretation are defined. An autocorrelation function for stochastic signals that randomly start and stop continuation is introduced. Both aircraft tracks and tracks originating from other objects or from random origin are taken in account. ESA

N88-20288# National Aerospace Lab., Amsterdam (Netherlands). Flight Div.
FLIGHT SIMULATIONS OF MLS INTERCEPTION PROCEDURES APPLICABLE TO LATERALLY SEGMENTED APPROACH PATHS
L. J. J. Erkelens and P. J. vanderGeest 26 May 1986 15 p Presented at the AIAA Atmospheric Flight Mech. Conference, Williamsburg, Va., 18-20 Aug. 1986 Sponsored by the Netherlands Directorate of Air Traffic Services and Aeronautical Telecommunications
(NLR-MP-86037-U; B8729624; ETN-88-91728) Avail: NTIS HC A03/MF A01

The design and implementation of microwave landing system (MLS) guided interception procedures, applicable to segmented approach paths were studied. Four MLS procedures were proposed for further evaluation. Guidance systems based on closed loop and open loop turn concepts were evaluated as to their capabilities of providing accurate tracking guidance. A simulator investigation was executed to analyze the feasibility of the four proposed interception procedures; turn techniques; and the avionics equipment required for these procedures. The avionics included an experimental navigation display, especially developed to be used with the MLS interception procedures. Test results consist of objective and subjective data. The objective data concern recorded path deviations and statistical data concerning tracking performance and control activity. Subjective data were derived from pilot effort ratings, questionnaire responses, and comments of pilots and air traffic controllers. ESA

N88-20691# Joint Publications Research Service, Arlington, Va.
GENERALIZED EXPRESSION FOR RADIO NAVIGATION PARAMETER ERROR Abstract Only
V. F. Ivashkevich and V. S. Tregubov *In its* JPRS Report: Science and Technology. USSR: Earth Sciences 26 Feb. 1988 p 20-21 Transl. into ENGLISH from Geodeziya i Kartografiya (Moscow, USSR), no. 3, Mar. 1987 p 45-48 (For primary document see N88-20674 13-42)
Avail: NTIS HC A04/MF A01

05 AIRCRAFT DESIGN, TESTING AND PERFORMANCE

Includes aircraft simulation technology.

For related information see also *18 Spacecraft Design, Testing and Performance* and *39 Structural Mechanics*.For land transportation vehicles see *85 Urban Technology and Transportation.*

N88-20289# General Accounting Office, Washington, D. C. National Security and International Affairs Div.
AQUILA REMOTELY PILOTED VEHICLE: ITS POTENTIAL BATTLEFIELD CONTRIBUTION STILL IN DOUBT
Oct. 1987 43 p
(PB88-120241; GAO/NSIAD-88-19; B-205804) Avail: NTIS HC A03/MF A01 CSCL 01C

The report contains an evaluation of the Army's Aquila remotely piloted vehicle program. It covers operational testing conducted at Fort Hood, Texas, from November 17, 1986 to March 25, 1987. The purpose of the test was to assess the Aquila's ability to accomplish its mission in its planned operational environment and to evaluate other key characteristics, such as reliability and maintainability. The report assesses the Aquila's readiness for production based primarily on its performance in operational testing and the adequacy of the test. GRA

N88-20290*# California Univ., Los Angeles. Dept. of Engineering and Applied Science.
CONTROL AUGMENTED STRUCTURAL SYNTHESIS
Robert V. Lust and Lucien A. Schmit Washington NASA Apr. 1988 193 p
(Grant NsG-1490)
(NASA-CR-4132; NAS 1.26:4132) Avail: NTIS HC A09/MF A01 CSCL 01C

A methodology for control augmented structural synthesis is proposed for a class of structures which can be modeled as an assemblage of frame and/or truss elements. It is assumed that both the plant (structure) and the active control system dynamics can be adequately represented with a linear model. The structural sizing variables, active control system feedback gains and nonstructural lumped masses are treated simultaneously as independent design variables. Design constraints are imposed on static and dynamic displacements, static stresses, actuator forces and natural frequencies to ensure acceptable system behavior. Multiple static and dynamic loading conditions are considered. Side constraints imposed on the design variables protect against the generation of unrealizable designs. While the proposed approach is fundamentally more general, here the methodology is developed and demonstrated for the case where: (1) the dynamic loading is harmonic and thus the steady state response is of primary interest; (2) direct output feedback is used for the control system model; and (3) the actuators and sensors are collocated. Author

N88-20291*# Houston Univ., Tex.
THE DESIGN OF AIRCRAFT USING THE DECISION SUPPORT PROBLEM TECHNIQUE
Farrokh Mistree, Stergios Marinopoulos, David M. Jackson, and Jon A. Shupe Apr. 1988 236 p
(Contract NAS1-18117)
(NASA-CR-4134; NAS 1.26:4134) Avail: NTIS HC A11/MF A01 CSCL 01C

The Decision Support Problem Technique for unified design, manufacturing and maintenance is being developed at the Systems Design Laboratory at the University of Houston. This involves the development of a domain-independent method (and the associated software) that can be used to process domain-dependent information and thereby provide support for human judgment. In a computer assisted environment, this support is provided in the form of optimal solutions to Decision Support Problems. Author

N88-20292# Air Force Wright Aeronautical Labs., Wright-Patterson AFB, Ohio.
AN INVESTIGATION OF CLASSICAL DYNAMIC SCALING TECHNIQUES APPLIED TO AN OLEO-PNEUMATIC LANDING GEAR STRUT Final Report, Oct. 1983 - Jul. 1985
Archie B. Clark, III Feb. 1987 157 p
(AD-A187664; AFWAL-TR-86-3058) Avail: NTIS HC A08/MF A01 CSCL 01C

A program was conducted to investigate the technical feasibility and practicality of using dynamic scale modeling techniques to design, fabricate, and test a scale model of an aircraft landing gear strut and tire. Dynamic scaling laws were developed and used to design a one-third model of an A-37 Nose Landing Gear (NLG) strut and tire. The A-37 NLG strut and the model gear were tested under dynamically similar conditions of weight, speed, and forcing function on a circular track, Dynamic Test Machine at the Mobility Development Laboratory, Wright-Patterson AFB, OH. Comparison of time history data, recorded during each phase of testing, indicated good correlation of the dynamic response of the model landing gear, in relation to the scaling laws and the A-37 NLG dynamic response. Presented in the report is the development and analytical verification of the scaling laws, test data and comparisons, conclusions, and recommendations. GRA

N88-20293# Aeronautical Research Labs., Melbourne (Australia).
CRACK DISTRIBUTION AND GROWTH RATES FOR CRITICAL FASTENER HOLES IN MIRAGE WING RH79
S. Bowles 18 Sep. 1987 42 p
(AD-A189080; ARL-MAT-TM-396; DODA-AR-004-560) Avail: NTIS HC A03/MF A01 CSCL 01C

Results of fractographic inspection of fatigue cracks found in the fastener holes (excepting hole 1 and SLAN rivet holes) in the inboard end of the lower flange of RH79 wing-spar, as a result of fatigue testing for 5600 hours, are presented. The largest crack found was only 2.18 mm deep and occurred in hole 10 in the rearward flange of the spar. Holes 1 to 4 remained crack-free as a result of the refurbishment procedures. GRA

N88-20294# Army Aviation Systems Command, St. Louis, Mo.
AVSCOM'S MODIFICATIONS TO TELEDYNE SYSTEMS COMPANY'S AIR-TO-AIR FIRE CONTROL SYSTEM SIMULATION MODEL
Daniel J. Breyer Nov. 1987 31 p
(AD-A189136; USAAVSCOM-TM-87-F-3) Avail: NTIS HC A03/MF A01 CSCL 19E

This report has been written to document the changes made to Teledyne Systems Company's (TSC) Attack Helicopter Air-to-Air (ATA) Fire Control System Simulation model (AIRTOAIR). The AIRTOAIR Simulation was used as a tool by TSC to assess the effectiveness of several mechanizations of fire control equations. These equations were being formulated with the intent of becoming a product improvement to the existing attack helicopters, the AH-1S COBRA and the AH-64 APACHE. The model simulates a one-on-one, non-dueling, close-in combat scenario using the automatic cannon. Since it is a fire control system representation, all of the sensors that feed information to the fire control computer (FCC) are modelled. The changes to AIRTOAIR are discussed at length and the coding required for each change is also provided. Applications of the changes to specific projects are briefly discussed when appropriate. GRA

N88-20295# National Aerospace Lab., Amsterdam (Netherlands). Structures and Materials Div.
HOW TO GENERATE EQUAL PROBABILITY DESIGN LOAD CONDITIONS
R. Noback 5 Dec. 1985 22 p
(Contract NIVR-1995)
(NLR-TR-86060-U; B8729597; ETN-88-91720) Avail: NTIS HC A03/MF A01

A method for the generation of design load conditions based on the design loads obtained with the power spectral density method and especially with the design envelope criterion is proposed. The generated design load conditions all have the same probability of occurrence. An example with only two loads is shown. The steps that have to be carried out to generate equal probability design load conditions for N loads are outlined. ESA

N88-20296*# National Aeronautics and Space Administration. Ames Research Center, Moffett Field, Calif.
A CORRELATION STUDY OF X-29A AIRCRAFT AND ASSOCIATED ANALYTICAL DEVELOPMENT Ph.D. Thesis. Final Contract Report
Ali Ahmadi, Kajal Gupta, and Paul Fortin (Kansas Univ. Center for Research, Inc., Lawrence.) Mar. 1988 282 p
(Contract NCC2-313)
(NASA-TM-89735; NAS 1.15:89735) Avail: NTIS HC A13/MF A01 CSCL 01C

Results of the contractor structural and aerodynamic analysis of the X-29A aircraft are verified. A brief history and potential advantages of the X-29A aircraft are discussed. The NASA developed computer package, STARS (STructures, Aerodynamics, and Related Systems), which is used in verifying contractor results is discussed. Enhancements of the STARS package are described, particularly the incorporation of the FASTEX computer program under STARS, and the development of a complete computer graphics system. A comparative study of free vibration and aerodynamic analysis of the X-29A aircraft is given. This study has shown that the natural frequencies and modeshapes determined analytically by STARS and the contractor compare relatively well with experimentally determined data. Also included in the study is the formulation and development of the higher-order plane-stress finite dynamic triangular element. Author

N88-20297*# National Aeronautics and Space Administration, Washington, D.C.
PROCEDURE FOR DETECTION AND IDENTIFICATION OF A HELICOPTER
Hans Siebecker Apr. 1988 9 p Transl. into ENGLISH from Verfahren Zur Detektion und Identifizierung Eines Hubschraubers, Federal Republic of Germany, Patent No. 2851205 Transl. by SCITRAN, Inc., Santa Barbara, Calif. Original document prepared for Eltro GmbH, Corporation for Radiation Technology
(Contract NASw-4307)
(NASA-TT-20234; NAS 1.77:20234) Avail: NTIS HC A02/MF A01 CSCL 01C

A procedure is described for detecting and identifying a helicopter based on its characteristic energy radiation in the visible and heat emitting range, as well as in the sonic range. This procedure uses a passive IR identification sensor. The procedure is discussed using illustrations and examples. Author

N88-20298# Messerschmitt-Boelkow-Blohm G.m.b.H., Ottobrunn (West Germany). Unternehmensgruppe Hubschrauber und Flugzeuge.
AEROELASTIC MODELS IN AIRCRAFT DESIGN [AEROELASTISCHE MODELLE IN DER FLUGZEUGENTWICKLUNG]
H. Hoenlinger and O. Sensburg Jun. 1986 10 p In GERMAN
(MBB/LKE-294/S/PUB/249; ETN-88-91439) Copyright Avail: NTIS HC A02/MF A01

The use of aeroelastic model tests in aircraft design is outlined. Aeroelastic models are economical for the development and testing of novel active-control technologies and measuring methods for aircraft vibration tests. The linearized dynamic calculation model of a flying elastic aircraft was realized in a wind tunnel using aeroelastic models. The validity domain of an aeroelastic model was substantially extended in a cryogenic wind tunnel. ESA

N88-20299# Bristol Univ. (England). Dept. of Aerospace Engineering.
AIR-JET SPOILER B.E. Thesis
K. N. Wolstencroft and A. E. J. Wood Jun. 1987 46 p
(BU-364; ETN-88-91903) Avail: NTIS HC A03/MF A01

The aerodynamic characteristics of a slender jet of air issuing transversely from a flat plate into the passing airflow was studied in anticipation of the use of such a jet to replace a conventional spoiler. The effects of air-jet momentum, mainstream velocity, and efflux angle of the jet on the separation bubble were investigated. Comparisons were made with the flow pattern of fluid passing over a simple fence. Two-dimensional and three-dimensional flow were created. Average Reynolds number was 193,500. The pressure distribution along the plate was determined at the centerline and at one position beyond the edge of the slot. The pressure variation on the centerline is consistent with the observed flow. A limited range of pressure variations beyond the slot edge is obtained. The two principal configurations adopted show characteristics similar to a fence. However, the net force over the whole plate is virtually zero and so the effect of the separation bubble was assessed. An air-jet angled upstream, instead of being normal to the plate, causes greater flow separation and is more effective. ESA

N88-20300# Fraunhofer-Inst. fuer Betriebsfestigkeit, Darmstadt (West Germany).
STANDARDIZED ENVIRONMENTAL FATIGUE SEQUENCE FOR THE EVALUATION OF COMPOSITE COMPONENTS IN COMBAT AIRCRAFT (ENSTAFF = ENVIRONMENTAL FALSTAFF)
J. J. Gerharz, comp., D. Schuetz, J. W. Bergmann, J. B. deJonge, J. N. Webb, and R. T. Potter (Royal Aircraft Establishment,

Farnborough, England) 1987 79 p Sponsored by BMFT, Bonn, Fed. Republic of Germany
(LBF-FB-179; IABG-B-TF-2194; NLR-TR-87053-U; RAE-TR-87048; ISSN-0721-5320; ETN-88-91936) Avail: NTIS HC A05/MF A01

An environmental fatigue loading standard was developed. It represents the mechanical loading and the environmental service conditions expected for wing root area structure of fighter aircraft. The standard, called ENSTAFF, utilizes the mechanical loading sequence FALSTAFF and connects defined temperatures to each peak and trough load on the basis of flight missions. It also includes rules for moisture conditioning and moisture control to account for the water picked up by the plastic matrix primarily during ground storage. The load and evironment sequence of ENSTAFF is presented in a form ready for application. ESA

N88-20301*# National Aeronautics and Space Administration. Hugh L. Dryden Flight Research Center, Edwards, Calif.
AIRCRAFT FLIGHT FLUTTER TESTING AT THE NASA AMES-DRYDEN FLIGHT RESEARCH FACILITY
Michael W. Kehoe May 1988 17 p Presented at the AIAA 4th Flight Test Conference, San Diego, Calif., 18-20 May 1988
(NASA-TM-100417; H-1445; NAS 1.15:100417) Avail: NTIS HC A03/MF A01 CSCL 01C

Many parameter identification techniques have been used at the NASA Ames Research Center, Dryden Research Facility at Edwards Air Force Base to determine the aeroelastic stability of new and modified research vehicles in flight. This paper presents a summary of each technique used with emphasis on fast Fourier transform methods. Experiences gained from application of these techniques to various flight test programs are discussed. Also presented are data-smoothing techniques used for test data distorted by noise. Data are presented for various aircraft to demonstrate the accuracy of each parameter identification technique discussed. Author

N88-20302*# National Aeronautics and Space Administration. Hugh L. Dryden Flight Research Facility, Edwards, Calif.
FORMULATION OF A GENERAL TECHNIQUE FOR PREDICTING PNEUMATIC ATTENUATION ERRORS IN AIRBORNE PRESSURE SENSING DEVICES
Stephen A. Whitmore May 1988 14 p Presented at the AIAA 4th Flight Test Conference, San Diego, Calif., 18-20 May 1988
(NASA-TM-100430; H-1462; NAS 1.15:100430) Avail: NTIS HC A03/MF A01 CSCL 01C

Presented is a mathematical model derived from the Navier-Stokes equations of momentum and continuity, which may be accurately used to predict the behavior of conventionally mounted pneumatic sensing systems subject to arbitrary pressure inputs. Numerical techniques for solving the general model are developed. Both step and frequency response lab tests were performed. These data are compared with solutions of the mathematical model and show excellent agreement. The procedures used to obtain the lab data are described. In-flight step and frequency response data were obtained. Comparisons with numerical solutions of the math model show good agreement. Procedures used to obtain the flight data are described. Difficulties encountered with obtaining the flight data are discussed. Author

06 AIRCRAFT INSTRUMENTATION

Includes cockpit and cabin display devices; and flight instruments.

For related information see also *19 Spacecraft Instrumentation* and *35 Instrumentation and Photography.*

N88-20303# Air Force Wright Aeronautical Labs., Wright-Patterson AFB, Ohio.
ARCHITECTURE SPECIFICATION FOR PAVE PILLAR AVIONICS Final Technical Report, Sep. 1985 - Oct. 1986
John Ostgaard, Ron Szkody, Steve Benning, Karl Purdy, and Gary Mauersberger Jan. 1987 399 p
(AD-A188722; AFWAL-TR-87-1114) Avail: NTIS HC A17/MF A01 CSCL 01B

This document establishes the functional requirements for the PAVE PILLAR Systems Architecture. This architecture is specifically targeted for advanced tactical fighters, and in general for all military aircraft applications. The PAVE PILLAR Architecture addresses those functions which could be implemented with common hardware and computer programs to allow adaptation to either air-to-air or air-to-ground missions. This document defines the major elements of the PAVE PILLAR Architecture, the mechanizations for inter-connecting those elements, a set of common modules from which those elements could be constructed, and the operation of the network constructed of these elements. The PAVE PILLAR core avionics exploits the commonality in air-to-air and air-to-ground missions. The PAVE PILLAR core avionics consists of the following functional areas: (1) Digital Signal Processing, (2) Mission Processing, (3) Vehicle Management Processing, and (4) Avionics Systems Control. GRA

N88-20304*# National Aeronautics and Space Administration. Hugh L. Dryden Flight Research Center, Edwards, Calif.
THE DESIGN AND USE OF A TEMPERATURE-COMPENSATED HOT-FILM ANEMOMETER SYSTEM FOR BOUNDARY-LAYER FLOW TRANSITION DETECTION ON SUPERSONIC AIRCRAFT
Harry R. Chiles May 1988 14 p Presented at the Aerospace Industries/Test Measurement Symposium, Albuquerque, N. Mex., 2-5 May 1988
(NASA-TM-100421; H-1451; NAS 1.15:100421) Avail: NTIS HC A03/MF A01 CSCL 01D

An airborne temperature-compensated hot-film anemometer system has been designed, fabricated, and used to obtain in-flight airfoil boundary-layer flow transition data by the NASA Ames-Dryden Flight Research Facility. Salient features of the anemometer include near constant sensitivity over the full flight envelope, installation without coaxial wiring, low-noise outputs, and self-contained signal conditioning with dynamic and steady-state outputs. The small size, low-power dissipation, and modular design make the anemometer suitable for use in modern high-performance research aircraft. Design of the temperature-compensated hot-film anemometer and its use for flow transition detection on a laminar flow flight research project are described. Also presented are data gathered in flight which is representative of the temperature-compensated hot-film anemometer operation at subsonic, transonic, and supersonic flight conditions. Author

07 AIRCRAFT PROPULSION AND POWER

Includes prime propulsion systems and systems components, e.g., gas turbine engines and compressors; and onboard auxilliary power plants for aircraft.

For related information see also *20 Spacecraft Propulsion and Power, 28 Propellants and Fuels,* and *44 Energy Production and Conversion.*

N88-20305# National Aerospace Lab., Amsterdam (Netherlands). Fluid Dynamics Div.
ENGINE FLOW SIMULATION FOR WIND TUNNEL TESTING AT NLR
W. B. deWolf 9 Feb. 1987 28 p Presented at the Symposium on Developments in Aircraft Propulsion, Haarlem, The Netherlands, 18 Mar. 1987
(NLR-MP-87011-U; B8729623; ETN-88-91737) Avail: NTIS HC A03/MF A01

Techniques for turbofan engine simulation like the blown nacelle and the turbo powered simulator are reviewed. Propeller model test techniques are discussed. ESA

N88-20306*# Hamilton Standard, Windsor Locks, Conn.
LARGE-SCALE ADVANCED PROP-FAN (LAP) Final Report
C. L. DeGeorge [1988] 255 p Original contains color illustrations

(Contract NAS3-23051)
(NASA-CR-182112; NAS 1.26:182112) Avail: NTIS HC A12/MF A01 CSCL 21E

In recent years, considerable attention has been directed toward improving aircraft fuel efficiency. Analytical studies and research with wind tunnel models have demonstrated that the high inherent efficiency of low speed turboprop propulsion systems may now be extended to the Mach .8 flight regime of today's commercial airliners. This can be accomplished with a propeller, employing a large number of thin highly swept blades. The term Prop-Fan has been coined to describe such a propulsion system. In 1983 the NASA-Lewis Research Center contracted with Hamilton Standard to design, build and test a near full scale Prop-Fan, designated the Large Scale Advanced Prop-Fan (LAP). This report provides a detailed description of the LAP program. The assumptions and analytical procedures used in the design of Prop-Fan system components are discussed in detail. The manufacturing techniques used in the fabrication of the Prop-Fan are presented. Each of the tests run during the course of the program are also discussed and the major conclusions derived from them stated. Author

N88-20307*# National Aeronautics and Space Administration. Hugh L. Dryden Flight Research Facility, Edwards, Calif.
EXHAUST-GAS PRESSURE AND TEMPERATURE SURVEY OF F404-GE-400 TURBOFAN ENGINE
James T. Walton and Frank W. Burcham, Jr. Dec. 1986 32 p
(NASA-TM-88273; H-1375; NAS 1.15:88273) Avail: NTIS HC A03/MF A01 CSCL 21E

An exhaust-gas pressure and temperature survey of the General Electric F404-GE-400 turbofan engine was conducted in the altitude test facility of the NASA Lewis Propulsion System Laboratory. Traversals by a survey rake were made across the exhaust-nozzle exit to measure the pitot pressure and total temperature. Tests were performed at Mach 0.87 and a 24,000-ft altitude and at Mach 0.30 and a 30,000-ft altitude with various power settings from intermediate to maximum afterburning. Data yielded smooth pressure and temperature profiles with maximum jet temperatures approximately 1.4 in. inside the nozzle edge and maximum jet temperatures from 1 to 3 in. inside the edge. A low-pressure region located exactly at engine center was noted. The maximum temperature encountered was 3800 R. Author

08 AIRCRAFT STABILITY AND CONTROL

Includes aircraft handling qualities; piloting; flight controls; and autopilots.

For related information see also *05 Aircraft Design, Testing and Performance.*

N88-20308*# Boeing Commercial Airplane Co., Seattle, Wash.
INTEGRATED AUTOPILOT/AUTOTHROTTLE BASED ON A TOTAL ENERGY CONTROL CONCEPT: DESIGN AND EVALUATION OF ADDITIONAL AUTOPILOT MODES
Kevin R. Bruce NASA Apr. 1988 111 p
(Contract NAS1-16300)
(NASA-CR-4131; NAS 1.26:4131) Avail: NTIS HC A06/MF A01 CSCL 01C

An integrated autopilot/autothrottle system was designed using a total energy control design philosophy. This design ensures that the system can differentiate between maneuvers requiring a change in thrust to accomplish a net energy change, and those maneuvers which only require elevator control to redistribute energy. The system design, the development of the system, and a summary of simulation results are defined. Author

N88-20309*# National Aeronautics and Space Administration. Langley Research Center, Hampton, Va.
LATERAL AND LONGITUDINAL STABILITY AND CONTROL PARAMETERS FOR THE SPACE SHUTTLE DISCOVERY AS DETERMINED FROM FLIGHT TEST DATA
William T. Suit and James R. Schiess Feb. 1988 24 p
(NASA-TM-100555; NAS 1.15:100555) Avail: NTIS HC A03/MF A01 CSCL 01C

The Discovery vehicle was found to have longitudinal and lateral aerodynamic characteristics similar to those of the Columbia and Challenger vehicles. The values of the lateral and longitudinal parameters are compared with the preflight data book. The lateral parameters showed the same trends as the data book. With the exception of C sub l sub Beta for Mach numbers greater than 15, C sub n sub delta r for Mach numbers greater than 2 and for Mach numbers less than 1.5, where the variation boundaries were not well defined, ninety percent of the extracted values of the lateral parameters fell within the predicted variations. The longitudinal parameters showed more scatter, but scattered about the preflight predictions. With the exception of the Mach 1.5 to .5 region of the flight envelope, the preflight predictions seem a reasonable representation of the Shuttle aerodynamics. The models determined accounted for ninety percent of the actual flight time histories. Author

09 RESEARCH AND SUPPORT FACILITIES (AIR)

Includes airports, hangars and runways; aircraft repair and overhaul facilities; wind tunnels; shock tubes; and aircraft engine test stands.

For related information see also *14 Ground Support Systems and Facilities (Space).*

N88-20310# Bristol Univ. (England). Dept. of Aerospace Engineering.
A WIND TUNNEL MODEL WITH DYNAMIC CONTROL B.E. Thesis
A. Anderson and P. Hannah Jun. 1987 42 p
(BU-352; ETN-88-91892) Avail: NTIS HC A03/MF A01

The use of a wind tunnel model for demonstrating how active control can augment stability of an unstable configuration is evaluated. A deliberately unstable delta wing with canard combination was tested. Interactive programs in two microcomputers are used to implement a pitch rate feedback controller with variable gains and motion display. A computer simulation package helps to compare flight test results with theoretical responses. Adequate performance of the system is achieved with similarities in frequency response and damping ratios, although more sensitive actuation of control surfaces and a reduction in friction in the model suspension would improve the reality of response when concentrating on the short period mode. ESA

N88-20311# Office National d'Etudes et de Recherches Aerospatiales, Paris (France). Large Testing Facilities Dept.
[ACTIVITIES REPORT OF THE LARGE TESTING FACILITIES DEPARTMENT] Annual Report, 1986
Sep. 1987 34 p Original contains color illustrations
(ETN-88-91982) Avail: NTIS HC A03/MF A01

Airbus A320 tests; preparatory testing for the Airbus A340; a balance for testing the motorized A320; store separation tests under fighters; flow survey in a fighter air intake; effects of protuberances from the surface of Ariane 4 on the aerodynamic coefficients of the launch vehicle; upgrading of the wind tunnel for Hermes tests; and breakage of a wind tunnel fan blade are discussed. ESA

12 ASTRONAUTICS (GENERAL)

For extraterrestrial exploration see *91 Lunar and Planetary Exploration.*

N88-20312# Joint Publications Research Service, Arlington, Va.
JPRS REPORT: SCIENCE AND TECHNOLOGY. USSR: SPACE
6 Apr. 1988 66 p Transl. into ENGLISH from various Russian

articles
(JPRS-USP-88-002) Copyright Avail: NTIS HC A04/MF A01

U.S.S.R. space science and technology topics are discussed. Manned space flight missions, Venus exploration, life sciences, space engineering, space applications and space policy and administration are discussed. For individual titles, see N88-20313 through N88-20329.

N88-20313# Joint Publications Research Service, Arlington, Va.
VEGA-1 AND VEGA-2 AUTOMATIC STATIONS: FUNCTIONING OF LANDING MODULES IN VENUSIAN ATMOSPHERE Abstract Only **c91**
V. A. Deryugin, V. P. Dolgopolov, V. P. Karyagin, V. M. Kovtunenko, R. S. Kremnev, K. M. Pichkhadze, G. N. Rogovskiy, and R. Z. Sagdeyev *In its* JPRS Report: Science and Technology. USSR: Space 6 Apr. 1988 p 14 Transl. into ENGLISH from Kosmicheskiye Issledovaniya (Moscow, USSR), v. 25, no. 5, Sep. - Oct. 1987 p 649-654 (For primary document see N88-20312 13-12)
Copyright Avail: NTIS HC A04/MF A01

A brief account is given of the Vega 1 and Vega 2 automatic interplanetary stations that were launched on 15 and 21 December 1984 for research on the Venusian atmosphere and surface and on Halley's comet. The two vehicles flew by the nucleus of the comet at distances of 8912 and 8036 km, conducting research from those distances that was used for more precise guidance of Giotto to the comet. During the descent into the atmosphere of Venus on June of 1985, balloons were released which made investigations of the planetary cloud layer independently of the descent module. The landing modules made determinations of the elemental composition of the ground, temperature, pressure, physical and optical properties of the atmosphere, cloud structure and composition. Author

N88-20314# Joint Publications Research Service, Arlington, Va.
VEGA-1 AND VEGA-2 AUTOMATIC STATIONS: FUNCTIONING OF FLYBY VEHICLES DURING ENCOUNTER WITH HALLEY'S COMET Abstract Only **c90**
V. P. Dolgopolov, V. P. Karyagin, V. M. Kovtunenko, R. S. Kremnev, O. V. Papkov, K. M. Pichkhadze, G. N. Rogovskiy, R. Z. Sagdeyev, and K. G. Sukhanov *In its* JPRS Report: Science and Technology. USSR: Space 6 Apr. 1988 p 14 Transl. into ENGLISH from Kosmicheskiye Issledovaniya (Moscow, USSR), v. 25, no. 5, Sep. - Oct. 1987 p 655-658 Original language document was announced in IAA as A88-17810 (For primary document see N88-20312 13-12)
Copyright Avail: NTIS HC A04/MF A01

The design of the Vega 1 and 2 probes is described, and the operation during the encounter with Comet Halley is discussed in detail with emphasis on solar array characteristics. Also considered is the use of the Vega probes to retarget the Giotto probe, assuring its flyby at a distance of about 600 km from the comet nucleus. Author

N88-20315# Joint Publications Research Service, Arlington, Va.
THERMAL STRUCTURE OF VENUSIAN ATMOSPHERE DETERMINED FROM RESULTS OF MEASUREMENTS FROM VEGA-2 LANDING MODULE Abstract Only **c91**
V. M. Linkin, G. Blamont, S. I. Devyatkin, S. P. Ignatova, V. V. Kerzhanovich, A. N. Lipatov, K. Malik, B. I. Stadnyk, Ya. V. Sanotskiy, and P. G. Stolyarchuk et al. *In its* JPRS Report: Science and Technology. USSR: Space 6 Apr. 1988 p 14-15 Transl. into ENGLISH from Kosmicheskiye Issledovaniya (Moscow, USSR), v. 25, no. 5, Sep. - Oct. 1987 p 659-672 Original language document was announced in IAA as A88-17811 (For primary document see N88-20312 13-12)
Copyright Avail: NTIS HC A04/MF A01

A description is given of the Meteo experiment which involved the measurement of the main thermodynamic characteristics of the Venus atmosphere using four temperature sensors and three pressure sensors on the Vega 2 lander. A table listing pressure and temperature values from about 430 separate measurements is presented. Data is also presented on the vertical thermal structure of the Venus atmosphere, the matching coefficient of hydrostatic and aerodynamic descent models, and the static stability profile. Author

N88-20316# Joint Publications Research Service, Arlington, Va.
RESEARCH ON ABSORPTION OF UV RADIATION IN VENUSIAN ATMOSPHERE FROM VEGA-1 AND VEGA-2 LANDING MODULES Abstract Only **c91**
Zh. L. Berto, A. P. Ekonomov, B. Mezh, V. I. Moroz, A. Aberzhal, V. I. Gnedykh, A. V. Grigoryev, B. Ye. Moshkin, A. Oshkorn, and Zh. P. Pommero et al. *In its* JPRS Report: Science and Technology. USSR: Space 6 Apr. 1988 p 15 Transl. into ENGLISH from Kosmicheskiye Issledovaniya (Moscow, USSR), v. 25, no. 5, Sep. - Oct. 1987 p 691-706 (For primary document see N88-20312 13-12)
Copyright Avail: NTIS HC A04/MF A01

The described experiment was for determining the vertical distribution of atmospheric gases exhibiting strong absorption in the UV spectral region. The Vega 1 and 2 landing modules carried an instrument consisting of an artificial source of UV radiation, cells through which atmospheric gas was passed and a spectrometer for measuring the spectrum of radiation passing through the cell. The objective of the research was a determination of the chemical composition of the Venusian atmosphere and the chemical processes transpiring there and identification of the so-called UV absorber, the substance or group of substances responsible for the drop-off of the albedo of single scattering with wavelength at different altitudes. Author

N88-20317# Joint Publications Research Service, Arlington, Va.
VERTICAL STRUCTURE OF VENUSIAN CLOUD LAYER AT LANDING SITES OF VEGA-1 AND VEGA-2 VEHICLES Abstract Only **c91**
V. I. Gnedykh, L. V. Zasova, V. I. Moroz, B. Ye. Moshkin, and A. P. Ekonomov *In its* JPRS Report: Science and Technology. USSR: Space 6 Apr. 1988 p 15 Transl. into ENGLISH from Kosmicheskiye Issledovaniya (Moscow, USSR), v. 25, no. 5, Sep. - Oct. 1987 p 707-714 Original language document was announced in IAA as A88-17815 (For primary document see N88-20312 13-12)
Copyright Avail: NTIS HC A04/MF A01

The objective of the Vega experiment was a study of parameters of aerosols in the Venusian atmosphere (particle size distribution and concentration of aerosols, shape of particles and refractive index of their material). Pioneer-Venus data seemed to indicate that the main cloud layer consisted of three types of particles forming three modes, the modal diameter of the third type being about 7.3 microns, asperical particles of unknown composition. The first mode is described by a Junge distribution from 0.5 to 5 microns and the second mode consists of particles measuring 2 to 5 microns. Author

N88-20318# Joint Publications Research Service, Arlington, Va.
GAS-CHROMATOGRAPHIC ANALYSIS OF PRODUCTS OF THERMAL REACTIONS OF AEROSOL IN VENUSIAN CLOUD LAYER ON VEGA-1 AND VEGA-2 AUTOMATIC INTERPLANETARY STATIONS Abstract Only **c91**
N. V. Porshnev, L. M. Mukhin, B. G. Gelman, D. F. Nenarokov, V. A. Rotin, A. V. Dyachkov, and V. B. Bondarev *In its* JPRS Report: Science and Technology. USSR: Space 6 Apr. 1988 p 16 Transl. into ENGLISH from Kosmicheskiye Issledovaniya (Moscow, USSR), v. 25, no. 5, Sep. - Oct. 1987 p 715-720 Original language document was announced in IAA as A88-17816 (For primary document see N88-20312 13-12)
Copyright Avail: NTIS HC A04/MF A01

Measurements made with the Sigma 3 gas chromatography setup led to the identification of CO2, H2O, and SO2 in the Venus cloud layer. The concentration of H2SO4 aerosol was found to be much less than 1 mg/cu m at heights of 61.5 to 54 km over the Vega 1 landing site. At heights of 61.5 to 48 km, the mean concentration of H2SO4 aerosol was 1.0 plus or minus 0.2 mg/cu over the Vega 2 landing site. In the absence of sulfur, the lower

limit for the H2SO4 concentration is 0.4 plus or minus 0.1 mg/cu m. Author

N88-20319# Joint Publications Research Service, Arlington, Va.
ROENTGENORADIOMETRIC ANALYSIS OF AEROSOL IN VENUSIAN CLOUDS BY VEGA-1 AND VEGA-2 AUTOMATIC INTERPLANETARY STATIONS Abstract Only **c91**
B. M. Andreychikov, I. K. Akhmetshin, B. N. Korchuganov, L. M. Mukhin, B. I. Ogorodnikov, I. V. Petryanov, and B. I. Skitovich *In its* JPRS Report: Science and Technology. USSR: Space 6 Apr. 1988 p 16 Transl. into ENGLISH from Kosmicheskiye Issledovaniya (Moscow, USSR), v. 25, no. 5, Sep. - Oct. 1987 p 721-736 (For primary document see N88-20312 13-12)
Copyright Avail: NTIS HC A04/MF A01

Vega 1 and 2 experiments on the elemental composition of cloud aerosols on Venus are discussed. The roentgenoradiometric instruments are described and the calibration procedures are outlined. Results of the chemical analysis of the three layers of distribution of aerosols are given. Author

N88-20320# Joint Publications Research Service, Arlington, Va.
CHEMICAL COMPOSITION AND STRUCTURE OF VENUSIAN CLOUDS DETERMINED FROM RESULTS OF ROENTGENO-RADIOMETRIC EXPERIMENTS CARRIED OUT BY LANDING MODULES OF VEGA-1 AND VEGA-2 AUTOMATIC INTER-PLANETARY STATIONS Abstract Only **c91**
B. M. Andreychikov *In its* JPRS Report: Science and Technology. USSR: Space 6 Apr. 1988 p 16-17 Transl. into ENGLISH from Kosmicheskiye Issledovaniya (Moscow, USSR), v. 25, no. 5, Sep. - Oct. 1987 p 737-743 Original language document was announced in IAA as A88-17818 (For primary document see N88-20312 13-12)
Copyright Avail: NTIS HC A04/MF A01

In the range of measurements made with the roentgenometric apparatus on the Vega 1 and 2, the cloud aerosol in the altitude range 62 to 51.5 km consists for the most part of components containing sulfur and chlorine. The altitude range 51.5 to 47 km is the region of occurrence of aerosol containing phosphorus and sulfur. The Venusian atmosphere may contain phosphorus oxides which are the products of hypergenesis and possibly volcanic activity. The active participation of phosphorus oxides in redox processes forms the profile water vapor, carbon monoxide and atmospheric components containing sulfur. Author

N88-20321# Joint Publications Research Service, Arlington, Va.
DETERMINING CHEMICAL COMPOSITION OF AEROSOL IN VENUSIAN CLOUD LAYER ON VEGA-1 AUTOMATIC INTERPLANETARY STATION USING MALAKHIT MASS SPECTRUM ANALYZER Abstract Only **c91**
Yu. A. Surkov, V. F. Ivanova, A. N. Pudov, E. P. Sheretov, B. I. Kolotilin, M. P. Safonov, R. Toma, G. Izrael, Zh. Lespanol, and D. Imbo et al. *In its* JPRS Report: Science and Technology. USSR: Space 6 Apr. 1988 p 17 Transl. into ENGLISH from Kosmicheskiye Issledovaniya (Moscow, USSR), v. 25, no. 5, Sep. - Oct. 1987 p 744-750 (For primary document see N88-20312 13-12)
Copyright Avail: NTIS HC A04/MF A01

The Malakhit instrument carried on the Vega 1 for the collection of more precise information concerning the chemical composition of the aerosol fraction of the Venusian cloud layer is described. The instrument consists of two independent modules: The collector-pyrolysis system for the collection and processing of the aerosol fraction of clouds and a mass spectrometer for analysis of the atmosphere or the gaseous products of the pyrolytic decomposition of aerosol. Author

N88-20322# Joint Publications Research Service, Arlington, Va.
ELEMENTAL COMPOSITION OF VENUSIAN ROCKS IN NORTHEASTERN PART OF TERRA APHRODITE (DETERMINED USING DATA FROM VEGA-2 LANDING MODULE) Abstract Only **c91**
Yu. A. Surkov, L. P. Moskaleva, V. P. Kharyukova, A. D. Dudin, G. G. Smirnov, S. Ye. Zaytseva, A. N. Tikhomirov, and O. S. Manvelyan *In its* JPRS Report: Science and Technology. USSR: Space 6 Apr. 1988 p 17-18 Transl. into ENGLISH from Kosmicheskiye Issledovaniya (Moscow, USSR), v. 25, no. 5, Sep. - Oct. 1987 p 751-761 (For primary document see N88-20312 13-12)
Copyright Avail: NTIS HC A04/MF A01

One of the main objectives of the Vega 2 landing module was the determination of the composition of Venusian rocks in a new geomorphological province of Venus using the roentgenoradiometric method used earlier by the Venera spacecraft. The concentrations of the principal rock-forming elements from Mg to Fe and some heavier rare elements were determined. The instrument, consisting of a detection module and a multichannel pulse analyzer module, is described, as is the preflight preparation of the experiment. Author

N88-20323# Joint Publications Research Service, Arlington, Va.
CONTENT OF NATURAL RADIOACTIVE ELEMENTS IN VENUSIAN ROCKS DETERMINED USING DATA FROM VEGA-1 AND VEGA-2 STATIONS Abstract Only **c91**
Yu. A. Surkov, F. F. Kirnozov, V. N. Glazov, A. G. Dunchenko, and L. P. Tatsiy *In its* JPRS Report: Science and Technology. USSR: Space 6 Apr. 1988 p 18 Transl. into ENGLISH from Kosmicheskiye Issledovaniya (Moscow, USSR), v. 25, no. 5, Sep. - Oct. 1987 p 762-767 Original language document was announced in IAA as A88-17821 (For primary document see N88-20312 13-12)
Copyright Avail: NTIS HC A04/MF A01

Vega 1 and 2 gamma ray spectroscopy data on the content of natural radioactive elements in Venus rocks are examined. Data are presented on the content of uranium, thorium, and potassium in near surface rocks at the Vega 1 and 2 landing sites. It is hypothesized that the rocks containing these elements probably correspond to terrestrial gabbroids and tholeiitic basalts. Author

N88-20324# Joint Publications Research Service, Arlington, Va.
SOME PERIODICITIES IN MOTION OF HALLEY'S COMET RELATIVE TO CENTER OF MASS Abstract Only **c91**
V. A. Sarychev, V. V. Sazonov, V. V. Savchenko, and V. I. Tarnopolskiy *In its* JPRS Report: Science and Technology. USSR: Space 6 Apr. 1988 p 18 Transl. into ENGLISH from Kosmicheskiye Issledovaniya (Moscow, USSR), v. 25, no. 5, Sep. - Oct. 1987 p 768-780 Original language document was announced in IAA as A88-17822 (For primary document see N88-20312 13-12)
Copyright Avail: NTIS HC A04/MF A01

Periodicities in three series of ground based observations of Comet Halley are investigated. One series consists of brightness measurements during January to February 1984; the other two series are residuals of observations of the right ascension and declination of the comet from December 1985 to February 1986. Harmonic analysis has revealed the periodic components of these series. In the first series, a component with a period of 2.36 plus or minus 0.084 days has been detected, which is explained by the self-rotation of the comet nucleus. Components with periods of 10.0 plus or minus 2.3 days and 9.1 plus or minus 2 days, respectively, were found for sections of the second and third series from December 12, 1985 to January 1986. Author

N88-20325# Joint Publications Research Service, Arlington, Va.
RESULTS OF INFRARED SPECTROMETER EXPERIMENT. 1: INFRARED RADIATION OF PARENT MOLECULES IN HALLEY'S COMET Abstract Only **c91**
V. I. Moroz, M. Combes, A. V. Grigoryev, J. F. Crifo, T. Encrenaz, J. Crovisier, J. P. Bibring, N. F. Sanko, N. Koron, and D. Bockelee-Morvan et al. *In its* JPRS Report: Science and Technology. USSR: Space 6 Apr. 1988 p 18-19 Transl. into ENGLISH from Kosmicheskiye Issledovaniya (Moscow, USSR), v. 25, no. 5, Sep. - Oct. 1987 p 781-792 (For primary document see N88-20312 13-12)
Copyright Avail: NTIS HC A04/MF A01

The infrared spectrometer experiment was for solving two problems: registry of IR emissions of parent molecules in the coma

surrounding the nucleus and research on the IR emission of the nucleus. Here, research on the parent nucleus is examined. The results obtained as of May 1987 are summarized. The technical specifications of the IR spectrometer are given, and the procedure for processing the measurement data are described. Author

N88-20326# Joint Publications Research Service, Arlington, Va.
RESULTS OF INFRARED SPECTROMETER EXPERIMENT. 2: INFRARED RADIOMETRY OF NUCLEUS OF HALLEY'S COMET Abstract Only **c91**
Yu. V. Nikolskiy, C. Emerich, J. M. Lamarre, N. F. Sanko, M. Combes, V. I. Moroz, J. Crovisier, T. Encrenaz, F. Rokar, and A. V. Grigoryev et al. *In its* JPRS Report: Science and Technology. USSR: Space 6 Apr. 1988 p 19 Transl. into ENGLISH from Kosmicheskiye Issledovaniya (Moscow, USSR), v. 25, no. 5, Sep. - Oct. 1987 p 793-809 (For primary document see N88-20312 13-12)
Copyright Avail: NTIS HC A04/MF A01

The IR radiometry of the nucleus of Halley's Comet is discussed. Since the data processing is still continuing, the results obtained as of May 1987 are given. The experiment was carried out only on the Vega 1. The infrared spectrometer was mounted on the platform, which by means of a TV system directed the optical instruments on the center of cometary brightness. It was assumed that the brightness coincided with the nucleus. The color temperature was T equals 420 plus or minus 60 K. It was found that the brightness temperature at the hottest points of the nucleus is close to the color temperature. It was found that there is little or no ice at the surface of the nucleus. The ice is covered by a thin layer of dark matter having a low thermal conductivity and a considerable degree of porosity, making it possible for water vapor to diffuse through it. Real proof of the presence of a dark mantle was obtained for the first time in the Vega observations. Author

N88-20327# Joint Publications Research Service, Arlington, Va.
ANALYSIS OF HYDROCARBON BAND 3.35 IN SPECTRUM OF HALLEY'S COMET USING DATA FROM INFRARED SPECTROMETER ON VEGA-1 SPACECRAFT Abstract Only **c91**
A. V. Grigoryev *In its* JPRS Report: Science and Technology. USSR: Space 6 Apr. 1988 p 19-20 Transl. into ENGLISH from Kosmicheskiye Issledovaniya (Moscow, USSR), v. 25, no. 5, Sep. - Oct. 1987 p 810-814 (For primary document see N88-20312 13-12)
Copyright Avail: NTIS HC A04/MF A01

The 3.35 micron hydrocarbon band is analyzed on the assumption that the emitting matter is in a gaseous state and the excitation source is solar ultraviolet radiation. The analysis method is described and qualitative estimates are given. The band was first broken down into three distinctive regions (3.22 to 3.25, 3.31 to 3.42 and 3.45 to 3.51 microns), corresponding to vibrations of different groups of atoms. Each of these three regions is analyzed in detail. Author

N88-20328# Joint Publications Research Service, Arlington, Va.
SOVIET SPACE TRANSPORT SYSTEMS **c16**
S. D. Grishin *In its* JPRS Report: Science and Technology. USSR: Space 6 Apr. 1988 p 26-31 Transl. into ENGLISH from Zemlya i Vselennaya (Moscow, USSR), no. 6, Nov. - Dec. 1987 p 18-26 (For primary document see N88-20312 13-12)
Copyright Avail: NTIS HC A04/MF A01

Several Soviet space transportation systems are discussed. The practical uses of cosmonautics; the Soyuz, Cosmos, Proton, and Energiya launch vehicles; and the prospects for interorbital space transport facilities are discussed. R.J.F.

N88-20329# Joint Publications Research Service, Arlington, Va.
FEATURES OF SOYUZ TM SPACECRAFT **c18**
Yu. Semenov and V. Timchenko *In its* JPRS Report: Science and Technology. USSR: Space 6 Apr. 1988 p 35-41 Transl. into ENGLISH from Pravda (Moscow, USSR), 5 Aug. 1987 p 3 (For primary document see N88-20312 13-12)
Copyright Avail: NTIS HC A04/MF A01

The Soyuz TM spacecraft is discussed. The descent module, propulsion system, inertial guidance system, and docking equipment and procedures are described. R.J.F.

N88-20330# Societe Nationale Industrielle Aerospatiale, Les Mureaux (France). Div. Systems Strategiques et Spatiaux.
STUDY ON LONG TERM EVOLUTION TOWARDS EUROPEAN AUTONOMOUS MANNED SPACEFLIGHT (STEAMS) Final Report
M. Grimard Paris, France ESA 22 Jun. 1987 169 p
(Contract ESTEC-6668/86-NL-PP)
(SNIAS-SE/LS/AP-35-073; ESA-CR(P)-2520; ETN-88-91962)
Avail: NTIS HC A08/MF A01

It is shown that a medium sized European space station (ESS) is achievable before 2010. This ESS should allow a permanent occupation by 2 to 4-men crews with a 3 months crew exchange cycle. Manned missions should focus on life sciences, materials, and bioprocessing. A coorbiting platform is required for processing in high quality microgravity environment. It will be a Columbus Man Tended Free Flyer or EURECA derivative. The polar infrastructure is independent of LEO manned one (only hardware commonality). Crew safety is a prime driver for the manned ESS and an escape means permanently docked at the station is required: a dedicated Escape Vehicle or Hermes if it can stay docked for a long time. The logistics support of ESS requires a combined use of Hermes and Ariane 5 flights. This implies high costs for the operations due to launch costs (2 to 4 Hermes flights per year and 1 Ariane 5 flight every 9 to 12 months). This first generation ESS does not allow efficient and intensive commercial activities because of the high operational costs. The reduction of these requires the introduction of new launching systems and the implementation in parallel of a 2nd generation manned infrastructure which might be foreseen in the post-2010 years. ESA

13 ASTRODYNAMICS

Includes powered and free-flight trajectories; and orbital and launching dynamics.

N88-20331# Instituto de Pesquisas Espaciais, Sao Jose dos Campos (Brazil).
ORBIT CORRECTION STRATEGY FOR AN EARTH OBSERVATION SATELLITE [ESTRATEGIA DE CORRECAO DE ORBITA PARA SATELITE DE OBSERVACAO DA TERRA]
Hans-Ulrich Pilchowski Aug. 1987 5 p In PORTUGUESE; ENGLISH summary Presented at the 9th Brazilian Congress of Mechanical Engineers: COBEM/87, Florianopolis, Brazil, 7-11 Dec. 1987
(INPE-4287-PRE/1159) Avail: NTIS HC A02/MF A01

It is possible to examine the required maneuvers for orbit adjust once a nominal orbit for an Earth observing satellite is established. The required orbital corrections are determined by estimating the orbital element perturbation caused by air drag, solar and lunar attraction and the solar radiation pressure. This perturbation changes the synchronicity with the Sun's apparent motion and the near-recurring property. To prevent this effect, orbit adjust maneuvers become necessary in order to keep the orbital elements as near as possible to the nominal values. Author

N88-20332# Messerschmitt-Boelkow-Blohm G.m.b.H., Ottobrunn (West Germany). Space Div.
STUDY OF THE OPTIMIZATION OF SATELLITE SYSTEM DESIGN FOR TRANSFER ORBIT Final Report
Baetz, K. Fetzer, W. Fink, H. Hufnagel, H. Kellermeier, Kleinau, W. Mueller, and H. Chalmers (Erno Raumfahrttechnik G.m.b.H., Bremen, West Germany) Paris, France ESA Apr. 1983 349 p
(Contract ESTEC-4908/81-NL-PP(SC))
(MBB-URV-135; ESA-CR(P)-2518; ETN-88-91960) Avail: NTIS HC A15/MF A01

Geostationary transfer orbit (GTO) characteristics of former geosynchronous satellites; satellite configurations as to GTO requirements; telemetry and telecommand, thermal, power, and attitude control subsystems as to stabilization modes and GTO constraints; and apogee injection strategies (single/multiple burn, steering law) were reviewed. The investigations were confined to 2 Ariane 4 payload classes (2500 kg in GTO, dual-launch and 4200 kg in GTO, single launch), three-axis or slow barbecue stabilization during transfer orbit, and use of a liquid apogee injection system with low thrust level (400 N). A recommendation for an overall system optimization is presented. ESA

N88-20499# Joint Publications Research Service, Arlington, Va.
ORBIT ACCURACY REQUIREMENT OF GPS FOR PRECISE POSITIONING AND ORBIT DETERMINATION WITHIN LOCAL AREA Abstract Only
Qifeng Xu *In its* JPRS Report: Science and Technology. China 12 Feb. 1988 p 81 Transl. into ENGLISH from Tianwen Xuebao (Beijing, People's Republic of China), v. 28, no. 3, Sep. 1987 p 226-236 (For primary document see N88-20495 13-31)
Avail: NTIS HC A07/MF A01

14 GROUND SUPPORT SYSTEMS AND FACILITIES (SPACE)

Includes launch complexes, research and production facilities; ground support equipment, e.g., mobile transporters; and simulators.

For related information see also *09 Research and Support Facilities (Air).*

N88-20333# Army Armament Research and Development Command, Watervliet, N. Y. Weapons Lab.
STRUCTURAL INTEGRITY OF METALLIC ARMATURE RAIL GUNS Final Report
G. P. OHara and M. Cascio Nov. 1987 28 p
(AD-A188735; ARCCB-TR-87031) Avail: NTIS HC A03/MF A01 CSCL 20C

The design of a rail system for an electromagnetic gun becomes more complicated when the transfer from a laboratory to a tactical system is considered. In the laboratory, weight and volume are not important and the system must be bolted together in order to be disassembled for study, modification, and repair. The tactical system must be of reasonable weight and volume, self supporting, safe to use, have a long life, and be factory assembled. This set of design requirements must be reconciled with the function as a projectile guide and an electrical conductor. The first crude prototype barrel must be manufactured from available materials which do not have the optimum properties. The design then becomes a series of compromises which are performed in the hope of a successful result. GRA

N88-20334# Illinois Univ., Urbana. Fusion Technology Lab.
APPLICATION OF RAILGUN PRINCIPLE TO HIGH-VELOCITY HYDROGEN PELLET INJECTION FOR MAGNETIC FUSION REACTOR REFUELING Technical Progress Report
Kyekyoon (Kevin) Kim Dec. 1987 110 p
(Contract DE-FG02-84ER-52111)
(DE88-005830; DOE/ER-52111/T2) Avail: NTIS HC A06/MF A01

This paper discusses the use of a railgun accelerator to inject hydrogen pellets into a magnetic fusion reactor for refueling purposes. Specific studies in this paper include: 1.5 mm-diameter two-stage fuseless plasma-arc-driven electromagnetic railgun, construction and testing of a 3.2 mm-diameter two-stage railgun and a theoretical analysis of the behavior of a railgun plasma-arc armature inside a railgun. DOE

N88-20335# Sandia National Labs., Albuquerque, N. Mex.
TRAJECTORY CODE STUDIES, 1987
J. W. Poukey Jan. 1988 47 p
(Contract DE-AC04-76DP-00789)
(DE88-006218; SAND-87-3068) Avail: NTIS HC A03/MF A01

The trajectory code TRAJ has been used extensively to study nonimmersed foilless electron diodes. The basic goal of the research is to design low-emittance injectors for electron linacs and propagation experiments. Systems studied during 1987 include Delphi, Recirc, and Troll. We also discuss a partly successful attempt to extend the same techniques to high currents (tens of kA). DOE

15 LAUNCH VEHICLES AND SPACE VEHICLES

Includes boosters; operating problems of launch/space vehicle systems; and reusable vehicles.

For related information see also *20 Spacecraft Propulsion and Power.*

N88-20336# Defence Technology and Procurement Group, Thun (Switzerland).
WHAT IS THE MAXIMUM LENGTH OF A SPIN STABILIZED PROJECTILE
B. Kneubuehl 1987 11 p
(PB88-130919) Avail: NTIS HC A03/MF A01 CSCL 16D

Among others, the well known gyroscopic stability factor of a projectile depends on its geometric and physical data as for example the moments of inertia. By calculating these moments and estimating the overturning moment by Munk's formula, the authors are able to determine the gyroscopic stability factor as a function of the length and the slenderness of the projectile. For simple shapes, the authors get a closed formula. For more complicated shapes, the function can be calculated with a numerical method with a computer program. GRA

N88-20337# Air Force Inst. of Tech., Wright-Patterson AFB, Ohio. School of Engineering.
EXPECTED VALUE ANALYSIS FOR AN UNMANNED EXPENDABLE LAUNCH VEHICLE PAYLOAD ESCAPE SYSTEM M.S. Thesis
Fred E. Wagner Dec. 1987 79 p
(AD-A189494; AFIT/GSO/ENS/87D-13) Avail: NTIS HC A05/MF A01 CSCL 22B

Since the beginning of the U.S. Space Program, there have been numerous schemes for humans to escape from spacecraft in distress. This has not been the case for payloads of unmanned, expendable launch vehicles (ELV). The literature review revealed no concepts or design in the U.S. Space Program for saving or salvaging unmanned payloads if an ELV failed during the boost phase. The purpose of this thesis was to develop a methodology to define a mathematical cost relation for a payload escape system (PES). That relation demonstrates when it is economically feasible to use a payload escape system. This methodology draws heavily upon Decision Analysis Techniques, although a classical decision analysis involving a decision maker was not performed. A mathematical relation was developed for two launch cases: the first assumed 100 percent insurance coverage for losses and the other assumed no insurance coverage for losses. The study found that the mathematical relations could be used to develop graphs defining when it is economically feasible to use a PES. The model is flexible and could be modified for use with a particular payload program. GRA

N88-20338# Army Armament Research and Development Command, Watervliet, N. Y. Weapons Lab.
EFFECT OF ROTATION ON THE LATERAL STABILITY OF A FREE-FLYING COLUMN SUBJECTED TO AN AXIAL THRUST WITH DIRECTIONAL CONTROL Final Report
J. D. Vasilakis and J. J. Wu Oct. 1987 20 p Presented at the 4th Army Conference on Applied Mathematics and Computing, Ithaca, N.Y., 27-30 May 1986
(AD-A188690; ARCCB-TR-87027) Avail: NTIS HC A03/MF A01 CSCL 16B

This report discusses some aspects of the stability problems of a free-flying column subjected to axial thrusts. In an age of spacecrafts and missiles, the stability of unsupported flying structures is of great importance. First the brief history of the lateral stability of a column is reviewed, and then the basic characteristic features of the stability problem of a free-free column are described. The mathematical techniques developed to solve these problems depend on a particular problem considered. The most general case requires the solution of a nonself-adjoint differential equation/boundary condition system, which is homogeneous and with zero eigenvalues. Numerical procedures for such a system appear to work well, although theoretical proof of convergence is still lacking. Results of these procedures are discussed. GRA

16 SPACE TRANSPORTATION

Includes passenger and cargo space transportation, e.g., shuttle operations; and space rescue techniques.

For related information see also *03 Air Transportation and Safety* and *18 Spacecraft Design, Testing and Performance*. For space suits see *54 Man/System Technology and Life Support*.

N88-20339*# Martin Marietta Corp., Denver, Colo. Astronautics Group.
ORBITAL TRANSFER VEHICLE CONCEPT DEFINITION AND SYSTEM ANALYSIS STUDY. VOLUME 2: OTV CONCEPT DEFINITION AND EVALUATION. BOOK 1: MISSION AND SYSTEM REQUIREMENTS Final Report, Jul. 1984 - Oct. 1985
Allen E. Kofal Jul. 1987 70 p Revised
(Contract NAS8-36108)
(NASA-CR-179321; NAS 1.26:179321; MCR-86-2601-Vol-2-Bk-1)
Avail: NTIS HC A04/MF A01 CSCL 22B

The mission and system requirements for the concept definition and system analysis of the Orbital Transfer Vehicle (OTV) are established. The requirements set forth constitute the single authority for the selection, evaluation, and optimization of the technical performance and design of the OTV. This requirements document forms the basis for the Ground and Space Based OTV concept definition analyses and establishes the physical, functional, performance and design relationships to STS, Space Station, Orbital Maneuvering Vehicle (OMV), and payloads. Author

N88-20340*# General Dynamics Corp., Huntsville, Ala. Advanced Space Programs.
TURNAROUND OPERATIONS ANALYSIS FOR OTV. VOLUME 1: EXECUTIVE SUMMARY Final Report
Feb. 1988 88 p
(Contract NAS8-36924)
(NASA-CR-179316; NAS 1.26:179316; GDSS-SP-87-018-Vol-1)
Avail: NTIS HC A05/MF A01 CSCL 22B

Anaylses performed for ground processing, both expendable and reusable ground-based Orbital Transfer Vehicles (OTVs) launched on the Space Transportation System (STS), a reusable space-based OTV (SBOTV) launched on the STS, and a reusable ground-based OTV (GBOTV) launched on an unmanned cargo vehicle and recovered by the Orbiter are summarized. Also summarized are the analyses performed for space processing the reusable SBOTV at the Space Station in low Earth orbit (LEO) as well as the maintenance and servicing of the SBOTV accommodations at the Space Station. In addition, the candidate OTV concepts, design and interface requirements, and the Space Station design, support, and interface requirements are summarized. A development schedule and associated costs for the required SBOTV accommodations at the Space Station are presented. Finallly, the technology development plan to develop the capability to process both GBOTVs and SBOTVs are summarized. Author

N88-20341*# General Dynamics Corp., Huntsville, Ala. Advanced Space Programs.
TURNAROUND OPERATIONS ANALYSIS FOR OTV. VOLUME 2: DETAILED TECHNICAL REPORT Final Report
Feb. 1988 263 p
(Contract NAS8-36924)
(NASA-CR-179317; NAS 1.26:179317; GDSS-SP-87-018-Vol-2)
Avail: NTIS HC A12/MF A01 CSCL 22B

The objectives and accomplishments were to adapt and apply the newly created database of Shuttle/Centaur ground operations. Previously defined turnaround operations analyses were to be updated for ground-based OTVs (GBOTVs) and space-based OTVs (SBOTVs), design requirements identified for both OTV and Space Station accommodations hardware, turnaround operations costs estimated, and a technology development plan generated to develop the required capabilities. Technical and programmatic data were provided for NASA pertinent to OTV round and space operations requirements, turnaround operations, task descriptions, timelines and manpower requirements, OTV modular design and booster and Space Station interface requirements. SBOTV accommodations development schedule, cost and turnaround operations requirements, and a technology development plan for ground and space operations and space-based accommodations facilities and support equipment. Significant conclusion are discussed. Author

N88-20342*# General Dynamics Corp., Huntsville, Ala. Advanced Space Programs.
TURNAROUND OPERATIONS ANALYSIS FOR OTV. VOLUME 3: TECHNOLOGY DEVELOPMENT PLAN Final Report
Feb. 1988 118 p
(Contract NAS8-36924)
(NASA-CR-179318; NAS 1.26:179318; GDSS-SP-87-018-Vol-3)
Avail: NTIS HC A06/MF A01 CSCL 22B

An integrated technology development plan for the technologies required to process both GBOTVs and SBOTVs are described. The plan includes definition of the tests and experiments to be accomplished on the ground, in a Space Shuttle Sortie Mission, on an Expendable Launch Vehicle, or at the Space Station as a Technology Development Mission (TDM). The plan reflects and accommodates current and projected research and technology programs where appropriate. Author

N88-20343*# General Dynamics Corp., Huntsville, Ala. Advanced Space Programs.
TURNAROUND OPERATIONS ANALYSIS FOR OTV. VOLUME 4: WBS AND DICTIONARY AND COST METHODOLOGY Final Report
Feb. 1988 65 p
(Contract NAS8-36924)
(NASA-CR-179319; NAS 1.26:179319; GDSS-SP-87-018-Vol-4)
Avail: NTIS HC A04/MF A01 CSCL 22B

The Work Breakdown Structure (WBS) and WBS Dictionary and a discussion of the cost methodology and ground rules employed for the cost analysis conducted, are documented. Author

N88-20328# Joint Publications Research Service, Arlington, Va.
SOVIET SPACE TRANSPORT SYSTEMS
S. D. Grishin *In its* JPRS Report: Science and Technology. USSR: Space 6 Apr. 1988 p 26-31 Transl. into ENGLISH from Zemlya i Vselennaya (Moscow, USSR), no. 6, Nov. - Dec. 1987 p 18-26 (For primary document see N88-20312 13-12)
Copyright Avail: NTIS HC A04/MF A01

17 SPACE COMM., SPACECRAFT COMM., COMMAND & TRACKING

Includes telemetry; space communications networks; astronavigation and guidance; and radio blackout.

For related information see also *04 Aircraft Communications and Navigation* and *32 Communications and Radar.*

N88-20344*# National Aeronautics and Space Administration. Hugh L. Dryden Flight Research Facility, Edwards, Calif.
DEVELOPMENT OF AN INTERACTIVE REAL-TIME GRAPHICS SYSTEM FOR THE DISPLAY OF VEHICLE SPACE POSITIONING
Robert Comperini and Donald C. Rhea May 1988 15 p Prepared for presentation at the 4th Flight Test Conference, San Diego, Calif., 18-20 May 1988
(Contract NAS2-12591)
(NASA-TM-100429; H-1460; NAS 1.15:100429; AIAA-88-2167)
Avail: NTIS HC A03/MF A01 CSCL 09F

Outlined is a new approach taken by the NASA Western Aeronautical Test Range to display real-time space positioning data using computer-generated images that produce a graphic representation of an area map integrated with the research flight test aircraft track. This display system supports research flight test requirements of research projects such as the advanced fighter technology integration (AFTI) F-16, F-18 high alpha research vehicle (HARV), AFTI F-111 mission adaptive wing (MAW), F-15, and X-29A forward-swept wing. This paper will discuss the requirements, system configuration and capability, and future system applications. Author

18 SPACECRAFT DESIGN, TESTING AND PERFORMANCE

Includes satellites; space platforms; space stations; spacecraft systems and components such as thermal and environmental controls; and attitude controls.

For life support systems see *54 Man/System Technology and Life Support.* For related information see also *05 Aircraft Design, Testing and Performance, 39 Structural Mechanics,* and *16 Space Transportation.*

N88-20345 New South Wales Univ., Kensington (Australia).
AN INVESTIGATION OF DOPPLER SATELLITE POSITIONING MULTI-STATION ADJUSTMENT SOFTWARE Abstract Only. M.S. Thesis
Gary Alan Jeffress 1986 118 p
Avail: Issuing Activity

The use of satellite positioning techniques is about to undergo accelerated growth with the introduction of the Global Positioning System (GPS). The forerunner to this system is the TRANSIT system which uses Doppler satellite positioning techniques. The body of knowledge pertaining to the TRANSIT system and the techniques that are used to derive accurate positions from the system were only investigated for the past 15 years or so. The number of computer software packages that are available to reduce Doppler satellite data in its most accurate mode, Multi-Station Adjustment, are very few. Very little comparison of these packages was undertaken and very little investigation of the use of Doppler satellite techniques was made on networks involving large distances. During the southern winter of 1982, a network of ten stations covering chord distances of over 2500 kilometers was observed in central Australia. This data set provided the ideal vehicle to investigate and compare the reduction of Doppler satellite observations using the GEODOP and MAGNET software packages. Author

N88-20346# Air Force Inst. of Tech., Wright-Patterson AFB, Ohio. School of Engineering.
OPTIMAL THRUST VECTOR CONTROL OF COPLANAR ORBITAL EVASIVE MANEUVERS M.S. Thesis
Sharon A. Eide Dec. 1987 140 p
(AD-A189544; AFIT/GA/AA/87D-2) Avail: NTIS HC A07/MF A01 CSCL 22C

Optimal inplane orbital maneuvers enabling a target spacecraft in geosynchronous orbit to avoid interception by a threat in direct coasting ascent are examined. Given constant magnitude, low thrust electric propulsion, the thrust vector control history is determined to propel the spacecraft to either a maximum or minimum orbit radius in a specified time of flight. The evasive maneuver is studied from two aspects. First, an orthogonality constraint is applied at the final time of the maneuver, such that the target spacecraft's position vector is orthogonal to its velocity vector. This requirement is then removed to allow the spacecraft to travel without influence of a terminal constraint. Results demonstrate the adverse shaping effect the orthogonality constraint applies over the entire evasive maneuver. Upon completion of the evasive maneuver, the spacecraft returns in minimum time to its nominal orbit, in a position as if no evasive thrusting had occurred. Results show the time required to rendezvous with the nominal orbit may be significantly greater than the time of flight of the evasive maneuver. GRA

N88-20347# National Aerospace Lab., Amsterdam (Netherlands). Space Div.
MOVEABLE THERMAL JOINTS FOR DEPLOYABLE OR STEERABLE SPACECRAFT RADIATOR SYSTEMS
A. A. M. Delil 20 Feb. 1987 16 p Presented at the 17th Intersoc. Conf. on Environmental Systems' European Thermal Control Session, Seattle, Wash., Jul. 1987 Previously announced as A88-21118
(NLR-MP-87016-U; B8725241; ETN-88-91739) Avail: NTIS HC A03/MF A01

Ways to handle the heat dissipated by the batteries of the Columbus Polar Platform are discussed. One solution is to equip each battery Orbital Replacement Unit with a dedicated heat pipe radiator. Such a radiator, being stowed during launch, has to be deployed in orbit and might be chosen to be steerable to achieve maximum radiator performance, hence minimum radiator size. The coupling between battery and deployable or steerable radiator has to incorporate a rotatable or flexible thermal joint. Drivers for the design of such joints optimize radiator size, and a small deployment/retraction torque or steering torque. Concepts for moveable thermal joints are described. Possible candidates for near-term application are: the flexible heat pipe; the braided conductor; the hydraulically or mechanically clamped joint; and the low melting point alloy filled, grease filled or (low pressure) gas filled (finned) heat exchanger. Concepts for non-near term applications include the radial heat pipe (condenser rotatable with respect to evaporator); the oscillating hydrodynamic joint (flexible or rotatable); the rollable membrane radiator; and the articulated or split heat pipe. ESA

N88-20348# Groningen Rijksuniversiteit (Netherlands). Systems and Control Group.
SIMSAT: SIMULATION PACKAGE FOR FLEXIBLE SYSTEMS. BEAMS IN SPACE M.S. Thesis
Martin H. Klompstra Apr. 1987 61 p
(TW-278; ETN-88-91868) Avail: NTIS HC A04/MF A01

A simulation package (SIMSAT) for flexible systems was developed to study the effects of flexibility, damping, and stabilizing (robust) compensators on these systems. Three partial differential equation models for flexible systems are simulated: Euler-Bernoulli beam with structural damping; Euler-Bernoulli beam with viscous damping; and two Euler-Bernoulli beams with viscous damping connected through a central disk. Possible simulations include simulate the models with or without damping, or connect a compensator to the models (closed loop systems). The SIMSAT calculates the state-evolution w(x,t) of the system, and the input, output, energy, and mean square error corresponding to these. All these calculations can either be shown in numbers (numerical results) or in curves. For the state-evolution two extra graphical facilities are present namely a motion picture and a three dimensional curve. If desired these numerical results and curves

can be sent to a printer. The package was developed in Turbo-Pascal for a personal computer with MS-DOS. ESA

N88-20349# Instituto de Pesquisas Espaciais, Sao Jose dos Campos (Brazil).
UTILIZATION OF STRAPDOWN INERTIAL AND NON-INERTIAL SENSORS IN DETERMINATION OF SATELLITE ATTITUDE BY KALMAN FILTERS M.S. Thesis [UTILIZACAO CONJUNTA DE SENSORES INERCIAIS E NAOINERCIAIS EM DETERMINACAO DE ATITUDE DE SATELITES VIA FILTRO DE KALMAN]
Valtair Antonio Ferraresi Aug. 1987 129 p In PORTUGUESE; ENGLISH summary
(INPE-4313-TDL/280) Avail: NTIS HC A07/MF A01

Four procedures utilizing inertial sensors (gyrometers) and non-inertial sensors (sun and horizon sensors) in the attitude determination of low-orbit artificial satellites are compared. The parameterized state estimation in quaternion is made through the Extended Kalman Filter. The use of the quaternion as state parameterization results in some problems in Kalman Filter application. These problems are due to the error covariance matrix singularity in the parameterized state, which is a difficult condition to be maintained numerically. Four procedures that avoid this difficulty are analyzed. Performance comparison and analysis of these procedures are made through digital simulation. Author

N88-20350# Instituto de Pesquisas Espaciais, Sao Jose dos Campos (Brazil).
GAS CONSUMPTION ESTIMATION OF AN ATTITUDE CONTROL SYSTEM OF AN ARTIFICIAL SATELLITE (UTILIZING DRF) IN LIMIT CYCLE PHASE Final Report Thesis [ESTIMACAO DO CONSUMO DE GAS DE UM SISTEMA DE CONTROLE DE ATITUDE DE SATELITES ARTIFICIAIS (UTILIZANDRO DRF) EM FASE DE CICLO-LIMITE]
Mauro Hissao Hashioka and Marcelo Lopes deOliv eSouza Sep. 1987 162 p In PORTUGUESE; ENGLISH summary
(INPE-4338-RPE/553) Avail: NTIS HC A08/MF A01

An important problem that appears when designing an artificial satellite attitude control system using the DRF (Derived Rate Feedback) controller is its gas consumption at limit cycle. This problem is solved: the gas consumption is calculated analytically and numerically either in the absence or in the presence of external torques. The numerical results agree with the analytical predictions perfectly. The effects of many system parameters on such gas consumption are analyzed through illustrative plots. They provide important background for designing those systems. The work also models the fluid system (which manipulates the gas) more precisely than in the available references to date, arriving at simple but useful models for the present calculations. Author

N88-20351*# Jet Propulsion Lab., California Inst. of Tech., Pasadena.
THE SPACE STATION ASSEMBLY PHASE: FLIGHT TELEROBOTIC SERVICER FEASIBILITY, VOLUME 1 Summary Report
Jeffrey H. Smith, Max A. Gyamfi, Kent Volkmer, and Wayne F. Zimmerman Sep. 1987 41 p
(Contract NAS7-918)
(NASA-CR-182689; JPL-Pub-87-42-Vol-1; NAS 1.26:182689)
Avail: NTIS HC A03/MF A01 CSCL 22B

The question is addressed which was raised by the Critical Evaluation Task Force (CETF) analysis of the space station: if a Flight Telerobotic Servicer (FTS) of a given technical risk could be built for use during space station assembly, could it save significant extravehicular (EVA) resources. Key issues and trade-offs associated with using an FTS to aid in space station assembly phase tasks such as construction and servicing are identified. A methodology is presented that incorporates assessment of candidate assembly phase tasks, telerobotics performance capabilities, development costs, operational constraints (STS and proximity operations), maintenance, attached payloads, and polar platforms. A discussion of the issues is presented with focus on potential FTS roles: (1) as a research-oriented test bed to learn more about space usage of telerobotics; (2) as a research-based test bed with an experimental demonstration orientation and limited assembly and servicing applications; or (3) as an operational system to augment EVA, to aid the construction of the space station, and to reduce the programmatic (schedule) risk by increasing the flexibility of mission operations. During the course of the study, the baseline configuration was modified into Phase 1 (a station assembled in 12 flights), and Phase 2 (a station assembled over a 30 flight period) configuration. Author

N88-20352*# Jet Propulsion Lab., California Inst. of Tech., Pasadena.
THE SPACE STATION ASSEMBLY PHASE: FLIGHT TELEROBOTIC SERVICER FEASIBILITY. VOLUME 2: METHODOLOGY AND CASE STUDY
Jeffrey H. Smith, Max A. Gyamfi, Kent Volkmer, and Wayne F. Zimmerman Sep. 1987 161 p
(Contract NAS7-918)
(NASA-CR-182690; JPL-Pub-87-42-Vol-2; NAS 1.26:182690)
Avail: NTIS HC A08/MF A01 CSCL 22B

A methodology is described for examining the feasibility of a Flight Telerobotic Servicer (FTS) using two assembly scenarios, defined at the EVA task level, for the 30 shuttle flights (beginning with MB-1) over a four-year period. Performing all EVA tasks by crew only is compared to a scenario in which crew EVA is augmented by FTS. A reference FTS concept is used as a technology baseline and life-cycle cost analysis is performed to highlight cost tradeoffs. The methodology, procedure, and data used to complete the analysis are documented in detail. Author

N88-20353*# Wyle Labs., Inc., Huntsville, Ala.
SPACECRAFT FIRE-SAFETY EXPERIMENTS FOR SPACE STATION: TECHNOLOGY DEVELOPMENT MISSION Final Contractor Report
Wallace W. Youngblood Apr. 1988 111 p
(Contract NAS3-25067)
(NASA-CR-182114; NAS 1.26:182114; Wyle-68300-1) Avail: NTIS HC A06/MF A01 CSCL 22B

Three concept designs for low-gravity, fire-safety related experiments are presented, as selected for the purpose of addressing key issues of enhancing safety and yet encouraging access to long-duration, manned spacecraft such as the NASA space station. The selected low-gravity experiments are the following: (1) an investigation of the flame-spread rate and combustion-product evolution of the burning of typical thicknesses of spacecraft materials in very low-speed flows; (2) an evaluation of the interaction of fires and candidate extinguishers in various fire scenarios; and (3) an investigation of the persistence and propagation of smoldering and deep-seated combustion. Each experiment is expected to provide fundamental combustion-science data, as well as the fire-safety applications, and each requires the unique long-duration, low-gravity environment of the space station. Two generic test facilities, i.e., the Combustion Tunnel Facility and the Combustion Facility, are proposed for space station accommodation to support the selected experiments. In addition, three near-term, fire-safety related experiments are described along with other related precursor activities. Author

N88-20354# Construcciones Aeronauticas S.A., Madrid (Spain). Space Div.
DEVELOPMENT OF ISOSTATIC MOUNTS AND ASSOCIATED GUIDELINES Final Report
Paris, France ESA Jun. 1987 318 p
(Contract ESA-5245/82-NL-PB(SC))
(CASA-IM-WP-301; ESA-CR(P)-2502; ETN-88-91955) Avail: NTIS HC A14/MF A01

Isostatic interfaces to alleviate load transfer effects between supporting structures and spacecraft payloads were studied. The mounting system of an infrared telescope primary mirror was taken as an example to develop devices. A top-down analysis methodology for device definition from the system requirements, materialized in a design optimization program. Two concepts, one in metal, one in carbon fiber reinforced plastic were developed.

The material characterization to guarantee the behavior of the latter was performed up to liquid helium cryogenic temperature. A manufacturing and testing methodology incorporating techniques to allow one-shot manufacturing of flexible devices in composites was defined. Data sheets to give designers a first approach were issued. ESA

N88-20329# Joint Publications Research Service, Arlington, Va.
FEATURES OF SOYUZ TM SPACECRAFT
Yu. Semenov and V. Timchenko *In its* JPRS Report: Science and Technology. USSR: Space 6 Apr. 1988 p 35-41 Transl. into ENGLISH from Pravda (Moscow, USSR), 5 Aug. 1987 p 3 (For primary document see N88-20312 13-12)
Copyright Avail: NTIS HC A04/MF A01

19 SPACECRAFT INSTRUMENTATION

For related information see also *06 Aircraft Instrumentation* and *35 Instrumentation and Photography.*

No abstracts in this category.

20 SPACECRAFT PROPULSION AND POWER

Includes main propulsion systems and components, e.g., rocket engines; and spacecraft auxilliary power sources.

For related information see also *07 Aircraft Propulsion and Power, 28 Propellants and Fuels, 44 Energy Production and Conversion,* and *15 Launch Vehicles and Space Vehicles.*

N88-20355# Hughes Research Labs., Malibu, Calif.
ADVANCED SPACE PROPULSION STUDY - ANTIPROTON AND BEAMED POWER PROPULSION Final Report, 1 May 1986 - 30 Jun. 1987
Robert L. Forward Oct. 1987 215 p
(Contract F04611-86-C-0039)
(AD-A189218; AFAL-TR-87-070) Avail: NTIS HC A10/MF A01 CSCL 21C

The contract objective was to monitor the research at the forefront of physics and engineering to discover new spacecraft propulsion concepts. The major topics covered were antiproton annihilation propulsion, laser thermal propulsion, laser-pushed lightsails, tether transportation systems, solar sails, and metallic hydrogen. Five papers were prepared and are included as appendices. They covered: (1) pellet, microwave, and laser beamed power systems for interstellar transport; (2) a design for a near-relativistic laser-pushed lightsail using near-term laser technology; (3) a survey of laser thermal propulsion, tether transportation systems, antiproton annihilation propulsion, exotic applications of solar sails, and laser-pushed interstellar lightsails; (4) the status of antiproton annihilation propulsion as of 1986, and (5) the prospects for obtaining antimatter ions heavier than antiprotons. Two additional appendices contain the first seven issues of the Mirror Matter Newsletter concerning the science and technology of antimatter, and an annotated bibliography of antiproton science and technology. GRA

N88-20356# Wisconsin Univ., Madison.
SOAR: SPACE ORBITING ADVANCED FUSION POWER REACTOR Final Report, Oct. 1986 - Jan. 1987
F. L. Kulcinski and J. F. Santarius Sep. 1987 57 p
(Contract F33615-86-C-2705)
(AD-A189234; AFWAL-TR-87-2048) Avail: NTIS HC A04/MF A01 CSCL 22B

The preconceptual design of a Space Orbiting Advanced Fusion Power Reactor (SOAR), which delivers up to 1000 MWe for at least 600 s from an orbited mass of about 500 tons, was accomplished. The power is produced by a magnetically confined D-3He plasma. Approximately 96 percent of the fusion energy is in charged particles, and a direct converter has been designed which converts much of this energy into electricity at high net efficiency (about 80 percent). An advanced shield design allows SOAR to deliver approximately 2 kilowatts of electricity for every kilogram of material orbited. The shield is designed to absorb all rejected heat during operation, and no active radiator is required. The SOAR reactor concept is designed to allow rapid startup and shutdown procedures. The lack of radioactivity on launch and the low radioactive inventory after operation make the SOAR concept attractive from maintenance, safety and environmental perspectives. The plasma physics approach extrapolates from the present plasma physics and fusion technology knowledge base using concepts which can be tested on existing or near-term devices. The symbiosis of burst mode requirements, D-3He tandem mirror fusion reactor characteristics, and the space environment leads to a very high performance design concept. GRA

N88-20357# Toronto Univ., Downsview (Ontario). Inst. for Aerospace Studies.
A STUDY OF COMBUSTION AND FLOW BEHAVIOUR IN SOLID-PROPELLANT ROCKET MOTORS
D. R. Greatrix Dec. 1987 166 p Sponsored by Natural Sciences and Engineering Research Council and DREV
(UTIAS-280; ISSN-0082-5255) Avail: NTIS HC A08/MF A01

A comprehensive study of several important aspects of the internal ballistics of solid-propellant rocket motors (SRMs) was undertaken. Numerical models were developed for the solution of the quasi-steady and unsteady, one-dimensional, hydrodynamic equations of motion governing the two-phase core flow behavior within the motor chamber and nozzle. A phenomenological model of erosive burning was develped and incorporated into an overall solid-propellant combustion model, which in turn is solved in conjunction with the equations of motion for the SRM. The quasi-steady internal ballistics predictions based on the phenomenological model was also developed for the description of normal acceleration effects on the combustion process, for the parametric study of spinning, composite-propellant SRM. The internal ballistics of an SRM within various longitudinal acceleration environments was studied numerically with the use of a comprehensive unsteady flow model. A numerical model for the description of ignition transient flow behavior of pellet-dispersion igniter systems was developed. The model was specifically created for the study of conventional bag and cartridge igniters employed for small-diameter, composite-propellant SRMs, but the model in its general form may be adapted for the study of a multitude of ignition transient problems. Good agreement is obtained between experimental firing data and the model prediction for the head-end pressure-time profile. Author

N88-20358 Utah Univ., Salt Lake City.
THE EFFECT OF COMBUSTION GAS FLOW ON THE ROTATIONAL DYNAMICS OF A SPINNING SOLID FUEL ROCKET Ph.D. Thesis
Paul Alexander Finlayson 1987 116 p
Avail: Univ. Microfilms Order No. DA8726533

The flow of combustion gases exerts a moment on a spinning solid fuel rocket. If the details of the internal combustion gas flow are known, accurate moment calculations may be obtained by means of a computationally expensive numerical volume integral. This internal gas flow model, however, is seldom available and represents a formidable problem in its own right. An alternative method developed describes the momentum induced by the combustion gas flow in terms of the angular momentum flux through a control volume. Computation of the lateral steady moment (jet damping) requires only the mass flow rates at the burning surface and at the nozzle exit. The axial steady moment requires, in addition, one component of the combustion gas velocity at the nozzle exit. Approximate equations describing the lateral moment induced by the steady combustion gas flow were available for over 40 years. Utilizing the theory described, modern jet damping

equations are derived which are accurate for a variety of realistic combustion chamber shapes and rocket geometries. For completeness, the moment induced by the unsteady flow is derived utilizing the angular momentum flux method. General rigid body dynamic models are developed for both the steady and unsteady moment cases, followed by an example simulation fo a STAR 48 rocket motor and vehicle dynamics. Dissert. Abstr.

N88-20359 Illinois Univ., Chicago.
BIPROPELLANT COMBUSTION IN A LIQUID ROCKET COMBUSTION CHAMBER Ph.D. Thesis
Tsung Leo Jiang 1987 159 p
Avail: Univ. Microfilms Order No. DA8726088

The combustion characteristics of bipropellants, including liquid fuel and liquid oxidizer, are studied on scales of droplet separation distance and droplet clouds analytically to provide the bases of bipropellant combustion modeling in the full scale computer simulation of a liquid rocket engine. A comprehensive computer simulation code is developed to analyze the complex bipropellant combustion in liquid rocket engines. A bipropellant group combustion model is built in the computer code to facilitate the determination of various combustion modes, including conjugate and normal droplet combustion and gas phase combustion. Physical submodels of the finite transport rates between droplet phase and gas phase are also adopted to account for the interactions between the two phases. An axisymmetric cylindrical liquid rocket combustion chamber installed in two annular ring injectors is selected to demonstrate the capabilities of the present computer simulation code. Two types of injection process are analyzed: one characterized by a nonpremixed spray process and the other a premixed spray process. Selected computations are conducted to illustrate the detailed structure, intensity and modes of combustion. Dissert. Abstr.

N88-20360 Utah Univ., Salt Lake City.
NUMERICAL MODEL OF THE TIME INDEPENDENT MEAN FLOW IN A ROTATING ROCKET MOTOR Ph.D. Thesis
Curtis David Clayton 1987 179 p
Avail: Univ. Microfilms Order No. DA8727896

The anlaysis of the time independent mean flow in the combustion chamber of a rotating PAM-D rocket motor is presented. The flow field is modeled using the Navier-Stokes equations for a viscous, incompressible, Newtonian fluid in an axisymmetric, non-inertial coordinate system. The resulting nonlinear differential equations are solved using the finite element method and a Newton-Raphson iteration technique with analytically derived derivatives. Streamlines are shown for nonrotating cases with Reynolds numbers from 0.8 to 15.0 and for rotating cases with Rossby numbers of 0.8 and 0.4. The analysis shows that the negative pressure gradient caused by the flow converging toward the nozzle effectively suppresses the flow separation in the aft end of the cavity and that the axial flow originating at the head end precludes the formation of a narrow vortex core along the axis. Source code for the analysis program is included.
Dissert. Abstr.

N88-20361*# Rockwell International Corp., Canoga Park, Calif. Rocketdyne Div.
SOLAR DYNAMIC POWER SYSTEM DEFINITION STUDY Final Report
Wayne E. Wallin and Jerry M. Friefeld Mar. 1988 322 p
Prepared for presentation at the National Aerospace and Electronics Conf., Dayton, Ohio, 18-22 May 1987
(Contract NAS3-24864)
(NASA-CR-180877; NAS 1.26:180877; RI/RD87-250) Avail: NTIS HC A14/MF A01 CSCL 10B

The solar dynamic power system design and analysis study compared Brayton, alkali-metal Rankine, and free-piston Stirling cycles with silicon planar and GaAs concentrator photovoltaic power systems for application to missions beyond the Phase 2 Space Station level of technology for all power systems. Conceptual designs for Brayton and Stirling power systems were developed for 35 kWe and 7 kWe power levels. All power systems were designed for 7-year end-of-life conditions in low Earth orbit. LiF was selected for thermal energy storage for the solar dynamic systems. Results indicate that the Stirling cycle systems have the highest performance (lowest weight and area) followed by the Brayton cycle, with photovoltaic systems considerably lower in performance. For example, based on the performance assumptions used, the planar silicon power system weight was 55 to 75 percent higher than for the Stirling system. A technology program was developed to address areas wherein significant performance improvements could be realized relative to the current state-of-the-art as represented by Space Station. In addition, a preliminary evaluation of hardenability potential found that solar dynamic systems can be hardened beyond the hardness inherent in the conceptual designs of this study. Author

23 CHEMISTRY AND MATERIALS (GENERAL)

N88-20362# Air Force Academy, Colo. Research Lab.
MOPAC MANUAL: A GENERAL MOLECULAR ORBITAL PACKAGE, FOURTH EDITION Technical Report, Jul. 1986 - Oct. 1987
James J. Stewart Oct. 1987 170 p
(AD-A188623; FJSRL-TR-87-0006) Avail: NTIS HC A08/MF A01 CSCL 07D

MOPAC is a general purpose, semi empirical molecular orbital program for the study of chemical reactions involving molecules, ions, and linear polymers. It implements the semi-empirical Hamiltonians MNDO, AM1, and MINDO/3 and combines the calculations of vibrational spectra, thermodynamic quantities, isotopic substitution effects, and force constants in a fully integrated program. Elements parameterized at the MNDO level include Hydrogen, Lithium, Beryllium, Boron, Carbon, Nitrogen, Oxygen, Fluorine, Aluminum, Silicon, Phosphorus, Sulfur, Chlorine, Chromium. Within the electronic part of the calculation, molecular and localized orbitals excited states up to sextets, chemical bond indices, charges, etc. are computed. Both intrinsic and dynamic reaction coordinates can be calculated. A transition-state location routine and two transition-state optimizing routines are available for studying chemical reactions. GRA

24 COMPOSITE MATERIALS

Includes physical, chemical, and mechanical properties of laminates and other composite materials.
For ceramic materials see *27 Nonmetallic Materials.*

N88-20363*# National Aeronautics and Space Administration. Langley Research Center, Hampton, Va.
SIMULATED IMPACT DAMAGE IN A THICK GRAPHITE/EPOXY LAMINATE USING SPHERICAL INDENTERS
C. C. Poe, Jr. Jan. 1988 35 p
(NASA-TM-100539; NAS 1.15:100539) Avail: NTIS HC A03/MF A01 CSCL 11D

A study was made to determine the extent of fiber damage caused by low-velocity impact of spherical impactors to a very thick graphite/epoxy laminate. The laminate was cut from a filament wound case being developed for the Space Shuttle solid rocket motors. The case was wound using a wet process with AS4W graphite fiber and HBRF-55A epoxy. Impacts were simulated under quasi-static conditions by pressing hemispherically shaped indenters against the laminate at different locations. The contact force and indenter diameter were varied from location to location. The forces were chosen for each indenter diameter to produce contact pressures below and above that required to initiate damage. After the forces were applied, the laminate was cut into smaller pieces so that each piece contained a test site. The pieces were then deplied and the individual plies examined to determine the extent of fiber damage. Broken fibers were found in the outer

layers directly beneath the contact site. The locus of broken fibers in each layer resembled a crack normal to the direction of the fibers. The maximum length and depth of the cracks increased with increasing contact pressure and indenter diameter. The internal stresses in the laminate were calculated using Hertz's law and Love's solution for pressure applied on part of the boundary of a semi-infinite body. The maximum length and depth of the cracks were predicted using a maximum shear stress criterion. Predictions and measurements were in good agreement. Author

N88-20364# Maryland Univ., College Park. Metallurgical Materials Lab.
COMPOSITES STRENGTHENING Final Report, 1985 - 1987
Richard J. Arsenault Nov. 1987 172 p
(Contract N00014-85-K-0007)
(AD-A189258; MML-1987-1) Avail: NTIS HC A08/MF A01 CSCL 11D

In all cases of discontinuous silicon carbide/aluminum metal matrix it was previously shown that classical composite strengthening mechanisms could not be used to explain the data. A high dislocation density model was proposed to account for the strengthening, but other factors such as residual stress and texture could contribute. These were investigated and it was shown that texture had no effect and residual stress reduced the tensile yield stress. The fracture process is matrix controlled up to SiC particle sizes of 20 micrometers and above where fracture of SiC begins to dominate. The matrix is influenced by residual hydrostatic tension and high density of dislocations generated at SiC/Al interfaces. Crack initiation fracture toughness does not depend on SiC particle size. Crack growth fracture toughness increases as the size of the SiC particles increases. GRA

N88-20365# Naval Ship Research and Development Center, Bethesda, Md. Ship Materials Engineering Dept.
COMPRESSION OF COMPOSITE MATERIALS: A REVIEW
E. T. Camponeschi, Jr. Nov. 1987 59 p
(AD-A189272; DTRC-87/050) Avail: NTIS HC A04/MF A01 CSCL 11D

This paper is a literature review of research on the compressive response of fiber-reinforced composite laminates. Emphasis is on recent research with papers from 1980 to the present included. The review is organized by subject and the papers are included in one of three main groups; compression test methods, failure theories and failure mechanisms and experimental investigations. Tables are presented summarizing the information included in the paper dealing with the evaluation of test methods and generation of experimental data. These tables provide an index for quick reference to the research discussed in this paper. GRA

N88-20366# Colorado Univ., Boulder. Dept. of Mechanical Engineering.
PHASE VELOCITY AND ATTENUATION OF PLANE ELASTIC WAVES IN A PARTICLE-REINFORCED COMPOSITE MEDIUM
S. K. Datta, H. M. Ledbetter, Y. Shindo, and A. H. Shah Aug. 1987 26 p
(Contract N00014-86-K-0280)
(AD-A189414; CUMER-87-3) Avail: NTIS HC A03/MF A01 CSCL 11D

Our study considered effective-plane-wave propagation, both longitudinal and shear, through a medium containing a random distribution of spherical inclusions. It was assumed that particles and matrix are separated by a thin layer of elastic material with different properties. For some systems, measurable effects were predicted for the thin layers. Especially, lead/epoxy and silicon carbine/aluminum were considered. The object of this study was to explore the practicality of using ultrasound to characterize properties of interface layers. Ultrasound is a practical tool for measuring properties of, and characterizing the state of, a material with microstructure (or changes in microstructure). GRA

N88-20367# Carnegie-Mellon Univ., Pittsburgh, Pa. Dept. of Metallurgical Engineering and Materials Science.
HIGH-TEMPERATURE METAL MATRIX COMPOSITES Annual Report, 15 Nov. 1986 - 30 Sep. 1987
A. W. Thompson, J. O. Parent, Hani Henein, Henry R. Piehler, and Daniel M. Watkins 30 Nov. 1987 130 p Prepared in cooperation with California Univ., Berkeley and Clemson Univ.
(Contract F49620-87-C-0017)
(AD-A189516; AFOSR-88-0089TR) Avail: NTIS HC A07/MF A01 CSCL 11D

The Annual Report for Year 1 of the University Research Initiative grant at Carnegie Mellon University on High-temperature Metal Matrix Structural Composites contains sections on processing, characterization, and mechanical properties. These are further divided into reports from individual tasks on powder blending and consolidation, composite performance, structure and composition of composite interfaces, fatigue crack growth, creep, and fracture behavior. GRA

N88-20368# Air Force Inst. of Tech., Wright-Patterson AFB, Ohio. School of Engineering.
VISCOELASTIC BEHAVIOR OF A POLYETHERETHERKETONE (PEEK) COMPOSITE M.S. Thesis
Richard P. Lockwood Dec. 1987 92 p
(AD-A189545; AFIT/GAE/AA/87D-10) Avail: NTIS HC A05/MF A01 CSCL 11D

The thermoplastic polyetheretherketone (PEEK) is being considered for structural applications in the Advanced Tactical Fighter. Previous efforts characterizing PEEK mechanical properties are reviewed. A study developing the viscoelastic frequency-temperature response to three point flexure of neat resin and PEEK/graphite fiber composites is detailed. The behavior of unidirectional laminates is compared to predictions from elastic plate theory, which also combines micro- and macromechanical approaches to predict transverse and longitudinal complex moduli. The experimental frequency-temperature shift factors, obtained under low strain in a Dynastat dynamic viscoelastic analyzer, are compared to shift factors predicted from the Williams-Landel-Ferry equation. Determining composite behavior from knowledge of matrix and fiber behavior is still applicable. The capability of the Dynastat to perform viscoelastic characterizations of stiff, unidirectional composites, based on comparisons of the various shift factors, is reduced due to the presence of the reinforcing fibers. Recommendations for future test and evaluations, including increasing the dynamic signal-to-noise ratio, are described. GRA

N88-20369# Oak Ridge National Lab., Tenn.
THE INFLUENCE OF THE FIBER-MATRIX BOND ON THE MECHANICAL BEHAVIOR OF NICALON/SiC COMPOSITES
R. A. Lowden and D. P. Stinton Dec. 1987 47 p
(Contract DE-AC05-84OR-21400)
(DE88-006155; ORNL/TM-10667) Avail: NTIS HC A03/MF A01

The effect of thin coatings deposited on NICALON fibers prior to densification with silicon carbide by chemical vapor infiltration was investigated. The thin films were applied to alter the strength of the fiber-matrix bond and to protect the fibers during processing. An indentation method developed to measure the strength of fiber-matrix bonding and frictional stresses was investigated and compared to a simple tensile test technique. The influence of the coatings on the bond strength and mechanical behavior of the composite products was examined. DOE

N88-20370# Indian Inst. of Tech., Bombay. Dept. of Civil Engineering.
TRANSIENT DYNAMICS OF FIBRE REINFORCED COMPOSITE PLATES Final Report
Tarun Kant Jan. 1987 426 p
(Grant Aero/RD-134/100/10/83-84/362)
(IIT-B/CE/RR/87-1) Avail: NTIS HC A19/MF A01

Higher-order shear deformation theories are developed for the elastostatic analyses of fiber reinforced laminated composite and sandwich plate structures. The theories are based on the Taylor's

series expansion of the generalized displacements and they account for cubic variation of inplane displacements and constant or parabolic variation of transverse displacement through the plate thickness. These assumed displacement fields lead to a parabolic variation of transverse shear stresses through the plate thickness. The use of the arbitrary shear correction coefficients which are problem dependent for laminated anisotropic plate and normally associated with the first-order shear deformation theories is avoided in the present development. A new approach to satisfying zero transverse shear conditions on top and bottom bounding planes of the plate by imposing these conditions in the shear rigidity matrix has been used to retain the simple C sup o continuity for the finite element formulation. The formulations for symmetric and unsymmetric laminates have been dealt with separately to achieve economy in computation. The accuracy and versatility of the theoretical and finite element formulations have been demonstrated through numerical examples. Author

N88-20371# National Aerospace Lab., Amsterdam (Netherlands). Structures and Materials Div.

FRACTURE CHARACTERISTICS OF CARBON AND ARAMID UNIDIRECTIONAL COMPOSITES IN INTERLAMINAR SHEAR AND OPEN HOLE TENSILE TESTS

A. C. Moss and W. G. J. tHart 26 Aug. 1986 39 p
(NLR-TR-86083-U; B8729598; ETN-88-91722) Avail: NTIS HC A03/MF A01

Carbon/epoxy and aramid/epoxy composites were examined in interlaminar shear and in open-hole tensile tests at 90 deg to the unidirectional fiber orientation. Epoxy resin was also tested under tension. Microscopy was used to study the fracture surfaces. Wet tests were performed to investigate the influence of moisture absorption on the strength of the composites. In the interlaminar shear tests, shear crippling and interlaminar delamination are seen for most of the specimens. The value of the interlaminar shear strength does not change with water absorption. In the open-hole tensile tests moisture uptake increases local plasticity of the resin and the size and number of voids in the material. In both the composites interfacial bonding decreases owing to water absorption. Kink bands are found on the compression sides of the aramid fibers in both the wet and dry specimens. ESA

N88-20372*# National Aeronautics and Space Administration. Langley Research Center, Hampton, Va.

PLY-LEVEL FAILURE ANALYSIS OF A GRAPHITE/EPOXY LAMINATE UNDER BEARING-BYPASS LOADING

R. A. Naik (PRC Kentron, Inc., Hampton, Va.) and J. H. Crews, Jr. 1988 37 p
(NASA-TM-100578; NAS 1.15:100578) Avail: NTIS HC A03/MF A01 CSCL 11D

A combined experimental and analytical study was conducted to investigate and predict the failure modes of a graphite/epoxy laminate subjected to combined bearing and bypass loading. Tests were conducted in a test machine that allowed the bearing-bypass load ratio to be controlled while a single-fastener coupon was loaded to failure in either tension or compression. Onset and ultimate failure modes and strengths were determined for each test case. The damage-onset modes were studied in detail by sectioning and micrographing the damaged specimens. A two-dimensional, finite-element analysis was conducted to determine lamina strains around the bolt hole. Damage onset consisted of matrix cracks, delamination, and fiber failures. Stiffness loss appeared to be caused by fiber failures rather than by matrix cracking and delamination. An unusual offset-compression mode was observed for compressive bearing-bypass laoding in which the specimen failed across its width along a line offset from the hole. The computed lamina strains in the fiber direction were used in a combined analytical and experimental approach to predict bearing-bypass diagrams for damage onset from a few simple tests. Author

N88-20373# California Univ., Berkeley. Lawrence Berkeley Lab.

TUNGSTEN-CARBON MULTILAYER SYSTEM STUDIED WITH X-RAY SCATTERING

J. B. Kortright and J. D. Denlinger Dec. 1987 8 p Presented at the Fall Meeting of the Materials Research Society, Boston, Mass., 30 Nov. 1987
(Contract DE-AC03-76SF-00098)
(DE88-005749; LBL-24356; CONF-871124-76) Avail: NTIS HC A02/MF A01

The tungsten-carbon multilayer system has been studied using X-ray scattering techniques as a function of multilayer period and annealing. Grazing incidence X-ray scattering shows that interatomic arrangements in the W-rich layers depend strongly on their proximity to the interface with the C-rich layers. Amorphous interface layers are stabilized by intermixing of W and C during deposition into local structures similar to those in the tungsten carbides. Further intermixing and structural relaxation in the amorphous state occurs on annealing these structures. This interatomic structural interpretation is consistent with trends in the observed X-ray optical properties. DOE

N88-20374*# National Aeronautics and Space Administration, Washington, D.C.

REINFORCING OF THERMOPLASTIC POLYCARBONATE AND POLYSULFONE WITH CARBON FIBERS: PRODUCTION AND CHARACTERISTICS OF UD-COMPOUND OBJECTS

E. Fitzer and H. Jaeger Apr. 1988 63 p Transl. into ENGLISH of paper presented at Arbeitsgemeinschaft Verstaerkte Kunststoffe, Open Annual Meeting, 20th International Meeting of Reinforced Plastics, 1986 Meeting held in Freudenstadt, Fed. Republic of Germany, 1986 Original language document was announced in IAA as A86-48094
(Contract NASw-4307)
(NASA-TT-20158; NAS 1.77:20158) Avail: NTIS HC A04/MF A01 CSCL 11D

The production and characteristics of the carbon fiber reinforced thermoplastics polycarbonate and polysulfone are described. The production of prepregs from defined polymer solutions is emphasized along with methods of optimizing the production of compounds. The characteristics of unidirectionally reinforced thermoplastics, such as shear strength, bending strength, and impact resistance are compared with regard to fracture behavior, the influence of intermediate layers, and the behavior under cryogenic conditions and under slightly elevated temperatures. The problem of adhesion between high strength carbon fibers and thermoplastics is examined, taking into account the effect of moisture on the shear strength and the impact resistance. E.R.

N88-20375*# National Aeronautics and Space Administration. Hugh L. Dryden Flight Research Facility, Edwards, Calif.

DELAMINATION STRESSES IN SEMICIRCULAR LAMINATED COMPOSITE BARS

William L. Ko Jan. 1988 27 p Submitted for publication
(NASA-TM-4026; H-1417; NAS 1.15:4026) Avail: NTIS HC A03/MF A01 CSCL 11D

Using anisotropic elasticity theory, delamination stresses in a semicircular laminated composite curved bar subjected to end forces and end moments were calculated, and their radial locations determined. A family of design curves was presented, showing variation of the intensity of delamination stresses and their radial locations with different geometry and different degrees of anisotropy of the curved bar. The effect of anisotropy on the location of peak delamination stress was found to be small. Author

25 INORGANIC AND PHYSICAL CHEMISTRY

Includes chemical analysis, e.g., chromatography; combustion theory; electrochemistry; and photochemistry.

For related information see also *77 Thermodynamics and Statistical Physics.*.

N88-20376# Purdue Univ., West Lafayette, Ind. Dept. of Chemistry.

ELECTROSORPTIVE DETECTION OF SIMPLE ORGANIC COMPOUNDS IN LIQUID CHROMATOGRAPHY Technical Report, Oct. 1986 - 30 Sep. 1987

T. Ramstad and M. J. Weaver 25 Sep. 1987 44 p

(Contract N00014-86-K-0556)

(AD-A188757) Avail: NTIS HC A03/MF A01 CSCL 07C

The detection of a range of neutral organic compounds in liquid chromatography based on decreases in differential double-layer capacitance, delta C(d), at a mercury-aqueous interface caused by analyte specific adsorption is described. The arrangement employs ac phase-selective measurements using a large-volume wall-jet configuration. The low-molecular-weight organic solutes examined include aliphatic alcohols, diols, mono- and dicarboxylic acids, amines, and alkanolamines. The differential capacitance measurements were conducted close to the potential of zero charge, where adsorption of such species is most extensive. Plots of delta C(d) versus analyte concentration were generally sigmoidal, in accordance with expectations from the Frumkin adsorption isotherm. A potential-step coulometric method, where variations in the nonfaradaic charge, delta(delta q), are measured, was found to be a useful alternative detection scheme. Methods based on measuring transient capacitive currents associated with tensammetric adsorption-desorption behavior were also briefly investigated. Analyte specific adsorption, Large volume wall jet, Frumkin adsorption isotherm, Potential step coulometric method. GRA

N88-20377# North Carolina Univ., Chapel Hill. Dept. of Chemistry.

THERMAL OXIDE GROWTH ON SILICON: INTRINSIC STRESS AND SILICON CLEANING EFFECTS

E. A. Irene 3 Dec. 1987 37 p

(Contract N00014-86-K-0305)

(AD-A188790; TR-19) Avail: NTIS HC A03/MF A01 CSCL 07B

This paper summarizes the experimental results and discusses the implications of recent research on two topics related to Si oxidation: mechanical stress effects and the influence of impurities on the Si surface. For stress measurement, a double beam optical technique is used to measure the strain in the Si substrate due to the film stress. An intrinsic SiO2 stress is measured which increases with decreasing oxidation temperature. Controversy exists about whether the intrinsic stress affects transport of oxidant or the interface reaction; arguments for both views are presented. A combination of in-situ ellipsometry and contact angle measurements performed on a Si surface which is immersed in various liquid media has been successfully used to determine the role of HF in Si cleaning process. A fluorocarbon film was found to replace the removed SiO2, and the fluorocarbon renders the Si surface hydrophobic and amenable to the growth of a high quality SiO2 film for device applications. GRA

N88-20378# Defence Research Establishment, Ottawa. (Ontario).

OBSERVATIONS ON ELECTROSTATIC EFFECTS IN A FILTER TEST SYSTEM

John R. Coleman Jun. 1987 36 p

(AD-A188797; DREO-TN-87-18) Avail: NTIS HC A03/MF A01 CSCL 11L

The filter test system FTS 400 was used to examine a variety of filter papers, using sodium chloride and dioctylphthalate as aerosols challenges. In nearly every case, minimum in penetration was observed at particle size in the vicinity of 0.02 micrometers. In the same region NaCl particles (but not DOP droplets) exhibited substantial in-line losses which could affect measured penetration results. Introduction of a radioactive neutralizer which removes most of the particle charge greatly reduced line losses. The effect of introducing the neutralizer on penetration was studied, using several types of filter paper. Conventional filter papers showed slight increase in penetration over the size range up to 0.3 micrometers. With electrets, which depend on electrical attraction for their effectiveness, introduction of a neutralizer increased penetration in the same range by several orders of magnitude. GRA

N88-20379# George Washington Univ., Washington, D.C. Dept. of Chemistry.

AN INTERPRETATION OF THE ETHYLENIC, CARBIDIC, AND GRAPHITE AUGER LINESHAPES OF CHEMISORBED CARBON SPECIES Interim Technical Report

F. L. Hutson and David E. Ramaker Dec. 1987 5 p

(Contract N00014-80-K-0852; Proj. RR0-1308)

(AD-A189092; TR-39) Avail: NTIS HC A02/MF A01 CSCL 07B

Recently, Koel reported the C KVV Auger lineshapes for Ethylene on nickel(100) at a temperature of 100 K and for the decomposition products at 250, 300, and 600 K. We present detailed interpretations of these lineshapes, as well as for other previously reported carbidic and graphitic lineshapes. The most significant results of this work can be summarized briefly as follows: (1) Although the lineshapes for the chemisorbed and comparable gas phase species are similar, they are composed of very different principal and satellite contributions; and (2) The Auger intensity arising from carbon hydrogen much higher two-hole binding energy than that from C-M (metal) bonds. Thus the amount of C-H and C-M bond character is seen to remain even at 600 K on the Ni(100) surface. GRA

N88-20380# Ballistic Research Labs., Aberdeen Proving Ground, Md.

A SIMPLIFIED COMPUTER CODE FOR REDUCTION TO BURNING RATES OF CLOSED BOMB PRESSURE-TIME DATA (MINICB)

William F. Oberle, Arpad A. Juhasz, and Teresa M. Griffie Aug. 1987 107 p

(AD-A189112; BRL-TR-2841) Avail: NTIS HC A06/MF A01 CSCL 07D

A closed bomb burning rate reduction code designed to operate on a microcomputer or programmable hand calculator is presented. To accommodate the needs of a minimal computational environment, simplifying assumptions were made in developing the theory and form functions. Typically, form function equations are valid only to the point of grain slivering. Evaluation of the program performed against synthetic data from a validated lumped parameter interior ballistics code indicates reasonable agreement with an overall mean error of 1.5 percent or less. The program also computes experimental impetus given the calculated value for co-volume. GRA

N88-20381# Princeton Univ., N. J. Dept. of Mechanical and Aerospace Engineering.

FUELS COMBUSTION RESEARCH Final Report, 1 Aug. 1986 - 31 Jul. 1987

Frederick L. Dryer, Irvin Glassman, and Forman A. Williams 8 Oct. 1987 16 p

(Grant AF-AFOSR-0240-86)

(AD-A189114; AFOSR-87-1894TR) Avail: NTIS HC A03/MF A01 CSCL 07C

The DOD equipment grant received by the Fuels Combustion Research Group has been used, in accord with the original intent of the award, to update an advance the analytic capabilities of the combustion laboratories. The newly purchased gas and liquid chromatographic instrumentation have become the center pieces of a DOD supported analytic facility that was recently shown to the Chairman of the Joint Chiefs of Staff, Admiral William J. Crowe, Jr. as an example of DOD supported research in the School of

Engineering. The chemical analysis instrumentation in the facility as well as the boron particle sizing and visualizing devices that have also been purchased are described briefly in this final report. Photographs of the installed equipment are used to facilitate the description of the various pieces of instrumentation. GRA

N88-20382# Cornell Univ., Ithaca, N.Y.
COMBUSTION THEORY AND RELATED QUESTIONS Final Report, 1 Dec. 1984 - 31 Aug. 1987
J. D. Buckmaster Oct. 1987 9 p
(Contract DAAG29-85-K-0022)
(AD-A189160; ARO-21306.14-MA) Avail: NTIS HC A02/MF A01 CSCL 21B

Modern asymptotic methods have been applied to a wide range of problems in combustion science and mechanics. Details are contained in the 22 Technical Reports and 5 Ph.D. thesis listed. A list of participating scientists is also given. GRA

N88-20383# Air Force Astronautics Lab., Edwards AFB, Calif.
KINETIC MECHANISMS FOR IONIZATION AND AFTERBURNING SUPPRESSION Final Report, Jun. 1985 - May 1987
David P. Weaver and T. Singh Nov. 1987 31 p
(AD-A189219; AFAL-TR-87-049) Avail: NTIS HC A03/MF A01 CSCL 21B

Currently, very little data exists detailing the chemical mechanisms associated with the addition of suppressants such as potassium sulfate or potassium nitrate and their impact on the production of ions in either typical laboratory flames or solid propellant exhaust flows. On an empirical basis, potassium-bearing salts (potassium sulfate, potassium nitrate, potassium chloride, etc.) have been found to be among the most general and most effective suppressants. The addition of such alkali metal salts to the plume gases, However, has been observed to increase ion/electron concentrations, which in turn may significantly affect the radar cross section and reduce the motor's performance (e.g., by producing a lower specific impulse). This report summarizes the results of a recent analytical investigation into the influence of the addition of potassium salts on both the inhibition effects and the production electrons in a Hydrogen/Air flame. GRA

N88-20384# Dayton Univ., Ohio.
AN ELECTROCHEMICAL AND SPECTROSCOPIC STUDY OF ELECTRODE SYSTEMS Final Report, May 1986 - Jan. 1987
R. G. Keil and Shyama P. Sinha Sep. 1987 54 p
(Contract F33615-86-C-2620)
(AD-A189274; AFWAL-TR-87-2047) Avail: NTIS HC A04/MF A01 CSCL 07D

This final report concerns research in the area of electrochemical and spectroscopic studies on electrode and electrolyte systems for use within nonaqueous battery systems from 1 May 1986 through 31 January, 1987. The research has as a unifying theme the use of electrochemical and spectroscopic methods in the pursuit of an understanding of the chemical processes which occur at the electrodes as well as within the solution phase. The work is divided into two distinct phases: (1) the study of imidazolium melts, and (2) the electrochemical reversibility of lithium. GRA

N88-20385# Battelle Columbus Labs., Research Triangle Park, N.C.
DETERMINATION OF THE PARTITION COEFFICIENTS OF ORGANOPHOSPHORUS COMPOUNDS USING HIGH-PERFORMANCE LIQUID CHROMATOGRAPHY Contractor Report, Mar. - Sep. 1985
S. E. Krikorian, Trevor A. Chorn, James W. King, and Michael W. Ellzy Dec. 1987 21 p Prepared in cooperation with Maryland Univ., Baltimore
(Contracts DAAG29-81-D-0100; DA Proj. 1L1-61101-A-71-A)
(AD-A189276; CRDEC-CR-88015) Avail: NTIS HC A02/MF A01 CSCL 07C

Octanol/water partition coefficients (log P) for a series of dialkyl alkylphosphonates, dialkyl alkylphosphonothionates, and an alkyl alkylphosphinate have been estimated using reversed-phase high-performance liquid chromatography. The test compounds proved to be readily amenable to the chromatographic procedures employed, although the more lipophilic compounds appeared to be more tolerant to variations in the chromatographic conditions and methods of data handling than were the less lipophilic compounds with regard to the precision and accuracy of the log P values obtained from the retention data. The methodology was validated by carrying out shake-flask experiments with two of the test samples. The rank order of log P values obtained was reasonably predictable, based on the sizes of the alkyl substituents present. The enhancement of lipophilic character attributable to replacement of oxygen by sulfur in the phosphorus oxygen group is also evident from the results. The data for the phosphonates permit the calculation of a value for the hydrophobic fragmental constant for the OPO2 group (f=2.79). GRA

N88-20386# Pittsburgh Univ., Pa. Dept. of Chemistry.
MEASUREMENT OF RATE CONSTANTS OF ELEMENTARY GAS REACTIONS OF IMPORTANCE TO UPPER ATMOSPHERE AND COMBUSTION SYSTEMS Final Report, 1 Mar. 1985 - 31 Aug. 1987
Michael F. Golde 31 Oct. 1987 22 p
(Grant AF-AFOSR-0166-85)
(AD-A189432; AFOSR-87-1725TR) Avail: NTIS HC A03/MF A01 CSCL 07D

Important elementary gas phase reactions have been studied by the discharge flow technique, utilizing laser induced fluorescence to detect radical species and mass spectrometry to monitor stable reaction products. Both rate constants and reaction products have been determined. The H-abstraction reactions of F atoms and of OH radicals with CH3OH favor different reaction channels: the former yields predominantly methoxy radicals (CH3O), whereas the latter strongly favors hydroxymethyl (CH2OH). The reaction of OH with CH3OH shows a large kinetic isotope effect for this channel. The kinetics of CH3O with NO resemble those of CH3O with NO2 studied previously, namely a weak positive pressure dependence and a strong inverse temperature dependence of the second order rate coefficient. Analysis of the rate data together with direct detection of reaction products have established that atom transfer to yield HNO + CH2O is the major channel at low pressures. A brief study of the reaction of NH2 with NO has shown that OH production is a minor channel, with a branching fraction of less than or equal to 0.04. GRA

N88-20387# State Univ. of New York, Buffalo. Dept. of Chemistry.
PHOTOCHEMISTRY AT STRUCTURED SURFACES: A CLASSICAL ELECTROMAGNETIC APPROACH
Daniel A. Jelski, P. T. Leung, and Thomas F. George Feb. 1988 68 p
(Contracts N00014-86-K-0043; F49620-86-C-0009; Grant NSF CHE-86-20274)
(AD-A189519; UBUFFALO/DC/88/TR-65) Avail: NTIS HC A04/MF A01 CSCL 07E

This review article discusses several important aspects of photochemistry at structured metallic surfaces. The electromagnetic field above the surface is calculated using the Rayleigh expansion. Conditions under which this expansion is valid and simplifying approximations which make it easier to use are discussed in detail. This formalism is then applied to three different but related phenomena. First, the photodissociation rate of a molecule above a surface is calculated for laser frequencies at or near the surface plasmon resonance. It is found that there is an optimal molecule-surface distance for photodissociation. Then the absorption lineshape of a molecule is considered, where both Fano and Lorentzian lineshapes are found to be distorted as the molecule approaches the surface. Finally, laser-induced periodic deposition is discussed, and a model is developed to describe the growth rate of a cadmium grating. GRA

N88-20388# University of Southern Illinois, Carbondale. Dept. of Mathematics.
MATERIAL INSTABILITIES IN SOLIDS Final Technical Report, 15 Jul. 1986 - 14 Jul. 1987
Scott J. Spector 12 Jan. 1988 13 p
(Grant AF-AFOSR-0184-86)
(AD-A189525; AFOSR-88-0125TR) Avail: NTIS HC A03/MF A01 CSCL 07F

The principal investigator considered a number of mathematical problems that may help explain material failures in polymers and ductile metals. In particular, useful results were obtained concerning the initiation and dynamic growth of holes, the static instability and surface cracking of a single hole and the linearized stability of a free surface in an elastic material. GRA

N88-20389# Argonne National Lab., Ill.
THE COORDINATION CLUSTER THEORY FOR METALLIC SOLUTIONS
Milton Blander and Marie Louise Saboungi Dec. 1987 7 p Presented at the NATO Advanced Study Institute on Alloy Phase Stability, Crete, Greece, 14 Jun. 1987
(Contract W-31-109-eng-38)
(DE88-005934; CONF-8706103-5) Avail: NTIS HC A02/MF A01

The coordination cluster theory (CCT) is a statistical mechanical theory for the thermodynamic properties of a dilute solute in a binary or higher order solvent. Although the CCT has been applied to liquids, it can be modified for solids. The theory permits one to describe the thermodynamic properties of a solute in a binary solvent in terms of the solute properties in the pure solvent components, the properties of the binary mixture and one unknown parameter. In principle, the properties of solutes in multicomponent solvents can be calculated from those in the subsidiary binary solvents. Modern quantum mechanical methods for the calculation of the energetics of metal solutions could be used to place the theory on a firm fundamental basis by testing the approximations in the theory and determining the unknown parameters. DOE

N88-20390# Sandia National Labs., Albuquerque, N. Mex.
NOVEL CATALYSTS FOR METHANE ACTIVATION
F. V. Stohl, J. A. Shelnutt, and B. Granoff 1987 19 p Presented at the Indirect Liquefaction Contractors' Conference, Pittsburgh, Pa., 7 Dec. 1987
(Contract DE-AC04-76DP-00789)
(DE88-003637; SAND-87-2836C; CONF-871249-1) Avail: NTIS HC A03/MF A01

Several naturally occurring enzymes, such as cytochrome P-450 and methane monooxygenase, catalyze the oxidation of alkanes to alcohols at low temperatures and pressures. We are attempting to develop catalysts that mimic the activity of these enzymes. Computer-aided design studies on unique carboranyl porphyrins have shown that they can have a pocket analogous to those of the enzymes. This work uses molecular-energy dynamics calculations to evaluate the methane interactions with the synthetic compounds. Activity tests have been devised for oxidation of cyclohexane, hexane and butane with iodosylbenzene as the oxidant, methylene chloride as the solvent, and Fe, Mn, Ni, and Rh tetraphenyl porphyrins and Fe and Mn tetra(pentafluorophenyl) porphyrins as catalysts. Results showed that Fe and Mn were the most active metals. With the Fe tetra(pentafluorophenyl) porphyrin, cyclohexanol, hexanol and butanol yields (based on oxidant) were 80, 64 and 40 percent, respectively. Additional tests are being developed for oxidation of ethane and methane. DOE

N88-20391# Colorado State Univ., Fort Collins. Dept. of Physics.
PROPERTIES OF MOLECULAR SOLIDS AND FLUIDS AT HIGH PRESSURE AND TEMPERATURE Annual Report
R. D. Etters 1987 39 p
(Contract DE-FG02-86ER-45238)
(DE88-004195; DOE/ER-45238/T2) Avail: NTIS HC A03/MF A01

Equilibrium structures, orientations, and magnetic order, lattice librational and vibrational mode frequencies, intramolecular vibron mode frequencies, sound velocities, equations of state, compressibilities, thermal expansion coefficients, and phase transitions in molecular solids over a wide range of temperatures and pressures were determined. Except for structures and orientations, which are not static, similar properties were calculated in the fluid, in addition to virial coefficients, viscosities, specific heats, and dynamic correlations of positions, orientation, and local magnetic order. Techniques used include several strategies to optimize multi-dimensional functions as a means to determine structures and orientations, as does constant pressure and constant volume. The Monte Carlo method also yields thermodynamic quantities and is a powerful means for characterizing phase transitions. Lattice dynamics, mean field methods, and classical perturbation theory are some of the analytic tools used to determine dynamical features. Systems studied include H2, N2, O2, CO, CO2, F2, I2, N2O, Cl2, Br2, HCL, HBr, and Hi. DOE

N88-20392# Brigham Young Univ., Provo, Utah. Dept. of Chemistry.
SUPERCRITICAL FLUID CHROMATOGRAPHY/SUPERSONIC JET SPECTROSCOPY Progress Report, 1 Sep. 1987 - 30 Nov. 1987
S. R. Goates and M. L. Lee 1987 8 p
(Contract DE-FG22-86PC-90534)
(DE88-004438; DOE/PC-90534/8) Avail: NTIS HC A02/MF A01

The thermal gradient of the heated nozzle interface was measured with the use of a thermocouple probe and this proved useful in characterizing configurations of the sheath nozzles. Further testing of the back-sealed pinhole restrictor resulted in a rejection of this configuration because of alignment difficulties with the pinhole. The adaptation of sheath flow nozzles for supersonic jet expansions with supercritical fluids is discussed along with the porous frit restrictor and electrical feedthroughs. Pulsed nozzle designs have also been studied and will be the object of further research. DOE

N88-20393# Yale Univ., New Haven, Conn. Dept. of Applied Physics.
MODEL CATALYST STUDIES OF SMSI (STRONG METAL/SUPPORT INTERACTIONS) AND THE ROLE OF D-ELECTRONS IN CHEMISORPTION AND CATALYSIS Final Report, 15 Jan. 1982 - 30 Sep. 1987
Victor E. Henrich Nov. 1987 14 p
(Contract DE-AC02-81ER-10830)
(DE88-004518; DOE/ER-10830/6) Avail: NTIS HC A03/MF A01

The origin of strong metal/support interactions (SMSI) in the Rh/TiO2 system through studies of model catalysts prepared on single-crystal supports has been investigated. The following areas were studied: processing and characterization of model Rh/TiO2 catalysts, theoretical basis for the charge transfer model of a Pt atom supported on TiO2, morphology of monolayer amounts of Rh and TiO2, and electronic interactions in the Rh/TiO2 system. Publications resulting from this research are appended. DOE

N88-20394# Pacific Northwest Labs., Richland, Wash.
DEVELOPMENT AND EVALUATION OF SUPERCRITICAL FLUID CHROMATOGRAPHY-MASS SPECTROMETRY Report, 1 Feb. 1984 - 1 Feb. 1988
E. K. Chess, R. D. Smith, and H. T. Kalinoski Oct. 1987 9 p Presented at the Advanced Research and Technology Development Direct Utilization, Morgantown, W. Va., 13 Oct. 1987
(Contract DE-AC06-76RL-01830)
(DE88-005122; PNL-SA-15272; CONF-871041-6) Avail: NTIS HC A02/MF A01

During FY87, we initiated research in the evaluation of SFC/MS with polar fluids and the quantification of polar materials by SFC/MS. We have investigated the performance of the supercritical fluid chromatograph-mass spectrometer interface and have made several modifications to the probe and ion source to improve

performance. We have continued to develop methodologies for fabricating capillary columns with bonded, crosslinked stationary phases that are suitable for use with polar fluids. Emphasis has also been placed on investigating the properties and range of utilities of mixed fluid systems in which a small percentage of a polar modifier has been added to a relatively nonpolar supercritical fluid. In addition, the SFC/MS methodologies developed in the past years have been applied to the characterization of fossil fuel materials. The use of polar supercritical fluids for the analysis of polar and high-molecular-weight fuel materials was actively pursued this year. Ammonia (NH3, T(sub c) = 133 C, P(sub c) = 144 bar) was found to solvate materials of higher molecular weight than were soluble in either pure hydrocarbon fluids (pentane or smaller alkanes) or alcohol-modified hydrocarbon fluids (e.g., pentane-ethanol). However, the use of ammonia was limited by the high reactivity of the fluid with the polymeric materials used in ferrules for unions and as coatings on fused silica capillary columns. In an effort to avoid the reactivity of supercritical ammonia, but still maintain a polar, highly solvating fluid, methylamine (CH3NH2) was chosen as a substitute. The critical temperature of methylamine is only slightly higher than that of ammonia (T(sub c) = 157 C); the critical pressure (P(sub c) = 75 bar) is lower. DOE

N88-20395# Sandia National Labs., Albuquerque, N. Mex.
UNCERTAINTIES IN HYDROGEN COMBUSTION
D. W. Stamps, C. C. Wong, and L. S. Nelson Oct. 1987 26 p Presented at the 15th Water Reactor Safety Information Meeting, Gaithersburg, Md., 26 Oct. 1987
(Contract DE-AC04-76DP-00789)
(DE88-005354; SAND-87-2277C; CONF-8710111-28) Avail: NTIS HC A03/MF A01

Three important areas of hydrogen combustion with uncertainties are identified: high-temperature combustion, flame acceleration and deflagration-to-detonation transition, and aerosol resuspension during hydrogen combustion. The uncertainties associated with high-temperature combustion may affect at least three different accident scenarios: the in-cavity oxidation of combustible gases produced by core-concrete interactions, the direct containment heating hydrogen problem, and the possibility of local detonations. How these uncertainties may affect the sequence of various accident scenarios is discussed and recommendations are made to reduce these uncertainties. DOE

N88-20396# Brown Univ., Providence, R. I. Materials Research Lab.
MATERIALS RESEARCH LABORATORY AT BROWN UNIVERSITY Annual Technical Report, 1 Jul. 1985 - 30 Apr. 1987
30 Apr. 1987 151 p
(Grant NSF DMR-83-16893)
(AD-A188006) Avail: NTIS HC A08/MF A01 CSCL 07D

Papers compiled have to do with the following topics: Plasticity and Fracture; Inorganic Glasses; and Solid Surfaces, are presented. GRA

N88-20397*# Ohio State Univ., Columbus. ElectroScience Lab.
MATERIAL PARAMETER MEASUREMENTS AT HIGH TEMPERATURES
A. Dominek, A. Park, and L. Peters, Jr. Mar. 1988 24 p
(Grant NAG3-784)
(NASA-CR-182707; NAS 1.26:182707; OS-TR-719300-2) Avail: NTIS HC A03/MF A01 CSCL 07D

Alternate fixtures of techniques for the measurement of the constitutive material parameters at elevated temperatures are presented. The technique utilizes scattered field data from material coated cylinders between parallel plates or material coated hemispheres over a finite size groundplane. The data acquisition is centered around the HP 8510B Network Analyzer. The parameters are then found from a numerical search algorithm using the Newton-Ralphson technique with the measured and calculated fields from these canonical scatters. Numerical and experimental results are shown. Author

N88-20398*# National Aeronautics and Space Administration, Washington, D.C.
MEASUREMENT OF DETONATION TEMPERATURE OF HYDROGEN-OXYGEN MIXTURE BY CARS (COHERENT ANTI-STOKES RAMAN SPECTROSCOPY)
Atsumu Tezaki, Hiroyuki Matsui, and Yoshiro Kawamura Apr. 1988 14 p Transl. into ENGLISH from Koatsu Gasu (Japan), v. 22, no. 3, 1985 p 106-111 Transl. by SCITRAN, Inc., Santa Barbara, Calif. Original document prepared by Tokyo Univ., Japan
(Contract NASw-4307)
(NASA-TT-20227; NAS 1.77:20227) Avail: NTIS HC A03/MF A01 CSCL 21B

It was confirmed that CARS is very useful as a temperature measurement method of detonation. By revising the detecting system so that a lot of information can be handled simultaneously like an optical multi-channel analyzer, it is possible to obtain information concerning the detailed three dimensional structure of detonation which has never been obtained. Author

N88-20399# Materials Research Labs., Melbourne (Australia).
ANOMALOUS SHOCK SENSITIVITY/DENSITY RELATIONSHIP FOR RDX-POLYETHYLENE WAX AND RELATED FORMULATIONS FROM MRL SMALL SCALE GAP TEST (SSGT) MEASUREMENTS
Robert J. Spear, Victor Nanut, Ian J. Dagley, and William S. Wilson Jan. 1988 29 p
(MRL-R-1099; AR-005-197) Avail: NTIS HC A03/MF A01

Shock sensitivity as measured by the Materials Research Laboratory Small Scale Gap Test (MRL SSGT) shows a consisient trend to lower values as percent TMD decreases for pressed RDX formulations and some pure explosives such as tetryl. Decrease in particle size, disruption of surface coating, critical diameter and run distance effects were all considered but found not to be the major cause. Comparison of MRL SSGT data for a series of production booster explosives with corresponding NOL SSGT data at 90 percent TMD suggested that the ability to undergo buildup is significantly more important for the MRL SSGT. Reasons for this difference are discussed, and limitations for assessment of data using the MRL SSGT are outlined. Author

N88-20400*# National Aeronautics and Space Administration, Washington, D.C.
FLAME RETARDANTS
J. Troitzsch Apr. 1988 10 p Transl. into ENGLISH from Kunststoffe (Fed. Republic of Germany), v. 77, no. 10, 1987 p 1078-1080 Transl. by Scientific Translation Service, Santa Barbara, Calif.
(Contract NASw-4307)
(NASA-TT-20250; NAS 1.77:20250) Avail: NTIS HC A02/MF A01 CSCL 21B

The use of flame retardants in plastics has grown only slightly in recent years and will probably grow slowly in the future. The reasons for this are slow economic growth and the absence of fundamentally new requirements for future fire prevention. The trends are toward the increasing use of easily handled, dust-free and well-dispersed flame retardant compounds and master batches; there are no spectacular new developments. In the future, questions of smoke evolution, toxicity and corrosiveness of combustion gases will become increasingly important, especially due to new regulations and rising requirements for environmental protection. Author

N88-20401*# National Aeronautics and Space Administration, Washington, D.C.
POTASSIUM CUPRATE (3)
Kurt Wahl and Wilhelm Klemm May 1988 13 p Transl. into ENGLISH from Zeitschrift fuer Anorganische und Allgemeine Chemie (Fed. Republic of Germany), v. 270, 1952 p 69-75 Transl. by Scientific Translation Service, Santa Barbara, Calif.
(Contract NASw-4307)
(NASA-TT-20246; NAS 1.77:20246) Avail: NTIS HC A03/MF A01 CSCL 07D

The reaction of KO2 and CuO in an O2 atmosphere at 400 to 450 C results in KCuO, which is a steel-blue and nonmagnetic compound. This substance exhibits a characteristic X-ray diagram; it decomposes in dilute acids to form O2 and Cu(II) salts. It decomposes thermally above 500 C. Author

N88-20402*# National Aeronautics and Space Administration, Washington, D.C.
QUANTITATIVE DETERMINATION OF A HYDROGEN IMPURITY IN A SODIUM COOLANT BY HYDRIDE THERMAL DISSOCIATION
M. N. Ivanovskiy, G. D. Pavlova, B. A. Shmatko, A. V. Milovidova, E. Ye. Konovalov, M. N. Arnoldov, and A. D. Pleshivtsev May 1988 12 p Transl. into ENGLISH from Tomnaya Energiya (USSR), v. 24, no. 3, 1968 p 227-230 Transl. by Scientific Translation Service, Santa Barbara, Calif.
(Contract NASw-4307)
(NASA-TT-20239; NAS 1.77:20239) Avail: NTIS HC A03/MF A01 CSCL 07D

A molten sodium coolant containing hydrogen was heated in a vacuum at 450 C, and the gases generated pumped through a liquid nitrogen trap, and the H2 was then oxidized on a copper oxide substrate heated to 400 C. The accuracy of the method is 1.5 percent and the sensitivity is 1x10 to the -5 wt percent hydrogen. Author

N88-20403*# National Aeronautics and Space Administration, Washington, D.C.
DECOMPOSITION OF HYPOCHLORITE IN THE PRESENCE OF COPPER IN A HOMOGENEOUS MEDIUM
A. Yu. Prokopchik and Yu. P. Butkyavichyus May 1988 16 p Transl. into ENGLISH from Trudy Akademii Nauk Litovskoy SSR, Seriya B (USSR), v. 3, no. 38, 1964 p 31-40 Transl. by Scientific Translation Service, Santa Barbara, Calif.
(Contract NASw-4307)
(NASA-TT-20199; NAS 1.77:20199) Avail: NTIS HC A03/MF A01 CSCL 07D

Spectrophotometric, spectrographic and chemical methods have demonstrated that yellow staining of a hypochlorite alkaline solution in the presence of sodium cuproate was determined by the formation of an unstable intermediate compound of trivalent copper of the type NaCu(OH)4 sorium cupriate. Author

26 METALLIC MATERIALS

Includes physical, chemical, and mechanical properties of metals, e.g., corrosion; and metallurgy.

N88-20404# Gosudarstvennyi Komitet po Ispolzovaniyu Atomnoi Energii, Obninsk (USSR). Fiziko-Ehnergeticheskij Inst.
VIBRATION SPECTRA OF OXYGEN AND VANADIUM ATOMS IN VANADIUM-OXYGEN DISORDERED INTERSTITIAL ALLOYS
S. A. Danilkin and T. V. Alenicheva 1986 12 p In RUSSIAN
(DE87-703166; FEI-1782) Avail: NTIS (US Sales Only) HC A03/MF A01

The results of calculations of weighed frequency distributions (WFD) of oxygen and vanadium atoms in the disordered solid vanadium-oxygen solution containing 17 percent of oxygen are presented in the paper. The oxygen atoms in the alloy are shown to vibrate mainly with optical frequencies, the spectrum of which differs from the proper part of the spectrum of the alloy frequencies. The acoustic region in the oxygen WFD is sufficiently deformed in comparison with the spectrum of the alloy frequencies and its weight relatively to the optical part of the oxygen WFD spectrum is 1/20 to 1/40. DOE

N88-20405# California Univ., Berkeley. Dept. of Chemistry.
TRANSITION METAL CLUSTER CHEMISTRY Final Report, 1 Aug. 1985 - 31 Jul. 1987
Peter B. Armentrout 21 Oct. 1987 6 p
(Contract DAAG29-85-K-0181)
(AD-A188731; ARO-22736.4-CH) Avail: NTIS HC A02/MF A01 CSCL 07B

Reactions of transition metal cluster ions are examined using guided ion beam techniques. These techniques allow ionic clusters of variable size and composition to be isolated. Measurement of reaction cross sections and branching ratios characterize the interactions of the clusters with a variety of neutral gases. By examining the variation of these quantities with the kinetic energy of the cluster ions, extensive thermochemical data for both ionic and neutral cluster species can be determined. Prototypical data for Mn(2)+ and Co(2)+ have been obtained. In addition, a new source of cold metal cluster ions (both bare and ligated) has been developed and demonstrated. GRA

N88-20406# Army Lab. Command, Watertown, Mass. Material Technology Lab.
HYDROGEN INDUCED CRACKS IN ARMOR STEEL WELDMENTS FABRICATED WITH AUSTENITIC FILLER ALLOYS Final Report
William S. Ricci Sep. 1987 16 p
(AD-A188733; MTL-TR-87-50) Avail: NTIS HC A03/MF A01 CSCL 19D

Hydrogen induced cracks have been identified in the weld metal of cast armor steel weldments fabricated with austenitic electrodes. Cracks propagated through a well defined band of materials located between the fusion boundary and the composite region of the weld metal. Martensite band formation was found to result from the combined effects of vigorous hydrodynamic forces, especially in large molten weld pools, and the interdiffusion of alloying elements in that system formed between the base metal and the weld metal. Methods of controlling this form of cracking include limiting base metal dilution, minimizing the concentration of available hydrogen in the welding arc atmosphere, or the selection of more suitable ferritic filler alloys. GRA

N88-20407# Army Armament Research, Development and Engineering Center, Watervliet, N.Y. Weapons Lab.
HYDROGEN EMBRITTLEMENT OF GUN STEEL Final Report
Gerald L. Spencer Nov. 1987 83 p
(AD-A188972; ARCCB-TR-87030) Avail: NTIS HC A05/MF A01 CSCL 11F

The objectives of this engineering project were to determine the critical concentration of hydrogen at which gun steel is embrittled, and to evaluate the effects of some acid solutions on gun steel to determine safe exposure parameters. GRA

N88-20408# Naval Postgraduate School, Monterey, Calif.
DEVELOPMENT OF A CONSTITUTIVE EQUATION FOR HSLA (HIGH-STRENGTH LOW-ALLOY)-100 AT CRYOGENIC TEMPERATURES M.S. Thesis
David M. Bissot Dec. 1987 89 p
(AD-A189243) Avail: NTIS HC A05/MF A01 CSCL 11F

HSLA-100 is a 100ksi nominal yield strength steel being developed by the Navy for Naval shipbuilding applications. To assist in ductile and brittle failure modelling of this low carbon steel, tensile tests were conducted at temperatures ranging from 37 C(99 F)to liquid nitrogen(-196 C/-321 F)to determine a constituitive equation for this alloy at low temperature. The Hollomon Power Equation and the Voce Equation are used to describe the true stress/true strain behavior to failure of individual tests. The Bridgman correction is applied to the true stress to compensate for the triaxial stress state that exists at and beyond the necking (maximum load) point. The power and Voce equations are then fit to the Bridgman corrected true stress versus true plastic strain. Relative comparisons are made between the two equations resulting in the conclusion that the Voce equation describes the stress-strain characteristics of this alloy better than the Holloman equation. The temperature dependence of the material constants So, Si, and A, in the Voce equation were determined producing a constituitive equation for the tensile behavior of HSLA-100 as a function of strain and temperature, at a strain rate of about .001 in/in sec. GRA

N88-20409# Kentucky Univ., Lexington. Dept. of Materials Engineering.
A DIRECT CORRELATION OF STRENGTH WITH IMPACT VELOCITY Technical Paper, Sep. - Nov. 1987
Peter P. Gillis and S. E. Jones Jan. 1988 15 p Prepared in cooperation with Alabama Univ., Tuscaloosa.
(Contract F08635-87-C-0125)
(AD-A189251; AFATL-TR-87-74) Avail: NTIS HC A03/MF A01 CSCL 11F

This paper presents a method for analyzing the results of a Taylor impact test. From post mortem measurements of final specimen length and final undeformed specimen length the dynamic material strength on impact is correlated with impact velocity. This correlation provides a rate-dependent constitutive law that is potentially useful in situations such as rod penetration. GRA

N88-20410# Battelle Columbus Labs., Research Triangle Park, N.C.
TEXTURE PROFILE IN THERMOMECHANICALLY PROCESSED 2-INCH-THICK 5 NI-STEEL ARMOR PLATE Final Report, 8 Jul. 1945 - 13 Sep. 1985
Hsun Hu Nov. 1987 28 p Prepared in cooperation with Pittsburgh Univ., Pa.
(Contract DAAG29-81-D-0100)
(AD-A189275; MTL-TR-87-59) Avail: NTIS HC A03/MF A01 CSCL 11F

The textural variation in the thickness direction of a 2-inch-thick 5 nickel steel plate, produced by controlled hot-rolling to 90 percent reduction, immediately water-quenched, then tempered, has been studied. Besides the surface texture, which differs from the interior texture at midthickness only in intensity and in rotational displacement, there is a drastic change in the nature of the texture at the intermediate sections. An analysis of the deformation-zone geometry of the rolling passes indicates that the present observations are consistent with those reported for cold-drawn or cold-rolled strips. The usefulness of this particular texture for textured armor research and future armor development is discussed. GRA

N88-20411# Purdue Univ., West Lafayette, Ind. Dept. of Chemistry.
CHARACTERIZATION OF REDOX STATES OF NICKEL HYDROXIDE FILM ELECTRODES BY IN-SITU RAMAN SPECTROSCOPY Technical Report, 1 Oct. 1986 - 30 Sep. 1987
J. Desilvestro, D. A. Corrigan, and M. J. Weaver 25 Sep. 1987 37 p
(Contract N00014-85-K-0556)
(AD-A189288; TR-65) Avail: NTIS HC A03/MF A01 CSCL 07D

Thin films of nickel hydroxide deposited on gold electrodes have been characterized in detail by in-situ surface Raman spectroscopy in conjunction with electrochemical techniques. Raman spectra were obtained for film thicknesses varying from less than one equivalent monolayer to several hundred monolayers, as determined from the faradaic charge for the cyclic voltammetric oxidation of Ni(OH)2. For the thinnest films, Raman bands at 455/cm and at 480 and 560/cm were obtained for the reduced and oxidized films, respectively, using 647.1 nm excitation at roughened gold. These signals, identified with Ni-OH and Ni-O vibrations from deuterium isotope data, were diagnosed as arising from surface-enhanced Raman scattering (SERS) in view of their absence for the reduced film when using the latter conditions for thicker oxidized films, which were consistent with resonance Raman scattering (RRS). GRA

N88-20412# Harvard Univ., Cambridge, Mass. Div. of Applied Sciences.
INTERACTION OF PARTICULATE AND TRANSFORMATION TOUGHENING
John C. Amazigo and Bernard Budiansky Dec. 1987 25 p
(Contract N00014-86-K-0753; DARPA Order 6065)
(AD-A189321; MECH-112) Avail: NTIS HC A03/MF A01 CSCL 07D

A theoretical study is made of the interaction between the fracture toughening effects of crack-bridging ductile particles and phase-transforming particles embedded in a brittle matrix. It is found that in certain parametric ranges the interaction can be synergistic, with an increase in toughness produced that is greater than the sum of the increases that would be provided separately by the two types of reinforcement. Quantitative results are provided for the toughening in terms of the individual toughening effects and coupling parameters that depend on the properties of the uncoupled systems. GRA

N88-20413# Johns Hopkins Univ., Baltimore, Md.
A FUNDAMENTAL UNDERSTANDING OF THE EFFECT OF ALLOYING ELEMENTS ON THE CORROSION RESISTANCE OF RAPIDLY SOLIDIFIED Mg ALLOYS Annual Report No. 2, 1 Nov. 1986 - 31 Oct. 1987
J. Kruger, G. G. Long, D. K. Tanaka, A. Joshi, and G. L. Makar 16 Nov. 1987 74 p
(Contract F49620-86-C-0014)
(AD-A189385; AFOSR-87-1892TR) Avail: NTIS HC A04/MF A01 CSCL 11F

During the second year of this project progress was made in the following areas concerned with the effect of alloying elements on the corrosion resistance of RSP Mg alloys: (1) The development of the surface reflection X-ray spectroscopic technique (EXAFS) to carry out structural studies on the films on Mg alloys that control corrosion was completed and applied in measurements at the oxygen K-edge of surface films on high purity Mg and AZ61 Mg alloys. The existence of magnesium hydroxide on these surfaces was found; (2) Electrochemical studies of the effect of Al, Zn, Ce, Nd, Y, Mn, Li, and Ca in melt-spun Mg alloy ribbons on corrosion behavior were carried out. The corrosion rate decreased with increased percentage of Al and small additions of Zn. It was found that rapid solidification improves the resistance of the alloy studied (AZ61) to localized Cl(-) attack; (3) Surface analytical studies found that only Li and Ca in the RSP Mg alloys have a tendency to be enriched in the films on these alloys. Hydroxides and carbonates were also found in the surface films along with oxides. GRA

N88-20414# Georgia Inst. of Tech., Atlanta. School of Materials Engineering.
THE EFFECT OF MICROSTRUCTURE ON THE FATIGUE CRACK GROWTH RESISTANCE OF NICKEL BASE SUPERALLOYS Final Technical Report, 1 May 1984 - 30 Sep. 1987
Stephen D. Antolovich Dec. 1987 102 p
(Grant AF-AFOSR-0101-84)
(AD-A189526; AFOSR-88-0176TR) Avail: NTIS HC A06/MF A01 CSCL 11F

The objective of this study is to determine the effect of microstructural properties on the fatigue crack propagation (FCP) response of nickel base superalloys. This report describes the results of four experimental alloys containing various amounts of aluminum, titanium, and molybdenum. Chemistry, precipitate size, and grain size were varied to produce systematically controlled microstructures. The four alloys were characterized for chemical composition, microstructure, tensile properties, low cycle fatigue (LCF), and FCP resistance. The FCP tests were performed under constant load (increasing K) conditions in air at a stress ratio (R) of 0.1 and 0.8. Closure loads were measured with a clip gage, back-face strain gage, and a laser extensometer. GRA

N88-20415# Air Force Inst. of Tech., Wright-Patterson AFB, Ohio. School of Engineering.
THRESHOLD FATIGUE CRACK GROWTH IN Ti-6Al-2Sn-4Zr-6Mo M.S. Thesis
Dale A. Nagy Dec. 1987 78 p
(AD-A189560; AFIT/GAE/AA/87D-13) Avail: NTIS HC A05/MF A01 CSCL 11F

The purpose of this study was to examine the effects of different loading histories, closure loads, and stress ratios on the

near-threshold crack growth rate of a titanium-aluminum alloy. Two different test types were conducted on four separate specimens to determine the threshold stress intensity of the material. The first test type maintained a constant maximum stress intensity factor, K(max) on a specimen with a growing crack. As the crack grew, the minimum stress intensity factor was increased until the crack growth rate reached the threshold level. The second test type also maintained a constant K(max). For this test a block of cycles was applied to the specimen and if the crack growth rate for the block of cycles was below the threshold level then K(min) was decreased by a small amount and another block of cycles was applied. This process was continued until the crack growth rate reached the threshold level. Once the threshold stress intensity was determined the cracks were grown under constant maximum load and stress ratio (R) to measure the threshold crack growth rate. Both test types were conducted over a wide range of stress ratios to investigate the effects of varying closure loads. GRA

N88-20416# Michigan Technological Univ., Houghton. Dept. of Metallurgical Engineering.
PROCESSING, STRUCTURE AND PROPERTIES OF HEAVILY DEFORMED IN SITU COMPOSITES Final Report, Aug. 1984 - 1 Oct. 1987
T. H. Courtney and J. K. Lee 5 Dec. 1987 25 p
(Contract DAAG29-84-K-0089)
(AD-A189611; ARO-21450.6-MS) Avail: NTIS HC A03/MF A01 CSCL 11F

This report describes the results of work conducted on the properties, structure, processing and thermal stability of heavily cold worked two phase metallic alloys. These are also known as heavily deformed in situ composites (HDISC). The primary reason for studying these kinds of materials is that two phase materials work harden more rapidly than do single phase ones. In fact, when subjected to true deformation strains greater than about three, strengths of two phase combinations usually significantly exceed those expected by volumetrically averaging the strengths developed in the single phase constituents subjected to the same strains. At true deformation strains on the order of ten, strengths approaching the theoretical ones are obtained in some two phase metal combinations. This enhanced strain hardening has been observed in a number of two phase metal alloys. Examples include silver-copper, silver-iron, copper-iron, copper-niobium, silver-nickel, copper-chromium, and nickel-tungsten. There is another reason for studying these materials. In particular, their fabrication takes place by relatively straightforward means, and thus they offer the potential for developing relatively inexpensive metal matrix composites. GRA

N88-20417*# National Aeronautics and Space Administration. Lewis Research Center, Cleveland, Ohio.
INTERFACIAL ADHESION: THEORY AND EXPERIMENT
John Ferrante, Guillermo H. Bozzolo, Clarence W. Finley (Pennsylvania State Univ., New Kensington.), and Amitava Banerjea 1988 32 p Presented at the Spring Meeting of the Materials Research Society, Reno, Nev., 5-9 Apr. 1988
(NASA-TM-100830; E-4019; NAS 1.15:100830) Avail: NTIS HC A03/MF A01 CSCL 11F

Adhesion, the binding of different materials at an interface, is of general interest to many branches of technology, e.g., microelectronics, tribology, manufacturing, construction, etc. However, there is a lack of fundamental understanding of such diverse interfaces. In addition, experimental techniques generally have practical objectives, such as the achievement of sufficient strength to sustain mechanical or thermal effects and/or have the proper electronic properties. In addition, the theoretical description of binding at interfaces is quite limited, and a proper data base for such theoretical analysis does not exist. This presentation will review both experimental and theoretical aspects of adhesion in nonpolymer materials. The objective will be to delineate the critical parameters needed, governing adhesion testing along with an outline of testing objectives. A distinction will be made between practical and fundamental objectives. Examples are given where interfacial bonding may govern experimental consideration. The present status of theory is presented along with recommendations for future progress and needs. Author

N88-20418# Lawrence Livermore National Lab., Calif.
USE OF THE LLNL 40 kV ELECTRIC GUN TO STUDY THE SHOCK RESPONSE OF 21-6-9 STAINLESS STEEL
J. A. Brusso, D. E. Mikkola, G. Bloom, R. S. Lee, and W. VonHolle 15 Jul. 1987 8 p Presented at the 5th Topical Conference of the American Physical Society on Shockwaves in Condensed Matter, Monterey, Calif., 20 Jul. 1987 Prepared in cooperation with Michigan Technological Univ., Houghton
(Contract W-7405-eng-48)
(DE87-014550; UCRL-96473; CONF-870753-72) Avail: NTIS HC A02

Exploding foil-flyer plate (electric gun) methods have been used to shock 21-6-9 stainless steel over a wide range of shock pulse amplitudes (20 to 53 GPa) and durations (10 to 70 ns). Dislocation generation and twinning have been studied in recovered specimens with the results providing support for the concept of finite rate plastic processes. DOE

N88-20419# Michigan Technological Univ., Houghton. Dept. of Metallurgical Engineering.
STRESS CORROSION CRACKING AND METAL-INDUCED EMBRITTLEMENT: COMPARATIVE STUDIES OF LOCAL CHEMISTRIES Progress Report, 16 Jan. 1987 - 15 Jan. 1988
L. A. Heldt and C. L. White Jan. 1988 17 p
(Contract DE-FG02-86ER-45255)
(DE88-003235; DOE/ER-45255/2) Avail: NTIS HC A03/MF A01

Brass crystals 6 mm diameter and 12 cm long were grown and cylindrical tensile specimens were prepared having reduced gauge sections. These samples were tested in distilled water at constant strain rate and at various electrochemical potentials. In addition, since fracture resulted in extremely large facets, the crystallography of fracture was determined. Crystals 3.8 cm diameter by 23 cm long were also prepared. Crack propagation studies were performed and propagation rates were determined. Plastic deformation and strain history effects were also investigated. DOE

N88-20420# Stanford Univ., Calif.
NON-DESTRUCTIVE EVALUATION TECHNIQUES APPLIED TO THE STUDY OF FATIGUE MICROCRACK GROWTH IN STEEL ALLOYS Final Report
B. London, H. Yuce, and D. Nelson Oct. 1987 397 p
(Contract DE-AS03-82ER-12092)
(DE88-004090; DOE/ER-12092/T1) Avail: NTIS HC A17/MF A01

In Part 1 of this study, an ultrasonic surface acoustic wave (SAW) technique was used to monitor the depth of surface fatigue microcracks in 300 M steel as they grew. This technique also provided information on the stress which must be applied to cause the cracks to fully open. Values of crack opening stress obtained by scanning electron microscope (SEM) measurements of crack tip opening displacements were compared with values determined acoustically. Good agreement was obtained, which may permit the conventional and tedious SEM measurements to be replaced by much faster acoustic measurements. The 300 M steel, heat treated to yield strength of 1737 MPa, was tested at two different zero-to-maximum tension stress levels. Effects of residual stresses produced by two different surface preparations on the growth of small cracks were studied. One preparation was electropolishings while the other was stress-relieving followed by diamond paste polishing. Fatigue microcrack growth rate agreed well with that of large cracks in electropolished specimens but, the presence of shallow compressive residual stresses in other specimens caused growth rates as much as an order of magnitude lower than in electropolished specimens. In Part 2, four different microstructures of 4140 steel were investigated. Small fatigue crack behavior was monitored using a surface acoustic wave ultrasonic technique to accurately measure crack depth and crack closure stress. Cracks

from 50 to 200 microns in depth in specially designed catilevered bending samples were investigated. DOE

N88-20421# Notre Dame Univ., Ind. Dept. of Materials Science and Engineering.
EROSION IN DUAL-PHASE MICROSTRUCTURES Final Report
T. H. Kosel Dec. 1987 65 p
(Contract DE-AC05-84OR-21400)
(DE88-004507; ORNL/Sub-83-43336/01) Avail: NTIS HC A04/MF A01

This project was designed to provide a systematic investigation of the effects of microstructural variables on particle impact erosion of two-phase metallic alloys containing large second-phase particles (SPPs). Commercial alloys that contain large hard carbides, such as high Cr-Mo white cast irons and Stellite alloys are known to be highly abrasion resistant. Since there are many similaries between abrasion and erosion, it was felt that a systematic examination of the erosion behavior of such alloys would be useful, especially since existing literature on the subject seemed to indicate that they offered little advantage in erosion. Work was divided into two major sections, on erosion of commercial alloys and of model alloys having artificial SPPs like Al2O3 dispersed in a Cu matrix. The model alloys allowed control of SPP size and second-phase volume fraction (SPVF), and permitted experiments comparing the erosion rates of the dispersed alloys with those of the pure phases. Under the wide range of erosion conditions investigated, this type of alloy offered no significant improvement of erosion resistance over simple, inexpensive low-carbon steels. This was concluded to be the result of the phenomenon of edge spalling from the edges of the SPPs, which was investigated in some detail. DOE

N88-20422# Johns Hopkins Univ., Baltimore, Md. Dept. of Materials Science and Engineering.
CORROSION, PASSIVITY AND BREAKDOWN OF ALLOYS USED IN HIGH ENERGY DENSITY BATTERIES Final Report
J. Kruger Oct. 1987 25 p
(Contract DE-AC03-76SF-00098)
(DE88-004891; LBL-24177) Avail: NTIS HC A03/MF A01

The objective of this research is to further the understanding of the passivity of metals and alloys in non-aqueous and mixed solvents. There is a lack of data in this area, despite its importance to applications such as the construction materials for high energy density batteries. There have been a number of corrosion-related problems reported in the construction materials of such batteries. As demands for longevity for these batteries increase, problems associated with corrosion will become increasingly important. This work is concerned with analyzing the nature, mode of formation, and mode of breakdown of passive films that exist on alloys in non-aqueous and mixed solvents. Work during Year 1 has concentrated upon generating cyclic voltammograms and potentiodynamic curves as baseline data on Au and Armco Fe in water/propylene carbonate mixtures. In addition, Scanning Electron Microscopy has been performed in order to characterize the attack observed and to correlate it to the electrochemical parameters measured. DOE

N88-20423# Rockwell International Corp., Golden, Colo.
GRAIN REFINEMENT DURING PRIMARY BREAKDOWN OF ALLOY 718
M. C. Mataya, M. L. Robinson, D. Chang, M. J. Weis, G. R. Edwards, and D. K. Matlock 1987 28 p Presented at the Iron and Steel Society of ATME, Toronto, Ontario, 23 Oct. 1987 Prepared in cooperation with Carpenter Technology Corp., Reading, Pa. and Colorado School of Mines, Golden
(Contract DE-AC04-76DP-03533)
(DE88-005193; RFP-4123; CONF-8710264-1) Avail: NTIS HC A03/MF A01

Grain refinement during primary breakdown of a production size alloy 718 ingot was investigated by compression testing of cylindrical specimens taken from various locations in the ingot cross section. Deformation was applied over a temperature range of 900 to 1150 C, at strain rates from 0.1/s to 1.0/s, and to strains of 0.25 to 1.0. Variations in grain morphology and orientation had a pronounced effect on the deformed sample geometry but little effect on recrystallization. Recrystallization was observed to nucleate at primary particles and high angle grain boundaries. Static recrystallization rather than dynamic recrystallization was the mechanism responsible for refinement of the coarse cast structure. The cycle time for one pass was identified as the critical processing variable with respect to microstructural evolution for a set of deformation conditions typically used during breakdown by radial forging. DOE

N88-20424# Edgerton, Germeshausen and Grier, Inc., Idaho Falls, Idaho.
CREEP BEHAVIOR OF CONSOLIDATED RAPIDLY SOLIDIFIED TYPE 304 STAINLESS STEEL POWDER CONTAINING HELIUM
J. E. Flinn, G. E. Korth, and R. N. Wright 1987 23 p Presented at the Fall Meeting of The Metallurgical Society of the American Institute of Mining and Metallurgical Engineers, Cincinnati, Ohio, 10 Oct. 1987
(Contract DE-AC07-76ID-01570)
(DE88-005536; EGG-M-05687; CONF-8710110-1) Avail: NTIS HC A03/MF A01

An investigation on the creep behavior of extrusion consolidated Type 304 SS powder containing approximately 7 appM helium was performed. The helium was entrapped during powder processing by centrifugal atomization (CA) and retained through consolidation. In comparison with a wrought ingot metallurgy (I/M) reference of Type 304 SS, the CA SS extruded powder material showed considerable creep resistance with nearly a factor of 30 extension in rupture time and a two order in magnitude decrease in minimum creep rate observed. No obvious embrittlement influences from the helium were observed. Preconditioning heat treatments on the CA 304 SS extruded powders influenced the creep properties. A 900 C,1-h heat treatment resulted in higher ductilities, shorter rupture times, and higher minimum creep rates compared to specimens heat treated for 1 h at 1200 C. The fracture patterns were also significantly different where highly elongated grains and grain boundary cavitation were observed for the 900 C heat treated specimens whereas the 1200 C heat treated specimens display wedge cracking and very little grain elongation. DOE

N88-20425# Edgerton, Germeshausen and Grier, Inc., Idaho Falls, Idaho.
EXPERIMENTAL AND THEORETICAL METHODS FOR INVESTIGATING HELIUM EFFECTS IN RAPIDLY SOLIDIFIED METALS
R. N. Wright and C. D. VanSiclen Jul. 1987 18 p
(Contract DE-AC07-76ID-01570)
(DE88-005542; EGG-MS-7734) Avail: NTIS HC A03/MF A01

Experimental and theoretical methods available for investigating helium-defect interactions in rapidly solidified materials are considered. Transmission electron microscopy and positron annihilation appear to be the most useful experimental techniques. The two techniques are generally complementary since the upper limit of resolution using positron annihilation is approximately of the scale where transmission microscopy becomes readily applied. The recently developed embedded atom method appears well suited to modeling helium-defect interactions. DOE

N88-20426# National Aerospace Lab., Amsterdam (Netherlands). Structures and Materials Div.
FRACTURE MECHANICS AND CREEP CRACK GROWTH OF 1 PERCENT Cr 1/2 PERCENT Mo STEEL WITH AND WITHOUT PRIOR EXPOSURE TO CREEP CONDITIONS
H. P. vanLeeuwen and L. Schra 14 Aug. 1986 36 p Original language document was announced as N87-15488 Submitted for publication
(NLR-TR-86051-U; B8729208; ETN-88-91729) Avail: NTIS HC A03/MF A01

A literature survey shows that of fracture mechanics parameters possible, the contour integral (CI) shows the best correlation with the creep crack propagation rate and would be a good basis for

relaible predictions of the rate. Prior exposure to creep conditions can have an important effect on the crack propagation resistance of the material. Creep crack growth tests were done on unexposed pipe material, pipe material from a pressure vessel exposed to creep conditions, and weld material from that vessel. The relation between the creep growth rate and CI appears to be independent of specimen thickness, initial crack length, and extent of prior exposure. The apparent predictability of the creep crack growth rate may justify a definition of the remnant life of high-temperature creep exposure industrial plants and components and can be the basis of the required inspection periods. ESA

N88-20427# National Aerospace Lab., Amsterdam (Netherlands). Structures and Materials Div.

AIRCRAFT CORROSION PROBLEMS AND RESEARCH IN THE NETHERLANDS

R. J. H. Wanhill 20 Nov. 1986 10 p Presented at the European Corrosion Meeting EUROCORR '87, Karlsruhe, Federal Republic of Germany, Apr. 1987

(NLR-MP-86066-U; B8725239; ETN-88-91732) Avail: NTIS HC A02/MF A01

Corrosion in aircraft landing gear, engines and fuel systems, and aluminum alloy rotor blades of helicopters is reviewed. Measures to alleviate corrosion are discussed. ESA

N88-20428# Brookhaven National Lab., Upton, N. Y.

STUDIES OF TRANSVERSE PHONON MODES IN PREMARTENSITIC INDIUM-THALLIUM ALLOYS

T. R. Finlayson, D. Donovan, J. Z. Larese, and H. G. Smith 1987 6 p Presented at the International Symposium of Neutron Scattering: Advances and Applications, Aedermaunsdorf, Switzerland, 8 Aug. 1987 Prepared in cooperation with Monash Univ., Clayton, Australia, Pennsylvania State Univ., University Park and ORNL, Tenn.

(Contracts DE-AC02-76CH-00016; DE-AC05-84OR-21400)

(DE88-003481; BNL-40534; CONF-8708199-1) Avail: NTIS HC A02/MF A01

The measured phonon dispersion relations along the high symmetry directions for a face-centered In-Tl alloy have been reasonably well fitted using a general Born-von Karman force constant model. However, for the (zeta zeta 0)(zeta anti zeta 0) branch at low zeta, there is poor agreement between the neutron measurements and the extrapolation of the line of initial slope determined from an ultrasonic velocity measurement. Phonon frequencies have been measured for wave vectors to within q = 0.033 (sq rt 2, 2 pi/a) of the zone center, and, contrary to the phonon softening with decreasing temperature, which might be expected from the known decrease in (C-11 - C-12 /2, phonon frequencies showed the normal trend of frequency increasing (hardening) as temperature was decreased in the premartensitic regime. To reconcile the disagreement between the extrapolation of the ultrasonic data and the measured (zeta zeta 0)(zeta anti zeta 0) phonon frequencies, there must exist a positive curvature in the dispersion relation at q less than 0.03 (sq rt 2, 2 /a). This is consistent with one recent theory for martensite nucleation. DOE

N88-20429# Argonne National Lab., Ill.

TEMPERATURE DEPENDENCE OF Kr PRECIPITATION IN Ni

R. C. Birtcher and A. S. Liu Nov. 1987 7 p Presented at the Fall Meeting of the Materials Research Society, Boston, Mass., 30 Nov. 1987

(Contract W-31-109-eng-38)

(DE88-005953; CONF-871124-74) Avail: NTIS HC A02/MF A01

The precipitation of Kr injected into Ni at temperatures between 25 and 560 C has been studied with transmission electron microscopy. The Kr precipitates in cavities which increase in size with Kr fluence. Electron diffraction and dark-field imaging demonstrate that small Kr precipitates are solid, fcc crystals aligned with each other and the Ni lattice. The Kr is held in the solid state by the pressure generated by the cavity walls, and this pressure decreases with increasing cavity size. The mismatch between the Kr and Ni lattices is as large as 55 percent. The average Kr lattice parameter, determined from electron diffraction at room temperature, increases with increasing Kr fluence from 0.515 nm to an asymptotic value of about 0.545 nm for implantations at temperatures of 300 C or less. This increase towards an asymptotic limit is due to expansion of the Kr lattices as precipitates grow, until the decrease in cavity pressures allows melting of solid Kr in large cavities. Diffuse electron scattering was observed from liquid Kr in large precipitates for fluences greater than 5 x 10 to the 20th Kr(+)/sq m. Implantations at temperatures of 400 C or higher result in a bi-modal size distribution containing small solid precipitates and an additional population of larger, faceted precipitates, a larger average Kr lattice parameter for a given Kr fluence, and a higher asymptotic lattice parameter of 0.550 nm. Solid Kr seems to inhibit motion of small precipitates, and Kr melting is a precursor to faceting and growth by coalescence. DOE

N88-20430# Tennessee Univ., Knoxville. Welding Research and Engineering.

TRANSFORMATION, METALLURGICAL RESPONSE AND BEHAVIOR OF THE WELD FUSION ZONE AND HEAT AFFECTED ZONE IN Cr-Mo STEELS FOR FOSSIL ENERGY APPLICATION Final Technical Report, Jan. 1985 - Sep. 1987

C. D. Lundin, J. A. Henning, R. Menon, and K. K. Khan 30 Sep. 1987 260 p

(Contract DE-AC05-84OR-21400)

(DE88-006037; ORNL/Sub-81-07685/02-77) Avail: NTIS HC A12/MF A01

The behavior of the heat affected zone (HAZ) in Cr-Mo steel welds as well as practical information on their relative weldability are investigated. The principal work was the evaluation of the post weld heat treatment (PWHT) cracking of Cr-Mo steels ranging in Cr content from 2.25 to 9 percent. Differences in observed cracking behavior were contrasted with composition, on cooling transformation behavior and HAZ microstructure. Hydrogen assisted cracking (HAC) studies using a large scale cracking test were conducted on 2.25 Cr and 3 Cr steels. Soft zone studies were conducted on 9 Cr NKK steel to determine the reason for the development of a low hardness region (Soft Zone) at the outer boundary of the HAZ. The literature review provides a concise historical review and the basis of theories for PWHT cracking and HAC in Cr-Mo steels which were employed to explain the weld cracking susceptibility of various Cr-Mo alloys. PWHT cracking susceptibility was investigated using Gleeble simulated heat affected zone (HAZ) specimens. A new test was developed at the University of Tennessee, the C-ring test to evaluate the PWHT cracking behavior. The C-ring test was found to be extremely useful in testing for PWHT cracking susceptibility and for verifying the results obtained from Gleeble tests. An excellent correlation was obtained for the two tests. The standard Y-groove test was selected for HAC susceptibility testing. This test is very suitable for evaluating the HAC of the base metal and is defined in Japanese Industrial Standard JIS Z 3158. DOE

N88-20431# Connecticut Univ., Storrs.

THE FATIGUE BEHAVIOR OF FERRITIC AND AUSTENITIC STEELS AT ELEVATED TEMPERATURES Progress Report

A. J. McEvily 1988 12 p

(Contract DE-FG02-84ER-45109)

(DE88-006304; DOE/ER-45109/T1) Avail: NTIS HC A03/MF A01

With type 304 austenitic steel we have observed no creep-fatigue interactions down to a frequency of 0.3 Hz. Crack closure occurs in 304 stainless at 538 C, whereas it does not in the ferritic alloys investigated. This is attributed to the greater resistance to creep of the austenitic material. The 304 material was also studied at room temperature with interesting results. Stress-induced phase transformation affects the nature of the crack closure process. In addition it reduces markedly the fatigue notch sensitivity of this alloy. With the 9Cr-2Mo ferritic alloy, a decrease in specimen thickness results in an increase in crack closure and a decrease in crack growth rate. DOE

N88-20432# International Atomic Energy Agency, Vienna (Austria).
STUDY OF DEFECTS IN METALS BY POSITRON ANNIHILATION Final Report, Dec. 1983 - Dec. 1986
N. AyresdeCampos Oct. 1987 4 p
(DE88-701042; IAEA-R-3650-F) Avail: NTIS (US Sales Only) HC A02/MF A01

Two techniques of positron annihilation, Doppler broadening and life-time measurements, were applied to studies of radiation damage effects in steels. The defects created in irradiation with deuterons and neutrons were observed at different stages of the annealing process, at different temperatures. The comparison with TEM was made. The vacancy clusters created in AISI316 steel by deuteron irradiation were observed to dissolve completely at 550 degrees C. The presence of deuterium in material has no influence on stabilization of these clusters. The neutron irradiation of steel, with the dose of 2 x 10 to the 19th power neutrons/sq cm formed in A533B steel microcavities containing around ten single vacancies. At 400 degrees C the shape decrease in positron trapping indicates a complete annealing; simultaneously, changes in the structure of carbide precipitates were observed. An interpretative model for these results was developed. DOE

N88-20433# Gosudarstvennyi Komitet po Ispolzovaniyu Atomnoi Energii, Moscow (USSR). Inst. Atomnoj Ehnergii.
STUDY OF ACTIVATIONLESS REACTIONS OF POINT DEFECTS WITH IMPURITIES AND IMPURITY-DEFECT COMPLEXES IN ALPHA-IRON
Yu. R. Kevorkyan 1986 8 p In RUSSIAN
(TI88-701028; IAE-4331/11) Avail: NTIS (US Sales Only) HC A02/MF A01

Using the method of molecular dynamics, instability region of intrinsic interstitial atom near the complex impurity-vacancy in alpha-iron is investigated. A great number of impurity atoms of substitution differing in the volumetric change, which they introduce into crystal, is considered. The effect of impurities on dimensions of the Frenkel couple recombination region is evaluated. Spatial positions of interstitial atoms and substitution impurities with a small volume, at which spontaneous replacement of the latter from lattice point to one of stable interstitial positions of matrix is realized, are determined. Certain peculiarities of recombination of mixed dumbbell-like and other interstitial configurations of impurity are considered. DOE

N88-20434*# National Aeronautics and Space Administration, Washington, D.C.
A CALORIMETRIC DETERMINATION OF THE ENTHALPY OF FORMATION AND A DESCRIPTION OF THE DEFECT STRUCTURE OF THE ORDERED BETA-PHASE /Ni, Cu/ /1-x/ Al/x/
E. T. Henig and H. L. Lukas Mar. 1988 38 p Transl. into ENGLISH from Zeitschrift fuer Metallkunde (Fed. Republic of Germany), v. 66, Feb. 1985 p 98-106 Transl. by Scientific Translation Service, Santa Barbara, Calif.
(Contract NASw-3047)
(NASA-TT-20157; NAS 1.77:20157) Avail: NTIS HC A03/MF A01 CSCL 11F

In order to describe thermodynamically the defect structure of an ordered B-Hume-Rothery phase, the heat of formation of (Ni,Cu)(1-x)Al(x) was measured at 1100 K as a function of concentration in the range x (sub Al) = 0.4 and 0.55 for three substitution rations x (sub Ni)/x (sub Cu) = infinity; 11; 5. The heat of formation of the NiAl beta-phase is strongly negative. For the stoichiometric composition it is -72.2 kJ/g-atom. On both the nickel-rich side and the aluminum-rich side the magnitude of the enthalpy of formation decreases linearly with concentration. Substitution of nickel for copper decreases the magnitude of the enthalpy of formation over the entire homogeneity range for the phase (Ni,Cu)(1-x)Al(x). The curve for the enthalpy of formation as well as the literature values for the chemical potential of aluminum are described with great accuracy by the disorder model of Wagner-Schottky. Author

N88-20435# Rhode Island Univ., Kingston. Chemical Lab.
GORDON CONFERENCE ON INTERMETALLIC COMPOUNDS HELD AT TILTON, NEW HAMPSHIRE ON 20-24 JULY 1987 Final Report, Jul. - Oct. 1987
David P. Pope, Harry A. Lipsitt, and Alexander Cruickshank 31 Oct. 1987 21 p Conference held in Tilton, N. Hamp., 20-24 Jul. 1987
(Grant AF-AFOSR-0195-87)
(AD-A188502; AFOSR-87-1749TR) Avail: NTIS HC A03/MF A01 CSCL 11F

The 1987 Gordon Research Conference on Physical Metallurgy was held 20-24 July 1987 at the Tilton School, Tilton, New Hampshire. The conference topic was intermetallic compounds. The primary purpose of the conference was to bring together three rather disparate groups: scientists and engineers concerned with the mechanical properties of intermetallic compounds; theoreticians interested in the problems of alloy stability and the calculation and prediction of the effects of chemical composition on alloy stability; and engineers interested in developing and producing new alloys based on intermetallic compounds for elevated temperature service. Topics include: Overview of Strength and Ductility of Intermetallic Compounds, Dislocation Core Structure and Slip Systems in Intermetallic Compounds, Strengthening Mechanisms in Intermetallic Compounds, Creep and Fatigue of Intermetallic Compounds, Deformation of Non-Cubic Intermetallic Compounds, Overview of Brittle-Ductile Transition Mechanisms, Mechanisms of Ductility Improvement in Lithium, Grain Boundary Accommodation of Slip, Grain Boundary Modeling, Limitations and Approximations of Electronic Structure Calculations, The Thermodynamics of Extended Defects in Intermetallic Compounds, and Quantum Mechanics and Fracture are presented. GRA

N88-20436# Office National d'Etudes et de Recherches Aerospatiales, Paris (France). Materials Dept.
[ACTIVITIES REPORT OF THE MATERIALS DEPARTMENT] Annual Report, 1986
Sep. 1987 26 p Original contains color illustrations
(ETN-88-91984) Avail: NTIS HC A03/MF A01

Alloys for single-crystal turbine blades; studies on conventional powder (100 micron) for the manufacture of turbine disks; alloys derived from microcrystalline powders obtained at rapid solidification rates; and studies on methods for protection against high-temperature corrosion and oxidation are discussed. ESA

N88-20437*# National Aeronautics and Space Administration, Washington, D.C.
FORMATION OF NUCLEI DURING PRECIPITATION IN METALLIC MIXED CRYSTALS
R. Becker Apr. 1988 18 p Transl. into ENGLISH from Annalen der Physik (Fed. Republic of Germany), no. 32, series 5, 1938 p 128-140 Transl. by Scientific Translation Service, Santa Barbara, Calif.
(Contract NASw-4307)
(NASA-TT-20248; NAS 1.77:20248) Avail: NTIS HC A03/MF A01 CSCL 11F

Assuming that the energy of a mixed crystal can be calculated by simple addition of neighboring bonds, the nuclear formation energy is calculated for precipation in a super-saturated binary mixed crystal. From this can be determined the frequency of the formation of nuclei. From the calculation of a numerical example we can obtain, for the degree of sub-cooling at which the frequency of the formation of nuclei reaches its maximum, satisfactory agreement with available measurements of the rate of precipitation. Author

27 NONMETALLIC MATERIALS

Includes physical, chemical, and mechanical properties of plastics, elastomers, lubricants, polymers, textiles, adhesives, and ceramic materials.

For composite materials see *24 Composite Materials.*

N88-20438*# Mega Engineering, Silver Spring, Md.
USE OF REINFORCED INORGANIC CEMENT MATERIALS FOR SPARK WIRE AND DRIFT CHAMBER WIRE FRAMES Final Report
3 Sep. 1987 33 p
(Contract NAS5-30051)
(NASA-CR-180759; NAS 1.26:180759) Avail: NTIS HC A03/MF A01 CSCL 11A

The results of a survey, materials test, and analysis study directed toward the development of an inorganic glass-fiber reinforced cement material for use in the construction of space qualified spark wire frames and drift chamber frames are presented. The purpose for this research was to evaluate the feasibility of using glass fiber reinforced cement (GFRC) for large dimensioned structural frames for supporting a number of precisely located spark wires in multiple planes. A survey of the current state of the art in fiber reinforced cement materials was made; material sample mixes were made and tested to determine their laboratory performances. Tests conducted on sample materials showed that compressive and flexural strengths of this material could approach values which would enable fabrication of structural spark wire frames. Author

N88-20439# Japan Atomic Energy Research Inst., Tokai.
IAEA SPECIALISTS' MEETING ON GRAPHITE COMPONENT STRUCTURAL DESIGN
Konomo Sanokawa, ed. Jan. 1987 257 p Meeting held in Tokai, Japan, 8-11 Sep. 1986
(DE88-780006; JAERI-M-86-192; IWGGCR-11; CONF-8609133-Summ) Avail: (US Sales Only) NTIS HC A12/MF A01

The purpose of this meeting was to provide an international forum to compare and discuss the state-of-the-art in the development of graphite components for gas cooled reactors in order to define critical issues and to give direction to future R and D programs. Specific technical sessions included design criteria, stress and strain analysis, material properties, graphite component tests, and inspection and surveillance of graphite components. All papers are provided along with conference and round-table discussion summaries. For individual titles, see N88-20440 through N88-20448.

N88-20440# Oak Ridge National Lab., Tenn.
THE STATISTICAL CHARACTERIZATION OF TENSILE STRENGTHS FOR A NUCLEAR-TYPE GRAPHITE
C. R. Kennedy and W. P. Eatherly *In* JAERI. IAEA Specialists' Meeting on Graphite Component Structural Design Jan. 1987 p 63-68 (For primary document see N88-20439 13-27)
Avail: (US Sales Only) NTIS HC A12/MF A01

A data set of tensile strengths comprising over 1200 experimental points has been analyzed statistically in conformance with the observed phenomena of background and disparate flaws. The data are consistent with a bimodal normal distribution. If corrections are made for strength dependence on density, the background mode is Weibull. It is proposed that the disparate mode can be represented by a combination of binomial and order statistics. The resultant bimodal model would show a strong dependence on stress volume. Author

N88-20441# Japan Atomic Energy Research Inst., Tokai.
STATISTICAL CONSIDERATIONS OF GRAPHITE STRENGTH FOR ASSESSING DESIGN ALLOWABLE STRESSES
M. Ishihara, H. Mogi, I. Ioka, T. Arai, and T. Oku *In its* IAEA Specialists' Meeting on Graphite Component Structural Design Jan. 1987 p 69-74 (For primary document see N88-20439 13-27)
Avail: (US Sales Only) NTIS HC A12/MF A01

Probability distribution functions of tensile and compressive strengths are investigated for candidate very high temperature graphites. Normal, logarithmic normal and Weibull distribution functions are compared in terms of coefficient of correlation to measured strength data. This leads to the adaptation of the normal distribution function. In addition, the relation between factor of safety and fracture probability is discussed for the following items: (1) as the graphite strength is more variable than that of metallic materials, the effect of strength variation on the fracture probability is evaluated; (2) fracture probability depending on survival probability of 99 to 99.9 percent with confidence level of 90 to 95 percent is discussed; and (3) as the material properties used in the design analysis are usually the mean values of their variation, the additional effect of these variations on the fracture probability is discussed. Finally, the way to assure the minimum ultimate strength with required survival probability with high confidence level is discussed in view of a statistical treatment of the strength data from varying sample numbers in a material acceptance test. Author

N88-20442# Ibaraki Univ., Hitachi (Japan). Faculty of Engineering.
FRACTURE CRITERION OF REACTOR GRAPHITE UNDER MULTIAXIAL STRESSES
S. Sato, H. Awaji, K. Kawasata, A. Kurusada, and T. Oku (Japan Atomic Energy Research Inst., Tokai.) *In* JAERI. IAEA Specialists' Meeting on Graphite Component Structural Design Jan. 1987 p 75-89 (For primary document see N88-20439 13-27)
Avail: (US Sales Only) NTIS HC A12/MF A01

Fracture criteria for graphite under multiaxial stresses are presented for designing core and support materials for a high temperature gas cooled reactor. Different kinds of fracture strength tests are carried out for a near isotropic graphite IG-11. Results show that, under the stress state in which tensile stresses are predominant, the maximum principle stress theory is seen as applicable for brittle fracture. Under the stress state in which compressive stresses are predominant, there may be two fracture modes for brittle fracture, namely, slipping fracture and mode II fracture. For the former fracture mode the maximum shear stress criterion is suitable, but for the later fracture mode a fracture criterion similar in form to the Coulomb-Mohr criterion and including a restraint effect for cracks is verified to be applicable. Also, a statistical correction for brittle fracture criteria under multiaxial stresses is discussed. By considering the allowable stress values for a safe design, the specified minimum ultimate strengths corresponding to a survival probability of 99 percent at the 95 percent confidence level are presented. Author

N88-20443# Japan Atomic Energy Research Inst., Tokai.
HIGH TEMPERATURE YOUNG'S MODULUS OF IG-110 GRAPHITE
T. Konishi, M. Eto, and T. Oku *In its* IAEA Specialists' Meeting on Graphite Component Structural Design Jan. 1987 p 133-137 (For primary document see N88-20439 13-27)
Avail: (US Sales Only) NTIS HC A12/MF A01

Data on Young's modulus of nuclear graphite at high temperature are required for the design and safety analysis of the VHTR (Very High Temperature Reactor). An ultrasonic wave pulse method was applied up to a temperature of 1400 C. The Young's modulus of oxidized materials was also measured. The results were compared with tensile strength at high temperture to estimate the tensile strength non-destructively. Tensile tests were carried out at 600 C and 1000 C in a vacuum chamber. Specimens were oxidized to three weight loss levels (3.5 percent, 5.0 percent, 7.0 percent) in air at 550 C. Young's modulus increased with increasing temperature. The temperature dependence of Young's modulus became less pronounced as the amount of oxidation increased. In the specimens oxidized to more than 5 percent, the Young's modulus first decreased slightly with increasing temperature and the temperature at which the Young's modulus started to rise shifted to a higher region with increasing weight loss. Young's modulus and tensile strength at high temperature up to 1000 C were correlated with each other using the equation: (sigma/sigma

sub 0) = (E/E sub 0) sup 1/2, where sigma, sigma sub 0, E, and E sub 0 denote tensile strength at a given temperature, tensile strength at room temperature, Young's modulus at a given temperature, and Young's modulus at room temperature, respectively. Author

N88-20444# Japan Atomic Energy Research Inst., Tokai.
EFFECTS OF HIGH TEMPERATURE NEUTRON IRRADIATION ON THE PHYSICAL, CHEMICAL AND MECHANICAL PROPERTIES OF FINE-GRAINED ISOTROPIC GRAPHITE
H. Matsuo, S Nomura, T. Oku, M. Eto, and H. Imai *In its* IAEA Specialists' Meeting on Graphite Component Structural Design Jan. 1987 p 138-143 (For primary document see N88-20439 13-27)
Avail: (US Sales Only) NTIS HC A12/MF A01

Effects of neutron irradiation on the dimensional change, coefficient of thermal expansion (CTE), thermal conductivity, corrosion rate, Young's modulus and strengths were studied for the candidate graphite material IG-110 of the experimental very high temperature gas-cooled reactor (VHTR) after irradiation at 585 to 1273 C to neutron fluences of up to about 3 x 10(25) n/sq m and 7 x 10(25) n/sq m (E greater than 29 fJ). The results were compared with irradiation behaviors of other graphites. Dimensional shrinkage was observed in the whole irradiation temperature range. The shrinkage rate showed the minimum in a temperature of around 850 C, followed by the increase for the samples irradiated at higher temperatures. The CTE, thermal resistivity and Young's modulus increased in the early stage of irradiation and then only the CTE decreased while the thermal resistivity and Young's modulus levelled off with further irradiation. The neutron fluence showing the maximum CTE shifted to the lower fluence with increasing irradiation temperature. The increases of both thermal resistivity and Young's modulus were very good for the samples irradiated at lower temperatures. Compressive and bending strengths measured at room temperature increased after irradiation as well. The corrosion rate with water vapor of 0.65 percent in helium at high temperatures decreased owing to irradiation. The activation energy for the reaction was estimated to be the same before and after irradiation. Author

N88-20445# Ibaraki Univ., Hitachi (Japan). Faculty of Engineering.
DEGRADATIONS OF THERMAL SHOCK RESISTANCE AND THE FRACTURE TOUGHNESS OF REACTOR GRAPHITE SUBJECTED TO NEUTRON IRRADIATION
S. Sato, K. Kawamata, A. Kurumada, H. Ugachi, and H. Awaji (Fukushima National Coll. of Tech., Iwaki, Japan) *In* JAERI. IAEA Specialists' Meeting on Graphite Component Structural Design Jan. 1987 p 144-157 (For primary document see N88-20439 13-27)
Avail: (US Sales Only) NTIS HC A12/MF A01

The effects of neutron irradiation on the thermal shock resistance delta = sigma(t) k/Ea (where sigma(t) is tensile strength, k is thermal conductivity, E is Young's modulus, and a is thermal expansivity) and the thermal shock fracture toughness del = K(Ic) k/Ea (where K(Ic) is the fracture toughness value of mode I) were investigated. In addition, other mechanical properties such as diametral compressive strength and fracture toughness were studied. Two kinds of near isotropic graphite subjected to irradiations of 1.1 to 1.5 x 10(21) n/sq cm (greater than 29 fJ) were prepared for the measurements. One was an isostatically molded graphite IG-11 with fine grain petroleum coke. The other is a binderless molded graphite HCB-18 which was prepared using mesophase pitch carbon of very fine grain size. Results show that, after irradiation, both the thermal shock resistance and the thermal shock fracture toughness of the two graphites decreased considerably in contrast with increases of the usual mechanical strengths. Author

N88-20446# Tohoku Univ., Sendai (Japan).
APPLICATION OF ISRM TESTING METHODS TO FRACTURE TOUGHNESS TESTING OF GRAPHITE
T. Hashida, S. Ishiyama (Japan Atomic Energy Research Inst., Tokai.), T. Fukasawa, H. Takahashi, and T. Oku *In* JAERI. IAEA Specialists' Meeting on Graphite Component Structural Design Jan. 1987 p 158-162 (For primary document see N88-20439 13-27)
Avail: (US Sales Only) NTIS HC A12/MF A01

Fracture toughness measurements of nuclear grade graphites, IG11 and PGX, were made using an acoustic emission (AE) technique. Tests were conducted on edge-notched round bend bars, edge-notched short bars and round compact tension specimens. These round-shaped specimens have been proposed as testing standards for rock fracture toughness tests by the International Society for Rock Mechanics (ISRM). Taking the observed nonlinear deformation behavior into account, a J-integral approach was utilized to determine the fracture toughness of the graphites. It is shown that the critical J integral determined by the AE technique, J(1AE), is independent of specimen geometry. Based on these experimental results, the fracture toughness, K(IC), of the graphites was determined from the J(1AE) values. The K(IC) value of IG11 was 1.04 MPa square root of m, and 0.77 MPa square root of m for PGX. Furthermore, the specimen size effect of the fracture toughness determined by the J-integral/AE method is discussed. Author

N88-20447# Fuji Electric Co. Ltd., Yokosuka (Japan).
NOTCH SENSITIVITY OF GRAPHITE MATERIALS FOR VHTR
Harao Kawakami *In* JAERI. IAEA Specialists' Meeting on Graphite Component Structural Design Jan. 1987 p 163-168 (For primary document see N88-20439 13-27)
Avail: (US Sales Only) NTIS HC A12/MF A01

Uniaxial tensile tests, compressive tests and thermal shock tests were performed to investigate the notch sensitivity of three nuclear grade graphite materials: PGX, IG-11 and Stackpole 2020. Results showed that: (1) the notch sensitivity of the graphite materials in the uniaxial tensile tests became smaller as the notch radius became smaller; (2) notch sensitivity of IG-11 was larger than that of PGX; (3) compressive fracture of PGX was in a shear mode, while that of IG-11 was in a mixed mode of shear and transverse splitting; and (4) the thermal shock fracture resistance (TSFR) parameter of IG-11 was larger than that of PGX, but, when a notch with a small radius existed, the TSFR of IG-11 could be smaller than that of PGX. M.G.

N88-20448# Tokyo Inst. of Tech. (Japan). Research Lab. for Nuclear Reactors.
NONDESTRUCTIVE TESTINGS OF HTGR GRAPHITES
T. Maruyama, H. Uragaki, M. Fujii, K. Ooka, T. Sakashita, H. Suzuki, and T. Oku (Japan Atomic Energy Research Inst., Ibaraki.) *In* JAERI, IAEA Specialists' Meeting on Graphite Component Structural Design Jan. 1987 p 169-175 (For primary document see N88-20439 13-27)
Avail: (US Sales Only) NTIS HC A12/MF A01

Results of nondestructive testing of fine-grained, high-density, isotropic graphites are described. The graphites tested are candidate materials to be used in the reactor cores of high temperature gas cooled reactors (HTGR). Specimens containing flaws of various shapes and sizes were fabricated and tested using a pulsed ultrasonic method and an X-ray computer tomography technique. The ultrasonic testing was done using high resolution transducers of longitudinal wave at frequencies of 1 and 2.25 MHz. The relationship between the ultrasonic echo amplitude and the dimension of flaws was obtained. The results were compared with calculated values. The X-ray computer tomography test was done using commercially available apparatus. Flaws in the graphites were clearly shown and the limits of detection for both lamellar and bulk flaws in the nuclear graphites were determined. Author

N88-20449# Air Force Wright Aeronautical Labs., Wright-Patterson AFB, Ohio. Materials Lab.
HIGH-TEMPERATURE THERMOSETS DERIVED FROM THE DIELS-ALDER POLYMERIZATION OF BISBENZOCYCLOBUTENES AND BIMALEIMIDES Final Report, Jan. 1986 - Jan. 1987

Loon-Seng Tan, Edward J. Soloski, and Fred E. Arnold Sep. 1987 29 p
(AD-A188800; AFWAL-TR-87-4073) Avail: NTIS HC A03/MF A01 CSCL 11I

A number of compatible mixtures of 2,2-bis4-(N-4-benzocyclobutenyl phthalimide-4-phenyl hexafluoropropane (BCB) and 1,1'-(methylene di-4, 1-phenylene) bismaleimide (BMI) were prepared. Complete compatibility of the mixtures was evidenced by a single initial t sub g. All mixtures showed relatively low initial t sub g's and characteristic polymerization exotherms of benzocyclobutene-based systems providing an excellent processing window. The cured sample of the mixtures, pure BCB and BMI were subjected to comparative isothermal gravimetric analysis (ITGA). After 200 hours at 650 F (343 C) in circulating air, the cured BMI exhibited similar thermo-oxidative stabilities to BCB. A model compound was synthesized from the intimate mixture of N-phenyl maleimide and N-benzocyclobutenyl phthalimide in 63 percent recrystallized yield. The ITGA results and isolation of the model Diels-Alder adduct render strong support to the conviction that Diels-Alder polymerization is the predominant curing process in the BCB/BMI system. GRA

N88-20450# Naval Air Development Center, Warminster, Pa. Air Vehicle and Crew Systems Technology Directorate.
OPTIMIZATION OF BINARY PIGMENT COATINGS Final Report, Sep. 1983 - Jun. 1985
Anthony T. Eng and Charles R. Hegedus 5 Jan. 1987 61 p
(AD-A189103; NADC-87008-60) Avail: NTIS HC A04/MF A01 CSCL 11C

In this effort, an approach was devised and utilized to theoretically predict optimum coating compositions using two parameters, the maximum pigment packing factor and the coating critical pigment volume concentration, (CPVC). Five binary pigment systems were evaluated in this study: (1) titanium dioxide - silicon dioxide, (2) titanium dioxide - antimony oxide, (3) titanium dioxide - zinc chromate, (4) titanium dioxide - vesiculated polymer beads, and (5) titanium dioxide - solid polymer beads. Each pigment systems was systematically formulated in a polyurethane resin using a simplex statistical design. After application and cure, the coatings were tested and evaluated for gloss and flexibility to experimentally determine the CPVC of the coating system. The correlation between the theoretical and experimental CPVC's was either good or fair for the five systems studied. These results indicate that theoretically predicting CPVC's along with a statistically designed formulation procedure will yield an optimum coating region for the given pigment system. GRA

N88-20451# AeroChem Research Labs., Inc., Princeton, N. J.
A NEW PROCESS FOR SYNTHESIS OF SILICON NITRIDE POWDERS FOR ADVANCED CERAMICS Final Report, 17 Sep. 1984 - 16 Sep. 1987
D. B. Olson and H. F. Calcote Nov. 1987 23 p
(Contract DAAG29-84-C-0023)
(AD-A189354; AEROCHEM-TP-469; ARO-21828.1-MS-S) Avail: NTIS HC A03/MF A01 CSCL 11B

A new self sustaining flame synthesis process for producing improved silicon nitride powders was experimentally tested. Mixtures of silane and ammonia could not be ignited, but mixtures of silane and hydrazine or silane, ammonia, and hydrazine were found to support stable flames over a wide range of pressures and reagent ratios. Flames with less than the stoichiometric amount of silane produced fine, white, amorphous powders of silicon nitride with specific surface areas from 90 to 150 m sq/g and intrinsic densities of about 3.0 grams/cubic centimeter. Yields greater than 90 precent and production rates of greater than 10 g/min were achieved. X-ray analysis, infrared spectra, and emission analysis for metals confirmed the material to be high purity. Samples typically contained 3 oxygen which was probably introduced in handling. GRA

N88-20452# Purdue Univ., West Lafayette, Ind. Dept. of Chemistry.
CONTRASTING CONDUCTANCE/VISCOSITY RELATIONS IN LIQUID STATES OF VITREOUS AND POLYMER SOLID ELECTROLYTES
M. McLin and C. A. Angell Nov. 1987 18 p
(Contract N00014-84-K-0289)
(AD-A189378; TR-14) Avail: NTIS HC A03/MF A01 CSCL 07F

In order to contrast conductivity mechanisms in fast ion glassy and rubbery polymer electrolytes, the liquid states of two prototypical cases have been studied. Viscosity and conductivity measurements have been performed on molten (as opposed to glassy) (AgCl) 0.35 (Ag(I)) 0.45 (CsCl) 0.20 and on solutions of sodium triflate in low molecular weight PPG (as opposed to high mw, 1,000,000 rubbery solid PPG - called PPO). Both types of system show non-Arrhenius viscosity with divergent behavior near T(g). The energetics of the conductivity processes, however, are very different. This is emphasized by reduced temperature scale (T/T(g)) plotting of (temperature-dependent) activation energies. For the polymer salt systems, as for normal molten salt systems and aqueous solutions, conductance and viscosity energetics are comparable - the processes are coupled. Reduced temperature plots of polymer solutions and glassforming aqueous solution data show the relative importance of T(g) and ion association factors in limiting polymer electrolyte performance. GRA

N88-20453# General Electric Co., Cincinnati, Ohio. Aircraft Engine Business Group.
NONDESTRUCTIVE EVALUATION OF CARBON-CARBON COATINGS Final Report, 1 Aug. 1984 - 23 Feb. 1987
D. C. Copley and M. Rooney Oct. 1987 94 p Prepared in cooperation with Southern Research Inst., Birmingham, Ala.
(Contract F33615-84-C-5007)
(AD-A189524; AFWAL-TR-87-4086) Avail: NTIS HC A05/MF A01 CSCL 11C

General Electric, with Southern Research Institute as subcontractor, completed this program to investigate differential-adsorption, nondestructive evaluation for carbon-carbon coatings. An optimum fluorescent particle and application method were developed to visualize crack patterns in the coatings. A stress-analysis model was developed to predict crack spacing as a function of coating properties, and this provided excellent agreement with experimental results. A study was made of the potential to improve oxidation life by adding glass-formers to the fluorescent particle suspension. A number of methods for measurement of coating thickness were investigated, and eddy current measurement was found to be the most accurate. GRA

N88-20454*# National Aeronautics and Space Administration. Lewis Research Center, Cleveland, Ohio.
DEVELOPMENT OF A TORSION BALANCE FOR ADHESION MEASUREMENTS
Kazuhisa Miyoshi, Chikayoshi Maeda, and Ryuichi Masuo (Osaka Inst. of Tech., Japan) 1988 21 p Proposed for presentation at IMEKO 11, Houston, Tex., 16-21 Oct. 1988; sponsored by Instrument Society of America
(NASA-TM-100799; E-3977; NAS 1.15:100799) Avail: NTIS HC A03/MF A01 CSCL 11B

A new torsion balance for study of adhesion in ceramics is discussed. A torsion wire and a linear variable differential transformer are used to monitor load and to measure pull-off force (adhesion force). The investigation suggests that this torsion balance is valuable in studying the interfacial properties of ceramics in controlled environments such as in ultrahigh vacuum. The pull-off forces measured in dry, moist, and saturated nitrogen atmosphere demonstrate that the adhesion of silicon nitride contacts remains low at humidities below 80 percent but rises rapidly above that. The adhesion at saturation is 10 times or more greater than that below 80 percent relative humidity. The adhesion in a saturated atmosphere arises primarily from the surface tension effects of a thin film of water adsorbed on the surface. The surface tension of the water film was 58 x 10 to the minus 5 to 65 x 10 to the

minus 5 power. The accepted value for water is 72.7 x 10 to the minus 5 power N/cm. Adhesion characteristics of silicon nitride in contact with metals, like the friction characteristics of silicon carbide to metal contacts, can be related to the relative chemical activity of metals in ultrahigh vacuum. The more active the metal, the higher the adhesion. Author

N88-20455*# National Aeronautics and Space Administration. Lewis Research Center, Cleveland, Ohio.
AVAILABILITY AND COST ESTIMATE OF A HIGH NAPHTHENE, MODIFIED AVIATION TURBINE FUEL
George M. Prok Apr. 1988 9 p
(NASA-TM-100823; E-4011; NAS 1.15:100823) Avail: NTIS HC A02/MF A01 CSCL 11B

Information from an Air Force study was used to determine the potential availability and cost of a modified conventional fuel with a naphthene content which could have a thermal stability near that of JP-7 for high-speed civil transports. Results showed sufficient capacity for a fuel made of a blend of 50 percent naphthenic straight run kerosene and 50 percent hydrocracked product, assuming a near-term requirement of 210,000 BBL per day. Fuel cost would be as low as 62.5 to 64.5 cents per gallon, assuming 20 dollars per barrel for crude. Author

N88-20456# Denver Univ., Colo. Dept. of Engineering.
CHARACTERIZATION AND FUNDAMENTAL STUDIES ON CuO SORBENT MATERIALS TO DETERMINE ATTRITION MECHANISMS ON SUBSTRATE GAMMA ALUMINA Technical Progress Report, 23 Mar. - 23 Jun. 1987
J. D. Mote, P. Eucker, and Zuming Zhu 1987 16 p
(Contract DE-AC22-86PC-91024)
(DE88-003674; DOE/PC-91024/T4; TPR-3) Avail: NTIS HC A03/MF A01

More detailed analysis of the impact properties of the sorbent materials in their various states were conducted during this quarter. Particle size determinations of sorbent spheres in various states were made by X-ray line broadening measurements. The materials examined indicate an increase in the particle size after sorption-desorption in the pilot facility. The possible effect of an increase in particle size on the mechanical properties is discussed. DOE

N88-20457# Brookhaven National Lab., Upton, N. Y.
THE EFFECT OF Ca(OH)2-TREATED CERAMIC MICROSPHERES ON THE MECHANICAL PROPERTIES OF HIGH-TEMPERATURE LIGHTWEIGHT CEMENT COMPOSITES
Toshifumi Sugama Oct. 1987 11 p Presented at the Symposium on Interfaces in Cementitious Composites, Boston, Mass., 2 Dec. 1987
(Contract DE-AC02-76CH-00016)
(DE88-004590; BNL-40419; CONF-871250-1) Avail: NTIS HC A03/MF A01

The compressive strength and water permeability of high-temperature lightweight cementing materials containing sillimanite-based hollow microspheres as a filler can be improved by treating the surfaces of the microspheres with a Ca(OH)2-saturated solution at temperatures up to 200 C. The precipitation of an epitaxial layer formed by an interaction between a hot calcium hydroxide solution and the surface of the sphere plays an essential role in developing favorable bonding characteristics at the interfaces and in promoting the hydration of the cement matrix. It was observed that tobermorite-truscottite transformation and anorthite formation during autoclave exposure for 180 days in brine at 300 C results in slight strength reductions and increased water permeability. DOE

N88-20458# Mound Lab., Miamisburg, Ohio.
IMPROVED GLASS-CERAMIC TO METAL SEALS IN ACTUATOR AND DETONATOR APPLICATIONS WITH AN ALUMINUM-CONTAINING AUSTENITIC STAINLESS STEEL
J. C. Birkbeck, R. T. Cassidy, P. N. Fagin, and W. E. Moddeman 1987 11 p Presented at the ASME Winter Meeting, Boston, Mass., 13 Dec. 1987
(Contract DE-AC04-76DP-00053)
(DE88-004691; MLM-3478(OP); CONF-871234-8) Avail: NTIS HC A03

Requirements for the formation of a strong, hermetic seal between a glass-ceramic and a metal, in actuator and detonator applications, were reviewed. The necessary parameters are: (1) a high strength metal; (2) a match in the thermal expansion coefficient between the metal and glass-ceramic; (3) wettability of the metal by the glass; and (4) the chemical compatibility at the glass-ceramic/metal interface at sealing temperatures. An Al2O3 layer, acting as a buffer between the glass and the metal, should be included to protect the metal from the glass attack. A model was proposed and tested with an aluminum-containing alloy (899) which formed a tightly adhering Al2O3 layer when pre-sealed heated in air. This Al2O3 layer was verified by Auger electron spectroscopy and is wettable by the glass and chemically compatible with it, as seen in the optical photomicrographs. The coefficients of thermal expansion for the oxide layer and the alumina-rich glass/oxide boundary were found to be acceptable. DOE

N88-20459# Edgerton, Germeshausen and Grier, Inc., Idaho Falls, Idaho.
ULTRASONIC CHARACTERIZATION OF NON-UNIFORM POROSITY DISTRIBUTIONS IN SiC CERAMIC
K. Telschow, J. Walter, and D. Kunerth 1987 15 p Presented at the Review of Progress in Quantitative NDE, Williamsburg, Va., 21 Jun. 1987
(Contract DE-AC07-76ID-01570)
(DE88-004814; EGG-M-11187; CONF-870691-10) Avail: NTIS HC A03/MF A01

During fabrication of monolithic ceramic silicon carbide very localized regions of high porosity can be produced. This porosity often consists of a very large density of small pores. Even at wavelengths considerably larger than the pore size, significant effects can be observed in the propagation of ultrasonic waves through these materials. These effects include attenuation, scattering and changes in wave velocity and anomalous wave amplitude modulation due to the non-uniformity of the porosity distribution. This paper describes the characterization of such a porosity distribution in SiC utilizing these ultrasonic techniques and their correlation with X-ray and optical microscopy measurements. Significant effects were observed due to the nonuniformity of the porosity which resulted in enhancement of signal amplitudes greatly exceeding attenuation effects due to scattering. This unexpected result proved to be most sensitive to the boundaries of the porosity distribution and provided one of the best techniques for delineating its extent. DOE

N88-20460# Lawrence Livermore National Lab., Calif.
KINETICS OF POLYMER DECOMPOSITION
A. K. Burnham and R. L. Braun Dec. 1987 29 p
(Contract W-7405-eng-48)
(DE88-005500; UCID-21293) Avail: NTIS HC A03/MF A01

Thermal decomposition rates at heating rates ranging from 5 to 60 C/min are reported for 11 polymers. Rates were measured using a Rock Eval II apparatus, which uses a flame ionization detector to detect total evolved non-oxygenated carbon. Reaction rates were fitted to a variety of kinetic models, some involving distributions of activation energies. We found that poly(methyl methacrylate), poly(ethyl methacrylate), and poly(vinyl acetate) required two distinct reactions, which we assumed to be parallel. Many of the polymers did not fit well to any of the rate laws considered. One common problem was that the reaction profile was narrower than a first order reaction with an activation energy that matches the shift of T(sub max) with heating rate, but it was often not the correct shape to be fitted satisfactorily by an nth-order reaction. We compare our observations with results for one Green River shale, whose decomposition is also sharper than a single first-order reaction, but whose profile is compatible with a fractional-order reaction. We discuss the implications of these problems on the ability to estimate decomposition rates at greatly different thermal histories. DOE

N88-20461# Pacific Northwest Labs., Richland, Wash.
INTERFACIAL CHEMISTRY-STRUCTURE AND FRACTURE OF CERAMIC COMPOSITES
R. H. Jones, C. H. Henager, Jr., C. H. Schilling, L. H. Schoenlein, and W. J. Weber Jan. 1988 13 p Presented at the Conference on Composite Materials and Structures, Cocoa Beach, Fla., 20 Jan. 1988 Prepared in cooperation with Los Alamos National Lab., N. Mex.
(Contract DE-AC06-76RL-01830)
(DE88-005516; PNL-SA-15269; CONF-880118-1) Avail: NTIS HC A03/MF A01

The interfacial chemistry and structure of SiC/Si3N4 composites has been evaluated using TEM/STEM and AES. Nicalon SiC fiber reinforced hot-pressed Si4N4 and VLS single crystal SiC reinforced reaction-bonded silicon nitride (RBSN) have been evaluated. An amorphous carbon-graphite interface structure was observed in the Nicalon SiC fiber-reinforced material resulting from sizing used to assist fiber handling. Fiber pull-out occurred upon fracture of the composite material with the fracture apparently occurring between the amorphous and graphitic carbon layers. The flexure strength of the composite was about 1/3 that of the matrix with the degradation apparently resulting from the development of a glass phase in the grain boundaries of the Nicalon during hot pressing. The interfaces of Si3N4 matrix composites with C, BN, SiO2 coated and untreated VLS whiskers were found to vary markedly. In the RBSN composites, the C was present in the form of a fibrous graphitic structure, the BN coating was nonexistent but large facets had formed on the whiskers while the SiO2 coating was present as a discontinuous glass phase. The composite with the SiO2 coated whiskers exhibited the highest fracture strength and toughness while the material made with BN-coated whiskers exhibited the lowest values. DOE

N88-20462# Pacific Northwest Labs., Richland, Wash.
PNL-1 IMPROVED CERAMIC COMPOSITES THROUGH CONTROLLED FIBER MATRIX INTERACTION
R. H. Jones, L. H. Schoenlein, C. H. Henager, Jr., C. H. Schilling, W. J. Weber, and J. L. Bates Oct. 1987 30 p
(Contract DE-AC06-76RL-01830)
(DE88-005680; PNL-SA-15419) Avail: NTIS HC A03/MF A01

In summary, the micromechanical models of composite fracture clearly indicate the desirability of a high-strength reinforcement such as the Los Alamos National Laboratory (LANL) SiC whiskers. Also, the models suggest that fracture toughness increases with increasing reinforcement diameter, although this benefit cannot be realized if the properties of the reinforcement are not independent of diameter. Since the reinforcement diameter and preparation method for fibers or whiskers are interdependent, it may not be possible to independently vary the reinforcement diameter without also changing the strength. The micromechanical fracture models also indicate that fiber pullout is more effective for increasing the fracture toughness of ceramic composite than crack bridging with strong fibers or whiskers. Interface strengths of 10 to 100 MPa and 100 to 1000 MPa produce optimum fracture toughness and fracture strength properties for fiber- and whisker-reinforced composites, respectively. Optimization of the interface chemistry and structure of ceramic composites requires a clear correlation between the interface and mechanical properties. Preparations are under way to make this correlation for fracture strength, fracture toughness, fracture resistance, and environmental effects on slow crack growth. DOE

N88-20463# Argonne National Lab., Ill.
LIQUID ALLOYS: NEW PERSPECTIVES AND CHALLENGES
Marie Louise Saboungi, Susan R. Leonard, Gerald K. Johnson, and David L. Price Dec. 1987 6 p Presented at the NATO Advanced Study Institute on Alloy Phase Stability, Crete, Greece, 14 Jun. 1987
(Contract W-31-109-eng-38)
(DE88-005935; CONF-8706103-6) Avail: NTIS HC A02/MF A01

One of many unusual liquid semiconducting alloys, K-Pb is examined. The thermodynamic and electrical properties will be discussed and analyzed in terms of a disorder model introduced first for crystalline semiconductors. The structure of the equiatomic alloy will be presented; interpretation of the first sharp diffraction peak in the total structure factor is based on the local structures in the crystalline phase and should be viewed as an example of the interrelation between the solid and liquid properties. DOE

N88-20464# Lawrence Livermore National Lab., Calif.
ABRASION AND IMPACT RESISTANT COATINGS
W. A. Steele, P. B. Mohr, and H. R. Leider Oct. 1987 21 p
(Contract W-7405-eng-48)
(DE88-003562; UCID-20839-87-3) Avail: NTIS HC A03

The study of the application of free filamentary composites in pile-like structures and linings is aimed at cost effective alternatives to the life limiting abrasive and galling wear experienced in solid member flow systems and system elements. The basic approach is to reduce the intensity of interaction between flowing fluid and container to a level which results in little or no abrasive or fretting wear. In the case of flow borne particulates especially, the objective is to select filament materials and geometries which singly and in composite are sufficiently strong to preclude single particle (event) failure but sufficiently flexible to allow essentially damage-free passage. Early evidence is that this condition is primarily dependent on particle energy and filament strength, although there may also be fatigue, especially acoustic involvement. Our thinking to date has been on wear and acoustic fatigue resistant linings for conduit, flow control, particle control, and separation and drag resistant sealing. Both analytic and test studies have been undertaken. Initial work has been aimed at direct determination of basic characteristics of drag and damage threshold. DOE

N88-20465# Maryland Univ., College Park. Dept. of Chemistry.
ADVANCES IN X-RAY LINE PROFILE ANALYSIS TO DETERMINE MICROSTRUCTURE INFORMATION ABOUT CERAMICS
Y. Zhang, J. M. Stewart, C. R. Hubbard, and B. Morosin 1987 7 p Presented at the 1st International Conference on Ceramic Powder Processing Sciences, Orlando, Fla., 1 Nov. 1987 Prepared in cooperation with National Bureau of Standards, Washington, D.C. and Sandia National Labs., Albuquerque, N. Mex.
(Contract DE-AC04-76DP-00789)
(DE88-003938; SAND-87-3036C; CONF-8711115-1) Avail: NTIS HC A02/MF A01

In order to obtain microstructural information on many ceramic materials by X-ray diffraction line broadening analysis, both separation of overlapping lines and accurate assessment of the broadened and inherent instrumental line profiles are necessary. A profile fitting code has been developed to overcome the difficulties usually encountered when applying line profile analysis to ceramics with overlapping X-ray diffraction lines. After the separation of the overlapping lines, the usual procedure for determining the crystallite size and microstrain information is employed. The results on the peak separation by using the profile fitting code as well as the results of the size and strain for shock-modified monoclinic ZrO2 are given as examples of the application of X-ray powder diffraction profile analysis. Such a procedure should be useful for assessing similar microstructural information on other ceramic materials. DOE

N88-20466# Oak Ridge National Lab., Tenn.
MOLECULAR DYNAMICS OF LASER ABLATION OF A POLYMER COATING
D. W. Noid and S. K. Gray 1987 7 p Presented at the 3rd International Laser Science Conference, Atlantic City, N.J., 1 Nov. 1987 Prepared in cooperation with University of Northern Illinois, DeKalb
(Contract DE-AC05-84OR-21400)
(DE88-004337; CONF-871147-4) Avail: NTIS HC A02/MF A01

Large-scale molecular dynamics calculations have been carried out to simulate laser ablation on a polymer surface. The model consisted of a polyethylene chain with 400 CH4 units placed on a

polymer surface. A laser excitation was simulated by giving a small portion of the polymer chain a nonequilibrium momentum distribution. The excitation energy threshold for fragmentation of the polymers was found to be quite large, owing to the tendency of the system to transfer large amounts of vibrational energy along the chain. DOE

N88-20467# Sandia National Labs., Albuquerque, N. Mex.
A NEW POLYMER-BASED HYDROGEN GETTER
L. R. Gilliom 1987 4 p Presented at the Fall Meeting of the Materials Research Society, Boston, Mass., 30 Nov. 1987
(Contract DE-AC04-76DP-00789)
(DE88-004538; SAND-87-1621C; CONF-871124-26) Avail: NTIS HC A02/MF A01

Styrene-butadiene triblock copolymer PS-PB-PS was hydrogenated in the bulk using the Crabtree catalyst (Ir(COD)(py)(tcyp))PF6 (COD = 1,5-cyclooctadiene, py = pyridene, tcyp = tricyclohexylphosphine). Since this polymer/catalyst mixture reacts rapidly with hydrogen at ambient temperature and low hydrogen pressures, it should act as an effective hydrogen getter. DOE

N88-20468# Mound Lab., Miamisburg, Ohio.
PROCESSING OF GLASS TO ALUMINUM (LOW MELTING METALS) SEALS VIA AN INJECTION MOLDING TECHNIQUE
D. P. Kramer, R. T. Massey, and D. L. Halcomb 1987 19 p Presented at the ASME Winter Meeting, Boston, Mass., 13 Dec. 1987
(Contract DE-AC04-76DP-00053)
(DE88-004689; MLM-3476(OP); CONF-871234-10) Avail: NTIS HC A03/MF A01

Injection molding-sealing is an innovative processing technique useful in the fabrication of complex glass or glass-ceramic-to-metal seals which use low melting metals such as aluminum. During injection molding-sealing, molten glass, which may have a higher melting temperature than that of the metal parts, is injected under pressure into the metal parts while they are held in a mold. The process, which for the first time allows the formation of seals with metals that have a lower melting temperature than the glass, allows the fabrication of seals of complex geometry. DOE

N88-20469# Dow Chemical Co., Walnut Creek, Calif.
IMPROVE THE LIFETIME OF THE HOLLOW FIBER SODIUM SULFUR CELL Final Report
P. Pierini, C. Nielsen, and F. Tsang Aug. 1987 103 p
(Contract DE-AC03-76SF-00098)
(DE88-004881; LBL-21343) Avail: NTIS HC A06/MF A01

This report is a continuation of work directed towards identifying potentially superior glass compositions for use as an electrolyte in the Dow sodium-sulfur cell. Prior work identified a glass candidate (T806) having superior resistance to metallic sodium and sodium polysulfides. However, lifetime testing of this glass was disappointing: mean lifetimes are only a few weeks for T806 cells versus ca. six months for cells employing the standard glass (D406). Thermodynamic calculations showed possible reactivity between the above mentioned glasses and sulfur. Work was undertaken in this report to test the hypothesis that T806 cells were failing sooner because of a more rapid reaction with sulfur. Glass-sulfur reactivities were measured at 300 C and 400 C by means of a sensitive ion chromatography method for fifteen glass compositions also in the ternary system: sodium oxide/boron trioxide/silicon dioxide system. Detailed comparisons of sulfur reactivities for T806 and D406 glass compositions permit the rejection of the above hypothesis. In addition, no clearly superior glasses of acceptable sodium ion conductivity were identified with respect to sulfur corrosion. Additional experiments are suggested that may shed light on the early failure of cells using T806 glass as the electrolyte. Attention is drawn to the possible involvement of the cathode foil, molybdenum coated aluminum foil. Specific experiments designed to test the influence of cathode foil are outlined. DOE

N88-20470# Sandia National Labs., Albuquerque, N. Mex.
INTEGRAL EQUATION THEORY OF HOMOPOLYMER MELTS
J. G. Curro and K. S. Schweizer 1987 25 p Presented at the Workshop on Neutron Scattering, Los Alamos, N. Mex., 3 Nov. 1987
(Contract DE-AC04-76DP-00789)
(DE88-005304; SAND-87-2333C; CONF-871190-3) Avail: NTIS HC A03/MF A01

A general theory is developed for the equilibrium structure of dense polymer melts. This theory is based on an integral equation approach developed for molecular liquids. We are able to construct a tractable formalism for the polymer problem by employing the fact that a polymer molecule in a melt is ideal. This leads to a set of integral equations for the intermolecular radial distribution functions. In the case of a long linear chain this set approximately reduces to a single integral equation which is solved numerically for the case of Gaussian and freely-jointed chain intramolecular statistics with repeat units interacting via hard core repulsions. From this solution we obtained the radial distribution function, structure factor, and compressibility as functions of liquid density and degree of polymerization. Unlike the random phase approximation (RPA) approach, the present theory allows for density fluctuations. These density fluctuations, which decay on a length scale comparable to a few monomer units, are crucial for the calculation of the structure factor and thermodynamic properties such as the equation-of-state of the polymer fluid. Generalizations of the present theory to include chain stiffness effects and attractive interactions are possible. DOE

N88-20471# Sandia National Labs., Albuquerque, N. Mex.
INTEGRAL EQUATION THEORY OF POLYMER BLENDS
K. S. Schweizer and J. G. Curro 1987 18 p Presented at the Workshop on Neutron Scattering, Los Alamos, N. Mex., 3 Nov. 1987
(Contract DE-AC04-76DP-00789)
(DE88-005305; SAND-87-2334C; CONF-871190-2) Avail: NTIS HC A03/MF A01

An off-lattice microscopic statistical mechanical theory of the equilibrium properties of polymer mixtures is developed based on modern integral equation methods. A rigorous derivation of the RPA scattering function is presented along with a fully microscopic, exact formula for the effective chi-parameter measured in SANS experiments. Numerical results for a hard core Gaussian polymer binary blend are presented. Chi is found to be a sensitive function of concentration, packing fraction, molecular weight, and structural asymmetry. DOE

N88-20472# Michigan Univ., Ann Arbor. Dept. of Materials Science and Engineering.
MICROMECHANICAL AND MICROSTRUCTURAL STUDIES OF CERAMIC SUPERPLASTICITY Progress Report, 1 May 1987 - 31 Jan. 1988
31 Jan. 1988 12 p
(Contract DE-FG02-87ER-45302)
(DE88-005793; DOE/ER-45302/1) Avail: NTIS HC A03/MF A01

Superplasticity of zirconia-mullito composites was studied. The strain rate of these composites decreases with the mullite fraction. YBa2Cu3O(sub x) was found to produce pronounced textures upon being hot pressed and extruded. DOE

N88-20473# Argonne National Lab., Ill.
RECENT DEVELOPMENTS IN NONDESTRUCTIVE EVALUATION FOR STRUCTURAL CERAMICS
W. A. Ellingson, R. A. Roberts, M. W. Vannier, J. L. Ackerman, B. D. Sawicka, S. Gronemeyer, and R. J. Kriz May 1987 29 p
(Contract W-31-109-eng-38)
(DE88-005889; ANL/FE-87-2) Avail: NTIS HC A03/MF A01

Advanced nondestructive evaluation methods are being developed to characterize ceramic materials and allow improvement of process technology. If one can determine porosity, map organic binder/plasticizer distributions, measure average through-volume and in-plane density, as well as detect inclusions, then process and machine operations may be modified to enhance the reliability of ceramics. Two modes of X-ray tomographic imaging - advanced

film tomography and computed tomography - are being developed to provide flaw detection and density profile mapping capability. Nuclear magnetic resonance imaging is being developed to determine porosity and map the distribution of organic binder/plasticizer. Ultrasonic backscatter and through-transmission are being developed to measure average through-thickness densities and detect surface inclusions. DOE

N88-20474# Argonne National Lab., Ill.
X-RAY COMPUTED TOMOGRAPHY FOR STRUCTURAL CERAMIC APPLICATIONS: BEAM HARDENING CORRECTIONS
W. A. Ellingson, E. Segal, and M. W. Vannier May 1987 29 p
(Contract W-31-109-eng-38)
(DE88-005891; ANL-87-24) Avail: NTIS HC A03/MF A01

Beam hardening (BH), caused by the energy dependence of X-ray attenuation in materials, reduces the reliability of images generated by computed tomographic (CT) when polychromatic X-ray sources are used. The magnitude of the BH effect was calculated, and four different approaches to BH correction for CT imaging of ceramics were investigated: the water bag approach, prehardening of the beam by use of a filter, linearization correction, and dual-energy methods. The dual-energy approach appears to be a promising means of BH correction for CT imaging of ceramics. DOE

N88-20475# Illinois Univ., Urbana. Materials Research Lab.
PROCESSING OF NANOPHASE CERAMICS
H. Hahn, J. A. Eastman, and R. W. Siegel Nov. 1987 11 p Presented at the 1st International Conference on Ceramic Powder Processing Sciences, Orlando, Fla., 1 Nov. 1987 Prepared in cooperation with Argonne National Lab., Ill.
(Contract W-31-109-eng-38)
(DE88-005985; CONF-8711115-5) Avail: NTIS HC A03/MF A01

The gas-condensation method for the production of small particles in the size range of 1 to 10 nm has recently enabled the synthesis of a new class of ultrafine-grained, nanophase ceramics. The first demonstrations of the synthesis of nanophase TiO2 have shown that these ceramics, while already rather well bonded on compaction at room temperature, sinter rapidly above 500 C, with only small increases in grain size, leading to Vickers hardness and fracture toughness values comparable to or greater than those of coarser-grained compacts, but at some 400 to 600 C lower temperatures and without the need for sintering aids. DOE

N88-20476*# National Aeronautics and Space Administration, Washington, D.C.
EVALUATION OF FLAMMABILITY FOR CABLE-LIKE POLYMERS
Tuneo Mikado and Kazuo Akita Apr. 1988 16 p Transl. into ENGLISH from Bulletin of Japanese Association of Fire Science and Engineering (Japan), v. 29, no. 1, 1979 p 17-25 Transl. by Scientific Translation Service, Santa Barbara, Calif.
(Contract NASw-4307)
(NASA-TT-20225; NAS 1.77:20225) Avail: NTIS HC A03/MF A01 CSCL 11B

A new test method is developed for the flammability of insulated electric cables as well as polymers formed in the cables. The rate of downward flame spread along the polymer surface is measured by a technique in which the flame is stopped at a particular position by winding up the cable at the same speed as the flame spreading rate, with external preheating by an electric furnace having oxidative gas flow. The polymer burns continuously without change of flame condition and the rate is obtained from the winding speed of the cable. A flame spread equation relates the flame spreading rate (V) of the cable-like polymer to O concentration (Yo) and the atmosphere, the preheating temperature, and the pyrolysis temperature for polymer burning. Plotting log V vs. log Yo for experimental results allows evaluation of the flammability of polymers, with discrimination between the effects of O concentration, heating temperature, and specimen shape. Results with various types of PVC electrical cable indicated the validity of the method. Application of the method to the cables in groups showed a flame retardation behavior different from the case of a single cable, in a atmosphere of high O concentration. Author

N88-20477*# National Aeronautics and Space Administration, Washington, D.C.
SAFETY RESEARCH OF INSULATING MATERIALS OF CABLE FOR NUCLEAR POWER GENERATING STATION
C. K. Lee, J. H. Choi, Y. K. Kong, and H. S. Chang Mar. 1988 49 p Transl. into ENGLISH of report (Seoul, North Korea, Korea Advanced Energy Research Inst.) p 1-48 Original language document was announced as N85-73183 Transl. by Scientific Translation Service, Santa Barbara, Calif.
(Contract NASw-4307)
(NASA-TT-20202; NAS 1.77:20202; KAERI/RR-325/81) Avail: NTIS HC A03/MF A01 CSCL 11B

The polymers PE, EPR, PVC, Neoprene, CSP, CLPE, EP and other similar substances are frequently used as insulation and protective covering for cables used in nuclear power generating stations. In order to test these materials for flame retardation, environmental resistance, and cable specifications, they were given the cable normal test, flame test, chemical tests, and subjected to design analysis and loss of coolant accident tests. Material was collected on spark tests and actual experience standards were established through these contributions and technology was accumulated. Author

N88-20478# Materials Research Labs., Melbourne (Australia).
EXAMINATION OF POLYSULFIDE SEALANTS BY SCANNING ELECTRON MICROSCOPY
W. Mazurek and V. M. Silva Dec. 1987 23 p
(MRL-R-1096; AR-005-193) Avail: NTIS HC A03/MF A01

A procedure was developed for the examination of polysulfide sealants by scanning electron microscopy. This procedure was applied to manganese dioxide and dichromate-cured elastomers. Calcium carbonate filler was identified in both types of sealants and the particle size was found to be less than 4 microns. A technique was developed for the removal of the surface calcium carbonate exposing other solid additives. Among these, manganese dioxide was most obvious due to the large particle size and abundance. The presence of chromium containing particles could not be established and in practical terms it can be considered as a solution in the polysulfide. This implies a homogeneous phase reaction between the dichromate curing agent and the prepolymer and consequently a greater likelihood of a more complete curing of the polymer than that effected by manganese dioxide. Author

N88-20479*# National Aeronautics and Space Administration, Washington, D.C.
AGING PROPERTIES OF CABLE POLMERS (2)
P. Chevassus Apr. 1988 32 p Transl. into ENGLISH from Propiedades de Envejecimiento de los Polimeros en Cables (2), Revista de Plasticos Modernos,(France), no. 287, May 1980 p 551-554, 559-564 Transl. by SCITRAN, Inc., Santa Barbara, Calif.
(Contract NASw-4307)
(NASA-TT-20228; NAS 1.77:20228) Avail: NTIS HC A03/MF A01 CSCL 11B

Notable improvement has been made in the past 20 years through the perfection of new polymers or through combined use of stabilizing agents making use of synergic action. The contribution of chemists in the field of insulation has been twofold. First, it has permitted a better understanding of the relationships between dielectric behavior (dielectric constant, the Debye theory) and chemical structure; and second, it has developed procedures to permit extension of useful life. Author

N88-20480*# National Aeronautics and Space Administration, Washington, D.C.
LUBRICATING PROPERTIES OF MOLYBDENUM DISULFIDE. PART 3: PERFORMANCE OF MOLYBDENUM DISULFIDE-CONTAINING OILS IN FLUID LUBRICATION
Norimune Soda and Yoshinori Miyahara May 1988 21 p Transl.

into ENGLISH from Junkatsu (Japan), v. 21, no. 2, 1976 p 90-97 Transl. by Scientific Translation Service, Santa Barbara, Calif.
(Contract NASw-4307)
(NASA-TT-20156; NAS 1.77:20156) Avail: NTIS HC A03/MF A01 CSCL 11H

The lubricating properties of a straight mineral oil with and without MoS2 powder were studied. Bearing testers of thrust-collar type and of journal bearing type were used for thin- and fluid-film conditions, respectively. The effectiveness of the MoS2 powder in the oil differed depending on the conditions of the rubbing surfaces. For fluid film conditions, considerable effects of the MoS2 were observed, in contrast to the thin-film cases. The addition of MoS2 powder was effective only when the lubricant film was formed between surfaces thickly enough to allow the inflow of MoS2 particles. Author

N88-20502# Joint Publications Research Service, Arlington, Va.
RECOMMENDATIONS ON DEVELOPING POLYCRYSTALLINE ALUMINA FIBER
Yulian Lin and Shouwei Xing *In its* JPRS Report: Science and Technology. China 7 Jul. 1987 p 15-17 Transl. into ENGLISH from Naihuo Cailiao (Luoyang, People's Republic of China), no. 1, 20 Jan. 1987 p 47-51 (For primary document see N88-20501 13-31)
Avail: NTIS HC A06/MF A01

28 PROPELLANTS AND FUELS

Includes rocket propellants, igniters, and oxidizers; their storage and handling procedures; and aircraft fuels.

For related information see also *07 Aircraft Propulsion and Power, 20 Spacecraft Propulsion and Power,* and *44 Energy Production and Conversion.*

N88-20481# General Accounting Office, Washington, D. C. Resources, Community and Economic Development Div.
ALTERNATIVE FUELS: INFORMATION ON DOE'S (DEPARTMENT OF ENERGY'S) METHANOL VEHICLE DEMONSTRATION PROGRAM
Oct. 1987 20 p
(PB88-118203; GAO/RCED-88-38BR; B-226783) Avail: NTIS HC A03/MF A01 CSCL 07D

The briefing report presents information on the status of the Department of Energy (DOE) program, which was begun in October 1984 to introduce methanol vehicles into the civilian federal fleet. Specifically, the report discusses why other federal agencies have not participated in the program, DOE's experience in acquiring and operating demonstration fleets, coordination between the DOE and DOD programs, and a recent initiative to acquire flexible-fueled vehicles that can operate on gasoline, methanol, or a combination of both fuels. GRA

N88-20482# Naval Surface Weapons Center, Silver Spring, Md.
SYNTHESIS OF ENERGETIC MATERIALS Annual Progress Report, 1 Jan. - 31 Dec. 1986
M. Chaykovsky and W. M. Koppes Mar. 1987 16 p
(DA Proj. RR0-24)
(AD-A189115) Avail: NTIS HC A03/MF A01 CSCL 07C

The chemistry of the 2,6-diazabicyclooctane ring system was studied toward the synthesis of tetra- and hexa-substituted derivatives. Stable dinitro derivatives were prepared but attempts to prepare tetranitro derivatives by oxidative nitration were unsuccessful, and work on the diazabicyclooctanes was terminated. Methylenedinitramine (MEDINA) was successfully condensed with glyoxal in acetic anhydride to give a substitute dinitroimidazolidine which shows promise as a precursor for the synthesis of bicyclo HMX. Trichloroacetamidine condensed with glyoxal and oxalyl chloride to give a trichloromethyl substituted dihydroxyimidazoline and imidazolinedione respectively. The imidazoline was unstable and could not be converted into the bistrichloromethyl substituted tetraazabicyclooctane ring system for further condensation with trichloroacetamidine. The stable imidazolinedione, on the other hand, is a potential intermediate for such a condensation reaction. Trihalomethyl-bisformamides and bisacetamides are also potential precursors for this substituted bicyclic ring system. The trihalomethyl groups should precursors for this substituted bicyclic ring system. The trihalomethyl groups should stabilize the ring during nitrolysis reactions leading to the bicyclo-HMX system. GRA

N88-20483# Pennsylvania State Univ., University Park. Dept. of Mechanical Engineering.
LASER IGNITION OF NITRAMINE COMPOSITE PROPELLANTS AND CRACK PROPAGATION AND BRANCHING IN BURNING SOLID PROPELLANTS Final Report, 1 Jan. 1986 - 31 Aug. 1987
K. K. Kuo, J. U. Kim, J. Nimis, J. Smedley, and J. M. Char Oct. 1987 196 p
(Contract N00014-79-C-0762)
(AD-A189260) Avail: NTIS HC A09/MF A01 CSCL 19A

Two major tasks performed during the investigation were: (1) laser ignition of nitramine-based composite propellants using a high-powered CO2 laser in (2) crack propagation and branching in burning solid propellants. The laser ignition of a series of RDX-based composite propellants was studied theoretically and experimentally. A comprehensive model for the radiative ignition of the nitramine composite propellants was formulated. The theoretical model was solved numerically. A radiative ignition test setup employing a high-powered CO2 laser was designed and constructed to study ignition characteristics of a series of RDX-based nitramine composite propellants. Interactions between the infrared laser beam and nitramine composite propellants revealed a number of interesting processes. The laser ignition of composite propellants involves many complex thermophysio-chemical processes including gasification, initiation of a luminous flame, propagation of the flame, and chemical reactions near the sample surface as well as heat conduction in solid phases. In general, the delay time based on the onset of light emission increases monotonically with the increase of incident laser energy flux. GRA

N88-20484# Ashland Petroleum Co., Ky.
AVIATION TURBINE FUELS FROM TAR SANDS BITUMEN AND HEAVY OILS. PART 3: LABORATORY SAMPLE PRODUCTION Interim Technical Report, 1 Jul. 1983 - 30 Sep. 1986
H. F. Moore, C. A. Johnson, R. M. Benslay, and W. A. Sutton Dec. 1987 89 p
(Contract F33615-83-C-2301)
(AD-A189278; AFWAL-TR-84-2070-Pt-3) Avail: NTIS HC A05/MF A01 CSCL 21D

The purpose of this research and development project is to provide sample quantities of aviation turbine fuel derived from tar sands and heavy oil feedstocks for testing and evaluation in programs sponsored by the Air Force Wright Aeronautical Laboratories (AFWAL). Samples of specification JP-4 Mil-T-5624L, JP-8 Mil-T-83133A, and variable quality JP-4 samples were produced via pilot plant operations. Data generated from Phases 1, 2, and 3, were used to: (1) optimize the processing scheme, (2) generate process material and energy balances for a commercial sized plant, and (3) provide a detailed final flow diagram of the processing scheme. A final economic analysis was performed based on all contract data available. GRA

N88-20485# Mueller Associates, Inc., Baltimore, Md.
STATUS OF ALCOHOL FUELS UTILIZATION TECHNOLOGY FOR HIGHWAY TRANSPORTATION: A 1986 PERSPECTIVE. VOLUME 2: COMPRESSION IGNITION ENGINES
Jan. 1988 442 p
(Contract DE-AC05-84OR-21400)
(DE88-006059; ORNL/Sub-85-22007/3-Vol-2) Avail: NTIS HC A19/MF A01

The current status of the technologies of alcohol utilization in highway transportation diesel engines is reviewed. The use of

methanol, ethanol, and certain of their derivatives in diesel-engine-powered vehicles is treated in this volume. Volume 1 covered alcohol utilization in vehicles powered by spark ignition engines. The results of engine, vehicle, and fuels testing are summarized. The topics of fuel properties, power output, fuel consumption, thermal efficiency, ignition delay, rate of pressure rise, engine noise, operability, exhaust emissions, smoke, materials compatibility, engine wear, and safety are discussed based on the data available at this time. The status of the technology at the time of the last comprehensive survey (1981) is summarized and discussed. Significant advances made since that time are delineated, as are remaining information gaps and areas in which more extensive investigation is still needed. DOE

N88-20486# Materials Research Labs., Melbourne (Australia).
A COMPARATIVE ASSESSMENT OF US AND UK EXPLOSIVES QUALIFIED AS REPLACEMENTS FOR TETRYL
Robert J. Spear and Victor Nanut Nov. 1987 27 p
(MRL-R-1094; AR-005-190) Avail: NTIS HC A03/MF A01

Three U.K. and seven U.S. production formulations qualified as replacments for tetryl in fuzes have been obtained. Characterization of powders, i.e., Rotter impact sensitivity, temperature of ignition, vacuum thermal stability and electrostatic spark sensitivity, and the shock sensitivity of pressed charges, has been carried out at the Materials Research Laboratories. Results compared well with U.K. and U.S. published data, producing probably the most complete comparative set published for production booster explosives. Author

N88-20487# Materials Research Labs., Melbourne (Australia).
A PYROTECHNIC DELAY IGNITION SYSTEM FOR A SUBMARINE LAUNCHED MARINE SIGNAL
B. W. Whiffen Sep. 1987 22 p
(MRL-R-1079; AR-005-170) Avail: NTIS HC A03/MF A01

This report describes the development of a delay ignition system for a submarine launched marine signal. The igniter, which incorporates a pyrotechnic delay element, was designed to transfer ignition from the payload expelling charge to the flare handle. The design eliminates ignition failures caused by water plumes extinguishing the igniters as the flare payload assembly is ejected from the signal canister. Author

N88-20488# Materials Research Labs., Melbourne (Australia).
A DEFECT INVESTIGATION OF THUNDERFLASH MK N5 (NAVY)
Scott Murdoch Sep. 1987 11 p
(MRL-TN-522; AR-005-164) Avail: NTIS HC A03/MF A01

This technical note describes the examination of Thunderflash devices which had been stored in sealed metal ammunition boxes. The ammunition boxes had exhibited severe swelling during storage and this was found to be due to a reaction between the photoflash composition in the device and moisture. The result of this reaction was the pressurization of the boxes with hydrogen gas. Author

N88-20489# Materials Research Labs., Melbourne (Australia).
RECOMMENDED REPLACEMENTS FOR TETRYL IN AUSTRALIAN PRODUCTION FUZES AND RELATED ORDNANCE
Robert J. Spear, Victor Nanut, Lance D. Redman, and Ian J. Dagley Nov. 1987 33 p
(MRL-R-1089; AR-005-184) Avail: NTIS HC A03/MF A01

The final phase of a study into RDX-based formulations suitable for replacement of tetryl in Australian ordnance is described. Three formulations using readily available AC629 emulsifiable polyethylene wax and processible on Australian production equipment are identified. It is recommended that pilot batch production and qualification of RDX/AC629 98.75:1.25 for leads and small pellets, RDX/AC629 96.5:3.5 for large boosters and RDX/AC629/zinc stearate/graphite 98.0:1.25:0.5:0.25 for high production rate automatic pelletting be carried out. Performance testing has included propagation in small channels, fuze train function in Fuze Mk 162 and production automatic pelletting. U.S. and U.K. qualified formulations have been similarly characterized and are compared. Author

N88-20490# Materials Research Labs., Melbourne (Australia).
SOME PROPERTIES OF AUSTRALIAN PRODUCED EXPLOSIVE COMPOSITION H-6
L. McVay and T. Bussell Oct. 1987 33 p
(MRL-TN-525; AR-005-189) Avail: NTIS HC A03/MF A01

This report describes an investigation to characterize the physical nature of cast H-6 and assess its stability and explosive properties. Scanning electron and optical microscopes were used to determine the aluminum and RDX distribution in the TNT matrix, while explosive stability was assessed from the results of vacuum stability and temperature of ignition tests and differential scanning calorimetry. H-6 sensitivity was assessed from the results of the gap test, Rotter impact test, train test, and jet sensitivity test. Some detonation parameters were determined experimentally and compared to BKW code estimates. The study showed that Australian produced H-6 exhibited similar stability and sensitivity characteristics to Composition B and that the results supported data published for equivalent U.S. tests. The aluminum was shown to be well distributed within the RDX/TNT system with only a small tendency to aggregate. Author

29 MATERIALS PROCESSING

Includes space-based development of products and processes for commercial applications.

For biological materials see *55 Space Biology*.

No abstracts in this category.

31 ENGINEERING (GENERAL)

Includes vacuum technology; control engineering; display engineering; cryogenics; and fire prevention.

N88-20491*# SatCon Technology Corp., Cambridge, Mass.
MODELLING AND CONTROL OF AN ANNULAR MOMENTUM CONTROL DEVICE
James R. Downer and Bruce G. Johnson NASA Apr. 1988 111 p Prepared in cooperation with Draper (Charles Stark) Lab., Inc., Cambridge, Mass.
(Contracts NAS9-16023; NAS9-17560)
(NASA-CR-4138; NAS 1.26:4138) Avail: NTIS HC A06/MF A01 CSCL 13I

The results of a modelling and control study for an advanced momentum storage device supported on magnetic bearings are documented. The control challenge posed by this device lies in its dynamics being such a strong function of flywheel rotational speed. At high rotational speed, this can lead to open loop instabilities, resulting in requirements for minimum and maximum control bandwidths and gains for the stabilizing controllers. Using recently developed analysis tools for systems described by complex coefficient differential equations, the closed properties of the controllers were analyzed and stability properties established. Various feedback controllers are investigated and discussed. Both translational and angular dynamics compensators are developed, and measures of system stability and robustness to plant and operational speed variations are presented. Author

N88-20492# SpecTran Corp., Sturbridge, Mass.
SBIR-LONG FLUORIDE FIBER Final Technical Report
Raymond E. Jaeger and Lubos J. Vacha Aug. 1987 38 p
(Contract F19628-86-C-0124)
(AD-A188595; RADC-TR-87-84) Avail: NTIS HC A03/MF A01 CSCL 11B

This report summarizes results obtained under a program aimed at develcping new techniques for fabricating long lengths of heavy

metal fluoride glass (HMFG) optical fiber. A new method for overcladding conventional HMFG preforms with a low melting oxide glass was developed, and improvements in the rotational casting method were made to increase preform length. The resulting composite glass canes consist of a fluoride glass overcoat layer to enhance strength and chemical durability. To show feasibility, prototype optical fiber preforms up to 1.6 cm in diameter with lengths of 22 cm were fabricated. These were drawn into optical fibers with lengths up to 900 meters. GRA

N88-20493# Carnegie-Mellon Univ., Pittsburgh, Pa. Dept. of Psychology.
UNDERSTANDING MACHINES FROM TEXT AND DIAGRAMS
Mary Hegarty and Marcel A. Just Dec. 1987 27 p
(Contract N00014-85-K-0584; DA Proj. RR0-4206)
(AD-A189034; Rept-87-9-ONR) Avail: NTIS HC A03/MF A01 CSCL 05I

Instructional materials typically use both text and diagrams to explain how machines work. In this paper we give an account of what information is involved in understanding a mechanical device and the role that diagrams might play in communicating this information. We propose a model of how people read a text and inspect an accompanying diagram which states that people inspect diagrams for three reasons: (1) to form a representation of information read in the text, (2) to reactivate information that has already been represented, and (3) to encode information that is absent from the text. Using data from subjects' eye fixations while they read a text and inspected an accompanying diagram, we find that low-ability subjects need to inspect diagrams more often than high-ability text. The data also suggest that knowledge of what is relevant in a diagram might be a prerequisite for encoding new information from a diagram. Instructional materials typically use both text and diagrams to explain how machines work. In this paper we give an account of what information is involved in understanding a mechanical device and the role that diagrams might play in communicating this information. We propose a model of how people read a text and inspect an accompanying diagram which states that people inspect diagrams for three reasons: (1) to form a representation of information read in the text; (2) to reactivate information that was alsready represented, and *3) to encode information that is absent from the text. Uinsg data from subjects' eye fixations while they read a text and inspected an accompanying diagram, we find that low-ability subjects need to inspect diagrmas more often than high-ability tesxt. The data also suggest that knowledge of what is relevant in a diagram might be a prerequisite and encoding information on a diagram. GRA

N88-20494# Army Foreign Science and Technology Center, Charlottesville, Va.
FEASIBILITY REPORT: OPERATION OF LIGHT AIR CUSHION VEHICLE AT MCMURDO SOUND, ANTARCTICA Letter Report
J. S. Dibbern 6 Feb. 1987 13 p
(AD-A189057) Avail: NTIS HC A03/MF A01 CSCL 13F

This report explores the viability of the use of an air cushion vehicle (ACV) or hovercraft to perform logistic and scientific support in the area of McMurdo Station, Antarctica. After a review of personnel assets and facilities at McMurdo Station to support the ACV plus a reconnaissance of the five major routes selected, it appears that an air cushion vehicle in the 1 to 1 1/2 ton payload class would be of significant value to support operations. It would reduce transit times for surface vehicle traverses on the routes selected and reduce requirements for expenditure of helicopter flight time in others. Of major significance is the ability to handle passenger/shuttle requirements between the Scott Base transition and Williams Field Skiway. Use of the ACV for high frequency passenger operations would help preserve the snow road for cargo operations during periods of road deterioration. GRA

N88-20495# Joint Publications Research Service, Arlington, Va.
JPRS REPORT: SCIENCE AND TECHNOLOGY. CHINA Abstracts Only
12 Feb. 1988 150 p Transl. into ENGLISH from various Chinese articles
(JPRS-CST-88-003) Avail: NTIS HC A07/MF A01

Articles and summaries from the open literature are presented in the areas of aerospace science, applied sciences, earth sciences, life sciences, and physical sciences. For individual titles, see N88-20496 through N88-20500.

N88-20496# Joint Publications Research Service, Arlington, Va.
SIMULATION OF EFFECT OF ANTI-RADAR STEALTH PRINCIPLE Abstract Only **c32**
Borao Zhao, Shuchen Xing, and Chunyi Li *In its* JPRS Report: Science and Technology. China 12 Feb. 1988 p 1 Transl. into ENGLISH from Xitong Gongcheng Lilun Yu Shijian (Beijing, People's Republic of China), v. 7, no. 1, 1987 p 43-48 (For primary document see N88-20495 13-31)
Avail: NTIS HC A07/MF A01

The paper presents simulation methods and results of the anti-radar stealth principle, proving that anti-radar stealth aircraft can drastically reduce the combat efficiency of an air defense radar system. In particular, when anti-radar stealth aircraft are coordinated with jamming as a self-defense soft weapon, the discovery probability, response time and hit rate of the air defense radar system are much lower, with extensive reduction in jamming power and maximum exposure distance of self-defense and long-range support. The paper describes an assumed combat situation and construction of a calculation model for the aircraft survival rate, as well as simulation results and analysis. Four figures show an enemy bomber attacking an airfield, as well as the effects of the radar effective reflecting surface on discovery probability, guidance radius, aircraft survival and exposure distance (for long-range support and jamming). Author

N88-20497# Joint Publications Research Service, Arlington, Va.
ADAPTIVE CONTROL OF SCIENTIFIC BALLOON-BORNE GONDOLA ATTITUDE Abstract Only **c02**
Yan Yan *In its* JPRS Report: Science and Technology. China 12 Feb. 1988 p 27 Transl. into ENGLISH from Kongjian Kexue Xuebao (Beijing, People's Republic of China), v. 7, no. 4, Oct. 1987 p 262-271 (For primary document see N88-20495 13-31)
Avail: NTIS HC A07/MF A01

The uncertainty of parameters of the mathematical model for the control system of a balloon-borne gondola attitude is analyzed. The effects of this uncertainty on the system performance are also verified through digital simulations and experiments. In searching for the ideal control characteristics, a model reference adaptive control for the gondola attitude is developed based on Popov's hyperstability theory. This paper presents the discrete adaptive algorithm which gives time varying adaptive gain, and a large number of digital simulations are conducted accordingly. The results show the advantages of this new method over the traditional one in coping with problems such as parameter variations over a wide range, unknown parameters and nonlinearities. The new approach also proves to have higher adaptive speed and is easier to implement than other adaptive control methods. Author

N88-20498# Joint Publications Research Service, Arlington, Va.
ANALYSIS OF SPECTRAL REFLECTANCE CHARACTERISTICS OF TARGETS UNDER SATELLITES AND AUTOMATIC CLOUD RECOGNITION Abstract Only **c43**
Li Wang *In its* JPRS Report: Science and Technology. China 12 Feb. 1988 p 28 Transl. into ENGLISH from Kongjian Kexue Xuebao (Beijing, People's Republic of China), v. 7, no. 4, Oct. 1987 p 321-326 (For primary document see N88-20495 13-31)
Avail: NTIS HC A07/MF A01

A method for real-time automatic classification of targets and the automatic control of camera shutters is discussed. A physical model computing the radiance is presented, the influences of the atmosphere are considered, and the spectral reflectance characteristics of five kinds of targets are analyzed. The radiance of 34 targets under 9 different atmospheric conditions is computed with the model. The best wavebands and also classification functions and classification flow diagrams for five kinds of targets are determined. The problem involving distinguishing clouds from

non-clouds is studied. Ten LANDSAT MSS pictures are measured with the TD504 densimeter, with the radiance distribution chart similar to the calculation results. A discussion is also presented regarding ways to realize the real-time automatic recognition of clouds on the satellite. Author

N88-20499# Joint Publications Research Service, Arlington, Va.
ORBIT ACCURACY REQUIREMENT OF GPS FOR PRECISE POSITIONING AND ORBIT DETERMINATION WITHIN LOCAL AREA Abstract Only **c13**
Qifeng Xu *In its* JPRS Report: Science and Technology. China 12 Feb. 1988 p 81 Transl. into ENGLISH from Tianwen Xuebao (Beijing, People's Republic of China), v. 28, no. 3, Sep. 1987 p 226-236 (For primary document see N88-20495 13-31)
Avail: NTIS HC A07/MF A01

The Global Positioning System (GPS) provides a new possibility for solving some problems relating to geodesy and geodynamics. As one powerful approach, the interferometric technique can be used for precise positioning without any knowledge of the precise code. As a matter of fact, it is difficult to get the ephemeris with a suitable accuracy, which is necessary for data processing. Therefore, the author discusses: (1) required accuracy of satellite position for precise positioning, and (2) satellite orbit accuracy obtainable within a local area, such as China. Currently, an empirical formula is applied to estimate the influence of orbit error on baseline determination. In this paper an analytical formula is derived and some simulations are given. These show that the analytical formula is more precise than the empirical formula. Then, according to the formula, an appropriate orbit accuracy is obtained through statistics within the China area. The advantages of GPS satellite distribution for orbit determination within a local area are discussed. Then the mathematical model of GPS orbit improvement using the interferometric technique and some simulation results relating to the geographic circumstances of China are given. These show that the satellite orbit obtained within China is sufficient for baseline determination with an accuracy of 0.000001 or better. Author

N88-20500# Joint Publications Research Service, Arlington, Va.
ON ERROR EQUATIONS FOR DETERMINING EARTH ROTATION PARAMETERS WITH VLBI NETWORK Abstract Only **c46**
Yifei Xia *In its* JPRS Report: Science and Technology. China 12 Feb. 1988 p 82 Transl. into ENGLISH from Tianwen Xuebao (Beijing, People's Republic of China), v. 28, no. 3, Sep. 1987 p 282-287 (For primary document see N88-20495 13-31)
Avail: NTIS HC A07/MF A01

In this paper the partial derivative matrix in the error equation for determining the Earth's rotation parameters with the VLBI network is described and the effect of the functional parameter constraint on solving the Earth's rotation parameters is discussed. It is pointed out that the expression for the delay and delay rate for computing partial derivatives should be in explicit function form of source position parameters in the space-fixed coordinate system and the baseline parameters in the body-fixed coordinate system. If the following expression of delay is adopted: tau = (-B/c)(sin psi sub B sin delta + cos psi sub B cos delta cos (S sub G + lambda sub B - alpha)), then the Celestial Ephemeris Pole will be used as the uniform pole for the space-fixed and body-fixed coordinate systems. The baseline parameters and clock polynomial coefficients must be examined before determination of the Earth's rotation parameters since they correlate highly. The functional parameters constraint imposed in the least squares adjustment may reduce the correlation of the Earth's rotation parameters with the baseline parameters and clock polynomial coefficients. All those parameters can be solved together and the precision of solving the Earth's rotation parameters can be increased if the functional parameter constraint is applied. Author

N88-20501# Joint Publications Research Service, Arlington, Va.
JPRS REPORT: SCIENCE AND TECHNOLOGY. CHINA
7 Jul. 1987 123 p Transl. into ENGLISH from various Chinese articles
(JPRS-CST-87-030) Avail: NTIS HC A06/MF A01

Articles and summaries from the open literature are presented in the areas of aerospace science, applied sciences, national developments, and physical sciences. For individual titles, see N88-20502 through N88-20503.

N88-20502# Joint Publications Research Service, Arlington, Va.
RECOMMENDATIONS ON DEVELOPING POLYCRYSTALLINE ALUMINA FIBER **c27**
Yulian Lin and Shouwei Xing *In its* JPRS Report: Science and Technology. China 7 Jul. 1987 p 15-17 Transl. into ENGLISH from Naihuo Cailiao (Luoyang, People's Republic of China), no. 1, 20 Jan. 1987 p 47-51 (For primary document see N88-20501 13-31)
Avail: NTIS HC A06/MF A01

Refractory fiber development in China is reviewed in terms of full-scale utilization in metallurgical furnaces, resistance furnace continuous melt/spray technique, breakthrough in polycrystalline alumina fiber production, and imported production facilities. Directions of foreign developments in polycrystalline refractory alumina fibers are reviewed. Five recommendations for further development in China are given. J.P.B.

N88-20503# Joint Publications Research Service, Arlington, Va.
COMPUTER-AIDED TRANSFORMATION OF DESCRIPTIVE MODE OF MATHEMATICAL MODELS OF A CONTROL SYSTEM **c61**
Wenjin Gu and Fuchun Sun *In its* JPRS Report: Science and Technology. China 7 Jul. 1987 p 18-27 Transl. into ENGLISH from Zidonghua Yibiao (Shanghai, People's Republic of China), v. 7, no. 8, Aug. 1986 p 29-33, 46 , 46 (For primary document see N88-20501 13-31)
Avail: NTIS HC A06/MF A01

The mode and program flow chart of computer-aided mathematical models of a control system are introduced. The transformation algorithm is simple and directly perceived, occupies less memory and features a wide application range. It has been used on the CAD library of PC-1500 computers. It is widely employed in research institutes and factories and enjoys favorable comments. Author

N88-20504# European Space Agency. European Space Research and Technology Center, ESTEC, Noordwijk (Netherlands). Materials and Processes Div.
THE PREPARATION, ASSEMBLY AND MOUNTING OF RF COAXIAL CABLES
Oct. 1987 33 p
(ESA-PSS-01-718-Iss-1; ISSN-0379-4059; ETN-88-91796)
Copyright Avail: NTIS HC A03/MF A01

European Space Agency standards to ensure the high reliability of radio-frequency coaxial-cable interconnections when the latter are exposed to normal terrestrial conditions and the vibrational g-loads and environment imposed by space flight are specified. The proper tools, correct materials, design, process steps, and workmanship are covered. ESA

N88-20505# Office National d'Etudes et de Recherches Aerospatiales, Paris (France). Systems Dept.
[ACTIVITIES REPORT OF THE SYSTEMS DEPARTMENT] Annual Report, 1986
Sep. 1987 24 p Original contains color illustrations
(ETN-88-91987) Avail: NTIS HC A03/MF A01

Control and handling qualities of transport aircraft; decision-making aid procedure by data aggregation; inertial guidance flight testing; statistical evaluation of an interception; optimal trajectory of Ariane 5 type launcher with first stage fallout constraint; real-time trajectory of an Ariane launch vehicle via a geostationary relay satellite; an adaptive optics concept; optical telecommunications by laser in the atmosphere; an optical sensor for space robotics; measurement of aircraft attitude during deck landing phase; SPOT image processing; an ultrasonic ice sensor on an airfoil; an optical temperature and ablation sensor; and nondestructive testing by photothermal or photoacoustic imaging are discussed. ESA

N88-20506*# National Aeronautics and Space Administration. Hugh L. Dryden Flight Research Facility, Edwards, Calif.
WESTERN AERONAUTICAL TEST RANGE REAL-TIME GRAPHICS SOFTWARE PACKAGE MAGIC
Jacqueline C. Malone and Archie L. Moore May 1988 10 p
Prepared for presentation at the AIAA 4th Flight Test Conference, San Diego, Calif., 18-20 May 1988
(NASA-TM-100425; H-1455; NAS 1.15:100425) Avail: NTIS HC A02/MF A01 CSCL 13B

The master graphics interactive console (MAGIC) software package used on the Western Aeronautical Test Range (WATR) of the NASA Ames Research Center is described. MAGIC is a resident real-time research tool available to flight researchers-scientists in the NASA mission control centers of the WATR at the Dryden Flight Research Facility at Edwards, California. The hardware configuration and capabilities of the real-time software package are also discussed. Author

32 COMMUNICATIONS AND RADAR

Includes radar; land and global communications; communications theory; and optical communications.

For related information see also *04 Aircraft Communications and Navigation* and *17 Space Communications, Spacecraft Communications, Command and Tracking.* For search and rescue see *03 Air Transportation and Safety,* and *16 Space Transportation.*

N88-20507# Academy of Sciences of the Armenian SSR, Erivan.
TRANSFORMATION COEFFICIENT IN WAVE-FIELD ACCELERATION SCHEME
V. M. Tsakanov 1986 14 p In RUSSIAN
(DE88-700158; EFI-893(44)-86) Avail: NTIS (US Sales Only) HC A03/MF A01

A few schemes for wake-field acceleration, allowing to have a high transformation coefficient are discussed. A wave-guide with electric filling is used as a moderator. DOE

N88-20508# Academy of Sciences of the Armenian SSR, Erivan.
SLOW WAVES IN WAVEGUIDE WITH ELLIPTICAL CROSS SECTION
V. M. Tsakanov 1986 12 p In RUSSIAN
(DE88-700159; EFI-894(45)-86) Avail: NTIS (US Sales Only) HC A03/MF

A dispersion equation for determination of the wave propagation constant E sub 11,C in a diaphragmed waveguide with elliptical cross section is obtained. Calculations are made to obtain slow waves able to accelerate particles in one of the ellipse foci. DOE

N88-20509# Academy of Sciences of the Armenian SSR, Erivan.
POLARIZATION OF ELECTRONS IN AN ELECTROMAGNETIC WAVE FIELD IN THE PRESENCE OF MAGNETIC FIELD
R. A. Melikyan 1986 16 p In RUSSIAN
(DE88-700169; EFI-914(65)-86) Avail: NTIS (US Sales Only) HC A03/MF A01

The possibility of electron polarization in the field of circularly polarized electromagnetic wave at its propagation along the direction of constant homogeneous magnetic field is discussed for the case of small transverse and large longitudinal momenta of electrons. It is shown that for large values of the wave intensity, definite direction of wave propagation as well as definite values of the ratio of wave cyclotron frequencies, the effect of electron beam polarization can be obtained during several periods of electron revolution in the transverse plane without notable charge in transverse dimensions of the beam. DOE

N88-20510# Carnegie-Mellon Univ., Pittsburgh, Pa. Dept. of Computer Science.
THE ACOUSTIC-MODELING PROBLEM IN AUTOMATIC SPEECH RECOGNITION Interim Report
Peter F. Brown Dec. 1987 126 p
(Contract F33615-84-K-1520)
(AD-A188529; CMU-CS-87-125; AFWAL-TR-87-1161) Avail: NTIS HC A07/MF A01 CSCL 25D

This thesis examines the acoustic-modeling problem in automatic speech recognition from an information-theoretic point of view. This problem is to design a speech-recognition system which can extract from the speech waveform as much information as possible about the corresponding word sequence. The information extraction process is broken down into two steps: a signal processing step which converts a speech waveform into a sequence of information bearing acoustic feature vectors, and a step which models such a sequence. This thesis is primarily concerned with the use of hidden Markov models to model sequences of feature vectors which lie in a continuous space such as R sub N. It explores the trade-off between packing a lot of information into such sequences and being able to model them accurately. The difficulty of developing accurate models of continuous parameter sequences is addressed by investigating a method of parameter estimation which is specifically designed to cope with inaccurate modeling assumptions. GRA

N88-20511# Massachusetts Inst. of Tech., Cambridge. Electronics Lab.
STATISTICAL SIGNAL PROCESSING USING A CLASS OF ITERATIVE ESTIMATION ALGORITHMS
Meir Feder Sep. 1987 208 p
(Contract N00014-81-K-0742)
(AD-A189050; TR-532) Avail: NTIS HC A10/MF A01 CSCL 12C

Many signal processing problems may be posed as statistical parameter estimation problems. A desired solution for the statistical problem is obtained by Maximum Likelihood (ML), the Maximum A-Posteriori (MAP) probability, or by optimizing other criterion, depending on the a-priori knowledge, and the risk criterion. However, in many practical situations, the original signal processing problem may generate a complicated optimization problem, e.g., when the observed signals are noisy and incomplete. A framework of iterative procedures for maximizing the likelihood, the Estimate Maximize (EM) algorithm, is widely used in statistics. In the EM algorithm, the observations are considered incomplete and the algorithm iterates between estimating the sufficient statistics of the complete data given the observations and a current estimate of the parameters (the E step) and maximizing the likelihood of the complete data, using the estimated sufficient statistics (the M step). When this algorithm is applied to signal processing problems, it yields, in many cases, an intuitively appealing processing scheme. GRA

N88-20512# Pennsylvania State Univ., University Park. Applied Research Lab.
ESTIMATION-CORRELATION MODELING, AND IDENTIFICATION IN ADAPTIVE ARRAY PROCESSORS Ph.D. Thesis
J. A. Tague and L. H. Sibul Oct. 1987 170 p
(Contract N00024-85-C-6041)
(AD-A189130; ARL/PSU/TR-87-005) Avail: NTIS HC A08/MF A01 CSCL 17K

Several issues involved with implementing adaptive array processors for signal detection and estimation are studied. The basic structure examined is the estimator-correlator processor. It establishes a fundamental connection between detection and estimation theory, and solves the detection problem for the generalized exponential class of signal and noise distributions. GRA

N88-20513# Naval Ocean Systems Center, San Diego, Calif.
HF (HIGH FREQUENCY) MAXIMUM USABLE FREQUENCY (MUF) MODEL UNCERTAINTY ASSESSMENT

T. N. Roy and D. B. Sailors Jun. 1987 116 p
(AD-A189132; NOSC/TR-1184) Avail: NTIS HC A06/MF A01 CSCL 20N

A statistical analysis of observed oblique sounder median maximum observed frequencies (MOF) and predicted maximum usable frequencies (MUF) was used to assess the accuracy of high-frequency MUF prediction. A database of 13,054 hours of oblique sounder MOFs measured on 70 paths was compared with the predicted MUF values from MINIMUF-3.5, MINIMUF 85, and an unrelated MUF model, the HF Broadcast WARC model (HFBC84). The data were screened into subsets to determine the effect of particular paths, path length and orientation, season, month, latitude, sunspot number, diurnal trends, geographic region, and sounder type. The accuracy of all three models was very close, with the MINIMUF-3.5 model having the lowest RMS error of 4.44 MHz. MINIMUF 85 was next, with an RMS error of 4.58 MHz, and HFBC84 was last, with an error of 4.67 MHz, and MINIMUF 85 last, with 1.28 MHZ. Correlation was good for all three models. Correlation coefficients were .824, .819, and .827 for MINIMUF-3.5, MINIMUF 85, and HFBC84, respectively. Future improvements to the MINIMUF model are discussed and current MUF computer algorithms are included in the appendices. GRA

N88-20514# Orincon Corp., La Jolla, Calif.
SIGNAL-FILTER DESIGN AND SYSTEM PERFORMANCE FOR POLARIMETRIC RADAR Final Report, Feb. 1984 - Feb. 1986
Richard A. Altes, Stephen F. Connelly, James R. Miller, Kishan G. Mehrotra, and H. Liu Jul. 1987 133 p
(Contract F30602-84-C-0017)
(AD-A189257; OCR-84-184041-A002; RADC-TR-87-3) Avail: NTIS HC A07/MF A01 CSCL 17I

Relatively simple expressions for the polarimetric scattering function of randomly oriented dipoles have yielded expressions for SIR (signal to interference ratio) in some simple but important cases, and these expressions have been analyzed in order to interpret the computational results. Some important insights have been obtained from the SIR expression for distributed planar targets and randomly oriented dipole clutter, i.e., for the typical target in chaff problem. These insights have resulted in the design of a new polarimetric clutter canceller which theoretically allows a polarimetric radar to see through chaff. Signal-to-interference ratio maximization has been used to obtain an optimum signal-filter pair for polarimetric radar when targets and/or clutter exhibit random polarization modulation. The results can easily be extended to include the design of a likelihood ratio receiver for the same problem. Considerable insight into the theoretical solutions has been obtained by implementation and test of a computer program to yield the maximum SIR and Bayesian systems, i.e., the best signal and receiver configurations in each case. GRA

N88-20515# Air Force Geophysics Lab., Hanscom AFB, Mass.
A POLARIZATION DIVERSITY METEOROLOGICAL RADAR SYSTEM Interim Report
James I. Metcalf, Graham M. Armstrong, and Alexander W. Bishop 19 Mar. 1987 302 p
(AD-A189291; AFGL-TR-87-0105) Avail: NTIS HC A14/MF A01 CSCL 17I

The AFGL 10-cm Doppler weather radar was modified to enable the measurement of the differential reflectivity between horizontal and vertical polarizations in addition to the absolute reflectivity and the Doppler mean velocity and spectrum variance. Polarization switching is achieved by means of a diplexer, which separates at the antenna the transmitted signals of two frequencies, 2710 and 2760 MHz, and permits nearly simultaneous transmission of signals of orthogonal polarizations. Signals of these frequencies can be transmitted either with horizontal and vertical polarization, respectively, or with left and right circular, polarization, respectively. We describe the design and performance of the diplexer and the performance of the real-time data processor, present examples of meteorological measurements, and discuss future developments of the radar system. GRA

N88-20516# Air Force Inst. of Tech., Wright-Patterson AFB, Ohio. School of Engineering.
ALTERNATIVE FORCE STRUCTURING STRATEGIES FOR MILITARY SATELLITE COMMUNICATION SYSTEMS M.S. Thesis
William P. Murdock, Jr Dec. 1987 102 p
(AD-A189492; AFIT/GSO/ENS/87D-8) Avail: NTIS HC A06/MF A01 CSCL 25E

The purpose of this study was to determine and examine alternative force structuring strategies for military satellite communication (MILSATCOM) systems. The study was undertaken due to the United States' reliance on relatively few, expensive satellites as critical communication links. Current anti-satellite weapons pose a definite threat to missions using this type of strategy. In response to this situation, proliferated MILSATCOM designs using low Earth circular orbits and a highly elliptical (Molniya) orbit were defined and analyzed. The objective of this effort was to compare the proliferated alternative systems' performance and cost with a current MILSATCOM system. The Fleet Satellite Communication (FLTSATCOM) system was used as the baseline system for comparison. Overall, both alternative force structuring strategies provided superior Earth coverage when subjected to satellite losses. This was especially evident in the European and Mideast theaters. The Molyniya constellation was the best alternative when considering system performance, system cost, current MILSATCOM system compatibility and the technology required for system implementation. GRA

N88-20517# Air Force Inst. of Tech., Wright-Patterson AFB, Ohio. School of Engineering.
MODIFICATION OF PARABOLIC DISH ANTENNA PATTERN USING TWO SYMMETRICALLY PLACED CIRCULAR FLAT PLATES M.S. Thesis
Glen C. Thorpe Dec. 1987 106 p
(AD-A189543; AFIT/GE/ENG/87D-67) Avail: NTIS HC A06/MF A01 CSCL 09A

This study aims to formulate a method of predicting the far field pattern of a parabolic dish antenna with two moveable flat plates mounted symmetrically on either side of the feed horn. The approach taken has been to first analyze the radiation pattern of the antenna with the disks at certain heights out from the surface of the dish. To do this the near-field radiation in amplitude and phase was measured over a plane surface in the near-field and the values were then transformed into the far field using a Fast Fourier Transform. Far field pattern values of the antenna were directly measured for each setting of the plates. The results obtained from the Fast Fourier Transform of the near field data were in good agreement with the values obtained by measurement. Finally, an approximate model of the antenna was developed and implemented as a computer program. This model, while relatively unsophisticated, provided some insights into the changes in the near field phase distribution caused by the moveable circular flat plates. GRA

N88-20518# Sandia National Labs., Albuquerque, N. Mex.
A HYBRID TRANSFORM/DPCM ENCODER FOR DATA COMPRESSION
S. D. Gray 11 Sep. 1987 23 p Presented at the IEEE International Conference on Robotics and Automation, Philadelphia, Pa., 25 Apr. 1988
(Contract DE-AC04-76DP-00789)
(DE87-014852; SAND-87-2255C; CONF-880424-1) Avail: NTIS HC A03/MF A01

A new technique for the transmission of video is presented. It incorporates several ideas that enable a significant reduction in the data rate over a straightforward pulse code modulation (PCM) system. Theoretical expressions are presented to give a firm background on how the procedure works and what are its limitations. Although the proposed system contains a considerable amount of computational sophistication, an emphasis has been placed on portable application. To back up these ideas and allow the reader to judge the effectiveness of this procedure, several photographs are included. DOE

N88-20519# National Bureau of Standards, Boulder, Colo. Electromagnetic Fields Div.
TIME-DOMAIN SYSTEM FOR IDENTIFICATION OF THE NATURAL RESONANT FREQUENCIES OF AIRCRAFT RELEVANT TO ELECTROMAGNETIC COMPATIBILITY TESTING
J. W. Adams, A. R. Ondrejka, and H. W. Medley Nov. 1987 54 p Sponsored by Army Aviation Systems Command, St. Louis, Mo.
(PB88-164520; NBSIR-87/3077) Avail: NTIS HC A04/MF A01 CSCL 20N

A method of measuring the natural resonant frequencies of a structure is described. The measurement involves irradiating this structure, in this case a helicopter, with an impulsive electromagnetic (EM) field and receiving the echo reflected from the helicopter. Resonances are identified by using a mathematical algorithm based on Prony's method to operate on the digitized reflected signal. The measurement system consists of special TEM horns, pulse generators, a time-domain system, and Prony's algorithm. The frequency range covered is 5 megahertz to 250 megahertz. This range is determined by antenna and circuit characteristics. The measurement system is demonstrated, and measured data from several different helicopters are presented in different forms. These different forms are needed to determine which of the resonant frequencies are real and which are false. The false frequencies are byproducts of Prony's algorithm. GRA

N88-20520 Illinois Univ., Chicago.
A POLARIMETRIC RAIN BACKSCATTER MODEL DEVELOPED FOR COHERENT POLARIZATION DIVERSITY RADAR APPLICATIONS Ph.D. Thesis
Amit Prakash Agrawal [1987] 254 p
Avail: Univ. Microfilms Order No. DA8726077

The electromagnetic direct and inverse scattering problem of plane wave backscattering from distributed fluctuating scatters, such as hydrometeors in rain, is analyzed for the monostatic case for which coherent dual polarization pulsed radar measurements are made available. Based on a critical assessment of the existing literature on polarimetric radar meteorology, it was found necessary to relate the polarimetric Doppler signatures of such distributed fluctuating scatterers in terms of the Kennaugh target characteristic radar polarization theory and its expressions. Using the resulting co/cross polarization null/max approach expressed in a linear (HV) polarization state basis in order to recover more useful information from such polarimetric L-to-W band radar data, the rain backscatter model of Stapor and Pratt is further developed. Using polarimetric scattering matrix pulse compression radar data in the X and Q bands, the derived polarimetric rain backscattering model is verified. The computer assisted data evaluation resulted in the findings that the simultaneous use of the co/cross-pol null and of the scattering matrix element spectral plots measured in the linear (HV) basis provide very useful information on identifying dynamic phase changes of fluctuating hydrometeors within moving sheets of rain showers. Dissert. Abstr.

N88-20521 Ohio State Univ., Columbus.
APPLICATIONS OF THE DIFFERENTIAL REFLECTIVITY RADAR TECHNIQUE: FOCUS ON ESTIMATION OF RAINFALL PARAMETERS AND MICROWAVE ATTENUATION PREDICTION Ph.D. Thesis
Haldun Direskeneli [1987] 270 p
Avail: Univ. Microfilms Order No. DA8726621

The application of the differential reflectivity radar method to estimate rainfall parameters by computing radar-derived estimates with ground-based disdrometer and rain gage measurements is explored. The derivation of the empirical relationships linking the rainfall parameters rainfall rate (R), water content (M), and median volume diameter (D sub 0) to the radar observables horizontal reflectivity factor (Z sub H) and/or differential reflectivity (Z sub DR) are described based on simulations employing disdrometer measurements made during a 1982 field experiment in central Illinois. Three case studies are described utilizing these relationships to compare radar estimates with ground-based measurements. Dissert. Abstr.

N88-20522 Drexel Univ., Philadelphia, Pa.
DETECTION AND ANGLE ESTIMATION OF COHERENT PLANE WAVES Ph.D. Thesis
Varaz Shahmirian [1987] 178 p
Avail: Univ. Microfilms Order No. DA8727456

The problem of detection and angle-of-arrival estimation of multiple coherent plane waves is addressed. A unified approach based on the singular value decomposition (SVD) is proposed to solve both the detection and angle estimation problems. A set of detection criteria for determining the number of coherent plane waves present in the field is developed and their performance of the case of two closely spaced coherent sources is analyzed. The probability of error for each criterion is derived as a function of the signal-to-noise ratio, the angle separation, the inter-signal correlation, and the number of snapshots. Using plots of these probability of error functions, thresholds of the above parameters for the correct detection are identified. For the problem of angle-of-arrival estimation, the SVD-based modified Forward-Backward Linear Prediction (FBLP) method of spectral estimation is applied and its performance under a multipath environment is analyzed. It is shown that, this method is capable of yielding high resolution estimates at low signal-to-noise ratios and with few number of snapshots. The advantage of this approach, besides its ability to solve the detection and angle estimation problem for the coherent signals, is its high computational efficiency and stability which is inherent to the SVD technique. Dissert. Abstr.

N88-20523 Arizona Univ., Tucson.
ELECTROMAGNETIC SCATTERING FROM AND NATURAL RESONANCES OF THE CIRCULAR STRIP Ph.D. Thesis
Jeffery Thomas Williams [1987] 174 p
Avail: Univ. Microfilms Order No. DA8726850

The formulation and calculation of the electromagnetic fields scattered from, and the natural resonances of, a thin, perfectly conducting circular strip mounted on a perfectly conducting ground plane is presented. The fields are excited by an axial electric dipole, oriented normal to the surface of the ground plane. An electric field integral equation is formulated in terms of the induced surface current and solved in closed form in the quasi-static limit as an expansion of Chebyshev polynomials. In addition, the integral equation is solved for the general case by the method of moments (MOM). Numerical results are given which show the excellent agreement between the quasi-static and method of moments solutions. The MOM currents are used to determine the field scattered from the circular strip, in both the frequency and time domains. The frequency domain analysis is applied to the problem of fencing small vertical broadcast antennas. Using the MOM formulation, the natural resonances of the circular strip were determined. These resonances are divided into two classes: the exterior resonances and the interior resonances. The pole trajectories are shown for the first layer of exterior resonances for a wide range of strip height-to-radius ratios. Using the transient scattered fields calculated from the MOM formulation as input and output data for a single input, single output identification algorithm, the dominant poles in the scattered fields were identified. Dissert. Abstr.

N88-20524*# Jet Propulsion Lab., California Inst. of Tech., Pasadena.
THE DEEP SPACE NETWORK
Jan. 1988 25 p
(NASA-CR-182700; JPL-400-333; NAS 1.26:182700) Avail: NTIS HC A03/MF A01 CSCL 17B

The Deep Space Network (DSN) is the largest and most sensitive scientific telecommunications and radio navigation network in the world. Its principal responsibilities are to support unmanned interplanetary spacecraft missions and to support radio and radar astronomy observations in the exploration of the solar

system and the universe. The DSN facilities and capabilities as of January 1988 are described. B.G.

N88-20525# Oak Ridge National Lab., Tenn.
OPTIMUM TRANSFORMER DESIGN FOR A PULSED POWER SYSTEM
A. Y. Broverman Nov. 1987 20 p
(Contract DE-AC05-84OR-21400)
(DE88-006054; ORNL/TM-10620) Avail: NTIS HC A03/MF A01

Electromagnetic forces resulting from peak pulsed current require special design consideration to prevent failure of the coils of the transformer. Procedures for interleaving transformer windings to reduce both electromagnetic short-circuit forces and reactive voltage drop while reducing procurement costs are described. The basics of transformer design principles and cost trade-offs are included to enhance understanding of the interleaving procedures. DOE

N88-20526*# National Aeronautics and Space Administration, Washington, D.C.
METHOD FOR SET-UP FOR RESEARCHING SIGNAL CURVE DEVELOPMENT
Emar Kreutz and Wilfred Koerber Apr. 1988 20 p Transl. into ENGLISH of Verfahren und Anordnung zur Untersuchung des Verlaufs Eines Signals, Federal Republic of Germany, Patent No. DE-3305425-A1 Transl. by SCITRAN, Inc., Santa Barbara, Calif. Original document prepared by Philips Patent Management Office GmbH, Hamburg, Federal Republic of Germany
(Contract NASw-4307)
(NASA-TT-20235; NAS 1.77:20235) Avail: NTIS HC A03/MF A01 CSCL 17B

A method is described for researching signal curve development. The signal is transformed into a delta-modulated signal, and the number of appearing signal changes are counted. Author

N88-20527# Wageningen Agricultural Univ. (Netherlands). Vakgroep Landmeetkunde en Teledetectie.
THE RADAR SCATTERING COEFFICIENT AS A FUNCTION OF FOREST STAND PARAMETERS AND VIEWING ANGLE. AN EMPIRICAL STUDY OF THE PINUS SYLVESTRIS L. IN THE KOOTWIJK FOREST (THE NETHERLANDS), EXTENDED WITH OBSERVATIONS IN THE SPEULDER AND SPRIELDER FOREST (THE NETHERLANDS) [DE RADARVERSTROOIINGSCOEFFICIENT ALS FUNCTIE VAN OPSTANDSPARAMETERS EN DE INKIJKHOEK. EEN EMPIRISCH ONDERZOEK AAN GROVE DEN (PINUS SYLVESTRIS L.) IN DE BOSWACHTERIJ KOOTWIJK, UITGEBREID MET ENIGE WAARNEMIINGEN IN HET SPEULDER-EN SPRIELDERBOS]
A. Huibert Visser Aug. 1986 85 p In DUTCH
(ETN-88-91348) Avail: NTIS HC A05/MF A01

The empirical relation between the radar scattering coefficient gamma and forest stand parameters and observation angle was investigated. The global procedure, the determination of the forest stand parameters, the airborne X-band side-looking radar observations, and the statistical processing of the data are described. The dependence of gamma on the observation angle is very clearly observed: for angles below 45 deg gamma depends less on the forest stand parameters than for larger angles. The correlation between gamma and these parameters generally increases after correction for the observation angle. Trunk-specific parameters show a significant correlation with gamma, in contrast with top-specific parameters and the number of trunks per hectare. ESA

N88-20528*# National Aeronautics and Space Administration, Washington, D.C.
SYSTEM FOR DETECTING OBJECTS THAT REPRESENT A THREAT
Guenther Riedl Mar. 1988 7 p Transl. into ENGLISH of German Patent no. DE-3233326-Al (8 Mar. 1984) Transl. by Scientific Translation Service, Santa Barbara, Calif.
(Contract NASw-4307)
(NASA-TT-20244; NAS 1.77:20244) Avail: NTIS HC A02/MF A01 CSCL 17B

A description is given of a panoramic receiver. It is used as a sensor containing several detectors that respond to various types of signal and sound. The system described can be used for detecting objects that represent a threat, by using a sensor and a system for discriminating characteristic signals. Author

N88-20529*# Smithsonian Astrophysical Observatory, Cambridge, Mass.
THEORETICAL INVESTIGATION OF EM WAVE GENERATION AND RADIATION IN THE ULF, ELF AND VLF BANDS BY THE ELECTRODYNAMIC ORBITING TETHER Semiannual Report, 1 May - 31 Oct. 1987
Robert D. Estes Apr. 1988 62 p
(Grant NAG8-638)
(NASA-CR-182720; NAS 1.26:182720; SAR-1) Avail: NTIS HC A04/MF A01 CSCL 20N

The goal is to extend the previous analysis of electromagnetic wave generation by an electrodynamic tethered satellite system to a more realistic model that includes the effects on wave propagation and reflection to the boundaries between ionosphere, atmosphere, and earth. One of the major activities was searching the scientific literature for publications that might be relevant to the problem. The software developed as SAO to follow the path of waves along field lines through the ionosphere to the atmosphere starting from an arbitary position in the atmosphere is described. Some preliminary results are presented from applying the code to the location of wave reception hot spots on the earth's surface for satellites operating at 300 and 600 km altitudes. A generalization of the Alfven wing analysis is presented to allow for arbitrary angles between the velocity vector, geomagnetic field, and the veritcal. This will be utilized in the modeling of the problem with boundaries included. B.G.

N88-20496# Joint Publications Research Service, Arlington, Va.
SIMULATION OF EFFECT OF ANTI-RADAR STEALTH PRINCIPLE Abstract Only
Borao Zhao, Shuchen Xing, and Chunyi Li *In its* JPRS Report: Science and Technology. China 12 Feb. 1988 p 1 Transl. into ENGLISH from Xitong Gongcheng Lilun Yu Shijian (Beijing, People's Republic of China), v. 7, no. 1, 1987 p 43-48 (For primary document see N88-20495 13-31)
Avail: NTIS HC A07/MF A01

N88-20707# Joint Publications Research Service, Arlington, Va.
INFLUENCE OF HYDROMETEOROLOGICAL FACTORS ON VISIBILITY OF OBJECTS DETECTED BY RADAR Abstract Only
A. A. Kotyukh *In its* JPRS Report: Science and Technology. USSR: Earth Sciences 26 Feb. 1988 p 56 Transl. into ENGLISH from Vestnik Leningradskogo Universiteta, Seriya 7: Geologiya, Geografiya (Leningrad, USSR), no. 1, Mar. 1987 p 92-97 (For primary document see N88-20674 13-42)
Avail: NTIS HC A04/MF A01

33 ELECTRONICS AND ELECTRICAL ENGINEERING

Includes test equipment and maintainability; components, e.g., tunnel diodes and transistors; microminiaturization; and integrated circuitry.

For related information see also *60 Computer Operations and Hardware* and *76 Solid-State Physics.*

N88-20530# Hughes Research Labs., Malibu, Calif.
INTERGRATED CIRCUIT DESIGN, PHASE 2 Final Report, Jul. - Sep. 1984
J. G. Nash Jul. 1987 32 p
(Contract N66001-84-C-0104)

(AD-A189060; NOSC-TD-1140) Avail: NTIS HC A03/MF A01 CSCL 09A

This report is in response to a request to provide an analysis on the design of an ultra-low power integrated circuit which will perform digital filtering on voice bandwidth signals. This chip will contain a 1024-tap linear phase filter with programmable weights, operate at a sample rate of 8 kHz, and will consume a maximum of 7.2 mW power with a 3.6-volt power supply. This monolithic filter will contain: an 8 to 12 bit a/d internal processing clock oscillator, and the digital filter. This study only reports on the power requirements of the digital filter portion of the chip, although all portions must be considered in the overall power budget. Preliminary device count and die size estimates are presented. The work presented here is based on an earlier study performed by Hughes Research Laboratories (HRL) for Naval Ocean Systems Center (NOSC). GRA

N88-20531# Rochester Univ., N. Y. Dept. of Computer Science.

DESCRIBING CONSTRAINTS ON A DIGITAL CIRCUIT'S BEHAVIOR

Doug Baldwin Jul. 1987 26 p

(Contract DACA76-85-C-0001; Grant NSF DMC-86-13489)

(AD-A189200; TR-222) Avail: NTIS HC A03/MF A01 CSCL 09A

Automatic design of circuits from high-level descriptions of their behavior requires that some physical constraints be included in behavioral specifications. This paper describes a simple but powerful mechanism for doing so. The key ideas behind this approach are attributes to represent physical parameters of a circuit and constraint statements to restrict the values that attributes may assume. Practical circuits have been described using these ideas. An algorithm for extracting constraints from specifications and deciding which parts of the specifications are subject to which constraints is also presented and proven correct. GRA

N88-20532# Princeton Univ., N. J. Dept. of Civil Engineering.

PARAMETRIC STUDY OF ACCELERATION-INDUCED STRESSES AND FREQUENCY CHANGES IN DOUBLY-ROTATED CRYSTAL RESONATORS Final Report, 16 Jul. 1984 - 30 Sep. 1987

P. C. Lee Nov. 1987 8 p

(Contract DAAG29-84-K-0133)

(AD-A189261; ARO-21353.7-EG) Avail: NTIS HC A02/MF A01 CSCL 09A

The objective of the research is to predict the acceleration sensitivity, i.e., the changes of resonance frequencies in crystal resonators due to applied, steady accelerations, and to identify the effects on the acceleration sensitivity from various parameters, such as the direction of acceleration, crystal plate orientation, plate thickness, support configuration and support structures. The ratios of the frequency shift to the thickness-shear resonance frequency are in the range of 10 to the -8th power to 10 to the -10th power. These frequency changes, although very small in numerical values, are regarded to be significant in applications in ultra-precision frequency control. The complexity of the problem mainly comes from the constitutive equations of the crystal: (1) For doubly-rotated cuts of quartz resonators, the stress-strain relations possess triclinic symmetry, the most general anisotropic relations; and (2) For accurate prediction of frequency changes, the third-order elastic stiffness coefficients, the nonlinear terms, must be taken into account. GRA

N88-20533# California Univ., Berkeley. Electronics Research Lab.

JOINT SERVICES ELECTRONICS PROGRAM Final Report, 1 May 1984 - 30 Apr. 1987

W. G. Oldham Jun. 1987 13 p

(Contract F49620-84-C-0057)

(AD-A189262; UCB/ERL-87/1; AFOSR-87-1155TR) Avail: NTIS HC A03/MF A01 CSCL 09A

The final report of the JSEP (Joint Services Electronics Program) in Electromagnetics, Quantum Electronics, Solid State Electronics, Materials and Devices, and Information Systems is presented. GRA

N88-20534# Kansas Univ. Center for Research, Inc., Lawrence. Telecommunications and Information Sciences Lab.

ADAPTIVE ALGORITHMS FOR HF ANTENNA ARRAYS Final Report, Jun. 1985 - Apr. 1986

D. Haegert, R. Spohn, V. Frost, K. Shanmugan, and G. Sargent Jul. 1987 221 p

(Contract F30602-81-C-0205)

(AD-A189329; TISL-5481; RADC-TR-86-159) Avail: NTIS HC A10/MF A01 CSCL 09A

The performance of an adaptive array system will not only be dependent upon the controlling algorithm, but also upon the specific environment in which the array is used. Isolating the contributions made solely by the control algorithm represents a formidable task, considering that adaptive array systems are inherently used in situations in which the interference environment is initially unknown, time-variant, or both. If an effective algorithm choice is to be made, it is important to be able to compare array performances in identical environments. The major focus of this study is to compare and contrast the performance of various control algorithms under identical conditions in a computer simulated adaptive HF antenna array system. After examining adaptive array systems and the role played by the controlling algorithms, this study concentrates on the selection and simulation of three specific algorithms. The simulation results are then presented in the form of a comparative evaluation of the selected control algorithms and relevant conclusions are drawn. GRA

N88-20535*# Jet Propulsion Lab., California Inst. of Tech., Pasadena.

BRAGG-CELL RECEIVER STUDY

Lonnie A. Wilson 10 Apr. 1987 113 p

(Contract NAS7-918)

(NASA-CR-182684; JPL-D-4307; NAS 1.26:182684; AD-A189361; TM-19; ALGO-PUB-0033) Avail: NTIS HC A06/MF A01 CSCL 17D

Bragg-cell receivers are employed in specialized Electronic Warfare (EW) applications for the measurement of frequency. Bragg-cell receiver characteristics are fully characterized for simple RF emitter signals. This receiver is early in its development cycle when compared to the IFM receiver. Functional mathematical models are derived and presented in this report for the Bragg-cell receiver. Theoretical analysis is presented and digital computer signal processing results are presented for the Bragg-cell receiver. Probability density function analysis are performed for output frequency. Probability density function distributions are observed to depart from assumed distributions for wideband and complex RF signals. This analysis is significant for high resolution and fine grain EW Bragg-cell receiver systems. GRA

N88-20536# Hughes Research Labs., Malibu, Calif.

PHASE PRESERVATION CLEANUP IN A DOUBLE-PASS RAMAN AMPLIFIER SBS (STIMULATED BRILLOUIN SCATTERING) CONJUGATOR Final Report, 1 Oct. 1985 - 31 May 1987

S. M. Jensen, M. L. Minden, C. D. Jones, S. M. Wandzura, and W. P. Brown 10 Dec. 1987 130 p

(Contract N00014-85-C-0839)

(AD-A189428; HAC-Ref-G0031) Avail: NTIS HC A07/MF A01 CSCL 09C

This report describes a one-year program to investigate phase-preservation and cleanup in a double-pass Raman amplifier (RA) by a stimulated Brillouin scattering (SBS) conjugator. The goal of this program was to determine the physical processes that limit the compensation of RA phase aberration by SBS conjugators. Departures from this ideal performance are caused by nonreciprocal aberrations and/or imperfect performance of the SBS conjugator. The purpose of this work was to quantify the distortions caused by nonreciprocal aberrations in the RA process for uniform as well as distorted pump and seed waves. GRA

N88-20537# Air Force Inst. of Tech., Wright-Patterson AFB, Ohio. School of Engineering.
LASER PROGRAMMING INTEGRATED CIRCUITS M.S. Thesis
Craig S. Spanburg Dec. 1987 117 p
(AD-A189590; AFIT/GE/ENG/87D-62) Avail: NTIS HC A06/MF A01 CSCL 09A

Programmable circuits are building blocks that improve design efficiency. Each mask and field programming technique has its own set of advantages and disadvantages. This thesis considers laser cutting as an alternative programming technique. This effort involves designing, assembling, and demonstrating a laser programming system. The laser system includes lasers and optics, a microprobe station, and a motion controller. Software for remote operation of the motion controller and for generating the cutting location coordinates is also developed during the research. Two applications of laser programming, a 32-bit comparator and a serial multiplier, are examined. The design of the two chips illustrates laser programmable circuit design and layout considerations. Programming the fabricated 32-bit comparator demonstrates the laser system. Testing the comparator verifies the performance of a laser programmable circuit. GRA

N88-20538# Westinghouse Research and Development Center, Pittsburgh, Pa.
VAPOR-MIST FOR LIGHTWEIGHT HIGH VOLTAGE SPACE INSULATION SYSTEMS Final Report
R. T. Harrold Mar. 1987 65 p
(Contract DE-AC03-85SF-15933)
(DE87-011704; DOE/SF-15933/T1) Avail: NTIS HC A04/MF A01

The purpose of this research was to assess whether the new and emerging technology of vapor-mist dielectrics would be applicable as a high voltage pulse insulation for space-borne weapons and radar. This is a very important area in which new and lightweight forms of high voltage insulation are critically needed. The research tasks addressed in this project are listed below: estimate the performance of vapor-mist under zero gravity conditions, develop rapid misting techniques, determine the electrical strength of vapor-mist at radar frequencies, examine the electrical strength of vapor-mist exposed to pulse voltages with nanosecond rise times, and examine the heat transfer and cooling properties of vapor-mist. In this report the experimental results, analyses and theoretical aspects associated with the above tasks are detailed. Also, included are some measurements of the ultraviolet absorbance properties of vapor-mist, and the results of a microscopic examination of the electrode surfaces after pulse voltage breakdown in vapor mist. DOE

N88-20539# California Univ., Berkeley. Lawrence Berkeley Lab.
A NEW CONCEPT IN AN ELECTRICALLY RECHARGEABLE ZINC-AIR ALKALINE BATTERY
P. N. Ross Oct. 1987 9 p Presented at the 8th Battery and Electrochemical Contractors Conference, Tyson Corner, Va., 16 Nov. 1987
(Contract DE-AC03-76SF-00098)
(DE88-003858; LBL-24181; CONF-871121-4) Avail: NTIS HC A02/MF A01

This paper describes a new idea for zinc-air battery design. The novel idea is a porous zinc electrode surrounded with a supersaturated zincate solution. DOE

N88-20540# Sandia National Labs., Albuquerque, N. Mex.
ELECTRICAL PROPERTIES OF MEDIUM FIELD, CHEM-PREP VARISTORS
B. A. Tuttle, J. A. Voigt, E. J. Binasiewicz, and K. M. Kimball Jan. 1988 82 p
(Contract DE-AC04-76DP-00789)
(DE88-006147; SAND-87-1824) Avail: NTIS HC A05/MF A01

Medium field, chem-prep, ZnO varistors were synthesized and electrically tested. Eight formulations were used with three dopants: (1) Co (0, 0.25, 0.5 mol percent), (2) Mn (0, 0.25, 0.5 mol percent) and (3) Al (0, 125, and 150 ppM by weight). Al doping produced two dramatic effects: (1) an increase in the electric switching field by factors of 5 to 10, and (2) a significant enhancement of the high current density nonlinearity coefficient. Firing temperatures of 800, 900 and 1000 C were used to densify materials and produce varistors with electrical switching fields in the 3 to 10 kV/cm range. Current density vs electric field measurements were made from 1 microA/sq cm to 10 A/sq cm using dc and pulse techniques. The varistor with the largest nonlinearity coefficient over this extended current density range was fired at 1000 C and contained 0.25 Co, 0.25 Mn, 0.56 Bi (mol percent) and 150 ppM Al (by weight). The nonlinearity coefficient was 14 at low current densities (0.1 mA/sq cm to 5 mA/sq cm) and 28 for high current densities (0.1 to 10 A/sq cm). Because of the large nonlinearity coefficient, this varistor is the best candidate for Sandia applications of all varistors synthesized. Further, the varistor had an electrical switch field of 5 kV/cm at 10 A/sq cm and was greater than 96 percent of theoretical density. Low field dielectric properties and J vs. E characteristics as a function of temperature were measured for this varistor. DOE

N88-20541# Sandia National Labs., Albuquerque, N. Mex.
SCALE-UP OF A BATCH-TYPE CHEMICAL POWDER PREPARATION PROCESS FOR HIGH FIELD VARISTOR FABRICATION
T. J. Gardner and S. J. Lockwood Feb. 1988 128 p
(Contract DE-AC04-76DP-00789)
(DE88-006601; SAND-87-2194) Avail: NTIS HC A07/MF A01

A batch-type chemical preparation process for the fabrication of high field varistor powders was scaled-up from laboratory to batch size (1 kg) deemed suitable for technology transfer to an appropriate manufacturing agency. Process development activities concerning batch preparation and reproducibility, impurity effects on varistor properties, electrical property degradation, and other scale-up problems were investigated. Detailed descriptions of the specific problems encountered and the resulting solutions are documented. A summary of the 1 kg inter-batch reproducibility with respect to both powder characteristics and sintered varistor properties is presented. In-depth process documentation is supplied in the appendices of this report. DOE

N88-20542# Eltech Systems, Inc., Fairport Harbor, Ohio. Research and Development Center.
ALUMINUM-AIR BATTERY DEVELOPMENT Final Report
20 Nov. 1987 137 p
(Contract W-7405-eng-48)
(DE88-006617; UCRL-21018-Vol-3) Avail: NTIS HC A07/MF A01

This document reports on the design and testing of aluminum anodes for aluminum-air batteries. DOE

N88-20543# Eltech Systems, Inc., Fairport Harbor, Ohio. Research and Development Center.
ALUMINUM-AIR BATTERY DEVELOPMENT Final Report
20 Nov. 1987 242 p
(Contract W-7405-eng-48)
(DE88-006618; UCRL-21018-Vol-4) Avail: NTIS HC A11/MF A01

This paper presents the results of investigations of the performance of aluminum-air battery electrodes. Different electrodes were built and tested, and their performance measured. The authors conclude that the present component development has been successful, and that future research be aimed at system integration. DOE

N88-20544# Argonne National Lab., Ill.
SODIUM-SULFUR TECHNOLOGY EVALUATION AT ARGONNE NATIONAL LABORATORY
T. P. Mulcahey, A. F. Tummillo, R. L. Hogrefe, C. C. Christianson, R. Biwer, C. E. Webster, J. Lee, J. F. Miller, J. J. Marr, and J. A. Smaga 1987 4 p Presented at the 8th Battery and Electrochemical Contractors' Conference, Tysons Corner, Va., 16 Nov. 1987

(Contract W-31-109-eng-38)
(DE88-002852; CONF-871121-2) Avail: NTIS HC A02/MF A01

The Analysis and Diagnostics Laboratory (ADL) at Argonne National Laboratory has completed evaluation of the Ford Aerospace and Communication Corp. (FACC) technology in the form of four load-levelling (LL) cells, five electric vehicle (EV) cells, and a sub-battery of 89 series connected EV cells. The ADL also has initiated evaluation of the Chloride Silent Power Limited (CSPL) sodium-sulfur (PB) battery technology in the form of 8 individual cells. The evaluation of the FACC-LL cells consisted of an abbreviated performance characterization followed by life-cycle tests on two individual cells and life-cycle tests only on the two other individual cells. The evaluation indicated that the technology was improving, but long-term (life) reliability was not yet adequate for utility applications. The cells exhibited individual cycle lives ranging from 659 to over 1366 cycles, which is equivalent to 2 1/2 to 5 1/2 years in utility use. It was also found that full-cell capacity could only be maintained by applying a special charge regime, regularly or periodically, that consisted of a constant-current followed by a constant-voltage. DOE

N88-20545# California Univ., Berkeley. Lawrence Berkeley Lab.
A NOVEL CLASS OF POSITIVE ELECTRODES FOR RECHARGEABLE BATTERIES Ph.D. Thesis
C. C. Mailhe Oct. 1987 139 p
(Contract DE-AC03-76SF-00098)
(DE88-004559; LBL-24244) Avail: NTIS HC A07/MF A01

A novel class of organosulfur positive electrodes for intermediate temperature rechargeable batteries is described here. High temperature batteries such as sodium/sulfur exhibit alluring and unrivaled power and energy densities but unfortunately are plagued by corrosion problems. A decrease in the operating temperature from 350 C to the 110 to 150 C temperature range resulted in a simplified cell technology allowing for the use of polymeric seals. The non-aggressive nature of the positive electrode lessened also considerably the corrosion issues. A tetraethylthiuram disulfide/diethyldithiocarbamate cell was first investigated because of its attractive theoretical energy density of 360 Wh/kg and because of the low melting point of the diethyldithiocarbamate sodium salt (145 C), condition necessary to maintain the electrode in the liquid state. (Sodium and Beta Alumina were respectively the negative electrode and the solid electrolyte). The low melting sodium salt requirement can be advantageously replaced by the use of a solvent in charge of solubilizing the sodium salt generated during discharge. Low viscosity and high dielectric constant were identified as two key factors in the solvent optimization. The addition of 20 percent in weight of dimethyl sulfoxide or of sulfolane permitted the cell charge and discharge at 5 mA/sq cm at 130 C. Peak current densities of 100 mA/sq cm at 1 Volt were also obtained. The perspectives opened by solvent addition, led to the concept of electroactive solvent where the electroactive material itself solvates the sulfide sodium salt. In this respect, the alkoxyalkyl disulfides are promising candidates because of their combined low viscosity, high energy density and thermal stability. DOE

N88-20546# Pinnacle Research Inst., Cupertino, Calif.
TECHNOLOGY BASE RESEARCH ON ZINC/AIR BATTERY SYSTEMS Final Report
H. B. SierraAlcazar, P. D. Nguyen, and A. A. Pinoli Sep. 1987 50 p
(Contract DE-AC03-76SF-00098)
(DE88-004893; LBL-23960) Avail: NTIS HC A03/MF A01

The capacity extension of additives was tested in a 200 cm^3 bi-cell and a Zn powder moving-bed slurry. It was found that for the Type A additives in 12 M KOH, 25 g/l of silicate provided higher capacity than stannate, titanate and aluminate additives. The optimum concentration of sorbitol (a Type B additive that stabilizes polymeric chains involving ZnO) was found to be 15 g/l in 12 M KOH. A silicate and sorbitol combination added to Zn powder slurry in 12 M KOH provided a 20 percent increase in discharge capacity (195 Ah/l at 200 A/cm^2) compared to the maximum capacity obtained with silicate alone. A much lower capacity (74 Ah/l) was realized with silicate as Type C additive (precipitation of ZnO away from the Zn surface, for low KOH concentrations). The mechanisms of passivation and capacity extension were discussed and a model presented. The cell voltage and power densities were determined for the discharge process as a function of: (1) current densities, (2) cathode depolarizer (air or oxygen), and (3) type of slurry (Zn powder or Zn coated polymeric bead). Air depolarization was observed to decrease the maximum power densities of both slurry types. The power densities obtained with Zn powder slurries were higher at all current densities investigated than those obtained with Zn coated polymeric beads (Zn-powder peak power densities more than doubled peak power densities obtained with Zn coated polymeric beads). The recharge process was studied with a planar electrode and with a rotating cylinder electrode. The current efficiency and cathode potentials were determined for glassy carbon and Mg cathodes. The dendritic Zn deposits were mechanically removed from the rotating cylinder electrode with fixed blades. Mechanical removal proved to be unsatisfactory in the embodiment investigated due to preferential dendritic growth on the baldes. Further investigations of discharge cell designs are underway. DOE

N88-20547# Pennsylvania Univ., Philadelphia. Dept. of Materials Science and Engineering.
POLYMERIC ELECTROLYTES FOR AMBIENT TEMPERATURE LITHIUM BATTERIES Final Report
G. C. Farrington Sep. 1987 27 p
(Contract DE-AC03-76SF-00098)
(DE88-004896; LBL-23959) Avail: NTIS HC A03/MF A01

During this reporting period a number of novel solid polymer electrolytes formed by salts of multivalent cations and polyethylene oxide (PEO) have been prepared and characterized. These materials are of interest not only because of their potential ionic conductivities, but also because some of them may have electronic conductivity and oxidizing power which would be useful for novel electrode materials in all-solid-state batteries. Two broad classes of materials were investigated: PEO solutions of Zn(2), Cd(2), and Pb(2), all of which are potential electrolytes for solid-state batteries, and PEO solutions of transition metal salts, which are of interest as possible cathode materials. Mixed compositions containing both divalent cations and lithium ions were also prepared. Electrolytes formed with small, highly-polarizing ions, such as Mg(2) and Ca(2), are essentially pure anion conductors. Electrolytes containing Zn(2) behave similarly, unless they are hydrated, in which case the Zn(2) ions are quite mobile. Electrolytes formed with larger, more polarizable cations, such as Pb(2) and Cd(2), conduct both anions and cations. Solutions of salts of transition metal cations form a third group of electrolytes. Of the electrolytes investigated so far, those formed with Ni(++) salts are the most unusual. It appears as if the transport number of Ni(2) and the electrolyte conductivity can be greatly enhanced by controlling the hydration and dehydration of the polymer. DOE

N88-20548# Edgerton, Germeshausen and Grier, Inc., Idaho Falls, Idaho.
MISSION DIRECTED GOALS FOR ELECTRIC VEHICLE BATTERY RESEARCH AND DEVELOPMENT: THE TASK FORCE ON ELECTRIC VEHICLE BATTERY GOALS
Nov. 1987 48 p
(Contract DE-AC07-76ID-01570)
(DE88-005601; DOE/CE-0148-Rev-1) Avail: NTIS HC A03/MF A01

This report on the Department of Energy (DOE) mission directed goals for electric vehicle battery research and development is a revision and update of report DOE/CE-0148. The original report was prepared by the Task Force on Electric Vehicle Battery Goals and published by the Electric and Hybrid Propulsion (EHP) Division of the Office of Transportation Systems. The EHP Division of the DOE formed the Task Force on Electric Vehicle Battery Goals to evaluate existing EV battery R and D goals and to recommend new battery goals targeted at the urban van mission. The original report (DOE/CE-0148) was distributed to government and industry

for review and comment. After consolidation of the comments, each comment was considered in the context of the project scope. INEL edited and published this document as the final report on the efforts of the Task Force on Electric Vehicle-Battery Goals. To the extent possible within the original scope of the project, the comments of government and industry are incorporated herein. This report will be updated periodically as results from current research, both federally and privately supported, become available. DOE

N88-20549# Technische Hogeschool, Eindhoven (Netherlands). Dept. of Electrical Engineering.
GRIDLESS ROUTING FOR GENERALIZED CELL ASSEMBLIES: REPORT AND USER MANUAL
Lukas P. P. P. Ginneken Sep. 1987 49 p Sponsored by the Commission of the European Communities
(Contract FOM-EEL-Proj-33.0417; ESPIRIT Proj. 999)
(EUT-87-E-180; ISBN-90-6144-180-3; ISSN-0167-9708; ETN-88-91827) Avail: NTIS HC A03/MF A01

A routing system for general custom cell layout style is presented. The system features construction of a floor plan topology by slicing, global routing by means of a Steiner tree heuristic, and gridless channel routing with rigorous contour compaction, which allows variable width wires and easy adaptation to the design rules. The router handles arbitrarily sized cells and takes advantage of irregular channel boundaries. Power and ground lines are routed planarly with variable width. An O(nlogn) algorithm for making contours irredundant is given. Benchmarks of the channel router and application to a small chip are included. ESA

N88-20550# Sandia National Labs., Albuquerque, N. Mex.
QUARTZ OSCILLATOR ANALYSIS
K. O. Wessendorf Jan. 1988 33 p
(Contract DE-AC04-76DP-00789)
(DE88-005886; SAND-87-0311) Avail: NTIS HC A03/MF A01

This paper develops an analytical modeling technique for a Pierce oscillator employing a quartz resonator and a bipolar transistor. The model is useful in predicting frequency, minimum gain required, and steady state signal levels of oscillation. This model is used to predict the operation of an actual 16MHz oscillator circuit. The circuit was modified to simulate changes in the resonator's motional resistance, R(sub m), and the bipolar's base to emitter resistance, h(sub ie). The model was used to show how well the oscillator's performance could be predicted. If the circuit is characterized well, the oscillator's frequency can be determined within 10 ppM and the oscillation amplitude can be calculated to within + or - 20 percent of actual measured values. DOE

N88-20551# Argonne National Lab., Ill.
TESTING AND DEVELOPMENT OF ELECTRIC VEHICLE BATTERIES FOR EPRI ELECTRIC TRANSPORTATION PROGRAM Technical Report, Jan. 1985 - Apr. 1986
J. Lee, comp. Jan. 1988 54 p
(Contract W-31-109-eng-38)
(DE88-005894; ANL-87-44) Avail: NTIS HC A04/MF A01

The battery is a key element in the acceptance of electric vehicles, and R and D efforts are being undertaken to improve battery performance and lifetime. In this electric-vehicle battery program, controlled laboratory tests were conducted to evaluate the effects of selected factors on the performance and life of the EV-2300 lead-acid battery manufactured by Johnson Controls, Inc. These factors included simulated driving profiles with different levels of peak power demands for vehicle acceleration, long rest times after charge or discharge, and different methods of recharging. The performance and cycle life of a 12-module full-scale battery pack and its support system were also evaluated. This report summarizes the work carried out on this program from January 1985 through April 1986. This work involved tests of the battery pack and support system, statistical analysis of capacity and power data from earlier tests of six-cell modules, and post-test analysis of selected modules and cells. DOE

N88-20552# Haut Commissariat a la Recherche, Algiers (Algeria). Centre d'Etudes Nucleaires et Solaires.
SIMPLIFIED PHYSICAL APPROACH OF THE CONTROL BY EDDY CURRENT M.S. Thesis
M. Zergoug Jan. 1986 124 p In FRENCH and ENGLISH
(TI88-701076; INIS-mf-11057) Avail: NTIS (US Sales Only) HC A06/MF A01

The variation was studied of the resistance of coil surrounding a nonferromagnetic cylindrical core in the presence of a flaw. The flaw is a longitudinal notch with an infinite length and a rectangular section. The impedance variation is to be calculated from the geometric repartition of the flow lines in the core. This repartition, as a function of the flaw, is given by the variation produced by the presence in the nonferromagnetic conducting core, of an emerging axial flaw with an infinite length. It is therefore possible to obtain in real time, on a computer screen, the image of a long standard flaw which may produce the observed impedance variation. DOE

N88-20553*# National Aeronautics and Space Administration, Washington, D.C.
EDF'S STUDIES AND FIRST CHOICES REGARDING THE DESIGN OF ELECTRICAL EQUIPMENT
Michel Paris, Gisele Metzger, Michel Pays, and Maurice Pasdeloup Mar. 1988 31 p Transl. into ENGLISH of Etudes et Premiers Choix d'EDF Concernant la Conception des Materiels Electriques (France, Electricite de France RGE), Jul. - Aug. 1984 p 465-474 Transl. by Scientific Translation Service, Santa Barbara, Calif.
(Contract NASw-4307)
(NASA-TT-20222; NAS 1.77:20222) Avail: NTIS HC A03/MF A01 CSCL 09C

In the performance of its studies and in its first choices, Electricite de France has taken into account the three parameters that have been judged essential for its electrical installations: flammability and flame propagation; smoke opacity; and corrosiveness and toxicity of emitted gases. In this research, materials tests have been widely developed in order to insure simple manufacturing controls, and to decrease the costly testing of near to full size models. Author

N88-20554# Instituto de Pesquisas Espaciais, Sao Jose dos Campos (Brazil).
NUMERICAL METHODS IN THE RESOLUTION OF CONTROL ELECTROVALVE MODEL [METODOS NUMERICOS NA RESOLUCAO DO MODELO DE UMA ELETROVALVULA DE CONTROLE]
Ismael E. deOliveira, Jr. and Eduardo AugustoGomesPereira Apr. 1987 7 p In PORTUGESE Presented at the 8th Regional Meeting of Applied Math and Computation, Belo Horizonte, Brazil, 26-28 Mar. 1987
(INPE-4154-RPE/540) Avail: NTIS HC A02/MF A01

This work shows the numerical method application in the resolution of the model of transistors in an electrovalve employed in the satellite attitude control. The primary support method is the curve approximation through third degree spline polynomials, used to approximate the curve characteristics of ferromagnetic materials. Two methods for localization of zero functions are used, the Newton-Raphson and the Regula Falsi. For the last, through a system of differential equations derived from the model, the predictor-corrector and the Runge-Kutta are applied, this final stage initiates the former. Also shown are some typical results obtained with this model. Author

N88-20555*# National Aeronautics and Space Administration. Lewis Research Center, Cleveland, Ohio.
OPTICAL RF DISTRIBUTION LINKS FOR MMIC PHASED ARRAY ANTENNAS
Richard R. Kunath, Kul B. Bhasin, and Charles A. Raquet 1987 7 p Presented at the IEEE AP-S International Symposium and URSI Radio Science Meeting, Blacksburg, Va., 15-19 Jun. 1987
(NASA-TM-100841; E-4031; NAS 1.15:100841) Avail: NTIS HC A02/MF A01 CSCL 09C

Conventional methods to distribute RF signals to GaAs Monolithic Microwave Integrated Circuits Phased Array Antennas are inadequate for arrays having large numbers of elements. Optical RF distribution links have been proposed as a lightweight, mechanically flexible, and low volume solution. Three candidate techniques for providing optical RF distribution are discussed along with the electro-optic devices required to configure them. A discussion of the present status of applicable electro-optics devices is also included. Author

34 FLUID MECHANICS AND HEAT TRANSFER

Includes boundary layers; hydrodynamics; fluidics; mass transfer; and ablation cooling.

For related information see also *02 Aerodynamics* and *77 Thermodynamics and Statistical Physics.*

N88-20556# Hokenson (Gustave J.), Los Angeles, Calif.
COHERENT STRUCTURE-REFLECTIVE TURBULENT VISCOUS FLOW MODELING Final Report, Mar. 1985 - Mar. 1987
Gustave J. Hokenson 7 Sep. 1987 94 p
(Contract F49620-85-C-0075)
(AD-A188339; HOKE-87-AF-01; AFOSR-87-1660TR) Avail: NTIS HC A05/MF A01 CSCL 20D

Three aspects of turbulent structure in shear flows were investigated theoretically. Both analytical and computational strategies were employed to extract new information on: (1) advection velocities of large-scale structure; (2) the velocity vector angle characteristics of turbulent fluctuations; and (3) the stability characteristics of the mean turbulent velocity profile. With regard to topic 1, the study of the propagation of a bulge in wall-bounded shear flow has exposed three characteristic propagation speeds. In (temporally and/or spatially) variable pressure flows, a unique inverse approach to the problem has exposed the critical value for the shape factor (H) of 2.0. This result impacts not only turbulent structure dynamics but flowfield separation as well. The work on topic 2, has served to clarify the importance of angular structure with respect to the interpretations of turbulence physics, the modeling thereof and advantages of those variables in numerical simulation. Finally, the mean turbulent velocity profile was found to support unstable modes of oscillation for the large-scale structure if the unresolved small scale processes are modeled appropriately. GRA

N88-20557# California Inst. of Tech., Pasadena. Div. of Engineering and Applied Science.
CAVITATION INCEPTION Final Report, 1Jul 1983 - 30 Jun. 1987
Allan J. Acosta 21 Dec. 1987 7 p
(Contract N00014-83-K-056)
(AD-A189220; E290.1) Avail: NTIS HC A02/MF A01 CSCL 20D

The present research effort on a special topic of Cavitation Inception was initiated on 1 July 1983 and was continued through June 30, 1987. This special area of interest was specifically directed towards the observation of microparticulates and microbubbles in the natural waters of the ocean. The motivation for this example of field work in the study of cavitation inception is that there is, even today, a great scarcity of information about the concentrations of microparticulates of all types in the natural waters that ships and all naval equipment may be expected to operate within. This is an important issue for several reasons; first of all it is known that an absence of microbubbles in laboratory cavitation test facilities leads to erroneous estimates of the inception of cavitation itself and the form and extent of the patterns that develop subsequent to the onset of cavitation. These kinds of laboratory cavitation scaling problems were beautifully exemplified in cavitation tests in the Netherlands vacuum towing tank where to achieve even rough cavitation similarity with prototypical propeller cavitation performance the waters of the towing tank had to be seeded with microbubbles formed by electrolysis. GRA

N88-20558# Pennsylvania State Univ., University Park. Applied Research Lab.
HIGH REYNOLDS NUMBER PUMP FACILITY FOR CAVITATION RESEARCH
K. J. Farrell, M. W. McBride, and M. L. Billet Sep. 1987 29 p Sponsored by the Naval Sea Systems Command, Washington, D.C.
(AD-A189310; PSU/ARL-TR-87-011) Avail: NTIS HC A03/MF A01 CSCL 13K

A High Reynolds Number Pump Facility (HIREP) designed for cavitation studies in the bladetip/endwall region of an axial flow pump is described. The facility consists of a 1.07-m diameter pump state driven by a 1.22-m diameter downstream turbine. An incompressible Reynolds Number of 6,000,000 at the rotor tip is achievable. The two units rotate on a common shaft and operate in the 1.22-m diameter test section of the Garfield Thomas Water Tunnel of the Applied Research Laboratory at Penn State. The facility was designed to accommodate laser velocimeter (LV) measurements in the pump stage, radially traversing five-hole probes in every stage, and a number of transducers in the rotating frame of reference: steady and unsteady pressure transducers force and torque cells, and accelerometers. The latter capability is provided by a slip-ring unit and hollow blade passage ways for conductors from the instrumentation in rotor-tip region. An optical quality window for LV measurements and other windows and ports are available for visual observation and instrumentation access. GRA

N88-20559# Imperial Coll. of Science and Technology, London (England).
TWO-PHASE FLOWS IN THE WAKE OF IN-CYLINDER PROJECTILES Final Technical Report, Jul. 1984 - Oct. 1987
J. H. Whitelaw Dec. 1987 74 p
(Contract DAJA45-84-C-0032; DA Proj. 1L1-61102-BH-57)
(AD-A189422; R/D-4352-R-AN) Avail: NTIS HC A04/MF A01 CSCL 19J

The contents of this report on two-phase flows is as follows: Two-Phase Flows in the Wake of In-Cylinder Projectiles; In-Bore Velocity Measurements in the Wake of a Subsonic Projectile; Velocity Characteristics of the Wake of an In-Cylinder Projectile; Subsonic Single-Phase Flow in a Gun Simulator; Subsonic Single- and Two-Phase Flow Characteristic of a Gun Simulator. GRA

N88-20560# Pennsylvania State Univ., University Park.
THE EULER-BERNOULLI BEAM EQUATION WITH BOUNDARY ENERGY DISSIPATION Report, 1 Sep. 1985 - 31 Aug. 1987
G. Chen, S. G. Krantz, D. W. Ma, C. E. Wayne, and H. H. West 5 Jan. 1988 31 p
(Grants AF-AFOSR-0253-85; NSF DMS-84-01297; NSF DMS-85-01306; NSF DMS-84-03664)
(AD-A189517; AFOSR-88-0147TR) Avail: NTIS HC A03/MF A01 CSCL 20K

Many problems in structural dynamics involve stabilizing the elastic energy of partial differential equations (PDE) such as the Euler-Bernoulli beam equation by boundary conditions. Exponential stability is a very desirable property in such elastic systems. The energy multiplier method has been successfully applied by several people to establish exponential stability for various PDEs and boundary conditions. However, it has also been found that for certain boundary conditions the energy multiplier method is not effective in proving the exponential stability property. A recent theorem of F. L. Huang introduces a frequency domain method to study such exponential decay problems. In this paper, we derive estimates of the resolvent operator on the imaginary axis and apply Huang's theorem to establish an exponential decay result for an Euler-Bernoulli beam with rate control of the bending moment only. We also derive asymptotic limits of eigenfrequencies, which was also done earlier by P. Rideau. Finally, we indicate the realizability of these boundary feedback stabilization schemes by

illustrating some mechanical designs of passive damping devices. GRA

N88-20561# Air Force Inst. of Tech., Wright-Patterson AFB, Ohio. School of Engineering.
INVESTIGATION OF HEAT TRANSFER TO A FLAT PLATE IN A SHOCK TUBE M.S. Thesis
Joseph T. Novak Dec. 1987 257 p
(AD-A189538; AFIT/GA/AA/87D-5) Avail: NTIS HC A12/MF A01 CSCL 20M

The heat transfer mechanisms taking place in the flow induced behind a shock wave travelling across a flat plate were investigated for flat plates with sharp and rounded leading edges. The boundary layer behind the shock is described by a transient boundary layer followed by a steady state boundary layer as the effects of the leading edge are transmitted downstream. The use of a multichannel high speed transient data recorder allowed thin film heat transfer gages at up to eight axial locations along the length of the flat plate to be simultaneously sampled. Heat transfer rate histories for each axial location were time correlated to the same flow conditions. The results indicate the existence of a threshold free system velocity (relative to the plate) above which are confined to some narrow interval. For Mach numbers below 1.22, the sharp leading edge flat plate experienced heat transfer rates in excess of theory, but the rounded leading edge flat plate data showed a consistent correlation between heat transfer magnitude and axial location on the plate; with limited data, the rounded plate showed no such correlation. GRA

N88-20562# Stanford Univ., Calif. Dept. of Mechanical Engineering.
CONTROL OF STRUCTURE IN TURBULENT FLOWS: BIFURCATING AND BLOOMING JETS Final Report, 1 Feb. 1984 - 31 May 1987
W. C. Reynolds, D. E. Parekh, and Mario J. Lee 10 Oct. 1987 49 p
(Contract F49620-84-K-0005; AF Proj. 2307)
(AD-A189607; AFOSR-88-0036TR) Avail: NTIS HC A03/MF A01 CSCL 20D

The general objective of this work is to control jet flows by properly organizing the dominant large-scale vortex structures. The work has focused on understanding the influence of excitation frequency and amplitude on the large-scale structures of these flows at various Reynolds numbers. Specifically, the effects of dual-mode forcing on the structure, momentum, and mixing characteristics of turbulent jets have been investigated using a combination of laboratory experiments and numerical simulations. The combination of properly-selected axial and orbital excitation has been shown to have dramatic effect on the structure and mixing of round jets. Experiments and numerical simulations show that these phenomena are due to interaction between the large-scale vortices in the jet near field. The position and phasing of these vortices can be altered by relatively weak excitation, causing the jet to divide into two separate jets (bifurcation) or to explode (bloom) in a shower of vortex rings. This report summarizes the key results of studies in water and low-speed air flows. GRA

N88-20563# University of Southern California, Los Angeles. Dept. of Mechanical Engineering.
FLUIDIZATION MECHANISMS IN SLURRY FLOWS Quarterly Report
C. S. Campbell Jan. 1988 9 p
(Contract DE-FG22-86PC-90957)
(DE88-005191; DOE/PC-90957/T5) Avail: NTIS HC A02/MF A01

There are two major events to report this time around. The first is the successful second startup of the slurry pipe loop which showed that the loop could accept particles in the dense phase region (around 50 percent by volume), but unfortunately, resulted in a failure in one of the rectangular channel sections after the pump had difficulty passing the particles at that density. The second involves a change in fluidization mechanism determination required by problems with drift in the commercial fiber-optic displacement transducers used in the particle pressure probes. Both mean that the project is falling behind schedule. DOE

N88-20564# Battelle Columbus Labs., Ohio.
PROCEEDINGS OF THE 1987 INTERNATIONAL SYMPOSIUM ON CONDENSING HEAT EXCHANGERS
Apr. 1987 224 p Symposium held in Columbus, Ohio, 14 Apr. 1987 Prepared in cooperation with Brookhaven National Lab., Upton, N.Y.
(Contract DE-AC02-76CH-00016)
(DE88-005230; BNL-52068-Vol-2; GRI-87/0091-2; CONF-8704247-Vol-2) Avail: NTIS HC A10/MF A01

Technology for advanced, high-efficiency heating equipment was discussed. Twenty-six papers from nine countries were presented, covering various aspects of such equipment designed to operate with condensing heat exchangers - including furnaces, boilers, water heaters, and fuel-fired heat pumps. The emphasis was on residential and commercial equipment, and both gas- and oil-firing were considered. Specific topics included: (1) condensate characterization; (2) metallic materials for condensing heat exchangers - aluminum and stainless steel; (3) non-metallic materials for heat exchangers and vents - ceramics and polymers; (4) example condensing units and systems; (5) experience with oil-fired condensing units; (6) field experience; (7) design techniques and efficiency test procedures. Papers are indexed separately. DOE

N88-20565# Cornell Univ., Ithaca, N.Y.
SYSTEMS NEAR THE ONSET AND IN THE WELL-DEVELOPED REGIMES OF TURBULENCE
E. D. Siggia 1987 12 p
(Contract DE-AC02-83ER-13044)
(DE88-005365; DOE/ER-13044/T2) Avail: NTIS HC A03/MF A01

This paper contains progress information on Painleve property and integrability, blow up in the three-dimensional Euler and Navier-Stokes equations, physics of disordered media and understanding of the interconnections between arbitrary objects constructed on binary trees, period doubling fixed points, presentation functions and scaling functions. DOE

N88-20566# Massachusetts Univ., Amherst.
MIXING OF VISCOUS FLUIDS: BEHAVIOR OF MICROSTRUCTURES AND CHAOS
1988 37 p
(Contract DE-FG02-85ER-13333)
(DE88-006287; DOE/ER-13333/1) Avail: NTIS HC A03/MF A01

In spite of its universality and practical implications, the understanding of mixing of viscous fluids remains rather incomplete. More work is necessary for the establishment of a comprehensive framework capable of addressing the many problems encountered in nature and technology. This proposal focuses on basic computational and experimental studies along two main themes towards the completion of such long-range goal: investigations of chaotic mixing of single fluids in deterministic two- and three-dimensional (slow) flows, and dynamics of active microstructures in such flows (e.g., stretching, breakup, coagulation, etc.). Work in the first area is underway and a clear picture is emerging; the theme of the second area is less well defined and the proposed ideas purely exploratory. Much work remains to mesh the two levels; in this proposal we elaborate on both aspects and indicate possible lines of attack. DOE

N88-20567# Naval Postgraduate School, Monterey, Calif. Dept. of Mechanical Engineering.
AN EXPERIMENTAL INVESTIGATION OF DECELERATING FLOW ABOUT TWO-DIMENSIONAL CAMBERED PLATES
T. Sarpkaya 30 Oct. 1987 54 p
(Contract DE-AC04-76DP-00789)
(DE88-006598; SAND-87-7159) Avail: NTIS HC A04/MF A01

Impulsively-started uniform flow, decelerating at specified rates, about two-dimensional cambered plates with included angles of

120, 180, and 240 degrees has been investigated experimentally in a vertical water tunnel. The forces acting on the plates have been determined as a function of the relative displacement of the fluid at subcritical Reynolds numbers. The evolution of the vortices was visualized by means of various dyes and polystyrene beads. The variation of the drag coefficient with time is interpreted in terms of the formation, growth, and motion of vortices. DOE

N88-20568# Pacific Northwest Labs., Richland, Wash.
HEAT PIPE TRANSIENT ANALYSIS: VAPOR DYNAMICS
J. M. Kelly and A. L. Schor Jan. 1988 48 p Presented at the 5th Symposium on Space Nuclear Power Systems, Albuquerque, N. Mex., 11 Jan. 1988 Prepared in cooperation with MIT, Cambridge
(Contract DE-AC06-76RL-01830)
(DE88-005132; PNL-SA-15374; CONF-880122-6) Avail: NTIS HC A03/MF A01

A multidimensional model for the analysis of heat pipe transients (HPTRAN) is being developed. The cornerstone of this model is a new partially implicit numerical algorithm for two phase flow. Time steps far in excess of the Courant limit (CFL number of 100 to 200) are allowed, without the computational burden per time step that accompanies a fully implicit treatment. The resulting computational efficiency renders transient multidimensional analysis practicable. This paper provides a brief description of the numerical method and presents the results of initial data comparisons. Bowman (1987) performed a series of experiments to investigate heat pipe vapor dynamics using a porous tube with blowing/suction. These tests were simulated using both distributed (2-D) and lumped (1-D) parameter models. Stable solutions were obtained using large time steps for a wide range of Reynolds (5 x 10 -10) and Mach (0.1 to 1.0) numbers. Good data comparisons were achieved, with the multidimensional model outperforming the one-dimensional model. Areas for future improvements were identified in both the turbulence model and the finite difference form of the momentum flux terms. DOE

N88-20569# National Aerospace Lab., Amsterdam (Netherlands). Space Div.
FEASIBILITY DEMONSTRATION OF A SENSOR FOR HIGH-QUALITY TWO-PHASE FLOW
A. A. M. Delil 9 Jan. 1987 32 p
(Contract NIVR-2502-N)
(NLR-TR-87009-U; B8729599; ETN-88-91724) Avail: NTIS HC A03/MF A01

Systems to control the liquid flow rates into evaporative cold plates in the two-phase flow heat transport systems for the Columbus Space Platform and the Space Station are discussed. Candidate components for such a control system are sensors monitoring the (very high) mixture quality at the cold plate exit lines, control algorithms, and actuators (valves) to adjust the liquid flow rates. The feasibility of a dedicated sensor is theoretically and experimentally demonstrated. Recommendations for the further development of the sensor are presented. ESA

N88-20570# National Aerospace Lab., Amsterdam (Netherlands). Fluid Dynamics Div.
THREE-DIMENSIONAL SHEAR LAYER EXPERIMENTS AND THEIR USE AS TEST CASES FOR CALCULATION METHODS
B. vandenBerg 23 May 1986 17 p Presented at the AGARD Special Course on Computation of Three-Dimensional Boundary Layers including Separation, Brussels, Belgium, 14-18 Apr. 1986 Previously announced as N87-22148
(NLR-MP-86036-U; B8725236; ETN-88-91727) Avail: NTIS HC A03/MF A01

Selection of experiments to test three-dimensional shear layer calculations is discussed. The fact that the three-dimensionality of the flow affects so strongly the turbulence properties can only be explained when realizing the important role of the large eddies in turbulent flows. The structure of the large eddies will be distorted when the mean velocity profile in the boundary layer is skewed and so their development may be obstructed, leading to a decreased turbulence level in three-dimensional boundary layers. As a consequence of the important role of the large eddies, whose properties are not easily generalized, universality of empirical assumptions about turbulence is difficult to achieve. Unfortunately many experiments do not simulate practical flow conditions. Generally the boundary layer is thick in the experiments relative to the length of the measurement region, which often leads to pressure forces which are comparatively large, and a tendency of turbulence history effects to dominate the turbulence development. There is a need for three-dimensional turbulent boundary layer experiments providing reliable data in flow conditions, which better resemble those in practical flows. Fundamental experiments should be carried out to shed more light on the turbulent processes in three-dimensional boundary layers. ESA

N88-20571# National Aerospace Lab., Amsterdam (Netherlands). Space Div.
DEVELOPMENT, MANUFACTURING AND TESTING OF A GAS-LOADED VARIABLE CONDUCTANCE METHANOL HEAT PIPE
R. I. J. vanBuggenum and D. H. W. Daniels 5 Feb. 1987 12 p Presented at the 6th International Heat Pipe Conference, Grenoble, France, May 1987
(Contract NIVR-02801-N)
(NLR-MP-87010-U; B8729620; ETN-88-91736) Avail: NTIS HC A03/MF A01

The experimental technology required to measure the performance of moderate temperature heat pipes is presented. The heat pipe manufacturing process is described. The hydrodynamic characteristics of the porous structure inside the heat pipe envelope were examined using a specially developed test rig, based upon a steady-state evaporation test. A fully automated test facility was developed and validated by testing constant conductance and variable conductance heat pipes (VCHP). Theoretical performance predictions are illustrated in terms of pressure, depicted in 3D-plots, and compared with the test results of the heat pipe performance tests. The design of the VCHP was directed towards the verification of the VCHP mathematical model. The VCHP design is validated and ready for the final testing and model verification. ESA

N88-20572# Deutsche Forschungs- und Versuchsanstalt fuer Luft- und Raumfahrt, Brunswick (West Germany). Abteilung Trans-Ueberschall-Entwurfsverfahren.
SOLUTION OF TWO-DIMENSIONAL EULER EQUATIONS: EXPERIENCE WITH A FINITE VOLUME CODE
Norbert Kroll and Romesh Kumar Jain Sep. 1987 144 p
(DFVLR-FB-87-41; ISSN-0171-1342; ETN-88-91924) Avail: NTIS HC A07/MF A01; DFVLR, VB-PL-DO, Postfach 90 60 58, 5000, Cologne, Federal Republic of Germany, 44.50 deutsche marks

A numerical method for the solution of two-dimensional Euler equations using a finite volume spatial discretization and Runge Kutta time stepping schemes, given by Jameson, Schmidt, and Turkel (1981) is described. Critical features of the algorithm like implementation of boundary conditions, influence of the artificial dissipation, multistage time stepping schemes, and acceleration techniques for the convergence to steady state, are analyzed. Accuracy and reliability of the computer code is tested in computing subsonic and transonic flows around various airfoils. Results are satisfactory. ESA

N88-20573*# Old Dominion Univ., Norfolk, Va. Dept. of Mechanical Engineering and Mechanics.
GRAPHICS AND FLOW VISUALIZATION OF COMPUTER GENERATED FLOW FIELDS Progress Report, 31 Jul. 1987
M. Kathong and S. N. Tiwari Aug. 1987 86 p
(Contract NCC1-68)
(NASA-CR-182679; NAS 1.26:182679) Avail: NTIS HC A05/MF A01 CSCL 20D

Flow field variables are visualized using color representations described on surfaces that are interpolated from computational grids and transformed to digital images. Techniques for displaying two and three dimensional flow field solutions are addressed. The

transformations and the use of an interactive graphics program for CFD flow field solutions, called PLOT3D, which runs on the color graphics IRIS workstation are described. An overview of the IRIS workstation is also described. Author

N88-20574*# Old Dominion Univ., Norfolk, Va. Dept. of Mechanical Engineering and Mechanics.
DEVELOPMENT OF DISTURBANCES IN SWEPT WING FLOWS Final Report, 1 Jun. 1987 - 15 Apr. 1988
Osama A. Kandil and Nabil M. El-Hady Apr. 1988 7 p
(Grant NAG1-729)
(NASA-CR-182675; NAS 1.26:182675) Avail: NTIS HC A02/MF A01 CSCL 20D

The development of a subharmonic secondary instability in a boundary layer with pressure gradients controlled by suction was investigated. The effect of suction control on this early stage leading to transition is evaluated. The secondary three-dimensional instability problem for compressible boundary layers was formulated to investigate theoretically the effect of finite amplitude two-dimensional wave on the growth of three-dimensional perturbations in compressible boundary layers. Only a range of Mach numbers up to the transonic, where the critical primary disturbance is two dimensional, was covered. Thr evolution of resonant triads in three-dimensional boundary layers was investigated. The triads investigated were comprised of different modes, stationary crossflow (CF), traveling crossflow, vertical vorticity (VV), and Tollmein-Schlichting (TS) modes. The mean flow used in the calculations is the boundary layer on a modern LFC transonic 23 swept wing. In the analysis the growth of the boundary layer is taken into account assuming that it is of the same order as the nonlinear effects. B.G.

N88-20575# Toronto Univ., Downsview (Ontario). Inst. for Aerospace Studies.
AN INTERFEROMETRIC INVESTIGATION OF THE DIFFRACTION OF PLANAR SHOCK WAVES OVER A HALF-DIAMOND CYLINDER IN AIR
D. L. Zhang and I. I. Glass Mar. 1988 107 p
(Contract DNA-001-85-C-0368; Grants AF-AFOSR-0124-87; NSERC-A1647)
(UTIAS-322; ISSN-0082-5255) Avail: NTIS HC A06/MF A01

An investigation is conducted on the diffraction of planar shock waves over a half-diamond (45 deg wedge angles) cylinder (28 mm x 28 mm x 56 mm cross section) in air at initial pressures ranging from 6.67 Kpa to 80.3 Kpa (50 torr to 605 torr), at an initial temperature near 300 K in all cases and at initial Mach numbers ranging from 1.35 equal to or less than M sub S equal to or less than 2.82. More than 150 experiments were conducted including models with smooth, spongy (plastic), rough (sandpaper) and saw-tooth surfaces. Infinite fringe interferograms were used throughout. The UTIAS 10 cm x 18 cm hypervelocity shock tube and the 23 cm diam field-of-view Mach-Zehnder interferometer were utilized for this purpose. The induced flows behind the incident shock waves were subsonic, transonic and supersonic. The subsequent intersections with the initial wedge produced regular, single Mach, complex Mach, and double Mach reflections. The isopycnics over the entire flowfields were evaluated and the pressure fields determined using the isentropic equation of state. A half-size model was also used to study the effects of longer flow durations. Author

N88-20576# Toronto Univ., Downsview (Ontario). Inst. for Aerospace Studies.
PSEUDO-STATIONARY OBLIQUE-SHOCK-WAVE REFLECTIONS IN LOW GAMMA GASES: ISOBUTANE AND SULPHUR HEXAFLUORIDE
J. T. Urbanowicz Feb. 1988 129 p Sponsored in cooperation with the Canadian Natural Sciences and Engineering Council
(Contract DNA-001-85-C-0368; Grant AF-AFOSR-0124-87)
(UTIAS-TN-267; ISSN-0082-5263) Avail: NTIS HC A07/MF A01

Nonstationary oblique-shock-wave reflections in sulfur hexafluoride and isobutane were investigated experimentally and numerically. Over 100 experiments were conducted in the UTIAS 10 x 18 cm Hypervelocity Shock Tube in order to investigate the RR-MR transition boundary and the features of terminal-double Mach reflection. Five types of shock wave reflections, i.e., regular (RR), single Mach (SMR), complex Mach (CMR), double Mach (DMR), and terminal double Mach (TDMR) reflections were observed. These were studied with infinite-fringe interferograms and shadowgraphs using a 23 cm diameter field of view Mach-Zehnder interferometer. The analytical transition boundaries were established up to an initial shock-wave Mach number M sub S = 10. The experimental results agree well with the predicted boundaries for the gases in vibrational equilibrium except for the MM-RR boundary where Mach reflections were observed up to 8 degrees above the detachment criterion line. Strong dependence of the initial test pressure on the first triple point trajectory angle chi was noted and investigated analytically. Author

N88-20577 California Univ., Berkeley.
TRANSPORT AND STABILITY PROPERTIES OF FREE SHEAR FLOWS Ph.D. Thesis
Jeffrey Daniel Lerner 1987 251 p
Avail: Univ. Microfilms Order No. DA8726270

Two models are posed and analytical perturbation theory is applied to analyze physically important issues such as linearized stability, and the free and driven response of a fluid sheared by plane parallel basic flows. The models are chosen because they are believed to describe basic physical mechanisms by which sheared fluids evolve. The point spectrum of the Rayleigh equation is analyzed for an inviscid, parallel shear flow describing a transition zone, or defect, in an unbounded uniform shear. The long wave expansion, a uniform perturbation method, is applied systematically. The second model addresses the dynamics of a compressible, strongly and uniformly sheared, dissipative fluid. Both the free and driven response are considered. The linearized stability is analyzed from several points of view. The system is quasi-asymptotically stable, with an initial period of algebraic growth in time followed by a fast, dissipative cutoff. The driven response analysis considers the system with a Gaussian, random stirring force. A perturbation theory is developed to allow calculation of cross correlation of physical quantities to any finite order of nonlinearity. Dissert. Abstr.

N88-20578 Louisiana State Univ., Baton Rouge.
BOUNDARY EFFECTS ON THE DRAG OF A CYLINDER IN AXIAL MOTION AT LOW REYNOLDS NUMBER Ph.D. Thesis
Elias George Wehbeh 1987 126 p
Avail: Univ. Microfilms Order No. DA8728226

An experimental study was performed of the Stokes drag on a right circular cylinder moving with constant velocity through a Newtonian viscous fluid. The cylinder velocity is parallel to its longitudinal axis, and the fluid is bounded on the outside by a fixed coaxial cylindrical tube of circular cross section. The length to diameter ratio of the moving cylinder ranges from 1.0 to 390, the ratio of width of the annular gap to the cylinder length ranges from 0.077 to 0.86, and the ratio, alpha, of the cylinder diameter to the tube diameter ranges from 0.022 to 0.91. Experimental values of the drag are compared with a theoretical expression which assumes a flow that is entirely axial in the annular region and a drag that is due entirely to the viscous stress on the cylinder side plus the effect of the dynamic pressure difference on the ends of the cylinder. An end correction term is obtained which is found to be proportional to the annular gap width and to the square root of alpha. This term is found to be consistent with previous numerical studies of the narrow gap case and with experimental studies of the wide gap case. Drag values are also presented for the situation in which the bottom of the tube is open to a larger fluid reservoir. Dissert. Abstr.

N88-20579 Cornell Univ., Ithaca, N.Y.
AN ADAPTIVE GRID TECHNIQUE FOR SOLUTION OF THE EULER EQUATIONS Ph.D. Thesis

Dun Charles Liu 1987 245 p
Avail: Univ. Microfilms Order No. DA8725831

To reduce errors associated with large solution gradients, under constraints of a fixed number of grid points, it is desirable to have the grid clustered in regions of large gradient and loosely arranged in regions of small gradient. Such mesh systems cannot be constructed without knowledge of the behavior of the solution. The grid equations are formed from linear combination of the Euler-Lagrange equations derived from functionals measuring smoothness, orthogonality and concentration. A directional concentration functional is proposed to take into consideration the effect of the direction of changing cell dimensions. Some salient features of the grid equations are explored by examining the existence of characteristic lines. The adaptive grid technique is applied to solve a finite volume approximation of the Euler equations for the transonic flow in quasi-one-dimensional nozzles and past two-dimensional airfoils. The multigrid method is incorporated to facilitate convergence when solving the grid equations. To speed up the convergence of the flow calculation, a new four stage coefficient set used in the Runge-Kutta scheme is derived, based upon the idea of reducing the growth factor in the high wavenumber region. Dissert. Abstr.

N88-20580 Princeton Univ., N. J.
CALCULATIONS OF VISCOUS FLOWS WITH A MULTIGRID METHOD Ph.D. Thesis
Luigi Martinelli 1987 190 p
Avail: Univ. Microfilms Order No. DA8727382

The continuing evolution of supercomputers is shifting the optimal tradeoff between computational costs and completeness of the mathematical model toward the solution of the full set of nonlinear conservation laws. During the last decade the development of effective methods for solving the inviscid form of the conservation laws has provided the necessary framework for attempting the analysis of viscous flows by solving the compressible Navier-Stokes and Reynolds averaged equations. The present work carries out this extension for 2-D transonic viscous flows past airfoils. Two multigrid schemes for the solution of the 2-D viscous compressible conservation equations were developed and validated. A finite volume formulation was used to discretize the spatial operators, and several discretization formulas for the viscous terms are studied. Several examples of applications to the Reynolds averaged equations in the transonic regime are presented and discussed. For these computations, closure was achieved by using a simple algebraic turbulence model widely accepted in computational aerodynamics. The validation of two efficient, robust, and accurate multigrid methods brings numerical simulation of the Navier-Stokes and Reynolds averaged equations to a new plateau. The combination of accuracy and speed provides a necessary tool for the study of turbulence modeling for aerodynamic flow, by making it possible to obtain a rapid and reliable assessment of the effects of substituting alternative models. Dissert. Abstr.

N88-20581 California Univ., Berkeley.
A FINITE-AMPLITUDE ANALYSIS OF THE BUOYANT INSTABILITY OF A HIGHLY VISCOUS FILM OVER A LESS VISCOUS HALF-SPACE Ph.D. Thesis
David Ralph Canright [1987] 137 p
Avail: Univ. Microfilms Order No. DA8726157

A fully nonlinear long-wave analysis is given for a buoyantly unstable horizontal layer of highly viscous fluid beneath a shear-free boundary and over a half-space of less dense, much less viscous fluid. For long waves, the creeping motion in the layer is horizontal and limited by normal viscous stresses. The main result is that the growth of disturbances of large amplitude is fundamentally different from that at small amplitude. While small-amplitude growth is exponential in time, the growth of large peaks (thickness maxima) in the layer is catastrophic, reaching infinite thickness in a finite time. Two cases are treated: the Rayleigh-Taylor instability with a dense viscous film over a half-space of lighter, much less viscous fluid; and a half-space of fluid whose viscosity depends strongly on temperature under a shear flow boundary which is impulsively cooled, forming an unstable, stiff thermal boundary. A large-slope analysis of the Rayleigh-Taylor problem shows that the same catastrophic growth continues even when slopes become large. Dissert. Abstr.

N88-20582 Cornell Univ., Ithaca, N.Y.
MULTIGRID SOLUTION OF THE EULER EQUATIONS Ph.D. Thesis
Wayne Allen Smith 1987 150 p
Avail: Univ. Microfilms Order No. DA8725792

A fast solver for 3-dimensional, inviscid, transonic flow in rotating domains is presented. The scheme is designed to be extended to the numerical simulation of viscous transonic flows about realistic geometries. The techniques employed are therefore chosen for their extensibility as well as for their efficiency. Spatial discretization of the governing equations is performed with a finite volume scheme to provide geometric generality and to facilitate the construction of a conservative scheme. Temporal discretization is performed with a multiple-stage time-stepping scheme to allow the calculation of both time-accurate and steady solutions. The use of multigrid plays a critical role in making the explicit scheme efficient. The effects of residual smoothing is found to be detrimental when used in multistage scheme. The efficiency of the scheme is demonstrated with representative computational results taken from a high speed compressor. The great potential of the scheme to exploit computational parallelism is demonstrated by implementing the scheme on a hypercube, a local memory multiprocessor computer. Dissert. Abstr.

N88-20583*# Stanford Univ., Calif. Center for Turbulence Research.
CENTER FOR TURBULENCE RESEARCH 1987 ACTIVITIES
Parviz Moin and William C. Reynolds Apr. 1988 59 p
(Contract NCC2-460)
(NASA-CR-182693; NAS 1.26:182693) Avail: NTIS HC A04/MF A01 CSCL 20D

Lagrangian techniques have found widespread application to the prediction and understanding of turbulent transport phenomena and have yielded satisfactory results for different cases of shear flow problems. However, it must be kept in mind that in most experiments what is really available are Eulerian statistics, and it is far from obvious how to extract from them the information relevant to the Lagrangian behavior of the flow; in consequence, Lagrangian models still include some hypothesis for which no adequate supporting evidence was until now available. Direct numerical simulation of turbulence offers a new way to obtain Lagrangian statistics and so verify the validity of the current predictive models and the accuracy of their results. After the pioneering work of Riley (Riley and Patterson, 1974) in the 70's, some such results have just appeared in the literature (Lee et al, Yeung and Pope). The present contribution follows in part similar lines, but focuses on two particle statistics and comparison with existing models. Author

N88-20584# West Virginia Univ., Morgantown. Dept. of Mechanical and Aerospace Engineering.
REDUCTION OF EROSION IN ELBOWS DUE TO FLOW MODIFICATIONS, PHASE 1 Final Report
E. K. Johnson, K. H. Means, R. L. Eyler, and J. D. Holtzworth Nov. 1987 96 p
(Contract DE-AC21-84MC-21349)
(DE88-001028; DOE/MC-21349/2531) Avail: NTIS HC A05/MF A01

The concept of flow-field modification as a method for reducing erosion in bends (elbows) used in pneumatic transport systems is investigated. Flow field modifications were primarily accomplished by injecting air at selected locations within the bends. Part 1 of this project shows the feasibility of the concept. Part 2 of this project will include further experiments and analysis, leading to a design methodology for incorporating this concept into piping systems. This is the final report for Part 1 of this project. It contains a survey of the literature dealing with the erosion in bends (elbows) and the fundamental subjects of erosion and two-phase, gas-solids, flow. Based on this literature survey, a pneumatic transport test

loop was constructed. Several bend designs were tested, using sand under a variety of operating conditions. The results of this exploratory effort indicate that modifying the flow field in a bend with jets may: (1) decrease erosion; (2) change the erosion pattern with the same amount of erosion; or (3) significantly increase the erosion process. Data indicate that the erosion rate may be reduced by low-velocity jets for high phase-density flow. Apparently, the interjection of jets with dilute phase-density flow tends to accelerate the erosion process. It is recommended that the project be continued in order to more fully understand the process and its capabilities to solve the difficult technical problem of erosion in bends (elbows). DOE

N88-20585# Aerojet Energy Conversion Co., Sacramento, Calif.
INNOVATIVE, COUNTERFLOW GAS/FINE SOLIDS, DIRECT CONTACT HEAT EXCHANGER Final Report
C. S. Mah Oct. 1987 125 p
(Contract DE-AC01-85CE-90232)
(DE88-004744; AECC-86-JAA-001-F) Avail: NTIS HC A06/MF A01

The Aerojet Energy Conversion Company has completed the first phase of study for development of a heat exchanger. The heat exchanger, a highly efficient, low cost concept, is a candidate for application in process manufacturing industries such as cement, lime, or glass. The analytical effort was to establish the heat exchanger performance via computer modeling and analysis; the experimental effort was to demonstrate the heat exchanger performance. DOE

N88-20586# Lawrence Livermore National Lab., Calif.
PARTICLE-DYNAMICS CALCULATIONS OF GRAVITY FLOW OF INELASTIC, FRICTIONAL SPHERES
O. R. Walton, R. L. Braun, R. G. Mallon, and D. M. Cervelli 17 Nov. 1987 10 p Presented at the US-Japan Symposium on Micromechanics of Granular Materials, Sendai, Japan, 26 Oct. 1987
(Contract W-7405-eng-48)
(DE88-005224; UCRL-97680; CONF-8710262-1) Avail: NTIS HC A02/MF A01

Three-dimensional discrete-particle computer models that calculate the motion of each individual grain in assemblies of hundreds of particles in steady shearing flows with either periodic or real boundaries have been modified to simulate gravity flow of particles through arrays of cylindrical horizontal rods and down inclined chutes. The particle interaction models reproduce experimentally measured recoil trajectories for colliding frictional particles, including rotation effects. Laboratory measurements of the flow of glass beads cascading down through an array of horizontal cylindrical rods correlate well with gravity flow calculations of inelastic, frictional spheres falling through a similar rod array. Less elastic particles are found to cascade through the array faster than nearly elastic particles. Likewise, smaller particles are found to flow faster than large ones. Model simulations of nearly two-dimensional inclined chute flow tests of 6mm diameter cellulose-acetate spheres flowing over a rough surface between parallel vertical glass plates, result in particle velocities that are considerably higher than values measured in similar laboratory tests at UCLA; however, inclusion of approximate air drag effects in the calculational model eliminates most of the discrepancy producing both density and velocity profiles that are close to the measured values. DOE

N88-20587# California Univ., Berkeley. Lawrence Berkeley Lab.
VERY LARGE VORTEX CALCULATIONS IN TWO DIMENSIONS
S. B. Baden Nov. 1987 28 p Presented at the UCLA Workshop on Vortex Methods, Los Angeles, Calif., 20 May 1987
(Contract DE-AC03-76SF-00098)
(DE88-005748; LBL-24334; CONF-8705256-1) Avail: NTIS HC A03/MF A01

We describe an implementation of Anderson's Method of Local Corrections running on the Cray X-MP multiprocessor with 4 CPUs. We will show how the code was vectorized and parallelized, including dynamic load balancing. We present computational results from very large runs of up to 25702 vortices. DOE

N88-20588# Oak Ridge National Lab., Tenn.
EFFICIENCY CHARACTERISTICS OF SPEED MODULATED DRIVES AT PREDICTED TORQUE CONDITIONS FOR AIR-TO-AIR HEAT PUMPS
C. K. Rice 1988 35 p Presented at the ASHRAE Winter Meeting, Dallas, Tex., 30 Jan. 1988
(Contract DE-AC05-84OR-21400)
(DE88-005846; CONF-880128-5) Avail: NTIS HC A03/MF A01

Examples of system (motor + inverter drive) efficiencies of two types of adjustable speed control are compared for predicted compressor and indoor blower load profiles. The two classifications are inverter-driven induction motors (IDIMs) and permanent-magnet electronically commutated motors (PM-ECMs). Reference sine-wave-driven induction motor (SWDIM) efficiencies are also given. Available bench data on late 70's IDIM compressor drives are compared to recent data on IDIM and PM-ECM drives. The drive efficiencies are compared over common operating torque requirements for heating and cooling. A modulating heat pump model was used to develop predicted reciprocating compressor torque/drive-frequency mappings and the expected operating torque ranges. The variation in modulating compressor torque requirements is analyzed. Ways to adjust the torque relation for different compressor types and sizing strategies are also discussed. Modulating blower performance data on an early '80s generation modulating heat pump with an IDIM drive (and SWDIM reference drive) were obtained and compared to bench data on recent IDIM and PM-ECM drives under similar torque conditions. In both compressor and blower applications, the combined system efficiency of the PM-ECM drives is nearly equal to or higher than that of the reference SWDIM cases and significantly better than IDIMs available in the late '70s. When compared to more recent IDIMs, the PM-ECM efficiency advantage over IDIM compressors has been reduced 40 to 50 percent between half and nominal speed (3600 rpm) but still remains 14 to 9 percent higher, respectively. DOE

N88-20589# Lovelace Foundation for Medical Education and Research, Albuquerque, N. Mex. Research Div.
VELOCITY AND CONCENTRATION MEASUREMENTS IN FLOWING SUSPENSIONS BY NUCLEAR MAGNETIC RESONANCE
P. D. Majors, S. A. Altobelli, Eiichi Fukushima, and R. C. Givler Jan. 1988 28 p Prepared in cooperation with Sandia National Labs., Albuquerque, N. Mex.
(Contract DE-AC04-76DP-00789)
(DE88-006225; SAND-88-7011) Avail: NTIS HC A03/MF A01

Noninvasive measurements are performed on fluid-particle flows with nuclear magnetic resonance techniques. These techniques are used to determine the characteristics of suspensions flowing axially in a cylindrical tube. The nonuniform velocity and concentration profiles, which result from the flow of a suspension of heavy particles, are presented. DOE

N88-20590*# National Aeronautics and Space Administration, Washington, D.C.
DETONATION VELOCITY OF THE HYDRAZINUM NITRATE-HYDRAZINE WATER SYSTEM
Shigeo Murata, Syuzo Fujiwara, Masao Kusakabe, and Kazauo Shiino Apr. 1988 7 p Transl. into ENGLISH from Kogyo Kayaku Kyokai (Japan), v. 37, no. 6, 1976 p 316-318 Transl. by Scientific Translation Service, Santa Barbara, Calif.
(Contract NASw-4307)
(NASA-TT-20213; NAS 1.77:20213) Avail: NTIS HC A02/MF A01 CSCL 20D

Detonation velocity of the ternary mixture, hydrazinium nitrate hydrazine water, was measured precisely under various conditions. The temperature coefficient, charge diameter effect, and the dependence on mixing ratio were determined. These results were

compared with those of a typical liquid explosive, nitromethane.
Author

N88-20591*# National Aeronautics and Space Administration. Langley Research Center, Hampton, Va.
NUMERICAL EXPERIMENTS ON THE STABILITY OF CONTROLLED BOUNDARY LAYERS Final Report
Thomas A. Zang and M. Y. Hussaini Mar. 1988 52 p Submitted for publication
(Contract NAS1-18107)
(NASA-CR-181649; ICASE-88-20; NAS 1.26:181649) Avail: NTIS HC A04/MF A01 CSCL 20D

Nonlinear simulations are presented for instability and transition in parallel water boundary layers subjected to pressure gradient, suction, or heating control. In the nonlinear regime, finite amplitude, 2-D Tollmein-Schlichting waves grow faster than is predicted by linear theory. Moreover, this discrepancy is greatest in the case of heating control. Likewise, heating control is found to be the least effective in delaying secondary instabilities of both the fundamental and subharmonic type. Flow field details (including temperature profiles) are presented for both the uncontrolled boundary layer and the heated boundary layer. Author

N88-20592*# National Aeronautics and Space Administration. Langley Research Center, Hampton, Va.
SLIP VELOCITY METHOD FOR THREE-DIMENSIONAL COMPRESSIBLE TURBULENT BOUNDARY LAYERS
Richard W. Barnwell and Richard A. Wahls (North Carolina State Univ., Raleigh.) Mar. 1988 22 p
(NASA-TM-100586; NAS 1.15:100586) Avail: NTIS HC A03/MF A01 CSCL 20D

A slip velocity method for 2-D incompressible turbulent boundary layers was presented in AIAA Paper 88-0137. The inner part of the boundary layer was characterized by a law of the wall and a law of the wake, and the outer part was characterized by an arbitrary eddy viscosity model. In the present study for compressible flows, only a law of the wall is considered. The problem of 2-D compressible flow is treated first; then the extension to 3-D flow is addressed. A formulation for primitive variables is presented.
Author

N88-20593*# National Aeronautics and Space Administration, Washington, D.C.
SOME PROBLEMS OF THE THEORY OF BUBBLE GROWTH AND CONDENSATION IN BUBBLE CHAMBERS
L. G. Tkachev Apr. 1988 16 p Transl. into ENGLISH of Nekotoryye Voprosy Teorii Rosta i Kondensatsii Puzyrkov v Puzyrkovykh Kamerakh, Joint Inst. for Nuclear Research, Dubna (USSR) p 1-17 Original language document was announced as N68-31970 Transl. by SCITRAN, Inc., Santa Barbara, Calif.
(Contract NASw-4307)
(NASA-TT-20232; NAS 1.77:20232; JINR-P-13-3726) Avail: NTIS HC A03/MF A01 CSCL 20D

This work is an attempt to explain the reasons for the discrepancies between the theoretical and experimental values of bubble growth rate in an overheated liquid, and to provide a brief formulation of the main premises of the theory on bubble growth in liquid before making a critical analysis. To simplify the problem, the floating upward of bubbles is not discussed; moreover, the study is based on the results of the theory of the behavior of fixed bubbles. Author

N88-20594*# National Aeronautics and Space Administration, Washington, D.C.
THE INFLUENCE OF MACH NUMBER AND HEAT TRANSFER ON THE TURBULENT FLOW WALL LAW
Julius Rotta Mar. 1988 30 p Transl. into ENGLISH from Uueber den Einfluss der Machschen Zahl und des Waermeuebergangs auf das Wandgesetz Turbulenter Stroemung, IN: Zeitschrift fuer Flugwissenschaften (Federal Republic of Germany), v. 9, Aug. 1959 p 264-274 Transl. by SCITRAN, Inc., Santa Barbara, Calif. Original document was prepared by Aerodynamic Test Facility, Goettingen (Federal Republic of Germany)
(Contract NASw-4307)
(NASA-TT-20230; NAS 1.77:20230) Avail: NTIS HC A03/MF A01 CSCL 20D

The similarity law of turbulent flow along a wall is extended to the case of compressible flow with heat transfer. After formulating the problem mathematically, some calculations are carried out with simplifying assumptions and compared with published experimental results. The results are discussed. Complete equations are given for the velocity and temperature distributions in the fully turbulent region. Author

N88-20595# Materials Research Labs., Melbourne (Australia).
THEORETICAL INVESTIGATION OF THE WAVE SHAPING PROCESS IN A SECTION OF LADDER FRACTURE TAPE
J. J. Masinskas and E. H. vanLeeuwen Sep. 1987 23 p
(MRL-R-1081; AR-005-172) Avail: NTIS HC A03/MF A01

Described is the modeling of the detonation process in a section of Fracture Tape using the 2-D reactive Lagrangian Hydrodynamic Code 2DL. The Forest Fire Burn Model of heterogeneous explosive shock initiation was used to model the explosive decomposition. The results show: (1) the time dependent pressures, (2) detonation wave shaping, and (3) deformation of the tape. Fracture tape is a channel-section neoprene molding designed to be filled with plastic explosive. The molding places barriers at regular intervals within the explosive which divide the detonation wave into two parts then focus both together to collide head on. Such a collision generates a narrow region of very high pressure, over 30 GPa in XTX-8003 compared with the normal detonation pressure of 19 GPa. Calculations indicate that with the ladder geometry Fracture Tape, the detonation wave propagates around the barriers, as well as creating a shock wave which is transmitted through the barrier itself. The transmitted shock wave may detonate the explosive immediately behind the barrier before the propagated detonation reaches it, thereby reducing the pressure enhancement from the expected collision for some distance from the barrier.
Author

N88-20596# Messerschmitt-Boelkow-Blohm G.m.b.H., Ottobrunn (West Germany). Unternehmensgruppe Hubschrauber und Flugzeuge.
GENERAL FUSELAGE COORDINATES FOR THE CALCULATION OF THREE-DIMENSIONAL BOUNDARY LAYERS Thesis - Technische Univ., Munich, Fed. Republic of Germany [ALLEGEMEINE RUMPFKOORDINATEN FUER DIE BERECHNUNG DREIDIMENSIONALER GRENZSCHICHTEN]
R. Hoeld 14 Jul. 1986 91 p In GERMAN
(MBB/LKE-122/S/PUB/244; ETN-88-91436) Copyright Avail: NTIS HC A05/MF A01

A programming package for the numerical calculation of three-dimensional boundary layers in aerodynamics was developed. It is suited for sub-, trans-, and supersonic flows. The fundamentals of general boundary layer coordinates and boundary layer theory are presented. The boundary layer calculation package consists of several programs, allowing a flexible application. Emphasis is placed on the control and the presentation of the results, facilitating the recognition and elimination of errors. A calculation network, adapted to the flow pattern about the body, was developed, with a view to the parabolic character of the boundary layer-equations. The developed program version was tested on a rotation ellipsoid; the calculated results agree with experimental results for an angle of attack of 0 deg, but differ substantially for increasing angles.
ESA

N88-20597# Office National d'Etudes et de Recherches Aerospatiales, Paris (France).
[ACTIVITIES REPORT OF THE LILLE INSTITUTE OF FLUID MECHANICS] Annual Report, 1986
Sep. 1987 15 p Original contains color illustrations
(ETN-88-91983) Avail: NTIS HC A03/MF A01

Analysis and modeling of flight dynamics at high angles of attack; composite blade models; turn over of light aircraft when landing; computation of elastomer structures; a cryogenic model

of the A320 aircraft for the wind tunnel; modeling of an isotropic explosion in a uniform flow; validation of tracer behavior models in a flow by holographic velocimetry; and qualification of the lift system of the NES 200 L surface effect ship are discussed.
ESA

N88-20598*# National Aeronautics and Space Administration. Hugh L. Dryden Flight Research Facility, Edwards, Calif.
PRELIMINARY IN-FLIGHT BOUNDARY LAYER TRANSITION MEASUREMENTS ON A 45 DEG SWEPT WING AT MACH NUMBERS BETWEEN 0.9 AND 1.8
J. Blair Johnson Mar. 1988 47 p
(NASA-TM-100412; H-1436; NAS 1.15:100412) Avail: NTIS HC A03/MF A01 CSCL 20D

A preliminary flight experiment was flown to generate a full-scale supersonic data base to aid the assessment of computational codes, to improve instrumentation for measuring boundary layer transition at supersonic speeds, and to provide preliminary information for the definition of follow-on programs. The experiment was conducted using an F-15 aircraft modified with a small cleanup test section on the right wing. Results are presented for Mach (M) numbers from 0.9 to 1.8 at altitudes from 25,000 to 55,000 ft. At M greater than or = 1.2, transition occurred near or at the leading edge for the clean configuration. The furthest aft that transition was measured was 20 percent chord at M = 0.9 and M = 0.97. No change in transition location was observed after the addition of a notch-bump on the leading edge of the inboard side of the test section which was intended to minimize attachment line transition problems. Some flow visualization was attempted during the flight experiment with both subliming chemicals and liquid crystals. However, difficulties arose from the limited time the test aircraft was able to hold test conditions and the difficulty of positioning the photo chase aircraft during supersonic test points. Therefore, no supersonic transition results were obtained.
Author

N88-20599*# National Aeronautics and Space Administration. Lewis Research Center, Cleveland, Ohio.
CRYOGENIC FLUID MANAGEMENT TECHNOLOGY WORKSHOP. VOLUME 2: ROUNDTABLE DISCUSSION OF TECHNOLOGY REQUIREMENTS
Mar. 1988 84 p Workshop held in Cleveland, Ohio, 28-30 Apr. 1987
(NASA-CP-10009; E-3987; NAS 1.55:10009) Avail: NTIS HC A05/MF A01 CSCL 20D

The Cryogenic Fluid Management Technology Workshop was held April 28 to 30, 1987, at the NASA Lewis Research Center in Cleveland, Ohio. The major objective of the workshop was to identify future NASA needs for technology concerning the management of subcritical cryogenic fluids in the low-gravity space environment. In addition, workshop participants were asked to identify those technologies which will require in-space experimentation and thus are candidates for inclusion in the flight experiment being defined at Lewis. The principal application for advanced fluid management technology is the Space-Based Orbit Transfer Vehicle (SBOTV) and its servicing facility, the On-Orbit Cryogenic Fuel Depot (OOCFD). Other potential applications include the replenishment of cryogenic coolants (with the exception of superfluid helium), reactants, and propellants on board a variety of spacecraft including the space station and space-based weapon systems. The last day was devoted to a roundtable discussion of cryogenic fluid management technology requirements by 30 representatives from NASA, industry, and academia. This volume contains a transcript of the discussion of the eight major technology categories.
Author

N88-20690# Joint Publications Research Service, Arlington, Va.
TURBULENT TRANSFER OF MOMENTUM AND HEAT IN BOUNDARY LAYER OF FLUID BEYOND AN OBSTACLE. 1: HYDRODYNAMIC CHARACTERISTICS Abstract Only
R. B. Shlyazhas and A. A. Shlanchyauskas *In its* JPRS Report: Science and Technology. USSR: Earth Sciences 26 Feb. 1988 p 19 Transl. into ENGLISH from Trudy Akademii Nauk Litovskoy SSR: Seriya B: Khimiya, Tekhnika, Fizicheskaya Geografiya (Vilnius, USSR), no. 6, Dec. 1986 p 92-103 (For primary document see N88-20674 13-42)
Avail: NTIS HC A04/MF A01

35 INSTRUMENTATION AND PHOTOGRAPHY

Includes remote sensors; measuring instruments and gages; detectors; cameras and photographic supplies; and holography.

For aerial photography see *43 Earth Resources and Remote Sensing*. For related information see also *06 Aircraft Instrumentation*, and *19 Spacecraft Instrumentation*.

N88-20600# Continuous Electron Beam Accelerator Facility, Newport New, Va.
PROGRESS IN DIAGNOSTIC TECHNIQUES FOR SC CAVITIES
Charles E. Reece [1988] 21 p
(Contract DE-AC05-84ER-40150)
(CEBAF-PR-88-003) Avail: NTIS HC A03/MF A01

While sizable efforts are now being directed toward large scale applications of RF superconductivity, the full promise is yet to be realized. Material screening techniques should aid in achieving improved reliability, and sensitive cavity thermometry useful below T sub lambda opens new possibilities for investigation into the behavior of superconducting materials. Perhaps the employment of these new tools will aid in understanding and surmounting the present performance limitations of superconducting cavities.
Author

N88-20601*# Infrared Labs., Inc., Tucson, Ariz.
ADVANCED COMPONENTS FOR SPACEBORNE INFRARED ASTRONOMY Final Report, Apr. 1985 - Jul. 1987
Arnold W. Davidson Jul. 1987 41 p
(Contract NAS2-12154)
(NASA-CR-177470; NAS 1.26:177470) Avail: NTIS HC A03/MF A01 CSCL 03A

Basic improvements in the technology of low noise read-out systems for low background detectors were demonstrated. Using discrete JFET integrating amplifiers at their optimum temperature of 55 K, read noise less than 7.5 electrons in 128 seconds of integration was obtained. Two models of single channel integrators are now available, the JF-77 for use between 50 and 80 K and the JF-4 for lower temperatures. A 1 x 15 linear array of complete integrators on a single integrated circuit was developed and will be made available in the near future. The successful operation of a superconducting stepper motor was demonstrated. The motor shows a three fold increase in torque over conventional motors operating at room temperature. The success of the motor stems from the use of superconducting coils in conjunction with developments in bearings for cryogenic use, rare-earth rotors, and motor cooling techniques. The current state of development will allow the rapid development of motors optimized for specific applications. An electronic switch capable of resetting cooled JFET integrating amplifiers was developed. The JFET integrating amplifiers that use this switch have demonstrated read noise of less than 10 electrons. The JFET reset device exhibits an extremely high open impedance and low leakage current. Capacitance is sufficiently low so as not to impair amplifier sensitivity. The effects of transient switching charges are minimized by a compensation technique and variable transient current problems inherent to devices of this type are overcome by external circuitry.
Author

N88-20602# Naval Research Lab., Washington, D.C.
MODE PRIMING IN AN OVERMODED GYROTRON OSCILLATOR
Alan H. McCurdy and Carter A. Armstrong 19 Oct. 1987 46 p
(AD-A189151; NRL-MR-6102) Avail: NTIS HC A03/MF A01 CSCL 20C

Axial mode control in a gyrotron oscillator is accomplished by injection of an external signal into the oscillator. The mechanism

by which the selection technique works is that of priming, where the injected signal is required only during the early stages of oscillation growth. Like phase priming, mode control can be obtained with an external mode than any other. It is found that the external signal can select a mode when the free gyrotron operation skips between modes from pulse to pulse. Also, in certain conditions, a single stable mode can be changed to a different mode by a priming signal. Finally, a case is studied where a bistable system (two simultaneous modes) is reduced to a single mode because of the external signal. Mode control is used as a diagnostic to investigate the coupling of an external electromagnetic wave to the electron beam via electron cyclotron resonance absorption. Beam-wave coupling is studied as a function of the polarization of the input drive signal. It is found that the external electromagnetic signal couples best when launched as a right-hand circularly polarized wave. The theoretical ratio (55.2) of the coupling factors for the right- and left-hand electromagnetic waves is found to be consistent with the experimentally value within the uncertainties of the measurement. GRA

N88-20603# Alabama Univ., Huntsville. Dept. of Mechanical Engineering.
DEVELOPMENT OF FIBER OPTIC SYSTEMS FOR RECORDING AND TRANSMITTING HOLOGRAPHIC INFORMATION Final Report, 1 Dec. 1985 - 30 Nov. 1987
John A. Gilbert 1 Dec. 1987 14 p
(Contract DAAL03-86-K-0014)
(AD-A189406; ARO-23573.18-EG) Avail: NTIS HC A03/MF A01 CSCL 20F

The work conducted under this research contract has allowed the principal investigator to develop a very strong research program in engineering mechanics and applied optics at the University of Alabama in Huntsville. To date, thirty publications and presentations have resulted. GRA

N88-20604# Lawrence Livermore National Lab., Calif.
REMOTE FIBER FLUORIMETRY TECHNIQUES FOR PRESSURE MEASUREMENTS
G. R. Haugen Nov. 1987 23 p
(Contract W-7405-eng-48)
(DE88-004486; UCID-21284) Avail: NTIS HC A03/MF A01

An optical remote sensor for temperature and pressure was constructed by affixing a ruby crystal to the tip of a single optical fiber. The temperature and pressure information is encoded onto the fluorescent signal back-scattered from the fibertip. Such an optical system is immune to electromagnetic noise. Changes in the lifetime of the emission are associated only with changes in the temperature of the ruby crystal, while frequency shifts of the emission lines are associated with both pressure and temperature changes. Measurements of frequency shifts and lifetime are not dependent on excitation beam intensity and/or losses in the optical fiber. This system will operate reliably and accurately in hostile and adverse non-isothermal environments. The sensor is able to measure pressure stresses at a minute point in a material with a resolution of a few tenths of kilobars. The dynamic range is one megabar. The doublet spacing also indicates whether the stresses are hydrostatic or non-hydrostatic. However, one disadvantage of the ruby sensor is its relatively long lifetime (3 msec at 300 K), limiting the time resolution of pressure wavefronts. Given the very favorable performance of the sensor, it would be significant improvement to develop a chromium ion activated crystal having a much faster mean lifetime. DOE

N88-20605# Nationaal Inst. voor Kernfysica en Hoge Energiefysica, Amsterdam (Netherlands).
HIGH RESOLUTION HADRON CALORIMETRY
Richard Wigmans 1987 53 p Presented at the International Conference on Advances in Experimental Methods for Colliding Beam Physics SLAC, 9-3 Mar. 1987
(NIKHEF-H/87-8; B8723613; ETN-88-91740) Avail: NTIS HC A04/MF A01

The components that contribute to the signal of a hadron calorimeter and the factors that affect its performance are discussed, concentrating on energy resolution and signal linearity. Both are decisively dependent on the relative response to the electromagnetic and the nonelectromagnetic shower components, the e/h signal ratio, which should be equal to 1.0 for optimal performance. The factors that determine the value of this ratio are examined. Calorimeter performance is crucially determined by its response to the abundantly present soft neutrons in the shower. The presence of a considerable fraction of hydrogen atoms in the active medium is essential for achieving the best possible results. Firstly, this allows one to tune e/h to the desired value by choosing the appropriate sampling fraction. Secondly, the efficient neutron detection via recoil protons in the readout medium itself reduces considerably the effect of fluctuations in binding energy losses at the nuclear level, which dominate the intrinsic energy resolution. Signal equalization, or compensation (e/h = 1.0) does not seem to be a property unique to U238, but can also be achieved with lead and probably even iron absorbers. ESA

N88-20606*# Morgan State Univ., Baltimore, Md.
THE CALIBRATION OF PHOTOGRAPHIC AND SPECTROSCOPIC FILMS: RECIPROCITY FAILURE AND THERMAL RESPONSES OF IIaO FILM AT LIQUID NITROGEN TEMPERATURES Seminannual Report
E. C. Hammond, Jr., K. A. Peters, S. O. Gunther, L. M. Cunningham, and D. D. Wright 26 Apr. 1985 15 p
(Grant NsG-5074)
(NASA-CR-181094; NAS 1.26:181094) Avail: NTIS HC A03/MF A01 CSCL 14E

Reciprocity failure was examined for IIaO spectroscopic film. The results indicate reciprocity failure occurs at three distinct minimum points in time; 15 min, 30 min and 90 min. The results are unique because theory suggests only one minimum reciprocity failure point should occur. When incubating 70mm IIaO film for 15 and 30 min at temperatures of 30, 40, 50, and 60 C and then placing in a liquid nitrogen bath at a temperature of -190 C the film demonstrated an increase of the optical density when developed at a warm-up time of 30 min. Longer warm-up periods of 1, 2 and 3 hrs yield a decrease in optical density of the darker wedge patterns; whereas, shorter warm-up times yield an overall increase in the optical densities. Author

N88-20607# Instituto de Pesquisas Espaciais, Sao Jose dos Campos (Brazil).
SYNTHESIS METHOD APPLIED TO THE DESIGN OF AN ELECTRON GUN FOR A GYROTRON M.S. Thesis [METODO DE SINTESE APLICADO AO PROJETO DE UM CANHAO DE ELECTRONS PARA GIROTRONS]
Carlos Alberto Bomfi Silva Sep. 1987 154 p In PORTUGUESE; ENGLISH summary
(INPE-4357-TDL/298) Avail: NTIS HC A08/MF A01

A synthesis method is applied to the design of an electron gun for a 94 GHz gyrotron. Using this method, an electrode shape is found compatible with the laminar flow, which minimizes the action of the space charge on electron velocity dispersion. A systematic procedure is presented to find the parameters of the synthesis method which, in turn, are closely related to the characteristics of the optoelectronic system. Finally, an electron gun is designed in which the velocity dispersion found is of the order of 1.5 percent and in which the beam power is 2.3 MW. Author

N88-20608*# Morgan State Univ., Baltimore, Md.
THE CALIBRATION OF PHOTOGRAPHIC AND SPECTROSCOPIC FILMS: THE RESPONSE OF 2aO FILM TO SMALL DOSAGES OF ALPHA PARTICLES FROM 3/10TH'S RAD TO 8 RADS AT ENERGY LEVELS 153 MeV, 79 MeV AND 47 MeV Semiannual Report, Jan. 1983 - Mar. 1984
E. C. Hammond, Jr., Kevin Peters, and Al Stober Mar. 1984 21 p
(Grant NsG-5074)
(NASA-CR-177830; NAS 1.26:177830) Avail: NTIS HC A03/MF A01 CSCL 14E

The 2aO film, pre-exposed to a series of neutral density filters which on development under standard conditions will produce the standard H-D curve for that film, were then exposed to Alpha paricles with a dose range of 3/10ths rads to 8 rads while varying the energy of the particles using 153 MeV, 70 MeV, and 47 MeV, respectively. An analysis of the film shows that the 3/10th rad dose produces the lowest optical density changes at 70 MeV and 47 MeV. While the optical density readings for the darker patterns seem to oscillate and decrease when exposed to radiation dosages of 3/10th rads to 8 rads. Author

N88-20609# California Univ., Berkeley. Lawrence Berkeley Lab.
IMPROVED METHODS FOR HIGH RESOLUTION ELECTRON MICROSCOPY Ph.D. Thesis
J. R. Taylor Apr. 1987 149 p
(Contract DE-AC03-76SF-00098)
(DE88-005731; LBL-24477) Avail: NTIS HC A07/MF A01

Existing methods of making support films for high resolution transmission electron microscopy are investigated and novel methods are developed. Existing methods of fabricating fenestrated, metal reinforced specimen supports (microgrids) are evaluated for their potential to reduce beam induced movement of monolamellar crystals of C44H90 paraffin supported on thin carbon films. Improved methods of producing hydrophobic carbon films by vacuum evaporation, and improved methods of depositing well ordered monolamellar paraffin crystals on carbon films are developed. A novel technique for vacuum evaporation of metals is described which is used to reinforce microgrids. A technique is also developed to bond thin carbon films to microgrids with a polymer bonding agent. Unique biochemical methods are described to accomplish site specific covalent modification of membrane proteins. Protocols are given which covalently convert the carboxy terminus of papain cleaved bacteriorhodopsin to a free thiol. DOE

N88-20610# Royal Netherlands Meteorological Inst., De Bilt. Instrumentele Afdeling.
THE EVALUATION OF AUTOMATIC BAROMETERS, ILLUSTRATED BY THE NAKAASA BAROMETER [HET BEOORDELEN VAN AUTOMATISCHE BAROMETERS MET ALS VOORBEELD DE NAKAASA BAROMETER]
A. vanLonden 1987 24 p In DUTCH
(KNMI-TR-95; B8713958; ISSN-0169-1708; ETN-88-91338)
Copyright Avail: NTIS HC A03/MF A01

The suitability of the Nakaasa model F-451 digital barometer for meteorological applications was evaluated. The test specifications are given, and the testing methods for the calibration of barometers are described. A technical description of the Nakaasa barometer is given. In spite of severe test conditions, the barometer works satisfactorily. Its quality is excellent, but the price is too high for operational use in weather stations. ESA

36 LASERS AND MASERS

Includes parametric amplifiers.
For related information see also *76 Solid-State Physics*.

N88-20611# Massachusetts Inst. of Tech., Cambridge. Research Lab. of Electronics.
FIBER-COUPLED EXTERNAL-CAVITY SEMICONDUCTOR HIGH POWER LASER Progress Report, Jan.-Dec. 1986
Robert H. Rediker, Kristin K. Anderson, So Kuen Liew, and Christopher J. Corcoran Jan. 1987 6 p Repr. from RLE Progress Report No. 129, Jan. 1987
(Contract N00014-80-C-0941; NR Proj. 395066)
(AD-A188454) Avail: NTIS HC A02/MF A01 CSCL 09C

Last year's annual report described the high spectral purity of the output from an ensemble of five discrete diode lasers when operated cw. The linewidth of the cw output of this external-cavity-controlled ensemble of diode lasers was shown to be less than 7.5 MHz (approx 2 x 10 to the -8th power of the center frequency). Also reported last year was high-spectral-purity pulsed output from this external cavity controlled laser. In 1986 the pulsed operation of this laser was investigated in detail both experimentally and theoretically. Linewidths of the order of the 7.5-MHz instrument resolution have been obtained. To achieve this high spectral purity in a pulse mode of operation, three alternate gain elements are operated cw and the intermediate two elements are pulsed. For a coherent ensemble of only three alternate gain elements, the spacing between the major intensity maxima in the Fourier plane (the filter plane) is decreased by a factor of 2 relative to the spacing with all five elements operating coherently. As a result, the lasing threshold of the three-element ensemble is much higher because significant radiation hits the opaque areas of the filter. A calculation of the single-pass filter transmission of this case yields a value of 0.48 as compared to the transmission of 0.92 when all five elements are running. GRA

N88-20612# Massachusetts Inst. of Tech., Cambridge. Research Lab. of Electronics.
COHERENT LASER RADAR SYSTEM THEORY Final Report, 1 Aug. 1984 - 30 Sep. 1987
Jeffrey H. Shapiro 5 Nov. 1987 26 p
(Contract DAAG29-84-K-0095)
(AD-A188759; ARO-21192.6-PH) Avail: NTIS HC A03/MF A01 CSCL 17I

This program is aimed at developing a system theory for the emerging technology of multifunction coherent CO2 laser radars. It builds upon previous work funded by U.S. Army Research Office contract DAAG29-80-K-0022. GRA

N88-20613# Texas Univ., Dallas. Center for Quantum Electronics and Applications.
PROOF OF THE FEASIBILITY OF COHERENT AND INCOHERENT SCHEMES FOR PUMPING A GAMMA-RAY LASER Quarterly Technical Progress Report, 1 Jul. - 30 Sep. 1987
Carl B. Collins Oct. 1987 113 p
(Contract N00014-86-C-2488)
(AD-A189238; UTD-GRL-8702) Avail: NTIS HC A06/MF A01 CSCL 07D

Recent approaches to the problem of the gamma ray laser have focused upon upconversion techniques in which metastable nuclei are pumped with long wavelength radiation. At the nuclear level the storage of energy can approach tera-Joules per liter for thousands of years. Any plan to use such a resource for a gamma ray laser poses problems requiring the fusion of concepts taken from relatively unrelated fields of physics. An approach has been pursued for the upconversion of longer wavelength radiation incident upon isomeric nuclear populations that can avoid many of the difficulties encountered with traditional concepts of single photon pumping. The present state-of-the-art has been adequate to identify 29 first-class candidate materials, but further evaluation cannot proceed without remeasurements of nuclear properties with higher precision. This report focuses upon continued development of one of the new technologies being developed for the screening of the laser candidates. It is the nuclear analog of the optical double resonance methods which produced much of the database at the molecular level that was such essential use in the development of conventional lasers. Applied most recently to the study of levels which might be used in dumping isomeric populations into freely radiating states, it produced an unexpected result of major importance. GRA

N88-20614# California Univ., Santa Barbara.
DEVELOPMENT OF ELECTROSTATIC-ACCELERATOR FREE-ELECTRON LASERS Final Report, 15 Jan. 1980 - 30 Apr. 1987
Luis R. Elias 30 Apr. 1987 62 p
(Contract N00014-80-C-0308)
(AD-A189507) Avail: NTIS HC A04/MF A01 CSCL 09C

A free-electron laser has been developed based on the utilization of a 6 MV electrostatic accelerator which has been modified to generate relatively high current electron pulses of sufficient intensity to allow its operation as an oscillator over a

wide range of frequencies from the infrared (IR) to the far-infrared (FIR) region. The FEL began with the development of a unique, high current, high brightness electron gun and continued with the successful demonstration of very high electron beam recovery efficiency in 1983 and culminated with the operation of the FEL as an oscillator at wavelengths longer than 400 microns, and with the demonstration of laser operation at wavelength longer than 120 micrometers after upgrading the accelerator voltage from 3 to 6 MV. The major goal of the program is to develop a new breed of free electron lasers based on the electron beams generated by electrostatic accelerators which would eventually be used as tools for scientific research in those regions of the spectrum where other coherent electromagnetic sources do not provide adequate power and/or continuous tunability. GRA

N88-20615# Air Force Inst. of Tech., Wright-Patterson AFB, Ohio. School of Engineering.

SEMICLASSICAL THEORY OF INJECTED LASERS WITH ARBITRARY STABLE AND UNSTABLE RESONATORS Ph.D. Thesis

Steven M. Rinaldi Dec. 1987 336 p
(AD-A189514; AFIT/DS/PH/76-3) Avail: NTIS HC A15/MF A01 CSCL 09C

A semiclassical analysis of injected lasers with stable and unstable resonators and arbitrary outcoupling fractions was performed. Homogeneously broadened lasers with Fabry-Perot and with positive branch, confocal unstable resonators were modeled. Both time-dependent and steady-state analyses of free-running and injected lasers were performed. Because of deficiencies in the standing wave semiclassical and the simple saturable gain models, a new semiclassical theory of homogeneously broadened lasers were developed. The theory is predicted upon the following assumptions: the atoms are two-level, a single longitudinal mode exists in the cavity, the transverse mode structure can be adequately modeled by the geometric optics mode, and the laser electric fields can be described by a pair of counterpropagating planar, cylindrical, or spherical traveling waves with different amplitudes. A general semiclassical theory was first developed, and then specialized to the Fabry-Perot and positive branch, confocal unstable resonator cases. Both the Maxwell-Bloch and rate equation approximation forms of the theory were derived. The theory was shown to reduce to the simple saturable gain and standing wave semiclassical models in the appropriate limits. GRA

N88-20616# Air Force Inst. of Tech., Wright-Patterson AFB, Ohio. School of Engineering.

RESONATOR COUPLING OF TWO RING CAVITY, ARGON-ION LASERS M.S. Thesis

Warren O. Abraham Dec. 1987 57 p
(AD-A189558; AFIT/GEO/ENP/87D-1) Avail: NTIS HC A04/MF A01 CSCL 09C

This thesis reports on a study of phasing two continuous-wave, resonator-coupled, argon-ion ring lasers. Rings with cavity lengths of about 3.4 meters were formed from Spectra Physics Model 164 and 165 lasers. These rings were coupled in several configurations, and portions of each ring output were combined to form a mixed beam, which was monitored for phase locking (frequency locking and coherence) with a Fabry-Perot scanning interferometer and a fast photodiode. Short term phase locking was achieved (2.5 msce) when at least one ring was operated in multimode. Precise frequency tuning of rigs operating in single mode was not possible, therefore phase locking of two single mode rings' lasing thresholds did not affect phase locking, but increasing the coupling strength between the resonators increased the duration of phase locking activity. Suppression of intracavity air turbulence increased the frequency range within which phase locking occurred. GRA

N88-20617# Air Force Inst. of Tech., Wright-Patterson AFB, Ohio. School of Engineering.

THEORY OF LASER COOLING AND SPECTROSCOPY OF HARMONICALLY TRAPPED SINGLE ATOMS Ph.D. Thesis

Ann L. Wells Dec. 1987 122 p
(AD-A189576; AFIT/DS/PH/87-5) Avail: NTIS HC A06/MF A01 CSCL 07D

The problem of laser cooling of a single ion or atom in a harmonic trap was considered. A simple theory of sideband cooling has been developed. In the limit that the particle's secular motion can be treated semiclassically, the theory allows the calculation of a logarithmic cooling rate either numerically or, for two special cases, analytically. The theory could be used to optimize the parameters of a cooling experiment. The spectroscopy of a single atom in the ladder configuration has been treated theoretically. A dressed atom approach was used to provide qualitative information about the system. GRA

N88-20618# Lawrence Livermore National Lab., Calif.

WIGGLER TAPER OPTIMIZATION FOR FREE-ELECTRON-LASER AMPLIFIERS WITH MODERATE SPACE-CHARGE EFFECTS

R. A. Jong, E. T. Scharlemann, and W. M. Fawley 1987 16 p Presented at the 9th International Free-Electron Laser Conference, Williamsburg, Va., 14 Sep. 1987
(Contract W-7405-eng-48)
(DE88-003758; UCRL-96735; CONF-8709110-15) Avail: NTIS HC A03/MF A01

The standard synchronous tapering method used to design the wiggler magnetic field for free-electron-laser (FEL) amplifiers operating in the Compton regime will not work for amplifier systems where space-charge effects are important. The space-charge effects lower the overall gain in the amplifier system and, even more importantly, shift the peak in the gain curve to magnetic field values that are significantly less than the synchronous magnetic field value. As a result, the overall predicted gain using the synchronous tapering method is too low. Moreover, the synchronous magnetic field corresponds to the peak in the gain curve for a frequency below the fundamental frequency. Consequently, shot noise at frequencies below the fundamental frequency can grow to levels that may prevent amplification of the fundamental. We have developed a new tapering strategy that improves the predicted amplifier gain and circumvents the shot-noise growth for systems with moderate space-charge effects. For this new strategy, we hold the wiggler magnetic field constant at a value below the synchronous value but near the peak of the gain curve for the fundamental frequency, for some optimized length at the front end of the wiggler. Beyond this constant wiggler section, the field is tapered using the standrd synchronous tapering algorithm. This new tapering scheme results in significant improvement in predicted amplifier gains and limits the growth of shot noise to insignificant levels. We demonstrate the effectiveness of this new tapering algorithm using the tapered wiggler design for the proposed microwave heating experiment (MTX) at the Lawrence Livermore National Laboratory (LLNL). DOE

N88-20619# Lawrence Livermore National Lab., Calif.

CAUSES OF DAMAGE IN MULTILAYER DIELECTRIC COATINGS EXPOSED TO HIGH AVERAGE POWER VISIBLE LASER RADIATION

D. M. Aikens and J. R. Taylor Oct. 1987 12 p Presented at the Boulder Damage Symposium, Boulder, Colo., 26 Oct. 1987
(Contract W-7405-eng-48)
(DE88-005363; UCRL-97573; CONF-8710165-6) Avail: NTIS HC A03/MF A01

Causes of damage in multilayer dielectric coatings exposed to high average power visible lasers have been examined. Damage has been seen to be related to coating defects, surface contamination, and coating absorption. Defects and contamination, particularly those larger than 4 microns, have been observed to significantly lower the damage threshold for high reflective coatings. Attempts have been made to visually evaluate defects and surface contamination prior to damage in order to find correlation with the damage threshold. The methods used to evaluate coating defects and conduct high average power damage testing as well as test results are presented. This work demonstrates the value of

controlling sources of defects in manufacture and contamination for use in high average power visible laser systems. DOE

N88-20620# Argonne National Lab., Ill.
LASER FLUORESCENCE SPECTROSCOPY OF ZINC NEUTRALS ORIGINATING FROM LASER-IRRADIATED AND ION-BOMBARDED ZINC SULFIDE AND ZINC SURFACES
H. F. Arlinghaus, W. F. Calaway, C. E. Young, M. J. Pellin, D. M. Gruen, and L. L. Chase 1987 13 p Presented at the 19th Annual Symposium on Optical Materials for High Power Lasers, Boulder, Colo., 26 Oct. 1987 Prepared in cooperation with Lawrence Livermore National Lab., Calif.
(Contracts W-31-109-eng-38; W-7405-eng-48)
(DE88-006033; CONF-8710254-3) Avail: NTIS HC A03/MF A01

Time-of-flight (TOF) measurements, employing high-resolution laser-induced fluorescence spectroscopy (LFS) as a probe, have been used to measure the yield and velocity distribution of Zn atoms ejected from a ZnS single crystal under irradiation by 308 nm photons. By comparison with the known ion sputtering yield for pure zinc, the absolute yield was determined to be 10 to the 10th power atoms/pulse at a laser fluence of 30 mJ/sq cm. The velocity distribution of the Zn atoms could be fitted by a Maxwell-Boltzmann distribution, having characteristic temperature of approx 2300 K. In addition, Doppler-shift techniques have been combined with TOF measurements in order to separate prompt from delayed emission of ablated atoms, as well as to probe possible molecular or cluster fragmentation. The results obtained suggest the possibility of molecular or cluster emission from ZnS. DOE

N88-20621# Sandia National Labs., Albuquerque, N. Mex.
REFRACTIVE INDEX GRADIENTS IN NUCLEAR-REACTOR-PUMPED LASERS: GASDYNAMIC EFFECTS
J. R. Torczynski and R. J. Gross 1987 26 p Presented at Lasers '87, Lake Tahoe, Nev., 7 Dec. 1987
(Contract DE-AC04-76DP-00789)
(DE88-006099; SAND-87-1252C; CONF-871254-3) Avail: NTIS HC A03

In nuclear-reactor-pumped lasers, the fission-fragment energy deposition is spatially nonuniform, with less energy deposited near the laser axis than is deposited near the side walls from which the fission fragments originate. This nonuniformity causes gas to move toward the laser axis and establish density and refractive index gradients perpendicular to the laser axis. In order to understand this phenomenon and describe it quantitatively, a numerical model of the gasdynamics of nuclear-reactor-pumped lasers has been developed. The numerical model simulates the 2-D motion of a perfect gas experiencing fission-fragment energy deposition in a rectangular or cylindrical enclosure. In addition to calculating mass density, temperature, pressure, velocity, and power density fields, ray-tracing calculations are performed to determine the beam steering caused by the varying gas density. The simulation of a representative 1-D rectangular case is found to be in excellent agreement with the existing analytical theory. In this case, the ray-tracing calculations indicate length limitations which result from internal focusing. Examination of cylindrical cases reveals that under certain circumstances gas motion reduces the on-axis power deposition to zero, a phenomenon termed axis-shielding. This phenomenon never occurs in rectangular cases. Simulations of experiments show good agreement between calculated and experimental Hartmann probe refractive index data. DOE

N88-20622# Sandia National Labs., Albuquerque, N. Mex.
MULTIMODE-WAVEGUIDE LASER BEAM DEFLECTOR
P. J. Brannon, G. R. Hadley, and A. Owyoung Feb. 1988 13 p
(Contract DE-AC04-76DP-00789)
(DE88-006222; SAND-88-0096) Avail: NTIS HC A03/MF A01

A LiNbO3 multimode-waveguide laser beam deflector using the electrooptic effect has been demonstrated. A full deflection angle of 0.23 degree is observed for 300 V applied. Propagation losses of 3 dB have been observed and full deflection times of 2 ns estimated. DOE

N88-20623# Sandia National Labs., Albuquerque, N. Mex.
PRACTICAL CONSTRAINTS ON SOURCES FOR PULSED BEAM LITHOGRAPHIES
J. Y. Tsao, S. T. Picraux, R. W. Light, and W. W. Hsing Mar. 1988 22 p
(Contract DE-AC04-76DP-00789)
(DE88-006594; SAND-87-1606) Avail: NTIS HC A03/MF A01

Many of the sources currently being considered for advanced microlithography are pulsed, rather than continuous. These sources are characterized not merely by brightness and lifetime, but more generally by shot-to-shot stability, lifetime, single-pulse fluence, and repetition rate. These four characteristics are constrained by practical considerations, and, within limits, can be traded off against each other. We describe these tradeoffs and optimal source operating regimes for lithographies based on broad- and narrow-band excimer laser sources and on pulsed X-ray sources. DOE

N88-20624# Purdue Univ., West Lafayette, Ind.
A STUDY OF THE INTERACTION OF LIGHT WITH SUB-MICRON METALLIC SURFACES Final Progress Report
R. G. Reifenberger 1987 26 p
(Contract DE-FG02-84ER-45162)
(DE88-003138; DOE/ER-45162/3) Avail: NTIS HC A03/MF A01

This program was largely concerned with the illumination of sub-micron metallic surfaces with intense laser light. This experimental arrangement, often referred to as photofield emission, is a technique that provides a convenient way of studying a variety of surface specific phenomena under intense laser illumination. Apart from the emphasis on small surfaces, the proposed experiments differ from conventional photoemission studies because a probe of the final state spectrum of emitted electrons populated by low photon energies can be readily achieved. Emphasis is therefore given to low photon energies and modest CW light intensities. An important feature of these experiments is the ability to investigate the effects of a strong applied electric field on the surface under illumination. DOE

N88-20625# Los Alamos National Lab., N. Mex.
PROJECTED PERFORMANCE OF RF-LINAC-DRIVEN FREE-ELECTRON LASERS IN THE VUV AND SOFT X-RAY REGIONS
B. E. Newnam Dec. 1987 8 p Presented at the Topical Meeting on Free-electron Laser Applications in the Ultraviolet, Cloudcroft, N. Mex., 2 Mar. 1988
(Contract W-7405-eng-36)
(DE88-004294; LA-UR-87-4245; CONF-880318-1) Avail: NTIS HC A02/MF A01

A multidisciplinary team of Los Alamos scientists, supported by the U.S. Department of Energy, has been developing the requisite technologies to extend free-electron laser (FEL) operation from infrared and visible wavelengths into the extreme-ultraviolet below 100 nm using RF-linear accelerator technology. The goal is to establish an XUV Free-Electron Laser User Facility, the next-generation light source that will make available to researchers optical power more than one-million times greater than provided by synchrotron light sources. Based primarily on a series of FEL oscillators driven by a single, RF-linac, the Los Alamos facility is designed to generate broadly tunable, picosecond-pulse, coherent radiation spanning the soft X-ray through the ultraviolet to the visible spectral ranges from 1 nm to 400 nm. The FEL facility design is discussed and performance predicted. DOE

N88-20626# Lawrence Livermore National Lab., Calif.
DATABASE OF AVERAGE-POWER DAMAGE THRESHOLDS AT 1064 nm
F. Rainer, E. A. Hildum, and D. Milam 14 Dec. 1987 22 p Presented at the Boulder Damage Symposium, Boulder, Colo., 26 Oct. 1987

(Contract W-7405-eng-48)
(DE88-004352; UCRL-97801; CONF-8710165-4) Avail: NTIS HC A03/MF A01

We have completed a database of average-power, laser-induced, damage thresholds at 1064 nm on a variety of materials. Measurements were made with a newly constructed laser to provide design input for moderate and high average-power laser projects. The measurements were conducted with 16-ns pulses at pulse-repetition frequencies ranging from 6 to 120 Hz. Samples were typically irradiated for time ranging from a fraction of a second up to 5 minutes (36,000 shots). We tested seven categories of samples which included antireflective coatings, high reflectors, polarizers, single and multiple layers of the same material, bare and overcoated metal surfaces, bare polished surfaces, and bulk materials. The measured damage threshold ranged from less than 1 J/sq cm for some metals to greater than 46 J/sq cm for a bare polished glass substrate. DOE

N88-20627# Oak Ridge National Lab., Tenn.
STUDIES OF COMPOUND STATES OF NEGATIVE IONS USING LASER BEAMS
R. N. Compton Dec. 1987 12 p Prepared in cooperation with Tennessee Univ., Knoxville
(Contract DE-AC05-84OR-21400)
(DE88-004708; ORNL/M-455) Avail: NTIS HC A03/MF A01

A brief discussion is given for the research effort in photodetachment spectroscopy and electron scattering in a laser field. DOE

N88-20628# Virginia Univ., Charlottesville. Dept. of Physics.
NONCONTACT THERMOMETRY VIA LASER PUMPED, THERMOGRAPHIC PHOSPHORS: CHARACTERIZATION OF SYSTEMATIC ERRORS AND INDUSTRIAL APPLICATIONS
G. T. Gillies, L. J. Dowell, W. N. Lutz, S. W. Allison, M. R. Cates, B. W. Noel, L. A. Franks, and H. M. Borella Oct. 1987 17 p Presented at the ICALEO '87: Conference on Electro-optic Sensing and Measurement, San Diego, Calif., 8 Nov. 1987 Prepared in cooperation with Los Alamos National Lab., N. Mex.; EG and G Energy Measurements, Goleta, Calif.; Oak Ridge Gaseous Diffusion Plant, Tenn.
(Contract DE-AC05-84OT-21400)
(DE88-005599; K/ETAC-32; CONF-8711118-2) Avail: NTIS HC A03/MF A01

There is a growing number of industrial measurement situations calling for a high precision, noncontact method of thermometry. Collaboration has been successful in developing one such method based on the laser-induced fluorescence of rare-earth-doped ceramic phosphors like Y2O3:Eu. In this paper, we summarize the results of characterization studies aimed at identifying the sources of systematic error in a laboratory-grade version of the method. We then go on to present data from measurements made in the afterburner plume of a jet turbine and inside an operating permanent magnet motor. DOE

N88-20629# Deutsche Forschungs- und Versuchsanstalt fuer Luft- und Raumfahrt, Stuttgart (West Germany). Inst. fuer Technische Physik.
DESIGN STUDIES FOR A SOLAR PUMPED LASER DEVICE
Werner Zittel Oct. 1987 65 p
(DFVLR-FB-87-39; ISSN-0171-1342; ETN-88-91922) Avail: NTIS HC A04/MF A01; DFVLR, VB-PL-DO, Postfach 90 60 58, 5000, Cologne, Federal Republic of Germany, 23 deutsche marks

Methods used for calculating solar pumped lasers are summarized. A central part is the numerical simulation with simple models for the power output in dependence of the power density of the concentrated sunlight. Solid state materials are investigated with respect to their temperature behavior. These include ruby, Nd:YAG, Nd:Cr:GSGG, Ti-sapphire and alexandrite. The calculations show that for ruby at T = 100 K efficiencies of 5 percent should be obtainable, for Nd:YAG 3 to 5 percent, and for Cr:Nd:GSGG up to 10 percent, if cooling problems are solved. The other materials investigated are not believed to be serious candidates for solar pumping. ESA

N88-20630*# Hampton Inst., Va.
DIRECT SOLAR-PUMPED IODINE LASER AMPLIFIER Progress Report, 1 Sep. 1987 - 29 Feb. 1988
Kwang S. Han, In Heon Hwang, Khong Hon Kim, and Larry V. Stock 28 Apr. 1988 81 p
(Grant NAG1-441)
(NASA-CR-182674; NAS 1.26:182674) Avail: NTIS HC A05/MF A01 CSCL 09C

A XeCl laser pumped iodine laser oscillator was developed which will be incorporated into the Master Oscillator Power Amplifier (MOPA) system. The developed XeCl laser produces output energy of about 60 mJ per pulse. The pulse duration was about 10 nsec. The kinetic model for the solar-pumped laser was refined and the algorithm for the calculation of a set of rate equations was improved to increase the accuracy and the efficiency of the calculation. The improved algorithm was applied to explain the existing experimental data taken from a flashlamp pumped iodine laser for three kinds of lasants, i-C3F7I, n-C4F9I, and t-C4F9I. Various solid laser materials were evaluated for solar-pumping. The materials studied were Nd:YAG, Nd:YLF, and Cr:Nd:GSGG crystals. The slope efficiency of 0.17 percent was measured for the Nd:YLF near the threshold pump intensity which was 211 solar constants (29W/sq cm). The threshold pump intensity of the Nd:YAG was measured to be 236 solar constants (32W/sq cm) and the near-threshold slope efficiency was 0.12 percent. True CW laser operation of Cr:Nd:GSGG was possible only at pump intensities less than or equal to 1,500 solar constants (203 W/sq cm). This fact was attributed to the high thermal focusing effect of the Cr:Nd:GSGG rod. B.G.

N88-20631 Cornell Univ., Ithaca, N.Y.
LOW THRESHOLD RIDGE WAVEGUIDE SINGLE QUANTUM WELL LASERS Ph.D. Thesis
Glen Anthony Beer Feak [1987] 282 p
Avail: Univ. Microfilms Order No. DA8725773

The goal was to produce a GaAs/AlGaAs laser suitable for short distance fiber communication as well as integrated optics. To accomplish this, a ridge waveguide, graded index separate confinement heterostructure with a single quantum well was chosen. Emphasis was placed on low power consumption of the device, and hence low threshold was a primary goal. Integrability, though not fully demonstrated, was also of key importance, as were ease and reproducibility of fabrication. In order to effectively couple to fibers, a narrow lateral beam width was also sought. For direct modulation, it was intended the device have linear power versus current characteristics, and high quantum efficiency. The devices fabricated met the goals set for them. Of 107 devices fabricated and tested, all had low thresholds, between 9.0 mA and 18.0 mA, with a 12.5 mA average. Above threshold linear power versus current curves with fairly high differential quantum efficiencies were measured up to 14 mW/facet for most devices, promising low-distortion direct modulation. The fabrication steps were relatively simple, compatible with eventual integration, and resulted in high uniformity and yield. Successful use of the device as an array element was also demonstrated. A three-laser array was fabricated. Single-lobed far-field emission was attained by introducing distributed saturable absorption regions in the outer cavities. The result was stable, in-phase coupled supermode operation of the ridge waveguide array up to 80 mW/facet, with a threshold current kept near 10 mA per ridge. Dissert. Abstr.

N88-20632# General Electric Co., Princeton, N.J. Astro-Space Div.
HIGH POWER, HIGH EFFICIENCY, 2D LASER DIODE ARRAYS FOR PUMPING SOLID STATE LASERS
A. Rosenberg, J. C. McShea, A. R. Bogdan, J. C. Petheram, and A. Rosen Nov. 1987 7 p Presented at CLEO '88: OSA/IEEE Conference on Lasers and Electro-Optics, Anaheim, Calif., 25 Apr. 1988 Prepared in cooperation with David Sarnoff Research Center, Princeton, N.J.
(Contract W-7405-eng-48)
(DE88-004042; UCRL-15982; CONF-880402-8) Avail: NTIS HC A02/MF A01

This document reports the current performance of 2D laser diode arrays operating at 770 nm and 808 nm for pumping promethium and neodymium solid state lasers, respectively. Typical power densities are in excess of 2kw/sq cm with overall efficiencies greater than 30 percent. DOE

N88-20633# Rochester Univ., N. Y. Inst. of Optics.
DOUBLY PERIODIC OUTPUT FROM A DYE LASER PUMPED BY A FREE-RUNNING ARGON LASER
I. A. McMackin, C. Radzewicz, and M. G. Raymer 1987 4 p Presented at the 15th International Conference on Quantum Electronics, Baltimore, Md., 27 Apr. 1987
(Contract DE-FG02-87ER-13761)
(DE88-005027; DOE/ER-13761/2; CONF-870488-2) Avail: NTIS HC A02/MF A01

Experiments were performed with a single-line argon-ion laser pumping a three-mirror, folded cavity dye laser containing a single-plate birefringent tuner. This resulted in multimode dye laser operation with a center frequency of 585 nm and a line width less than 1 A. The dye laser field and the power spectra were modulated with a period of n delta, where delta is the dye laser mode spacing. As predicted, the strength of the modulation is larger for the n = 7 case. DOE

N88-20634# Paris-Sud Univ., Orsay (France). Lab. de Spectroscopie Atomique et Ionique.
WAVELENGTH SCALING OF LITHIUM-LIKE RECOMBINATION SCHEME FOR X-UV GAIN PRODUCTION
A. Carillon, F. Gadi, B. Gauthe, H. Guennou, P. Jaegle, G. Jamel, A. Klisnick, C. Moeller, and A. Sureau 1987 5 p Presented at the 14th International Conference on X-Ray and Inner Shell Processes, Paris, France, 14-18 Sep. 1987
(ETN-88-92002) Avail: NTIS HC A02/MF A01

Observed and predicted values of gain for 3d-5f, 3d-4f and 4d-5f transitions of lithium-like ions in laser-produced plasmas are reported. Experimental results concerning the S13(+) ion are reported. A gain coefficient of the order of 1/cm is measured for the 3d-5f transition of S XIV at the wavelength of 65.2 A. Calculations concerning the K16(+), CA17(+), and Ti19(+) ions are also presented. ESA

37 MECHANICAL ENGINEERING

Includes auxiliary systems (nonpower); machine elements and processes; and mechanical equipment.

N88-20635# IIT Research Inst., Chicago, Ill.
CORROSION-WEAR PROCESS UNDER ROLLING-SLIDING MOTION Final Report, 30 Aug. 1985 - 28 Feb. 1987
Binayak Panda Aug. 1987 104 p
(Contract N62269-85-C-0265)
(AD-A189603; IITRI-M06140-6; NADC-87151-60) Avail: NTIS HC A06/MF A01 CSCL 13I

To advance the understanding of the corrosion-wear process under rolling and rolling-sliding motion, a dynamic corrosion-wear electrochemical cell was designed and constructed. This cell is capable of monitoring the electrochemical behavior under simultaneously occurring corrosion and wear processes simulating naval aircraft bearings. With this test apparatus, complete polarization diagrams were obtained for various rolling and rolling-sliding conditions along with the corrosion current density and open-circuit potential of the system. Even under pure rolling conditions, the effect of wear was significant in removing the passive film, as indicated by the increase in corrosion current and decrease in open-circuit potential. Increase in load and introduction of a few percent sliding generated more severe wear conditions, reflected in the results of electrochemical measurements. Results from the statistical analysis of the tests based on the Plackett-Burman test matrix indicated that more than one variable exerts significant influence on the electrochemical parameters. Addition of 500 ppm sodium dichromate into the electrolyte was the most significant factor statistically. A combination inhibitor consisting of 500 ppm sodium nitrite and 500 ppm sodium dichromate had the most dramatic effect in reducing corrosion in the absence of lubricating oil. GRA

N88-20636# Edgerton, Germeshausen and Grier, Inc., Idaho Falls, Idaho.
AN EXPERIMENTAL METHOD FOR SPECIES CONCENTRATION MEASUREMENTS IN A WELDING ARC USING LASER-INDUCED FLUORESCENCE
S. C. Snyder, C. B. Shaw, Jr., and C. L. Shull 1987 6 p Presented at the Spring Meeting of the Materials Research Society, Anaheim, Calif., 21 Apr. 1987
(Contract DE-AC07-76ID-01570)
(DE88-005638; EGG-M-36386; CONF-870438-39) Avail: NTIS HC A02/MF A01

An experimental method using laser-induced fluorescence (LIF) to determine the distribution of neutral manganese in a gas tungsten welding arc is described. The theoretical consideration and experimental difficulties encountered when extending LIF techniques from flames to thermal plasmas are discussed, and preliminary results are presented. DOE

N88-20637# Argonne National Lab., Ill.
OVERVIEW OF THE DOE-ECUT TRIBOLOGY PROGRAM
F. A. Nichols and A. I. Michaels 1987 13 p Presented at the Coatings for Advanced Heat Engines Workshop, Castine, Maine, 27 Jul. 1987
(Contract W-31-109-eng-38)
(DE88-002878; CONF-870762-1) Avail: NTIS HC A03/MF A01

This paper describes the ECUT Tribology Program which seeks to provide the base technology required to achieve savings in US annual energy consumption by means of major tribological advances. This may be achieved through direct energy savings, by increasing efficiency or productivity, or through savings of the energy embodied in materials and devices by reducing wear. The mission also seeks to reduce the significant limitations in the operation of existing and advanced tribological systems which have to operate in severe environments such as high temperature, high speeds, high loads, corrosive gases and liquids and combinations thereof. The ECUT Tribology Program has established close ties with US industry and universities to determine current and future needs for advances of tribological systems and to facilitate the transfer of any new technology which is developed within the program. DOE

N88-20638# Sandia National Labs., Albuquerque, N. Mex.
INTELLIGENT CONTROL OF ROBOT MANIPULATORS IN HAZARDOUS ENVIRONMENTS
R. W. Harrigan 1988 5 p Presented at COMPCON Spring '88, San Francisco, Calif., 29 Feb. 1988
(Contract DE-AC04-76DP-00789)
(DE88-003305; SAND-87-2780C; CONF-880236-1) Avail: NTIS HC A02/MF A01

The characteristics of hazardous environments and the impact these have on robot manipulator system control are reviewed. In particular, computer based reasoning must be integrated into the control of robot manipulators to allow successful application to such environments. Computing architectures and the concomitant software structures necessary to support both the high level reasoning and low level servo control requirements are discussed in the context of prototype robot systems. DOE

N88-20639# National Aerospace Lab., Amsterdam (Netherlands). Space Div.
MODELLING AND SIMULATION OF A RATE CONTROLLED MANIPULATOR ARM
M. Guelman 15 Dec. 1986 29 p
(NLR-TR-87010-U; B8729600; ETN-88-91725) Avail: NTIS HC A03/MF A01

The mathematical model of a space based manipulator arm with a rate controlled end effector is defined and the recursive algorithms for the computation of the basic dynamic functions are formulated. Digital simulation results are presented. Actual running

times for the simulation in a VAX 750 computer for the six degrees of freedom rate controlled manipulator are faster than real time. ESA

N88-20640# Polish Academy of Sciences, Warsaw. Inst. of Fundamental Technological Research.
STRUCTURAL CLEARANCES AND INTERNAL FRICTION: SIMULATION BY EIGEN DISTORTIONS
Jan HolnickiSzulc 1987 23 p
(ISSN-0208-5658) Avail: NTIS HC A03/MF A01

The variational principles and computational methods of analysis of initially slackened and stiffened structures are discussed. The simulation of clearences or internal dry friction in the structural elements by eigen distortions is applied. Presented considerations will be used in the problem of nonstandard design of structural setting (with clearances or friction in the structural joints) for load capacity maximization. Author

N88-20641 Wisconsin Univ., Milwaukee.
DYNAMIC MODELLING OF FLEXIBLE ROTOR SHAFTS MOUNTED ON HYDRODYNAMIC BEARINGS Ph.D. Thesis
Vicente Alfonso Feria-Kaiser 1987 201 p
Avail: Univ. Microfilms Order No. DA8725275

A general dynamic stability analysis for flexible rotors mounted on hydrodynamic journal bearings is developed. The general equations of motion of the system are obtained from Lagrange's equation of motion. The system kinetic, potential, and dissipation functions are found based on the generalized coordinates of the system. The loads acting at the journals of the shaft are integrated from the fluid film pressure distribution in the journal bearings. The journal displacements are related to the overall dynamics of the rotor using deformable bearings. A mathematical model is formulated and solved. This model includes the elastic and inertial properties of the flexible rotor, the elastic, damping, and inertial properties of the supports and the hydrodynamic characteristics of the journal-bearings. Dissert. Abstr.

N88-20642 Ohio State Univ., Columbus.
FORCE DISTRIBUTION AND TRAJECTORY CONTROL FOR CLOSED KINEMATIC CHAINS WITH APPLICATIONS TO WALKING MACHINES Ph.D. Thesis
John F. Gardner 1987 308 p
Avail: Univ. Microfilms Order No. DA8726634

Most industrial robotic applications utilize kinematic chains which are open loops. However, many applications arise in which closed kinematic chains are incorporated. Work cells containing two or more robot manipulators and legged vehicles are two such applications. The control of these closed kinematics chains is made more difficult by the fact that the system is statically indeterminate by virtue of the closed chains. Another way to express this is that the force distribution of these systems is underspecified and the controller must somehow compute an appropriate force distribution. An effective and simple solution is proposed, called the Partitioned Actuator Set Control Technique (PASC), forms a framework within which additional constraint equations may be specified. The method is applied to a walking machine application which is similar to the Adaptive Suspension Vehicle, currently being tested. A simplified, planar version of the vehicle is defined so that the method may be applied and studied. The multivariate trajectory control problem is also considered for this example system. Effective control stategies are derived and applied in simulation. Dissert. Abstr.

N88-20643 Minnesota Univ., Minneapolis.
DYNAMICS OF HIGH-SPEED MECHANISMS WITH ELASTIC MEMBERS Ph.D. Thesis
Fue-Wen Liou 1987 241 p
Avail: Univ. Microfilms Order No. DA8727424

Techniques are presented to study the dynamic effect of an electromechanical system which includes a dc motor, a gear box, and a flexible four-bar linkage. Computer simulation is used to demonstrate the idea. A new experimental technique is developed to verify the analytical result. The vibration of the linkage and the nonlinear characteristics of the dc motor are simulated on a computer. Based on the equation of motion derived from the principle of virtual displacement, a general planar motion finite element analysis computer code FEMAP is developed on the Apollo computer. The dynamic behavior of the mechanism is displayed on the screen. The simulation also takes care of the dynamic response of the electromechanical system: the effect of the torque of the mechanism on the motor performance. By knowing the standard motor specifications and the design parameters of the mechanism, we can predict the performance of the motor while driving the mechanism. A high-speed cinephotogrammetry combined with digital image processing experimental technique was also used to study the entire motion of the flexible linkage. The reflectors placed on the four-bar linkages are monitored by the high-speed camera. The pictures are then digitized and analyzed by the computer. The entire motion of the experimental flexible linkage computer animation is displayed on the Apollo screen and compared with the analytical results. Dissert. Abstr.

N88-20644 Ohio State Univ., Columbus.
FINITE ELEMENT METHODS FOR QUASI-PRISMATIC BODIES WITH APPLICATION TO GEARS Ph.D. Thesis
Sandeep M. Vijayakar 1987 188 p
Avail: Univ. Microfilms Order No. DA8726743

A three-dimensional finite element is developed to efficiently model quasi-prismatic bodies using shape functions based on Chebyshev polynomials. The element is used in several numerical examples, including three-dimensional gear models. A method of imposing contact constraints on finite element models of kinematically constrained multibody systems using a Simplex type of algorithm is also developed. This contact algorithm is demonstrated on a two-dimensional gearing problem. Dissert. Abstr.

N88-20645# Southwest Research Inst., San Antonio, Tex.
ENGINE TESTING FOR SYNFUEL OPERATION
D. W. Dickey, S. Vinyard, T. J. Callahan, T. W. Ryan, III, M. A. Warner-Selph, and N. R. Sefer Jan. 1988 336 p
(DE88-006044; ORNL/Sub-85-28609/1) Avail: NTIS HC A15/MF A01

A heavy duty diesel engine was tested for operation on minimally processed synthetic fuels. Fuels included in this test were a reference No. 2 diesel fuel and liquid products derived from shale, tar sands, and coal. Performance, gaseous and particulate emissions, cold startability and deposit formation with extended idle were tested. Phase 1 includes baseline testing of a state-of-the-art heavy duty diesel engine meeting current Federal emissions standards. Phase 2 includes determining practical engine modifications to enhance synfuel operation and a repeat of selected Phase 1 tests. This report is the result of Phases 1 and 2. DOE

N88-20646*# Massachusetts Inst. of Tech., Cambridge. Dept. of Mechanical Engineering.
THE DYNAMIC CONTROL OF ROBOTIC MANIPULATORS IN SPACE Semiannual Report, 31 Jul. 1987 - 31 Jan. 1988
S. Dubowsky 29 Apr. 1988 30 p
(Grant NAG1-801)
(NASA-CR-182710; NAS 1.26:182710; SAR-1) Avail: NTIS HC A03/MF A01 CSCL 13I

Described briefly is the work done during the first half year of a three-year study on dynamic control of robotic manipulators in space. The research focused on issues for advanced control of space manipulators including practical issues and new applications for the Virtual Manipulator. In addition, the development of simulations and graphics software for space manipulators, begun during the first NASA proposal in the area, has continued. The fabrication of the Vehicle Emulator System (VES) is completed and control algorithms are in process of development. Author

N88-20647# Imperial Coll. of Science and Technology, London (England). Computational Fluid Dynamics Unit.
COMPARISON BETWEEN COMPUTED AND MEASURED SWIRL AND TURBULENCE IN RECIPROCATING ENGINES
J. Z. Y. Wu Jun. 1987 27 p

(PDR/IC-CFDU/32; ETN-88-91916) Avail: NTIS HC A03/MF A01

Measurements made by Witze (1974) and Bracco (1987) in reciprocating engines under motoring conditions and predictions of the same flow obtained with the PHOENICS computer code were compared. Acceptable agreement is obtained, when the PHOENICS built-in k-epsilon model was used, with the same model constants for both engines. ESA

38 QUALITY ASSURANCE AND RELIABILITY

Includes product sampling procedures and techniques; and quality control.

N88-20648# Atomic Energy Research Establishment, Harwell (England). National NDT Centre.

ULTRASONIC INSPECTION OF IRREGULAR SURFACES

G. B. Hesketh Feb. 1987 38 p

(AERE-R-12465; HL87/1057(C14)) Avail: NTIS HC A03/MF A01

A technique and instrument are described to overcome a number of problems in examining complex irregular surfaces. The instrument is a portable, highly accurate position-sensing arm. It can be interrogated under program control to yield a position with respect to an arbitrary set of orthogonal axes. The technique involves transformation of these coordinates into a much more useful set of values, based on a non-orthogonal set of axes derived from a triangle of points located on the specimen surface. Inspection of individual areas on the sample is done on a fine triangular matrix, whereas coverage of the whole surface is achieved by linking larger triangles of arbitrary shape in a manner not dissimilar to a patchwork quilt. Ultrasonic waveforms are collected under program control, and the data are stored in a direct-access structure on disk. Entries into the structure are calculated with respect to the triangular matrix. This facilitates rapid reconstruction of section views (in particular B-scans). The technique has been successfully demonstrated using a prototype arm. Author

N88-20649# Atomic Energy Research Establishment, Harwell (England). Materials Physics and Metallurgy Div.

INVESTIGATION OF THE USE OF HORIZONTALLY POLARISED SHEAR WAVES FOR TOFD STUDIES ON AUSTENITIC STEEL

M. G. Silk, K. F. Bainton, M. J. Hillier, and N. Robertson Feb. 1986 37 p

(AERE-R-12145; HL86/1146) Avail: NTIS HC A03/MF A01

The time of flight diffraction technique (TOFD) has been used to investigate two austenitic welds containing fatigue cracks. In this work, however, the horizontally polarized shear (SH) wave has been employed rather than the usual compressional wave. It is shown that in each case the use of SH waves results in a lower level of weld reflections and other acoustic scatter and gives a clearer and more easily resolved response from the true defect. In one specimen the interpretation of the nature of the defect has been materially altered. Author

39 STRUCTURAL MECHANICS

Includes structural element design and weight analysis; fatigue; and thermal stress.

For applications see *05 Aircraft Design, Testing and Performance* and *18 Spacecraft Design, Testing and Performance.*

N88-20650# Atomic Energy Research Establishment, Harwell (England). Materials Physics and Metallurgy Div.

A STUDY OF THE DYNAMICS OF HIGH TEMPERATURE BRITTLE INTERGRANULAR FRACTURE BY ACOUSTIC EMISSION

C. A. Hippsley, D. J. Buttle, and C. B. Scruby Mar. 1987 40 p

(AERE-R-12479; HL87/1113) Avail: NTIS HC A03/MF A01

A study of high temperature brittle intergranular fracture (HTBIGF) in which acoustic emission (AE) data and fractography were used together to make deductions about the dynamics of fracture is discussed. The AE event rate was proportional to the rate of overall crack growth, and the average crack increment per AE event correlated well with spacing of striations observed on the fracture surface. The AE from HTBIGF was also compared with ambient temperature intergranular fracture and high temperature ductile fracture. HTBIGF generated about 50 percent of the emission of fully brittle fracture, and at least an order of magnitude more than that from ductile fracture. The observation of discrete bursts of AE of this magnitude, coupled with the striation on the fracture surface, indicates that HTBIGF takes place in discrete brittle steps. This is consistent with the segregation of sulfur as an embrittling species to the region of the crack tip, promoting stepwise decohesion, rather than a continuous crack growth process. Author

N88-20651 New Hampshire Univ., Durham.

BODY TENSOR FORMALISM IN FINITE DEFORMATION ELASTICITY AND APPLICATION TO THE TORSION OF A CIRCULAR CYLINDER Ph.D. Thesis

Alexander Sachs [1987] 188 p

Avail: Univ. Microfilms Order No. DA8722439

The body tensor formalism was developed for homogeneous, isotropic elastic materials. This formalism is general and not limited to small deformations. The physlical laws and the constitutive equation which relates the stress to the strain are examined with the help ot the two Lame coefficients and the three third order elastic constants. Although the body tensor formalism was used before to describe finite deformation elasticity, it was not used to generalize the constitutive equation for the stress-strain relationship. The body tensor formalism and the generalized constitutive equation are applied to the torsion of a right circular cylinder whose length is prevented from changing by the application of an end force. The solution of the torsion problem leads to a second order nonlinear differential equation which is valid to all orders in the torsion parameter. When linearized this equation can be solved to the first two orders in a dimensionaless torsion parameter. Using the values of the third order elastic constants found in the ultrasonic literature values are calculated to first order for the radius, the torque, and the force at the end of the cylinder for six metallic compounds and three nonmetallic ones.

Dissert. Abstr.

N88-20652*# Computer Software Management and Information Center, Athens, Ga.

SIXTEENTH NASTRAN (TRADEMARK) USERS' COLLOQUIUM

Mar. 1988 196 p Colloquium held in Arlington, Va., 25-29 Apr. 1988

(NASA-CP-2505; NAS 1.55:2505) Avail: NTIS HC A09/MF A01 CSCL 20K

These are the proceedings of the Sixteenth NASTRAN Users' Colloquium held in Arlington, Virginia from 25 to 29 April, 1988. Technical papers contributed by participants review general application of finite element methodology and the specific application of the NASA Structural Analysis System (NASTRAN) to a variety of static and dynamic structural problems. Author

N88-20653# South Carolina Univ., Columbia. Dept. of Statistics.

ESTIMATING SYSTEM AND COMPONENT RELIABILITIES UNDER PARTIAL INFORMATION ON CAUSE OF FAILURE

Frank M. Guess, John S. Usher, and Thom J. Hodgson Nov. 1987 19 p

(Grant AF-AFOSR-0156-84)

(AD-A189107; TR-136; AFOSR-87-1864TR) Avail: NTIS HC A03/MF A01 CSCL 12C

Estimating component reliabilities along with the system reliability frequently requires using lifetimes from the system level. Due to cost and time constraints, however, the exact cause of

system failure may be unknown. Instead, it may only be ascertained that the cause of failure is due to one component in a subset of components, e.g., the subset forms a subsystem. Confronted with such data, this article discusses how to exploit fully the available information using a maximum likelihood approach. We extend and clarify the useful work of Miyakawa (1984). A small Monte Carlo study indicates the helpfulness of this approach. GRA

N88-20654# Brown Univ., Providence, R. I.
DUCTILE FAILURE Summary Report
A. S. Kushner 28 Sep. 1987 8 p
(Contract N00014-86-K-0262)
(AD-A189429) Avail: NTIS HC A02/MF A01 CSCL 11F

Ductile failure is studied to provide a framework for quantitatively relating macroscopic measures of fracture toughness and ductility to micro-structural mechanisms of ductile fracture. Microvoid nucleation and growth is the principal mechanism of ductile fracture in metals; the voids mainly nucleate at second phase particles, by particle cracking or by decohesion of the particle-matrix interface, and final rupture involves the growth of neighboring voids to coalescence. Although the role of void nucleation and growth in ductile failure of metals is now well known, the details of the mechanism governing this failure process are not fully understood. A detailed characterization of porosity evolution is necessary to relate microstructural descriptions of the ductile rupture process quantitatively to macroscopic measures of ductility. GRA

N88-20655# Air Force Inst. of Tech., Wright-Patterson AFB, Ohio. School of Engineering.
CYCLIC CRACK GROWTH EMANATING AT A ROUND NOTCH CONSIDERING VISCOPLASTICITY M.S. Thesis
Gary L. Chestnut Dec. 1987 108 p
(AD-A189577; AFIT/GAE/AA/87D-3) Avail: NTIS HC A06/MF A01 CSCL 20K

A finite element investigation was conducted to analyze a crack growing from a round (large radius) notch under cyclic conditions at 1200 F. The results of the finite element analysis were compared to previously published results obtained for a crack emanating from a blunt notch and a single-edge-cracked specimen. The finite element program used was a two-dimensional materially and geometrically nonlinear finite element code called SNAP. The program has the capability to release fixed nodes to allow crack growth and the ability to simulate crack closure under cyclic conditions. Constitutive equations set forth by Bodner and Partom were used to account for the nonlinear, viscoplastic material behavior exhibited by IN-718 at 1200 F. Finite element analysis of a crack growing from a round notch under cyclic loading provided crack opening profile information, opening and closing loads, stress and strain profiles and plastic zone estimations. GRA

N88-20656*# National Aeronautics and Space Administration. Langley Research Center, Hampton, Va.
A PRELIMINARY INVESTIGATION OF FINITE-ELEMENT MODELING FOR COMPOSITE ROTOR BLADES
Renee C. Lake and Mark W. Nixon (Army Aviation Research and Development Command, Hampton, Va.) Jan. 1988 11 p
(NASA-TM-100559; AVSCOM-TM-88-B-001; NAS 1.15:100559)
Avail: NTIS HC A03/MF A01 CSCL 20K

The results from an initial phase of an in-house study aimed at improving the dynamic and aerodynamic characteristics of composite rotor blades through the use of elastic couplings are presented. Large degree of freedom shell finite element models of an extension twist coupled composite tube were developed and analyzed using MSC/NASTRAN. An analysis employing a simplified beam finite element representation of the specimen with the equivalent engineering stiffness was additionally performed. Results from the shell finite element normal modes and frequency analysis were compared to those obtained experimentally, showing an agreement within 13 percent. There was appreciable degradation in the frequency prediction for the torsional mode, which is elastically coupled. This was due to the absence of off-diagonal coupling terms in the formulation of the equivalent engineering stiffness. Parametric studies of frequency variation due to small changes in ply orientation angle and ply thickness were also performed. Results showed linear frequency variations less than 2 percent per 1 degree variation in the ply orientation angle, and 1 percent per 0.0001 inch variation in the ply thickness. Author

N88-20657# Sandia National Labs., Albuquerque, N. Mex.
COMPONENT MODE SYNTHESIS USING EXPERIMENTAL MODES ENHANCED BY MASS LOADING
K. W. Gwinn, J. P. Lauffer, and A. K. Miller 1988 8 p Presented at the 6th International Modal Analysis Conference, Orlando, Fla., 1 Feb. 1988
(Contract DE-AC04-76DP-00789)
(DE88-006097; SAND-87-1518C; CONF-880220-15) Avail: NTIS HC A02/MF A01

A technique is presented for synthesis of mathematical models of structural systems using experimentally measured component modes that have been enhanced by mass interface loading. With this technique, individual components are tested with arbitrary discrete masses added to interface points. This generates mode shape vectors with increased curvature near the interface to better account for local flexibility effects, and concentrates additional flexible body modes in the measurement frequency bandwidth. The effect of the interface mass is then analytically removed before the component is assembled into the global system. Results of an analytical study, using this technique on a simple beam structure, are given that show significant improvement in predicting system modes compared to using only free-free interface modes. An example is provided which assembles the same structure using an experimentally defined component with a finite element model. Results from this study indicate significant improvement in the assembled system properties. DOE

N88-20658# Oak Ridge National Lab., Tenn.
DYNAMIC TENSILE CYCLIC FATIGUE OF Si3N4
K. C. Liu and C. R. Brinkman 1987 10 p Presented at the 25th Automotive Technology Development Contractor's Coordination Meeting, Dearborn, Mich., 26 Oct. 1987
(Contract DE-AC05-84OR-21400)
(DE88-003919; CONF-8710116-2) Avail: NTIS HC A02

A series of tensile fast fracture and dynamic tension-tension cyclic fatigue tests were performed on a commercial grade of sintered silicon nitride at elevated temperatures above 1000 C. Small amounts of plasticity were observed when this material was cycled under tension-tension loading at 1200 C. Because of the plasticity, the fatigue behavior at 1200 C was found to be more complex compared to that at lower temperatures. Further, studies of the fatigue behavior showed that this material may be strain hardened slightly, such that increasing the cycling load via multiple step loading with intermittent cycling, i.e., coaxing resulted in increased fatigue life under certain conditions. An alternate explanation is that at elevated temperatures, some localized recrystallization may occur, thereby strengthening the material and increasing the fatigue life. The fracture surfaces of test specimens were examined using optical and scanning electron microscopy techniques to determine fracture origin and modes. These examinations have shown that all fractures were initiated at internal flaws, suggesting that the equipment and test methods are reliable and the data are indicative of material performance. DOE

N88-20659# Brown Univ., Providence, R. I. Div. of Engineering.
THEORY AND EXPERIMENTS OF FRACTURE IN CYCLIC COMPRESSION: SINGLE PHASE CERAMICS, TRANSFORMING CERAMICS AND CERAMIC COMPOSITES Annual Report, 31 Jul. 1987
S. Suresh and J. R. Brockenbrough 28 Aug. 1987 52 p
(Contract DE-FG02-84ER-45167)
(DE88-005792; DOE/ER-45167/7) Avail: NTIS HC A04/MF A01

We present experimental results and constitutive models aimed at developing the framework for a general theory of compression fatigue in notched brittle solids. Firstly, the results of a recent constitutive model for microcracking brittle solids in cyclic compression are briefly summarized in the light of new experimental

information on compression fatigue. Next, an experimentally-substantiated, generalized constitutive formulation, which incorporates both volumetric and shear strains produced by martensitic transformation, is developed. A finite element analysis is performed whereby the near-tip residual stress field is determined in notched plates of magnesia-partially stabilized zirconia subject to cyclic compression. Numerical results obtained for microcracking single phase ceramics and transformation-toughened ceramics clearly illustrate the inducement of notch-tip residual tensile stresses upon unloading from a far-field compressive stress. The residual tensile stresses, of magnitude considerably greater than the tensile strength of the solid, are created over a distance which is substantially larger than any characteristic microstructural dimension, but comparable to the experimentally-observed distance of crack growth after one compression cycle. The results obtained for ceramics are compared and contrasted with our previous studies of notch-tip residual tensile fields for metallic materials. DOE

N88-20660# National Aerospace Lab., Amsterdam (Netherlands). Structures and Materials Div.

FATIGUE LOAD MEASUREMENTS AND EVALUATION OF THE 25M HORIZONTAL AXIS WIND TURBINE (HAWT) AT PETTEN, THE NETHERLANDS

H. H. vanderLinden, L. Hartsuiker, A. A. tenHave, J. W. M. Dekker, and H. Ch. Rieffe 8 Sep. 1986 10 p Presented at the European Wind Energy Association EWEC 86 Conference and Exhibition, Rome, Italy, 7-9 Oct. 1986

(NLR-MP-86054-U; B8729621; ETN-88-91730) Avail: NTIS HC A02/MF A01

Load measurements on the 25 m Horizontal Axis Wind Turbine were carried out to establish fatigue load spectra for 7 load channels in 9 modes of operation, i.e., 7 wind speed classes and the start and stop at the cutout wind speed. Special attention was paid to the location of the zero levels for the different recordings. The fatigue load data were reduced and counted by the Rainflow method, resulting in 32 x 32 Markov (from-to) matrices for each combination of wind speed/event class and load channel. Rainflow matrices for 1 yr of operation were derived. Results are presented as load-exceedance spectra. ESA

N88-20661# National Aerospace Lab., Amsterdam (Netherlands). Structures and Materials Div.

EUROPEAN APPROACHES IN STANDARD SPECTRUM DEVELOPMENT

A. A. tenHave 26 Jan. 1987 17 p Presented at the ASTM Symposium on Development of Fatique Loading Spectra, Cincinnati, Ohio, 29 Apr. 1987

(NLR-MP-87007-U; B8729622; ETN-88-91735) Avail: NTIS HC A03/MF A01

Typical characteristics of various types of aircraft service loading are presented as they were discussed during the establishment of standardized test load sequences. Counting methods are reviewed and a simple and powerful algorithm is given to perform rainflow counting and to store the counting results afterwards. Synthesis procedures that generate rainflow consistent load sequences from matrix-based counting results are discussed. ESA

N88-20662*# Clemson Univ., S.C. Dept. of Mechanical Engineering.

FRACTURE CRITERIA FOR DISCONTINUOUSLY REINFORCED METAL MATRIX COMPOSITES Annual Report, 18 Nov. 1986 - 17 Nov. 1988

H. J. Rack, J. G. Goree, J. Albritton, and P. Ratnarparkhi 13 Apr. 1988 28 p

(Grant NAG1-724)

(NASA-CR-182665; NAS 1.26:182665) Avail: NTIS HC A03/MF A01 CSCL 20K

The effect of sample configuration on the details of initial crack propagation in discontinuously whisker reinforced aluminum metal matrix composites was investigated. Care was taken to allow direct comparison of fracture toughness values utilizing differing sample configurations and orientations, holding all materials variables constant, e.g., extrusion ration, heat treatment, and chemistry. B.G.

N88-20663 Old Dominion Univ., Norfolk, Va.

FINITE ELEMENT METHODOLOGY FOR NONLINEAR FREE AND HARMONIC FORCED VIBRATIONS OF BEAM AND PLATE STRUCTURES Ph.D. Thesis

Kamolphan Decha-Umphai 1987 157 p

Avail: Univ. Microfilms Order No. DA8719137

The literature and experiments have shown that nonlinear vibrations produce significant effects in structural analysis, especially the frequency-amplitude-force relation and the analysis of strain. An analysis was developed to predict both the frequency-amplitude-force relation and strains of beam and plate structures. Two finite element methods were developed, namely, the iterative single-mode method and the multiple-mode method. The harmonic force matrix was developed to analyze nonlinear forced vibrations. The study showed that the effects of midplate stretching due to large deflection is to increase the nonlinearity. However, the effects of plane displacements and inertia (IDI) are to reduce nonlinearity. For beams, both method 1 and 2 converge into a true deflection shape, provided the number of modes for method 2 is high enough. Similarly, both methods yield accurate strains provided the number of modes for method 2 is high enough. Dissert. Abstr.

N88-20664 Cornell Univ., Ithaca, N.Y.

AN ANALYSIS OF LARGE DEFORMATION AXISYMMETRIC INELASTIC PROBLEMS BY FINITE ELEMENT AND BOUNDARY ELEMENT METHODS Ph.D. Thesis

Harindra Rajiyah 1987 131 p

Avail: Univ. Microfilms Order No. DA8725797

A boundary element method is developed and implemented for elastoviscoplastic axisymmetric problems in the presence of large strains and rotations. A finite element method is implemented for the same class of problems mainly for comparison. The methods are capable of using any of a class of combined creep plasticity state variable models for the description of material behavior. An updated Lagrangian description is used for both methods. Both linear and quadratic versions of tractions and displacements on the boundary and linear variation of nonelastic deformation rates are implemented in the boundary element method. As for the finite element method, T6 elements are used. Numerical results are presented for various axisymmetric problems using the constitutive model originally proposed by Anand. Problems such as uniaxial tension tests, expansion of conical cylinders and spherical shells and radial extension of tapered discs are considered in an initial attempt to compare the two numerical techniques. Some direct solutions are also used to check the BEM program for its numerical accuracy. The results presented are obtained after careful convergence study. Dissert. Abstr.

N88-20665*# National Aeronautics and Space Administration. Langley Research Center, Hampton, Va.

OPTIMAL PLACEMENT OF TUNING MASSES FOR VIBRATION REDUCTION IN HELICOPTER ROTOR BLADES

Jocelyn I. Pritchard (Army Aviation Research and Development Command, Hampton, Va.) and Howard M. Adelman Mar. 1988 16 p Presented at the 29th AIAA/ASME/ASCE/AHS/ASC Structures, Structural Dynamics and Materials Conference, Williamsburg, Va., 18-20 Apr. 1988

(NASA-TM-100562; NAS 1.15:100562; AVSCOM-TM-88-B-003) Avail: NTIS HC A03/MF A01 CSCL 20K

Described are methods for reducing vibration in helicopter rotor blades by determining optimum sizes and locations of tuning masses through formal mathematical optimization techniques. An optimization procedure is developed which employs the tuning masses and corresponding locations as design variables which are systematically changed to achieve low values of shear without a large mass penalty. The finite-element structural analysis of the blade and the optimization formulation require development of discretized expressions for two performance parameters: modal shaping parameter and modal shear amplitude. Matrix expressions

for both quantities and their sensitivity derivatives are developed. Three optimization strategies are developed and tested. The first is based on minimizing the modal shaping parameter which indirectly reduces the modal shear amplitudes corresponding to each harmonic of airload. The second strategy reduces these amplitudes directly, and the third strategy reduces the shear as a function of time during a revolution of the blade. The first strategy works well for reducing the shear for one mode responding to a single harmonic of the airload, but has been found in some cases to be ineffective for more than one mode. The second and third strategies give similar results and show excellent reduction of the shear with a low mass penalty. Author

N88-20666*# National Aeronautics and Space Administration. Langley Research Center, Hampton, Va.
FLUID-THERMAL-STRUCTURAL STUDY OF AERODYNAMICALLY HEATED LEADING EDGES
Pramote Deuchamphai, Earl A. Thornton (Old Dominion Univ., Norfolk, Va.), and Allan R. Wieting Apr. 1988 16 p Presented at the AIAA/ASME/ASCS/AHS 29th Structures, Structural Dynamics and Materials Conference, Williamsburg, Va., 18-20 Apr. 1988
(NASA-TM-100579; NAS 1.15:100579) Avail: NTIS HC A03/MF A01 CSCL 20K

A finite element approach for integrated fluid-thermal-structural analysis of aerodynamically heated leading edges is presented. The Navier-Stokes equations for high speed compressible flow, the energy equation, and the quasi-static equilibrium equations for the leading edge are solved using a single finite element approach in one integrated, vectorized computer program called LIFTS. The fluid-thermal-structural coupling is studied for Mach 6.47 flow over a 3-in diam cylinder for which the flow behavior and the aerothermal loads are calibrated by experimental data. Issues of the thermal-structural response are studied for hydrogen-cooled, super thermal conducting leading edges subjected to intense aerodynamic heating. Author

N88-20667*# Wisconsin Univ., Milwaukee. Dept. of Mechanical Engineering.
IMPROVEMENT OF THE REYNOLDS-STRESS MODEL BY A NEW PRESSURE-STRAIN CORRELATION Status Report
Ryoichi S. Amano and John C. Chai Apr. 1988 25 p
(Grant NAG8-617)
(NASA-CR-182699; NAS 1.26:182699) Avail: NTIS HC A03/MF A01 CSCL 20K

A study is made to improve the predictions of Reynolds stresses in backward facing step flows, through modifications of the pressure-strain correlation. The mean-strain term of the pressure-strain correlation is formulated only in terms of nonisotropic turbulence in order to take the severe nonisotropic effect caused by a separating flow. This model is compared with other models and results are verified with experimental results. Author

N88-20668*# Georgia Inst. of Tech., Atlanta. School of Aerospace Engineering.
ANALYSIS OF SHELL-TYPE STRUCTURES SUBJECTED TO TIME-DEPENDENT MECHANICAL AND THERMAL LOADING Semiannual Status Report
G. J. Simitses and R. Riff Apr. 1988 57 p
(Grant NAG3-534)
(NASA-CR-182705; NAS 1.26:182705) Avail: NTIS HC A04/MF A01 CSCL 20K

This research is performed to develop a general mathematical model and solution methodologies for analyzing structural response of thin, metallic shell-type structures under large transient, cyclic or static thermomechanical loads. Among the system responses, which are associated with these load conditions, are thermal buckling, creep buckling, and ratcheting. Thus, geometric as well as material-type nonlinearities (of high order) can be anticipated and must be considered in the development of the mathematical model. Furthermore, this must also be accommodated in the solution procedures. Author

N88-20669*# National Aeronautics and Space Administration. Langley Research Center, Hampton, Va.
ACTIVE COOLING DESIGN FOR SCRAMJET ENGINES USING OPTIMIZATION METHODS
Stephen J. Scotti, Carl J. Martin, and Stephen H. Lucas (Vigyan Research Associates, Inc., Hampton, Va.) Mar. 1988 13 p Presented at the AIAA/ASME 29th Structures, Structural Dynamics and Materials Conference, Williamsburg, Va., 18-20 Apr. 1988
(NASA-TM-100581; NAS 1.15:100581) Avail: NTIS HC A03/MF A01 CSCL 20K

A methodology for using optimization in designing metallic cooling jackets for scramjet engines is presented. The optimal design minimizes the required coolant flow rate subject to temperature, mechanical-stress, and thermal-fatigue-life constraints on the cooling-jacket panels, and Mach-number and pressure contraints on the coolant exiting the panel. The analytical basis for the methodology is presented, and results for the optimal design of panels are shown to demonstrate its utility. Author

N88-20670# Technische Hogeschool, Delft (Netherlands). Inst. voor Windenergie.
DESIGN GRAPHS FOR THE FIRST TWO BENDING EIGENVIBRATION FORMS OF ROTATING BEAMS CONSISTING OF TWO BEAM POINTS [ONTWERPGRAFIEKEN VOOR DE EERSTE TWEE BUIGEIGENTRILLINGSVORMEN VAN DRAAIENDE BALKEN BESTAANDE UIT TWEE BALKDELEN]
P. A. Joosse Jun. 1987 35 p In DUTCH Sponsored by Stichting Projektbeheerbureau Energieonderzoek, The Netherlands
(IW-86006R; B8719780; ETN-88-91340) Avail: NTIS NC A03/MF A01

Design graphs for the first and second mode of the uncoupled bending eigenvibration form of a two-part rotating, vibrating beam for wind turbines and helicopter blades are given. The bar diagram, showing for several vibration directions the eigenfrequencies as a function of rpm, and the Southwell relation and beam parameters are explained. The design graphs allow a fast determination of the nonrotating eigenfrequencies and a bar diagram. The calculated frequencies have a maximum error of 5 percent and can hence be used in the preliminary design of wind turbine blades. The effect of velocity on the first vibration mode of the stiff flexbeam is maximum for short beam lengths. ESA

N88-20671# Messerschmitt-Boelkow-Blohm G.m.b.H., Ottobrunn (West Germany).
BUCKLING AND BREAKDOWN PROBLEMS IN STRUCTURAL MECHANICS. FAILURE OF PRESTRESSED DOUBLE-WALLED CONTAINERS OR RINGS [VERZWEIGUNGS- UND DURCHSCHLAGSPROBLEME IN DER STRUKTURMECHANIK. DAS VERSAGEN VORGESPANNTER DOPPELWANDIGER BEHAELTER ODER RINGE]
W. Huessler 1987 82 p In GERMAN Presented at a seminar, Munich, Federal Republic of Germany, 29 Jan. 1987
(MBB-UR-E-956/87; ETN-88-91382) Avail: NTIS HC A05/MF A01

The equilibrium of double-walled containers with rigid interwall layer was determined using variational calculus with variable boundaries. The solution for the linear-elastic case with classical buckling form, for the double ring in neutral equilibrium, and for the equilibrium of the double ring with an ideal joint at the inner ring, are discussed. The effect of a plastic residual moment in the inner ring on the load-carrying capacity of the double ring is discussed. ESA

N88-20672# Office National d'Etudes et de Recherches Aerospatiales, Paris (France). Structures Dept.
[ACTIVITIES REPORT OF THE STRUCTURES DEPARTMENT] Annual Report, 1986
Jul. 1987 25 p Original contains color illustrations
(ETN-88-91986) Avail: NTIS HC A03/MF A01

Finite element computation of composite plates with a nonlinear model of degradation and fracture related to a behavior instability; response of an elasto-acoustical structure to a diffuse, low

frequency noise; and random vibrations in the medium frequency domain of the main elements of the SA 365 Dauphin helicopter are discussed. Active control of a deformable aircraft subjected to turbulence: numerical simulation; multicontrols in unsteady aerodynamics with spoilers; flight test systems for flutter study; technical assistance to aircraft builders for dynamic identification of aeronautic structures; unsteady aerodynamic forces induced on an oscillating jet engine with jet flow; aeroelasticity of compressor blades; and prediction of helicopter rotor loads are reviewed. Prediction of lifetime of structures operating at high temperature; damage mechanics and local approaches to cracking; synthesis of plastic and viscoplastic constitutive equations; and the strength of the fiber-matrix interface in a composite material are considered. ESA

N88-20673*# Strainoptic Technologies, Inc., Norristown, Pa.
SPECTRAL CONTENTS READOUT OF BIREFRINGENT SENSORS Final Report
Alex S. Redner and Arkady S. Voloshin Apr. 1988 40 p
(Contract NAS2-12351)
(NASA-CR-179430; H-1444; NAS 1.26:179430) Avail: NTIS HC A03/MF A01 CSCL 20K

The objective of the research performed was to establish the feasibility of using spectral contents analysis to measure accurately, strains and retardation in birefringent sensors, and more generally, on transparent materials. Author

42 GEOSCIENCES (GENERAL)

N88-20674# Joint Publications Research Service, Arlington, Va.
JPRS REPORT: SCIENCE AND TECHNOLOGY. USSR: EARTH SCIENCES Abstracts Only
26 Feb. 1988 67 p Transl. into ENGLISH from various Russian articles
(JPRS-UES-88-001) Avail: NTIS HC A04/MF A01

Translations are presented of articles from Soviet scientific and technical books and journals. The predominate area of concern is the Earth Sciences. Headings under which the articles are divided are: oceanography, geology, physics of the atmosphere and Arctic and Antarctic research. For individual titles, see N88-20675 through N88-20707.

N88-20675# Joint Publications Research Service, Arlington, Va.
DETERMINATION OF MEAN THERMOHALINE CHARACTERISTICS OF THE OCEAN Abstract Only **c48**
S. A. Dobrolyubov *In its* JPRS Report: Science and Technology. USSR: Earth Sciences 26 Feb. 1988 p 1 Transl. into ENGLISH from Vestnik Moskovskogo Universiteta, Seriya 5: Geografiya (Moscow, USSR), no. 3, May - Jun. 1987 p 65-71 (For primary document see N88-20674 13-42)
Avail: NTIS HC A04/MF A01

There are two major approaches to determination of average hydrologic characteristics and energy potential of the ocean: averaging over the water area of the ocean using a file of data on the temperature and salinity of the water at standard depths after preliminary averaging for each latitude band or spherical square and construction of so-called volumetric T, S diagrams, in which the volumes of water falling into certain intervals of temperature and salinity or T, S classes are summed for each selected station. The second method is simpler than the first in terms of volume of computation work because it does not require preliminary averaging measurements. However, errors result from differences between hydrologic conditions of a specific survey and mean climatic characteristics. The error is calculated for the North Atlantic and Pacific Oceans. Results of previous computations of the mean temperature and salinity of the ocean obtained by different authors are compared. Mean temperatures and salinities for the Pacific, Atlantic and Indian Oceans and for the entire ocean are presented. Differences in mean characteristics between ocean basins are analyzed. Author

N88-20676# Joint Publications Research Service, Arlington, Va.
SPECTRAL REFLECTIVE CHARACTERISTICS OF SEA SURFACE Abstract Only **c48**
V. V. Kazaryan and V. P. Korovin *In its* JPRS Report: Science and Technology. USSR: Earth Sciences 26 Feb. 1988 p 1-2 Transl. into ENGLISH from Vestnik Leningradskogo Universiteta, Seriya 7: Geologiya, Geografiya (Leningrad, USSR), no. 1, Mar. 1987 p 97-99 (For primary document see N88-20674 13-42)
Avail: NTIS HC A04/MF A01

A multichannel type SP-4 spectropolarimeter operating in the 400 to 760 nm band from an aircraft was used to measure the spectral brightness of the sea surface and study the brightness variation as a function of various hydrophysical characteristics. It was found that the spatial resolution of the instrument increased with decreasing measurement altitude, but that this increased dispersion and standard deviation of the measured values. The spectral distribution of sea surface brightness differed for various water areas. Over the ocean there was a characteristic maximum at 470 to 490 nm, in littoral waters it is shifted to 490 to 535 nm. Author

N88-20677# Joint Publications Research Service, Arlington, Va.
ANISOTROPY OF MICROSTRUCTURAL EDDY MOTION IN SURFACE LAYER DURING CALM Abstract Only
Yu. B. Shaub *In its* JPRS Report: Science and Technology. USSR: Earth Sciences 26 Feb. 1988 p 2 Transl. into ENGLISH from Doklady Akademii Nauk SSSR (Moscow, USSR), v. 292, no. 4, Feb. 1987 p 975-977 (For primary document see N88-20674 13-42)
Avail: NTIS HC A04/MF A01

The use of vector measurements of resistivity variations makes it possible to detect and register rotational motions of nonuniform water masses, including in the dynamic nonuniform surface layer. At scales of several centimeters the eddy disturbances detectable from the rotational motions of projections of the total of three vector onto three corresponding coordinate planes do not have any dominant direction. However, it was discovered that during a calm the rotation of two vectors decreases relatively in the vertical planes and rotation of the other vector in the horizontal plane is dominant. This phenomenon was studied using experimental vector records containing 512 discrete readings at time intervals 0.1 and 1 s. Analysis of resulting and other data confirmed the possibility of dynamics of water masses in the surface layer. Such measurements make it possible to trace the formation of anisotropic microstructural eddy motion in the horizontal plane during a calm and its subsequent destruction upon restoration of wind waves. Author

N88-20678# Joint Publications Research Service, Arlington, Va.
MUSHROOM-SHAPED CURRENTS (EDDY DIPOLES) UNDER ROTATION AND STRATIFICATION CONDITIONS Abstract Only **c48**
A. I. Ginzburg, A. G. Kostyanoy, A. M. Pavlov, and K. N. Fedorov *In its* JPRS Report: Science and Technology. USSR: Earth Sciences 26 Feb. 1988 p 3 Transl. into ENGLISH from Doklady Akademii Nauk SSSR (Moscow, USSR), v. 292, no. 4, Feb. 1987 p 971-974 (For primary document see N88-20674 13-42)
Avail: NTIS HC A04/MF A01

The mushroom shaped currents detected from satellite images are a combination of narrow jet flows and plane eddy dipoles. A study was made to clarify the following aspects of this phenomenon: behavior of eddy dipoles under different conditions related to the presence or absence of stratification and different methods for inducing a disturbance allowing the possibility of a change in the sign and intensity of a relative angular momentum locally introduced into a fluid rotating as a solid body. The experimental apparatus included a rotating platform and a cylindrical basin filled with fresh water or a two layer fluid which was spun in a clockwise direction until solid body rotation was attained. The experimental configuration corresponded to an f-plane for which the beta-effect due to parabolic level curvature is negligible. A dye was used to ease observation of disturbance development. Various means were

used to generate disturbances. The experiments revealed that in a fluid rotating system it is possible to stimulate currents on the f-plane by any of the various types of local disturbance in either a uniform or stratified fluid resulting in the formation of eddy dipole(s). Author

N88-20679# Joint Publications Research Service, Arlington, Va.
ESTIMATES OF OCEAN-ATMOSPHERE THERMAL INTERACTION IN GULF STREAM ENERGY-ACTIVE TEST RANGE IN WINTER OF 1984 Abstract Only **c48**
S. S. Yefimov, G. G. Panteleyev, and Ye. V. Semenov *In its* JPRS Report: Science and Technology. USSR: Earth Sciences 26 Feb. 1988 p 3-4 Transl. into ENGLISH from Izvestiya Akademii Nauk SSSR: Fizika Atmosfery i Okeana (Moscow, USSR), v. 23, no. 3, Mar. 1987 p 309-313 (For primary document see N88-20674 13-42)
Avail: NTIS HC A04/MF A01

Data collected on the temperature and salinity fields were used in an analysis of the hydrology of the Gulf Stream energy active test range in winter. Two complete hydrological surveys of these fields were made. The first survey was from Dec. 1983 to Jan. 1984 and the second was from Feb. to Mar. 1984. The grid used measured 15 x 10 points of intersection horizontally with a uniform interval of 0.5 deg with 12 vertical levels. Eulerian and Lagrangian descriptions of the motion of particles were used in estimating thermal interactions between the ocean and atmosphere. Maps were constructed showing the heat flows at the ocean surface for the end of the first and second surveys. The main region of heat transfer into the atmosphere is the Gulf Stream flow proper, evidently resulting from the more intensive mixing of the upper layer and more active heat transfer by the cooling ocean surface. The intensity of the heat flow was up to 960 W/sq m for the first survey and to 1,350 W/sq m for the second. The regions where the ocean receives heat are situated to the north of the Gulf Stream jet and in the southwestern and eastern parts of the test range. The heat flow from the atmosphere to the ocean is less than the opposite flow. Author

N88-20680# Joint Publications Research Service, Arlington, Va.
DETERMINING LANGMUIR CIRCULATION PARAMETERS ON BASIS OF SIMILARITY THEORY Abstract Only **c48**
V. P. Krasitskiy and B. N. Filyushkin *In its* JPRS Report: Science and Technology. USSR: Earth Sciences 26 Feb. 1988 p 4-5 Transl. into ENGLISH from Izvestiya Akademii Nauk SSSR: Fizika Atmosfery i Okeana (Moscow, USSR), v. 23, no. 3, Mar. 1987 p 293-299 (For primary document see N88-20674 13-42)
Avail: NTIS HC A04/MF A01

A variant of similarity theory is proposed for describing Langmuir circulations. The determining parameters used were mean wind speed at the sea surface, mean height of wind waves, frequency of the wave spectrum maximum and corresponding wave number, and kinematic coefficient of turbulent viscosity of water. It is shown that when using this set of determining parameters the universal functions of similarity theory are dependent on only a single argument, the dimensionless frequency of the wave spectrum maximum. An analysis of observational data indicated an important dependence of the characteristics of Langmuir circulations on this dimensionless logic. It is evident that the degree of development of waves is important. It is now possible to formulate the main requirements for carrying out in situ study of such circulations. Synchronous vertical measurements of the distribution of hydrophysical characteristics make possible a more complete study of the role of circulations in the formation of active layer structure. Author

N88-20681# Joint Publications Research Service, Arlington, Va.
THERMODYNAMIC THEORY OF FLUCTUATIONS AND RAYLEIGH LIGHT SCATTERING IN SOLUTIONS Abstract Only **c48**
V. A. Durov *In its* JPRS Report: Science and Technology. USSR: Earth Sciences 26 Feb. 1988 p 5 Transl. into ENGLISH from Vestnik Moskovskogo Universiteta, Seriya 2: Khimiya (Moscow, USSR), v. 28, no. 1, Jan. - Feb. 1987 p 54-61 (For primary document see N88-20674 13-42)
Avail: NTIS HC A04/MF A01

Research on Rayleigh light scattering yields much information on the thermodynamic and kinetic properties of fluid systems, their molecular structure and the mechanisms of its restructuring in the course of thermal motion. This study is limited to the isotropic component of Rayleigh light scattering. It is shown that computations of the intensity of scattered light within the framework of macroscopic theory essentially involves computation of the mean squares and mean products of fluctuations of solution parameters. Computations are given of a number of parameters of solutions of interest in the theory of Rayleigh light scattering using the methods of the thermodynamic theory of fluctuations. It was found that the expressions for fluctuations of such intensive parameters as temperature and pressure in solutions coincide with the corresponding expressions for single component systems. The expressions for fluctuations of extensive parameters and such intensive variables as density are different in solutions and pure fluids. These and other results make it possible to derive general expressions for the intensity of the isotropic component of Rayleigh light scattering in solutions. Author

N88-20682# Joint Publications Research Service, Arlington, Va.
RESEARCH ON INFLUENCE OF INDIVIDUAL SEA WATER COMPONENTS ON SPECTRAL BRIGHTNESS COEFFICIENT OF OUTGOING RADIATION Abstract Only **c48**
Ye. K. Naumenko *In its* JPRS Report: Science and Technology. USSR: Earth Sciences 26 Feb. 1988 p 6 Transl. into ENGLISH from Zhurnal Prikladnoy Spektroskopii (Minsk, USSR), v. 46, no. 1, Jan. 1987 p 80-86 (For primary document see N88-20674 13-42)
Avail: NTIS HC A04/MF A01

There is a correlation between phytoplankton content and the brightness of radiation emanating from the water. However, the correlations obtained by different authors differ considerably. A study was therefore made of the factors exerting an influence on the brightness of outgoing radiation which cannot be experimentally controlled. The basis for the study was an optical model of sea water, including the spectral properties of water itself, dissolved organic matter and hydrosol, constituting a two component mixture of particles of mineral and biological origin. Formulas are derived which can be used in computing the spectral brightness coefficients for different mass concentration of particles. An analysis was made to determine the influence of individual components on the spectral brightness coefficient value. The analysis was made for directions of illumination and observation close to the optimal conditions for detecting color contrasts in a visual study of the sea surface from space in the observation plane perpendicular to the plane of the solar vertical. Important information was obtained concerning the contributions of these components. Author

N88-20683# Joint Publications Research Service, Arlington, Va.
RELATIONSHIP BETWEEN OCEANIC GEOLOGICAL FORMATIONS AND TECTONIC STRUCTURES Abstract Only **c46**
I. O. Murdmaa *In its* JPRS Report: Science and Technology. USSR: Earth Sciences 26 Feb. 1988 p 6-7 Transl. into ENGLISH from Geotektonika (Moscow, USSR), no. 2, Mar. - Apr. 1987 p 35-45 (For primary document see N88-20674 13-42)
Avail: NTIS HC A04/MF A01

In a review made of information published in recent years, it is made clear that each of the major structural elements of the ocean crust (mid-oceanic ridges, ocean floor basins and marginal ocean mobile zones) is characterized by a specific set of magmatic and sedimentary formations. There is a definite oceanic type of crust and lithosphere. There is a distinctive combination of predominantly abyssal (pelagic or adjacent to the continents) sedimentary formations with specific magmatic formations of the oceanic crust belonging to the ophiolotic association. On the other hand, in the marginal oceanic mobile zones, where the oceanic crust is destroyed and transformed into a continental crust, there is a special group of sedimentary formations associated with both the ophiolites of the oceanic crust and with an island arc complex

of magmatic rocks of the calc-alkali (andesite) series. Each of the major structural elements of the oceanic crust in the evolution series from a spreading zone through an oceanic plate plunged to abyssal depths to a subduction zone is characterized by its own formation types, making it possible to reconstruct these structures themselves, and also their stages of evolution in the past. Author

N88-20684# Joint Publications Research Service, Arlington, Va.
NUMERICAL MODELING OF WAVE MIGRATION OF SEISMIC DATA Abstract Only **c48**
V. V. Perekhvatov, Yu. A. Byakov, V. A. Kemelman, and G. F. Seleznev *In its* JPRS Report: Science and Technology. USSR: Earth Sciences 26 Feb. 1988 p 7 Transl. into ENGLISH from Geologiya i Geofizika (Novosibirsk, USSR), no. 2, Feb. 1987 p 99-106 (For primary document see N88-20674 13-42)
Avail: NTIS HC A04/MF A01

A study was made of the applicability of wave migration for processing time sections obtained in abyssal zones of the world ocean. Numerical modeling of wave fields was carried out using materials collected in the course of work along the Angolan-Brazilian geotraverse. Much of this geotraverse intersects the Mid-Atlantic Ridge and adjacent regions where ocean depths vary in the range of 3 to 5 km due to the great dissection of bottom relief. Most of the time sections for the geotraverse are characterized by a strong background of regular noise which in some cases virtually completely masks the images of useful structures and the wave pattern is very difficult to interpret. The wave migration procedure was used for transforming the time sections into seismic images of the medium, thereby simplifying the wave field. An algorithm was written for processing time sections by this procedure. Several examples of application of the algorithm are presented. These examples show that the wave migration procedure is an effective tool for retrieving the structure of the upper part of the section, including the bathymetric characteristics of the ocean floor, but the deep boundaries are retrieved with distortions attributable to inadequate allowance for the influence of the upper part of the section. Author

N88-20685# Joint Publications Research Service, Arlington, Va.
NEGATIVE VISCOSITY IN GLOBAL CIRCULATIONS Abstract Only **c91**
A. S. Monin *In its* JPRS Report: Science and Technology. USSR: Earth Sciences 26 Feb. 1988 p 9 Transl. into ENGLISH from Doklady Akademii Nauk SSSR (Moscow, USSR), v. 293, no. 1, Mar. 1987 p 70-74 Original language document was announced in AIAA as A87-35842 (For primary document see N88-20674 13-42)
Avail: NTIS HC A04/MF A01

Published studies of negative viscosity (NV) are briefly reviewed. It is noted that NV can explain a number of peculiar phenomena connected with the global circulations on the Sun, Jupiter, Saturn as well as in the Earth's atmosphere and ocean, and in the upper layers of the Venus atmosphere. E.R.

N88-20686# Joint Publications Research Service, Arlington, Va.
PROPAGATION OF SUBSURFACE SALINITY MAXIMUM IN TROPICAL ATLANTIC Abstract Only **c48**
S. Ye. Navrotskaya and V. F. Dubravin *In its* JPRS Report: Science and Technology. USSR: Earth Sciences 26 Feb. 1988 p 11 Transl. into ENGLISH from Okeanologiya (Moscow, USSR), v. 27, no. 2, Mar. - Apr. 1987 p 197-203 (For primary document see N88-20674 13-42)
Avail: NTIS HC A04/MF A01

Temperature and salinity indices of the northern tropical and equatorial water masses and the deep North Atlantic water mass were taken for the Northern Hemisphere and used in the study of spatial distribution of the subsurface salinity maximum between 30 N and 30 S, calculating the percent content in the core of the tropical water mass. The subsurface salinity maximum is formed primarily due to Southern Hemisphere water at the equator throughout the year, though there is a significant seasonal variation in the maximum near the equator in response to surface and subsurface currents. The topography of the subsurface salinity maximum is diagramed for summer and winter. In the spring, the dynamic relief of the maximum near the equator in the Northern Hemisphere is complicated by a doubling of the equatorial trough due to the dynamics of the Lomonosov Current associated with the weakened Southeast Trades. Author

N88-20687# Joint Publications Research Service, Arlington, Va.
SPACE-TIME ANALYSIS OF OCEANOGRAPHIC FIELDS BY MODIFIED EMPIRICAL ORTHOGONAL FUNCTIONS METHOD Abstract Only **c48**
A. O. Artemyev *In its* JPRS Report: Science and Technology. USSR: Earth Sciences 26 Feb. 1988 p 12 Transl. into ENGLISH from Okeanologiya (Moscow, USSR), v. 27, no. 2, Mar. - Apr. 1987 p 204-211 (For primary document see N88-20674 13-42)
Avail: NTIS HC A04/MF A01

The characteristic dynamics of temperature and salinity in the Artic Basin from year to year was determined and the possibility of their prediction was evaluated. Studies were based on a changing of the widely used method of empirical orthogonal functions. Dynamics of the anomalies were discovered with periods of about 5 to 6 years. The expanded method of empirical orthogonal function analysis allows prediction of the dynamics of these variables, revealing peculiarities of their space-time structure which are not obvious when traditional analysis methods are used. The variations in temperature and salinity anomaly fields in the surface layer of the Arctic Basin are determined from year to year primarily by surface circulation of water, water exchanged with the Arctic seas and the inflow of Pacific water. Author

N88-20688# Joint Publications Research Service, Arlington, Va.
INTRATHERMOCLINE LENS OF MEDITERRANEAN WATER IN TROPICAL NORTH ATLANTIC Abstract Only **c48**
V. D. Yegorikhin, Yu. A. Ivanov, V. G. Kort, M. N. Koshlyakov, Yu. F. Lukashev, Ye. G. Morozov, I. M. Ovchinnikov, V. T. Paka, T. B. Tsybaneva, and I. F. Shadrin et al. *In its* JPRS Report: Science and Technology. USSR: Earth Sciences 26 Feb. 1988 p 16 Transl. into ENGLISH from Okeanologiya (Moscow, USSR), v. 27, no. 2, Mar. - Apr. 1987 p 165-175 (For primary document see N88-20674 13-42)
Avail: NTIS HC A04/MF A01

Intrathermocline anticyclonic vortices located within the intermediate layer of the ocean may carry waters from the area of their formation within themselves for hundreds of thousands of kilometers. Traces of such lenses containing Mediterranean water have been found in the subtropical North Atlantic, and some have been extensively studied. A lens of Mediterranean water with record values of temperature and salinity was found and studied in detail in the eastern tropical North Atlantic near 20 N, 37 W. Charts illustrate the distribution of temperature, salinity and water density in this formation. The lens was apparently formed on the outer or oceanic edge of the intrusive flow of Mediterranean water moving generally westward, then northward, along the continental slope along the southwestern and western coast of the Iberian Peninsula as a continuation of the deep current through the Strait of Gibraltar. Movement of perhaps as many as several hundred such lenses per year is probably the main mechanism of penetration of Mediterranean waters into the deep Atlantic Ocean. Author

N88-20689# Joint Publications Research Service, Arlington, Va.
DYNAMICS OF SYNOPTIC OCEAN EDDIES Abstract Only **c48**
M. N. Koshlyakov *In its* JPRS Report: Science and Technology. USSR: Earth Sciences 26 Feb. 1988 p 18-19 Transl. into ENGLISH from Vestnik Akademii Nauk SSSR (Moscow, USSR), no. 2, Feb. 1987 p 22-35 (For primary document see N88-20674 13-42)
Avail: NTIS HC A04/MF A01

The results are briefly presented of an analysis of the properties of synoptic eddies observed during the American-Soviet POLYMODE project, covering their origin, dynamics and interaction with large scale ocean currents. The basis of the Soviet work

was 19 anchored automonous buoy stations in a equilateral triangle grid spaced at distances of 72 km, with the center of the grid at 29 N, 70 W. The area covered is in the vicinity of the Gulf Stream, where large quantities of heat are transmitted from the ocean to the atmosphere in Winter. The interaction of Gulf Stream eddies with each other and with the main current is described. Additional work was done in 1982 to 1983 in the Subantarctic. The behavior of two cyclonic eddies in this area is described. There is a direct interrelationship between oceanic eddies and atmospheric processes. Bottom relief is said to directly influence the formation of eddies, although the eddy pattern does not repeat from year to year in the same area. Author

N88-20690# Joint Publications Research Service, Arlington, Va.
TURBULENT TRANSFER OF MOMENTUM AND HEAT IN BOUNDARY LAYER OF FLUID BEYOND AN OBSTACLE. 1: HYDRODYNAMIC CHARACTERISTICS Abstract Only **c34**
R. B. Shlyazhas and A. A. Shlanchyauskas *In its* JPRS Report: Science and Technology. USSR: Earth Sciences 26 Feb. 1988 p 19 Transl. into ENGLISH from Trudy Akademii Nauk Litovskoy SSR: Seriya B: Khimiya, Tekhnika, Fizicheskaya Geografiya (Vilnius, USSR), no. 6, Dec. 1986 p 92-103 (For primary document see N88-20674 13-42)
Avail: NTIS HC A04/MF A01

Experimental studies were carried out to analyze the distribution of mean velocity, correlation moments of velocity pulsations up to third order and balance terms in the energy equation in a turbulent boundary layer with separating flow around an obstacle situated on a plate. Mean velocity profiles, turbulent energy profiles, profiles of third order correlation moments and turbulent energy dissipation profiles are presented. It is found that the main source of the increase in turbulent energy is similar in energy transfer properties to a flat mixing layer developing in the initial portion of a flooded jet. Attachment of the flow involves redistribution of energy among velocity pulsation components. The energy of vertical pulsations is transferred to pulsation movement parallel to the wall, while the turbulent flow of momentum near the wall is reduced.
Author

N88-20691# Joint Publications Research Service, Arlington, Va.
GENERALIZED EXPRESSION FOR RADIO NAVIGATION PARAMETER ERROR Abstract Only **c04**
V. F. Ivashkevich and V. S. Tregubov *In its* JPRS Report: Science and Technology. USSR: Earth Sciences 26 Feb. 1988 p 20-21 Transl. into ENGLISH from Geodeziya i Kartografiya (Moscow, USSR), no. 3, Mar. 1987 p 45-48 (For primary document see N88-20674 13-42)
Avail: NTIS HC A04/MF A01

An analysis of physical factors influencing the accuracy of radio navigation measurements in low frequency systems such as Loran-C was made in deriving a generalized expression for the error in measuring the radio navigation parameter, which can be used in referencing objects during hydrographic and topographic-geodetic work on the continental self. All parameter measurement errors are considered to fall in three main groups: instrumental, noise in the measurement zone, and those caused by the influence of the environment on the radio wave propagation. An evaluation of measurement accuracy of the radio navigation parameter, since the correction for the propagation conditions for surface radio waves cannot be constant for the entire zone of action of the radio navigation system due to changing path length and effective conductivity, can be made using the equation derived, which consists of three components: the rms measurement error of the parameter and two mean square errors for excluding systematic components. The effects of this evaluation accuracy are given. Author

N88-20692# Joint Publications Research Service, Arlington, Va.
EXPERIENCE WITH AND WAYS TO UPGRADE ACCURACY OF HYDROMAGNETIC SURVEYS IN OCEAN Abstract Only **c48**
N. N. Rzhevskiy *In its* JPRS Report: Science and Technology. USSR: Earth Sciences 26 Feb. 1988 p 23 Transl. into ENGLISH from Ekspress-Informatsiya. Seriya: Morskaya Geologiya i Geofizika (Moscow, USSR), no. 12, 1986 p 1-4 (For primary document see N88-20674 13-42)
Avail: NTIS HC A04/MF A01

In geophysical magnetometric research there is a lack of consistency between the instrumental accuracy of measurements and the accuracy of compiled maps of the anomalous magnetic field. There is also a disproportion between the random and systematic errors of these maps. Because of this, the highly successful work of scientists and engineers in developing new instruments for measuring the magnetic field is largely defeated. A number of measures can be proposed for increasing the efficiency of hydromagnetic surveys in the ocean which can be used in the planning of work and the processing of measurement data. Methods for reducing random errors and systematic error are given. Author

N88-20693# Joint Publications Research Service, Arlington, Va.
VERTICAL TURBULENT TRANSFER OF MATTER IN THIN OCEAN SURFACE LAYER DURING DAYTIME HEATING Abstract Only **c48**
K. A. Korotenko *In its* JPRS Report: Science and Technology. USSR: Earth Sciences 26 Feb. 1988 p 25 Transl. into ENGLISH from Okeanologiya (Moscow, USSR), v. 27, no. 1, Jan. - Feb. 1987 p 47-51 (For primary document see N88-20674 13-42)
Avail: NTIS HC A04/MF A01

The long wave part of the solar radiation spectrum responsible for the heating of water is almost entirely absorbed in the upper 5 m layer of the ocean and this can give rise to considerable temperature (density) gradients. An increase in the density gradient during heating results in definite changes in the characteristics of vertical diffusion of impurities in this ocean layer. This effect was observed during diffusion experiments in the Black Sea in which a dye was used. It was found that the penetration of matter into the depths of the ocean is dependent to a considerable degree on the nature of temperature field variability in the layer in the course of radiation heating. Three regimes of this process are defined; each is described and analyzed. These regimes are associated with the rate of increase in the temperature gradient in the layer of volumetric absorption of solar radiation. Author

N88-20694# Joint Publications Research Service, Arlington, Va.
PHENOMENOLOGICAL DESCRIPTION OF EDDY REGISTERED IN GULF STREAM Abstract Only **c48**
V. A. Bubnov, N. P. Kuzmina, and I. S. Podymov *In its* JPRS Report: Science and Technology. USSR: Earth Sciences 26 Feb. 1988 p 26 Transl. into ENGLISH from Okeanologiya (Moscow, USSR), v. 27, no. 1, Jan. - Feb. 1987 p 25-29 (For primary document see N88-20674 13-42)
Avail: NTIS HC A04/MF A01

A cruise was carried out in the Gulf Stream frontal zone in a region of intensive meandering. Measurements were made with an STD complex to a depth of 1,000 m and a thermistor towed at the surface. Macro- and mesoscale characteristics of the zone were determined. A cyclonic eddy formation of relatively small horizontal dimensions, with anomalously low temperature and salinity and high orbital velocities, was discovered at the center of the meander. The measured parameters indicate that this eddy is a new type, not observed earlier in the frontal zone. The eddy had an elliptical shape with the longer axis oriented in a SW-NE direction. The horizontal scales of the formation at the 0 and 200 m horizons were about 60 and 30 miles respectively. The ships drift rate was the same as the orbital velocity of eddy motion; this eddy orbital motion is cyclostrophic, rather than geostrophic. Sections through the eddy reveal a sharp frontal nature of its boundaries. In the upper layer the horizontal temperature and salinity gradients attain 2 C/mile and 0.2/oo mile. Numerous inversions on the temperature and salinity profiles indicate strong transfrontal heat and mass transfer in peripheral portions of the eddy. The mechanism of formation of this eddy may be similar to the generation of cyclones and anticyclones in the North Atlantic Current region. Author

N88-20695# Joint Publications Research Service, Arlington, Va.
CONTRIBUTION TO THEORY OF QUASIGEOSTROPHIC MOTIONS OF FINITE AMPLITUDE IN VISCOUS STRATIFIED OCEAN Abstract Only **c48**
G. I. Shapiro *In its* JPRS Report: Science and Technology. USSR: Earth Sciences 26 Feb. 1988 p 27 Transl. into ENGLISH from Okeanologiya (Moscow, USSR), v. 27, no. 1, Jan. - Feb. 1987 p 18-24 (For primary document see N88-20674 13-42)
Avail: NTIS HC A04/MF A01

A study was made of quasigeostrophic motions of finite amplitude, with allowance for viscosity forces, in the approximation of a multilayer stratified fluid. A generalized quasigeostrophic equation is derived which describes motion of different spatial scales: mesoscale, synoptic and planetary. There are no restrictions on the amplitude of displacement of the isopycnic line. In the theoretical analysis two types of nonlinearity are examined: dynamic, characterized by the Kibel number, and kinematic, associated with finite deflection of the isopycnic line from its equilibrium position. The case of a three layer fluid is examined in detail. A classification of quasigeostrophic motions is proposed as a function of the relationship between the Kibel and Ekman numbers and the dimensionless amplitude of perturbations. Estimates for the rate of viscous degeneration of intrathermocline eddies are given. The temporal evolution and the three dimensional field of velocities of an axisymmetric intrathermocline eddy are computed. Author

N88-20696# Joint Publications Research Service, Arlington, Va.
NUMERICAL MODEL OF RAYLEIGH INSTABILITY AND SPIN-OFF EDDIES ON FRONTS Abstract Only **c47**
V. F. Kozlov and Ye. V. Yaroshchuk *In its* JPRS Report: Science and Technology. USSR: Earth Sciences 26 Feb. 1988 p 28 Transl. into ENGLISH from Okeanologiya (Moscow, USSR), v. 27, no. 1, Jan. - Feb. 1987 p 12-17 (For primary document see N88-20674 13-42)
Avail: NTIS HC A04/MF A01

A contour dynamics model of baroclinic instability of a front is proposed. It is represented in the form of a linear shear layer with constant vorticity within. Numerical experiments not only confirm the known Rayleigh instability criteria, but also make it possible to trace a decay process in a highly nonlinear stage in development of the process. This spin-off eddy phenomenon has been observed in the Florida Current. These are cyclonic eddies of an intermediate scales extending to a depth of 100 to 200 m. A linear analysis of stability and the numerical experiments described show that such an unstable shear layer decays into a train of eddies, whereas the stable layer, in the case of perturbations of the boundaries, may experience deformations resembling the tiled structures observed in the ocean. It is shown that an extremely probable cause of appearance of spin-off eddies is shear barotropic instability on fronts, developing in the upper layer. It appears that the contour dynamics model can serve as an effective tool in modeling the dynamics of fronts and can be useful in interpreting satellite observation data. Author

N88-20697# Joint Publications Research Service, Arlington, Va.
RESEARCH ON TURBULENCE IN BOTTOM BOUNDARY LAYER IN OCEAN Abstract Only **c48**
V. N. Nabatov and R. V. Ozmidov *In its* JPRS Report: Science and Technology. USSR: Earth Sciences 26 Feb. 1988 p 29 Transl. into ENGLISH from Okeanologiya (Moscow, USSR), v. 27, no. 1, Jan. - Feb. 1987 p 5-11 (For primary document see N88-20674 13-42)
Avail: NTIS HC A04/MF A01

The results of turbulence measurements in the bottom layer of an ocean are presented. The measurements were made using a probe with sensors for measuring temperature, water conductivity, pressure and fluctuations of current velocity shear. The measurements were made over a sloping bottom in the Norwegian Sea. The records revealed a turbulent upper ocean layer coinciding in thickness with the upper homogeneous layer. In this layer, turbulence was caused for the most part by wind waves whose height during the measurements was 1 to 2 m. Below the upper turbulent layer it was common to observe individual spots of turbulent fluid. Since these spots appeared and disappeared spontaneously, during repeated soundings the position of these spots and their intensity changed. These spots are evidently a result of generation of turbulence by the instability of internal waves and shear currents. These and other data were analyzed for clarifying the characteristics of the bottom turbulent layer. A model is proposed which is based on the equation for the balance of turbulent energy in a density stratified flow. Author

N88-20698# Joint Publications Research Service, Arlington, Va.
INVARIANT CHARACTERISTICS OF ACOUSTIC FIELD IN STRATIFIED OCEAN Abstract Only **c48**
B. A. Kasatkin *In its* JPRS Report: Science and Technology. USSR: Earth Sciences 26 Feb. 1988 p 30 Transl. into ENGLISH from Doklady Akademii Nauk SSSR (Moscow, USSR), v. 291, no. 6, Dec. 1986 p 1483-1487 (For primary document see N88-20674 13-42)
Avail: NTIS HC A04/MF A01

The acoustic fields formed under waveguide propagation conditions have considerable spatial frequency variability caused by the interference of normal waves. Although variability of a signal and its phase have been well studied under these conditions, little study has been made of invariant relations in such an acoustic field, these being the most stable under intermode interference conditions. Little has been known of the invariant characteristics corresponding to these relations. Expressions are derived which make it possible to determine the invariant kinematic characteristics of a nonuniform waveguide with the speed of sound profile. For such a waveguide there is a functional dependence which for a waveguide with ideal boundaries is not dependent on the normal wave nor on frequency. In the limiting case of a uniform waveguide the invariant velocity undergoes transition into mean harmonic velocity, whose invariance in the case of relatively low variability of the kinematic characteristics follows from the invariance of mean geometrical velocity. It is shown that the invariant characteristics are not dependent on sea depth, making it useful under both model and real conditions of an irregular depth waveguide.
Author

N88-20699# Joint Publications Research Service, Arlington, Va.
STUDY OF SPECTRA OF SEA WAVES ON HORIZONTALLY NONUNIFORM CURRENT IN RIP ZONE Abstract Only **c48**
I. A. Leykin *In its* JPRS Report: Science and Technology. USSR: Earth Sciences 26 Feb. 1988 p 33 Transl. into ENGLISH from Izvestiya Akademii Nauk SSSR: Fizika Atmosfery i Okeana (Moscow, USSR), v. 23, no. 1, Jan. 1987 p 52-58 (For primary document see N88-20674 13-42)
Avail: NTIS HC A04/MF A01

A study was made of the spectra of sea waves on a horizontally nonuniform current. The work was done in the White Sea, where rips are common, and in shallow waters in a strait with regular semidiurnal tides. Wave measurements were made in a frontal rip which developed near an elongated bank, an underwater ridge with a width of about 100 m, extending almost perpendicular to the direction of the tidal current. The depth of the strait was 40 to 50 m, decreasing over the bank to 5 to 10 m. Wave measurements were made using a string wave recorder. Simultaneous registry was in 2 channels: a LF channel for the total signal and a HF channel for the signal passed through a HF filter with a cutoff frequency of 1 Hz. Each record had a duration of 80 to 120 s. Sixteen wave records were registered during 2 occurrences of a rip when there was a weak wind and opposite directions of the wind and current. The record provided data on the following rip zones: collapse zone, transition zone, calm water zone, toicheya zone. It is demonstrated that the transformation of surface waves on a horizontally nonuniform current is decisive in the development of a frontal rip. Author

N88-20700# Joint Publications Research Service, Arlington, Va.
MODEL OF HYDRODYNAMIC ADJUSTMENT OF TEMPERATURE, SALINITY AND CURRENT FIELDS Abstract Only **c48**

A. S. Sarkisyan, Yu. L. Demin, and D. I. Trukhchev *In its* JPRS Report: Science and Technology. USSR: Earth Sciences 26 Feb. 1988 p 34 Transl. into ENGLISH from Izvestiya Akademii Nauk SSSR: Fizika Atmosfery i Okeana (Moscow, USSR), v. 23, no. 1, Jan. 1987 p 45-51 (For primary document see N88-20674 13-42)
Avail: NTIS HC A04/MF A01

A numerical model for diagnosis of state of a sea or ocean basin is proposed, as well as a method for hydrodynamic adaptation of the temperature, salinity and current fields. Since diagnostic models have a number of shortcomings, it was decided to combine the advantages of diagnostic and prognostic models and at the same time to eliminate such shortcomings as the mismatching of fields, presence of noise and idealization. The approach is based on successive use of diagnostic and prognostic models. The temperature and salinity fields stipulated from observations and the current fields computed using a diagnostic model are used as the initial approximation in the prognostic model. The proposed model is formulated for adaptation of the temperature, salinity, density and current fields. Using this model, the results are given of two numerical experiments for the Black Sea. The adaptation mechanism, role of bottom relief, nonlinear effects and methods for the parameterization of turbulence are examined. Author

N88-20701# Joint Publications Research Service, Arlington, Va.
RESOLUTION OF THE MAGNETOTELLURIC METHOD FOR DETERMINING LOCAL INHOMOGENEITIES IN THE SEDIMENTARY COVER Abstract Only **c46**

V. M. Kobzova, I. P. Moroz, and A. I. Bilinskiy *In its* JPRS Report: Science and Technology. USSR: Earth Sciences 26 Feb. 1988 p 45 Transl. into ENGLISH from Geofizicheskiy Zhurnal (Kiev, USSR), no. 1, Jan. - Feb. 1987 p 65-70 (For primary document see N88-20674 13-42)
Avail: NTIS HC A04/MF A01

Experiments were carried out with physical modeling of the electromagnetic field of local inclusions in the sedimentary cover for ascertaining the possibilities and resolution of the magnetotelluric method when determining structures of such a type. The investigated inclusions were of a cylindrical or complex isometrix configuration corresponding to certain types of deposits. The high resistance inclusions were fabricated of rubber and conducting inclusions were simulated by Duralumin objects. The various experimental parameters and the strength of the induced field were varied. It was revealed that local inhomogeneities of the sedimentary cover can be mapped by the magnetotelluric method. The minimum size of the inclusions is determined using nomograms constructed during physical modeling. The resolution of the MTS method is much higher for conducting inclusions than for high resistance inclusions and is determined by the relation of the horizontal extent and depth of occurrence and is dependent on inclusion thickness. Author

N88-20702# Joint Publications Research Service, Arlington, Va.
INTERACTIVE AUTOMATED SYSTEM FOR TESTING ANALOG UNITS OF DIGITAL SEISMIC STATIONS Abstract Only **c46**

L. I. Orlov *In its* JPRS Report: Science and Technology. USSR: Earth Sciences 26 Feb. 1988 p 47 Transl. into ENGLISH from Pribory i Sistemy Upravleniya (Moscow, USSR), no. 11, Nov. 1986, p 11-12 (For primary document see N88-20674 13-42)
Avail: NTIS HC A04/MF A01

Seismic and electric exploration often uses low frequency multichannel geophysical data measurement systems. Such systems includes tens to hundreds of measurement channels, high and low frequency filters, analog-to-digital converters and devices for recording and processing data. The great number of systems in production and planning require highly reliable and sensitive automated test systems (ATS) for ensuring that the system meet the required rigorous technical specifications. An ATS system for this purpose is modular in design and interactive with the operator. The modular design minimizes costs in adapting the system to testing new systems. In 1985, an ATS was developed for the analog units in seismic exploration equipment. A 16 bit microcomputer with floppy disk storage is the central computer in this system and auxiliary units include SM-4 and DVK-2. The programming is designed for the RAFOS operating system. System hardware used for checking and adjusting digital, analog-to-digital and analog components is given and the programs used with this system are named. Author

N88-20703# Joint Publications Research Service, Arlington, Va.
TRAJECTORY SYNTHESIS OF IONOGRAMS IN PRESENCE OF ARTIFICIAL IONOSPHERIC INHOMOGENEITIES Abstract Only **c46**

N. P. Danilkin, D. S. Lukin, and V. I. Stasevich *In its* JPRS Report: Science and Technology. USSR: Earth Sciences 26 Feb. 1988 p 51 Transl. into ENGLISH from Geomagnetizm i Aeronomiya (Moscow, USSR), v. 27, no. 2, Feb. 1987 p 217-221 Original language document was announced in AIAA as A87-42006 (For primary document see N88-20674 13-42)
Avail: NTIS HC A04/MF A01

The present study examines the digital synthesis of complex ionograms formed in the presence of a large local disturbance of ionospheric electron density during active injection experiments. The dependence of the ionogram on various parameters of the irregularity is investigated, and the main types and characteristic features of the possible ionogram are determined. Also considered is the optimal positioning of an additional receiver for obtaining ionograms with maximum information content. E.R.

N88-20704# Joint Publications Research Service, Arlington, Va.
EFFECT OF NITROGEN DIOXIDE RELEASE ON THERMOSPHERE Abstract Only **c45**

M. N. Vlasov and S. A. Pokhunkov *In its* JPRS Report: Science and Technology. USSR: Earth Sciences 26 Feb. 1988 p 52 Transl. into ENGLISH from Geomagnetizm i Aeronomiya (Moscow, USSR), v. 27, no. 2, Feb. 1987 p 237-241 Original language document was announced in AIAA as A87-42010 (For primary document see N88-20674 13-42)
Avail: NTIS HC A04/MF A01

A theoretical assessment is made of the possible effect of the emission on an NO2 cloud in the region of the main ionospheric maximum, numerical integration is used to study the effect of NO2 on ionospheric electron density with allowance for diffusion and photochemistry. It is shown that the emission of NO2 in quantities the order of hundreds of moles can lead to a considerable decrease (several fold) in several minutes. Also considered are effects connected with an increase in NO concentration in the upper atmosphere accompanying the NO2 emission. E.R.

N88-20705# Joint Publications Research Service, Arlington, Va.
INFLUENCE OF NONLINEAR SPECTROSCOPIC EFFECTS ON ATMOSPHERIC PROPAGATION OF INTENSE LASER RADIATION AT 10.6 MICRONS WAVELENGTH Abstract Only **c46**

A. A. Mitsel, Yu. N. Ponomarev, and K. M. Firsov *In its* JPRS Report: Science and Technology. USSR: Earth Sciences 26 Feb. 1988 p 53 Transl. into ENGLISH from Izvestiya Akademii Nauk SSSR: Fizika Atmosfery i Okeana (Moscow, USSR), v. 23, no. 2, Feb. 1987 p 165-169 Original language document was announced in AIAA as A87-35834 (For primary document see N88-20674 13-42)
Avail: NTIS HC A04/MF A01

Numerical methods are utilized to study the influence of nonlinear spectroscopic effects on the propagation in the Earth's atmosphere of short high power pulses of radiation from a CO2 laser at 10.6 microns. Allowance is made for the dependence of the molecular absorption coefficient of air on the intensity. It is shown that nonlinear effects led to a reduction of the energy losses on the propagation path. The energy gain depends on the divergence radius and on the weather, this gain being greater at the beam axis than at its edge. E.R.

N88-20706# Joint Publications Research Service, Arlington, Va.
SYNCHRONOUS MEASUREMENTS OF EFFECTIVE PHOTON PATH LENGTH IN VISIBLE AND NEAR-IR SPECTRAL REGIONS IN REAL CLOUD SYSTEMS Abstract Only **c46**
Ye. I. Grechko, S. V. Dvoryashin, and V. I. Dianov-Klokov *In its* JPRS Report: Science and Technology. USSR: Earth Sciences 26 Feb. 1988 p 54 Transl. into ENGLISH from Izvestiya Akademii Nauk SSSR: Fizika Atmosfery i Okeana (Moscow, USSR), v. 23, no. 2, Feb. 1987 p 115-120 (For primary document see N88-20674 13-42)
Avail: NTIS HC A04/MF A01

The first results are presented from synchronous measurements of the effective photon path length in two spectral intervals centered at 0.76 and 2.06 micron wavelength. The study was made using reflected and transmitted fluxes measured from an aircraft. The results analyzed and compared with model calculations. In order to estimate the influence of scattering index on photon path length in a cloud with conservative scattering, model calculations were performed on a computer by the Monte Carlo method for two scattering indices. Mean photon path lengths were computed as functions of the scattering coefficient and with a bottom altitude of 1 km. Calculated estimates and the first synchronous measurements made at 0.76 and 2.06 microns show that the effective photon cloud cover coincide within the limits of measurement error. Author

N88-20707# Joint Publications Research Service, Arlington, Va.
INFLUENCE OF HYDROMETEOROLOGICAL FACTORS ON VISIBILITY OF OBJECTS DETECTED BY RADAR Abstract Only **c32**
A. A. Kotyukh *In its* JPRS Report: Science and Technology. USSR: Earth Sciences 26 Feb. 1988 p 56 Transl. into ENGLISH from Vestnik Leningradskogo Universiteta, Seriya 7: Geologiya, Geografiya (Leningrad, USSR), no. 1, Mar. 1987 p 92-97 (For primary document see N88-20674 13-42)
Avail: NTIS HC A04/MF A01

Hydrometeorological factors exert a significant influence on the operation of radars, changing the maximum range of detection of relief elements by ships' radars in the Arctic and reducing the level of detail visible on PPI's. A theoretical discussion is presented on the influence of hydrometeorological factors on the range of detection of objects. Rain, snow and fog decreases radar visibility. Rain is virtually inpenetrable to centimeterband radar signals, wet snow causes significant interference, and fog reduces radar visibility somewhat. A gently sloping snow covered shore seen through falling precipitation may be quite difficult to detect by radar. The influence of precipitation on radar can be decreased by the use of vertical polarization and by techniques for suppressing interference from sidelobes of the radiated radar signal. Author

43 EARTH RESOURCES AND REMOTE SENSING

Includes remote sensing of earth resources by aircraft and spacecraft; photogrammetry; and aerial photography.

For instrumentation see *35 Instrumentation and Photography.*

N88-20708# Instituto de Pesquisas Espaciais, Sao Jose dos Campos (Brazil).
A PROCEDURE FOR AUTOMATIC CLASSIFICATION OF CROP AREAS [UM PROCEDIMENTO PARA CLASSIFICACAO AUTOMATICA DE AREAS AGRICOLAS]
Flavio Roberto DiasVelasco, Leonardo SantAnnaBins, Virginia RagonideMoraesCorrea, Fernando Augusta Mitsuoli, and Maria Helena Costa Feb. 1988 8 p In PORTUGUESE; ENGLISH summary Presented at the 2nd Latin-American Symposium on Remote Sensors, Bogata, Columbia, 16-21 Nov. 1987
(INPE-4467-PRE/1240) Avail: NTIS HC A02/MF A01

A procedure is presented for image classification used in the SIAG project for crop statistics. The classification is performed using LANDSAT/TM images in areas with same land use within the same orbit and in small regions where local information is gathered. The classification of the segments permit errors which occur in the district classification to be corrected. The procedure consists of the following: window extraction, field digitization, training, analysis district determination and classification. The window extraction step is performed using SITIM, a general purpose image processing system based on a IBM-PC compatible microcomputer. The remaining steps are executed on a VAX 780 computer. Author

N88-20709# New Mexico State Univ., Las Cruces. Dept. of Mathematical Sciences.
CONFORMAL GEOMETRY, HOTINE'S CONJECTURE, AND DIFFERENTIAL GEODESY
Joseph D. Zund and Wayne A. Moore 27 Jul. 1987 128 p
(Contract F19628-86-K-0028)
(AD-A189265; AFGL-TR-87-0233; SR-1) Avail: NTIS HC A07/MF A01 CSCL 08E

This report, based on the Ph.D. dissertation of Wayne Moore together with a supplement describing details of the recent resolution of Hotine's Conjecture, is a more comprehensive version of a paper to appear in Bulletin Geodesique. It includes a detailed development of conformal geometry which is more complete than that given in Chapter 10 of Martin Hotine's Mathematical Geodesy (1969), and numerous technical aspects of Hotine's work on his conjecture. It is hoped that this report will be helpful to mathematical geodesists who wish to further explore the contributions of Hotine and Marussi to differential geodesy. GRA

N88-20710# Army Research Inst. for the Behavioral and Social Sciences, Alexandria, Va.
A COMPARISON OF TERRAIN ASSOCIATION AND RESECTION AS METHODS OF POSITION LOCATION Technical Report, Feb. 1986 - May 1986
Gerald I. Dewey and Joseph T. OHanlan, Jr. Aug. 1987 31 p
(AD-A189480; ARI-TR-756) Avail: NTIS HC A03/MF A01 CSCL 08B

This research examined two methods of position fixing, terrain association and resection to determine which would result in faster and more accurate judgments of location. The research was conducted in the Surface Navigation and Orientation Trainer (SURNOT), which projects slide images a full 360 degree field of view. Two groups of soldiers (n = 12 each) were shown terrain scenes, given a 1:50,000 topographic map of the area, and asked to locate their position by terrain association and resection. Overall, performance was poor: There was no significant difference in accuracy of solution between the two groups (723 meters average error), but terrain association was approximately 3 minutes faster. The results were interpreted in terms of a two-stage position fixing model, and suggest that errors in position fixing occur early in the process. GRA

N88-20711*# Massachusetts Inst. of Tech., Cambridge. Research Lab. of Electronics.
REMOTE SENSING OF EARTH TERRAIN Semiannual Report, 1 Sep. 1987 - 29 Feb. 1988
J. A. Kong 28 Apr. 1988 17 p
(Grant NAG5-270)
(NASA-CR-182677; NAS 1.26:182677) Avail: NTIS HC A03/MF A01 CSCL 08B

A systematic approach for the identification of terrain media such as vegetation canopy, forest, and snow covered fields is developed using the optimum polarimetric classifier. The covariance matrices for the various terrain covers are computed from the theoretical models of random medium by evaluating the full polarimetric scattering matrix elements. The optimal classification scheme makes use of a quadratic distance measure and is applied to classify a vegetation canopy consisting of both trees and grass. Experimentally measured data are used to validate the classification scheme. Theoretical probability of classification error using the full polarimetric matrix are compared with classification based on single features including the phase difference between the VV and HH polarization returns. It is shown that the full polarimetric

results are optimal and provide better classification performance than single feature measurements. A systematic approach is presented for obtaining the optimal polarimetric matched filter which produces maximum contrast between two scattering classes, each represented by its respective covariance matrix. Author

N88-20712# Instituto de Pesquisas Espaciais, Sao Jose dos Campos (Brazil).
RESTORATION TECHNIQUES FOR REDISPLAY OF LANDSAT-5 SATELLITE IMAGERY [TECNICAS DE RESTAURACAO PARA REAMOSTRAGEM DE IMAGENS DO SATELITE LANDSAT-5]
Leila Maria Garcia Fonseca, Nelson Delfino dAvil Mascarenhas, and Gerald Jean Francis Banon Jun. 1987 14 p In PORTUGESE Presented at the 5th Brazilian Symposium of Telecommunication Campinas, Brazil, 8-10 Sep. 1987
(INPE-4189-PRE/1076) Avail: NTIS HC A03/MF A01

Some results are shown of restoration for redisplayed images of the Thematic Mapper, utilizing Fourier domain techniques. A restored image is compared to the redisplayed image with cubic convolution interpolation. The comparison is done visually and through radiometric profile of the line imagery. Author

N88-20713*# Ohio State Univ., Columbus. Dept. of Geodetic Science and Surveying.
DETERMINATION OF EARTH ROTATION BY THE COMBINATION OF DATA FROM DIFFERENT SPACE GEODETIC SYSTEMS
Brent Allen Archinal Feb. 1987 104 p
(Grant NsG-5265)
(NASA-CR-181388; NAS 1.26:181388; Rept-375) Avail: NTIS HC A06/MF A01 CSCL 08E

Formerly, Earth Rotation Parameters (ERP), i.e., polar motion and UTI-UTC values, have been determined using data from only one observational system at a time, or by the combination of parameters previously obtained in such determinations. The question arises as to whether a simultaneous solution using data from several sources would provide an improved determination of such parameters. To pursue this reasoning, fifteen days of observations have been simulated using realistic networks of Lunar Laser Ranging (LLR), Satellite Laser Ranging (SLR) to Lageos, and Very Long Baseline Interferometry (VLBI) stations. A comparison has been done of the accuracy and precision of the ERP obtained from: (1) the individual system solutions, (2) the weighted means of those values, (3) all of the data by means of the combination of the normal equations obtained in 1, and (4) a grand solution with all the data. These simulations show that solutions done by the normal equation combination and grand solution methods provide the best or nearly the best ERP for all the periods considered, but that weighted mean solutions provide nearly the same accuracy and precision. VLBI solutions also provide similar accuracies. Author

N88-20714*# National Aeronautics and Space Administration. Goddard Space Flight Center, Greenbelt, Md.
THE 1987 AIRBORNE ANTARCTIC OZONE EXPERIMENT: THE NIMBUS-7 TOMS DATA ATLAS
Arlin J. Krueger, Philip E. Ardanuy, Frank S. Sechrist, Lanning M. Penn, David E. Larko, Scott D. Doiron, and Reginald N. Galimore (Science Applications Research, Lanham, Md.) Mar. 1988 246 p
(NASA-RP-1201; Rept-88B0107; NAS 1.61:1201) Avail: NTIS HC A11/MF A01 CSCL 04B

Total ozone data taken by the Nimbus-7 Total Ozone Mapping Spectrometer (TOMS) played a central role in the successful outcome of the 1987 Airborne Antarctic Ozone Experiment. The near-real-time TOMS total ozone observations were suppled within hours of real time to the operations center in Punta Arenas, Chile, over a telecommunications network designed specifically for this purpose. The TOMS data preparation and method of transfer over the telecommunications links are reviewed. This atlas includes a complete set of the near-real-time TOMS orbital overpass data over regions around the Palmer Peninsula of Antarctica for the period of August 8 through September 29, 1987. Also provided are daily polar orthographic projections of TOMS total ozone measurements over the Southern Hemisphere from August through November 1987. In addition, a chronology of the salient points of the experiment, along with some latitudinal cross sections and time series at locations of interest of the TOMS total ozone observations are presented. The TOMS total ozone measurements are evaluated along the flight tracks of each of the ER-2 and DC-8 missions during the experiment. The ozone hole is shown here to develop in a monotonic progression throughout late August and September. The minimum total ozone amount was found on 5 October, when its all-time lowest value of 109 DU is recorded. The hole remains well defined, but fills gradually from mid-October through mid-November. The hole's dissolution is observed here to begin in mid-November, when it elongates and begins to rotate. By the end of November, the south pole is no longer located within the ozone hole. Author

N88-20715# Instituto de Pesquisas Espaciais, Sao Jose dos Campos (Brazil).
ANALYSIS FOR ARCHITECTURE FOR IMAGE PROCESSING [ANALISE DE ARQUITETURAS PARA PROCESSAMENTO DE IMAGENS]
Celso Luiz Mendes, Gilberto GamaraNeto, Jose Claudio Mura, Juan Carlos PintodeGarrido, and Ricardo CartaxoModestodeSouza Aug. 1987 18 p In PORTUGESE Presented at the 1st Brazilian Symposium Computer Architecture-Parallel Processing, Gramado, RS, 13-15 May 1987
(INPE-4294-PRE/1165) Avail: NTIS HC A03/MF A01

After a brief introduction on image processing activities at INPE, the principal characteristics of the system family SITIM are presented, followed by a presentation of procedure types most utilized in image processing. Discussed are some options already tested for augmentation on the system execution, through the use of accelerator plates and, lastly, the perspectives for future development are presented, some in the areas of accelerator plates, as systems based on parallel architecture, associated unity of advanced images. Author

N88-20716*# National Aeronautics and Space Administration, Washington, D.C.
THE USE OF FOUR-PHOTON RAMAN SPECTROSCOPY FOR THE REMOTE SENSING OF NATURAL OBJECTS
A. F. Bunkin, A. S. Galumyan, Kh. A. Zhumanov, and D. V. Maltsev May 1988 16 p Transl. into ENGLISH from Izvestiya Akademii Nauk SSSR, Seriya Fizicheskaya (USSR), v. 51, no. 8, 1987 p 1256-1262 Original language document was announced in IAA as A88-12154 Transl. by Scientific Translation Service, Santa Barbara, Calif.
(Contract NASw-4307)
(NASA-TT-20257; NAS 1.77:20257) Avail: NTIS HC A03/MF A01 CSCL 08B

The results of the laboratory simulation of optical Kerr effect/Raman spectroscopy for the purpose of remote sensing are presented. The experimental setup is described, and measurements of the vibrational spectra of various liquids obtained. Attention is paid to the possibility of using the proposed method to detect trace hydrocarbons in water, and the spectrum of petroleum is obtained. Full-scale measurements using a laser spectrometer were made on the Black Sea. Author

N88-20498# Joint Publications Research Service, Arlington, Va.
ANALYSIS OF SPECTRAL REFLECTANCE CHARACTERISTICS OF TARGETS UNDER SATELLITES AND AUTOMATIC CLOUD RECOGNITION Abstract Only
Li Wang *In its* JPRS Report: Science and Technology. China 12 Feb. 1988 p 28 Transl. into ENGLISH from Kongjian Kexue Xuebao (Beijing, People's Republic of China), v. 7, no. 4, Oct. 1987 p 321-326 (For primary document see N88-20495 13-31)
Avail: NTIS HC A07/MF A01

44 ENERGY PRODUCTION AND CONVERSION

Includes specific energy conversion systems, e.g., fuel cells; global sources of energy; geophysical conversion; and windpower.

For related information see also *07 Aircraft Propulsion and Power, 20 Spacecraft Propulsion and Power,* and *28 Propellants and Fuels.*

N88-20717# Army Lab. Command, Watertown, Mass. Material Technology Lab.
A CASE STUDY OF THE DEVELOPMENT OF A MILITARY SPECIFICATION - ZIRCONIUM POWDER FOR THERMAL BATTERIES Final Report
Mary T. Burgess Oct. 1987 19 p
(AD-A188751; MTL-TR-87-55) Avail: NTIS HC A03/MF A01 CSCL 11F

Thermal batteries are used as the critical power source in nuclear fuses, missiles, and aircraft. Heat sources in thermal batteries use a fine zirconium powder. This report focuses on the zirconium problem and the development of a military specification for zirconium powder as produced by the magnesium reduction method. GRA

N88-20718# Chicago Univ., Ill.
PERFORMANCE AND COST BENEFITS ASSOCIATED WITH NONIMAGING SECONDARY CONCENTRATORS USED IN POINT-FOCUS DISH SOLAR THERMAL APPLICATIONS
J. OGallagher and R. Winston Sep. 1987 72 p Prepared in cooperation with Midwest Research Inst., Golden, Colo.
(Contract DE-AC02-83CH-10093)
(DE88-001104; SERI/STR-253-3113) Avail: NTIS HC A04/MF A01

Using nonimaging secondary concentrators in point-focus applications may permit the development of more cost-effective concentrator systems by either improving performance or reducing costs. Secondaries may also increase design flexibility. The major objective of this study was to develop as complete an understanding as possible of the quantitative performance and cost effects associated with deploying nonimaging secondary concentrators at the focal zone of point-focus solar thermal concentrators. A performance model was developed that uses a Monte Carlo ray-trace procedure to determine the focal plane distribution of a paraboloidal primary as a function of optical parameters. It then calculates the corresponding optimized concentration and thermal efficiency as a function of temperature with and without the secondary. To examine the potential cost benefits associated with secondaries, a preliminary model for the rational optimization of performance versus cost trade-offs was developed. This model suggests a possible 10 to 20 percent reduction in the cost of delivered energy when secondaries are used. This is a lower limit, and the benefits may even be greater if using a secondary permits the development of inexpensive primary technologies for which the performance would not otherwise be viable. DOE

N88-20719# Sandia National Labs., Albuquerque, N. Mex.
STATUS OF THE MAGMA ENERGY PROJECT
J. C. Dunn 1987 7 p Presented at the Symposium on Geothermal Energy, New Orleans, La., 10 Jan. 1988
(Contract DE-AC04-76DP-00789)
(DE88-002413; SAND-87-2560C; CONF-880103-3) Avail: NTIS HC A02

The current magma energy project is assessing the engineering feasibility of extracting thermal energy directly from crustal magma bodies. The estimated size of the U.S. resource (50,000 to 500,000 quads) suggests a considerable potential impact on future power generation. In a previous seven-year study, we concluded that there are no insurmountable barriers that would invalidate the magma energy concept. Several concepts for drilling, energy extraction, and materials survivability were successfully demonstrated in Kilauea Iki lava lake, Hawaii. The present program is addressing the engineering design problems associated with accessing magma bodies and extracting thermal energy for power generation. The normal stages for development of a geothermal resource are being investigated: exploration, drilling and completions, production, and surface power plant design. Current status of the engineering program and future plans are described. DOE

N88-20720# Solar Kinetics, Inc., Dallas, Tex.
POINT-FOCUS CONCENTRATOR REFLECTOR ASSEMBLY, PHASE 1
Nov. 1987 153 p
(Contract DE-AC04-76DP-00789)
(DE88-003616; SAND-87-7014) Avail: NTIS HC A08/MF A01

A point-focus concentrator reflective assembly was developed in Phase 1 on contract 21-3695 under the direction of Sandia National Laboratories, Albuquerque. This concentrator is conventional in presentation, yet innovative in detail. The development concentrated on structural efficiency and production design to achieve a high performance at minimum cost. The concentrator design achieves stiffness and strength through the integration of two structural elements. The optical element provides the reflective surface accuracy; a secondary support structure provides resistance to uniform and non-uniform load conditions. A retractable receiver strut, which moves the power conversion assembly out of focus in emergency power loss, was also incorporated. This same assembly provides maintenance access to the engine near ground level. A full-scale optical element was fabricated. Slope error was measured at 1 mrad. Concentrator performance was projected to be 88 percent, optical. This point-focus concentrator reflector assembly design provides low weight, low cost, and simplicity. Our analysis indicates these benefits are gained without impairing performance. DOE

N88-20721# Chevron Research Co., Richmond, Calif.
RESEARCH ON MULTIBANDGAP SOLAR CELLS Final Subcontract Report, 1 Mar. 1984 - 31 Jan. 1987
J. A. Cape, L. M. Fraas, P. S. McLeod, and L. D. Partain Jul. 1987 91 p Prepared in cooperation with Midwest Research Inst., Golden, Colo.
(Contract DE-AC02-83CH-10093)
(DE87-012261; SERI/STR-211-3189) Avail: NTIS HC A05/MF A01

This report describes research in multibandgap solar cells. In early work, two-color solar cells with efficiencies exceeding 20 percent were grown monolithically, comprising a GaAsP top junction over a GaAs or GaAsSb bottom junction. Researchers attempted to understand the effects of lattice mismatch and optimize growth conditions for these structures. Severe unreproducibility was encountered and traced to source material impurities. CP2Mg, the p-dopant, was found to be undependable, and efforts were made to purify it. Impurity effects were also traced to the arsine (predominantly water vapor) and the gallium alkyls. Efforts were also made to purify these. Work focused on optimizing component cells of GaAsP and GaAsSb and on developing the growth process. This, though, did not lead to higher efficiencies. In developing component cells, work was also done on optimizing vacuum chemical epitaxy growth conditions (temperatures, flow rates, III-V ratios, chamber designs, etc.); on developing cell transition layers and reducing lattice-mismatch effects; on improving cell processing; on reducing impurities; and on improving material and cell characterization. DOE

N88-20722# Meridian Corp., Falls Church, Va.
FEDERAL OCEAN ENERGY TECHNOLOGY Program Summary Report, fiscal year 1986
Oct. 1987 59 p Prepared in cooperation with Science Applications International Corp., McLean, Va.
(Contracts DE-AC02-83CH10093; DE-AC01-86CE-30844)
(DE87-012279; DOE/CH-10093/14) Avail: NTIS HC A04/MF A01

The Department of Energy's (DOE) Ocean Energy Technology (OET) Program is looking for cost-effective ways to harness ocean

energy to help power tomorrow's world. Federally sponsored researchers are studying methods to transform the solar heat stored in the ocean's surface waters into electricity as well as new ways to convert wave energy into mechanical energy or electricity. This report provides a summary of research completed during FY86. Four major research areas are addressed in the work covered by this report: Thermodynamic Research and Analysis addresses the process and system analyses which provide the underlying understanding of physical effects which constitute the energy conversion processes, Experimental Verification and Testing provides confirmation of the analytical projections and empirical relationships, Materials and Structural Research addresses special materials compatibility issues related to operation in the sea. Much of its focus is on concepts for the system CWP which is a major technology cost driver, and Oceanographic, Environmental, and Geotechnical Research addresss those unique design requirements imposed by construction in steep slope coastal areas. DOE

N88-20723# Spire Corp., Bedford, Mass.
RESEARCH ON HIGH-EFFICIENCY, STACKED, MULTIJUNCTION, AMORPHOUS SILICON ALLOY THIN-FILM SOLAR CELLS Final Subcontract Report, 11 Oct. 1983 - 30 Oct. 1986
J. Bragagnolo Oct. 1987 125 p
(Contract DE-AC02-83CH-10093)
(DE88-001108; SERI/STR-211-3231) Avail: NTIS HC A06/MF A01

This report covers the third year of a three-year project to develop high-efficiency, stable, multijunction amorphous silicon alloy solar cells. It describes new deposition techniques to obtain pinhole-free, a-Si:H alloy films by avoiding dust formation in the plasma; the deposition of low-absorptance, textured SnO2 layers by thermal CVD of Sn(CH3)4; a more stable, high-reflectance Ti/Ag back contact; the application of the new deposition techniques to achieve efficiencies of 10.5, 10.1, and 9.4 percent for a-Si:H p-i-n devices; the development of a-(Si,Ge):H cells with efficiencies from 5.4 percent for a-(Si,Ge):H cells to 7.5 percent for graded-bandgap cells; and the development of a-Si/a-(Si,Ge) tandem cells with 6.5 and 7.2 percent efficiencies are presented. DOE

N88-20724# Ford Aerospace and Communications Corp., Newport Beach, Calif.
CdZnTe AS A WIDE-BAND-GAP ABSORBER FOR A TANDEM, THIN-FILM SOLAR CELL Final Subcontract Report, 1 Apri 1986 - 31 Aug. 1987
K. R. Zanio Oct. 1987 16 p
(Contract DE-AC02-83CH-10093)
(DE88-001114; SERI/STR-211-3217) Avail: NTIS HC A03/MF A01

The objective of this program was to prepare by low-cost ultra-high-vacuum (UHV) methods on all-thin-film (approximately 1.6 eV) wide-bandgap solar cell using CdZnTe as the absorber layer. ZnTe/CdZnTe/n-CdS/ITO/glass structures were prepared by congruent evaporation in UHV. Ohmic contact to the ZnTe with HgZnTe and conversion of the high-resistivity ZnTe and CdZnTe was simultaneously undertaken by the closed-space vapor deposition of HgZnTe. Mesa structures did not show blocking action. Single-crystal cells were prepared by the deposition of CdS on bulk p-CdTe and thin-film, single-crystal p-CdTe-on-sapphire and p-CdZnTe-on-sapphire. A comparison of results suggests that the all-thin-film polycrystalline structure is limited by the CdZnTe. DOE

N88-20725# Rensselaer Polytechnic Inst., Troy, N.Y.
RESEARCH ON SINGLE-CRYSTAL CdTe SOLAR CELLS Final Subcontract Report, 1 Feb. 1985 - 1 Feb. 1987
J. M. Borrego and S. K. Ghandhi Oct. 1987 100 p
(Contract DE-AC02-83CH-10093)
(DE88-001115; SERI/STR-211-3224) Avail: NTIS HC A05/MF A01

This report outlines two years of work on the growth and characterization of single-crystal CdTe layers, to explore their potential for high-efficiency solar cells. It was demonstrated that high-quality layers can be grown by organometallic vapor phase epitaxy (OMVPE), whose photoluminescence peak has a FWHM of 5.8 MeV, the lowest value for them yet achieved. CdTe layers were extrinsically doped both n- and p-type with indium and arsenic, respectively. The doping level achieved for p-type is the highest yet reported in the literature, achieved for the first time in an OMVPE system. A hole lifetime of 2.0 microns was measured. In the n-type material, five deep levels were isolated; their capture cross section, energy level, and concentration were determined. A thermodynamic analysis was made to identify their defect character. Both Schottky and p-n junction devices were produced on these layers. The diode characteristics were superior to those of GaAs so this is a potentially superior material for solar cells. DOE

N88-20726# Delaware Univ., Newark. Inst. of Energy Conversion.
STABLE, HIGH-EFFICIENCY, CuInSe2-BASED, POLYCRYSTALLINE, THIN-FILM TANDEM SOLAR CELLS Final Subcontract Report, 16 Mar. 1984 - 15 Mar. 1987
R. W. Birkmire and J. E. Phillips Oct. 1987 124 p
(Contract DE-AC02-83CH-10093)
(DE88-001116; SERI/STR-211-3249) Avail: NTIS HC A06/MF A01

The long-term objective of this research was to obtain a stable, thin-film solar cell based on polycrystalline materials with an efficiency of 15 percent. The approach was to make a tandem cell based on CuInSe2/CdS as the bottom cell and CdTe/CdS as the top cell. An essential feature was to develop a CdTe cell with transport contacts. A suitable contacting system was developed using transparent conducting oxides (ITO and SnO2) in conjunction with a thin layer of copper. Cells were made with efficiencies over 8.5 percent. A reproducible fabrication process for CuInSe2/(CdZn)S cells was developed based on CuInSe2 films grown by vacuum evaporation using Knudsen-type effusion sources. These cells were made with efficiencies over 10 percent. The composition of the CuInSe2 films can be varied over a considerable range and still yield high-efficiency cells. Adding Zn to the CdS did not increase the V(sub oc) of the devices; analysis showed that the V(sub oc) is not controlled by interface recombination. The effect of oxidizing and reducing heat treatments on CuInSe2 cells is to change carrier concentration and thus V(sub oc). Analysis suggests that J(sub o) is controlled by band-to-band recombination. Monolithic tandem CuInSe2 CdTe cells have been made with efficiencies of approximately 3 percent, demonstrating the feasibility of this approach. DOE

N88-20727# Boeing Co., Seattle, Wash. High Technology Center.
CADMIUM SULFIDE/COPPER TERNARY HETEROJUNCTION CELL RESEARCH Final Subcontract Report, 1 Oct. 1984 - 31 May 1987
W. E. Devaney, R. A. Mickelsen, W. S. Chen, B. J. Stanbery, J. M. Stewart, F. W. Lytle, and A. F. Burnett Nov. 1987 130 p
(Contract DE-AC02-83CH-10093)
(DE88-001122; SERI/STR-211-3230) Avail: NTIS HC A07/MF A01

This is the final technical progress report on a thirty-two month research program on CuInSe2 and CuInGaSe2 based thin-film polycrystalline heterojunction solar cells. CuInGaSe2 films incorporating Ga fractions (x in CuIn(1-x)Ga(x)Se2) from 0.04 to 1.0 have been prepared and characterized. CuInGaSe2/CdZnS heterojunction devices have been fabricated for a range of Ga contents and show the expected variations in Voc and spectral response with Ga content. An efficiency of 10.2 percent (SERI test, ASTM87) has been measured for a cell with Ga fraction of 0.23, the highest efficiency reported for this material. A CuInSe2/CdZnS monolithically interconnected four cell series string of 91 sq cm area has been fabricated with a total area efficiency of 9.5 percent (SERI test, ASTM87). Results are presented on Ion-Assisted Deposition of the selenide and sulfide, on a new design for the Se evaporation source, on ITO reactive sputter deposition, and on CdZnS films prepared from an E-Gun

Evaporation source. Spectral response and I-V characteristic variations with selenide composition before and after heat-treatment are discussed for the CuInSe2/CdZnS devices. The highest AM1 total area efficiency for the CuInSe2/CdZnS cell is now 11.9 percent (Boeing test, AM1 spectrum) with five cells measured over the previously reported high of 10.9 percent. Room Temperature Photoluminescence, Voltage Contrast Imaging of junction cross sections, Raman spectroscopy, and EXAFS measurements on the CuInSe2/CdZnS devices are also presented and discussed. DOE

N88-20728# Midwest Research Inst., Golden, Colo. Solar Energy Research Inst.
SERI'S PHOTOVOLTAIC R AND D PROJECT: RECENT PROGRESS AND FUTURE DIRECTIONS
T. Surek Nov. 1987 14 p Presented at the Special Meeting of the Kansai Section of the Japan Solar Energy Society and the Japan Applied Physics Society, Osaka, Japan, 10 Nov. 1987
(Contract DE-AC02-83CH-10093)
(DE88-001129; SERI/TP-211-3272; CONF-8711127-1) Avail: NTIS HC A03/MF A01

Photovoltaic (PV) research efforts at the Solar Energy Research Institute (SERI) focus on developing improved generations of photovoltaic technologies having the potential for low cost, high performance, and long-term reliability. The new PV technology generations are thin-film single-junction and multijunction devices suitable for either flat-plate or concentrator systems, and advanced crystalling silicon sheet materials. Improvements in materials and processing, solar cell design, and cell fabrication techniques have led to remarkable progress for these new generations of photovoltaic devices leading to record cell efficiencies in nearly all material areas. Current research identified the criticality of source material purity and the device processing conditions for a number of different PV materials. Furthermore, attention to total device design and processing helped to realize greater understanding of metallic contacts, transparent conductors, and interlayers. The development of sophisticated models enabled quick assessment of device concepts. Another characteristic of current research directions is increased collaboration among PV experts. Enhanced measurement and characterization techniques, along with interaction among PV scientists, are adding to a strong scientific foundation for the photovoltaic future. DOE

N88-20729# Sandia National Labs., Albuquerque, N. Mex.
DESIGN OF THE SANDIA-ISRAEL 20-kW REFLUX HEAT-PIPE SOLAR RECEIVER/REACTOR
R. B. Diver and W. C. Ginn Sep. 1987 81 p
(Contract DE-AC04-76DP-00789)
(DE88-001312; SAND-87-1533) Avail: NTIS HC A05/MF A01

This report describes the design and fabrication of a 20-kW sodium reflux heat-pipe solar receiver/reactor for CO2 reforming of methane. This project is part of a bilateral agreement between the United States and Israel. Under the terms of the agreement the solar receiver/reactor has been designed and built by Sandia National Laboratories for testing in the 7-meter solar furnace facility at the Weizmann Institute of Science in Rehovot, Israel. DOE

N88-20730# Hawaii Univ., Honolulu. Renewable Resources Research Lab.
PHOTOLYTIC FORMATION OF FREE RADICALS AND THEIR EFFECT ON HYDROCARBON PYROLYSIS CHEMISTRY IN A CONCENTRATED SOLAR ENVIRONMENT Final Report
M. Hunjan, W. S. Mok, and M. J. Antal, Jr. 1987 133 p
(Contract DE-AC03-84SF-12221)
(DE88-004129; DOE/SF-12221/T8) Avail: NTIS HC A07/MF A01

The objective of this research was two-fold: (1) to determine whether UV photons available in a concentrated solar environment can be used as a photolytic source to dissociate vapor phase acetone; and (2) to explore the effects of photolysis on rate and selectivity of free radical reactions. The experiments were conducted in a 1 kW arc image furnace/tubular flow reactor system. The results obtained conclusively showed that acetone readily photodissociates in a 1000 sun environment, leading to the formation of free radicals. It was further observed that Beer-Lambert law can be used to predict the rate of photolysis of acetone. Furthermore, acetone, when used as source of methyl radicals, sensitized the reaction chemistry of alkanes and alkenes at a temperature of 350 C. The methyl radicals from photolysis of acetone enhanced the cracking reactions of the alkanes yielding smaller alkanes and alkenes. When the initial hydrocarbon reactant was an alkene, a sensitization of the addition reaction was observed leading to formation of next higher alkene. To gain a theoretical insight into the reaction chemistry of alkanes, a numerical simulation model was developed to study the photosensitized decomposition of n-butane and the simulation results thus obtained were found to be in close agreement with experimental results. DOE

N88-20731# Sandia National Labs., Albuquerque, N. Mex.
CONTROL STRATEGIES AND HARDWARE USED IN SOLAR THERMAL APPLICATIONS
D. R. Adkins Nov. 1987 136 p
(Contract DE-AC04-76DP-00789)
(DE88-004631; SAND-86-1943) Avail: NTIS HC A07/MF A01

The control technology used in solar power production has gone through several changes over the past decade. To highlight some current aspects of solar collector control technologies, this report examines procedures and hardware for tracking the Sun and regulating receiver temperatures. Requirements placed on controls for system protection and reliability are also reviewed. Control experiences in point- and line-focus concentrators, central receiver systems, and photovoltaic arrays are included. DOE

N88-20732# Pacific Northwest Labs., Richland, Wash.
AN ASSESSMENT METHODOLOGY FOR THERMAL ENERGY STORAGE EVALUATION
D. R. Brown, J. A. Dirks, M. K. Drost, G. E. Spanner, and T. A. Williams Nov. 1987 107 p
(Contract DE-AC06-76RL-01830)
(DE88-004642; PNL-6372) Avail: NTIS HC A06/MF A01

This report documents an assessment methodology for evaluating the cost, performance, and overall economic feasibility of thermal energy storage (TES) concepts. The methodology was developed by Thermal Energy Storage Evaluation Program personnel at Pacific Northwest Laboratory (PNL) for use by PNL and other TES concept evaluators. The methodology is generically applicable to all TES concepts; however, specific analyses may require additional or more detailed definition of the ground rules, assumptions, and analytical approach. The overall objective of the assessment methodology is to assist in preparing equitable and proper evaluations of TES concepts that will allow developers and end-users to make valid decisions about research and development (R and D) and implementation. The methodology meets this objective by establishing standard approaches, ground rules, assumptions, and definitions that are analytically correct and can be consistently applied by concept evaluators. DOE

N88-20733# Midwest Research Inst., Golden, Colo. Solar Energy Research Inst.
PROGRESS OF AMORPHOUS SILICON BASED SOLAR CELLS AND MODULES
J. L. Stone 1987 18 p Presented at the 3rd International Photovoltaic Science and Engineering Conference, Tokyo, Japan, 3 Nov. 1987
(Contract DE-AC02-83CH-10093)
(DE88-004666; CONF-871112-3) Avail: NTIS HC A03

It is clear that amorphous silicon photovoltaic technology has entered a new era, having emerged from the research labs to commercialization of energy producing applications. Although effort still must be placed on improving the device performance, more emphasis is now being devoted to questions of cost and reliability. More system and subsystem experiments are being deployed to gain field experience with this relatively new technology. This is particularly true with the U.S. utility companies who are examining PV for consideration as a future generating option. What was only a few years ago a promise, is now becoming a reality. This paper

reviews significant accomplishments in research and technology in the United States' research and production community. DOE

N88-20734# Sandia National Labs., Albuquerque, N. Mex.
CRYSTALLINE PHOTOVOLTAIC CELL TECHNOLOGY: PRESENT AND FUTURE
D. E. Arvizu 1988 9 p Presented at the 15th Annual Energy Technology Conference and Exposition, Washington, D.C., 17 Feb. 1988
(Contract DE-AC04-76DP-00789)
(DE88-004684; SAND-87-3086C; CONF-880212-2) Avail: NTIS HC A02/MF A01

This paper summarizes the status of crystalline cell research in the program managed by Sandia National Laboratories and sponsored by the U.S. Department of Energy (DOE). Recent advances in high efficiency and program direction are discussed for each of the three program elements which include one-sun crystalline silicon, concentrator silicon, and concentrator 3-5 material cells. DOE

N88-20735# Rasor Associates, Inc., Sunnyvale, Calif.
THERMIONIC TECHNOLOGY PROGRAM. A: INSULATOR TEST AND EVALUATION Final Report
J. C. Dobson and T. Witt 30 Nov. 1987 91 p
(Contract DE-AC03-86SF-15954)
(DE88-004707; DOE/SF-15954/T2; NSR-25-15) Avail: NTIS HC A05/MF A01

The Thermionic Technology Program (TTP) consisted of two major efforts, evaluation of insulators and evaluation of thermionic converters. This report details the work performed on the insulator phase of the program. Efforts were made to better understand the mechanisms involved in the electrochemistry of insulators at elevated temperatures by modelling the ionic transport through the various layers of the insulator package. Although rigorous analytic solutions could not be obtained owing to a lack of detailed data, a simplified model indicated that alumina should not fail by depletion of aluminum for thousands of years, whereas calculations for yttria revealed a far more rapid depletion of oxygen and consequently earlier failure. Methods for microscopic and electrical testing of cylindrical insulator samples were developed, and an improved test oven design was initiated. Testing of alumina/niobium cermet samples revealed rapid failure contrary to the theoretical predictions for alumina. Large discrepancies in the initial conduction activation energy among the various samples suggested that different mechanisms could have controlled the conduction and hence the failure in different samples, although all had undergone nominally identical processing. The short lifetimes reveal how rapidly ambient conditions in thermionic power conversion can degrade the performance of insulating oxides. It was concluded that minor dopants could have been responsible for the early breakdowns. Thus, high purity materials with precise quality control will be necessary for trilayer package development. DOE

N88-20736# Midwest Research Inst., Golden, Colo. Solar Energy Research Inst.
POWER FROM THE SUN: PRINCIPLES OF HIGH TEMPERATURE SOLAR THERMAL TECHNOLOGY
W. B. Stine May 1987 55 p
(Contract DE-AC02-83CH-10093)
(DE87-001104; SERI/SP-273-3054) Avail: NTIS HC A04/MF A01

This report describes the development of solar thermal technoloGy by looking at the fundamental principles of solar thermal components and systems, discussing the technical issues that enhance or limit their behavior, and describing their evolution to its current state. It is written for those who want to understand the solar thermal conversion process. The reader should realize that many concepts here are highly simplified so that only the major points are emphasized. Detailed engineering, mathematics, and physics underlies this simplicity. DOE

N88-20737# Sandia National Labs., Albuquerque, N. Mex.
DIRECT ABSORPTION RECEIVER CONTROL STUDIES
C. E. Tyner and G. J. Kolb Sep. 1987 18 p Presented at the ASME Solar Energy Conference, Denver, Colo., 1 Mar. 1988
(Contract DE-AC04-76DP-00789)
(DE87-013653; SAND-87-1424C; CONF-880320-1) Avail: NTIS HC A03/MF A01

In a solar central receiver system Direct Absorption Receiver (DAR), the heat absorbing fluid (a blackened molten nitrate salt) flows in a thin film down a vertical panel (rather than through tubes as in conventional receiver designs) and absorbs the concentrated solar flux directly. This unique flow system presents different control requirements from other receiver systems. These requirements are discussed, including analyses of multiple control zones for various receiver geometries and steady-state flux patterns. The results show that as few as 9 to 13 control zones can provide adequate operation of the receiver under nearly all conditions. Also discussed is the simple outlet-temperature feedback-control algorithm developed to control the DAR during cloud transients and present system thermal/hydraulic responses to various transient conditions. DOE

N88-20738# Edgerton, Germeshausen and Grier, Inc., Idaho Falls, Idaho.
OVERVIEW OF RECENT ACTIVITIES IN THE HEAT CYCLE RESEARCH PROGRAM
C. J. Bliem and G. L. Mines 1987 7 p Presented at the 5th Geothermal Program Review, Washington, D.C., 14 Apr. 1987
(Contract DE-AC07-76ID-01570)
(DE88-005544; EGG-M-10887; CONF-8704110-15) Avail: NTIS HC A02

The Heat Cycle Research Program being conducted for DOE has as its objective the development of technology to improve the utilization of moderate temperature geothermal resources. The program hopes to improve the performance of geothermal binary cycles to levels approaching the practicable thermodynamic maximum. Tests are being conducted at the Heat Cycle Research Facility located at the DOE Geothermal Test Facility, East Mesa, California. The current testing involves the investigation of binary power cycle performance utilizing mixtures of non-adjacent hydrocarbons as the working fluids, with supercritical vaporization and in-tube condensation of the working fluid. In addition to the present test program, preparations are being made to investigate the binary cycle performance improvements which can be achieved by allowing supersaturated vapor expansions in the turbine. These efforts are anticipated to verify that through the utilization of these advanced power cycle comcepts and allowing the supersaturated turbine expansions, improvements of up to 28 percent in the net geofluid effectiveness (net watt hours plant output per pound of geofluid) over conventional binary power plants can be achieved. Results presented for the recent testing, including those tests examining the performance of the countercurrent condenser at different tube inclinations, support the assumptions used in projected performance improvements. DOE

N88-20739# Sandia National Labs., Albuquerque, N. Mex.
OXIDATION/SULFIDATION OF MATERIALS IN AN SO3/SO2/O2 THERMOCHEMICAL-TRANSPORT, DISTRIBUTED-RECEIVER, SOLAR-ENERGY SYSTEM Final Report
L. J. Weirick Dec. 1987 24 p
(Contract DE-AC04-76DP-00789)
(DE88-005875; SAND-87-1753) Avail: NTIS HC A03/MF A01

Metals for potential use in the dissociator and the synthesizer reactors of a distributed solar-receiver, thermochemical-transport loop using SO3/SO2/O2 molecular chemistry were tested in SO3 gas at 500 C and 900 C, respectively, for periods up to 8 weeks and in a cyclic-temperature mode from 200 C to 900 C, representing the diurnal solar cycle, for 35 days. They included iron-base, nickel-base, and cobalt-base superalloys. Weight-gain measurements were used to determine the oxidation/sulfidation kinetics. Electron-microprobe analysis identified any possible penetration of oxygen and sulfur into the metal and the formation of internal oxides and sulfides. Selected iron-base, nickel-base, and cobalt-base alloys look promising as candidates for the synthesizer reactor which operates at approx 500 C. The most

promising candidate for the dissociator reactor operating above 900 C is Kanthal A-1, which contains sufficient quantities of both aluminum and chromium alloying additions to be an alumina and chromia former. DOE

N88-20740# Commission of the European Communities, Ispra (Italy). Joint Research Centre.
A FIVE YEAR WEATHERING EXPERIMENT WITH SOLAR COLLECTORS
R. Bauch, ed., M. Brovelli, ed., and P. Weisgerber, ed. 1987 16 p
(DE88-900369; EUR-10906) Avail: NTIS (US Sales Only) HC A03/MF A01

Two solar collectors were exposed for five years in a weathering experiment, keeping the maximum temperature under solar irradiation limited by simple thermoregulated heat exchange circuits in order to simulate real user conditions. The installation used was a prototype for operational tests, and preceeded another experiment of the same type, which is still running in two zones of different environment regarding corrosivity of the atmosphere, for the study of atmospheric corrosion and degradation. Observations made during operation and the results are given of the examinations of the collectors after five year's exposure. DOE

45 ENVIRONMENT POLLUTION

Includes atmospheric, noise, thermal, and water pollution.

N88-20741*# Jet Propulsion Lab., California Inst. of Tech., Pasadena.
ENVIRONMENTAL PROJECTS. VOLUME 5, PART 1: STUDY OF SUBSURFACE CONTAMINATION. PART 2: GUIDE TO IMPLEMENT ENVIRONMENTAL COMPLIANCE PROGRAMS
I. Bengelsdorf 15 Apr. 1988 224 p
(Contract NAS7-918)
(NASA-CR-182691; JPL-Pub-87-4-Vol-5-Pt-1-Pt-2; NAS 1.26:182691) Avail: NTIS HC A10/MF A01 CSCL 13B

In support of the national goal for the preservation of the environment and the protection of human health and safety, NASA, the Jet Propulsion Laboratory, and the Goldstone Deep Space Communications Complex have adopted the position that their operating installations shall maintain a high level of compliance in regard to regulations concerning environmental hazards. An investigation carried out by Engineering Science, Inc. focused on possible underground contamination that may have resulted from leaks and/or spills from storage facilities at the Goldstone Communications Complex. It also involved the cleanup of a non-hazardous waste dumpsite at the Mojave Base Site at the Goldstone complex. The report also includes details of the management duties and responsibilities needed to maintain compliance with environmental laws and regulations. Author

N88-20704# Joint Publications Research Service, Arlington, Va.
EFFECT OF NITROGEN DIOXIDE RELEASE ON THERMOSPHERE Abstract Only
M. N. Vlasov and S. A. Pokhunkov *In its* JPRS Report: Science and Technology. USSR: Earth Sciences 26 Feb. 1988 p 52 Transl. into ENGLISH from Geomagnetizm i Aeronomiya (Moscow, USSR), v. 27, no. 2, Feb. 1987 p 237-241 Original language document was announced in AIAA as A87-42010 (For primary document see N88-20674 13-42)
Avail: NTIS HC A04/MF A01

46 GEOPHYSICS

Includes aeronomy; upper and lower atmosphere studies; ionospheric and magnetospheric physics; and geomagnetism.

For space radiation see *93 Space Radiation.*

N88-20742*# Cornell Univ., Ithaca, N.Y. Dept. of Geological Sciences.
CORRELATION OF DATA ON STRAIN ACCUMULATION ADJACENT TO THE SAN ANDREAS FAULT WITH AVAILABLE MODELS Final Technical Report, 9 Sep. 1982 - 14 Oct. 1986
Donald L. Turcotte 14 Oct. 1986 8 p
(Contract NAS5-27340)
(NASA-CR-180757; NAS 1.26:180757) Avail: NTIS HC A02/MF A01 CSCL 08G

Theoretical and numerical studies of deformation on strike slip faults were performed and the results applied to geodetic observations performed in the vicinity of the San Andreas Fault in California. The initial efforts were devoted to an extensive series of finite element calculations of the deformation associated with cyclic displacements on a strike-slip fault. Measurements of strain accumulation adjacent to the San Andreas Fault indicate that the zone of strain accumulation extends only a few tens of kilometers away from the fault. There is a concern about the tendency to make geodetic observations along the line to the source. This technique has serious problems for strike slip faults since the vector velocity is also along the fault. Use of a series of stations lying perpendicular to the fault whose positions are measured relative to a reference station are suggested to correct the problem. The complexity of faulting adjacent to the San Andreas Fault indicated that the homogeneous elastic and viscoelastic approach to deformation had serious limitations. These limitation led to the proposal of an approach that assumes a fault is composed of a distribution of asperities and barriers on all scales. Thus, an earthquake on a fault is treated as a failure of a fractal tree. Work continued on the development of a fractal based model for deformation in the western United States. In order to better understand the distribution of seismicity on the San Andreas Fault system a fractal analog was developed. The fractal concept also provides a means of testing whether clustering in time or space is a scale-invariant process. B.G.

N88-20743# Instituto de Pesquisas Espaciais, Sao Jose dos Campos (Brazil).
ROYS AND RADIOSONDES IN THE REGION [O TOVS E AS RADIOSSONDAGENS NO PAIS]
Paulo Roberto Foster, Yoshihiro Yamazaki, Carlos Ho Shih Ning, and Maria Roseli Cabral Sep. 1987 18 p In PORTUGUESE; ENGLISH summary Presented at the 6th Selper Conference, Gramada, 10-15 Aug. 1986
(INPE-4362-PRE/1188) Avail: NTIS HC A03/MF A01

The Environmental Satellite Service of the U.S. (ESSA) has the capacity today to produce around 20,000 vertical soundings of the atmosphere over the globe for every 24 hours using imformation from the satellite sensors (TOVS) of two polar orbit operational satellite series of NOAA. The processed satellite data from ESSA and the simultaneously selected local time conventional meteorological radiosondes of some meteorological stations of Brazil are analyzed for two seasons of the year (summer and winter). The comparison between the two vertical thermal structures obtained by these distinct methods are presented. Within a certain limit, the short range forecast by meteorologists is perfectly acceptable for practical purposes. This demonstrates that the orbital polar satellites have great potential. Author

N88-20744# Rockwell International Corp., Thousand Oaks, Calif.
ULTRASONIC PHYSICAL MODELING OF SEISMIC WAVE PROPAGATION FROM GRABEN-LIKE STRUCTURES Final Report, 19 Feb. 1985 - 30 Jun. 1987
M. S. Vassiliou, Monem Abdel-Gawad, and B. R. Tittmann Nov. 1987 51 p
(Contract F19628-85-C-0034; DARPA Order 5307)

(AD-A189066; SC5420.FR; AFGL-TR-87-0256) Avail: NTIS HC A04/MF A01 CSCL 08K

This report describes ultrasonic experiments intended to help clarify the problem of seismic wave propagation in cases where sources are excited in a graben-like structure with significantly different material properties from those of the surrounding propagation medium. Ultrasonic waves are produced using a breaking pencil lead as a source (step unloading of the surface) and a true-displacement conical transducer as a receiver. We have made measurements by exciting the source on the half space (made of fine grained gabbro, with V sub p = 6.2 km/s) and within two graben-like structures: a cylindrical plug graben of 13 mm diameter and 2 mm depth; and a scale model (1 mm = 1 km) of Yucca Flat. In the case of cylindrical graben, the presence of a source region with significantly slower velocities than the surrounding region appears to lead to a more complex signal, with more ringing than would be apparant if there were no such region. The presence of such a source appears to result in a relative amplification of the high frequency part (200 to 400 KHz) of the signal. If we scale the results so that they correspond to a cylindrical basin roughly the size of Yucca Flat, this means that frequencies analogous to 3 to 10 s in the earth appear to be amplified relative to lower frequencies. Experiments on the scale model of Yucca Flat yield, in general, less dramatic results. The loss of symmetry apparently leads to less opportunity for focussing, and amplifications are not as great. GRA

N88-20745# Atmospheric and Environmental Research, Inc., Cambridge, Mass.

A STUDY OF SATELLITE EMISSION COMPUTED TOMOGRAPHY Final Report, 16 May 1986 - 15 Aug. 1987

Ross N. Hoffman, Ronald G. Isaacs, and Christopher Grassotti 15 Sep. 1987 102 p

(Contract F19628-86-C-0084)

(AD-A189567; AFGL-TR-87-0321) Avail: NTIS HC A06/MF A01 CSCL 04A

We have performed a study to assess the capability of tomography to infer the temperature structure of the atmosphere when realistic instrument geometry and noise characteristics are taken into consideration. Fleming (1982) demonstrated a significant improvement using his tomographic retrieval technique in an idealized simulation experiment. The present study rectifies a number of shortcomings of Fleming's (1982) experiment, following Fleming's (1985) suggestions. In particular, geometric effects of the instantaneous field of view of the sensor are properly accounted for in our study. In addition, realistic instrumental noise is included in our simulations. Finally, we have used realistic atmospheric cross sections and realistic geometry and simulation codes appropriate for the HIRS2 sensor. Our atmospheric cross sections are based on National Meteorological Center analyses during the Global Weather Experiment. The simulation code we used is a linearization of the HIRS2 rapid algorithm developed by J. Susskind (Susskind et al., 1982) of NASA/GSFC. We have exclusively used Fleming's (1982) row action method of solution of the satellite tomography problem, but a number of modifications to improve convergence were necessary. GRA

N88-20746# Air Force Inst. of Tech., Wright-Patterson AFB, Ohio. School of Engineering.

SPECIFICATION FOR AN INFRARED SATELLITE SURVEILLANCE SYSTEM FOR THE DETECTION OF AIRCRAFT M.S. Thesis

Timothy J. Lawder Nov. 1987 95 p

(AD-A189592; AFIT/GSO/ENP/87D-1) Avail: NTIS HC A05/MF A01 CSCL 17A

This report gives a methodology for designing an infrared satellite surveillance system for detection of aircraft against a background of the earth. Values for target intensity and background radiance have been assumed, and a satellite focal plane array configuration has been designed. System calculations have been performed and indicate that detection of aircraft against a background of the earth appears feasible. This report contains limited actual data due to its unclassified level. GRA

N88-20747# National Academy of Sciences - National Research Council, Washington, D. C.

[ACTIVITIES AND OBJECTIVES OF THE POLAR RESEARCH BOARD] Annual Report, 1986

1987 66 p

(Contract DE-FG01-81ER-60013)

(DE88-004543; DOE/ER-60013/T1) Avail: NTIS HC A04/MF A01

This annual report describes the Polar Research Board, its origin and objectives, its work and plans, and its principal activities and accomplishments during calendar year 1986. The report presents a summary of the various aspects of the Board's program and of its responsibilities as U.S. National Committee for the Scientific Committee on Antarctic Research (SCAR) of the International Council of Scientific Unions. DOE

N88-20748# Center for Mathematics and Computer Science, Amsterdam (Netherlands). Dept. of Applied Mathematics.

LOW-ORDER SPECTRAL MODELS OF ATMOSPHERIC CIRCULATION: A SURVEY

H. E. deSwart Jun. 1987 45 p Sponsored by the Netherlands Foundation for the Technical Sciences

(CWI-AM-R8705; B8723966; ETN-88-91791) Copyright Avail: NTIS HC A03/MF A01

A quasi-geostrophic potential vorticity equation is derived from the Navier-Stokes equations for atmospheric motions. It describes the evolution of a quasi-horizontal flow on time scales of a few days and more. The associated boundary value problem is analyzed by projection of the equation onto orthonormal eigenfunctions (modes) of a Sturm-Liouville operator. The result is a spectral model, consisting of an infinite number of nonlinear ordinary differential equations for the evolution of the mode amplitudes. Low-order spectral models, in which only a few modes are resolved, appear to have properties which agree with observations of atmospheric circulation. However, little justification is available for truncating the spectral expansion at low resolution numbers. It is argued that stochastic forcing terms should be added to the equations, but it is not clear how they should be specified. A derivation of a specific low-order spectral model of the quasi-geostrophic potential vorticity equation is presented. ESA

N88-20749 Drexel Univ., Philadelphia, Pa.

STRATOSPHERIC TRACE GAS DISTRIBUTIONS FROM FAIR INFRARED THERMAL EMISSION SPECTROSCOPY Ph.D. Thesis

Jing Guo 1987 259 p

Avail: Univ. Microfilms Order No. DA8727453

An inversion algorithm was developed to retrieve stratospheric trace gas distributions from high resolution far infrared limb thermal emission spectral data. The algorithm follows an onion peel approach and employs a non-linear least-square-fit spectral analysis technique. The infrared radiative transfer model used to compute the spectrum is based on full line-by-line and layer-by-layer calculations and includes curvature and refraction effects. Finite instrument field of view effects have been studied. An inversion algorithm has also been developed to correct observation angles. Details of spectra of stratospheric O3, H2O, HDO, HCN, O(16) and O(18) are presented. Dissert. Abstr.

N88-20750 Colorado Univ., Boulder.

DYNAMICAL MODELING OF MARINE BOUNDARY LAYER CONVECTION Ph.D. Thesis

Hung-chi Kuo 1987 142 p

Avail: Univ. Microfilms Order No. DA8725632

The interaction between dynamics and infrared radiation is investigated, as well as the problem of entrainment instability in the cloud-topped marine boundary layer. A two-dimensional Boussinesq moist model with a numerical technique (Fourier-Chebysheve tau method) and resolution sufficient to simulate cloud top processes was developed. Previous measurements suggest that the cloud-top radiative cooling is likely to undergo significant horizontal and vertical variability. To investigate the impact of infrared cooling on the boundary layer

dynamics, numerical experiments on marine boundary layer convection under various radiative forcings are performed. The results indicate that the model steady state does not depend on the horizontal and the vertical distribution of the cooling when the cooling is confined to the turbulent region. The thermodynamic theory and observations taken during the last fifteen years are summarized. The results indicate that stratocumulus remain solid even when the theoretical entrainment instability criterion is satisfied. Radiatively forced numerical simulations are performed. The cloud cells can decay and reform in a finite time. The appearance and disappearance of cloud holes may have nothing to do with entrainment instability. Signs of stratocumulus breakup were not ovserved even in the situation of strong entrainment.
Dissert. Abstr.

N88-20751 California Univ., Los Angeles.
SEASONAL VARIATIONS AND EXCITATION MECHANISMS OF THE EQUATORIALLY TRAPPED WAVES Ph.D. Thesis
Mong-Ming Lu 1987 351 p
Avail: Univ. Microfilms Order No. DA8719932

The seasonal variation and excitation mechanisms of the equatorially trapped waves (ETWs) are studied using the wind, geopotential, and outgoing longwave radiation (OLR) data during the First and Second Special Observing Periods (SOP-1 and SOP-2) of the First GARP Global Experiment (FGGE). Some properties of the low-frequency (30 to 50 day) oscillation in the equatorial region are also examined. The intensity of equatorial disturbances in the wind field is found to be closely related to the configurations of the mean zonal flow. The dominant zonal wavenumbers (s) and periods (tau) of ETWs are determined by examining the spectra of equatorial zonal and meridional winds. Both the spectral analysis of meridional wave energy flux (WEF) and the time series of the zonally averaged wave amplitude and meridional WEF show that the convergence of WEF between 14 deg S and 14 deg N is often associated with ETWs. Then, frequency bandpass filtering and zonal wavenumber decomposition are employed. The convergence of WEF produced by the eddies appears to be crucial for exciting the Kelvin waves. The trough and ridge axes of mixed Rossby-gravity waves at 200 mb are tilted in such a way that these eddies transport wave energy meridionally. The amplitudes and the associated meridional WEF of the Kelvin waves are found to have the same longitudinal difference. In constrast, the convective activity and the amplitude of the Kelvin waves are negatively correlated. Dissert. Abstr.

N88-20752*# Ohio State Univ., Columbus. Dept. of Geodetic Science and Surveying.
COMPARISONS OF GLOBAL TOPOGRAPHIC/ISOSTATIC MODELS TO THE EARTH'S OBSERVED GRAVITY FIELD
Reiner Rummel, Richard H. Rapp, Hans Suenkel, and C. Christian Tscherning (Geodetic Inst., Charlottenlund, Denmark) Mar. 1988 38 p
(Grant NGR-36-008-161)
(NASA-CR-182696; NAS 1.26:182696; OSU-388) Avail: NTIS HC A03/MF A01 CSCL 08G

The Earth's gravitational potential, as described by a spherical harmonic expansion to degree 180, was compared to the potential implied by the topography and its isostatic compensation using five different hypothesis. Initially, series expressions for the Airy/Heiskanen topographic isostatic model were developed to the third order in terms of (h/R), where h is equivalent rock topography and R is a mean Earth radius. Using actual topographic developments for the Earth, it was found that the second and third terms of the expansion contributed 30 and 3 percents, of the first of the expansion. With these new equations it is possible to compute depths (D) of compensation, by degree, using 3 different criteria. The results show that the average depth implied by criterion I is 60 km while it is about 33 km for criteria 2 and 3 with smaller compensation depths at the higher degrees. Another model examined was related to the Vening-Meinesz regional hypothesis implemented in the spectral domain. Finally, oceanic and continental response functions were derived for the global data sets and comparisons made to locally determined values.
Author

N88-20753*# National Aeronautics and Space Administration. Goddard Space Flight Center, Greenbelt, Md.
CRUSTAL DYNAMICS PROJECT DATA ANALYSIS, 1987. VOLUME 2: MOBILE VLBI GEODETIC RESULTS 1982-1986
C. Ma and J. W. Ryan Nov. 1987 130 p
(NASA-TM-100689-Vol-2; Rept-88B0042; NAS 1.15:100689-Vol-2)
Avail: NTIS HC A07/MF A01 CSCL 08G

The Goddard VLBI group reports the results of analyzing 101 Mark 111 data sets acquired from mobile observing sites through the end of 1986 and available to the Crustal Dynamics Project. The fixed VLBI observations at Hat Creek, Ft. Davis, Mojave, and OVRO are included since they participate heavily in the mobile schedules. One large solution GLB171 was used to obtain baseline length and transverse evolutions. Radio source positions were estimated globally, while nutation offsets were estimated from each data set. The results include 28 mobile sites. Author

N88-20754*# Massachusetts Inst. of Tech., Cambridge.
GEODETIC MEASUREMENT OF DEFORMATION EAST OF THE SAN ANDREAS FAULT IN CENTRAL CALIFORNIA
Jeanne M. Sauber, Michael Lisowski, and Sean C. Solomon [1988] 39 p Prepared in cooperation with Geological Survey, Menlo Park, Calif.
(Grants NAG5-814; NGT5-0103)
(NASA-CR-182709; NAS 1.26:182709) Avail: NTIS HC A03/MF A01 CSCL 08E

Triangulation and trilateration data from two geodetic networks located between the western edge of the Great Valley and the San Andreas fault have been used to calculate shear strain rates in the Diablo Range and to estimate the slip rate along the Calaveras and Paicines faults in Central California. Within the Diablo Range the average shear strain rate was determined for the time period between 1962 and 1982 to be 0.15 + or - 0.08 microrad/yr, with the orientation of the most compressive strain at N 16 deg E + or - 14 deg. The orientation of the principal compressive strain predicted from the azimuth of the major structures in the region is N 25 deg E. It is inferred that the measured strain is due to compression across the folds of this area: the average shear straining corresponds to a relative shortening rate of 4.5 + or - 2.4 mm/yr. From an examination of wellbore breakout orientations and the azimuths of P-axes from earthquake focal mechanisms the inferred orientation of maximum compressive stress was found to be similar to the direction of maximum compressive strain implied by the trend of local fold structures. Results do not support the hypothesis of uniform fault-normal compression within the Coast Ranges. From trilateration measurements made between 1972 and 1987 on lines that are within 10 km of the San Andreas fault, a slip rate of 10 to 12 mm/yr was calculated for the Calaveras-Paicines fault south of Hollister. The slip rate of the Paicines fault decreases to 4 mm/yr near Bitter. Author

N88-20755# International Meteorological Inst., Stockholm (Sweden).
[ACTIVITIES REPORT IN METEOROLOGY] Annual Report, Jul. 1986 - Jun. 1987
Oct. 1987 52 p
(AR-86-87; ISSN-0349-0068; ETN-88-91880) Avail: NTIS HC A04/MF A01

Research in dynamic meteorology, chemical meteorology, biogeochemistry, geophysical fluid dynamics, atmospheric physics, and chemical glaciology is summarized. ESA

N88-20756# Kernforschungsanlage, Juelich (West Germany). Inst. fuer Chemie der Belastenden Atmosphaere.
COMPUTER SIMULATION OF TROPOSPHERIC CHEMISTRY
Christian Holzapfel Jul. 1987 133 p In GERMAN; ENGLISH summary
(JUEL-2144; ISSN-0366-0885; ETN-88-91931) Avail: NTIS HC A07/MF A01

A one-dimensional time dependent photochemical model of the troposphere, with vertical turbulent transport, was used to study the influence of light intensity of summer and wintertime on the diurnal and seasonal variation of O3 and HNO3. Below 2 to 3 km the model of the polluted troposphere O3 shows strong diurnal variation in summertime with an increase at daytime due to the photochemistry of hydrocarbons and NOx and a decrease at night. The HO2-concentration at noon-time shows a maximum in the summer due to the photodissociation of O3. The O3-concentration is lower in summertime than in winter in the remote troposphere and in the upper levels of the polluted troposphere. Only below 3 km in the model of the polluted troposphere is the O3-concentration higher in summertime than in wintertime. In summertime the HNO3-concentration increases during the day and decreases at night. In wintertime the HNO3-concentration decreases during the day and increases at night. The HNO3-concentration strongly depends on water content and on precipitation in the troposphere. ESA

N88-20500# Joint Publications Research Service, Arlington, Va.
ON ERROR EQUATIONS FOR DETERMINING EARTH ROTATION PARAMETERS WITH VLBI NETWORK Abstract Only
Yifei Xia *In its* JPRS Report: Science and Technology. China 12 Feb. 1988 p 82 Transl. into ENGLISH from Tianwen Xuebao (Beijing, People's Republic of China), v. 28, no. 3, Sep. 1987 p 282-287 (For primary document see N88-20495 13-31)
Avail: NTIS HC A07/MF A01

N88-20683# Joint Publications Research Service, Arlington, Va.
RELATIONSHIP BETWEEN OCEANIC GEOLOGICAL FORMATIONS AND TECTONIC STRUCTURES Abstract Only
I. O. Murdmaa *In its* JPRS Report: Science and Technology. USSR: Earth Sciences 26 Feb. 1988 p 6-7 Transl. into ENGLISH from Geotektonika (Moscow, USSR), no. 2, Mar. - Apr. 1987 p 35-45 (For primary document see N88-20674 13-42)
Avail: NTIS HC A04/MF A01

N88-20701# Joint Publications Research Service, Arlington, Va.
RESOLUTION OF THE MAGNETOTELLURIC METHOD FOR DETERMINING LOCAL INHOMOGENEITIES IN THE SEDIMENTARY COVER Abstract Only
V. M. Kobzova, I. P. Moroz, and A. I. Bilinskiy *In its* JPRS Report: Science and Technology. USSR: Earth Sciences 26 Feb. 1988 p 45 Transl. into ENGLISH from Geofizicheskiy Zhurnal (Kiev, USSR), no. 1, Jan. - Feb. 1987 p 65-70 (For primary document see N88-20674 13-42)
Avail: NTIS HC A04/MF A01

N88-20702# Joint Publications Research Service, Arlington, Va.
INTERACTIVE AUTOMATED SYSTEM FOR TESTING ANALOG UNITS OF DIGITAL SEISMIC STATIONS Abstract Only
L. I. Orlov *In its* JPRS Report: Science and Technology. USSR: Earth Sciences 26 Feb. 1988 p 47 Transl. into ENGLISH from Pribory i Sistemy Upravleniya (Moscow, USSR), no. 11, Nov. 1986, p 11-12 (For primary document see N88-20674 13-42)
Avail: NTIS HC A04/MF A01

N88-20703# Joint Publications Research Service, Arlington, Va.
TRAJECTORY SYNTHESIS OF IONOGRAMS IN PRESENCE OF ARTIFICIAL IONOSPHERIC INHOMOGENEITIES Abstract Only
N. P. Danilkin, D. S. Lukin, and V. I. Stasevich *In its* JPRS Report: Science and Technology. USSR: Earth Sciences 26 Feb. 1988 p 51 Transl. into ENGLISH from Geomagnetizm i Aeronomiya (Moscow, USSR), v. 27, no. 2, Feb. 1987 p 217-221 Original language document was announced in AIAA as A87-42006 (For primary document see N88-20674 13-42)
Avail: NTIS HC A04/MF A01

N88-20705# Joint Publications Research Service, Arlington, Va.
INFLUENCE OF NONLINEAR SPECTROSCOPIC EFFECTS ON ATMOSPHERIC PROPAGATION OF INTENSE LASER RADIATION AT 10.6 MICRONS WAVELENGTH Abstract Only
A. A. Mitsel, Yu. N. Ponomarev, and K. M. Firsov *In its* JPRS Report: Science and Technology. USSR: Earth Sciences 26 Feb. 1988 p 53 Transl. into ENGLISH from Izvestiya Akademii Nauk SSSR: Fizika Atmosfery i Okeana (Moscow, USSR), v. 23, no. 2, Feb. 1987 p 165-169 Original language document was announced in AIAA as A87-35834 (For primary document see N88-20674 13-42)
Avail: NTIS HC A04/MF A01

N88-20706# Joint Publications Research Service, Arlington, Va.
SYNCHRONOUS MEASUREMENTS OF EFFECTIVE PHOTON PATH LENGTH IN VISIBLE AND NEAR-IR SPECTRAL REGIONS IN REAL CLOUD SYSTEMS Abstract Only
Ye. I. Grechko, S. V. Dvoryashin, and V. I. Dianov-Klokov *In its* JPRS Report: Science and Technology. USSR: Earth Sciences 26 Feb. 1988 p 54 Transl. into ENGLISH from Izvestiya Akademii Nauk SSSR: Fizika Atmosfery i Okeana (Moscow, USSR), v. 23, no. 2, Feb. 1987 p 115-120 (For primary document see N88-20674 13-42)
Avail: NTIS HC A04/MF A01

47 METEOROLOGY AND CLIMATOLOGY

Includes weather forecasting and modification.

N88-20757# Massachusetts Inst. of Tech., Cambridge. Lincoln Lab.
A PRELIMINARY ASSESSMENT OF THUNDERSTORM OUTFLOW WIND MEASUREMENT WITH AIRPORT SURVEILLANCE RADARS
Mark E. Weber and William R. Moser 15 May 1987 90 p
(Contract F19628-85-C-0002)
(AD-A189064; ATC-140; DOT/FAA/PM-86-38) Avail: NTIS HC A05/MF A01 CSCL 17I

Modern airport surveillance radars (ASR) situated on or near most major air terminals, feature coherent pulse Doppler processing, a vertical fan beam and rapid azimuthal antenna scanning for detection and tracking of aircraft. These radars might serve an additional useful role by making radial wind measurements in the immediate vicinity of an airport so as to provide data on thunderstorm outflow winds. This report presents a preliminary analysis of the capabilities and limitations of ASRs in measuring outflow winds. Principal results are: (1) radar sensitivity is adequate to measure winds associated with weakly reflecting (5 to 20 dBZ) thunderstorm outflows at ranges less than 20 km provided that appropriate operating parameters are chosen; (2) overhanging precipitation, often moving at a markedly different radial velocity than the outflow, will be a significant source of interference owing to the vertical-fan antenna pattern. If radar reflectivity is approximately constant with altitude, this interference will limit the maximum range for reliable outflow velocity measurements to about 20 km for an outflow that extends 1000 m above the surface and to 7 km for an outflow that extends only 300 m above the surface; (3) At two example major air terminals (Memphis International and Denver Stapleton) ground clutter suppression of approximately 40 dB, combined with the use of inter-clutter visibility techniques, would result in an adequate signal-to-interference ratio for thunderstorm outflow velocity measured over the significant approach/departure corridors. GRA

N88-20758*# South Dakota School of Mines and Technology, Rapid City. Inst. of Atmospheric Sciences.
ATMOSPHERIC ELECTRICAL MODELING IN SUPPORT OF THE NASA F-106 STORM HAZARDS PROJECT Final Report, 15 Mar. 1984 - 14 Jun. 1987
John H. Helsdon, Jr. Mar. 1988 137 p
(Grant NAG1-463)
(NASA-CR-181639; NAS 1.26:181639; SDSMT/IAS/R-87/02)
Avail: NTIS HC A07/MF A01 CSCL 04B

A recently developed storm electrification model (SEM) is used to investigate the operating environment of the F-106 airplane during the NASA Storm Hazards Project. The model is 2-D, time dependent and uses a bulkwater microphysical parameterization

scheme. Electric charges and fields are included, and the model is fully coupled dynamically, microphysically and electrically. One flight showed that a high electric field was developed at the aircraft's operating altitude (28 kft) and that a strong electric field would also be found below 20 kft; however, this low-altitude, high-field region was associated with the presence of small hail, posing a hazard to the aircraft. An operational procedure to increase the frequency of low-altitude lightning strikes was suggested. To further the understanding of lightning within the cloud environment, a parameterization of the lightning process was included in the SEM. It accounted for the initiation, propagation, termination, and charge redistribution associated with an intracloud discharge. Finally, a randomized lightning propagation scheme was developed, and the effects of cloud particles on the initiation of lightning investigated. Author

N88-20759# Brown Univ., Providence, R. I. Dept. of Geological Sciences.
MODEL VALIDATION RESEARCH: COMPARISON OF SIMULATED AND OBSERVED CLIMATE PATTERNS FOR THE PAST 18,000 YEARS Progress Report, 1 Feb. 1987 - 31 Jan. 1988
T. Webb, III and W. L. Prell Jan. 1988 16 p
(Contract DE-FG02-85ER-60304)
(DE88-004945; DOE/ER-60304/3) Avail: NTIS HC A03/MF A01

General circulation models (GCM's) for the atmosphere and oceans are being used to provide predictions for the potential climatic effects of increased concentrations of atmospheric carbon dioxide. Confidence in the GCM predictions will be much enhanced once the models are thoroughly tested in terms of their ability to simulate climates that differ significantly from today's climate. Simulating the climate of the past 18,000 years provides one opportunity to test the models. As one index of climate change, the magnitude of the global mean temperature change during the past 18,000 years was similar to that predicted for carbon dioxide doubling. The comparison of model results with paleoclimatic data can illustrate the sensitivity of the model's response to variations in the seasonal radiation budget as well as to changes in other boundary conditions. These comparisons also provide the opportunity to check the sensitivity of the climatic response of critical components of the climate system such as sea-ice. During the past several years, we have used paleoclimatic data to test the NCAR CCM, a model used in CO2 research, after changing its boundary conditions to those appropriate for simulating past climates. We have assembled global paleoclimatic data sets of pollen, lake level, and marine plankton data, and calibrated many of the data in climatic terms. We have also developed methods that permit direct quantitative comparisons between the data and model results. Our comparisons have shown both some of the strengths and weaknesses of the model. DOE

N88-20760# Sandia National Labs., Albuquerque, N. Mex.
CHARACTERISTICS OF THE POSITIVE LIGHTING FLASH
R. J. Fisher Jan. 1988 26 p
(Contract DE-AC04-76DP-00789)
(DE88-005854; SAND-87-2615) Avail: NTIS HC A03/MF A01

This report summarizes and documents the available data on key positive lightning parameters such as peak channel current, rise times and rise rates, continuing currents, and overall charge transfer. While the body of existing data in this area was found to be relatively sparse, it is generally consistent and indicates positive flash distributions with average values of peak currents in excess of those of negative ground flashes by about 50 percent. In comparison with those of negative ground flashes, these distributions are broader and are weighted by numbers of more severe flashes. Positive flashes very often combine long stroke current decay times with high level continuing currents to produce extraordinary stroke charge transfers of 300 C or more. Peak currents as high as 400 kA have been reported, a factor of 2 greater than the accepted one percentile level severe negative flash amplitude. Averaged over all factors (geographic, seasonal, ans storm phase), positive flashes constitute between 10 to 20 percent of all ground flashes. Under certain circumstances, however, up to 100 percent of all observed flashes in given storms and storm phases are positive. Key areas of uncertainty include: (1) the frequency of occurrence of the more severe positive flashes, (2) definition of the details of the severe continuing currents which have been found to accompany over 60 percent of all such flashes, and (3) the distribution of the current derivatives associated with the fast transition portion of the return stroke current front. Recommendations are given for possible practical research efforts addressing each of these data gaps. DOE

N88-20761# Pacific Northwest Labs., Richland, Wash.
SIMULATING HIGH-RESOLUTION VERTICAL PLANE ARRAY WIND CHARACTERISTICS USING LOWER-SPATIAL-RESOLUTION WIND MEASUREMENTS
D. C. Powell and J. R. Connell Oct. 1987 7 p Presented at the 7th Wind Energy Symposium, New Orleans, La., 10 Jan. 1988
(Contract DE-AC06-76RL-01830)
(DE88-005626; PNL-SA-15370; CONF-880132-6) Avail: NTIS HC A02/MF A01

Several sets of 12-anemometer rotational wind data from the Clayton, New Mexico, vertical plane array were reduced to 6-anemometer rotational data by including every other anemometer. Statistics of these reduced data were compared to statistics of the original 12-anemometer rotational data. Also, techniques based on assumptions were employed to simulate the original 12-anemometer data by using the reduced data as part of constructed 12-point data series. Good statistical comparisons were conditionally, but not consistently, obtained. DOE

N88-20762# National Weather Service, Garden City, N.Y.
WIND SHEAR AS A PREDICTOR OF SEVERE WEATHER FOR THE EASTERN UNITED STATES
H. M. Stone Jan. 1988 27 p
(PB88-157144; NOAA-TM-NWS-ER-75) Avail: NTIS HC A03/MF A01 CSCL 04B

Various numerical and observational studies have indicated that wind shear may be useful in explaining and possibly forecasting the type of convective storms that develop under unstable atmospheric conditions. Most of the observational data supporting the results of the numerical experiments are taken from the Great Plains region of the United States, an area well known for strong thunderstorm activity. In the study the authors seek to identify relationships between various measures of wind shear and stability and the occurrence of severe weather in the eastern United States. The authors show that some good relationships do exist that may be useful in assessing afternoon severe weather potential. GRA

N88-20763 Princeton Univ., N. J.
THE PRESSURE DRAG AND MOMENTUM FLUX DURING A COLD FRONTAL PASSAGE OVER THE ALPS Ph.D. Thesis
Bertrand Charles Carissimo 1987 186 p
Avail: Univ. Microfilms Order No. DA8727374

The strong pressure drag, the momentum flux, and the air flow changes occurring during the interaction of a cold front with a mesoscale mountain are investigated using a combination of observations from the Alpine Experiment and theoretical models. The surface pressure observations are analyzed every three hours to derive the pressure drag and reveal that peak values are reached when tight pressure gradients are located on steep orography. These values would be underestimated by conventional synoptic analyses or coarse resolution numerical models. The momentum flux above the topography is estimated from aircraft measurements taken during the strong drag events. Compared with the surface pressure drag, the observed momentum fluxes are small. The accuracy of these fluxes is discussed. In order to understand these observations, the dynamics of the interaction between a cold front and the mountain is further investigated. A dynamical explanation for the large observed drag during frontal passage is therefore sought using a simple layer model. Although this model is somewhat deficient in simulating the prefrontal stage in the interaction, it is capable of reproducing the observed frontal retardation and drag. An additional series of numerical experiments with a continuously

stratified model is performed to compare the air flow over the mountain with and without the presence of a front and the evolution of the front with and without the mountain. Dissert. Abstr.

N88-20764 Princeton Univ., N. J.
SAMPLE MODELS OF STEADY AND LOW FREQUENCY CIRCULATIONS IN THE TROPICAL ATMOSPHERE, WITH APPLICATION TO TROPICAL AIR-SEA INTERACTIONS Ph.D. Thesis
James David Neelin 1987 240 p
Avail: Univ. Microfilms Order No. DA8727383

A steady state model of the large flow in the tropical atmosphere is developed and tested by comparison to a general circulation model. The development proceeds in two stages: the first half of the model gives surface stress when forced by a given mid-tropospheric vertical velocity. Since vertical velocity is closely related to diabatic heating in the tropics, the model can also be forced by latent heating as measured by precipitation. The model is highly successful at simulating GCM results for both the total climatology and El Nino anomalies. This success is largely due to the fact that the boundary layer flow is effectively decoupled from that at upper levels. The second half of the model relates the mid-tropospheric vertical velocity or diabatic heating to the sea surface temperature. It is argued that the strong upward motions of the tropical convergence zones are associated with minima in the gross moist stability, a vertically integrated measure of the moist static stability. The model is based on a parameterization of this quantity in which the positions of these minima are determined by the time-mean moisture field. A mechanism for exciting the 30 to 50 day oscillation is examined in a simple model. It is tested in a series of GCM experiments and proves to be important to the maintenance of the oscillation when fixed sea surface temperature lower boundary conditions are used. Finally, the steady state atmospheric model is coupled to a cut-down version of a tropical ocean GCM and preliminary tests are run. Dissert. Abstr.

N88-20765 Missouri Univ., Columbia.
NORTHERN HEMISPHERE CIRCULATION AND THE PRINCIPAL COMPONENTS OF SUBSEQUENT SUMMER PATTERNS IN NORTH AMERICA AND WEST AFRICA Ph.D. Thesis
Chung Kyu Park 1987 116 p
Avail: Univ. Microfilms Order No. DA8726949

The winter and spring patterns of the Northern Hemisphere circulation are related to the principal components of the following summer temperature of North America and the summer precipitation of sub-Saharan West Africa. The first two components of the North American temperature and the first component of the West African precipitation are used to describe the dominant modes of the summer atmosphere. The results of correlation analysis incidate that the planetary scale circulation over the North Pacific during winter and spring is significantly related to the following summer circulation of North America. In particular the sea surface temperature in the central North Pacific is found to be a useful predictor of the following North American summer temperature. Examination of the West African precipitation shows that the summer rainfall fluctuation is closely related to the atmospheric moisture contents in the tropics during the preceding winter and spring. A possible impact of the El Nino-Southern Oscillation (ENSO) on the summer circulation is discussed. A teleconnection between the upper tropospheric geopotential field over North America and the precipitation in West Africa may suggest that quasi-stationary waves are important to determine the regional summer circulation patterns in the tropics and the middle latitudes. Dissert. Abstr.

N88-20766 Utah Univ., Salt Lake City.
PLANETARY SCALE BAROTROPIC SPECTRAL MODEL Ph.D. Thesis
Eugene Anthony Robl 1987 191 p
Avail: Univ. Microfilms Order No. DA8726797

A highly truncated spectral baratropic model which is used to qualitatively reproduce certain recurrent planetary scale atmospheric flow configurations, in particular, quasistationary states having high and low zonal index is evaluated. The model includes single spectral component topography and suitably parameterized eddy divergence due to latent heating; both the topography and the eddy divergence possess Zonal Wavenumber 2 and therefore represent important spectral terms for the actual large scale mountains and patterns of tropical heating. Zonally-symmetric momentum forcing and linear clamping are also included in the model. Equilibrium solutions for several different cases of external forcing are presented. Stability properties of the equilibria are also determined and the physical mechanisms generating any unstable behavior are inferred. The sets of solutions derived from the model are checked for consistency with realistic mid-tropospheric flow conditions. External forcing conditions giving rise to multiple equilibrium solutions are determined and the flow profiles of the resulting multiple equilibria are described in detail. The spectral system is also applied to real data in order to, first, determine the degree of validity of the model and, second, to provide some physical interpretation to a case of actual atmospheric flow in the planetary-scale regime. Dissert. Abstr.

N88-20767 Cornell Univ., Ithaca, N.Y.
UPWARD PROPAGATING ELECTRIC FIELDS FROM THUNDERSTORMS AND VLF TRANSMITTERS Ph.D. Thesis
Carl Lewis Siefring 1987 252 p
Avail: Univ. Microfilms Order No. DA8725832

In an experiment, simultaneous rocket-borne electric field observations were made in the ionosphere and atmosphere over a nighttime thunderstorm. Lightning-induced transient electric fields were measured in the ionosphere with amplitudes of tens of mV/m with rise times as fast as 0.2 ms and typical durations of approx. 10 ms. The transients had significant components parallel to the Earth's magnetic field in the ionosphere. Both the parallel and perpendicular electric fields are large by ionospheric standards. An analysis shows that the lightning induced transients result from an electrostatic source. A lightning stroke moves large quantities of charge from one location to another. This sets up a different electrostatic configuration that propagates upward as an electromagnetic disturbance and drives currents in the atmosphere and ionosphere. The data suggest a new model for whistler generation wherein the ionosphere is viewed as an aperture antenna. Other whistler observations are also presented. Also detected were standing wave patterns from two VLF transmitter signals. These were generated by reflections off a sporatic E layer, and were used to determine electron concentration.
Dissert. Abstr.

N88-20768 Utah Univ., Salt Lake City.
MULTIPLE SCATTERING OF POLARIZED LIGHT IN CIRRUS CLOUDS Ph.D. Thesis
Yoshihide Takano 1987 136 p
Avail: Univ. Microfilms Order No. DA8726537

The correct formula for superimposing diffracted and reflected/refracted light rays is derived on the basis of the geometric ray technique for light scattering by hexagonal ice crystals. The scattering phase matrix for randomly oriented ice crystals, including the effect of birefringence, is formulated. In addition, a theory for the symmetrical property of the scattering phase matrix for horizontally oriented ice crystals is presented. Computations of the scattering phase matrix for randomly and horizontally oriented ice crystals are then carried out and the results are presented and discussed. Using the resulting single-scattering properties derived from the present study, the radiative transfer of polarized light through randomly and horizontally oriented ice crystals is theoretically formulated and numerically computed. A comparison was made between the radiative properties of randomly oriented ice crystals, area equivalent ice spheres, and horizontally oriented ice crystals. The computational scheme and results presented could be useful for the development of parameterizations for the radiative properties of cirrus clouds in climate models, as well as remote sensing of the composition and structure of cirrus clouds by meteorological satellites. Dissert. Abstr.

N88-20769*# National Aeronautics and Space Administration, Washington, D.C.
METHOD FOR DETERMINATION OF THE WIND VELOCITY AND DIRECTION
Goesta Johan Dahlin Mar. 1988 13 p Transl. into ENGLISH from Saett Att Bestaemma Vindhastighet Och Vindriktning, Swedish Patent No. SE-8201788-0 Transl. by SCITRAN, Inc., Santa Barbara, Calif.
(Contract NASw-4307)
(NASA-TT-20233; NAS 1.77:20233) Avail: NTIS HC A03/MF A01 CSCL 04B

Accurate determination of the position of an artillery piece, for example, using sound measurement systems through measurement of the muzzle noise requires access to wind data that is representative of the portion of the air from where the sound wave is propagated up the microphone base of the system. The invention provides a system for determining such representative wind data. Author

N88-20770# Technische Hogeschool, Eindhoven (Netherlands). Vakgroep Transportfysica.
WIND VELOCITY MEASUREMENT DATA. ZIMBABWE, 4 MEASURING STATIONS [WINDSNELHEIDSMEETGEGEVENS. ZIMBABWE, 4 MEETSTATIONS]
P. Smulders Mar. 1987 60 p In DUTCH
(R-845-D; ETN-88-91316) Avail: NTIS HC A04/MF A01

Wind velocity data, measured at four stations around a place in Zimbabwe where a wind mill is planned, are given in the form of histograms, per month. Data concerning geographical situation and climatic conditions are also presented. ESA

N88-20771# Gesellschaft fuer Strahlen- und Umweltforschung m.b.H., Munich (West Germany).
OZONE SONDE AND DOBSON SPECTROMETER DATA OBTAINED DURING THE MAP/GLOBUS 1983 CAMPAIGN OVER WESTERN EUROPE
W. Attmannspracher, J. Cisneros, H. Claude, C. DeBakker, D. DeMuer, R. Hartmannsgruber, A. Lovisa, P. Marche, G. Megie, and K. Munzert (Fraunhofer-Inst. fuer Atmosphaerische Umweltforschung, Garmisch-Partenkirchen, West Germany) et al. 1987 274 p
(BPT-5/87; ISSN-0176-0777; ETN-88-91935) Copyright Avail: NTIS HC A12/MF A01

During the international MAP/GLOBUS campaign in September 1983 in Southern France simultaneous ozone soundings and total ozone measurements were performed at ozone stations in Western Europe. Pressure, altitude, temperature, humidity, and wind were also measured. The results are given in tables and maps. ESA

N88-20772*# National Aeronautics and Space Administration. Langley Research Center, Hampton, Va.
SUMMARY OF ALONG-TRACK DATA FROM THE EARTH RADIATION BUDGET SATELLITE FOR SEVERAL MAJOR DESERT REGIONS
David R. Brooks and Marta A. Fenn May 1988 147 p
(NASA-RP-1197; L-16401; NAS 1.61:1197) Avail: NTIS HC A07/MF A01 CSCL 04B

For several days in January and August 1985, the Earth Radiation Budget Satellite, a component of the Earth Radiation Budget Experiment (ERBE), was operated in an along-track scanning mode. A survey of radiance measurements is given for four desert areas in Africa, the Arabian Peninsula, Australia, and the Sahel region of Africa. Each overflight provides radiance information for four scene categories: clear, partly cloudy, mostly cloudy, and overcast. The data presented include the variation of radiance in each scene classification as a function of viewing zenith angle during each overflight of the five target areas. Several features of interest in the development of anisotropic models are evident, including day-night differences in longwave limb darkening and the azimuthal dependence of short wave radiance. There is some evidence that surface features may introduce thermal or visible shadowing that is not incorporated in the usual descriptions of the anisotropic behavior of radiance as viewed from space. The data also demonstrate that the ERBE scene classification algorithms give results that, at least for desert surfaces, are a function of viewing geometry. Author

N88-20773*# Michigan Technological Univ., Houghton. Dept. of Mechanical Engineering and Engineering Mechanics.
POWER SPECTRAL DENSITY ANALYSIS OF WIND-SHEAR TURBULENCE FOR RELATED FLIGHT SIMULATIONS M.S. Thesis
Tony R. Laituri [1988] 219 p
(Grant NAG1-717)
(NASA-CR-182721; NAS 1.26:182721) Avail: NTIS HC A10/MF A01 CSCL 04B

Meteorological phenomena known as microbursts can produce abrupt changes in wind direction and/or speed over a very short distance in the atmosphere. These changes in flow characteristics have been labelled wind shear. Because of its adverse effects on aerodynamic lift, wind shear poses its most immediate threat to flight operations at low altitudes. The number of recent commercial aircraft accidents attributed to wind shear has necessitated a better understanding of how energy is transferred to an aircraft from wind-shear turbulence. Isotropic turbulence here serves as the basis of comparison for the anisotropic turbulence which exists in the low-altitude wind shear. The related question of how isotropic turbulence scales in a wind shear is addressed from the perspective of power spectral density (psd). The role of the psd in related Monte Carlo simulations is also considered. Author

N88-20696# Joint Publications Research Service, Arlington, Va.
NUMERICAL MODEL OF RAYLEIGH INSTABILITY AND SPIN-OFF EDDIES ON FRONTS Abstract Only
V. F. Kozlov and Ye. V. Yaroshchuk *In its* JPRS Report: Science and Technology. USSR: Earth Sciences 26 Feb. 1988 p 28 Transl. into ENGLISH from Okeanologiya (Moscow, USSR), v. 27, no. 1, Jan. - Feb. 1987 p 12-17 (For primary document see N88-20674 13-42)
Avail: NTIS HC A04/MF A01

48 OCEANOGRAPHY

Includes biological, dynamic, and physical oceanography; and marine resources.

For related information see also *43 Earth Resources and Remote Sensing.*

N88-20774# Instituto de Pesquisas Espaciais, Sao Jose dos Campos (Brazil).
THE USE OF A BAROTROPIC FINITE ELEMENT MODEL FOR THE STUDY OF CIRCULATION ON THE CONTINENTAL SHELF OF THE SOUTHEAST COAST OF BRAZIL [USO DE UM MODELO BAROTROPICO DE ELEMENTOS FINITOS PARA O ESTUDO DA CIRCULACAO NA PLATAFORMA DA COSTA SUDESTE DO BRASIL]
Joao Antonio Lorenzzetti, Jose Luiz Stech, and John D. Wang (Miami Univ., Coral Gables, Fla.) Oct. 1987 21 p In PORTUGUESE; ENGLISH summary Presented at the 2nd Latin American Congress on Ocean Sciences, Lima, Peru, 17-21 Aug. 1987 Submitted for publication
(INPE-4401-PRE/1218) Avail: NTIS HC A03/MF A01

Numerical modeling is an important tool which is increasingly being used in the study of coastal dynamics. At present, with the availability of high-speed computers with great memory capacity, many models have been developed which make use of different techniques and numerical schemes. In this work, a barotropic finite elment model is implemented for the simulation of the wind-forced circulation on the continental shelf of the southeast coast of Brazil. Numerical experiments are made to evaluate the region's response to different forcings. The results of these experiments, such as current field, sea surface anomalies and momentum balances, are analyzed and discussed. Author

N88-20775# Naval Research Lab., Washington, D.C.
BATHYMETRIC HAZARD SURVEY TEST Final Report No. 3, 1982 - 1984
F. T. Erskine, G. M. Bernstein, S. M. Brylow, W. T. Newbold, and R. C. Gauss 20 Aug. 1987 64 p Original contains color illustrations
(AD-A189150; NRL-9048) Avail: NTIS HC A04/MF A01 CSCL 08C

NRL is developing a long range active acoustics technique for estimating seamount heights and mapping undersea topography over an entire ocean basin region. A concept demonstration, the BHST, was conducted in the eastern Atlantic in 1980. The technique uses explosive shot acoustic sources and a large aperture, towed acoustic receiver array. Reverberation data are output to an imaging system to study the spatial distribution of acoustic backscatter. These images are in the form of 2-D maps of reverberation, each typically 2000 km on a side. After correction of maps from individual shot detonations for range-dependent propagation loss, and scattering area, maps are averaged together on a pixel by pixel basis for a clear picture of major bathymetry. Measured backscattering strengths are used to estimate seamount heights for all major seamounts in a deep (5 km) basin to within + or - 1.3 km. This result is comparable to, or better than, that available from other wide area bathymetry surveying methods. All major (within about 2 km of the surface) seamounts can be detected and located to within + or - 20 km and smaller ones can be identified as well. Reported in detail are the analysis of BHST data for FY 1982-84. GRA

N88-20776# Naval Ocean Research and Development Activity, Bay St. Louis, Miss.
PREDICTIONS AND STUDIES WITH A ONE-DIMENSIONAL ICE/OCEAN MODEL Final Report
Shelley H. Riedlinger and Alex Warn-Varnas Apr. 1987 124 p
(AD-A189158; NORDA-195) Avail: NTIS HC A06/MF A01 CSCL 08C

A coupled one-dimensional ice/ocean model is developed in differential form. The ice/snow system is represented by the simplified thermodynamic model of Semtner and a dynamic approximation that neglects the internal stresses. The ocean is represented by the Mellor-Yamada Level- 2 turbulence mixed-layer model. The thermodynamic coupling considers a moving ice/ocean interface and salinity flux generated by the freezing or melting of ice. The dynamic coupling occurs via the turbulent stress that exists in the mixed-layer beneath the ice. The test cases are used for model validation and scientific studies. One is the standard climatological test used by Semtner and others. The other test case is with the AIDJEX data. The ice/ocean model is compared to Semtner's ice model to determine the effect of a variable-depth mixed layer as opposed to an isothermal, fixed-depth mixed layer. The sensitivity of the ice/ocean model to changes in certain parameters and forcing is also examined. Finally, the ability of the model simulate Arctic conditions is shown by comparison of model results of data obtained during AIDJEX. GRA

N88-20777# SACLANT ASW Research Center, La Spezia (Italy).
DEEP WATER MASS CIRCULATION IN THE ALBORAN BASIN. MEASUREMENTS - JANUARY TO APRIL 1982: ALBORAN 2
P. Pistek Sep. 1987 89 p
(AD-A189205; SACLANTCEN-SM-195) Avail: NTIS HC A05/MF A01 CSCL 08C

Alboran Sea circulation between 220 m and 1100 m depth is studied. Interactions among 3 sea water types, Atlantic water, Levantine water, and western Mediterranean deep water cause complicated flow patterns. Atlantic water flowing as a jet through the Strait of Gibraltar forms a variable anticyclonic gyre down to a depth of 200 m. Measurements by moored current meters and free-floating vertical current meters deployed and acoustically tracked in the western part of the Moroccan continental slope revealed an enhanced current along this slope toward Gibraltar. The study of the total deep circulation pattern in the Alboran basin used a combination of current meter and free float measurements. Tracks of the floats at all depths from 220 m to 1100 m revealed broad and slow (approx. 2.5 cm/s) cyclonic circulation located under the surface anticyclonic gyre. Floats revealed the boundary current along the Moroccan continental slope to have a complicated pattern, moving eastward or westward after reaching the slope east or west of 4.0 deg W respectively. The time-dependent vector field of currents created from all the float and current-meter readings shows periods of enhanced and extended cyclonic motion followed by stagnation and even reversal of current direction in external positions, with only the small cyclonic vortex. GRA

N88-20778# Massachusetts Inst. of Tech., Cambridge. Dept. of Earth Atmospheric and Planetary Sciences.
STUDIES TOWARD OBSERVING AND MODELLING LARGE ENERGETIC OCEAN REGIONS Annual Report, 1 Oct. 1986 - 30 Sep. 1987
Carl Wunsch 2 Nov. 1987 5 p
(Contract N00014-85-G-0241)
(AD-A189267) Avail: NTIS HC A02/MF A01 CSCL 08C

Studies have been made directed at: modelling high energy, near Gulf Stream regions; optimally combining data with general models, including inverse and control methods; reducing satellite data (altimetry and scatterometry) for combination into the models; and developing a new generation of operational tomographic instruments. GRA

N88-20779# Army Cold Regions Research and Engineering Lab., Hanover, N.H.
MICROWAVE AND STRUCTURAL PROPERTIES OF SALINE ICE
Anthony J. Gow, Steven A. Arcone, and Seth G. McGrew Oct. 1987 39 p
(AD-A189307; CRREL-87-20) Avail: NTIS HC A03/MF A01 CSCL 08L

The structure and salinity characteristics of saline ice slabs removed from ice sheets grown in an outdoor pool have been studied and related to the complex relative dielectric permittivity measured with free-space transmission techniques at 4.80 and 9.50 GHz. The saline ice closely simulated arctic sea ice in its structural and salinity characteristics, which were regularly monitored in a number of ice sheets grown during the winters of 1983, 1984 and 1985. In situ transmission measurements at similar frequencies were also made on the ice sheets themselves using antennas located above and beneath the ice. The slab measurements were made during warming from -29 to -2 C on slabs grown during the winter of 1983 and 1984 (4.75 GHz) and during a warming and cooling cycle over a slightly larger temperature range on slabs grown during the winter of 1984 and 1985 (4.80 and 9.50 GHz). GRA

N88-20780*# National Aeronautics and Space Administration. Goddard Space Flight Center, Greenbelt, Md.
TIDAL ESTIMATION IN THE PACIFIC WITH APPLICATION TO SEASAT ALTIMETRY
Braulio V. Sanchez and David E. Cartwright (National Academy of Sciences - National Research Council, Washington, D. C.) Dec. 1987 27 p
(NASA-TM-100694; Rept-88B0061; NAS 1.15:100694) Avail: NTIS HC A03/MF A01 CSCL 08C

The techniques for computing the eigenfunctions of the velocity potential (Proudman functions) set out in Sanchez, et al. (1986) in relation to the Atlantic-Indian Oceans are here applied to the Pacific Ocean, using a 6x6 degree grid of 510 points (455 points for the associated stream functions). Normal modes are computed from the first Proudman functions and have natural periods from 43.9h downward. Tidal syntheses are derived from these modes by direct application of the (frictionless) dynamic equations and by least-squares fitting of Proudman functions to the dynamically interpolated tide-gauge data of Schwiderski (1983). The modes contributing the most energy to the principal harmonic tidal constituents are different in the two computations: their natural periods are typically in the range of 9 to 16h for semidiurnal, and

14 to 43h for diurnal tides. The rms of fit for the Proudman functions is, in all cases, better than the corresponding value for the same number of spherical harmonics. Author

N88-20781# Miami Univ., Coral Gables, Fla. Div. of Meteorology and Physical Oceanography.
CIRCULATION AND EXCHANGE PROCESSES ON THE SOUTH ATLANTIC BIGHT CONTINENTAL SHELF Progress Report, 1 Jul. 1987 - 30 Jun. 1988
T. N. Lee Dec. 1987 33 p
(Contract DE-FG05-85ER-60355)
(DE88-003330; DOE/ER-60355/3) Avail: NTIS HC A03/MF A01

This report describes an investigation of the physical processes regulating the transport and exchange of materials in the shelf waters. The objective is to improve the capability for prediction of the physical environment. The principal scientific task is to determine the relative importance of the forces driving shelf circulation and exchange and to measure the shelf waters' response over variable time and space scales. The influence of physical processes on chemical and biological distributions and their interactions is studied through interdisciplinary investigations, joint analysis and interpretation of data and joint publications. DOE

N88-20782# Alaska Univ., Fairbanks. Geophysical Inst.
MECHANICAL PROPERTIES OF SEA ICE AND SEA ICE DEFORMATION IN THE NEAR-SHORE ZONE Final Report
L. H. Shapiro Dec. 1987 263 p Sponsored in part by Bureau of Land Management, Anchorage, Alaska
(Grant NA81RA-C-00046)
(PB88-147889) Avail: NTIS HC A12/MF A01 CSCL 08L

The areas of interest are the strength and mechanical properties of sea ice and ice deformation in the near-shore area. Objectives were to: (1) develop and test procedures and hardware required for in situ measurement of the strength and other mechanical properties of sea ice; (2) determine some aspects of the deformational behavior of sea ice; and (3) combine experimental results with existing data to define a stress-strain law and failure criterion for sea ice. Information was collected on uniaxial and biaxial compression, direct shear and indirect tension ice strength, ice-push and ice-override, ice sheet vibration as an indicator of rising stress levels, nearshore ice motion patterns, coefficients of static and kinetic friction between sea ice and unfrozen beach gravel, and correlation of ice movement with sea-bed ice gouges. GRA

N88-20783# National Oceanic and Atmospheric Administration, Boulder, Colo. Wave Propagation Lab.
SURVEY OF ACOUSTIC TECHNIQUES FOR MONITORING EL NINO
T. M. Georges, D. R. Palmer, R. M. Jones, and J. P. Riley Jan. 1988 61 p
(PB88-157615; NOAA-TM-ERL-WPL-149) Avail: NTIS HC A04/MF A01 CSCL 08C

The challenge of understanding the El Nino-Southern Oscillation (ENSO) cycle in the equatorial Pacific Ocean is a test of our abilities to observe, model and forecast the processes of global climate change. The author examines how the following acoustic techniques might be used to monitor ENSO-induced changes in the upper ocean: (1) ocean acoustic tomography; (2) a long-range acoustic thermometer; (3) passive monitoring of ambient acoustic noise level; (4) an occultation technique that depends on bottom absorption; and (5) space-time scintillation analysis. Pulse tomography, applied to vertical ocean slices, could adequately sample the temperature and currents in the upper ocean if appropriate receiving arrays were used. GRA

N88-20784 Minnesota Univ., Minneapolis.
EXPERIMENTAL AND THEORETICAL CONSTRAINTS ON THE ORIGIN OF MID-OCEAN RIDGE GEOTHERMAL FLUIDS Ph.D. Thesis
Michael Eugene Berndt 1987 168 p
Avail: Univ. Microfilms Order No. DA8727403

Hydrothermal experiments were performed using basalt, diabase, and two synthetic plagioclase bearing assemblages and Na-Ca-K-Cl fluids of seawater chlorinity at conditions from 350 to 425 C and 250 to 400 bars. Dissolved Ca, Na, SiO2 and pH appear to be controlled by equilibrium with plagioclase and epidote. High SiO2 activities during basalt alteration lead to high Ca and base metal concentrations and low pH compared to diabase alteration at the same conditions. Dissolved Li, K, Rb, and Ba concentrations reach higher levels during basalt alteration than during diabase alteration. These elements all precipitate to a small degree into secondary alteration phases, K, Rb, and Li in particular appear to be taken up in Mg-silicate alteration phases. Na-Ca-pH-SiO2 relationships in vent fluids can be used to constrain reaction zone conditions assuming the fluids are equilibrated with plagioclase and epidote. Calculations suggest that most of the vent fluids may be slightly undersaturated with respect to quartz in the reaction zone similar to what has been noted in diabase alteration experiments. Dissolved Sr/Ca ratios for ridge crest fluids are similar to those produced during diabase alterations and higher than those produced during basalt alteration. Dissert. Abstr.

N88-20785# Hawaii Univ., Honolulu. Inst. of Geophysics.
DYNAMICS OF THE OCEANIC SURFACE MIXED LAYER
Peter Muller, ed. and Diane Henderson, ed. 1987 308 p The 4th 'Aha Huliko'a Hawaiian Winter Workshop was held in Manoa, Hawaii, 14-16 Jan. 1987
(Grant N00014-87-G-0091)
(AD-A188348) Avail: NTIS HC A14/MF A01 CSCL 08C

Topics relative to the oceanic surface mixed layer are discussed. Equatorial turbulence, the mixed layer of the Western Equatorial Pacific Ocean, observations of waves and Langmuir circulation with Doppler sonars, mixed layer shears, horizontal scales of wind forced inertial motions and energy and momentum fluxes through the sea surface are among the topics considered. For individual titles, see N88-20786 through N88-20803.

N88-20786# Washington Univ., Seattle. Applied Physics Lab.
STRUCTURES AND FLUXES IN A DEEP CONVECTING MIXED LAYER
M. C. Gregg *In* Hawaii Univ., Dynamics of the Oceanic Surface Mixed Layer 1987 p 1-23 (For primary document see N88-20785 13-48)
Avail: NTIS HC A14/MF A01 CSCL 08C

A sequence of microstructure profiles observed a strongly convecting mixed layer deepen from 25 m to over 140 m in two days. Dissipation rates and overturning scales reveal mixing rates and mechanisms in the layer and in the entrainment zone below. Preliminary analysis shows the strong role of convection and of entrainment. Author

N88-20787# Washington Univ., Seattle. Applied Physics Lab.
EQUATORIAL TURBULENCE: MIXED LAYER AND THERMOCLINE
Hartmut Peters and Michael C. Gregg *In* Hawaii Univ., Dynamics of the Oceanic Surface Mixed Layer 1987 p 25-45 Sponsored in part by NSF (For primary document see N88-20785 13-48)
Avail: NTIS HC A14/MF A01 CSCL 08C

In November 1984, the equatorial undercurrent in the central Pacific was strongly developed with mean Richardson numbers as low as 1/4. Intense mixing in the shear zone above the core produced a diapycnal turbulent heat flux of 80 W m(-2). A diurnal cycle with changes in dissipation rates of a factor of 100 extended well into the thermocline. Internal waves radiating from the nighttime convecting mixed layer probably produced the deep component of the diurnal cycle. Owing to the low mean Richardson numbers, any additional shear from internal waves was likely to cause breaking. The depth-integrated dissipation rate between 15 m and the undercurrent core at 110 m was largest near the equator and smallest at plus or minus 1.5 degrees latitude. Author

N88-20788# Oregon State Univ., Corvallis. Coll. of Oceanography.
ON THE ZONAL MOMENTUM BALANCE AT THE EQUATOR
T. M. Dillon, J. N. Moum, T. K. Chereskin, and D. R. Caldwell *In* Hawaii Univ., Dynamics of the Oceanic Surface Mixed Layer 1987 p 47-66 (For primary document see N88-20785 13-48)
(Contract N00014-84-C-0218; Grant NSF OCE-82-14639)
Avail: NTIS HC A14/MF A01 CSCL 08C

It is shown that the momentum budget at 30 m depth and above on the equator at 140 degrees W cannot be balanced using typical estimates of large scale forces (zonal pressure gradients, upwelling of eastward momentum, convergence of westward momentum, and meridional eddy transport) and conventional estimates of the turbulent stress. Researchers believe that eddy viscosities estimated from measured dissipation rates must be treated with caution. Estimates of anomalies in the large scale forces which could explain the imbalance are unrealistically large, and do not have a realistic depth structure. It is possible that internal wave interactions play a crucial role in near surface equatorial dynamics, either by transporting momentum directly, or by radiating energy and invalidating the hypothesis of a local production-dissipation balance. Author

N88-20789# Hawaii Univ., Honolulu. Inst. of Geophysics.
THE MIXED LAYER OF THE WESTERN EQUATORIAL PACIFIC OCEAN
Roger Lukas and Eric Lindstrom (Commonwealth Scientific and Industrial Research Organization, Hobart, Australia) *In its* Dynamics of the Oceanic Surface Mixed Layer 1987 p 67-94 (For primary document see N88-20785 13-48)
(HIG-1861; IMA-87-0132) Avail: NTIS HC A14/MF A01 CSCL 08C

The new observations from the Western Equatorial Pacific Ocean Circulation Study show that the mixed layer in this important region is shallower than previously thought, averaging only about 30 m. This appears to be a result of strong pasitive buoyancy forcing associated with heavy precipitation combined with highly intermittent wind forcing. The vertical scale of temperature in the upper ocean of the western equatorial Pacific is larger than for salinity, which is probably a reflection of the larger zonal scale for SST along the equator than for precipitation. A hypothesis of subduction of saltier mixed layer waters from the east below the fresh mixed layer of the western equatorial Pacific appears to explain this aspect of the observations. Author

N88-20790# Scripps Institution of Oceanography, La Jolla, Calif. Marine Physical Lab.
OBSERVATIONS OF WAVES AND LANGMUIR CIRCULATION WITH DOPPLER SONARS
J. A. Smith and R. Pinkel *In* Hawaii Univ., Dynamics of the Oceanic Surface Mixed Layer 1987 p 95-118 (For primary document see N88-20785 13-48)
(Contract N00014-79-C-0472)
Avail: NTIS HC A14/MF A01 CSCL 08C

In October to November 1983, Doppler sonars mounted on the research platform FLIP were used to scatter 75 kHz sound from the underside of the sea surface at low angle, as well as from the interior of the mixed layer. Surface gravity waves were easily seen in velocity from the surface scattering sonar, even though the wave conditions were unusually calm. Valid measurements of sea surface motion were obtained over the range interval 600 to 1400 m from FLIP. A second sonar, which transmitted horizontally and scattered from the interior of the mixed layer, also sensed surface waves, although with amplitude reduced in proportion to the decay of the motions with depth. Wavenumber frequency spectra of the observed motions are consistent with linear theory. In addition, lower frequency motions were detected, which are consistent with Langmuir circulation. Author

N88-20791# Naval Postgraduate School, Monterey, Calif. Dept. of Oceanography.
UNSTEADY SHALLOWING MIXED LAYER
Roland W. Garwood, Jr. *In* Hawaii Univ., Dynamics of the Oceanic Surface Mixed Layer 1987 p 119-129 (For primary document see N88-20785 13-48)
Avail: NTIS HC A14/MF A01 CSCL 08C

The purpose was to examine the unsteady ocean surface mixed layer which shallows in response to a change in atmospheric forcing. An analytical analysis of the mechanical energy balance for an unsteady shallowing oceanic surface mixed layer with a downward surface buoyancy flux B sub o and a water surface friction velocity u sub asterisk provides insight into the relative roles of vertical mixing by turbulence generated within the Obukhov depth zone, L equals 2 u sub asterisk (3)/B sub o, and by turbulence generated by a mean flow dynamic instability below L. Author

N88-20792# Woods Hole Oceanographic Institution, Mass.
SOME EFFECTS OF HEATING ON THE WIND-DRIVEN VELOCITY IN THE UPPER OCEAN
James F. Price, Robert A. Weller, and Rebecca R. Schudlich *In* Hawaii Univ., Dynamics of the Oceanic Surface Mixed Layer 1987 p 131-139 (For primary document see N88-20785 13-48)
(Contracts N00014-76-C-0197; N00014-84-C-0134; NR 083-400; NR 083-400)
Avail: NTIS HC A14/MF A01 CSCL 08C

The relationship between the mean wind stress and the mean, wind driven, upper ocean velocity is analyzed using measurements made by a surface mooring in the open Sargasso Sea. Mean values are estimated by ensemble averaging daily averages which have been rotated to a common wind direction. Velocity is referenced to 50 m depth to suppress tides and eddies. The resulting mean velocity is strongly surface trapped and rotating slightly to the right with increasing depth. This vertical structure of the mean velocity spiral is a result of diurnal cycling, and can be simulated well by a one-dimensional model driven with the estimated wind stress and diurnally varying surface heat flux. Volume transport is within about 10 percent of that expected from a steady Ekman balance, and is nearly 90 degrees to the right of the wind. Author

N88-20793# Hawaii Univ., Honolulu. Dept. of Oceanography.
MIXED-LAYER SHEAR RELATED TO WIND STRESS IN THE CENTRAL EQUATORIAL PACIFIC
Fernando Santiago-Mandujano and Eric Firing *In its* Dynamics of the Oceanic Surface Mixed Layer 1987 p 141-152 (For primary document see N88-20785 13-48)
(Grant NSF OCE-83-14486)
Avail: NTIS HC A14/MF A01 CSCL 08C

Sixteen months of wind and current profile observations in the central equatorial Pacific show the response of the upper ocean shear to local wind forcing. The shear at the ocean surface is significantly correlated with the wind stress in direction, but not in magnitude. This implies that the vertical eddy viscosity coefficient is proportional to the square of the wind speed or to the stress. Using this variable eddy viscosity coefficient in Stommel's model of the Equatorial Undercurrent, researchers calculated shears in the mixed layer that compare well with the calculations. The flow is downwind of the equator and tends toward an Ekman spiral off the equator. The depth to which the model applies increases with the wind speed and is close to the Ekman depth at 2 degrees from the equator. The application of the model to the observations is insensitive to the method of estimating the layer depth.
Author

N88-20794# Woods Hole Oceanographic Institution, Mass.
MIXED-LAYER FRONTS IN THE CALIFORNIA CURRENT
Pierre Flament *In* Hawaii Univ., Dynamics of the Oceanic Surface Mixed Layer 1987 p 153-157 (For primary document see N88-20785 13-48)
Avail: NTIS HC A14/MF A01 CSCL 08C

Observations of the structure of the mixed layer in regions of large horizontal shear are presented. Cyclonic shears were found to be associated with strong surface convergences. Several possible driving mechanisms are proposed and scaled. Author

N88-20795# Washington Univ., Seattle. Applied Physics Lab.
HORIZONTAL SCALES OF WIND FORCED INERTIAL MOTIONS
Eric A. DAsaro *In* Hawaii Univ., Dynamics of the Oceanic Surface Mixed Layer 1987 p 159-179 (For primary document see N88-20785 13-48)
(Contract N00014-84-C-0111)
Avail: NTIS HC A14/MF A01 CSCL 08C

Wind forced upper ocean inertial motions are simulated using a theory appropriate for regions of low oceanic mesoscale activity with the goal of identifying the causes of horizontal variability in inertial currents. Mixed layer inertial currents are modeled as a uniform slab forced by wind stress. The subsequent evolution of these currents and their propagation below the mixed layer is analyzed using a perturbation analysis of the linearized equations. The resulting equations allow only near-inertial frequency dynamics and suppress other classes of motion. Author

N88-20796# Florida State Univ., Tallahassee. Dept. of Oceanography.
SUBDUCTION
Benoit Cushman-Roisin *In* Hawaii Univ., Dynamics of the Oceanic Surface Mixed Layer 1987 p 181-196 (For primary document see N88-20785 13-48)
Avail: NTIS HC A14/MF A01 CSCL 08C

The purpose is to elucidate the kinematics and dynamics of subduction (and of its twin process, entrainment) by inductive reasoning through a series of increasingly more comprehensive models. Some likely pitfalls (e.g., the common belief that the rate of suduction is the Ekman pumping velocity) are identified, and several dimensionless numbers are noted. Author

N88-20797# Washington Univ., Seattle. School of Oceanography.
WIND FORCING AND OBSERVED OCEANIC WAVENUMBER SPECTRA
Charles C. Eriksen *In* Hawaii Univ., Dynamics of the Oceanic Surface Mixed Layer 1987 p 197-205 (For primary document see N88-20785 13-48)
Avail: NTIS HC A14/MF A01 CSCL 08C

If internal waves are forced by wind stress applied as a body force in a surface layer, their spectrum has a vertical wavenumber shape of the Garrett-Munk internal wave spectrum. Bandwidth and high wavenumber shape are functions of the layer thickness and shape, respectively. Conversely, if the Garrett-Munk wavenumber shape is determined by wind forced waves at near inertial frequencies, then the observed shape implies that the vertical gradient of stress from the surface is nearly uniform and cuts off sharply at a depth comparable to observed seasonal thermocline depths. Author

N88-20798# Royal Netherlands Meteorological Inst., De Bilt.
ENERGY AND MOMENTUM FLUXES THROUGH THE SEA SURFACE
Gerbrand Komen *In* Hawaii Univ., Dynamics of the Oceanic Surface Mixed Layer 1987 p 207-217 (For primary document see N88-20785 13-48)
(Grant NATO-523/85)
Avail: NTIS HC A14/MF A01 CSCL 08C

Progress in the understanding of the energy and momentum balance in wind driven surface waves is discussed. A new estimate is given for the energy and momentum flux to and from the waves. Author

N88-20799# La Jolla Inst., Calif. Center for Studies of Nonlinear Dynamics.
HAMILTONIAN DESCRIPTION OF THE INTERACTION OF SURFACE WAVES WITH MIXED-LAYER CURRENTS
Frank S. Henyey and Jon Wright *In* Hawaii Univ., Dynamics of the Oceanic Surface Mixed Layer 1987 p 219-228 (For primary document see N88-20785 13-48)
Avail: NTIS HC A14/MF A01 CSCL 08C

The Hamiltonian for the dynamics of water motion with a free surface is constructed by combining the irrotational flow surface Hamiltonian and the interior rotational flow Hamiltonian. This Hamiltonian is then specialized to the effect of a depth dependent current on small amplitude surface waves. The dispersion relation and an associated variational principle are presented. The modification of the gravity-capillary group velocity by wind drift layer is remarkable. Author

N88-20800# Scripps Institution of Oceanography, La Jolla, Calif. Space Inst.
RADIATIVE PROCESSES AFFECTING OCEAN MIXED-LAYER HEAT CONTENT AND THEIR MONITORING FROM SATELLITE
Catherine Gautier *In* Hawaii Univ., Dynamics of the Oceanic Surface Mixed Layer 1987 p 229-247 (For primary document see N88-20785 13-48)
(Contract N00014-86-K-0752; Grant NSF OCE-82-14791)
Avail: NTIS HC A14/MF A01 CSCL 08C

Radiation flux observations (satellite and surface) from various studies are examined to assess their possible roles in modifying the ocean's mixed layer heat content. Several processes are investigated. First, observations indicate that the magnitude and extent of sea surface temperature (SST) diurnal warming events (changes of up to 3 degrees C), which affect air-sea heat fluxes, can be effectively monitored by satellite. Second, although still not well understood, a mechanism is suggested that would involve convective lines in upper ocean turbulent mixing generation. The mechanism has a strong diurnal variability, resulting in nighttime cooling in bursts concurrent with wind stress bursts, and might generate bursts of turbulent mixing. Third, mixings effect on photosynthesis and the potential influence of photoplankton distribution on mixing and thermal stratification are discussed. Lastly, several satellite methods for computing net surface radiation flux are reviewed and assessed. Author

N88-20801# National Center for Atmospheric Research, Boulder, Colo.
MONITORING OCEAN SURFACE LAYER PROCESSES
W. G. Large *In* Hawaii Univ., Dynamics of the Oceanic Surface Mixed Layer 1987 p 249-263 (For primary document see N88-20785 13-48)
Avail: NTIS HC A14/MF A01 CSCL 08C

The monitoring of several upper ocean processes over large spatial scales on monthly and longer time scales is discussed. The surface forcing functions of wind stress, heat flux, and freshwater flux are treated in terms of the potential roles that in situ observations, satellites and atmospheric general circulation models might play in producing the most useful fields on a regular basis globally. Thermocline mixing and daily cycling are presented as examples of phenomena that, once understood from intensive regional studies, could be observed from a much wider perspective using relatively easily measured data. Specifically, episodic cooling, a symptom of intense thermocline mixing in the North Pacific during autumn, appears to occur over large regions of the Southern Hemisphere, depending on the annual cycle of wind forcing. Also, the daily cycle of equatorial oceanic turbulence seen in the short Tropic Heat study of 1984 appears to persist throughout the year over 20 degrees of longitude. A similar cycle is not evident during heating season in the Sargasso Sea. Author

N88-20802# Pennsylvania State Univ., University Park. Dept. of Meteorology.
SIMILARITY THEORIES AND MICROTURBULENCE IN THE ATMOSPHERIC MIXED LAYER
C. W. Fairall *In* Hawaii Univ., Dynamics of the Oceanic Surface Mixed Layer 1987 p 265-290 (For primary document see N88-20785 13-48)
(Contracts N00014-85-K-0250; N00014-86-K-0688; Grant AF-AFOSR-0049-86)
Avail: NTIS HC A14/MF A01 CSCL 08C

The cloud-free, convective mixed layer is the simplest and best understood atmospheric boundary layer regime. Many of the mean and turbulent properties can be well represented by similarity

models based on scaling in terms of the basic forcing processes (e.g., the surface and tropospheric interfacial fluxes). The boundary layer can be divided into three scaling height regimes which, historically, are described with different scaling models: the surface layer (Monin-Obukhov similarity), the mixed layer (top-down/bottom-up diffusion), and the inversion layer (Wyngaard-Lemone entrainment similarity). These models are known to be particularly successful when used to describe the small scale turbulence properties (dissipation rates and structure function parameters for velocity and passive scalers). Combined with these simple models, measurement of small scale turbulence can be used to infer surface fluxes, entrainment rate, and flux profiles. Author

N88-20803# Hawaii Univ., Honolulu. Dept. of Oceanography.
GLOBAL MIXED-LAYER NATURAL AND ANTHROPOGENIC FLUXES
Fred T. Mackenzie *In its* Dynamics of the Oceanic Surface Mixed Layer 1987 p 291-310 (For primary document see N88-20785 13-48)
(Grant ACE-PRF-17371-AC2)
Avail: NTIS HC A14/MF A01 CSCL 08C

The oceanic surface mixed layer is generally the initial reservoir for materials that enter the ocean from the land and atmosphere. Here, a number of global biogeochemical cycles of dissolved constituents, gases and particulates are portrayed. Some brief comments are made concerning the role of the mixed layer in the cycling behavior in the ocean of the chemical species H, O, C, N, P, S, Ca, Si, and As, and of particulate materials. It is demonstrated that the open ocean mixed layer can undergo chemical changes induced by perturbations of processes and fluxes on land on a time scale of decades. These perturbations may result from natural causes or may be due to the industrial and agricultural activities of society. Author

N88-20804# Royal Netherlands Meteorological Inst., De Bilt. Oceanografisch Onderzoek.
EVALUATION OF WAVE CALCULATIONS USING GONO IN THE PERIOD OCTOBER 1985 - APRIL 1986 [EVALUATIE VAN DE GOLFBEREKENINGEN MET GONO OVER DE PERIODE OKTOBER 1985 - APRIL 1986]
E. Bouws, G. J. Komen, P. Kruseman, and R. A. vanMoerkerken 1986 68 p In DUTCH; ENGLISH summary
(KNMI-TR-96; B8715224; ISSN-0169-1708; ETN-88-91339)
Copyright Avail: NTIS HC A04/MF A01

Results of the wave model GONO on wave height, low frequency wave height, wind velocity, and wind direction were compared with observations. The comparison was made for the period October 1985 until April 1986 for the following locations: Euro, Ymuiden, and Pennzoil in the southern North Sea, and Auk and Brent in the northern North Sea. The time series, contained in a separate supplement, are discussed. The quality of the GONO forecasts are stable, and the limit of what is attainable with such a model is reached. ESA

N88-20675# Joint Publications Research Service, Arlington, Va.
DETERMINATION OF MEAN THERMOHALINE CHARACTERISTICS OF THE OCEAN Abstract Only
S. A. Dobrolyubov *In its* JPRS Report: Science and Technology. USSR: Earth Sciences 26 Feb. 1988 p 1 Transl. into ENGLISH from Vestnik Moskovskogo Universiteta, Seriya 5: Geografiya (Moscow, USSR), no. 3, May - Jun. 1987 p 65-71 (For primary document see N88-20674 13-42)
Avail: NTIS HC A04/MF A01

N88-20676# Joint Publications Research Service, Arlington, Va.
SPECTRAL REFLECTIVE CHARACTERISTICS OF SEA SURFACE Abstract Only
V. V. Kazaryan and V. P. Korovin *In its* JPRS Report: Science and Technology. USSR: Earth Sciences 26 Feb. 1988 p 1-2 Transl. into ENGLISH from Vestnik Leningradskogo Universiteta, Seriya 7: Geologiya, Geografiya (Leningrad, USSR), no. 1, Mar. 1987 p 97-99 (For primary document see N88-20674 13-42)
Avail: NTIS HC A04/MF A01

N88-20678# Joint Publications Research Service, Arlington, Va.
MUSHROOM-SHAPED CURRENTS (EDDY DIPOLES) UNDER ROTATION AND STRATIFICATION CONDITIONS Abstract Only
A. I. Ginzburg, A. G. Kostyanoy, A. M. Pavlov, and K. N. Fedorov *In its* JPRS Report: Science and Technology. USSR: Earth Sciences 26 Feb. 1988 p 3 Transl. into ENGLISH from Doklady Akademii Nauk SSSR (Moscow, USSR), v. 292, no. 4, Feb. 1987 p 971-974 (For primary document see N88-20674 13-42)
Avail: NTIS HC A04/MF A01

N88-20679# Joint Publications Research Service, Arlington, Va.
ESTIMATES OF OCEAN-ATMOSPHERE THERMAL INTERACTION IN GULF STREAM ENERGY-ACTIVE TEST RANGE IN WINTER OF 1984 Abstract Only
S. S. Yefimov, G. G. Panteleyev, and Ye. V. Semenov *In its* JPRS Report: Science and Technology. USSR: Earth Sciences 26 Feb. 1988 p 3-4 Transl. into ENGLISH from Izvestiya Akademii Nauk SSSR: Fizika Atmosfery i Okeana (Moscow, USSR), v. 23, no. 3, Mar. 1987 p 309-313 (For primary document see N88-20674 13-42)
Avail: NTIS HC A04/MF A01

N88-20680# Joint Publications Research Service, Arlington, Va.
DETERMINING LANGMUIR CIRCULATION PARAMETERS ON BASIS OF SIMILARITY THEORY Abstract Only
V. P. Krasitskiy and B. N. Filyushkin *In its* JPRS Report: Science and Technology. USSR: Earth Sciences 26 Feb. 1988 p 4-5 Transl. into ENGLISH from Izvestiya Akademii Nauk SSSR: Fizika Atmosfery i Okeana (Moscow, USSR), v. 23, no. 3, Mar. 1987 p 293-299 (For primary document see N88-20674 13-42)
Avail: NTIS HC A04/MF A01

N88-20681# Joint Publications Research Service, Arlington, Va.
THERMODYNAMIC THEORY OF FLUCTUATIONS AND RAYLEIGH LIGHT SCATTERING IN SOLUTIONS Abstract Only
V. A. Durov *In its* JPRS Report: Science and Technology. USSR: Earth Sciences 26 Feb. 1988 p 5 Transl. into ENGLISH from Vestnik Moskovskogo Universiteta, Seriya 2: Khimiya (Moscow, USSR), v. 28, no. 1, Jan. - Feb. 1987 p 54-61 (For primary document see N88-20674 13-42)
Avail: NTIS HC A04/MF A01

N88-20682# Joint Publications Research Service, Arlington, Va.
RESEARCH ON INFLUENCE OF INDIVIDUAL SEA WATER COMPONENTS ON SPECTRAL BRIGHTNESS COEFFICIENT OF OUTGOING RADIATION Abstract Only
Ye. K. Naumenko *In its* JPRS Report: Science and Technology. USSR: Earth Sciences 26 Feb. 1988 p 6 Transl. into ENGLISH from Zhurnal Prikladnoy Spektroskopii (Minsk, USSR), v. 46, no. 1, Jan. 1987 p 80-86 (For primary document see N88-20674 13-42)
Avail: NTIS HC A04/MF A01

N88-20684# Joint Publications Research Service, Arlington, Va.
NUMERICAL MODELING OF WAVE MIGRATION OF SEISMIC DATA Abstract Only
V. V. Perekhvatov, Yu. A. Byakov, V. A. Kemelman, and G. F. Seleznev *In its* JPRS Report: Science and Technology. USSR: Earth Sciences 26 Feb. 1988 p 7 Transl. into ENGLISH from Geologiya i Geofizika (Novosibirsk, USSR), no. 2, Feb. 1987 p 99-106 (For primary document see N88-20674 13-42)
Avail: NTIS HC A04/MF A01

N88-20686# Joint Publications Research Service, Arlington, Va.
PROPAGATION OF SUBSURFACE SALINITY MAXIMUM IN TROPICAL ATLANTIC Abstract Only
S. Ye. Navrotskaya and V. F. Dubravin *In its* JPRS Report: Science and Technology. USSR: Earth Sciences 26 Feb. 1988 p 11 Transl. into ENGLISH from Okeanologiya (Moscow, USSR),

v. 27, no. 2, Mar. - Apr. 1987 p 197-203 (For primary document see N88-20674 13-42)
Avail: NTIS HC A04/MF A01

N88-20687# Joint Publications Research Service, Arlington, Va.
SPACE-TIME ANALYSIS OF OCEANOGRAPHIC FIELDS BY MODIFIED EMPIRICAL ORTHOGONAL FUNCTIONS METHOD Abstract Only
A. O. Artemyev *In its* JPRS Report: Science and Technology. USSR: Earth Sciences 26 Feb. 1988 p 12 Transl. into ENGLISH from Okeanologiya (Moscow, USSR), v. 27, no. 2, Mar. - Apr. 1987 p 204-211 (For primary document see N88-20674 13-42)
Avail: NTIS HC A04/MF A01

N88-20688# Joint Publications Research Service, Arlington, Va.
INTRATHERMOCLINE LENS OF MEDITERRANEAN WATER IN TROPICAL NORTH ATLANTIC Abstract Only
V. D. Yegorikhin, Yu. A. Ivanov, V. G. Kort, M. N. Koshlyakov, Yu. F. Lukashev, Ye. G. Morozov, I. M. Ovchinnikov, V. T. Paka, T. B. Tsybaneva, and I. F. Shadrin et al. *In its* JPRS Report: Science and Technology. USSR: Earth Sciences 26 Feb. 1988 p 16 Transl. into ENGLISH from Okeanologiya (Moscow, USSR), v. 27, no. 2, Mar. - Apr. 1987 p 165-175 (For primary document see N88-20674 13-42)
Avail: NTIS HC A04/MF A01

N88-20689# Joint Publications Research Service, Arlington, Va.
DYNAMICS OF SYNOPTIC OCEAN EDDIES Abstract Only
M. N. Koshlyakov *In its* JPRS Report: Science and Technology. USSR: Earth Sciences 26 Feb. 1988 p 18-19 Transl. into ENGLISH from Vestnik Akademii Nauk SSSR (Moscow, USSR), no. 2, Feb. 1987 p 22-35 (For primary document see N88-20674 13-42)
Avail: NTIS HC A04/MF A01

N88-20692# Joint Publications Research Service, Arlington, Va.
EXPERIENCE WITH AND WAYS TO UPGRADE ACCURACY OF HYDROMAGNETIC SURVEYS IN OCEAN Abstract Only
N. N. Rzhevskiy *In its* JPRS Report: Science and Technology. USSR: Earth Sciences 26 Feb. 1988 p 23 Transl. into ENGLISH from Ekspress-Informatsiya. Seriya: Morskaya Geologiya i Geofizika (Moscow, USSR), no. 12, 1986 p 1-4 (For primary document see N88-20674 13-42)
Avail: NTIS HC A04/MF A01

N88-20693# Joint Publications Research Service, Arlington, Va.
VERTICAL TURBULENT TRANSFER OF MATTER IN THIN OCEAN SURFACE LAYER DURING DAYTIME HEATING Abstract Only
K. A. Korotenko *In its* JPRS Report: Science and Technology. USSR: Earth Sciences 26 Feb. 1988 p 25 Transl. into ENGLISH from Okeanologiya (Moscow, USSR), v. 27, no. 1, Jan. - Feb. 1987 p 47-51 (For primary document see N88-20674 13-42)
Avail: NTIS HC A04/MF A01

N88-20694# Joint Publications Research Service, Arlington, Va.
PHENOMENOLOGICAL DESCRIPTION OF EDDY REGISTERED IN GULF STREAM Abstract Only
V. A. Bubnov, N. P. Kuzmina, and I. S. Podymov *In its* JPRS Report: Science and Technology. USSR: Earth Sciences 26 Feb. 1988 p 26 Transl. into ENGLISH from Okeanologiya (Moscow, USSR), v. 27, no. 1, Jan. - Feb. 1987 p 25-29 (For primary document see N88-20674 13-42)
Avail: NTIS HC A04/MF A01

N88-20695# Joint Publications Research Service, Arlington, Va.
CONTRIBUTION TO THEORY OF QUASIGEOSTROPHIC MOTIONS OF FINITE AMPLITUDE IN VISCOUS STRATIFIED OCEAN Abstract Only
G. I. Shapiro *In its* JPRS Report: Science and Technology. USSR: Earth Sciences 26 Feb. 1988 p 27 Transl. into ENGLISH from Okeanologiya (Moscow, USSR), v. 27, no. 1, Jan. - Feb. 1987 p 18-24 (For primary document see N88-20674 13-42)
Avail: NTIS HC A04/MF A01

N88-20697# Joint Publications Research Service, Arlington, Va.
RESEARCH ON TURBULENCE IN BOTTOM BOUNDARY LAYER IN OCEAN Abstract Only
V. N. Nabatov and R. V. Ozmidov *In its* JPRS Report: Science and Technology. USSR: Earth Sciences 26 Feb. 1988 p 29 Transl. into ENGLISH from Okeanologiya (Moscow, USSR), v. 27, no. 1, Jan. - Feb. 1987 p 5-11 (For primary document see N88-20674 13-42)
Avail: NTIS HC A04/MF A01

N88-20698# Joint Publications Research Service, Arlington, Va.
INVARIANT CHARACTERISTICS OF ACOUSTIC FIELD IN STRATIFIED OCEAN Abstract Only
B. A. Kasatkin *In its* JPRS Report: Science and Technology. USSR: Earth Sciences 26 Feb. 1988 p 30 Transl. into ENGLISH from Doklady Akademii Nauk SSSR (Moscow, USSR), v. 291, no. 6, Dec. 1986 p 1483-1487 (For primary document see N88-20674 13-42)
Avail: NTIS HC A04/MF A01

N88-20699# Joint Publications Research Service, Arlington, Va.
STUDY OF SPECTRA OF SEA WAVES ON HORIZONTALLY NONUNIFORM CURRENT IN RIP ZONE Abstract Only
I. A. Leykin *In its* JPRS Report: Science and Technology. USSR: Earth Sciences 26 Feb. 1988 p 33 Transl. into ENGLISH from Izvestiya Akademii Nauk SSSR: Fizika Atmosfery i Okeana (Moscow, USSR), v. 23, no. 1, Jan. 1987 p 52-58 (For primary document see N88-20674 13-42)
Avail: NTIS HC A04/MF A01

N88-20700# Joint Publications Research Service, Arlington, Va.
MODEL OF HYDRODYNAMIC ADJUSTMENT OF TEMPERATURE, SALINITY AND CURRENT FIELDS Abstract Only
A. S. Sarkisyan, Yu. L. Demin, and D. I. Trukhchev *In its* JPRS Report: Science and Technology. USSR: Earth Sciences 26 Feb. 1988 p 34 Transl. into ENGLISH from Izvestiya Akademii Nauk SSSR: Fizika Atmosfery i Okeana (Moscow, USSR), v. 23, no. 1, Jan. 1987 p 45-51 (For primary document see N88-20674 13-42)
Avail: NTIS HC A04/MF A01

51 LIFE SCIENCES (GENERAL)

N88-20805# Pennsylvania Hospital, Philadelphia. Dept. of Molecular Biology.
MOLECULAR AND ELECTRONIC MECHANISM IN THE CONTROL OF Na+ AND K+ PERMEABILITY OF EXCITABLE CELL MEMBRANE BY LIGAND BINDING ON RECEPTOR SITES Annual Report, 1 Jul. 1986 - 31 Oct. 1987
Gilbert N. Ling 12 Nov. 1987 7 p
(Contract N00014-85-K-0573; Proj. RR0-4108)
(AD-A188725) Avail: NTIS HC A02/MF A01 CSCL 06A

Our objective is to investigate the control of cell membrane permeability to Sodium (Na+), Potassium (K+), and other ions by transmitters, drugs, and other biologically potent ligands: to extend and test a general electronic theory of the control of physiological activities. GRA

N88-20806# California Univ., Berkeley. Lawrence Berkeley Lab.
BIOPHYSICAL APPLICATIONS OF SOLID STATE AND TRITIUM NMR Ph.D. Thesis
Sun Un Oct. 1987 193 p
(Contract DE-AC03-76SF-00098)
(DE88-005328; LBL-24384) Avail: NTIS HC A09/MF A01

Novel applications of Magic Angle Sample Spinning (MASS) and Tritium (H-3) NMR to the study of mammalian tissue and in vivo metabolism, respectively, are described. The solid state P-31 MASS NMR spectra of sodium, magnesium, and calcium complexes of adenosine triphosphate (ATP) were recorded. These spectra indicate that the terminal phosphate group of the sodium complex is protonated in contrast to the unprotonated divalent complexes. The chemical shift tensors of a large variety of phosphates and phosphate esters were measured. The magnitude of the sigma sub 33, the low field, elements of the P-31 chemical shift tensors in these phosphates were linearly related to the longest P-O bonds and the sigma sub 11, the high field, elements to the shortest bonds. Similar relationships were found when these tensor elements were plotted against bond angles. The implications of these observations are discussed in the context of phosphorus-oxygen d-p pi bonding interactions. The P-31 and H-1 MASS NMR were applied to the study of lyophilized rat tissue. The ^{31}P spectra exhibit resonances from phospholipids, DNA, ATP and NAD. The MASS results were compared to chemical analysis data obtained by others and to calculated spectra based on MASS data of model compounds. The H-1 MASS spectra of these tissue samples exhibited lines with widths less than 40 Hz, and were assigned to phospholipid protons. The intensity distribution of the H-1 spectra supported this assignment. Motionally narrowed P-31 and H-1 resonances suggest that the phospholipids undergo varying degrees of motion with correlation times ranging from 0.5 ns to 2 microsec. The degree of hydration of the DNA was also established. DOE

N88-20807*# National Aeronautics and Space Administration, Washington, D.C.
USE OF DIPHOSPHONATES TO CORRECT DISORDERS IN CALCIUM METABOLISM AND MINERAL COMPOSITION OF BONE TISSUE WITH 60-DAY HYPOKINESIA IN RATS
B. V. Morukov, V. Ye. Zaychik, V. M. Ivanov, and O. I. Orlov Mar. 1988 12 p Transl. into ENGLISH from Patologicheskaya Fiziologiya i Eksperimental'naya Terapiya (USSR), no. 2, 1987 p 75-77 Transl. by Scientific Translation Service, Santa Barbara, Calif.
(Contract NASw-4307)
(NASA-TT-20220; NAS 1.77:20220) Avail: NTIS HC A03/MF A01 CSCL 06C

Compounds of the diphosphonate group suppress bone resorption and bone tissue metabolism, from which it was assumed that they can be used for the prevention of osteoporosis and disorders of calcium homeostasis in humans during space flight. Two compounds of this group were used for preventive purposes in 60 day hypokinesia in rats. The results showed that diphosphonates have a marked effect on calcium metabolism and the condition of the bone tissues under conditions of long term hypokinesia: they reduce the content of ionized calcium in blood, delay the loss of calcium and phosphorus by the bone tissue, and to a considerable degree prevent reduction of bone density. This confirms the possibility of using compounds of this group for correcting and preventing changes of bone tissue and mineral metabolism during long term hypokinesia. Author

52 AEROSPACE MEDICINE

Includes physiological factors; biological effects of radiation; and effects of weightlessness on man and animals.

N88-20808# Naval Health Research Center, San Diego, Calif.
LIFTING AND CARRYING CAPACITIES RELATIVE TO PHYSICAL FITNESS MEASURES Final Report
Marcie B. Beckett and James A. Hodgdon 21 Oct. 1987 49 p
(AD-A189305; NHRC-87-26) Avail: NTIS HC A03/MF A01 CSCL 05I

Through the Physical Readiness Test (PRT), the Navy assesses the physical fitness and body composition of its members. Those fitness attributes which contribute to optimal Navy job performance have not yet been fully identified. The purpose of this study was to determine the extent to which performance of simulated general shipboard work can be predicted by measures of physical capacity. Three tasks representative of general shipboard work were developed - a long duration carry and two maximal box lifting tests. These tasks, as well as, PRT items (including lean body mass LBM from body circumference and weight), other field fitness measures, and Incremental Lift Machine (ILM) tests were performed by 102 Navy men and women. Substitution of broad jump score for LBM offers a small improvement in task prediction. ILM scores offer lift capacity prediction comparable to that obtained from PRT and broad jump scores. LBM, broad jump and ILM scores are all strong indicators of overall body strength. If these prediction methods are to be implemented as screening or selection tools, critical lifting and carrying task parameters for Navy jobs must be defined. In addition, further research is needed to cross-validate results obtained in this study and to expand prediction application. GRA

N88-20809# Letterman Army Inst. of Research, San Francisco, Calif.
PURSUIT TRACKING PERFORMANCE DECREMENTS ASSOCIATED WITH DECREASING AMBIENT ILLUMINATION Final Report, Feb. - Jul. 1987
Jerome W. Molchany, David A. Stamper, and David J. Lund Aug. 1987 30 p
(AD-A189336; LAIR-243) Avail: NTIS HC A03/MF A01 CSCL 17E

Reduction in ambient illumination alters one's ability to acquire and track moving targets. In this study we have attempted to describe the relationship between decreasing ambient illumination and pursuit tracking performance. Eight male volunteers used an optical tracking device to track targets at a constant angular velocity of 5 mrad/sec under bright and reduced ambient light levels in the BLASER tracking simulator. Reduction of the ambient light level was accomplished by inserting neutral density filters into the optics of the tracking device. Volunteers were assigned randomly to a schedule of 6 levels of reduced ambient illumination. Analysis of Variance for the Percent Time-on-Target (Percent TOT), horizontal Root Mean Square (RMS) error, and Maximum Absolute Error (MAE) revealed highly significant main effects. Ambient light levels below 0.075 cd/sq.m. produced large tracking error scores (e.g., Percent TOT less than 68 percent). The use of direct view optics below luminance levels of 0.18 cd/sq.m. could seriously jeopardize the success of the mission. GRA

N88-20810# Army Research Inst. of Environmental Medicine, Natick, Mass.
PLASMA CORTISOL, RENIN AND ALDOSTERONE DURING AN INTENSE HEAT ACCLIMATION PROGRAM
Lawrence E. Armstrong, Ralph P. Francesconi, William J. Kraemer, Natalie Leva, and Jane P. DeLuca Sep. 1987 20 p
(AD-A189387) Avail: NTIS HC A03/MF A01 CSCL 06J

The effects of an intense, intermittent heat acclimation (HA) regimen on stress and fluid balance hormones responses were examined in 13 unacclimated male volunteers. Venous blood samples were collected before (PRE) and after (POST) exercise and analyzed for plasma renin activity (PRA), aldosterone (ALD), cortisol (PC), plasma volume shifts (delta PV percent), sodium (Na+) and potassium (K+). Subjects exhibited physiological adaptions typical of HA decreased heart rate, rectal temperature, skin temperature, and improved defense of PV. While plasma Na+ demonstrated no change during daily exercise, K+, PC, PRA, and ALD increased more than delta PV percent accounted for. PRA and ALD did not change as a result of HA, but PRE vs POST PC responses were attenuated. The dissociation of PRA and ALD levels on day 4 of HA (POST) may be explained by differences in splanchnic clearance mechanisms. It was concluded that during an intense HA regimen, electrolyte and hormonal responses to exercise in the heat are modulated by the acquisition of acclimation. GRA

N88-20811# Air Force Inst. of Tech., Wright-Patterson AFB, Ohio. School of Engineering.
RETINOTOPIC MAPPING OF THE HUMAN VISUAL SYSTEM WITH MAGNETOENCEPHALOGRAPHY M.S. Thesis
Michael G. Dowler Dec. 1987 72 p
(AD-A189557; AFIT/GEP/ENP/87D-6) Avail: NTIS HC A04/MF A01 CSCL 06D

A retinotopic mapping was verified using magnetoencephalography as the means to observe brain activity in one human subject. The stimulus consisted of 12 sectors of a hemicircle, 6 foveal and 6 peripheral out to about 17 degrees visual field angle. The sectors flashed individually for 63 milliseconds with an inter-stimulus-interval between .8 and 1.8 seconds. The recording computer was syncronized to the stimulus and recorded for .5 seconds after onset of stimulus. Thirty averages were taken for each stimulus section, for each of about 45 grid points on the scalp. The sectors were localized to distinct points in the primary visual cortex (area 17). The results did not verify the cruciform model of retinotopic mapping nor the theory that more visually eccentric stimuli produce deeper responses. The data seem to suggest and different type of mapping for foveal stimuli than peripheral, but this could also be due to the fold structure of the primary visual cortex. GRA

N88-20812# Air Force Inst. of Tech., Wright-Patterson AFB, Ohio. School of Engineering.
AN ANALYSIS OF PHYSIOLOGICAL DATA RELATED TO MOTION SICKNESS FOR USE IN A REAL-TIME MOTION SICKNESS INDICATOR M.S. Thesis
Michael E. Drylie Dec. 1987 86 p
(AD-A189589; AFIT/GE/ENG/87D-16) Avail: NTIS HC A05/MF A01 CSCL 06E

The goal of this thesis project was to continue to collect physiological data on volunteers as motion sickness was induced, analyze the data collected, test and improve motion sickness indicators previously developed, for use in a real-time processor, and develop a method for testing the susceptibility to motion sickness for individuals. The existing data acquisition system was modified to produce better accuracy of the measured data. Additional sensors were added, sensor types and placements were modified. Circuits were modified to prevent overloading and to allow better tracking of the full range of expected physiological data points. Previous indicators were evaluated as to their accuracy and degree of their usefulness in a real-time processor. A susceptibility test was developed to allow the classification of a person as to their level of motion sickness susceptibility. Physiological data were analyzed on the basis of their relationship with the onset of motion sickness, to develop a motion sickness indicator. GRA

N88-20813*# National Aeronautics and Space Administration, Washington, D.C.
CHANGES IN THE STATUS OF THE HUMAN TIBIA DURING ANTIORTHOSTATIC HYPOKINESIA
A. M. Tatarinov, A. I. Grigoryev, V. V. Dzenis, Kh. A. Yanson, V. S. Oganov, and A. S. Rakhmanov Mar. 1988 20 p Transl. into ENGLISH from Mekhanika Kompozitnykh Materialov (Riga, USSR, Zimatne), 1986 p 134-143 Transl. by Scientific Translation Service, Santa Barbara, Calif.
(Contract NASw-4307)
(NASA-TT-20221; NAS 1.77:20221) Avail: NTIS HC A03/MF A01 CSCL 06P

Changes were studied in biomechanical properties of the human tibia during prolonged antiorthostatic hypokinesia with different modes of motor activity and pharmacotherapy and comparison of results obtained with parallel examinations using ultrasonic diagnosis and photon absorptiometry. Author

N88-20814* National Aeronautics and Space Administration, Washington, D.C.
AEROSPACE MEDICINE AND BIOLOGY: A CONTINUING BIBLIOGRAPHY WITH INDEXES (SUPPLEMENT 309)
Apr. 1988 57 p
(NASA-SP-7011(309); NAS 1.21:7011(309)) Avail: NTIS HC A04 CSCL 06E

This bibliography lists 136 reports, articles and other documents introduced into the NASA scientific and technical information system in February, 1988. Author

N88-20815 Joint Publications Research Service, Arlington, Va.
JPRS REPORT: SCIENCE AND TECHNOLOGY. USSR: LIFE SCIENCES Abstracts Only
15 Mar. 1988 36 p Transl. into ENGLISH from various Russian articles
(JPRS-ULS-88-004) Copyright Avail: Issuing Activity

Translations of scientific and technological articles from Russian journals, books, and other publications are presented. The subject heading is Life Sciences. Subheadings include: Biochemistry, Biophysics, Biotechnology, Epidemiology, Human Factors, Immunology, Laser Bioeffects, Medicine, Microbiology, Molecular Biology, Pharmacology and Toxicology, Physiology, and Public Health. For individual titles, see N88-20816 through N88-20817.

N88-20816 Joint Publications Research Service, Arlington, Va.
INCREASE IN INFLUENCE OF OXYGEN ON THE BODY IN THE PRESENCE OF HELIUM Abstract Only
M. M. Seredenko and Ye. V. Rozova *In its* JPRS Report: Science and Technology. USSR: Life Sciences 15 Mar. 1988 p 26 Transl. into ENGLISH from Fiziologiya Cheloveka (Moscow, USSR), v. 13, no. 3, May - Jun. 1987 p 463-468 (For primary document see N88-20815 13-52)
Copyright Avail: Issuing Activity

An attempt is made to estimate the combined influence of oxygen and helium on the body over a broad range of oxygen concentrations in the gas mixture breathed, using 105 healthy volunteers and 78 subjects with chronic pulmonary insufficiency. The subjects breathed mixtures containing 40, 21, 14.5 and 11 percent oxygen in nitrogen or helium. Subjects with pulmonary insufficiency were given mixtures containing 40 and 21 percent oxygen only. Exposure time was 20 minutes. Helium increased the hyperoxic effect, decreasing the level of gas metabolism. Systems supporting the body with oxygen concentrations when mixed with helium, and hyperoxia is increased at higher oxygen concentrations. Author

N88-20817 Joint Publications Research Service, Arlington, Va.
REGULATION OF HEMODYNAMICS UPON IMITATION OF THE TRANSITION TO WEIGHTLESSNESS (MATHEMATICAL MODELING) Abstract Only
B. L. Palets, A. A. Popov, M. A. Tikhonov, and V. S. Panchenko *In its* JPRS Report: Science and Technology. USSR: Life Sciences 15 Mar. 1988 p 26 Transl. into ENGLISH from Fiziologiya Cheloveka (Moscow, USSR), v. 13, no. 4, Jul. - Aug. 1987 p 627-632 Original language document was announced in IAA as A88-14728 (For primary document see N88-20815 13-52)
Copyright Avail: Issuing Activity

A mathematical model of human circulation dynamics, based on the model of Palets et al., was used to study rapid responses of the cardiovascular system to the onset of weightlessness. The model was also used to study the effects on circulation of some weightlessness counteracting methods, such as hypovolumia, lower body negative pressure (LBNP), and hip cuffs. The analytical results show that upon the onset of weightlessness, the right heart ventricle, due to the blood volume overload, starts to function in a plateau range of the accretion function. Hypovolumia, LBNP, and occlusion cuffs all function to decrease the volume load of the right ventricle. Among the counter weightlessness methods, the LBNP is the most effective. E.R.

N88-20818*# National Aeronautics and Space Administration, Washington, D.C.
THE EFFECTS OF NORMAL AND THERAPEUTIC BATHS ON THE CENTRAL VASCULAR ORGANS OF PERSONS WITH HEALTHY HEARTS, AS MEASURED BY X-RAY
G. Boehm and Fr. Ekert Apr. 1988 21 p Transl. into ENGLISH from Deutsches Archiv F. Klin. Med. (Fed. Republic of Germany), v. 182, 1938 p 598-610 Transl. by Scientific Translation Service, Santa Barbara, Calif.
(Contract NASw-4307)
(NASA-TT-20252; NAS 1.77:20252) Avail: NTIS HC A03/MF A01 CSCL 06P

According to current information, baths have a four-fold effect on the circulation: (1) Dilation or constriction is produced in the area of the blood vessels in the skin as a result of thermal, chemical or mechanical stimuli; (2) This reaction in the dermal vascular system produces a further effect on the central vessels in the extremities, the area of the splanchnicus, and other body cavities; (3) The reflect transposition of other organ systems, i.e., the respiratory organs, has a reaction on the circulation; and (4) The water pressure of the bath has a hydrostatic effect, i.e., on the one hand it empties peripheral veins more rapidly, and on the other it increases the intra-abdominal pressure and this reduces once again the circulation in the area of the splanchnicus.
Author

53 BEHAVIORAL SCIENCES

Includes psychological factors; individual and group behavior; crew training and evaluation; and psychiatric research.

N88-20819 New South Wales Univ., Kensington (Australia).
COMPUTERISED MEASUREMENT OF HUMAN HORIZONTAL SMOOTH PURSUIT EYE MOVEMENTS Abstract Only. M.S. Thesis
M. J. Todd Mar. 1987 249 p
Avail: Issuing Activity

Smooth pursuit is one type of compensatory eye movement which maintains gaze on a moving target and ensures clear vision. There is clinical evidence that abnormalities of pursuit are an early and sensitive index of brain disease and measurement of smooth pursuit responses could be important for diagnosis and for assessment of progress and treatment. Clinical testing so far has measured only steady-state pursuit responses to predictable target motion but recent research in monkeys has indicated that the response to transient stimuli may be clinically more significant. The development of a computerized system for generating precisely controlled transient smooth pursuit stimuli and for accurately recording and analyzing the eye movements produced are described. The type of target motion used was a step-ramp, first described by Rashbass in 1961. Clinical tests of the final system showed that it performs as well as the best contemporary systems in the world for recording smooth pursuit transients and that it is a useful tool for intensively studying the normal and abnormal responses to these stimuli.
Author

N88-20820# Decision Science Consortium, Inc., Falls Church, Va.
A PERSONALIZED AND PRESCRIPTIVE DECISION AID FOR CHOICE FROM A DATABASE OF OPTIONS Final Technical Report, Jul. 1983 - Sep. 1986
Marvin S. Cohen, Kathryn B. Laskey, and Martin A. Tolcott 23 Nov. 1987 71 p
(Contract N00014-83-C-0485; Proj. F66-701)
(AD-A188726; DSCI-87-18) Avail: NTIS HC A04/MF A01 CSCL 05H

In many decision making contexts there is a need for aids which cater flexibly to individual users in their preferred ways of organizing information and solving problems, but which guard against potential errors or biases inherent in common approaches to decision making. DSC has developed principles of personalized and prescriptive decision aiding which respond to this need, and which are based on experimental findings and theoretical models in cognitive psychology. In Phase 1 of this project, those principles were applied to the development of an aid for attack submarine approach and attack. In Phase 2, the principles have been generalized and extended to the development of a generic personalized and prescriptive evaluation system. The system incorporates five basic cognitive interface modules to customize the user's interaction with the aid to provide prescriptive guidance, as well as a set of interactive dialogues or guides which blend all five functions in support of specific user-selected decision-making strategies. The aid has been tested and demonstrated in the context of a personnel application.
GRA

N88-20821# Katholieke Universiteit, Nijmegen (Netherlands). Psychologisch Lab.
DISTRACTION AND INHIBITION IN CONTINUOUS CRT PERFORMANCE: A REPLICATION AND SOME NEW FINDINGS
R. W. T. L. Jansen and G. J. P. vanBreukelen 1987 37 p
(PB88-150941; Rept-87-MA-01) Avail: NTIS HC A03/MF A01 CSCL 05I

The present study replicates findings of van Breukelen and Jansen (1987) concerning the role of distractions and inhibition in response times, but using a different task. The distraction hypothesis states that a fair amount of the reaction time consists of distraction, i.e., time not serving the task performance. The inhibition hypothesis states that the tendency of being distracted increases during mental processing time and decreases during distraction. An experimental comparison of massed (continuous work) versus spaced (work with regular resting periods) served to test the two main hypotheses. Subjects were 16 male and 16 female student volunteers. A digit addition task was used. The experimental setting was as in van Breukelen and Jansen (1987). Specific predictions were derived from the inhibition model of Van der Ven, Smit, and Jansen (1987). The results supported most of these predictions. Furthermore, a few explorative analyses are reported concerning learning effects. Finally, the task independence of speed, error rate and concentration was explored by calculating correlations between the corresponding conditions of the van Breukelen and Jansen (1987) and the present experiment with respect to these variables. All correlations were significant, varying between .40 and .80.
GRA

54 MAN/SYSTEM TECHNOLOGY AND LIFE SUPPORT

Includes human engineering; biotechnology; and space suits and protective clothing.

For related information see also *16 Space Transportation.*

N88-20822*# Charles River Analytics, Inc., Cambridge, Mass.
IDENTIFICATION OF VISUAL EVOKED RESPONSE PARAMETERS SENSITIVE TO PILOT MENTAL STATE Final Report, Mar. 1985 - Aug. 1987
G. L. Zacharias NASA Apr. 1988 182 p
(Contract NAS1-17816)
(NASA-CR-4140; NAS 1.26:4140; R8701) Avail: NTIS HC A09/MF A01 CSCL 05H

Systems analysis techniques were developed and demonstrated for modeling the electroencephalographic (EEG) steady state visual evoked response (ssVER), for use in EEG data compression and as an indicator of mental workload. The study focused on steady state frequency domain stimulation and response analysis, implemented with a sum-of-sines (SOS) stimulus generator and an off-line describing function response analyzer. Three major tasks were conducted: (1) VER related systems identification material was reviewed; (2) Software for experiment control and data analysis was developed and implemented; and (3) ssVER identification and modeling was demonstrated, via a mental loading experiment. It was found that a systems approach to ssVER functional modeling can serve as the basis for eventual

development of a mental workload indicator. The review showed how transient visual evoked response (tVER) and ssVER research are related at the functional level, the software development showed how systems techniques can be used for ssVER characterization, and the pilot experiment showed how a simple model can be used to capture the basic dynamic response of the ssVER, under varying loads. Author

N88-20823# Carnegie-Mellon Univ., Pittsburgh, Pa. Dept. of Psychology.
MENTAL MODELS OF MECHANICAL SYSTEMS: INDIVIDUAL DIFFERENCES IN QUALITATIVE AND QUANTITATIVE REASONING
Mary Hegarty, Marcel A. Just, and Ian R. Morrison Dec. 1987 36 p
(Contract N00014-85-K-0584; DA Proj. RR0-4206)
(AD-A189035; Rept-87-8-ONR) Avail: NTIS HC A03/MF A01 CSCL 05H

People who understand mechanical systems can infer the principles of operation of an unfamiliar device from their knowledge of the device's components and their mechanical interactions. Individuals vary considerably in their ability to make this type of inference. This paper describes studies of performance in psychometric tests of mechanical ability. Based on subjects' retrospective protocols and response patterns, it was possible to identify rules of mechanical reasoning that accounted for the performance of subjects of different levels of mechanical ability. The rules are explicitly stated in a simulation model which demonstrates the sufficiency of the rules by producing the kinds of responses observed in the subjects. Three abilities are proposed as the sources of individual differences in performance: (1) ability to correctly identify which attributes of a system are relevant to its mechanical function, (2) ability to use rules consistently, and (3) ability to quantitatively combine information about two or more relevant attributes. GRA

N88-20824# Boeing Military Airplane Development, Seattle, Wash.
MULTI-CREW PICTORIAL FORMAT DISPLAY EVALUATION Final Report, May 1984 - Jan. 1987
T. C. Way, R. L. Martin, J. D. Gilmour, M. E. Hornsby, and R. E. Edwards Mar. 1987 203 p
(Contract F33615-83-C-3618)
(AD-A189349; AFWAL-TR-87-3047) Avail: NTIS HC A10/MF A01 CSCL 23B

The Multi-Crew Format evaluation was designed to evaluate pictorial formats in a two-seat fighter, to determine their usability as a function of color, and determine their acceptability. The study consisted of designing the formats, evaluation of formats in part-task, part-mission, and full-mission simulation, and redesigning formats based on air crew feedback if needed. GRA

N88-20825# Carlow Associates, Inc., Fairfax, Va.
ADVANCED HUMAN FACTORS ENGINEERING TOOL TECHNOLOGIES Final Report, 18 Jul. 1986 - 2 Apr. 1987
Stephen A. Fleger, Kathryn E. Permenter, and Thomas B. Malone 20 Mar. 1987 276 p
(Contract DAAA15-86-C-0064)
(AD-A189390) Avail: NTIS HC A13/MF A01 CSCL 23B

Presented are the results of a study to identify the human factors engineering (HFE) technologies or tools presently used, and projected for use, by HFE specialists. Both traditional and advanced tools were candidates for inclusion in the report, although the emphasis of the study was on advanced computer applications. Human factors practitioners representing the government, the military, academe and private industry were surveyed to identify those tools most frequently used or viewed as most important for conducting human factors engineering related work. If advanced tool capabilities did not meet existing job requirements, the specialists identified the types of tools they would like to see developed to fill the existing technology gaps. The advanced tools were categorized using an eight point classification scheme, which included the phase(s) of the material acquisition process in which the tools' application would be most appropriate. All of the tools were ranked to facilitate tool selection, and entered into a database to accommodate future revisions. The survey resulted in the identification of 113 advanced human factors engineering tools. GRA

N88-20826# Georgia Inst. of Tech., Atlanta. Center for Man-Machine Systems Research.
HUMAN PROBLEM SOLVING IN DYNAMIC ENVIRONMENTS. UNDERSTANDING AND SUPPORTING OPERATORS IN LARGE-SCALE, COMPLEX SYSTEMS Final Report, Jun. 1982 - Dec. 1986
Richard L. Henneman and William B. Rouse Oct. 1987 75 p
(Contracts MDA903-82-C-0145; DA Proj. 2Q1-61102-B-74-F)
(AD-A189539; ARI-RN-87-51) Avail: NTIS HC A04/MF A01 CSCL 05H

This research note seeks an empirical understanding of the relationship between the physical characteristics of a large-scale system and human performance and a formalization of empirical results into several measures of large scale complexity. Behavioral computer models of the human operator in a large-scale environment were then constructed, and the models were found consistent with human behavior. This approach showed subtle performance improvement for aided subjects. GRA

N88-20827# Douglas Aircraft Co., Inc., Long Beach, Calif.
PROCEEDINGS OF THE WORKSHOP ON THE ASSESSMENT OF CREW WORKLOAD MEASUREMENTS METHODS, TECHNIQUES AND PROCEDURES. VOLUME 1: PRELIMINARY SELECTION OF MEASURES Final Report, 24 - 25 Feb. 1987
Michael A. Biferno and George P. Boucek, Jr. (Boeing Commercial Airplane Co., Seattle, Wash.) Jun. 1987 386 p Workshop held in Long Beach, Calif., 24-25 Feb. 1987
(Contract F33615-86-C-3600)
(AD-A189004; AFWAL-TR-3043-Vol-1) Avail: NTIS HC A17/MF A01 CSCL 05H

The objectives of the workshop were to: gather information from workload experts regarding which measures have evidence supporting their reliability or validity; provide an independent review of the facts concerning the validity and reliability of workload measures; and provide a means for systematically reviewing and modifying the fact matrices. A schedule of the events is included. GRA

N88-20828# Messerschmitt-Boelkow-Blohm G.m.b.H., Ottobrunn (West Germany). Unternehmensgruppe Hubschrauber und Flugzeuge.
PRESSURIZING SYSTEMS AND AIR CONDITIONING SYSTEMS [DRUCK- UND KLIMAANLAGEN]
Senoner 11 Apr. 1986 55 p In GERMAN
(MBB/LKE-312/S/PUB/246; ETN-88-91440) Copyright Avail: NTIS HC A04/MF A01

The development of pressurizing and air conditioning systems for aircraft is outlined. The requirements for an air conditioning system are explained. The data and parameters for the design of a pressurized air conditioning system are given. The investigations required for the design of such a system are outlined. The pneumatic supply units and subunits for pressurizing and air conditioning systems are described. The coolant processing unit, the air distribution system, and the heat transport cycle are described. The testing, problem solving, and improvement of pressurizing and air conditioning systems are explained. ESA

55 SPACE BIOLOGY

Includes exobiology; planetary biology; and extraterrestrial life.

No abstracts in this category.

59 MATHEMATICAL AND COMPUTER SCIENCES (GENERAL)

N88-20829*# National Aeronautics and Space Administration. Langley Research Center, Hampton, Va.
ON THE SENSITIVITY OF COMPLEX, INTERNALLY COUPLED SYSTEMS
Jaroslaw SobieszczanskiSobieski Jan. 1988 13 p Prepared for presentation at the 29th AIAA ASME/ASCE/AHS Structures, Structural Dynamics and Materials Conference, Williamsburg, Va., 18-20 Apr. 1988
(NASA-TM-100537; AIAA-88-2378; NAS 1.15:100537) Avail: NTIS HC A03/MF A01 CSCL 12A

A method is presented for computing sensitivity derivatives with respect to independent (input) variables for complex, internally coupled systems, while avoiding the cost and inaccuracy of finite differencing performed on the entire system analysis. The method entails two alternative algorithms: the first is based on the classical implicit function theorem formulated on residuals of governing equations, and the second develops the system sensitivity equations in a new form using the partial (local) sensitivity derivatives of the output with respect to the input of each part of the system. A few application examples are presented to illustrate the discussion. Author

N88-20830*# National Aeronautics and Space Administration. Langley Research Center, Hampton, Va.
A NEW ALGORITHM FOR GENERAL MULTIOBJECTIVE OPTIMIZATION
Jaroslaw Sobieszczanski-Sobieski, Augustine R. Dovi, and Gregory A. Wrenn (Planning Research Corp., Hampton, Va.) Mar. 1988 11 p Presented at the 29th AIAA/ASME/ASCE/AHS Structures, Structural Dynamics and Materials Conference, Williamsburg, Va., 18-20 Apr. 1988
(NASA-TM-100536; NAS 1.15:100536; AIAA-88-2434) Avail: NTIS HC A03/MF A01 CSCL 12A

Described is a new technique for converting a constrained optimization problem to an unconstrained one, and a new method for multiobjective optimization based on that technique. The technique transforms the objective functions into goal constraints. The goal constraints are appended to the set of behavior constraints and the envelope of all functions in the set is searched for an unconstrained minimum. The technique may be categorized as a SUMT algorithm. In multiobjective applications, the approach has the advantage of locating a compromise minimum without the need to optimize for each individual objective function separately. The constrained to unconstrained conversion is described, followed by a description of the multiobjective problem. Two example problems are presented to demonstrate the robustness of the method. Author

N88-20831*# National Aeronautics and Space Administration. Langley Research Center, Hampton, Va.
DATA TRAFFIC REDUCTION SCHEMES FOR SPARSE CHOLESKY FACTORIZATIONS Final Report
Vijay K. Naik and Merrell L. Patrick Feb. 1988 35 p Submitted for publication Prepared in cooperation with Duke Univ., Durham, N.C.
(Contract NAS1-18107)
(NASA-CR-181626; ICASE-88-14; NAS 1.26:181626) Avail: NTIS HC A03/MF A01 CSCL 12A

Load distribution schemes are presented which minimize the total data traffic in the Cholesky factorization of dense and sparse, symmetric, positive definite matrices on multiprocessor systems with local and shared memory. The total data traffic in factoring an n x n sparse, symmetric, positive definite matrix representing an n-vertex regular 2-D grid graph using n (sup alpha), alpha is equal to or less than 1, processors are shown to be O(n(sup 1 + alpha/2)). It is O(n(sup 3/2)), when n (sup alpha), alpha is equal to or greater than 1, processors are used. Under the conditions of uniform load distribution, these results are shown to be asymptotically optimal. The schemes allow efficient use of up to O(n) processors before the total data traffic reaches the maximum value of O(n(sup 3/2)). The partitioning employed within the scheme, allows a better utilization of the data accessed from shared memory than those of previously published methods. Author

N88-20832*# National Aeronautics and Space Administration. Hugh L. Dryden Flight Research Center, Edwards, Calif.
CONFIGURATION MANAGEMENT ISSUES AND OBJECTIVES FOR A REAL-TIME RESEARCH FLIGHT TEST SUPPORT FACILITY
Stephen Yergensen and Donald C. Rhea May 1988 12 p Presented at the AIAA 4th Flight Test Conference, San Diego, Calif., 18-20 May 1988
(NASA-TM-100437; H-1463; NAS 1.15:100437) Avail: NTIS HC A03/MF A01 CSCL 12A

Presented are some of the critical issues and objectives pertaining to configuration management for the NASA Western Aeronautical Test Range (WATR) of Ames Research Center. The primary mission of the WATR is to provide a capability for the conduct of aeronautical research flight test through real-time processing and display, tracking, and communications systems. In providing this capability, the WATR must maintain and enforce a configuration management plan which is independent of, but complimentary to, various research flight test project configuration management systems. A primary WATR objective is the continued development of generic research flight test project support capability, wherein the reliability of WATR support provided to all project users is a constant priority. Therefore, the processing of configuration change requests for specific research flight test project requirements must be evaluated within a perspective that maintains this primary objective. Author

60 COMPUTER OPERATIONS AND HARDWARE

Includes hardware for computer graphics, firmware, and data processing.

For components see *33 Electronics and Electrical Engineering.*

N88-20833*# National Aeronautics and Space Administration. Langley Research Center, Hampton, Va.
DIGITAL ENHANCEMENT OF FLOW FIELD IMAGES
Robert A. Kudlinski and Stephen K. Park Mar. 1988 25 p Original contains color illustrations
(NASA-TP-2770; L-16318; NAS 1.60:2770) Avail: NTIS HC A03/MF A01 CSCL 09B

Most photographs of experimentally generated fluid flow fields have inherently poor photographic quality, specifically low contrast. Thus, there is a need to establish a process for quickly and accurately enhancing these photographs to provide improved versions for physical interpretation, analysis, and publication. A sequence of digital image processing techniques which have been demonstrated to effectively enhance such photographs is described. Author

N88-20834# Aeronautical Systems Div., Wright-Patterson AFB, Ohio.
A COMPARISON OF TWO CHORD KEYBOARD CODING SYSTEMS FOR ALPHANUMERIC DATA ENTRY Final Report
John R. Amell and Eric E. Crawford Jun. 1987 90 p
(AD-A189230; ASD-TR-87-5006) Avail: NTIS HC A05/MF A01 CSCL 12G

Chord keyboards are alphanumeric data entry devices that generally have fewer keys than a standard typewriter keyboard. Characters are produced by pressing either a single key or several keys simultaneously. Two coding systems, both using one-handed operation, were implemented on a commercially available chord keyboard, the Microwriter. The coding system resident on the Microwriter was compared to the coding system developed by Sidorsky (1974), known as the Alpha-dot system. Measures of

time to learn, time to reach a 35 character per minute criterion entry rate, text entry speed and accuracy, and cognitive workload were collected from two groups of ten subjects. Cognitive workload was measured using two auditory tasks in a secondary task paradigm. The results of initial code learning indicated that the two groups did not differ in the amount of time needed to reach a 95 percent accuracy criterion. The Alpha-dot group was, however, quicker in reaching the 35 character per minute speed criterion. Text entry was measured three times during the experiment. The first test, immediately after initial learning of the codes, indicated that the Alpha-dot group was typing at a faster rate, with no difference in errors. The second and third tests showed no differences in speed or accuracy. GRA

N88-20835# California Inst. of Tech., Pasadena.
THE PHYSICAL STRUCTURE OF CONCURRENT PROBLEMS AND CONCURRENT COMPUTERS
G. C. Fox and W. Furmanski 1988 60 p
(Contracts DE-AC04-76DP-00789; DE-FG03-85ER-25009)
(DE88-005812; DOE/ER-25009/493) Avail: NTIS HC A04/MF A01

We introduce a physical analogy to describe problems and high performance concurrent computers on which they are run. We show that the spatial characteristics of problems lead to their parallelism and review the lessons from use of the early hypercubes and a natural particle-process analogy. We generalize this picture to include the temporal structure of problems and show how this allows us to unify distributed, shared, and hierarchical memories as well as SIMD architectures. We also show how neural network methods can be used to analyze a general formalism based on interacting strings and these lead to possible real-time schedulers and decomposers for massively parallel machines. DOE

N88-20836# Center for Mathematics and Computer Science, Amsterdam (Netherlands). Dept. of Computer Science/Dept. of Interactive Systems.
LOGICAL INPUT DEVICES AND INTERACTION
R. vanLiere and P. J. W. tenHagen Aug. 1987 18 p Submitted for publication
(CWI-CS-R8738; B8729657; ETN-88-91784) Copyright Avail: NTIS HC A03/MF A01

The functionality provided by the logical input device model when brought in conjunction with interaction is questioned. The logical input device model does not support the notion of input/output symmetry: the input model is completely separated from the corresponding graphical output model. It is shown that the ad hoc relationships provided by the graphics kernel system that interrelate these two models are insufficient. Suggestions based on the notion of input/output-symmetry, to improve the input model, are made. ESA

61 COMPUTER PROGRAMMING AND SOFTWARE

Includes computer programs, routines, alogorithms, and specific applications, e.g., CAD/CAM.

N88-20837*# RSIC Associates, Belmont, Mass.
PARALLEL IMAGE COMPRESSION
John H. Reif 1987 42 p
(Contract NAS5-30056)
(NASA-CR-180758; NAS 1.26:180758) Avail: NTIS HC A03/MF A01 CSCL 09B

A parallel compression algorithm for the 16,384 processor MPP machine was developed. The serial version of the algorithm can be viewed as a combination of on-line dynamic lossless test compression techniques (which employ simple learning strategies) and vector quantization. These concepts are described. How these concepts are combined to form a new strategy for performing dynamic on-line lossy compression is discussed. Finally, the implementation of this algorithm in a massively parallel fashion on the MPP is discussed. B.G.

N88-20838# CD Metrology, Inc., Germantown, Md.
COMPUTER SOFTWARE FOR THE COMPUTATION OF THE SCATTERED FIELD AND THE OPTICAL MICROSCOPE IMAGE OF LINE OBJECTS PATTERNED IN THICK LAYERS
D. Nyyssonen Dec. 1987 89 p Sponsored by National Bureau of Standards, Gaithersburg, Md.
(PB88-153705; NBSIR-87/3618) Avail: NTIS HC A05/MF A01 CSCL 09B

The report contains computer software for calculating optical microscope images of line objects patterned in thick layers (greater than lambda/4 thick). The algorithms used are based on a monochromatic, waveguide model which can predict the images of line objects with arbitrary edge geometry including multilayer structures with sloped, curved, asymmetric, and undercut edges. Along with the computer software listing, the mathematics of the model, a short description of its structure and use, and test cases for help in implementation are given. The computer software described in the report was written in conjunction with the National Bureau of Standards project to develop fundamentally accurate optical measurement techniques for the width of micrometer and submicrometer lines patterned on integrated circuit wafers. GRA

N88-20839# Science Applications International Corp., McLean, Va.
BROADBAND CORRELATION ANALYSIS Final Report
X. A. Zabal 13 Nov. 1987 6 p
(Contract N00014-86-D-0701)
(AD-A188732; SAIC-87/1873) Avail: NTIS HC A02/MF A01 CSCL 12A

The work under this contract was conducted by Science Applications International Corporation (SAIC) during the period from 28 April 1987 through 13 November 1987. The bulk of the work under this contract has been reported to PMW180-42 during the Broadband Workshop meetings. These results have been documented in SAIC report No. MDCD 87:3107. SAIC developed system performance models to evaluate different broadband correlation algorithms. These included the Smooth COherence Transform (SCOT) algorithm, the PHAse Transform (PHAT) algorithm and the Clipped Correlator. Algorithm performance was evaluated in terms of sensitivity to direct and surface path detection as well as robustness against CW tonal contamination. GRA

N88-20840# Rochester Univ., N. Y. Dept. of Computer Science.
ON RELAXATION ALGORITHMS BASED ON MARKOV RANDOM FIELDS
Paul B. Chou and Rajeev Raman 10 Jul. 1987 32 p
(Contracts N00014-82-K-0193; DACA76-85-C-0001)
(AD-A189043; TR-212) Avail: NTIS HC A03/MF A01 CSCL 23C

Many computer vision problems can be formulated as computing the minimum energy states of thermal dynamic systems. However, due to the complexity of the energy functions, the solutions to the minimization problem are very difficult to acquire in practice. Stochastic and deterministic methods exist to approximate the solutions, but they fail to be both efficient and robust. This paper describes a new deterministic method, the Highest Confidence First algorithm, to approximate the minimum energy solution to the image labeling problem under the Maximum A Posteriori (MAP) criterion. This method uses Markov Random Fields to model spatial prior knowledge of images and likelihood probabilities to represent external observations regarding hypotheses of image entities. Following an order decided by a dynamic stability measure, the image entities make make local estimates based on the combined knowledge of priors and observations. The solutions so constructed compare favorably to the ones produced by existing methods and that the computation is more predictable and less expensive. GRA

N88-20841# Rochester Univ., N. Y. Dept. of Computer Science.
DESIGN OF THE CONSUL PROGRAMMING LANGUAGE
Doug Baldwin Feb. 1987 29 p
(Contract DACA76-85-C-0001)
(AD-A189202; TR-208) Avail: NTIS HC A03/MF A01 CSCL 12E

The problem of automatically exploiting parallelism in computer programs, with particular emphasis on linguistic barriers to parallelism detection is studied. Although functional languages and Prolog have many desirable characteristics in this respect, they are not entirely ideal. We therefore offer constraint-based programming as a generalization of logic programming. By virtue of the more flexible ways in which they allow relations to be defined, constraint languages support more natural descriptions of potentially parallel algorithms than do existing logic or functional languages. We introduce a prototype constraint language called CONSUL, which demonstrates features that we feel make constraint languages well-suited for general-purpose programming of multi-processors. The extra expressiveness of constraint languages comes at a price, namely that satisfaction of general constraints can be much more difficult than satisfaction of predicates for a language like Prolog. Nonetheless, we believe that effective compilers for constraint languages can be built, and we outline some ideas on which they could be based. on which they could be based. GRA

N88-20842# Michigan Univ., Ann Arbor. Center for Ergonomics.
ONLINE AIDING FOR HUMAN-COMPUTER INTERFACES Technical Report, 15 Aug. 1987 - 14 Aug. 1988
Jay Elkerton 9 Oct. 1987 47 p
(Contracts N00014-87-K-0740; DA Proj. RR0-4209)
(AD-A189239; C4E-ONR-1) Avail: NTIS HC A03/MF A01 CSCL 23B

Current research is surveyed on interfaces which aid the computer user online. Results show that many online aiding dialogues fall far short of the ultimate goal of helping users with their current problems, while also supporting continued skill acquisition at the computer interface. To address this problem, a task-analytic approach is presented which is based on the GOMS model of human computer interaction. This model will provide an opportunity for usability problems to be identified analytically, as well as to allow assistance and instructional dialogues to be simulated in order to predict improvements due to online aiding. GRA

N88-20843# Naval Postgraduate School, Monterey, Calif.
MACCAD (MACINTOSH COMPUTER AIDED DESIGN), COMPUTER AIDED DESIGN TOOL FOR SYSTEM ANALYSIS M.S. Thesis
Kenneth MacDonald Dec. 1987 288 p
(AD-A189241) Avail: NTIS HC A13/MF A01 CSCL 12E

MacCAD, a computer aided design program, was developed as an analysis tool of continuous, linear control systems for the graduate level controls or electrical engineering student. A variety of programs are presently available for the IBM-PC and the IBM Mainframe. MacCAD is written in Pascal and operates on the Apple Macintosh. It was developed in order to meet the need for a powerful yet simple to use program with high quality graphics and multiple window capabilities. It offers a highly flexible block manipulator capable of handling virtually unlimited blocks and loops, along with the standard analysis tools, Bode, Nyguist, Root Locus and Time response plots. Mouse and menu driven, it offers user defined plotting and calculation parameters which include multiple plot overlapping and linear or logarithmic plot point intervals. GRA

N88-20844# Rochester Univ., N. Y. Dept. of Computer Science.
AN INTERFACE BETWEEN OBJECT-ORIENTED SYSTEMS
Lawrence A. Crowl Apr. 1987 23 p
(Contract DACA76-85-C-0001; Grant NSF DCR-83-20136)
(AD-A189245; TR-211) Avail: NTIS HC A03/MF A01 CSCL 12E

The Chrysalis operating system for the Butterfly Parallel Processor presents an object-oriented programming environment based on shared memory. However, because of Chrysalis's low level orientation and its use of type-unsafe features of the C programming language, programs using the environment are difficult to program and highly error-prone. Using C as the primary programming language for the Butterfly does not fully realize the benefit of Chrysalis's object orientation. An object-oriented programming language is natural candidate for improving the Chrysalis environment. The C(++) programming language provides a number of advantages in developing such an interface. This paper reports the successes and problems encountered in the development of Chrysalis(++) a C(++) interface to Chrysalis(++) uncovered many strengths and weakness in C(++). Some apply to C(++) in general, others apply only to its adaptation to a parallel programming environment. It is important to note that C(++) is a sequential language; it is used in a parallel programming environment is therefore outside the bounds of its design. GRA

N88-20845# Naval Research Lab., Washington, D.C.
INVERSION ALGORITHMS FOR GEOPHYSICAL PROBLEMS Final Report, Aug. 1986 - Jul. 1987
Paolo Lanzano 16 Dec. 1987 14 p
(AD-A189252; NRL-MR-6138) Avail: NTIS HC A03/MF A01 CSCL 08C

We discuss procedures for the iterative solution of an integral equation of the Fredholm type of generic kernel and provide details for two particular geophysical problems. We study the inversion of gravity data in order to retrieve the profile of the underlying topography by searching for solutions giving rise to the most compact configuration. We invert radar measurements to obtain ocean spectra: this is achieved according to a perturbation procedure by minimizing a functional of errors which also expresses the deviation of the solution from an expected spectral density. GRA

N88-20846*# Jet Propulsion Lab., California Inst. of Tech., Pasadena. Algorithm Analysis Subgroup.
PASSIVE DF: A TUTORIAL, PART 1 Final Report
Bill Buckles 30 Apr. 1987 30 p
(Contract NAS7-918)
(NASA-CR-182669; JPL-D-4625; NAS 1.26:182669; AD-A189447; ALGO-PUB-0098-Pt-1) Avail: NTIS HC A03/MF A01 CSCL 17K

This memo introduces passive intercept and emitter identification problems. Then precission Direction of Arrival (DOA) methods and algorithms are introduced. The algorithms for amplitude comparison and phase interferometry are discussed in detail. Four other types of location algorithms are also examined. The memo concludes with a cross-comparison of these methods. GRA

N88-20847*# Jet Propulsion Lab., California Inst. of Tech., Pasadena.
TWO DIMENSIONAL UNCORRELATED BIAS IN FIX ALGORITHMS Final Report
Michael W. Rennie 10 Jun. 1987 48 p
(Contract NAS7-918)
(NASA-CR-182683; JPL-D-4492; NAS 1.26:182683; AD-A189473; ALSO-PUB-0045) Avail: NTIS HC A03/MF A01 CSCL 09B

Bias in Location Estimation Algorithms is defined to be a vector from the estimated fix site to the true Fix site. Four Fix Algorithms are examined in this report: Least Squares (Stanfield Approximation), Weighted Least Squares, Minimization of Angular Error, and minimization of the Site of the Angular Error. Analysis expressions for the First-Order error are derived for two specific cases: Two Lines-of-Bearing (LOB's) and infinite LOB's. The analytic derivations are relegated to appendices. Three questions are answered by this report. First, which algorithms cause the largest bias? Second, how sensitive is this bias to sample size,

system noise, and variance? Third, which algorithms (if any) are asymptotically unbiased? All conclusions are then verified by simulation. GRA

N88-20848# Oak Ridge National Lab., Tenn.
IMPLEMENTATION OF A 3-D NONLINEAR MHD (MAGNETOHYDRODYNAMICS) CALCULATION ON THE INTEL HYPERCUBE
V. E. Lynch, B. A. Carreras, J. B. Drake, H. R. Hicks, and W. F. Lawkins 1987 6 p Presented at the 12th Conference on the Numerical Simulation of Plasmas, San Francisco, Calif., 20 Sep. 1987
(Contract DE-AC05-84OR-21400)
(DE88-000625; CONF-870947-9) Avail: NTIS HC A02/MF A01

The optimization of numerical schemes and increasing computer capabilities in the last ten years have improved the efficiency of 3-D nonlinear resistive MHD calculations by about two to three orders of magnitude. However, we are still very limited in performing these types of calculations. Hypercubes have a large number of processors with only local memory and bidirectional links among neighbors. The Intel Hypercube at Oak Ridge has 64 processors with 0.5 megabytes of memory per processor. The multiplicity of processors opens new possibilities for the treatment of such computations. The constraint on time and resources favored the approach of using the existing RSF code which solves as an initial value problem the reduced set of MHD equations for a periodic cylindrical geometry. This code includes minimal physics and geometry, but contains the basic three dimensionality and nonlinear structure of the equations. The code solves the reduced set of MHD equations by Fourier expansion in two angular coordinates and finite differences in the radial one. Due to the continuing interest in these calculations and the likelihood that future supercomputers will take greater advantage of parallelism, the present study was initiated by the ORNL Exploratory Studies Committee and funded entirely by Laboratory Discretionary Funds. The objectives of the study were: to ascertain the suitability of MHD calculation for parallel computation, to design and implement a parallel algorithm to perform the computations, and to evaluate the hypercube, and in particular, ORNL's Intel iPSC, for use in MHD computations. DOE

N88-20849# Texas Univ., Austin. Center for Numerical Analysis.
PRECONDITIONED CONJUGATE GRADIENT ALGORITHMS AND SOFTWARE FOR SOLVING LARGE SPARSE LINEAR SYSTEMS
D. M. Young, K. C. Jea, and Tsun-Zee Mai Mar. 1987 31 p Presented at the SIAM Meeting on Linear Algebra in Signals and Control, Boston, Mass., 1 Aug. 1986
(Contract DE-AS05-81ER-10954)
(DE88-002180; CONF-8608206-1-Draft; CNA-207) Avail: NTIS HC A03/MF A01

The classical form of the conjugate gradient method (CG method), developed by Hestenes and Stiefel, for solving the linear system Au = b is applicable when the coefficient matrix A is symmetric and positive definite (SPD). In this paper we consider various alternative forms of the CG method as well as generalizations to cases where A is not necessarily SPD. This analysis includes the preconditioned conjugate gradient method which is equivalent to conjugate gradient acceleration of a basic iterative method corresponding to a preconditioned system. Both the symmetrizable case and the nonsymmetrizable case are considered. For the nonsymmetrizable case there are very few useful theoretical results available. A package of programs, known as ITPACK, has been developed as a tool for carrying out experimental studies on various algorithms. Preliminary conclusions based on experimental results are given. DOE

N88-20850# Washington State Univ., Pullman. Dept. of Pure and Applied Mathematics.
CONIC ALGORITHMS FOR UNCONSTRAINED MINIMIZATION WITH SPECIAL CONSIDERATION OF PROBLEMS WITH LARGE SPARSE HESSIANS: A SUMMARY OF RESEARCH PERFORMED
K. A. Ariyawansa 31 Oct. 1987 8 p
(Contract DE-FG06-85ER-25007)
(DE88-002549; DOE/ER-25007/T1) Avail: NTIS HC A02/MF A01

This paper contains a brief description of research activities on conic algorithms for unconstrained minimization. Line search termination criteria and the rate of convergence for a certain class of conic algorithms for sparse problems are discussed. DOE

N88-20851# Argonne National Lab., Ill.
ALGORITHMS WITH CONIC TERMINATION FOR NONLINEAR OPTIMIZATION
Dong C. Liu and Jorge Nocedal Dec. 1987 22 p
(Contracts W-31-109-eng-38; DE-FG02-87ER-25047; Grant NSF DCR-86-02071)
(DE88-005893; ANL/MCS-TM-104) Avail: NTIS HC A03/MF A01

This paper describes algorithms for unconstrained optimization which have the property of minimizing conic objective functions in a finite number of steps, when line searches are exact. This work extends the algorithms of Davidon and Gourgeon and Nocedal to general nonlinear objective functions, paying much attention to the practical behavior of the new methods. Three types of algorithms are described; they are extensions of the conjugate gradient method, the BFGS method and a limited memory BFGS method. The numerical results show that new methods are very effective in solving practical problems. DOE

N88-20852# Wisconsin Univ., Madison. Torsatron/Stellarator Lab.
PROPAGATOR SOLUTIONS OF PARTIAL DIFFERENTIAL EQUATIONS APPLIED TO PLASMA TRANSPORT
W. N. G. Hitchon, D. J. Koch, and J. B. Adams Nov. 1987 26 p
(Contract DE-FG02-85ER-53201)
(DE88-006432; DOE/ER-53201/T4; TSL-87-4) Avail: NTIS HC A03/MF A01

A variety of partial differential equations may be solved efficiently and easily, using a single algorithm which is based on the propagator (or Green's function) for equations of the Fokker-Planck type. The numerical method employed is always at least as fast as finite differencing, but is especially efficient in cases where flow dominates over diffusion, and is consequently potentially widely applicable in fluid dynamics. Two transport problems in a small toroidal magnetic confinement device (IMS) have been considered. First, the ion distribution function and the potential in the sheath were calculated in the presence of charge exchange collisions for a wide range of neutral densities. Second, radial particle transport was modeled allowing for strong convection in the bulk plasma, and the density n(r,theta) was obtained for various plausible forms of the flow velocity, consistent with the observed average radial velocity. The best agreement with experiment is obtained with a vertical flow, which is also suggested by the measured potential profiles. DOE

N88-20853# Los Alamos National Lab., N. Mex.
METHOD TO EVALUATE IMAGE-RECOVERY ALGORITHMS BASED ON TASK PERFORMANCE
K. M. Hanson 1988 9 p Presented at the Medical Imaging 2 Conference, Newport Beach, Calif., 31 Jan. 1988
(Contract W-7405-eng-36)
(DE88-005382; LA-UR-88-111; CONF-880153-1) Avail: NTIS HC A02/MF A01

A method for evaluating image-recovery algorithms is presented, which is based on the numerical assessment of how well a specified visual task may be performed using the reconstructed images. A Monte Carlo technique is used to simulate the complete imaging

process including the generation of scenes appropriate to the desired application, subsequent data taking, image recovery, and performance of the stated task based on the final image. The use of a pseudo-random simulation process permits one to assess the response of an image-recovery algorithm to many different scenes. Nonlinear algorithms are readily evaluated. The usefulness of this method is demonstrated through a study of the algebraic reconstruction technique (ART), the nonnegativity constraint in ART can dramatically increase the detectability of objects in some instances, especially when the data consist of a limited number of noiseless projections. DOE

N88-20854# Arizona State Univ., Tempe. Dept. of Computer Science.
COMPUTER AIDED SURFACE REPRESENTATION
R. E. Barnhill Feb. 1987 39 p
(Contract DE-AC02-82ER-12046)
(DE88-005408; DOE/ER-12046/T4) Avail: NTIS HC A03/MF A01

The proposed Surfaces research can be classified into two general categories involving the creation of new surface forms, and the determination of geometric and physical properties of these and other surfaces. The specific research problems to be addressed in this project for the Department of Energy, include the following surface construction: piecewise polynomial interpolants, scattered data interpolants, and surfaces defined on surfaces; geometric and physical properties, numerical integration and surface interrogation. DOE

N88-20855# Lawrence Livermore National Lab., Calif.
GAUSSIAN TECHNIQUES ON SHARED MEMORY MULTIPROCESSOR COMPUTERS
G. A. Darmohray and E. D. Brooks, III Jan. 1988 9 p Presented at the 3rd SIAM Conference on Parallel Processing for Scientific Computing, Los Angeles, Calif., 1 Dec. 1987
(Contract W-7405-eng-48)
(DE88-005426; UCRL-97939; CONF-871251-3) Avail: NTIS HC A02/MF A01

Performance results are presented for parallel Gauss and Gauss-Jordan elimination algorithms on a shared memory multiprocessor. The Cerberus multiprocessor simulator, a simulator for a scalable shared memory multiprocessor with fully pipelined functional units, is used to evaluate algorithm performance. Our parallel implementations of these linear system solvers make extensive use of barrier synchronization. We show the need for barrier synchronization supported directly in hardware for tightly coupled algorithms. For a fixed problem size, the performance of Gauss-Jordan elimination crosses that of Gauss elimination as we increase the number of processors, even though the latter algorithm has a lower operation count. Sometimes, one can profit by trading operations for a better load balance and lower relative synchronization cost in a parallel algorithm. DOE

N88-20856# Sandia National Labs., Albuquerque, N. Mex.
MASPLT: A ONE-DIMENSIONAL GRAPHICS POST PROCESSOR FOR WAVE PROPAGATION CODES
J. S. Rottler and S. L. Thompson Nov. 1987 47 p
(Contract DE-AC04-76DP-00789)
(DE88-005506; SAND-87-0652) Avail: NTIS HC A03/MF A01

MASPLT is a one-dimensional graphics post processor for wave propagation codes. MASPLT employs a simple database structure that allows the program to be adapted to process data generated by dissimilar wave propagation codes. This report provides a complete set of input instructions for MASPLT, as well as a description of the structure of the MASPLT database. The report also provides examples of the types of plotted output that can be generated using MASPLT. DOE

N88-20857# Sandia National Labs., Albuquerque, N. Mex.
HISPLT: A HISTORY GRAPHICS POST PROCESSOR FOR WAVE PROPAGATION CODES
J. S. Rottler and S. L. Thompson Nov. 1987 49 p
(Contract DE-AC04-76DP-00789)
(DE88-005507; SAND-87-0653) Avail: NTIS HC A03/MF A01

HISPLT is a history graphics post processor for wave propagation codes. HISPLT employs a database structure that allows the program to be used without modification to process data generated by any wave propagation code. This report provides a complete set of input instructions for HISPLT, as well as a description of the structure of the HISPLT database. The report also provides examples of the types of plotted output that can be generated using HISPLT. DOE

N88-20858# Sandia National Labs., Albuquerque, N. Mex.
CSQPLT: A GRAPHICS POST PROCESSOR FOR MULTIDIMENSIONAL WAVE PROPAGATION CODES
J. S. Rottler and S. L. Thompson Nov. 1987 65 p
(Contract DE-AC04-76DP-00789)
(DE88-005508; SAND-87-2018) Avail: NTIS HC A04/MF A01

CSQPLT is a graphics post processor for multidimensional wave propagation codes. CSQPLT employs a database structure that allows the program to be adapted to process data generated by dissimilar multidimensional wave propagation codes. This report provides a complete set of input instructions for CSQPLT, as well as a description of the structure of the CSQPLT database. The report also provides examples of the types of plotted output that can be generated using CSQPLT. DOE

N88-20859# Lawrence Livermore National Lab., Calif.
EXPERIMENTAL VERIFICATION OF A FINITE-DIFFERENCE TIME-DOMAIN THIN SLOT ALGORITHM
S. T. Pennock, K. S. Yee, and J. C. Kasher Jan. 1988 27 p
(Contract W-7405-eng-48)
(DE88-005572; UCID-21327) Avail: NTIS HC A03/MF A01

A current area of interest in finite-difference time-domain computer codes is in developing the ability to model items of less than one cell in extent. A special case is an attempt to provide an algorithm to model thin slots, (much less than one cell dimension), without resorting to small cells which would increase storage and time requirements. Such an algorithm has been written and seems to work well. However, to lend real confidence to the algorithm's effectiveness, comparison with experimental data was deemed necessary. To this end, a series of experiments was carried out in the Lawrence Livermore National Laboratory's EMPEROR facility. This report will describe the measurements, the facility in which they were taken, and will conclude with a comparison of the experimental data and the results obtained from a finite-difference code with the thin slot algorithm. The comparison shows that the thin slot algorithm performs as well or better than expected, with generally less than a factor of 2 difference in amplitude. DOE

N88-20860# Stanford Univ., Calif. Systems Optimization Lab.
CONSTRAINED NONLINEAR PROGRAMMING
P. E. Gill, W. Murray, M. A. Saunders, and M. H. Wright Dec. 1987 40 p
(Contract DE-FG03-87ER-25030)
(DE88-005695; SOL-87-13) Avail: NTIS HC A03/MF A01

Aspects of constrained nonlinear programming are reviewed. Selected optimality conditions are derived and discussed. Also presented are algorithms for constrained nonlinear programming, including their theoretical and practical properties. DOE

N88-20861# Center for Mathematics and Computer Science, Amsterdam (Netherlands). Dept. of Operations Research and System Theory.
APPROXIMATION ALGORITHMS FOR SCHEDULING UNRELATED PARALLEL MACHINES
Jan Karel Lenstra, David B. Shmoys, and Eva Tardos (Massachusetts Inst. of Tech., Cambridge.) Sep. 1987 13 p Presented at the 28th Annual IEEE Symposium on the Foundations of Computer Science Submitted for publication
(Grants AF-AFOSR-0078-86; NSF MCS-83-11422; NSF ECS-85-01988; NSF MCS-81-20790)

(CWI-OS-R8714; B8731194; ETN-88-91752) Copyright Avail: NTIS HC A03/MF A01

A scheduling problem is considered. There are m parallel machines and n independent jobs. Each job is to be assigned to one of the machines. The processing of job j on machine i requires time p sub ij. The objective is to find a schedule that minimizes the makespan. A polynomial algorithm which constructs a schedule that is guaranteed to be no longer than twice the optimum is found. A polynomial approximation scheme for the case that the number of machines is fixed is presented. Both approximation results are corollaries of a theorem about the relationship of a class of integer programming problems and their linear programming relaxations. A polynomial method to round the fractional extreme points of the linear program to integral points that nearly satisfy the constraints is given. In contrast to the main result, it is proved that no polynomial algorithm can achieve a worst-case ratio less than 3/2 unless P = NP. A complexity classification for all special cases with a fixed number of processing times is obtained. ESA

N88-20862# Center for Mathematics and Computer Science, Amsterdam (Netherlands). Dept. of Computer Science/Dept. of Algorithmics and Architecture.

ON PROVING REGISTER ATOMICITY

Baruch Awerbuch, Lefteris M. Kirousis, Evangelos Kranakis, and Paul M. B. Vitanyi May 1987 27 p Submitted for publication

(Contracts N00014-83-K-0125; N00014-85-K-0168; DAAG29-84-K-0058; Grants AF-AFOSR-0078-86; NSF DCR-83-02391)

(CWI-CS-R8707; B8723967; ETN-88-91753) Copyright Avail: NTIS HC A03/MF A01

It is suggested that since concurrent access of shared variables by asynchronous processes does not require mutual exclusion, but can be solved with no waiting, a fruitful paradigm in this context is the notion of a shared register satisfying a niceness condition called atomicity. The model is presented, and a method for proving register atomicity is given. It is used to give simple proofs of the atomicity of two register constructions, the matrix register and the Bloom register, without assuming the existence of a global clock. The matrix construction shows how to implement an atomic, n-writer, n-reader register with value domain V from n squared atomic or even regular 1-writer, 1-reader registers with value domain N x V, with N the set of nonnegative integers. Bloom's construction shows how to implement an atomic, 2-writer, n-reader register with value domain V, from two atomic, 1-writer, n-1-reader registers with value domain (0,1)xV. These constructions are so simple that they may be even practical. ESA

N88-20863# Center for Mathematics and Computer Science, Amsterdam (Netherlands). Dept. of Computer Science/Dept. of Algorithmics and Architecture.

USING DESIGN AXIOMS AND TOPOLOGY TO MODEL DATABASE SEMANTICS

Arno Siebes and Martin L. Kersten Mar. 1987 17 p

(CWI-CS-R8711; B8711196; ETN-88-91757) Copyright Avail: NTIS HC A03/MF A01

A formal model that explicates database semantics through entity definitions and limits their use along well-defined paths is developed. The approach is based on six design axioms and concepts borrowed topology. This achieves a unified description of the database intension and its extension. It is shown that generalization/specialization hierarchies are naturally cast into proper subset hierarchies in the entity type topology. The limitations imposed on the construction of entity types preserve the Armstrong axioms for functional dependencies. This way the model captures much of the real-world semantic constraints and remains sound and complete. ESA

N88-20864# Center for Mathematics and Computer Science, Amsterdam (Netherlands). Dept. of Computer Science/Dept. of Software Technology.

A PARSER GENERATOR FOR FINITELY AMBIGUOUS CONTEXT-FREE GRAMMARS

Jan Rekers Mar. 1987 20 p Sponsored in part by the European Economic Commission ESPRIT Project 348

(CWI-CS-R8712; B8711197; ETN-88-91758) Copyright Avail: NTIS HC A03/MF A01

An implementation of the syntax definition formalism (SDF) is described. The SDF combines the specification of lexical syntax, context-free syntax, and abstract syntax in a single formalism. From an SDF definition a lexical scanner and parse tables are generated. These parse tables together with a universal parser form a parser for the defined language. The algorithm used in the universal parser allows finitely ambiguous context-free grammars. ESA

N88-20865# Center for Mathematics and Computer Science, Amsterdam (Netherlands). Dept. of Computer Science/Dept. of Interactive Systems.

THE CONCEPT OF INTELLIGENT INTEGRATED INTERACTIVE CAD SYSTEMS

Tetsuo Tomiyama and Paul J. W. tenHagen Apr. 1987 32 p Submitted for publication

(CWI-CS-R8717; B8717222; ETN-88-91762) Copyright Avail: NTIS HC A03/MF A01

The concept of Intelligent Integrated Interactive Computer Aided Design (IIICAD) systems is proposed. The IIICAD is expected to be a large software system based on knowledge engineering technology. The architecture of IIICAD was defined and its subsystems were clarified. The framework of IIICAD will be constructed having supervisor, integrated data description schema which has a language called integrated data description language, intelligent user interface, and application program interface. However, to achieve intelligence required to IIICAD, intelligent design subsystems must be implemented on top of the framework. ESA

N88-20866# Center for Mathematics and Computer Science, Amsterdam (Netherlands). Dept. of Computer Science/Dept. of Interactive Systems.

A MODEL FOR GRAPHICAL INTERACTION

P. J. W. tenHagen and R. vanLiere Apr. 1987 29 p Submitted for publication

(CWI-CS-R8718; B8717223; ETN-88-91763) Copyright Avail: NTIS HC A03/MF A01

A model for graphical interaction to be used to precisely and formally describe aspects of graphical input, graphical output and various correlations between the two is presented. The model encapsulates the fundamental properties of elementary graphics input devices and their feedback. It also encompasses the operational modes of such devices and the screen resources they occupy. It allows the description of compound inputs leading to the description of arbitrary complex interaction techniques. These interaction techniques can very precisely be controlled by the application program. One of the main achievements of the model is the encapsulation of the concept called I/O-symmetry. It is shown how the model can be used to describe concepts such as user freedom, direct manipulation, error recovery, and dialog scheduling. Directions for further development of the I/O-unit model are outlined. ESA

N88-20867# Center for Mathematics and Computer Science, Amsterdam (Netherlands). Dept. of Computer Science/Dept. of Interactive Systems.

PARALLEL GRAPHICAL OUTPUT FROM DIALOGUE CELLS

P. J. W. tenHagen and H. J. Schouten Apr. 1987 18 p

(CWI-CS-R8719; B8717224; ETN-88-91764) Copyright Avail: NTIS HC A03/MF A01

A system that accepts and processes graphical output from parallel processes using a single workstation, and its use in a user interface management system called dialog cells, is described. It allows for a programmer to easily, concisely, and precisely describe pictures and operations on them in a highly interactive environment. Each parallel process can do output independently, but pictures can also be moved from one process to another. Each process has its own graphical output environment. The

description and implementation of the system is based on graphical kernel system. ESA

N88-20868# Center for Mathematics and Computer Science, Amsterdam (Netherlands). Dept. of Computer Science/Dept. of Interactive Systems.
ORGANIZATION OF DESIGN KNOWLEDGE IN AN INTELLIGENT CAD ENVIRONMENT
T. Tomiyama and P. J. W. tenHagen Apr. 1987 31 p Presented at the IFIP Working Group 5.2 Working Conference on Expert Systems in Computer-Aided Design, Sydney, Australia, 16-20 Feb. 1987 Submitted for publication
(CWI-CS-R8720; B87239968; ETN-88-91765) Copyright Avail: NTIS HC A03/MF A01

The concept of intelligent integrated interactive computer aided design (CAD) systems is proposed. A language based on predicate logic and the object oriented programming paradigm is introduced: the mechanisms of the system are described in this language. The possibility to describe and organize design knowledge using this language is assessed, and it is shown how design knowledge should work and be embedded in an intelligent, integrated, and interactive CAD environment. ESA

N88-20869# Center for Mathematics and Computer Science, Amsterdam (Netherlands). Dept. of Computer Science.
ALGEBRA OF COMMUNICATING PROCESSES (ACP)TAU: A UNIVERSAL AXIOM SYSTEM FOR PROCESS SPECIFICATION
J. A. Bergstra (Amsterdam Univ., Netherlands) and J. W. Klop May 1987 21 p
(ESPRIT Proj. 432)
(CWI-CS-R8725; B8723973; ETN-88-91770) Copyright Avail: NTIS HC A03/MF A01

Starting with Basic Process Algebra (BPA), an axiom system for alternative composition (+) and sequential composition (x) of processes, a presentation in several intermediate stages leading to ACP tau, Algebra of Communicating Processes with abstraction is given. At each successive stage an example showing that the specification power is increased is presented. Graph models for the respective axiom systems are informally presented. The finite specification theorem for ACP tau, stating that each finitely branching, effectively presented process (as an element of the graph model) can be specified in ACP tau by means of a finite system of guarded recursion equations, is outlined. ESA

N88-20870# Center for Mathematics and Computer Science, Amsterdam (Netherlands). Dept. of Computer Science.
STEPS INTO A GEOMETER'S WORKBENCH
Varol Akman May 1987 24 p Submitted for publication
(CWI-CS-R8726; B8723974; ETN-88-91771) Copyright Avail: NTIS HC A03/MF A01

Use of computational geometry techniques in environments where graphics and robotics are natural candidates is discussed. This is a nontrivial task since computational geometry concerns itself with asymptotic analysis, and in search of elegance it ignores the special cases which are the bugbear of practical applications. Experimentation is a way to resolve these difficulties. A software system to act as a Geometer's Workbench is proposed. This entails the integration of geometric knowledge with algorithm animation and object-oriented graphics. The workbench should allow improvisation with geometric objects and is expected to broaden the way geometry is used in the style Macsyma accomplished for algebra. ESA

N88-20871# Center for Mathematics and Computer Science, Amsterdam (Netherlands). Dept. of Computer Science.
AN INTEGRATED DATA DESCRIPTION LANGUAGE FOR CODING DESIGN KNOWLEDGE
B. Veth Jul. 1987 22 p
(CWI-CS-R8731; B8729650; ETN-88-91776) Copyright Avail: NTIS HC A03/MF A01

A framework to describe design knowledge is presented. The theory of computer aided design (CAD) is used to formulate design maxims which were converted into Integrated Data Description Language specifications. Theory of CAD is also used to understand, clarify, model, and formalize design processes and design knowledge in an intelligent CAD environment. ESA

N88-20872# Center for Mathematics and Computer Science, Amsterdam (Netherlands). Dept. of Computer Science/Dept. of Software Technology.
DESIGNING EQUIVALENT SEMANTIC MODELS FOR PROCESS CREATION
Pierre America (Phillips International B.V., Eindhoven, Netherlands) and Jaco W. deBakker Jul. 1987 70 p Sponsored in part by the European Economic Commission ESPRIT Project 415
(CWI-CS-R8732; B8729651; ETN-88-91777) Copyright Avail: NTIS HC A05/MF A01

Operational and denotational semantic models are designed for languages with process creation, and the relationships between the two semantics are investigated. A uniform and static, a uniform and dynamic, a nonuniform and static, and a nonuniform and dynamic language are considered. The contrast between uniform and nonuniform is reflected in the use of linear time versus branching time models, the latter employing a version of Plotkin's resumptions. The operational semantics use Hennessy and Plotkin's transition systems. All models are built on metric structures, and involve continuations in an essential way. The languages studied are abstractions of the parallel object-oriented language POOL. The relationship between the two semantics for these abstractions is analyzed. A key role is played by an operator which decides dynamically whether it should act as sequential or parallel composition. ESA

N88-20873# Center for Mathematics and Computer Science, Amsterdam (Netherlands). Dept. of Computer Science/Dept. of Software Technology.
VERIFICATION OF A SYSTOLIC ALGORITHM FOR STRING COMPARISON
L. Kossen and W. P. Weijland (Amsterdam Univ., Netherlands) Jul. 1987 37 p Submitted for publication Sponsored in part by the European Economic Commission ESPRIT Project 432
(CWI-CS-R8734; B8729653; ETN-88-91779) Copyright Avail: NTIS HC A03/MF A01

A self-timed systolic system computing the edit distance between two strings is proved correct by means of the algebraical concurrency theory algebra of communicating processes. A systolic system is a system consisting of a great number of concurrently operating and cooperating elements. In the system described the flow of control is regulated by the elements themselves: the system is self-timed. A formal approach can be helpful to construct complex systems such as VLSI-circuits. ESA

N88-20874# Center for Mathematics and Computer Science, Amsterdam (Netherlands). Dept. of Computer Science/Dept. of Software Technology.
TWO NORMAL FORM THEOREMS FOR COMMUNICATING SEQUENTIAL PROCESSES (CSP) PROGRAM
K. R. Apt, L. Bouge, and Ph. Clermont (Etablissement Technique Central de l'Armement, Arcueil, France) Jul. 1987 15 p Sponsored in part by CNRS, France
(CNRS Proj. C3)
(CWI-CS-R8735; B8729654; ETN-88-91780) Copyright Avail: NTIS HC A03/MF A01

Two normal forms for Communicating Sequential Processes (CSP) programs are defined. In the first normal form, each process contains only one I/O repetitive command and all its I/O commands appear as guards of this command. In the second normal form, it is moreover required that all guards of this I/O repetitive command are in fact I/O guards. An inductive method which transforms any CSP program into an equivalent program in first or second normal form is described. The involved equivalence notion is discussed. It is shown that no transformation into second normal form can preserve deadlock-freedom. ESA

N88-20875# Technische Hogeschool, Eindhoven (Netherlands). Dept. of Electrical Engineering.
GM: A GATE MATRIX LAYOUT GENERATOR M.S. Thesis
G. J. P. vanLieshout and L. P. P. P. vanGinneken Sep. 1987 66 p
(EUT-87-E-179; ISBN-90-6144-179-X; ISSN-0167-9708; ETN-88-91826) Avail: NTIS HC A04/MF A01

A gate matrix cell generator which can layout any nMOS circuit is presented. The circuit is specified as a netlist of parametrizable transistors. The size of the transistors can be freely specified thereby giving the opportunity of optimizing parameters as power, speed, and fanout. Shape, pinout, and design rules can be parametrized. The pinout can be determined while building the gate matrix structure, by extending certain gates or nets to the correct side. The design rule parameters can be satisfied by a simple two dimensional grid-based compaction algorithm. The horizontal connections are realized in the metal layer and are called the nets. The vertical connections are realized in polysilicon and are called the gates. A two dimensional folding algorithm was used to improve the layout density and to manipulate the shape of the cell. Two dimensional folding allows nets to be assigned to the same row, as well as gates assigned to the same column. The area used for small logic examples is smaller on average (up to 40 percent smaller) than the area used by a pluri cell style random logic generator. ESA

N88-20876# Groningen Rijksuniversiteit (Netherlands). Dept. of Mathematics and Computing Science.
PREDICATE-TRANSFORMER SEMANTICS OF GENERAL RECURSION
Wim H. Hesselink 1987 27 p
(CS-8709; ETN-88-91867) Avail: NTIS HC A03/MF A01

The semantics of a language with arbitrary atomic statements, unbounded nondeterminacy, and mutual recursion is developed. The semantics is expressed in weakest preconditions and weakest liberal preconditions. Individual states are not mentioned. The predicates on the state space are treated as elements of a distributive lattice. The semantics of recursion is constructed by means of the theorem of Knaster-Tarski. It is proved that the law of the excluded miracle can be preserved, if that is wanted. The universal conjunctivity of the weakest liberal precondition, and the connection between the weakest precondition and the weakest liberal precondition are proved to remain valid. Hoare-triple methods for proving correctness and conditional correctness of programs are treated. ESA

N88-20877# Instituto de Pesquisas Espaciais, Sao Jose dos Campos (Brazil).
INTERPOLATION ALGORITHMS FOR DIGITAL TERRAIN MODELS [ALGORITMO DE INTERPOLACAO PARA MODELOS DIGITAIS DE TERRENO]
Luiz Alberto Vieira Dias Sep. 1987 12 p In PORTUGESE Presented at the 4th ERMAC, 14 Aug. 1987, Recife, Brazil
(INPE-4373-PRE/1196) Avail: NTIS HC A03/MF A01

Some methods of interpolation appropriate for use in digital elevation models are reviewed. For the case of interpolation of a 3-D surface, special emphasis is on the data in the Hermite model, with the calculation of routine tangents done through the Akima method. This model utilizes the Geographic Information System at INPE. Author

N88-20878*# Massachusetts Inst. of Tech., Cambridge. Dept. of Mechanical Engineering.
SPECTRAL ELEMENT METHODS: ALGORITHMS AND ARCHITECTURES
Paul Fischer, Einar M. Ronquist, Daniel Dewey, and Anthony T. Patera [1988] 33 p
(Grant NAG1-574)
(NASA-CR-182701; NAS 1.26:182701) Avail: NTIS HC A03/MF A01 CSCL 09B

Spectral element methods are high-order weighted residual techniques for partial differential equations that combine the geometric flexibility of finite element methods with the rapid convergence of spectral techniques. Spectral element methods are described for the simulation of incompressible fluid flows, with special emphasis on implementation of spectral element techniques on medium-grained parallel processors. Two parallel architectures are considered: the first, a commercially available message-passing hypercube system; the second, a developmental reconfigurable architecture based on Geometry-Defining Processors. High parallel efficiency is obtained in hypercube spectral element computations, indicating that load balancing and communication issues can be successfully addressed by a high-order technique/medium-grained processor algorithm-architecture coupling. Author

N88-20879# Los Alamos National Lab., N. Mex.
DYNAMIC RUN-TIME GRAPHICS
J. Tabor 1987 16 p Presented at the Cray User Group Spring Meeting, New York, N.Y., 21 Apr. 1987
(Contract W-7405-eng-36)
(DE87-008997; LA-UR-87-1270; CONF-8704165-3) Avail: NTIS HC A03/MF A01

The major components of the Instant Graphics Package (IGP) have been integrated with the Dynamic Debugging Tool (DDT). IGP and DDT can produce 1D, 2D, and 3D plots; 2D contour plots; and array-versus-array plots at run time for a CTSS controllee memory image. These plots can be used to graphically inspect any array and to satisfy many of the user community's routine graphics requirements. A brief overview of the USERPORT feature, which can dynamically interface to any fragment of a CTSS controllee, will be presented. DOE

N88-20880# Idaho State Univ., Pocatello. Coll. of Engineering.
A REPORT ON THE STUDY OF ALGORITHMS TO ENHANCE VECTOR COMPUTER PERFORMANCE FOR THE DISCRETIZED ONE-DIMENSIONAL TIME-DEPENDENT HEAT CONDUCTION EQUATION: EPIC RESEARCH, PHASE 1
A. Majumdar and H. Makowitz Oct. 1987 40 p Presented at the Joint Meeting of the American Nuclear Society and the Atomic Industrial Forum, Los Angeles, Calif., 15 Nov. 1987 Prepared in cooperation with Edgerton, Germeshausen and Grier, Inc., Idaho Falls, Idaho
(Contract DE-AC07-76ID-01570)
(DE88-005642; EGG-M-38987; CONF-871101-81) Avail: NTIS HC A03/MF A01

With the development of modern vector/parallel supercomputers and their lower performance clones it has become possible to increase computational performance by several orders of magnitude compared to the previous generation of scalar computers. These performance gains are not observed when production versions of current thermal-hydraulic codes are implemented on modern supercomputers. It is our belief that this is due in part to the inappropriateness of using old thermal-hydraulic algorithms with these new computer architectures. It is believed that a new generation of algorithms needs to be developed for thermal-hydraulics simulation optimized for vector/parallel architectures, and not the scalar computers of the previous generation. A study is begun to investigate several approaches for designing such optimal algorithms. These approaches are based on the following concepts: minimize recursion; utilize predictor-corrector iterative methods; maximize the convergence rate of iterative methods used; use physical approximations as well as numerical means to accelerate convergence; utilize explicit methods (i.e., marching) where stability will permit. We call this approach the EPIC methodology (i.e., Explicit Predictor Iterative Corrector methods). Utilizing the above ideas, work was begun on the investigation of the one-dimensional transient heat conduction equation. Algorithms based on variations of the Hopscotch concept are developed, which are discussed in the body of this report. DOE

N88-20881# Fermi National Accelerator Lab., Batavia, Ill.
FINITE STATE TABLES FOR GENERAL COMPUTER PROGRAMMING APPLICATIONS
M. Leininger Jan. 1988 16 p

(Contract DE-AC02-76CH-03000)
(DE88-006254; FNAL-TM-1508) Avail: NTIS HC A03/MF A01

The Finite State Table is a computer programming technique which offers a faster and more compact alternative to traditional logical control structures such as the IF-THEN-ELSE statement. A basic description of this technique is presented. The application example is the creation of plot output from engineering analysis and design models generated by I-DEAS, a commercial software package used for solid modeling, finite element analysis, design and drafting. DOE

N88-20882# Instituto de Pesquisas Espaciais, Sao Jose dos Campos (Brazil).
AN IMPLEMENTATION OF THE OPS5 LANGUAGE FOR COMPUTERS COMPATIBLE WITH IBM-PC [UMA IMPLEMENTACAO DA LINGUAGEM OPS5 PARA COMPUTADORES COMPATIVEIS COM O IBM-PC]
Flavio Roberto DiasVelasco Aug. 1987 11 p In PORTUGESE Presented at the 4th Brazilian Symposium on Artificial Intelligence, Uberlandia, M.G., 13-16 Oct. 1987
(INPE-4291-PRE/1162) Avail: NTIS HC A03/MF A01

The OPS5 language is a programming language based on rules reserved for implementation of expert systems. The most important characteristics of the OPS5 language are: efficiency (through the use of the Rete algorithm), generality (lending itself to various applications), and powerful mechanisms of model harmony. This work describes the implementation of the OPS5 language for microcomputers (IBM compatible). The internal structure of the data implementation is displayed, with emphasis on decision design. Author

N88-20883# Technische Hogeschool, Eindhoven (Netherlands).
SIMULATION OF MEASURING POINTS FOR THREE DIMENSIONAL MEASUREMENTS [SIMULATIE VAN MEETPUNTEN BIJ DRIEDIMENSIONALE METINGEN]
J. Koning Aug. 1986 9 p In DUTCH
(WPB-0115; ETN-88-91319) Avail: NTIS HC A02/MF A01

A method for the introduction of numerical values in a measuring apparatus in order to test its behavior, and especially the calculation methods was developed. The method can be used to test algotithms in computer programs, as well as for didactic applications. For didactic purposes the measured value can be introduced using a simple addressable program. The method is less suited to test algorithms because many (1000) measuring points have to be introduced, which increases the error probability drastically. The details of the program, as well as an example are given. ESA

N88-20884# Wageningen Agricultural Univ. (Netherlands). Vakgroep Informatica.
EXPERT SYSTEM TECHNIQUES AND DECISION SUPPORT SYSTEM: A CASE STUDY (DEC. 1985 - JUN. 1986) [EXPERT SYSTEM TECHNIEKEN EN DECISION SUPPORT SYSTEM; EEN CASE STUDIE. DEC. 85 - JUN. 86]
W. J. H. Geraets 1986 70 p In DUTCH
(ETN-88-91347) Avail: NTIS HC A04/MF A01

The possibilities to improve the Decision Support System (DSS) program VLUCHT using Expert System (ES) techniques were investigated. It is explained how a DSS and an ES function. The program was modified for use on a VAX computer. The effects of the use of ES techniques on the existing DSS program system are presented. The behavior of an experienced user with respect to the program was formalized, and the resulting rules were implemented in the program. It is concluded that ES techniques can be a meaningful supplement for existing DSS program systems. ESA

N88-20503# Joint Publications Research Service, Arlington, Va.
COMPUTER-AIDED TRANSFORMATION OF DESCRIPTIVE MODE OF MATHEMATICAL MODELS OF A CONTROL SYSTEM
Wenjin Gu and Fuchun Sun *In its* JPRS Report: Science and Technology. China 7 Jul. 1987 p 18-27 Transl. into ENGLISH from Zidonghua Yibiao (Shanghai, People's Republic of China), v. 7, no. 8, Aug. 1986 p 29-33, 46 , 46 (For primary document see N88-20501 13-31)
Avail: NTIS HC A06/MF A01

62 COMPUTER SYSTEMS

Includes computer networks and special application computer systems.

N88-20885# Carnegie-Mellon Univ., Pittsburgh, Pa. Dept. of Computer Science.
DISTRIBUTED TRANSACTION PROCESSING AND THE CAMELOT SYSTEM Interim Report
Alfred Z. Spector Dec. 1987 30 p
(Contract F33615-84-K-1520)
(AD-A188614; CMU-CS-87-100; AFWAL-TR-87-1163) Avail: NTIS HC A03/MF A01 CSCL 12E

This paper describes distributed transaction processing, a technique used for simplifying the construction of reliable distributed systems. After introducing transaction processing, the paper presents models describing the structure of distributed systems, and the transactional computations on them. The layered software architecture model contains five layers, including an intermediate layer that provides a common set of useful functions for supporting the highly reliable operation of system services, such as data management, file management, and mail. The functions of this layer can be realized in what is termed a distributed transaction facility. The paper then describes one such facility - Camelot. Camelot provides flexible and high performance commit supervision, disk management, and recovery mechanisms that are useful for implementing a wide class of data types, including large databases. It runs on the Unix-compatible Mach operating system and uses the standard Arpanet IP communication protocols. Presently, Camelot runs on RT PC's and Vaxes, but it should also run on other computers including shared memory multiprocessors. GRA

N88-20886# Rochester Univ., N. Y. Dept. of Computer Science.
COMPUTING WITH STRUCTURED CONNECTIONS NETWORKS
Jerome A. Feldman, Mark A. Fanty, Nigel Goddard, and Kenton Lynne Apr. 1987 39 p
(Contracts N00014-82-K-0193; N00014-84-K-0655; Grant NSF DCR-83-20136)
(AD-A189244; TR-213) Avail: NTIS HC A03/MF A01 CSCL 12I

Rapid advances both in the neurosciences and in computer science lead to a new interest in computational models linking animal brains and behavior. In computer science, there is a large and growing body of knowledge about parallel computation and another, largely separate, science of artificial intelligence. Massively parallel realizations of intelligent activity promises to be fruitful for the study of both natural and artificial computations. Much attention has been directed towards the biological implications of this interdisciplinary effort, but there are equally important relations with computational theory, hardware and software. The focus here is on the design and use of massively parallel computational models, particularly in artificial intelligence. Much of the recent work on massively parallel computation has been carried out by physicists and examines the emergent behavior of large, unstructured collections of computing units. We are more concerned with how one can design, realize and analyze networks that embody the specific computational structures needed to solve hard problems. Adaptation and learning are treated as ways to improve structured networks, not as a replacement for analysis and design. GRA

N88-20887# Air Force Inst. of Tech., Wright-Patterson AFB, Ohio. School of Engineering.
A SIMULATION STUDY OF A PARALLEL PROCESSOR WITH UNBALANCED LOADS M.S. Thesis
Timothy S. Moore Dec. 1987 115 p Original contains color illustrations
(AD-A189573; AFIT/GCS/ENG/87D-20) Avail: NTIS HC A06/MF A01 CSCL 12F

The purpose of this thesis was twofold: to estimate the impact of unbalanced computational loads on a parallel processing architecture via Monte Carlo simulation; and second to investigate the impact of representing the dynamics of the parallel processing problem via animated simulation. It is constrained to the hypercube architecture in which each node is connected in a predetermined topology and allowed to communicate to other nodes through calls to the operating system. Routing of messages through the network is fixed and specified within the operating system. Message transmission preempts nodal processing causing internodal communications to complicate the concurrent operation of the network. Two independent variables are defined: (1) the degree of imbalance characterizes the nature or severity of the load imbalance, and (2) the degree of locality characterizes the node loadings with respect to node locations across the cube. A SLAM II simulation model of a generic 16 node hypercube was constructed in which each node processes a predetermined number of computational tasks and, following each task, sends a message to a single randomly chosen receiver node. GRA

N88-20888# Illinois Univ., Urbana. Center for Supercomputing Research and Development.
ON THE DESIGN OF PARALLEL NUMERICAL METHODS IN MESSAGE PASSING AND SHARED MEMORY ENVIRONMENTS
Y. Saad Feb. 1987 24 p Presented at the International Seminar on Scientific Supercomputers, Paris, France, 2 Feb. 1987
(Contract DE-FG02-85ER-25001)
(DE88-003566; DOE/ER-25001/58; CONF-870294-2; CSRD-614) Avail: NTIS HC A03/MF A01

This paper presents a comparative view of the methodologies used in parallel methods for scientific computing. Our goal is to put in contrast the approaches taken when developing scientific software for two broad classes of parallel machines namely shared memory machines and distributed memory machines. We will illustrate our discussion with two specific algorithms namely the Alternating Directions Implicit method and the Preconditioned Conjugate Gradient method. DOE

N88-20889# Center for Mathematics and Computer Science, Amsterdam (Netherlands). Dept. of Operations Research and System Theory.
PERSPECTIVES ON PARALLEL COMPUTING
G. A. P. Kindervater, J. K. Lenstra, and A. H. G. RinnooyKan (Erdmagnetisches Observatorium Wingst, Hoeftgrube , West Germany) Jun. 1987 8 p Submitted for publication. Sponsored by a NSF Presidential Young Investigator Award
(CWI-OS-R8709; B8723354; ETN-88-91748) Copyright Avail: NTIS HC A02/MF A01

Perspectives for operations research using parallel processing are assessed. More realism in theoretical models of parallel computation and more uniformity in available architectures are required. Formal techniques have to be developed for the design and implementation of efficient parallel algorithms. ESA

N88-20890# Center for Mathematics and Computer Science, Amsterdam (Netherlands). Dept. of Computer Science/Dept. of Algorithmics and Architecture.
LOCALITY, COMMUNICATION AND INTERCONNECT LENGTH IN MULTICOMPUTERS
Paul M. B. Vitanyi Feb. 1987 14 p Submitted for publication
(Contracts N00014-85-K-0168; DAAG29-84-K-0058; N00014-83-K-0125; Grant NSF DCR-83-02391)
(CWI-CS-R8708; B8711193; ETN-88-91754) Copyright Avail: NTIS HC A03/MF A01

The lower bound on the average interconnect (wire) length in d-dimensional embeddings of symmetric circuits is proved to be within a small constant multiplicative factor of the obvious worst-case upper bound. The proof is simple, geometrical, and works for wires with zero volume, thus increasing the range of applicability of the results, e.g., to optical (fiber) or photonic (fiberless, laser) communication. While getting rid or the von Neumann bottleneck in the shift from sequential to nonsequential computation, a new communication bottleneck arises from the interplay between locality of computation, communication, and the number of dimensions of physical space. ESA

N88-20891# Center for Mathematics and Computer Science, Amsterdam (Netherlands). Dept. of Computer Science/Dept. of Software Technology.
A PROOF RULE PROCESS CREATION
Frank S. deBoer Feb. 1987 45 p
(CWI-CS-R8710; B8711195; ETN-88-91756) Copyright Avail: NTIS HC A03/MF A01

A Hoare-style proof system for partial correctness is defined for a language which embodies the kind of parallelism which stems from process-creation. The proof theoretic concepts of cooperation test, global invariant, bracketed section, and auxiliary variables are used. The proof theory of a language with a generalization of the synchronous message-passing mechanism of CSP is studied. The syntactic construct of process creation and its semantic definition is taken from the language POOL. One of the main characteristics of this language is that the communication partner referred to by an output statement (or input statement) is not syntactically identifiable, in contrast with the mentioned languages. The proof system is built upon the way the semantic mechanism of process identification is brought to the syntactic level. The proof system is shown to be sound and relatively complete. ESA

N88-20892# Center for Mathematics and Computer Science, Amsterdam (Netherlands). Dept. of Computer Science.
AN AMOEBA REPLICATED SERVICE ORGANISATION
Irvin Shizgal May 1987 10 p
(ESPRIT Proj. 432)
(CWI-CS-R8723; B8723971; ETN-88-91768) Copyright Avail: NTIS HC A02/MF A01

A distributed algorithm which allows replicated instances of an amoeba local area network server at distinct sites to dynamically locate other currently active server sites, and for these to cooperate in the maintenance of replicated data is described. The technique eliminates dependence on other services such as name servers, requires no multicast support, and does not assume the availability of any other means of information sharing, such as a common file system. ESA

N88-20893# Center for Mathematics and Computer Science, Amsterdam (Netherlands). Dept. of Computer Science.
A FULLY ABSTRACT SEMANTICS FOR DATA FLOW NETS
Joost N. Kok May 1987 21 p Presented at the PARLE Conference Submitted for publication
(Grant ZWO-125-20-04)
(CWI-CS-R8724; B8723972; ETN-88-91769) Copyright Avail: NTIS HC A03/MF A01

Two semantic models for data flow nets are given. The first model is an intuitive, operational model. This model has an important drawback: it is not compositional. An example given in Brock and Ackerman (1981) shows the noncompositionality of the model. There exist two nets that have the same semantics, but when they are placed in a specific context, the semantics of the resulting nets differ. The second one is obtained by adding information to the first model. The amount of information is enough to make it compositional. It is shown that the minimal amount of information to make the model compositional is added. The second model is fully abstract with respect to the equivalence generated by the first model. The first model describes the semantics of data flow net as a function from (tuples of) sequences of tokens to sets of (tuples of) sequences of tokens. The second one maps a data flow net to a function from (tuples of) infinite sequences of

finite words to sets of (tuples of) infinite sequences of finite words. ESA

N88-20894*# National Aeronautics and Space Administration. Langley Research Center, Hampton, Va.
A SURVEY OF PROVABLY CORRECT FAULT-TOLERANT CLOCK SYNCHRONIZATION TECHNIQUES
Ricky W. Butler Feb. 1988 28 p
(NASA-TM-100553; NAS 1.15:100553) Avail: NTIS HC A03/MF A01 CSCL 09B

Six provably correct fault-tolerant clock synchronization algorithms are examined. These algorithms are all presented in the same notation to permit easier comprehension and comparison. The advantages and disadvantages of the different techniques are examined and issues related to the implementation of these algorithms are discussed. The paper argues for the use of such algorithms in life-critical applications. Author

N88-20895*# Research Triangle Inst., Research Triangle Park, N.C. Center for Digital Systems Research.
A FAULT INJECTION EXPERIMENT USING THE AIRLAB DIAGNOSTIC EMULATION FACILITY
Robert Baker, Scott Mangum, and Charlotte Scheper Mar. 1988 130 p
(Contract NAS1-17964)
(NASA-CR-178390; NAS 1.26:178390) Avail: NTIS HC A07/MF A01 CSCL 09B

The preparation for, conduct of, and results of a simulation based fault injection experiment conducted using the AIRLAB Diagnostic Emulation facilities is described. An objective of this experiment was to determine the effectiveness of the diagnostic self-test sequences used to uncover latent faults in a logic network providing the key fault tolerance features for a flight control computer. Another objective was to develop methods, tools, and techniques for conducting the experiment. More than 1600 faults were injected into a logic gate level model of the Data Communicator/Interstage (C/I). For each fault injected, diagnostic self-test sequences consisting of over 300 test vectors were supplied to the C/I model as inputs. For each test vector within a test sequence, the outputs from the C/I model were compared to the outputs of a fault free C/I. If the outputs differed, the fault was considered detectable for the given test vector. These results were then analyzed to determine the effectiveness of some test sequences. The results established coverage of selt-test diagnostics, identified areas in the C/I logic where the tests did not locate faults, and suggest fault latency reduction opportunities. Author

N88-20896*# National Aeronautics and Space Administration. Hugh L. Dryden Flight Research Center, Edwards, Calif.
THE USE OF AN AUTOMATED FLIGHT TEST MANAGEMENT SYSTEM IN THE DEVELOPMENT OF A RAPID-PROTOTYPING FLIGHT RESEARCH FACILITY
Eugene L. Duke, Marie D. Hewett, Randal W. Brumbaugh, David M. Tartt, Robert F. Antoniewicz, and Arvind K. Agarwal May 1988 21 p Presented at the 4th Conference on Artificial Intelligence Applications, Long Beach, Calif., 4-6 May 1988
(NASA-TM-100435; H-1477; NAS 1.15:100435) Avail: NTIS HC A03/MF A01 CSCL 09B

An automated flight test management system (ATMS) and its use to develop a rapid-prototyping flight research facility for artificial intelligence (AI) based flight systems concepts are described. The ATMS provides a flight test engineer with a set of tools that assist in flight planning and simulation. This system will be capable of controlling an aircraft during the flight test by performing closed-loop guidance functions, range management, and maneuver-quality monitoring. The rapid-prototyping flight research facility is being developed at the Dryden Flight Research Facility of the NASA Ames Research Center (Ames-Dryden) to provide early flight assessment of emerging AI technology. The facility is being developed as one element of the aircraft automation program which focuses on the qualification and validation of embedded real-time AI-based systems. Author

63 CYBERNETICS

Includes feedback and control theory, artificial intelligence, robotics and expert systems.

For related information see also *54 Man/System Technology and Life Support.*

N88-20897# Instituto de Pesquisas Espaciais, Sao Jose dos Campos (Brazil).
MATHEMATIC MODELING OF VISUAL PERCEPTION PROBLEMS [MODELAGEM MATEMATICA DE PROBLEMAS DE PERCEPCAO VISUAL]
Paulo Ouvera Simoni Sep. 1987 9 p In PORTUGUESE; ENGLISH summary Presented at the 10th National Congress of Applied Mathematics and Computation, Gramado, RS, 21-25 Sep. 1987
(INPE-4355-PRE/1186) Avail: NTIS HC A02/MF A01

Some Artificial Intelligence problems which occur at the preliminary steps of the vision process are presented. They require a mathematical formulation in terms of differential equations, as well as solutions by variational calculus. The way that these problems were modeled is described, mainly the subjects concerning the search of constraints which allow the generation of computational rules, and the difficulty in dealing with situations in which more than one phenomenon is important. Author

N88-20898# Carnegie-Mellon Univ., Pittsburgh, Pa. Dept. of Computer Science.
SOAR: AN ARCHITECTURE FOR GENERAL INTELLIGENCE Interim Report
Allen Newell, Paul S. Rosenbloom, and John E. Laird Dec. 1987 68 p
(Contract F33615-84-K-1520; AF Proj. 4976)
(AD-A188742; CMU-CS-86-171; AFWAL-TR-87-1177) Avail: NTIS HC A04/MF A01 CSCL 12I

The ultimate goal of work in cognitive architecture is to provide the foundation for a system capable of general intelligent behavior, i.e., to provide the underlying structure that would enable a system to perform the full range of cognitive tasks, employ the full range of problem-solving methods and representations appropriate to the tasks, and learn about all aspects of the tasks and its performance on them. This article presents Soar, an implemented proposal for such an architecture. We describe its organizational principles, the system as currently implemented, and demonstrations of its capabilities. Soar embodies 11 basic hypothesis about the structure of an architecture for general intelligence: (1) Physical symbol-system: A general intelligence must be realized with a symbolic system; (2) Goal-structure: Control in a general intelligence is maintained by a symbolic goal system; (3) Uniform elementary-representation: There is a single elementary representation for declarative knowledge; (4) Problem-space: Problem spaces are the fundamental organizational unit of all goal-directed behavior; (5) Production-system: Production systems are the appropriate organization for encoding all long-term knowledge; and (6) Universal-subgoaling: Any decision can be an object of goal-oriented attention; (7) Automatic-subgoaling: All goals arise dynamically in response to impasses and are generated automatically by the architecture; (8) Control-knowledge: Any decision can be controlled by indefinite amounts of knowledge, both domain dependent and independent; (9) Weak-method: The weak methods form the basic methods of intelligence; (10) Weak-method emergence: The weak methods arise directly from the system responding based on its knowledge of the task; and (11) Uniform-learning: Goal-based chunking is the general learning mechanism, all having varying standing in current research in artificial intelligence. Many aspects of the Soar architecture are not reflected in these eleven hypotheses, and are discussed in detail. GRA

N88-20899# Rochester Univ., N. Y. Dept. of Computer Science.
KNOWLEDGE RETRIEVAL AS SPECIALIZED INFERENCE
Alan M. Frisch May 1987 105 p
(Contract N00014-80-C-0197; Grant NSF-DCR-83-51665)

(AD-A189042; TR-214) Avail: NTIS HC A06/MF A01 CSCL 12I

Artificial intelligence reasoning systems commonly contain a large corpus of declarative knowledge, called a knowledge base (KB), and provide facilities with which the system's components can retrieve this knowledge. Formal specifications that capture certain informal intuitions about retrieval are developed, studied, and implemented by retrieval algorithms. Consistent with the necessity for fast retrieval is the guiding intuition that a retriever is, at least in simple cases, a pattern matcher, though in more complex cases it may perform selected inferences such as property inheritance. The entire process of retrieval can be reviewed as a form of inference and hence the KB as a representation, not merely a data structure. A retriever makes a limited attempt to prove that a queried sentence is a logical consequence of the KB. When constrained by the no-chaining-restriction, inference becomes indistinguishable from pattern matching. Imagining the KB divided into quanta, a retriever that respects this restriction cannot combine two quanta in order to derive a third. The techniques of model theory will build non-procedural specifications of retrievability relations, which determine what sentences are retrievable from what KBs. Model-theoretic specifications are presented for four retrievers, each extending the capabilities of the previous one. GRA

N88-20900# Oak Ridge National Lab., Tenn.
A DARWINIAN APPROACH TO ARTIFICIAL NEURAL SYSTEMS
W. B. Dress and J. R. Knisley 1987 7 p Presented at the IEEE International Conference on Systems, Man and Cybernetics, Alexandria, Va., 20 Oct. 1987
(Contract DE-AC05-84OR-21400)
(DE87-013184; CONF-8710124-4) Avail: NTIS HC A02/MF A01

Self-organization in artificial neural systems and simulated genetic methods for determining functional parameters of such systems have been combined. This leads to a model of the genome as a self-organizing system on a supra-organism level, and to suggestions for a number of experiments to be performed on the abstract genetic space. The problem of the open system is also addressed in this model. A synthetic intelligent system is viewed as an extensible set of parameters-the evolved genome. This set also serves as a specification file for individual synthetic organisms, and algorithms for network-construction use this set as data for creating specific networks. It is this set of parameters that undergoes mutation and selection leading to a synthetic organism fulfilling the goals of the systems designer. DOE

N88-20901# Edgerton, Germeshausen and Grier, Inc., Idaho Falls, Idaho.
QUALITY ENHANCEMENT WITH MACHINE INTELLIGENCE
M. R. Johnson 1988 9 p Presented at the International Symposium on Computer-aided Quality Assurance, Leipzig, German Democratic Republic, 17 Mar. 1988
(Contract DE-AC07-76ID-01570)
(DE88-005639; EGG-M-40187; CONF-880345-1) Avail: NTIS HC A02/MF A01

This paper discussed applications of machine intelligence for quality enhancement in several areas of technology including signal verification and validation, control systems, fault tolerance, artificial intelligence, and medical research. The purpose of this general presentation is to set the stage for the more detailed ideas that will follow in the symposium, and to encourage participants to broaden their views, definitions, and thinking in regard to quality. DOE

N88-20902# Lawrence Livermore National Lab., Calif.
ROBUST DECENTRALIZED CONTROL OF LARGE FLEXIBLE STRUCTURES
S. C. Lu, I. K. Fong, S. H. Wang, and S. Bumpus 17 Nov. 1987 48 p Prepared in cooperation with California Univ., Davis.
(Contract W-7405-eng-48)
(DE88-005416; UCRL-15980) Avail: NTIS HC A03/MF A01

This report studies the problem of controlling a large flexible structure with robust decentralized feedback control. A decentralized optimal control algorithm is applied to compute the parameters of the robust controller. The proposed method is tested on the ACOSS Model No. 2, which is a realistic evaluation model for active structure control methods. Twelve co-located sensors and actuators are applied in order to suppress vibrations which are caused by two external disturbances. It is demonstrated that the proposed method can stabilize the closed-loop system via decentralized feedback. Other performance measures are also discussed. DOE

N88-20903# Center for Mathematics and Computer Science, Amsterdam (Netherlands). Dept. of Computer Science.
GEOMETRY AND GRAPHICS APPLIED TO ROBOTICS
Varol Akman May 1987 22 p Submitted for publication
(CWI-CS-R8727; B8723975; ETN-88-91772) Copyright Avail: NTIS HC A03/MF A01

Efforts on integrating robotics and computer science ideas are reviewed. The view that applying results from areas of computer science such as concrete complexity, symbolic computation, and computational geometry will simplify the work of robot programmers is advocated. For model-based robotics, it is argued that the time has come to build a Geometer's Workbench, a system integrating geometric knowhow with algorithm animation techniques and interactive graphics to visualize complex situations as encountered in robotics. Such a system is expected to broaden the way geometry is practiced in the style Macsyma accomplished for algebra. ESA

N88-20904# Groningen Rijksuniversiteit (Netherlands). Dept. of Mathematics and Computing Science.
USING TRACE THEORY TO MODEL DISCRETE EVENTS
Rein Smedinga Aug. 1987 28 p
(CS-8708; ETN-88-91866) Avail: NTIS HC A03/MF A01

Discrete processes are defined by means of trace structures. Every symbol in a trace denotes (the occurrence of) a discrete event. The trace alphabet is split into two disjoint sets, one denoting the communication events, the other denoting the exogenous events. Control of a discrete process means constructing a second discrete process having as alphabet the communication events only, so that the connection of the two discrete processes results in a desired exogenous trace set. Connection of discrete processes means blending of the corresponding trace structures. An algorithm to construct a controller, given a process to be controlled and specifications of the desired exogenous behavior is derived. Two examples of the use of this algorithm are presented: the dining philosophers and ships passing through a lock with two gates. ESA

N88-20905*# Jet Propulsion Lab., California Inst. of Tech., Pasadena.
PREDICTIVE MONITORING RESEARCH: SUMMARY OF THE PREMON SYSTEM
Richard J. Doyle, Suzanne M. Sellers, and David J. Atkinson 15 Dec. 1987 16 p
(Contract NAS7-918)
(NASA-CR-182687; JPL-Pub-87-40; NAS 1.26:182687) Avail: NTIS HC A03/MF A01 CSCL 09B

Traditional approaches to monitoring are proving inadequate in the face of two important issues: the dynamic adjustment of expectations about sensor values when the behavior of the device is too complex to enumerate beforehand, and the selective but effective interpretation of sensor readings when the number of sensors becomes overwhelming. This system addresses these issues by building an explicit model of a device and applying common-sense theories of physics to model causality in the device. The resulting causal simulation of the device supports planning decisions about how to efficiently yet reliably utilize a limited number of sensors to verify correct operation of the device. Author

64 NUMERICAL ANALYSIS

Includes iteration, difference equations, and numerical approximation.

N88-20906# Stanford Univ., Calif. Dept. of Statistics.
SURVIVAL ANALYSIS USING ADDITIVE RISK MODELS
Fred W. Huffer and Ian W. McKeague 6 Oct. 1987 37 p
(Contract N00014-86-K-0156)
(AD-A189053; SU-TR-396) Avail: NTIS HC A03/MF A01 CSCL 12C

In this paper we study Aalen's additive risk model for the regression analysis of censored survival data. The additive risk model provides a useful alternative to Cox's (1972) proportional hazards model when large sample size makes its application feasible. It is capable of providing detailed information concerning the temporal influence of each covariate. The temporal influences of the covariates are not assumed to be proportional as they are in Cox's model. Buckley has pointed out that additive risk models are biologically more plausible than proportional hazard models. Also, the use of the proportional hazards model when the true model is additive risk has been found by O'Neil to result in serious asymptiotic bias. The first purpose of the present paper is to apply the additive risk model to the analysis of grouped data in which only the person-years at risk and number of uncensored deaths over successive time intervals, tabulated for various levels of the covariates, are available. This kind of data typically arises in epidemiological cohort studies involving the follow-up of large population groups over many years, see Breslow. Our approach is to use an estimator, constructed using the method of sieves, for which an asymptotic distribution theory was developed by McKeague. GRA

N88-20907# Naval Postgraduate School, Monterey, Calif.
ROBUSTIFYING THE KALMAN FILTER M.S. Thesis
D. P. Gaver and P. A. Jacobs Nov. 1987 22 p
(AD-A189240; NPS55-87-014) Avail: NTIS HC A03/MF A01 CSCL 12C

Kalman filters are tracking and prediction algorithms based on Gaussian measurement errors and structural models. The Kalman filter performance may degrade if the measurement errors come from a thicker-tailed-than Gaussian distribution. In this report non-linear procedures are described which are based on Kalman-type models, but work with student-t measurement errors. GRA

N88-20908# Florida Univ., Gainesville. Center for Mathematical System Theory.
RESEARCH IN APPLIED MATHEMATICS RALATED TO IDENTIFICATION OF NOISY SYSTEMS Final Report, 1 Apr. 1985 - 30 Sep. 1987
Rudolf E. Kalman 12 Jan. 1988 24 p
(Contract DAAG29-85-K-0099)
(AD-A189355; ARO-22356.12-MA) Avail: NTIS HC A03/MF A01 CSCL 12E

The research program for noisy analysis and noisy realization theory is only about half way complete. An extensive amount of data analysis by computer was performed during the past two years, supplementing spot-checks in 1981 to 1984 on real data. These previous data analyses were important in showing that new research is needed. The empirical analysis of real data is related to the present build-up of the Center's own computer facilities and serves as a check on the programs being developed. The results of the theoretical and computer investigations on the identification of static systems (linear relations) will appear soon in the research monograph KALMAN that has been in preparation for several years. The objective of the monograph is not only to explain the facts of life but also to enable the reader to duplicate the quite sophisticated data and analysis procedures which have been developed. In short, the objective of the monograph is not polemical but tutorial. GRA

N88-20909# Iowa State Univ. of Science and Technology, Ames. Dept. of Mathematics.
NUMERICAL SOLUTION OF ILL POSED PROBLEMS IN PARTIAL DIFFERENTIAL EQUATIONS Final Technical Report, 1 Oct. 1984 - 30 Sep. 1987
Howard A. Levine Sep. 1987 27 p
(Grant AF-AFOSR-0252-84)
(AD-A189383; AFOSR-87-1917TR) Avail: NTIS HC A03/MF A01 CSCL 12A

This project is concerned with several questions concerning the existence, uniqueness, continuous data dependence and numerical computation of solutions of various ill-posed problems in partial differential equations. Several problems involving reaction diffusion equations with and without convection terms present were studied. In the latter case the ability of finite element approximate solutions to reproduce the continuous time dynamics was investigated. In the former case a convective diffusion equation with a similar source in the boundary condition was analyzed. A fairly complete picture of the dynamics was obtained. With the source term in the equation, computations revealed a rich structure which has been partially analyzed theoretically. Several problems for reaction diffusion equations in unbounded regimes were also investigated. It was shown that under certain conditions in the rate law all nonzero solutions blow up in finite time, while for other conditions in the rate law, solutions damp out. GRA

N88-20910# North Carolina Univ., Chapel Hill. Psychometric Lab.
MEASURES OF SIMILARITY BETWEEN FUZZY CONCEPTS: A COMPARATIVE ANALYSIS Interim Report, Aug. 1985 - Aug. 1986
Rami Zwick, Edward Carlstein, and David Budescu Dec. 1987 35 p
(Contract MDA903-83-K-0347; DA Proj. 2Q6-1102-B-74-F)
(AD-A189430; ARI-RN-87-68) Avail: NTIS HC A03/MF A01 CSCL 12I

This research note discusses the selection of an appropriate index to measure the similarity between fuzzy subsets (concepts). The note reviews 19 measures of linguistic approximation procedures, and compares their performance in a behavioral experiment. For categorizing pairs of fuzzy concepts as similar or dissimilar all measures performed well. For distinguishing degrees of similarity or dissimilarity, however, certain measures were superior. The best measures focus on only one slice of membership function. GRA

N88-20911# Air Force Inst. of Tech., Wright-Patterson AFB, Ohio. School of Engineering.
PREDICTING OSCILLATORY FINITE DIFFERENCE SOLUTIONS TO THE HEAT EQUATION: A COMPARATIVE STUDY OF THE COEFFICIENT AND MATRIX METHODS M.S. Thesis
Thomas M. Dipp Dec. 1987 121 p
(AD-A189591; AFIT/GEP/ENP/87D-5) Avail: NTIS HC A06/MF A01 CSCL 12A

coefficient and matrix methods For individual titles, see N88-20816 through N88-20815.

This thesis compared the coefficient method with the full matrix method for predicting stability and oscillatory behavior of Finite Difference Methods (FDMs) used in solving the one and two dimensional transient heat (diffusion) equation with Dirichlet boundary conditions. Five FDMs were used: the fully implicit, fully explicit, DuFort-Frankel, Crank-Nicolson, and Peaceman-Rachford ADI. Analytically, the Pade' method was found to be equivalent to the matrix method in predicting stability and oscillations. The matrix method was shown to be more severe than the coefficient method in predicting both stable and non-oscillatory step size constraints. Also, the matrix method, while mathematically more rigorous, proved to be more difficult to derive and analyze, possibly limiting its usefulness. Ultimately, it was found that the coefficient method's predictions could be derived from the matrix method for two-level FDMs. Numerically, all methods were solved repeatedly and the results investigated for oscillatory behavior and maximum errors in the h-k, or space and time step, domain. GRA

N88-20912# Stanford Univ., Calif. Systems Optimization Lab.
ELIMINATION OF QUANTIFIERS OF LINEAR VARIABLES AND CORRESPONDING TRANSFER PRINCIPLES
B. C. Eaves and U. G. Rothblum Nov. 1987 17 p
(Contract DE-FG03-87ER-25028)
(DE88-005692; SU-SOL-87-17) Avail: NTIS HC A03/MF A01

Given a first order formula for ordered fields whose quantified variables are linear with respect to each other, we show how to eliminate the quantifiers and obtain a quantifier-free formula that is equivalent to the original one over all ordered fields. The result parallels Tarski's Theorem that concerns the elimination of quantifiers for first order formula for ordered fields applied to real closed fields. Like Tarski's Theorem, our results yield transfer principles for drawing conclusions in one ordered field that are established for another. Applications of this transfer principle are discussed. DOE

N88-20913# Brookhaven National Lab., Upton, N. Y.
ON THE NORM EQUIVALENCE OF SINGULARLY PERTURBED ELLIPTIC DIFFERENCE OPERATORS
C. I. Goldstein and S. V. Parter 1988 25 p
(Contract DE-AC02-76CH-00016)
(DE88-006353; BNL-40740) Avail: NTIS HC A03/MF A01

Consider the system of linear algebraic equations L(sub h,k)U = f which arises from the finite-difference discretization of the singularly perturbed elliptic operator where 1 much less than K leass than infinity, 0 less than or equal to sigma less than or equal to 1. In this work we are concerned with preconditioning operators L(sub K,h) so that: the condition number ((L(sub K,h)) sup 1 L(sub K,h)) and the condition number (L(sub K,h)(L(sub K,h))sup-1) is bounded independently of h and there are bounds on the growth of these condition numbers as a function of K. DOE

N88-20914# Sandia National Labs., Albuquerque, N. Mex.
A KNOWLEDGE SYSTEM FOR AUTOMATIC FINITE ELEMENT MESH GENERATION: AMEKS
L. R. Phillips, J. L. Mitchiner, and T. D. Blacker 1988 16 p Presented at the 4th IEEE Conference on Artificial Intelligence Applications, San Diego, Calif., 14 Mar. 1988
(Contract DE-AC04-76DP-00789)
(DE87-014894; SAND-87-2242C; CONF-880315-1) Avail: NTIS HC A03/MF A01

Finite element analysis is widely employed by the engineering community for the numerical analysis of complex structures. It involves the partitioning of an object into small elements for which applicable physical responses can be readily formulated. The generation of this partition, or mesh, is a tedious and often difficult part of the analysis. This paper presents a knowledge-based system, AMEKS, which, in conjunction with existing software, automatically meshes objects using the transfinite mapping technique. This technique requires tha analyst to decompose complex objects into primitive shapes and prepare each primitive for algorithmic meshing based on problem geometry and mesh requirements. AMEKS now performs these tasks. Several characteristics of this problem indicate the need for artificial intelligence techniques. Decomposition is non-algorithmic and expertise intensive. The number of possible decompositions is usually too large for exhaustive search. Locally acceptable decompositions can prove to be globally unacceptable. The concept of primitive is ill-defined, and once a region is classified as primitive, its acceptability for meshing is case-by-case dependent on geometry, physics, and the available alternatives. AMEKS currently accepts two-dimensional straight-sided objects. It uses frames to represent the geometry, rules to classify regions and evaluate region quality, heuristic search control to prune the large search space, and assumption-based truth maintenance to simultaneously examine multiple contexts during the decomposition. DOE

N88-20915# Lawrence Livermore National Lab., Calif.
STOCHASTICITY IN NONLINEAR HAMILTONIAN SYSTEMS Ph.D. Thesis
R. C. White 1 Oct. 1987 147 p
(Contract W-7405-eng-48)
(DE88-005499; UCRL-53838) Avail: NTIS HC A07/MF A01

Principles involved in the research of nonlinear Hamiltonian systems in a few dimensions are described, and both standard and new examples of such dynamical systems that exhibit chaotic behavior provided. Analytical theories are discussed, which are not new, but which are measured accurately with modern computers. With the tools of computers and perturbation methods, the geometry of the phase space can be described. DOE

N88-20916# Center for Mathematics and Computer Science, Amsterdam (Netherlands). Dept. of Computer Science/Dept. of Software Technology.
ALGEBRAIC SPECIFICATIONS FOR PARAMETERIZED DATA TYPES: THE CASE OF MINIMAL COMPUTABLE ALGEBRAS AND PARAMETERS WITH EQUALITY
P. H. Rodenburg Mar. 1987 17 p Submitted for publication
Sponsored in part by the European Economic Commission ESPRIT Project 432
(CWI-CS-R8714; B8717219; ETN-88-91759) Copyright Avail: NTIS HC A03/MF A01

For minimal algebras, and under certain assumptions on the domain of parameters, it is shown that a persistent parametrized data type with computable parameters is effective if it has a finite equational specification. ESA

N88-20917# Center for Mathematics and Computer Science, Amsterdam (Netherlands). Dept. of Computer Science/Dept. of Algorithmics and Architecture.
ON EFFECTIVELY LABELING PLANAR PROJECTIONS OF POLYHEDRA
Lefteris M. Kirousis Mar. 1987 19 p
(CWI-CS-R8715; B8717220; ETN-88-91760) Copyright Avail: NTIS HC A03/MF A01

The method for interpreting planar projections (images) of three dimensional polyhedra by labeling their lines by the Clowes-Huffman scheme is discussed. The question of whether there is such a labeling is shown to be NP-complete. A linear in time algorithm that answers the labelability question under the assumption that information is known about those edges of the polyhedron whose both faces are visible is given. In many cases, this information can be derived from the image itself. The algorithm has an effective parallel version, i.e., with polynomially many processors it can be executed in time polynomial in logn. ESA

N88-20918# Center for Mathematics and Computer Science, Amsterdam (Netherlands). Dept. of Computer Science/Dept. of Software Technology.
MERGE AND TERMINATION IN PROCESS ALGEBRA
J. C. M. Baeten (Amsterdam Univ., Netherlands) and R. J. vanGlabbeek Apr. 1987 29 p Submitted for publication
Sponsored in part by the European Economic Commission ESPRIT Project 432
(CWI-CS-R8716; B8717221; ETN-88-91761) Copyright Avail: NTIS HC A03/MF A01

The empty process added to the algebra of communicating processes (ACP) of Bergstra and Klop (1984, 86) are considered. Reconsidering the definition of the parallel composition operator merge, it is found that it is preferable to explicitly state the termination option. This gives an extra summand in the defining equation of merge, using the auxiliary operator tick. Tick can be defined in terms of the encapsulation operator. An operational and a denotational semantics for the resulting system ACP tick is given, and it is proved that they are equal. The limit rule is proved to hold in the models. ESA

N88-20919# Center for Mathematics and Computer Science, Amsterdam (Netherlands). Dept. of Computer Science.
ABSTRACTION AND EMPTY PROCESS IN PROCESS ALGEBRA
J. C. M. Baeten and R. J. vanGlabbeek Apr. 1987 27 p Submitted for publication

(ESPRIT Proj. 432)
(CWI-CS-R8721; B8723969; ETN-88-91766) Copyright Avail: NTIS HC A03/MF A01

Baeten and Glabbeek's (B and G, 1987) hidden step eta is combined with the empty process of Vrancken (1986) and Band G (1987). A system algebra of communicating processes, ACPc, which is a conservative extension of the systems ACP eta, tick, and tau is formulated. It is a general system, in which most relevant issues can be discussed. Abstraction from internal steps can be achieved in two ways, in two stages: one can abstract to the hidden step eta and then from eta to Milner's silent step tau. ESA

N88-20920# Center for Mathematics and Computer Science, Amsterdam (Netherlands). Dept. of Computer Science/Dept. of Software Technology.
A CONVERGENCE THEOREM IN PROCESS ALGEBRA
J. A. Bergstra (Amsterdam Univ., Netherlands) and J. W. Klop Jul. 1987 35 p Sponsored in part by the European Economic Commission ESPRIT Project 432
(CWI-CS-R8733; B8729652; ETN-88-91778) Copyright Avail: NTIS HC A03/MF A01

A convergence phenomenon in the projective limit model A sup inf for process algebra, an axiom system in the framework of process algebra for processes built from atomic actions by means of alternative composition (+) and sequential composition (x), and subject to the operations merge and left-merge is studied. The model is also a complete metric space. It is shown that for every element q is a member of the set A sup inf the sequence q, s(q), s sq(q) ..., s sup n(q) ... converges to a solution of the (possibly unguarded) recursion equation X = s(X) where s(X) is an expression in the signature of PA involving the recursion variable X. As the convergence holds for arbitrary starting points q, this result does not seem readily obtainable by the usual convergence proof techniques. The connection is between projective models and models based on process graphs is studied. These models are compared with the process model introduced by De Bakker and Zucker (1982). ESA

N88-20921# Center for Mathematics and Computer Science, Amsterdam (Netherlands). Dept. of Computer Science/Dept. of Software Technology.
TYPE-CHECKING MINI-ML: AN ALGEBRAIC SPECIFICATION WITH USER-DEFINED SYNTAX
P. R. H. Hendriks Aug. 1987 35 p Submitted for publication Sponsored in part by the European Economic Commission ESPRIT Project 348
(CWI-CS-R8737; B8729656; ETN-88-91783) Copyright Avail: NTIS HC A03/MF A01

An algebraic specification of a type-checker for Mini-ML, a sublanguage of ML, is given. As specification formalism a combination of the algebraic specification formalism and the syntax definition formalism is used. ESA

N88-20922# Center for Mathematics and Computer Science, Amsterdam (Netherlands). Dept. of Numerical Mathematics.
A LAGRANGIAN MOVING GRID SCHEME FOR ONE-DIMENSIONAL EVOLUTIONARY PARTIAL DIFFERENTIAL EQUATIONS
J. G. Blom, J. M. Sanz-Serna, and J. G. Verwer Jun. 1987 22 p Submitted for publication
(CWI-NM-R8713; B8723961; ETN-88-91785) Copyright Avail: NTIS HC A03/MF A01

A Lagrangian moving grid finite difference method for one-space dimensional, evolutionary partial differential equations which exhibit sharp transitions in space and time is developed. The method is based on a Crank-Nicolson type difference scheme derived via a coordinate transformation governed by equidistribution of the second space derivative. Each time step involves two stages. First, a static grid numerical integration is carried out, immediately followed by a de Boor type redistribution of nodes at the forward time level. This stage serves only to compute the transformation. Second, a moving grid numerical integration is carried out with the Crank-Nicolson scheme. Numerical experiments show that the method automatically concentrates the grid in regions of high spatial activity and can also step in time with stepsizes larger than those needed by static methods, i.e., methods which for intervals of time work on a fixed, nonuniform grid. The method achieves high accuracy with few gridpoints in space and time. ESA

N88-20923# Center for Mathematics and Computer Science, Amsterdam (Netherlands). Dept. of Numerical Mathematics.
STABILIZATION OF EXPLICIT DIFFERENCE SCHEMES BY SMOOTHING TECHNIQUES
P. J. vanderHouwen Jul. 1987 14 p
(CWI-NM-R8714; B8723762; ETN-88-91786) Copyright Avail: NTIS HC A03/MF A01

Applications of smoothing techniques to difference schemes for partial differential equations are reviewed. Smoothing techniques may improve the stability or convergence of the difference scheme considerably. Smoothing of the numerical solution itself, smoothing of the right-hand side of the differential equation, and residue smoothing are distinguished. Examples are given for parabolic, hyperbolic and elliptic equations. ESA

N88-20924# Center for Mathematics and Computer Science, Amsterdam (Netherlands). Dept. of Numerical Mathematics.
CONVERGENCE OF RUNGE-KUTTA METHODS ON CLASSES OF STIFF INITIAL VALUE PROBLEMS
Willem H. Hundsdorfer Sep. 1987 12 p Presented at the International Symposium on Numerical Analysis, Ankara, Turkey, 1-4 Sep. 1987
(CWI-NM-R8717; B8729648; ETN-88-91789) Copyright Avail: NTIS HC A03/MF A01

For classes of stiff initial value problems, convergence results which are independent of the stiffness, such as the B-convergence results for nonlinear dissipative problems are considered. The classes contain problems with arbitrarily large Lipschitz constants, so the error bounds obtained are not affected by stiffness. ESA

N88-20925# Technische Hogeschool, Eindhoven (Netherlands). Dept. of Electrical Engineering.
FURTHER RESULTS ON THE MCMILLAN DEGREE AND THE KRONECKER INDICES OF ARMA MODELS
P. H. M. Janssen Jun. 1987 21 p
(EUT-87-E-175; ISBN-9-06-144175-7; ISSN-0167-9708; ETN-88-91822) Avail: NTIS HC A03/MF A01

It is shown that the McMillan degree and the Kronecker indices of ARMA models can easily be related to the determinantal degree and the row degrees of a suitable submatrix of the polynomial factors in the ARMA model. For systems having no poles at the origin, these quantities can even be inferred from the determinantal degree and the row degrees of the polynominal AR factor. ESA

N88-20926# Technische Hogeschool, Eindhoven (Netherlands). Dept. of Electrical Engineering.
MODEL STRUCTURE SELECTION FOR MULTIVARIABLE SYSTEMS BY CROSS-VALIDATION METHODS
Peter H. M. Janssen, Petre Stoica, Torsten Soderstrom (Uppsala Univ., Sweden), and Pieter Eykhoff Jun. 1987 41 p
(EUT-87-E-176; ISBN-9-06-144176-5; ISSN-0167-9708; ETN-88-91823) Avail: NTIS HC A03/MF A01

Using cross-validation ideas, two procedures for choosing between different model structures used for (approximate) modeling of multivariable systems are proposed. The procedures are derived under fairly general conditions: the true system does not need to be contained in the model set; model structures do not need to be nested; and different criteria may be used for model estimation and validation. The proposed structure selection rules are shown to be invariant to parameter scaling. Under certain conditions (essentially requiring that the system belongs to the model set and that the maximum likelihood method is used for parameter estimation) they are shown to be asymptotically equivalent to the (generalized) Akaike structure selection criteria. ESA

N88-20927# Technische Hogeschool, Eindhoven (Netherlands). Dept. of Electrical Engineering.
ON THE EXPECTATION OF THE PRODUCT OF FOUR MATRIX-VALUED GAUSSIAN RANDOM VARIABLES
Peter H. M. Janssen and Petre Stoica (Polytechnic Inst. of Bucharest, Rumania) Jul. 1987 16 p
(EUT-87-E-178; ISBN-90-6144-178-1; ISSN-0167-9708; ETN-88-91825) Avail: NTIS HC A03/MF A01

The formula for the expectation of the product of four scalar real Gaussian random variables is generalized to matrix-valued (real or complex) Gaussian random variables. As an application of the extended formula, a simple derivation of the covariance matrix of instrumental variable estimates of parameters in multivariate linear regression models is presented. ESA

N88-20928# Groningen Rijksuniversiteit (Netherlands). Dept. of Mathematics and Computing Science.
UNFOLDINGS OF QUASI-PERIODIC TORI
H. W. Broer, G. B. Huitema, and F. Takens 1987 79 p
(Grant ZWO-10-70-10)
(ZW-8706; B8731945; ETN-88-91869) Avail: NTIS HC A05/MF A01

Dynamical systems depending on parameters in conservative and dissipative settings are considered. For such systems integrability is defined as equivariance with respect to an appropriate torus action. Persistence of invariant, quasi-periodic tori in such integrable systems under nearly integrable perturbation is studied. With KAM perturbation theory an unfolding theory is developed for these tori. ESA

N88-20929# Instituto de Pesquisas Espaciais, Sao Jose dos Campos (Brazil).
A STUDY OF DATA COMPACTATION USING NUMERICAL METHODS M.S. Thesis [UM ESTUDO DE COMPACTACAO DE DADOS USANDO METODOS NUMERICOS]
Joao Eduardo Oliveir daSilva Aug. 1987 186 p In PORTUGUESE; ENGLISH summary
(INPE-4317-TDL/284) Avail: NTIS HC A09/MF A01

Three methods of data compactation by using numerical analysis techniques are described. Each method presents practical results contained in Burroughs 6800, as well as suggestions on how to improve the performance of the implementations. Author

N88-20930# Instituto de Pesquisas Espaciais, Sao Jose dos Campos (Brazil).
LOCAL REFINEMENT OF STRESS FIELD BY FINITE ELEMENT METHOD M.S. Thesis [REFINAMENTO LOCAL DO CAMPO DE TENSOES NO METODO DE ELEMENTOS FINITOS]
Celso Figueiredo Nogueira Aug. 1987 115 p In PORTUGUESE; ENGLISH summary
(INPE-4321-TDL/288) Avail: NTIS HC A06/MF A01

A stress refinement technique, for the Finite Element Method, is presented. This technique uses a principle of the Variational Calculus to profit on the better precision obtained for the nodal displacements via finite elements (Displacement Method). A finite element routine was developed for testing the technique and also to verify clearly what kind of problems would arise if the technique was implemented in a Finite Element Software, developed in the usual fashion. The results obtained are excellent compared both to a similar technique by Gilbert and Gorge (1981) and to a simple, but more expensive technique of adding more nodes to the mesh. Author

N88-20931# Helsinki Univ. of Technology, Espoo (Finland). Inst. of Mathematics.
NEW WAY TO SOLVE VOLTERRA EQUATIONS OF THE SECOND KIND
J. Tuomela Aug. 1987 15 p
(PB88-148820; HTKK-MAT-A250; ISBN-951-754-247-X) Avail: NTIS HC A03/MF A01 CSCL 12A

A new way is proposed to solve Volterra equations of second kind. The given kernel is approximated with a degenerate one using finite elements, and the integral equation is reduced to a system of ordinary differential equations. Because of the local nature of the finite elements, the amount of work needed to solve the system remains small, although the system itself can be quite large. GRA

N88-20932# Helsinki Univ. of Technology, Espoo (Finland). Inst. of Mathematics.
WHAT DO MULTISTEP METHODS APPROXIMATE
Timo Eirola and Olavi Nevanlinna Sep. 1987 21 p
(PB88-148838; HTKKK-MAT-A251; ISBN-951-754-252-6; ISSN-0784-3143) Avail: NTIS HC A03/MF A01 CSCL 12A

Standard analysis of multistep methods for ODE's assumes the application of an initialization routine that generates the starting points. Here a k-step method is considered directly as a mapping (R sup kn) maps onto (R sup n). It is shown to approximate a mapping which is expressible directly in terms of the flow of the vector field. Some useful properties of that mapping are shown, and, for strictly stable methods, these are applied to the question of invariant circles near a hyperbolic periodic solution. GRA

N88-20933# Oak Ridge National Lab., Tenn.
NONLINEAR DIFFERENTIAL EQUATIONS
L. Dresner Jan. 1988 132 p
(Contract DE-AC05-84OR-21400)
(DE88-006047; ORNL/TM-10655) Avail: NTIS HC A07/MF A01

This report is the text of a graduate course on nonlinear differential equations given by the author at the University of Wisconsin-Madison during the summer of 1987. The topics covered are: direction fields of first-order differential equations; the Lie (group) theory of ordinary differential equations; similarity solutions of second-order partial differential equations; maximum principles and differential inequalities; monotone operators and iteration; complementary variational principles; and stability of numerical methods. The report should be of interest to graduate students, faculty, and practicing scientists and engineers. No prior knowledge is required beyond a good working knowledge of the calculus. The emphasis is on practical results. Most of the illustrative examples are taken from the fields of nonlinear diffusion, heat and mass transfer, applied superconductivity, and helium cryogenics. DOE

N88-20934*# Old Dominion Univ., Norfolk, Va. Dept. of Mechanical Engineering and Mechanics.
CONSERVATIVE FINITE VOLUME SOLUTIONS OF A LINEAR HYPERBOLIC TRANSPORT EQUATION IN TWO AND THREE DIMENSIONS USING MULTIPLE GRIDS Progress Report, 30 Jun. 1987
Surendra N. Tiwari and Monchai Kathong Jul. 1987 53 p
(Contract NCC1-68)
(NASA-CR-182715; NAS 1.26:182715) Avail: NTIS HC A04/MF A01 CSCL 12A

The feasibility of the multiple grid technique is investigated by solving linear hyperbolic equations for simple two- and three-dimensional cases. The results are compared with exact solutions and those obtained from the single grid calculations. It is demonstrated that the technique works reasonably well when two grid systems contain grid cells of comparative sizes. The study indicates that use of the multiple grid does not introduce any significant error and that it can be used to attack more complex problems. Author

65 STATISTICS AND PROBABILITY

Includes data sampling and smoothing; Monte Carlo method; and stochastic processes.

N88-20935# Stanford Univ., Calif. Dept. of Statistics.
TESTS FOR UNIFORMITY ARISING FROM A SERIES OF EVENTS
Michael A. Stephens 28 Jan. 1988 23 p
(Contract N00014-86-K-0156)

(AD-A189069; TR-400) Avail: NTIS HC A03/MF A01 CSCL 12C

Test procedures are reviewed for testing whether events in time are occurring randomly. When this is so, a well-known transformation takes the times of occurrence to uniform order statistics, and the problem reduces to finding tests for uniformity which are sensitive to those alternative patterns of events which might be met in practice. Some alternatives are described and use is discussed of Neyman's test procedure, EDF tests, and spacings. Some recent work on spacings is examined in this context, and throughout the paper suggestions are made for future work. GRA

N88-20936# Florida Univ., Gainesville. Dept. of Statistics.
THE PARAMETERIZATION OF ORTHOGONAL MATRICES: A REVIEW MAINLY FOR STATISTICIANS
I. J. Good and A. I. Khuri Nov. 1987 19 p
(Contract N00014-86-K-0059)
(AD-A189144; R-293) Avail: NTIS HC A03/MF A01 CSCL 12B

This paper reviews methods for the parameterization of orthogonal matrices. Examples of where such parameterization can be used are presented. GRA

N88-20937# Florida State Univ., Tallahassee. Dept. of Statistics.
BIAS REDUCTION WHEN THERE IS NO UNBIASED ESTIMATE
Hani Doss and Jayaram Sethuraman Jan. 1988 8 p
(Contracts DAAL03-86-K-0094; F49620-85-C-0007)
(AD-A189407; FSU-TR-M777; AFOSR-87-0219TR;
ARO-23699.17-MA) Avail: NTIS HC A02/MF A01 CSCL 12C

Let phi be a parameter for which there is no unbiased estimator. This note shows that for an arbitrary sequence of estimators T sup (k), if the bias of T sup (k) tend to O then their variances must tend to infinity. GRA

N88-20938# Florida State Univ., Tallahassee. Dept. of Statistics.
STOCHASTIC COMPARISONS OF ORDER STATISTICS, WITH APPLICATIONS IN RELIABILITY
Jee S. Kim, Frank Proschan, and Jayaram Sethuraman Nov. 1987 19 p
(Contracts DAAL03-86-K-0094; F49620-85-C-0007)
(AD-A189408; FSU-TR-M773; AFOSR-87-0217TR;
ARO-23699.16-MA) Avail: NTIS HC A03/MF A01 CSCL 12C

Recent advances in stochastic comparisons of order statistics are surveyed along with reliability applications. Section 2 presents inequalities for linear combinations of order statistics from restricted families. Comparisons of linear combinations of order statistics from distributions F and G are obtained for G(sup equivalent to 1) F convex and for G(sup equivalent to 1) F starshaped. These results yield conservative upper and lower tolerance limits. For G exponential and F IFR or IFRA, stochastic comparisons are presented for total test time. Section 3 presents stochastic comparisons of order statistics from underlying heterogeneous distributions. Given two sets of independent components (possibly unlike), majorization conditions are given which insure that any k-out-of-n system constructed from components in the first set will have reliability at least as great as that of a corresponding system constructed from components in the second set. Since the ordered failure times of the components represent order statistics from heterogeneous distributions, the order statistics from one set of underlying distributions (F1,...,Fn) can be compared stochastically with those of another set. GRA

N88-20939# Environmental Research Inst. of Michigan, Ann Arbor. Optical Science Lab.
REDUCED TOLERANCE IMAGING 2, VOLUME 2 Final Technical Report, 15 Oct. 1984 - 14 Oct. 1986
James R. Fienup, Jack N. Cederquist, Thomas R. Crimmins, Richard G. Paxman, and David L. Neuhoff 29 Jan. 1988 292 p
(Contract F33615-83-C-1046; DARPA Order 5205)
(AD-A189604; ERIM-167400-101-F-Vol-2; AFWAL-TR-87-1148-Vol-2) Avail: NTIS HC A13/MF A01 CSCL 12I

Reduced tolerance imaging is a concept wherein an imaging system is designed with reduced performance requirements permitting large phase errors in the received signal, and the full performance level is recovered through use of post-detection processing using phase retrieval techniques yielding a diffraction-limited reconstructed image. This report describes an effort to develop reduced-tolerance imaging techniques. An estimation theoretic (Cramer-Rao) lower bound on the error in estimating a coherent image from: (1) far-field (Fourier) intensity (squared modulus) measurements, and (2) electromagnetic field measurements with phase errors were derived for the case of additive Gaussian detector noise. Uniqueness of reconstruction from Fourier modulus assuming a support constraint known a priori was proven for a particular class of objects- sampled objects whose support (the area in which the object has non-zero values) has a convex hull with no parallel sides. A closed-form recursive reconstruction algorithm was developed for reconstructing such objects. retrieval; Image reconstruction. GRA

N88-20940# Center for Mathematics and Computer Science, Amsterdam (Netherlands). Dept. of Applied Mathematics.
STOCHASTIC AND CHAOTIC OSCILLATIONS
J. Grasman and J. B. T. M. Roerdink May 1987 18 p Submitted for publication
(CWI-AM-R8704; B8723965; ETN-88-91790) Copyright Avail: NTIS HC A03/MF A01

For relaxation oscillators stochastic and chaotic dynamics are investigated. The effect of random perturbations upon the period is computed. For an extended system with additional state variables chaotic behavior can be expected. As an example the Van der Pol oscillator is changed into a third order system admitting period doubling and chaos in a certain parameter range. The distinction between chaotic oscillation and oscillation with noise is explored by studying a time series of one of the variables. Return maps, power spectra, and Lyapunov exponents are analyzed. ESA

N88-20941# Center for Mathematics and Computer Science, Amsterdam (Netherlands). Dept. of Mathematical Statistics.
NON- AND SEMI-PARAMETRIC MAXIMUM LIKELIHOOD ESTIMATORS AND THE VON MISIS METHOD, PART 1
Richard D. Gill Jul. 1987 29 p
(CWI-MS-R8709; B8731189; ETN-88-91798) Copyright Avail: NTIS HC A03/MF A01

The approach to von Mises derivatives based on compact differentiation due to Reeds (1976) is introduced, and it is shown how nonparametric maximum likelihood estimators can often be defined by solving infinite dimensional score equations. Each component of the score equation corresponds to the derivative of the log likelihood for a one-dimensional parametric submodel. Examples show that it usually not possible to base consistency and asymptotic normality theorems on the implicit function theorem. ESA

N88-20942# Oak Ridge National Lab., Tenn.
DETERMINISTIC UNCERTAINTY ANALYSIS
B. A. Worley Dec. 1987 53 p
(Contract DE-AC05-84OR-21400)
(DE88-006139; ORNL-6428) Avail: NTIS HC A04/MF A01

This paper presents a deterministic uncertainty analysis (DUA) method for calculating uncertainties that has the potential to significantly reduce the number of computer runs compared to conventional statistical analysis. The method is based on the availability of derivative and sensitivity data such as that calculated using the well known direct or adjoint sensitivity analysis techniques. Formation of response surfaces using derivative data and the propagation of input probability distributions are discussed relative to their role in the DUA method. A sample problem that models the flow of water through a borehole is used as a basis to compare the cumulative distribution function of the flow rate as calculated by the standard statistical methods and the DUA method. Propagation of uncertainties by the DUA method is compared for

ten cases in which the number of reference model runs was varied from one to ten. The DUA method gives a more accurate representation of the true cumulative distribution of the flow rate based on as few as two model executions compared to fifty model executions using a statistical approach. DOE

N88-20943# Florida Univ., Gainesville. Dept. of Statistics.
REGIONAL CONFERENCE ON THE ANALYSIS OF THE UNBALANCED MIXED MODEL Report, 6 Jan. - 31 Dec. 1987
Andre I. Khuri and Ramon C. Littell 31 Dec. 1987 7 p Conference held at Gainesville, Fla., 6-10 Apr. 1987
(N00014-87-G-0090)
(AD-A188747) Avail: NTIS HC A02/MF A01 CSCL 12C

The main objective of the conference was to bring together leading statisticians who have done significant research work in the area of variance components and linear models in general. Of particular interest was the analysis concerning the unbalanced mixed linear model. This is a rather difficult area in statistics that has been the subject of investigation by many researchers. Unfortunately, however, there is no general consensus among research workers on the most efficient method to analyze data from an unbalanced experiment. The conference was a necessary step in the process of solving this complicated problem. Paper titles: The Present Status of Confidence Interval Estimation on Variance Components in Balanced and Unbalanced Random Models; Prediction-Interval Procedures and (Fixed Effects) Confidence-Interval Procedures for Mixed Linear Models; The Use of Equivalent Linear Models in Mixed Model Estimation and Prediction; Estimation of Variance Components in Unbalanced Mixed Models; On the Role of MINQUE in Testing of Hypothese Under Mixed Linear Models; Practical Computation of MINQUE Estimators in Mixed Model Analysis of Variance; Confidence Intervals and Tests on the Variance Ratio in Random Models with Two Variance Components; Robust Tests and Confidence Intervals for Functions of Variance Components in the Nested Error Regression Model; Estimation for Variance Component Models; Small and Large Sample Properties; and Mixed Models and Unbalanced Data: Wherefrom and Whereto. GRA

66 SYSTEMS ANALYSIS

Includes mathematical modeling; network analysis; and operations research.

N88-20944# Los Alamos National Lab., N. Mex.
SEAT: A STRATEGIC ENGAGEMENT ANALYSIS TOOL
J. Dreicer, C. Michelsen, and D. Morgeson 1988 6 p Presented at the 4th IEEE Conference on Artificial Intelligence Applications, San Diego, Calif., 14 Mar. 1988
(Contract W-7405-eng-36)
(DE88-000498; LA-UR-87-3131; CONF-880315-2) Avail: NTIS HC A02/MF A01

The Strategic Engagement Analysis Tool (SEAT) is a prototype of an expert system knowledge-based discrete event simulation. SEAT realistically represents the interrelationships between the eight major subsystems in the strategic targeting and assault domain. Some of the subsystems employ run-time cognitive decision making and reasoning capabilities to represent human tactical and operational strategy decisions. SEAT's goal is to allow analysts to conduct sensitivity analysis and to determine cause-effect relationships. An intelligent interface mechanism is provided to aid the analyst in scenario creation. The interface was designed to provide on-line documentation, support for model input, logic control, and data validation prior to simulation execution. DOE

N88-20945# Lawrence Livermore National Lab., Calif.
THE AUTOMATED SYMBOLIC DERIVATION OF STATE EQUATIONS FOR DYNAMIC SYSTEMS
J. Macfarlane and M. Donath Sep. 1987 15 p Presented at the 4th IEEE Conference on Artificial Intelligence Applications, San Diego, Calif., 14 Mar. 1988 Prepared in cooperation with Minnesota Univ., Minneapolis
(Contract W-7405-eng-48)
(DE88-000968; UCRL-97418; CONF-880315-3) Avail: NTIS HC A03/MF A01

A system which is capable of generating symbolic state equations for dynamic systems is described. The underlying object-oriented knowledge representation structure is based on the bond graph modelling methodology which abstracts a complex system into a network of simple relations that describe the behavior of the system. Constraint propagation techniques provide a method for determining the causal relationships that must exist between system variables in a state determined system, thereby identifying a set of state variables for the system. The relation network and the state variables are manipulated by MACSYMA to define the state equations for the physical system dynamics. The availability of state equations in symbolic form allows the engineer to assess the influence of component parameters on the overall function of the physical system without having to resort to simulation iterations. This representation establishes the foundation for a model based reasoning system currently under development. DOE

N88-20946# National Aerospace Lab., Amsterdam (Netherlands). Flight Div.
EXPERT SYSTEMS FOR DECISION SUPPORT IN MILITARY AIRCRAFT MISSION PREPARATION
P. J. M. Urlings and A. L. Spijkervet 10 Feb. 1987 25 p Presented at the COMPAS 87 Conf. on Computer Aided Design, Manufacture and Operation in the Aeronautics and Space Industries, Paris, France, 16-18 Jun. 1987
(NLR-MP-87013-U; B8729209; ETN-88-91738) Avail: NTIS HC A03/MF A01

Characteristics of military aircraft mission preparation that make it desirable to use expert systems are elaborated. An approach from operations research which provides an operational environment for expert system applications is described. An inventory of the state-of-the-art of expert systems in computer aided mission preparation is presented. ESA

N88-20947# Center for Mathematics and Computer Science, Amsterdam (Netherlands). Dept. of Operations Research and System Theory.
SOJOURN TIMES IN FEEDBACK QUEUES
J. L. vandenBerg and O. J. Boxma Jun. 1987 19 p Submitted for publication
(CWI-OS-R8710; B8723355; ETN-88-91749) Copyright Avail: NTIS HC A03/MF A01

An M/M/1 queue with a very general feedback mechanism is considered. When a customer completes his i-th service, he departs from the system with probability 1-p(i) and he cycles back with probability p(i). A formula for the joint distribution of the successive sojourn times of a customer in the system is derived. It is shown that the sojourn times in all individual cycles are identically, negative exponentially, distributed. The correlation between the sojourn times of the j-th and k-th cycle of a customer is calculated. The distribution of the total sojourn time is derived. ESA

N88-20948# Center for Mathematics and Computer Science, Amsterdam (Netherlands). Dept. of Operations Research and System Theory.
LOCAL SEARCH FOR CONSTRAINED ROUTING PROBLEMS
Martin W. P. Savelsbergh Jul. 1987 13 p
(CWI-OS-R8711; B8723356; ETN-88-91750) Copyright Avail: NTIS HC A03/MF A01

Local search algorithms for routing problems with various side constraints such as time windows on vertices and precedence relations between vertices are developed. The algorithms are based on the k-exchange concept. The presence of side constraints introduces feasibility problems. Checking the feasibility of a given solution in the straightforward way requires time which is linear in the number of vertices. The method reduces this effort to constant time. ESA

N88-20949# Center for Mathematics and Computer Science, Amsterdam (Netherlands). Dept. of Operations Research and System Theory.
TWO QUEUES WITH ALTERNATING SERVICE AND SWITCHING TIMES
O. J. Boxma and W. P. Groenendijk Jul. 1987 23 p Submitted for publication
(CWI-OS-R8712; B8731192; ETN-88-91751) Copyright Avail: NTIS HC A03/MF A01

A system of two queues, attended by a single server who alternately serves one customer of each queue (if not empty) is considered. The server experiences switching times in his transition from one queue to the other. It is shown that the joint stationary queue-length distribution, at the instants at which the server becomes available to a queue, can be determined via transformation to a Riemann boundary value problem. The latter problem can be completely solved for general service and switching-time distributions. The stationary distributions of the waiting times at both queues, and of the cycle times of the server, are also derived. The results, particularly the extensive numerical data for moments of waiting times and cycle times, yield insight into the behavior of more general cyclic-service models as used to analyze polling systems. ESA

N88-20950# Center for Mathematics and Computer Science, Amsterdam (Netherlands). Dept. of Computer Science/Dept. of Software Technology.
CONSISTENCY OF RULE-BASED EXPERT SYSTEMS
Marc Bezem Jul. 1987 13 p Sponsored in part by the Dutch Stimulerings-Projectteam Informatica-Onderzoek Prepared in cooperation with Philips International B.V., Eindhoven, The Netherlands
(CWI-CS-R8736; B8729655; ETN-88-91782) Copyright Avail: NTIS HC A03/MF A01

A theoretical framework in which the semantics and the consistency of a knowledge base can be studied is presented. The framework is based on first order many-sorted predicate logic and is sufficiently rich to capture an interesting class of rule based expert systems and deductive databases. Criteria to isolate cases in which the consistency test is feasible are given. ESA

67 THEORETICAL MATHEMATICS

Includes topology and number theory.

N88-20951# Texas Univ., Austin. Inst. for Fusion Studies.
WKB THEORY OF WAVE TUNNELING FOR HERMITIAN VECTOR SYSTEMS OF INTEGRAL EQUATIONS
H. J. Kull, R. J. Kashuba, and H. L. Berk Jan. 1988 54 p
(Contract DE-FG05-80ET-53088)
(DE88-005332; DOE/ET-53088/307; IFSR-307) Avail: NTIS HC A04/MF A01

A general theory of wave tunneling in one dimension for Hermitian vector systems of integral equations is presented. It describes mode conversion in terms of the general dielectric tensor of the medium, and without regard to specific models gives a proper account to the forward and backward nature of the waves. Energy conservation in the WKB approximation can be obtained for general linear systems by a consistent treatment of the vector polarization and by the use of modified Furry rules, which are similar to those used by Heading for second order differential equations. Operational graphical rules are developed to construct global wave solutions and to determine the direction of energy flow for spatially disconnected roots. In principle these rules could be applied to systems with arbitrary mode complexity. Coupling coefficients for wave tunneling problems with up to four interacting modes are calculated explicitly. DOE

N88-20952# Sandia National Labs., Albuquerque, N. Mex.
CAMPAIGN GRAPHS
G. J. Simmons 1988 16 p Presented at the 19th Southeastern International Conference on Combinatorics Graph Theory and Computing, Baton Rouge, La., 15 Feb. 1988
(Contract DE-AC04-76DP-00789)
(DE88-005336; SAND-88-0113C; CONF-880238-1) Avail: NTIS HC A03/MF A01

We define a class of geometrical constructions in the plane in which each (unextended) line lies on (precisely) k points, and every point is an endpoint of (precisely) one line. We will refer to any construction satisfying these conditions as a campaign graph, or as a k-campaign graph if the value of k isn't clear from the context. A k-campaign graph, G, is said to be critical if no subgraph of G is also a k-campaign graph. DOE

N88-20953# Massachusetts Univ., Amherst.
COMPUTATION AND GRAPHICS IN MATHEMATICAL RESEARCH Progress Report, 1 Jun. - 31 Dec. 1987
D. A. Hoffman, J. Spruck, and W. H. Meeks, III Jan. 1988 23 p
(Contract DE-FG02-86ER-25015)
(DE88-005796; DOE/ER-25015/12) Avail: NTIS HC A03

Increasingly, research in differential geometry, calculus of variations, and applied mathematics has taken on a computational component, while still addressing problems of current theoretical interest in these subjects. This computational side has two important aspects: implementation of algorithms to solve problems in partial differential equations (arising from physical problems) and scientific graphics. Some of the research done and under way is described. Critical to this research is the ongoing use of advanced computing equipment and the development of new graphics algorithms and interfaces tailored to the solution of computational problems in science. Connections are made between surfaces of constant mean curvature and surface interfaces in block copolymers. DOE

N88-20954# Center for Mathematics and Computer Science, Amsterdam (Netherlands). Dept. of Pure Mathematics.
GROUP THEORETIC INTERPRETATIONS OF ASKEY'S SCHEME OF HYPERGEOMETRIC ORTHOGONAL POLYNOMIALS
Tom H. Koornwinder Jun. 1987 32 p Presented at the International Congress on Orthogonal Polynomials and their Applications, Segovia, Spain, 22-27 Sep. 1986 Submitted for publication
(CWI-PM-R8703; B8723958; ETN-88-91745) Copyright Avail: NTIS HC A03/MF A01

Group theoretical interpretations of the classical hypergeometric orthogonal polynomials which occur in the Askey scheme are reviewed. A natural extension of the scheme where families of hypergeometric functions are allowed which may be orthogonal in a generalized sense and which may be of nonpolynomial nature is discussed. Limit transitions and group theoretic interpretations are also given for this extended scheme. It turns out that the scheme contains many triples of kernels of integral transforms for which the composition yields identity. ESA

N88-20955# Center for Mathematics and Computer Science, Amsterdam (Netherlands). Dept. of Pure Mathematics.
ACTION-ANGLE MAPS AND SCATTERING THEORY FOR SOME FINITE-DIMENSIONAL INTEGRABLE SYSTEMS. THE PURE SOLUTION CASE
S. N. M. Ruijsenaars Jun. 1987 37 p Submitted for publication. Sponsored by the Netherlands Organization for the Advancement of Pure Research
(CWI-PM-R8704; B8723959; ETN-88-91746) Copyright Avail: NTIS HC A03/MF A01

An action-angle transformation for the Calogero-Moser systems with repulsive potentials, and for relativistic generalizations thereof is constructed. This map is shown to be closely related to the wave transformations for a large class C of Hamiltonians, and is shown to have remarkable duality properties. All dynamics in C lead to the same scattering transformation, which is obtained explicitly and exhibits a soliton structure. An auxiliary result concerns the spectral asymptotics of matrices of the form Mexp(tD) as t tends to infinity. It pertains to diagonal matrices D whose

diagonal elements have pairwise different real parts and to matrices M for which certain principal minors are non-zero. ESA

N88-20956# Center for Mathematics and Computer Science, Amsterdam (Netherlands). Dept. of Computer Science/Dept. of Software Technology.
SOLVING REFLEXIVE DOMAIN EQUATIONS IN A CATEGORY OF COMPLETE METRIC SPACES
Pierre America and Jan J. M. M. Rutten Feb. 1987 36 p Sponsored by the European Economic Commission ESPRIT Project 415
(CWI-CS-R8709; B8711194; ETN-88-91755) Copyright Avail: NTIS HC A03/MF A01

A technique by which solutions to reflexive domain equations can be found in a certain category of complete metric spaces is presented. The objects in this category are the (nonempty) metric spaces and the arrows consist of two maps: an isometric embedding and a non-distance-increasing left inverse to it. The solution of the equation is constructed as a fixed point of a functor over this category associated with the equation. The fixed point obtained is the direct limit (colimit) of a convergent tower. This construction works if the functor is contracting, which roughly amounts to the condition that it maps every embedding to an even denser one. Two additional conditions, each of which is sufficient to ensure that the functor has a unique fixed point (up to isomorphism) are given. For a large class of functors, including function space constructions, it is shown that these conditions are satisfied, so that they are guaranteed to have a unique fixed point. The techniques are reminiscent of Banach's fixed-point theorem, and are considered as a category-theoretic version of it. ESA

N88-20957# Gosudarstvennyj Komitet po Ispolzovaniyu Atomnoi Energii, Serpukhov (USSR). Inst. Fiziki Vysokikh Ehnergij.
INTRODUCTION TO CLASSICAL MECHANICS OF SYSTEMS WITH CONSTRAINTS, PART 1
A. V. Razumov 1986 30 p In RUSSIAN; ENGLISH summary
(TI88-701055; IFVE-OTF-86-212-Pt-1) Avail: NTIS (US Sales Only) HC A03/MF A-1

Classical theory of mechanical systems with constraints is consistently considered. The following problems are treated. Lagrangian equations are derived. The connection of symmetry transformations with conserved quantities is demonstrated. Lagrangian and Hamilton's equation of motion for the system with nondegenerate Lagrangians are proved to be equivalent. Restrictions for the choice of noncanonical coordinates in the extended phase space are studied. One-parameter groups of time dependent canonical transformations are considered. DOE

70 PHYSICS (GENERAL)

For precision time and time interval (PTTI) see *35 Instrumentation and Photography;* for geophysics, astrophysics or solar physics see *46 Geophysics, 90 Astrophysics,* or *92 Solar Physics.*

N88-20958# Lawrence Livermore National Lab., Calif.
PHYSICS OF CONDENSED MATTER AT EXTREME CONDITIONS
M. Ross Feb. 1988 9 p Presented at SPIE O-E Lase '88: Optoelectronics and Laser Applications in Science and Engineering, Los Angeles, Calif., 10 Jan. 1988
(Contract W-7405-eng-48)
(DE88-006232; UCRL-98170; CONF-880110-20) Avail: NTIS HC A02/MF A01

The study of matter under extreme conditions is a highly interdisciplinary subject with broad applications to materials science, geophysics and astrophysics. High-pressure properties are studied in the laboratory using static and dynamic techniques. The two differ drastically in the methods of generating and measuring pressure and in the fundamentally different nature of the final compressed state. This article covers a very broad range of conditions, intended to present an overview of important recent developments and to emphasize the behavior of materials and the kinds of properties now being studied. DOE

N88-20959# Washington Univ., Seattle. Dept. of Physics.
SEARCHES FOR FORCES WEAKER THAN GRAVITY
E. G. Adelberger 1987 12 p
(Contract DE-AC06-81ER-40048)
(DE88-003579; DOE/ER-40048/209-L7) Avail: NTIS HC A03/MF A01

This paper discusses experiments that are searching for field particles associated with a new force that is weaker than gravity. DOE

N88-20960# Warsaw Technical Univ. (Poland). Inst. of Physics.
DOUBLE LAYER POLARIZATION OF NONCONDUCTING SPHEROIDAL PARTICLES AND ITS APPLICATION TO KERR EFFECT
Krystyna Szumilin and Sonja Krause (Rensselaer Polytechnic Inst., Troy, N.Y.) [1987] 39 p
(ISSN-0208-05658) Avail: NTIS HC A03/MF A01

The problem of the double layer polarization of elongated spheroidal charged particles in an electrolyte solution is discussed. The nonconducting elongate ellipsoidal particle, embedded in the electrolyte, is assumed to acquire a surface charge, compensated by the surrounding counterion atmosphere, forming a double layer. The double layer thickness is assumed to be small. The electric potential is found inside the particle for the case of the constant external electric field, applied parallel to the symmetry axis of the particle. The Laplace equations are solved for the distribution of the potential and the electrolyte concentration with the boundary conditions describing the diffuse double layer in the model of Dukhin and Shilov. The effective electric field is then found inside the ellipsoidal particle. The polarization energy, associated with the induced polarization of the ellipsoid and the surrounding medium is calculated, then the steady-state specific Kerr constant is found, following the O'Konski and Krause approach. Author

N88-20961# Helsinki Univ. of Technology, Espoo (Finland). Dept. of Technical Physics.
PERIOD-DOUBLING UNIVERSALITY IN MULTIDIMENSIONAL DISSIPATIVE AND CONSERVATIVE SYSTEMS
J. A. Ketoja 4 Sep. 1987 54 p
(PB88-148812; TKK-F-B109; ISBN-951-754-256-9) Avail: NTIS HC A04/MF A01 CSCL 20C

The standard renormalization theories of dissipative and conservative dynamical systems do not explain all of the observed universal features of two dimensional maps, for example the universal crossover of the Feigenbaum constants before the period-doubling accumulation line. The universal crossover has a counterpart on the other side of the period-doubling accumulation line: universal effective values of the Jacobian control the crossings of the MSS windows away from the strictly one dimensional dissipative limit. All this suggests that there should exist a general renormalization scheme which incorporates a Jacobian as a special parameter and applies everywhere from dissipative to conservative maps. A straightforward generalization of the ideas current in one dimension leads to a candidate for such a generalized theory. GRA

N88-20962*# Ohio State Univ., Columbus. ElectroScience Lab.
MEASUREMENT OF THE PROPERTIES OF LOSSY MATERIALS INSIDE A FINITE CONDUCTING CYLINDER Semiannual Report
A. Dominek, A. Park, and R. Caldecott Mar. 1988 34 p
(Grant NAG3-784)
(NASA-CR-182664; NAS 1.26:182664; ESL-719300-1) Avail: NTIS HC A03/MF A01 CSCL 20C

Broadband, swept frequency measurement techniques were investigated for the evaluation of the electrical performance of thin, high temperature material coatings. Reflections and transmission measurements using an HP8510B Network Analyzer were developed for an existing high temperature test rig at NASA

Lewis Research Center. Reflection measurements will be the initial approach used due to fixture simplicity even though surface wave transmission measurements would be more sensitive. The minimum goal is to monitor the electrical change of the material's performance as a function of temperature. If possible, the materials constitutive parameters, epsilon and muon will be found. Author

N88-20963# California Univ., Berkeley. Lawrence Berkeley Lab.
MODELING THE BEHAVIOR OF ORIENTED PERMANENT MAGNET MATERIAL USING CURRENT DOUBLE THEORY
M. A. Green Nov. 1987 6 p Presented at the 10th International Conference on Magnet Technology (MT-10), Boston, Mass., 21 Sep. 1987
(Contract DE-AC03-76SF-00098)
(DE88-004446; LBL-23972; CONF-870901-28) Avail: NTIS HC A02

This paper presents a method for modeling two dimensional dipoles, quadrupoles and other higher multipoles built using oriented permanent magnet materials such as samarium cobalt (one of the rare earth cobalt REC materials). The technique presented here uses complex current doublet to model the magnetized material. This technique can be used in conjunction with an infinitely permeable circular iron shield which lies outside the REC material. Examples of two types of dipoles and quadrupoles are presented in this report. DOE

N88-20964# Office National d'Etudes et de Recherches Aerospatiales, Paris (France). Physics Dept.
[ACTIVITIES REPORT OF THE PHYSICS DEPARTMENT] Annual Report, 1986
Sep. 1987 40 p Original contains color illustrations
(ETN-88-91985) Avail: NTIS HC A03/MF A01

An antistatic coating tester; measurement of tip clearance in turbomachines; the GRADIO Project and electrostatic three-axis accelerometers for space applications; a dedicated processor for correcting the signal from CCD array; and improvement of barometric and accelerometric sensitivities of quartz-crystal resonators are discussed. Effects of aerodynamic flows on image generation; bispectral infrared imaging; infrared cameras; and wavefront analysis are reviewed. Impulsive noise of main helicopter rotors is treated. Application of holographic interferometry on two wavelengths to measuring the density of a plasma; and a secondary emission electron gun are described. Lightning monitoring and warning by radioelectric interferometry and electrostatic measurements; space-time analysis of the electromagnetic radiation associated with lightning discharges; airborne lightning characterization; electromagnetic interference generated on the fly-by-wire controls of an Airbus aircraft by a simulated direct lightning strike; electromagnetic radiation generated by junction of a lightning channel with ground; and determination of the charge distribution within an E-irradiated dielectric are considered. ESA

71 ACOUSTICS

Includes sound generation, transmission and attenuation. For noise pollution see *45 Environmental Pollution.*

N88-20965# Naval Underwater Systems Center, New London, Conn.
OPTIMAL AND CONVENTIONAL SPACE-TIME PROCESSING IN FLOW NOISE Ph.D. Thesis
John W. Fay 10 Nov. 1987 210 p
(AD-A189104; NUSC-TR-7997) Avail: NTIS HC A10/MF A01 CSCL 20A

A systematic approach is developed as a means of characterizing optimal and conventional space-time detection of a Gaussian signal in colored Gaussian flow noise with line arrays. Discrete arrays of sensors, as well as continuous finite observation intervals, are considered. Using the likelihood ratio as a starting point, exact solutions are formulated, specifying the optimal instrumentation for a rational noise model. These solutions provide the theoretical framework to determine upperbound detection performance and permit examination of the role played by the noise spectra in influencing the optimal instrumentation and its performance. The study describes potential gains achievable with optimal processing over conventional processing. Flow noise spectral parameters are identified, for which either the detection gains with optimal processing are significant or conventional processing is sufficiently close to optimal. The best narrowband robust performance is nearly achieved with conventional processing alone, especially if the spatial bandwidth-length product is large. A simple modification is examined of basic Eckart frequency filtering at a conventional beamformer output. GRA

N88-20966# Applied Research Lab., State College, Pa.
MEASUREMENT AND ANALYSIS OF THE NOISE RADIATED BY LOW MACH NUMBERS CENTRIFUGAL BLOWERS Ph.D. Thesis
D. M. Yeager and G. C. Lauchle Nov. 1987 222 p Prepared in cooperation with IBM Corp., Poughkeepsie, N.Y.
(Contract N00024-85-C-6041)
(AD-A189226; ARL/PSU/TR-87-009) Avail: NTIS HC A10/MF A01 CSCL 20A

The broad band, aerodynamically generated noise in low tip-speed Mach number, centrifugal air moving devices is investigated. An interdisciplinary approach was taken which involved investigation of the aerodynamic and acoustic fields, and their mutual relationship. The noise generation process was studied using two experimental vehicles: (1) a scale model of a homologous family of centrifugal blowers typical of those used to cool computer and business equipment, and (2) a single blade from a centrifugal blower impeller which was placed in a known, controllable flow field. The radiation characteristics of the model blower were investigated by measuring the acoustic intensity distribution near the blower inlet and comparing it with the intensity near the inlet to an axial flow fan. Aerodynamic studies of the flow field in the inlet and at the discharge to the rotating impeller were used to assess the mean flow distribution through the impeller blade channels and to identify regions of excessive turbulence near the rotating blade row. New frequency-domain expressions for the correlation area and dipole source strength per unit area on a surface immersed in turbulence were developed which can be used to characterize the noise generation process over a rigid surface immersed in turbulence. An investigation of the noise radiated from the single, isolated airfoil (impeller blade) was performed using modern correlation and spectral analysis techniques. GRA

N88-20967# Admiralty Research Establishment, Teddington (England).
FLOW/ACOUSTIC INTERACTION IN DUCT INFLOW
M. C. Quinn Sep. 1987 80 p
(AD-A189264; ARE-TM-(UHA)-87511; DRIC-BR-103850) Avail: NTIS HC A05/MF A01 CSCL 20A

Sound generation in the convection of turbulence into a flow intake duct is discussed by examination of an idealized problem. Ideal fluid is in motion with uniform low, subsonic velocity above and parallel to a plane, rigid wall. A thin, rigid, semi-infinite plate is parallel to the wall and the fluid flows past its leading edge. The radiated sound is calculated for a turbulent eddy modelled by a weak line vortex which is allowed to convect passively past the leading edge of the plate. Account is taken of the contribution to the radiated sound from the disturbance produced by the convecting vortex in the boundary layers on each side of the plate by means of the theory of displacement thickness fluctuations, the strength of the disturbance being fixed by a leading edge Kutta condition. The predicted level of the radiated sound is substantially reduced due to the boundary layer disturbances relative to when they are neglected. The case of the convection of a frozen 2-D gust is also considered. Examination of the analogous problem of plane wave radiation from the duct shows that the presence of displacement waves enhanced both the far-field intensity in the ambient fluid and the reflected field in the duct. GRA

N88-20968# Harvard Univ., Cambridge, Mass.
MATHEMATICAL MODELS OF SOUND WAVES IN FLUIDS Final Technical Report
Garrett Birkhoff 12 Aug. 1987 9 p
(Contract N00014-85-C-0466)
(AD-A189270) Avail: NTIS HC A02/MF A01 CSCL 20A

The research discusses mathematical problems of numerical ocean acoustics. These concern the propagation of sound waves in (generally inhomogeneous) elastic fluids, with special reference ot the consistency of the elastic fluid model with ray theory (Fermat-Huygens), in predicting reflection, refraction, and diffraction. The standard modern explanation in terms of relaxation times, although sixty years old, has not yet been substantiated (especially in liquids) by clear answers to many basic questions. These include the following: To what extent is the absorption of sound per wave length, alpha lambda, in air, CO2, and other dilute gases determined by the absolute temperature, T, and the ratio f/p of the frequency to the pressure. To what extent are contributions to alpha from different causes demonstrably additive, in gases and in liquids. GRA

N88-20969# Pennsylvania State Univ., University Park. Applied Research Lab.
ACOUSTIC RADIATION FROM LINE- AND POINT-LOADED PLATES: UNIFORMLY ASYMPTOTIC SOLUTIONS Ph.D. Thesis
H. Y. Hsu and S. I. Hayek Nov. 1987 142 p
(Contract N00024-85-C-6041)
(AD-A189367; ARL/PSU/TR-87-010) Avail: NTIS HC A07/MF A01 CSCL 20A

The theoretical analysis for predicting the acoustic radiation from an infinite fluid-loaded elastic plate excited by a line or a point force is presented. The acoustic pressure radiated by this coupled plate-fluid system is obtained by the use of the Fourier transform method for line force excitation and a Hankel transform for point force excitation. The integral representation of the radiated acoustic pressure is evaluated by three methods based on the steepest descent path (SDP). The first is the widely used saddle point method which can only lead to the far-field solution. The first-order approximation due to the contribution at the saddle point is obtained with the assumption that all the poles of the integrand are located far away from the saddle point and SDP. However the leaky wave pole may approach the saddle point when the frequency is above the coincidence frequency. Thus the saddle point method is modified such that all the singularities of the integrand are explicitly isolated regardless of their proximity to the saddle point. GRA

N88-20970# Sandia National Labs., Albuquerque, N. Mex.
MEASURING THIN FILM PROPERTIES USING SAW (SURFACE ACOUSTIC WAVE) DEVICES: DIFFUSIVITY AND SURFACE AREA
S. J. Martin, G. C. Frye, A. J. Ricco, and T. E. Zipperian 1987 6 p Presented at the IEEE Ultrasonics Symposium, Denver, Colo., 13 Oct. 1987
(Contract DE-AC04-76DP-00789)
(DE88-002216; SAND-87-2539C; CONF-8710201-1) Avail: NTIS HC A02

Surface acoustic wave (SAW) devices have been used in two new techniques for the characterization of thin film properties. By monitoring the change in surface wave propagation velocity, the sorption of gases and vapors by a film can be recorded. In the first technique, the absorption transient for gas and vapor molecules diffusing into polymer films is observed. These transient data can be fit to a one-dimensional diffusion equation and a diffusivity extracted. In the second technique, the adsorption of nitrogen by a porous film is measured at 77 K as a function of partial pressure. The effective surface area of porous thin films can be extracted from such adsorption isotherms using standard BET analysis. DOE

N88-20971# Edgerton, Germeshausen and Grier, Inc., Idaho Falls, Idaho.
MODELING OF LASER ULTRASOUND GENERATION IN A WELD POOL
J. A. Johnson 1987 8 p Presented at the Review of Progress in Quantitative NDE, Williamsburg, Va., 21 Jun. 1987
(Contract DE-AC07-76ID-01570)
(DE88-005546; EGG-M-08887; CONF-870691-9) Avail: NTIS HC A02/MF A01

Finite element techniques are used to model laser generation of ultrasound and its propagation through a weld pool. The laser generation is modeled by assuming the reactive force to the laser ablation of the liquid is a stress perpendicular to the surface of the pool. The boundary of the pool is assumed to be spherical. The propagation of the sound waves from the laser source through the boundary into the solid metal is calculated assuming homogeneous properties in both the liquid and solid metal and temperature gradient effects are neglected. The results are compared to a series of experiments on real and simulated weld pools. DOE

N88-20972*# National Aeronautics and Space Administration, Washington, D.C.
METHOD FOR DETERMINING THE COORDINATES OF SOUND SOURCES BY MEANS OF A SOUND MEASUREMENT SYSTEM
Goesta Johan Dahlin Apr. 1988 18 p Transl. into ENGLISH of Swedish Patent no. SE-8204061 (30 Jun. 1982) Transl. by Scientific Translation Service, Santa Barbara, Calif.
(Contract NASw-4307)
(NASA-TT-20242; NAS 1.77:20242) Avail: NTIS HC A03/MF A01 CSCL 20A

A procedure for determining the coordinates of sound sources by means of a sound measurement system is described. Microphone grouping and procedure, sorting with larger measurement systems, and sorting of times in a hyperbola systems are discussed. Author

N88-20973*# National Aeronautics and Space Administration, Washington, D.C.
METHOD FOR DETERMINING ARTILLERY POSITION
Wilfried Meuser Apr. 1988 19 p Transl. into ENGLISH of German Patent no. DE-3216183-A1 (17 Jul. 1986) Transl. by Scientific Translation Service, Santa Barbara, Calif.
(Contract NASw-4307)
(NASA-TT-20238; NAS 1.77:20238) Avail: NTIS HC A03/MF A01 CSCL 20A

A method is described for determining the position of artillery in which a circle of four closely spaced microphones is located at two measurement sites for acoustic radio direction finding of muzzle blasts. A method for determining the position of artillery using this procedure is discussed. Author

N88-20974*# National Aeronautics and Space Administration, Washington, D.C.
METHOD FOR DETERMINING ARTILLERY POSITION
Johannes Fischer and Wilfried Meuser Apr. 1988 25 p Transl. into ENGLISH of German Patent no. DE-3239240 A1 (26 Apr. 1984) Transl. by Scientific Translation Service, Santa Barbara, Calif.
(Contract NASw-4307)
(NASA-TT-20237; NAS 1.77:20237) Avail: NTIS HC A03/MF A01 CSCL 20A

A method is described for determinig artillery positions. Two groups of four closely spaced microphones are placed at known positions, and radio bearings are determined by projectile flight time differences of muzzle blasts. The advantages of the method are discussed. Author

72 ATOMIC AND MOLECULAR PHYSICS

Includes atomic structure, electron properties, and molecular spectra.

N88-20975# State Univ. of New York, Buffalo. Dept. of Chemistry.
SPONTANEOUS DECAY AND ATOMIC FLUORESCENCE NEAR A METAL SURFACE OF AN ABSORBING DIELECTRIC
Henk F. Arnoldus and Thomas F. George Oct. 1987 36 p
(Contract N00014-86-K-0043)
(AD-A187508; UBUFFALO/DC/87/TR-54) Avail: NTIS HC A03/MF A01 CSCL 20E

Optical properties of an atom in the vicinity of a metal or dielectric are different from those in free space. The spontaneous decay of an atom with two degenerate levels is studied, where the relaxation operator is obtained as a function of the atom-surface separation and the complex bulk dielectric constant epsilon(omega). The Einstein coefficient A(m)(e) of an excited state j(e)m(e) (right arrow) appears to depend on the magnetic quantum number m(e). A sum rule for A(m)(e) is derived, and from the rotational symmetry with respect to the surface normal it is found that A(m)(e) = A(-m)(e). A general expression for the fluorescent radiation field in the far zone is then derived, which incorporates the polarization properties of the fluorescence, as they are modified by the presence of the dielectric. It is shown that the angular distribution of the emitted intensity depends strongly on epsilon(omega), and it is pointed out how information about the substrate, e.g., epsilon(omega), can be extracted from the temporal statistical behavior of the emitted photons. It is emphasized that the major surface effects are purely geometrical, despite the essential quantum nature of the problem. GRA

N88-20976# California Inst. of Tech., Pasadena.
PROPERTIES OF REACTIVELY SPUTTERED WNx FILMS ZHAO, X. -A.
E. Kolawa, F. C. So, X.-A. Zhao, and M.-A. Nicolet 1987 8 p
(Contract DAAG29-85-K-1092)
(AD-A188711; ARO-22281.11-MS) Avail: NTIS HC A02/MF A01 CSCL 07B

Tungsten nitride (WNx) films were prepared by reactive rf sputtering of a tungsten target in N2/Ar plasma. The resistivity, intrinsic stress and atomic composition of the films were studied as functions of various sputtering parameters: sputtering power, gas pressure, gas composition and substrate bias. The atomic percentage of nitrogen (x) of the WNx films was found to decrease with sputtering power and to increase with the partial pressure of nitrogen. The intrinsic stress if WNx is compressive. The dependence of film properties upon sputtering parameters for WNx differs significantly from that of reactively sputtered TiN films, and may be attributed to the difference in the formation mechanisms of TiN and WNx. GRA

N88-20977# California Univ., Berkeley.
QUANTUM MONTE CARLO STUDY OF THE MIES ASSOCIATED WITH H2 (X 1 SIGMA SUB G (+)) AND H2 (B 1 SIGMA SUB U (+)) Final Report, 1 Jul. 1985 - 30 Jun. 1987
William A. Lester Oct. 1987 30 p Sponsored by Air Force Space Div., Edwards AFB, Calif.
(AD-A189063; AFAL-TR-87-075) Avail: NTIS HC A03/MF A01 CSCL 20J

Initial efforts to characterize the electronically excited state of H4 that correlates in one asymptotic limit to H2(X 1 Sigma(+) sub q + H2(B1 sigma(+) sub u are described. Multiconfiguration self consistent field (MCSCF) and fixed-node quantum Monte Carlo (FNQMC) methods have been used to explore the suggested region of stability. The minimum on the excited-state potential energy surface for pyramidal geometries is found to have an isoceles base. Initial estimates of nonadiabiatic coupling matrix elements needed for the determination of lifetimes and stability are determined using normal mode distortions. GRA

N88-20978# George Washington Univ., Washington, D.C. Dept. of Chemistry.
ELECTRON STIMULATED DESORPTION AND COHERENT ELECTRON SCATTERING Interim Technical Report
Hideo Sambe, David E. Ramaker, L. Parenteau, and L. Sanche Dec. 1987 5 p
(Contract N00014-80-K-0852; Proj. RR0-1308)
(AD-A189091; TR-40) Avail: NTIS HC A02/MF A01 CSCL 07B

We have studied electron-stimulated 0(-) desorption from O2 condensed on thick rare-gas (Ar, Kr, or Xe) films, which were previously deposited on a Pt substrate. For ordered rare-gas layers with a fixed O2 coverage, the 0(-) yield increases almost linearly as the thickness of the rare gas layer increases, particularly near the Bragg reflection energies. This is shown to arise from coherent scattering of electrons in the rare gas film. GRA

N88-20979# George Washington Univ., Washington, D.C. Dept. of Chemistry.
IMAGE CHARGE, COHERENT SCATTERING, AND SYMMETRY EFFECTS IN ELECTRON STIMULATED DESORPTION: O(-) FROM O SUB 2 CONDENSED ON METALS Interim Technical Report
David E. Ramaker and Hideo Sambe Dec. 1987 8 p
(Contract N00014-80-K-0852; Proj. RR0-1308)
(AD-A189093; TR-38) Avail: NTIS HC A02/MF A01 CSCL 07B

This work examines environmental effects, which do not arise from alteration of the excited-state lifetime, but rather from the image charge induced in the metal substrate, adsorbate-adsorbate interactions which reduce the symmetry and hence cause certain selection rules to breakdown, and coherent scattering of electrons in the substrate. GRA

N88-20980# George Washington Univ., Washington, D.C. Dept. of Chemistry.
THE MAGNITUDE OF SECONDARY ELECTRON CONTRIBUTIONS IN PHOTON STIMULATED DESORPTION Interim Technical Report
David E. Ramaker, T. E. Madey, R. L. Kurtz, and Hideo Sambe Dec. 1987 5 p
(Contract N00014-80-K-0852; Proj. RR0-1308)
(AD-A189094; TR-36) Avail: NTIS HC A02/MF A01 CSCL 07D

Recent reports on the extent of secondary electron contributions in electron/photon stimulated desorption (ESD/PSD) appear to be contradictory. JAEGER et al. suggested that secondary electrons provide the dominant contribution to the H+ yield from NH3/Ni and called the process X-ray induced ESD (XESD). Others have concluded that the XESD process is the dominant mechanism in the PSD of N+ and O+ ions from the mixed condensed gases such as N2 and O2 and in the PSD of H+ ions from OH/YbO-Sm. On the other hand, considerable evidence exists in the literature for the dominance of the direct photon excitation mechanisms. This paper presents a re-examination of the three systems mentioned above where a dominant XESD effect has been postulated to determine the validity of the conclusions previously reached. GRA

N88-20981# Kent State Univ., Ohio. Liquid Crystal Inst.
LARGE MOMENTUM PAIRING IN ONE-DIMENSIONAL SYSTEMS Final Report, 1 Jul. 1984 - 31 Dec. 1985
D. W. Allender 1987 6 p
(Grant AF-AFOSR-0185-86)
(AD-A189228; AFOSR-87-1724TR) Avail: NTIS HC A02/MF A01 CSCL 20E

The primary objective was to determine the correlation function describing large momentum pairing. A comparison of this correlation function with other correlations (such as singlet pairing, triplet pairing, charge density wave, and spin density wave) is now possible. In light of the recent discovery of high temperature superconductivity (T(C) 95K) in rare earth copper oxide materials,

it is apparent that a revolution in superconductivity research is beginning. GRA

N88-20982# Yale Univ., New Haven, Conn.
MOLECULAR COLLISION PROCESSES IN GASES AND AT SURFACES Final Report, 1 Mar. 1985 - 31 Jul. 1987
John B. Fenn 12 Dec. 1987 18 p
(Contract F49620-85-C-0065)
(AD-A189518; AFOSR-88-0132TR) Avail: NTIS HC A03/MF A01 CSCL 07D

Results have been obtained by Fourier Transform Infrared Emission Spectrometry (FTIES) to determine the internal energy distribution in molecules whose states are consequent to three kinds of inelastic and/or reactive collision processes. Gas that is vibrationally excited in the source by heating, corona discharge or chemical reaction is interrogated by FTIES after free jet expansion into vacuum. The observed marked departures from equilibrium give insight on RR, RT, RV and VV exchanges where R, T and V refer to rotational, vibrational and translational energy. When free jets of CO2, CO2, N2O, and OCS are incident on a hot Pt surface the reflected molecule have enough vibrational excitation to be analyzed by FTIES. Vibrational and rotational accommodation coefficients have been determined for these species over a range of surface temperatures. FTIES analysis has been carried out on nascent carbon dioxide molecules formed by the catalytic oxidation of carbon monoxide molecules incident on a Pt surface bathed in oxygen. Results indicated vibrational and rotational temperatures much higher than surface temperatures. GRA

N88-20983# Boston Univ., Mass. Dept. of Chemistry.
MECHANISMS OF PHOTOINDUCED ELECTRON TRANSFER Final Report, 1 Jul. 1977 - 30 Sep. 1987
Guilford Jones, II Dec. 1987 28 p
(Contract DE-AC02-77ER-04380)
(DE88-004917; DOE/ER-04380/8) Avail: NTIS HC A03/MF A01

Work on photoinduced electron transfer reactions in organic compounds conducted under Department of Energy sponsorship over the past ten years at Boston University is described. Early studies in the series were directed to the development of new mechanisms for driving isomerization processes which store light energy as latent heat. Other investigations were devoted to an understanding of the dynamics of charge separation for photoexcited (charge-transfer) complexes or ion-pairs. Recent studies focused on the development of charge relays such as dithioethers and viologen or pyridinium ions, the electron transfer photochemistry of high potential quinones, and the photophysical properties of organic dyes bound to water-soluble polymers. DOE

N88-20984# Los Alamos National Lab., N. Mex.
INTERMEDIATE ENERGY NEUTRINO PHYSICS
D. H. White 1987 31 p Presented at the Theoretical Advanced Summer Institute, Santa Fe, N. Mex., 6 Jul. 1987
(Contract W-7405-eng-36)
(DE88-005378; LA-UR-88-97; CONF-8707141-3) Avail: NTIS HC A03/MF A01

Occasionally, our understanding of a situation in physics is apparently so clear that consequences of a particular experimental result can imply a substantial confrontation with our view of the physical world. The standard model of electroweak interactions is now so clear that a number of experimental consequences are precisely predicted. This seems like a delightful situation for experimenters, but the bad news is that the experiments on which the predictions rest are at least hard and certainly expensive. We will focus on one such experiment; the principal goal of the experiment was to measure neutrino-electron scattering, and also to measure a number of other exclusive channels in neutrino scattering which have bearing on our view of hadronic electroweak interactions. Study of neutrino-proton scattering and neutrino oscillation is also reported. DOE

N88-20985# Lawrence Livermore National Lab., Calif.
ELECTRON EMISSION FROM CONDUCTORS SUBJECTED TO INTENSE, SHORT-PULSE ELECTRIC FIELDS
R. D. Scarpetti, D. A. Goerz, P. R. Bowen, R. L. Hodgin, K. C. Wong, and P. D'A. Champney Jun. 1987 6 p Presented at the 6th Inst. of Electrical and Electronic Engineers Pulsed Power Conference, Arlington, Va., 29 Jun. 1987 Prepared in cooperation with Pulse Sciences, Inc., San Leandro, Calif.
(Contract W-7405-eng-48)
(DE88-005412; UCRL-96204; CONF-870656-49) Avail: NTIS HC A02

We studied electron emission from metal electrodes subjected to electric fields ranging from 0.5 to 2.5 MV/cm for pulse durations of 3 to 10 ns. We used two high-voltage pulsers for these tests; a 500 to 700 kV, 72 ohm pulser that generated a 3 ns Gaussian pulse; and a 2 MV, 60 ohm pulser that generated a 10 ns flat-top pulse with a 1-ns risetime. The high voltage levels allowed emission studies using electrode spacings of several millimeters to several centimeters. Our studies emphasized bare and anodized aluminum surface shaving surface finishes that ranged from rolled stock to machined finishes of 2 to 400 micron-in roughness. We also investigated polished stainless steel and brass. Emphasis was on first-shot performance with subsequent pulses applied to check for possible conditioning. The background pressure was typically .00005 Torr. Our studies showed that for 10 ns pulse lengths, anodized aluminum surfaces could hold off more than twice the electric field strength of bare aluminum surfaces without appreciable electron emission. Anodized surfaces performed well at 1.0 to 1.5 MV/cm, while bare surfaces emitted at 0.5 to 0.7 MV/cm. For the shorter, 3 ns pulse lengths, anodizing was less effective at improving suppression of electron emission, while surface finish became the important factor. Electrodes with surface finishes of 40 micro-in or better roughness performed well at field strengths of up to 2.4 MV/cm. The behavior of velvet cloth as an emitter was also investigated using the 3 ns pulser. We found that velvet would emit within 3 ns at field strengths approaching 100 kV/cm. DOE

N88-20986# California Univ., Berkeley. Lawrence Berkeley Lab.
PHYSICS AT LARGE TRANSVERSE MOMENTA
I. Hinchliffe Dec. 1987 20 p Presented at the Workshop on Experiments, Detectors, and Experimental Areas for the Supercollider, Berkeley, Calif., 7 Jul. 1987
(Contract DE-AC03-76SF-00098)
(DE88-005758; LBL-24375; CONF-870739-15) Avail: NTIS HC A03/MF A01

The methods used in estimating the signals and backgrounds involved in searches for new particles at the SSC are reviewed. A brief summary is given of the problems involved in these searches. The required detector parameters are summarized and an indication of the open problems given. DOE

N88-20987# Nationaal Inst. voor Kernfysica en Hoge Energiefysica, Amsterdam (Netherlands).
PROTON/ANTIPROTON YIELDS W(+/-)BOSON GAMMA X AS A TEST OF THE QUARK CHARGES
R. M. Godbole, J. Smith, W. L. vanNeerven, and J. A. M. Vermaseren 1987 9 p
(NIKHEF-H/87-11; ITP-SB-87-28; DO-TM-87/5; B8729110; ETN-88-91742) Avail: NTIS HC A02/MF A01

The suggestion that radiation zeroes can be used to test the difference between fractional and integer-charged quarks is examined. Since the amplitude zeroes for fractionally-charged quarks are altered by the effect of higher order QCD corrections, the test is likely to be difficult. ESA

N88-20988# Nationaal Inst. voor Kernfysica en Hoge Energiefysica, Amsterdam (Netherlands).
ENERGY LOSS OF PARTICLES IN DENSE MATTER-CALORIMETRY
Richard Wigmans Aug. 1987 112 p Presented at the ICFA School on Instrumentation in Elementary Particle Physics Lecture,

Trieste, Italy, 8-19 Jun. 1987
(NIKHEF-H/87-12; B8729553; ETN-88-91743) Avail: NTIS HC A06/MF A01

Factors that limit the performance of calorimeters used in supercollider experiments are considered. Calorimeters for detecting electromagnetic (em) showers are discussed. Physics processes relevant to em shower development, and the factors that limit the performance of em calorimeters are examined. Readout techniques for sampling calorimeters are reviewed. Hadron calorimeters are assessed. Physics processes relevant to hadron shower development, their consequences for the calorimeter signals, and the possibilities for optimizing the performance of hadron calorimeters are examined. Future developments are considered. ESA

N88-20989# Colorado Univ., Boulder.
EXCIMER LASER PHOTOLYSIS STUDIES OF T-V (TRANSLATION-TO-VIBRATION) ENERGY TRANSFER Final Report, 21 Dec. 1984 - 20 Dec. 1987
Stephen R. Leone 21 Dec. 1987 24 p
(Contract DAAG29-85-K-0033)
(AD-A189613; ARO-21970.2-PH) Avail: NTIS HC A03/MF A01 CSCL 07D

Under the previous grant, research has been carried out on translation-to-vibration, rotation (T-VR) transfer excitation processes and reactive events of photolytically-produced hot atoms which have accomplishments of laser and infrared probing in systems such as hydrogen + nitrogen oxide, hydrogen, deuterium + hydrogen fluoride, and collisional dissociation of bromine (B, V prime, J prime). We then discuss recent successful efforts to construct an apparatus to produce even more highly energetic neutral atoms and radicals by laser ablation techniques and the first results in obtaining translationally fast molecular and radical species. GRA

N88-20990# Lawrence Livermore National Lab., Calif.
NUMERICAL SIMULATIONS OF MULTIPHOTON PROCESSES IN MANY ELECTRON ATOMS
K. C. Kulander and C. Cerjan 1 Sep. 1987 10 p Presented at the NATO Workshop on Atomic and Molecular Processes with Short Intense Laser Pulse, Sherbrooke, Quebec, 19 Jul. 1987
(Contract W-7405-eng-48)
(DE88-003293; UCRL-97493; CONF-870784-4) Avail: NTIS HC A02/MF A01

In this report, we will present some details of two numerical methods which we have been pursuing for treating the multi-electron case. Both involve a numerical representation of the time dependent Hartree Fock electronic orbitals and a direct time integration of the coupled equations. Using these methods we will be able to determine the dynamics of the energy absorption process (preionization dynamics and the mechanism of ionization, i.e., whether it is direct multi-electron emission or sequential). DOE

N88-20991# Los Alamos National Lab., N. Mex.
FRAGMENTATION AND FLOW IN CENTRAL COLLISIONS
B. V. Jacak, K. G. R. Doss, H. A. Gustafsson, H. Gutbrod, J. W. Harris, K. H. Kampert, B. Kolb, A. M. Poskanzer, H. G. Ritter, and H. R. Schmidt 1987 15 p Presented at the Symposium on Hot Nuclei, College Station, Tex., 7 Dec. 1987 Prepared in cooperation with Gesellschaft fuer Schwerionenforschung m.b.H., Darmstadt, Fed. Republic of Germany and California Univ., Berkeley, Lawrence Berkeley Lab.
(Contract W-7405-eng-36)
(DE88-005386; LA-UR-88-153; CONF-871243-5) Avail: NTIS HC A03/MF A01

Investigation of the fragmentation mechanism requires the measurement of complicated observables. To identify what part of the reacting system gives rise to the fragments, it would be useful to tag them as participants or spectators. A large acceptance for all the reaction products and an event-by-event measurement of the fragment multiplicity is required to distinguish fragment formation via sequential emission from a large equilibrated system and multifragmentation. In order to address whether fragments are formed early or late in the collision, information about the dynamical evolution of the reaction is necessary. This can be provided by study of the global properties of the events. This paper discusses experimental techniques applicable to studying fragmentation processes. DOE

N88-20992# Argonne National Lab., Ill.
DIFFRACTION THEORY IN QCD AND BEYOND
Alan R. White 11 Dec. 1987 18 p Presented at the 2nd International Conference on Elastic and Diffractive Scattering, New York, N.Y., 15 Oct. 1987
(Contract W-31-109-eng-38)
(DE88-005958; ANL-HEP-CP-87-120; CONF-8710274-1) Avail: NTIS HC A03/MF A01

A study of the Pomeron in QCD is briefly outlined. Implications for the production of W(+)W(-) and Z(0)Z(0) pairs are described and the possibility that the electroweak scale is a major strong-interaction threshold discussed. The application of Pomeron phase-transition theory to SU(5) dynamical symmetry breaking is suggested and the related strong-interaction properties of the photon briefly mentioned. DOE

N88-20993# Georgia Univ., Athens. Dept. of Physics and Astronomy.
OPTICAL STUDIES OF DYNAMICAL PROCESSES IN DISORDERED SYSTEM Progress Report, Mar. 1987 - Feb. 1988
W. M. Yen Jan. 1988 16 p
(Contract DE-FG09-87ER-45291)
(DE88-005965; DOE/ER-45291/T1) Avail: NTIS HC A03/MF A01

In this document, we present a brief summary of the progress archieved during the present grant period and an outline of the various projects currently under way including new initiatives we have undertaken. Progress has been attained in several areas: it would appear that we are nearing a complete theoretical understanding of the relaxation properties of ions in glasses as they manifest themselves in the homogeneous optical linewidth; a number of experiments currently in progress would yield definitive evidence of the validity of various theoretical predictions. Additionally, we are in the process of concluding measurements of absolute quantum efficiencies of Cr3+ doped transparent ceramics and extending the studies to include energy transfer processes in trivalent Nd, Cr doubly doped systems. We have obtained preliminary results in our attempts to isolate single optically active ions in a glass optical fiber. DOE

N88-20994# Florida Univ., Gainesville.
RESEARCH IN HIGH ENERGY ELEMENTARY PARTICLE PHYSICS Annual Progress Report, 1 Mar. 1986 - 29 Feb. 1988
R. Field, P. Ramond, C. Thorn, P. Avery, J. Walker, D. Tanner, P. Sikivie, N. Sullivan, and S. Majeswki 11 Jan. 1988 93 p
(Contract DE-FG05-86ER-40272)
(DE88-006065; DOE/ER-40272/49) Avail: NTIS HC A05

This is a progress report covering the period March 1, 1986 through February 29, 1988 for the High Energy Physics program at the University of Florida (DOE Florida Demonstration Project grant FG05-86-ER40272). The research program covers a broad range of topics in theoretical and experimental physics and includes detector development and an Axion search. Included in this report is a summary of the program and a discussion of the research progress. DOE

N88-20995# Netherlands Energy Research Foundation, Petten.
COMPUTER PROGRAMS FOR CALCULATING GROUP CROSS-SECTION COVARIANCES FROM UNCERTAINTY PARAMETERS IN THE ENDF/B-V FORMAT. UNC 32/33
H. J. Nolthenius Oct. 1987 34 p
(ECN-202; B8729608; ETN-88-91718) Avail: NTIS HC A03/MF A01

Calculation programs for neutron metrology are described. Cross-section libraries in the ENDF/B-V format contain uncertainty

information for a number of cross-section sets. The programs UNC 32/33 read this information and convert it to a group structure of interest for further calculations. The output of the programs becomes available in the form of a set of covariance matrices. These programs are useful for estimating the role of covariances in the calculation of reaction rates and adjusted neutron spectra, since the programs provide a convenient tool for deriving covariance matrices of cross-sections in a selected coarse group structure directly from libraries in the ENDF/B-V format. ESA

73 NUCLEAR AND HIGH-ENERGY PHYSICS

Includes elementary and nuclear particles; and reactor theory.

For space radiation see *93 Space Radiation.*

N88-20996# Continuous Electron Beam Accelerator Facility, Newport New, Va.

THE CONTINUOUS ELECTRON BEAM ACCELERATOR FACILITY

H. A. Grunder, J. J. Bisognano, W. I. Diamond, B. K. Hartline, C. W. Leemann, J. Mougey, R. M. Sundelin, and R. C. York [1987] 8 p

(Contract DE-AC05-84ER-40150)

(CEBAF-PR-87-017) Avail: NTIS HC A02/MF A01

On February 13, 1987, construction started on the Continuous Electron Beam Accelerator Facility, a 4-GeV, 200 microA, continuous beam, electron accelerator facility designed for nuclear physics research. The machine has a racetrack configuration with two antiparallel, 500-MeV, superconducting linac segments connected by beam lines to allow four passes of recirculation. The accelerating structure consists of 1500-MHz, five-cell niobium cavities developed at Cornell University. A liquid helium cryogenic system cools the cavities to an operating temperature of 2 K. Beam extraction after any three of the four passes allows simultaneous delivery of up to three beams of independently variable currents and different, but correlated, energies to the three experimental areas. Beam breakup thresholds exceed the design current by nearly two orders of magnitude. Project completion and the start of physics operations are scheduled for 1993. The total estimated cost is 255 million dollars. Author

N88-20997# Los Alamos National Lab., N. Mex.

A SEGMENTED CALORIMETER FOR LOW-ENERGY PARTICLE BEAMS IN SPACE

M. H. Barron, T. O. Gallagher, C. A. Goulding, R. O. Hedges, K. M. Henneke, C. E. Moss, K. C. Shrouf, and G. E. Slentz Oct. 1987 4 p Presented at the Nuclear Science Symposium, San Francisco, Calif., 21 Oct. 1987

(Contract W-7405-eng-36)

(DE88-001806; LA-UR-87-3575; CONF-871006-5) Avail: NTIS HC A02/MF A01

We describe a segmented calorimeter for determining the spatial intensity distribution of a neutral particle beam. Our instrument for a 1-MeV H^0 beam consists of a 5 x 5 array of boron nitride (BN) blocks, each block 0.975 cm by 0.975 cm by 0.053 cm thick, glued onto a polyimide printed circuit board. The temperature sensor behind each block is a special integrated circuit (AD590). The sensor data are multiplexed into an IBM AT computer for laboratory testing or into a telemetry system and a microVAX II computer for flight. Special features include protection against beam-induced sparking and the launch and space environment. DOE

N88-20998# Cornell Univ., Ithaca, N.Y.

COLLECTIVE ACCELERATION OF ELECTRONS AND IONS IN A HIGH RELATIVISTIC ELECTRON BEAM Progress Report

J. A. Nation and C. E. Seyler 1988 19 p

(Contract DE-AC02-80ER-10569)

(DE88-005261; DOE/ER-10569/5) Avail: NTIS HC A03/MF A01

This paper discusses progress in the acceleration of electrons and ions to high relativistic speeds. Most of the current research time has been spent in the development of a new pulsed power, low repetition rate source for electron wave acceleration. Other projects discussed are investigations in slow space charge waves, fast wave excitation and a phase slip accelerator concept. DOE

N88-20999# Sandia National Labs., Albuquerque, N. Mex.

DESIGN OF ELECTRON BEAM ACCELERATOR FOR MICROWAVE APPLICATION

K. R. Prestwich 1988 40 p Presented at the Pulsed Power Short Course, Lubbock, Tex., 18 Jan. 1988

(Contract DE-AC04-76DP-00789)

(DE88-005252; SAND-88-0091C; CONF-880149-1) Avail: NTIS HC A03/MF A01

Relativistic electron beams are used for generating high power microwaves. These microwave sources require electron beam generators spanning significant ranges in voltage and impedance. The pulsed power technology used to generate these electron beams is presented. Electron beam generators that produce beams with pulse durations in the 10 ns to 100 ns regime consist of an energy storage section, pulse shaping section, and an electron beam diode. The energy storage section is either a Marx generator or capacitor bank-pulsed transformer. The pulse shaping is done with high-voltage transmission lines. The electron beam diode is usually a cold-cathode, space-charge-limited flow device. For longer pulses (approx 1 microsec) the energy storage and pulse shaping can be combined. Lumped-element pulsed-forming networks (PFN) can be designed to produce the desired pulse shape. The Marx generator becomes one of the elements of the PFN. Alternatively, a low voltage PFN followed by a highly coupled transformer can be used. Basic design principles for all of the above subsystems are discussed. Both PFLs and PFNs can also be operated as inductive storage systems with opening switches. DOE

N88-21000# GA Technologies, Inc., San Diego, Calif.

A HIGH FIELD LAUNCH FOR ELECTRON CYCLOTRON HEATING USING AN EXTERNAL WINDOW

C. P. Moeller, R. Prater, A. C. Riviere, N. R. G. Ainsworth, A. N. Dellis, and P. C. Johnson Sep. 1987 9 p Presented at the Joint Workshop on Electron Cyclotron Emission and the Electron Cyclotron Resonance Heating, Oxford, United Kingdom, 16 Sep. 1987 Prepared in cooperation with UKAEA Culham Lab., Abingdon

(Contract DE-AC03-84ER-51044)

(DE88-005350; GA-A-19056; CONF-8709157-3) Avail: NTIS HC A02/MF A01

Electron cyclotron heating experiments in which the extraordinary mode is launched from the inside (high field side) of the torus have required a vacuum window on the high field side of the resonance, with the part of the waveguide passing through the resonance layer pressurized, in order to avoid a breakdown at the resonance layer. We have installed a launcher in the DITE tokamak which tests an alternative scheme permitting an external vacuum window to be used. In this system, resonant breakdown is avoided by means of an electrostatic field, applied by means of a longitudinally split TE(sub 11) mode waveguide, which sweeps electrons into the waveguide wall. In tests using long pulses from a 200 kW, 60 GHz gyrotron, a field as low as 25 V/cm was found to be effective in suppressing breakdown. In the unbaked DITE vessel, it was found that in addition to an electric field, an initial glow discharge cleaning was necessary before long pulses could be transmitted. A similar approach, but with the addition of high temperature baking of the waveguide within the vacuum vessel, will be used on the DIII-D2 MW inside launch ECH experiment. DOE

N88-21001# Nationaal Inst. voor Kernfysica en Hoge Energiefysica, Amsterdam (Netherlands).

HADRONIC OVERLAP AND TOTAL MULTIPLICITY DISTRIBUTIONS IN HIGH ENERGY PHYSICS COLLISIONS

G. F. Wolters Jun. 1987 33 p

(NIKHEF-H/87-10; B8723612; ETN-88-91741) Avail: NTIS HC A03/MF A01

In the realm of Chou and Yang's (1985) geometrical description of hadron collisions at high energy, the total multiplicity distribution of negative binomial type for nonleading secondaries is compounded from a Poisson and a gamma distribution. The latter is attributed to overlap in space-time of the colliding hadrons. The overlap is defined in terms of local interaction probabilities for each incident hadron. These probabilities are assumed to be similar but not identical to hadron constituent quark densities. They are predicted to approach the densities for growing energy. This, and the resulting integrated overlap, are borne out by the empirical data on the negative binomial distribution in an unambiguous way. The preponderance of the latter at very high energies thus reflects nonrelativistic spatial hadron structure and incoherence of event-like excitations throughout the overlap region. ESA

N88-21002# General Electric Co., San Jose, Calif. Astro Space Div.

CERMET-FUELED REACTORS FOR ADVANCED SPACE APPLICATIONS

C. L. Cowan, R. S. Palmer, I. N. Taylor, S. Vaidyanathan, S. K. Bhattacharyya, and J. O. Barner Dec. 1987 7 p Presented at the 5th Symposium on Space Nuclear Power Systems, Albuquerque, N. Mex., 11 Jan. 1988 Prepared in cooperation with Argonne National Lab., Ill. and Pacific Northwest Lab., Richland, Wash.

(Contract DE-AC06-76RL-01830)

(DE88-005528; PNL-SA-15224; CONF-880122-8) Avail: NTIS HC A02

Cermet-fueled nuclear reactors are attractive candidates for high-performance advanced space power systems. The cermet consists of a hexagonal matrix of a refractory metal and a ceramic fuel, with multiple tubular flow channels. The high performance characteristics of the fuel matrix come from its high strength at elevated temperatures and its high thermal conductivity. The cermet fuel concept evolved in the 1960s with the objective of developing a reactor design that could be used for a wide range of mobile power generating sytems, including both Brayton and Rankine power conversion cycles. High temperature thermal cycling tests for the cermet fuel were carried out by General Electric as part of the 710 Project (General Electric 1966), and by Argonne National Laboratory in the Direct Nuclear Rocket Program (1965). Development programs for cermet fuel are currently under way at Argonne National Laboratory and Pacific Northwest Laboratory. The high temperature qualification tests from the 1960s have provided a base for the incorporation of cermet fuel in advanced space applications. The status of the cermet fuel development activities and descriptions of the key features of the cermet-fueled reactor design are summarized. DOE

N88-21003# Pacific Northwest Labs., Richland, Wash.

MOLYBDENUM-BASE CERMET FUEL DEVELOPMENT

W. E. Gurwell, R. W. Moss, J. P. Pilger, and G. D. White Jul. 1987 7 p Presented at the 5th Symposium on Space Nuclear Power Systems, Albuquerque, N. Mex., 11 Jan. 1988

(Contract DE-AC06-76RL-01830)

(DE88-005529; PNL-SA-15107; CONF-880122-7) Avail: NTIS HC A02/MF A01

Development of a multimegawatt (MMW) space nuclear power system requires identification and resolution of several technical feasibility issues before selecting one or more promising system concepts. Demonstration of reactor fuel fabrication technology is required for cermet-fueled reactor concepts. MMW reactor fuel development activity at Pacific Northwest Laboratory (PNL) is focused on producing a molybdenum-matrix uranium-nitride (UN) fueled cermet. This cermet is to have a high matrix density (greater than or equal to 95 percent) for high strength and high thermal conductance coupled with a high particle (UN) porosity (approximately 25 percent) for retention of released fission gas at high burnup. Fabrication process development involves the use of porous TiN microspheres as surrogate fuel material until porous UN microspheres become available. Process development has been conducted in the areas of microsphere synthesis, particle sealing/coating, and high-energy-rate forming (HERF) and vacuum hot press consolidation techniques. This paper summarizes the status of these activities. DOE

N88-21004# Los Alamos National Lab., N. Mex.

COMPATIBILITY IN SPACE REACTOR FUEL SYSTEMS

R. E. Mason and R. B. Matthews Mar. 1988 38 p

(Contract W-7405-eng-36)

(DE88-005698; LA-11071-MS) Avail: NTIS HC A03/MF A01

Isothermal out-of-pile tests for compatibility between Nb-1Zr, tungsten or rhenium, and UN identified high-temperature interactions. These tests demonstrated uranium transport to the inner surface of the cladding and zirconium transport from the cladding to the pellet surface. A URe sub 2 layer was found on the rhenium barrier of tests performed at 1800 K. No other reactions between UN and rhenium were observed. Interdiffusion of rhenium and tungsten with Nb-1Zr was consistent with rates reported in the literature. Significant cladding grain growth was observed in specimens tested at or above 1600 K. One compatibility pin was heated until the cladding melted and the pin was breached. The pin components began melting below the melting point of Nb-1Zr. The cladding and end caps were first to melt; then the liquid partially dissolved the tungsten in barrier and disks and the UN from the surface of the pellet. DOE

74 OPTICS

Includes light phenomena; and optical devices.
For lasers see *36 Lasers and Masers.*

N88-21005# Honeywell Systems and Research Center, Minneapolis, Minn.

PASSIVE AUTONOMOUS INFRARED SENSOR TECHNOLOGY Final Report, 9 Aug. 1985 - 9 May 1987

Firooz Sadjadi Oct. 1987 139 p

(Contract DAAL02-85-C-0134)

(AD-A188698; Rept-87SRC17) Avail: NTIS HC A07/MF A01 CSCL 17E

This study was conducted in response to the DoD's need for establishing understanding of algorithm's modules for passive infrared sensors and seekers and establishing a standardized systematic procedure for applying this understanding to DoD applications. We quantified the performances of Honeywell's Background Adaptive Convexity Operator Region Extractor (BACORE) detection and segmentation modules, as functions of a set of image metrics for both single-frame and multiframe processing. We established an understanding of the behavior of the BACORE's internal parameters. We characterized several sets of stationary and sequential imagery and extracted TIR squared, TBIR squared, ESR, and range for each target. We generated a set of performance models for multi-frame processing BACORE that could be used to predict the behavior of BACORE in image metric space. A similar study was conducted for another of Honeywell's segmentors, namely Texture Boundary Locator (TBL), and its performances were quantified. Finally, a comparison of TBL and BACORE on the same data base and same number of frames was made. GRA

N88-21006# San Diego State Univ., Calif. Dept. of Physics.

STUDY OF PHOTOCHROMIC MATERIALS FOR USE IN OPTICAL SIGNAL PROCESSING Final Technical Report, Jun. 1986 - Jun. 1987

Jeffrey A. Davis and Richard L. Lee Nov. 1987 89 p Sponsored by RADC, Griffiss AFB, N.Y.

(AD-A189068; RADC-TR-87-206) Avail: NTIS HC A05/MF A01 CSCL 20F

This report summarizes 12 months of investigation into the feasibility of using photochromic materials for programmable spatial filters and optical data storage applications. Write and erase times, optical density, and laser power intensity measurements were made. GRA

N88-21007# Rochester Univ., N. Y. Dept. of Physics and Astronomy.
COHERENCE EFFECTS IN OPTICAL PHYSICS WITH SPECIAL REFERENCE TO SPECTROSCOPY Final Report, Nov. 1984 - Jan. 1988
Emil Wolf Jan. 1988 78 p
(Contract F19628-85-K-0005)
(AD-A189520; AFGL-TR-88-0006) Avail: NTIS HC A05/MF A01 CSCL 20F

Results are reported of an investigation in the area of light propagation and spectroscopy from sources of arbitrary states of coherence. The research undertaken has completely clarified the foundations of the radiometric model. It was demonstrated conclusively that spatial coherence properties of a source influence the nature of the spectrum of the emitted radiation. A number of results were derived relating to effects of a random medium on the state of polarization of light transmitted through it. GRA

N88-21008# Air Force Inst. of Tech., Wright-Patterson AFB, Ohio. School of Engineering.
ABERRATIONS: THEIR EFFECT ON OFF-AXIS BEAM STEERING M.S. Thesis
Christina N. Walton Dec. 1987 114 p
(AD-A189601; AFIT/GEP/ENP/87D-10) Avail: NTIS HC A06/MF A01 CSCL 17E

The effect of aberrations on off-axis beam steering for multi-aperture systems was qualitatively investigated. A new expression analogous to Goodman's Thin Lens is proposed which shows the beam degradation that occurs at angles, with respect to the optic axis, much greater than five degrees for a thin lens, and two degrees for a thick lens. This expression was then applied to three multi-aperture configurations as a way to correctly predict the field-of-view for various optical systems. Analytical predictions supported by computational and experimental results are included. Although the beam degradation as the field-of-view or field angle is increased has a dramatic effect on the image quality, the power loss as the field angle is increased will be the major factor in designing a system of this type. GRA

N88-21009# Lawrence Livermore National Lab., Calif.
NONLINEAR REFRACTIVE INDEX MEASUREMENTS OF GLASSES AND CRYSTALS
R. Adair, L. L. Chase, and S. A. Payne Dec. 1987 5 p Presented at the International Laser Science Conference, Seattle, Wash., 20 Oct. 1987
(Contract W-7405-eng-48)
(DE88-005673; UCRL-96104; CONF-8710273-1) Avail: NTIS HC A02/MF A01

We have measured the nonlinear index for numerous glasses and crystals with the goal of determining the material properties that contribute to the magnitude and dispersion of n sub 2. We have found that a nearly-degenerate three-wave-mixing (TWM) process is the most useful method since it can provide both rapid and accurate n sub 2 measurements. DOE

N88-21010# Lawrence Livermore National Lab., Calif.
GUIDELINES FOR ESTIMATION AND CHARACTERIZATION OF THE THERMO-MECHANICAL PROPERTIES OF NEW OPTICAL MATERIALS
J. Marion 18 Nov. 1987 8 p Presented at the Fall Meeting of the Materials Research Society, Boston, Mass., 30 Nov. 1987
(Contract W-7405-eng-48)
(DE88-004359; UCRL-97813; CONF-871124-36) Avail: NTIS HC A02/MF A01

Methods are discussed for the estimation and determination of the thermomechanical properties of new optical materials for laser and nonlinear applications. The goal is to characterize the important properties before materials synthesis, where possible, or for properties where no reliable estimation method is available, a secondary goal is to perform accurate measurements on small samples. The thermomechanical properties of primary emphasis for these applications are fracture toughness, an intrinsic measure of the strength of brittle materials, thermal conductivity, thermal expansion and the elastic constants. DOE

N88-21011# Brookhaven National Lab., Upton, N. Y.
APPLICATIONS OF THE LATERAL SHEARING INTERFEROMETER IN MEASUREMENT OF SYNCHROTRON RADIATION OPTICAL ELEMENTS
Wu-ming Liu, P. Z. Takacs, and D. P. Siddons Nov. 1987 20 p
(Contract DE-AC02-76CH-00016)
(DE88-005184; BNL-40626) Avail: NTIS HC A03/MF A01

The use of a single plate shearing, or Murty, interferometer for measuring the surface quality of several optical elements is reviewed and results given. The principle of the Murty interferometer is also explained. DOE

N88-21012# Connecticut Univ., Storrs.
ENERGY TRANSFER AND NON-LINEAR OPTICAL PROPERTIES AT NEAR ULTRAVIOLET WAVELENGTHS: RARE EARTH 4f YIELDS 5d TRANSITIONS IN CRYSTALS AND GLASSES Progress Report, 1 Jun. 1987 - 31 May 1988
D. S. Hamilton Jan. 1988 45 p
(Contract DE-FG02-84ER-45056)
(DE88-005403; DOE/ER-45056/7) Avail: NTIS HC A03/MF A01

Aspects of the optical properties of lanthanide (rare-earth) doped crystals and glasses at near ultraviolet wavelengths are considered. Measurements of the optical gain and loss at 325 nm in Ce3+:LiYF4 are presented. In addition to creating a cerium ion population inversion, the ultraviolet pumping forms transient and stable color centers via the excited cerium states. Crystals of Cr3+ GSGG show several sharp absorption lines in the 310 nm to 340 nm region which we have identified as transitions of the Gd3+ ion. Excitation spectra taken by monitoring the Cr3+ luminescence shows that a Gd3+ yields Cr3+ energy transfer process is active in this material. Measurements of the time dependance of the Cr3+ fluorescence following pulsed laser excitation of the Gd3+ ions indicates the characteristic time over which this energy transfer occurs. The 5d yields 4f transitions of cerium doped crystals are generally thought to have unity quantum efficiency of luminescence at room temperature. Measurements of the fluorescence lifetimes of the 5d yields 4f fluorescence transitions in Ce3+:CaF2, Ce3+;LiYF4, Ce3+:YAG, Ce3+:-fluoroberyllate glass, and Ce3+:ZBLA glass at 300 K and 77 K are presented. Progress in the construction of a high temperature oven with full optical access is also discussed. Cerium doped solids have the potential for laser action on the 5d yields 4f transitions. Such laser would be broadly tunable toward the near ultraviolet. DOE

N88-21013# Lawrence Livermore National Lab., Calif.
ENZYME-BASED FIBER OPTIC SENSORS
T. J. Kulp, I. Camins, and S. M. Angel Dec. 1987 6 p Presented at the SPIE O-E Lase '88 Optoelectronics and Laser Applications in Science and Engineering, Los Angeles, Calif., 10 Jan. 1988
(Contract W-7405-eng-48)
(DE88-005674; UCRL-97907; CONF-880110-19) Avail: NTIS HC A02/MF A01

Fiber optic chemical sensors capable of detecting glucose and penicillin were developed. Each consists of a polymer membrane that is covalently attached to the tip of a glass optical fiber. The membrane contains the enzyme and a pH-sensitive fluorescent dye (fluorescein). A signal is produced when the enzyme catalyzes the conversion of the analyte (glucose or penicillin) into a product (gluconic or penicilloic acid, respectively) that lowers the microenvironmental pH of the membrane and consequently, lowers the fluorescence intensity of the dye. Each sensor is capable of responding to analyte concentrations in the range of approx. 0.1 to 100 mM. The penicillin optrode response time is 40 to 60 s while that for glucose is approx. 5 to 12 min. DOE

N88-21014 Arizona Univ., Tucson.
OPTICS FOR LARGE TELESCOPE Ph.D. Thesis

Der-Shen Wan 1987 752 p
Avail: Univ. Microfilms Order No. DA8727940

Two topics are discussed: development of phase reduction algorithms for test interferograms especially of large optics, and accurate analytical expression of surface deflection due to gravity when the mirror is supported in the axial direction. Two algorithms for generating phase maps from interferograms were developed. The first method is designed to generate phase from an interferogram that is sampled and digitized only along fringe centers. The second algorithm was developed as an automatic phase reduction process which works on test interferograms recorded by a CCD camera and transferred digitally to a personal computer through a frame grabber. A model was developed to calculate analytically the surface deflection of a mirror supported axially on multiple points. It is based on the thin plate theory, but considerations of thickness variation of a curved mirror, lightweight honeycomb structure and shear are included. These additions improve the accuracy of the calculated surface deflection, giving results close to those obtained form the accurate but computer intensive finite element method. Dissert. Abstr.

N88-21015# Instituto de Pesquisas Espaciais, Sao Jose dos Campos (Brazil).
ASPECTS AND APPLICATIONS OF PRIMARY PROCESSING OF VISUAL INFORMATION [ASPECTOS E APLICACOES DO PROCESSAMENTO PRIMARIO DA INFORMACAO VISUAL]
Antonio Miguel VieiraMonteiro and Flavio Roberto DiasVelasco Aug. 1987 12 p In PORTUGESE Presented at the 4th Brazilian Symposium on Artificial Intelligence, Uberlandia, M.G., 13-16 Oct. 1987
(INPE-4290-PRE/1161) Avail: NTIS HC A03/MF A01

An organization proposal is analyzed for systems which handle visual data. Based on the biological visual system, the initial (primary) processing of visual information is discussed. The primary design, now a possible symbolic scene representation is presented and a possible application in satellite imagery analyzed. Author

N88-21016# National Aerospace Lab., Amsterdam (Netherlands). Space Div.
DEVELOPMENT OF AN OPTICAL DIAGNOSTIC INSTRUMENT. PART 2: INSTRUMENT DEVELOPMENT Final Report
D. vandenAssem and R. H. Huijser Paris, France ESA 15 Jun. 1987 243 p
(Contracts ESA-5188/82/NL-HP(SC); ESA-6533/85-NL-IW(SC); NIVR-423-020405N)
(NLR-TR-87079-L-Pt-2; ESA-CR(P)-2509-Pt-2; ETN-88-91956)
Avail: NTIS HC A11/MF A01

An optical diagnostic instrument is being developed for fluid physics research in the microgravity environment of a space laboratory. The instrument offers a whole field observation system with a Schlieren overlay combined with a local narrow field observation capability, the stake system. The latter allows for operation of a variety of optical instruments, of which two types were evaluated in a test setup: an equal path interferometer and a Moire deflectometer. Development of the narrow field stake system with its accommodation capability of easily exchangeable optical diagnostics is described. The whole field Schlieren system and stake sytem performance was tested. A preliminary design is given for a flight instrument suited for accommodation in a space laboratory. ESA

75 PLASMA PHYSICS

Includes magnetohydrodynamics and plasma fusion.

For ionospheric plasmas see *46 Geophysics*. For space plasmas see *90 Astrophysics*.

N88-21017 California Univ., Davis.
EXPERIMENTAL STUDIES OF PLASMA HEATING DUE TO THE PARAMETRIC DECAY OF A LARGE AMPLITUDE PUMP INTO LOWER HYBRID WAVES Ph.D. Thesis
Victor Jozef Harper-Slaboszewicz 1987 132 p
Avail: Univ. Microfilms Order No. DA8723395

Plasma heating of a high density, low temperature linear plasma by the parametric decay instability of lower hybrid waves excited in a parallel-plate geometry is studied experimentally for omega/omega sub lh = 3 and 10. The electric field distribution is modeled considering the higher-order modes produced in this geometry. A method of measuring bulk electron temperature in the presence of an oscillating potential is developed and validated. Electron heating results show that the prametric decay instability in this geometry is strongly driven and strongly convectively damped, resulting in very rapid electron heating which saturates in a time of 20 to 30/omega. Bulk electron heating consistent with a recent theory of parametric decay of a large amplitude driver near the lower hybrid frequency is also observed. Control of the instability by use of a finite bandwidth driver is also studied, and the results show that the threshold of the parametric decay instability in this geometry can be increased by a factor of 3 by a noise-modulated driver with delta omega/omega = .7. These results are contrasted with earlier studies. Dissert. Abstr.

N88-21018# Indiana Univ., Bloomington. Dept. of Chemistry.
DEVELOPMENT AND EVALUATION OF INSTRUMENTATION AND METHODS FOR MULTI-ELEMENT ANALYSIS Final Report, 1 May 1976 - 30 Apr. 1986
Gary M. Hieftje 13 Jan. 1988 21 p
(Contract N00014-76-C-0838)
(AD-A189345) Avail: NTIS HC A03/MF A01 CSCL 20I

The principal focus of work is to develop and characterize new methods for multielement analysis. Three such methods were originally emphasized and included the development of low flow, high-efficiency torches for use in inductively coupled plasma (ICP) spectrometry, the exploration of novel microwave-induced plasmas (MIP) for elemental analysis, and the exploration of a new technique for the spectral selection of atomic or ionic emission lines, termed selective spectral line modulation (SLM). GRA

N88-21019# Texas Univ., Austin. Inst. for Fusion Studies.
OBSERVATIONS ON ENERGY TRANSPORT IN TOKAMAKS: A NEW FORMULA FOR TURBULENT TRANSPORT
Y. Z. Zhang and S. M. Mahajan Dec. 1987 20 p
(Contract DE-FG05-80ET-53088)
(DE88-005309; DOE/ET-53088/304; IFSR-304) Avail: NTIS HC A03/MF A01

Arguments for a new, modified Ohkawa type formula of anomalous electron energy transport due to electromagnetic microturbulence are presented and its predictions are compared with tokamak experiments. DOE

N88-21020# Edgerton, Germeshausen and Grier, Inc., Idaho Falls, Idaho.
ANALYTICALLY MODELING THE CARBOTHERMIC REDUCTION OF ALUMINA IN A THERMAL PLASMA
D. J. Varacalle, Jr., W. C. Schutte, C. D. VanSiclen, and R. W. Bartlett 1987 26 p Presented at the Extractive and Process Metallurgy Fall Meeting, Palm Springs, Calif., 29 Nov. 1987
(Contract DE-AC07-76ID-01570)
(DE88-005535; EGG-M-11787; CONF-8711148-1) Avail: NTIS HC A03/MF A01

The in-flight carbothermic reduction of vaporized alumina (Al2O3) particles to aluminum was analytically investigated in an argon nontransferred plasma torch. The computational procedure for approximating the plasma physics, particle dynamics, and plasma chemistry of the process is presented. The equations that govern the energy and mass transport in the plasma column and plume are solved numerically to determine the plasma temperature and velocity. The plasma/particle interaction analysis procedure then approximates the trajectories and vaporization of injected particulates in the plasma jet. The results obtained to date indicate the potential of vaporizing a significant amount of alumina and carbon in a plasma, if the particles are small. The thermochemistry analysis indicates that the carbothermic reduction of alumina is possible for in-flight chemical reactions in a dc nontransferred arc

configuration. The economics of the process using a nontransferred configuration is discussed on the assumption that quenching to liquid metal can be achieved. DOE

N88-21021# California Univ., Los Angeles. Dept. of Mechanical, Aerospace and Nuclear Engineering.
HYDROGEN PUMPING AND RELEASE BY GRAPHITE UNDER HIGH FLUX PLASMA BOMBARDMENT
Y. Hirooka, W. K. Leung, R. W. Conn, D. M. Goebel, B. LaBombard, R. Nygren, and K. L. Wilson Jan. 1988 41 p Prepared in cooperation with Sandia National Labs., Livermore, Calif.
(Contract DE-AS03-84ER-52104)
(DE88-005880; UCLA/PPG-1123) Avail: NTIS HC A03

Inert gas (helium or argon) plasma bombardment has been found to increase the surface gas adsorptivity of isotropic graphite (POCO-graphite), which can then getter residual gases in a high vacuum system. The inert gas plasma bombardment was carried out at a flux approx. = 1 x 10 to the 18th /s/sq cm to a fluence of the order of 10 to the 21st ions/sq cm. and at temperatures around 800 C. The gettering capability of graphite can be easily recovered by repeating inert gas plasma bombardment. The activated graphite surface exhibits a smooth, sponge-like morphology with significantly increased pore openings, which correlates with the observed increase in the surface gas adsorptivity. The activated graphite surface has been observed to pump hydrogen plasma particles as well. From calibrated H-alpha measurements, the dynamic hydrogen retention capacity is evaluated to be as large as 2 x 10 to the 18th H/sq cm. at temperatures below 100C and at a plasma bombarding energy of 300 eV. The graphite temperature was varied between 15 and 180 C to the plasma particle pumping capability, hydrogen recycling from the activated graphite surface is significantly reduced, relative to that from a pre-saturated surface. A pre-saturated surface was also observed to reproducibly pump a hydrogen plasma to a concentration of 9.5 x 10 to the 17th H/sq cm. The hydrogen retention capacity of graphite is found to decrease with increasing temperature. A transient pumping mechanism associated with the sponge-like surface morphology is conjectured to explain the large hydrogen retention capacity. Hydrogen release behavior under helium and argon plasma bombardment was also investigated, and the result indicated the possibility of some in-pore retrapping effect. DOE

N88-21022# Massachusetts Inst. of Tech., Cambridge. Plasma Fusion Center.
EVOLUTION OF POLOIDAL VARIATION OF IMPURITY DENSITY AND AMBIPOLAR POTENTIAL IN ROTATING TOKAMAK PLASMA, PART 1
D. J. Sigmar, R. Zanino, and C. T. Hsu Sep. 1987 17 p
(Contract DE-AC02-78ET-51013)
(DE88-006263; DOE/ET-51013/225-Pt-1; PFC/RR-87-8-Pt-1)
Avail: NTIS HC A03/MF A01

When the beam driven toroidal plasma rotation reaches thermal velocity the particle density and the ambipolar potential can develop strong poloidal variations in the flux surface. The rapid time evolution of the thermal velocity, the change in toroidal plasma rotation, and the plasma flow velocity components in the flux surface are calculated. These results are evaluated numerically using a spectral code to describe the strong poloidal couplings. Results are compared to data from the ASDEX tokamak. DOE

N88-21023# Oak Ridge National Lab., Tenn.
FULLY IMPLICIT THREE-DIMENSIONAL MHD (MAGNETOHYDRODYNAMICS) STABILITY AND EVOLUTION IN TOROIDAL GEOMETRY
J. A. Holmes, L. A. Charlton, B. A. Carreras, and V. E. Lynch 1987 4 p Presented at the 12th Conference on the Numerical Simulation of Plasmas, San Francisco, Calif., 20 Sep. 1987
(Contract DE-AC05-84OR-21400)
(DE88-000624; CONF-870947-10) Avail: NTIS HC A02/MF A01

The FAR family of computer codes has been developed at Oak Ridge National Laboratory to solve ideal and resistive, linear and nonlinear, 3-D full MHD problems in toroidal geometry. Extensive application of an incompressible version of these codes has been made to the linear stability of tokamaks and stellarators, and nonlinear studies have also been recently completed. Present work includes generalization of the physical model in several respects to incorporate the effects of compressibility, long mean free path, and thermal conductivity. DOE

N88-21024# Edgerton, Germeshausen and Grier, Inc., Idaho Falls, Idaho.
POTENTIAL OFF-NORMAL EVENTS AND ASSOCIATED RADIOLOGICAL SOURCE TERMS FOR THE COMPACT IGNITION TOKAMAK: FUSION SAFETY PROGRAM
D. F. Holland and R. E. Lyon Oct. 1987 57 p
(Contract DE-AC07-76ID-01570)
(DE88-004112; EGG-FSP-7872) Avail: NTIS HC A04/MF A01

The Compact Ignition Tokamak (CIT), the latest step in the United States program to develop the commercial application of fusion power, is designed as the first fusion device to achieve ignition conditions. It is to be constructed near Princeton, New Jersey on the site of the existing Tokamak Fusion Test Reactor (TFTR). To address the environmental impact and public safety concerns, a preliminary analysis was performed of potential off-normal radiological releases. Operational occurrences, natural phenomena, accidents with external origins, and accidents external to the PPPL site were considered as potential sources for off-normal events. Based on an initial screening, events were selected for preliminary analysis. Included in these events were tritium releases from the tritium delivery and recovery system, tritium releases from the torus, releases of activated nitrogen from the test cell or cryostat, seismic events, and shipping accidents. In each case, the design considerations related to the event were reviewed and the release scenarios discussed. Because of the complexity of some of the proposed safety systems, in some cases event trees were used to describe the accident scenarios. For each scenario, the probability was estimated as well as the release magnitude, isotope, chemical form, and release mode. DOE

N88-21025# Oak Ridge National Lab., Tenn.
COMPARISON OF ANALYTIC AND FULL GUIDING CENTER BEHAVIOR AT A TRAPPED-PASSING INTERFACE IN STELLARATORS
C. L. Hedrick, J. S. Tolliver, and J. R. Cary 1987 31 p Presented at the Meeting of the Division of Plasma Physics of the American Physical Society, San Diego, Calif., 2 Nov. 1987 Prepared in cooperation with Colorado Univ., Boulder
(Contract DE-AC05-84OR-21400)
(DE88-004174; CONF-871105-2) Avail: NTIS HC A03/MF A01

The toroidal adiabatic invariant, can be used to describe both trapped and passing particle motion. Analytic expressions have also been developed to treat transitional particles, which are sometimes trapped, and sometimes passing. We have developed analytic descriptions using a non-canonical Hamiltonian formalism. Here we compare analytic approaches with solutions to the full guiding center equations of motion for a model stellarator magnetic and electric field. We also develop the analytic result directly from the equations of motion, since this clarifies some points, particularly for transitional particles. DOE

N88-21026# Michigan Univ., Ann Arbor. Dept. of Nuclear Engineering.
THE MAGNETICALLY INSULATED INERTIAL CONFINEMENT FUSION (MICF): A NOVEL APPROACH Progress Report, 1 Jun. - 31 Dec. 1987
T. Kammash Jan. 1988 10 p
(Contract DE-FG02-87ER-13723)
(DE88-005460; DOE/ER-13723/1) Avail: NTIS HC A02/MF A01

The Magnetically Insulated Inertial Confinement Fusion (MICF) concept represents a new and a novel approach to fusion power. It combines the favorable aspects of both magnetic and inertial fusions in that physical containment of the plasma is provided by the metallic shell that surrounds the solid fuel pellet, while insulation

of its thermal energy is provided by a very strong, self-generated magnetic field. The plasma of interest is formed at the core of the pellet as a result of ablation of the solid fuel wall by a laser beam that enters the target through a hole. In addition to heating the plasma the laser beam contributes to the formation of the instantaneous magnetic field that serves to impede the energy flow from the hot plasma to the wall. In a reactor scenario the core plasma would be a high beta (ratio of plasma pressure to magnetic field pressure) plasma and as a result the magnetic field does not provide confinement as in magnetic fusion but serves as a thermal insulator. The major thrust thus far has been to model the plasma in such a system and, in so doing, identify the major physics and technological problems that must be addressed in order for MICF to become a viable fusion reactor. DOE

N88-21027# GA Technologies, Inc., San Diego, Calif.
REVERSED FIELD PINCH OPERATION WITH A THIN SHELL
S. Ortolani, V. Antoni, S. Martini, R. LaHaye, M. Schaffer, T. Tamano, and P. Taylor Dec. 1987 8 p Presented at the 14th European Conference on Controlled Fusion and Plasma Physics, Madrid, Spain, 22 Jun. 1987 Prepared in cooperation with Consiglio Nazionale delle Ricerche, Padua (Italy)
(Contract DE-FG03-86ER-53228)
(DE88-005521; GA-A-18834; CONF-870629-14) Avail: NTIS HC A02/MF A01

This paper discusses the possible use of a thin conducting shell to achieve accurate active plasma position control. This is important for minimizing plasma-wall interactions. DOE

N88-21028# Technische Hogeschool, Eindhoven (Netherlands). Dept. of Electrical Engineering.
ARCS IN CESIUM SEEDED NOBLE GASES RESULTING FROM A MAGNETICALLY INDUCED ELECTRIC FIELD
B. Stefanov, A. Veefkind (Bulgarian Academy of Sciences, Sofia.), and L. Zarkova Jul. 1987 36 p
(EUT-87-E-177; ISBN-9-06-144177-3; ISSN-0167-9708; ETN-88-91824) Avail: NTIS HC A03/MF A01

The filaments which form the substructure in the moving discharges in noble gas magnetohydrodynamic generators are considered as free arcs. The spatial distributions of the important plasma quantities are calculated by solving the balance equations. Solutions for cesium seeded argon, helium, xenon, and pure argon are obtained. The solutions yield characteristic radial dimensions which agree with experimental values. The effects of variations of important arc parameters are discussed for the case of cesium seeded argon. The effects of parameter variations can be explained by a simplified expression for the radial dimension of the arc. Deviation from local thermodynamic equilibrium is only significant in the outer region of the arc and has practically no influence on the arc properties. ESA

N88-21029# National Academy of Sciences - National Research Council, Washington, D. C.
OUTLOOK FOR THE FUSION HYBRID AND TRITIUM-BREEDING FUSION REACTORS
J. M. Richardson, R. Cohen, and J. W. Simpson 1987 173 p
(Contract DE-FG05-85ER-52121)
(PB88-149281) Avail: NTIS HC A08/MF A01 CSCL 20I

The study examines the outlook for fusion hybrid reactors. The study evaluates the status of fusion hybrid technology in the United States and analyzes the circumstances under which such reactors might be deployed. The study also examines a related concept, the tritium-breeding fusion reactor. The study examined two potential applications for fusion hybrid technology: (1) the production of fissile material to fuel light-water reactors, and (2) the direct production of baseload electricity. For both applications, markets were sufficiently problematical or remote (mid-century or later) to warrant only modest current research and development emphasis on technology specific to the fusion hybrid reactor. For the tritium-breeding fusion reactor, a need for tritium for use in nuclear weapons might arise well before the middle of the next century, so that a program of design studies, experimentation, and evaluation should be undertaken. GRA

N88-21030 California Univ., Berkeley.
ON THE STRUCTURE OF PULSED PLASMA JETS Ph.D. Thesis
John Arthur Cavolowsky [1987] 229 p
Avail: Univ. Microfilms Order No. DA8726159

A pulsed plasma jet is a turbulent, inhomogeneous fluid mechanical discharge capable of initiating and inhancing combustion. Having shown the ability to ignite lean fuel mixtures, is now offers the potential for real-time control of combustion processes. The fluid mechanical and chemical properties of such jets are explored. The fluid mechanical structure of the jet was examined using two optical diagnostic techniques. Self-light streak photography provided information on the motion of luminous gas particles in its core. The turbulent, thermal evolution of the jet was explored using high speed laser schlieren cinematography. By examine plasma jet generators with both opaque and transparent plasma cavities, detailed information on plasma formation and jet structure, beginning with the electric arc discharge in the cavity, was obtained. Molecular beam mass spectroscopy was used to determine temperature and species concentration in the jet. Both noncombustible and combustible jets were studied. Species measurements in combustible jets revealed significant concentrations of radicals and products of complete as well as incomplete combustion. Dissert. Abstr.

N88-21031# Wisconsin Univ., Madison. Torsatron/Stellarator Lab.
HELICAL RIPPLE TRANSPORT IN STELLARATORS AT LOW COLLISION FREQUENCY Ph.D. Thesis
C. D. Beidler Dec. 1987 157 p
(Contracts DE-FG02-85ER-53201; DE-FG02-86ER-53216)
(DE88-006431; DOE/ER-53201/T3; TSL-87-7) Avail: NTIS HC A08/MF A01

Numerical and analytical techniques were developed to investigate the plasma transport which is due to particles trapping/detrapping in the local helical ripple wells of a stellarator's magnetic field. This process is of considerable importance as it provides the dominant transport mechanism in a stellarator plasma at low collision frequency: that is, when the frequency with which a particle is collisionally detrapped from a local ripple well is less than the bounce frequency of the particle in that well. A form of the longitudinal adiabatic invariant, J, is constructed and shown to describe accurately the orbits of ripple trapped particles. Unlike previous expressions for J, the form derived here correctly accounts for the local toroidal variation of the magnetic field. The expression for J is incorporated into a rapid hybrid Monte Carlo simulation of ripple transport in stellarators. The simulation is a hybrid in the sense that particle orbits in the narrow region of phase space on either side of the ripple trapping/detrapping boundary are followed using guiding center equations of motion while orbits in the remainder of phase space are described using adiabatic invariants. An analytical expression for the distribution function of ripple trapped particles in a stellarator - valid at all low collision frequencies - has been obtained by series solution of the bounce - averaged kinetic equation. This solution has been applied to both standard and a class of transport optimized stellarator magnetic fields. Analytical estimates of the diffusion coefficient obtained from the series solution show excellent agreement with the numerical results of the hybrid Monte Carlo code in all cases studied. DOE

N88-21032# Materials Research Labs., Melbourne (Australia).
TEMPERATURE ESTIMATES FOR A FREE FLOWING RAILGUN PLASMA
G. A. Clark and V. Kowalenko Jun. 1987 49 p
(MRL-R-1054; AR-005-132) Avail: NTIS HC A03/MF A01

In-bore spectroscopic observations of a free-flowing plasma for wavelengths between 3000 and 6250 A were made for a series of railgun firings. The experimental arrangement for the series is described and the results presented. Atomic species present in the plasma are identified from absorption and emission spectra. Calculations of the degree of ionization of these species are then used to produce a temperature estimate between 11 x 10 to the

3rd to 25 x 10 to the 3rd K for the railgun plasma. A comparison of the theoretical values of the plasma electrical conductivity with values obtained from muzzle voltage records indicate that the peak plasma temperature is approximately 11 x 10 to the 3rd K, which is consistent with estimates obtained from the spectra.
Author

N88-21033# Paris-Sud Univ., Orsay (France). Lab. de Spectroscopie Atomique et Ionique.
EXPERIMENTAL STUDY OF THE ROLE OF PLASMA POLARIZATION ON LINE SHAPE IN DENSE LABORATORY PLASMAS
G. Jamelot, P. Jaegle, P. Lemaire, and A. Carillon 1987 19 p Presented at the Workshop on Spectral Line Formation in Plasmas under Extreme or Unusual Conditions, Nice, France, 31 Aug. - 4 Nov. 1987 Submitted for publication
(ETN-88-92001) Avail: NTIS HC A03/MF A01

The spectral line profiles emitted by multicharged ions in dense laser-produced plasmas were studied. The time and/or space integrated spectra of the Lyman series of H-like lithium show a strong red asymmetry and a red shift of the top of the lines. It is shown that such profiles have to be interpreted as due to space and time integration of mostly symmetric profiles, which are red shifted in an amount depending on the emitting plasma zone. Theoretically built profiles show the role, in the observed profiles, of plasma polarization shift, due to the penetration of atomic orbits by the plasma free electrons. ESA

76 SOLID-STATE PHYSICS

Includes superconductivity.

For related information, see also *33 Electronics and Electrical Engineering* and *36 Lasers and Masers.*

N88-21034# Cincinnati Univ., Ohio.
SILICON-GERMANIUM HETEROSTRUCTURES Ph.D. Thesis
Jih-Chen Chian [1987] 160 p
Avail: Univ. Microfilms Order No. DA8722083

First of all, it was found that the semiempirical LCAO method (second-nearest-neighbor interactions included) only gives qualitative results for the Si-Ge(x)Si(1-x) superlattice band structures. To improve this, it will be necessary to include the third-nearest-neighbor interactions for the semiempirical LCAO method. Secondly, the effective mass method (EMM) was generalized and used to calculate the band structures of indirect-indirect Si-Ge(x)Si(1-x) (001) superlattice (x is less than 75 percent). In comparing the band structures of Si-Ge(x)Si(1-x) (001) superlattices calculated by the EMM with those calculated by the semiempirical LCAO method very good agreement was found between these two methods for the energy bands nearest to the forbidden gap. The conduction band discontinuity of the strained-layer Si-Ge(x)Si(1-x) superlattices was calculated by including only one interface load effect (the deformations of both Si and Ge(x)Si(1-x) layers caused by interface lattice mismatch. The results are in very good agreement with the experimental data. This good agreement also implies that the nature valence band discontinuity between Si and Ge is approximately equal to 0.18 eV. Dissert. Abstr.

N88-21035# California Inst. of Tech., Pasadena.
THIN-FILM DIFFUSION BARRIERS FOR METAL-SEMICONDUCTOR CONTACTS
M.-A. Nicolet 1987 9 p
(Contract DAAG29-85-K-0192)
(AD-A188712; ARO-22281.9-MS) Avail: NTIS HC A02/MF A01 CSCL 20L

The notion of a diffusion barrier is discussed as it applies to thin films, and to metal semiconductor contacts in particular. The electrical requirements on the barrier material are easily met; those of the thermodynamic stability of the barrier and the low atomic diffusivity in the barrier are not. The critical influence of the deposition process on the latter property is pointed out. Several different ways to solve the problem are discussed by examples.
GRA

N88-21036# Rockwell International Science Center, Anaheim, Calif.
SOLID-STATE ELECTROCHEMICAL PROCESSES IN DYE FILMS Final Report, 1 Sep. 1977 - 31 Aug. 1987
M. M. Nicholson Nov. 1987 9 p
(Contract N00014-77-C-0636)
(AD-A188756; SC5384.FR) Avail: NTIS HC A02/MF A01 CSCL 07C

Research on solid state electrochemistry of lanthanide diphthalocyanine electrochromic films in the period 1977 to 1987 is summarized. Highlights include characterization of the ion-insertion processes with a novel solid-state moving-boundary technique, study of ambient-atmosphere effects on the anodic reactions, and investigation of solid polymer electrolytes for use in contact with diphthalocyanine electrode films. Future applications of these electrochromic systems in multicolor flat-panel information displays for military purposes are anticipated. GRA

N88-21037# Arizona State Univ., Tempe.
MODELING AND TRANSPORT IN SEMICONDUCTOR DEVICES Final Report, 1 Sep. 1984 - 31 Aug. 1987
D. K. Ferry Nov. 1987 88 p
(Contract DAAG29-84-K-0146)
(AD-A188760; ARO-21057.5-EL) Avail: NTIS HC A05/MF A01 CSCL 20L

Time resolved, subpisecond laser pulse techniques were used to experimentally study the ultrafast relaxation process in the far-from equilibrium electron-hole plasma in Gallium Arsenide. Several theoretical studies have been carried out to explain these experimental measurements. The novel ensemble Monte Carlo simulation technique was used to investigate the cooling process of the hot laser-excited carriers, considering the roles of the carrier-phonon interaction, electron-hole interaction, and the hot phonon effects. The effects of different excitation energies and excitation levels were examined without applying external electric fields. Screening effects were investigated separately and electron-electron and hole-hole interactions were ignored in the calculations to emphasize the electron-hole interaction and hot phonon effects. Degeneracy was taken into account while the excitation level was greater than 1 x 10 to the 17th power cc. The study showed that the hot phonon effects do slow down the cooling rates as expected and the electron-hole interaction slows the cooling rate at low excitation levels while enhancing it at high excitation levels. GRA

N88-21038# State Univ. of New York, Buffalo. Dept. of Chemistry.
THE SYNTHESIS, CHARACTERIZATION AND STRUCTURAL STUDIES OF In(C5H4Me) BY X-RAY DIFFRACTION AND ELECTRON DIFFRACTION TECHNIQUES AND A REINVESTIGATION OF THE CRYSTALLINE STATE OF In(C5H5) BY X-RAY DIFFRACTION STUDIES
O. T. Beachley, Jr., J. C. Pazik, T. E. Glassman, Melvyn R. Churchill, and James C. Fettinger 17 Dec. 1987 50 p
(Contract N00014-87-K-0266)
(AD-A189110; TR-18) Avail: NTIS HC A03/MF A01 CSCL 07C

The compound In(C5H4Me) has been prepared from InCl and Li(C5H4Me) in diethyl ether and fully characterized according to its physical and solubility properties, reaction with dilute HCl, a cryoscopic molecular weight study in cyclohexane, infrared and 1H nuclear magnetic resonance (NMR) spectroscopic properties, an X-ray structural study and a gas-phase electron diffraction study. In addition, a quantitative X-ray structural study has been used to reinvestigate the nature of the solid state of In(C5H5). The compound In(C5H4Me) crystallizes in the centrosymmetric space group P21/n (N0. 14var) with a = 6.1636(14), b = 11.5684(17), c = 9.1723(15)A, beta = 103.561(15), V = 635.78(19)A3 and Z = 4. GRA

N88-21039# Rensselaer Polytechnic Inst., Troy, N.Y.
RESEARCH ON MERCURY CADMIUM TELLURIDE Annual Letter Report, 15 Feb. 1986 - 15 Feb. 1987
Sorab K. Ghandhi 15 Nov. 1987 94 p
(Contract N00014-85-K-0151)
(AD-A189155) Avail: NTIS HC A05/MF A01 CSCL 07B

Accomplishments during this reporting period include the design of a new epitaxial reactor, the growth of high quality cadmium telluride and HgCdTe on both gallium arsenide and CdTe substrates, and the development of a comprehensive theory for the growth of CdTe in OMCVD systems. GRA

N88-21040# Massachusetts Inst. of Tech., Cambridge. Research Lab. of Electronics.
FOCUSED ION BEAM FABRICATION OF GRADED CHANNEL FET'S IN GaAs AND Si Semiannual Technical Report, 1 Jan. - 30 Jun. 1987
John Melngailis 30 Jun. 1987 7 p
(Contract MDA903-85-C-0215)
(AD-A189166) Avail: NTIS HC A02/MF A01 CSCL 20L

The focused ion beam is a unique semiconductor fabrication tool with many applications. Of these, markless/resistless implantation is perhaps the one with the greatest potential impact. It permits implant dose to be varied from point to point on a wafer. Thus, devices can be fabricated side by side with different doping densities, and the doping density can be varied from point to point within a device. Thus, lateral gradients of doping are possible. The aim of this contract is to produce field effect transistors in GaAs and Si with graded implants from source to drain. To achieve this, alignment procedures have to be developed to permit the focused ion beam implant to be positioned precisely relative to features fabricated by conventional means. In addition, models of the behavior of graded devices have to be developed. GRA

N88-21041# Societe Anonyme de Telecommunications, Paris (France).
STUDY FOR THE DETERMINATION OF GENERAL AND SPECIFIC PROPERTIES OF WIDE ENERGY-BAND GAP HgHdTe IN THE 1-2 MICROMETER WAVELENGTH RANGE Interim Report, Jul. - Sep. 1987
A. Durand, M. Royer, A. Gauthier, and F. Raymond 9 Sep. 1987 8 p
(Contract DAJA45-87-C-0020)
(AD-A189177; IR-1) Avail: NTIS HC A02/MF A01 CSCL 07B

During this initial contract phase we concentrated on the study of physical properties of wide energy-band gap Hg(1-x)Cd(x)Te on the one hand and on growth techniques for very high-grade material, on the other hand. GRA

N88-21042# Georgia Univ., Athens. Dept. of Chemistry.
THE RELATIONSHIP OF THE CHEMICAL BONDING TOPOLOGY OF HIGH CRITICAL TEMPERATURE COPPER OXIDE SUPERCONDUCTORS TO THAT OF THE CHEVREL PHASES AND THE TERNARY LANTHANIDE RHODIUM BORIDES
R. B. King 11 Dec. 1987 9 p
(Contract N00014-84-K-0365)
(AD-A189255; TR-56) Avail: NTIS HC A02/MF A01 CSCL 20C

The high critical temperature copper oxide superconductors exhibit chemical bonding topologies closely related to those of the ternary molybdenum chalcogenides and ternary lanthanide rhodium borides in which the conducting skeleton is constructed from metal-oxygen-metal rather than direct metal-metal bonds and antiferromagnetic metal-metal interactions occur rather than direct metal-metal bonding. GRA

N88-21043# STAR Microwave, Campbell, Calif.
MODULATABLE THIN FILM FIELD EMISSION SPACE GUN Final Technical Report, Oct. 1985 - Jun. 1986
Robert M. Phillips Nov. 1987 54 p
(Contract F19628-85-C-0088)
(AD-A189279; RADC-TR-87-41) Avail: NTIS HC A04/MF A01 CSCL 20L

The feasibility is examined of using a Spindt type thin film emitter chip to produce amperes of low voltage modulated current at tens of kilovolt beam voltage for a space application. The specific requirement was for a pulse modulated column of electrons of 10 amperes current at 50 kilovolts voltage. A design effort determined that a 2-inch diameter chip would be required to provide this current with conservative emission current density. A conceptual design was developed consisting of an array of emitting regions producing beamlets which were to be accelerated through a gridded or perforated anode at approximately 3 kilovolt voltage, followed by post-acceleration to 50 kilovolts. Feasibility was to be demonstrated by using smaller (1/2-inch square) standard emitter chip of the type produced by SRI International for their field emissions research program. This chip was to be tested to the same current density as would be required of the 2-inch chip. A test electron gun employing a standard emitter chip was designed and fabricated based on the results of a computer-derive electron optics model. Of five emitter chips started, two were successful and were delivered for use in the test gun. One chip was lost during assembly of the test gun due to breakdown of the chip, apparently from RF leakage while a welding process was being performed. After modifying the construction procedure, the test gun was successfully assembled. However, during tests this chip failed catastrophically at one percent of the current emission which was required to demonstrate feasibility of the approach. GRA

N88-21044# Hughes Research Labs., Malibu, Calif.
DEVELOPMENT OF Si/SiGe HETEROSTRUCTURES Quarterly Report, Sep. - Dec. 1987
R. J. Hauenstein and O. J. Marsh Jan. 1988 17 p
(Contract F49620-87-C-0104; DARPA Order 6140)
(AD-A189527; HAC-Ref-G3810; AFOSR-88-0093TR) Avail: NTIS HC A03/MF A01 CSCL 20L

With the recent advances in Si molecular beam epitaxy (MBE), a heterojunction-based device technology for Si may soon be at hand. Strained-layer Si(1-x)Ge(x) epitaxial alloy films and coherently strained Si(1-x)Ge(x)/Si multilayer structures have been grown very successfully by MBE. Si(1-x)Ge(x) systems are of considerable interest because they promise to extend the capabilities of heterojunction-based devices to the already well established realm of Si technology. The major impact of heterojunction technology applied to Si electronic devices is expected to be twofold: in the performance improvement of certain conventional Si devices such as the n-p-n bipolar transistor, and in the development within Si technology of novel device structures such as the High Electron-Mobility Transistor (HEMT). GRA

N88-21045# Air Force Inst. of Tech., Wright-Patterson AFB, Ohio. School of Engineering.
OPTICAL STUDY OF GERMANIUM, GERMANIUM PLUS ARSENIC, AND GERMANIUM PLUS GALLIUM IMPLANTS IN GALLIUM ARSENIDE M.S. Thesis
Thomas G. Alley Dec. 1987 108 p
(AD-A189600; AFIT/GEP/ENP/87D-1) Avail: NTIS HC A06/MF A01 CSCL 20L

rsenide For individual titles, see N88-20816 through N88-20815.

The low temperature photoluminescence (PL) properties of single implants of Germanium and dual implants of Ge+Arsenic or Ge+Gallium into semi-insulating Chromium-doped Gallium Arsenide have been analyzed. Room temperature implantation was performed at 120 keV. When dual implantation was used, samples were implanted at the same dose and energy. Ion doses ranged from 1 x 10 to the 13th power to 1 x 10 to the 15th power/cm2. Samples were encapsulated with Silicon Nitride and then annealed at temperatures ranging from 700 to 950 C. Si3N4 was removed prior to PL measurements. A PL peak due to Ge-acceptors was identified. A bound exciton peak related to Ge-donors was also observed. An acceptor peak due to residual Silicon was found in all samples. The heights of the Ge-acceptor peak and exciton peak were compared to the height of the intrinsic Si-acceptor

peak. The height comparison was used in an effort to find trends of Ge-acceptor and Ge-donor transitions as a function of anneal temperature and ion dose. GRA

N88-21046# Oak Ridge National Lab., Tenn.
DISCUSSION OF RADIATION EFFECTS AND HIGH-TEMPERATURE OXIDE SUPERCONDUCTORS
D. K. Christen 1987 11 p Presented at the Division of Materials Sciences Contractors Meeting, Oak Ridge, Tenn., 30 Jul. 1987
(Contract DE-AC05-84OR-21400)
(DE88-001427; CONF-8707125-1) Avail: NTIS HC A03/MF A01

Physical radiation effects on high temperature superconductors La(sub 1.85)Sr(sub 0.15)CuO4 and YBa2Cu3O7 are presented. The importance of, and evidence for 2D superconductivity is also addressed. Most of this document consists of viewgraphs. DOE

N88-21047# Missouri Univ., Columbia. Research Reactor Facility.
PRESSURE-DEPENDENT DLTS (DEEP LEVEL TRANSIENT SPECTROSCOPY) EXPERIMENTS ON Si-DOPED AlGaAs
J. W. Farmer, H. P. Hjalmarson, and G. A. Samara 1987 9 p Presented at the Fall Meeting of the Materials Research Society, Boston, Mass., 30 Nov. 1987 Prepared in cooperation with Sandia National Labs., Albuquerque, N. Mex.
(Contract DE-AC04-76DP-00789)
(DE88-003842; SAND-87-1591C; CONF-871124-27) Avail: NTIS HC A02/MF A01

Pressure dependent Deep Level Transient Spectroscopy (DLTS) experiments are used to measure the properties of the deep donors (DX-centers) responsible for the persistent photoconductivity effect in Si-doped AlGaAs. The sample dependence of the DLTS spectra shows evidence for a defect complex involved in the DX-center. DOE

N88-21048# California Univ., Berkeley. Lawrence Berkeley Lab.
RECENT PROGRESS IN STRUCTURE DETERMINATION BY LEED (LOW-ENERGY ELECTRON DIFFRACTION) MEASURE THE PROPERTIES OF THE DEEP DONORS (DX-CENT)
M. A. VanHove and G. A. Somorjai Oct. 1987 13 p Presented at the 4th International Symposium on Surface Physics, Bechyne, Czechoslovakia, 7 Sep. 1987
(Contract DE-AC03-76SF-00098)
(DE88-003851; LBL-23927; CONF-8709212-1) Avail: NTIS HC A03/MF A01

Surface crystallography with low-energy electron diffraction (LEED) is shown to be developing fast towards solving more complex and diverse kinds of surfaces. This progress is exemplified here with solved structures in three very diverse categories: (1) metal surface reconstructions with multi-layer relaxations; (2) coadsorption of different molecules on metal surfaces; and (3) incommensurate overlayers of graphite on Pt(111). DOE

N88-21049# Missouri Univ., Kansas City.
THEORETICAL STUDIES ON THE ELECTRONIC STRUCTURE AND PROPERTIES OF COMPLEX CERAMIC CRYSTALS AND GLASSES Annual Progress Report, 1 Jul. 1987 - 30 Jun. 1988
Wai-Yim Ching Jan. 1988 17 p
(Contract DE-FG02-84ER-45170)
(DE88-005837; DOE/ER-45170/4) Avail: NTIS HC A03/MF A01

Because of the unexpected discovery of the high T sub c superconductivity in perovskite oxides about a year ago and the subsequent intensified research effort world-wide, our major effort during this period has been in the area of high T sub c superconducting oxides. The major accomplishments covered in this report are: (1) study of electronic structure and optical properties of YBa2Cu3O7 and the formulation of an excitonic-enhancement model for high T sub c superconductivity; (2) study of ground-state properties of alpha-SiO2, beta-Si3N4 and ZrO2 based on accurate self-consistent calculations; (3) comparative study of electronic and magnetic properties of Nd2Fe14B, Nd2Co14B, Y2Fe14B and Y2Co14B crystals; (4) first-principles calculation of electronic structure and transport properties of Mg(x)Zn(1-x) metallic glasses; and (5) calculation of vibrational, infrared and Raman spectra of amorphous SiO2 glass. DOE

N88-21050# Southern Methodist Univ., Dallas, Tex.
THIN-FILM CADMIUM TELLURIDE SOLAR CELLS Annual Subcontract Report, 1 May 1986 - 31 May 1987
T. L. Chu Oct. 1987 36 p
(Contract DE-AC02-83CH-10093)
(DE88-001107; SERI/STR-211-3229) Avail: NTIS HC A03/MF A01

Cadmium telluride, with a room-temperature band-gap energy of 1.5 eV, is a promising thin-film photovoltaic material. The major objective of this research has been to demonstrate thin-film CdTe heterojunction solar cells with a total area greater than 1 sq cm and photovoltaic efficiencies of 13 percent or more. Thin-film p-CdTe/CdS/SnO2:F/glass solar cells with an AM1.5 efficiency of 10.5 percent have been reported previously. This report contains results of work done on: (1) the deposition, resistivity control, and characterization of p-CdTe films by the close-spaced sublimation process; (2) the deposition of large-band-gap window materials; (3) the electrical properties of CdS/CdTe heterojunctions; (4) the formation of stable, reproducible, ohmic contacts (such as p-HgTe) to p-CdTe; and (5) the preparation and evaluation of heterojunction solar cells. DOE

N88-21051# Oregon Univ., Eugene. Dept. of Physics.
INVESTIGATIONS OF THE ORIGINS OF METASTABLE, LIGHT-INDUCED CHANGES IN HYDROGENATED AMORPHOUS SILICON Annual Subcontract Report, 1 Feb. 1986 - 28 Feb. 1987
J. D. Cohen Oct. 1987 32 p
(Contract DE-AC02-83CH-10093)
(DE88-001117; SERI/STR-211-3256) Avail: NTIS HC A03/MF A01

This report presents results of an investigation into the metastable changes in the density of deep mobility gap states in hydrogenated amorphous silicon, using a variety of junction capacitance techniques. This work extends previous studies (using drive-level capacitance profiling) to some new samples. With these measurements, researchers examined how the distribution of occupied gap states changes with light soaking and partial annealing through a series of intermediate states between states A and B. The results on two phosphorus-free samples indicate no qualitative change from previous results, which revealed a large metastable increase in the concentration of D (sup -) centers with light soaking, so phosphorus contamination is not crucial to this increase. Because such an increase is inconsistent with the Si-Si bond-breaking model, this result favors a model in which local configurational changes shift the gap-state energies of existing defects. Transient photocapacitance was applied to undoped films to investigate metastable changes in more detail. Results seemed to confirm the magnitude of the metastable defect creation found by drive-level analysis on the same samples. DOE

N88-21052# Sandia National Labs., Albuquerque, N. Mex.
A HYDROXYCARBONATE ROUTE TO SUPERCONDUCTOR PRECURSOR POWDERS
J. A. Voigt, B. C. Bunker, D. H. Doughty, D. L. Lamppa, and K. M. Kimball 1987 5 p Presented at the Fall Meeting of the Materials Research Society, Boston, Mass., 30 Nov. 1987
(Contract DE-AC04-76DP-00789)
(DE88-003638; SAND-87-2922C; CONF-871124-35) Avail: NTIS HC A02/MF A01

A precipitation process is described for the preparation of powders that can be thermally decomposed to form high critical temperature superconductors such as YBa2Cu3O7. In the process, a cationic solution (a concentrated chloride or nitrate solution) is instantaneously mixed with an anionic solution (a mixture of tetramethylammonium hydroxide and carbonate) to produce a

metal-hydroxycarbonate precipitate having the metal stoichiometry of the desired superconducting oxide. The calcining and sintering of the precipitates is critical in controlling the structural integrity and morphology of the superconducting ceramics made from the chem-prep powders, as well as controlling superconducting properties. Under appropriate conditions, high density (greater than 95 percent) materials that exhibit good superconducting characteristics can be prepared with the chem-prep powders.
DOE

N88-21053# Sandia National Labs., Albuquerque, N. Mex.
ELECTRICAL CHARACTERISTICS OF MBE (MOLECULAR BEAM EPITAXYL)-GROWN GaAs/SUB 1-x/Sb/SUB x ON InP AND CORRELATION WITH FILM MICROSTRUCTURE
J. Klem, J. I. Chyi, H. Morkoc, Y. E. Ihm, and N. Otsuka 1988 6 p Presented at the Innovative Science and Technology Symposium, Los Angeles, Calif., 13 Jan. 1988 Prepared in cooperation with Illinois Univ., Urbana and Purdue Univ., West Lafayette, Ind.
(Contract DE-AC04-76DP-00789)
(DE88-003841; SAND-87-2590C; CONF-880141-1) Avail: NTIS HC A02

GaAs(0.5)Sb(0.5) grown on InP by molecular beam epitaxy (MBE) has been characterized by transmission electron microscopy and variable temperature Hall measurements. Unintentionally doped layers are p-type with measured hole concentrations of 1 to 3 x 10 to the 16th/cu cm at 300 K. The behavior of the Hall coefficient as a function of temperature is found to be well-described in the temperature range 30 K is less than T is less than 300 K by a two-acceptor model. Intentional Si doping of the GaAs(0.5)Sb(0.5) layers leads to relatively uncompensated p-type conductivity. Hole mobilities in these layers are generally less than 100 sq cm/Vs at 300 K as a result of compositional fluctuations which result from the metastable nature of these films. In addition, hole mobilities are anisotropic and reflect an unusual asymmetry in the film microstructure which can be observed by transmission electron microscopy.
DOE

N88-21054# Oak Ridge National Lab., Tenn.
PHOTON-CONTROLLED GROWTH OF MULTILAYERED STRUCTURES
D. H. Lowndes, D. B. Geohegan, D. Eres, D. N. Mashburn, and S. J. Pennycook 1987 7 p Presented at the Symposium on Multilayers: Synthesis, Properties and Nonelectronic Applications, Boston, Mass., 30 Nov. 1987
(Contract DE-AC05-84OR-21400)
(DE88-005061; CONF-8711143-1) Avail: NTIS HC A02/MF A01

Pulsed ArF excimer laser (193 nm) photolysis has been used to deposit entirely amorphous and mixed amorphous/polycrystalline superlattice structures containing Si, Ge and Si3N4. High-resolution in-situ optical reflectivity measurements were used to monitor and/or control deposition. Transmission electron microscope cross-section views demonstrate that amorphous superlattice structures having highly reproducible layer thicknesses (from 70 to several hundred A), and sharp interlayer boundaries, can be deposited at low substrate temperatures under laser photolytic control.
DOE

N88-21055# Oak Ridge National Lab., Tenn.
X-RAY DIFFRACTION STUDY OF A THIN GaAs FILM ON Si(100)
A. S. Bommannavar, C. J. Sparks, A. Habenschuss, G. E. Ice, A. Dhere, H. Morkoc, and H. Zabel 1987 6 p Presented at the Fall Meeting of the Materials Research Society, Boston, Mass., 30 Nov. 1987 Prepared in cooperation with Illinois Univ., Urbana
(Contract DE-AC05-84OR-21400)
(DE88-005290; CONF-871124-62) Avail: NTIS HC A02/MF A01

A 900 A single crystalline GaAs film deposited by molecular beam epitaxy (MBE) on a silicon crystal cut 4.1 deg from (001) surface was characterized with X-ray diffraction measurements of the mosaic spread, particle size and strain distribution, and lattice parameter. The GaAs film had a larger mosaic spread in the direction of the steps of the silicon surface and coherent particle sizes of about 900 A compared to the estimated film thickness of approximately 1000 A. Superlattice reflections gave an ordered domain size of about 330 A. There is a residual strain gradient in the film which is nearly linear with the lattice constant differing by about 0.044 A between the surface of the film and its interface with the silicon substrate. Lattice parameter measurements indicate a small expansion of 0.13 percent perpendicular to the plane of the film.
DOE

N88-21056# Los Alamos National Lab., N. Mex.
A SYMMETRIC SET OF EULER ANGLES AND OBLIQUE ORIENTATION SPACE SECTIONS
U. F. Kocks 1987 7 p Presented at the 8th International Conference on Textures of Materials, Santa Fe, N. Mex., 21 Sep. 1987
(Contract W-7405-eng-36)
(DE88-005317; LA-UR-88-5; CONF-8709172-4) Avail: NTIS HC A02/MF A01

A slight variation of conventional definitions is proposed which treats the relation between crystal and sample systems as symmetrical and simplifies the procedure of plotting or identifying individual orientations. The specific convention proposed uses the Roe angles psi and theta, but replaces Roe's PHI by phi identical to pi- PHI. For plotting the oblique sections proposed at this conference to avoid the remaining distortions near theta = 0, one may define nu identical (psi + phi)/2; the aximuthal angle in the sections may then be either = identical (psi - phi)/2 for maximum symmetry, or psi for obtaining partial pole figures, or phi for partial inverse pole figures. Any of the sections follow from any other by a simple turning of the figure, by an amount that depends on the section parameter.
DOE

N88-21057# Arizona Univ., Tucson.
COMPETING INTERACTIONS IN METALLIC SUPERLATTICES
C. M. Falco, J. L. Makous, J. A. Bell, W. R. Bennett, R. Zanoni, G. I. Stegeman, and C. T. Seaton 1987 7 p Presented at the Workshop on Competing Interactions and Microstructures: Statics and Dynamics, Los Alamos, N. Mex., 5 May 1987
(Contract DE-FG02-87ER-45297)
(DE88-005344; DOE/ER-45297/4; CONF-8705168-7) Avail: NTIS HC A02/MF A01

Metallic superlattices provide an excellent system to study in a controlled manner a variety of physical phenomena, including superconductivity, magnetism, and electrical transport properties. As will be discussed in this paper, changes in certain of these properties as a function of superlattice modulation wavelength lambda hyperon are found to be correlated with structural changes and elastic property anomalies. The properties of two particular metallic superlattices, Cu/Nb and Mo/Ta, are discussed in this paper as examples of how competing interactions manifest themselves in the physical properties of these superlattices.
DOE

N88-21058# Arizona Univ., Tucson.
SUPERCONDUCTING SUPERLATTICE STRUCTURES
J. L. Makous, J. A. Leavitt, L. C. McIntyre, Jr., L. Maritato, R. Vaglio, A. Cucolo, and C. M. Falco 1987 7 p Presented at the Fall Meeting of the Materials Research Society, Boston, Mass., 30 Nov. 1987 Prepared in cooperation with Istituto Nazionale di Fisica Nucleare, Frascati (Italy), and Salerno Univ.
(Contract DE-FG02-87ER-45297)
(DE88-005346; DOE/ER-45297/7; CONF-871124-64) Avail: NTIS HC A02/MF A01

Superlattice superconductors exhibit behavior different from other homogeneous superconductors because of their layered structures. Sputtering has proved to be an excellent technique for producing such multilayered systems. Also, systems naturally having layered structures, such as the new high-Tc materials, can be fabricated by sputtering. Here we describe the preparation of superconducting superlattices by dc triode sputtering and techniques useful for characterizing them. In particular, we discuss

Mo/Ta superconducting superlattices and high-Tc thin films of YBa2Cu3O(sub 7-x). DOE

N88-21059# Lawrence Livermore National Lab., Calif.
INITIAL STAGES OF SILICON GROWTH ON THE (100) SURFACE OF SILICON BY LOCALIZED LASER CVD
D. E. Kotecki and I. P. Herman 18 Dec. 1987 8 p Presented at the Laser and Particle-beam Chemical Processing for Microelectronics, Boston, Mass., 30 Nov. 1987 Prepared in cooperation with Columbia Univ., New York, N.Y.
(Contract W-7405-eng-48)
(DE88-005420; UCRL-97894; CONF-8711147-1) Avail: NTIS HC A02/MF A01

This paper reports initial results of an experimental study of the early stages of silicon thin film growth on well prepared (100) c-Si surfaces by pyrolytic deposition from silane (SiH4) during localized laser chemical vapor deposition (LLCVD). The rate of silicon thin film growth during low pressure (less than 10 Torr) deposition using tightly focussed laser beams (514.5 nm, approximately 2.5 micron FWHM) is characterized and is shown to be much slower than expected based on the previously measured silane decomposition rate. Hybrid-heating experiments, in which laser heating induces a slight temperature increase on a uniformly heated substrate in the presence of silane gas, shows that growth is inhibited within the laser irradiation region. This result suggests that a nonpyrolytic mechanism contributes to silicon growth in laser CVD. Possible explanations for this nonpyrolytic growth mechanism are discussed. DOE

N88-21060# Lawrence Livermore National Lab., Calif.
EXPLORING THE RELATION BETWEEN INTERFACE STRUCTURE AND MECHANICAL PROPERTIES IN MULTILAYER STRUCTURES
A. F. Jankowski, D. M. Makowiecki, M. A. McKernan, and S. R. Nutt Nov. 1987 8 p Presented at the Fall Meeting of the Materials Research Society, Boston, Mass., 30 Nov. 1987 Prepared in cooperation with Brown Univ., Providence, R.I.
(Contract W-7405-eng-48)
(DE88-005428; UCRL-97761; CONF-871124-63) Avail: NTIS HC A02

The relationship between microstructure and physical behavior is especially pronounced in synthetic multilayer materials. Insight to the mechanisms responsible for changes in the mechanical properties can be investigated through an examination of the inherent microstructure. A dominant feature of the multilayer structure is the interface. The population of interlayer boundaries, that is interfaces, is directly controlled by the multilayer period for any given film thickness. In this paper, we will present TEM images of multilayer systems. The interface structure will be viewed in cross-section. A range of layer thicknesses should be considered as variations in the elastic modules, yield stress, and microhardness. These have been observed for many noble-transition metal systems over a wide range of multilayer periods, from less than 1 nm to greater than 1000 nm. In epitaxial systems, the extent of superlattice perfection (coherency effects) is closely tied with changes in physical behavior. In summation, emphasis will be placed on the structure and strain distribution from the interface, and its role in determining the mechanical properties of multilayers. DOE

N88-21061# Lawrence Livermore National Lab., Calif.
LATTICE RELAXATION OF THE DX CENTERS IN Ga/SUB 1-x/Al/SUB x/As AND OF THE PRESSURE-INDUCED DEEP DONORS IN GaAs
M. F. Li, W. Shan, P. Y. Yu, W. L. Hansen, E. R. Weber, and E. Bauser Nov. 1987 7 p Presented at the Fall Meeting of the Materials Research Society, Boston, Mass., 30 Nov. 1987 Prepared in cooperation with Max-Planck-Institut fuer Festkoerperforschung, Stuttgart (Federal Republic of Germany)
(Contract DE-AC03-76SF-00098)
(DE88-005452; LBL-24523; CONF-871124-66) Avail: NTIS HC A02/MF A01

Deep Level Transient Spectroscopies (DLTS) and capacitance transient techniques have been applied to GaAs:Si and to Ga(sub 1-x)Al(sub x) s:Te (x = 0.35) under quasi-hydrostatic pressure using a diamond anvil cell. By substituting the experimental pressure coefficients of the defect energies into a model proposed by Li and Yu (Solid State Commun. 61, 13 (1987)) it is concluded that both the DX center in the GaAlAs alloy and the pressure-induced deep donor (PIDD) in GaAs have large lattice relaxations associated with them. DOE

N88-21062# Sandia National Labs., Albuquerque, N. Mex.
ENERGY LOSS RATES FOR LIGHT HOLES IN InGaAs/GaAs STRAINED LAYER SINGLE QUANTUM WELLS
M. C. Smith, E. D. Jones, I. J. Fritz, T. J. Drummond, T. E. Zipperian, and J. E. Schirber 1987 6 p Presented at the Fall Meeting of the Materials Research Society, Boston, Mass., 30 Nov. 1987
(Contract DE-AC04-76DP-00789)
(DE88-005744; SAND-87-1592C; CONF-871124-72) Avail: NTIS HC A02/MF A01

Energy relaxation rates for light holes in InGaAs/GaAs strained layer quantum wells are measured. Two techniques were used to measure light hole temperatures as a function of power dissipated in the hole gas. For T(sub h) less than 20K, Shubnikov-de Haas oscillations were used and for T(sub h) greater than 20K, a photoluminescence technique was employed. DOE

N88-21063 California Univ., Berkeley.
MOSFET PERFORMANCE DEGRADATION DUE TO HOT CARRIERS Ph.D. Thesis
Jeong Yeol Choi [1987] 82 p
Avail: Univ. Microfilms Order No. DA8726170

Hot-carrier-induced degradation of short-channel MOSFETs is investigated. It is shown that both charge trapping and interface-state generation take place. The relative importance of these two mechanisms depends on the bias condition and the electron trap density in the oxide. The device degradation was studied using a constant field method. The effects of gate and drain voltage waveforms on the hot-carrier-induced MOSFET degradation are studied. Guidelines for the lifetime prediction of hot-carrier-induced MOSFET degradation are presented. An empirical model is found. The lifetime versus substrate current plot is a convenient tool. Several potential pitfalls are pointed out by considereing the effects of oxide thickness, oxide field, and device structures. Dissert. Abstr.

N88-21064# North Carolina State Univ., Raleigh. Dept. of Nuclear Engineering.
A NOVEL METHOD FOR SPUTTER-DEPOSITION OF HIGH T(SUB c) SUPERCONDUCTOR FILMS VIA A COMPUTER-CONTROLLED MASS ANALYZED TON BEAM
O. Auciello and A. R. Krauss 1987 9 p Presented at the 34th National Vacuum Symposium and Topical Conference, Anaheim, Calif., 2 Nov. 1987 Prepared in cooperation with Argonne National Lab., Ill.
(Contract W-31-109-eng-38)
(DE88-006001; CONF-871125-21) Avail: NTIS HC A02/MF A01

A novel concept is demonstrated for ion beam sputter-induced deposition of high T(sub c) superconductor films, involving the use of a well-focused ion beam which can be sequentially directed via a set of x-y electrostatic deflection plates onto three or more different elemental or compound targets which are constituents of the desired composite film. The deflection plates are driven by two + or - 1000 volt bipolar programmable power supplies controllable by a DEC LSI 11/73 computer. A custom program drives two D/A converters to provide the + or - 10 volt analog signal used to drive the power supplies in such a way that the ion beam is positioned on selected spots on the different targets. By programming the dwell time for each target according to the known sputtering yield and desired layer thickness for each material, it is possible to deposit composite films from a

well-controlled sub-monolayer up to thicknesses determined only by available deposition time. Initial results on the deposition of Y-Ba-CuO films are presented to demonstrate the concept, which in principle can be applied to the deposition of high T(sub c) superconducting films by electron- and laser induced evaportation of elemental ot oxide targets. DOE

77 THERMODYNAMICS AND STATISTICAL PHYSICS

Includes quantum mechanics; theoretical physics; and Bose and Fermi statistics.

For related information see also *25 Inorganic and Physical Chemistry* and *34 Fluid Mechanics and Heat Transfer.*

N88-21065# IIT Research Inst., Bartlesville, Okla. National Inst. for Petroleum and Energy Research.

THE THERMODYNAMIC PROPERTIES OF ORGANIC OXYGEN COMPOUNDS

R. D. Chirico, W. V. Steele, A. Hossenlopp, A. Nguyen, D. G. Archer, and M. M. Strube Jan. 1988 24 p

(Contract DE-FC22-83FE-60149)

(DE88-001208; NIPER-271) Avail: NTIS HC A03/MF A01

The principles of group additivity are used to compare a series of cyclic hydrocarbons with the corresponding oxygen-containing analogs. The strengths and limitations of the group-additivity method are demonstrated and recommendations are made for measurements essential to the improvement of the accuracy of the predicted properties. The ideal-gas enthalpies of formation and ideal-gas entropies (which are used in combination to calculate Gibbs energies) are considered. DOE

N88-21066# Sandia National Labs., Albuquerque, N. Mex.

RAPID e-BEAM HEATING FOR MEASURING THERMODYNAMICS OF METASTABLE MATERIALS

J. A. Knapp and D. M. Follstaedt 1987 12 p Presented at the Fall Meeting of the Materials Research Society, Boston, Mass., 30 Nov. 1987

(Contract DE-AC04-76DP-00789)

(DE88-003565; SAND-87-1577C; CONF-871124-47) Avail: NTIS HC A03/MF A01

A line-source electron-beam system has been used to heat thin surface layers of metastable phases at a rate which precludes solid-state transformation to stable phases, thus permitting the observation of melting transitions normally missed with slow heating. A detailed example of a new approach to this method is shown for metastable icosahedral Al-Re and crystalline Al6Re. DOE

N88-21067# Brown Univ., Providence, R. I. Div. of Engineering.

TWO STUDIES OF NONLINEAR PROCESSES IN IRREVERSIBLE THERMODYNAMICS Annual Performance Report, 1 May 1987 - 30 Apr. 1988

J. Kestin Jan. 1988 6 p

(Contract DE-FG02-87ER-13687)

(DE88-005794; DOE/ER-13687/1) Avail: NTIS HC A02/MF A01

This paper discusses two nonlinear irreversible processes: Inelastic deformation and two-phase flow. DOE

N88-21068# Battelle Pacific Northwest Labs., Richland, Wash.

REVIEW OF SELENIUM THERMODYNAMIC DATA Final Report

C. E. Cowan Feb. 1988 73 p

(Contract DE-AC06-76RL-01830; EPRI Proj. 2020-3)

(DE88-006194; EPRI-EA-5655) Avail: NTIS HC A04/MF A01

This report assesses the accuracy and completeness of available thermodynamic data on selenium. A review of experimental methods from published literature on selenium thermodynamic data focused on chemical reactions responsible for the formation of both aqueous complexes and solid phases of selenate, selenite, and selenide. The reviewer selected best data values, based on the methods used for estimating thermodynamic data. After inclusion of these values into the MINTEQ model, a validation study evaluated model performance for selenite and selenide solid phases. Lack of selenate data precluded model validation for this compound. The review furnished data on 22 aqueous complexes of selenite, 15 of selenide, and 17 of selenate, as well as 21 solid phases of selenite, 20 of selenide and 8 of selenate. These data proved inadequate to represent the formation of species in the solid phase. The validation study gave inconclusive predictions of selenite and selenide solubility and could not be used to assess the accuracy or completeness of the thermodynamic data. DOE

N88-21069# California Univ., Berkeley. Lawrence Berkeley Lab.

PREDICTION OF HIGH-TEMPERATURE THERMODYNAMIC PROPERTIES OF MIXED ELECTROLYTE SOLUTIONS INCLUDING SOLUBILITY EQUILIBRIA, VAPOR PRESSURE DEPRESSION AND BOILING POINT ELEVATION

R. T. Pabalan and K. S. Pitzer Jan. 1988 18 p Presented at the Temperature Aqueous Solutions, Provo, Utah, 25 Aug. 1987

(Contract DE-AC03-76SF-00098)

(DE88-006344; LBL-24627; CONF-8708178-2) Avail: NTIS HC A03/MF A01

The Pitzer ion-interaction model, which is theoretically derived but uses empirical parameters evaluated from experimental data on binary and ternary aqueous mixtures, is shown to accurately predict thermodynamic properties of aqueous electrolytes to high temperatures and concentrations and for more complex compositions. Applications of the model include calculations of solubility equilibria, vapor pressures and boiling points of electrolyte mixtures. Examples of these calculations are given. DOE

N88-21070# Center for Mathematics and Computer Science, Amsterdam (Netherlands). Dept. of Pure Mathematics.

STRING THEORY AND ALGEBRAIC GEOMETRY OF MODULI SPACES

Dirk-Jan Smit Jul. 1987 38 p Sponsored by Stichting voor Fundamenteel Onderzoek der Materie

(CWI-PM-R8705; B8723960; ETN-88-91747) Copyright Avail: NTIS HC A03/MF A01

It is shown how the algebraic geometry of the moduli space of Riemann surfaces entirely determines the partition function of Polyakov's string theory. This is done by using elements of Arakelov's intersection theory applied to determinants of families of differential operators parameterized by moduli space. As a result the partition function is written in terms of exponentials of Arakelov's Green functions and Faltings' invariant on Riemann surfaces. Generalizing to arithmetic surfaces, i.e., surfaces which are associated to an algebraic number field K, a connection between string theory and the infinite primes of K is established. It is conjectured that the usual partition function is a special case of a partition function on the moduli space defined over K. ESA

N88-21071# Gosudarstvennyi Komitet po Ispolzovaniyu Atomnoi Energii, Moscow (USSR). Inst. Atomnoj Ehnergii.

CHRONOMETRICALLY INVARIANT FORMULATION OF ELECTRODYNAMICS EQUATION

B. Ya. Lyubimov and L. V. Matveev 1986 17 p In RUSSIAN

(TI88-701030; IAE-4347/1) Avail: NTIS (US Sales Only) HC A03/MF A01

Chronometrically invariant combinations of components for 4-tensor electrodynamic objects corresponding to the observed three-dimensional values are constructed. The Maxwell equations and material relations are described by means of chronoinvariant differential operations. In general, the equation for fields contain acceleration and the angular velocity of a frame of reference. DOE

N88-21072# Gosudarstvennyj Komitet po Ispolzovaniyu Atomnoi Energii, Serpukhov (USSR). Inst. Fiziki Vysokikh Ehnergij.

INTRODUCTION TO CLASSICAL MECHANICS OF SYSTEMS WITH CONSTRAINTS, PART 2

A. V. Razumov and L. D. Solovev 1986 28 p In RUSSIAN;

ENGLISH summary
(TI88-701056; IFVE-OTF-86-213-Pt-2) Avail: NTIS (US Sales Only) HC A03/MF A01

Lagrangians whose symmetry transformations include arbitrary functions on time are shown to be, with necessity, degenerate. The Hamiltonian formalism for mechanical systems with degenerate Lagrangians is presented. The algorithm of producing the constraints and the total Hamiltonian is described. The reduction of a Hamiltonian mechanical system to a surface in the extended phase space and application of Dirac brackets to calculate poisson brackets of the reduced system are considered. DOE

N88-21073# Gosudarstvennyj Komitet po Ispolzovaniyu Atomnoi Energii, Serpukhov (USSR). Inst. Fiziki Vysokikh Ehnergij.
INTRODUCTION TO CLASSICAL MECHANICS OF SYSTEMS WITH CONSTRAINTS, PART 3
A. V. Razumov and L. D. Solovev 1986 36 p In RUSSIAN; ENGLISH summary
(TI88-701057; IFVE-OTF-86-214-Pt-3) Avail: NTIS (US Sales Only) HC A03/MF A01

For systems with second class constraints the reduced phase space is constructed. It is shown that physically equivalent points of the phase space for systems with first class constraints are connected by canonical transformations generated by linear combinations of the first class constraints. For every system with first class constraints a physically equivalent system with second class constraints is constructed. As an illustrative application of the theory the relativistic straightline string is considered. DOE

80 SOCIAL SCIENCES (GENERAL)

Includes educational matters.

No abstracts in this category.

81 ADMINISTRATION AND MANAGEMENT

Includes management planning and research.

N88-21074*# Boeing Aerospace Co., Seattle, Wash.
APPLICATION OF EXPERT SYSTEMS IN PROJECT MANAGEMENT DECISION AIDING Final Technical Report No. 2092
Regina Harris, Steven Shaffer, James Stokes, and David Goldstein Aug. 1987 122 p
(Contract NAS5-30040)
(NASA-CR-180762; NAS 1.26:180762) Avail: NTIS HC A06/MF A01 CSCL 05A

The feasibility of developing an expert systems-based project management decision aid to enhance the performance of NASA project managers was assessed. The research effort included extensive literature reviews in the areas of project management, project management decision aiding, expert systems technology, and human-computer interface engineering. Literature reviews were augmented by focused interviews with NASA managers. Time estimation for project scheduling was identified as the target activity for decision augmentation, and a design was developed for an Integrated NASA System for Intelligent Time Estimation (INSITE). The proposed INSITE design was judged feasible with a low level of risk. A partial proof-of-concept experiment was performed and was successful. Specific conclusions drawn from the research and analyses are included. The INSITE concept is potentially applicable in any management sphere, commercial or government, where time estimation is required for project scheduling. As project scheduling is a nearly universal management activity, the range of possibilities is considerable. The INSITE concept also holds potential for enhancing other management tasks, especially in areas such as cost estimation, where estimation-by-analogy is already a proven method. Author

N88-21075# Allen Corp. of America, Alexandria, Va.
MANPRINT HANDBOOK FOR RFP (REQUEST FOR PROPOSAL) DEVELOPMENT Final Report, 30 Jun. 1986 - 15 Sep. 1987
Jacob L. Barber, Robert E. Jones, Jr., Harry L. Ching, and John L. Miles, Jr. (Army Research Inst. for the Behavioral and Social Sciences, Alexandria, Va.) 15 Sep. 1987 156 p
(Contract OPM-85-75)
(AD-A188321) Avail: NTIS HC A08/MF A01 CSCL 05A

This handbook is designed to assist personnel tasked with preparing a Request for Proposal (RFP) for any phase of a major system development program. It specifically focuses on how to include Manpower and Personnel Integration (MANPRINT) requirements in the RFP. The Handbook is organized into four chapters and an appendix section. Chapter 1, discusses the six domains that comprise MANPRINT and explains how the domains and their integrated products relate to the materiel acquisition process. Chapter 2, examines each of the six domains separately and identifies both documents and agencies that can provide assistance in RFP preparation. Chapter 3, identifies preceding events and activities that shape the structure and content of the MANPRINT requirements in the RFP. It describes the linkages that should exist and what can be done in the event critical MANPRINT elements are non-existent. Illustrative paragraphs as they should appear in the RFP are provided. Chapter 4, is a summation of activities described in Chapter 3. An RFP for a major notional Army weapon system with significant MANPRINT implications is presented. GRA

N88-21076*# National Aeronautics and Space Administration. Lyndon B. Johnson Space Center, Houston, Tex.
JOHNSON SPACE CENTER'S STRATEGIC GAME PLAN: CHARTING A COURSE TO THE YEAR 2000 AND BEYOND
Oct. 1987 45 p
(NASA-TM-89733; NAS 1.15:89733) Avail: NTIS HC A03/MF A01 CSCL 05A

The Johnson Space Center has established five major goals to meet the Nation's expectation of maintaining U.S. preeminence in space. The first three are technical in nature. They define the basic mission-the reason for being. The two goals relating to the Space Shuttle and Space Station are obviously the most demanding in their immediate claim for major resources. The third goal is equally important in that the technical competence must be maintained and enhanced. The remaining two goals address the two critical success factors required for achieving the first three. One goal pertains to maintaining and enhancing the highly skilled work force. The other goal concerns the important relations with other key members of the U.S. space team. Each goal is listed along with a proposed strategy or approach for implementing each goal. Subsequently, each goal is accompanied by a brief explanation and a set of objectives. These objectives provide the specific targets of opportunity for focusing the immediate efforts. B.G.

N88-21077# Office National d'Etudes et de Recherches Aerospatiales, Paris (France).
[ACTIVITIES REPORT OF THE TOULOUSE RESEARCH CENTER] Annual Report, 1986
Sep. 1987 21 p Original contains color illustrations
(ETN-88-91988) Avail: NTIS HC A03/MF A01

The OASYS tool for analysis of production systems by simulation; processing of the A320 fluttering tests by telemetering; aerothermodynamics 3D flows and transonic flows; and activities in the framework of the supercomputer project are described. Analysis of the dynamic behavior of a fuel injector subjected to acoustic interference; measurement apparatus for surface effect ships; intensimetry applied to underwater acoustics; millimetric radiometers, a velocity sensor for spectral imaging system by Fourier transform; an automatic granulometric sensor; and a simultaneous irradiation device are presented. ESA

82 DOCUMENTATION AND INFORMATION SCIENCE

Includes information management; information storage and retrieval technology; technical writing; graphic arts; and micrography.

For computer documentation see *61 Computer Programming and Software.*

N88-21078# Office of the Under Secretary of Defense (Acquisitions), Washington, D.C.
REPORT OF THE DEFENSE SCIENCE BOARD SUMMER STUDY ON TECHNOLOGY BASE MANAGEMENT
Aug. 1987 60 p
(AD-A188560) Avail: NTIS HC A04/MF A01 CSCL 05B

The 1987 Defense Science Board (DSB) Summer Study on Technology Base Management was charged with evaluating the management of the technology base of Department of Defense (DOD) and making recommendations on ways to improve the effectiveness and efficiency of the management process. The thrust of this study was to develop management principles that could guide the Technology Base rather than to develop a more detailed set of recommendations. The conclusions of the panel are derived from a qualitative evaluation of the present system coupled with an understanding of how well (or poorly) recommendations of past studies have been implemented. It was evident that implementation of any recommendations will face substantial institutional resistance and political difficulties. Accordingly the Study has, in some cases, adopted the mechanism of proposing a series of experiments or demonstrations of major change which point in the right direction. It is important to understand that the leadership and vision of motivated individuals and groups are a critical part of technical management. The study has been as concerned with this aspect of Technology Base management as with more institutional or bureaucratic processes. GRA

N88-21079# Oak Ridge National Lab., Tenn.
A MENU-DRIVEN KNOWLEDGE RETRIEVAL SYSTEM ACCESSING ASCII DATA
N. E. Clapp, Jr., A. W. Renshaw, and C. E. Snyder Aug. 1987 13 p Presented at the Conference on User-oriented Content-based Text and Image Handling, Cambridge, Mass., 21 Mar. 1988
(Contract DE-AC05-84OR-21400)
(DE88-001742; CONF-880327-1) Avail: NTIS HC A03/MF A01

The knowledge retrieval system reported here consists of two elements: a utility program and a data set containing the knowledge base. The utility program provides the capability of retrieving and displaying information using layered menus. The layered menu system is similar to a logical tree structure, with each menu being a major node of the tree. The system is designed to be data driven, which allows it to be maintained, refined, and expanded by modifying the data set. DOE

N88-21080# National Bureau of Standards, Gaithersburg, Md.
REFERENCE MODEL FOR DBMS (DATABASE MANAGEMENT SYSTEM) USER FACILITY
E. N. Fong, J. Gersting, and K. Kinsley Jan. 1988 39 p
(PB88-169446; NBSIR-88/3709) Avail: NTIS HC A03/MF A01 CSCL 05B

A reference model is presented for the user facility portion of a database management system. The User Facility Reference Model offers a separation between the Data Management Tools and the User. The User Data Language and the Internal User Data Language are candidates for standardization. Since the Data Management tool layer is continually evolving and current technology often embeds a user interface in each tool, the process of standardization must be staged. The work here indicates that the User Data Language can provide a focus for the start of the process. The report also provides a theoretical basis from which a User Data Language could be developed. GRA

N88-21081# Office of Naval Research Liason Office, Far East, APO, San Francisco, Calif.
ONR FAR EAST SCIENTIFIC BULLETIN, VOLUME 12, NUMBER 3, JULY-SEPTEMBER 1987
George B. Wright and Sandy Kawano Sep. 1987 122 p
(AD-A188554) Avail: NTIS HC A06/MF A01 CSCL 05B

This quarterly publication presents articles covering recent developments in Far Eastern (particularly Japanese) scientific research. Partial contents: Perpendicular magnetic recording by anodic oxidation; The Marine Science Division of the Center for Earth Science Studies (Trivandrum, India); Status of fracture mechanics methodology for ceramic materials; Ship and hydraulic research and development institutions in the People's Republic of China; Advanced telerobotic systems under development in Japan; Marine science in Bombay; Permanent magnets in Japan and the 1987 Tokoyo INTERMAG Conference; Materials engineering research in Taiwan; Phase, electron holography, and a conclusive demonstration of the Aharonov-Bohm effect; and International meetings in the Far East, 1987 to 1994. GRA

N88-21082# Deutsche Forschungs- und Versuchsanstalt fuer Luft- und Raumfahrt, Cologne (West Germany).
THE GERMAN PROCESSING AND ARCHIVING FACILITY FOR ERS-1 Final Report
W. Bosch, comp. (Deutsches Geodaetisches Forschungsinst., Munich, West Germany), J. Gredel, comp., W. Noack, comp., C. Reigber, comp., G. Schreier, comp., and H. Schroeter, comp. Paris, France ESA May 1987 252 p
(Contract ESA-6292/85-HGE-I(SC))
(ESA-CR(P)-2531; ETN-88-91967) Avail: NTIS HC A12/MF A01

A center for processing and archiving ERS-1 SAR, radar altimeter (RA) and precise range and range rate equipment (PRARE) laser tracking data is described. The hardware architecture, which forms a distributed processing system, includes a high performance, vendor-independent local area network; workstations for all interactive tasks such as image processing; high speed array processors for signal processing; large solid-state memories as data buffers for near real-time processing; optical disk storage technology for archival and distribution of data; and use of large scale computers (IBM) and vector processors (CRAY-1/S). The software technology used enables developments which are to a large degree hardware-independent. This includes: extensive use of the UNIX operating system; Ada as programming language for new software developments; use of LISP-based knowledge engineering software on UNIX workstations for operations support; and use of commercial database management software for all data management aspects. Algorithmic features include use of the range/Doppler algorithm for the generation of radiometrically accurate digital SAR images; use of digital elevation models for the precise geometric registration of SAR images over land and their presentation in map projections; application enhanced software for the generation of highly precise ERS-1 orbits, making use of PRARE and laser tracking data and derivation of an ERS-1 dedicated Earth gravity field; and with the precision orbit as prerequisite, accurate geophysical ocean products derivation from the RA data. ESA

83 ECONOMICS AND COST ANALYSIS

Includes cost effectiveness studies.

N88-21083# Stanford Univ., Calif. Systems Optimization Lab.
ON THE ROLE OF COMPLETE REDUCIBILITY IN GENERAL COMPETITIVE EQUILIBRIUM MODELS
K. T. Krenzin Jan. 1988 35 p
(Contract DE-FG03-87ER-25028)
(DE88-005693; SU-SOL-88-1) Avail: NTIS HC A03/MF A01

In this report a class of economic models is defined which properly includes most of the popular forms used in general equilibrium modelling. For these models, conditions are derived which are sufficient to insure the existence of an equilibrium in

positive prices, fulfilling the natural expectation that a model is defined over economically relevant entities. The conditions are somewhat weaker than those historically imposed, and represent, for the most part, a combinatorial restriction of the data describing the model. As such, the large part of the conditions can be tested by a strongly polynomial algorithm presented herein. Moreover, there are derived necessary conditions which are apparently only slight relaxations of those sufficient conditions. DOE

84 LAW, POLITICAL SCIENCE AND SPACE POLICY

Includes NASA appropriation hearings; aviation law; space law and policy; international law; international cooperation; and patent policy.

No abstracts in this category.

85 URBAN TECHNOLOGY AND TRANSPORTATION

Includes applications of space technology to urban problems; technology transfer; technology assessment; and surface and mass transportation.

For related information see also *03 Air Transportation and Safety, 16 Space Transportation,* and *44 Energy Production and Conversion.*

N88-21084# Department of Energy, Washington, D. C.
TECHNOLOGY '87: RESEARCH AND DEVELOPMENT LABORATORY TECHNOLOGY TRANSFER PROGRAM Annual Report
Jan. 1988 113 p
(DE88-003142; DOE/ER-0355) Avail: NTIS HC A06/MF A01

An overview of technology transfer of U.S. Department of Energy's National Laboratories is presented. Areas specifically presented are: Materials Science and Manufacturing; Analysis and Instrumentation; Energy Technology; Environment and Waste Management; Biology and Medicine; and Computers and Communication. Specific research accomplishments are discussed. DOE

N88-21085# Edgerton, Germeshausen and Grier, Inc., Idaho Falls, Idaho.
SPIN OFF BUSINESSES AS MECHANISMS FOR TRANSFERRING TECHNOLOGIES
J. M. Welch 1987 7 p Presented at the FLC Semi Annual Meeting: Headed for the Future, Sacramento, Calif., 3 Nov. 1987
(Contract DE-AC07-76ID-01570)
(DE88-005640; EGG-M-39887; CONF-8711153-1) Avail: NTIS HC A02/MF A01

Federal Laboratories, especially those in rural settings, have the opportunity to participate in local economic development through spin off businesses based on laboratory technologies. Quite often, it is a laboratory employee who is one of the principals in the spin off business. Transferring technology to an employee can add a degree of complexity that is not normally faced in a transfer to an external requestor. Procedures followed at the Idaho National Engineering Laboratory by one of the prime contractors there, EG and G Idaho Inc., are discussed in this article. DOE

N88-21086# Kentucky Univ., Lexington. Dept. of Metallurgical Engineering and Materials Science.
APPLICABILITY OF AEROSPACE THERMAL INSULATION TECHNOLOGIES TO THE CIVILIAN SECTOR Final Report
H. A. Fine Oct. 1987 93 p
(Contract DE-AC05-84OR-21400)
(DE88-003717; ORNL/Sub-86-55951/1) Avail: NTIS HC A05/MF A01

The thermal insulation-related technology developed and documented in past research and development programs in aerospace and other federally-funded programs and the international community, was identified and located using the NASA/RECON system and through personal contacts to facilitate technology transfer. In addition, the literature was reviewed to identify specific concepts that seemed to have the potential for substantial energy conservation and which fit into the ECUT mission. These concepts were separated into the following categories: fibrous insulation materials, evacuated microsphere insulation, multi-layer insulation, other insulation concepts, coatings, transport models, measurement technology, and patent literature. Citations to the pertinent literature and suggestions for future research are presented. DOE

N88-21087# Executive Office of the President, Washington D.C.
AERONAUTICS AND SPACE REPORT OF THE PRESIDENT: 1986 ACTIVITIES
[1986] 141 p
Avail: NTIS HC A07/MF A01

The achievements of aeronautics and space programs in the United States for 1986 are summarized in the areas of communications: Earth atmosphere, environment, and resources; space science; space transportation; commercial use of space; space tracking and data systems, space station; and aeronautics and space research and technology. The achievements of each of the following organizations are described: NASA, the Departments of Defense, Commerce, Energy, Interior, Agriculture, Transportation and State, the Federal Communications Commission, Environmental Protection Agency, National Science Foundation, Smithsonian Institution, Arms Control and Disarmament Agency and USIA. Appendices provide historical information on launches, satellites, manned and unmanned spacecraft, and Federal budgets for aeronautical and astronautical activities.
Author

88 SPACE SCIENCES (GENERAL)

No abstracts in this category.

89 ASTRONOMY

Includes radio, gamma-ray, and infrared astronomy, and astrometry.

N88-21088# Pennsylvania State Univ., University Park. Dept. of Astronomy.
DEVELOPMENT OF HIGH STABILITY FIBER OPTIC SPECTROPHOTOMETRIC SYSTEMS FOR STUDY OF SOLAR/STELLAR MAGNETIC ACTIVITY Final Report, 15 Jun. 1983 - 15 Jun. 1986
Lawrence W. Ramsey 17 Feb. 1987 25 p
(Contract F19628-83-K-0038)
(AD-A189327; AFGL-TR-87-0218) Avail: NTIS HC A03/MF A01 CSCL 03A

A program to study magnetic activity cycles in solar-type stars, including the Sun, is described. The goal is to establish the relationships between a star's magnetic cycle morphology (i.e., amplitude, period, shape, regularity, etc.) and its age, rotation rate, and if possible, differential rotation rate, for a variety of solar like stars. Basic empirical input will be provided for the construction of a viable dynamical dynamo theory for the Sun and the stars, leading to a deeper understanding of the ultimate origins of solar and stellar magnetism. Only when a realistic theory of magnetic

field generation is available can one understand fully the physics of magnetic activity, which manifests itself on all temporal and spatial scales, from transients such as flares to long-lived structures such as quiescent prominences, from flux-tubes at the limit of resolution to complex groups of sunspots. A critical first step in this effort was the development of an appropriate instrument. What follows describes an advanced-design, special-purpose, fiber fed spectrograph carefully optimized to make the required observations with maximum efficiency. This contract designs, fabricates and tests the breadboard instrument. GRA

N88-21089# Massachusetts Univ., Amherst. Dept. of Physics and Astronomy.
ANALYSIS OF DEEP SKY SOURCES FOUND BY THE INFRARED ASTRONOMY SATELLITE Final Technical Report, 30 Jan. 1985 - 29 Jul. 1987
Susan G. Kleinmann 15 Dec. 1987 16 p
(Grant AF-AFOSR-0057-85)
(AD-A189605; AFOSR-88-0038TR) Avail: NTIS HC A03/MF A01 CSCL 03A

This program was aimed at understanding the number and types of sources found in the fields observed with greatest sensitivity by the IRAS satellite. The initial phase of the study emphasized observation and analysis of sources found in the less sensitive all sky survey carried out with Infrared Astronomy Satellite. Significant differences between the bright and faint 12 um sources were found, which constrain their relative spatial distributions and luminosities. A study focussed on one, large population of infrared-bright stars - those whose atmospheres are rich in carbon - yielded measurements of their space distribution range of mass loss rates, and lifetimes. An analysis of 60 um sources from the IRAS survey showed that eighty-five percent of those located more than thirty degrees above the plane of the Galaxy are extragalactic objects, provided a measure of the space density of galaxies of different infrared luminosities, and showed that there are significant differences in the environment and infrared properties of the most luminous and least luminous galaxies. Studies of galaxies with particularly strong mid-infrared emission resulted in the discovery of ultraluminous objects. Initial studies of results from the IRAS pointed observations show effects of contamination by low-surface-brightness intestellar clouds. GRA

N88-21090*# National Aeronautics and Space Administration. Goddard Space Flight Center, Greenbelt, Md.
RELATIVISTIC JET MODELS FOR THE BL LACERTAE OBJECT Mrk 421 DURING THREE EPOCHS OF OBSERVATION Final Technical Report
S. L. Mufson, D. J. Hutter, Y. Kondo, and W. Z. Wisniewski (Arizona Univ., Tucson.) 5 Apr. 1988 31 p
(Grant NAG5-198)
(NASA-TM-89727; NAS 1.15:89727) Avail: NTIS HC A03/MF A01 CSCL 03A

Coordinated observation of the nearby BL Lacertae object Mrk 421 obtained during May 1980, January 1984, and March 1984 are described. These observations give a time-frozen picture of the continuous spectrum of Mrk 421 at X-ray, ultraviolet, optical, and radio wavelengths. The observed spectra have been fitted to an inhomogeneous relativistic jet model. In general, the models reproduce the data well. Many of the observed differences during the three epochs can be attributed to variations in the opening angle of the jet and in the angle that the jet makes to the line of sight. The jet models obtained here are compared with the homogeneous, spherically symmetric, synchrotron self-Compton models for this source. The models are also compared with the relativistic jet models obtained for other active galactic nuclei.
Author

N88-21091*# Columbia Univ., New York, N.Y. Astrophysics Lab.
VARIABLE SPECTRA OF ACTIVE GALAXIES Final Technical Report
Jules P. Halpern May 1988 11 p
(Grant NAG8-570)
(NASA-CR-182694; NAS 1.26:182694; CAL-1683) Avail: NTIS HC A03/MF A01 CSCL 03A

The analysis of EXOSAT spectra of active galaxies are presented. The objects examined for X-ray spectral variability were MR 2251-178 and 3C 120. The results of these investigations are described, as well as additional results on X-ray spectral variability related to EXOSAT observations of active galaxies. Additionally, the dipping X-ray source 4U1624-49 was also investigated.
Author

N88-21092*# Smithsonian Astrophysical Observatory, Cambridge, Mass.
SPACE INFRARED TELESCOPE FACILITY WIDE FIELD AND DIFFRACTION LIMITED ARRAY CAMERA (IRAC) Final Report, 1 Sep. 1984 - 31 Oct. 1987
Giovanni G. Fazio Apr. 1988 117 p
(Grant NAG2-316)
(NASA-CR-182704; NAS 1.26:182704) Avail: NTIS HC A06/MF A01 CSCL 03A

The wide-field and diffraction limited array camera (IRAC) is capable of two-dimensional photometry in either a wide-field or diffraction-limited mode over the wavelength range from 2 to 30 microns with a possible extension to 120 microns. A low-doped indium antimonide detector was developed for 1.8 to 5.0 microns, detectors were tested and optimized for the entire 1.8 to 30 micron range, beamsplitters were developed and tested for the 1.8 to 30 micron range, and tradeoff studies of the camera's optical system performed. Data are presented on the performance of InSb, Si:In, Si:Ga, and Si:Sb array detectors bumpbonded to a multiplexed CMOS readout chip of the source-follower type at SIRTF operating backgrounds (equal to or less than 1 x 10 to the 8th ph/sq cm/sec) and temperature (4 to 12 K). Some results at higher temperatures are also presented for comparison to SIRTF temperature results. Data are also presented on the performance of IRAC beamsplitters at room temperature at both 0 and 45 deg angle of incidence and on the performance of the all-reflecting optical system baselined for the camera. Author

N88-21093# Tuebingen Univ. (West Germany). Inst. fuer Astronomie.
PREPARATION OF PHOTOMETRIC MEASUREMENTS ON A MILLION STARS IN THE FRAMEWORK OF THE SATELLITE PROJECT HIPPARCOS/TYCHO Thesis [VORBEREITUNG PHOTOMETRISCHER MESSUNGEN AN EINER MILLION STERNEN MIT DEM SATELLITENPROJEKT HIPPARCOS/TYCHO]
Dominic R. Scales Jun. 1986 117 p In GERMAN
(ETN-88-91502) Avail: NTIS HC A06/MF A01

The satellite project HIPPARCOS/TYCHO, aiming at an improvement of the accuracy of astrometric measurements, is presented. The spacecraft, its payload, and its instrumentation are described. The scientific objectives of the HIPPARCOS mission are presented. The TYCHO experiment, the data flow, and data evaluation are presented. A computer program was developed and implemented to solve the special problem related to the calibration of the photometric data from more than 1 million stars in the TYCHO experiment. The results show that, in spite of the large number of measurements, all the data can be calibrated and reduced. ESA

90 ASTROPHYSICS

Includes cosmology; celestial mechanics; space plasmas; and interstellar and interplanetary gases and dust.
For related information see also *75 Plasma Physics*.

N88-21094# Lockheed Missiles and Space Co., Palo Alto, Calif.
STIMULATED EMISSION OF ENERGETIC PARTICLES (SEEP) Final Report, 30 Sep. 1987
William L. Imhof, Henry D. Voss, Joseph Mobilia, Dayton W. Datlowe, and Edward E. Gaines 30 Nov. 1987 202 p Original contains color illustrations

(Contract N00014-79-C-0824)
(AD-A188724; LMSC/D068456) Avail: NTIS HC A10/MF A01 CSCL 04A

An active satellite-ground coordinated space plasma experiment was conducted in which electrons were precipitated from the radiation belts into the ionosphere by the controlled injection of VLF signals from ground-based transmitters. In this experiment Stimulated Emission of Energetic Particles (SEEP), four operational VLF transmitters were operated in special controlled formats at times of overpasses of the low-altitude polar- orbiting satellite S81-1. The results confirm the hypothesis that electrons can be precipitated from the radiation belts by ground-based VLF transmitters, and they provide information relating to the effects of such precipitation on the ionosphere. In addition, the precipitation of electrons by VLF waves associated with lightning was measured for the first time from a satellite. Many other important findings were made with the SEEP data. These include the following: (1) an assessment was made of the relative contributions of hiss, lightning and VLF transmitter waves to electron precipitation from the slot region, (2) discovery of the frequent occurrence of multiple peaks in the energy spectra of electrons trapped at low altitudes, (3) observation of electron pulsations near the trapping boundary, and (4) discovery of bremsstrahlung X-ray images of small isolated patches of energetic electron precipitation at high latitude. GRA

N88-21095# Iowa State Univ. of Science and Technology, Ames.
VERY HIGH ENERGY GAMMA RAY ASTROPHYSICS Progress Report, 1 May 1987 - 1 Feb. 1988
R. G. Lamb and D. A. Lewis Feb. 1988 16 p
(Contract DE-AC02-80ER-10774)
(DE88-005821; DOE/ER-10774/8) Avail: NTIS HC A03/MF A01

The Whipple observatory Gamma Ray Collaboration has continued to make steady progress in its development of a highly sensitive stereoscopic imaging gamma-ray telescope (known as the HERCULES project). The milestones in this year's development include: the demonstration of the success of the imaging concept with a single camera by the detection of a very weak flux of gamma rays from the Crab Nebula at a high level of statistical significance (7 sigma), the confirmation of our detection of an anomalous pulsed flux from Hercules X-1 in the summer of 1986 by two other groups; this result has serious implications for the mechanism for gamma-ray emission in this binary source. The construction and installation of the new high resolution camera on the 10 m reflector; the realistic simulation of the sensitivity of this camera as well as that of the full HERCULES system was also undertaken. These, and other highlights of this year's program at the Iowa State University and the Smithsonian Astrophysical Observatory, are discussed in this paper. DOE

N88-21096# Chicago Univ., Ill.
PARTICLE PHYSICS AND COSMOLOGY Progress Report, Jan. 1986 - Jan. 1988
M. S. Turner Jan. 1988 14 p
(Contract DE-AC02-80ER-10587)
(DE88-004944; DOE/ER-10587/T6) Avail: NTIS HC A03/MF A01

This paper briefly discusses research at the University of Chicago in the following areas: Supernova 1987a, inflation, cosmic strings, primordial nucleosynthesis, dark matter/structure formation and MSW neutrino oscillations. DOE

N88-21097 Minnesota Univ., Minneapolis.
A MASS SPECTROMETER EVOLVED GAS ANALYSIS EXPERIMENT FOR IN-SITU ANALYSIS OF COMETARY DUST VOLATILES Ph.D. Thesis
Brian Jay Anderson 1987 152 p
Avail: Univ. Microfilms Order No. DA8726027

The recent encounters with comets Giacobini-Zinner and Halley mark the beginning of an exciting new step in space exploration. Future cometary missions will attempt to perform systematic studies of the structure, composition, and behavior of comets in ways not possible with fast flybys. In anticipation of such a mission, an instrument for repeated in-situ dust collection and evolved gas analysis has been constructed and tested. The instrument employs a high efficiency dust collector incorporated in a furnace which can maintain a temperature of 900 C with only 30 watts of power. A simple mass spectrometer with a single ion collector and a dynamic range of 10 to the 5th power was used in laboratory tests of the furnace. Tests performed with Ivuna meteorite material show that volatile releases employing linear temperature ramping are reproducible and have a detection limit of 10 ppm of the volatile fraction. Use of a more sophisticated mass spectrometer should reduce detection levels to less than 1 ppm by improving the statistics and increasing the dynamic range. Dissert. Abstr.

N88-21098 Arizona Univ., Tucson.
ASYMPTOTIC GIANT BRANCH POPULATIONS IN COMPOSITE STELLAR SYSTEMS Ph.D. Thesis
Kem Holland Cook 1987 266 p
Avail: Univ. Microfilms Order No. DA8727922

A technique is presented for the identification and classification of late-type stars and for the estimation of M star metallicities. The technique uses broadband, V and I, CCD images to identify red stars and two intermediate band CCD images to classify these as carbon or M types. One of the intermediate passbands is centered on a TiO absorption band at 7705 A and the other is centered on a CN absorption band at 8100 A. Color-color plots of V-I versus the intermediate band index, 77-81, clearly distinguishes carbon from M stars. Observations of both early and late type stars were used to define the 77-81 system based upon the intermediate band filters. The TiO band strength deduced from the 77-81 color as a function of V-I color was investigated for field giants and giants in 12 globular clusters. A linear correlation between (Fe/H) and the V-I color at a given TiO band strength was found. The correlation can be used to estimate the metallicity of M giants. The stellar population of a field in Baade's Window was examined using this technique. The stellar population of the Sagittarius Dwarf Irregular galaxy (Sagdig) was examined using the 77-81 system. A method for estimating reddening based upon the color mode of foreground stars was developed for the analysis of the Sagdig data. Bright blue and red stars in Sagdig are evidence for recent star formation. Carbon stars were identified in Sagdig. The spatial distribution of carbon stars and bright red stars in Sagdig shows this galaxy to be much larger than previously thought. Dissert. Abstr.

N88-21099 California Univ., Berkeley.
VELOCITY RESOLVED FAR-INFRARED SPECTROSCOPY OF GALACTIC SOURCES Ph.D. Thesis
John Butterfield Lugten 1987 114 p
Avail: Univ. Microfilms Order No. DA8726285

The far-infrared spectrum is very rich with atomic fine-structure lines of abundant elements and rotational lines of simple molecules, many of which were observed with the second generation of Berkeley Fabry-Perot spectrometer described here. The CO, OH, and (OI) line emission was observed from Orion-KL with 15 to 30 km/s spectral resolution. The far-infrared lines have wings of blue-shifted emission extending to about -60 km/s LSR, similar to the H2 lines observed in the near-infrared. The first detection of a rare isotope in the far-infrared, OH-18 and the first far-infrared detection of CH were made toward SgrB2. Far-infrared CO line emission was observed from a thin ring in the central 10 pc of the Galaxy. The CO line intensities indicate T sub gas is approximately 300 K and n sub H2 is approximately few x 10 to the 4th /cu cm at 2 pc from the galactic center. The thermal energy density in the ring decreases slowly with increasing galactocentric radius, suggesting that at the present epock, the ring is heated predominantly by turbulence or UV photons, rather than by mass outflow from a central source. Dissert. Abstr.

N88-21100 Pennsylvania Univ., Philadelphia.
TOPICS IN CURVED AND FLAT SPACE ELECTROMAGNETISM Ph.D. Thesis

Errol Mustafa 1987 134 p
Avail: Univ. Microfilms Order No. DA8725192

Several problems in curved space and flat space electromagnetism are discussed and resolved. The use of the Hertz and Debye bivector potential schemes for the solution of Maxwell's equations for source-free electromagnetic test fields in general relativity is further developed. A new method for classifying such schemes is presented and the Debye schemes are given with respect to an orthonormal tetrad (basis). The electromagnetic properties of a slowly rotating charged thin shell are considered in both curved and flat space. The g-factor g, magnetic moment and angular momentum of such a shell are computed as a function of the charge-to-mass and radius-to-mass ratios. In the general relativistic case it is found that for a charge-to-mass ratio which exceeds unity g is not bounded and the magnetic moment and net angular momentum of such a shell may vanish or change sign. In the flat space case it is shown that classical physics can give a g-factor which exceeds unity for such a system. The electromagnetic properties of the classical electron modeled as a thin charged shell are considered. A solution to the problem that the energy and linear momentum of such an extended system do not transform properly under Lorentz transformations is given. It is shown that the energy and linear momentum of such a system naturally constitute components of a four vector if the cohesive stress in the shell is included correctly in the calculation. An application of flat space electromagnetism to pulsar astrophysics is given. Dissert. Abstr.

N88-21101 Michigan Univ., Ann Arbor.
GALAXY EVOLUTION IN DENSE CLUSTERS Ph.D. Thesis
Michael Van Newberry 1987 233 p
Avail: Univ. Microfilms Order No. DA8720319

In order to substantiate the observation that the fraction of blue galaxies in the cores of dense clusters increases with redshift (the Butcher-Oemler effect), spectra were obtained for 61 galaxies in seven dense clusters over the redshift range 0.195 less than z less than 0.38. Results verified the effect at better than a 99.5 percent confidence level. Models for the evolution of the integrated spectra of stellar populations were constructed in order to ascertain the nature of the stellar populations within the observed galaxies. It is concluded that it is impossible to distinguish between two considered starburst models and the evolution of a stripped late-type galaxy using mean Balmer strength and B-V alone. The present models suggest that Dressler and Gunn's interpretation is not a unique explanation for previous observations. For galaxies having a larger bulge contribution, or for which stripping terminates star formation over a long timescale of approximately one billion years, the starburst scenario would be preferred. Also, it is possible to distinguish between the alternative evolutionary scenarios on the basis of comparisons between H beta and CaII H+K, the G band and the 4000 A break. Of all cluster galaxies observed, only one shows sufficiently strong Balmer absorption lines to be considered a starburst or stripped galaxy. Dissert. Abstr.

N88-21102 Cornell Univ., Ithaca, N.Y.
INFRARED CONSTRAINTS ON THE NATURE OF DARK MATTER Ph.D. Thesis
Michael F. Skrutskie 1987 289 p
Avail: Univ. Microfilms Order No. DA8725804

Observations of the dynamics of galaxies reveal a universe dominated by unseen matter. This dark matter problem manifests itself in the galactic disk, galaxy halos, galaxy clusters, and intergalactic space. The results are presented of near infrared observations directed at determining a variety of environments where dynamical observations betray the existence of a substantial underluminous component. Near-infrared imaging of stars within 12 parsecs of the Sun reveals a deficit of low mass companions in the solar neighborhood, ruling out a simple extrapolation of the observed luminosity function for low mass stars as an explanation for the Oort discrepancy within the galactic disk. Direct imaging of GL644C denies the existence of the only substellar candidate yet reported. Simultaneous large aperture photometry at visible and near-infrared wavelengths in the halos of three nearby late-type edge-on spiral galaxies eliminates low mass stars from consideration as the main constituent of massive galactic halos. Similar photometry of the newly discovered intergalactic HI cloud in LEO reveals this object to be substantially underluminous with respect to its HI mass. These observations require stars to play a minor role in contributing to dark matter in the universe, suggesting that either cool substellar objects, or any one of a number of known or postulated weakly interacting massive particles, constitute dark matter. Dissert. Abstr.

N88-21103 California Univ., Berkeley.
EARLY REHEATING AND COSMIC STRINGS Ph.D. Thesis
Albert Joseph Stebbins, III 1987 173 p
Avail: Univ. Microfilms Order No. DA8726379

Possible thermal histories of the universe during the epoch z = 10 to 1000 are studied. Expressions for the fractional ionization and electron temperature are given in the case of homogeneous heating as a function of the parameters of arbitrary ionizing sources. The accretion of matter onto the wakes left behind by horizon-size pieces of cosmic string is examined. It was found that in a universe containing cold dissipationless matter (CDM), accretion onto wakes produces a network of sheet-like regions with a nonlinear density enhancement. A formalism for calculating the microwave anisotropy produced by cosmic string loops in Minkowski space was developed. The final formalism involves doing a one-dimensional integral along the string for each point on the sky. Exact solutions were found for a circular loop seen face-on. The equations were integrated for one particular loop configuration at nine points in its evolution. Dissert. Abstr.

N88-21104 California Univ., Berkeley.
RESONANT ALFVEN WAVE INSTABILITIES DRIVEN BY STREAMING FAST PARTICLES Ph.D. Thesis
Andrew Lee Zachary 1987 254 p
Avail: Univ. Microfilms Order No. DA8726421

A plasma simulation code is used to study the resonant interactions between streaming ions and Alfven waves. The medium which supports the Alfven waves is treated as a single, one dimensional, ideal MHD fluid, while the ions are treated as kinetic particles. The code is used to study three ion distributions: a cold beam; a monoenergetic shell; and a drifting distribution with a power-law dependence on momentum. These distributions represent: the field-aligned beams upstream of the earth's bow shock; the diffuse ions upstream of the bow shock; and the cosmic ray distribution function near a supernova remnant shock. Dissert. Abstr.

N88-20314# Joint Publications Research Service, Arlington, Va.
VEGA-1 AND VEGA-2 AUTOMATIC STATIONS: FUNCTIONING OF FLYBY VEHICLES DURING ENCOUNTER WITH HALLEY'S COMET Abstract Only
V. P. Dolgopolov, V. P. Karyagin, V. M. Kovtunenko, R. S. Kremnev, O. V. Papkov, K. M. Pichkhadze, G. N. Rogovskiy, R. Z. Sagdeyev, and K. G. Sukhanov *In its* JPRS Report: Science and Technology. USSR: Space 6 Apr. 1988 p 14 Transl. into ENGLISH from Kosmicheskiye Issledovaniya (Moscow, USSR), v. 25, no. 5, Sep. - Oct. 1987 p 655-658 Original language document was announced in IAA as A88-17810 (For primary document see N88-20312 13-12)
Copyright Avail: NTIS HC A04/MF A01

91 LUNAR AND PLANETARY EXPLORATION

Includes planetology; and manned and unmanned flights. For spacecraft design or space stations see *18 Spacecraft Design, Testing and Performance.*

N88-21105*# Alabama A & M Univ., Normal.
MODEL OF JOVIAN F REGION IONOSPHERE Annual Status Report
A. Tan Mar. 1988 18 p

(Grant NAGw-1067)
(NASA-CR-182587; NAS 1.26:182587; AAMU-NAG-88-1) Avail: NTIS HC A03/MF A01 CSCL 03B

To date, seven electron density profiles of the Jovian ionosphere have been furnished by the radio occultation experiments aboard the Pioneer and Voyager space probes. The data correspond to various localities (latitudes and longitudes) and times (dawn and dusk) and phases of sunspot cycle (high and low). This renders comparative studies difficult. Nevertheless, the possibility of existence of diurnal variation, equatorial anomaly, and auroral particle precipitation in the Jovian ionosphere have been put forth. The grand magnitude and depth of the equatorial anomaly, in particular, is a matter of great interest and speculation. Correct interpretations of the data and the physical processes in the complex Jovian atmospheric environment will remain a major task for the Aeronomer for decades to come. Model studies of a Jovian ionosphere created by solar EUV radiation and subjected to model ExB drifts showed that equatorial anomaly similar to that in the terrestrial ionosphere can indeed be produced in the Jovian ionosphere. However, owing to the difference in size and rotation period of the two planets and the ionic compositions, much larger drift velocities are required to produce a comparable anomaly in the Jovian atmosphere. Author

N88-21106# Air Force Inst. of Tech., Wright-Patterson AFB, Ohio. School of Engineering.
FROZEN ORBIT ANALYSIS IN THE MARTIAN SYSTEM M.S. Thesis
James W. Foister, III Dec. 1987 189 p
(AD-A189574; AFIT/GSO/AA/87D-2) Avail: NTIS HC A09/MF A01 CSCL 03C

A frozen orbit is an orbit whose time rate of change of the argument of the periapsis, the eccentricity, the semi major axis, or the angle of inclination (i) is approximately equal to zero. Martian frozen orbits are known to exist for polar trajectories with altitudes from 300 km to 1000 km. The objective of this study was to determine if other regions with characteristics similar to the known frozen orbits exist, taking into account the perturbative effects due to a 6 x 6 gravity field and atmospheric drag. First, the geopotential equation was derived for both spherical coordinates and the classical orbital elements. Next, a model for the atmospheric drag was developed. Using these two models, a FORTRAN computer model named ASAP (Artificial Satellite Analysis Program) was analyzed for accuracy. This program proved to be highly reliable, and was used to carry out further analysis. Two of the three trajectories planned for the future Mars Geoscience/Climatology Orbiter (MGCO) are frozen orbits. In order to determine the characteristics of w, e, a, and i of a frozen orbit, one of the MGCO frozen orbits was examined in both a 6 x 0 and a 6 x 6 gravity field. The analysis showed that the above orbital elements are not periodic over one orbital period (when in the presence of a 6 x 6 gravity field), but they are bounded over one axial period. GRA

N88-21107*# Johns Hopkins Univ., Baltimore, Md. Center for Astrophysical Sciences.
IUE PROGRAM SUGSD: VARABILITY TIME SCALE OF H Ly-ALPHA FROM URANUS Final Technical Report
Samuel T. Durrance, J. T. Clarke, H. W. Moss, and S. Boyer 27 Apr. 1988 14 p
(Grant NAG5-435)
(NASA-CR-182706; NAS 1.26:182706) Avail: NTIS HC A03/MF A01 CSCL 03B

The scientific motivation for this program was to determine the time scale for the variability of the H Lyman-alpha emission from Uranus. The purpose of this series of observation is to determine its variability on shorter time scales. A series of observations was carried out in coordination with ESA to cover as completely as possible one 24 hour period of the Uranian H Lyman-alpha emission. The observations were obtained on April 23 and 24. Two additional ovservations on April 25 and 26 were obtained to search for longer term trends. A small modulation in the brightness was observed and the results presented. Author

N88-20313# Joint Publications Research Service, Arlington, Va.
VEGA-1 AND VEGA-2 AUTOMATIC STATIONS: FUNCTIONING OF LANDING MODULES IN VENUSIAN ATMOSPHERE Abstract Only
V. A. Deryugin, V. P. Dolgopolov, V. P. Karyagin, V. M. Kovtunenko, R. S. Kremnev, K. M. Pichkhadze, G. N. Rogovskiy, and R. Z. Sagdeyev *In its* JPRS Report: Science and Technology. USSR: Space 6 Apr. 1988 p 14 Transl. into ENGLISH from Kosmicheskiye Issledovaniya (Moscow, USSR), v. 25, no. 5, Sep. - Oct. 1987 p 649-654 (For primary document see N88-20312 13-12)
Copyright Avail: NTIS HC A04/MF A01

N88-20315# Joint Publications Research Service, Arlington, Va.
THERMAL STRUCTURE OF VENUSIAN ATMOSPHERE DETERMINED FROM RESULTS OF MEASUREMENTS FROM VEGA-2 LANDING MODULE Abstract Only
V. M. Linkin, G. Blamont, S. I. Devyatkin, S. P. Ignatova, V. V. Kerzhanovich, A. N. Lipatov, K. Malik, B. I. Stadnyk, Ya. V. Sanotskiy, and P. G. Stolyarchuk et al. *In its* JPRS Report: Science and Technology. USSR: Space 6 Apr. 1988 p 14-15 Transl. into ENGLISH from Kosmicheskiye Issledovaniya (Moscow, USSR), v. 25, no. 5, Sep. - Oct. 1987 p 659-672 Original language document was announced in IAA as A88-17811 (For primary document see N88-20312 13-12)
Copyright Avail: NTIS HC A04/MF A01

N88-20316# Joint Publications Research Service, Arlington, Va.
RESEARCH ON ABSORPTION OF UV RADIATION IN VENUSIAN ATMOSPHERE FROM VEGA-1 AND VEGA-2 LANDING MODULES Abstract Only
Zh. L. Berto, A. P. Ekonomov, B. Mezh, V. I. Moroz, A. Aberzhal, V. I. Gnedykh, A. V. Grigoryev, B. Ye. Moshkin, A. Oshkorn, and Zh. P. Pommero et al. *In its* JPRS Report: Science and Technology. USSR: Space 6 Apr. 1988 p 15 Transl. into ENGLISH from Kosmicheskiye Issledovaniya (Moscow, USSR), v. 25, no. 5, Sep. - Oct. 1987 p 691-706 (For primary document see N88-20312 13-12)
Copyright Avail: NTIS HC A04/MF A01

N88-20317# Joint Publications Research Service, Arlington, Va.
VERTICAL STRUCTURE OF VENUSIAN CLOUD LAYER AT LANDING SITES OF VEGA-1 AND VEGA-2 VEHICLES Abstract Only
V. I. Gnedykh, L. V. Zasova, V. I. Moroz, B. Ye. Moshkin, and A. P. Ekonomov *In its* JPRS Report: Science and Technology. USSR: Space 6 Apr. 1988 p 15 Transl. into ENGLISH from Kosmicheskiye Issledovaniya (Moscow, USSR), v. 25, no. 5, Sep. - Oct. 1987 p 707-714 Original language document was announced in IAA as A88-17815 (For primary document see N88-20312 13-12)
Copyright Avail: NTIS HC A04/MF A01

N88-20318# Joint Publications Research Service, Arlington, Va.
GAS-CHROMATOGRAPHIC ANALYSIS OF PRODUCTS OF THERMAL REACTIONS OF AEROSOL IN VENUSIAN CLOUD LAYER ON VEGA-1 AND VEGA-2 AUTOMATIC INTERPLANETARY STATIONS Abstract Only
N. V. Porshnev, L. M. Mukhin, B. G. Gelman, D. F. Nenarokov, V. A. Rotin, A. V. Dyachkov, and V. B. Bondarev *In its* JPRS Report: Science and Technology. USSR: Space 6 Apr. 1988 p 16 Transl. into ENGLISH from Kosmicheskiye Issledovaniya (Moscow, USSR), v. 25, no. 5, Sep. - Oct. 1987 p 715-720 Original language document was announced in IAA as A88-17816 (For primary document see N88-20312 13-12)
Copyright Avail: NTIS HC A04/MF A01

N88-20319# Joint Publications Research Service, Arlington, Va.
ROENTGENORADIOMETRIC ANALYSIS OF AEROSOL IN VENUSIAN CLOUDS BY VEGA-1 AND VEGA-2 AUTOMATIC INTERPLANETARY STATIONS Abstract Only
B. M. Andreychikov, I. K. Akhmetshin, B. N. Korchuganov, L. M. Mukhin, B. I. Ogorodnikov, I. V. Petryanov, and B. I. Skitovich *In*

its JPRS Report: Science and Technology. USSR: Space 6 Apr. 1988 p 16 Transl. into ENGLISH from Kosmicheskiye Issledovaniya (Moscow, USSR), v. 25, no. 5, Sep. - Oct. 1987 p 721-736 (For primary document see N88-20312 13-12)
Copyright Avail: NTIS HC A04/MF A01

N88-20320# Joint Publications Research Service, Arlington, Va.
CHEMICAL COMPOSITION AND STRUCTURE OF VENUSIAN CLOUDS DETERMINED FROM RESULTS OF ROENTGENO-RADIOMETRIC EXPERIMENTS CARRIED OUT BY LANDING MODULES OF VEGA-1 AND VEGA-2 AUTOMATIC INTERPLANETARY STATIONS Abstract Only
B. M. Andreychikov *In its* JPRS Report: Science and Technology. USSR: Space 6 Apr. 1988 p 16-17 Transl. into ENGLISH from Kosmicheskiye Issledovaniya (Moscow, USSR), v. 25, no. 5, Sep. - Oct. 1987 p 737-743 Original language document was announced in IAA as A88-17818 (For primary document see N88-20312 13-12)
Copyright Avail: NTIS HC A04/MF A01

N88-20321# Joint Publications Research Service, Arlington, Va.
DETERMINING CHEMICAL COMPOSITION OF AEROSOL IN VENUSIAN CLOUD LAYER ON VEGA-1 AUTOMATIC INTERPLANETARY STATION USING MALAKHIT MASS SPECTRUM ANALYZER Abstract Only
Yu. A. Surkov, V. F. Ivanova, A. N. Pudov, E. P. Sheretov, B. I. Kolotilin, M. P. Safonov, R. Toma, G. Izrael, Zh. Lespanol, and D. Imbo et al. *In its* JPRS Report: Science and Technology. USSR: Space 6 Apr. 1988 p 17 Transl. into ENGLISH from Kosmicheskiye Issledovaniya (Moscow, USSR), v. 25, no. 5, Sep. - Oct. 1987 p 744-750 (For primary document see N88-20312 13-12)
Copyright Avail: NTIS HC A04/MF A01

N88-20322# Joint Publications Research Service, Arlington, Va.
ELEMENTAL COMPOSITION OF VENUSIAN ROCKS IN NORTHEASTERN PART OF TERRA APHRODITE (DETERMINED USING DATA FROM VEGA-2 LANDING MODULE) Abstract Only
Yu. A. Surkov, L. P. Moskaleva, V. P. Kharyukova, A. D. Dudin, G. G. Smirnov, S. Ye. Zaytseva, A. N. Tikhomirov, and O. S. Manvelyan *In its* JPRS Report: Science and Technology. USSR: Space 6 Apr. 1988 p 17-18 Transl. into ENGLISH from Kosmicheskiye Issledovaniya (Moscow, USSR), v. 25, no. 5, Sep. - Oct. 1987 p 751-761 (For primary document see N88-20312 13-12)
Copyright Avail: NTIS HC A04/MF A01

N88-20323# Joint Publications Research Service, Arlington, Va.
CONTENT OF NATURAL RADIOACTIVE ELEMENTS IN VENUSIAN ROCKS DETERMINED USING DATA FROM VEGA-1 AND VEGA-2 STATIONS Abstract Only
Yu. A. Surkov, F. F. Kirnozov, V. N. Glazov, A. G. Dunchenko, and L. P. Tatsiy *In its* JPRS Report: Science and Technology. USSR: Space 6 Apr. 1988 p 18 Transl. into ENGLISH from Kosmicheskiye Issledovaniya (Moscow, USSR), v. 25, no. 5, Sep. - Oct. 1987 p 762-767 Original language document was announced in IAA as A88-17821 (For primary document see N88-20312 13-12)
Copyright Avail: NTIS HC A04/MF A01

N88-20324# Joint Publications Research Service, Arlington, Va.
SOME PERIODICITIES IN MOTION OF HALLEY'S COMET RELATIVE TO CENTER OF MASS Abstract Only
V. A. Sarychev, V. V. Sazonov, V. V. Savchenko, and V. I. Tarnopolskiy *In its* JPRS Report: Science and Technology. USSR: Space 6 Apr. 1988 p 18 Transl. into ENGLISH from Kosmicheskiye Issledovaniya (Moscow, USSR), v. 25, no. 5, Sep. - Oct. 1987 p 768-780 Original language document was announced in IAA as A88-17822 (For primary document see N88-20312 13-12)
Copyright Avail: NTIS HC A04/MF A01

N88-20325# Joint Publications Research Service, Arlington, Va.
RESULTS OF INFRARED SPECTROMETER EXPERIMENT. 1: INFRARED RADIATION OF PARENT MOLECULES IN HALLEY'S COMET Abstract Only
V. I. Moroz, M. Combes, A. V. Grigoryev, J. F. Crifo, T. Encrenaz, J. Crovisier, J. P. Bibring, N. F. Sanko, N. Koron, and D. Bockelee-Morvan et al. *In its* JPRS Report: Science and Technology. USSR: Space 6 Apr. 1988 p 18-19 Transl. into ENGLISH from Kosmicheskiye Issledovaniya (Moscow, USSR), v. 25, no. 5, Sep. - Oct. 1987 p 781-792 (For primary document see N88-20312 13-12)
Copyright Avail: NTIS HC A04/MF A01

N88-20326# Joint Publications Research Service, Arlington, Va.
RESULTS OF INFRARED SPECTROMETER EXPERIMENT. 2: INFRARED RADIOMETRY OF NUCLEUS OF HALLEY'S COMET Abstract Only
Yu. V. Nikolskiy, C. Emerich, J. M. Lamarre, N. F. Sanko, M. Combes, V. I. Moroz, J. Crovisier, T. Encrenaz, F. Rokar, and A. V. Grigoryev et al. *In its* JPRS Report: Science and Technology. USSR: Space 6 Apr. 1988 p 19 Transl. into ENGLISH from Kosmicheskiye Issledovaniya (Moscow, USSR), v. 25, no. 5, Sep. - Oct. 1987 p 793-809 (For primary document see N88-20312 13-12)
Copyright Avail: NTIS HC A04/MF A01

N88-20327# Joint Publications Research Service, Arlington, Va.
ANALYSIS OF HYDROCARBON BAND 3.35 IN SPECTRUM OF HALLEY'S COMET USING DATA FROM INFRARED SPECTROMETER ON VEGA-1 SPACECRAFT Abstract Only
A. V. Grigoryev *In its* JPRS Report: Science and Technology. USSR: Space 6 Apr. 1988 p 19-20 Transl. into ENGLISH from Kosmicheskiye Issledovaniya (Moscow, USSR), v. 25, no. 5, Sep. - Oct. 1987 p 810-814 (For primary document see N88-20312 13-12)
Copyright Avail: NTIS HC A04/MF A01

N88-20685# Joint Publications Research Service, Arlington, Va.
NEGATIVE VISCOSITY IN GLOBAL CIRCULATIONS Abstract Only
A. S. Monin *In its* JPRS Report: Science and Technology. USSR: Earth Sciences 26 Feb. 1988 p 9 Transl. into ENGLISH from Doklady Akademii Nauk SSSR (Moscow, USSR), v. 293, no. 1, Mar. 1987 p 70-74 Original language document was announced in AIAA as A87-35842 (For primary document see N88-20674 13-42)
Avail: NTIS HC A04/MF A01

92 SOLAR PHYSICS

Includes solar activity, solar flares, solar radiation and sunspots.

For related information see *93 Space Radiation.*

N88-21108# Helsinki Univ. of Technology, Kylmaelae (Finland). Raidio Lab.
SOLAR MICROWAVE RADIATION MAPS MEASURED AT METSAEHOVI RADIO RESEARCH STATION IN 1978-1979
S. Urop, S. Pohjolainen, and H. Teraesranta 1987 75 p (PB88-127543; SER-A-1; ISBN-951-754-201-1) Avail: NTIS HC A04/MF A01 CSCL 03B

The Radio Laboratory of the Helsinki University of Technology operates at the Metsahovi Radio Research Station a 14-m diameter radio telescope. The Cassegrain telescope system can be used at frequencies 10 to 100 GHz (wavelengths 3 cm to 3 mm). The telescope has been used for solar research irregularly since 1976. Solar mapping with minicomputer-based recordings started in 1978. Measurements include maps of all or part of the sun, tracking of active regions, and solar oscillation monitoring. Most of the solar maps have been measured using receivers operating at 22.2 GHz or at 36.8 GHz. The purpose of the report series is to publish at least one map for each of the days when measurements were

performed. The volume contains selected maps measured in 1978 and 1979. GRA

N88-21109 Alabama Univ., Huntsville.
MAGNETOHYDRODYNAMIC (MHD) SIMULATION OF SOLAR PROMINENCE FORMATION Ph.D. Thesis
Jinjun Bao 1987 217 p
Avail: Univ. Microfilms Order No. DA8724337

The formation of Kippenhahn-Schluter type solar prominences by chromospheric mass injection is studied via numerical simulation. The numerical model is based on a two-dimensional, time dependent, magnetohydrodynamic (MHD) theory. In addition, an analysis of gravitational thermal MHD instabilities related to condensation is performed by using the small perturbation method. Dissert. Abstr.

N88-21110 Arizona Univ., Tucson.
GLOBAL SOLAR OSCILLATIONS OBSERVED IN THE VISIBLE TO NEAR INFRARED CONTINUUM Ph.D. Thesis
Paul Harvey Oglesby 1987 151 p
Avail: Univ. Microfilms Order No. DA8726834

A technique for detecting solar oscillations in the visible to near infrared continuum was developed and tested. In 1985, measurements of the solar radiation intensity near disk center were made. The results of these observations were compared to the reported detections and classifications by Hill (1984, 1985) and Rabaey and Hill (1987) of the low-order, low-degree acoustic modes, the intermediate degree f-modes; and the low-order g-modes. For the low-order, low-degree, acoustic modes and the intermediate f-modes, a total of 40 multiplets were used in the analysis. The coincidence rates between the peaks in the power spectrum of the 1985 observations and the classified frequency spectrum for multiplets taken in subgroups of approximately 5 are typically 4 to 5 sigma above the accidental coincidence rate. Also included is a comparison of diameter measurements obtained at SCLERA in 1978 with the classified modes. Agreement in this case is at the 3.1 sigma level for both the f-mode (n = 0) multiplets with 21 is equal to or less than t is equal to or greater than 12 acoustic modes. The confirmation of the detection and classification of the low-order g-modes of oscillation was found to be at the 3.1 sigma level. Additionally, the m dependence of the 1985 power spectrum was found to behave in the manner expected for the proper classifications in m for the g-modes. Dissert. Abstr.

93 SPACE RADIATION

Includes cosmic radiation; and inner and outer earth's radiation belts.

For biological effects of radiation see *52 Aerospace Medicine*. For theory see *73 Nuclear and High-Energy Physics*.

N88-21111 Ohio State Univ., Columbus.
THE ASTROPHYSICS OF NEBULAE AND ACTIVE GALACTIC NUCLEAR EMISSION-LINE REGIONS: NEW METHODS AND APPLICATIONS Ph.D. Thesis
Stephen Andrew Cota 1987 274 p
Avail: Univ. Microfilms Order No. DA8726612

The effects of electron collisions on the populations of the highly excited states of ions are examined. It is demonstrated that three-body recombinations to these states enhance the total recombination rate in cold nova shells and broad-line regions of active galactic nuclei (AGN). The treatment of the hydrogen atom in photoionization models is then considered. The applicability and accuracy of l-mixing and the published collision rates are discussed. A general method to treat a 100-level atom as a 10-level atom, increasing accuracy but not calculation time is presented. Next, the helium singlet recombination spectrum for cases of finite optical depth is predicted with allowance for the destruction of He I resonance photons through photoionization of neutral hydrogen. The H beta emissivity for cases of finite optical depth is then predicted, allowing for the destruction of Lyman photons on dust grains before they can attain case B. It is demonstrated that for dusty H II regions, helium abundance measurements made relative to H beta have been overestimated by 5 to 15 percent. Finally, it is demonstrated through photoionization modeling of its fine structure line spectrum, that the center of our galaxy, Sgr A West, is ionized by a soft spectrum like that of a 35,000 K star. An AGN-like ionizing spectrum is ruled out. This suggests that our galaxy's nucleus is similar to starburst nuclei. Dissert. Abstr.

N88-21112 California Univ., Berkeley.
A LOW-FREQUENCY MEASUREMENT OF THE SPECTRUM OF THE COSMIC MICROWAVE BACKGROUND RADIATION Ph.D. Thesis
Steven Mark Levin 1987 139 p
Avail: Univ. Microfilms Order No. DA8726274

As part of a larger effort to measure the spectrum of the Cosmic Background Radiation (CBR) at low frequencies, the intensity of the CBR was measured at a frequency of 1.410 GHz. The measurement was made by comparing the power received from the sky with the power received from a specially designed cooled calibration target with know properties. Sources of radiation other than the CBR were then identified and subtracted to calculate the antenna temperature of the CBR at 1.410 GHz. The instrument used to measure the CBR was a total power microwave radiometer with a noise temperature of 80 K. The sources of error were predominantly systematic in nature, and the largest error was due to uncertainty in the reflection characteristics of the cold-load calibrator. Identification and subtraction of signals from the Galaxy (0.7 K) and the Earth's atmosphere (0.8 K) were also significant parts of the data reduction and error analysis. The brightness temperature of the CBR at 1.410 GHz is 2.22 + or - 0.55 K. The spectrum is consistent with a blackbody spectrum of temperature 2.741 + or - 0.016. Constraints on the amount by which the CBR spectrum deviates from the Planck spectrum are used to place limits on energy releases early in the history of the universe. The experimental error could be reduced by changes in the instrument and measurement procedures, and several possible improvements are described. Dissert. Abstr.

N88-21113 Massachusetts Univ., Amherst.
POLARIZATION PROPERTIES OF SiO MASERS Ph.D. Thesis
Gordon Campbell McIntosh 1987 241 p
Avail: Univ. Microfilms Order No. DA8727082

The measurement of circular polarization in silicon monoxide masers provides a probe of the magnitude of the magnetic field in the near stellar environment. Calculations indicate the masers originate in regions where the magnetic field is on the order of 10 to 80 gauss. The linear polarization directions combined with the high resolution spatial maps from the very long baseline interferometry (VLBI) experiments indicate there may be some organization to the magnetic field in the circumstellar region. The VLBI results indicate maser emission occurs over a region several stellar radii in extent. These results also show that the circumstellar region is clumpy, not isotropic as many models assume. The combination of time monitoring with high resolution spatial maps indicates features separated by several stellar radii vary synchronously. This observation constrains pumping mechanisms to those that travel with velocities of approximately 100,000,000 cm/s or greater. If more than one pumping mechanism is active in these sources, this constraint does not apply. A limited fringe amplitude analysis of a linearly polarized VLBI experiment was performed. The analysis indicates the linear polarization characteristics of a maser feature observed at high spatial resolution are comparable to lower spatial resolution polarization measurements. Dissert. Abstr.

99 GENERAL

N88-21114# Department of Defense, Washington, D. C.
SOVIET MILITARY POWER, 1987

1987 161 p Original contains color illustrations
Avail: NTIS HC A08/MF A01; also available SOD HC $7.50 as 008-000-00464-1

Developments in the U.S.S.R. armed forces over the past year are reviewed and placed in the context of current doctrine and strategy. The U.S.S.R. strategic defense program is updated. The realities of the Soviet military power are documented. It is clear that the Soviet Union, together with Soviet-backed forces, is fully capable of simultaneous agression in multiple regions of the world and of threatening U.S. vital interests. The U.S. national security strategies and the capabilities required to execute them must take into account the reality of the Soviet military power. B.G.

N88-21115# National Aerospace Lab., Amsterdam (Netherlands).
[ACTIVITIES REPORT IN AERONAUTICS AND ASTRONAUTICS] Annual Report, 1986 [VERSLAG OVER HET JAAR 1986]
1986 104 p In DUTCH Original document contains color illustrations
(ETN-88-91332) Avail: NTIS HC A06/MF A01

Research concerning flow (inlet channel of the Fokker-50 engine, development of computer programs); aircraft (development of a measuring, registration, and processing system for the evaluation of the Fokker-50 and Fokker-100); aircraft structures and composite materials; spacecraft control and remote sensing; applied computer sciences; and environment management is summarized. Technical facilities are described. The properties and applications of composites, and the development of satellite ground stations are discussed. ESA

☆ U.S. GOVERNMENT PRINTING OFFICE: 1988— 202-150/80011

Typical Subject Index Listing

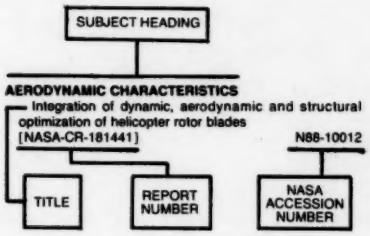

The subject heading is the key to the subject content of the document. Titles, report numbers, and accession numbers of pertinent documents are provided under each subject heading. When the title is insufficiently descriptive of the document content, a title extension has been added, separated from the title by three hyphens. The report number helps to indicate the type of document cited (e.g., NASA report, NASA translation, NASA contractor report). The NASA accession number is the number by which the document abstracts are arranged in this journal and by which the document is sold or requested. The titles, with title extensions if present, are arranged under each subject heading in ascending accession number order. The subject headings have been selected from the latest revision of the *NASA Thesaurus* (NASA SP-7053).

A

ABERRATION
Aberrations: Their effect on off-axis beam steering
[AD-A189601] N88-21008
ABLATION
Molecular dynamics of laser ablation of a polymer coating
[DE88-004337] N88-20466
ABRASION RESISTANCE
Abrasion and impact resistant coatings
[DE88-003562] N88-20464
ABSORPTION SPECTRA
Influence of nonlinear spectroscopic effects on atmospheric propagation of intense laser radiation at 10.6 microns wavelength N88-20705
ACCELERATION (PHYSICS)
Parametric study of acceleration-induced stresses and frequency changes in doubly-rotated crystal resonators
[AD-A189261] N88-20532
An experimental investigation of decelerating flow about two-dimensional cambered plates
[DE88-006598] N88-20567
ACCESS CONTROL
On proving register atomicity
[CWI-CS-R8707] N88-20862
Two queues with alternating service and switching times
[CWI-OS-R8712] N88-20949
ACCIDENTS
Potential off-normal events and associated radiological source terms for the compact ignition tokamak: Fusion Safety Program
[DE88-004112] N88-21024
ACCURACY
Experience with and ways to upgrade accuracy of hydromagnetic surveys in ocean N88-20692
ACOUSTIC EMISSION
Application of ISRM testing methods to fracture toughness testing of graphite N88-20446
A study of the dynamics of high temperature brittle intergranular fracture by acoustic emission
[AERE-R-12479] N88-20650
ACOUSTIC EXCITATION
Acoustic radiation from line- and point-loaded plates: Uniformly asymptotic solutions
[AD-A189367] N88-20969
ACOUSTIC FATIGUE
Abrasion and impact resistant coatings
[DE88-003562] N88-20464
ACOUSTIC MEASUREMENT
Application of ISRM testing methods to fracture toughness testing of graphite N88-20446
Method for determination of the wind velocity and direction
[NASA-TT-20233] N88-20769
Survey of acoustic techniques for monitoring El Nino
[PB88-157615] N88-20783
Measurement and analysis of the noise radiated by low Mach numbers centrifugal blowers
[AD-A189226] N88-20966
Method for determining the coordinates of sound sources by means of a sound measurement system
[NASA-TT-20242] N88-20972
Method for determining artillery position
[NASA-TT-20238] N88-20973
ACOUSTICS
Invariant characteristics of acoustic field in stratified ocean N88-20698
Survey of acoustic techniques for monitoring El Nino
[PB88-157615] N88-20783
Flow/acoustic interaction in duct inflow
[AD-A189264] N88-20967
ACOUSTO-OPTICS
Bathymetric hazard survey test
[AD-A189150] N88-20775
ACTIVATION ENERGY
Novel catalysts for methane activation
[DE88-003637] N88-20390
Kinetics of polymer decomposition
[DE88-005500] N88-20460
ACTIVE CONTROL
Control augmented structural synthesis
[NASA-CR-4132] N88-20290
ACTIVE GALAXIES
Variable spectra of active galaxies
[NASA-CR-182694] N88-21091
ACTIVITY (BIOLOGY)
Biophysical applications of solid state and tritium NMR
[DE88-005328] N88-20806
ADAPTIVE CONTROL
A wind tunnel model with dynamic control
[BU-352] N88-20310
Estimation-correlation, modeling, and identification in adaptive array processors
[AD-A189130] N88-20512
Adaptive algorithms for HF antenna arrays
[AD-A189329] N88-20534
ADDITIVES
Lattice relaxation of the DX centers in Ga/sub 1-x/Al/sub x/As and of the pressure-induced deep donors in GaAs
[DE88-005452] N88-21061
ADHESION
Interfacial adhesion: Theory and experiment
[NASA-TM-100830] N88-20417
Development of a torsion balance for adhesion measurements
[NASA-TM-100799] N88-20454
ADSORBENTS
Characterization and fundamental studies on CuO sorbent materials to determine attrition mechanisms on substrate gamma alumina
[DE88-003674] N88-20456
ADSORPTION
Electrosorptive detection of simple organic compounds in liquid chromatography
[AD-A188757] N88-20376
Measuring thin film properties using SAW (Surface Acoustic Wave) devices: Diffusivity and surface area
[DE88-002216] N88-20970
Recent progress in structure determination by LEED (Low-Energy Electron Diffraction) measure the properties of the deep donors (DX-cent)
[DE88-003851] N88-21048
ADVECTION
Coherent structure-reflective turbulent viscous flow modeling
[AD-A188339] N88-20556
AERODYNAMIC CHARACTERISTICS
Australian aerodynamic design codes for aerial tow bodies
[AD-A189048] N88-20258
Nonaxisymmetric body supersonic, aerodynamic prediction
[AD-A189338] N88-20259
A correlation study of X-29A aircraft and associated analytical development
[NASA-TM-89735] N88-20296
Lateral and longitudinal stability and control parameters for the space shuttle discovery as determined from flight test data
[NASA-TM-100555] N88-20309
AERODYNAMIC COEFFICIENTS
Finite element calculations for aerodynamic coefficients of a 3-dimensional body in subsonic flow using Green's function method
[NASA-TT-20208] N88-20272
AERODYNAMIC CONFIGURATIONS
A review of technologies applicable to low-speed flight of high-performance aircraft investigated in the Langley 14- x 22-foot subsonic tunnel
[NASA-TP-2796] N88-20264
AERODYNAMIC DRAG
Flight tests of external modifications used to reduce blunt base drag
[NASA-TM-100433] N88-20279
Frozen orbit analysis in the Martian system
[AD-A189574] N88-21106
AERODYNAMIC HEATING
Fluid-thermal-structural study of aerodynamically heated leading edges
[NASA-TM-100579] N88-20666
AERODYNAMIC LOADS
Nonaxisymmetric body supersonic, aerodynamic prediction
[AD-A189338] N88-20259
Calculation of the distributed loads on the blades of individual multiblade propellers in axial flow using linear and nonlinear lifting surface theories
[NASA-TT-20173] N88-20278
AERODYNAMIC NOISE
Measurement and analysis of the noise radiated by low Mach numbers centrifugal blowers
[AD-A189226] N88-20966
AERODYNAMIC STABILITY
A correlation study of X-29A aircraft and associated analytical development
[NASA-TM-89735] N88-20296
AERODYNAMICS
Aeronautical engineering: A continuing bibliography with indexes (supplement 224)
[NASA-SP-7037(224)] N88-20254
Australian aerodynamic design codes for aerial tow bodies
[AD-A189048] N88-20258
Activities report of the Lille Institute of Fluid Mechanics
[ETN-88-91983] N88-20597
AEROELASTICITY
An experimental investigation of the flap-lag-torsion aeroelastic stability of a small-scale hingeless helicopter rotor in hover
[NASA-TP-2546] N88-20257
Application of a nonisentropic full potential method to AGARD standard airfoils
[NASA-TM-100560] N88-20263
Aeroelastic models in aircraft design
[MBB/LKE-294/S/PUB/249] N88-20298
Activities report of the Structures Department
[ETN-88-91986] N88-20672

AERONAUTICAL ENGINEERING
Aeronautical engineering: A continuing bibliography with indexes (supplement 224)
[NASA-SP-7037(224)] N88-20254
Aeronautics and space report of the President: 1986 activities N88-21087
AEROSOLS
Vertical structure of Venusian cloud layer at landing sites of Vega-1 and Vega-2 vehicles N88-20317
Roentgenoradiometric analysis of aerosol in Venusian clouds by Vega-1 and Vega-2 automatic interplanetary stations N88-20319
Determining chemical composition of aerosol in Venusian cloud layer on Vega-1 automatic interplanetary station using Malakhit mass spectrum analyzer N88-20321
Observations on electrostatic effects in a filter test system
[AD-A188797] N88-20378
AEROSPACE ENGINEERING
JPRS report: Science and technology. USSR: Space
[JPRS-USP-88-002] N88-20312
JPRS report: Science and technology. China
[JPRS-CST-88-003] N88-20495
JPRS report: Science and technology. China
[JPRS-CST-87-030] N88-20501
Aeronautics and space report of the President: 1986 activities N88-21087
AEROSPACE MEDICINE
Aerospace medicine and biology: A continuing bibliography with indexes (supplement 309)
[NASA-SP-7011(309)] N88-20814
AEROSPACE SYSTEMS
Activities report of the Systems Department
[ETN-88-91987] N88-20505
Vapor-mist for lightweight high voltage space insulation systems
[DE87-011704] N88-20538
Compatibility in space reactor fuel systems
[DE88-005698] N88-21004
AEROTHERMODYNAMICS
Activities report of the Toulouse Research Center
[ETN-88-91986] N88-21077
AFRICA
Northern Hemisphere circulation and the principal components of subsequent summer patterns in North America and West Africa N88-20765
AFTERBURNING
Kinetic mechanisms for ionization and afterburning suppression
[AD-A189219] N88-20383
AGING (MATERIALS)
Aging properties of cable polmers (2)
[NASA-TT-20228] N88-20479
AGRICULTURE
Global mixed-layer natural and anthropogenic fluxes N88-20803
AIR
An interferometric investigation of the diffraction of planar shock waves over a half-diamond cylinder in air
[UTIAS-322] N88-20575
AIR CONDITIONING EQUIPMENT
Pressurizing systems and air conditioning systems
[MBB/LKE-312/S/PUB/246] N88-20828
AIR DEFENSE
Simulation of effect of anti-radar stealth principle N88-20496
AIR FLOW
Air-jet spoiler
[BU-364] N88-20299
Control of structure in turbulent flows: Bifurcating and blooming jets
[AD-A189607] N88-20562
The pressure drag and momentum flux during a cold frontal passage over the Alps N88-20763
AIR JETS
Air-jet spoiler
[BU-364] N88-20299
AIR POLLUTION
Computer simulation of tropospheric chemistry
[JUEL-2144] N88-20756
AIR TRAFFIC CONTROL
Activities report in civil aeronautics
[ETN-88-91344] N88-20255
A method and measures to evaluate trackers for air traffic control
[NLR-TR-86072-U] N88-20287
AIR TRANSPORTATION
Activities report in civil aeronautics
[ETN-88-91344] N88-20255
AIR WATER INTERACTIONS
Estimates of ocean-atmosphere thermal interaction in Gulf Stream energy-active test range in winter of 1984 N88-20679
Sample models of steady and low frequency circulations in the tropical atmosphere, with application to tropical air-sea interactions N88-20764
Dynamics of the Oceanic Surface Mixed Layer
[AD-A188348] N88-20785
Structures and fluxes in a deep convecting mixed layer N88-20786
On the zonal momentum balance at the equator N88-20788
The mixed layer of the western equatorial Pacific Ocean
[HIG-1861] N88-20789
Unsteady shallowing mixed layer N88-20791
Some effects of heating on the wind-driven velocity in the upper ocean N88-20792
Mixed-layer shear related to wind stress in the central equatorial Pacific N88-20793
Wind forcing and observed oceanic wavenumber spectra N88-20797
Energy and momentum fluxes through the sea surface N88-20798
Radiative processes affecting ocean mixed-layer heat content and their monitoring from satellite N88-20800
AIRCRAFT ACCIDENT INVESTIGATION
Aircraft accident report: Midair collision of Cessna-340A, N8716K, and North American SNJ-4N, N711SQ, Orlando, Florida, May 1, 1987
[PB88-910402] N88-20282
AIRCRAFT ACCIDENTS
Aircraft accident report: Midair collision of Cessna-340A, N8716K, and North American SNJ-4N, N711SQ, Orlando, Florida, May 1, 1987
[PB88-910402] N88-20282
AIRCRAFT COMPARTMENTS
Pressurizing systems and air conditioning systems
[MBB/LKE-312/S/PUB/246] N88-20828
AIRCRAFT CONFIGURATIONS
Steady and unsteady transonic small disturbance analysis of realistic aircraft configurations
[NASA-TM-100557] N88-20269
CODAC (Cockpit Oriented Display of Aircraft Configurations) version 1.4 user's guide
[NASA-CR-181650] N88-20273
Configuration management issues and objectives for a real-time research flight test support facility
[NASA-TM-100437] N88-20832
AIRCRAFT CONSTRUCTION MATERIALS
Viscoelastic behavior of a polyetheretherketone (PEEK) composite
[AD-A189545] N88-20368
AIRCRAFT DESIGN
The design of aircraft using the decision support problem technique
[NASA-CR-4134] N88-20291
How to generate equal probability design load conditions --- aircraft design
[NLR-TR-86060-U] N88-20295
Aeroelastic models in aircraft design
[MBB/LKE-294/S/PUB/249] N88-20298
Activities report in aeronautics and astronautics
[ETN-88-91332] N88-21115
AIRCRAFT ENGINES
Engine flow simulation for wind tunnel testing at NLR
[NLR-MP-87011-U] N88-20305
Aircraft corrosion problems and research in the Netherlands
[NLR-MP-86066-U] N88-20427
AIRCRAFT FUELS
Large-Scale Advanced Prop-Fan (LAP)
[NASA-CR-182112] N88-20306
Aviation turbine fuels from tar sands bitumen and heavy oils. Part 3: Laboratory sample production
[AD-A189278] N88-20484
AIRCRAFT GUIDANCE
Flight simulations of MLS interception procedures applicable to laterally segmented approach paths
[NLR-MP-86037-U] N88-20288
AIRCRAFT LANDING
An investigation of classical dynamic scaling techniques applied to an oleo-pneumatic landing gear strut
[AD-A187664] N88-20292
AIRCRAFT MAINTENANCE
The design of aircraft using the decision support problem technique
[NASA-CR-4134] N88-20291
AIRCRAFT MODELS
Aeroelastic models in aircraft design
[MBB/LKE-294/S/PUB/249] N88-20298
Activities report of the Lille Institute of Fluid Mechanics
[ETN-88-91983] N88-20597
AIRCRAFT NOISE
Activities report of the Physics Department
[ETN-88-91985] N88-20964
AIRCRAFT PERFORMANCE
Aquila remotely piloted vehicle: Its potential battlefield contribution still in doubt
[PB88-120241] N88-20289
AIRCRAFT SAFETY
Atmospheric electrical modeling in support of the NASA F-106 storm hazards project
[NASA-CR-181639] N88-20758
Proceedings of the Workshop on the Assessment of Crew Workload Measurements Methods, Techniques and Procedures. Volume 1: Preliminary Selection of Measures
[AD-A189004] N88-20827
AIRCRAFT STRUCTURES
Standardized environmental fatigue sequence for the evaluation of composite components in combat aircraft (ENSTAFF = ENvironmental faISTAFF)
[LBF-FB-179] N88-20300
European approaches in standard spectrum development --- aircraft load spectra
[NLR-MP-87007-U] N88-20661
Activities report of the Structures Department
[ETN-88-91986] N88-20672
Activities report in aeronautics and astronautics
[ETN-88-91332] N88-21115
AIRFOIL OSCILLATIONS
Application of a nonisentropic full potential method to AGARD standard airfoils
[NASA-TM-100560] N88-20263
AIRFOILS
Application of a nonisentropic full potential method to AGARD standard airfoils
[NASA-TM-100560] N88-20263
On the Kutta condition for flows around lifting airfoils and wings
[DFVLR-FB-87-40] N88-20268
AIRFRAMES
Aircraft corrosion problems and research in the Netherlands
[NLR-MP-86066-U] N88-20427
ALASKA
Alaska Loran C probe test results
[AD-A189131] N88-20284
ALCOHOLS
Status of alcohol fuels utilization technology for highway transportation: A 1986 perspective. Volume 2: Compression ignition engines
[DE88-006059] N88-20485
ALDOSTERONE
Plasma cortisol, renin and aldosterone during an intense heat acclimation program
[AD-A189387] N88-20810
ALGORITHMS
An L-U implicit multigrid algorithm to solve the Euler equations for transonic flow in rotating turbomachinery passages N88-20270
A method and measures to evaluate trackers for air traffic control
[NLR-TR-86072-U] N88-20287
Material parameter measurements at high temperatures
[NASA-CR-182707] N88-20397
Adaptive control of scientific balloon-borne gondola attitude N88-20497
Statistical signal processing using a class of iterative estimation algorithms
[AD-A189050] N88-20511
Adaptive algorithms for HF antenna arrays
[AD-A189329] N88-20534
Systems near the onset and in the well-developed regimes of turbulence
[DE88-005365] N88-20565
Finite element methods for quasi-prismatic bodies with application to gears N88-20644
Numerical modeling of wave migration of seismic data N88-20684
Stratospheric trace gas distributions from fair infrared thermal emission spectroscopy N88-20749
A new algorithm for general multiobjective optimization
[NASA-TM-100536] N88-20830
The physical structure of concurrent problems and concurrent computers
[DE88-005812] N88-20835
Parallel image compression
[NASA-CR-180758] N88-20837
Broadband correlation analysis
[AD-A188732] N88-20839
On relaxation algorithms based on Markov random fields
[AD-A189043] N88-20840
Passive DF: A tutorial, part 1
[NASA-CR-182669] N88-20846
Two dimensional uncorrelated bias in fix algorithms
[NASA-CR-182683] N88-20847

Preconditioned conjugate gradient algorithms and software for solving large sparse linear systems
[DE88-002180] N88-20849
Conic algorithms for unconstrained minimization with special consideration of problems with large sparse Hessians: A summary of research performed
[DE88-002549] N88-20850
Algorithms with conic termination for nonlinear optimization
[DE88-005893] N88-20851
Method to evaluate image-recovery algorithms based on task performance
[DE88-005382] N88-20853
Experimental verification of a finite-difference time-domain thin slot algorithm
[DE88-005572] N88-20859
Approximation algorithms for scheduling unrelated parallel machines
[CWI-OS-R8714] N88-20861
Verification of a systolic algorithm for string comparison
[CWI-CS-R8734] N88-20873
Interpolation algorithms for digital terrain models
[INPE-4373-PRE/1196] N88-20877
Spectral element methods: Algorithms and architectures
[NASA-CR-182701] N88-20878
A report on the study of algorithms to enhance vector computer performance for the discretized one-dimensional time-dependent heat conduction equation: EPIC research, phase 1
[DE88-005642] N88-20880
An implementation of the OPS5 language for computers compatible with IBM-PC
[INPE-4291-PRE/1162] N88-20882
On the design of parallel numerical methods in message passing and shared memory environments
[DE88-003566] N88-20888
An amoeba replicated service organisation --- Amoeba operating system
[CWI-CS-R8723] N88-20892
Robustifying the Kalman filter
[AD-A189240] N88-20907
A study of data compactation using numerical methods
[INPE-4317-TDL/284] N88-20929
Local search for constrained routing problems --- traveling salesman
[CWI-OS-R8711] N88-20948
Passive autonomous infrared sensor technology
[AD-A188698] N88-21005
Optics for large telescope N88-21014
On the role of complete reducibility in general competitive equilibrium models
[DE88-005693] N88-21083

ALIPHATIC COMPOUNDS
Electrosorptive detection of simple organic compounds in liquid chromatography
[AD-A188757] N88-20376

ALKALI METALS
Kinetic mechanisms for ionization and afterburning suppression
[AD-A189219] N88-20383

ALKALINE BATTERIES
A new concept in an electrically rechargeable zinc-air alkaline battery
[DE88-003858] N88-20539

ALKANES
Photolytic formation of free radicals and their effect on hydrocarbon pyrolysis chemistry in a concentrated solar environment
[DE88-004129] N88-20730

ALKENES
Photolytic formation of free radicals and their effect on hydrocarbon pyrolysis chemistry in a concentrated solar environment
[DE88-004129] N88-20730

ALPHA PARTICLES
The calibration of photographic and spectroscopic films: The response of 2aO film to small dosages of alpha particles from 3/10th's rad to 8 rads at energy levels 153 MeV, 79 MeV and 47 MeV
[NASA-CR-177830] N88-20608

ALPHANUMERIC CHARACTERS
A comparison of two chord keyboard coding systems for alphanumeric data entry
[AD-A189230] N88-20834

ALTIMETRY
Tidal estimation in the Pacific with application to SEASAT altimetry
[NASA-TM-100694] N88-20780

ALUMINUM
The effect of microstructure on the fatigue crack growth resistance of nickel base superalloys
[AD-A189526] N88-20414
Aluminum-air battery development
[DE88-006617] N88-20542
Aluminum-air battery development
[DE88-006618] N88-20543

ALUMINUM ALLOYS
Composites strengthening
[AD-A189258] N88-20364
Threshold fatigue crack growth in Ti-6Al-2Sn-4Zr-6Mo
[AD-A189560] N88-20415
A calorimetric determination of the enthalpy of formation and a description of the defect structure of the ordered beta-phase /Ni, Cu/ /1-x/ Al/x/
[NASA-TT-20157] N88-20434
Processing of glass to aluminum (low melting metals) seals via an injection molding technique
[DE88-004689] N88-20468

ALUMINUM GALLIUM ARSENIDES
Pressure-dependent DLTS (Deep Level Transient Spectroscopy) experiments on Si-doped AlGaAs
[DE88-003842] N88-21047

ALUMINUM OXIDES
Characterization and fundamental studies on CuO sorbent materials to determine attrition mechanisms on substrate gamma alumina
[DE88-003674] N88-20456
Recommendations on developing polycrystalline alumina fiber N88-20502
Analytically modeling the carbothermic reduction of alumina in a thermal plasma
[DE88-005535] N88-21020

AMBIENT TEMPERATURE
Polymeric electrolytes for ambient temperature lithium batteries
[DE88-004896] N88-20547

AMORPHOUS SILICON
Research on high-efficiency, stacked, multijunction, amorphous silicon alloy thin-film solar cells
[DE88-001108] N88-20723
Progress of amorphous silicon based solar cells and modules
[DE88-004666] N88-20733
Investigations of the origins of metastable, light-induced changes in hydrogenated amorphous silicon
[DE88-001117] N88-21051

AMPLIFICATION
Fiber-coupled external-cavity semiconductor high power laser
[AD-A188454] N88-20611
Wavelength scaling of lithium-like recombination scheme for X-UV gain production --- X-ray lasers
[ETN-88-92002] N88-20634

AMPLIFIERS
Phase preservation cleanup in a double-pass Raman amplifier SBS (Stimulated Brillouin Scattering) conjugator
[AD-A189428] N88-20536
Advanced components for spaceborne infrared astronomy
[NASA-CR-177470] N88-20601
Wiggler taper optimization for free-electron-laser amplifiers with moderate space-charge effects
[DE88-003758] N88-20618

AMPLITUDES
Passive DF: A tutorial, part 1
[NASA-CR-182669] N88-20846

ANALOG TO DIGITAL CONVERTERS
Method for set-up for researching signal curve development
[NASA-TT-20235] N88-20526

ANALYSIS (MATHEMATICS)
Research in applied mathematics ralated to identification of noisy systems
[AD-A189355] N88-20908
Computation and graphics in mathematical research
[DE88-005796] N88-20953

ANALYSIS OF VARIANCE
The statistical characterization of tensile strengths for a nuclear-type graphite N88-20440

ANALYTIC GEOMETRY
Steps into a geometer's workbench
[CWI-CS-R8726] N88-20870
Geometry and graphics applied to robotics
[CWI-CS-R8727] N88-20903

ANEMOMETERS
Simulating high-resolution vertical plane array wind characteristics using lower-spatial-resolution wind measurements
[DE88-005626] N88-20761

ANGLES (GEOMETRY)
Reduction of erosion in elbows due to flow modifications, phase 1
[DE88-001028] N88-20584
A symmetric set of Euler angles and oblique orientation space sections
[DE88-005317] N88-21056

ANGULAR MOMENTUM
Modelling and control of an annular momentum control device
[NASA-CR-4138] N88-20491

ANHYDRIDES
Synthesis of energetic materials
[AD-A189115] N88-20482

ANISOTROPY
Anisotropy of microstructural eddy motion in surface layer during calm N88-20677
Electrical characteristics of MBE (Molecular Beam Epitaxyl)-grown GaAs/sub 1-x/Sb/sub x on InP and correlation with film microstructure
[DE88-003841] N88-21053
Early reheating and cosmic strings N88-21103

ANNEALING
Study of defects in metals by positron annihilation
[DE88-701042] N88-20432
Optical study of germanium, germanium plus arsenic, and germanium plus gallium implants in gallium arsenide
[AD-A189600] N88-21045

ANNIHILATION REACTIONS
Advanced space propulsion study - antiproton and beamed power propulsion
[AD-A189218] N88-20355
Proton/antiproton yields W(+/-)boson gamma X as a test of the quark charges
[NIKHEF-H/87-11] N88-20987

ANNUAL VARIATIONS
Seasonal variations and excitation mechanisms of the equatorially trapped waves N88-20751
Computer simulation of tropospheric chemistry
[JUEL-2144] N88-20756
Northern Hemisphere circulation and the principal components of subsequent summer patterns in North America and West Africa N88-20765

ANODES
Aluminum-air battery development
[DE88-006617] N88-20542

ANODIC COATINGS
ONR Far East Scientific Bulletin, volume 12, number 3, July-September 1987
[AD-A188554] N88-21081

ANOMALIES
Anomalous shock sensitivity/density relationship for RDX-polyethylene wax and related formulations from MRL Small Scale Gap Test (SSGT) measurements
[MRL-R-1099] N88-20399
Sample models of steady and low frequency circulations in the tropical atmosphere, with application to tropical air-sea interactions N88-20764
Computerised measurement of human horizontal smooth pursuit eye movements N88-20819

ANTARCTIC REGIONS
Feasibility report: Operation of light air cushion vehicle at McMurdo Sound, Antarctica
[AD-A189057] N88-20494
The 1987 Airborne Antarctic Ozone Experiment: The Nimbus-7 TOMS data atlas
[NASA-RP-1201] N88-20714
Activities and objectives of the Polar Research Board
[DE88-004543] N88-20747

ANTENNA ARRAYS
Estimation-correlation, modeling, and identification in adaptive array processors
[AD-A189130] N88-20512
Adaptive algorithms for HF antenna arrays
[AD-A189329] N88-20534

ANTENNA FEEDS
Modification of parabolic dish antenna pattern using two symmetrically placed circular flat plates
[AD-A189543] N88-20517

ANTENNA RADIATION PATTERNS
Modification of parabolic dish antenna pattern using two symmetrically placed circular flat plates
[AD-A189543] N88-20517

ANTENNAS
The evaluation and selection of a 5th ground antenna site for the global positioning system
[AD-A189495] N88-20286
Electromagnetic scattering from and natural resonances of the circular strip N88-20523
Optical RF distribution links for MMIC phased array antennas
[NASA-TM-100841] N88-20555

ANTIFRICTION BEARINGS
Corrosion-wear process under rolling-sliding motion
[AD-A189603] N88-20635

ANTIMONY ALLOYS
Electrical characteristics of MBE (Molecular Beam Epitaxyl)-grown GaAs/sub 1-x/Sb/sub x on InP and correlation with film microstructure
[DE88-003841] N88-21053

ANTIPROTONS
Advanced space propulsion study - antiproton and beamed power propulsion
[AD-A189218] N88-20355
APERTURES
Aberrations: Their effect on off-axis beam steering
[AD-A189601] N88-21008
APPLICATIONS PROGRAMS (COMPUTERS)
Dynamics of high-speed mechanisms with elastic members N88-20643
Computer software for the computation of the scattered field and the optical microscope image of line objects patterned in thick layers
[PB88-153705] N88-20838
APPROACH CONTROL
Flight simulations of MLS interception procedures applicable to laterally segmented approach paths
[NLR-MP-86037-U] N88-20288
APPROXIMATION
Approximation algorithms for scheduling unrelated parallel machines
[CWI-OS-R8714] N88-20861
Predicting oscillatory finite difference solutions to the heat equation: A comparative study of the coefficient and matrix methods
[AD-A189591] N88-20911
What do multistep methods approximate
[PB88-148838] N88-20932
ARC DISCHARGES
Arcs in cesium seeded noble gases resulting from a magnetically induced electric field
[EUT-87-E-177] N88-21028
ARCHITECTURE (COMPUTERS)
NAVLAB: An autonomous navigation testbed
[AD-A189049] N88-20283
Architecture specification for PAVE PILLAR avionics
[AD-A188722] N88-20303
Analysis for architecture for image processing
[INPE-4294-PRE/1165] N88-20715
Spectral element methods: Algorithms and architectures
[NASA-CR-182701] N88-20878
Distributed transaction processing and the Camelot system
[AD-A188614] N88-20885
A simulation study of a parallel processor with unbalanced loads
[AD-A189573] N88-20887
On the design of parallel numerical methods in message passing and shared memory environments
[DE88-003566] N88-20888
Locality, communication and interconnect length in multicomputers
[CWI-CS-R8708] N88-20890
Soar: An architecture for general intelligence
[AD-A188742] N88-20898
ARCTIC OCEAN
Predictions and studies with a one-dimensional ice/ocean model
[AD-A189158] N88-20776
Microwave and structural properties of saline ice
[AD-A189307] N88-20779
ARCTIC REGIONS
Activities and objectives of the Polar Research Board
[DE88-004543] N88-20747
ARGON
Electron stimulated desorption and coherent electron scattering
[AD-A189091] N88-20978
ARGON LASERS
Resonator coupling of two ring cavity, argon-ion lasers
[AD-A189558] N88-20616
Doubly periodic output from a dye laser pumped by a free-running argon laser
[DE88-005027] N88-20633
ARMATURES
Structural integrity of metallic armature rail guns
[AD-A188735] N88-20333
ARMED FORCES (FOREIGN)
Soviet military power, 1987 N88-21114
ARMOR
Hydrogen induced cracks in armor steel weldments fabricated with austenitic filler alloys
[AD-A188733] N88-20406
Texture profile in thermomechanically processed 2-inch-thick 5 Ni-steel armor plate
[AD-A189275] N88-20410
ARRAYS
Control strategies and hardware used in solar thermal applications
[DE88-004631] N88-20731
Simulating high-resolution vertical plane array wind characteristics using lower-spatial-resolution wind measurements
[DE88-005626] N88-20761
ARSENIC
Optical study of germanium, germanium plus arsenic, and germanium plus gallium implants in gallium arsenide
[AD-A189600] N88-21045
ARTIFICIAL INTELLIGENCE
Intelligent control of robot manipulators in hazardous environments
[DE88-003305] N88-20638
An implementation of the OPS5 language for computers compatible with IBM-PC
[INPE-4291-PRE/1162] N88-20882
The use of an automated flight test management system in the development of a rapid-prototyping flight research facility
[NASA-TM-100435] N88-20896
Mathematic modeling of visual perception problems
[INPE-4355-PRE/1186] N88-20897
Soar: An architecture for general intelligence
[AD-A188742] N88-20898
Knowledge retrieval as specialized inference
[AD-A189042] N88-20899
A Darwinian approach to artificial neural systems
[DE87-013184] N88-20900
Quality enhancement with machine intelligence
[DE88-005639] N88-20901
Aspects and applications of primary processing of visual information
[INPE-4290-PRE/1161] N88-21015
Application of expert systems in project management decision aiding
[NASA-CR-180762] N88-21074
ARTIFICIAL SATELLITES
Utilization of strapdown inertial and non-inertial sensors in determination of satellite attitude by Kalman filters
[INPE-4313-TDL/280] N88-20349
Aeronautics and space report of the President: 1986 activities N88-21087
ARTILLERY
Method for determining artillery position
[NASA-TT-20238] N88-20973
Method for determining artillery position
[NASA-TT-20237] N88-20974
ASCENT TRAJECTORIES
Optimal thrust vector control of coplanar orbital evasive maneuvers
[AD-A189544] N88-20346
ASSEMBLING
The space station assembly phase: Flight telerobotic servicer feasibility, volume 1
[NASA-CR-182689] N88-20351
The space station assembly phase: Flight telerobotic servicer feasibility. Volume 2: Methodology and case study
[NASA-CR-182690] N88-20352
ASTROMETRY
Preparation of photometric measurements on a million stars in the framework of the satellite project HIPPARCOS/TYCHO
[ETN-88-91502] N88-21093
ASTRONAUTICS
Soviet space transport systems N88-20328
ASTRONOMICAL MAPS
Solar microwave radiation maps measured at Metsaehovi Radio Research Station in 1978-1979
[PB88-127543] N88-21108
ASTROPHYSICS
Physics of condensed matter at extreme conditions
[DE88-006232] N88-20958
Very high energy gamma ray astrophysics
[DE88-005821] N88-21095
ASYMPTOTIC GIANT BRANCH STARS
Asymptotic giant branch populations in composite stellar systems N88-21098
ASYMPTOTIC METHODS
Steps into a geometer's workbench
[CWI-CS-R8726] N88-20870
ASYMPTOTIC SERIES
Survival analysis using additive risk models
[AD-A189053] N88-20906
Acoustic radiation from line- and point-loaded plates: Uniformly asymptotic solutions
[AD-A189367] N88-20969
ATLANTIC OCEAN
Propagation of subsurface salinity maximum in tropical Atlantic N88-20686
The use of a barotropic finite element model for the study of circulation on the continental shelf of the southeast coast of Brazil
[INPE-4401-PRE/1218] N88-20774
ATMOSPHERIC BOUNDARY LAYER
Similarity theories and microturbulence in the atmospheric mixed layer N88-20802
ATMOSPHERIC CHEMISTRY
Gas-chromatographic analysis of products of thermal reactions of aerosol in Venusian cloud layer on Vega-1 and Vega-2 automatic interplanetary stations N88-20318
Roentgenoradiometric analysis of aerosol in Venusian clouds by Vega-1 and Vega-2 automatic interplanetary stations N88-20319
Effect of nitrogen dioxide release on thermosphere N88-20704
Activities report in meteorology
[AR-86-87] N88-20755
Computer simulation of tropospheric chemistry
[JUEL-2144] N88-20756
ATMOSPHERIC CIRCULATION
Negative viscosity in global circulations N88-20685
Low-order spectral models of atmospheric circulation: A survey
[CWI-AM-R8705] N88-20748
Seasonal variations and excitation mechanisms of the equatorially trapped waves N88-20751
Model validation research: Comparison of simulated and observed climate patterns for the past 18,000 years
[DE88-004945] N88-20759
Sample models of steady and low frequency circulations in the tropical atmosphere, with application to tropical air-sea interactions N88-20764
Northern Hemisphere circulation and the principal components of subsequent summer patterns in North America and West Africa N88-20765
Planetary scale barotropic spectral model N88-20766
ATMOSPHERIC COMPOSITION
Vega-1 and Vega-2 automatic stations: Functioning of landing modules in Venusian atmosphere N88-20313
Research on absorption of UV radiation in Venusian atmosphere from Vega-1 and Vega-2 landing modules N88-20316
Gas-chromatographic analysis of products of thermal reactions of aerosol in Venusian cloud layer on Vega-1 and Vega-2 automatic interplanetary stations N88-20318
Chemical composition and structure of Venusian clouds determined from results of roentgenoradiometric experiments carried out by landing modules of Vega-1 and Vega-2 automatic interplanetary stations N88-20320
Effect of nitrogen dioxide release on thermosphere N88-20704
ATMOSPHERIC EFFECTS
Analysis of spectral reflectance characteristics of targets under satellites and automatic cloud recognition N88-20498
ATMOSPHERIC MODELS
A polarimetric rain backscatter model developed for coherent polarization diversity radar applications N88-20520
Low-order spectral models of atmospheric circulation: A survey
[CWI-AM-R8705] N88-20748
Dynamical modeling of marine boundary layer convection N88-20750
Computer simulation of tropospheric chemistry
[JUEL-2144] N88-20756
Model validation research: Comparison of simulated and observed climate patterns for the past 18,000 years
[DE88-004945] N88-20759
Sample models of steady and low frequency circulations in the tropical atmosphere, with application to tropical air-sea interactions N88-20764
Similarity theories and microturbulence in the atmospheric mixed layer N88-20802
Model of Jovian F region ionosphere
[NASA-CR-182587] N88-21105
ATMOSPHERIC OPTICS
Influence of nonlinear spectroscopic effects on atmospheric propagation of intense laser radiation at 10.6 microns wavelength N88-20705
ATMOSPHERIC PHYSICS
JPRS report: Science and technology. USSR: Earth sciences
[JPRS-UES-88-001] N88-20674
Activities report in meteorology
[AR-86-87] N88-20755
ATMOSPHERIC SCATTERING
Ozone sonde and Dobson spectrometer data obtained during the MAP/GLOBUS 1983 campaign over Western Europe
[BPT-5/87] N88-20771
ATMOSPHERIC SOUNDING
Roys and radiosondes in the region
[INPE-4362-PRE/1188] N88-20743
ATMOSPHERIC STRATIFICATION
Chemical composition and structure of Venusian clouds determined from results of roentgenoradiometric experiments carried out by landing modules of Vega-1 and Vega-2 automatic interplanetary stations N88-20320

ATMOSPHERIC TEMPERATURE
Thermal structure of Venusian Atmosphere determined from results of measurements from Vega-2 landing module N88-20315
Roys and radiosondes in the region [INPE-4362-PRE/1188] N88-20743
A study of satellite emission computed tomography [AD-A189567] N88-20745
ATMOSPHERIC TURBULENCE
Similarity theories and microturbulence in the atmospheric mixed layer N88-20802
ATOMIC INTERACTIONS
Competing interactions in metallic superlattices [DE88-005344] N88-21057
ATOMIC STRUCTURE
Tungsten-carbon multilayer system studied with X-ray scattering [DE88-005749] N88-20373
Model catalyst studies of SMSI (Strong Metal/Support Interactions) and the role of D-electrons in chemisorption and catalysis [DE88-004518] N88-20393
Properties of reactively sputtered WNx films Zhao, X. -A. [AD-A188711] N88-20976
Theoretical studies on the electronic structure and properties of complex ceramic crystals and glasses [DE88-005837] N88-21049
ATOMS
Theory of laser cooling and spectroscopy of harmonically trapped single atoms [AD-A189576] N88-20617
Spontaneous decay and atomic fluorescence near a metal surface of an absorbing dielectric [AD-A187508] N88-20975
ATTENUATION
Formulation of a general technique for predicting pneumatic attenuation errors in airborne pressure sensing devices [NASA-TM-100430] N88-20302
Phase velocity and attenuation of plane elastic waves in a particle-reinforced composite medium [AD-A189414] N88-20366
ATTITUDE CONTROL
Laser gyro attitude control system feasibility [AD-A189368] N88-20285
Utilization of strapdown inertial and non-inertial sensors in determination of satellite attitude by Kalman filters [INPE-4313-TDL/280] N88-20349
AUGER SPECTROSCOPY
An interpretation of the ethylenic, carbidic, and graphite auger lineshapes of chemisorbed carbon species [AD-A189092] N88-20379
AUSTENITE
Hydrogen induced cracks in armor steel weldments fabricated with austenitic filler alloys [AD-A188733] N88-20406
AUSTENITIC STAINLESS STEELS
The fatigue behavior of ferritic and austenitic steels at elevated temperatures [DE88-006304] N88-20431
Improved glass-ceramic to metal seals in actuator and detonator applications with an aluminum-containing austenitic stainless steel [DE88-004691] N88-20458
Investigation of the use of horizontally polarised shear waves for TOFD studies on austenitic steel [AERE-R-12145] N88-20649
AUSTRALIA
Recommended replacements for tetryl in Australian production fuzes and related ordnance [MRL-R-1089] N88-20489
Some properties of Australian produced explosive composition H-6 [MRL-TN-525] N88-20490
AUTOMATIC CONTROL
AVSCOM'S modifications to Teledyne Systems Company's air-to-air fire control system simulation model [AD-A189136] N88-20294
Analysis of spectral reflectance characteristics of targets under satellites and automatic cloud recognition N88-20498
The evaluation of automatic barometers, illustrated by the Nakaasa barometer [KNMI-TR-95] N88-20610
The use of an automated flight test management system in the development of a rapid-prototyping flight research facility [NASA-TM-100435] N88-20896
The automated symbolic derivation of state equations for dynamic systems [DE88-000968] N88-20945
AUTOMATIC PILOTS
Integrated autopilot/autothrottle based on a total energy control concept: Design and evaluation of additional autopilot modes [NASA-CR-4131] N88-20306
AUTONOMOUS NAVIGATION
NAVLAB: An autonomous navigation testbed [AD-A189049] N88-20283
AVIONICS
Architecture specification for PAVE PILLAR avionics [AD-A188722] N88-20303
AXIAL COMPRESSION LOADS
Fracture criterion of reactor graphite under multiaxial stresses N88-20442
AXIAL FLOW
Boundary effects on the drag of a cylinder in axial motion at low Reynolds number N88-20578
AXIAL FLOW PUMPS
High Reynolds number pump facility for cavitation research [AD-A189310] N88-20558
AXIAL LOADS
Fracture criterion of reactor graphite under multiaxial stresses N88-20442
Notch sensitivity of graphite materials for VHTR N88-20447
AXIOMS
Using design axioms and topology to model database semantics [CWI-CS-R8711] N88-20863
Algebra of Communicating Processes (ACP)tau: A universal axiom system for process specification [CWI-CS-R8725] N88-20869
A convergence theorem in process algebra [CWI-CS-R8733] N88-20920
AXISYMMETRIC BODIES
Nonaxisymmetric body supersonic, aerodynamic prediction [AD-A189338] N88-20259
Static performance of an axisymmetric nozzle with post-exit vanes for multiaxis thrust vectoring [NASA-TP-2800] N88-20280

B

BACKGROUND RADIATION
Specification for an infrared satellite surveillance system for the detection of aircraft [AD-A189592] N88-20748
A low-frequency measurement of the spectrum of the cosmic microwave background radiation N88-21112
BACKSCATTERING
A polarimetric rain backscatter model developed for coherent polarization diversity radar applications N88-20520
BALANCE
The effect of sting interference at low speeds on the drag coefficient of an ellipsoidal body using a magnetic suspension and balance system [NASA-CR-181611] N88-20274
Development of a torsion balance for adhesion measurements [NASA-TM-100799] N88-20454
BALLISTICS
A simplified computer code for reduction to burning rates of closed bomb pressure-time data (MINICB) [AD-A189112] N88-20380
BALLOONS
Adaptive control of scientific balloon-borne gondola attitude N88-20497
BAROCLINIC INSTABILITY
Numerical model of Rayleigh instability and spin-off eddies on fronts N88-20696
BAROMETERS
The evaluation of automatic barometers, illustrated by the Nakaasa barometer [KNMI-TR-95] N88-20610
BAROTROPISM
The use of a barotropic finite element model for the study of circulation on the continental shelf of the southeast coast of Brazil [INPE-4401-PRE/1218] N88-20774
BARS
Delamination stresses in semicircular laminated composite bars [NASA-TM-4026] N88-20375
BASE PRESSURE
Flight tests of external modifications used to reduce blunt base drag [NASA-TM-100433] N88-20279
BATCH PROCESSING
Scale-up of a batch-type chemical powder preparation process for high field varistor fabrication [DE88-006601] N88-20541
BATHING
The effects of normal and therapeutic baths on the central vascular organs of persons with healthy hearts, as measured by X-ray [NASA-TT-20252] N88-20818
BATHYMETERS
Bathymetric hazard survey test [AD-A189150] N88-20775
Inversion algorithms for geophysical problems [AD-A189252] N88-20845
BATTERY CHARGERS
A novel class of positive electrodes for rechargeable batteries [DE88-004559] N88-20545
BAYES THEOREM
Signal-filter design and system performance for polarimetric radar [AD-A189257] N88-20514
BEAM SPLITTERS
Space infrared telescope facility wide field and diffraction limited array camera (IRAC) [NASA-CR-182704] N88-21092
BEAMS (RADIATION)
Multimode-waveguide laser beam deflector [DE88-006222] N88-20622
Practical constraints on sources for pulsed beam lithographies [DE88-006594] N88-20623
Studies of compound states of negative ions using laser beams [DE88-004708] N88-20627
Aberrations: Their effect on off-axis beam steering [AD-A189601] N88-21008
BEAMS (SUPPORTS)
The Euler-Bernoulli beam equation with boundary energy dissipation [AD-A189517] N88-20560
Component mode synthesis using experimental modes enhanced by mass loading [DE88-006097] N88-20657
Finite element methodology for nonlinear free and harmonic forced vibrations of beam and plate structures N88-20663
Design graphs for the first two bending Eigenvibration forms of rotating beams consisting of two beam points [IW-86006R] N88-20670
BEARING (DIRECTION)
A comparison of terrain association and resection as methods of position location [AD-A189480] N88-20710
BEARINGS
Ply-level failure analysis of a graphite/epoxy laminate under bearing-bypass loading [NASA-TM-100578] N88-20372
BEHAVIOR
Describing constraints on a digital circuit's behavior [AD-A189200] N88-20531
BENDING DIAGRAMS
Design graphs for the first two bending Eigenvibration forms of rotating beams consisting of two beam points [IW-86006R] N88-20670
BENDING MOMENTS
The Euler-Bernoulli beam equation with boundary energy dissipation [AD-A189517] N88-20560
BIAS
Two dimensional uncorrelated bias in fix algorithms [NASA-CR-182683] N88-20847
Bias reduction when there is no unbiased estimate [AD-A189407] N88-20937
BIBLIOGRAPHIES
Aeronautical engineering: A continuing bibliography with indexes (supplement 224) [NASA-SP-7037(224)] N88-20254
Aerospace medicine and biology: A continuing bibliography with indexes (supplement 309) [NASA-SP-7011(309)] N88-20814
BIDIRECTIONAL REFLECTANCE
Summary of along-track data from the Earth radiation budget satellite for several major desert regions [NASA-RP-1197] N88-20772
BIG BANG COSMOLOGY
Particle physics and cosmology [DE88-004944] N88-21095
BINARY ALLOYS
Processing, structure and properties of heavily deformed in situ composites [AD-A189611] N88-20416
Erosion in dual-phase microstructures [DE88-004507] N88-20421
BINARY STARS
Very high energy gamma ray astrophysics [DE88-005821] N88-21095

BIOCHEMISTRY
Improved methods for high resolution electron microscopy
[DE88-005731] N88-20609
JPRS report: Science and technology. USSR: Life sciences
[JPRS-ULS-88-004] N88-20815
Technology '87: Research and Development Laboratory Technology Transfer Program
[DE88-003142] N88-21084
BIOGEOCHEMISTRY
Global mixed-layer natural and anthropogenic fluxes N88-20803
BIOLOGICAL EFFECTS
Aerospace medicine and biology: A continuing bibliography with indexes (supplement 309)
[NASA-SP-7011(309)] N88-20814
BIOLOGICAL MODELS (MATHEMATICS)
Regulation of hemodynamics upon imitation of the transition to weightlessness (mathematical modeling) N88-20817
BIOLOGY
JPRS report: Science and technology. China
[JPRS-CST-88-003] N88-20495
BIOPHYSICS
Biophysical applications of solid state and tritium NMR
[DE88-005328] N88-20806
JPRS report: Science and technology. USSR: Life sciences
[JPRS-ULS-88-004] N88-20815
BIOTECHNOLOGY
JPRS report: Science and technology. USSR: Life sciences
[JPRS-ULS-88-004] N88-20815
BIPOLAR TRANSISTORS
Quartz oscillator analysis
[DE88-005886] N88-20550
BIREFRINGENCE
Spectral contents readout of birefringent sensors
[NASA-CR-179430] N88-20673
Multiple scattering of polarized light in cirrus clouds N88-20768
BITUMENS
Aviation turbine fuels from tar sands bitumen and heavy oils. Part 3: Laboratory sample production
[AD-A189278] N88-20484
BL LACERTAE OBJECTS
Relativistic jet models for the BL Lacertae object Mrk 421 during three epochs of observation
[NASA-TM-89727] N88-21090
BLOOD CIRCULATION
The effects of normal and therapeutic baths on the central vascular organs of persons with healthy hearts, as measured by X-ray
[NASA-TT-20252] N88-20818
BLOOD PLASMA
Plasma cortisol, renin and aldosterone during an intense heat acclimation program
[AD-A189387] N88-20810
BLOOD VOLUME
Plasma cortisol, renin and aldosterone during an intense heat acclimation program
[AD-A189387] N88-20810
BLOWERS
Measurement and analysis of the noise radiated by low Mach numbers centrifugal blowers
[AD-A189226] N88-20966
BLUNT BODIES
Nonaxisymmetric body supersonic, aerodynamic prediction
[AD-A189338] N88-20259
Flight tests of external modifications used to reduce blunt base drag
[NASA-TM-100433] N88-20279
BODIES OF REVOLUTION
The effect of sting interference at low speeds on the drag coefficient of an ellipsoidal body using a magnetic suspension and balance system
[NASA-CR-181611] N88-20274
BODY TEMPERATURE
Plasma cortisol, renin and aldosterone during an intense heat acclimation program
[AD-A189387] N88-20810
BOILERS
Proceedings of the 1987 International Symposium on Condensing Heat Exchangers
[DE88-005230] N88-20564
BOILING
Prediction of high-temperature thermodynamic properties of mixed electrolyte solutions including solubility equilibria, vapor pressure depression and boiling point elevation
[DE88-006344] N88-21089
BOMBS (ORDNANCE)
A simplified computer code for reduction to burning rates of closed bomb pressure-time data (MINICB)
[AD-A189112] N88-20380
BONDING
Interfacial adhesion: Theory and experiment
[NASA-TM-100830] N88-20417
BONE MINERAL CONTENT
Use of diphosphonates to correct disorders in calcium metabolism and mineral composition of bone tissue with 60-day hypokinesia in rats
[NASA-TT-20220] N88-20807
BORIDES
The relationship of the chemical bonding topology of high critical temperature copper oxide superconductors to that of the chevrel phases and the ternary lanthanide rhodium borides
[AD-A189255] N88-21042
BORON NITRIDES
A segmented calorimeter for low-energy particle beams in space
[DE88-001806] N88-20997
BOSON FIELDS
Searches for forces weaker than gravity
[DE88-003579] N88-20959
BOSONS
Searches for forces weaker than gravity
[DE88-003579] N88-20959
Proton/antiproton yields W(+/-)boson gamma X as a test of the quark charges
[NIKHEF-H/87-11] N88-20987
BOUNDARY ELEMENT METHOD
An analysis of large deformation axisymmetric inelastic problems by finite element and boundary element methods N88-20664
BOUNDARY LAYER CONTROL
Development of disturbances in swept wing flows
[NASA-CR-182675] N88-20574
BOUNDARY LAYER EQUATIONS
Pseudo-stationary oblique-shock-wave reflections in low gamma gases: Isobutane and sulphur hexafluoride
[UTIAS-TN-267] N88-20576
General fuselage coordinates for the calculation of three-dimensional boundary layers
[MBB/LKE-122/S/PUB/244] N88-20596
BOUNDARY LAYER FLOW
The design and use of a temperature-compensated hot-film anemometer system for boundary-layer flow transition detection on supersonic aircraft
[NASA-TM-100421] N88-20304
Numerical experiments on the stability of controlled boundary layers
[NASA-CR-181649] N88-20591
General fuselage coordinates for the calculation of three-dimensional boundary layers
[MBB/LKE-122/S/PUB/244] N88-20596
BOUNDARY LAYER SEPARATION
Interaction between two-dimensional sonic jets and supersonic flow to model heat addition in a supersonic combustor
[AD-A189572] N88-20261
Coherent structure-reflective turbulent viscous flow modeling
[AD-A188339] N88-20556
BOUNDARY LAYER TRANSITION
Development of disturbances in swept wing flows
[NASA-CR-182675] N88-20574
Preliminary in-flight boundary layer transition measurements on a 45 deg swept wing at Mach Numbers between 0.9 and 1.8
[NASA-TM-100412] N88-20598
Turbulent transfer of momentum and heat in boundary layer of fluid beyond an obstacle. 1: Hydrodynamic characteristics N88-20690
BOUNDARY LAYERS
A finite-amplitude analysis of the buoyant instability of a highly viscous film over a less viscous half-space N88-20581
Dynamical modeling of marine boundary layer convection N88-20750
BOUNDARY VALUE PROBLEMS
Predicting oscillatory finite difference solutions to the heat equation: A comparative study of the coefficient and matrix methods
[AD-A189591] N88-20911
Convergence of Runge-Kutta methods on classes of stiff initial value problems
[CWI-NM-R8717] N88-20924
Double layer polarization of nonconducting spheroidal particles and its application to Kerr effect
[ISSN-0208-05658] N88-20960
BRAZIL
The use of a barotropic finite element model for the study of circulation on the continental shelf of the southeast coast of Brazil
[INPE-4401-PRE/1218] N88-20774
BREAKING
Buckling and breakdown problems in structural mechanics. Failure of prestressed double-walled containers or rings
[MBB-UR-E-956/87] N88-20671
BREEDER REACTORS
Outlook for the fusion hybrid and tritium-breeding fusion reactors
[PB88-149281] N88-21029
BRIGHTNESS
Research on influence of individual sea water components on spectral brightness coefficient of outgoing radiation N88-20682
IUE program SUGSD: Varability time scale of H Ly-alpha from Uranus
[NASA-CR-182706] N88-21107
BRIGHTNESS DISTRIBUTION
Some periodicities in motion of Halley's Comet relative to center of mass N88-20324
Spectral reflective characteristics of sea surface N88-20676
BRILLOUIN EFFECT
Phase preservation cleanup in a double-pass Raman amplifier SBS (Stimulated Brillouin Scattering) conjugator
[AD-A189428] N88-20536
BRITTLENESS
A study of the dynamics of high temperature brittle intergranular fracture by acoustic emission
[AERE-R-12479] N88-20650
Guidelines for estimation and characterization of the thermo-mechanical properties of new optical materials
[DE88-004359] N88-21010
BROADBAND
Bragg-cell receiver study
[NASA-CR-182684] N88-20535
Broadband correlation analysis
[AD-A188732] N88-20839
Optimal and conventional space-time processing in flow noise
[AD-A189104] N88-20965
BROKEN SYMMETRY
Diffraction theory in QCD and beyond
[DE88-005958] N88-20992
BUBBLES
Cavitation inception
[AD-A189220] N88-20557
Some problems of the theory of bubble growth and condensation in bubble chambers
[NASA-TT-20232] N88-20593
BUCKLING
Buckling and breakdown problems in structural mechanics. Failure of prestressed double-walled containers or rings
[MBB-UR-E-956/87] N88-20671
BURNING RATE
A simplified computer code for reduction to burning rates of closed bomb pressure-time data (MINICB)
[AD-A189112] N88-20380
BUTANES
Pseudo-stationary oblique-shock-wave reflections in low gamma gases: Isobutane and sulphur hexafluoride
[UTIAS-TN-267] N88-20576
BUTENES
High-temperature thermosets derived from the Diels-Alder polymerization of bisbenzocyclobutenes and bimaleimides
[AD-A188800] N88-20449

C

CADMIUM TELLURIDES
CdZnTe as a wide-band-gap absorber for a tandem, thin-film solar cell
[DE88-001114] N88-20724
Research on single-crystal CdTe solar cells
[DE88-001115] N88-20725
Thin-film cadmium telluride solar cells
[DE88-001107] N88-21050
CALCIUM METABOLISM
Use of diphosphonates to correct disorders in calcium metabolism and mineral composition of bone tissue with 60-day hypokinesia in rats
[NASA-TT-20220] N88-20807
CALCULUS OF VARIATIONS
Inversion algorithms for geophysical problems
[AD-A189252] N88-20845
Nonlinear differential equations
[DE88-006047] N88-20933
CALIBRATING
A low-frequency measurement of the spectrum of the cosmic microwave background radiation N88-21112
CALORIMETERS
High resolution hadron calorimetry
[NIKHEF-H/87-8] N88-20605

Energy loss of particles in dense matter-calorimetry
[NIKHEF-H/87-12] N88-20988
A segmented calorimeter for low-energy particle beams in space
[DE88-001806] N88-20997

CAMBER
An experimental investigation of decelerating flow about two-dimensional cambered plates
[DE88-006598] N88-20567

CAMERA SHUTTERS
Analysis of spectral reflectance characteristics of targets under satellites and automatic cloud recognition N88-20498

CAMERAS
Space infrared telescope facility wide field and diffraction limited array camera (IRAC)
[NASA-CR-182704] N88-21092

CANONICAL FORMS
Introduction to classical mechanics of systems with constraints, part 1
[TI88-701055] N88-20957
Introduction to classical mechanics of systems with constraints, part 3
[TI88-701057] N88-21073

CANOPIES (VEGETATION)
Remote sensing of earth terrain
[NASA-CR-182677] N88-20711

CARBON
Tungsten-carbon multilayer system studied with X-ray scattering
[DE88-005749] N88-20373
An interpretation of the ethylenic, carbidic, and graphite auger lineshapes of chemisorbed carbon species
[AD-A189092] N88-20379
Improved methods for high resolution electron microscopy
[DE88-005731] N88-20609

CARBON DIOXIDE CONCENTRATION
Model validation research: Comparison of simulated and observed climate patterns for the past 18,000 years
[DE88-004945] N88-20759

CARBON DIOXIDE LASERS
Coherent laser radar system theory
[AD-A188759] N88-20612
Influence of nonlinear spectroscopic effects on atmospheric propagation of intense laser radiation at 10.6 microns wavelength N88-20705

CARBON FIBER REINFORCED PLASTICS
Reinforcing of thermoplastic polycarbonate and polysulfone with carbon fibers: Production and characteristics of UD-compound objects
[NASA-TT-20158] N88-20374

CARBON STARS
Asymptotic giant branch populations in composite stellar systems N88-21098

CARBON STEELS
Development of a constitutive equation for HSLA (High-Strength Low-Alloy)-100 at cryogenic temperatures
[AD-A189243] N88-20408

CARBON-CARBON COMPOSITES
Nondestructive evaluation of carbon-carbon coatings
[AD-A189524] N88-20453

CARDIOVASCULAR SYSTEM
The effects of normal and therapeutic baths on the central vascular organs of persons with healthy hearts, as measured by X-ray
[NASA-TT-20252] N88-20818

CASTING
SBIR-Long fluoride fiber
[AD-A188595] N88-20492

CASTINGS
Hydrogen induced cracks in armor steel weldments fabricated with austenitic filler alloys
[AD-A188733] N88-20406

CATALYSIS
Model catalyst studies of SMSI (Strong Metal/Support Interactions) and the role of D-electrons in chemisorption and catalysis
[DE88-004516] N88-20393

CATALYSTS
Novel catalysts for methane activation
[DE88-003637] N88-20390
A new polymer-based hydrogen getter
[DE88-004538] N88-20467

CATHODES
A novel class of positive electrodes for rechargeable batteries
[DE88-004559] N88-20545

CAVITATION FLOW
Cavitation inception
[AD-A189220] N88-20557
High Reynolds number pump facility for cavitation research
[AD-A189310] N88-20558

CAVITY RESONATORS
Progress in diagnostic techniques for SC cavities
[CEBAF-PR-88-003] N88-20600
Resonator coupling of two ring cavity, argon-ion lasers
[AD-A189556] N88-20616

CEMENTS
Use of reinforced inorganic cement materials for spark wire and drift chamber wire frames
[NASA-CR-180759] N88-20438
The effect of Ca(OH)2-treated ceramic microspheres on the mechanical properties of high-temperature lightweight cement composites
[DE88-004590] N88-20457

CENTER OF MASS
Some periodicities in motion of Halley's Comet relative to center of mass N88-20324

CENTRIFUGAL FORCE
Measurement and analysis of the noise radiated by low Mach numbers centrifugal blowers
[AD-A189226] N88-20966

CERAMIC MATRIX COMPOSITES
Activities report of the Materials Department
[ETN-88-91984] N88-20436

CERAMIC NUCLEAR FUELS
Cermet-fueled reactors for advanced space applications
[DE88-005528] N88-21002

CERAMICS
A new process for synthesis of silicon nitride powders for advanced ceramics
[AD-A189354] N88-20451
Development of a torsion balance for adhesion measurements
[NASA-TM-100799] N88-20454
The effect of Ca(OH)2-treated ceramic microspheres on the mechanical properties of high-temperature lightweight cement composites
[DE88-004590] N88-20457
Improved glass-ceramic to metal seals in actuator and detonator applications with an aluminum-containing austenitic stainless steel
[DE88-004691] N88-20458
Ultrasonic characterization of non-uniform porosity distributions in SiC ceramic
[DE88-004814] N88-20459
Interfacial chemistry-structure and fracture of ceramic composites
[DE88-005516] N88-20461
PNL-1 improved ceramic composites through controlled fiber matrix interaction
[DE88-005680] N88-20462
Abrasion and impact resistant coatings
[DE88-003562] N88-20464
Advances in X-ray line profile analysis to determine microstructure information about ceramics
[DE88-003938] N88-20465
Micromechanical and microstructural studies of ceramic superplasticity
[DE88-005793] N88-20472
Recent developments in nondestructive evaluation for structural ceramics
[DE88-005889] N88-20473
X-ray computed tomography for structural ceramic applications: Beam hardening corrections
[DE88-005891] N88-20474
Processing of nanophase ceramics
[DE88-005985] N88-20475
Theory and experiments of fracture in cyclic compression: Single phase ceramics, transforming ceramics and ceramic composites
[DE88-005792] N88-20659
Fracture criteria for discontinuously reinforced metal matrix composites
[NASA-CR-182665] N88-20662
Theoretical studies on the electronic structure and properties of complex ceramic crystals and glasses
[DE88-005837] N88-21049
A hydroxycarbonate route to superconductor precursor powders
[DE88-003638] N88-21052
ONR Far East Scientific Bulletin, volume 12, number 3, July-September 1987
[AD-A188554] N88-21081

CEREBRAL CORTEX
Retinotopic mapping of the human visual system with magnetoencephalography
[AD-A189557] N88-20811

CERMETS
Cermet-fueled reactors for advanced space applications
[DE88-005528] N88-21002
Molybdenum-base cermet fuel development
[DE88-005529] N88-21003

CESIUM
Arcs in cesium seeded noble gases resulting from a magnetically induced electric field
[EUT-87-E-177] N88-21028

CHAOS
Stochastic and chaotic oscillations
[CWI-AM-R8704] N88-20940

CHARACTERIZATION
The synthesis, characterization and structural studies of In(C5H4Me) by X-ray diffraction and electron diffraction techniques and a reinvestigation of the crystalline state of In(C5H5) by X-ray diffraction studies
[AD-A189110] N88-21038

CHARGE TRANSFER
Mode priming in an overmoded gyrotron oscillator
[AD-A189151] N88-20602
Characteristics of the positive lighting flash
[DE88-005854] N88-20760

CHARGED PARTICLES
Velocity and concentration measurements in flowing suspensions by nuclear magnetic resonance
[DE88-006225] N88-20589

CHEBYSHEV APPROXIMATION
Electromagnetic scattering from and natural resonances of the circular strip N88-20523
A study of data compactation using numerical methods
[INPE-4317-TDL/284] N88-20929

CHEMICAL ANALYSIS
Fuels combustion research
[AD-A189114] N88-20381
Development and evaluation of supercritical fluid chromatography-mass spectrometry
[DE88-005122] N88-20394
Improved methods for high resolution electron microscopy
[DE88-005731] N88-20609
Plasma cortisol, renin and aldosterone during an intense heat acclimation program
[AD-A189387] N88-20810
On the structure of pulsed plasma jets N88-21030

CHEMICAL BONDS
Properties of molecular solids and fluids at high pressure and temperature
[DE88-004195] N88-20391
Improved glass-ceramic to metal seals in actuator and detonator applications with an aluminum-containing austenitic stainless steel
[DE88-004691] N88-20458
The relationship of the chemical bonding topology of high critical temperature copper oxide superconductors to that of the chevrel phases and the ternary lanthanide rhodium borides
[AD-A189255] N88-21042

CHEMICAL COMPOSITION
Gas-chromatographic analysis of products of thermal reactions of aerosol in Venusian cloud layer on Vega-1 and Vega-2 automatic interplanetary stations N88-20318
Roentgenoradiometric analysis of aerosol in Venusian clouds by Vega-1 and Vega-2 automatic interplanetary stations N88-20319
Determining chemical composition of aerosol in Venusian cloud layer on Vega-1 automatic interplanetary station using Malakhit mass spectrum analyzer N88-20321
Elemental composition of Venusian rocks in northeastern part of Terra Aphrodite (determined using data from Vega-2 landing module) N88-20322
Content of natural radioactive elements in Venusian rocks determined using data from Vega-1 and Vega-2 stations N88-20323
Results of infrared spectrometer experiment. 1: Infrared radiation of parent molecules in Halley's Comet N88-20325
The effect of microstructure on the fatigue crack growth resistance of nickel base superalloys
[AD-A189526] N88-20414
On the structure of pulsed plasma jets N88-21030

CHEMICAL ENERGY
Molecular collision processes in gases and at surfaces
[AD-A189518] N88-20982

CHEMICAL REACTIONS
MOPAC manual: A general molecular orbital package, fourth edition
[AD-A188623] N88-20362
Combustion theory and related questions
[AD-A189160] N88-20382
Kinetic mechanisms for ionization and afterburning suppression
[AD-A189219] N88-20383
Potassium cuprate (3)
[NASA-TT-20246] N88-20401
Scale-up of a batch-type chemical powder preparation process for high field varistor fabrication
[DE88-006601] N88-20541

Experimental and theoretical constraints on the origin of mid-ocean ridge geothermal fluids N88-20784
Solid-state electrochemical processes in dye films [AD-A188756] N88-21036

CHEMISORPTION
An interpretation of the ethylenic, carbidic, and graphite auger lineshapes of chemisorbed carbon species [AD-A189092] N88-20379
Model catalyst studies of SMSi (Strong Metal/Support Interactions) and the role of D-electrons in chemisorption and catalysis [DE88-004518] N88-20393

CHINA
JPRS report: Science and technology. China [JPRS-CST-87-030] N88-20501

CHIPS (ELECTRONICS)
Laser programming integrated circuits [AD-A189590] N88-20537
Gridless routing for generalized cell assemblies: Report and user manual [EUT-87-E-180] N88-20549
Modulatable thin film field emission space gun [AD-A189279] N88-21043

CHLORINE COMPOUNDS
Decomposition of hypochlorite in the presence of copper in a homogeneous medium [NASA-TT-20199] N88-20403

CHOLESKY FACTORIZATION
Data traffic reduction schemes for sparse Cholesky factorizations [NASA-CR-181626] N88-20831

CHROMATOGRAPHY
Fuels combustion research [AD-A189114] N88-20381

CHRONOLOGY
Early reheating and cosmic strings N88-21103

CIRCULAR CYLINDERS
Nonaxisymmetric body supersonic, aerodynamic prediction [AD-A189338] N88-20259
Body tensor formalism in finite deformation elasticity and application to the torsion of a circular cylinder N88-20651

CIRCULAR POLARIZATION
Mode priming in an overmoded gyrotron oscillator [AD-A189151] N88-20602
Polarization properties of SiO masers N88-21113

CIVIL AVIATION
Activities report in civil aeronautics [ETN-88-91344] N88-20255
Availability and cost estimate of a high naphthene, modified aviation turbine fuel [NASA-TM-100823] N88-20455

CLADDING
SBIR-Long fluoride fiber [AD-A186595] N88-20492

CLASSICAL MECHANICS
Introduction to classical mechanics of systems with constraints, part 1 [TI86-701055] N88-20957
Introduction to classical mechanics of systems with constraints, part 2 [TI86-701056] N88-21072
Introduction to classical mechanics of systems with constraints, part 3 [TI86-701057] N88-21073

CLASSIFICATIONS
Asymptotic giant branch populations in composite stellar systems N88-21098

CLASSIFYING
Method for determining the coordinates of sound sources by means of a sound measurement system [NASA-TT-20242] N88-20972

CLEANING
Thermal oxide growth on silicon: Intrinsic stress and silicon cleaning effects [AD-A188790] N88-20377

CLIMATE
Predictions and studies with a one-dimensional ice/ocean model [AD-A189158] N88-20776

CLIMATOLOGY
JPRS report: Science and technology. USSR: Earth sciences [JPRS-UES-88-001] N88-20674
Sample models of steady and low frequency circulations in the tropical atmosphere, with application to tropical air-sea interactions N88-20764
Predictions and studies with a one-dimensional ice/ocean model [AD-A189158] N88-20776

CLINICAL MEDICINE
Technology '87: Research and Development Laboratory Technology Transfer Program [DE88-003142] N88-21084

CLOCKS
A survey of provably correct fault-tolerant clock synchronization techniques [NASA-TM-100553] N88-20894

CLOUD PHYSICS
Gas-chromatographic analysis of products of thermal reactions of aerosol in Venusian cloud layer on Vega-1 and Vega-2 automatic interplanetary stations N88-20318

CLOUDS
Chemical composition and structure of Venusian clouds determined from results of roentgenoradiometric experiments carried out by landing modules of Vega-1 and Vega-2 automatic interplanetary stations N88-20320
Determining chemical composition of aerosol in Venusian cloud layer on Vega-1 automatic interplanetary station using Malakhit mass spectrum analyzer N88-20321
Synchronous measurements of effective photon path length in visible and near-IR spectral regions in real cloud systems N88-20706

CLOUDS (METEOROLOGY)
Analysis of spectral reflectance characteristics of targets under satellites and automatic cloud recognition N88-20498

CLUSTER ANALYSIS
The coordination cluster theory for metallic solutions [DE88-005934] N88-20389

CLUSTERS
Transition metal cluster chemistry [AD-A188731] N88-20405

CLUTTER
Signal-filter design and system performance for polarimetric radar [AD-A189257] N88-20514
A preliminary assessment of thunderstorm outflow wind measurement with airport surveillance radars [AD-A189064] N88-20757

COAL DERIVED LIQUIDS
Development and evaluation of supercritical fluid chromatography-mass spectrometry [DE88-005122] N88-20394

COASTAL CURRENTS
The use of a barotropic finite element model for the study of circulation on the continental shelf of the southeast coast of Brazil [INPE-4401-PRE/1218] N88-20774

COASTAL WATER
Circulation and exchange processes on the South Atlantic Bight Continental Shelf [DE88-003330] N88-20781
Mechanical properties of sea ice and sea ice deformation in the near-shore zone [PB88-147889] N88-20782
Mixed-layer fronts in the California current N88-20794

COATING
Molecular dynamics of laser ablation of a polymer coating [DE88-004337] N88-20466

COATINGS
The influence of the fiber-matrix bond on the mechanical behavior of NICALON/SiC composites [DE88-006155] N88-20369
Optimization of binary pigment coatings [AD-A189103] N88-20450
PNL-1 improved ceramic composites through controlled fiber matrix interaction [DE88-005680] N88-20462
Causes of damage in multilayer dielectric coatings exposed to high average power visible laser radiation [DE88-005363] N88-20619

COAXIAL CABLES
The preparation, assembly and mounting of RF coaxial cables [ESA-PSS-01-718-ISS-1] N88-20504

COCKPITS
CODAC (Cockpit Oriented Display of Aircraft Configurations) version 1.4 user's guide [NASA-CR-181650] N88-20273

CODERS
A hybrid transform/DPCM encoder for data compression [DE87-014852] N88-20518

CODING
Trajectory code studies, 1987 [DE88-008218] N88-20335
A comparison of two chord keyboard coding systems for alphanumeric data entry [AD-A189230] N88-20834
MASPLT: A one-dimensional graphics post processor for wave propagation codes [DE88-005506] N88-20856
CSOPLT: A graphics post processor for multidimensional wave propagation codes [DE88-005508] N88-20858
An integrated data description language for coding design knowledge [CWI-CS-R8731] N88-20871

COEFFICIENTS
Determination of the partition coefficients of organophosphorus compounds using high-performance liquid chromatography [AD-A189276] N88-20385
Transformation coefficient in wave-field acceleration scheme [DE88-700158] N88-20507
Predicting oscillatory finite difference solutions to the heat equation: A comparative study of the coefficient and matrix methods [AD-A189591] N88-20911

COGNITION
A personalized and prescriptive decision aid for choice from a database of options [AD-A188726] N88-20820
Mental models of mechanical systems: Individual differences in qualitative and quantitative reasoning [AD-A189035] N88-20823
Human problem solving in dynamic environments. Understanding and supporting operators in large-scale, complex systems [AD-A189539] N88-20826
Online aiding for human-computer interfaces [AD-A189239] N88-20842
Soar: An architecture for general intelligence [AD-A188742] N88-20898

COHERENT RADAR
Coherent laser radar system theory [AD-A188759] N88-20612

COHERENT SCATTERING
Electron stimulated desorption and coherent electron scattering [AD-A189091] N88-20978
Image charge, coherent scattering, and symmetry effects in electron stimulated desorption: O(-) from O sub 2 condensed on metals [AD-A189093] N88-20979

COLD PLASMAS
Experimental studies of plasma heating due to the parametric decay of a large amplitude pump into lower hybrid waves N88-21017

COLLISION RATES
Helical ripple transport in stellarators at low collision frequency [DE88-006431] N88-21031

COLLISIONLESS PLASMAS
Helical ripple transport in stellarators at low collision frequency [DE88-006431] N88-21031

COLOR
Graphics and flow visualization of computer generated flow fields [NASA-CR-182679] N88-20573

COLUMBUS SPACE STATION
Feasibility demonstration of a sensor for high-quality two-phase flow — Space Station [NLR-TR-87009-U] N88-20569

COMBUSTIBLE FLOW
Measurement of rate constants of elementary gas reactions of importance to upper atmosphere and combustion systems [AD-A189432] N88-20388

COMBUSTION
The effect of combustion gas flow on the rotational dynamics of a spinning solid fuel rocket N88-20358
Combustion theory and related questions [AD-A189160] N88-20382
Uncertainties in hydrogen combustion [DE88-005354] N88-20395

COMBUSTION CHAMBERS
Interaction between two-dimensional sonic jets and supersonic flow to model heat addition in a supersonic combustor [AD-A189572] N88-20261

COMBUSTION PHYSICS
A study of combustion and flow behaviour in solid-propellant rocket motors [UTIAS-280] N88-20357

COMBUSTION PRODUCTS
Fuels combustion research [AD-A189114] N88-20381

COMET NUCLEI
Results of infrared spectrometer experiment. 1: Infrared radiation of parent molecules in Halley's Comet N88-20325
Results of infrared spectrometer experiment. 2: Infrared radiometry of nucleus of Halley's Comet N88-20326

COMETARY ATMOSPHERES
A mass spectrometer evolved gas analysis experiment for in-situ analysis of cometary dust volatiles N88-21097

COMMERCE
Spin off businesses as mechanisms for transferring technologies
[DE88-005640] N88-21085
COMMINUTION
Characterization and fundamental studies on CuO sorbent materials to determine attrition mechanisms on substrate gamma alumina
[DE88-003674] N88-20456
COMMUNICATING
Online aiding for human-computer interfaces
[AD-A189239] N88-20842
COMMUNICATION CABLES
Aging properties of cable polmers (2)
[NASA-TT-20228] N88-20479
COMMUNICATION NETWORKS
Alternative force structuring strategies for military satellite communication systems
[AD-A189492] N88-20516
Human problem solving in dynamic environments. Understanding and supporting operators in large-scale, complex systems
[AD-A189539] N88-20826
COMPARISON
A comparative assessment of US and UK explosives qualified as replacements for tetryl
[MRL-R-1094] N88-20486
A comparison of terrain association and resection as methods of position location
[AD-A189480] N88-20710
Stochastic comparisons of order statistics, with applications in reliability
[AD-A189408] N88-20938
COMPATIBILITY
High-temperature thermosets derived from the Diels-Alder polymerization of bisbenzocyclobutenes and bimaleimides
[AD-A188800] N88-20449
Compatibility in space reactor fuel systems
[DE88-005698] N88-21004
COMPETITION
Competing interactions in metallic superlattices
[DE88-005344] N88-21057
COMPLEX SYSTEMS
On the sensitivity of complex, internally coupled systems
[NASA-TM-100537] N88-20829
COMPONENT RELIABILITY
Estimating system and component reliabilities under partial information on cause of failure
[AD-A189107] N88-20653
COMPOSITE MATERIALS
Compression of composite materials: A review
[AD-A189272] N88-20365
Phase velocity and attenuation of plane elastic waves in a particle-reinforced composite medium
[AD-A189414] N88-20366
The influence of the fiber-matrix bond on the mechanical behavior of NICALON/SiC composites
[DE88-006155] N88-20369
Delamination stresses in semicircular laminated composite bars
[NASA-TM-4026] N88-20375
The effect of Ca(OH)2-treated ceramic microspheres on the mechanical properties of high-temperature lightweight cement composites
[DE88-004590] N88-20457
PNL-1 improved ceramic composites through controlled fiber matrix interaction
[DE88-005680] N88-20462
Micromechanical and microstructural studies of ceramic superplasticity
[DE88-005793] N88-20472
Theory and experiments of fracture in cyclic compression: Single phase ceramics, transforming ceramics and ceramic composites
[DE88-005792] N88-20659
Activities report in aeronautics and astronautics
[ETN-88-91332] N88-21115
COMPOSITE PROPELLANTS
Laser ignition of nitramine composite propellants and crack propagation and branching in burning solid propellants
[AD-A189260] N88-20483
COMPOSITE STRUCTURES
Standardized environmental fatigue sequence for the evaluation of composite components in combat aircraft (ENSTAFF = ENvironmental falSTAFF)
[LBF-FB-179] N88-20300
A preliminary investigation of finite-element modeling for composite rotor blades
[NASA-TM-100559] N88-20656
COMPRESSIBILITY
Compression of composite materials: A review
[AD-A189272] N88-20365
COMPRESSIBLE FLOW
Computational technique for compressible vortex flows using the integral equation solution
[NASA-CR-182695] N88-20271
Slip velocity method for three-dimensional compressible turbulent boundary layers
[NASA-TM-100586] N88-20592
COMPRESSING
Theory and experiments of fracture in cyclic compression: Single phase ceramics, transforming ceramics and ceramic composites
[DE88-005792] N88-20659
Parallel image compression
[NASA-CR-180758] N88-20837
COMPRESSION LOADS
Geodetic measurement of deformation east of the San Andreas fault in Central California
[NASA-CR-182709] N88-20754
COMPRESSION TESTS
Compression of composite materials: A review
[AD-A189272] N88-20365
Notch sensitivity of graphite materials for VHTR
N88-20447
COMPRESSIVE STRENGTH
Statistical considerations of graphite strength for assessing design allowable stresses N88-20441
Effects of high temperature neutron irradiation on the physical, chemical and mechanical properties of fine-grained isotropic graphite N88-20444
The effect of Ca(OH)2-treated ceramic microspheres on the mechanical properties of high-temperature lightweight cement composites
[DE88-004590] N88-20457
COMPRESSOR EFFICIENCY
Efficiency characteristics of speed modulated drives at predicted torque conditions for air-to-air heat pumps
[DE88-005846] N88-20588
COMPUTATION
Application of a flux vector splitting methodology towards the solution of unsteady transonic flows, with future emphasis on the blade flutter problem
[AD-A189500] N88-20260
Implementation of a 3-D nonlinear MHD (magnetohydrodynamics) calculation on the Intel hypercube
[DE88-000625] N88-20848
Computing with structured connections networks
[AD-A189244] N88-20886
Numerical solution of ill posed problems in partial differential equations
[AD-A189383] N88-20909
Algebraic specifications for parameterized data types: The case of minimal computable algebras and parameters with equality
[CWI-CS-R8714] N88-20916
Computation and graphics in mathematical research
[DE88-005796] N88-20953
A low-frequency measurement of the spectrum of the cosmic microwave background radiation N88-21112
COMPUTATIONAL FLUID DYNAMICS
Application of a nonisentropic full potential method to AGARD standard airfoils
[NASA-TM-100560] N88-20263
Computational technique for compressible vortex flows using the integral equation solution
[NASA-CR-182695] N88-20271
Mixing of viscous fluids: Behavior of microstructures and chaos
[DE88-006287] N88-20566
Three-dimensional shear layer experiments and their use as test cases for calculation methods
[NLR-MP-86036-U] N88-20570
Solution of two-dimensional Euler equations: Experience with a finite volume code
[DFVLR-FB-87-41] N88-20572
Graphics and flow visualization of computer generated flow fields
[NASA-CR-182679] N88-20573
Pseudo-stationary oblique-shock-wave reflections in low gamma gases: Isobutane and sulphur hexafluoride
[UTIAS-TN-267] N88-20576
Calculations of viscous flows with a multigrid method
N88-20580
General fuselage coordinates for the calculation of three-dimensional boundary layers
[MBB/LKE-122/S/PUB/244] N88-20596
Activities report of the Lille Institute of Fluid Mechanics
[ETN-88-91983] N88-20597
Comparison between computed and measured swirl and turbulence in reciprocating engines
[PDR/IC-CFDU/32] N88-20647
COMPUTATIONAL GRIDS
An L-U implicit multigrid algorithm to solve the Euler equations for transonic flow in rotating turbomachinery passages N88-20270
The construction of a three-dimensional finite volume grid generator for a wing in a wind tunnel with application to Navier-Stokes flow solvers
[FFA-TN-1987-58] N88-20277
An adaptive grid technique for solution of the Euler equations N88-20579
Calculations of viscous flows with a multigrid method
N88-20580
Multigrid solution of the Euler equations N88-20582
Data traffic reduction schemes for sparse Cholesky factorizations
[NASA-CR-181626] N88-20831
A knowledge system for automatic finite element mesh generation: AMEKS
[DE87-014894] N88-20914
A Lagrangian moving grid scheme for one-dimensional evolutionary partial differential equations
[CWI-NM-R8713] N88-20922
Conservative finite volume solutions of a linear hyperbolic transport equation in two and three dimensions using multiple grids
[NASA-CR-182715] N88-20934
COMPUTER AIDED DESIGN
Australian aerodynamic design codes for aerial tow bodies
[AD-A189048] N88-20258
Computer-aided transformation of descriptive mode of mathematical models of a control system N88-20503
Gridless routing for generalized cell assemblies: Report and user manual
[EUT-87-E-180] N88-20549
On the sensitivity of complex, internally coupled systems
[NASA-TM-100537] N88-20829
MacCAD (Macintosh Computer Aided Design), computer aided design tool for system analysis
[AD-A189241] N88-20843
Computer aided surface representation
[DE88-005408] N88-20854
The concept of intelligent integrated interactive CAD systems
[CWI-CS-R8717] N88-20865
Organization of design knowledge in an intelligent CAD environment
[CWI-CS-R8720] N88-20868
An integrated data description language for coding design knowledge
[CWI-CS-R8731] N88-20871
GM: A gate matrix layout generator
[EUT-87-E-179] N88-20875
Finite State Tables for general computer programming applications
[DE88-006254] N88-20881
COMPUTER AIDED TOMOGRAPHY
Nondestructive testings of HTGR graphites
N88-20448
Recent developments in nondestructive evaluation for structural ceramics
[DE88-005889] N88-20473
X-ray computed tomography for structural ceramic applications: Beam hardening corrections
[DE88-005891] N88-20474
COMPUTER ANIMATION
Dynamics of high-speed mechanisms with elastic members N88-20643
COMPUTER GRAPHICS
CODAC (Cockpit Oriented Display of Aircraft Configurations) version 1.4 user's guide
[NASA-CR-181650] N88-20273
Western aeronautical test range real-time graphics software package MAGIC
[NASA-TM-100425] N88-20506
Graphics and flow visualization of computer generated flow fields
[NASA-CR-182679] N88-20573
Analysis for architecture for image processing
[INPE-4294-PRE/1165] N88-20715
Logical input devices and interaction --- computer graphics
[CWI-CS-R8738] N88-20836
MASPLT: A one-dimensional graphics post processor for wave propagation codes
[DE88-005506] N88-20856
HISPLT: A history graphics post processor for wave propagation codes
[DE88-005507] N88-20857
CSQPLT: A graphics post processor for multidimensional wave propagation codes
[DE88-005508] N88-20858
A model for graphical interaction --- computer graphics
[CWI-CS-R8718] N88-20866
Parallel graphical output from dialogue cells
[CWI-CS-R8719] N88-20867
Steps into a geometer's workbench
[CWI-CS-R8726] N88-20870

Dynamic run-time graphics
[DE87-008997] N88-20879
Geometry and graphics applied to robotics
[CWI-CS-R8727] N88-20903
Computation and graphics in mathematical research
[DE88-005796] N88-20953

COMPUTER NETWORKS
Computing with structured connections networks
[AD-A189244] N88-20886
A fully abstract semantics for data flow nets
[CWI-CS-R8724] N88-20893
Two queues with alternating service and switching times
[CWI-OS-R8712] N88-20949
A menu-driven knowledge retrieval system accessing ASCII data
[DE88-001742] N88-21079

COMPUTER PROGRAMMING
Intergrated circuit design, phase 2
[AD-A189060] N88-20530
Laser programming integrated circuits
[AD-A189590] N88-20537
Finite State Tables for general computer programming applications
[DE88-006254] N88-20881
Expert system techniques and decision support system: A case study (Dec. 1985 - Jun. 1986)
[ETN-88-91347] N88-20884
Research in applied mathematics ralated to identification of noisy systems
[AD-A189355] N88-20908

COMPUTER PROGRAMS
Fully-coupled analysis of jet mixing problems. Three-dimensional PNS model, SCIP3D
[NASA-CR-4139] N88-20256
Australian aerodynamic design codes for aerial tow bodies
[AD-A189048] N88-20258
CODAC (Cockpit Oriented Display of Aircraft Configurations) version 1.4 user's guide
[NASA-CR-181650] N88-20273
Documentation and installation of the hypersonic arbitrary-body computer program (Mark 3 version) of A.E. Gentry on the IBM computer system
[MBB/LKE-127/S/PUB/256] N88-20276
Architecture specification for PAVE PILLAR avionics
[AD-A188722] N88-20303
Trajectory code studies, 1987
[DE88-006218] N88-20335
MOPAC manual: A general molecular orbital package, fourth edition
[AD-A188623] N88-20362
A simplified computer code for reduction to burning rates of closed bomb pressure-time data (MINICB)
[AD-A189112] N88-20380
Interactive automated system for testing analog units of digital seismic stations N88-20702
MacCAD (Macintosh Computer Aided Design), computer aided design tool for system analysis
[AD-A189241] N88-20843
Preconditioned conjugate gradient algorithms and software for solving large sparse linear systems
[DE88-002180] N88-20849
A report on the study of algorithms to enhance vector computer performance for the discretized one-dimensional time-dependent heat conduction equation: EPIC research, phase 1
[DE88-005642] N88-20880
Distributed transaction processing and the Camelot system
[AD-A188614] N88-20885
Local refinement of stress field by finite element method
[INPE-4321-TDL/288] N88-20930
A novel method for sputter-deposition of high T(sub c) superconductor films via a computer-controlled mass analyzed ion beam
[DE88-006001] N88-21064

COMPUTER STORAGE DEVICES
An interface between object-oriented systems
[AD-A189245] N88-20844

COMPUTER SYSTEMS DESIGN
The concept of intelligent integrated interactive CAD systems
[CWI-CS-R8717] N88-20865
Organization of design knowledge in an intelligent CAD environment
[CWI-CS-R8720] N88-20868
The German processing and archiving facility for ERS-1
[ESA-CR(P)-2531] N88-21082

COMPUTER SYSTEMS PERFORMANCE
A report on the study of algorithms to enhance vector computer performance for the discretized one-dimensional time-dependent heat conduction equation: EPIC research, phase 1
[DE88-005642] N88-20880

COMPUTER SYSTEMS PROGRAMS
SIMSAT: Simulation package for flexible systems. Beams in space
[TW-278] N88-20348

COMPUTER TECHNIQUES
A simplified computer code for reduction to burning rates of closed bomb pressure-time data (MINICB)
[AD-A189112] N88-20380
A study of satellite emission computed tomography
[AD-A189567] N88-20745
Advanced human factors engineering tool technologies
[AD-A189390] N88-20825
Computer aided surface representation
[DE88-005408] N88-20854
Quality enhancement with machine intelligence
[DE88-005639] N88-20901

COMPUTER VISION
Retinotopic mapping of the human visual system with magnetoencephalography
[AD-A189557] N88-20811
On relaxation algorithms based on Markov random fields
[AD-A189043] N88-20840
Mathematic modeling of visual perception problems
[INPE-4355-PRE/1186] N88-20897
Aspects and applications of primary processing of visual information
[INPE-4290-PRE/1161] N88-21015

COMPUTERIZED SIMULATION
AVSCOM'S modifications to Teledyne Systems Company's air-to-air fire control system simulation model
[AD-A189136] N88-20294
Trajectory code studies, 1987
[DE88-006218] N88-20335
SIMSAT: Simulation package for flexible systems. Beams in space
[TW-278] N88-20348
Bipropellant combustion in a liquid rocket combustion chamber N88-20359
Mixing of viscous fluids: Behavior of microstructures and chaos
[DE88-006287] N88-20586
Multigrid solution of the Euler equations N88-20582
Particle-dynamics calculations of gravity flow of inelastic, frictional spheres
[DE88-005224] N88-20586
Dynamics of high-speed mechanisms with elastic members N88-20643
Human problem solving in dynamic environments. Understanding and supporting operators in large-scale, complex systems
[AD-A189539] N88-20826
Simulation of measuring points for three dimensional measurements
[WPB-0115] N88-20883
A fault injection experiment using the AIRLAB Diagnostic Emulation Facility
[NASA-CR-178390] N88-20895
SEAT: A strategic engagement analysis tool
[DE88-000498] N88-20944
Physics at large transverse momenta
[DE88-005758] N88-20986
Numerical simulations of multiphoton processes in many electron atoms
[DE88-003293] N88-20990
Activities report of the Toulouse Research Center
[ETN-88-91988] N88-21077
Resonant Alfven wave instabilities driven by streaming fast particles N88-21104

COMPUTERS
Online aiding for human-computer interfaces
[AD-A189239] N88-20842

CONCENTRATION (COMPOSITION)
Hydrogen embrittlement of gun steel
[AD-A188972] N88-20407
An experimental method for species concentration measurements in a welding arc using laser-induced fluorescence
[DE88-005638] N88-20636
Research on influence of individual sea water components on spectral brightness coefficient of outgoing radiation N88-20682

CONCENTRATORS
Performance and cost benefits associated with nonimaging secondary concentrators used in point-focus dish solar thermal applications
[DE88-001104] N88-20718
Point-focus concentrator reflector assembly, phase 1
[DE88-003616] N88-20720

CONCURRENT PROCESSING
The physical structure of concurrent problems and concurrent computers
[DE88-005812] N88-20835
On proving register atomicity
[CWI-CS-R8707] N88-20862
A proof rule process creation
[CWI-CS-R8710] N88-20891
Merge and termination in process algebra
[CWI-CS-R8716] N88-20918
Abstraction and empty process in process algebra
[CWI-CS-R8721] N88-20919

CONDENSED MATTER PHYSICS
Physics of condensed matter at extreme conditions
[DE88-006232] N88-20958

CONDENSERS (LIQUEFIERS)
Proceedings of the 1987 International Symposium on Condensing Heat Exchangers
[DE88-005230] N88-20564

CONDENSING
Some problems of the theory of bubble growth and condensation in bubble chambers
[NASA-TT-20232] N88-20593

CONDUCTION BANDS
Silicon-germanium heterostructures N88-21034

CONDUCTIVE HEAT TRANSFER
A report on the study of algorithms to enhance vector computer performance for the discretized one-dimensional time-dependent heat conduction equation: EPIC research, phase 1
[DE88-005642] N88-20880

CONDUCTIVITY
Electromagnetic scattering from and natural resonances of the circular strip N88-20523

CONDUCTORS
Measurement of the properties of lossy materials inside a finite conducting cylinder
[NASA-CR-182664] N88-20962

CONFERENCES
Gordon Conference on Intermetallic Compounds held at Tilton, New Hampshire on 20-24 July 1987
[AD-A188502] N88-20435
IAEA Specialists' Meeting on Graphite Component Structural Design
[DE88-780006] N88-20439
Proceedings of the 1987 International Symposium on Condensing Heat Exchangers
[DE88-005230] N88-20564
Cryogenic Fluid Management Technology Workshop. Volume 2: Roundtable Discussion of Technology Requirements
[NASA-CP-10009] N88-20599
Sixteenth NASTRAN (trademark) Users' Colloquium
[NASA-CP-2505] N88-20652
Dynamics of the Oceanic Surface Mixed Layer
[AD-A188348] N88-20785
Regional Conference on the Analysis of the Unbalanced Mixed Model
[AD-A188747] N88-20943
ONR Far East Scientific Bulletin, volume 12, number 3, July-September 1987
[AD-A188554] N88-21081

CONFIDENCE LIMITS
Regional Conference on the Analysis of the Unbalanced Mixed Model
[AD-A188747] N88-20943

CONFIGURATION MANAGEMENT
Configuration management issues and objectives for a real-time research flight test support facility
[NASA-TM-100437] N88-20832

CONFORMAL MAPPING
Conformal geometry, Hotine's conjecture, and differential geodesy
[AD-A189265] N88-20709
What do multistep methods approximate
[PB88-148838] N88-20932
Action-angle maps and scattering theory for some finite-dimensional integrable systems. The pure solution case
[CWI-PM-R8704] N88-20955

CONICS
Conic algorithms for unconstrained minimization with special consideration of problems with large sparse Hessians: A summary of research performed
[DE88-002549] N88-20850
Algorithms with conic termination for nonlinear optimization
[DE88-005893] N88-20851

CONJUGATE GRADIENT METHOD
Preconditioned conjugate gradient algorithms and software for solving large sparse linear systems
[DE88-002180] N88-20849

CONSERVATION
Period-doubling universality in multidimensional dissipative and conservative systems
[PB88-148812] N88-20961

CONSISTENCY
Consistency of rule-based expert systems
[CWI-CS-R8736] N88-20950
CONSOLES
Western aeronautical test range real-time graphics software package MAGIC
[NASA-TM-100425] N88-20506
CONSTANTS
Measurement of rate constants of elementary gas reactions of importance to upper atmosphere and combustion systems
[AD-A189432] N88-20386
CONSTRAINTS
Describing constraints on a digital circuit's behavior
[AD-A189200] N88-20531
Practical constraints on sources for pulsed beam lithographies
[DE88-006594] N88-20623
Active cooling design for scramjet engines using optimization methods
[NASA-TM-100581] N88-20669
Constrained nonlinear programming
[DE88-005695] N88-20860
CONSTRUCTION
The space station assembly phase: Flight telerobotic servicer feasibility, volume 1
[NASA-CR-182689] N88-20351
Campaign graphs
[DE88-005336] N88-20952
CONTAINERS
Buckling and breakdown problems in structural mechanics. Failure of prestressed double-walled containers or rings
[MBB-UR-E-956/87] N88-20671
CONTINENTAL SHELVES
Circulation and exchange processes on the South Atlantic Bight Continental Shelf
[DE88-003330] N88-20781
CONTINUOUS RADIATION
The continuous electron beam accelerator facility
[CEBAF-PR-87-017] N88-20996
CONTROL EQUIPMENT
Western aeronautical test range real-time graphics software package MAGIC
[NASA-TM-100425] N88-20506
CONTROL SIMULATION
Integrated autopilot/autothrottle based on a total energy control concept: Design and evaluation of additional autopilot modes
[NASA-CR-4131] N88-20308
CONTROL STABILITY
Modelling and control of an annular momentum control device
[NASA-CR-4138] N88-20491
Mode priming in an overmoded gyrotron oscillator
[AD-A189151] N88-20602
CONTROL SYSTEMS DESIGN
Control augmented structural synthesis
[NASA-CR-4132] N88-20290
Integrated autopilot/autothrottle based on a total energy control concept: Design and evaluation of additional autopilot modes
[NASA-CR-4131] N88-20308
Computer-aided transformation of descriptive mode of mathematical models of a control system N88-20503
Numerical methods in the resolution of control electrovalve model
[INPE-4154-RPE/540] N88-20554
Control of structure in turbulent flows: Bifurcating and blooming jets
[AD-A189607] N88-20562
Feasibility demonstration of a sensor for high-quality two-phase flow --- Space Station
[NLR-TR-87009-U] N88-20569
Control strategies and hardware used in solar thermal applications
[DE88-004631] N88-20731
Robust decentralized control of large flexible structures
[DE88-005416] N88-20902
Using trace theory to model discrete events
[CS-8708] N88-20904
CONTROL THEORY
Integrated autopilot/autothrottle based on a total energy control concept: Design and evaluation of additional autopilot modes
[NASA-CR-4131] N88-20308
Using trace theory to model discrete events
[CS-8708] N88-20904
CONTROLLED FUSION
SOAR: Space orbiting advanced fusion power reactor
[AD-A189234] N88-20356
CONTROLLERS
NAVLAB: An autonomous navigation testbed
[AD-A189049] N88-20283
Control of structure in turbulent flows: Bifurcating and blooming jets
[AD-A189607] N88-20562
Force distribution and trajectory control for closed kinematic chains with applications to walking machines N88-20642
CONVECTION
Dynamical modeling of marine boundary layer convection N88-20750
CONVECTIVE HEAT TRANSFER
Structures and fluxes in a deep convecting mixed layer N88-20786
The mixed layer of the western equatorial Pacific Ocean
[HIG-1861] N88-20789
Similarity theories and microturbulence in the atmospheric mixed layer N88-20802
CONVERGENCE
A convergence theorem in process algebra
[CWI-CS-R8733] N88-20920
Convergence of Runge-Kutta methods on classes of stiff initial value problems
[CWI-NM-R8717] N88-20924
CONVERGENT-DIVERGENT NOZZLES
Static performance of an axisymmetric nozzle with post-exit vanes for multiaxis thrust vectoring
[NASA-TP-2800] N88-20280
COOLANTS
Quantitative determination of a hydrogen impurity in a sodium coolant by hydride thermal dissociation
[NASA-TT-20239] N88-20402
COOLING
Theory of laser cooling and spectroscopy of harmonically trapped single atoms
[AD-A189576] N88-20617
COOLING SYSTEMS
Active cooling design for scramjet engines using optimization methods
[NASA-TM-100581] N88-20669
COORDINATION
The coordination cluster theory for metallic solutions
[DE88-005934] N88-20389
COPOLYMERS
A new polymer-based hydrogen getter
[DE88-004538] N88-20467
COPPER
A direct correlation of strength with impact velocity
[AD-A189251] N88-20409
COPPER COMPOUNDS
Decomposition of hypochlorite in the presence of copper in a homogeneous medium
[NASA-TT-20199] N88-20403
COPPER OXIDES
Potassium cuprate (3)
[NASA-TT-20246] N88-20401
Characterization and fundamental studies on CuO sorbent materials to determine attrition mechanisms on substrate gamma alumina
[DE88-003674] N88-20456
Large momentum pairing in one-dimensional systems
[AD-A189228] N88-20981
The relationship of the chemical bonding topology of high critical temperature copper oxide superconductors to that of the chevrel phases and the ternary lanthanide rhodium borides
[AD-A189255] N88-21042
CORONAGRAPHS
Development of high stability fiber optic spectrophotometric systems for study of solar/stellar magnetic activity
[AD-A189327] N88-21088
CORRECTION
Orbit correction strategy for an Earth observation satellite
[INPE-4287-PRE/1159] N88-20331
CORRELATION
A direct correlation of strength with impact velocity
[AD-A189251] N88-20409
Estimation-correlation, modeling, and identification in adaptive array processors
[AD-A189130] N88-20512
CORRELATION DETECTION
Broadband correlation analysis
[AD-A188732] N88-20839
CORROSION
Corrosion, passivity and breakdown of alloys used in high energy density batteries
[DE88-004891] N88-20422
Improve the lifetime of the hollow fiber sodium sulfur cell
[DE88-004881] N88-20469
A five year weathering experiment with solar collectors
[DE88-900369] N88-20740
CORROSION PREVENTION
Corrosion-wear process under rolling-sliding motion
[AD-A189603] N88-20635
CORROSION RESISTANCE
Hydrogen embrittlement of gun steel
[AD-A188972] N88-20407
A fundamental understanding of the effect of alloying elements on the corrosion resistance of rapidly solidified Mg alloys
[AD-A189385] N88-20413
Optimization of binary pigment coatings
[AD-A189103] N88-20450
COSMIC DUST
A mass spectrometer evolved gas analysis experiment for in-situ analysis of cometary dust volatiles N88-21097
COSMIC RAYS
A low-frequency measurement of the spectrum of the cosmic microwave background radiation N88-21112
COST ANALYSIS
Expected value analysis for an unmanned expendable launch vehicle payload escape system
[AD-A189494] N88-20337
Turnaround operations analysis for OTV. Volume 3: Technology development plan
[NASA-CR-179318] N88-20342
Performance and cost benefits associated with nonimaging secondary concentrators used in point-focus dish solar thermal applications
[DE88-001104] N88-20718
COST EFFECTIVENESS
EDF's studies and first choices regarding the design of electrical equipment
[NASA-TT-20222] N88-20553
COST ESTIMATES
Turnaround operations analysis for OTV. Volume 2: Detailed technical report
[NASA-CR-179317] N88-20341
Turnaround operations analysis for OTV. Volume 4: WBS and dictionary and cost methodology
[NASA-CR-179319] N88-20343
COUNTERFLOW
Innovative, counterflow gas/fine solids, direct contact heat exchanger
[DE88-004744] N88-20585
COUPLING
Interaction of particulate and transformation toughening
[AD-A189321] N88-20412
COVARIANCE
Computer programs for calculating group cross-section covariances from uncertainty parameters in the ENDF/B-V format. UNC 32/33 --- neutron physics
[ECN-202] N88-20995
CRACK CLOSURE
The fatigue behavior of ferritic and austenitic steels at elevated temperatures
[DE88-006304] N88-20431
Cyclic crack growth emanating at a round notch considering viscoplasticity
[AD-A189577] N88-20655
CRACK PROPAGATION
Crack distribution and growth rates for critical fastener holes in Mirage wing RH79
[AD-A189080] N88-20293
Composites strengthening
[AD-A189258] N88-20364
High-temperature metal matrix composites
[AD-A189516] N88-20367
Fracture characteristics of carbon and aramid unidirectional composites in interlaminar shear and open hole tensile tests
[NLR-TR-86083-U] N88-20371
Materials Research Laboratory at Brown University
[AD-A188006] N88-20396
Hydrogen induced cracks in armor steel weldments fabricated with austenitic filler alloys
[AD-A188733] N88-20406
The effect of microstructure on the fatigue crack growth resistance of nickel base superalloys
[AD-A189526] N88-20414
Threshold fatigue crack growth in Ti-6Al-2Sn-4Zr-6Mo
[AD-A189560] N88-20415
Stress corrosion cracking and metal-induced embrittlement: Comparative studies of local chemistries
[DE88-003235] N88-20419
Non-destructive evaluation techniques applied to the study of fatigue microcrack growth in steel alloys
[DE88-004090] N88-20420
Fracture mechanics and creep crack growth of 1 percent Cr 1/2 percent Mo steel with and without prior exposure to creep conditions
[NLR-TR-86051-U] N88-20426
PNL-1 improved ceramic composites through controlled fiber matrix interaction
[DE88-005680] N88-20462

Laser ignition of nitramine composite propellants and crack propagation and branching in burning solid propellants
[AD-A189260] N88-20483
A study of the dynamics of high temperature brittle intergranular fracture by acoustic emission
[AERE-R-12479] N88-20650
Cyclic crack growth emanating at a round notch considering viscoplasticity
[AD-A189577] N88-20655
Theory and experiments of fracture in cyclic compression: Single phase ceramics, transforming ceramics and ceramic composites
[DE88-005792] N88-20659
Fracture criteria for discontinuously reinforced metal matrix composites
[NASA-CR-182665] N88-20662

CRACKS
Crack distribution and growth rates for critical fastener holes in Mirage wing RH79
[AD-A189080] N88-20293
Material instabilities in solids
[AD-A189525] N88-20388
Hydrogen induced cracks in armor steel weldments fabricated with austenitic filler alloys
[AD-A188733] N88-20406
Threshold fatigue crack growth in Ti-6Al-2Sn-4Zr-6Mo
[AD-A189560] N88-20415
Nondestructive evaluation of carbon-carbon coatings
[AD-A189524] N88-20453
Ductile failure
[AD-A189429] N88-20654

CRAY COMPUTERS
Dynamic run-time graphics
[DE87-006997] N88-20879

CREEP PROPERTIES
High-temperature metal matrix composites
[AD-A189516] N88-20367
Creep behavior of consolidated rapidly solidified Type 304 stainless steel powder containing helium
[DE88-005536] N88-20424
Fracture mechanics and creep crack growth of 1 percent Cr 1/2 percent Mo steel with and without prior exposure to creep conditions
[NLR-TR-86051-U] N88-20426
The fatigue behavior of ferritic and austenitic steels at elevated temperatures
[DE88-006304] N88-20431

CROP IDENTIFICATION
A procedure for automatic classification of crop areas
[INPE-4467-PRE/1240] N88-20708

CROP INVENTORIES
A procedure for automatic classification of crop areas
[INPE-4467-PRE/1240] N88-20708

CRUDE OIL
Aviation turbine fuels from tar sands bitumen and heavy oils. Part 3: Laboratory sample production
[AD-A189278] N88-20484

CRUSTAL FRACTURES
Correlation of data on strain accumulation adjacent to the San Andreas Fault with available models
[NASA-CR-180757] N88-20742

CRYOGENIC FLUIDS
Cryogenic Fluid Management Technology Workshop. Volume 2: Roundtable Discussion of Technology Requirements
[NASA-CP-10009] N88-20599

CRYOGENICS
Development of a constitutive equation for HSLA (High-Strength Low-Alloy)-100 at cryogenic temperatures
[AD-A189243] N88-20408
Advanced components for spaceborne infrared astronomy
[NASA-CR-177470] N88-20601

CRYSTAL DEFECTS
Experimental and theoretical methods for investigating helium effects in rapidly solidified metals
[DE88-005542] N88-20425
A calorimetric determination of the enthalpy of formation and a description of the defect structure of the ordered beta-phase /Ni, Cu/ /1-x/ Al/x/
[NASA-TT-20157] N88-20434

CRYSTAL GROWTH
Research on mercury cadmium telluride
[AD-A189155] N88-21039
Initial stages of silicon growth on the (100) surface of silicon by localized laser CVD
[DE88-005420] N88-21059

CRYSTAL LATTICES
Temperature dependence of Kr precipitation in Ni
[DE88-005953] N88-20429
Lattice relaxation of the DX centers in Ga/sub 1-x/Al/sub x/As and of the pressure-induced deep donors in GaAs
[DE88-005452] N88-21061

CRYSTAL STRUCTURE
CdZnTe as a wide-band-gap absorber for a tandem, thin-film solar cell
[DE88-001114] N88-20724

CRYSTALLINITY
Crystalline photovoltaic cell technology: Present and future
[DE88-004684] N88-20734

CRYSTALLOGRAPHY
Stress corrosion cracking and metal-induced embrittlement: Comparative studies of local chemistries
[DE88-003235] N88-20419
Recent progress in structure determination by LEED (Low-Energy Electron Diffraction) measure the properties of the deep donors (DX-cent)
[DE88-003851] N88-21048

CRYSTALS
Parametric study of acceleration-induced stresses and frequency changes in doubly-rotated crystal resonators
[AD-A189261] N88-20532
Thermionic Technology Program. A: Insulator test and evaluation
[DE88-004707] N88-20735
Multiple scattering of polarized light in cirrus clouds
N88-20768
Nonlinear refractive index measurements of glasses and crystals
[DE88-005673] N88-21009

CURING
High-temperature thermosets derived from the Diels-Alder polymerization of bisbenzocyclobutenes and bimaleimides
[AD-A188800] N88-20449

CURRENT DENSITY
A novel class of positive electrodes for rechargeable batteries
[DE88-004559] N88-20545
Simplified physical approach of the control by eddy current
[TI88-701076] N88-20552

CURVED BEAMS
Delamination stresses in semicircular laminated composite bars
[NASA-TM-4026] N88-20375

CYCLES
Global mixed-layer natural and anthropogenic fluxes
N88-20803

CYCLIC COMPOUNDS
Synthesis of energetic materials
[AD-A189115] N88-20482

CYCLIC HYDROCARBONS
High-temperature thermosets derived from the Diels-Alder polymerization of bisbenzocyclobutenes and bimaleimides
[AD-A188800] N88-20449

CYCLIC LOADS
Cyclic crack growth emanating at a round notch considering viscoplasticity
[AD-A189577] N88-20655

CYCLOTRON RESONANCE
Mode priming in an overmoded gyrotron oscillator
[AD-A189151] N88-20602

CYCLOTRON RESONANCE DEVICES
Mode priming in an overmoded gyrotron oscillator
[AD-A189151] N88-20602
Synthesis method applied to the design of an electron gun for a gyrotron
[INPE-4357-TDL/298] N88-20607

CYLINDERS
An interferometric investigation of the diffraction of planar shock waves over a half-diamond cylinder in air
[UTIAS-322] N88-20575
Measurement of the properties of lossy materials inside a finite conducting cylinder
[NASA-CR-182664] N88-20962

D

DAMAGE ASSESSMENT
Activities report of the Structures Department
[ETN-88-91986] N88-20672

DARK MATTER
Infrared constraints on the nature of dark matter
N88-21102

DATA ACQUISITION
An analysis of physiological data related to motion sickness for use in a real-time motion sickness indicator
[AD-A189589] N88-20812

DATA BASE MANAGEMENT SYSTEMS
HISPLT: A history graphics post processor for wave propagation codes
[DE88-005507] N88-20857
CSQPLT: A graphics post processor for multidimensional wave propagation codes
[DE88-005508] N88-20858
Using design axioms and topology to model database semantics
[CWI-CS-R8711] N88-20863
Distributed transaction processing and the Camelot system
[AD-A188614] N88-20885
Reference model for DBMS (database management system) user facility
[PB88-169446] N88-21080

DATA BASES
Database of average-power damage thresholds at 1064 nm
[DE88-004352] N88-20626
An analysis of physiological data related to motion sickness for use in a real-time motion sickness indicator
[AD-A189589] N88-20812
Knowledge retrieval as specialized inference
[AD-A189042] N88-20899

DATA COMPRESSION
A hybrid transform/DPCM encoder for data compression
[DE87-014852] N88-20518
A study of data compactation using numerical methods
[INPE-4317-TDL/284] N88-20929

DATA FLOW ANALYSIS
Verification of a systolic algorithm for string comparison
[CWI-CS-R8734] N88-20873
A fully abstract semantics for data flow nets
[CWI-CS-R8724] N88-20893

DATA PROCESSING
A comparison of two chord keyboard coding systems for alphanumeric data entry
[AD-A189230] N88-20834
Distributed transaction processing and the Camelot system
[AD-A188614] N88-20885
Optimal and conventional space-time processing in flow noise
[AD-A189104] N88-20965
Aspects and applications of primary processing of visual information
[INPE-4290-PRE/1161] N88-21015
The German processing and archiving facility for ERS-1
[ESA-CR(P)-2531] N88-21082

DATA PROCESSING EQUIPMENT
A comparison of two chord keyboard coding systems for alphanumeric data entry
[AD-A189230] N88-20834

DATA REDUCTION
Data traffic reduction schemes for sparse Cholesky factorizations
[NASA-CR-181626] N88-20831

DATA SIMULATION
Simulation of measuring points for three dimensional measurements
[WPB-0115] N88-20883

DATA SMOOTHING
Stabilization of explicit difference schemes by smoothing techniques
[CWI-NM-R8714] N88-20923

DATA TRANSMISSION
A hybrid transform/DPCM encoder for data compression
[DE87-014852] N88-20518

DECELERATION
An experimental investigation of decelerating flow about two-dimensional cambered plates
[DE88-006598] N88-20567

DECISION MAKING
The design of aircraft using the decision support problem technique
[NASA-CR-4134] N88-20291
Expected value analysis for an unmanned expendable launch vehicle payload escape system
[AD-A189494] N88-20337
A personalized and prescriptive decision aid for choice from a database of options
[AD-A188726] N88-20820
SEAT: A strategic engagement analysis tool
[DE88-000498] N88-20944
Expert systems for decision support in military aircraft mission preparation
[NLR-MP-87013-U] N88-20946
Application of expert systems in project management decision aiding
[NASA-CR-180762] N88-21074

DECISION THEORY
Expert system techniques and decision support system: A case study (Dec. 1985 - Jun. 1986)
[ETN-88-91347] N88-20884

DECOMPOSITION
Decomposition of hypochlorite in the presence of copper in a homogeneous medium
[NASA-TT-20199] N88-20403
Molecular dynamics of laser ablation of a polymer coating
[DE88-004337] N88-20466
DEEP SPACE NETWORK
The Deep Space Network
[NASA-CR-182700] N88-20524
DEEP WATER
Deep water mass circulation in the Alboran Basin. Measurements - January to April 1982: ALBORAN 2
[AD-A189205] N88-20777
DEFECTS
Study of defects in metals by positron annihilation
[DE88-701042] N88-20432
Gordon Conference on Intermetallic Compounds held at Tilton, New Hampshire on 20-24 July 1987
[AD-A188502] N88-20435
A defect investigation of Thunderflash MK N5 (Navy)
[MRL-TN-522] N88-20488
DEFLECTORS
Multimode-waveguide laser beam deflector
[DE88-006222] N88-20622
DEFORMATION
Processing, structure and properties of heavily deformed in situ composites
[AD-A189611] N88-20416
Use of the LLNL 40 kV electric gun to study the shock response of 21-6-9 stainless steel
[DE87-014550] N88-20418
Grain refinement during primary breakdown of alloy 718
[DE88-005193] N88-20423
Gordon Conference on Intermetallic Compounds held at Tilton, New Hampshire on 20-24 July 1987
[AD-A188502] N88-20435
Geodetic measurement of deformation east of the San Andreas fault in Central California
[NASA-CR-182709] N88-20754
Mechanical properties of sea ice and sea ice deformation in the near-shore zone
[PB88-147889] N88-20782
DEGRADATION
MOSFET performance degradation due to hot carriers N88-21063
DELAMINATING
Ply-level failure analysis of a graphite/epoxy laminate under bearing-bypass loading
[NASA-TM-100578] N88-20372
Delamination stresses in semicircular laminated composite bars
[NASA-TM-4026] N88-20375
DELAY
A pyrotechnic delay ignition system for a submarine launched marine signal
[MRL-R-1079] N88-20487
DELTA MODULATION
Method for set-up for researching signal curve development
[NASA-TT-20235] N88-20526
DELTA WINGS
Tests on the AFWAL 65 deg delta wing at NLR: A study of vortex flow development between Mach = 0.4 and 4
[NLR-MP-86058-U] N88-20266
The international vortex flow experiment: A test case for compressible Euler codes
[NLR-MP-86076-U] N88-20267
Computational technique for compressible vortex flows using the integral equation solution
[NASA-CR-182695] N88-20271
DEMOGRAPHY
Survival analysis using additive risk models
[AD-A189053] N88-20906
DENSITY MEASUREMENT
Study of photochromic materials for use in optical signal processing
[AD-A189068] N88-21006
DEPLOYMENT
The evaluation and selection of a 5th ground antenna site for the global positioning system
[AD-A189495] N88-20286
DEPOSITION
Thin-film diffusion barriers for metal-semiconductor contacts
[AD-A188712] N88-21035
Photon-controlled growth of multilayered structures
[DE88-005061] N88-21054
A novel method for sputter-deposition of high T(sub c) superconductor films via a computer-controlled mass analyzed ion beam
[DE88-006001] N88-21064
DESERTS
Summary of along-track data from the Earth radiation budget satellite for several major desert regions
[NASA-RP-1197] N88-20772
DESIGN ANALYSIS
The design and use of a temperature-compensated hot-film anemometer system for boundary-layer flow transition detection on supersonic aircraft
[NASA-TM-100421] N88-20304
Turnaround operations analysis for OTV. Volume 1: Executive summary
[NASA-CR-179316] N88-20340
Turnaround operations analysis for OTV. Volume 2: Detailed technical report
[NASA-CR-179317] N88-20341
Synthesis method applied to the design of an electron gun for a gyrotron
[INPE-4357-TDL/298] N88-20607
On the sensitivity of complex, internally coupled systems
[NASA-TM-100537] N88-20829
A new algorithm for general multiobjective optimization
[NASA-TM-100536] N88-20830
Potential off-normal events and associated radiological source terms for the compact ignition tokamak: Fusion Safety Program
[DE88-004112] N88-21024
DESIGN TO COST
The space station assembly phase: Flight telerobotic servicer feasibility, volume 1
[NASA-CR-182689] N88-20351
DESORPTION
Electron stimulated desorption and coherent electron scattering
[AD-A189091] N88-20978
Image charge, coherent scattering, and symmetry effects in electron stimulated desorption: O(-) from O sub 2 condensed on metals
[AD-A189093] N88-20979
The magnitude of secondary electron contributions in photon stimulated desorption
[AD-A189094] N88-20980
Hydrogen pumping and release by graphite under high flux plasma bombardment
[DE88-005880] N88-21021
DETECTION
Specification for an infrared satellite surveillance system for the detection of aircraft
[AD-A189592] N88-20746
Reduced tolerance imaging 2, volume 2
[AD-A189604] N88-20939
Searches for forces weaker than gravity
[DE88-003579] N88-20959
Optimal and conventional space-time processing in flow noise
[AD-A189104] N88-20965
Physics at large transverse momenta
[DE88-005758] N88-20986
Enzyme-based fiber optic sensors
[DE88-005674] N88-21013
DETERMINANTS
Deterministic uncertainty analysis
[DE88-006139] N88-20942
DETONABLE GAS MIXTURES
Measurement of detonation temperature of hydrogen-oxygen mixture by CARS (Coherent Anti-Stokes Raman Spectroscopy)
[NASA-TT-20227] N88-20398
DETONATION
Measurement of detonation temperature of hydrogen-oxygen mixture by CARS (Coherent Anti-Stokes Raman Spectroscopy)
[NASA-TT-20227] N88-20398
Theoretical investigation of the wave shaping process in a section of ladder fracture tape
[MRL-R-1081] N88-20595
DETONATION WAVES
Combustion theory and related questions
[AD-A189160] N88-20382
Detonation velocity of the hydrazinum nitrate-hydrazine water system
[NASA-TT-20213] N88-20590
DEUTERIUM PLASMA
SOAR: Space orbiting advanced fusion power reactor
[AD-A189234] N88-20356
DEUTERON IRRADIATION
Study of defects in metals by positron annihilation
[DE88-701042] N88-20432
DIAGNOSIS
Progress in diagnostic techniques for SC cavities
[CEBAF-PR-88-003] N88-20600
DIELECTRIC POLARIZATION
Spontaneous decay and atomic fluorescence near a metal surface of an absorbing dielectric
[AD-A187508] N88-20975
DIELECTRIC PROPERTIES
Microwave and structural properties of saline ice
[AD-A189307] N88-20779
DIELECTRICS
Transformation coefficient in wave-field acceleration scheme
[DE88-700158] N88-20507
Vapor-mist for lightweight high voltage space insulation systems
[DE87-011704] N88-20538
Causes of damage in multilayer dielectric coatings exposed to high average power visible laser radiation
[DE88-005363] N88-20619
Spontaneous decay and atomic fluorescence near a metal surface of an absorbing dielectric
[AD-A187508] N88-20975
DIELS-ALDER REACTIONS
High-temperature thermosets derived from the Diels-Alder polymerization of bisbenzocyclobutenes and bimaleimides
[AD-A188800] N88-20449
DIESEL ENGINES
Engine testing for synfuel operation
[DE88-006044] N88-20645
DIESEL FUELS
Engine testing for synfuel operation
[DE88-006044] N88-20645
DIFFERENCE EQUATIONS
Predicting oscillatory finite difference solutions to the heat equation: A comparative study of the coefficient and matrix methods
[AD-A189591] N88-20911
DIFFERENCES
On the norm equivalence of singularly perturbed elliptic difference operators
[DE88-006353] N88-20913
DIFFERENTIAL EQUATIONS
What do multistep methods approximate
[PB88-148838] N88-20932
DIFFRACTION
An interferometric investigation of the diffraction of planar shock waves over a half-diamond cylinder in air
[UTIAS-322] N88-20575
Space infrared telescope facility wide field and diffraction limited array camera (IRAC)
[NASA-CR-182704] N88-21092
DIFFUSION
Vertical turbulent transfer of matter in thin ocean surface layer during daytime heating N88-20693
Thin-film diffusion barriers for metal-semiconductor contacts
[AD-A188712] N88-21035
DIGITAL DATA
Interpolation algorithms for digital terrain models
[INPE-4373-PRE/1196] N88-20877
DIGITAL ELECTRONICS
Describing constraints on a digital circuit's behavior
[AD-A189200] N88-20531
DIGITAL FILTERS
Intergrated circuit design, phase 2
[AD-A189060] N88-20530
DIGITAL SYSTEMS
Architecture specification for PAVE PILLAR avionics
[AD-A188722] N88-20303
DIGITAL TECHNIQUES
Digital enhancement of flow field images
[NASA-TP-2770] N88-20833
DIODES
High power, high efficiency, 2D laser diode arrays for pumping solid state lasers
[DE88-004042] N88-20632
DIPHOSPHATES
Use of diphosphonates to correct disorders in calcium metabolism and mineral composition of bone tissue with 60-day hypokinesia in rats
[NASA-TT-20220] N88-20807
DIPLEXERS
A polarization diversity meteorological radar system
[AD-A189291] N88-20515
DIPOLES
Mushroom-shaped currents (eddy dipoles) under rotation and stratification conditions N88-20678
DIRAC EQUATION
Polarization of electrons in an electromagnetic wave field in the presence of magnetic field
[DE88-700169] N88-20509
DIRECTION FINDING
Method for determining artillery position
[NASA-TT-20238] N88-20973
Method for determining artillery position
[NASA-TT-20237] N88-20974
DIRECTIONAL CONTROL
Effect of rotation on the lateral stability of a free-flying column subjected to an axial thrust with directional control
[AD-A188690] N88-20338

DISCOVERY (ORBITER)
Lateral and longitudinal stability and control parameters for the space shuttle discovery as determined from flight test data
[NASA-TM-100555] N88-20309
DISCRETE FUNCTIONS
Using trace theory to model discrete events
[CS-8708] N88-20904
DISK GALAXIES
Infrared constraints on the nature of dark matter N88-21102
DISPLAY DEVICES
CODAC (Cockpit Oriented Display of Aircraft Configurations) version 1.4 user's guide
[NASA-CR-181650] N88-20273
Development of an interactive real-time graphics system for the display of vehicle space positioning
[NASA-TM-100429] N88-20344
Restoration techniques for redisplay of LANDSAT-5 satellite imagery
[INPE-4189-PRE/1076] N88-20712
Multi-crew pictorial format display evaluation
[AD-A189349] N88-20624
Solid-state electrochemical processes in dye films
[AD-A188756] N88-21036
DISSIPATION
Period-doubling universality in multidimensional dissipative and conservative systems
[PB88-148812] N88-20961
DISSOCIATION
Excimer laser photolysis studies of T-V (Translation-to-Vibration) energy transfer
[AD-A189613] N88-20989
DISTRIBUTED PARAMETER SYSTEMS
Calculation of the distributed loads on the blades of individual multiblade propellers in axial flow using linear and nonlinear lifting surface theories
[NASA-TT-20173] N88-20278
DISTRIBUTED PROCESSING
Two normal form theorems for Communicating Sequential Processes (CSP) program
[CWI-CS-R8735] N88-20874
Distributed transaction processing and the Camelot system
[AD-A188614] N88-20885
On the design of parallel numerical methods in message passing and shared memory environments
[DE88-003566] N88-20888
An amoeba replicated service organisation — Amoeba operating system
[CWI-CS-R8723] N88-20892
DISTRIBUTION (PROPERTY)
Stratospheric trace gas distributions from fair infrared thermal emission spectroscopy N88-20749
DISTURBANCES
A finite-amplitude analysis of the buoyant instability of a highly viscous film over a less viscous half-space N88-20581
DIURNAL VARIATIONS
Computer simulation of tropospheric chemistry
[JUEL-2144] N88-20756
DOPED CRYSTALS
Pressure-dependent DLTS (Deep Level Transient Spectroscopy) experiments on Si-doped AlGaAs
[DE88-003842] N88-21047
DOPPLER EFFECT
A polarization diversity meteorological radar system
[AD-A189291] N88-20515
Observations of waves and Langmuir circulation with Doppler sonars N88-20790
DRAG COEFFICIENTS
The effect of sting interference at low speeds on the drag coefficient of an ellipsoidal body using a magnetic suspension and balance system
[NASA-CR-181611] N88-20274
DRAG REDUCTION
Flight tests of external modifications used to reduce blunt base drag
[NASA-TM-100433] N88-20279
DUALITY THEOREM
Action-angle maps and scattering theory for some finite-dimensional integrable systems. The pure solution case
[CWI-PM-R8704] N88-20955
DUCTILITY
Material instabilities in solids
[AD-A189525] N88-20388
Development of a constitutive equation for HSLA (High-Strength Low-Alloy)-100 at cryogenic temperatures
[AD-A189243] N88-20408
Ductile failure
[AD-A189429] N88-20654
DUCTS
Flow/acoustic interaction in duct inflow
[AD-A189264] N88-20987
DYE LASERS
Doubly periodic output from a dye laser pumped by a free-running argon laser
[DE88-005027] N88-20633
DYNAMIC CHARACTERISTICS
Dynamics of high-speed mechanisms with elastic members N88-20643
DYNAMIC CONTROL
A wind tunnel model with dynamic control
[BU-352] N88-20310
Modelling and control of an annular momentum control device
[NASA-CR-4138] N88-20491
The dynamic control of robotic manipulators in space
[NASA-CR-182710] N88-20646
DYNAMIC LOADS
Changes in the status of the human tibia during antiorthostatic hypokinesia
[NASA-TT-20221] N88-20813
DYNAMIC RESPONSE
Dynamics of high-speed mechanisms with elastic members N88-20643
DYNAMIC STABILITY
On relaxation algorithms based on Markov random fields
[AD-A189043] N88-20840
DYNAMIC STRUCTURAL ANALYSIS
Control augmented structural synthesis
[NASA-CR-4132] N88-20290
The Euler-Bernoulli beam equation with boundary energy dissipation
[AD-A189517] N88-20560
DYNAMICAL SYSTEMS
Transient dynamics of fibre reinforced composite plates
[IIT-B/CE/RR/87-1] N88-20370
Unfoldings of quasi-periodic tori
[ZW-8706] N88-20928
Period-doubling universality in multidimensional dissipative and conservative systems
[PB88-148812] N88-20961
Optical studies of dynamical processes in disordered system
[DE88-005965] N88-20993

E

EARTH CRUST
Crustal dynamics project data analysis, 1987. Volume 2: Mobile VLBI geodetic results 1982-1986
[NASA-TM-100689-VOL-2] N88-20753
EARTH GRAVITATION
Comparisons of global topographic/isostatic models to the Earth's observed gravity field
[NASA-CR-182696] N88-20752
EARTH PLANETARY STRUCTURE
Ultrasonic physical modeling of seismic wave propagation from graben-like structures
[AD-A189066] N88-20744
EARTH RADIATION BUDGET EXPERIMENT
Summary of along-track data from the Earth radiation budget satellite for several major desert regions
[NASA-RP-1197] N88-20772
EARTH RESOURCES
The use of four-photon Raman spectroscopy for the remote sensing of natural objects
[NASA-TT-20257] N88-20716
EARTH ROTATION
On error equations for determining Earth rotation parameters with VLBI network N88-20500
Determination of Earth rotation by the combination of data from different space geodetic systems
[NASA-CR-181388] N88-20713
EARTH SURFACE
Resolution of the magnetotelluric method for determining local inhomogeneities in the sedimentary cover N88-20701
Remote sensing of earth terrain
[NASA-CR-182677] N88-20711
EARTHQUAKES
Correlation of data on strain accumulation adjacent to the San Andreas Fault with available models
[NASA-CR-180757] N88-20742
ECONOMIC ANALYSIS
An assessment methodology for thermal energy storage evaluation
[DE88-004642] N88-20732
ECONOMIC DEVELOPMENT
Spin off businesses as mechanisms for transferring technologies
[DE88-005640] N88-21085
ECONOMICS
On the role of complete reducibility in general competitive equilibrium models
[DE88-005693] N88-21093
EDDY CURRENTS
Simplified physical approach of the control by eddy current
[TI88-701076] N88-20552
EDDY VISCOSITY
Determining Langmuir circulation parameters on basis of similarity theory N88-20680
On the zonal momentum balance at the equator N88-20788
EFFICIENCY
High power, high efficiency, 2D laser diode arrays for pumping solid state lasers
[DE88-004042] N88-20632
EIGENVALUES
Design graphs for the first two bending Eigenvibration forms of rotating beams consisting of two beam points
[IW-86006R] N88-20670
Numerical solution of ill posed problems in partial differential equations
[AD-A189383] N88-20909
ELASTIC DEFORMATION
Body tensor formalism in finite deformation elasticity and application to the torsion of a circular cylinder N88-20651
An analysis of large deformation axisymmetric inelastic problems by finite element and boundary element methods N88-20664
ELASTIC PLATES
Acoustic radiation from line- and point-loaded plates: Uniformly asymptotic solutions
[AD-A189367] N88-20969
ELASTIC PROPERTIES
The Euler-Bernoulli beam equation with boundary energy dissipation
[AD-A189517] N88-20560
Dynamics of high-speed mechanisms with elastic members N88-20643
Mathematical models of sound waves in fluids
[AD-A189270] N88-20968
Guidelines for estimation and characterization of the thermo-mechanical properties of new optical materials
[DE88-004359] N88-21010
ELASTIC SCATTERING
Intermediate energy neutrino physics
[DE88-005378] N88-20984
ELASTIC WAVES
Phase velocity and attenuation of plane elastic waves in a particle-reinforced composite medium
[AD-A189414] N88-20366
ELASTOPLASTICITY
An analysis of large deformation axisymmetric inelastic problems by finite element and boundary element methods N88-20664
ELECTRETS
Observations on electrostatic effects in a filter test system
[AD-A188797] N88-20378
ELECTRIC BATTERIES
An electrochemical and spectroscopic study of electrode systems
[AD-A189274] N88-20384
Corrosion, passivity and breakdown of alloys used in high energy density batteries
[DE88-004891] N88-20422
Polymeric electrolytes for ambient temperature lithium batteries
[DE88-004896] N88-20547
Mission directed goals for electric vehicle battery research and development: The Task Force on electric vehicle battery goals
[DE88-005601] N88-20548
Testing and development of electric vehicle batteries for EPRI Electric Transportation Program
[DE88-005894] N88-20551
ELECTRIC CONDUCTORS
Contrasting conductance/viscosity relations in liquid states of vitreous and polymer solid electrolytes
[AD-A189378] N88-20452
Electron emission from conductors subjected to intense, short-pulse electric fields
[DE88-005412] N88-20985
ELECTRIC CONTACTS
Corrosion-wear process under rolling-sliding motion
[AD-A189603] N88-20635
Stable, high-efficiency, CuInSe2-based, polycrystalline, thin-film tandem solar cells
[DE88-001116] N88-20726
Thin-film diffusion barriers for metal-semiconductor contacts
[AD-A188712] N88-21035
ELECTRIC CORONA
Molecular collision processes in gases and at surfaces
[AD-A189518] N88-20982
ELECTRIC DIPOLES
Electromagnetic scattering from and natural resonances of the circular strip N88-20523

ELECTRIC EQUIPMENT TESTS
EDF's studies and first choices regarding the design of electrical equipment
[NASA-TT-20222] N88-20553
ELECTRIC FIELDS
Atmospheric electrical modeling in support of the NASA F-106 storm hazards project
[NASA-CR-181639] N88-20758
Upward propagating electric fields from thunderstorms and VLF transmitters N88-20767
Double layer polarization of nonconducting spheroidal particles and its application to Kerr effect
[ISSN-0208-05658] N88-20960
Comparison of analytic and full guiding center behavior at a trapped-passing interface in stellarators
[DE88-004174] N88-21025
Arcs in cesium seeded noble gases resulting from a magnetically induced electric field
[EUT-87-E-177] N88-21028
Competing interactions in metallic superlattices
[DE88-005344] N88-21057
ELECTRIC MOTOR VEHICLES
Mission directed goals for electric vehicle battery research and development: The Task Force on electric vehicle battery goals
[DE88-005601] N88-20548
Testing and development of electric vehicle batteries for EPRI Electric Transportation Program
[DE88-005894] N88-20551
ELECTRIC POWER TRANSMISSION
Safety research of insulating materials of cable for nuclear power generating station
[NASA-TT-20202] N88-20477
ELECTRIC PULSES
Optimum transformer design for a pulsed power system
[DE88-006054] N88-20525
ELECTRIC WIRE
Evaluation of flammability for cable-like polymers
[NASA-TT-20225] N88-20476
ELECTRICAL ENGINEERING
MacCAD (Macintosh Computer Aided Design), computer aided design tool for system analysis
[AD-A189241] N88-20843
ELECTRICAL INSULATION
Evaluation of flammability for cable-like polymers
[NASA-TT-20225] N88-20476
Vapor-mist for lightweight high voltage space insulation systems
[DE87-011704] N88-20538
ELECTRICAL PROPERTIES
Electrical properties of medium field, chem-prep varistors
[DE88-006147] N88-20540
Scale-up of a batch-type chemical powder preparation process for high field varistor fabrication
[DE88-006601] N88-20541
Measurement of the properties of lossy materials inside a finite conducting cylinder
[NASA-CR-182664] N88-20962
ELECTRICAL RESISTIVITY
Simplified physical approach of the control by eddy current
[TI88-701076] N88-20552
ELECTROCHEMICAL CORROSION
Corrosion-wear process under rolling-sliding motion
[AD-A189603] N88-20635
ELECTROCHEMICAL OXIDATION
Characterization of redox states of nickel hydroxide film electrodes by in-situ Raman spectroscopy
[AD-A189288] N88-20411
ELECTROCHEMISTRY
An electrochemical and spectroscopic study of electrode systems
[AD-A189274] N88-20384
A fundamental understanding of the effect of alloying elements on the corrosion resistance of rapidly solidified Mg alloys
[AD-A189385] N88-20413
Thermionic Technology Program. A: Insulator test and evaluation
[DE88-004707] N88-20735
Solid-state electrochemical processes in dye films
[AD-A188756] N88-21036
ELECTRODEPOSITION
Technology base research on zinc/air battery systems
[DE88-004893] N88-20546
ELECTRODES
An electrochemical and spectroscopic study of electrode systems
[AD-A189274] N88-20384
Aluminum-air battery development
[DE88-006618] N88-20543
Electron emission from conductors subjected to intense, short-pulse electric fields
[DE88-005412] N88-20985
ELECTRODYNAMICS
Theoretical investigation of EM wave generation and radiation in the ULF, ELF and VLF bands by the electrodynamic orbiting tether
[NASA-CR-182720] N88-20529
Chronometrically invariant formulation of electrodynamics equation
[TI88-701030] N88-21071
ELECTROENCEPHALOGRAPHY
Retinotopic mapping of the human visual system with magnetoencephalography
[AD-A189557] N88-20811
Identification of visual evoked response parameters sensitive to pilot mental state
[NASA-CR-4140] N88-20822
ELECTROLYSIS
Cavitation inception
[AD-A189220] N88-20557
ELECTROLYTES
Contrasting conductance/viscosity relations in liquid states of vitreous and polymer solid electrolytes
[AD-A189378] N88-20452
Polymeric electrolytes for ambient temperature lithium batteries
[DE88-004896] N88-20547
Double layer polarization of nonconducting spheroidal particles and its application to Kerr effect
[ISSN-0208-05658] N88-20960
Prediction of high-temperature thermodynamic properties of mixed electrolyte solutions including solubility equilibria, vapor pressure depression and boiling point elevation
[DE88-006344] N88-21069
ELECTROMAGNETIC ABSORPTION
Photochemistry at structured surfaces: A classical electromagnetic approach
[AD-A189519] N88-20387
ELECTROMAGNETIC FIELDS
Structural integrity of metallic armature rail guns
[AD-A188735] N88-20333
Photochemistry at structured surfaces: A classical electromagnetic approach
[AD-A189519] N88-20387
Transformation coefficient in wave-field acceleration scheme
[DE88-700158] N88-20507
Optimum transformer design for a pulsed power system
[DE88-006054] N88-20525
Resolution of the magnetotelluric method for determining local inhomogeneities in the sedimentary cover N88-20701
Reduced tolerance imaging 2, volume 2
[AD-A189604] N88-20939
Numerical simulations of multiphoton processes in many electron atoms
[DE88-003293] N88-20990
Topics in curved and flat space electromagnetism N88-21100
ELECTROMAGNETIC INTERFERENCE
Influence of hydrometeorological factors on visibility of objects detected by radar N88-20707
ELECTROMAGNETIC MEASUREMENT
Microwave and structural properties of saline ice
[AD-A189307] N88-20779
ELECTROMAGNETIC PROPERTIES
Joint services electronics program
[AD-A189262] N88-20533
Topics in curved and flat space electromagnetism N88-21100
ELECTROMAGNETIC PULSES
Electron emission from conductors subjected to intense, short-pulse electric fields
[DE88-005412] N88-20985
ELECTROMAGNETIC RADIATION
Time-domain system for identification of the natural resonant frequencies of aircraft relevant to electromagnetic compatibility testing
[PB88-164520] N88-20519
Theoretical investigation of EM wave generation and radiation in the ULF, ELF and VLF bands by the electrodynamic orbiting tether
[NASA-CR-182720] N88-20529
ELECTROMAGNETIC SCATTERING
Electromagnetic scattering from and natural resonances of the circular strip N88-20523
ELECTROMAGNETISM
Topics in curved and flat space electromagnetism N88-21100
ELECTROMECHANICAL DEVICES
Dynamics of high-speed mechanisms with elastic members N88-20843
ELECTRON ACCELERATION
Collective acceleration of electrons and ions in a high relativistic electron beam
[DE88-005261] N88-20998
ELECTRON ACCELERATORS
Trajectory code studies, 1987
[DE88-006218] N88-20335
The continuous electron beam accelerator facility
[CEBAF-PR-87-017] N88-20996
Design of electron beam accelerator for microwave application
[DE88-005252] N88-20999
ELECTRON BEAMS
Mode priming in an overmoded gyrotron oscillator
[AD-A189151] N88-20602
Development of electrostatic-accelerator free-electron lasers
[AD-A189507] N88-20614
The continuous electron beam accelerator facility
[CEBAF-PR-87-017] N88-20996
Rapid e-beam heating for measuring thermodynamics of metastable materials
[DE88-003565] N88-21066
ELECTRON CYCLOTRON HEATING
A high field launch for electron cyclotron heating using an external window
[DE88-005350] N88-21000
ELECTRON DENSITY (CONCENTRATION)
Upward propagating electric fields from thunderstorms and VLF transmitters N88-20767
ELECTRON DENSITY PROFILES
Arcs in cesium seeded noble gases resulting from a magnetically induced electric field
[EUT-87-E-177] N88-21028
ELECTRON DIFFRACTION
Recent progress in structure determination by LEED (Low-Energy Electron Diffraction) measure the properties of the deep donors (DX-cent)
[DE88-003851] N88-21048
ELECTRON EMISSION
Electron emission from conductors subjected to intense, short-pulse electric fields
[DE88-005412] N88-20985
ELECTRON ENERGY
Experimental studies of plasma heating due to the parametric decay of a large amplitude pump into lower hybrid waves N88-21017
Arcs in cesium seeded noble gases resulting from a magnetically induced electric field
[EUT-87-E-177] N88-21028
ELECTRON GUNS
Synthesis method applied to the design of an electron gun for a gyrotron
[INPE-4357-TDL/298] N88-20607
Development of electrostatic-accelerator free-electron lasers
[AD-A189507] N88-20614
Modulatable thin film field emission space gun
[AD-A189279] N88-21043
ELECTRON MICROSCOPY
Examination of polysulfide sealants by scanning electron microscopy
[MRL-R-1096] N88-20478
Improved methods for high resolution electron microscopy
[DE88-005731] N88-20609
ELECTRON ORBITALS
Numerical simulations of multiphoton processes in many electron atoms
[DE88-003293] N88-20990
ELECTRON PLASMA
Arcs in cesium seeded noble gases resulting from a magnetically induced electric field
[EUT-87-E-177] N88-21028
ELECTRON PRECIPITATION
Stimulated Emission of Energetic Particles (SEEP)
[AD-A188724] N88-21094
ELECTRON SCATTERING
Electron stimulated desorption and coherent electron scattering
[AD-A189091] N88-20978
ELECTRON SPECTROSCOPY
An interpretation of the ethylenic, carbidic, and graphite auger lineshapes of chemisorbed carbon species
[AD-A189092] N88-20379
ELECTRON TRANSFER
Mechanisms of photoinduced electron transfer
[DE88-004917] N88-20983
ELECTRONIC EQUIPMENT
Joint services electronics program
[AD-A189262] N88-20533
ELECTRONIC WARFARE
Bragg-cell receiver study
[NASA-CR-182684] N88-20535
ELECTRONS
Polarization of electrons in an electromagnetic wave field in the presence of magnetic field
[DE88-700169] N88-20509

Image charge, coherent scattering, and symmetry effects in electron stimulated desorption: O(-) from O sub 2 condensed on metals
[AD-A189093] N88-20979
The magnitude of secondary electron contributions in photon stimulated desorption
[AD-A189094] N88-20980
Topics in curved and flat space electromagnetism N88-21100

ELECTROSTATICS
Observations on electrostatic effects in a filter test system
[AD-A188797] N88-20378
Development of electrostatic-accelerator free-electron lasers
[AD-A189507] N88-20614

ELEMENTARY PARTICLES
Research in high energy elementary particle physics
[DE88-006065] N88-20994

ELEVATION
Interpolation algorithms for digital terrain models
[INPE-4373-PRE/1196] N88-20877
Prediction of high-temperature thermodynamic properties of mixed elctrolyte solutions including solubility equilibria, vapor pressure depression and boiling point elevation
[DE88-006344] N88-21069

ELIMINATION
Elimination of quantifiers of linear variables and corresponding transfer principles
[DE88-005692] N88-20912

ELLIPSOIDS
The effect of sting interference at low speeds on the drag coefficient of an ellipsoidal body using a magnetic suspension and balance system
[NASA-CR-181611] N88-20274

ELLIPTIC FUNCTIONS
On the norm equivalence of singularly perturbed elliptic difference operators
[DE88-006353] N88-20913

EMBRITTLEMENT
Stress corrosion cracking and metal-induced embrittlement: Comparative studies of local chemistries
[DE88-003235] N88-20419
Creep behavior of consolidated rapidly solidified Type 304 stainless steel powder containing helium
[DE88-005536] N88-20424
A study of the dynamics of high temperature brittle intergranular fracture by acoustic emission
[AERE-R-12479] N88-20650

EMISSION
A study of satellite emission computed tomography
[AD-A189567] N88-20745

EMISSION SPECTRA
Stratospheric trace gas distributions from fair infrared thermal emission spectroscopy N88-20749
IUE program SUGSD: Varability time scale of H Ly-alpha from Uranus
[NASA-CR-182706] N88-21107
The astrophysics of nebulae and active galactic nuclear emission-line regions: New methods and applications N88-21111

EMITTERS
Bragg-cell receiver study
[NASA-CR-182684] N88-20535
Passive DF: A tutorial, part 1
[NASA-CR-182669] N88-20646
Modulatable thin film field emission space gun
[AD-A189279] N88-21043

ENERGETIC PARTICLES
Stimulated Emission of Energetic Particles (SEEP)
[AD-A188724] N88-21094

ENERGY CONSERVATION
Large-Scale Advanced Prop-Fan (LAP)
[NASA-CR-182112] N88-20306
Overview of the DOE-ECUT Tribology Program
[DE88-002878] N88-20637
Applicability of aerospace thermal insulation technologies to the civilian sector
[DE88-003717] N88-21086

ENERGY CONVERSION
Point-focus concentrator reflector assembly, phase 1
[DE88-003616] N88-20720

ENERGY CONVERSION EFFICIENCY
Research on multibandgap solar cells
[DE87-012261] N88-20721
Stable, high-efficiency, CuInSe2-based, polycrystalline, thin-film tandem solar cells
[DE88-001116] N88-20726
Crystalline photovoltaic cell technology: Present and future
[DE88-004684] N88-20734
Overview of recent activities in the Heat Cycle Research Program
[DE88-005544] N88-20738
Thin-film cadmium telluride solar cells
[DE88-001107] N88-21050

ENERGY DISSIPATION
The Euler-Bernoulli beam equation with boundary energy dissipation
[AD-A189517] N88-20560
On the zonal momentum balance at the equator N88-20788

ENERGY DISTRIBUTION
Procedure for detection and identification of a helicopter
[NASA-TT-20234] N88-20297

ENERGY GAPS (SOLID STATE)
Research on multibandgap solar cells
[DE87-012261] N88-20721
Study for the determination of general and specific properties of wide energy-band gap HgHdTe in the 1-2 micrometer wavelength range
[AD-A189177] N88-21041

ENERGY LEVELS
An experimental method for species concentration measurements in a welding arc using laser-induced fluorescence
[DE88-005638] N88-20636
Quantum Monte Carlo study of the MIES associated with H2 (X 1 sigma sub g (+)) and H2 (B 1 sigma sub u (+))
[AD-A189063] N88-20977
Image charge, coherent scattering, and symmetry effects in electron stimulated desorption: O(-) from O sub 2 condensed on metals
[AD-A189093] N88-20979

ENERGY SPECTRA
Vibration spectra of oxygen and vanadium atoms in vanadium-oxygen disordered interstitial alloys
[DE87-703166] N88-20404
Study of spectra of sea waves on horizontally nonuniform current in rip zone N88-20699

ENERGY STORAGE
Proof of the feasibility of coherent and incoherent schemes for pumping a gamma-ray laser
[AD-A189238] N88-20613

ENERGY TECHNOLOGY
Federal Ocean Energy Technology
[DE87-012279] N88-20722
Power from the sun: Principles of high temperature solar thermal technology
[DE87-001104] N88-20736
Technology '87: Research and Development Laboratory Technology Transfer Program
[DE88-003142] N88-21084

ENERGY TRANSFER
Molecular dynamics of laser ablation of a polymer coating
[DE88-004337] N88-20488
Turbulent transfer of momentum and heat in boundary layer of fluid beyond an obstacle. 1: Hydrodynamic characteristics N88-20690
Power spectral density analysis of wind-shear turbulence for related flight simulations
[NASA-CR-182721] N88-20773
Energy and momentum fluxes through the sea surface N88-20798
Excimer laser photolysis studies of T-V (Translation-to-Vibration) energy transfer
[AD-A189613] N88-20989
Observations on energy transport in tokamaks: A new formula for turbulent transport
[DE88-005309] N88-21019

ENGINE FAILURE
Flight simulator experiments concerning take-off visibility minima
[NLR-TR-86050-U] N88-20281

ENGINE PARTS
Aircraft corrosion problems and research in the Netherlands
[NLR-MP-86066-U] N88-20427

ENGINE TESTS
Engine testing for synfuel operation
[DE88-006044] N88-20645

ENGINES
Advanced components for spaceborne infrared astronomy
[NASA-CR-177470] N88-20601

ENTHALPY
A calorimetric determination of the enthalpy of formation and a description of the defect structure of the ordered beta-phase /Ni, Cu/ /1-x/ Al/x/
[NASA-TT-20157] N88-20434
Radiative processes affecting ocean mixed-layer heat content and their monitoring from satellite N88-20800
The thermodynamic properties of organic oxygen compounds
[DE88-001208] N88-21065

ENTRAINMENT
Structures and fluxes in a deep convecting mixed layer N88-20786
Subduction N88-20796

ENTROPY
The thermodynamic properties of organic oxygen compounds
[DE88-001208] N88-21065

ENVIRONMENT EFFECTS
Review of selenium thermodynamic data
[DE88-006194] N88-21068

ENVIRONMENT MANAGEMENT
Activities report in aeronautics and astronautics
[ETN-88-91332] N88-21115

ENVIRONMENT PROTECTION
Environmental projects. Volume 5, part 1: Study of subsurface contamination. Part 2: Guide to implement environmental compliance programs
[NASA-CR-182691] N88-20741

ENVIRONMENTAL TESTS
Cavitation inception
[AD-A189220] N88-20557

ENZYMES
Enzyme-based fiber optic sensors
[DE88-005674] N88-21013

EPOXY MATRIX COMPOSITES
Fracture characteristics of carbon and aramid unidirectional composites in interlaminar shear and open hole tensile tests
[NLR-TR-86083-U] N88-20371

EQUATIONS
On error equations for determining Earth rotation parameters with VLBI network N88-20500

EQUATIONS OF MOTION
Contribution to theory of quasigeostrophic motions of finite amplitude in viscous stratified ocean N88-20695

EQUATIONS OF STATE
The automated symbolic derivation of state equations for dynamic systems
[DE88-000968] N88-20945

EQUATORIAL REGIONS
Equatorial turbulence: Mixed layer and thermocline N88-20787
On the zonal momentum balance at the equator N88-20788
Mixed-layer shear related to wind stress in the central equatorial Pacific N88-20793

EQUIVALENCE
On the norm equivalence of singularly perturbed elliptic difference operators
[DE88-006353] N88-20913

EROSION
Erosion in dual-phase microstructures
[DE88-004507] N88-20421
Reduction of erosion in elbows due to flow modifications, phase 1
[DE88-001028] N88-20584
Hydrogen pumping and release by graphite under high flux plasma bombardment
[DE88-005880] N88-21021

ERROR ANALYSIS
Formulation of a general technique for predicting pneumatic attenuation errors in airborne pressure sensing devices
[NASA-TM-100430] N88-20302
Generalized expression for radio navigation parameter error N88-20691

ERRORS
On error equations for determining Earth rotation parameters with VLBI network N88-20500
Two dimensional uncorrelated bias in fix algorithms
[NASA-CR-182683] N88-20847
A low-frequency measurement of the spectrum of the cosmic microwave background radiation N88-21112

ERS-1 (ESA SATELLITE)
The German processing and archiving facility for ERS-1
[ESA-CR(P)-2531] N88-21082

ESCAPE SYSTEMS
Expected value analysis for an unmanned expendable launch vehicle payload escape system
[AD-A189494] N88-20337

ESTIMATES
Estimation-correlation, modeling, and identification in adaptive array processors
[AD-A189130] N88-20512
Detection and angle estimation of coherent plane waves N88-20522
Energy and momentum fluxes through the sea surface N88-20798
Bias reduction when there is no unbiased estimate
[AD-A189407] N88-20937
Regional Conference on the Analysis of the Unbalanced Mixed Model
[AD-A188747] N88-20943

Temperature estimates for a free flowing railgun plasma
[MRL-R-1054] N88-21032

ESTIMATING
Tidal estimation in the Pacific with application to SEASAT altimetry
[NASA-TM-100694] N88-20780

EULER EQUATIONS OF MOTION
An L-U implicit multigrid algorithm to solve the Euler equations for transonic flow in rotating turbomachinery passages N88-20270
Solution of two-dimensional Euler equations: Experience with a finite volume code
[DFVLR-FB-87-41] N88-20572
Multigrid solution of the Euler equations N88-20582
A symmetric set of Euler angles and oblique orientation space sections
[DE88-005317] N88-21056

EULER-LAGRANGE EQUATION
An adaptive grid technique for solution of the Euler equations N88-20579
Introduction to classical mechanics of systems with constraints, part 1
[TI88-701055] N88-20957
Introduction to classical mechanics of systems with constraints, part 2
[TI88-701056] N88-21072

EUROPE
Ozone sonde and Dobson spectrometer data obtained during the MAP/GLOBUS 1983 campaign over Western Europe
[BPT-5/87] N88-20771

EUROPEAN COMMUNICATIONS SATELLITE
Alternative force structuring strategies for military satellite communication systems
[AD-A189492] N88-20516

EUROPEAN SPACE AGENCY
The preparation, assembly and mounting of RF coaxial cables
[ESA-PSS-01-718-ISS-1] N88-20504

EVALUATION
Combustion theory and related questions
[AD-A189160] N88-20382
Method to evaluate image-recovery algorithms based on task performance
[DE88-005382] N88-20853
Development and evaluation of instrumentation and methods for multi-element analysis
[AD-A189345] N88-21018

EVAPORATION
Model catalyst studies of SMSI (Strong Metal/Support Interactions) and the role of D-electrons in chemisorption and catalysis
[DE88-004518] N88-20393
The thermodynamic properties of organic oxygen compounds
[DE88-001208] N88-21065

EVOKED RESPONSE (PSYCHOPHYSIOLOGY)
Identification of visual evoked response parameters sensitive to pilot mental state
[NASA-CR-4140] N88-20822

EXCIMER LASERS
Practical constraints on sources for pulsed beam lithographies
[DE88-006594] N88-20623

EXCITATION
Seasonal variations and excitation mechanisms of the equatorially trapped waves N88-20751
Image charge, coherent scattering, and symmetry effects in electron stimulated desorption: O(-) from O sub 2 condensed on metals
[AD-A189093] N88-20979
The magnitude of secondary electron contributions in photon stimulated desorption
[AD-A189094] N88-20980

EXHAUST GASES
Exhaust-gas pressure and temperature survey of F404-GE-400 turbofan engine
[NASA-TM-88273] N88-20307

EXHAUST NOZZLES
Exhaust-gas pressure and temperature survey of F404-GE-400 turbofan engine
[NASA-TM-88273] N88-20307

EXOBIOLOGY
Aerospace medicine and biology: A continuing bibliography with indexes (supplement 309)
[NASA-SP-7011(309)] N88-20814

EXPECTATION
On the expectation of the product of four matrix-valued Gaussian random variables
[EUT-87-E-178] N88-20927

EXPERIMENT DESIGN
Interfacial adhesion: Theory and experiment
[NASA-TM-100830] N88-20417
Three-dimensional shear layer experiments and their use as test cases for calculation methods
[NLR-MP-86036-U] N88-20570
Experimental verification of a finite-difference time-domain thin slot algorithm
[DE88-005572] N88-20859

EXPERT SYSTEMS
The concept of intelligent integrated interactive CAD systems
[CWI-CS-R8717] N88-20865
Organization of design knowledge in an intelligent CAD environment
[CWI-CS-R8720] N88-20868
An integrated data description language for coding design knowledge
[CWI-CS-R8731] N88-20871
An implementation of the OPS5 language for computers compatible with IBM-PC
[INPE-4291-PRE/1162] N88-20882
Expert system techniques and decision support system: A case study (Dec. 1985 - Jun. 1986)
[ETN-88-91347] N88-20884
The use of an automated flight test management system in the development of a rapid-prototyping flight research facility
[NASA-TM-100435] N88-20896
SEAT: A strategic engagement analysis tool
[DE88-000498] N88-20944
Expert systems for decision support in military aircraft mission preparation
[NLR-MP-87013-U] N88-20946
Consistency of rule-based expert systems
[CWI-CS-R8736] N88-20950
Application of expert systems in project management decision aiding
[NASA-CR-180762] N88-21074
A menu-driven knowledge retrieval system accessing ASCII data
[DE88-001742] N88-21079

EXPLOSIONS
Theoretical investigation of the wave shaping process in a section of ladder fracture tape
[MRL-R-1081] N88-20595

EXPLOSIVES
Anomalous shock sensitivity/density relationship for RDX-polyethylene wax and related formulations from MRL Small Scale Gap Test (SSGT) measurements
[MRL-R-1099] N88-20399
A comparative assessment of US and UK explosives qualified as replacements for tetryl
[MRL-R-1094] N88-20486
Some properties of Australian produced explosive composition H-6
[MRL-TN-525] N88-20490

EXTRAGALACTIC RADIO SOURCES
Relativistic jet models for the BL Lacertae object Mrk 421 during three epochs of observation
[NASA-TM-89727] N88-21090

EXTRATERRESTRIAL RADIO WAVES
Analysis of deep sky sources found by the infrared astronomy satellite
[AD-A189605] N88-21089

EXTRAVEHICULAR ACTIVITY
The space station assembly phase: Flight telerobotic servicer feasibility. Volume 2: Methodology and case study
[NASA-CR-182690] N88-20352

EXTREME ULTRAVIOLET RADIATION
Projected performance of RF-linac-driven free-electron lasers in the VUV and soft X-ray regions
[DE88-004294] N88-20625

F

F REGION
Model of Jovian F region ionosphere
[NASA-CR-182587] N88-21105

F-106 AIRCRAFT
Atmospheric electrical modeling in support of the NASA F-106 storm hazards project
[NASA-CR-181639] N88-20758

FABRICATION
Use of reinforced inorganic cement materials for spark wire and drift chamber wire frames
[NASA-CR-180759] N88-20438
A new process for synthesis of silicon nitride powders for advanced ceramics
[AD-A189354] N88-20451
Scale-up of a batch-type chemical powder preparation process for high field varistor fabrication
[DE88-006601] N88-20541
Low threshold ridge waveguide single quantum well lasers N88-20631
Research on high-efficiency, stacked, multijunction, amorphous silicon alloy thin-film solar cells
[DE88-001108] N88-20723
Research on single-crystal CdTe solar cells
[DE88-001115] N88-20725
Stable, high-efficiency, CuInSe2-based, polycrystalline, thin-film tandem solar cells
[DE88-001116] N88-20726
Design of the Sandia-Israel 20-kW reflux heat-pipe solar receiver/reactor
[DE88-001312] N88-20729
Molybdenum-base cermet fuel development
[DE88-005529] N88-21003
Focused ion beam fabrication of graded channel FET's in GaAs and Si
[AD-A189166] N88-21040
Thin-film cadmium telluride solar cells
[DE88-001107] N88-21050

FABRY-PEROT SPECTROMETERS
Velocity resolved far-infrared spectroscopy of galactic sources N88-21099

FAILURE
Estimating system and component reliabilities under partial information on cause of failure
[AD-A189107] N88-20653

FAILURE ANALYSIS
Ply-level failure analysis of a graphite/epoxy laminate under bearing-bypass loading
[NASA-TM-100578] N88-20372
Improve the lifetime of the hollow fiber sodium sulfur cell
[DE88-004881] N88-20469
Fracture criteria for discontinuously reinforced metal matrix composites
[NASA-CR-182665] N88-20662

FAR INFRARED RADIATION
Development of electrostatic-accelerator free-electron lasers
[AD-A189507] N88-20614
Stratospheric trace gas distributions from fair infrared thermal emission spectroscopy N88-20749
Velocity resolved far-infrared spectroscopy of galactic sources N88-21099

FAR ULTRAVIOLET RADIATION
Wavelength scaling of lithium-like recombination scheme for X-UV gain production --- X-ray lasers
[ETN-88-92002] N88-20634

FASTENERS
Crack distribution and growth rates for critical fastener holes in Mirage wing RH79
[AD-A189080] N88-20293

FATIGUE (MATERIALS)
Crack distribution and growth rates for critical fastener holes in Mirage wing RH79
[AD-A189080] N88-20293
High-temperature metal matrix composites
[AD-A189516] N88-20367
The effect of microstructure on the fatigue crack growth resistance of nickel base superalloys
[AD-A189526] N88-20414
Threshold fatigue crack growth in Ti-6Al-2Sn-4Zr-6Mo
[AD-A189560] N88-20415

FATIGUE LIFE
Dynamic tensile cyclic fatigue of Si3N4
[DE88-003919] N88-20658
Fatigue load measurements and evaluation of the 25m Horizontal Axis Wind Turbine (HAWT) at Petten, The Netherlands
[NLR-MP-86054-U] N88-20660
European approaches in standard spectrum development --- aircraft load spectra
[NLR-MP-87007-U] N88-20661

FATIGUE TESTS
Crack distribution and growth rates for critical fastener holes in Mirage wing RH79
[AD-A189080] N88-20293
Dynamic tensile cyclic fatigue of Si3N4
[DE88-003919] N88-20658

FAULT TOLERANCE
A survey of provably correct fault-tolerant clock synchronization techniques
[NASA-TM-100553] N88-20894
A fault injection experiment using the AIRLAB Diagnostic Emulation Facility
[NASA-CR-178390] N88-20895

FEASIBILITY
Laser gyro attitude control system feasibility
[AD-A189368] N88-20285
Feasibility report: Operation of light air cushion vehicle at McMurdo Sound, Antarctica
[AD-A189057] N88-20494

FEASIBILITY ANALYSIS
An investigation of classical dynamic scaling techniques applied to an oleo-pneumatic landing gear strut
[AD-A187664] N88-20292

Proof of the feasibility of coherent and incoherent schemes for pumping a gamma-ray laser
[AD-A189238] N88-20613
Federal Ocean Energy Technology
[DE87-012279] N88-20722
An assessment methodology for thermal energy storage evaluation
[DE88-004842] N88-20732
Conservative finite volume solutions of a linear hyperbolic transport equation in two and three dimensions using multiple grids
[NASA-CR-182715] N88-20934
Molybdenum-base cermet fuel development
[DE88-005529] N88-21003
Modulatable thin film field emission space gun
[AD-A189279] N88-21043

FEEDBACK
Robust decentralized control of large flexible structures
[DE88-005416] N88-20902

FEEDBACK CONTROL
Gas consumption estimation of an attitude control system of an artificial satellite (utilizing DRF) in limit cycle phase
[INPE-4338-RPE/553] N88-20350
Sojourn times in feedback queues
[CWI-OS-R8710] N88-20947

FERRITIC STAINLESS STEELS
The fatigue behavior of ferritic and austenitic steels at elevated temperatures
[DE88-006304] N88-20431

FERROMAGNETISM
Simplified physical approach of the control by eddy current
[TI88-701076] N88-20552

FIBER COMPOSITES
Viscoelastic behavior of a polyetheretherketone (PEEK) composite
[AD-A189545] N88-20368
Transient dynamics of fibre reinforced composite plates
[IIT-B/CE/RR/87-1] N88-20370
Interfacial chemistry-structure and fracture of ceramic composites
[DE88-005516] N88-20461

FIBER OPTICS
Development of fiber optic systems for recording and transmitting holographic information
[AD-A189406] N88-20603
Remote fiber fluorimetry techniques for pressure measurements
[DE88-004486] N88-20604
Enzyme-based fiber optic sensors
[DE88-005674] N88-21013
Development of high stability fiber optic spectrophotometric systems for study of solar/stellar magnetic activity
[AD-A189327] N88-21088

FIBER ORIENTATION
Reinforcing of thermoplastic polycarbonate and polysulfone with carbon fibers: Production and characteristics of UD-compound objects
[NASA-TT-20158] N88-20374

FIBERS
The influence of the fiber-matrix bond on the mechanical behavior of NICALON/SiC composites
[DE88-006155] N88-20369
Recommendations on developing polycrystalline alumina fiber N88-20502

FIELD EFFECT TRANSISTORS
Focused ion beam fabrication of graded channel FET's in GaAs and Si
[AD-A189166] N88-21040
Energy loss rates for light holes in InGaAs/GaAs strained layer single quantum wells
[DE88-005744] N88-21062
MOSFET performance degradation due to hot carriers N88-21063

FIELD EMISSION
A study of the interaction of light with sub-micron metallic surfaces
[DE88-003138] N88-20624
Modulatable thin film field emission space gun
[AD-A189279] N88-21043

FIELD OF VIEW
Space infrared telescope facility wide field and diffraction limited array camera (IRAC)
[NASA-CR-182704] N88-21092

FIELD THEORY (ALGEBRA)
String theory and algebraic geometry of moduli spaces
[CWI-PM-R8705] N88-21070

FIGHTER AIRCRAFT
Crack distribution and growth rates for critical fastener holes in Mirage wing RH79
[AD-A189080] N88-20293
Viscoelastic behavior of a polyetheretherketone (PEEK) composite
[AD-A189545] N88-20368

FILLERS
Hydrogen induced cracks in armor steel weldments fabricated with austenitic filler alloys
[AD-A188733] N88-20406

FILTRATION
Observations on electrostatic effects in a filter test system
[AD-A188797] N88-20378

FINITE DIFFERENCE THEORY
Experimental verification of a finite-difference time-domain thin slot algorithm
[DE88-005572] N88-20859
Predicting oscillatory finite difference solutions to the heat equation: A comparative study of the coefficient and matrix methods
[AD-A189591] N88-20911
A Lagrangian moving grid scheme for one-dimensional evolutionary partial differential equations
[CWI-NM-R8713] N88-20922

FINITE ELEMENT METHOD
Finite element calculations for aerodynamic coefficients of a 3-dimensional body in subsonic flow using Green's function method
[NASA-TT-20208] N88-20272
Effect of rotation on the lateral stability of a free-flying column subjected to an axial thrust with directional control
[AD-A188890] N88-20338
Nondestructive evaluation of carbon-carbon coatings
[AD-A189524] N88-20453
Dynamics of high-speed mechanisms with elastic members N88-20643
Finite element methods for quasi-prismatic bodies with application to gears N88-20644
A preliminary investigation of finite-element modeling for composite rotor blades
[NASA-TM-100559] N88-20656
Theory and experiments of fracture in cyclic compression: Single phase ceramics, transforming ceramics and ceramic composites
[DE88-005792] N88-20659
Finite element methodology for nonlinear free and harmonic forced vibrations of beam and plate structures N88-20663
An analysis of large deformation axisymmetric inelastic problems by finite element and boundary element methods N88-20664
Correlation of data on strain accumulation adjacent to the San Andreas Fault with available models
[NASA-CR-180757] N88-20742
The use of a barotropic finite element model for the study of circulation on the continental shelf of the southeast coast of Brazil
[INPE-4401-PRE/1218] N88-20774
Finite State Tables for general computer programming applications
[DE88-006254] N88-20881
A knowledge system for automatic finite element mesh generation: AMEKS
[DE87-014894] N88-20914
Local refinement of stress field by finite element method
[INPE-4321-TDL/288] N88-20930
Modeling of laser ultrasound generation in a weld pool
[DE88-005546] N88-20971

FINITE VOLUME METHOD
The construction of a three-dimensional finite volume grid generator for a wing in a wind tunnel with application to Navier-Stokes flow solvers
[FFA-TN-1987-58] N88-20277
Solution of two-dimensional Euler equations: Experience with a finite volume code
[DFVLR-FB-87-41] N88-20572
Conservative finite volume solutions of a linear hyperbolic transport equation in two and three dimensions using multiple grids
[NASA-CR-182715] N88-20934

FIRE CONTROL
AVSCOM'S modifications to Teledyne Systems Company's air-to-air fire control system simulation model
[AD-A189136] N88-20294

FIRE PREVENTION
Spacecraft fire-safety experiments for space station: Technology development mission
[NASA-CR-182114] N88-20353
Flame retardants
[NASA-TT-20250] N88-20400

FISSURES (GEOLOGY)
Experimental and theoretical constraints on the origin of mid-ocean ridge geothermal fluids N88-20784

FIXED POINTS (MATHEMATICS)
Solving reflexive domain equations in a category of complete metric spaces
[CWI-CS-R8709] N88-20956

FLAME IONIZATION
Kinetic mechanisms for ionization and afterburning suppression
[AD-A189219] N88-20383

FLAME PROPAGATION
Evaluation of flammability for cable-like polymers
[NASA-TT-20225] N88-20476

FLAME RETARDANTS
Kinetic mechanisms for ionization and afterburning suppression
[AD-A189219] N88-20383
Flame retardants
[NASA-TT-20250] N88-20400

FLAMES
Laser ignition of nitramine composite propellants and crack propagation and branching in burning solid propellants
[AD-A189260] N88-20483

FLAMMABILITY
Evaluation of flammability for cable-like polymers
[NASA-TT-20225] N88-20476

FLANGES
Crack distribution and growth rates for critical fastener holes in Mirage wing RH79
[AD-A189080] N88-20293

FLAPS (CONTROL SURFACES)
An experimental investigation of the flap-lag-torsion aeroelastic stability of a small-scale hingeless helicopter rotor in hover
[NASA-TP-2546] N88-20257

FLAT PLATES
Modification of parabolic dish antenna pattern using two symmetrically placed circular flat plates
[AD-A189543] N88-20517
Investigation of heat transfer to a flat plate in a shock tube
[AD-A189538] N88-20561

FLEXIBILITY
PNL-1 improved ceramic composites through controlled fiber matrix interaction
[DE88-005680] N88-20462

FLEXIBLE BODIES
Moveable thermal joints for deployable or steerable spacecraft radiator systems
[NLR-MP-87016-U] N88-20347
Dynamic modelling of flexible rotor shafts mounted on hydrodynamic bearings N88-20641

FLEXIBLE SPACECRAFT
SIMSAT: Simulation package for flexible systems. Beams in space
[TW-278] N88-20348
Robust decentralized control of large flexible structures
[DE88-005416] N88-20902

FLIGHT CONTROL
A fault injection experiment using the AIRLAB Diagnostic Emulation Facility
[NASA-CR-178390] N88-20895

FLIGHT CREWS
Multi-crew pictorial format display evaluation
[AD-A189349] N88-20824
Proceedings of the Workshop on the Assessment of Crew Workload Measurements Methods, Techniques and Procedures. Volume 1: Preliminary Selection of Measures
[AD-A189004] N88-20827

FLIGHT ENVELOPES
Australian aerodynamic design codes for aerial tow bodies
[AD-A189048] N88-20258

FLIGHT OPTIMIZATION
Optimal thrust vector control of coplanar orbital evasive maneuvers
[AD-A189544] N88-20346

FLIGHT PATHS
Development of an interactive real-time graphics system for the display of vehicle space positioning
[NASA-TM-100429] N88-20344
Method for determining artillery position
[NASA-TT-20237] N88-20974

FLIGHT SAFETY
Proceedings of the Workshop on the Assessment of Crew Workload Measurements Methods, Techniques and Procedures. Volume 1: Preliminary Selection of Measures
[AD-A189004] N88-20827

FLIGHT SIMULATION
Standardized environmental fatigue sequence for the evaluation of composite components in combat aircraft (ENSTAFF = ENvironmental falSTAFF)
[LBF-FB-179] N88-20300

Power spectral density analysis of wind-shear turbulence for related flight simulations
[NASA-CR-182721] N88-20773

FLIGHT TESTS
A review of technologies applicable to low-speed flight of high-performance aircraft investigated in the Langley 14- x 22-foot subsonic tunnel
[NASA-TP-2796] N88-20264
Flight tests of external modifications used to reduce blunt base drag
[NASA-TM-100433] N88-20279
A correlation study of X-29A aircraft and associated analytical development
[NASA-TM-89735] N88-20296
Aircraft flight flutter testing at the NASA Ames-Dryden Flight Research Facility
[NASA-TM-100417] N88-20301
The design and use of a temperature-compensated hot-film anemometer system for boundary-layer flow transition detection on supersonic aircraft
[NASA-TM-100421] N88-20304
Lateral and longitudinal stability and control parameters for the space shuttle discovery as determined from flight test data
[NASA-TM-100555] N88-20309
Western aeronautical test range real-time graphics software package MAGIC
[NASA-TM-100425] N88-20506
Preliminary in-flight boundary layer transition measurements on a 45 deg swept wing at Mach Numbers between 0.9 and 1.8
[NASA-TM-100412] N88-20598
Atmospheric electrical modeling in support of the NASA F-106 storm hazards project
[NASA-CR-181639] N88-20758
Configuration management issues and objectives for a real-time research flight test support facility
[NASA-TM-100437] N88-20832
The use of an automated flight test management system in the development of a rapid-prototyping flight research facility
[NASA-TM-100435] N88-20896
Predictive monitoring research: Summary of the PREMON system
[NASA-CR-182687] N88-20905

FLIR DETECTORS
Passive autonomous infrared sensor technology
[AD-A188698] N88-21005

FLOW COEFFICIENTS
Measurement of rate constants of elementary gas reactions of importance to upper atmosphere and combustion systems
[AD-A189432] N88-20386

FLOW DISTRIBUTION
On the Kutta condition for flows around lifting airfoils and wings
[DFVLR-FB-87-40] N88-20268
Air-jet spoiler
[BU-364] N88-20299
Numerical model of the time independent mean flow in a rotating rocket motor N88-20360
Coherent structure-reflective turbulent viscous flow modeling
[AD-A188339] N88-20556
Graphics and flow visualization of computer generated flow fields
[NASA-CR-182679] N88-20573
Reduction of erosion in elbows due to flow modifications, phase 1
[DE88-001028] N88-20584
Measurement and analysis of the noise radiated by low Mach numbers centrifugal blowers
[AD-A189226] N88-20966

FLOW EQUATIONS
On the Kutta condition for flows around lifting airfoils and wings
[DFVLR-FB-87-40] N88-20268

FLOW MEASUREMENT
Tests on the AFWAL 65 deg delta wing at NLR: A study of vortex flow development between Mach = 0.4 and 4
[NLR-MP-86058-U] N88-20266
Verification of the momentum theory for rotors using measurements on a model helicopter
[R-840-S] N88-20275
Comparison between computed and measured swirl and turbulence in reciprocating engines
[PDR/IC-CFDU/32] N88-20647
Deep water mass circulation in the Alboran Basin. Measurements - January to April 1982: ALBORAN 2
[AD-A189205] N88-20777

FLOW STABILITY
Measurement of rate constants of elementary gas reactions of importance to upper atmosphere and combustion systems
[AD-A189432] N88-20386
Development of disturbances in swept wing flows
[NASA-CR-182675] N88-20574

FLOW VELOCITY
Boundary effects on the drag of a cylinder in axial motion at low Reynolds number N88-20578
Turbulent transfer of momentum and heat in boundary layer of fluid beyond an obstacle. 1: Hydrodynamic characteristics N88-20690
Contribution to theory of quasigeostrophic motions of finite amplitude in viscous stratified ocean N88-20695

FLOW VISUALIZATION
An experimental investigation of decelerating flow about two-dimensional cambered plates
[DE88-006598] N88-20567
Graphics and flow visualization of computer generated flow fields
[NASA-CR-182679] N88-20573
Digital enhancement of flow field images
[NASA-TP-2770] N88-20833

FLUID DYNAMICS
Structures and fluxes in a deep convecting mixed layer N88-20786
Hamiltonian description of the interaction of surface waves with mixed-layer currents N88-20799
Development of an optical diagnostic instrument. Part 2: Instrument development --- space laboratories
[NLR-TR-87079-L-PT-2] N88-21016

FLUID FILMS
Lubricating properties of molybdenum disulfide. Part 3: Performance of molybdenum disulfide-containing oils in fluid lubrication
[NASA-TT-20156] N88-20480

FLUID FLOW
Fluidization mechanisms in slurry flows
[DE88-005191] N88-20563
Velocity and concentration measurements in flowing suspensions by nuclear magnetic resonance
[DE88-006225] N88-20589
Subduction N88-20796
Hamiltonian description of the interaction of surface waves with mixed-layer currents N88-20799

FLUID MANAGEMENT
Cryogenic Fluid Management Technology Workshop. Volume 2: Roundtable Discussion of Technology Requirements
[NASA-CP-10009] N88-20599

FLUID MECHANICS
Fluidization mechanisms in slurry flows
[DE88-005191] N88-20563
Fluid-thermal-structural study of aerodynamically heated leading edges
[NASA-TM-100579] N88-20666
On the structure of pulsed plasma jets N88-21030

FLUID-SOLID INTERACTIONS
Abrasion and impact resistant coatings
[DE88-003562] N88-20464

FLUIDS
Experimental and theoretical constraints on the origin of mid-ocean ridge geothermal fluids N88-20784

FLUORESCENCE
Nondestructive evaluation of carbon-carbon coatings
[AD-A189524] N88-20453
Remote fiber fluorimetry techniques for pressure measurements
[DE88-004486] N88-20604
Laser fluorescence spectroscopy of zinc neutrals originating from laser-irradiated and ion-bombarded zinc sulfide and zinc surfaces
[DE88-006033] N88-20620
Noncontact thermometry via laser pumped, thermographic phosphors: Characterization of systematic errors and industrial applications
[DE88-005599] N88-20628
Spontaneous decay and atomic fluorescence near a metal surface of an absorbing dielectric
[AD-A187508] N88-20975

FLUORIDES
SBIR-Long fluoride fiber
[AD-A188595] N88-20492

FLUOROHYDROCARBONS
Thermal oxide growth on silicon: Intrinsic stress and silicon cleaning effects
[AD-A188790] N88-20377

FLUTTER
Application of a flux vector splitting methodology towards the solution of unsteady transonic flows, with future emphasis on the blade flutter problem
[AD-A189500] N88-20260

FLUTTER ANALYSIS
Aircraft flight flutter testing at the NASA Ames-Dryden Flight Research Facility
[NASA-TM-100417] N88-20301

FLUX (RATE)
Energy and momentum fluxes through the sea surface N88-20798
Radiative processes affecting ocean mixed-layer heat content and their monitoring from satellite N88-20800

FLUX DENSITY
Corrosion, passivity and breakdown of alloys used in high energy density batteries
[DE88-004891] N88-20422

FLUX VECTOR SPLITTING
Application of a flux vector splitting methodology towards the solution of unsteady transonic flows, with future emphasis on the blade flutter problem
[AD-A189500] N88-20260

FOCUSING
Geodetic measurement of deformation east of the San Andreas fault in Central California
[NASA-CR-182709] N88-20754
Focused ion beam fabrication of graded channel FET's in GaAs and Si
[AD-A189166] N88-21040

FOKKER-PLANCK EQUATION
Propagator solutions of partial differential equations applied to plasma transport
[DE88-006432] N88-20852

FORCE DISTRIBUTION
Force distribution and trajectory control for closed kinematic chains with applications to walking machines N88-20642

FORCED VIBRATION
Finite element methodology for nonlinear free and harmonic forced vibrations of beam and plate structures N88-20663

FOREST MANAGEMENT
The radar scattering coefficient as a function of forest stand parameters and viewing angle. An empirical study of the Pinus sylvestris L. in the Kootwijk forest (The Netherlands), extended with observations in the Speulder and Sprielder forest (The Netherlands)
[ETN-88-91348] N88-20527

FORESTS
Remote sensing of earth terrain
[NASA-CR-182677] N88-20711

FORMALISM
Body tensor formalism in finite deformation elasticity and application to the torsion of a circular cylinder N88-20651
Early reheating and cosmic strings N88-21103

FORMULAS
Orbit accuracy requirement of GPS for precise positioning and orbit determination within local area N88-20499

FOSSIL FUELS
Fluidization mechanisms in slurry flows
[DE88-005191] N88-20563

FOURIER TRANSFORMATION
Restoration techniques for redisplay of LANDSAT-5 satellite imagery
[INPE-4189-PRE/1076] N88-20712
Numerical simulations of multiphoton processes in many electron atoms
[DE88-003293] N88-20990

FOVEA
Retinotopic mapping of the human visual system with magnetoencephalography
[AD-A189557] N88-20811

FRACTIONATION
Aviation turbine fuels from tar sands bitumen and heavy oils. Part 3: Laboratory sample production
[AD-A189278] N88-20484

FRACTOGRAPHY
Crack distribution and growth rates for critical fastener holes in Mirage wing RH79
[AD-A189080] N88-20293
Fracture characteristics of carbon and aramid unidirectional composites in interlaminar shear and open hole tensile tests
[NLR-TR-86083-U] N88-20371
A study of the dynamics of high temperature brittle intergranular fracture by acoustic emission
[AERE-R-12479] N88-20650

FRACTURE MECHANICS
High-temperature metal matrix composites
[AD-A189516] N88-20367
Fracture characteristics of carbon and aramid unidirectional composites in interlaminar shear and open hole tensile tests
[NLR-TR-86083-U] N88-20371
Materials Research Laboratory at Brown University
[AD-A188006] N88-20396
Stress corrosion cracking and metal-induced embrittlement: Comparative studies of local chemistries
[DE88-003235] N88-20419
Non-destructive evaluation techniques applied to the study of fatigue microcrack growth in steel alloys
[DE88-004090] N88-20420

Fracture mechanics and creep crack growth of 1 percent Cr 1/2 percent Mo steel with and without prior exposure to creep conditions
[NLR-TR-86051-U] N88-20426
Use of reinforced inorganic cement materials for spark wire and drift chamber wire frames
[NASA-CR-180759] N88-20438
Fracture criterion of reactor graphite under multiaxial stresses N88-20442
A study of the dynamics of high temperature brittle intergranular fracture by acoustic emission
[AERE-R-12479] N88-20650
Theory and experiments of fracture in cyclic compression: Single phase ceramics, transforming ceramics and ceramic composites
[DE88-005792] N88-20659
Fracture criteria for discontinuously reinforced metal matrix composites
[NASA-CR-182665] N88-20662
ONR Far East Scientific Bulletin, volume 12, number 3, July-September 1987
[AD-A188554] N88-21081

FRACTURE STRENGTH
Composites strengthening
[AD-A189258] N88-20364
Fracture criterion of reactor graphite under multiaxial stresses N88-20442
Degradations of thermal shock resistance and the fracture toughness of reactor graphite subjected to neutron irradiation N88-20445
Application of ISRM testing methods to fracture toughness testing of graphite N88-20446
Notch sensitivity of graphite materials for VHTR N88-20447
Guidelines for estimation and characterization of the thermo-mechanical properties of new optical materials
[DE88-004359] N88-21010

FRACTURES (MATERIALS)
Interfacial chemistry-structure and fracture of ceramic composites
[DE88-005516] N88-20461

FRACTURING
A study of the dynamics of high temperature brittle intergranular fracture by acoustic emission
[AERE-R-12479] N88-20650

FRAGMENTATION
Fragmentation and flow in central collisions
[DE88-005386] N88-20991

FRAMES
Control augmented structural synthesis
[NASA-CR-4132] N88-20290
Use of reinforced inorganic cement materials for spark wire and drift chamber wire frames
[NASA-CR-180759] N88-20438

FRANCE
EDF's studies and first choices regarding the design of electrical equipment
[NASA-TT-20222] N88-20553

FREE ELECTRON LASERS
Development of electrostatic-accelerator free-electron lasers
[AD-A189507] N88-20614
Wiggler taper optimization for free-electron-laser amplifiers with moderate space-charge effects
[DE88-003758] N88-20618
Projected performance of RF-linac-driven free-electron lasers in the VUV and soft X-ray regions
[DE88-004294] N88-20625

FREE FLIGHT
Australian aerodynamic design codes for aerial tow bodies
[AD-A189048] N88-20258
Effect of rotation on the lateral stability of a free-flying column subjected to an axial thrust with directional control
[AD-A188690] N88-20338

FREE FLOW
Transport and stability properties of free shear flows N88-20577
Temperature estimates for a free flowing railgun plasma
[MRL-R-1054] N88-21032

FREE JETS
Molecular collision processes in gases and at surfaces
[AD-A189518] N88-20982

FREE RADICALS
Photolytic formation of free radicals and their effect on hydrocarbon pyrolysis chemistry in a concentrated solar environment
[DE88-004129] N88-20730

FREE VIBRATION
Finite element methodology for nonlinear free and harmonic forced vibrations of beam and plate structures N88-20663

FREQUENCIES
Theoretical investigation of EM wave generation and radiation in the ULF, ELF and VLF bands by the electrodynamic orbiting tether
[NASA-CR-182720] N88-20529
Optimal and conventional space-time processing in flow noise
[AD-A189104] N88-20965

FREQUENCY CONTROL
Fiber-coupled external-cavity semiconductor high power laser
[AD-A188454] N88-20611

FREQUENCY MEASUREMENT
Material parameter measurements at high temperatures
[NASA-CR-182707] N88-20397

FRICTION
Particle-dynamics calculations of gravity flow of inelastic, frictional spheres
[DE88-005224] N88-20586
Structural clearances and internal friction: Simulation by Eigen distortions
[ISSN-0208-5658] N88-20640

FRONTS (METEOROLOGY)
Numerical model of Rayleigh instability and spin-off eddies on fronts N88-20696
The pressure drag and momentum flux during a cold frontal passage over the Alps N88-20763
Mixed-layer fronts in the California current N88-20794

FUEL COMBUSTION
Fuels combustion research
[AD-A189114] N88-20381

FUEL CONSUMPTION
Large-Scale Advanced Prop-Fan (LAP)
[NASA-CR-182112] N88-20306
Gas consumption estimation of an attitude control system of an artificial satellite (utilizing DRF) in limit cycle phase
[INPE-4338-RPE/553] N88-20350
Status of alcohol fuels utilization technology for highway transportation: A 1986 perspective. Volume 2: Compression ignition engines
[DE88-006059] N88-20485

FUELS
Alternative fuels: Information on DOE's (Department of Energy's) methanol vehicle demonstration program
[PB88-118203] N88-20481
Status of alcohol fuels utilization technology for highway transportation: A 1986 perspective. Volume 2: Compression ignition engines
[DE88-006059] N88-20485
Molybdenum-base cermet fuel development
[DE88-005529] N88-21003

FUNCTIONAL DESIGN SPECIFICATIONS
Algebra of Communicating Processes (ACP)tau: A universal axiom system for process specification
[CWI-CS-R8725] N88-20869

FUNCTIONS (MATHEMATICS)
Large momentum pairing in one-dimensional systems
[AD-A189226] N88-20981

FURNACES
Proceedings of the 1987 International Symposium on Condensing Heat Exchangers
[DE88-005230] N88-20564

FUSELAGES
General fuselage coordinates for the calculation of three-dimensional boundary layers
[MBB/LKE-122/S/PUB/244] N88-20596

FUSES
A comparative assessment of US and UK explosives qualified as replacements for tetryl
[MRL-R-1094] N88-20486

FUSES (ORDNANCE)
Recommended replacements for tetryl in Australian production fuzes and related ordnance
[MRL-R-1089] N88-20489

FUSION REACTORS
Application of railgun principle to high-velocity hydrogen pellet injection for magnetic fusion reactor refueling
[DE88-005830] N88-20334
The Magnetically Insulated Inertial Confinement Fusion (MICF): A novel approach
[DE88-005460] N88-21026
Outlook for the fusion hybrid and tritium-breeding fusion reactors
[PB88-149281] N88-21029

FUZZY SETS
Measures of similarity between fuzzy concepts: A comparative analysis
[AD-A189430] N88-20910

G

GALACTIC CLUSTERS
Galaxy evolution in dense clusters N88-21101
Infrared constraints on the nature of dark matter N88-21102

GALACTIC EVOLUTION
Galaxy evolution in dense clusters N88-21101

GALACTIC MASS
Infrared constraints on the nature of dark matter N88-21102

GALACTIC NUCLEI
The astrophysics of nebulae and active galactic nuclear emission-line regions: New methods and applications N88-21111

GALLIUM ARSENIDES
Modeling and transport in semiconductor devices
[AD-A188760] N88-21037
Research on mercury cadmium telluride
[AD-A189155] N88-21039
Focused ion beam fabrication of graded channel FET's in GaAs and Si
[AD-A189166] N88-21040
Optical study of germanium, germanium plus arsenic, and germanium plus gallium implants in gallium arsenide
[AD-A189600] N88-21045
Electrical characteristics of MBE (Molecular Beam Epitaxyl)-grown GaAs/sub 1-x/Sb/sub x on InP and correlation with film microstructure
[DE88-003841] N88-21053
X-ray diffraction study of a thin GaAs film on Si(100)
[DE88-005290] N88-21055
Lattice relaxation of the DX centers in Ga/sub 1-x/Al/sub x/As and of the pressure-induced deep donors in GaAs
[DE88-005452] N88-21061
Energy loss rates for light holes in InGaAs/GaAs strained layer single quantum wells
[DE88-005744] N88-21062

GAMMA RAY ASTRONOMY
Very high energy gamma ray astrophysics
[DE88-005821] N88-21095
Topics in curved and flat space electromagnetism N88-21100

GAMMA RAY SPECTROMETERS
Content of natural radioactive elements in Venusian rocks determined using data from Vega-1 and Vega-2 stations N88-20323

GAMMA RAYS
Proof of the feasibility of coherent and incoherent schemes for pumping a gamma-ray laser
[AD-A189238] N88-20613

GAS ANALYSIS
A mass spectrometer evolved gas analysis experiment for in-situ analysis of cometary dust volatiles N88-21097

GAS CHROMATOGRAPHY
Gas-chromatographic analysis of products of thermal reactions of aerosol in Venusian cloud layer on Vega-1 and Vega-2 automatic interplanetary stations N88-20318
Fuels combustion research
[AD-A189114] N88-20381

GAS COOLED REACTORS
IAEA Specialists' Meeting on Graphite Component Structural Design
[DE88-780006] N88-20439

GAS DYNAMICS
Heat pipe transient analysis: Vapor dynamics
[DE88-005132] N88-20568

GAS EXPANSION
Molecular collision processes in gases and at surfaces
[AD-A189518] N88-20982

GAS FLOW
The effect of combustion gas flow on the rotational dynamics of a spinning solid fuel rocket N88-20358
Innovative, counterflow gas/fine solids, direct contact heat exchanger
[DE88-004744] N88-20585

GAS PRESSURE
Measurement of rate constants of elementary gas reactions of importance to upper atmosphere and combustion systems
[AD-A189432] N88-20386

GAS TUNGSTEN ARC WELDING
An experimental method for species concentration measurements in a welding arc using laser-induced fluorescence
[DE88-005638] N88-20636

GAS VISCOSITY
Negative viscosity in global circulations N88-20685

GAS-GAS INTERACTIONS
Transition metal cluster chemistry
[AD-A188731] N88-20405

GAS-LIQUID INTERACTIONS
Bipropellant combustion in a liquid rocket combustion chamber N88-20359
GASEOUS DIFFUSION
Measuring thin film properties using SAW (Surface Acoustic Wave) devices: Diffusivity and surface area [DE88-002216] N88-20970
GASES
Gas consumption estimation of an attitude control system of an artificial satellite (utilizing DRF) in limit cycle phase [INPE-4338-RPE/553] N88-20350
Stratospheric trace gas distributions from fair infrared thermal emission spectroscopy N88-20749
GATES (CIRCUITS)
GM: A gate matrix layout generator [EUT-87-E-179] N88-20875
GAUSS EQUATION
Gaussian techniques on shared memory multiprocessor computers [DE88-005426] N88-20855
GEARS
Finite element methods for quasi-prismatic bodies with application to gears N88-20644
GENETICS
A Darwinian approach to artificial neural systems [DE87-013184] N88-20900
GEODESY
Conformal geometry, Hotine's conjecture, and differential geodesy [AD-A189265] N88-20709
Determination of Earth rotation by the combination of data from different space geodetic systems [NASA-CR-181388] N88-20713
Crustal dynamics project data analysis, 1987. Volume 2: Mobile VLBI geodetic results 1982-1986 [NASA-TM-100689-VOL-2] N88-20753
GEODETIC ACCURACY
Generalized expression for radio navigation parameter error N88-20691
GEODETIC SURVEYS
Geodetic measurement of deformation east of the San Andreas fault in Central California [NASA-CR-182709] N88-20754
GEODYNAMICS
Crustal dynamics project data analysis, 1987. Volume 2: Mobile VLBI geodetic results 1982-1986 [NASA-TM-100689-VOL-2] N88-20753
GEOLOGICAL FAULTS
Ultrasonic physical modeling of seismic wave propagation from graben-like structures [AD-A189066] N88-20744
GEOLOGY
JPRS report: Science and technology. China [JPRS-CST-88-003] N88-20495
JPRS report: Science and technology. USSR: Earth sciences [JPRS-UES-88-001] N88-20674
Activities and objectives of the Polar Research Board [DE88-004543] N88-20747
GEOMETRICAL OPTICS
Semiclassical theory of injected lasers with arbitrary stable and unstable resonators [AD-A189514] N88-20615
GEOMETRY
Conformal geometry, Hotine's conjecture, and differential geodesy [AD-A189265] N88-20709
Campaign graphs [DE88-005336] N88-20952
GEOPHYSICS
Interactive automated system for testing analog units of digital seismic stations N88-20702
Inversion algorithms for geophysical problems [AD-A189252] N88-20845
Physics of condensed matter at extreme conditions [DE88-006232] N88-20958
ONR Far East Scientific Bulletin, volume 12, number 3, July-September 1987 [AD-A188554] N88-21081
GEOSTROPHIC WIND
Contribution to theory of quasigeostrophic motions of finite amplitude in viscous stratified ocean N88-20695
GEOSYNCHRONOUS ORBITS
Study of the optimization of satellite system design for transfer orbit [MBB-URV-135] N88-20332
GEOTHERMAL ENERGY CONVERSION
Status of the Magma Energy Project [DE88-002413] N88-20719
Overview of recent activities in the Heat Cycle Research Program [DE88-005544] N88-20738
GEOTHERMAL ENERGY EXTRACTION
Status of the Magma Energy Project [DE88-002413] N88-20719
GEOTHERMAL RESOURCES
Overview of recent activities in the Heat Cycle Research Program [DE88-005544] N88-20738
GERMANIUM
Development of Si/SiGe heterostructures [AD-A189527] N88-21044
Optical study of germanium, germanium plus arsenic, and germanium plus gallium implants in gallium arsenide [AD-A189600] N88-21045
GERMANIUM COMPOUNDS
Silicon-germanium heterostructures N88-21034
GETTERS
A new polymer-based hydrogen getter [DE88-004538] N88-20487
GLASS
Materials Research Laboratory at Brown University [AD-A188006] N88-20396
Processing of glass to aluminum (low melting metals) seals via an injection molding technique [DE88-004689] N88-20468
Nonlinear refractive index measurements of glasses and crystals [DE88-005673] N88-21009
Theoretical studies on the electronic structure and properties of complex ceramic crystals and glasses [DE88-005837] N88-21049
GLASS COATINGS
Improved glass-ceramic to metal seals in actuator and detonator applications with an aluminum-containing austenitic stainless steel [DE88-004691] N88-20458
SBIR-Long fluoride fiber [AD-A188595] N88-20492
GLASS FIBERS
Use of reinforced inorganic cement materials for spark wire and drift chamber wire frames [NASA-CR-180759] N88-20438
SBIR-Long fluoride fiber [AD-A188595] N88-20492
GLOBAL ATMOSPHERIC RESEARCH PROGRAM
Seasonal variations and excitation mechanisms of the equatorially trapped waves N88-20751
GLOBAL POSITIONING SYSTEM
The evaluation and selection of a 5th ground antenna site for the global positioning system [AD-A189495] N88-20286
An investigation of Doppler satellite positioning multi-station adjustment software N88-20345
Orbit accuracy requirement of GPS for precise positioning and orbit determination within local area N88-20499
GLOW DISCHARGES
Measurement of rate constants of elementary gas reactions of importance to upper atmosphere and combustion systems [AD-A189432] N88-20386
GOALS
Johnson Space Center's strategic game plan: Charting a course to the year 2000 and beyond [NASA-TM-89733] N88-21076
GONDOLAS
Adaptive control of scientific balloon-borne gondola attitude N88-20497
GOVERNMENT PROCUREMENT
MANPRINT handbook for RFP (Request For Proposal) development [AD-A188321] N88-21075
GRAIN BOUNDARIES
Gordon Conference on Intermetallic Compounds held at Tilton, New Hampshire on 20-24 July 1987 [AD-A188502] N88-20435
GRAIN SIZE
Processing of nanophase ceramics [DE88-005985] N88-20475
GRAMMARS
A parser generator for finitely ambiguous context-free grammars [CWI-CS-R8712] N88-20864
GRAND UNIFIED THEORY
Diffraction theory in QCD and beyond [DE88-005958] N88-20992
GRAPHIC ARTS
MacCAD (Macintosh Computer Aided Design), computer aided design tool for system analysis [AD-A189241] N88-20843
GRAPHITE
An interpretation of the ethylenic, carbidic, and graphite auger lineshapes of chemisorbed carbon species [AD-A189092] N88-20379
IAEA Specialists' Meeting on Graphite Component Structural Design [DE88-780006] N88-20439
The statistical characterization of tensile strengths for a nuclear-type graphite N88-20440
Statistical considerations of graphite strength for assessing design allowable stresses N88-20441
Fracture criterion of reactor graphite under multiaxial stresses N88-20442
High temperature Young's modulus of IG-110 graphite N88-20443
Effects of high temperature neutron irradiation on the physical, chemical and mechanical properties of fine-grained isotropic graphite N88-20444
Degradations of thermal shock resistance and the fracture toughness of reactor graphite subjected to neutron irradiation N88-20445
Application of ISRM testing methods to fracture toughness testing of graphite N88-20446
Notch sensitivity of graphite materials for VHTR N88-20447
Nondestructive testings of HTGR graphites N88-20448
Recent progress in structure determination by LEED (Low-Energy Electron Diffraction) measure the properties of the deep donors (DX-cent) [DE88-003851] N88-21048
GRAPHITE-EPOXY COMPOSITES
Simulated impact damage in a thick graphite/epoxy laminate using spherical indenters [NASA-TM-100539] N88-20363
Ply-level failure analysis of a graphite/epoxy laminate under bearing-bypass loading [NASA-TM-100578] N88-20372
GRAPHS (CHARTS)
Design graphs for the first two bending Eigenvibration forms of rotating beams consisting of two beam points [IW-88006R] N88-20670
Campaign graphs [DE88-005336] N88-20952
GRAVITATIONAL FIELDS
Comparisons of global topographic/isostatic models to the Earth's observed gravity field [NASA-CR-182696] N88-20752
GRAVITATIONAL PHYSIOLOGY
Regulation of hemodynamics upon imitation of the transition to weightlessness (mathematical modeling) N88-20817
GRAVITY WAVES
Seasonal variations and excitation mechanisms of the equatorially trapped waves N88-20751
Observations of waves and Langmuir circulation with Doppler sonars N88-20790
GREEN'S FUNCTIONS
Finite element calculations for aerodynamic coefficients of a 3-dimensional body in subsonic flow using Green's function method [NASA-TT-20208] N88-20272
GROUND EFFECT MACHINES
Feasibility report: Operation of light air cushion vehicle at McMurdo Sound, Antarctica [AD-A189057] N88-20494
GROUND HANDLING
Turnaround operations analysis for OTV. Volume 2: Detailed technical report [NASA-CR-179317] N88-20341
Turnaround operations analysis for OTV. Volume 3: Technology development plan [NASA-CR-179318] N88-20342
Turnaround operations analysis for OTV. Volume 4: WBS and dictionary and cost methodology [NASA-CR-179319] N88-20343
GROUND SUPPORT SYSTEMS
The German processing and archiving facility for ERS-1 [ESA-CR(P)-2531] N88-21082
GROUND WATER
Environmental projects. Volume 5, part 1: Study of subsurface contamination. Part 2: Guide to implement environmental compliance programs [NASA-CR-182691] N88-20741
GROUP THEORY
Group theoretic interpretations of Askey's scheme of hypergeometric orthogonal polynomials [CWI-PM-R8703] N88-20954
GROWTH
Thermal oxide growth on silicon: Intrinsic stress and silicon cleaning effects [AD-A188790] N88-20377
Some problems of the theory of bubble growth and condensation in bubble chambers [NASA-TT-20232] N88-20593
GULF STREAM
Estimates of ocean-atmosphere thermal interaction in Gulf Stream energy-active test range in winter of 1984 N88-20679
Phenomenological description of eddy registered in Gulf Stream N88-20694
Studies toward observing and modelling large energetic ocean regions [AD-A189267] N88-20778

GUNS (ORDNANCE)
Hydrogen embrittlement of gun steel
[AD-A188972] N88-20407
GYROSCOPES
Laser gyro attitude control system feasibility
[AD-A189368] N88-20285
GYROSCOPIC STABILITY
What is the maximum length of a spin stabilized projectile
[PB88-130919] N88-20336

H

H BETA LINE
The astrophysics of nebulae and active galactic nuclear emission-line regions: New methods and applications N88-21111
H LINES
Experimental study of the role of plasma polarization on line shape in dense laboratory plasmas
[ETN-88-92001] N88-21033
HADRONS
High resolution hadron calorimetry
[NIKHEF-H/87-8] N88-20605
Energy loss of particles in dense matter-calorimetry
[NIKHEF-H/87-12] N88-20988
Hadronic overlap and total multiplicity distributions in high energy physics collisions
[NIKHEF-H/87-10] N88-21001
HALF SPACES
A finite-amplitude analysis of the buoyant instability of a highly viscous film over a less viscous half-space N88-20581
HALL EFFECT
Electrical characteristics of MBE (Molecular Beam Epitaxyl)-grown GaAs/sub 1-x/Sb/sub x on InP and correlation with film microstructure
[DE88-003841] N88-21053
HALLEY'S COMET
JPRS report: Science and technology. USSR: Space
[JPRS-USP-88-002] N88-20312
Vega-1 and Vega-2 automatic stations: Functioning of landing modules in Venusian atmosphere N88-20313
Vega-1 and Vega-2 automatic stations: Functioning of flyby vehicles during encounter with Halley's comet N88-20314
Some periodicities in motion of Halley's Comet relative to center of mass N88-20324
Results of infrared spectrometer experiment. 1: Infrared radiation of parent molecules in Halley's Comet N88-20325
Results of infrared spectrometer experiment. 2: Infrared radiometry of nucleus of Halley's Comet N88-20326
Analysis of hydrocarbon band 3.35 in spectrum of Halley's Comet using data from infrared spectrometer on Vega-1 spacecraft N88-20327
HAMILTON-JACOBI EQUATION
Introduction to classical mechanics of systems with constraints, part 2
[TI88-701056] N88-21072
HAMILTONIAN FUNCTIONS
Systems near the onset and in the well-developed regimes of turbulence
[DE88-005365] N88-20565
Hamiltonian description of the interaction of surface waves with mixed-layer currents N88-20799
Stochasticity in nonlinear Hamiltonian systems
[DE88-005499] N88-20915
Introduction to classical mechanics of systems with constraints, part 2
[TI88-701056] N88-21072
HANDBOOKS
MANPRINT handbook for RFP (Request For Proposal) development
[AD-A188321] N88-21075
HARMONIC ANALYSIS
Comparisons of global topographic/isostatic models to the Earth's observed gravity field
[NASA-CR-182696] N88-20752
HARMONIC MOTION
Theory of laser cooling and spectroscopy of harmonically trapped single atoms
[AD-A189576] N88-20617
HARTREE APPROXIMATION
Numerical simulations of multiphoton processes in many electron atoms
[DE88-003293] N88-20990
HAZARDS
Atmospheric electrical modeling in support of the NASA F-106 storm hazards project
[NASA-CR-181639] N88-20758
Bathymetric hazard survey test
[AD-A189150] N88-20775
HEAD-UP DISPLAYS
Multi-crew pictorial format display evaluation
[AD-A189349] N88-20824
HEALTH
The effects of normal and therapeutic baths on the central vascular organs of persons with healthy hearts, as measured by X-ray
[NASA-TT-20252] N88-20818
HEART
The effects of normal and therapeutic baths on the central vascular organs of persons with healthy hearts, as measured by X-ray
[NASA-TT-20252] N88-20818
HEAT ACCLIMATIZATION
Plasma cortisol, renin and aldosterone during an intense heat acclimation program
[AD-A189387] N88-20810
HEAT AFFECTED ZONE
Transformation, metallurgical response and behavior of the weld fusion zone and heat affected zone in Cr-Mo steels for fossil energy application
[DE88-006037] N88-20430
HEAT EXCHANGERS
Proceedings of the 1987 International Symposium on Condensing Heat Exchangers
[DE88-005230] N88-20564
Innovative, counterflow gas/fine solids, direct contact heat exchanger
[DE88-004744] N88-20585
HEAT FLUX
Some effects of heating on the wind-driven velocity in the upper ocean N88-20792
HEAT MEASUREMENT
A calorimetric determination of the enthalpy of formation and a description of the defect structure of the ordered beta-phase /Ni, Cu/ /1-x/ Al/x/
[NASA-TT-20157] N88-20434
High resolution hadron calorimetry
[NIKHEF-H/87-8] N88-20605
HEAT OF FORMATION
A calorimetric determination of the enthalpy of formation and a description of the defect structure of the ordered beta-phase /Ni, Cu/ /1-x/ Al/x/
[NASA-TT-20157] N88-20434
HEAT PIPES
Moveable thermal joints for deployable or steerable spacecraft radiator systems
[NLR-MP-87016-U] N88-20347
Heat pipe transient analysis: Vapor dynamics
[DE88-005132] N88-20568
Development, manufacturing and testing of a gas-loaded variable conductance methanol heat pipe
[NLR-MP-87010-U] N88-20571
Design of the Sandia-Israel 20-kW reflux heat-pipe solar receiver/reactor
[DE88-001312] N88-20729
HEAT PUMPS
Proceedings of the 1987 International Symposium on Condensing Heat Exchangers
[DE88-005230] N88-20564
Efficiency characteristics of speed modulated drives at predicted torque conditions for air-to-air heat pumps
[DE88-005846] N88-20588
HEAT RESISTANT ALLOYS
Gordon Conference on Intermetallic Compounds held at Tilton, New Hampshire on 20-24 July 1987
[AD-A188502] N88-20435
Activities report of the Materials Department
[ETN-88-91984] N88-20436
HEAT SOURCES
A case study of the development of a military specification - zirconium powder for thermal batteries
[AD-A188751] N88-20717
HEAT STORAGE
An assessment methodology for thermal energy storage evaluation
[DE88-004642] N88-20732
HEAT TRANSFER
Vapor-mist for lightweight high voltage space insulation systems
[DE87-011704] N88-20538
Investigation of heat transfer to a flat plate in a shock tube
[AD-A189538] N88-20561
Heat pipe transient analysis: Vapor dynamics
[DE88-005132] N88-20568
The influence of Mach number and heat transfer on the turbulent flow wall law
[NASA-TT-20230] N88-20594
Estimates of ocean-atmosphere thermal interaction in Gulf Stream energy-active test range in winter of 1984 N88-20679
Compatibility in space reactor fuel systems
[DE88-005698] N88-21004
HEATING
Some effects of heating on the wind-driven velocity in the upper ocean N88-20792
Rapid e-beam heating for measuring thermodynamics of metastable materials
[DE88-003565] N88-21066
Early reheating and cosmic strings N88-21103
HELICOPTER DESIGN
Verification of the momemtum theory for rotors using measurements on a model helicopter
[R-840-S] N88-20275
HELICOPTERS
An experimental investigation of the flap-lag-torsion aeroelastic stability of a small-scale hingeless helicopter rotor in hover
[NASA-TP-2546] N88-20257
Procedure for detection and identification of a helicopter
[NASA-TT-20234] N88-20297
Time-domain system for identification of the natural resonant frequencies of aircraft relevant to electromagnetic compatibility testing
[PB88-164520] N88-20519
Optimal placement of tuning masses for vibration reduction in helicopter rotor blades
[NASA-TM-100562] N88-20665
HELIUM
Creep behavior of consolidated rapidly solidified Type 304 stainless steel powder containing helium
[DE88-005536] N88-20424
Experimental and theoretical methods for investigating helium effects in rapidly solidified metals
[DE88-005542] N88-20425
Increase in influence of oxygen on the body in the presence of helium N88-20816
The astrophysics of nebulae and active galactic nuclear emission-line regions: New methods and applications N88-21111
HELIUM PLASMA
SOAR: Space orbiting advanced fusion power reactor
[AD-A189234] N88-20356
HELIUM-NEON LASERS
Fuels combustion research
[AD-A189114] N88-20381
HEMODYNAMIC RESPONSES
Regulation of hemodynamics upon imitation of the transition to weightlessness (mathematical modeling) N88-20817
HERMES MANNED SPACEPLANE
Modelling and simulation of a rate controlled manipulator arm — Hermes
[NLR-TR-87010-U] N88-20639
HERMETIC SEALS
Improved glass-ceramic to metal seals in actuator and detonator applications with an aluminum-containing austenitic stainless steel
[DE88-004691] N88-20458
HESSIAN MATRICES
Conic algorithms for unconstrained minimization with special consideration of problems with large sparse Hessians: A summary of research performed
[DE88-002549] N88-20850
HETEROJUNCTION DEVICES
Low threshold ridge waveguide single quantum well lasers N88-20631
Cadmium sulfide/copper ternary heterojunction cell research
[DE88-001122] N88-20727
HETEROJUNCTIONS
Silicon-germanium heterostructures N88-21034
Development of Si/SiGe heterostructures
[AD-A189527] N88-21044
HIGH ENERGY ELECTRONS
Modeling and transport in semiconductor devices
[AD-A188760] N88-21037
HIGH ENERGY INTERACTIONS
Energy loss of particles in dense matter-calorimetry
[NIKHEF-H/87-12] N88-20988
Hadronic overlap and total multiplicity distributions in high energy physics collisions
[NIKHEF-H/87-10] N88-21001
Modeling and transport in semiconductor devices
[AD-A188760] N88-21037
HIGH FREQUENCIES
HF (High Frequency) Maximum Usable Frequency (MUF) model uncertainty assessment
[AD-A189132] N88-20513
Adaptive algorithms for HF antenna arrays
[AD-A189329] N88-20534
HIGH LEVEL LANGUAGES
Design of the CONSUL programming language
[AD-A189202] N88-20841
An integrated data description language for coding design knowledge
[CWI-CS-R8731] N88-20871

HIGH POWER LASERS
Phase preservation cleanup in a double-pass Raman amplifier SBS (Stimulated Brillouin Scattering) conjugator
[AD-A189428] N88-20536
Fiber-coupled external-cavity semiconductor high power laser
[AD-A188454] N88-20611
Causes of damage in multilayer dielectric coatings exposed to high average power visible laser radiation
[DE88-005363] N88-20619
High power, high efficiency, 2D laser diode arrays for pumping solid state lasers
[DE88-004042] N88-20632
HIGH PRESSURE
Properties of molecular solids and fluids at high pressure and temperature
[DE88-004195] N88-20391
HIGH RESOLUTION
High resolution hadron calorimetry
[NIKHEF-H/87-8] N88-20605
Improved methods for high resolution electron microscopy
[DE88-005731] N88-20609
Simulating high-resolution vertical plane array wind characteristics using lower-spatial-resolution wind measurements
[DE88-005626] N88-20761
Velocity resolved far-infrared spectroscopy of galactic sources N88-21099
HIGH REYNOLDS NUMBER
High Reynolds number pump facility for cavitation research
[AD-A189310] N88-20558
HIGH SPEED
Dynamics of high-speed mechanisms with elastic members N88-20643
HIGH STRENGTH STEELS
Development of a constitutive equation for HSLA (High-Strength Low-Alloy)-100 at cryogenic temperatures
[AD-A189243] N88-20408
HIGH TEMPERATURE
Properties of molecular solids and fluids at high pressure and temperature
[DE88-004195] N88-20391
Material parameter measurements at high temperatures
[NASA-CR-182707] N88-20397
Effects of high temperature neutron irradiation on the physical, chemical and mechanical properties of fine-grained isotropic graphite N88-20444
A study of the dynamics of high temperature brittle intergranular fracture by acoustic emission
[AERE-R-12479] N88-20650
Power from the sun: Principles of high temperature solar thermal technology
[DE87-001104] N88-20736
Discussion of radiation effects and high-temperature oxide superconductors
[DE88-001427] N88-21046
Prediction of high-temperature thermodynamic properties of mixed electrolyte solutions including solubility equilibria, vapor pressure depression and boiling point elevation
[DE88-006344] N88-21069
HIGH TEMPERATURE NUCLEAR REACTORS
IAEA Specialists' Meeting on Graphite Component Structural Design
[DE88-780006] N88-20439
HIGH TEMPERATURE PLASMAS
Modeling and transport in semiconductor devices
[AD-A188760] N88-21037
HIGH TEMPERATURE SUPERCONDUCTORS
The relationship of the chemical bonding topology of high critical temperature copper oxide superconductors to that of the chevrel phases and the ternary lanthanide rhodium borides
[AD-A189255] N88-21042
HIGH TEMPERATURE TESTS
High temperature Young's modulus of IG-110 graphite N88-20443
HIGH VOLTAGES
Vapor-mist for lightweight high voltage space insulation systems
[DE87-011704] N88-20538
HIPPARCOS SATELLITE
Preparation of photometric measurements on a million stars in the framework of the satellite project HIPPARCOS/TYCHO
[ETN-88-91502] N88-21093
HISTORIES
HISPLT: A history graphics post processor for wave propagation codes
[DE88-005507] N88-20857
HOLE DISTRIBUTION (MECHANICS)
Crack distribution and growth rates for critical fastener holes in Mirage wing RH79
[AD-A189080] N88-20293
HOLES (ELECTRON DEFICIENCIES)
Modeling and transport in semiconductor devices
[AD-A188760] N88-21037
HOLOGRAPHY
Development of fiber optic systems for recording and transmitting holographic information
[AD-A189406] N88-20603
ONR Far East Scientific Bulletin, volume 12, number 3, July-September 1987
[AD-A188554] N88-21081
HOMOGENEITY
Decomposition of hypochlorite in the presence of copper in a homogeneous medium
[NASA-TT-20199] N88-20403
HOMOGENEOUS TURBULENCE
Center for Turbulence Research 1987 activities
[NASA-CR-182693] N88-20583
HORIZONTAL ORIENTATION
A polarization diversity meteorological radar system
[AD-A189291] N88-20515
Fatigue load measurements and evaluation of the 25m Horizontal Axis Wind Turbine (HAWT) at Petten, The Netherlands
[NLR-MP-88054-U] N88-20660
HOT PRESSING
Molybdenum-base cermet fuel development
[DE88-005529] N88-21003
HOT-FILM ANEMOMETERS
The design and use of a temperature-compensated hot-film anemometer system for boundary-layer flow transition detection on supersonic aircraft
[NASA-TM-100421] N88-20304
HOVERING
An experimental investigation of the flap-lag-torsion aeroelastic stability of a small-scale hingeless helicopter rotor in hover
[NASA-TP-2546] N88-20257
HUMAN BEINGS
Pursuit tracking performance decrements associated with decreasing ambient illumination
[AD-A189336] N88-20809
HUMAN BODY
Lifting and carrying capacities relative to physical fitness measures
[AD-A189305] N88-20808
HUMAN FACTORS ENGINEERING
Multi-crew pictorial format display evaluation
[AD-A189349] N88-20824
Advanced human factors engineering tool technologies
[AD-A189390] N88-20825
HUMAN PERFORMANCE
Lifting and carrying capacities relative to physical fitness measures
[AD-A189305] N88-20808
Proceedings of the Workshop on the Assessment of Crew Workload Measurements Methods, Techniques and Procedures. Volume 1: Preliminary Selection of Measures
[AD-A189004] N88-20827
A comparison of two chord keyboard coding systems for alphanumeric data entry
[AD-A189230] N88-20834
HYBRID STRUCTURES
Outlook for the fusion hybrid and tritium-breeding fusion reactors
[PB88-149281] N88-21029
HYDRAULIC EQUIPMENT
High Reynolds number pump facility for cavitation research
[AD-A189310] N88-20558
HYDRAZINE NITRATE
Detonation velocity of the hydrazinum nitrate-hydrazine water system
[NASA-TT-20213] N88-20590
HYDRAZINIUM COMPOUNDS
Detonation velocity of the hydrazinum nitrate-hydrazine water system
[NASA-TT-20213] N88-20590
HYDRIDES
Quantitative determination of a hydrogen impurity in a sodium coolant by hydride thermal dissociation
[NASA-TT-20239] N88-20402
HYDROCARBONS
Analysis of hydrocarbon band 3.35 in spectrum of Halley's Comet using data from infrared spectrometer on Vega-1 spacecraft N88-20327
HYDRODYNAMICS
Dynamic modelling of flexible rotor shafts mounted on hydrodynamic bearings N88-20641
Model of hydrodynamic adjustment of temperature, salinity and current fields N88-20700
HYDROGEN
Uncertainties in hydrogen combustion
[DE88-005354] N88-20395
Quantitative determination of a hydrogen impurity in a sodium coolant by hydride thermal dissociation
[NASA-TT-20239] N88-20402
Hydrogen induced cracks in armor steel weldments fabricated with austenitic filler alloys
[AD-A188733] N88-20406
HYDROGEN ATOMS
The astrophysics of nebulae and active galactic nuclear emission-line regions: New methods and applications N88-21111
HYDROGEN EMBRITTLEMENT
Hydrogen embrittlement of gun steel
[AD-A188972] N88-20407
HYDROGEN IONS
The magnitude of secondary electron contributions in photon stimulated desorption
[AD-A189094] N88-20980
HYDROGEN PLASMA
Hydrogen pumping and release by graphite under high flux plasma bombardment
[DE88-005880] N88-21021
HYDROGENATION
A new polymer-based hydrogen getter
[DE88-004538] N88-20467
Investigations of the origins of metastable, light-induced changes in hydrogenated amorphous silicon
[DE88-001117] N88-21051
HYDROMETEOROLOGY
Influence of hydrometeorological factors on visibility of objects detected by radar N88-20707
HYDROSTATICS
Composites strengthening
[AD-A189258] N88-20364
HYDROTHERMAL SYSTEMS
Experimental and theoretical constraints on the origin of mid-ocean ridge geothermal fluids N88-20784
HYDROXIDES
Characterization of redox states of nickel hydroxide film electrodes by in-situ Raman spectroscopy
[AD-A189288] N88-20411
HYDROXYL RADICALS
Measurement of rate constants of elementary gas reactions of importance to upper atmosphere and combustion systems
[AD-A189432] N88-20386
HYPERBOLIC DIFFERENTIAL EQUATIONS
Conservative finite volume solutions of a linear hyperbolic transport equation in two and three dimensions using multiple grids
[NASA-CR-182715] N88-20934
HYPERCUBE MULTIPROCESSORS
Implementation of a 3-D nonlinear MHD (magnetohydrodynamics) calculation on the Intel hypercube
[DE88-000825] N88-20848
HYPEROXIA
Increase in influence of oxygen on the body in the presence of helium N88-20816
HYPERSONIC FLOW
Documentation and installation of the hypersonic arbitrary-body computer program (Mark 3 version) of A.E. Gentry on the IBM computer system
[MBB/LKE-127/S/PUB/256] N88-20276
HYPERSPACES
Group theoretic interpretations of Askey's scheme of hypergeometric orthogonal polynomials
[CWI-PM-R8703] N88-20954
HYPERVELOCITY GUNS
Structural integrity of metallic armature rail guns
[AD-A188735] N88-20333
HYPOKINESIA
Use of diphosphonates to correct disorders in calcium metabolism and mineral composition of bone tissue with 60-day hypokinesia in rats
[NASA-TT-20220] N88-20807
Changes in the status of the human tibia during antiorthostatic hypokinesia
[NASA-TT-20221] N88-20813

I

IBM COMPUTERS
Documentation and installation of the hypersonic arbitrary-body computer program (Mark 3 version) of A.E. Gentry on the IBM computer system
[MBB/LKE-127/S/PUB/256] N88-20276
ICE
Multiple scattering of polarized light in cirrus clouds N88-20768
Predictions and studies with a one-dimensional ice/ocean model
[AD-A189158] N88-20776

ICE ENVIRONMENTS
JPRS report: Science and technology. USSR: Earth sciences
[JPRS-UES-88-001] N88-20674
IDENTIFYING
Estimation-correlation, modeling, and identification in adaptive array processors
[AD-A189130] N88-20512
A comparison of terrain association and resection as methods of position location
[AD-A189480] N88-20710
Passive DF: A tutorial, part 1
[NASA-CR-182669] N88-20646
IGNITION
A pyrotechnic delay ignition system for a submarine launched marine signal
[MRL-R-1079] N88-20487
IMAGE ANALYSIS
A procedure for automatic classification of crop areas
[INPE-4467-PRE/1240] N88-20708
IMAGE ENHANCEMENT
Digital enhancement of flow field images
[NASA-TP-2770] N88-20833
IMAGE PROCESSING
Recent developments in nondestructive evaluation for structural ceramics
[DE88-005899] N88-20473
A hybrid transform/DPCM encoder for data compression
[DE87-014852] N88-20518
Dynamics of high-speed mechanisms with elastic members N88-20643
Analysis for architecture for image processing
[INPE-4294-PRE/1165] N88-20715
Bathymetric hazard survey test
[AD-A189150] N88-20775
Retinotopic mapping of the human visual system with magnetoencephalography
[AD-A189557] N88-20811
Digital enhancement of flow field images
[NASA-TP-2770] N88-20833
On relaxation algorithms based on Markov random fields
[AD-A189043] N88-20840
Method to evaluate image-recovery algorithms based on task performance
[DE88-005382] N88-20853
Parallel graphical output from dialogue cells
[CWI-CS-R8719] N88-20867
On effectively labeling planar projections of polyhedra
[CWI-CS-R8715] N88-20917
Passive autonomous infrared sensor technology
[AD-A188698] N88-21005
IMAGE RECONSTRUCTION
Restoration techniques for redisplay of LANDSAT-5 satellite imagery
[INPE-4189-PRE/1076] N88-20712
Method to evaluate image-recovery algorithms based on task performance
[DE88-005382] N88-20853
IMAGES
Reduced tolerance imaging 2, volume 2
[AD-A189604] N88-20939
Aberrations: Their effect on off-axis beam steering
[AD-A189601] N88-21008
IMAGING TECHNIQUES
Bathymetric hazard survey test
[AD-A189150] N88-20775
Parallel image compression
[NASA-CR-180758] N88-20837
Reduced tolerance imaging 2, volume 2
[AD-A189604] N88-20939
IMMUNOLOGY
JPRS report: Science and technology. USSR: Life sciences
[JPRS-ULS-88-004] N88-20815
IMPACT DAMAGE
Simulated impact damage in a thick graphite/epoxy laminate using spherical indenters
[NASA-TM-100539] N88-20363
IMPACT LOADS
Use of the LLNL 40 kV electric gun to study the shock response of 21-6-9 stainless steel
[DE87-014550] N88-20418
IMPACT RESISTANCE
Abrasion and impact resistant coatings
[DE88-003562] N88-20464
IMPACT STRENGTH
A direct correlation of strength with impact velocity
[AD-A189251] N88-20409
IMPACT TESTS
A direct correlation of strength with impact velocity
[AD-A189251] N88-20409
IMPURITIES
Thermal oxide growth on silicon: Intrinsic stress and silicon cleaning effects
[AD-A188790] N88-20377
Quantitative determination of a hydrogen impurity in a sodium coolant by hydride thermal dissociation
[NASA-TT-20239] N88-20402
Study of activationless reactions of point defects with impurities and impurity-defect complexes in alpha-iron
[TI88-701028] N88-20433
Research on multibandgap solar cells
[DE87-012261] N88-20721
Evolution of poloidal variation of impurity density and ambipolar potential in rotating tokamak plasma, part 1
[DE88-006263] N88-21022
INCLUSIONS
Resolution of the magnetotelluric method for determining local inhomogeneities in the sedimentary cover N88-20701
INCOMPRESSIBLE FLOW
High Reynolds number pump facility for cavitation research
[AD-A189310] N88-20558
INCONEL (TRADEMARK)
Grain refinement during primary breakdown of alloy 718
[DE88-005193] N88-20423
INDEPENDENT VARIABLES
On error equations for determining Earth rotation parameters with VLBI network N88-20500
INDIUM ALLOYS
Studies of transverse phonon modes in premartensitic indium-thallium alloys
[DE88-003481] N88-20428
INDIUM COMPOUNDS
The synthesis, characterization and structural studies of In(C5H4Me) by X-ray diffraction and electron diffraction techniques and a reinvestigation of the crystalline state of In(C5H5) by X-ray diffraction studies
[AD-A189110] N88-21038
INDUSTRIAL WASTES
Global mixed-layer natural and anthropogenic fluxes N88-20803
INDUSTRIES
Some properties of Australian produced explosive composition H-6
[MRL-TN-525] N88-20490
INELASTIC COLLISIONS
Particle-dynamics calculations of gravity flow of inelastic, frictional spheres
[DE88-005224] N88-20586
INERTIA
Horizontal scales of wind forced inertial motions N88-20795
INERTIAL CONFINEMENT FUSION
The Magnetically Insulated Inertial Confinement Fusion (MICF): A novel approach
[DE88-005460] N88-21026
INERTIAL GUIDANCE
Features of Soyuz TM spacecraft N88-20329
INFERENCE
Knowledge retrieval as specialized inference
[AD-A189042] N88-20899
INFORMATION DISSEMINATION
Applicability of aerospace thermal insulation technologies to the civilian sector
[DE88-003717] N88-21086
INFORMATION MANAGEMENT
Distributed transaction processing and the Camelot system
[AD-A188614] N88-20885
INFORMATION PROCESSING (BIOLOGY)
A personalized and prescriptive decision aid for choice from a database of options
[AD-A188726] N88-20820
INFORMATION RETRIEVAL
The acoustic-modeling problem in automatic speech recognition
[AD-A188529] N88-20510
Knowledge retrieval as specialized inference
[AD-A189042] N88-20899
A menu-driven knowledge retrieval system accessing ASCII data
[DE88-001742] N88-21079
INFORMATION THEORY
Research in applied mathematics related to identification of noisy systems
[AD-A189355] N88-20908
INFRARED ASTRONOMY
Advanced components for spaceborne infrared astronomy
[NASA-CR-177470] N88-20601
Analysis of deep sky sources found by the infrared astronomy satellite
[AD-A189605] N88-21089
INFRARED ASTRONOMY SATELLITE
Analysis of deep sky sources found by the infrared astronomy satellite
[AD-A189605] N88-21089
INFRARED DETECTORS
Procedure for detection and identification of a helicopter
[NASA-TT-20234] N88-20297
Advanced components for spaceborne infrared astronomy
[NASA-CR-177470] N88-20601
Passive autonomous infrared sensor technology
[AD-A188698] N88-21005
Analysis of deep sky sources found by the infrared astronomy satellite
[AD-A189605] N88-21089
INFRARED IMAGERY
Passive autonomous infrared sensor technology
[AD-A188698] N88-21005
INFRARED INSTRUMENTS
Specification for an infrared satellite surveillance system for the detection of aircraft
[AD-A189592] N88-20746
INFRARED LASERS
Influence of nonlinear spectroscopic effects on atmospheric propagation of intense laser radiation at 10.6 microns wavelength N88-20705
INFRARED PHOTOMETRY
Infrared constraints on the nature of dark matter N88-21102
INFRARED RADIATION
Results of infrared spectrometer experiment. 1: Infrared radiation of parent molecules in Halley's Comet N88-20325
Analysis of hydrocarbon band 3.35 in spectrum of Halley's Comet using data from infrared spectrometer on Vega-1 spacecraft N88-20327
Dynamical modeling of marine boundary layer convection N88-20750
Analysis of deep sky sources found by the infrared astronomy satellite
[AD-A189605] N88-21089
INFRARED SPECTRA
Synchronous measurements of effective photon path length in visible and near-IR spectral regions in real cloud systems N88-20706
Stratospheric trace gas distributions from fair infrared thermal emission spectroscopy N88-20749
INFRARED SPECTROMETERS
Results of infrared spectrometer experiment. 1: Infrared radiation of parent molecules in Halley's Comet N88-20325
Velocity resolved far-infrared spectroscopy of galactic sources N88-21099
INFRARED SPECTROSCOPY
Results of infrared spectrometer experiment. 2: Infrared radiometry of nucleus of Halley's Comet N88-20326
Analysis of hydrocarbon band 3.35 in spectrum of Halley's Comet using data from infrared spectrometer on Vega-1 spacecraft N88-20327
Molecular collision processes in gases and at surfaces
[AD-A189518] N88-20982
INFRARED STARS
Analysis of deep sky sources found by the infrared astronomy satellite
[AD-A189605] N88-21089
INFRARED TRACKING
Passive autonomous infrared sensor technology
[AD-A188698] N88-21005
INHIBITION (PSYCHOLOGY)
Distraction and inhibition in continuous CRT performance: A replication and some new findings
[PB88-150941] N88-20821
INJECTION
Application of railgun principle to high-velocity hydrogen pellet injection for magnetic fusion reactor refueling
[DE88-005830] N88-20334
INJECTION MOLDING
Processing of glass to aluminum (low melting metals) seals via an injection molding technique
[DE88-004689] N88-20468
INPUT
Logical input devices and interaction --- computer graphics
[CWI-CS-R8738] N88-20836
INPUT/OUTPUT ROUTINES
A comparison of two chord keyboard coding systems for alphanumeric data entry
[AD-A189230] N88-20834
INSPECTION
Ultrasonic inspection of irregular surfaces
[AERE-R-12465] N88-20648
INSULATION
Safety research of insulating materials of cable for nuclear power generating station
[NASA-TT-20202] N88-20477

Aging properties of cable polmers (2)
[NASA-TT-20228] N88-20479
The Magnetically Insulated Inertial Confinement Fusion (MICF): A novel approach
[DE88-005460] N88-21026

INSULATORS
Thermionic Technology Program. A: Insulator test and evaluation
[DE88-004707] N88-20735

INTAKE SYSTEMS
Measurement and analysis of the noise radiated by low Mach numbers centrifugal blowers
[AD-A189226] N88-20966
Flow/acoustic interaction in duct inflow
[AD-A189264] N88-20967

INTEGRAL EQUATIONS
Computational technique for compressible vortex flows using the integral equation solution
[NASA-CR-182695] N88-20271
Integral equation theory of homopolymer melts
[DE88-005304] N88-20470
Integral equation theory of polymer blends
[DE88-005305] N88-20471
Inversion algorithms for geophysical problems
[AD-A189252] N88-20845
WKB theory of wave tunneling for Hermitian vector systems of integral equations
[DE88-005332] N88-20951

INTEGRATED CIRCUITS
Intergrated circuit design, phase 2
[AD-A189060] N88-20530
Laser programming integrated circuits
[AD-A189590] N88-20537
Optical RF distribution links for MMIC phased array antennas
[NASA-TM-100841] N88-20555

INTERCEPTION
Optimal thrust vector control of coplanar orbital evasive maneuvers
[AD-A189544] N88-20346
Passive DF: A tutorial, part 1
[NASA-CR-182669] N88-20846

INTERFACES
Interfacial adhesion: Theory and experiment
[NASA-TM-100830] N88-20417
Interfacial chemistry-structure and fracture of ceramic composites
[DE88-005516] N88-20461
Component mode synthesis using experimental modes enhanced by mass loading
[DE88-006097] N88-20657
An interface between object-oriented systems
[AD-A189245] N88-20844
Exploring the relation between interface structure and mechanical properties in multilayer structures
[DE88-005428] N88-21060

INTERFEROMETERS
Applications of the lateral shearing interferometer in measurement of synchrotron radiation optical elements
[DE88-005184] N88-21011
Development of an optical diagnostic instrument. Part 2: Instrument development --- space laboratories
[NLR-TR-87079-L-PT-2] N88-21016

INTERFEROMETRY
An interferometric investigation of the diffraction of planar shock waves over a half-diamond cylinder in air
[UTIAS-322] N88-20575
Passive DF: A tutorial, part 1
[NASA-CR-182669] N88-20846
Optics for large telescope N88-21014

INTERIOR BALLISTICS
A study of combustion and flow behaviour in solid-propellant rocket motors
[UTIAS-280] N88-20357
Two-phase flows in the wake of in-cylinder projectiles
[AD-A189422] N88-20559

INTERMETALLICS
Gordon Conference on Intermetallic Compounds held at Tilton, New Hampshire on 20-24 July 1987
[AD-A188502] N88-20435

INTERNAL COMBUSTION ENGINES
Status of alcohol fuels utilization technology for highway transportation: A 1986 perspective. Volume 2: Compression ignition engines
[DE88-006059] N88-20485

INTERNAL WAVES
Wind forcing and observed oceanic wavenumber spectra N88-20797

INTERPOLATION
Interpolation algorithms for digital terrain models
[INPE-4373-PRE/1196] N88-20877

INTERPROCESSOR COMMUNICATION
Locality, communication and interconnect length in multicomputers
[CWI-CS-R8708] N88-20890

INTERSTELLAR SPACECRAFT
Advanced space propulsion study - antiproton and beamed power propulsion
[AD-A189218] N88-20355

INVARIANCE
Invariant characteristics of acoustic field in stratified ocean N88-20698
Chronometrically invariant formulation of electrodynamics equation
[TI88-701030] N88-21071

INVESTIGATION
Experimental and theoretical methods for investigating helium effects in rapidly solidified metals
[DE88-005542] N88-20425
A defect investigation of Thunderflash MK N5 (Navy)
[MRL-TN-522] N88-20488

INVISCID FLOW
Application of a flux vector splitting methodology towards the solution of unsteady transonic flows, with future emphasis on the blade flutter problem
[AD-A189500] N88-20260
Multigrid solution of the Euler equations N88-20582

ION BEAMS
Focused ion beam fabrication of graded channel FET's in GaAs and Si
[AD-A189166] N88-21040
A novel method for sputter-deposition of high T(sub c) superconductor films via a computer-controlled mass analyzed ion beam
[DE88-006001] N88-21064

ION EXCHANGING
Molecular and electronic mechanism in the control of Na+ and K+ permeability of excitable cell membrane by ligand binding on receptor sites
[AD-A188725] N88-20805
Solid-state electrochemical processes in dye films
[AD-A188756] N88-21036

ION IMPLANTATION
Temperature dependence of Kr precipitation in Ni
[DE88-005953] N88-20429
Focused ion beam fabrication of graded channel FET's in GaAs and Si
[AD-A189166] N88-21040
Optical study of germanium, germanium plus arsenic, and germanium plus gallium implants in gallium arsenide
[AD-A189600] N88-21045

ION IRRADIATION
Laser fluorescence spectroscopy of zinc neutrals originating from laser-irradiated and ion-bombarded zinc sulfide and zinc surfaces
[DE88-006033] N88-20620

ION MOTION
Theory of laser cooling and spectroscopy of harmonically trapped single atoms
[AD-A189576] N88-20617

ION RECOMBINATION
Wavelength scaling of lithium-like recombination scheme for X-UV gain production --- X-ray lasers
[ETN-88-92002] N88-20634

IONIZATION
Kinetic mechanisms for ionization and afterburning suppression
[AD-A189219] N88-20383
Studies of compound states of negative ions using laser beams
[DE88-004708] N88-20627

IONOGRAMS
Trajectory synthesis of ionograms in presence of artificial ionospheric inhomogeneities N88-20703

IONOSPHERIC DISTURBANCES
Trajectory synthesis of ionograms in presence of artificial ionospheric inhomogeneities N88-20703

IONOSPHERIC ELECTRON DENSITY
Trajectory synthesis of ionograms in presence of artificial ionospheric inhomogeneities N88-20703
Effect of nitrogen dioxide release on thermosphere N88-20704

IONOSPHERIC PROPAGATION
Upward propagating electric fields from thunderstorms and VLF transmitters N88-20767

IRON
Study of activationless reactions of point defects with impurities and impurity-defect complexes in alpha-iron
[TI88-701028] N88-20433

IRRADIATION
Hydrogen pumping and release by graphite under high flux plasma bombardment
[DE88-005880] N88-21021

IRREGULAR GALAXIES
Asymptotic giant branch populations in composite stellar systems N88-21098

IRREGULARITIES
Ultrasonic inspection of irregular surfaces
[AERE-R-12465] N88-20648

IRREVERSIBLE PROCESSES
Two studies of nonlinear processes in irreversible thermodynamics
[DE88-005794] N88-21067

ISOLATORS
Development of isostatic mounts and associated guidelines --- spacecraft payloads
[CASA-IM-WP-301] N88-20354

ISOPYCNIC PROCESSES
Contribution to theory of quasigeostrophic motions of finite amplitude in viscous stratified ocean N88-20695

ISOSTASY
Comparisons of global topographic/isostatic models to the Earth's observed gravity field
[NASA-CR-182696] N88-20752

ISOTHERMAL FLOW
Determining Langmuir circulation parameters on basis of similarity theory N88-20680

ISOTROPIC TURBULENCE
Center for Turbulence Research 1987 activities
[NASA-CR-182693] N88-20583

ISRAEL
Design of the Sandia-Israel 20-kW reflux heat-pipe solar receiver/reactor
[DE88-001312] N88-20729

ITERATION
Statistical signal processing using a class of iterative estimation algorithms
[AD-A189050] N88-20511
Nonlinear differential equations
[DE88-006047] N88-20933

ITERATIVE SOLUTION
Data traffic reduction schemes for sparse Cholesky factorizations
[NASA-CR-181626] N88-20831
Inversion algorithms for geophysical problems
[AD-A189252] N88-20845

J

J INTEGRAL
Fracture mechanics and creep crack growth of 1 percent Cr 1/2 percent Mo steel with and without prior exposure to creep conditions
[NLR-TR-86051-U] N88-20426

JET ENGINE FUELS
Availability and cost estimate of a high naphthene, modified aviation turbine fuel
[NASA-TM-100823] N88-20455
Aviation turbine fuels from tar sands bitumen and heavy oils. Part 3: Laboratory sample production
[AD-A189278] N88-20484

JET EXHAUST
Fully-coupled analysis of jet mixing problems. Three-dimensional PNS model, SCIP3D
[NASA-CR-4139] N88-20256

JET FLOW
Mushroom-shaped currents (eddy dipoles) under rotation and stratification conditions N88-20678

JET MIXING FLOW
Fully-coupled analysis of jet mixing problems. Three-dimensional PNS model, SCIP3D
[NASA-CR-4139] N88-20256
Control of structure in turbulent flows: Bifurcating and blooming jets
[AD-A189607] N88-20562

JFET
Advanced components for spaceborne infrared astronomy
[NASA-CR-177470] N88-20601

JOINTS (JUNCTIONS)
Reduction of erosion in elbows due to flow modifications, phase 1
[DE88-001028] N88-20584
Structural clearances and internal friction: Simulation by Eigen distortions
[ISSN-0208-5658] N88-20640

JOURNAL BEARINGS
Dynamic modelling of flexible rotor shafts mounted on hydrodynamic bearings N88-20641

JUPITER ATMOSPHERE
Model of Jovian F region ionosphere
[NASA-CR-182587] N88-21105

K

KALMAN FILTERS
Utilization of strapdown inertial and non-inertial sensors in determination of satellite attitude by Kalman filters
[INPE-4313-TDL/280] N88-20349
Robustifying the Kalman filter
[AD-A189240] N88-20907

KEROSENE
Availability and cost estimate of a high naphthene, modified aviation turbine fuel
[NASA-TM-100823] N88-20455
KERR ELECTROOPTICAL EFFECT
Double layer polarization of nonconducting spheroidal particles and its application to Kerr effect
[ISSN-0208-05658] N88-20960
KEVLAR (TRADEMARK)
Fracture characteristics of carbon and aramid unidirectional composites in interlaminar shear and open hole tensile tests
[NLR-TR-86063-U] N88-20371
KINEMATICS
Force distribution and trajectory control for closed kinematic chains with applications to walking machines N88-20642
Subduction N88-20796
KINETIC ENERGY
Unsteady shallowing mixed layer N88-20791
KINETICS
Thermodynamic theory of fluctuations and Rayleigh light scattering in solutions N88-20681
KNOWLEDGE REPRESENTATION
A knowledge system for automatic finite element mesh generation: AMEKS
[DE87-014894] N88-20914
KRYPTON
Temperature dependence of Kr precipitation in Ni
[DE88-005953] N88-20429
Electron stimulated desorption and coherent electron scattering
[AD-A189091] N88-20978
KUTTA-JOUKOWSKI CONDITION
On the Kutta condition for flows around lifting airfoils and wings
[DFVLR-FB-87-40] N88-20268

L

LABORATORIES
Aviation turbine fuels from tar sands bitumen and heavy oils. Part 3: Laboratory sample production
[AD-A189278] N88-20484
LABORATORY EQUIPMENT
Development of an optical diagnostic instrument. Part 2: Instrument development --- space laboratories
[NLR-TR-87079-L-PT-2] N88-21016
LAGRANGE COORDINATES
A Lagrangian moving grid scheme for one-dimensional evolutionary partial differential equations
[CWI-NM-R8713] N88-20922
LAGRANGE SIMILARITY HYPOTHESIS
Center for Turbulence Research 1987 activities
[NASA-CR-182693] N88-20583
LAMINAR BOUNDARY LAYER
Development of disturbances in swept wing flows
[NASA-CR-182675] N88-20574
LAMINATES
Simulated impact damage in a thick graphite/epoxy laminate using spherical indenters
[NASA-TM-100539] N88-20363
Transient dynamics of fibre reinforced composite plates
[IIT-B/CE/RR/87-1] N88-20370
Delamination stresses in semicircular laminated composite bars
[NASA-TM-4026] N88-20375
Nondestructive evaluation of carbon-carbon coatings
[AD-A189524] N88-20453
Exploring the relation between interface structure and mechanical properties in multilayer structures
[DE88-005426] N88-21060
LANDING GEAR
An investigation of classical dynamic scaling techniques applied to an oleo-pneumatic landing gear strut
[AD-A187664] N88-20292
Aircraft corrosion problems and research in the Netherlands
[NLR-MP-86066-U] N88-20427
LAPLACE EQUATION
Double layer polarization of nonconducting spheroidal particles and its application to Kerr effect
[ISSN-0208-05658] N88-20960
LARGE SPACE STRUCTURES
Robust decentralized control of large flexible structures
[DE88-005416] N88-20902
LASER APPLICATIONS
Molecular dynamics of laser ablation of a polymer coating
[DE88-004337] N88-20466
Studies of compound states of negative ions using laser beams
[DE88-004708] N88-20627
Noncontact thermometry via laser pumped, thermographic phosphors: Characterization of systematic errors and industrial applications
[DE88-005599] N88-20628
Low threshold ridge waveguide single quantum well lasers N88-20631
Study of photochromic materials for use in optical signal processing
[AD-A189068] N88-21006
LASER CAVITIES
Fiber-coupled external-cavity semiconductor high power laser
[AD-A188454] N88-20611
Resonator coupling of two ring cavity, argon-ion lasers
[AD-A189558] N88-20616
LASER CUTTING
Laser programming integrated circuits
[AD-A189590] N88-20537
LASER DAMAGE
Causes of damage in multilayer dielectric coatings exposed to high average power visible laser radiation
[DE88-005363] N88-20619
Database of average-power damage thresholds at 1064 nm
[DE88-004352] N88-20626
LASER GYROSCOPES
Laser gyro attitude control system feasibility
[AD-A189368] N88-20285
LASER INDUCED FLUORESCENCE
An experimental method for species concentration measurements in a welding arc using laser-induced fluorescence
[DE88-005638] N88-20636
LASER MATERIALS
Database of average-power damage thresholds at 1064 nm
[DE88-004352] N88-20626
Design studies for a solar pumped laser device
[DFVLR-FB-87-39] N88-20629
Guidelines for estimation and characterization of the thermo-mechanical properties of new optical materials
[DE88-004359] N88-21010
LASER OUTPUTS
Advanced space propulsion study - antiproton and beamed power propulsion
[AD-A189218] N88-20355
Laser ignition of nitramine composite propellants and crack propagation and branching in burning solid propellants
[AD-A189260] N88-20483
Laser fluorescence spectroscopy of zinc neutrals originating from laser-irradiated and ion-bombarded zinc sulfide and zinc surfaces
[DE88-006033] N88-20620
Refractive index gradients in nuclear-reactor-pumped lasers: Gasdynamic effects
[DE88-006099] N88-20621
Multimode-waveguide laser beam deflector
[DE88-006222] N88-20622
Database of average-power damage thresholds at 1064 nm
[DE88-004352] N88-20626
Studies of compound states of negative ions using laser beams
[DE88-004708] N88-20627
Direct solar-pumped iodine laser amplifier
[NASA-CR-182674] N88-20630
Low threshold ridge waveguide single quantum well lasers N88-20631
Doubly periodic output from a dye laser pumped by a free-running argon laser
[DE88-005027] N88-20633
Initial stages of silicon growth on the (100) surface of silicon by localized laser CVD
[DE88-005420] N88-21059
LASER PLASMAS
Wavelength scaling of lithium-like recombination scheme for X-UV gain production --- X-ray lasers
[ETN-88-92002] N88-20634
Experimental study of the role of plasma polarization on line shape in dense laboratory plasmas
[ETN-88-92001] N88-21033
LASER PROPULSION
Advanced space propulsion study - antiproton and beamed power propulsion
[AD-A189218] N88-20355
LASER PUMPING
Proof of the feasibility of coherent and incoherent schemes for pumping a gamma-ray laser
[AD-A189238] N88-20613
Design studies for a solar pumped laser device
[DFVLR-FB-87-39] N88-20629
LASER SPECTROSCOPY
Theory of laser cooling and spectroscopy of harmonically trapped single atoms
[AD-A189576] N88-20617
Laser fluorescence spectroscopy of zinc neutrals originating from laser-irradiated and ion-bombarded zinc sulfide and zinc surfaces
[DE88-006033] N88-20620
LASER STABILITY
Semiclassical theory of injected lasers with arbitrary stable and unstable resonators
[AD-A189514] N88-20615
LASER WELDING
Modeling of laser ultrasound generation in a weld pool
[DE88-005546] N88-20971
LASERS
Laser programming integrated circuits
[AD-A189590] N88-20537
Proof of the feasibility of coherent and incoherent schemes for pumping a gamma-ray laser
[AD-A189238] N88-20613
Semiclassical theory of injected lasers with arbitrary stable and unstable resonators
[AD-A189514] N88-20615
LATERAL CONTROL
Lateral and longitudinal stability and control parameters for the space shuttle discovery as determined from flight test data
[NASA-TM-100555] N88-20309
LATTICE VIBRATIONS
Vibration spectra of oxygen and vanadium atoms in vanadium-oxygen disordered interstitial alloys
[DE87-703166] N88-20404
LAUNCH VEHICLES
Soviet space transport systems N88-20328
Expected value analysis for an unmanned expendable launch vehicle payload escape system
[AD-A189494] N88-20337
LAUNCHING
A pyrotechnic delay ignition system for a submarine launched marine signal
[MRL-R-1079] N88-20487
LAYOUTS
Gridless routing for generalized cell assemblies: Report and user manual
[EUT-87-E-180] N88-20549
GM: A gate matrix layout generator
[EUT-87-E-179] N88-20875
LEADERSHIP
Report of the Defense Science Board Summer Study on Technology Base Management
[AD-A188560] N88-21078
LEADING EDGE SWEEP
Large-Scale Advanced Prop-Fan (LAP)
[NASA-CR-182112] N88-20306
LEADING EDGES
The international vortex flow experiment: A test case for compressible Euler codes
[NLR-MP-86076-U] N88-20267
Fluid-thermal-structural study of aerodynamically heated leading edges
[NASA-TM-100579] N88-20666
LEARNING
Soar: An architecture for general intelligence
[AD-A188742] N88-20898
LEAST SQUARES METHOD
Two dimensional uncorrelated bias in fix algorithms
[NASA-CR-182683] N88-20847
Survival analysis using additive risk models
[AD-A189053] N88-20906
LENGTH
Locality, communication and interconnect length in multicomputers
[CWI-CS-R8708] N88-20890
LENSES
Aberrations: Their effect on off-axis beam steering
[AD-A189601] N88-21008
LIE GROUPS
Nonlinear differential equations
[DE88-006047] N88-20933
LIFE (DURABILITY)
Improve the lifetime of the hollow fiber sodium sulfur cell
[DE88-004881] N88-20469
LIFE CYCLE COSTS
The space station assembly phase: Flight telerobotic servicer feasibility. Volume 2: Methodology and case study
[NASA-CR-182690] N88-20352
LIFE SCIENCES
JPRS report: Science and technology. USSR: Life sciences
[JPRS-ULS-88-004] N88-20815
LIFT
Calculation of the distributed loads on the blades of individual multiblade propellers in axial flow using linear and nonlinear lifting surface theories
[NASA-TT-20173] N88-20278

LIFT DEVICES
On the Kutta condition for flows around lifting airfoils and wings
[DFVLR-FB-87-40] N88-20268
LIGANDS
Molecular and electronic mechanism in the control of Na+ and K+ permeability of excitable cell membrane by ligand binding on receptor sites
[AD-A188725] N88-20805
LIGHT MODULATION
Study of photochromic materials for use in optical signal processing
[AD-A189068] N88-21006
LIGHT SCATTERING
Thermodynamic theory of fluctuations and Rayleigh light scattering in solutions N88-20681
Multiple scattering of polarized light in cirrus clouds N88-20768
LIGHT TRANSMISSION
Influence of nonlinear spectroscopic effects on atmospheric propagation of intense laser radiation at 10.6 microns wavelength N88-20705
Coherence effects in optical physics with special reference to spectroscopy
[AD-A189520] N88-21007
LIGHTNING
Atmospheric electrical modeling in support of the NASA F-106 storm hazards project
[NASA-CR-181639] N88-20758
Characteristics of the positive lighting flash
[DE88-005854] N88-20760
Upward propagating electric fields from thunderstorms and VLF transmitters N88-20767
Activities report of the Physics Department
[ETN-88-91985] N88-20964
LINE SPECTRA
An interpretation of the ethylenic, carbidic, and graphite auger lineshapes of chemisorbed carbon species
[AD-A189092] N88-20379
The astrophysics of nebulae and active galactic nuclear emission-line regions: New methods and applications N88-21111
LINEAR ACCELERATORS
Projected performance of RF-linac-driven free-electron lasers in the VUV and soft X-ray regions
[DE88-004294] N88-20625
The continuous electron beam accelerator facility
[CEBAF-PR-87-017] N88-20996
LINEAR ARRAYS
Optimal and conventional space-time processing in flow noise
[AD-A189104] N88-20985
LINEAR EQUATIONS
Conservative finite volume solutions of a linear hyperbolic transport equation in two and three dimensions using multiple grids
[NASA-CR-182715] N88-20934
LINEAR POLARIZATION
Polarization properties of SiO masers N88-21113
LINEAR SYSTEMS
Preconditioned conjugate gradient algorithms and software for solving large sparse linear systems
[DE88-002180] N88-20849
Further results on the McMillan degree and the Kronecker indices of ARMA models --- input-output relations of linear systems
[EUT-87-E-175] N88-20925
Regional Conference on the Analysis of the Unbalanced Mixed Model
[AD-A188747] N88-20943
LINEARIZATION
Transport and stability properties of free shear flows N88-20577
LINKAGES
Dynamics of high-speed mechanisms with elastic members N88-20643
LIOUVILLE THEOREM
Systems near the onset and in the well-developed regimes of turbulence
[DE88-005365] N88-20565
LIPSCHITZ CONDITION
Convergence of Runge-Kutta methods on classes of stiff initial value problems
[CWI-NM-R8717] N88-20924
LIQUID ALLOYS
Liquid alloys: New perspectives and challenges
[DE88-005935] N88-20463
LIQUID CHROMATOGRAPHY
Electrosorptive detection of simple organic compounds in liquid chromatography
[AD-A188757] N88-20376
Fuels combustion research
[AD-A189114] N88-20381
Determination of the partition coefficients of organophosphorus compounds using high-performance liquid chromatography
[AD-A189276] N88-20385
Development and evaluation of supercritical fluid chromatography-mass spectrometry
[DE88-005122] N88-20394
LIQUID HYDROGEN
Some problems of the theory of bubble growth and condensation in bubble chambers
[NASA-TT-20232] N88-20593
LIQUID METALS
Liquid alloys: New perspectives and challenges
[DE88-005935] N88-20463
LIQUID OXIDIZERS
Bipropellant combustion in a liquid rocket combustion chamber N88-20359
LIQUID ROCKET PROPELLANTS
Bipropellant combustion in a liquid rocket combustion chamber N88-20359
LIQUIDS
Contrasting conductance/viscosity relations in liquid states of vitreous and polymer solid electrolytes
[AD-A188378] N88-20452
Mathematical models of sound waves in fluids
[AD-A189270] N88-20968
LITHIUM
Polymeric electrolytes for ambient temperature lithium batteries
[DE88-004896] N88-20547
Wavelength scaling of lithium-like recombination scheme for X-UV gain production --- X-ray lasers
[ETN-88-92002] N88-20634
LITHIUM COMPOUNDS
The synthesis, characterization and structural studies of In(C5H4Me) by X-ray diffraction and electron diffraction techniques and a reinvestigation of the crystalline state of In(C5H5) by X-ray diffraction studies
[AD-A189110] N88-21038
LITHOGRAPHY
Content of natural radioactive elements in Venusian rocks determined using data from Vega-1 and Vega-2 stations N88-20323
Practical constraints on sources for pulsed beam lithographies
[DE88-006594] N88-20623
LOAD TESTS
Application of ISRM testing methods to fracture toughness testing of graphite N88-20446
European approaches in standard spectrum development --- aircraft load spectra
[NLR-MP-87007-U] N88-20661
LOADS (FORCES)
Ply-level failure analysis of a graphite/epoxy laminate under bearing-bypass loading
[NASA-TM-100578] N88-20372
Dynamic modelling of flexible rotor shafts mounted on hydrodynamic bearings N88-20641
Component mode synthesis using experimental modes enhanced by mass loading
[DE88-006097] N88-20657
Analysis of shell-type structures subjected to time-dependent mechanical and thermal loading
[NASA-CR-182705] N88-20668
LOGIC CIRCUITS
Describing constraints on a digital circuit's behavior
[AD-A189200] N88-20531
A fault injection experiment using the AIRLAB Diagnostic Emulation Facility
[NASA-CR-178390] N88-20895
LOGICAL ELEMENTS
Logical input devices and interaction --- computer graphics
[CWI-CS-R8738] N88-20836
LOMONOSOV CURRENT
Propagation of subsurface salinity maximum in tropical Atlantic N88-20686
LONGITUDINAL CONTROL
Lateral and longitudinal stability and control parameters for the space shuttle discovery as determined from flight test data
[NASA-TM-100555] N88-20309
LORAN C
Alaska Loran C probe test results
[AD-A189131] N88-20284
LOSSY MEDIA
Measurement of the properties of lossy materials inside a finite conducting cylinder
[NASA-CR-182664] N88-20962
LOW SPEED
A review of technologies applicable to low-speed flight of high-performance aircraft investigated in the Langley 14- x 22-foot subsonic tunnel
[NASA-TP-2796] N88-20264
The effect of sting interference at low speeds on the drag coefficient of an ellipsoidal body using a magnetic suspension and balance system
[NASA-CR-181611] N88-20274
LOW VISIBILITY
Flight simulator experiments concerning take-off visibility minima
[NLR-TR-86050-U] N88-20281
LUBRICANTS
Lubricating properties of molybdenum disulfide. Part 3: Performance of molybdenum disulfide-containing oils in fluid lubrication
[NASA-TT-20156] N88-20480
LUBRICATING OILS
Corrosion-wear process under rolling-sliding motion
[AD-A189603] N88-20635
LUBRICATION
Overview of the DOE-ECUT Tribology Program
[DE88-002878] N88-20637
LUMINAIRES
A defect investigation of Thunderflash MK N5 (Navy)
[MRL-TN-522] N88-20488
LUMINANCE
Pursuit tracking performance decrements associated with decreasing ambient illumination
[AD-A189336] N88-20809
LYMAN ALPHA RADIATION
IUE program SUGSD: Varability time scale of H Ly-alpha from Uranus
[NASA-CR-182706] N88-21107
LYMAN SPECTRA
Experimental study of the role of plasma polarization on line shape in dense laboratory plasmas
[ETN-88-92001] N88-21033

M

M STARS
Asymptotic giant branch populations in composite stellar systems N88-21098
MACH NUMBER
Nonaxisymmetric body supersonic, aerodynamic prediction
[AD-A189338] N88-20259
The influence of Mach number and heat transfer on the turbulent flow wall law
[NASA-TT-20230] N88-20594
Preliminary in-flight boundary layer transition measurements on a 45 deg swept wing at Mach Numbers between 0.9 and 1.8
[NASA-TM-100412] N88-20598
Measurement and analysis of the noise radiated by low Mach numbers centrifugal blowers
[AD-A189226] N88-20966
MAGMA
Status of the Magma Energy Project
[DE88-002413] N88-20719
MAGNESIUM ALLOYS
A fundamental understanding of the effect of alloying elements on the corrosion resistance of rapidly solidified Mg alloys
[AD-A189385] N88-20413
MAGNETIC BEARINGS
Modelling and control of an annular momentum control device
[NASA-CR-4138] N88-20491
MAGNETIC DIPOLES
Modeling the behavior of oriented permanent magnet material using current double theory
[DE88-004446] N88-20963
MAGNETIC FIELD CONFIGURATIONS
Fully implicit three-dimensional MHD (magnetohydrodynamics) stability and evolution in toroidal geometry
[DE88-000624] N88-21023
MAGNETIC FIELDS
Wiggler taper optimization for free-electron-laser amplifiers with moderate space-charge effects
[DE88-003758] N88-20618
Experience with and ways to upgrade accuracy of hydromagnetic surveys in ocean N88-20692
The Magnetically Insulated Inertial Confinement Fusion (MICF): A novel approach
[DE88-005460] N88-21026
Helical ripple transport in stellarators at low collision frequency
[DE88-006431] N88-21031
MAGNETIC PROPERTIES
Theoretical studies on the electronic structure and properties of complex ceramic crystals and glasses
[DE88-005837] N88-21049
MAGNETIC SURVEYS
Experience with and ways to upgrade accuracy of hydromagnetic surveys in ocean N88-20692

Resolution of the magnetotelluric method for determining local inhomogeneities in the sedimentary cover N88-20701
MAGNETIC SUSPENSION
The effect of sting interference at low speeds on the drag coefficient of an ellipsoidal body using a magnetic suspension and balance system [NASA-CR-181611] N88-20274
MAGNETIC VARIATIONS
Development of high stability fiber optic spectrophotometric systems for study of solar/stellar magnetic activity [AD-A189327] N88-21088
MAGNETICALLY TRAPPED PARTICLES
Helical ripple transport in stellarators at low collision frequency [DE88-006431] N88-21031
MAGNETOHYDRODYNAMIC GENERATORS
Arcs in cesium seeded noble gases resulting from a magnetically induced electric field [EUT-87-E-177] N88-21028
MAGNETOHYDRODYNAMIC STABILITY
Fully implicit three-dimensional MHD (magnetohydrodynamics) stability and evolution in toroidal geometry [DE88-000624] N88-21023
Magnetohydrodynamic (MHD) simulation of solar prominence formation N88-21109
MAGNETOHYDRODYNAMIC WAVES
Resonant Alfven wave instabilities driven by streaming fast particles N88-21104
MAGNETOHYDRODYNAMICS
Experience with and ways to upgrade accuracy of hydromagnetic surveys in ocean N88-20692
Implementation of a 3-D nonlinear MHD (magnetohydrodynamics) calculation on the Intel hypercube [DE88-000625] N88-20848
MAINTENANCE
Turnaround operations analysis for OTV. Volume 1: Executive summary [NASA-CR-179316] N88-20340
Turnaround operations analysis for OTV. Volume 3: Technology development plan [NASA-CR-179318] N88-20342
MAN MACHINE SYSTEMS
NAVLAB: An autonomous navigation testbed [AD-A189049] N88-20283
A personalized and prescriptive decision aid for choice from a database of options [AD-A188726] N88-20820
Mental models of mechanical systems: Individual differences in qualitative and quantitative reasoning [AD-A189035] N88-20823
Human problem solving in dynamic environments. Understanding and supporting operators in large-scale, complex systems [AD-A189539] N88-20826
MAN-COMPUTER INTERFACE
Online aiding for human-computer interfaces [AD-A189239] N88-20842
A model for graphical interaction --- computer graphics [CWI-CS-R8718] N88-20866
Parallel graphical output from dialogue cells [CWI-CS-R8719] N88-20867
Application of expert systems in project management decision aiding [NASA-CR-180762] N88-21074
MANAGEMENT
Report of the Defense Science Board Summer Study on Technology Base Management [AD-A188560] N88-21078
MANAGEMENT INFORMATION SYSTEMS
Report of the Defense Science Board Summer Study on Technology Base Management [AD-A188560] N88-21078
MANAGEMENT METHODS
Distributed transaction processing and the Camelot system [AD-A188614] N88-20885
Application of expert systems in project management decision aiding [NASA-CR-180762] N88-21074
MANGANESE
An experimental method for species concentration measurements in a welding arc using laser-induced fluorescence [DE88-005638] N88-20636
MANIPULATORS
Intelligent control of robot manipulators in hazardous environments [DE88-003305] N88-20638
Modelling and simulation of a rate controlled manipulator arm --- Hermes [NLR-TR-87010-U] N88-20639
Force distribution and trajectory control for closed kinematic chains with applications to walking machines N88-20642
Dynamics of high-speed mechanisms with elastic members N88-20643
The dynamic control of robotic manipulators in space [NASA-CR-182710] N88-20646
MANNED SPACE FLIGHT
JPRS report: Science and technology. USSR: Space [JPRS-USP-88-002] N88-20312
Study on long term evolution Towards European Autonomous Manned Spaceflight (STEAMS) [SNIAS-SE/LS/AP-35-073] N88-20330
Aeronautics and space report of the President: 1986 activities N88-21087
MANPOWER
MANPRINT handbook for RFP (Request For Proposal) development [AD-A188321] N88-21075
MANUFACTURING
The design of aircraft using the decision support problem technique [NASA-CR-4134] N88-20291
MANY BODY PROBLEM
Very large vortex calculations in two dimensions [DE88-005748] N88-20587
MAPPING
Development of an interactive real-time graphics system for the display of vehicle space positioning [NASA-TM-100429] N88-20344
The 1987 Airborne Antarctic Ozone Experiment: The Nimbus-7 TOMS data atlas [NASA-RP-1201] N88-20714
Bathymetric hazard survey test [AD-A189150] N88-20775
Retinotopic mapping of the human visual system with magnetoencephalography [AD-A189557] N88-20811
MARINE ENVIRONMENTS
Cavitation inception [AD-A189220] N88-20557
MARINE METEOROLOGY
Dynamical modeling of marine boundary layer convection N88-20750
Predictions and studies with a one-dimensional ice/ocean model [AD-A189158] N88-20776
MARINE PROPULSION
Cavitation inception [AD-A189220] N88-20557
MARKOV PROCESSES
The acoustic-modeling problem in automatic speech recognition [AD-A188529] N88-20510
On relaxation algorithms based on Markov random fields [AD-A189043] N88-20840
MARS (PLANET)
Frozen orbit analysis in the Martian system [AD-A189574] N88-21106
MARTENSITE
Studies of transverse phonon modes in premartensitic indium-thallium alloys [DE88-003481] N88-20428
MASERS
Polarization properties of SiO masers N88-21113
MASS
Optimal placement of tuning masses for vibration reduction in helicopter rotor blades [NASA-TM-100562] N88-20665
MASS SPECTROSCOPY
Determining chemical composition of aerosol in Venusian cloud layer on Vega-1 automatic interplanetary station using Malakhit mass spectrum analyzer N88-20321
Development and evaluation of supercritical fluid chromatography-mass spectrometry [DE88-005122] N88-20394
A mass spectrometer evolved gas analysis experiment for in-situ analysis of cometary dust volatiles N88-21097
MATHEMATICAL LOGIC
Measures of similarity between fuzzy concepts: A comparative analysis [AD-A189430] N88-20910
Abstraction and empty process in process algebra [CWI-CS-R8721] N88-20919
MATHEMATICAL MODELS
Fully-coupled analysis of jet mixing problems. Three-dimensional PNS model, SCIP3D [NASA-CR-4139] N88-20256
A study of combustion and flow behaviour in solid-propellant rocket motors [UTIAS-280] N88-20357
Bipropellant combustion in a liquid rocket combustion chamber N88-20359
Numerical model of the time independent mean flow in a rotating rocket motor N88-20360
Erosion in dual-phase microstructures [DE88-004507] N88-20421
PNL-1 improved ceramic composites through controlled fiber matrix interaction [DE88-005680] N88-20462
Molecular dynamics of laser ablation of a polymer coating [DE88-004337] N88-20466
Computer-aided transformation of descriptive mode of mathematical models of a control system N88-20503
Theoretical investigation of EM wave generation and radiation in the ULF, ELF and VLF bands by the electrodynamic orbiting tether [NASA-CR-182720] N88-20529
Aluminum-air battery development [DE88-006617] N88-20542
Development, manufacturing and testing of a gas-loaded variable conductance methanol heat pipe [NLR-MP-87010-U] N88-20571
Transport and stability properties of free shear flows N88-20577
Calculations of viscous flows with a multigrid method N88-20580
Direct solar-pumped iodine laser amplifier [NASA-CR-182674] N88-20630
Modelling and simulation of a rate controlled manipulator arm --- Hermes [NLR-TR-87010-U] N88-20639
Dynamic modelling of flexible rotor shafts mounted on hydrodynamic bearings N88-20641
Finite element methods for quasi-prismatic bodies with application to gears N88-20644
Numerical modeling of wave migration of seismic data N88-20684
Numerical model of Rayleigh instability and spin-off eddies on fronts N88-20696
Model of hydrodynamic adjustment of temperature, salinity and current fields N88-20700
Performance and cost benefits associated with nonimaging secondary concentrators used in point-focus dish solar thermal applications [DE88-001104] N88-20718
Correlation of data on strain accumulation adjacent to the San Andreas Fault with available models [NASA-CR-180757] N88-20742
Ultrasonic physical modeling of seismic wave propagation from graben-like structures [AD-A189066] N88-20744
The pressure drag and momentum flux during a cold frontal passage over the Alps N88-20763
Planetary scale barotropic spectral model N88-20766
The use of a barotropic finite element model for the study of circulation on the continental shelf of the southeast coast of Brazil [INPE-4401-PRE/1218] N88-20774
Studies toward observing and modelling large energetic ocean regions [AD-A189267] N88-20778
Evaluation of wave calculations using GONO in the period October 1985 - April 1986 [KNMI-TR-96] N88-20804
A model for graphical interaction --- computer graphics [CWI-CS-R8718] N88-20866
Interpolation algorithms for digital terrain models [INPE-4373-PRE/1196] N88-20877
Mathematic modeling of visual perception problems [INPE-4355-PRE/1186] N88-20897
A Darwinian approach to artificial neural systems [DE87-013184] N88-20900
Further results on the McMillan degree and the Kronecker indices of ARMA models --- input-output relations of linear systems [EUT-87-E-175] N88-20925
Model structure selection for multivariable systems by cross-validation methods [EUT-87-E-176] N88-20926
Regional Conference on the Analysis of the Unbalanced Mixed Model [AD-A188747] N88-20943
The automated symbolic derivation of state equations for dynamic systems [DE88-000968] N88-20945
Double layer polarization of nonconducting spheroidal particles and its application to Kerr effect [ISSN-0208-05658] N88-20960
Modeling the behavior of oriented permanent magnet material using current double theory [DE88-004446] N88-20963
Mathematical models of sound waves in fluids [AD-A189270] N88-20968
Modeling of laser ultrasound generation in a weld pool [DE88-005546] N88-20971
Optics for large telescope N88-21014

Electrical characteristics of MBE (Molecular Beam Epitaxyl)-grown GaAs/sub 1-x/Sb/sub x on InP and correlation with film microstructure
[DE88-003841] N88-21053
The thermodynamic properties of organic oxygen compounds
[DE88-001208] N88-21065
Review of selenium thermodynamic data
[DE88-006194] N88-21068
On the role of complete reducibility in general competitive equilibrium models
[DE88-005693] N88-21083
Magnetohydrodynamic (MHD) simulation of solar prominence formation N88-21109

MATRICES (MATHEMATICS)
Further results on the McMillan degree and the Kronecker indices of ARMA models --- input-output relations of linear systems
[EUT-87-E-175] N88-20925
The parameterization of orthogonal matrices: A review mainly for statisticians
[AD-A189144] N88-20936

MATRIX THEORY
Predicting oscillatory finite difference solutions to the heat equation: A comparative study of the coefficient and matrix methods
[AD-A189591] N88-20911

MAXIMUM LIKELIHOOD ESTIMATES
Statistical signal processing using a class of iterative estimation algorithms
[AD-A189050] N88-20511
Estimating system and component reliabilities under partial information on cause of failure
[AD-A189107] N88-20653
Non- and semi-parametric maximum likelihood estimators and the von Misis Method, part 1
[CWI-MS-R8709] N88-20941

MAXIMUM USABLE FREQUENCY
HF (High Frequency) Maximum Usable Frequency (MUF) model uncertainty assessment
[AD-A189132] N88-20513

MAXWELL EQUATION
Chronometrically invariant formulation of electrodynamics equation
[TI88-701030] N88-21071
Topics in curved and flat space electromagnetism N88-21100

MEASURING INSTRUMENTS
Development of a torsion balance for adhesion measurements
[NASA-TM-100799] N88-20454

MECHANICAL DEVICES
Understanding machines from text and diagrams
[AD-A189034] N88-20493
Mental models of mechanical systems: Individual differences in qualitative and quantitative reasoning
[AD-A189035] N88-20823

MECHANICAL PROPERTIES
Nonaxisymmetric body supersonic, aerodynamic prediction
[AD-A189338] N88-20259
Viscoelastic behavior of a polyetheretherketone (PEEK) composite
[AD-A189545] N88-20368
The influence of the fiber-matrix bond on the mechanical behavior of NICALON/SiC composites
[DE88-006155] N88-20369
A fundamental understanding of the effect of alloying elements on the corrosion resistance of rapidly solidified Mg alloys
[AD-A189385] N88-20413
Gordon Conference on Intermetallic Compounds held at Tilton, New Hampshire on 20-24 July 1987
[AD-A188502] N88-20435
PNL-1 improved ceramic composites through controlled fiber matrix interaction
[DE88-005680] N88-20462
Analysis of shell-type structures subjected to time-dependent mechanical and thermal loading
[NASA-CR-182705] N88-20668
Mechanical properties of sea ice and sea ice deformation in the near-shore zone
[PB88-147889] N88-20782
On the structure of pulsed plasma jets N88-21030
Exploring the relation between interface structure and mechanical properties in multilayer structures
[DE88-005428] N88-21060

MEDITERRANEAN SEA
Deep water mass circulation in the Alboran Basin. Measurements - January to April 1982: ALBORAN 2
[AD-A189205] N88-20777

MELTING
Integral equation theory of homopolymer melts
[DE88-005304] N88-20470
Rapid e-beam heating for measuring thermodynamics of metastable materials
[DE88-003565] N88-21066

MELTING POINTS
Processing of glass to aluminum (low melting metals) seals via an injection molding technique
[DE88-004689] N88-20468

MEMBRANES
Molecular and electronic mechanism in the control of Na+ and K+ permeability of excitable cell membrane by ligand binding on receptor sites
[AD-A188725] N88-20805
Enzyme-based fiber optic sensors
[DE88-005674] N88-21013

MEMORY (COMPUTERS)
Gaussian techniques on shared memory multiprocessor computers
[DE88-005426] N88-20855

MENTAL PERFORMANCE
Understanding machines from text and diagrams
[AD-A189034] N88-20493
A comparison of terrain association and resection as methods of position location
[AD-A189480] N88-20710
Distraction and inhibition in continuous CRT performance: A replication and some new findings
[PB88-150941] N88-20821
Identification of visual evoked response parameters sensitive to pilot mental state
[NASA-CR-4140] N88-20822
Mental models of mechanical systems: Individual differences in qualitative and quantitative reasoning
[AD-A189035] N88-20823
Knowledge retrieval as specialized inference
[AD-A189042] N88-20899

MERCURY CADMIUM TELLURIDES
Research on mercury cadmium telluride
[AD-A189155] N88-21039
Study for the determination of general and specific properties of wide energy-band gap HgHdTe in the 1-2 micrometer wavelength range
[AD-A189177] N88-21041

MERGING ROUTINES
Merge and termination in process algebra
[CWI-CS-R8716] N88-20918

MERIDIONAL FLOW
Seasonal variations and excitation mechanisms of the equatorially trapped waves N88-20751

MEROMORPHIC FUNCTIONS
Systems near the onset and in the well-developed regimes of turbulence
[DE88-005365] N88-20565

MESOSCALE PHENOMENA
Phenomenological description of eddy registered in Gulf Stream N88-20694

MESSAGE PROCESSING
A simulation study of a parallel processor with unbalanced loads
[AD-A189573] N88-20887

METAL AIR BATTERIES
Aluminum-air battery development
[DE88-006617] N88-20542
Aluminum-air battery development
[DE88-006618] N88-20543
Technology base research on zinc/air battery systems
[DE88-004893] N88-20546

METAL BONDING
Improved glass-ceramic to metal seals in actuator and detonator applications with an aluminum-containing austenitic stainless steel
[DE88-004691] N88-20458
The relationship of the chemical bonding topology of high critical temperature copper oxide superconductors to that of the chevrel phases and the ternary lanthanide rhodium borides
[AD-A189255] N88-21042

METAL FATIGUE
Non-destructive evaluation techniques applied to the study of fatigue microcrack growth in steel alloys
[DE88-004090] N88-20420
The fatigue behavior of ferritic and austenitic steels at elevated temperatures
[DE88-006304] N88-20431
Investigation of the use of horizontally polarised shear waves for TOFD studies on austenitic steel
[AERE-R-12145] N88-20649

METAL FILMS
Characterization of redox states of nickel hydroxide film electrodes by in-situ Raman spectroscopy
[AD-A189288] N88-20411
Properties of reactively sputtered WNx films Zhao, X. -A.
[AD-A188711] N88-20976

METAL IONS
Transition metal cluster chemistry
[AD-A188731] N88-20405
Wavelength scaling of lithium-like recombination scheme for X-UV gain production --- X-ray lasers
[ETN-88-92002] N88-20634

METAL MATRIX COMPOSITES
Composites strengthening
[AD-A189258] N88-20364
High-temperature metal matrix composites
[AD-A189516] N88-20367
Processing, structure and properties of heavily deformed in situ composites
[AD-A189611] N88-20416
Fracture criteria for discontinuously reinforced metal matrix composites
[NASA-CR-182665] N88-20662

METAL OXIDE SEMICONDUCTORS
GM: A gate matrix layout generator
[EUT-87-E-179] N88-20875

METAL POWDER
A case study of the development of a military specification - zirconium powder for thermal batteries
[AD-A188751] N88-20717

METAL SURFACES
A study of the interaction of light with sub-micron metallic surfaces
[DE88-003138] N88-20624
Spontaneous decay and atomic fluorescence near a metal surface of an absorbing dielectric
[AD-A187508] N88-20975
Recent progress in structure determination by LEED (Low-Energy Electron Diffraction) measure the properties of the deep donors (DX-cent)
[DE88-003851] N88-21048

METAL-METAL BONDING
The relationship of the chemical bonding topology of high critical temperature copper oxide superconductors to that of the chevrel phases and the ternary lanthanide rhodium borides
[AD-A189255] N88-21042

METALLOGRAPHY
Processing, structure and properties of heavily deformed in situ composites
[AD-A189611] N88-20416

METALS
Photochemistry at structured surfaces: A classical electromagnetic approach
[AD-A189519] N88-20387
Material instabilities in solids
[AD-A189525] N88-20388
The coordination cluster theory for metallic solutions
[DE88-005934] N88-20389
Formation of nuclei during precipitation in metallic mixed crystals
[NASA-TT-20248] N88-20437
Spontaneous decay and atomic fluorescence near a metal surface of an absorbing dielectric
[AD-A187508] N88-20975
Image charge, coherent scattering, and symmetry effects in electron stimulated desorption: O(-) from O sub 2 condensed on metals
[AD-A189093] N88-20979

METASTABLE STATE
Quantum Monte Carlo study of the MIES associated with H2 (X 1 sigma sub g (+)) and H2 (B 1 sigma sub u (+))
[AD-A189063] N88-20977
Investigations of the origins of metastable, light-induced changes in hydrogenated amorphous silicon
[DE88-001117] N88-21051

METEOROLOGICAL RADAR
A polarization diversity meteorological radar system
[AD-A189291] N88-20515

METEOROLOGY
A study of satellite emission computed tomography
[AD-A189567] N88-20745

METHANE
Novel catalysts for methane activation
[DE88-003637] N88-20390

METHOD OF MOMENTS
Electromagnetic scattering from and natural resonances of the circular strip N88-20523

METHODOLOGY
Active cooling design for scramjet engines using optimization methods
[NASA-TM-100581] N88-20669

METHYL ALCOHOL
Alternative fuels: Information on DOE's (Department of Energy's) methanol vehicle demonstration program
[PB88-118203] N88-20481

METRIC SPACE
Solving reflexive domain equations in a category of complete metric spaces
[CWI-CS-R8709] N88-20956

MICROBURSTS (METEOROLOGY)
Power spectral density analysis of wind-shear turbulence for related flight simulations
[NASA-CR-182721] N88-20773

MICROCOMPUTERS
A simplified computer code for reduction to burning rates of closed bomb pressure-time data (MINICB)
[AD-A189112] N88-20380
Interactive automated system for testing analog units of digital seismic stations N88-20702
MICROCRACKS
Non-destructive evaluation techniques applied to the study of fatigue microcrack growth in steel alloys
[DE88-004090] N88-20420
MICROMECHANICS
Micromechanical and microstructural studies of ceramic superplasticity
[DE88-005793] N88-20472
MICROMETERS
Study for the determination of general and specific properties of wide energy-band gap HgHdTe in the 1-2 micrometer wavelength range
[AD-A189177] N88-21041
MICROPARTICLES
The effect of Ca(OH)2-treated ceramic microspheres on the mechanical properties of high-temperature lightweight cement composites
[DE88-004590] N88-20457
MICROPOROSITY
Ultrasonic characterization of non-uniform porosity distributions in SiC ceramic
[DE88-004814] N88-20459
MICROSCOPY
Computer software for the computation of the scattered field and the optical microscope image of line objects patterned in thick layers
[PB88-153705] N88-20838
MICROSTRUCTURE
The effect of microstructure on the fatigue crack growth resistance of nickel base superalloys
[AD-A189526] N88-20414
Processing, structure and properties of heavily deformed in situ composites
[AD-A189611] N88-20416
Use of the LLNL 40 kV electric gun to study the shock response of 21-6-9 stainless steel
[DE87-014550] N88-20418
Non-destructive evaluation techniques applied to the study of fatigue microcrack growth in steel alloys
[DE88-004090] N88-20420
Erosion in dual-phase microstructures
[DE88-004507] N88-20421
Grain refinement during primary breakdown of alloy 718
[DE88-005193] N88-20423
Advances in X-ray line profile analysis to determine microstructure information about ceramics
[DE88-003936] N88-20465
Micromechanical and microstructural studies of ceramic superplasticity
[DE88-005793] N88-20472
Mixing of viscous fluids: Behavior of microstructures and chaos
[DE88-006287] N88-20566
Ductile failure
[AD-A189429] N88-20654
Anisotropy of microstructural eddy motion in surface layer during calm N88-20677
Electrical characteristics of MBE (Molecular Beam Epitaxyl)-grown GaAs/sub 1-x/Sb/sub x on InP and correlation with film microstructure
[DE88-003841] N88-21053
MICROWAVE AMPLIFIERS
Wiggler taper optimization for free-electron-laser amplifiers with moderate space-charge effects
[DE88-003758] N88-20618
MICROWAVE CIRCUITS
Optical RF distribution links for MMIC phased array antennas
[NASA-TM-100841] N88-20555
MICROWAVE LANDING SYSTEMS
Flight simulations of MLS interception procedures applicable to laterally segmented approach paths
[NLR-MP-86037-U] N88-20288
MICROWAVES
Microwave and structural properties of saline ice
[AD-A189307] N88-20779
Design of electron beam accelerator for microwave application
[DE88-005252] N88-20999
Solar microwave radiation maps measured at Metsaehovi Radio Research Station in 1978-1979
[PB88-127543] N88-21108
MIDAIR COLLISIONS
Aircraft accident report: Midair collision of Cessna-340A, N8716K, and North American SNJ-4N, N711SQ, Orlando, Florida, May 1, 1987
[PB88-910402] N88-20282
MILITARY HELICOPTERS
AVSCOM'S modifications to Teledyne Systems Company's air-to-air fire control system simulation model
[AD-A189136] N88-20294
MILITARY OPERATIONS
Expert systems for decision support in military aircraft mission preparation
[NLR-MP-87013-U] N88-20946
MANPRINT handbook for RFP (Request For Proposal) development
[AD-A188321] N88-21075
Soviet military power, 1987 N88-21114
MILITARY SPACECRAFT
Alternative force structuring strategies for military satellite communication systems
[AD-A189492] N88-20516
MILITARY TECHNOLOGY
Soviet military power, 1987 N88-21114
MILKY WAY GALAXY
The astrophysics of nebulae and active galactic nuclear emission-line regions: New methods and applications N88-21111
MINERAL OILS
Lubricating properties of molybdenum disulfide. Part 3: Performance of molybdenum disulfide-containing oils in fluid lubrication
[NASA-TT-20156] N88-20480
MINERALS
Experimental and theoretical constraints on the origin of mid-ocean ridge geothermal fluids N88-20764
MIRRORS
Optics for large telescope N88-21014
MISSILE COMPONENTS
Nonaxisymmetric body supersonic, aerodynamic prediction
[AD-A189338] N88-20259
MISSILE DEFENSE
SEAT: A strategic engagement analysis tool
[DE88-000498] N88-20944
MISSILE TRAJECTORIES
Effect of rotation on the lateral stability of a free-flying column subjected to an axial thrust with directional control
[AD-A188690] N88-20338
MISSION PLANNING
Orbital transfer vehicle concept definition and system analysis study. Volume 2: OTV concept definition and evaluation. Book 1: Mission and system requirements
[NASA-CR-179321] N88-20339
Turnaround operations analysis for OTV. Volume 1: Executive summary
[NASA-CR-179316] N88-20340
Turnaround operations analysis for OTV. Volume 2: Detailed technical report
[NASA-CR-179317] N88-20341
Turnaround operations analysis for OTV. Volume 3: Technology development plan
[NASA-CR-179318] N88-20342
Development of an interactive real-time graphics system for the display of vehicle space positioning
[NASA-TM-100429] N88-20344
Expert systems for decision support in military aircraft mission preparation
[NLR-MP-87013-U] N88-20946
Johnson Space Center's strategic game plan: Charting a course to the year 2000 and beyond
[NASA-TM-89733] N88-21076
MIXED CRYSTALS
Formation of nuclei during precipitation in metallic mixed crystals
[NASA-TT-20248] N88-20437
MIXING
Mixing of viscous fluids: Behavior of microstructures and chaos
[DE88-006287] N88-20566
Structures and fluxes in a deep convecting mixed layer N88-20786
Equatorial turbulence: Mixed layer and thermocline N88-20787
The mixed layer of the western equatorial Pacific Ocean
[HIG-1861] N88-20789
MIXTURES
Prediction of high-temperature thermodynamic properties of mixed electrolyte solutions including solubility equilibria, vapor pressure depression and boiling point elevation
[DE88-006344] N88-21089
MOBILITY
An investigation of classical dynamic scaling techniques applied to an oleo-pneumatic landing gear strut
[AD-A187664] N88-20292
Crustal dynamics project data analysis, 1987. Volume 2: Mobile VLBI geodetic results 1982-1986
[NASA-TM-100689-VOL-2] N88-20753
MODEL REFERENCE ADAPTIVE CONTROL
Adaptive control of scientific balloon-borne gondola attitude N88-20497
MODELS
Nonaxisymmetric body supersonic, aerodynamic prediction
[AD-A189338] N88-20259
Understanding machines from text and diagrams
[AD-A189034] N88-20493
Estimation-correlation, modeling, and identification in adaptive array processors
[AD-A189130] N88-20512
Numerical methods in the resolution of control electrovalve model
[INPE-4154-RPE/540] N88-20554
Improvement of the Reynolds-stress model by a new pressure-strain correlation
[NASA-CR-182699] N88-20667
Atmospheric electrical modeling in support of the NASA F-106 storm hazards project
[NASA-CR-181639] N88-20758
Broadband correlation analysis
[AD-A188732] N88-20839
Relativistic jet models for the BL Lacertae object Mrk 421 during three epochs of observation
[NASA-TM-89727] N88-21090
MODULATION
Signal-filter design and system performance for polarimetric radar
[AD-A189257] N88-20514
Efficiency characteristics of speed modulated drives at predicted torque conditions for air-to-air heat pumps
[DE88-005846] N88-20588
MODULES
Component mode synthesis using experimental modes enhanced by mass loading
[DE88-006097] N88-20657
MODULUS OF ELASTICITY
High temperature Young's modulus of IG-110 graphite N88-20443
Effects of high temperature neutron irradiation on the physical, chemical and mechanical properties of fine-grained isotropic graphite N88-20444
MOLECULAR BEAM EPITAXY
Research on multibandgap solar cells
[DE87-012261] N88-20721
Development of Si/SiGe heterostructures
[AD-A189527] N88-21044
Electrical characteristics of MBE (Molecular Beam Epitaxyl)-grown GaAs/sub 1-x/Sb/sub x on InP and correlation with film microstructure
[DE88-003841] N88-21053
MOLECULAR BEAMS
A study of the interaction of light with sub-micron metallic surfaces
[DE88-003138] N88-20624
MOLECULAR COLLISIONS
Molecular collision processes in gases and at surfaces
[AD-A189518] N88-20982
Excimer laser photolysis studies of T-V (Translation-to-Vibration) energy transfer
[AD-A189613] N88-20989
MOLECULAR EXCITATION
Molecular and electronic mechanism in the control of Na+ and K+ permeability of excitable cell membrane by ligand binding on receptor sites
[AD-A188725] N88-20805
Quantum Monte Carlo study of the MIES associated with H2 (X 1 sigma sub g (+)) and H2 (B 1 sigma sub u (+))
[AD-A189063] N88-20977
Excimer laser photolysis studies of T-V (Translation-to-Vibration) energy transfer
[AD-A189613] N88-20989
MOLECULAR GASES
Molecular collision processes in gases and at surfaces
[AD-A189518] N88-20982
MOLECULAR INTERACTIONS
Photochemistry at structured surfaces: A classical electromagnetic approach
[AD-A189519] N88-20387
MOLECULAR STRUCTURE
Novel catalysts for methane activation
[DE88-003637] N88-20390
Properties of molecular solids and fluids at high pressure and temperature
[DE88-004195] N88-20391
Gordon Conference on Intermetallic Compounds held at Tilton, New Hampshire on 20-24 July 1987
[AD-A188502] N88-20435
Thermodynamic theory of fluctuations and Rayleigh light scattering in solutions N88-20681
MOLECULES
Results of infrared spectrometer experiment. 1: Infrared radiation of parent molecules in Halley's Comet N88-20325

MOPAC manual: A general molecular orbital package, fourth edition
[AD-A188623] N88-20362

MOLTEN SALTS
Quantitative determination of a hydrogen impurity in a sodium coolant by hydride thermal dissociation
[NASA-TT-20239] N88-20402

MOLYBDENUM
The effect of microstructure on the fatigue crack growth resistance of nickel base superalloys
[AD-A189526] N88-20414
The relationship of the chemical bonding topology of high critical temperature copper oxide superconductors to that of the chevrel phases and the ternary lanthanide rhodium borides
[AD-A189255] N88-21042

MOLYBDENUM DISULFIDES
Lubricating properties of molybdenum disulfide. Part 3: Performance of molybdenum disulfide-containing oils in fluid lubrication
[NASA-TT-20156] N88-20480

MOMENTS OF INERTIA
What is the maximum length of a spin stabilized projectile
[PB88-130919] N88-20336

MOMENTUM
The pressure drag and momentum flux during a cold frontal passage over the Alps N88-20763
Energy and momentum fluxes through the sea surface N88-20798
Large momentum pairing in one-dimensional systems
[AD-A189228] N88-20981

MOMENTUM TRANSFER
Turbulent transfer of momentum and heat in boundary layer of fluid beyond an obstacle. 1: Hydrodynamic characteristics N88-20690
On the zonal momentum balance at the equator N88-20788
Energy and momentum fluxes through the sea surface N88-20798
Fragmentation and flow in central collisions
[DE88-005386] N88-20991

MONTE CARLO METHOD
Estimating system and component reliabilities under partial information on cause of failure
[AD-A189107] N88-20653
Performance and cost benefits associated with nonimaging secondary concentrators used in point-focus dish solar thermal applications
[DE88-001104] N88-20718
Biophysical applications of solid state and tritium NMR
[DE88-005328] N88-20806
The physical structure of concurrent problems and concurrent computers
[DE88-005812] N88-20835
A simulation study of a parallel processor with unbalanced loads
[AD-A189573] N88-20887
Quantum Monte Carlo study of the MIES associated with H2 (X 1 sigma sub g (+)) and H2 (B 1 sigma sub u (+))
[AD-A189063] N88-20977
Modeling and transport in semiconductor devices
[AD-A188760] N88-21037

MOTION PERCEPTION
Computerised measurement of human horizontal smooth pursuit eye movements N88-20819

MOTION SICKNESS
An analysis of physiological data related to motion sickness for use in a real-time motion sickness indicator
[AD-A189589] N88-20812

MOTION SIMULATION
Dynamics of high-speed mechanisms with elastic members N88-20643

MOTOR VEHICLES
Alternative fuels: Information on DOE's (Department of Energy's) methanol vehicle demonstration program
[PB88-118203] N88-20481

MOTORS
Dynamics of high-speed mechanisms with elastic members N88-20643

MULTIPROCESSING (COMPUTERS)
NAVLAB: An autonomous navigation testbed
[AD-A189049] N88-20283
Very large vortex calculations in two dimensions
[DE88-005748] N88-20587
Data traffic reduction schemes for sparse Cholesky factorizations
[NASA-CR-181626] N88-20831
Gaussian techniques on shared memory multiprocessor computers
[DE88-005426] N88-20855
Locality, communication and interconnect length in multicomputers
[CWI-CS-R8708] N88-20890

MULTIVARIATE STATISTICAL ANALYSIS
Force distribution and trajectory control for closed kinematic chains with applications to walking machines N88-20642

N

NAPHTHENES
Availability and cost estimate of a high naphthene, modified aviation turbine fuel
[NASA-TM-100823] N88-20455

NARROWBAND
Optimal and conventional space-time processing in flow noise
[AD-A189104] N88-20965

NASA PROGRAMS
The Deep Space Network
[NASA-CR-182700] N88-20524
Application of expert systems in project management decision aiding
[NASA-CR-180762] N88-21074
Johnson Space Center's strategic game plan: Charting a course to the year 2000 and beyond
[NASA-TM-89733] N88-21076

NASA SPACE PROGRAMS
Aeronautics and space report of the President: 1986 activities N88-21087

NASTRAN
Sixteenth NASTRAN (trademark) Users' Colloquium
[NASA-CP-2505] N88-20652
A preliminary investigation of finite-element modeling for composite rotor blades
[NASA-TM-100559] N88-20656

NAVIER-STOKES EQUATION
Fully-coupled analysis of jet mixing problems. Three-dimensional PNS model, SCIP3D
[NASA-CR-4139] N88-20256
The construction of a three-dimensional finite volume grid generator for a wing in a wind tunnel with application to Navier-Stokes flow solvers
[FFA-TN-1987-58] N88-20277
Numerical model of the time independent mean flow in a rotating rocket motor N88-20360
Calculations of viscous flows with a multigrid method N88-20580
Numerical experiments on the stability of controlled boundary layers
[NASA-CR-181649] N88-20591

NAVIGATION
Alaska Loran C probe test results
[AD-A189131] N88-20284

NEAR INFRARED RADIATION
Global solar oscillations observed in the visible to near infrared continuum N88-21110

NEBULAE
The astrophysics of nebulae and active galactic nuclear emission-line regions: New methods and applications N88-21111

NEGATIVE IONS
Studies of compound states of negative ions using laser beams
[DE88-004708] N88-20627

NETHERLANDS
Activities report in civil aeronautics
[ETN-88-91344] N88-20255

NETWORK CONTROL
Sojourn times in feedback queues
[CWI-OS-R8710] N88-20947
Two queues with alternating service and switching times
[CWI-OS-R8712] N88-20949

NEURAL NETS
A Darwinian approach to artificial neural systems
[DE87-013184] N88-20900

NEUROLOGY
Computing with structured connections networks
[AD-A189244] N88-20886

NEUTRAL BEAMS
A segmented calorimeter for low-energy particle beams in space
[DE88-001806] N88-20997

NEUTRINOS
Intermediate energy neutrino physics
[DE88-005378] N88-20984

NEUTRON CROSS SECTIONS
Computer programs for calculating group cross-section covariances from uncertainty parameters in the ENDF/B-V format. UNC 32/33 --- neutron physics
[ECN-202] N88-20995

NEUTRON IRRADIATION
Effects of high temperature neutron irradiation on the physical, chemical and mechanical properties of fine-grained isotropic graphite N88-20444
Degradations of thermal shock resistance and the fracture toughness of reactor graphite subjected to neutron irradiation N88-20445

NEUTRON SPECTRA
Computer programs for calculating group cross-section covariances from uncertainty parameters in the ENDF/B-V format. UNC 32/33 --- neutron physics
[ECN-202] N88-20995

NEWTON-RAPHSON METHOD
Numerical methods in the resolution of control electrovalve model
[INPE-4154-RPE/540] N88-20554

NEWTONIAN FLUIDS
Boundary effects on the drag of a cylinder in axial motion at low Reynolds number N88-20578

NICKEL
The effect of microstructure on the fatigue crack growth resistance of nickel base superalloys
[AD-A189526] N88-20414
Temperature dependence of Kr precipitation in Ni
[DE88-005953] N88-20429

NICKEL ALLOYS
The effect of microstructure on the fatigue crack growth resistance of nickel base superalloys
[AD-A189526] N88-20414

NICKEL COMPOUNDS
Characterization of redox states of nickel hydroxide film electrodes by in-situ Raman spectroscopy
[AD-A189288] N88-20411

NICKEL STEELS
Texture profile in thermomechanically processed 2-inch-thick 5 Ni-steel armor plate
[AD-A189275] N88-20410

NIMBUS 7 SATELLITE
The 1987 Airborne Antarctic Ozone Experiment: The Nimbus-7 TOMS data atlas
[NASA-RP-1201] N88-20714

NITRAMINE PROPELLANTS
Laser ignition of nitramine composite propellants and crack propagation and branching in burning solid propellants
[AD-A189260] N88-20483

NITRIDES
Properties of reactively sputtered WNx films Zhao, X. -A.
[AD-A188711] N88-20976

NITROGEN DIOXIDE
Effect of nitrogen dioxide release on thermosphere N88-20704

NITROGEN IONS
The magnitude of secondary electron contributions in photon stimulated desorption
[AD-A189094] N88-20980

NITROGEN POLYMERS
MOPAC manual: A general molecular orbital package, fourth edition
[AD-A188623] N88-20362

NOCTURNAL VARIATIONS
Computer simulation of tropospheric chemistry
[JUEL-2144] N88-20756

NOISE
Research in applied mathematics related to identification of noisy systems
[AD-A189355] N88-20908

NOISE SPECTRA
Optimal and conventional space-time processing in flow noise
[AD-A189104] N88-20965

NOISE TEMPERATURE
A study of satellite emission computed tomography
[AD-A189567] N88-20745

NONDESTRUCTIVE TESTS
Non-destructive evaluation techniques applied to the study of fatigue microcrack growth in steel alloys
[DE88-004090] N88-20420
High temperature Young's modulus of IG-110 graphite N88-20443
Nondestructive testings of HTGR graphites N88-20448
Nondestructive evaluation of carbon-carbon coatings
[AD-A189524] N88-20453
Recent developments in nondestructive evaluation for structural ceramics
[DE88-005889] N88-20473
X-ray computed tomography for structural ceramic applications: Beam hardening corrections
[DE88-005891] N88-20474
Noncontact thermometry via laser pumped, thermographic phosphors: Characterization of systematic errors and industrial applications
[DE88-005599] N88-20628
Thermionic Technology Program. A: Insulator test and evaluation
[DE88-004707] N88-20735

NONLINEAR EQUATIONS
Nonlinear differential equations
[DE88-006047] N88-20933
NONLINEAR OPTICS
Influence of nonlinear spectroscopic effects on atmospheric propagation of intense laser radiation at 10.6 microns wavelength N88-20705
NONLINEAR PROGRAMMING
Constrained nonlinear programming
[DE88-005695] N88-20860
NONLINEAR SYSTEMS
Robustifying the Kalman filter
[AD-A189240] N88-20907
Stochasticity in nonlinear Hamiltonian systems
[DE88-005499] N88-20915
Period-doubling universality in multidimensional dissipative and conservative systems
[PB88-146812] N88-20961
NONLINEARITY
Finite element methodology for nonlinear free and harmonic forced vibrations of beam and plate structures N88-20663
Algorithms with conic termination for nonlinear optimization
[DE88-005893] N88-20851
Nonlinear refractive index measurements of glasses and crystals
[DE88-005673] N88-21009
Energy transfer and non-linear optical properties at near ultraviolet wavelengths: Rare earth 4f yields 5d transitions in crystals and glasses
[DE88-005403] N88-21012
Two studies of nonlinear processes in irreversible thermodynamics
[DE88-005794] N88-21067
NORMS
On the norm equivalence of singularly perturbed elliptic difference operators
[DE88-006353] N88-20913
NORTH AMERICA
Northern Hemisphere circulation and the principal components of subsequent summer patterns in North America and West Africa N88-20765
NORTHERN HEMISPHERE
Northern Hemisphere circulation and the principal components of subsequent summer patterns in North America and West Africa N88-20765
NOTCH SENSITIVITY
Notch sensitivity of graphite materials for VHTR N88-20447
Cyclic crack growth emanating at a round notch considering viscoplasticity
[AD-A189577] N88-20655
NOTCH TESTS
Application of ISRM testing methods to fracture toughness testing of graphite N88-20446
Notch sensitivity of graphite materials for VHTR N88-20447
NOTCHES
Cyclic crack growth emanating at a round notch considering viscoplasticity
[AD-A189577] N88-20655
NOZZLE FLOW
Application of a flux vector splitting methodology towards the solution of unsteady transonic flows, with future emphasis on the blade flutter problem
[AD-A189500] N88-20260
An adaptive grid technique for solution of the Euler equations N88-20579
NUCLEAR FUELS
Compatibility in space reactor fuel systems
[DE88-005698] N88-21004
NUCLEAR FUSION
Application of railgun principle to high-velocity hydrogen pellet injection for magnetic fusion reactor refueling
[DE88-005830] N88-20334
SOAR: Space orbiting advanced fusion power reactor
[AD-A189234] N88-20356
NUCLEAR MAGNETIC RESONANCE
Recent developments in nondestructive evaluation for structural ceramics
[DE88-005889] N88-20473
Velocity and concentration measurements in flowing suspensions by nuclear magnetic resonance
[DE88-006225] N88-20589
Biophysical applications of solid state and tritium NMR
[DE88-005328] N88-20806
NUCLEAR MEDICINE
Technology '87: Research and Development Laboratory Technology Transfer Program
[DE88-003142] N88-21084
NUCLEAR PHYSICS
Intermediate energy neutrino physics
[DE88-005378] N88-20984
Research in high energy elementary particle physics
[DE88-006065] N88-20994
Particle physics and cosmology
[DE88-004944] N88-21096
NUCLEAR POWER PLANTS
Uncertainties in hydrogen combustion
[DE88-005354] N88-20395
NUCLEAR PUMPED LASERS
Refractive index gradients in nuclear-reactor-pumped lasers: Gasdynamic effects
[DE88-006099] N88-20621
NUCLEAR WEAPONS
Characteristics of the positive lighting flash
[DE88-005854] N88-20760
NUCLEATION
Cavitation inception
[AD-A189220] N88-20557
Ductile failure
[AD-A189429] N88-20654
NUMERICAL ANALYSIS
Numerical simulation of subsonic and transonic propeller flow
[NASA-TM-100163] N88-20262
Detection and angle estimation of coherent plane waves N88-20522
Numerical methods in the resolution of control electrovalve model
[INPE-4154-RPE/540] N88-20554
Control of structure in turbulent flows: Bifurcating and blooming jets
[AD-A189607] N88-20562
Center for Turbulence Research 1987 activities
[NASA-CR-182693] N88-20583
Numerical experiments on the stability of controlled boundary layers
[NASA-CR-181649] N88-20591
Structural clearances and internal friction: Simulation by Eigen distortions
[ISSN-0208-5658] N88-20640
Dynamical modeling of marine boundary layer convection N88-20750
Multiple scattering of polarized light in cirrus clouds N88-20768
Computer aided surface representation
[DE88-005408] N88-20854
Numerical solution of ill posed problems in partial differential equations
[AD-A189383] N88-20909
Elimination of quantifiers of linear variables and corresponding transfer principles
[DE88-005692] N88-20912
Numerical simulations of multiphoton processes in many electron atoms
[DE88-003293] N88-20990
Silicon-germanium heterostructures N88-21034
NUMERICAL CONTROL
Intelligent control of robot manipulators in hazardous environments
[DE88-003305] N88-20638
A novel method for sputter-deposition of high T(sub c) superconductor films via a computer-controlled mass analyzed ion beam
[DE88-006001] N88-21064
NUMERICAL STABILITY
Transport and stability properties of free shear flows N88-20577
Stabilization of explicit difference schemes by smoothing techniques
[CWI-NM-R8714] N88-20923
Nonlinear differential equations
[DE88-006047] N88-20933

O

OCEAN BOTTOM
Relationship between oceanic geological formations and tectonic structures N88-20683
Experience with and ways to upgrade accuracy of hydromagnetic surveys in ocean N88-20692
Research on turbulence in bottom boundary layer in ocean N88-20697
Bathymetric hazard survey test
[AD-A189150] N88-20775
Experimental and theoretical constraints on the origin of mid-ocean ridge geothermal fluids N88-20784
OCEAN CURRENTS
Anisotropy of microstructural eddy motion in surface layer during calm N88-20677
Mushroom-shaped currents (eddy dipoles) under rotation and stratification conditions N88-20678
Determining Langmuir circulation parameters on basis of similarity theory N88-20680
Space-time analysis of oceanographic fields by modified empirical orthogonal functions method N88-20687
Intrathermocline lens of Mediterranean water in tropical North Atlantic N88-20688
Dynamics of synoptic ocean eddies N88-20689
Contribution to theory of quasigeostrophic motions of finite amplitude in viscous stratified ocean N88-20695
Research on turbulence in bottom boundary layer in ocean N88-20697
Study of spectra of sea waves on horizontally nonuniform current in rip zone N88-20699
Model validation research: Comparison of simulated and observed climate patterns for the past 18,000 years
[DE88-004945] N88-20759
Deep water mass circulation in the Alboran Basin. Measurements - January to April 1982: ALBORAN 2
[AD-A189205] N88-20777
Survey of acoustic techniques for monitoring El Nino
[PB88-157615] N88-20783
Dynamics of the Oceanic Surface Mixed Layer
[AD-A188348] N88-20785
Equatorial turbulence: Mixed layer and thermocline N88-20787
On the zonal momentum balance at the equator N88-20788
The mixed layer of the western equatorial Pacific Ocean
[HIG-1861] N88-20789
Observations of waves and Langmuir circulation with Doppler sonars N88-20790
Some effects of heating on the wind-driven velocity in the upper ocean N88-20792
Mixed-layer shear related to wind stress in the central equatorial Pacific N88-20793
Mixed-layer fronts in the California current N88-20794
Horizontal scales of wind forced inertial motions N88-20795
Subduction N88-20796
Wind forcing and observed oceanic wavenumber spectra N88-20797
Hamiltonian description of the interaction of surface waves with mixed-layer currents N88-20799
OCEAN DYNAMICS
Negative viscosity in global circulations N88-20685
Propagation of subsurface salinity maximum in tropical Atlantic N88-20686
Intrathermocline lens of Mediterranean water in tropical North Atlantic N88-20688
Dynamics of synoptic ocean eddies N88-20689
Structures and fluxes in a deep convecting mixed layer N88-20786
Equatorial turbulence: Mixed layer and thermocline N88-20787
On the zonal momentum balance at the equator N88-20788
The mixed layer of the western equatorial Pacific Ocean
[HIG-1861] N88-20789
Some effects of heating on the wind-driven velocity in the upper ocean N88-20792
Subduction N88-20796
OCEAN MODELS
Model validation research: Comparison of simulated and observed climate patterns for the past 18,000 years
[DE88-004945] N88-20759
Predictions and studies with a one-dimensional ice/ocean model
[AD-A189158] N88-20776
Wind forcing and observed oceanic wavenumber spectra N88-20797
Evaluation of wave calculations using GONO in the period October 1985 - April 1986
[KNMI-TR-96] N88-20804
OCEAN SURFACE
Spectral reflective characteristics of sea surface N88-20676
Anisotropy of microstructural eddy motion in surface layer during calm N88-20677
Vertical turbulent transfer of matter in thin ocean surface layer during daytime heating N88-20693
Dynamics of the Oceanic Surface Mixed Layer
[AD-A188348] N88-20785
Structures and fluxes in a deep convecting mixed layer N88-20786
Equatorial turbulence: Mixed layer and thermocline N88-20787
Observations of waves and Langmuir circulation with Doppler sonars N88-20790
Unsteady shallowing mixed layer N88-20791
Some effects of heating on the wind-driven velocity in the upper ocean N88-20792
Mixed-layer shear related to wind stress in the central equatorial Pacific N88-20793
Mixed-layer fronts in the California current N88-20794
Horizontal scales of wind forced inertial motions N88-20795
Energy and momentum fluxes through the sea surface N88-20798

Monitoring ocean surface layer processes N88-20801
Global mixed-layer natural and anthropogenic fluxes N88-20803

OCEAN TEMPERATURE
Determination of mean thermohaline characteristics of the ocean N88-20675
Estimates of ocean-atmosphere thermal interaction in Gulf Stream energy-active test range in winter of 1984 N88-20679
Propagation of subsurface salinity maximum in tropical Atlantic N88-20686
Space-time analysis of oceanographic fields by modified empirical orthogonal functions method N88-20687
Intrathermocline lens of Mediterranean water in tropical North Atlantic N88-20688
Model of hydrodynamic adjustment of temperature, salinity and current fields N88-20700
Dynamics of the Oceanic Surface Mixed Layer
[AD-A188348] N88-20785
Structures and fluxes in a deep convecting mixed layer N88-20786
Equatorial turbulence: Mixed layer and thermocline N88-20787
The mixed layer of the western equatorial Pacific Ocean
[HIG-1861] N88-20789
Mixed-layer fronts in the California current N88-20794
Wind forcing and observed oceanic wavenumber spectra N88-20797
Radiative processes affecting ocean mixed-layer heat content and their monitoring from satellite N88-20800
Monitoring ocean surface layer processes N88-20801

OCEAN THERMAL ENERGY CONVERSION
Federal Ocean Energy Technology
[DE87-012279] N88-20722

OCEANOGRAPHIC PARAMETERS
Predictions and studies with a one-dimensional ice/ocean model
[AD-A189158] N88-20776

OCEANOGRAPHY
JPRS report: Science and technology. USSR: Earth sciences
[JPRS-UES-88-001] N88-20674
Studies toward observing and modelling large energetic ocean regions
[AD-A189267] N88-20778
Dynamics of the Oceanic Surface Mixed Layer
[AD-A188348] N88-20785
Inversion algorithms for geophysical problems
[AD-A189252] N88-20845
ONR Far East Scientific Bulletin, volume 12, number 3, July-September 1987
[AD-A188554] N88-21081

OCEANS
Determination of mean thermohaline characteristics of the ocean N88-20675
Structures and fluxes in a deep convecting mixed layer N88-20786
On the zonal momentum balance at the equator N88-20788
Subduction N88-20796
Wind forcing and observed oceanic wavenumber spectra N88-20797
Energy and momentum fluxes through the sea surface N88-20798
Global mixed-layer natural and anthropogenic fluxes N88-20803

ON-LINE SYSTEMS
Parallel image compression
[NASA-CR-180758] N88-20837
Online aiding for human-computer interfaces
[AD-A189239] N88-20842

OPERATING SYSTEMS (COMPUTERS)
An interface between object-oriented systems
[AD-A189245] N88-20844
An amoeba replicated service organisation --- Amoeba operating system
[CWI-CS-R8723] N88-20892

OPERATIONS RESEARCH
Perspectives on parallel computing
[CWI-OS-R8709] N88-20889

OPERATOR PERFORMANCE
Human problem solving in dynamic environments. Understanding and supporting operators in large-scale, complex systems
[AD-A189539] N88-20826

OPERATORS (MATHEMATICS)
On the norm equivalence of singularly perturbed elliptic difference operators
[DE88-006353] N88-20913

OPERATORS (PERSONNEL)
Human problem solving in dynamic environments. Understanding and supporting operators in large-scale, complex systems
[AD-A189539] N88-20826

OPTICAL DATA PROCESSING
Study of photochromic materials for use in optical signal processing
[AD-A189068] N88-21006

OPTICAL EQUIPMENT
Laser gyro attitude control system feasibility
[AD-A189368] N88-20285
Aberrations: Their effect on off-axis beam steering
[AD-A189601] N88-21008
Applications of the lateral shearing interferometer in measurement of synchrotron radiation optical elements
[DE88-005184] N88-21011

OPTICAL FILTERS
Study of photochromic materials for use in optical signal processing
[AD-A189068] N88-21006

OPTICAL MEASUREMENT
Computer software for the computation of the scattered field and the optical microscope image of line objects patterned in thick layers
[PB88-153705] N88-20838

OPTICAL MEASURING INSTRUMENTS
Activities report of the Physics Department
[ETN-88-91985] N88-20964

OPTICAL MICROSCOPES
Computer software for the computation of the scattered field and the optical microscope image of line objects patterned in thick layers
[PB88-153705] N88-20838

OPTICAL POLARIZATION
Spontaneous decay and atomic fluorescence near a metal surface of an absorbing dielectric
[AD-A187508] N88-20975

OPTICAL PROPERTIES
Tungsten-carbon multilayer system studied with X-ray scattering
[DE88-005749] N88-20373
Materials Research Laboratory at Brown University
[AD-A188006] N88-20396
Optical studies of dynamical processes in disordered system
[DE88-005965] N88-20993
Energy transfer and non-linear optical properties at near ultraviolet wavelengths: Rare earth 4f yields 5d transitions in crystals and glasses
[DE88-005403] N88-21012

OPTICAL PUMPING
High power, high efficiency, 2D laser diode arrays for pumping solid state lasers
[DE88-004042] N88-20632

OPTICAL RADAR
Coherent laser radar system theory
[AD-A188759] N88-20612

OPTICAL TRACKING
Pursuit tracking performance decrements associated with decreasing ambient illumination
[AD-A189336] N88-20809

OPTIMIZATION
Control augmented structural synthesis
[NASA-CR-4132] N88-20290
The design of aircraft using the decision support problem technique
[NASA-CR-4134] N88-20291
Optimization of binary pigment coatings
[AD-A189103] N88-20450
Optimal placement of tuning masses for vibration reduction in helicopter rotor blades
[NASA-TM-100562] N88-20665
Active cooling design for scramjet engines using optimization methods
[NASA-TM-100581] N88-20669
On the sensitivity of complex, internally coupled systems
[NASA-TM-100537] N88-20829
A new algorithm for general multiobjective optimization
[NASA-TM-100536] N88-20830
Conic algorithms for unconstrained minimization with special consideration of problems with large sparse Hessians: A summary of research performed
[DE88-002549] N88-20850
Algorithms with conic termination for nonlinear optimization
[DE88-005893] N88-20851
Constrained nonlinear programming
[DE88-005695] N88-20860
Deterministic uncertainty analysis
[DE88-006139] N88-20942
Optimal and conventional space-time processing in flow noise
[AD-A189104] N88-20965

ORBIT CALCULATION
Orbit correction strategy for an Earth observation satellite
[INPE-4287-PRE/1159] N88-20331
Orbit accuracy requirement of GPS for precise positioning and orbit determination within local area N88-20499

ORBIT PERTURBATION
Orbit correction strategy for an Earth observation satellite
[INPE-4287-PRE/1159] N88-20331

ORBIT TRANSFER VEHICLES
Orbital transfer vehicle concept definition and system analysis study. Volume 2: OTV concept definition and evaluation. Book 1: Mission and system requirements
[NASA-CR-179321] N88-20339
Turnaround operations analysis for OTV. Volume 1: Executive summary
[NASA-CR-179316] N88-20340
Turnaround operations analysis for OTV. Volume 2: Detailed technical report
[NASA-CR-179317] N88-20341
Turnaround operations analysis for OTV. Volume 3: Technology development plan
[NASA-CR-179318] N88-20342
Turnaround operations analysis for OTV. Volume 4: WBS and dictionary and cost methodology
[NASA-CR-179319] N88-20343

ORBITAL MANEUVERS
Orbit correction strategy for an Earth observation satellite
[INPE-4287-PRE/1159] N88-20331
Optimal thrust vector control of coplanar orbital evasive maneuvers
[AD-A189544] N88-20346

ORBITAL MECHANICS
Orbit correction strategy for an Earth observation satellite
[INPE-4287-PRE/1159] N88-20331
Study of the optimization of satellite system design for transfer orbit
[MBB-URV-135] N88-20332
Frozen orbit analysis in the Martian system
[AD-A189574] N88-21106

ORBITAL SERVICING
Turnaround operations analysis for OTV. Volume 1: Executive summary
[NASA-CR-179316] N88-20340
Turnaround operations analysis for OTV. Volume 3: Technology development plan
[NASA-CR-179318] N88-20342
Turnaround operations analysis for OTV. Volume 4: WBS and dictionary and cost methodology
[NASA-CR-179319] N88-20343

ORDER-DISORDER TRANSFORMATIONS
A calorimetric determination of the enthalpy of formation and a description of the defect structure of the ordered beta-phase /Ni, Cu/ /1-x/ Al/x/
[NASA-TT-20157] N88-20434
Optical studies of dynamical processes in disordered system
[DE88-005965] N88-20993

ORDNANCE
Texture profile in thermomechanically processed 2-inch-thick 5 Ni-steel armor plate
[AD-A189275] N88-20410

ORGANIC COMPOUNDS
Electrosorptive detection of simple organic compounds in liquid chromatography
[AD-A188757] N88-20376
Mechanisms of photoinduced electron transfer
[DE88-004917] N88-20983
The thermodynamic properties of organic oxygen compounds
[DE88-001208] N88-21065

ORGANIC PHOSPHORUS COMPOUNDS
Determination of the partition coefficients of organophosphorus compounds using high-performance liquid chromatography
[AD-A189276] N88-20385

ORTHOGONAL FUNCTIONS
Space-time analysis of oceanographic fields by modified empirical orthogonal functions method N88-20687
Group theoretic interpretations of Askey's scheme of hypergeometric orthogonal polynomials
[CWI-PM-R8703] N88-20954

ORTHOGONALITY
The parameterization of orthogonal matrices: A review mainly for statisticians
[AD-A189144] N88-20936

ORTHOSTATIC TOLERANCE
Changes in the status of the human tibia during antiorthostatic hypokinesia
[NASA-TT-20221] N88-20813

OSCILLATIONS
Predicting oscillatory finite difference solutions to the heat equation: A comparative study of the coefficient and matrix methods
[AD-A189591] N88-20911
Stochastic and chaotic oscillations
[CWI-AM-R8704] N88-20940
OSCILLATORS
Quartz oscillator analysis
[DE88-005886] N88-20550
Direct solar-pumped iodine laser amplifier
[NASA-CR-182674] N88-20630
OXIDATION
Thermal oxide growth on silicon: Intrinsic stress and silicon cleaning effects
[AD-A188790] N88-20377
Novel catalysts for methane activation
[DE88-003637] N88-20390
High-temperature thermosets derived from the Diels-Alder polymerization of bisbenzocyclobutenes and bimaleimides
[AD-A188800] N88-20449
Oxidation/sulfidation of materials in an SO3/SO2/O2 thermochemical-transport, distributed-receiver, solar-energy system
[DE88-005875] N88-20739
OXIDATION RESISTANCE
Nondestructive evaluation of carbon-carbon coatings
[AD-A189524] N88-20453
OXIDE FILMS
Thermal oxide growth on silicon: Intrinsic stress and silicon cleaning effects
[AD-A188790] N88-20377
OXIDES
Discussion of radiation effects and high-temperature oxide superconductors
[DE88-001427] N88-21046
OXIDIZERS
Thermal oxide growth on silicon: Intrinsic stress and silicon cleaning effects
[AD-A188790] N88-20377
OXYGEN ATOMS
Measurement of rate constants of elementary gas reactions of importance to upper atmosphere and combustion systems
[AD-A189432] N88-20386
OXYGEN CONSUMPTION
Increase in influence of oxygen on the body in the presence of helium N88-20816
OXYGEN METABOLISM
Increase in influence of oxygen on the body in the presence of helium N88-20816
OZONE
Ozone sonde and Dobson spectrometer data obtained during the MAP/GLOBUS 1983 campaign over Western Europe
[BPT-5/87] N88-20771
OZONE DEPLETION
The 1987 Airborne Antarctic Ozone Experiment: The Nimbus-7 TOMS data atlas
[NASA-RP-1201] N88-20714
OZONOMETRY
Ozone sonde and Dobson spectrometer data obtained during the MAP/GLOBUS 1983 campaign over Western Europe
[BPT-5/87] N88-20771

P

P-I-N JUNCTIONS
Research on high-efficiency, stacked, multijunction, amorphous silicon alloy thin-film solar cells
[DE88-001106] N88-20723
PACIFIC OCEAN
Tidal estimation in the Pacific with application to SEASAT altimetry
[NASA-TM-100694] N88-20780
Dynamics of the Oceanic Surface Mixed Layer
[AD-A188348] N88-20785
Equatorial turbulence: Mixed layer and thermocline N88-20787
The mixed layer of the western equatorial Pacific Ocean
[HIG-1861] N88-20789
Mixed-layer shear related to wind stress in the central equatorial Pacific N88-20793
Monitoring ocean surface layer processes N88-20801
PAIR PRODUCTION
Diffraction theory in QCD and beyond
[DE88-005958] N88-20992
PALEOCLIMATOLOGY
Model validation research: Comparison of simulated and observed climate patterns for the past 18,000 years
[DE88-004945] N88-20759
PANEL METHOD (FLUID DYNAMICS)
ARSPNSC: A method to calculate subsonic steady and unsteady potential flow about complex configurations
[NLR-TR-86122-U] N88-20265
PANORAMIC SCANNING
System for detecting objects that represent a threat
[NASA-TT-20244] N88-20528
PAPER (MATERIAL)
Observations on electrostatic effects in a filter test system
[AD-A188797] N88-20378
PARABOLIC ANTENNAS
Modification of parabolic dish antenna pattern using two symmetrically placed circular flat plates
[AD-A189543] N88-20517
PARABOLIC REFLECTORS
Modification of parabolic dish antenna pattern using two symmetrically placed circular flat plates
[AD-A189543] N88-20517
Point-focus concentrator reflector assembly, phase 1
[DE88-003616] N88-20720
PARALLEL PROCESSING (COMPUTERS)
Analysis for architecture for image processing
[INPE-4294-PRE/1165] N88-20715
The physical structure of concurrent problems and concurrent computers
[DE88-005812] N88-20835
Parallel image compression
[NASA-CR-180758] N88-20837
Implementation of a 3-D nonlinear MHD (magnetohydrodynamics) calculation on the Intel hypercube
[DE88-000625] N88-20848
Gaussian techniques on shared memory multiprocessor computers
[DE88-005426] N88-20855
Approximation algorithms for scheduling unrelated parallel machines
[CWI-OS-R8714] N88-20861
Computing with structured connections networks
[AD-A189244] N88-20886
A simulation study of a parallel processor with unbalanced loads
[AD-A189573] N88-20887
On the design of parallel numerical methods in message passing and shared memory environments
[DE88-003566] N88-20888
Perspectives on parallel computing
[CWI-OS-R8709] N88-20889
Locality, communication and interconnect length in multicomputers
[CWI-CS-R8708] N88-20890
PARALLEL PROGRAMMING
Design of the CONSUL programming language
[AD-A189202] N88-20841
An interface between object-oriented systems
[AD-A189245] N88-20844
Designing equivalent semantic models for process creation
[CWI-CS-R8732] N88-20872
PARAMETER IDENTIFICATION
Aircraft flight flutter testing at the NASA Ames-Dryden Flight Research Facility
[NASA-TM-100417] N88-20301
Material parameter measurements at high temperatures
[NASA-CR-182707] N88-20397
On error equations for determining Earth rotation parameters with VLBI network N88-20500
PARAMETERIZATION
Parametric study of acceleration-induced stresses and frequency changes in doubly-rotated crystal resonators
[AD-A189261] N88-20532
Generalized expression for radio navigation parameter error N88-20691
Algebraic specifications for parameterized data types: The case of minimal computable algebras and parameters with equality
[CWI-CS-R8714] N88-20916
Model structure selection for multivariable systems by cross-validation methods
[EUT-87-E-176] N88-20926
The parameterization of orthogonal matrices: A review mainly for statisticians
[AD-A189144] N88-20936
Non- and semi-parametric maximum likelihood estimators and the von Mises Method, part 1
[CWI-MS-R8709] N88-20941
PARSING ALGORITHMS
A parser generator for finitely ambiguous context-free grammars
[CWI-CS-R8712] N88-20864
PARTIAL DIFFERENTIAL EQUATIONS
The Euler-Bernoulli beam equation with boundary energy dissipation
[AD-A189517] N88-20560
Propagator solutions of partial differential equations applied to plasma transport
[DE88-006432] N88-20852
Spectral element methods: Algorithms and architectures
[NASA-CR-182701] N88-20878
Numerical solution of ill posed problems in partial differential equations
[AD-A189383] N88-20909
A Lagrangian moving grid scheme for one-dimensional evolutionary partial differential equations
[CWI-NM-R8713] N88-20922
Stabilization of explicit difference schemes by smoothing techniques
[CWI-NM-R8714] N88-20923
Nonlinear differential equations
[DE88-006047] N88-20933
PARTICLE ACCELERATORS
Development of electrostatic-accelerator free-electron lasers
[AD-A189507] N88-20614
Collective acceleration of electrons and ions in a high relativistic electron beam
[DE88-005261] N88-20998
PARTICLE COLLISIONS
Fragmentation and flow in central collisions
[DE88-005386] N88-20991
Hadronic overlap and total multiplicity distributions in high energy physics collisions
[NIKHEF-H/87-10] N88-21001
The astrophysics of nebulae and active galactic nuclear emission-line regions: New methods and applications N88-21111
PARTICLE DENSITY (CONCENTRATION)
Fluidization mechanisms in slurry flows
[DE88-005191] N88-20563
Velocity and concentration measurements in flowing suspensions by nuclear magnetic resonance
[DE88-006225] N88-20589
PARTICLE INTERACTIONS
Research in high energy elementary particle physics
[DE88-006065] N88-20994
PARTICLE MOTION
Theory of laser cooling and spectroscopy of harmonically trapped single atoms
[AD-A189576] N88-20617
Fragmentation and flow in central collisions
[DE88-005386] N88-20991
Comparison of analytic and full guiding center behavior at a trapped-passing interface in stellarators
[DE88-004174] N88-21025
PARTICLE PRECIPITATION
Formation of nuclei during precipitation in metallic mixed crystals
[NASA-TT-20248] N88-20437
Stimulated Emission of Energetic Particles (SEEP)
[AD-A188724] N88-21094
PARTICLE PRODUCTION
Physics at large transverse momenta
[DE88-005758] N88-20986
PARTICLE SIZE DISTRIBUTION
Vertical structure of Venusian cloud layer at landing sites of Vega-1 and Vega-2 vehicles N88-20317
Erosion in dual-phase microstructures
[DE88-004507] N88-20421
Characterization and fundamental studies on CuO sorbent materials to determine attrition mechanisms on substrate gamma alumina
[DE88-003674] N88-20456
Processing of nanophase ceramics
[DE88-005985] N88-20475
PARTICLE THEORY
Theory of laser cooling and spectroscopy of harmonically trapped single atoms
[AD-A189576] N88-20617
Particle physics and cosmology
[DE88-004944] N88-21096
PARTICLE TRAJECTORIES
Particle-dynamics calculations of gravity flow of inelastic, frictional spheres
[DE88-005224] N88-20586
PARTICLES
Global mixed-layer natural and anthropogenic fluxes N88-20803
Double layer polarization of nonconducting spheroidal particles and its application to Kerr effect
[ISSN-0208-05658] N88-20960
PARTICULATES
Interaction of particulate and transformation toughening
[AD-A189321] N88-20412
Cavitation inception
[AD-A189220] N88-20557

PASSIVITY
Corrosion, passivity and breakdown of alloys used in high energy density batteries
[DE88-004891] N88-20422
PATTERN RECOGNITION
A procedure for automatic classification of crop areas
[INPE-4467-PRE/1240] N88-20708
Measures of similarity between fuzzy concepts: A comparative analysis
[AD-A189430] N88-20910
PAYLOADS
Expected value analysis for an unmanned expendable launch vehicle payload escape system
[AD-A189494] N88-20337
Orbital transfer vehicle concept definition and system analysis study. Volume 2: OTV concept definition and evaluation. Book 1: Mission and system requirements
[NASA-CR-179321] N88-20339
PELLETS
Application of railgun principle to high-velocity hydrogen pellet injection for magnetic fusion reactor refueling
[DE88-005830] N88-20334
PENETRATION
Observations on electrostatic effects in a filter test system
[AD-A188797] N88-20378
A direct correlation of strength with impact velocity
[AD-A189251] N88-20409
PERFORMANCE PREDICTION
Robustifying the Kalman filter
[AD-A189240] N88-20907
PERFORMANCE TESTS
An investigation of classical dynamic scaling techniques applied to an oleo-pneumatic landing gear strut
[AD-A187664] N88-20292
Combustion theory and related questions
[AD-A189160] N88-20382
Materials Research Laboratory at Brown University
[AD-A188006] N88-20396
Optimization of binary pigment coatings
[AD-A189103] N88-20450
Improve the lifetime of the hollow fiber sodium sulfur cell
[DE88-004881] N88-20469
Aluminum-air battery development
[DE88-006618] N88-20543
Testing and development of electric vehicle batteries for EPRI Electric Transportation Program
[DE88-005894] N88-20551
The evaluation of automatic barometers, illustrated by the Nakaasa barometer
[KNMI-TR-95] N88-20610
Stable, high-efficiency, CuInSe2-based, polycrystalline, thin-film tandem solar cells
[DE88-001116] N88-20726
Cadmium sulfide/copper ternary heterojunction cell research
[DE88-001122] N88-20727
Pursuit tracking performance decrements associated with decreasing ambient illumination
[AD-A189336] N88-20809
Electron emission from conductors subjected to intense, short-pulse electric fields
[DE88-005412] N88-20985
Space infrared telescope facility wide field and diffraction limited array camera (IRAC)
[NASA-CR-182704] N88-21092
PERIOD DOUBLING
Period-doubling universality in multidimensional dissipative and conservative systems
[PB88-148812] N88-20961
PERMANENT MAGNETS
Modeling the behavior of oriented permanent magnet material using current double theory
[DE88-004446] N88-20963
ONR Far East Scientific Bulletin, volume 12, number 3, July-September 1987
[AD-A188554] N88-21081
PERMEABILITY
The effect of Ca(OH)2-treated ceramic microspheres on the mechanical properties of high-temperature lightweight cement composites
[DE88-004590] N88-20457
Molecular and electronic mechanism in the control of Na+ and K+ permeability of excitable cell membrane by ligand binding on receptor sites
[AD-A188725] N88-20805
PERSONNEL
A comparison of terrain association and resection as methods of position location
[AD-A189480] N88-20710
PERTURBATION THEORY
Horizontal scales of wind forced inertial motions N88-20795
Unfoldings of quasi-periodic tori
[ZW-8706] N88-20928
PHARMACOLOGY
Changes in the status of the human tibia during antiorthostatic hypokinesia
[NASA-TT-20221] N88-20813
PHASE COHERENCE
Reduced tolerance imaging 2, volume 2
[AD-A189604] N88-20939
PHASE DIAGRAMS
Transformation, metallurgical response and behavior of the weld fusion zone and heat affected zone in Cr-Mo steels for fossil energy application
[DE88-006037] N88-20430
PHASE ERROR
Reduced tolerance imaging 2, volume 2
[AD-A189604] N88-20939
PHASE LOCKED SYSTEMS
Resonator coupling of two ring cavity, argon-ion lasers
[AD-A189558] N88-20616
PHASE SHIFT
Optics for large telescope N88-21014
PHASE SHIFT CIRCUITS
Intergrated circuit design, phase 2
[AD-A189060] N88-20530
PHASE TRANSFORMATIONS
Interaction of particulate and transformation toughening
[AD-A189321] N88-20412
Transformation, metallurgical response and behavior of the weld fusion zone and heat affected zone in Cr-Mo steels for fossil energy application
[DE88-006037] N88-20430
Diffraction theory in QCD and beyond
[DE88-005958] N88-20992
Rapid e-beam heating for measuring thermodynamics of metastable materials
[DE88-003565] N88-21066
PHASE VELOCITY
Phase velocity and attenuation of plane elastic waves in a particle-reinforced composite medium
[AD-A189414] N88-20386
Two-phase flows in the wake of in-cylinder projectiles
[AD-A189422] N88-20559
PHASE-SPACE INTEGRAL
Introduction to classical mechanics of systems with constraints, part 3
[TI88-701057] N88-21073
PHASED ARRAYS
Optical RF distribution links for MMIC phased array antennas
[NASA-TM-100841] N88-20555
PHONONS
Studies of transverse phonon modes in premartensitic indium-thallium alloys
[DE88-003481] N88-20428
PHOSPHONIUM COMPOUNDS
Use of diphosphonates to correct disorders in calcium metabolism and mineral composition of bone tissue with 60-day hypokinesia in rats
[NASA-TT-20220] N88-20807
PHOSPHORS
Noncontact thermometry via laser pumped, thermographic phosphors: Characterization of systematic errors and industrial applications
[DE88-005599] N88-20628
PHOTOCHEMICAL REACTIONS
Photochemistry at structured surfaces: A classical electromagnetic approach
[AD-A189519] N88-20387
Mechanisms of photoinduced electron transfer
[DE88-004917] N88-20983
PHOTOCONDUCTIVITY
Pressure-dependent DLTS (Deep Level Transient Spectroscopy) experiments on Si-doped AlGaAs
[DE88-003842] N88-21047
PHOTOGRAMMETRY
Dynamics of high-speed mechanisms with elastic members N88-20643
PHOTOGRAPHIC DEVELOPERS
The calibration of photographic and spectroscopic films: Reciprocity failure and thermal responses of IIaO film at liquid nitrogen temperatures
[NASA-CR-181094] N88-20606
PHOTOGRAPHIC FILM
The calibration of photographic and spectroscopic films: Reciprocity failure and thermal responses of IIaO film at liquid nitrogen temperatures
[NASA-CR-181094] N88-20606
The calibration of photographic and spectroscopic films: The response of 2aO film to small dosages of alpha particles from 3/10th's rad to 8 rads at energy levels 153 MeV, 79 MeV and 47 MeV
[NASA-CR-177830] N88-20608
PHOTOGRAPHIC PROCESSING
Digital enhancement of flow field images
[NASA-TP-2770] N88-20833
PHOTOIONIZATION
The astrophysics of nebulae and active galactic nuclear emission-line regions: New methods and applications N88-21111
PHOTOLUMINESCENCE
Optical study of germanium, germanium plus arsenic, and germanium plus gallium implants in gallium arsenide
[AD-A189600] N88-21045
PHOTOLYSIS
Photolytic formation of free radicals and their effect on hydrocarbon pyrolysis chemistry in a concentrated solar environment
[DE88-004129] N88-20730
Excimer laser photolysis studies of T-V (Translation-to-Vibration) energy transfer
[AD-A189613] N88-20989
Photon-controlled growth of multilayered structures
[DE88-005061] N88-21054
PHOTON BEAMS
Synchronous measurements of effective photon path length in visible and near-IR spectral regions in real cloud systems N88-20706
PHOTONS
Proof of the feasibility of coherent and incoherent schemes for pumping a gamma-ray laser
[AD-A189238] N88-20613
The use of four-photon Raman spectroscopy for the remote sensing of natural objects
[NASA-TT-20257] N88-20716
The magnitude of secondary electron contributions in photon stimulated desorption
[AD-A189094] N88-20980
Diffraction theory in QCD and beyond
[DE88-005958] N88-20992
PHOTOVOLTAIC CELLS
SERI's Photovoltaic R and D Project: Recent progress and future directions
[DE88-001129] N88-20728
Control strategies and hardware used in solar thermal applications
[DE88-004631] N88-20731
Progress of amorphous silicon based solar cells and modules
[DE88-004666] N88-20733
Crystalline photovoltaic cell technology: Present and future
[DE88-004684] N88-20734
PHOTOVOLTAIC CONVERSION
SERI's Photovoltaic R and D Project: Recent progress and future directions
[DE88-001129] N88-20728
Progress of amorphous silicon based solar cells and modules
[DE88-004666] N88-20733
PHYSICAL FITNESS
Lifting and carrying capacities relative to physical fitness measures
[AD-A189305] N88-20808
PHYSICAL OPTICS
Coherence effects in optical physics with special reference to spectroscopy
[AD-A189520] N88-21007
PHYSICAL WORK
Lifting and carrying capacities relative to physical fitness measures
[AD-A189305] N88-20808
PHYSICS
JPRS report: Science and technology. China
[JPRS-CST-88-003] N88-20495
PHYSIOLOGICAL RESPONSES
Plasma cortisol, renin and aldosterone during an intense heat acclimation program
[AD-A189387] N88-20810
PHYTOPLANKTON
Research on influence of individual sea water components on spectral brightness coefficient of outgoing radiation N88-20682
PIGMENTS
Optimization of binary pigment coatings
[AD-A189103] N88-20450
PILOT PERFORMANCE
Flight simulator experiments concerning take-off visibility minima
[NLR-TR-86050-U] N88-20281
PILOT PLANTS
Aviation turbine fuels from tar sands bitumen and heavy oils. Part 3: Laboratory sample production
[AD-A189278] N88-20484
PIONEER VENUS SPACECRAFT
Vertical structure of Venusian cloud layer at landing sites of Vega-1 and Vega-2 vehicles N88-20317
PIPES (TUBES)
Reduction of erosion in elbows due to flow modifications, phase 1
[DE88-001028] N88-20584

PISTON ENGINES
Comparison between computed and measured swirl and turbulence in reciprocating engines
[PDR/IC-CFDU/32] N88-20647
PLANAR STRUCTURES
Nonaxisymmetric body supersonic, aerodynamic prediction
[AD-A189338] N88-20259
On effectively labeling planar projections of polyhedra
[CWI-CS-R8715] N88-20917
PLANE WAVES
Phase velocity and attenuation of plane elastic waves in a particle-reinforced composite medium
[AD-A189414] N88-20366
Detection and angle estimation of coherent plane waves N88-20522
PLANETARY ATMOSPHERES
Negative viscosity in global circulations N88-20685
PLANETARY ENVIRONMENTS
Model of Jovian F region ionosphere
[NASA-CR-182587] N88-21105
PLANETARY IONOSPHERES
Model of Jovian F region ionosphere
[NASA-CR-182587] N88-21105
PLANETARY WAVES
Seasonal variations and excitation mechanisms of the equatorially trapped waves N88-20751
PLASMA CONTROL
SOAR: Space orbiting advanced fusion power reactor
[AD-A189234] N88-20356
Reversed field pinch operation with a thin shell
[DE88-005521] N88-21027
PLASMA COOLING
Modeling and transport in semiconductor devices
[AD-A188760] N88-21037
PLASMA EQUILIBRIUM
Fully implicit three-dimensional MHD (magnetohydrodynamics) stability and evolution in toroidal geometry
[DE88-000624] N88-21023
PLASMA HEATING
Experimental studies of plasma heating due to the parametric decay of a large amplitude pump into lower hybrid waves N88-21017
PLASMA INTERACTIONS
Hydrogen pumping and release by graphite under high flux plasma bombardment
[DE88-005880] N88-21021
Reversed field pinch operation with a thin shell
[DE88-005521] N88-21027
Modeling and transport in semiconductor devices
[AD-A188760] N88-21037
PLASMA JETS
On the structure of pulsed plasma jets N88-21030
Relativistic jet models for the BL Lacertae object Mrk 421 during three epochs of observation
[NASA-TM-89727] N88-21090
PLASMA SPECTRA
Experimental study of the role of plasma polarization on line shape in dense laboratory plasmas
[ETN-88-92001] N88-21033
Stimulated Emission of Energetic Particles (SEEP)
[AD-A188724] N88-21094
PLASMA TEMPERATURE
Temperature estimates for a free flowing railgun plasma
[MRL-R-1054] N88-21032
PLASMA-PARTICLE INTERACTIONS
Analytically modeling the carbothermic reduction of alumina in a thermal plasma
[DE88-005535] N88-21020
PLASMAS (PHYSICS)
Propagator solutions of partial differential equations applied to plasma transport
[DE88-006432] N88-20852
PLASTIC DEFORMATION
Stress corrosion cracking and metal-induced embrittlement: Comparative studies of local chemistries
[DE88-003235] N88-20419
PLASTIC PROPERTIES
Materials Research Laboratory at Brown University
[AD-A188006] N88-20396
PLASTICS
Flame retardants
[NASA-TT-20250] N88-20400
Kinetics of polymer decomposition
[DE88-005500] N88-20460
PLATES
Transient dynamics of fibre reinforced composite plates
[IIT-B/CE/RR/87-1] N88-20370
An experimental investigation of decelerating flow about two-dimensional cambered plates
[DE88-006598] N88-20567
Finite element methodology for nonlinear free and harmonic forced vibrations of beam and plate structures N88-20663
PLATES (TECTONICS)
Relationship between oceanic geological formations and tectonic structures N88-20683
PLATING
Hydrogen embrittlement of gun steel
[AD-A188972] N88-20407
PLUMES
Kinetic mechanisms for ionization and afterburning suppression
[AD-A189219] N88-20383
PLY ORIENTATION
Ply-level failure analysis of a graphite/epoxy laminate under bearing-bypass loading
[NASA-TM-100578] N88-20372
A preliminary investigation of finite-element modeling for composite rotor blades
[NASA-TM-100559] N88-20656
PNEUMATIC EQUIPMENT
Reduction of erosion in elbows due to flow modifications, phase 1
[DE88-001026] N88-20584
PNEUMATIC PROBES
Formulation of a general technique for predicting pneumatic attenuation errors in airborne pressure sensing devices
[NASA-TM-100430] N88-20302
POINT DEFECTS
Study of activationless reactions of point defects with impurities and impurity-defect complexes in alpha-iron
[TI88-701028] N88-20433
POISSON DENSITY FUNCTIONS
Tests for uniformity arising from a series of events
[AD-A189069] N88-20935
Bias reduction when there is no unbiased estimate
[AD-A189407] N88-20937
POISSON EQUATION
Propagator solutions of partial differential equations applied to plasma transport
[DE88-006432] N88-20852
POLAR ORBITS
Frozen orbit analysis in the Martian system
[AD-A189574] N88-21106
POLAR REGIONS
The 1987 Airborne Antarctic Ozone Experiment: The Nimbus-7 TOMS data atlas
[NASA-RP-1201] N88-20714
POLARIMETERS
A polarimetric rain backscatter model developed for coherent polarization diversity radar applications N88-20520
POLARIMETRY
Signal-filter design and system performance for polarimetric radar
[AD-A189257] N88-20514
POLARIZATION (CHARGE SEPARATION)
Spontaneous decay and atomic fluorescence near a metal surface of an absorbing dielectric
[AD-A187508] N88-20975
POLARIZATION (WAVES)
A polarization diversity meteorological radar system
[AD-A189291] N88-20515
POLARIZED ELECTROMAGNETIC RADIATION
Polarization of electrons in an electromagnetic wave field in the presence of magnetic field
[DE88-700169] N88-20509
Mode priming in an overmoded gyrotron oscillator
[AD-A189151] N88-20602
POLARIZED LIGHT
Multiple scattering of polarized light in cirrus clouds N88-20768
POLOIDAL FLUX
Evolution of poloidal variation of impurity density and ambipolar potential in rotating tokamak plasma, part 1
[DE88-006263] N88-21022
POLYCARBONATES
Reinforcing of thermoplastic polycarbonate and polysulfone with carbon fibers: Production and characteristics of UD-compound objects
[NASA-TT-20158] N88-20374
POLYCRYSTALS
Recommendations on developing polycrystalline alumina fiber N88-20502
Photon-controlled growth of multilayered structures
[DE88-005061] N88-21054
POLYHEDRONS
On effectively labeling planar projections of polyhedra
[CWI-CS-R8715] N88-20917
POLYMER CHEMISTRY
Contrasting conductance/viscosity relations in liquid states of vitreous and polymer solid electrolytes
[AD-A189378] N88-20452
Examination of polysulfide sealants by scanning electron microscopy
[MRL-R-1096] N88-20478
Aging properties of cable polmers (2)
[NASA-TT-20228] N88-20479
POLYMER PHYSICS
Integral equation theory of homopolymer melts
[DE88-005304] N88-20470
Integral equation theory of polymer blends
[DE88-005305] N88-20471
POLYMERIC FILMS
Molecular dynamics of laser ablation of a polymer coating
[DE88-004337] N88-20466
Safety research of insulating materials of cable for nuclear power generating station
[NASA-TT-20202] N88-20477
Measuring thin film properties using SAW (Surface Acoustic Wave) devices: Diffusivity and surface area
[DE88-002216] N88-20970
POLYMERIZATION
Reinforcing of thermoplastic polycarbonate and polysulfone with carbon fibers: Production and characteristics of UD-compound objects
[NASA-TT-20158] N88-20374
High-temperature thermosets derived from the Diels-Alder polymerization of bisbenzocyclobutenes and bimaleimides
[AD-A188800] N88-20449
POLYNOMIALS
Elimination of quantifiers of linear variables and corresponding transfer principles
[DE88-005692] N88-20912
Group theoretic interpretations of Askey's scheme of hypergeometric orthogonal polynomials
[CWI-PM-R8703] N88-20954
POLYSTATION DOPPLER TRACKING SYSTEM
A preliminary assessment of thunderstorm outflow wind measurement with airport surveillance radars
[AD-A189064] N88-20757
POLYSTYRENE
A new polymer-based hydrogen getter
[DE88-004538] N88-20467
POLYSULFIDES
Examination of polysulfide sealants by scanning electron microscopy
[MRL-R-1096] N88-20478
POLYURETHANE RESINS
Optimization of binary pigment coatings
[AD-A189103] N88-20450
POLYVINYL CHLORIDE
Evaluation of flammability for cable-like polymers
[NASA-TT-20225] N88-20476
POPULATIONS
Galaxy evolution in dense clusters N88-21101
POROUS MATERIALS
Development, manufacturing and testing of a gas-loaded variable conductance methanol heat pipe
[NLR-MP-87010-U] N88-20571
PORPHYRINS
Novel catalysts for methane activation
[DE88-003637] N88-20390
PORTABLE EQUIPMENT
A hybrid transform/DPCM encoder for data compression
[DE87-014852] N88-20518
Ultrasonic inspection of irregular surfaces
[AERE-R-12465] N88-20648
POSITION (LOCATION)
The evaluation and selection of a 5th ground antenna site for the global positioning system
[AD-A189495] N88-20286
A comparison of terrain association and resection as methods of position location
[AD-A189480] N88-20710
POSITION ERRORS
A method and measures to evaluate trackers for air traffic control
[NLR-TR-86072-U] N88-20267
A comparison of terrain association and resection as methods of position location
[AD-A189480] N88-20710
POSITION INDICATORS
Procedure for detection and identification of a helicopter
[NASA-TT-20234] N88-20297
Development of an interactive real-time graphics system for the display of vehicle space positioning
[NASA-TM-100429] N88-20344
POSITION SENSING
Procedure for detection and identification of a helicopter
[NASA-TT-20234] N88-20297
POSITIONING
Method for determining artillery position
[NASA-TT-20237] N88-20974

POSITRON ANNIHILATION
Study of defects in metals by positron annihilation
[DE88-701042] N88-20432
POTASSIUM COMPOUNDS
Potassium cuprate (3)
[NASA-TT-20246] N88-20401
POTENTIAL ENERGY
Quantum Monte Carlo study of the MIES associated with H2 (X 1 sigma sub g (+)) and H2 (B 1 sigma sub u (+))
[AD-A189063] N88-20977
POTENTIAL FLOW
ARSPNSC: A method to calculate subsonic steady and unsteady potential flow about complex configurations
[NLR-TR-86122-U] N88-20265
POTENTIAL THEORY
Application of a nonisentropic full potential method to AGARD standard airfoils
[NASA-TM-100560] N88-20263
Numerical solution of ill posed problems in partial differential equations
[AD-A189383] N88-20909
POWDER (PARTICLES)
Creep behavior of consolidated rapidly solidified Type 304 stainless steel powder containing helium
[DE88-005536] N88-20424
A new process for synthesis of silicon nitride powders for advanced ceramics
[AD-A189354] N88-20451
Processing of nanophase ceramics
[DE88-005985] N88-20475
Scale-up of a batch-type chemical powder preparation process for high field varistor fabrication
[DE88-006601] N88-20541
A hydroxycarbonate route to superconductor precursor powders
[DE88-003638] N88-21052
POWDER METALLURGY
Activities report of the Materials Department
[ETN-88-91984] N88-20436
A case study of the development of a military specification - zirconium powder for thermal batteries
[AD-A188751] N88-20717
POWER LINES
Safety research of insulating materials of cable for nuclear power generating station
[NASA-TT-20202] N88-20477
POWER SPECTRA
How to generate equal probability design load conditions — aircraft design
[NLR-TR-86060-U] N88-20295
European approaches in standard spectrum development — aircraft load spectra
[NLR-MP-87007-U] N88-20661
Power spectral density analysis of wind-shear turbulence for related flight simulations
[NASA-CR-182721] N88-20773
PRECIPITATION (CHEMISTRY)
Temperature dependence of Kr precipitation in Ni
[DE88-005953] N88-20429
A hydroxycarbonate route to superconductor precursor powders
[DE88-003638] N88-21052
PRECIPITATION (METEOROLOGY)
The mixed layer of the western equatorial Pacific Ocean
[HIG-1861] N88-20789
PREDICTION ANALYSIS TECHNIQUES
A study of combustion and flow behaviour in solid-propellant rocket motors
[UTIAS-280] N88-20357
Ply-level failure analysis of a graphite/epoxy laminate under bearing-bypass loading
[NASA-TM-100578] N88-20372
Detection and angle estimation of coherent plane waves N88-20522
Pseudo-stationary oblique-shock-wave reflections in low gamma gases: Isobutane and sulphur hexafluoride
[UTIAS-TN-267] N88-20576
Predictions and studies with a one-dimensional ice/ocean model
[AD-A189158] N88-20776
Aberrations: Their effect on off-axis beam steering
[AD-A189601] N88-21008
PREDICTIONS
Formulation of a general technique for predicting pneumatic attenuation errors in airborne pressure sensing devices
[NASA-TM-100430] N88-20302
Predictive monitoring research: Summary of the PREMON system
[NASA-CR-182687] N88-20905
MOSFET performance degradation due to hot carriers N88-21063
PRESSURE
A simplified computer code for reduction to burning rates of closed bomb pressure-time data (MINICB)
[AD-A189112] N88-20380
Lattice relaxation of the DX centers in Ga/sub 1-x/Al/sub x/As and of the pressure-induced deep donors in GaAs
[DE88-005452] N88-21061
PRESSURE DEPENDENCE
Pressure-dependent DLTS (Deep Level Transient Spectroscopy) experiments on Si-doped AlGaAs
[DE88-003842] N88-21047
PRESSURE DISTRIBUTION
Nonaxisymmetric body supersonic, aerodynamic prediction
[AD-A189336] N88-20259
PRESSURE DRAG
The pressure drag and momentum flux during a cold frontal passage over the Alps N88-20763
PRESSURE GRADIENTS
Numerical model of the time independent mean flow in a rotating rocket motor N88-20360
PRESSURE MEASUREMENT
Verification of the momemtum theory for rotors using measurements on a model helicopter
[R-840-S] N88-20275
Formulation of a general technique for predicting pneumatic attenuation errors in airborne pressure sensing devices
[NASA-TM-100430] N88-20302
Exhaust-gas pressure and temperature survey of F404-GE-400 turbofan engine
[NASA-TM-88273] N88-20307
Remote fiber fluorimetry techniques for pressure measurements
[DE88-004486] N88-20604
PRESSURE RATIO
Improvement of the Reynolds-stress model by a new pressure-strain correlation
[NASA-CR-182699] N88-20667
PRESSURE SENSORS
Formulation of a general technique for predicting pneumatic attenuation errors in airborne pressure sensing devices
[NASA-TM-100430] N88-20302
High Reynolds number pump facility for cavitation research
[AD-A189310] N88-20558
PRESSURE VESSELS
Fracture mechanics and creep crack growth of 1 percent Cr 1/2 percent Mo steel with and without prior exposure to creep conditions
[NLR-TR-86051-U] N88-20426
PRESSURIZING
Pressurizing systems and air conditioning systems
[MBB/LKE-312/S/PUB/246] N88-20828
PRESTRESSING
Buckling and breakdown problems in structural mechanics. Failure of prestressed double-walled containers or rings
[MBB-UR-E-956/87] N88-20671
PROBABILITY DENSITY FUNCTIONS
Bragg-cell receiver study
[NASA-CR-182684] N88-20535
PROBABILITY DISTRIBUTION FUNCTIONS
Bragg-cell receiver study
[NASA-CR-182684] N88-20535
Hadronic overlap and total multiplicity distributions in high energy physics collisions
[NIKHEF-H/87-10] N88-21001
PROBABILITY THEORY
Characteristics of the positive lighting flash
[DE88-005854] N88-20760
PROBLEM SOLVING
Finite element methods for quasi-prismatic bodies with application to gears N88-20644
A personalized and prescriptive decision aid for choice from a database of options
[AD-A188726] N88-20820
An implementation of the OPS5 language for computers compatible with IBM-PC
[INPE-4291-PRE/1162] N88-20882
New way to solve Volterra equations of the second kind
[PB88-148820] N88-20931
PROCESS CONTROL (INDUSTRY)
Recommended replacements for tetryl in Australian production fuzes and related ordnance
[MRL-R-1089] N88-20489
EDF's studies and first choices regarding the design of electrical equipment
[NASA-TT-20222] N88-20553
PRODUCT DEVELOPMENT
Pressurizing systems and air conditioning systems
[MBB/LKE-312/S/PUB/246] N88-20828
PROGRAM VERIFICATION (COMPUTERS)
Dynamic run-time graphics
[DE87-008997] N88-20879
PROGRAMMING LANGUAGES
Design of the CONSUL programming language
[AD-A189202] N88-20841
An interface between object-oriented systems
[AD-A189245] N88-20844
Algebra of Communicating Processes (ACP)tau: A universal axiom system for process specification
[CWI-CS-R8725] N88-20869
Designing equivalent semantic models for process creation
[CWI-CS-R8732] N88-20872
Two normal form theorems for Communicating Sequential Processes (CSP) program
[CWI-CS-R8735] N88-20874
Predicate-transformer semantics of general recursion
[CS-8709] N88-20876
An implementation of the OPS5 language for computers compatible with IBM-PC
[INPE-4291-PRE/1162] N88-20882
A proof rule process creation
[CWI-CS-R8710] N88-20891
Type-checking Mini-ML: An algebraic specification with user-defined syntax
[CWI-CS-R8737] N88-20921
PROGRAMS
Alternative fuels: Information on DOE's (Department of Energy's) methanol vehicle demonstration program
[PB88-118203] N88-20481
PROJECT MANAGEMENT
Application of expert systems in project management decision aiding
[NASA-CR-180762] N88-21074
PROJECTILES
What is the maximum length of a spin stabilized projectile
[PB88-130919] N88-20336
Simulated impact damage in a thick graphite/epoxy laminate using spherical indenters
[NASA-TM-100539] N88-20383
Two-phase flows in the wake of in-cylinder projectiles
[AD-A189422] N88-20559
PROJECTIVE GEOMETRY
On effectively labeling planar projections of polyhedra
[CWI-CS-R8715] N88-20917
PROP-FAN TECHNOLOGY
Large-Scale Advanced Prop-Fan (LAP)
[NASA-CR-182112] N88-20306
PROPAGATION VELOCITY
Coherent structure-reflective turbulent viscous flow modeling
[AD-A188339] N88-20556
Detonation velocity of the hydrazinum nitrate-hydrazine water system
[NASA-TT-20213] N88-20590
PROPELLANT COMBUSTION
Bipropellant combustion in a liquid rocket combustion chamber N88-20359
PROPELLER BLADES
Numerical simulation of subsonic and transonic propeller flow
[NASA-TM-100163] N88-20262
Calculation of the distributed loads on the blades of individual multiblade propellers in axial flow using linear and nonlinear lifting surface theories
[NASA-TT-20173] N88-20278
Large-Scale Advanced Prop-Fan (LAP)
[NASA-CR-182112] N88-20306
PROPELLER SLIPSTREAMS
Numerical simulation of subsonic and transonic propeller flow
[NASA-TM-100163] N88-20262
PROPELLERS
Cavitation inception
[AD-A189220] N88-20557
PROTECTIVE COATINGS
Nondestructive evaluation of carbon-carbon coatings
[AD-A189524] N88-20453
Abrasion and impact resistant coatings
[DE88-003562] N88-20464
Safety research of insulating materials of cable for nuclear power generating station
[NASA-TT-20202] N88-20477
Aging properties of cable polmers (2)
[NASA-TT-20228] N88-20479
Measurement of the properties of lossy materials inside a finite conducting cylinder
[NASA-CR-182664] N88-20962
PROTOTYPES
The use of an automated flight test management system in the development of a rapid-prototyping flight research facility
[NASA-TM-100435] N88-20896

PROVING
A correlation study of X-29A aircraft and associated analytical development
[NASA-TM-89735] N88-20296
Experimental verification of a finite-difference time-domain thin slot algorithm
[DE88-005572] N88-20859
PULSARS
Topics in curved and flat space electromagnetism N88-21100
PULSE AMPLITUDE MODULATION
Bragg-cell receiver study
[NASA-CR-182684] N88-20535
PULSE GENERATORS
Optimum transformer design for a pulsed power system
[DE88-006054] N88-20525
PULSE MODULATION
Modulatable thin film field emission space gun
[AD-A189279] N88-21043
PULSED LASERS
Modeling and transport in semiconductor devices
[AD-A188760] N88-21037
PULSED RADIATION
Practical constraints on sources for pulsed beam lithographies
[DE88-006594] N88-20623
PURSUIT TRACKING
Pursuit tracking performance decrements associated with decreasing ambient illumination
[AD-A189336] N88-20809
PYROLYSIS
Photolytic formation of free radicals and their effect on hydrocarbon pyrolysis chemistry in a concentrated solar environment
[DE88-004129] N88-20730
PYROTECHNICS
A pyrotechnic delay ignition system for a submarine launched marine signal
[MRL-R-1079] N88-20487
A defect investigation of Thunderflash MK N5 (Navy)
[MRL-TN-522] N88-20488

Q

QUADRUPOLES
Modeling the behavior of oriented permanent magnet material using current double theory
[DE88-004446] N88-20963
QUALITATIVE ANALYSIS
Predictive monitoring research: Summary of the PREMON system
[NASA-CR-182687] N88-20905
QUALITY CONTROL
Quality enhancement with machine intelligence
[DE88-005639] N88-20901
QUANTITATIVE ANALYSIS
Quantitative determination of a hydrogen impurity in a sodium coolant by hydride thermal dissociation
[NASA-TT-20239] N88-20402
QUANTUM CHROMODYNAMICS
Diffraction theory in QCD and beyond
[DE88-005958] N88-20992
QUANTUM EFFICIENCY
Low threshold ridge waveguide single quantum well lasers N88-20631
QUANTUM ELECTRONICS
Joint services electronics program
[AD-A189262] N88-20533
QUANTUM MECHANICS
Gordon Conference on Intermetallic Compounds held at Tilton, New Hampshire on 20-24 July 1987
[AD-A188502] N88-20435
QUANTUM THEORY
Spontaneous decay and atomic fluorescence near a metal surface of an absorbing dielectric
[AD-A187508] N88-20975
Quantum Monte Carlo study of the MIES associated with H2 (X 1 sigma sub g (+)) and H2 (B 1 sigma sub u (+))
[AD-A189063] N88-20977
QUANTUM WELLS
Low threshold ridge waveguide single quantum well lasers N88-20631
Energy loss rates for light holes in InGaAs/GaAs strained layer single quantum wells
[DE88-005744] N88-21062
QUARKS
Proton/antiproton yields W(+/-)boson gamma X as a test of the quark charges
[NIKHEF-H/87-11] N88-20987
QUARTZ
Quartz oscillator analysis
[DE88-005886] N88-20550
QUATERNARY ALLOYS
Cadmium sulfide/copper ternary heterojunction cell research
[DE88-001122] N88-20727
QUERY LANGUAGES
Reference model for DBMS (database management system) user facility
[PB88-169446] N88-21080
QUEUEING THEORY
Sojourn times in feedback queues
[CWI-OS-R8710] N88-20947
Two queues with alternating service and switching times
[CWI-OS-R8712] N88-20949

R

RADAR
Simulation of effect of anti-radar stealth principle N88-20496
Signal-filter design and system performance for polarimetric radar
[AD-A189257] N88-20514
RADAR DETECTION
Aircraft accident report: Midair collision of Cessna-340A, N8716K, and North American SNJ-4N, N711SQ, Orlando, Florida, May 1, 1987
[PB88-910402] N88-20282
Influence of hydrometeorological factors on visibility of objects detected by radar N88-20707
RADAR EQUIPMENT
A preliminary assessment of thunderstorm outflow wind measurement with airport surveillance radars
[AD-A189064] N88-20757
RADAR IMAGERY
A polarimetric rain backscatter model developed for coherent polarization diversity radar applications N88-20520
RADAR MEASUREMENT
Applications of the differential reflectivity radar technique: Focus on estimation of rainfall parameters and microwave attenuation prediction N88-20521
A preliminary assessment of thunderstorm outflow wind measurement with airport surveillance radars
[AD-A189064] N88-20757
Inversion algorithms for geophysical problems
[AD-A189252] N88-20845
RADAR SCATTERING
The radar scattering coefficient as a function of forest stand parameters and viewing angle. An empirical study of the Pinus sylvestris L. in the Kootwijk forest (The Netherlands), extended with observations in the Speulder and Sprielder forest (The Netherlands)
[ETN-88-91348] N88-20527
RADAR SIGNATURES
A polarimetric rain backscatter model developed for coherent polarization diversity radar applications N88-20520
RADAR TRACKING
Aircraft accident report: Midair collision of Cessna-340A, N8716K, and North American SNJ-4N, N711SQ, Orlando, Florida, May 1, 1987
[PB88-910402] N88-20282
A method and measures to evaluate trackers for air traffic control
[NLR-TR-86072-U] N88-20287
RADIAL VELOCITY
A preliminary assessment of thunderstorm outflow wind measurement with airport surveillance radars
[AD-A189064] N88-20757
RADIATION ABSORPTION
Research on absorption of UV radiation in Venusian atmosphere from Vega-1 and Vega-2 landing modules N88-20316
Spontaneous decay and atomic fluorescence near a metal surface of an absorbing dielectric
[AD-A187508] N88-20975
RADIATION BELTS
Stimulated Emission of Energetic Particles (SEEP)
[AD-A188724] N88-21094
RADIATION DAMAGE
Study of defects in metals by positron annihilation
[DE88-701042] N88-20432
RADIATION DOSAGE
The calibration of photographic and spectroscopic films: The response of 2aO film to small dosages of alpha particles from 3/10th's rad to 8 rads at energy levels 153 MeV, 79 MeV and 47 MeV
[NASA-CR-177830] N88-20608
RADIATION EFFECTS
Effects of high temperature neutron irradiation on the physical, chemical and mechanical properties of fine-grained isotropic graphite N88-20444
Degradations of thermal shock resistance and the fracture toughness of reactor graphite subjected to neutron irradiation N88-20445
Computer simulation of tropospheric chemistry
[JUEL-2144] N88-20756
Discussion of radiation effects and high-temperature oxide superconductors
[DE88-001427] N88-21046
RADIATION MEASUREMENT
Global solar oscillations observed in the visible to near infrared continuum N88-21110
A low-frequency measurement of the spectrum of the cosmic microwave background radiation N88-21112
RADIATION PRESSURE
Acoustic radiation from line- and point-loaded plates: Uniformly asymptotic solutions
[AD-A189367] N88-20969
RADIATION PROTECTION
Vega-1 and Vega-2 automatic stations: Functioning of flyby vehicles during encounter with Halley's comet N88-20314
RADIATION SHIELDING
SOAR: Space orbiting advanced fusion power reactor
[AD-A189234] N88-20356
RADIATIVE TRANSFER
Multiple scattering of polarized light in cirrus clouds N88-20768
RADIO ASTRONOMY
The Deep Space Network
[NASA-CR-182700] N88-20524
RADIO FREQUENCIES
The preparation, assembly and mounting of RF coaxial cables
[ESA-PSS-01-718-ISS-1] N88-20504
Optical RF distribution links for MMIC phased array antennas
[NASA-TM-100841] N88-20555
Progress in diagnostic techniques for SC cavities
[CEBAF-PR-88-003] N88-20600
RADIO NAVIGATION
Generalized expression for radio navigation parameter error N88-20691
RADIO WAVES
Generalized expression for radio navigation parameter error N88-20691
Trajectory synthesis of ionograms in presence of artificial ionospheric inhomogeneities N88-20703
RADIOACTIVE DECAY
Spontaneous decay and atomic fluorescence near a metal surface of an absorbing dielectric
[AD-A187508] N88-20975
RADIOACTIVE ISOTOPES
Content of natural radioactive elements in Venusian rocks determined using data from Vega-1 and Vega-2 stations N88-20323
RADIOMETERS
Roentgenoradiometric analysis of aerosol in Venusian clouds by Vega-1 and Vega-2 automatic interplanetary stations N88-20319
Coherence effects in optical physics with special reference to spectroscopy
[AD-A189520] N88-21007
Activities report of the Toulouse Research Center
[ETN-88-91988] N88-21077
RADIOMETRIC RESOLUTION
Restoration techniques for redisplay of LANDSAT-5 satellite imagery
[INPE-4189-PRE/1076] N88-20712
RADIOSONDES
Roys and radiosondes in the region
[INPE-4362-PRE/1188] N88-20743
RAILGUN ACCELERATORS
Structural integrity of metallic armature rail guns
[AD-A188735] N88-20333
Application of railgun principle to high-velocity hydrogen pellet injection for magnetic fusion reactor refueling
[DE88-005830] N88-20334
Temperature estimates for a free flowing railgun plasma
[MRL-R-1054] N88-21032
RAILS
Structural integrity of metallic armature rail guns
[AD-A188735] N88-20333
RAIN
A polarimetric rain backscatter model developed for coherent polarization diversity radar applications N88-20520
Applications of the differential reflectivity radar technique: Focus on estimation of rainfall parameters and microwave attenuation prediction N88-20521
RAMAN LASERS
Phase preservation cleanup in a double-pass Raman amplifier SBS (Stimulated Brillouin Scattering) conjugator
[AD-A189428] N88-20536

RAMAN SPECTRA
Phase preservation cleanup in a double-pass Raman amplifier SBS (Stimulated Brillouin Scattering) conjugator
[AD-A189428] N88-20536
RAMAN SPECTROSCOPY
Measurement of detonation temperature of hydrogen-oxygen mixture by CARS (Coherent Anti-Stokes Raman Spectroscopy)
[NASA-TT-20227] N88-20398
Characterization of redox states of nickel hydroxide film electrodes by in-situ Raman spectroscopy
[AD-A189288] N88-20411
The use of four-photon Raman spectroscopy for the remote sensing of natural objects
[NASA-TT-20257] N88-20716
RANDOM NOISE
Optimal and conventional space-time processing in flow noise
[AD-A189104] N88-20965
RANDOM NUMBERS
A study of data compactation using numerical methods
[INPE-4317-TDL/284] N88-20929
RANDOM VARIABLES
On the expectation of the product of four matrix-valued Gaussian random variables
[EUT-87-E-178] N88-20927
RANGE (EXTREMES)
Physics of condensed matter at extreme conditions
[DE88-006232] N88-20958
RARE EARTH COMPOUNDS
Large momentum pairing in one-dimensional systems
[AD-A189228] N88-20961
RARE EARTH ELEMENTS
Energy transfer and non-linear optical properties at near ultraviolet wavelengths: Rare earth 4f yields 5d transitions in crystals and glasses
[DE88-005403] N88-21012
RATES (PER TIME)
Measurement of rate constants of elementary gas reactions of importance to upper atmosphere and combustion systems
[AD-A189432] N88-20386
RAYLEIGH SCATTERING
Thermodynamic theory of fluctuations and Rayleigh light scattering in solutions N88-20681
RAYLEIGH WAVES
Numerical model of Rayleigh instability and spin-off eddies on fronts N88-20696
RDX
Laser ignition of nitramine composite propellants and crack propagation and branching in burning solid propellants
[AD-A189260] N88-20483
REACTION KINETICS
Kinetic mechanisms for ionization and afterburning suppression
[AD-A189219] N88-20383
Measurement of rate constants of elementary gas reactions of importance to upper atmosphere and combustion systems
[AD-A189432] N88-20386
Kinetics of polymer decomposition
[DE88-005500] N88-20460
Experimental and theoretical constraints on the origin of mid-ocean ridge geothermal fluids N88-20784
Analytically modeling the carbothermic reduction of alumina in a thermal plasma
[DE88-005535] N88-21020
REACTION PRODUCTS
Proton/antiproton yields W(+/-)boson gamma X as a test of the quark charges
[NIKHEF-H/87-11] N88-20987
REACTIVITY
Properties of reactively sputtered WNx films Zhao, X. -A.
[AD-A188711] N88-20976
Molecular collision processes in gases and at surfaces
[AD-A189518] N88-20982
REACTOR MATERIALS
IAEA Specialists' Meeting on Graphite Component Structural Design
[DE88-780006] N88-20439
Fracture criterion of reactor graphite under multiaxial stresses N88-20442
High temperature Young's modulus of IG-110 graphite N88-20443
Effects of high temperature neutron irradiation on the physical, chemical and mechanical properties of fine-grained isotropic graphite N88-20444
Degradations of thermal shock resistance and the fracture toughness of reactor graphite subjected to neutron irradiation N88-20445
Application of ISRM testing methods to fracture toughness testing of graphite N88-20446
Notch sensitivity of graphite materials for VHTR N88-20447
Nondestructive testings of HTGR graphites N88-20448
REACTOR SAFETY
Uncertainties in hydrogen combustion
[DE88-005354] N88-20395
Potential off-normal events and associated radiological source terms for the compact ignition tokamak: Fusion Safety Program
[DE88-004112] N88-21024
REACTOR TECHNOLOGY
IAEA Specialists' Meeting on Graphite Component Structural Design
[DE88-780006] N88-20439
REAL TIME OPERATION
Development of an interactive real-time graphics system for the display of vehicle space positioning
[NASA-TM-100429] N88-20344
Western aeronautical test range real-time graphics software package MAGIC
[NASA-TM-100425] N88-20506
The 1987 Airborne Antarctic Ozone Experiment: The Nimbus-7 TOMS data atlas
[NASA-RP-1201] N88-20714
Configuration management issues and objectives for a real-time research flight test support facility
[NASA-TM-100437] N88-20832
Dynamic run-time graphics
[DE87-008997] N88-20879
RECEIVERS
Signal-filter design and system performance for polarimetric radar
[AD-A189257] N88-20514
System for detecting objects that represent a threat
[NASA-TT-20244] N88-20528
Bragg-cell receiver study
[NASA-CR-182684] N88-20535
RECEPTION DIVERSITY
A polarization diversity meteorological radar system
[AD-A189291] N88-20515
RECHARGING
A new concept in an electrically rechargeable zinc-air alkaline battery
[DE88-003858] N88-20539
RECIPROCITY THEOREM
The calibration of photographic and spectroscopic films: Reciprocity failure and thermal responses of IIaO film at liquid nitrogen temperatures
[NASA-CR-181094] N88-20606
RECOMBINATION REACTIONS
Study of activationless reactions of point defects with impurities and impurity-defect complexes in alpha-iron
[TI88-701028] N88-20433
The astrophysics of nebulae and active galactic nuclear emission-line regions: New methods and applications N88-21111
RECONNAISSANCE
Feasibility report: Operation of light air cushion vehicle at McMurdo Sound, Antarctica
[AD-A189057] N88-20494
RECONNAISSANCE AIRCRAFT
Aquila remotely piloted vehicle: Its potential battlefield contribution still in doubt
[PB88-120241] N88-20269
RECONNAISSANCE SPACECRAFT
Specification for an infrared satellite surveillance system for the detection of aircraft
[AD-A189592] N88-20746
RECORDING
Development of fiber optic systems for recording and transmitting holographic information
[AD-A189406] N88-20603
RECRYSTALLIZATION
Grain refinement during primary breakdown of alloy 718
[DE88-005193] N88-20423
RECURSIVE FUNCTIONS
Predicate-transformer semantics of general recursion
[CS-8709] N88-20876
RED SHIFT
Coherence effects in optical physics with special reference to spectroscopy
[AD-A189520] N88-21007
Galaxy evolution in dense clusters N88-21101
REDUCED GRAVITY
Development of an optical diagnostic instrument. Part 2: Instrument development --- space laboratories
[NLR-TR-87079-L-PT-2] N88-21016
REDUCTION (CHEMISTRY)
Analytically modeling the carbothermic reduction of alumina in a thermal plasma
[DE88-005535] N88-21020
REENTRY VEHICLES
Features of Soyuz TM spacecraft N88-20329
REFINING
Aviation turbine fuels from tar sands bitumen and heavy oils. Part 3: Laboratory sample production
[AD-A189278] N88-20484
REFLECTANCE
Applications of the differential reflectivity radar technique: Focus on estimation of rainfall parameters and microwave attenuation prediction N88-20521
Pseudo-stationary oblique-shock-wave reflections in low gamma gases: Isobutane and sulphur hexafluoride
[UTIAS-TN-267] N88-20576
REFLECTED WAVES
Flow/acoustic interaction in duct inflow
[AD-A189264] N88-20967
REFLECTION
Solving reflexive domain equations in a category of complete metric spaces
[CWI-CS-R8709] N88-20956
REFRACTED WAVES
Mathematical models of sound waves in fluids
[AD-A189270] N88-20968
REFRACTIVITY
Refractive index gradients in nuclear-reactor-pumped lasers: Gasdynamic effects
[DE88-006099] N88-20621
Nonlinear refractive index measurements of glasses and crystals
[DE88-005673] N88-21009
REFRACTORY MATERIALS
High-temperature metal matrix composites
[AD-A189516] N88-20367
Statistical considerations of graphite strength for assessing design allowable stresses N88-20441
Fracture criterion of reactor graphite under multiaxial stresses N88-20442
High temperature Young's modulus of IG-110 graphite N88-20443
Effects of high temperature neutron irradiation on the physical, chemical and mechanical properties of fine-grained isotropic graphite N88-20444
Degradations of thermal shock resistance and the fracture toughness of reactor graphite subjected to neutron irradiation N88-20445
REFUELING
Application of railgun principle to high-velocity hydrogen pellet injection for magnetic fusion reactor refueling
[DE88-005830] N88-20334
REGISTERS (COMPUTERS)
On proving register atomicity
[CWI-CS-R8707] N88-20862
REGRESSION ANALYSIS
Survival analysis using additive risk models
[AD-A189053] N88-20906
REGULATIONS
Deterministic uncertainty analysis
[DE88-006139] N88-20942
REINFORCING FIBERS
Use of reinforced inorganic cement materials for spark wire and drift chamber wire frames
[NASA-CR-180759] N88-20438
PNL-1 improved ceramic composites through controlled fiber matrix interaction
[DE88-005680] N88-20462
REINFORCING MATERIALS
Viscoelastic behavior of a polyetheretherketone (PEEK) composite
[AD-A189545] N88-20368
Fracture criteria for discontinuously reinforced metal matrix composites
[NASA-CR-182665] N88-20662
RELATIVISTIC EFFECTS
Relativistic jet models for the BL Lacertae object Mrk 421 during three epochs of observation
[NASA-TM-89727] N88-21090
Topics in curved and flat space electromagnetism N88-21100
RELATIVISTIC ELECTRON BEAMS
Collective acceleration of electrons and ions in a high relativistic electron beam
[DE88-005261] N88-20998
Design of electron beam accelerator for microwave application
[DE88-005252] N88-20999
RELATIVISTIC PARTICLES
Action-angle maps and scattering theory for some finite-dimensional integrable systems. The pure solution case
[CWI-PM-R8704] N88-20955
RELATIVISTIC VELOCITY
Collective acceleration of electrons and ions in a high relativistic electron beam
[DE88-005261] N88-20998
RELATIVITY
Topics in curved and flat space electromagnetism N88-21100

RELAXATION (MECHANICS)
Lattice relaxation of the DX centers in Ga/sub 1-x/Al/sub x/As and of the pressure-induced deep donors in GaAs
[DE88-005452] N88-21061
RELIABILITY
Estimating system and component reliabilities under partial information on cause of failure
[AD-A189107] N88-20653
Stochastic comparisons of order statistics, with applications in reliability
[AD-A189408] N88-20938
RELIABILITY ANALYSIS
A fault injection experiment using the AIRLAB Diagnostic Emulation Facility
[NASA-CR-178390] N88-20695
REMOTE SENSING
The radar scattering coefficient as a function of forest stand parameters and viewing angle. An empirical study of the Pinus sylvestris L. in the Kootwijk forest (The Netherlands), extended with observations in the Speulder and Sprielder forest (The Netherlands)
[ETN-88-91348] N88-20527
Remote fiber fluorimetry techniques for pressure measurements
[DE88-004486] N88-20604
Remote sensing of earth terrain
[NASA-CR-182677] N88-20711
Determination of Earth rotation by the combination of data from different space geodetic systems
[NASA-CR-181388] N88-20713
The use of four-photon Raman spectroscopy for the remote sensing of natural objects
[NASA-TT-20257] N88-20716
Activities and objectives of the Polar Research Board
[DE88-004543] N88-20747
Summary of along-track data from the Earth radiation budget satellite for several major desert regions
[NASA-RP-1197] N88-20772
Activities report in aeronautics and astronautics
[ETN-88-91332] N88-21115
REMOTELY PILOTED VEHICLES
Aquila remotely piloted vehicle: Its potential battlefield contribution still in doubt
[PB88-120241] N88-20289
REPLACING
A comparative assessment of US and UK explosives qualified as replacements for tetryl
[MRL-R-1094] N88-20486
Recommended replacements for tetryl in Australian production fuzes and related ordnance
[MRL-R-1089] N88-20489
REQUIREMENTS
Turnaround operations analysis for OTV. Volume 1: Executive summary
[NASA-CR-179316] N88-20340
Turnaround operations analysis for OTV. Volume 2: Detailed technical report
[NASA-CR-179317] N88-20341
Intergrated circuit design, phase 2
[AD-A189060] N88-20530
RESEARCH AIRCRAFT
A correlation study of X-29A aircraft and associated analytical development
[NASA-TM-89735] N88-20296
RESEARCH FACILITIES
A review of technologies applicable to low-speed flight of high-performance aircraft investigated in the Langley 14- x 22-foot subsonic tunnel
[NASA-TP-2796] N88-20264
Aircraft flight flutter testing at the NASA Ames-Dryden Flight Research Facility
[NASA-TM-100417] N88-20301
High Reynolds number pump facility for cavitation research
[AD-A189310] N88-20558
The use of an automated flight test management system in the development of a rapid-prototyping flight research facility
[NASA-TM-100435] N88-20896
The continuous electron beam accelerator facility
[CEBAF-PR-87-017] N88-20996
RESEARCH MANAGEMENT
Mission directed goals for electric vehicle battery research and development: The Task Force on electric vehicle battery goals
[DE88-005601] N88-20548
The use of an automated flight test management system in the development of a rapid-prototyping flight research facility
[NASA-TM-100435] N88-20896
Computation and graphics in mathematical research
[DE88-005796] N88-20953
Aeronautics and space report of the President: 1986 activities N88-21087
RESONANCE
Electromagnetic scattering from and natural resonances of the circular strip N88-20523
RESONANT FREQUENCIES
Time-domain system for identification of the natural resonant frequencies of aircraft relevant to electromagnetic compatibility testing
[PB88-164520] N88-20519
RESONATORS
Parametric study of acceleration-induced stresses and frequency changes in doubly-rotated crystal resonators
[AD-A189261] N88-20532
Quartz oscillator analysis
[DE88-005886] N88-20550
Semiclassical theory of injected lasers with arbitrary stable and unstable resonators
[AD-A189514] N88-20615
Resonator coupling of two ring cavity, argon-ion lasers
[AD-A189558] N88-20616
RESPIRATION
Increase in influence of oxygen on the body in the presence of helium N88-20816
RESPONSES
Distraction and inhibition in continuous CRT performance: A replication and some new findings
[PB88-150941] N88-20821
REVERSE FIELD PINCH
Reversed field pinch operation with a thin shell
[DE88-005521] N88-21027
REYNOLDS EQUATION
Calculations of viscous flows with a multigrid method N88-20580
REYNOLDS STRESS
Improvement of the Reynolds-stress model by a new pressure-strain correlation
[NASA-CR-182699] N88-20667
RHENIUM
Compatibility in space reactor fuel systems
[DE88-005696] N88-21004
RHODIUM
Model catalyst studies of SMSI (Strong Metal/Support Interactions) and the role of D-electrons in chemisorption and catalysis
[DE88-004518] N88-20393
The relationship of the chemical bonding topology of high critical temperature copper oxide superconductors to that of the chevrel phases and the ternary lanthanide rhodium borides
[AD-A189255] N88-21042
RIDGES
Experimental and theoretical constraints on the origin of mid-ocean ridge geothermal fluids N88-20784
RIEMANN MANIFOLD
String theory and algebraic geometry of moduli spaces
[CWI-PM-R8705] N88-21070
RIGID ROTORS
An experimental investigation of the flap-lag-torsion aeroelastic stability of a small-scale hingeless helicopter rotor in hover
[NASA-TP-2546] N88-20257
RING LASERS
Laser gyro attitude control system feasibility
[AD-A189368] N88-20285
Resonator coupling of two ring cavity, argon-ion lasers
[AD-A189558] N88-20616
RING STRUCTURES
Buckling and breakdown problems in structural mechanics. Failure of prestressed double-walled containers or rings
[MBB-UR-E-956/87] N88-20671
RIPPLES
Helical ripple transport in stellarators at low collision frequency
[DE88-006431] N88-21031
RISK
The space station assembly phase: Flight telerobotic servicer feasibility, volume 1
[NASA-CR-182689] N88-20351
Survival analysis using additive risk models
[AD-A189053] N88-20906
RIVETS
Crack distribution and growth rates for critical fastener holes in Mirage wing RH79
[AD-A189080] N88-20293
ROBOTICS
The space station assembly phase: Flight telerobotic servicer feasibility, volume 1
[NASA-CR-182689] N88-20351
The space station assembly phase: Flight telerobotic servicer feasibility. Volume 2: Methodology and case study
[NASA-CR-182690] N88-20352
Modelling and simulation of a rate controlled manipulator arm — Hermes
[NLR-TR-87010-U] N88-20639
The dynamic control of robotic manipulators in space
[NASA-CR-182710] N88-20646
Ultrasonic inspection of irregular surfaces
[AERE-R-12465] N88-20648
Geometry and graphics applied to robotics
[CWI-CS-R8727] N88-20903
ONR Far East Scientific Bulletin, volume 12, number 3, July-September 1987
[AD-A188554] N88-21081
ROBOTS
Intelligent control of robot manipulators in hazardous environments
[DE88-003305] N88-20638
Force distribution and trajectory control for closed kinematic chains with applications to walking machines N88-20642
Ultrasonic inspection of irregular surfaces
[AERE-R-12465] N88-20648
ROCKET ENGINES
Numerical model of the time independent mean flow in a rotating rocket motor N88-20360
ROCKET EXHAUST
Kinetic mechanisms for ionization and afterburning suppression
[AD-A189219] N88-20383
ROCKET VEHICLES
Effect of rotation on the lateral stability of a free-flying column subjected to an axial thrust with directional control
[AD-A188690] N88-20338
ROCKS
Elemental composition of Venusian rocks in northeastern part of Terra Aphrodite (determined using data from Vega-2 landing module) N88-20322
Content of natural radioactive elements in Venusian rocks determined using data from Vega-1 and Vega-2 stations N88-20323
RODS
A direct correlation of strength with impact velocity
[AD-A189251] N88-20409
ROLLER BEARINGS
Corrosion-wear process under rolling-sliding motion
[AD-A189603] N88-20635
ROTARY WINGS
Verification of the momemtum theory for rotors using measurements on a model helicopter
[R-840-S] N88-20275
ROTATING BODIES
An L-U implicit multigrid algorithm to solve the Euler equations for transonic flow in rotating turbomachinery passages N88-20270
Topics in curved and flat space electromagnetism N88-21100
ROTATING FLUIDS
Mushroom-shaped currents (eddy dipoles) under rotation and stratification conditions N88-20678
ROTATING PLASMAS
Evolution of poloidal variation of impurity density and ambipolar potential in rotating tokamak plasma, part 1
[DE88-006263] N88-21022
ROTATION
The effect of combustion gas flow on the rotational dynamics of a spinning solid fuel rocket N88-20358
Numerical model of the time independent mean flow in a rotating rocket motor N88-20360
Parametric study of acceleration-induced stresses and frequency changes in doubly-rotated crystal resonators
[AD-A189261] N88-20532
ROTOR AERODYNAMICS
Verification of the momemtum theory for rotors using measurements on a model helicopter
[R-840-S] N88-20275
ROTOR BLADES
A preliminary investigation of finite-element modeling for composite rotor blades
[NASA-TM-100559] N88-20656
Optimal placement of tuning masses for vibration reduction in helicopter rotor blades
[NASA-TM-100562] N88-20665
ROTOR BLADES (TURBOMACHINERY)
Design graphs for the first two bending Eigenvibration forms of rotating beams consisting of two beam points
[IW-86006R] N88-20670
Measurement and analysis of the noise radiated by low Mach numbers centrifugal blowers
[AD-A189226] N88-20966
ROTORS
Dynamic modelling of flexible rotor shafts mounted on hydrodynamic bearings N88-20641
RUNGE-KUTTA METHOD
Numerical methods in the resolution of control electrovalve model
[INPE-4154-RPE/540] N88-20554
An adaptive grid technique for solution of the Euler equations N88-20579

Convergence of Runge-Kutta methods on classes of stiff initial value problems
[CWI-NM-R8717] N88-20924
RUPTURING
Ductile failure
[AD-A189429] N88-20654

S

S MATRIX THEORY
Action-angle maps and scattering theory for some finite-dimensional integrable systems. The pure solution case
[CWI-PM-R8704] N88-20955
S WAVES
Investigation of the use of horizontally polarised shear waves for TOFD studies on austenitic steel
[AERE-R-12145] N88-20649
SAFETY
Characteristics of the positive lighting flash
[DE88-005854] N88-20760
SAFETY MANAGEMENT
Spacecraft fire-safety experiments for space station: Technology development mission
[NASA-CR-182114] N88-20353
Flame retardants
[NASA-TT-20250] N88-20400
Safety research of insulating materials of cable for nuclear power generating station
[NASA-TT-20202] N88-20477
EDF's studies and first cnoices regarding the design of electrical equipment
[NASA-TT-20222] N88-20553
Environmental projects. Volume 5, part 1: Study of subsurface contamination. Part 2: Guide to implement environmental compliance programs
[NASA-CR-182691] N88-20741
SALINITY
Determination of mean thermohaline characteristics of the ocean N88-20675
Estimates of ocean-atmosphere thermal interaction in Gulf Stream energy-active test range in winter of 1984 N88-20679
Propagation of subsurface salinity maximum in tropical Atlantic N88-20686
Space-time analysis of oceanographic fields by modified empirical orthogonal functions method N88-20687
Intrathermocline lens of Mediterranean water in tropical North Atlantic N88-20688
Model of hydrodynamic adjustment of temperature, salinity and current fields N88-20700
Microwave and structural properties of saline ice
[AD-A189307] N88-20779
SAN ANDREAS FAULT
Correlation of data on strain accumulation adjacent to the San Andreas Fault with available models
[NASA-CR-180757] N88-20742
Geodetic measurement of deformation east of the San Andreas fault in Central California
[NASA-CR-182709] N88-20754
SATELLITE ATTITUDE CONTROL
Gas consumption estimation of an attitude control system of an artificial satellite (utilizing DRF) in limit cycle phase
[INPE-4338-RPE/553] N88-20350
SATELLITE COMMUNICATION
Alternative force structuring strategies for military satellite communication systems
[AD-A189492] N88-20516
SATELLITE DESIGN
Study of the optimization of satellite system design for transfer orbit
[MBB-URV-135] N88-20332
SATELLITE IMAGERY
An investigation of Doppler satellite positioning multi-station adjustment software N88-20345
Restoration techniques for redisplay of LANDSAT-5 satellite imagery
[INPE-4189-PRE/1076] N88-20712
Analysis for architecture for image processing
[INPE-4294-PRE/1165] N88-20715
Aspects and applications of primary processing of visual information
[INPE-4290-PRE/1161] N88-21015
IUE program SUGSD: Varability time scale of H Ly-alpha from Uranus
[NASA-CR-182706] N88-21107
SATELLITE OBSERVATION
An investigation of Doppler satellite positioning multi-station adjustment software N88-20345
Analysis of spectral reflectance characteristics of targets under satellites and automatic cloud recognition N88-20498
Radiative processes affecting ocean mixed-layer heat content and their monitoring from satellite N88-20800
SATELLITE ORBITS
The evaluation and selection of a 5th ground antenna site for the global positioning system
[AD-A189495] N88-20286
Orbit accuracy requirement of GPS for precise positioning and orbit determination within local area N88-20499
SATELLITE SOUNDING
Roys and radiosondes in the region
[INPE-4362-PRE/1188] N88-20743
SATELLITE TEMPERATURE
A study of satellite emission computed tomography
[AD-A189567] N88-20745
SCALARS
On the expectation of the product of four matrix-valued Gaussian random variables
[EUT-87-E-178] N88-20927
SCALE MODELS
An investigation of classical dynamic scaling techniques applied to an oleo-pneumatic landing gear strut
[AD-A187664] N88-20292
SCALING LAWS
Cavitation inception
[AD-A189220] N88-20557
Similarity theories and microturbulence in the atmospheric mixed layer N88-20802
SCATTERING COEFFICIENTS
The radar scattering coefficient as a function of forest stand parameters and viewing angle. An empirical study of the Pinus sylvestris L. in the Kootwijk forest (The Netherlands), extended with observations in the Speulder and Sprielder forest (The Netherlands)
[ETN-88-91348] N88-20527
SCATTERING CROSS SECTIONS
Vibration spectra of oxygen and vanadium atoms in vanadium-oxygen disordered interstitial alloys
[DE87-703166] N88-20404
SCATTERING FUNCTIONS
Synchronous measurements of effective photon path length in visible and near-IR spectral regions in real cloud systems N88-20706
SCHEDULING
Approximation algorithms for scheduling unrelated parallel machines
[CWI-OS-R8714] N88-20861
SCHLIEREN PHOTOGRAPHY
Development of an optical diagnostic instrument. Part 2: Instrument development — space laboratories
[NLR-TR-87079-L-PT-2] N88-21016
SEA ICE
Predictions and studies with a one-dimensional ice/ocean model
[AD-A189158] N88-20776
Microwave and structural properties of saline ice
[AD-A189307] N88-20779
Mechanical properties of sea ice and sea ice deformation in the near-shore zone
[PB88-147889] N88-20782
SEA WATER
Cavitation inception
[AD-A189220] N88-20557
Determination of mean thermohaline characteristics of the ocean N88-20675
Research on influence of individual sea water components on spectral brightness coefficient of outgoing radiation N88-20682
Predictions and studies with a one-dimensional ice/ocean model
[AD-A189158] N88-20776
Experimental and theoretical constraints on the origin of mid-ocean ridge geothermal fluids N88-20784
SEALERS
Examination of polysulfide sealants by scanning electron microscopy
[MRL-R-1096] N88-20478
SEALING
Processing of glass to aluminum (low melting metals) seals via an injection molding technique
[DE88-004689] N88-20468
SEAMOUNTS
Bathymetric hazard survey test
[AD-A189150] N88-20775
SEARCH RADAR
A preliminary assessment of thunderstorm outflow wind measurement with airport surveillance radars
[AD-A189064] N88-20757
SEASAT SATELLITES
Tidal estimation in the Pacific with application to SEASAT altimetry
[NASA-TM-100694] N88-20780
SECONDARY EMISSION
The magnitude of secondary electron contributions in photon stimulated desorption
[AD-A189094] N88-20980
SEDIMENTS
Resolution of the magnetotelluric method for determining local inhomogeneities in the sedimentary cover N88-20701
SEISMIC WAVES
Ultrasonic physical modeling of seismic wave propagation from graben-like structures
[AD-A189066] N88-20744
Geodetic measurement of deformation east of the San Andreas fault in Central California
[NASA-CR-182709] N88-20754
SEISMOLOGY
Numerical modeling of wave migration of seismic data N88-20684
Interactive automated system for testing analog units of digital seismic stations N88-20702
Correlation of data on strain accumulation adjacent to the San Andreas Fault with available models
[NASA-CR-180757] N88-20742
SELECTION
Advanced human factors engineering tool technologies
[AD-A189390] N88-20825
SELENIUM COMPOUNDS
Review of selenium thermodynamic data
[DE88-006194] N88-21068
SEMANTICS
Using design axioms and topology to model database semantics
[CWI-CS-R8711] N88-20863
Algebra of Communicating Processes (ACP)tau: A universal axiom system for process specification
[CWI-CS-R8725] N88-20869
Designing equivalent semantic models for process creation
[CWI-CS-R8732] N88-20872
Predicate-transformer semantics of general recursion
[CS-8709] N88-20876
A fully abstract semantics for data flow nets
[CWI-CS-R8724] N88-20893
A convergence theorem in process algebra
[CWI-CS-R8733] N88-20920
SEMICONDUCTOR DEVICES
Electrical properties of medium field, chem-prep varistors
[DE88-006147] N88-20540
SEMICONDUCTOR LASERS
Fiber-coupled external-cavity semiconductor high power laser
[AD-A188454] N88-20811
High power, high efficiency, 2D laser diode arrays for pumping solid state lasers
[DE88-004042] N88-20832
SEMICONDUCTOR PLASMAS
Modeling and transport in semiconductor devices
[AD-A188760] N88-21037
SEMICONDUCTORS (MATERIALS)
Thin-film diffusion barriers for metal-semiconductor contacts
[AD-A188712] N88-21035
SENSITIVITY
Anomalous shock sensitivity/density relationship for RDX-polyethylene wax and related formulations from MRL Small Scale Gap Test (SSGT) measurements
[MRL-R-1099] N88-20399
Some properties of Australian produced explosive composition H-6
[MRL-TN-525] N88-20490
SENSORS
Spectral contents readout of birefringent sensors
[NASA-CR-179430] N88-20673
SEPARATED FLOW
Numerical model of the time independent mean flow in a rotating rocket motor N88-20360
SERVICE LIFE
Sodium-sulfur technology evaluation at Argonne National Laboratory
[DE88-002852] N88-20544
SET THEORY
Measures of similarity between fuzzy concepts: A comparative analysis
[AD-A189430] N88-20910
SHAFTS (MACHINE ELEMENTS)
Dynamic modelling of flexible rotor shafts mounted on hydrodynamic bearings N88-20641
SHARP LEADING EDGES
Tests on the AFWAL 65 deg delta wing at NLR: A study of vortex flow development between Mach = 0.4 and 4
[NLR-MP-86058-U] N88-20266
SHEAR FLOW
Transport and stability properties of free shear flows N88-20577
Research on turbulence in bottom boundary layer in ocean N88-20697
Mixed-layer shear related to wind stress in the central equatorial Pacific N88-20793

Mixed-layer fronts in the California current N88-20794

SHEAR LAYERS
Three-dimensional shear layer experiments and their use as test cases for calculation methods [NLR-MP-86036-U] N88-20570
Numerical model of Rayleigh instability and spin-off eddies on fronts N88-20696

SHEAR PROPERTIES
Parametric study of acceleration-induced stresses and frequency changes in doubly-rotated crystal resonators [AD-A189261] N88-20532

SHEAR STRAIN
Geodetic measurement of deformation east of the San Andreas fault in Central California [NASA-CR-182709] N88-20754

SHEARING
Applications of the lateral shearing interferometer in measurement of synchrotron radiation optical elements [DE88-005184] N88-21011

SHIPS
A pyrotechnic delay ignition system for a submarine launched marine signal [MRL-R-1079] N88-20487

SHOCK TUBES
Investigation of heat transfer to a flat plate in a shock tube [AD-A189538] N88-20561

SHOCK WAVE INTERACTION
Resonant Alfven wave instabilities driven by streaming fast particles N88-21104

SHOCK WAVES
Anomalous shock sensitivity/density relationship for RDX-polyethylene wax and related formulations from MRL Small Scale Gap Test (SSGT) measurements [MRL-R-1099] N88-20399
Use of the LLNL 40 kV electric gun to study the shock response of 21-6-9 stainless steel [DE87-014550] N88-20418
Investigation of heat transfer to a flat plate in a shock tube [AD-A189538] N88-20561
An interferometric investigation of the diffraction of planar shock waves over a half-diamond cylinder in air [UTIAS-322] N88-20575
Pseudo-stationary oblique-shock-wave reflections in low gamma gases: Isobutane and sulphur hexafluoride [UTIAS-TN-267] N88-20576
Theoretical investigation of the wave shaping process in a section of ladder fracture tape [MRL-R-1081] N88-20595

SHORT TAKEOFF AIRCRAFT
A review of technologies applicable to low-speed flight of high-performance aircraft investigated in the Langley 14- x 22-foot subsonic tunnel [NASA-TP-2796] N88-20264

SIGNAL DETECTION
Detection and angle estimation of coherent plane waves N88-20522
Method for set-up for researching signal curve development [NASA-TT-20235] N88-20526

SIGNAL MEASUREMENT
Alaska Loran C probe test results [AD-A189131] N88-20284
Bragg-cell receiver study [NASA-CR-182664] N88-20535

SIGNAL PROCESSING
Architecture specification for PAVE PILLAR avionics [AD-A188722] N88-20303
The acoustic-modeling problem in automatic speech recognition [AD-A188529] N88-20510
Statistical signal processing using a class of iterative estimation algorithms [AD-A189050] N88-20511
System for detecting objects that represent a threat [NASA-TT-20244] N88-20528
Bragg-cell receiver study [NASA-CR-182664] N88-20535
Analysis for architecture for image processing [INPE-4294-PRE/1165] N88-20715
Study of photochromic materials for use in optical signal processing [AD-A189068] N88-21006

SIGNAL TO NOISE RATIOS
Signal-filter design and system performance for polarimetric radar [AD-A189257] N88-20514
Detection and angle estimation of coherent plane waves N88-20522
A preliminary assessment of thunderstorm outflow wind measurement with airport surveillance radars [AD-A189064] N88-20757

SIGNAL TRANSMISSION
Method for set-up for researching signal curve development [NASA-TT-20235] N88-20526
Upward propagating electric fields from thunderstorms and VLF transmitters N88-20767

SILICON
Thermal oxide growth on silicon: Intrinsic stress and silicon cleaning effects [AD-A188790] N88-20377
Focused ion beam fabrication of graded channel FET's in GaAs and Si [AD-A189166] N88-21040
Pressure-dependent DLTS (Deep Level Transient Spectroscopy) experiments on Si-doped AlGaAs [DE88-003842] N88-21047
X-ray diffraction study of a thin GaAs film on Si(100) [DE88-005290] N88-21055
Initial stages of silicon growth on the (100) surface of silicon by localized laser CVD [DE88-005420] N88-21059

SILICON CARBIDES
Composites strengthening [AD-A189258] N88-20364
The influence of the fiber-matrix bond on the mechanical behavior of NICALON/SiC composites [DE88-006155] N88-20369
Nondestructive evaluation of carbon-carbon coatings [AD-A189524] N88-20453
Ultrasonic characterization of non-uniform porosity distributions in SiC ceramic [DE88-004814] N88-20459

SILICON COMPOUNDS
Silicon-germanium heterostructures N88-21034

SILICON NITRIDES
A new process for synthesis of silicon nitride powders for advanced ceramics [AD-A189354] N88-20451
Dynamic tensile cyclic fatigue of Si3N4 [DE88-003919] N88-20658

Optical study of germanium, germanium plus arsenic, and germanium plus gallium implants in gallium arsenide [AD-A189600] N88-21045
Photon-controlled growth of multilayered structures [DE88-005061] N88-21054

SILICON OXIDES
Thermal oxide growth on silicon: Intrinsic stress and silicon cleaning effects [AD-A188790] N88-20377
Polarization properties of SiO masers N88-21113

SILICON TRANSISTORS
Development of Si/SiGe heterostructures [AD-A189527] N88-21044

SIMD (COMPUTERS)
The physical structure of concurrent problems and concurrent computers [DE88-005812] N88-20835

SIMILARITY THEOREM
Determining Langmuir circulation parameters on basis of similarity theory N88-20680

SIMULATION
Interaction between two-dimensional sonic jets and supersonic flow to model heat addition in a supersonic combustor [AD-A189572] N88-20261
Numerical simulation of subsonic and transonic propeller flow [NASA-TM-100163] N88-20262
The effect of combustion gas flow on the rotational dynamics of a spinning solid fuel rocket N88-20358
Simulated impact damage in a thick graphite/epoxy laminate using spherical indenters [NASA-TM-100539] N88-20363
Model catalyst studies of SMSI (Strong Metal/Support Interactions) and the role of D-electrons in chemisorption and catalysis [DE88-004518] N88-20393
Applications of the differential reflectivity radar technique: Focus on estimation of rainfall parameters and microwave attenuation prediction N88-20521
Center for Turbulence Research 1987 activities [NASA-CR-182693] N88-20583
Corrosion-wear process under rolling-sliding motion [AD-A189603] N88-20635
Structural clearances and internal friction: Simulation by Eigen distortions [ISSN-0208-5658] N88-20640
Two dimensional uncorrelated bias in fix algorithms [NASA-CR-182683] N88-20847
Predictive monitoring research: Summary of the PREMON system [NASA-CR-182687] N88-20905
Very high energy gamma ray astrophysics [DE88-005821] N88-21095

SIMULATORS
Engine flow simulation for wind tunnel testing at NLR [NLR-MP-87011-U] N88-20305

SINTERING
Processing of nanophase ceramics [DE88-005985] N88-20475

SITE SELECTION
The evaluation and selection of a 5th ground antenna site for the global positioning system [AD-A189495] N88-20286

SKY
Analysis of deep sky sources found by the infrared astronomy satellite [AD-A189605] N88-21089

SLIP FLOW
Slip velocity method for three-dimensional compressible turbulent boundary layers [NASA-TM-100586] N88-20592

SLOTS
Experimental verification of a finite-difference time-domain thin slot algorithm [DE88-005572] N88-20859

SLURRIES
Fluidization mechanisms in slurry flows [DE88-005191] N88-20563

SMALL PERTURBATION FLOW
Steady and unsteady transonic small disturbance analysis of realistic aircraft configurations [NASA-TM-100557] N88-20269

SNOW COVER
Remote sensing of earth terrain [NASA-CR-182677] N88-20711

SODIUM
Quantitative determination of a hydrogen impurity in a sodium coolant by hydride thermal dissociation [NASA-TT-20239] N88-20402

SODIUM COMPOUNDS
Corrosion-wear process under rolling-sliding motion [AD-A189603] N88-20635

SODIUM SULFUR BATTERIES
Improve the lifetime of the hollow fiber sodium sulfur cell [DE88-004881] N88-20469
Sodium-sulfur technology evaluation at Argonne National Laboratory [DE88-002852] N88-20544
A novel class of positive electrodes for rechargeable batteries [DE88-004559] N88-20545

SOFTWARE ENGINEERING
Theoretical investigation of EM wave generation and radiation in the ULF, ELF and VLF bands by the electrodynamic orbiting tether [NASA-CR-182720] N88-20529
Algebra of Communicating Processes (ACP)tau: A universal axiom system for process specification [CWI-CS-R8725] N88-20869
Two normal form theorems for Communicating Sequential Processes (CSP) program [CWI-CS-R8735] N88-20874
Type-checking Mini-ML: An algebraic specification with user-defined syntax [CWI-CS-R8737] N88-20921

SOFTWARE TOOLS
Western aeronautical test range real-time graphics software package MAGIC [NASA-TM-100425] N88-20506
Advanced human factors engineering tool technologies [AD-A189390] N88-20825
MacCAD (Macintosh Computer Aided Design), computer aided design tool for system analysis [AD-A189241] N88-20843
Steps into a geometer's workbench [CWI-CS-R8726] N88-20870

SOLAR ACTIVITY
Development of high stability fiber optic spectrophotometric systems for study of solar/stellar magnetic activity [AD-A189327] N88-21088

SOLAR ARRAYS
Vega-1 and Vega-2 automatic stations: Functioning of flyby vehicles during encounter with Halley's comet N88-20314
Direct absorption receiver control studies [DE87-013653] N88-20737

SOLAR ATMOSPHERE
Negative viscosity in global circulations N88-20685

SOLAR CELLS
Research on multibandgap solar cells [DE87-012261] N88-20721
Research on high-efficiency, stacked, multijunction, amorphous silicon alloy thin-film solar cells [DE88-001108] N88-20723

CdZnTe as a wide-band-gap absorber for a tandem, thin-film solar cell
[DE88-001114] N88-20724
Research on single-crystal CdTe solar cells
[DE88-001115] N88-20725
Stable, high-efficiency, CuInSe2-based, polycrystalline, thin-film tandem solar cells
[DE88-001116] N88-20726
Cadmium sulfide/copper ternary heterojunction cell research
[DE88-001122] N88-20727
SERI's Photovoltaic R and D Project: Recent progress and future directions
[DE88-001129] N88-20728
Progress of amorphous silicon based solar cells and modules
[DE88-004666] N88-20733
Thin-film cadmium telluride solar cells
[DE88-001107] N88-21050
Investigations of the origins of metastable, light-induced changes in hydrogenated amorphous silicon
[DE88-001117] N88-21051

SOLAR COLLECTORS
Control strategies and hardware used in solar thermal applications
[DE88-004631] N88-20731
Direct absorption receiver control studies
[DE87-013653] N88-20737
A five year weathering experiment with solar collectors
[DE88-900369] N88-20740

SOLAR DYNAMIC POWER SYSTEMS
Solar dynamic power system definition study
[NASA-CR-180877] N88-20361

SOLAR ENERGY CONVERSION
Design of the Sandia-Israel 20-kW reflux heat-pipe solar receiver/reactor
[DE88-001312] N88-20729
Control strategies and hardware used in solar thermal applications
[DE88-004631] N88-20731
Oxidation/sulfidation of materials in an SO3/SO2/O2 thermochemical-transport, distributed-receiver, solar-energy system
[DE88-005875] N88-20739

SOLAR FURNACES
Photolytic formation of free radicals and their effect on hydrocarbon pyrolysis chemistry in a concentrated solar environment
[DE88-004129] N88-20730

SOLAR GENERATORS
Oxidation/sulfidation of materials in an SO3/SO2/O2 thermochemical-transport, distributed-receiver, solar-energy system
[DE88-005875] N88-20739

SOLAR MAGNETIC FIELD
Development of high stability fiber optic spectrophotometric systems for study of solar/stellar magnetic activity
[AD-A189327] N88-21088

SOLAR OSCILLATIONS
Global solar oscillations observed in the visible to near infrared continuum N88-21110

SOLAR PROMINENCES
Magnetohydrodynamic (MHD) simulation of solar prominence formation N88-21109

SOLAR RADIATION
Vertical turbulent transfer of matter in thin ocean surface layer during daytime heating N88-20693
Direct absorption receiver control studies
[DE87-013653] N88-20737
Radiative processes affecting ocean mixed-layer heat content and their monitoring from satellite N88-20800

SOLAR REFLECTORS
Point-focus concentrator reflector assembly, phase 1
[DE88-003616] N88-20720

SOLAR THERMAL ELECTRIC POWER PLANTS
Power from the sun: Principles of high temperature solar thermal technology
[DE87-001104] N88-20736

SOLAR-PUMPED LASERS
Design studies for a solar pumped laser device
[DFVLR-FB-87-39] N88-20629
Direct solar-pumped iodine laser amplifier
[NASA-CR-182674] N88-20630

SOLID ELECTROLYTES
Contrasting conductance/viscosity relations in liquid states of vitreous and polymer solid electrolytes
[AD-A189378] N88-20452

SOLID PROPELLANT COMBUSTION
Combustion theory and related questions
[AD-A189160] N88-20382
Laser ignition of nitramine composite propellants and crack propagation and branching in burning solid propellants
[AD-A189260] N88-20483

SOLID PROPELLANT IGNITION
Laser ignition of nitramine composite propellants and crack propagation and branching in burning solid propellants
[AD-A189260] N88-20483

SOLID PROPELLANT ROCKET ENGINES
A study of combustion and flow behaviour in solid-propellant rocket motors
[UTIAS-280] N88-20357
The effect of combustion gas flow on the rotational dynamics of a spinning solid fuel rocket N88-20358

SOLID STATE DEVICES
Solid-state electrochemical processes in dye films
[AD-A188756] N88-21036

SOLID STATE LASERS
Direct solar-pumped iodine laser amplifier
[NASA-CR-182674] N88-20630
High power, high efficiency, 2D laser diode arrays for pumping solid state lasers
[DE88-004042] N88-20632
Energy transfer and non-linear optical properties at near ultraviolet wavelengths: Rare earth 4f yields 5d transitions in crystals and glasses
[DE88-005403] N88-21012

SOLIDIFICATION
A fundamental understanding of the effect of alloying elements on the corrosion resistance of rapidly solidified Mg alloys
[AD-A189385] N88-20413
Experimental and theoretical methods for investigating helium effects in rapidly solidified metals
[DE88-005542] N88-20425

SOLIDS
Material instabilities in solids
[AD-A189525] N88-20388
Properties of molecular solids and fluids at high pressure and temperature
[DE88-004195] N88-20391
Innovative, counterflow gas/fine solids, direct contact heat exchanger
[DE88-004744] N88-20585
Particle-dynamics calculations of gravity flow of inelastic, frictional spheres
[DE88-005224] N88-20586

SOLUTES
The coordination cluster theory for metallic solutions
[DE88-005934] N88-20389

SOLUTIONS
The coordination cluster theory for metallic solutions
[DE88-005934] N88-20389
Prediction of high-temperature thermodynamic properties of mixed electrolyte solutions including solubility equilibria, vapor pressure depression and boiling point elevation
[DE88-006344] N88-21069

SONAR
Observations of waves and Langmuir circulation with Doppler sonars N88-20790

SOUND FIELDS
Invariant characteristics of acoustic field in stratified ocean N88-20698
Measurement and analysis of the noise radiated by low Mach numbers centrifugal blowers
[AD-A189226] N88-20966
Flow/acoustic interaction in duct inflow
[AD-A189264] N88-20967
Acoustic radiation from line- and point-loaded plates: Uniformly asymptotic solutions
[AD-A189367] N88-20969

SOUND LOCALIZATION
Method for determining the coordinates of sound sources by means of a sound measurement system
[NASA-TT-20242] N88-20972

SOUND WAVES
Method for determination of the wind velocity and direction
[NASA-TT-20233] N88-20769
Flow/acoustic interaction in duct inflow
[AD-A189264] N88-20967
Mathematical models of sound waves in fluids
[AD-A189270] N88-20968
Acoustic radiation from line- and point-loaded plates: Uniformly asymptotic solutions
[AD-A189367] N88-20969
Modeling of laser ultrasound generation in a weld pool
[DE88-005546] N88-20971
Method for determining artillery position
[NASA-TT-20238] N88-20973

SOUNDING
HF (High Frequency) Maximum Usable Frequency (MUF) model uncertainty assessment
[AD-A189132] N88-20513

SOUTHERN OSCILLATION
Survey of acoustic techniques for monitoring El Nino
[PB88-157615] N88-20783

SOYUZ SPACECRAFT
Soviet space transport systems N88-20328
Features of Soyuz TM spacecraft N88-20329

SPACE CHARGE
Wiggler taper optimization for free-electron-laser amplifiers with moderate space-charge effects
[DE88-003758] N88-20618

SPACE ENVIRONMENT SIMULATION
Activities report of the Toulouse Research Center
[ETN-88-91988] N88-21077

SPACE EXPLORATION
Soviet space transport systems N88-20328
The Deep Space Network
[NASA-CR-182700] N88-20524

SPACE FLIGHT
Advanced space propulsion study - antiproton and beamed power propulsion
[AD-A189218] N88-20355

SPACE LABORATORIES
Development of an optical diagnostic instrument. Part 2: Instrument development --- space laboratories
[NLR-TR-87079-L-PT-2] N88-21016

SPACE POWER REACTORS
Molybdenum-base cermet fuel development
[DE88-005529] N88-21003

SPACE PROGRAMS
Aeronautics and space report of the President: 1986 activities N88-21087

SPACE SHUTTLES
Lateral and longitudinal stability and control parameters for the space shuttle discovery as determined from flight test data
[NASA-TM-100555] N88-20309
Soviet space transport systems N88-20328

SPACE STATIONS
Vega-1 and Vega-2 automatic stations: Functioning of flyby vehicles during encounter with Halley's comet N88-20314
Study on long term evolution Towards European Autonomous Manned Spaceflight (STEAMS)
[SNIAS-SE/LS/AP-35-073] N88-20330
Turnaround operations analysis for OTV. Volume 1: Executive summary
[NASA-CR-179316] N88-20340
Turnaround operations analysis for OTV. Volume 2: Detailed technical report
[NASA-CR-179317] N88-20341
The space station assembly phase: Flight telerobotic servicer feasibility, volume 1
[NASA-CR-182689] N88-20351
The space station assembly phase: Flight telerobotic servicer feasibility. Volume 2: Methodology and case study
[NASA-CR-182690] N88-20352
Spacecraft fire-safety experiments for space station: Technology development mission
[NASA-CR-182114] N88-20353
Solar dynamic power system definition study
[NASA-CR-180877] N88-20361
The dynamic control of robotic manipulators in space
[NASA-CR-182710] N88-20646

SPACE TRANSPORTATION
Soviet space transport systems N88-20328

SPACE WEAPONS
Vapor-mist for lightweight high voltage space insulation systems
[DE87-011704] N88-20538

SPACE-TIME FUNCTIONS
Space-time analysis of oceanographic fields by modified empirical orthogonal functions method N88-20687

SPACEBORNE ASTRONOMY
Preparation of photometric measurements on a million stars in the framework of the satellite project HIPPARCOS/TYCHO
[ETN-88-91502] N88-21093

SPACEBORNE EXPERIMENTS
Thermal structure of Venusian Atmosphere determined from results of measurements from Vega-2 landing module N88-20315

SPACECRAFT COMMUNICATION
The evaluation and selection of a 5th ground antenna site for the global positioning system
[AD-A189495] N88-20286

SPACECRAFT COMPONENTS
SOAR: Space orbiting advanced fusion power reactor
[AD-A189234] N88-20356

SPACECRAFT CONTROL
Activities report in aeronautics and astronautics
[ETN-88-91332] N88-21115

SPACECRAFT DEFENSE
Alternative force structuring strategies for military satellite communication systems
[AD-A189492] N88-20516

SPACECRAFT DESIGN
Study on long term evolution Towards European Autonomous Manned Spaceflight (STEAMS)
[SNIAS-SE/LS/AP-35-073] N88-20330
On the sensitivity of complex, internally coupled systems
[NASA-TM-100537] N88-20829
SPACECRAFT EQUIPMENT
The preparation, assembly and mounting of RF coaxial cables
[ESA-PSS-01-718-ISS-1] N88-20504
SPACECRAFT INSTRUMENTS
Roentgenoradiometric analysis of aerosol in Venusian clouds by Vega-1 and Vega-2 automatic interplanetary stations N88-20319
SPACECRAFT ORBITS
Optimal thrust vector control of coplanar orbital evasive maneuvers
[AD-A189544] N88-20346
SPACECRAFT PERFORMANCE
Predictive monitoring research: Summary of the PREMON system
[NASA-CR-182667] N88-20905
SPACECRAFT POWER SUPPLIES
Solar dynamic power system definition study
[NASA-CR-180877] N88-20361
SPACECRAFT PROPULSION
Soviet space transport systems N88-20328
Advanced space propulsion study - antiproton and beamed power propulsion
[AD-A189218] N88-20355
Cermet-fueled reactors for advanced space applications
[DE88-005528] N88-21002
SPACECRAFT RADIATORS
Moveable thermal joints for deployable or steerable spacecraft radiator systems
[NLR-MP-87016-U] N88-20347
SPACECRAFT STRUCTURES
Development of isostatic mounts and associated guidelines --- spacecraft payloads
[CASA-IM-WP-301] N88-20354
SPACECRAFT TEMPERATURE
Moveable thermal joints for deployable or steerable spacecraft radiator systems
[NLR-MP-87016-U] N88-20347
Feasibility demonstration of a sensor for high-quality two-phase flow --- Space Station
[NLR-TR-87009-U] N88-20569
SPACECRAFT TRAJECTORIES
Optimal thrust vector control of coplanar orbital evasive maneuvers
[AD-A189544] N88-20346
SPARK CHAMBERS
Use of reinforced inorganic cement materials for spark wire and drift chamber wire frames
[NASA-CR-180759] N88-20438
SPARK IGNITION
Status of alcohol fuels utilization technology for highway transportation: A 1986 perspective. Volume 2: Compression ignition engines
[DE88-006059] N88-20485
SPATIAL DISTRIBUTION
A segmented calorimeter for low-energy particle beams in space
[DE88-001806] N88-20997
Arcs in cesium seeded noble gases resulting from a magnetically induced electric field
[EUT-87-E-177] N88-21028
SPECIFICATIONS
Engine testing for synfuel operation
[DE88-006044] N88-20645
Algebraic specifications for parameterized data types: The case of minimal computable algebras and parameters with equality
[CWI-CS-R8714] N88-20916
Type-checking Mini-ML: An algebraic specification with user-defined syntax
[CWI-CS-R8737] N88-20921
SPECIMEN GEOMETRY
Application of ISRM testing methods to fracture toughness testing of graphite N88-20446
SPECTRA
Inversion algorithms for geophysical problems
[AD-A189252] N88-20845
SPECTRAL BANDS
Analysis of hydrocarbon band 3.35 in spectrum of Halley's Comet using data from infrared spectrometer on Vega-1 spacecraft N88-20327
SPECTRAL EMISSION
Research on influence of individual sea water components on spectral brightness coefficient of outgoing radiation N88-20682
SPECTRAL ENERGY DISTRIBUTION
Power spectral density analysis of wind-shear turbulence for related flight simulations
[NASA-CR-182721] N88-20773
Inversion algorithms for geophysical problems
[AD-A189252] N88-20845
SPECTRAL METHODS
How to generate equal probability design load conditions --- aircraft design
[NLR-TR-86060-U] N88-20295
Low-order spectral models of atmospheric circulation: A survey
[CWI-AM-R8705] N88-20748
Spectral element methods: Algorithms and architectures
[NASA-CR-182701] N88-20878
SPECTRAL REFLECTANCE
Analysis of spectral reflectance characteristics of targets under satellites and automatic cloud recognition N88-20498
Spectral reflective characteristics of sea surface N88-20676
SPECTRAL RESOLUTION
Velocity resolved far-infrared spectroscopy of galactic sources N88-21099
SPECTROMETERS
The 1987 Airborne Antarctic Ozone Experiment: The Nimbus-7 TOMS data atlas
[NASA-RP-1201] N88-20714
SPECTROPHOTOGRAPHY
The calibration of photographic and spectroscopic films: Reciprocity failure and thermal responses of IIaO film at liquid nitrogen temperatures
[NASA-CR-181094] N88-20606
SPECTROPHOTOMETRY
Development of high stability fiber optic spectrophotometric systems for study of solar/stellar magnetic activity
[AD-A189327] N88-21088
SPECTROSCOPIC ANALYSIS
An experimental method for species concentration measurements in a welding arc using laser-induced fluorescence
[DE88-005638] N88-20636
SPECTROSCOPY
An electrochemical and spectroscopic study of electrode systems
[AD-A189274] N88-20384
Supercritical fluid chromatography/supersonic jet spectroscopy
[DE88-004438] N88-20392
Coherence effects in optical physics with special reference to spectroscopy
[AD-A189520] N88-21007
Development and evaluation of instrumentation and methods for multi-element analysis
[AD-A189345] N88-21018
SPECTRUM ANALYSIS
Elemental composition of Venusian rocks in northeastern part of Terra Aphrodite (determined using data from Vega-2 landing module) N88-20322
Analysis of hydrocarbon band 3.35 in spectrum of Halley's Comet using data from infrared spectrometer on Vega-1 spacecraft N88-20327
Spectral contents readout of birefringent sensors
[NASA-CR-179430] N88-20673
Stratospheric trace gas distributions from fair infrared thermal emission spectroscopy N88-20749
Planetary scale barotropic spectral model N88-20766
Computer programs for calculating group cross-section covariances from uncertainty parameters in the ENDF/B-V format. UNC 32/33 --- neutron physics
[ECN-202] N88-20995
Development and evaluation of instrumentation and methods for multi-element analysis
[AD-A189345] N88-21018
SPEECH RECOGNITION
The acoustic-modeling problem in automatic speech recognition
[AD-A188529] N88-20510
SPHERES
Simulated impact damage in a thick graphite/epoxy laminate using spherical indenters
[NASA-TM-100539] N88-20363
SPIN DYNAMICS
The effect of combustion gas flow on the rotational dynamics of a spinning solid fuel rocket N88-20358
SPOILERS
Air-jet spoiler
[BU-364] N88-20299
SPUTTERING
Properties of reactively sputtered WNx films Zhao, X. -A.
[AD-A188711] N88-20976
Superconducting superlattice structures
[DE88-005346] N88-21058
A novel method for sputter-deposition of high T(sub c) superconductor films via a computer-controlled mass analyzed ion beam
[DE88-006001] N88-21064
STABILITY
An experimental investigation of the flap-lag-torsion aeroelastic stability of a small-scale hingeless helicopter rotor in hover
[NASA-TP-2546] N88-20257
Some properties of Australian produced explosive composition H-6
[MRL-TN-525] N88-20490
Numerical experiments on the stability of controlled boundary layers
[NASA-CR-181649] N88-20591
STABILITY AUGMENTATION
A wind tunnel model with dynamic control
[BU-352] N88-20310
STABILIZED PLATFORMS
Vega-1 and Vega-2 automatic stations: Functioning of flyby vehicles during encounter with Halley's comet N88-20314
STABLE OSCILLATIONS
Mode priming in an overmoded gyrotron oscillator
[AD-A189151] N88-20602
STAINLESS STEELS
Hydrogen induced cracks in armor steel weldments fabricated with austenitic filler alloys
[AD-A188733] N88-20406
Use of the LLNL 40 kV electric gun to study the shock response of 21-6-9 stainless steel
[DE87-014550] N88-20418
Creep behavior of consolidated rapidly solidified Type 304 stainless steel powder containing helium
[DE88-005536] N88-20424
Study of defects in metals by positron annihilation
[DE88-701042] N88-20432
STANDARDIZATION
European approaches in standard spectrum development --- aircraft load spectra
[NLR-MP-87007-U] N88-20661
STANDARDS
Standardized environmental fatigue sequence for the evaluation of composite components in combat aircraft (ENSTAFF = ENvironmental faiSTAFF)
[LBF-FB-179] N88-20300
Orbital transfer vehicle concept definition and system analysis study. Volume 2: OTV concept definition and evaluation. Book 1: Mission and system requirements
[NASA-CR-179321] N88-20339
The preparation, assembly and mounting of RF coaxial cables
[ESA-PSS-01-718-ISS-1] N88-20504
STARBURST GALAXIES
Galaxy evolution in dense clusters N88-21101
STARS
Galaxy evolution in dense clusters N88-21101
STATIC STABILITY
Material instabilities in solids
[AD-A189525] N88-20388
STATIC TESTS
Static performance of an axisymmetric nozzle with post-exit vanes for multiaxis thrust vectoring
[NASA-TP-2800] N88-20280
STATICS
Research in applied mathematics ralated to identification of noisy systems
[AD-A189355] N88-20908
STATISTICAL ANALYSIS
Statistical considerations of graphite strength for assessing design allowable stresses N88-20441
Statistical signal processing using a class of iterative estimation algorithms
[AD-A189050] N88-20511
HF (High Frequency) Maximum Usable Frequency (MUF) model uncertainty assessment
[AD-A189132] N88-20513
Tests for uniformity arising from a series of events
[AD-A189069] N88-20935
Stochastic comparisons of order statistics, with applications in reliability
[AD-A189408] N88-20938
Application of expert systems in project management decision aiding
[NASA-CR-180762] N88-21074
STATISTICAL MECHANICS
Integral equation theory of polymer blends
[DE88-005305] N88-20471
STEELS
Hydrogen embrittlement of gun steel
[AD-A188972] N88-20407
Non-destructive evaluation techniques applied to the study of fatigue microcrack growth in steel alloys
[DE88-004090] N88-20420

Transformation, metallurgical response and behavior of the weld fusion zone and heat affected zone in Cr-Mo steels for fossil energy application
[DE88-006037] N88-20430
Corrosion-wear process under rolling-sliding motion
[AD-A189603] N88-20835

STEERING
Aberrations: Their effect on off-axis beam steering
[AD-A189601] N88-21008

STELLAR ENVELOPES
Polarization properties of SiO masers N88-21113

STELLAR MAGNETIC FIELDS
Polarization properties of SiO masers N88-21113

STELLAR MASS EJECTION
Magnetohydrodynamic (MHD) simulation of solar prominence formation N88-21109

STELLAR MODELS
Galaxy evolution in dense clusters N88-21101

STELLAR SPECTROPHOTOMETRY
Preparation of photometric measurements on a million stars in the framework of the satellite project HIPPARCOS/TYCHO
[ETN-88-91502] N88-21093

STELLAR SYSTEMS
Asymptotic giant branch populations in composite stellar systems N88-21098

STELLAR TEMPERATURE
The astrophysics of nebulae and active galactic nuclear emission-line regions: New methods and applications N88-21111

STELLARATORS
Comparison of analytic and full guiding center behavior at a trapped-passing interface in stellarators
[DE88-004174] N88-21025
Helical ripple transport in stellarators at low collision frequency
[DE88-006431] N88-21031

STIMULATED EMISSION
Stimulated Emission of Energetic Particles (SEEP)
[AD-A188724] N88-21094

STIMULATION
Phase preservation cleanup in a double-pass Raman amplifier SBS (Stimulated Brillouin Scattering) conjugator
[AD-A189428] N88-20536

STOCHASTIC PROCESSES
On relaxation algorithms based on Markov random fields
[AD-A189043] N88-20840
Stochasticity in nonlinear Hamiltonian systems
[DE88-005499] N88-20915
Stochastic comparisons of order statistics, with applications in reliability
[AD-A189408] N88-20938
Stochastic and chaotic oscillations
[CWI-AM-R8704] N88-20940

STOKES LAW (FLUID MECHANICS)
Boundary effects on the drag of a cylinder in axial motion at low Reynolds number N88-20578

STOPPING
Algorithms with conic termination for nonlinear optimization
[DE88-005893] N88-20851
Merge and termination in process algebra
[CWI-CS-R8716] N88-20918

STORAGE BATTERIES
A novel class of positive electrodes for rechargeable batteries
[DE88-004559] N88-20545

STRAIN HARDENING
Processing, structure and properties of heavily deformed in situ composites
[AD-A189611] N88-20416

STRAIN MEASUREMENT
Correlation of data on strain accumulation adjacent to the San Andreas Fault with available models
[NASA-CR-180757] N88-20742

STRAPDOWN INERTIAL GUIDANCE
Utilization of strapdown inertial and non-inertial sensors in determination of satellite attitude by Kalman filters
[INPE-4313-TDL/280] N88-20349

STRATEGY
Alternative force structuring strategies for military satellite communication systems
[AD-A189492] N88-20516
Parallel image compression
[NASA-CR-180758] N88-20837
Johnson Space Center's strategic game plan: Charting a course to the year 2000 and beyond
[NASA-TM-89733] N88-21076

STRATIFICATION
Dynamics of the Oceanic Surface Mixed Layer
[AD-A188348] N88-20785
Structures and fluxes in a deep convecting mixed layer N88-20786
Equatorial turbulence: Mixed layer and thermocline N88-20787
On the zonal momentum balance at the equator N88-20788
The mixed layer of the western equatorial Pacific Ocean
[HIG-1861] N88-20789
Unsteady shallowing mixed layer N88-20791
Horizontal scales of wind forced inertial motions N88-20795
Subduction N88-20796
Hamiltonian description of the interaction of surface waves with mixed-layer currents N88-20799
Monitoring ocean surface layer processes N88-20801

STRATIFIED FLOW
Mushroom-shaped currents (eddy dipoles) under rotation and stratification conditions N88-20678

STRATOSPHERE
Stratospheric trace gas distributions from fair infrared thermal emission spectroscopy N88-20749

STREAM FUNCTIONS (FLUIDS)
Resonant Alfven wave instabilities driven by streaming fast particles N88-21104

STRESS (PHYSIOLOGY)
Plasma cortisol, renin and aldosterone during an intense heat acclimation program
[AD-A189387] N88-20810

STRESS ANALYSIS
Delamination stresses in semicircular laminated composite bars
[NASA-TM-4026] N88-20375

STRESS CONCENTRATION
Cyclic crack growth emanating at a round notch considering viscoplasticity
[AD-A189577] N88-20655

STRESS CORROSION
Aircraft corrosion problems and research in the Netherlands
[NLR-MP-86066-U] N88-20427

STRESS CORROSION CRACKING
Stress corrosion cracking and metal-induced embrittlement: Comparative studies of local chemistries
[DE88-003235] N88-20419

STRESS DISTRIBUTION
Local refinement of stress field by finite element method
[INPE-4321-TDL/288] N88-20930

STRESS FUNCTIONS
Non- and semi-parametric maximum likelihood estimators and the von Misis Method, part 1
[CWI-MS-R8709] N88-20941

STRESS INTENSITY FACTORS
Threshold fatigue crack growth in Ti-6Al-2Sn-4Zr-6Mo
[AD-A189560] N88-20415

STRESS-STRAIN RELATIONSHIPS
Development of a constitutive equation for HSLA (High-Strength Low-Alloy)-100 at cryogenic temperatures
[AD-A189243] N88-20408
Parametric study of acceleration-induced stresses and frequency changes in doubly-rotated crystal resonators
[AD-A189261] N88-20532
Body tensor formalism in finite deformation elasticity and application to the torsion of a circular cylinder N88-20651
Improvement of the Reynolds-stress model by a new pressure-strain correlation
[NASA-CR-182699] N88-20667

STRESSES
Thermal oxide growth on silicon: Intrinsic stress and silicon cleaning effects
[AD-A188790] N88-20377

STRING THEORY
String theory and algebraic geometry of moduli spaces
[CWI-PM-R8705] N88-21070
Introduction to classical mechanics of systems with constraints, part 3
[TI88-701057] N88-21073
Early reheating and cosmic strings N88-21103

STRINGS
Verification of a systolic algorithm for string comparison
[CWI-CS-R8734] N88-20873

STRONGLY COUPLED PLASMAS
Development and evaluation of instrumentation and methods for multi-element analysis
[AD-A189345] N88-21018

STRUCTURAL ANALYSIS
A correlation study of X-29A aircraft and associated analytical development
[NASA-TM-89735] N88-20296
Viscoelastic behavior of a polyetheretherketone (PEEK) composite
[AD-A189545] N88-20368
Materials Research Laboratory at Brown University
[AD-A188006] N88-20396
A fundamental understanding of the effect of alloying elements on the corrosion resistance of rapidly solidified Mg alloys
[AD-A189385] N88-20413
Recent developments in nondestructive evaluation for structural ceramics
[DE88-005889] N88-20473
Time-domain system for identification of the natural resonant frequencies of aircraft relevant to electromagnetic compatibility testing
[PB88-164520] N88-20519
Control of structure in turbulent flows: Bifurcating and blooming jets
[AD-A189607] N88-20562
Structural clearances and internal friction: Simulation by Eigen distortions
[ISSN-0208-5658] N88-20640
Sixteenth NASTRAN (trademark) Users' Colloquium
[NASA-CP-2505] N88-20652
A preliminary investigation of finite-element modeling for composite rotor blades
[NASA-TM-100559] N88-20656
Component mode synthesis using experimental modes enhanced by mass loading
[DE88-006097] N88-20657
Finite element methodology for nonlinear free and harmonic forced vibrations of beam and plate structures N88-20663
Fluid-thermal-structural study of aerodynamically heated leading edges
[NASA-TM-100579] N88-20666
Analysis of shell-type structures subjected to time-dependent mechanical and thermal loading
[NASA-CR-182705] N88-20668
Activities report of the Structures Department
[ETN-88-91986] N88-20672
Microwave and structural properties of saline ice
[AD-A189307] N88-20779
Biophysical applications of solid state and tritium NMR
[DE88-005328] N88-20806
Robustifying the Kalman filter
[AD-A189240] N88-20907
The synthesis, characterization and structural studies of In(C5H4Me) by X-ray diffraction and electron diffraction techniques and a reinvestigation of the crystalline state of In(C5H5) by X-ray diffraction studies
[AD-A189110] N88-21038
Exploring the relation between interface structure and mechanical properties in multilayer structures
[DE88-005428] N88-21060

STRUCTURAL BASINS
Bathymetric hazard survey test
[AD-A189150] N88-20775

STRUCTURAL DESIGN
Orbital transfer vehicle concept definition and system analysis study. Volume 2: OTV concept definition and evaluation. Book 1: Mission and system requirements
[NASA-CR-179321] N88-20339
Development of isostatic mounts and associated guidelines --- spacecraft payloads
[CASA-IM-WP-301] N88-20354
X-ray computed tomography for structural ceramic applications: Beam hardening corrections
[DE88-005891] N88-20474
Aluminum-air battery development
[DE88-006617] N88-20542
Structural clearances and internal friction: Simulation by Eigen distortions
[ISSN-0208-5658] N88-20640
Potential off-normal events and associated radiological source terms for the compact ignition tokamak: Fusion Safety Program
[DE88-004112] N88-21024
Space infrared telescope facility wide field and diffraction limited array camera (IRAC)
[NASA-CR-182704] N88-21092

STRUCTURAL DESIGN CRITERIA
How to generate equal probability design load conditions --- aircraft design
[NLR-TR-86060-U] N88-20295

STRUCTURAL FAILURE
Buckling and breakdown problems in structural mechanics. Failure of prestressed double-walled containers or rings
[MBB-UR-E-956/87] N88-20671

STRUCTURAL PROPERTIES (GEOLOGY)
Relationship between oceanic geological formations and tectonic structures N88-20683

STRUCTURAL RELIABILITY
Structural integrity of metallic armature rail guns
[AD-A188735] N88-20333

STRUTS
An investigation of classical dynamic scaling techniques applied to an oleo-pneumatic landing gear strut
[AD-A187664] N88-20292

SUBDUCTION (GEOLOGY)
Relationship between oceanic geological formations and tectonic structures N88-20683
SUBMARINES
A pyrotechnic delay ignition system for a submarine launched marine signal
[MRL-R-1079] N88-20487
SUBROUTINES
Computer programs for calculating group cross-section covariances from uncertainty parameters in the ENDF/B-V format. UNC 32/33 — neutron physics
[ECN-202] N88-20995
SUBSONIC FLOW
Numerical simulation of subsonic and transonic propeller flow
[NASA-TM-100163] N88-20262
ARSPNSC: A method to calculate subsonic steady and unsteady potential flow about complex configurations
[NLR-TR-86122-U] N88-20265
Finite element calculations for aerodynamic coefficients of a 3-dimensional body in subsonic flow using Green's function method
[NASA-TT-20208] N88-20272
SUBSTRATES
Research on mercury cadmium telluride
[AD-A189155] N88-21039
X-ray diffraction study of a thin GaAs film on Si(100)
[DE88-005290] N88-21055
SULFIDATION
Oxidation/sulfidation of materials in an SO3/SO2/O2 thermochemical-transport, distributed-receiver, solar-energy system
[DE88-005875] N88-20739
SULFONES
Reinforcing of thermoplastic polycarbonate and polysulfone with carbon fibers: Production and characteristics of UD-compound objects
[NASA-TT-20158] N88-20374
SULFUR FLUORIDES
Pseudo-stationary oblique-shock-wave reflections in low gamma gases: Isobutane and sulphur hexafluoride
[UTIAS-TN-267] N88-20576
SUN
Solar microwave radiation maps measured at Metsaehovi Radio Research Station in 1978-1979
[PB88-127543] N88-21108
SUNSPOT CYCLE
Development of high stability fiber optic spectrophotometric systems for study of solar/stellar magnetic activity
[AD-A189327] N88-21086
SUPERCOMPUTERS
A report on the study of algorithms to enhance vector computer performance for the discretized one-dimensional time-dependent heat conduction equation: EPIC research, phase 1
[DE88-005642] N88-20880
Activities report of the Toulouse Research Center
[ETN-88-91988] N88-21077
SUPERCONDUCTING SUPER COLLIDER
Physics at large transverse momenta
[DE88-005758] N88-20986
SUPERCONDUCTIVITY
Progress in diagnostic techniques for SC cavities
[CEBAF-PR-88-003] N88-20600
Large momentum pairing in one-dimensional systems
[AD-A189228] N88-20981
Theoretical studies on the electronic structure and properties of complex ceramic crystals and glasses
[DE88-005837] N88-21049
Competing interactions in metallic superlattices
[DE88-005344] N88-21057
Superconducting superlattice structures
[DE88-005346] N88-21058
SUPERCONDUCTORS
Large momentum pairing in one-dimensional systems
[AD-A189228] N88-20981
The relationship of the chemical bonding topology of high critical temperature copper oxide superconductors to that of the chevrel phases and the ternary lanthanide rhodium borides
[AD-A189255] N88-21042
Discussion of radiation effects and high-temperature oxide superconductors
[DE88-001427] N88-21046
A hydroxycarbonate route to superconductor precursor powders
[DE88-003638] N88-21052
Superconducting superlattice structures
[DE88-005346] N88-21058
A novel method for sputter-deposition of high T(sub c) superconductor films via a computer-controlled mass analyzed ion beam
[DE88-006001] N88-21064
SUPERCRITICAL FLUIDS
Supercritical fluid chromatography/supersonic jet spectroscopy
[DE88-004436] N88-20392
Development and evaluation of supercritical fluid chromatography-mass spectrometry
[DE88-005122] N88-20394
SUPERLATTICES
Silicon-germanium heterostructures N88-21034
Photon-controlled growth of multilayered structures
[DE88-005061] N88-21054
Competing interactions in metallic superlattices
[DE88-005344] N88-21057
Superconducting superlattice structures
[DE88-005346] N88-21058
SUPERNOVA 1987A
Particle physics and cosmology
[DE88-004944] N88-21096
SUPERPLASTICITY
Micromechanical and microstructural studies of ceramic superplasticity
[DE88-005793] N88-20472
SUPERSONIC AIRCRAFT
The design and use of a temperature-compensated hot-film anemometer system for boundary-layer flow transition detection on supersonic aircraft
[NASA-TM-100421] N88-20304
SUPERSONIC COMBUSTION
Interaction between two-dimensional sonic jets and supersonic flow to model heat addition in a supersonic combustor
[AD-A189572] N88-20261
SUPERSONIC COMBUSTION RAMJET ENGINES
Active cooling design for scramjet engines using optimization methods
[NASA-TM-100581] N88-20689
SUPERSONIC FLOW
Nonaxisymmetric body supersonic, aerodynamic prediction
[AD-A189338] N88-20259
Interaction between two-dimensional sonic jets and supersonic flow to model heat addition in a supersonic combustor
[AD-A189572] N88-20261
Tests on the AFWAL 65 deg delta wing at NLR: A study of vortex flow development between Mach = 0.4 and 4
[NLR-MP-86058-U] N88-20266
The international vortex flow experiment: A test case for compressible Euler codes
[NLR-MP-86076-U] N88-20267
Supercritical fluid chromatography/supersonic jet spectroscopy
[DE88-004438] N88-20392
SUPERSONIC SPEED
Nonaxisymmetric body supersonic, aerodynamic prediction
[AD-A189338] N88-20259
SUPPORTS
Development of isostatic mounts and associated guidelines — spacecraft payloads
[CASA-IM-WP-301] N88-20354
SUPPRESSORS
Kinetic mechanisms for ionization and afterburning suppression
[AD-A189219] N88-20383
SURFACE ACOUSTIC WAVE DEVICES
Measuring thin film properties using SAW (Surface Acoustic Wave) devices: Diffusivity and surface area
[DE88-002216] N88-20970
SURFACE DEFECTS
Ultrasonic inspection of irregular surfaces
[AERE-R-12465] N88-20648
SURFACE LAYERS
Characterization of redox states of nickel hydroxide film electrodes by in-situ Raman spectroscopy
[AD-A189288] N88-20411
Vertical turbulent transfer of matter in thin ocean surface layer during daytime heating N88-20693
SURFACE NAVIGATION
A comparison of terrain association and resection as methods of position location
[AD-A189480] N88-20710
SURFACE PROPERTIES
A study of the interaction of light with sub-micron metallic surfaces
[DE88-003138] N88-20624
Computer aided surface representation
[DE88-005408] N88-20854
Optics for large telescope N88-21014
Hydrogen pumping and release by graphite under high flux plasma bombardment
[DE88-005880] N88-21021
SURFACE REACTIONS
Photochemistry at structured surfaces: A classical electromagnetic approach
[AD-A189519] N88-20387
Model catalyst studies of SMSI (Strong Metal/Support Interactions) and the role of D-electrons in chemisorption and catalysis
[DE88-004518] N88-20393
SURFACE TEMPERATURE
Radiative processes affecting ocean mixed-layer heat content and their monitoring from satellite N88-20800
Monitoring ocean surface layer processes N88-20801
SURFACE VEHICLES
Feasibility report: Operation of light air cushion vehicle at McMurdo Sound, Antarctica
[AD-A189057] N88-20494
SURFACE WAVES
Energy and momentum fluxes through the sea surface N88-20798
Hamiltonian description of the interaction of surface waves with mixed-layer currents N88-20799
SURFACES
Calculation of the distributed loads on the blades of individual multiblade propellers in axial flow using linear and nonlinear lifting surface theories
[NASA-TT-20173] N88-20278
SURVEILLANCE
Specification for an infrared satellite surveillance system for the detection of aircraft
[AD-A189592] N88-20746
A preliminary assessment of thunderstorm outflow wind measurement with airport surveillance radars
[AD-A189064] N88-20757
SURVIVAL
Survival analysis using additive risk models
[AD-A189053] N88-20906
SUSPENDING (MIXING)
Velocity and concentration measurements in flowing suspensions by nuclear magnetic resonance
[DE88-006225] N88-20589
SWEEP FREQUENCY
Material parameter measurements at high temperatures
[NASA-CR-182707] N88-20397
SWEPT FORWARD WINGS
A correlation study of X-29A aircraft and associated analytical development
[NASA-TM-89735] N88-20296
SWEPT WINGS
Development of disturbances in swept wing flows
[NASA-CR-182675] N88-20574
Preliminary in-flight boundary layer transition measurements on a 45 deg swept wing at Mach Numbers between 0.9 and 1.8
[NASA-TM-100412] N88-20598
SWITCHING
Two queues with alternating service and switching times
[CWI-OS-R8712] N88-20949
SYMMETRY
A symmetric set of Euler angles and oblique orientation space sections
[DE88-005317] N88-21056
SYNCHRONISM
On proving register atomicity
[CWI-CS-R8707] N88-20862
A survey of provably correct fault-tolerant clock synchronization techniques
[NASA-TM-100553] N88-20894
SYNCHRONIZED OSCILLATORS
Mode priming in an overmoded gyrotron oscillator
[AD-A189151] N88-20802
SYNCHROTRON RADIATION
Applications of the lateral shearing interferometer in measurement of synchrotron radiation optical elements
[DE88-005184] N88-21011
SYNOPTIC METEOROLOGY
Dynamics of synoptic ocean eddies N88-20689
SYNTAX
A parser generator for finitely ambiguous context-free grammars
[CWI-CS-R8712] N88-20864
SYNTHESIS (CHEMISTRY)
Synthesis of energetic materials
[AD-A189115] N88-20482
A hydroxycarbonate route to superconductor precursor powders
[DE88-003638] N88-21052
SYNTHETIC FUELS
Engine testing for synfuel operation
[DE88-006044] N88-20645
SYSTEMS ANALYSIS
Study of the optimization of satellite system design for transfer orbit
[MBB-URV-135] N88-20332
Solar dynamic power system definition study
[NASA-CR-180877] N88-20361
Activities report of the Systems Department
[ETN-88-91987] N88-20505

Coherent laser radar system theory
[AD-A188759] N88-20812
On the sensitivity of complex, internally coupled systems
[NASA-TM-100537] N88-20829
MacCAD (Macintosh Computer Aided Design), computer aided design tool for system analysis
[AD-A189241] N88-20843
Further results on the McMillan degree and the Kronecker indices of ARMA models --- input-output relations of linear systems
[EUT-87-E-175] N88-20925
MANPRINT handbook for RFP (Request For Proposal) development
[AD-A188321] N88-21075

SYSTEMS ENGINEERING
Activities report of the Systems Department
[ETN-88-91987] N88-20505
The acoustic-modeling problem in automatic speech recognition
[AD-A188529] N88-20510

SYSTEMS SIMULATION
AVSCOM'S modifications to Teledyne Systems Company's air-to-air fire control system simulation model
[AD-A189136] N88-20294
SIMSAT: Simulation package for flexible systems. Beams in space
[TW-278] N88-20348
Activities report of the Systems Department
[ETN-88-91987] N88-20505
Model structure selection for multivariable systems by cross-validation methods
[EUT-87-E-176] N88-20926

SYSTEMS STABILITY
Modelling and control of an annular momentum control device
[NASA-CR-4138] N88-20491

T

TAKEOFF
Flight simulator experiments concerning take-off visibility minima
[NLR-TR-86050-U] N88-20281

TAR SANDS
Aviation turbine fuels from tar sands bitumen and heavy oils. Part 3: Laboratory sample production
[AD-A189278] N88-20484

TARGET RECOGNITION
Analysis of spectral reflectance characteristics of targets under satellites and automatic cloud recognition N88-20498
Passive autonomous infrared sensor technology
[AD-A188698] N88-21005

TARGETS
Properties of reactively sputtered WNx films Zhao, X. -A.
[AD-A188711] N88-20976

TASK COMPLEXITY
Distraction and inhibition in continuous CRT performance: A replication and some new findings
[PB88-150941] N88-20821

TASKS
The space station assembly phase: Flight telerobotic servicer feasibility. Volume 2: Methodology and case study
[NASA-CR-182690] N88-20352
Lifting and carrying capacities relative to physical fitness measures
[AD-A189305] N88-20808
Proceedings of the Workshop on the Assessment of Crew Workload Measurements Methods, Techniques and Procedures. Volume 1: Preliminary Selection of Measures
[AD-A189004] N88-20827
Method to evaluate image-recovery algorithms based on task performance
[DE88-005382] N88-20853

TECHNOLOGICAL FORECASTING
Study on long term evolution Towards European Autonomous Manned Spaceflight (STEAMS)
[SNIAS-SE/LS/AP-35-073] N88-20330

TECHNOLOGIES
JPRS report: Science and technology. China
[JPRS-CST-88-003] N88-20495
JPRS report: Science and technology. China
[JPRS-CST-87-030] N88-20501

TECHNOLOGY ASSESSMENT
A review of technologies applicable to low-speed flight of high-performance aircraft investigated in the Langley 14- x 22-foot subsonic tunnel
[NASA-TP-2796] N88-20264
Spacecraft fire-safety experiments for space station: Technology development mission
[NASA-CR-182114] N88-20353
A comparative assessment of US and UK explosives qualified as replacements for tetryl
[MRL-R-1094] N88-20486
Cryogenic Fluid Management Technology Workshop. Volume 2: Roundtable Discussion of Technology Requirements
[NASA-CP-10009] N88-20599
The evaluation of automatic barometers, illustrated by the Nakaasa barometer
[KNMI-TR-95] N88-20610
Power from the sun: Principles of high temperature solar thermal technology
[DE87-001104] N88-20736
Biophysical applications of solid state and tritium NMR
[DE88-005328] N88-20806
The concept of intelligent integrated interactive CAD systems
[CWI-CS-R8717] N88-20865
Energy loss of particles in dense matter-calorimetry
[NIKHEF-H/87-12] N88-20988
Johnson Space Center's strategic game plan: Charting a course to the year 2000 and beyond
[NASA-TM-89733] N88-21076

TECHNOLOGY TRANSFER
Technology '87: Research and Development Laboratory Technology Transfer Program
[DE88-003142] N88-21084
Spin off businesses as mechanisms for transferring technologies
[DE88-005640] N88-21085
Applicability of aerospace thermal insulation technologies to the civilian sector
[DE88-003717] N88-21086

TECHNOLOGY UTILIZATION
Johnson Space Center's strategic game plan: Charting a course to the year 2000 and beyond
[NASA-TM-89733] N88-21076

TECTONICS
Crustal dynamics project data analysis, 1987. Volume 2: Mobile VLBI geodetic results 1982-1986
[NASA-TM-100689-VOL-2] N88-20753
Experimental and theoretical constraints on the origin of mid-ocean ridge geothermal fluids N88-20784

TELECOMMUNICATION
A simulation study of a parallel processor with unbalanced loads
[AD-A189573] N88-20887

TELEOPERATORS
The space station assembly phase: Flight telerobotic servicer feasibility, volume 1
[NASA-CR-182689] N88-20351
The space station assembly phase: Flight telerobotic servicer feasibility. Volume 2: Methodology and case study
[NASA-CR-182690] N88-20352

TELESCOPES
Optics for large telescope N88-21014
Very high energy gamma ray astrophysics
[DE88-005821] N88-21095

TEMPERATURE COMPENSATION
The design and use of a temperature-compensated hot-film anemometer system for boundary-layer flow transition detection on supersonic aircraft
[NASA-TM-100421] N88-20304

TEMPERATURE CONTROL
Moveable thermal joints for deployable or steerable spacecraft radiator systems
[NLR-MP-87016-U] N88-20347
Feasibility demonstration of a sensor for high-quality two-phase flow --- Space Station
[NLR-TR-87009-U] N88-20569
Development, manufacturing and testing of a gas-loaded variable conductance methanol heat pipe
[NLR-MP-87010-U] N88-20571

TEMPERATURE DISTRIBUTION
Roys and radiosondes in the region
[INPE-4362-PRE/1188] N88-20743
Arcs in cesium seeded noble gases resulting from a magnetically induced electric field
[EUT-87-E-177] N88-21028

TEMPERATURE EFFECTS
The fatigue behavior of ferritic and austenitic steels at elevated temperatures
[DE88-006304] N88-20431
The calibration of photographic and spectroscopic films: Reciprocity failure and thermal responses of IIaO film at liquid nitrogen temperatures
[NASA-CR-181094] N88-20606
A study of the dynamics of high temperature brittle intergranular fracture by acoustic emission
[AERE-R-12479] N88-20650

TEMPERATURE GRADIENTS
Vertical turbulent transfer of matter in thin ocean surface layer during daytime heating N88-20693
The mixed layer of the western equatorial Pacific Ocean
[HIG-1881] N88-20789

TEMPERATURE MEASUREMENT
Exhaust-gas pressure and temperature survey of F404-GE-400 turbofan engine
[NASA-TM-88273] N88-20307
Measurement of detonation temperature of hydrogen-oxygen mixture by CARS (Coherent Anti-Stokes Raman Spectroscopy)
[NASA-TT-20227] N88-20398
Remote fiber fluorimetry techniques for pressure measurements
[DE88-004486] N88-20604
Noncontact thermometry via laser pumped, thermographic phosphors: Characterization of systematic errors and industrial applications
[DE88-005599] N88-20628
Phenomenological description of eddy registered in Gulf Stream N88-20694
Monitoring ocean surface layer processes N88-20801
On the structure of pulsed plasma jets N88-21030
The astrophysics of nebulae and active galactic nuclear emission-line regions: New methods and applications N88-21111

TENSILE PROPERTIES
Development of a constitutive equation for HSLA (High-Strength Low-Alloy)-100 at cryogenic temperatures
[AD-A189243] N88-20408
The effect of microstructure on the fatigue crack growth resistance of nickel base superalloys
[AD-A189526] N88-20414

TENSILE STRENGTH
Materials Research Laboratory at Brown University
[AD-A188006] N88-20396
A direct correlation of strength with impact velocity
[AD-A189251] N88-20409
Use of reinforced inorganic cement materials for spark wire and drift chamber wire frames
[NASA-CR-180759] N88-20438
The statistical characterization of tensile strengths for a nuclear-type graphite N88-20440
Statistical considerations of graphite strength for assessing design allowable stresses N88-20441
High temperature Young's modulus of IG-110 graphite N88-20443
Dynamic tensile cyclic fatigue of Si3N4
[DE88-003919] N88-20658

TENSILE STRESS
Fracture criterion of reactor graphite under multiaxial stresses N88-20442

TENSILE TESTS
Development of a constitutive equation for HSLA (High-Strength Low-Alloy)-100 at cryogenic temperatures
[AD-A189243] N88-20408
High temperature Young's modulus of IG-110 graphite N88-20443
Notch sensitivity of graphite materials for VHTR N88-20447

TENSORS
Body tensor formalism in finite deformation elasticity and application to the torsion of a circular cylinder N88-20651

TERRAIN ANALYSIS
A comparison of terrain association and resection as methods of position location
[AD-A189480] N88-20710
Remote sensing of earth terrain
[NASA-CR-182677] N88-20711
Interpolation algorithms for digital terrain models
[INPE-4373-PRE/1196] N88-20877

TEST FACILITIES
Aircraft flight flutter testing at the NASA Ames-Dryden Flight Research Facility
[NASA-TM-100417] N88-20301
Western aeronautical test range real-time graphics software package MAGIC
[NASA-TM-100425] N88-20506
Overview of recent activities in the Heat Cycle Research Program
[DE88-005544] N88-20738
Configuration management issues and objectives for a real-time research flight test support facility
[NASA-TM-100437] N88-20832
Activities report of the Physics Department
[ETN-88-91985] N88-20964

TETHERLINES
Theoretical investigation of EM wave generation and radiation in the ULF, ELF and VLF bands by the electrodynamic orbiting tether
[NASA-CR-182720] N88-20529

TETRYL
A comparative assessment of US and UK explosives qualified as replacements for tetryl
[MRL-R-1094] N88-20486

Recommended replacements for tetryl in Australian production fuzes and related ordnance
[MRL-R-1089] N88-20489

TEXTURES
Texture profile in thermomechanically processed 2-inch-thick 5 Ni-steel armor plate
[AD-A189275] N88-20410
Micromechanical and microstructural studies of ceramic superplasticity
[DE88-005793] N88-20472
A symmetric set of Euler angles and oblique orientation space sections
[DE88-005317] N88-21056

THALLIUM ALLOYS
Studies of transverse phonon modes in premartensitic indium-thallium alloys
[DE88-003481] N88-20428

THEOREM PROVING
A proof rule process creation
[CWI-CS-R8710] N88-20891

THERAPY
The effects of normal and therapeutic baths on the central vascular organs of persons with healthy hearts, as measured by X-ray
[NASA-TT-20252] N88-20818

THERMAL ANALYSIS
Fluid-thermal-structural study of aerodynamically heated leading edges
[NASA-TM-100579] N88-20666
Analysis of shell-type structures subjected to time-dependent mechanical and thermal loading
[NASA-CR-182705] N88-20668

THERMAL BATTERIES
A case study of the development of a military specification - zirconium powder for thermal batteries
[AD-A188751] N88-20717

THERMAL CONDUCTIVITY
Effects of high temperature neutron irradiation on the physical, chemical and mechanical properties of fine-grained isotropic graphite N88-20444
A segmented calorimeter for low-energy particle beams in space
[DE88-001806] N88-20997
Guidelines for estimation and characterization of the thermo-mechanical properties of new optical materials
[DE88-004359] N88-21010

THERMAL CYCLING TESTS
Dynamic tensile cyclic fatigue of Si3N4
[DE88-003919] N88-20658
Overview of recent activities in the Heat Cycle Research Program
[DE88-005544] N88-20738

THERMAL DECOMPOSITION
Kinetics of polymer decomposition
[DE88-005500] N88-20460
Analytically modeling the carbothermic reduction of alumina in a thermal plasma
[DE88-005535] N88-21020

THERMAL DEGRADATION
Degradations of thermal shock resistance and the fracture toughness of reactor graphite subjected to neutron irradiation N88-20445
Interfacial chemistry-structure and fracture of ceramic composites
[DE88-005516] N88-20461

THERMAL DISSOCIATION
Quantitative determination of a hydrogen impurity in a sodium coolant by hydride thermal dissociation
[NASA-TT-20239] N88-20402

THERMAL EMISSION
Stratospheric trace gas distributions from fair infrared thermal emission spectroscopy N88-20749

THERMAL ENERGY
An assessment methodology for thermal energy storage evaluation
[DE88-004642] N88-20732

THERMAL EXPANSION
Effects of high temperature neutron irradiation on the physical, chemical and mechanical properties of fine-grained isotropic graphite N88-20444
Guidelines for estimation and characterization of the thermo-mechanical properties of new optical materials
[DE88-004359] N88-21010

THERMAL INSULATION
Applicability of aerospace thermal insulation technologies to the civilian sector
[DE88-003717] N88-21086

THERMAL PLASMAS
Analytically modeling the carbothermic reduction of alumina in a thermal plasma
[DE88-005535] N88-21020

THERMAL RESISTANCE
Degradations of thermal shock resistance and the fracture toughness of reactor graphite subjected to neutron irradiation N88-20445

THERMAL SHOCK
Degradations of thermal shock resistance and the fracture toughness of reactor graphite subjected to neutron irradiation N88-20445
Notch sensitivity of graphite materials for VHTR N88-20447

THERMAL STABILITY
A novel class of positive electrodes for rechargeable batteries
[DE88-004559] N88-20545

THERMIONICS
Thermionic Technology Program. A: Insulator test and evaluation
[DE88-004707] N88-20735

THERMOCLINES
Intrathermocline lens of Mediterranean water in tropical North Atlantic N88-20688
Dynamics of the Oceanic Surface Mixed Layer
[AD-A188348] N88-20785
Structures and fluxes in a deep convecting mixed layer N88-20786
Equatorial turbulence: Mixed layer and thermocline N88-20787
Subduction N88-20796
Wind forcing and observed oceanic wavenumber spectra N88-20797
Monitoring ocean surface layer processes N88-20801

THERMODYNAMIC COUPLING
Predictions and studies with a one-dimensional ice/ocean model
[AD-A189158] N88-20776

THERMODYNAMIC PROPERTIES
MOPAC manual: A general molecular orbital package, fourth edition
[AD-A188623] N88-20362
High-temperature metal matrix composites
[AD-A189516] N88-20367
Properties of molecular solids and fluids at high pressure and temperature
[DE88-004195] N88-20391
Liquid alloys: New perspectives and challenges
[DE88-005935] N88-20463
Thermodynamic theory of fluctuations and Rayleigh light scattering in solutions N88-20681
The thermodynamic properties of organic oxygen compounds
[DE88-001208] N88-21065
Rapid e-beam heating for measuring thermodynamics of metastable materials
[DE88-003565] N88-21066
Review of selenium thermodynamic data
[DE88-006194] N88-21068
Prediction of high-temperature thermodynamic properties of mixed electrolyte solutions including solubility equilibria, vapor pressure depression and boiling point elevation
[DE88-006344] N88-21069

THERMODYNAMICS
Oxidation/sulfidation of materials in an SO3/SO2/O2 thermochemical-transport, distributed-receiver, solar-energy system
[DE88-005875] N88-20739
Dynamical modeling of marine boundary layer convection N88-20750
Predicting oscillatory finite difference solutions to the heat equation: A comparative study of the coefficient and matrix methods
[AD-A189591] N88-20911
Two studies of nonlinear processes in irreversible thermodynamics
[DE88-005794] N88-21067

THERMOGRAPHY
Noncontact thermometry via laser pumped, thermographic phosphors: Characterization of systematic errors and industrial applications
[DE88-005599] N88-20628

THERMOMECHANICAL TREATMENT
Grain refinement during primary breakdown of alloy 718
[DE88-005193] N88-20423

THERMOPLASTIC RESINS
Reinforcing of thermoplastic polycarbonate and polysulfone with carbon fibers: Production and characteristics of UD-compound objects
[NASA-TT-20158] N88-20374

THERMOSETTING RESINS
High-temperature thermosets derived from the Diels-Alder polymerization of bisbenzocyclobutenes and bimaleimides
[AD-A188800] N88-20449
Optimization of binary pigment coatings
[AD-A189103] N88-20450

THERMOSPHERE
Effect of nitrogen dioxide release on thermosphere N88-20704

THICKNESS
Simulated impact damage in a thick graphite/epoxy laminate using spherical indenters
[NASA-TM-100539] N88-20363

THIN FILMS
Characterization of redox states of nickel hydroxide film electrodes by in-situ Raman spectroscopy
[AD-A189288] N88-20411
Improved methods for high resolution electron microscopy
[DE88-005731] N88-20609
Research on high-efficiency, stacked, multijunction, amorphous silicon alloy thin-film solar cells
[DE88-001108] N88-20723
CdZnTe as a wide-band-gap absorber for a tandem, thin-film solar cell
[DE88-001114] N88-20724
Stable, high-efficiency, CuInSe2-based, polycrystalline, thin-film tandem solar cells
[DE88-001116] N88-20726
Cadmium sulfide/copper ternary heterojunction cell research
[DE88-001122] N88-20727
Direct absorption receiver control studies
[DE87-013653] N88-20737
Measurement of the properties of lossy materials inside a finite conducting cylinder
[NASA-CR-182664] N88-20962
Measuring thin film properties using SAW (Surface Acoustic Wave) devices: Diffusivity and surface area
[DE88-002216] N88-20970
Thin-film diffusion barriers for metal-semiconductor contacts
[AD-A188712] N88-21035
Modulatable thin film field emission space gun
[AD-A189279] N88-21043
Thin-film cadmium telluride solar cells
[DE88-001107] N88-21050
X-ray diffraction study of a thin GaAs film on Si(100)
[DE88-005290] N88-21055
Superconducting superlattice structures
[DE88-005346] N88-21058
Initial stages of silicon growth on the (100) surface of silicon by localized laser CVD
[DE88-005420] N88-21059
A novel method for sputter-deposition of high T(sub c) superconductor films via a computer-controlled mass analyzed ion beam
[DE88-006001] N88-21064

THIN WALLED SHELLS
Analysis of shell-type structures subjected to time-dependent mechanical and thermal loading
[NASA-CR-182705] N88-20668
Reversed field pinch operation with a thin shell
[DE88-005521] N88-21027
Topics in curved and flat space electromagnetism N88-21100

THREAT EVALUATION
System for detecting objects that represent a threat
[NASA-TT-20244] N88-20528

THREE DIMENSIONAL BOUNDARY LAYER
General fuselage coordinates for the calculation of three-dimensional boundary layers
[MBB/LKE-122/S/PUB/244] N88-20596

THREE DIMENSIONAL FLOW
Numerical simulation of subsonic and transonic propeller flow
[NASA-TM-100163] N88-20262
The construction of a three-dimensional finite volume grid generator for a wing in a wind tunnel with application to Navier-Stokes flow solvers
[FFA-TN-1987-58] N88-20277
Three-dimensional shear layer experiments and their use as test cases for calculation methods
[NLR-MP-86036-U] N88-20570
Development of disturbances in swept wing flows
[NASA-CR-182675] N88-20574
Slip velocity method for three-dimensional compressible turbulent boundary layers
[NASA-TM-100586] N88-20592

THREE DIMENSIONAL MOTION
Simulation of measuring points for three dimensional measurements
[WPB-0115] N88-20883

THROTTLING
Integrated autopilot/autothrottle based on a total energy control concept: Design and evaluation of additional autopilot modes
[NASA-CR-4131] N88-20308

THRUST VECTOR CONTROL
Static performance of an axisymmetric nozzle with post-exit vanes for multiaxis thrust vectoring
[NASA-TP-2800] N88-20280
Optimal thrust vector control of coplanar orbital evasive maneuvers
[AD-A189544] N88-20346

THUNDERSTORMS
A preliminary assessment of thunderstorm outflow wind measurement with airport surveillance radars
[AD-A189064] N88-20757
Wind shear as a predictor of severe weather for the eastern United States
[PB88-157144] N88-20762
Upward propagating electric fields from thunderstorms and VLF transmitters N88-20767

TIBIA
Changes in the status of the human tibia during antiorthostatic hypokinesia
[NASA-TT-20221] N88-20813

TIDES
Tidal estimation in the Pacific with application to SEASAT altimetry
[NASA-TM-100694] N88-20780

TIME DEPENDENCE
Numerical model of the time independent mean flow in a rotating rocket motor N88-20360
The calibration of photographic and spectroscopic films: Reciprocity failure and thermal responses of IIaO film at liquid nitrogen temperatures
[NASA-CR-181094] N88-20606
Analysis of shell-type structures subjected to time-dependent mechanical and thermal loading
[NASA-CR-182705] N88-20668

TIME LAG
Sojourn times in feedback queues
[CWI-OS-R8710] N88-20947

TIN
Properties of reactively sputtered WNx films Zhao, X. -A.
[AD-A188711] N88-20976

TISSUES (BIOLOGY)
Biophysical applications of solid state and tritium NMR
[DE88-005328] N88-20806

TITANIUM ALLOYS
Threshold fatigue crack growth in Ti-6Al-2Sn-4Zr-6Mo
[AD-A189560] N88-20415

TITANIUM OXIDES
Model catalyst studies of SMSI (Strong Metal/Support Interactions) and the role of D-electrons in chemisorption and catalysis
[DE88-004518] N88-20393

TOKAMAK DEVICES
A high field launch for electron cyclotron heating using an external window
[DE88-005350] N88-21000
Observations on energy transport in tokamaks: A new formula for turbulent transport
[DE88-005309] N88-21019
Evolution of poloidal variation of impurity density and ambipolar potential in rotating tokamak plasma, part 1
[DE88-006263] N88-21022
Potential off-normal events and associated radiological source terms for the compact ignition tokamak: Fusion Safety Program
[DE88-004112] N88-21024

TOLLMEIN-SCHLICHTING WAVES
Development of disturbances in swept wing flows
[NASA-CR-182675] N88-20574

TOMOGRAPHY
A study of satellite emission computed tomography
[AD-A189567] N88-20745
Studies toward observing and modelling large energetic ocean regions
[AD-A189267] N88-20778
Survey of acoustic techniques for monitoring El Nino
[PB88-157615] N88-20783

TOPOGRAPHY
A comparison of terrain association and resection as methods of position location
[AD-A189480] N88-20710
Comparisons of global topographic/isostatic models to the Earth's observed gravity field
[NASA-CR-182696] N88-20752
Planetary scale barotropic spectral model N88-20766
Bathymetric hazard survey test
[AD-A189150] N88-20775

TOPOLOGY
Using design axioms and topology to model database semantics
[CWI-CS-R8711] N88-20863

TOROIDAL PLASMAS
Fully implicit three-dimensional MHD (magnetohydrodynamics) stability and evolution in toroidal geometry
[DE88-000624] N88-21023

TORQUE
Efficiency characteristics of speed modulated drives at predicted torque conditions for air-to-air heat pumps
[DE88-005846] N88-20588

TORSION
An experimental investigation of the flap-lag-torsion aeroelastic stability of a small-scale hingeless helicopter rotor in hover
[NASA-TP-2546] N88-20257
Development of a torsion balance for adhesion measurements
[NASA-TM-100799] N88-20454

TORUSES
Unfoldings of quasi-periodic tori
[ZW-8706] N88-20928
A high field launch for electron cyclotron heating using an external window
[DE88-005350] N88-21000

TOUGHNESS
Interaction of particulate and transformation toughening
[AD-A189321] N88-20412
Degradations of thermal shock resistance and the fracture toughness of reactor graphite subjected to neutron irradiation N88-20445

TOWED BODIES
Australian aerodynamic design codes for aerial tow bodies
[AD-A189048] N88-20258

TRACE ELEMENTS
Stratospheric trace gas distributions from fair infrared thermal emission spectroscopy N88-20749

TRACKING (POSITION)
An investigation of Doppler satellite positioning multi-station adjustment software N88-20345
Robustifying the Kalman filter
[AD-A189240] N88-20907

TRAJECTORY ANALYSIS
A method and measures to evaluate trackers for air traffic control
[NLR-TR-86072-U] N88-20287
Trajectory code studies, 1987
[DE88-006218] N88-20335

TRAJECTORY OPTIMIZATION
Optimal thrust vector control of coplanar orbital evasive maneuvers
[AD-A189544] N88-20346

TRANSFER FUNCTIONS
Elimination of quantifiers of linear variables and corresponding transfer principles
[DE88-005692] N88-20912

TRANSFER ORBITS
Study of the optimization of satellite system design for transfer orbit
[MBB-URV-135] N88-20332

TRANSFORMATIONS (MATHEMATICS)
Introduction to classical mechanics of systems with constraints, part 1
[TI88-701055] N88-20957
Introduction to classical mechanics of systems with constraints, part 2
[TI88-701056] N88-21072
Introduction to classical mechanics of systems with constraints, part 3
[TI88-701057] N88-21073

TRANSFORMERS
Optimum transformer design for a pulsed power system
[DE88-006054] N88-20525

TRANSIENT LOADS
Transient dynamics of fibre reinforced composite plates
[IIT-B/CE/RR/87-1] N88-20370

TRANSISTORS
Numerical methods in the resolution of control electrovalve model
[INPE-4154-RPE/540] N88-20554

TRANSITION FLOW
The design and use of a temperature-compensated hot-film anemometer system for boundary-layer flow transition detection on supersonic aircraft
[NASA-TM-100421] N88-20304

TRANSITION METALS
Transition metal cluster chemistry
[AD-A188731] N88-20405

TRANSITION TEMPERATURE
Rapid e-beam heating for measuring thermodynamics of metastable materials
[DE88-003565] N88-21066

TRANSMISSION
Development of fiber optic systems for recording and transmitting holographic information
[AD-A189406] N88-20603

TRANSMISSION LINES
Safety research of insulating materials of cable for nuclear power generating station
[NASA-TT-20202] N88-20477

TRANSONIC FLOW
Application of a flux vector splitting methodology towards the solution of unsteady transonic flows, with future emphasis on the blade flutter problem
[AD-A189500] N88-20260
Numerical simulation of subsonic and transonic propeller flow
[NASA-TM-100163] N88-20262
Tests on the AFWAL 65 deg delta wing at NLR: A study of vortex flow development between Mach = 0.4 and 4
[NLR-MP-86058-U] N88-20266
The international vortex flow experiment: A test case for compressible Euler codes
[NLR-MP-86076-U] N88-20267
Steady and unsteady transonic small disturbance analysis of realistic aircraft configurations
[NASA-TM-100557] N88-20269
An L-U implicit multigrid algorithm to solve the Euler equations for transonic flow in rotating turbomachinery passages N88-20270
An adaptive grid technique for solution of the Euler equations N88-20579
Multigrid solution of the Euler equations N88-20582

TRANSPORT PROPERTIES
Competing interactions in metallic superlattices
[DE88-005344] N88-21057

TRANSPORT THEORY
Propagator solutions of partial differential equations applied to plasma transport
[DE88-006432] N88-20852
Conservative finite volume solutions of a linear hyperbolic transport equation in two and three dimensions using multiple grids
[NASA-CR-182715] N88-20934

TRAPPED MAGNETIC FIELDS
Comparison of analytic and full guiding center behavior at a trapped-passing interface in stellarators
[DE88-004174] N88-21025

TRAPPED PARTICLES
Theory of laser cooling and spectroscopy of harmonically trapped single atoms
[AD-A189576] N88-20617
Comparison of analytic and full guiding center behavior at a trapped-passing interface in stellarators
[DE88-004174] N88-21025

TRAPPING
MOSFET performance degradation due to hot carriers N88-21063

TRAVELING SALESMAN PROBLEM
Local search for constrained routing problems --- traveling salesman
[CWI-OS-R8711] N88-20948

TRIBOLOGY
Overview of the DOE-ECUT Tribology Program
[DE88-002878] N88-20637

TRITIUM
Biophysical applications of solid state and tritium NMR
[DE88-005328] N88-20806
Outlook for the fusion hybrid and tritium-breeding fusion reactors
[PB88-149281] N88-21029

TROPOSPHERE
Computer simulation of tropospheric chemistry
[JUEL-2144] N88-20756

TRUSSES
Control augmented structural synthesis
[NASA-CR-4132] N88-20290

TUNABLE LASERS
Projected performance of RF-linac-driven free-electron lasers in the VUV and soft X-ray regions
[DE88-004294] N88-20625

TUNGSTEN
Tungsten-carbon multilayer system studied with X-ray scattering
[DE88-005749] N88-20373
Properties of reactively sputtered WNx films Zhao, X. -A.
[AD-A188711] N88-20976
Compatibility in space reactor fuel systems
[DE88-005698] N88-21004

TUNING
Optimal placement of tuning masses for vibration reduction in helicopter rotor blades
[NASA-TM-100562] N88-20665

TURBINE BLADES
Fatigue load measurements and evaluation of the 25m Horizontal Axis Wind Turbine (HAWT) at Petten, The Netherlands
[NLR-MP-86054-U] N88-20660

TURBOFAN ENGINES
Engine flow simulation for wind tunnel testing at NLR
[NLR-MP-87011-U] N88-20305
Exhaust-gas pressure and temperature survey of F404-GE-400 turbofan engine
[NASA-TM-88273] N88-20307

TURBOFANS
Measurement and analysis of the noise radiated by low Mach numbers centrifugal blowers
[AD-A189226] N88-20966
TURBOMACHINE BLADES
High Reynolds number pump facility for cavitation research
[AD-A189310] N88-20558
TURBOMACHINERY
An L-U implicit multigrid algorithm to solve the Euler equations for transonic flow in rotating turbomachinery passages N88-20270
TURBULENCE
Systems near the onset and in the well-developed regimes of turbulence
[DE88-005365] N88-20565
Calculations of viscous flows with a multigrid method N88-20580
Power spectral density analysis of wind-shear turbulence for related flight simulations
[NASA-CR-182721] N88-20773
On the zonal momentum balance at the equator N88-20788
Observations on energy transport in tokamaks: A new formula for turbulent transport
[DE88-005309] N88-21019
TURBULENT BOUNDARY LAYER
Interaction between two-dimensional sonic jets and supersonic flow to model heat addition in a supersonic combustor
[AD-A189572] N88-20261
Coherent structure-reflective turbulent viscous flow modeling
[AD-A188339] N88-20556
Slip velocity method for three-dimensional compressible turbulent boundary layers
[NASA-TM-100586] N88-20592
Research on turbulence in bottom boundary layer in ocean N88-20697
Unsteady shallowing mixed layer N88-20791
Flow/acoustic interaction in duct inflow
[AD-A189264] N88-20967
TURBULENT FLOW
Coherent structure-reflective turbulent viscous flow modeling
[AD-A188339] N88-20556
Control of structure in turbulent flows: Bifurcating and blooming jets
[AD-A189607] N88-20562
The influence of Mach number and heat transfer on the turbulent flow wall law
[NASA-TT-20230] N88-20594
TURBULENT HEAT TRANSFER
Turbulent transfer of momentum and heat in boundary layer of fluid beyond an obstacle. 1: Hydrodynamic characteristics N88-20690
Vertical turbulent transfer of matter in thin ocean surface layer during daytime heating N88-20693
Equatorial turbulence: Mixed layer and thermocline N88-20787
TURBULENT JETS
Control of structure in turbulent flows: Bifurcating and blooming jets
[AD-A189607] N88-20562
TURBULENT MIXING
Unsteady shallowing mixed layer N88-20791
Radiative processes affecting ocean mixed-layer heat content and their monitoring from satellite N88-20800
TWO DIMENSIONAL FLOW
Application of a flux vector splitting methodology towards the solution of unsteady transonic flows, with future emphasis on the blade flutter problem
[AD-A189500] N88-20260
Solution of two-dimensional Euler equations: Experience with a finite volume code
[DFVLR-FB-87-41] N88-20572
TWO PHASE FLOW
Two-phase flows in the wake of in-cylinder projectiles
[AD-A189422] N88-20559

U

U.S.S.R.
Soviet military power, 1987 N88-21114
U.S.S.R. SPACE PROGRAM
JPRS report: Science and technology. USSR: Space
[JPRS-USP-88-002] N88-20312
Soviet space transport systems N88-20328
Features of Soyuz TM spacecraft N88-20329
ULTRASONIC FLAW DETECTION
Nondestructive testings of HTGR graphites N88-20448
Ultrasonic inspection of irregular surfaces
[AERE-R-12465] N88-20648
ULTRASONIC SCANNERS
Ultrasonic inspection of irregular surfaces
[AERE-R-12465] N88-20648
ULTRASONIC TESTS
Ultrasonic characterization of non-uniform porosity distributions in SiC ceramic
[DE88-004814] N88-20459
Changes in the status of the human tibia during antiorthostatic hypokinesia
[NASA-TT-20221] N88-20813
ULTRASONIC WELDING
Modeling of laser ultrasound generation in a weld pool
[DE88-005546] N88-20971
ULTRASONICS
Ultrasonic physical modeling of seismic wave propagation from graben-like structures
[AD-A189066] N88-20744
ULTRAVIOLET PHOTOGRAPHY
The calibration of photographic and spectroscopic films: The response of 2aO film to small dosages of alpha particles from 3/10th's rad to 8 rads at energy levels 153 MeV, 79 MeV and 47 MeV
[NASA-CR-177830] N88-20608
ULTRAVIOLET RADIATION
Research on absorption of UV radiation in Venusian atmosphere from Vega-1 and Vega-2 landing modules N88-20316
Energy transfer and non-linear optical properties at near ultraviolet wavelengths: Rare earth 4f yields 5d transitions in crystals and glasses
[DE88-005403] N88-21012
UNDERWATER ACOUSTICS
Observations of waves and Langmuir circulation with Doppler sonars N88-20790
Mathematical models of sound waves in fluids
[AD-A189270] N88-20968
UNITED KINGDOM
A comparative assessment of US and UK explosives qualified as replacements for tetryl
[MRL-R-1094] N88-20486
UNITED STATES
A comparative assessment of US and UK explosives qualified as replacements for tetryl
[MRL-R-1094] N88-20486
UNIVERSE
Early reheating and cosmic strings N88-21103
UNMANNED SPACECRAFT
Expected value analysis for an unmanned expendable launch vehicle payload escape system
[AD-A189494] N88-20337
UNSTEADY AERODYNAMICS
Steady and unsteady transonic small disturbance analysis of realistic aircraft configurations
[NASA-TM-100557] N88-20269
UNSTEADY FLOW
Application of a flux vector splitting methodology towards the solution of unsteady transonic flows, with future emphasis on the blade flutter problem
[AD-A189500] N88-20260
ARSPNSC: A method to calculate subsonic steady and unsteady potential flow about complex configurations
[NLR-TR-86122-U] N88-20265
UPPER ATMOSPHERE
Measurement of rate constants of elementary gas reactions of importance to upper atmosphere and combustion systems
[AD-A189432] N88-20386
UPWELLING WATER
Circulation and exchange processes on the South Atlantic Bight Continental Shelf
[DE88-003330] N88-20781
URANUS (PLANET)
IUE program SUGSD: Varability time scale of H Ly-alpha from Uranus
[NASA-CR-182706] N88-21107
USER MANUALS (COMPUTER PROGRAMS)
Documentation and installation of the hypersonic arbitrary-body computer program (Mark 3 version) of A.E. Gentry on the IBM computer system
[MBB/LKE-127/S/PUB/256] N88-20276
MOPAC manual: A general molecular orbital package, fourth edition
[AD-A188823] N88-20362
MASPLT: A one-dimensional graphics post processor for wave propagation codes
[DE88-005506] N88-20856
USER REQUIREMENTS
Orbital transfer vehicle concept definition and system analysis study. Volume 2: OTV concept definition and evaluation. Book 1: Mission and system requirements
[NASA-CR-179321] N88-20339
Online aiding for human-computer interfaces
[AD-A189239] N88-20842

V

V/STOL AIRCRAFT
A review of technologies applicable to low-speed flight of high-performance aircraft investigated in the Langley 14- x 22-foot subsonic tunnel
[NASA-TP-2796] N88-20264
VACUUM
Molecular collision processes in gases and at surfaces
[AD-A189518] N88-20982
A high field launch for electron cyclotron heating using an external window
[DE88-005350] N88-21000
VALVES
Numerical methods in the resolution of control electrovalve model
[INPE-4154-RPE/540] N88-20554
VANADIUM ALLOYS
Vibration spectra of oxygen and vanadium atoms in vanadium-oxygen disordered interstitial alloys
[DE87-703166] N88-20404
VANADIUM OXIDES
Vibration spectra of oxygen and vanadium atoms in vanadium-oxygen disordered interstitial alloys
[DE87-703166] N88-20404
VANES
Static performance of an axisymmetric nozzle with post-exit vanes for multiaxis thrust vectoring
[NASA-TP-2800] N88-20280
VAPOR DEPOSITION
Research on mercury cadmium telluride
[AD-A189155] N88-21039
Initial stages of silicon growth on the (100) surface of silicon by localized laser CVD
[DE88-005420] N88-21059
VAPOR PHASE EPITAXY
Research on single-crystal CdTe solar cells
[DE88-001115] N88-20725
VAPOR PHASES
An interpretation of the ethylenic, carbidic, and graphite auger lineshapes of chemisorbed carbon species
[AD-A189092] N88-20379
Measurement of rate constants of elementary gas reactions of importance to upper atmosphere and combustion systems
[AD-A189432] N88-20386
VAPOR PRESSURE
Prediction of high-temperature thermodynamic properties of mixed electrolyte solutions including solubility equilibria, vapor pressure depression and boiling point elevation
[DE88-006344] N88-21069
VAPORS
Heat pipe transient analysis: Vapor dynamics
[DE88-005132] N88-20568
VARIABILITY
A new algorithm for general multiobjective optimization
[NASA-TM-100536] N88-20830
VARIATIONAL PRINCIPLES
Structural clearances and internal friction: Simulation by Eigen distortions
[ISSN-0208-5658] N88-20640
Hamiltonian description of the interaction of surface waves with mixed-layer currents N88-20799
VARIATIONS
Evolution of poloidal variation of impurity density and ambipolar potential in rotating tokamak plasma, part 1
[DE88-006263] N88-21022
VARISTORS
Electrical properties of medium field, chem-prep varistors
[DE88-006147] N88-20540
Scale-up of a batch-type chemical powder preparation process for high field varistor fabrication
[DE88-006601] N88-20541
VECTOR ANALYSIS
Deep water mass circulation in the Alboran Basin. Measurements - January to April 1982: ALBORAN 2
[AD-A189205] N88-20777
VEGA PROJECT
JPRS report: Science and technology. USSR: Space
[JPRS-USP-88-002] N88-20312
Vega-1 and Vega-2 automatic stations: Functioning of landing modules in Venusian atmosphere N88-20313
Vega-1 and Vega-2 automatic stations: Functioning of flyby vehicles during encounter with Halley's comet N88-20314
Thermal structure of Venusian Atmosphere determined from results of measurements from Vega-2 landing module N88-20315
Research on absorption of UV radiation in Venusian atmosphere from Vega-1 and Vega-2 landing modules N88-20316
Vertical structure of Venusian cloud layer at landing sites of Vega-1 and Vega-2 vehicles N88-20317

Gas-chromatographic analysis of products of thermal reactions of aerosol in Venusian cloud layer on Vega-1 and Vega-2 automatic interplanetary stations N88-20318

Roentgenoradiometric analysis of aerosol in Venusian clouds by Vega-1 and Vega-2 automatic interplanetary stations N88-20319

Chemical composition and structure of Venusian clouds determined from results of roentgenoradiometric experiments carried out by landing modules of Vega-1 and Vega-2 automatic interplanetary stations N88-20320

Determining chemical composition of aerosol in Venusian cloud layer on Vega-1 automatic interplanetary station using Malakhit mass spectrum analyzer N88-20321

Elemental composition of Venusian rocks in northeastern part of Terra Aphrodite (determined using data from Vega-2 landing module) N88-20322

Content of natural radioactive elements in Venusian rocks determined using data from Vega-1 and Vega-2 stations N88-20323

Results of infrared spectrometer experiment. 2: Infrared radiometry of nucleus of Halley's Comet N88-20326

Analysis of hydrocarbon band 3.35 in spectrum of Halley's Comet using data from infrared spectrometer on Vega-1 spacecraft N88-20327

VELOCITY

Erosion in dual-phase microstructures [DE88-004507] N88-20421

Reduction of erosion in elbows due to flow modifications, phase 1 [DE88-001028] N88-20584

Some effects of heating on the wind-driven velocity in the upper ocean N88-20792

VELOCITY DISTRIBUTION

Coherent structure-reflective turbulent viscous flow modeling [AD-A188339] N88-20556

VELOCITY MEASUREMENT

Velocity and concentration measurements in flowing suspensions by nuclear magnetic resonance [DE88-006225] N88-20589

Observations of waves and Langmuir circulation with Doppler sonars N88-20790

VENTS

Experimental and theoretical constraints on the origin of mid-ocean ridge geothermal fluids N88-20784

VENUS (PLANET)

Vega-1 and Vega-2 automatic stations: Functioning of landing modules in Venusian atmosphere N88-20313

Elemental composition of Venusian rocks in northeastern part of Terra Aphrodite (determined using data from Vega-2 landing module) N88-20322

VENUS ATMOSPHERE

Vega-1 and Vega-2 automatic stations: Functioning of landing modules in Venusian atmosphere N88-20313

Thermal structure of Venusian Atmosphere determined from results of measurements from Vega-2 landing module N88-20315

Research on absorption of UV radiation in Venusian atmosphere from Vega-1 and Vega-2 landing modules N88-20316

Vertical structure of Venusian cloud layer at landing sites of Vega-1 and Vega-2 vehicles N88-20317

Gas-chromatographic analysis of products of thermal reactions of aerosol in Venusian cloud layer on Vega-1 and Vega-2 automatic interplanetary stations N88-20318

Roentgenoradiometric analysis of aerosol in Venusian clouds by Vega-1 and Vega-2 automatic interplanetary stations N88-20319

Chemical composition and structure of Venusian clouds determined from results of roentgenoradiometric experiments carried out by landing modules of Vega-1 and Vega-2 automatic interplanetary stations N88-20320

Determining chemical composition of aerosol in Venusian cloud layer on Vega-1 automatic interplanetary station using Malakhit mass spectrum analyzer N88-20321

VENUS CLOUDS

Roentgenoradiometric analysis of aerosol in Venusian clouds by Vega-1 and Vega-2 automatic interplanetary stations N88-20319

VENUS SURFACE

JPRS report: Science and technology. USSR: Space [JPRS-USP-88-002] N88-20312

Vega-1 and Vega-2 automatic stations: Functioning of landing modules in Venusian atmosphere N88-20313

Elemental composition of Venusian rocks in northeastern part of Terra Aphrodite (determined using data from Vega-2 landing module) N88-20322

Content of natural radioactive elements in Venusian rocks determined using data from Vega-1 and Vega-2 stations N88-20323

VERTICAL DISTRIBUTION

Vertical structure of Venusian cloud layer at landing sites of Vega-1 and Vega-2 vehicles N88-20317

VERTICAL ORIENTATION

A polarization diversity meteorological radar system [AD-A189291] N88-20515

VERY LARGE SCALE INTEGRATION

Gridless routing for generalized cell assemblies: Report and user manual [EUT-87-E-180] N88-20549

GM: A gate matrix layout generator [EUT-87-E-179] N88-20875

VERY LONG BASE INTERFEROMETRY

Crustal dynamics project data analysis, 1987. Volume 2: Mobile VLBI geodetic results 1982-1986 [NASA-TM-100689-VOL-2] N88-20753

Polarization properties of SiO masers N88-21113

VIBRATION

Vibration spectra of oxygen and vanadium atoms in vanadium-oxygen disordered interstitial alloys [DE87-703166] N88-20404

VIBRATION DAMPING

Optimal placement of tuning masses for vibration reduction in helicopter rotor blades [NASA-TM-100562] N88-20665

VISCOELASTICITY

Viscoelastic behavior of a polyetheretherketone (PEEK) composite [AD-A189545] N88-20368

An analysis of large deformation axisymmetric inelastic problems by finite element and boundary element methods N88-20664

VISCOPLASTICITY

Cyclic crack growth emanating at a round notch considering viscoplasticity [AD-A189577] N88-20655

VISCOSITY

Contrasting conductance/viscosity relations in liquid states of vitreous and polymer solid electrolytes [AD-A189378] N88-20452

VISCOUS DRAG

Boundary effects on the drag of a cylinder in axial motion at low Reynolds number N88-20578

VISCOUS FLOW

Mixing of viscous fluids: Behavior of microstructures and chaos [DE88-006287] N88-20566

Calculations of viscous flows with a multigrid method N88-20580

VISCOUS FLUIDS

Properties of molecular solids and fluids at high pressure and temperature [DE88-004195] N88-20391

VISIBILITY

Influence of hydrometeorological factors on visibility of objects detected by radar N88-20707

VISIBLE SPECTRUM

Synchronous measurements of effective photon path length in visible and near-IR spectral regions in real cloud systems N88-20706

Global solar oscillations observed in the visible to near infrared continuum N88-21110

VISION

Computerised measurement of human horizontal smooth pursuit eye movements N88-20819

VISUAL PERCEPTION

Computerised measurement of human horizontal smooth pursuit eye movements N88-20819

Identification of visual evoked response parameters sensitive to pilot mental state [NASA-CR-4140] N88-20822

Mathematic modeling of visual perception problems [INPE-4355-PRE/1186] N88-20897

VISUAL SIGNALS

A pyrotechnic delay ignition system for a submarine launched marine signal [MRL-R-1079] N88-20487

VISUAL STIMULI

Computerised measurement of human horizontal smooth pursuit eye movements N88-20819

VOIDS

Material instabilities in solids [AD-A189525] N88-20388

VOLATILITY

A mass spectrometer evolved gas analysis experiment for in-situ analysis of cometary dust volatiles N88-21097

VOLTERRA EQUATIONS

New way to solve Volterra equations of the second kind [PB88-148820] N88-20931

VORTEX SHEETS

Computational technique for compressible vortex flows using the integral equation solution [NASA-CR-182695] N88-20271

VORTICES

The international vortex flow experiment: A test case for compressible Euler codes [NLR-MP-86076-U] N88-20267

Control of structure in turbulent flows: Bifurcating and blooming jets [AD-A189607] N88-20562

An experimental investigation of decelerating flow about two-dimensional cambered plates [DE88-006598] N88-20567

Very large vortex calculations in two dimensions [DE88-005748] N88-20587

Mushroom-shaped currents (eddy dipoles) under rotation and stratification conditions N88-20678

Dynamics of synoptic ocean eddies N88-20689

Phenomenological description of eddy registered in Gulf Stream N88-20694

W

WAKES

Two-phase flows in the wake of in-cylinder projectiles [AD-A189422] N88-20559

WALKING

Force distribution and trajectory control for closed kinematic chains with applications to walking machines N88-20642

WALL FLOW

The influence of Mach number and heat transfer on the turbulent flow wall law [NASA-TT-20230] N88-20594

WASTES

Technology '87: Research and Development Laboratory Technology Transfer Program [DE88-003142] N88-21084

WATER

Numerical experiments on the stability of controlled boundary layers [NASA-CR-181649] N88-20591

WATER CIRCULATION

Numerical model of Rayleigh instability and spin-off eddies on fronts N88-20696

WATER CURRENTS

Model of hydrodynamic adjustment of temperature, salinity and current fields N88-20700

Circulation and exchange processes on the South Atlantic Bight Continental Shelf [DE88-003330] N88-20781

WATER POLLUTION

Environmental projects. Volume 5, part 1: Study of subsurface contamination. Part 2: Guide to implement environmental compliance programs [NASA-CR-182691] N88-20741

Global mixed-layer natural and anthropogenic fluxes N88-20803

WATER TREATMENT

Review of selenium thermodynamic data [DE88-006194] N88-21068

WATER TUNNEL TESTS

High Reynolds number pump facility for cavitation research [AD-A189310] N88-20558

An experimental investigation of decelerating flow about two-dimensional cambered plates [DE88-006598] N88-20567

WATER WAVES

Anisotropy of microstructural eddy motion in surface layer during calm N88-20677

Numerical modeling of wave migration of seismic data N88-20684

Invariant characteristics of acoustic field in stratified ocean N88-20698

Study of spectra of sea waves on horizontally nonuniform current in rip zone N88-20699

Dynamics of the Oceanic Surface Mixed Layer [AD-A186348] N88-20785

Wind forcing and observed oceanic wavenumber spectra N88-20797

Energy and momentum fluxes through the sea surface N88-20798

Hamiltonian description of the interaction of surface waves with mixed-layer currents N88-20799

Evaluation of wave calculations using GONO in the period October 1985 - April 1986 [KNMI-TR-96] N88-20804

WAVE DISPERSION

Slow waves in waveguide with elliptical cross section [DE88-700159] N88-20508

WAVE EQUATIONS

A finite-amplitude analysis of the buoyant instability of a highly viscous film over a less viscous half-space N88-20581

WKB theory of wave tunneling for Hermitian vector systems of integral equations [DE88-005332] N88-20951

WAVE FRONTS
Theoretical investigation of the wave shaping process in a section of ladder fracture tape
[MRL-R-1081] N88-20595
WAVE FUNCTIONS
Polarization of electrons in an electromagnetic wave field in the presence of magnetic field
[DE88-700169] N88-20509
WKB theory of wave tunneling for Hermitian vector systems of integral equations
[DE88-005332] N88-20951
Numerical simulations of multiphoton processes in many electron atoms
[DE88-003293] N88-20990
WAVE GENERATION
Theoretical investigation of EM wave generation and radiation in the ULF, ELF and VLF bands by the electrodynamic orbiting tether
[NASA-CR-182720] N88-20529
WAVE INTERACTION
Flow/acoustic interaction in duct inflow
[AD-A189264] N88-20967
WAVE PROPAGATION
Slow waves in waveguide with elliptical cross section
[DE88-700159] N88-20508
Detonation velocity of the hydrazinum nitrate-hydrazine water system
[NASA-TT-20213] N88-20590
Numerical modeling of wave migration of seismic data
N88-20684
Invariant characteristics of acoustic field in stratified ocean N88-20698
Ultrasonic physical modeling of seismic wave propagation from graben-like structures
[AD-A189066] N88-20744
Method for determination of the wind velocity and direction
[NASA-TT-20233] N88-20769
MASPLT: A one-dimensional graphics post processor for wave propagation codes
[DE88-005506] N88-20856
HISPLT: A history graphics post processor for wave propagation codes
[DE88-005507] N88-20857
CSQPLT: A graphics post processor for multidimensional wave propagation codes
[DE88-005508] N88-20858
Mathematical models of sound waves in fluids
[AD-A189270] N88-20968
Method for determining artillery position
[NASA-TT-20238] N88-20973
WAVE SCATTERING
Transport and stability properties of free shear flows
N88-20577
WAVEFORMS
MOSFET performance degradation due to hot carriers
N88-21063
WAVEGUIDES
Transformation coefficient in wave-field acceleration scheme
[DE88-700158] N88-20507
Slow waves in waveguide with elliptical cross section
[DE88-700159] N88-20508
Multimode-waveguide laser beam deflector
[DE88-006222] N88-20622
Low threshold ridge waveguide single quantum well lasers N88-20631
WAVELENGTHS
Study for the determination of general and specific properties of wide energy-band gap HgHdTe in the 1-2 micrometer wavelength range
[AD-A189177] N88-21041
WEAK INTERACTIONS (FIELD THEORY)
Searches for forces weaker than gravity
[DE88-003579] N88-20959
Intermediate energy neutrino physics
[DE88-005378] N88-20984
WEAPONS
Soviet military power, 1987 N88-21114
WEAR
Characterization and fundamental studies on CuO sorbent materials to determine attrition mechanisms on substrate gamma alumina
[DE88-003674] N88-20456
Corrosion-wear process under rolling-sliding motion
[AD-A189603] N88-20835
Overview of the DOE-ECUT Tribology Program
[DE88-002878] N88-20637
WEAR RESISTANCE
Reduction of erosion in elbows due to flow modifications, phase 1
[DE88-001028] N88-20584
WEATHER FORECASTING
Activities report in meteorology
[AR-86-87] N88-20755
Wind shear as a predictor of severe weather for the eastern United States
[PB88-157144] N88-20762
WEATHERING
A five year weathering experiment with solar collectors
[DE88-900369] N88-20740
WEDGES
An interferometric investigation of the diffraction of planar shock waves over a half-diamond cylinder in air
[UTIAS-322] N88-20575
WEIBULL DENSITY FUNCTIONS
Tests for uniformity arising from a series of events
[AD-A189069] N88-20935
WEIGHTING FUNCTIONS
Two dimensional uncorrelated bias in fix algorithms
[NASA-CR-182683] N88-20847
Robustifying the Kalman filter
[AD-A189240] N88-20907
WEIGHTLESSNESS SIMULATION
Regulation of hemodynamics upon imitation of the transition to weightlessness (mathematical modeling)
N88-20817
WELDED JOINTS
Transformation, metallurgical response and behavior of the weld fusion zone and heat affected zone in Cr-Mo steels for fossil energy application
[DE88-006037] N88-20430
WELDED STRUCTURES
Hydrogen induced cracks in armor steel weldments fabricated with austenitic filler alloys
[AD-A188733] N88-20406
WELDING
Investigation of the use of horizontally polarised shear waves for TOFD studies on austenitic steel
[AERE-R-12145] N88-20649
WELLS
Status of the Magma Energy Project
[DE88-002413] N88-20719
WENTZEL-KRAMER-BRILLOUIN METHOD
WKB theory of wave tunneling for Hermitian vector systems of integral equations
[DE88-005332] N88-20951
WHISKER COMPOSITES
Composites strengthening
[AD-A189258] N88-20364
Interfacial chemistry-structure and fracture of ceramic composites
[DE88-005516] N88-20461
WIGGLER MAGNETS
Wiggler taper optimization for free-electron-laser amplifiers with moderate space-charge effects
[DE88-003758] N88-20618
WIND (METEOROLOGY)
Simulating high-resolution vertical plane array wind characteristics using lower-spatial-resolution wind measurements
[DE88-005626] N88-20761
Circulation and exchange processes on the South Atlantic Bight Continental Shelf
[DE88-003330] N88-20781
WIND DIRECTION
Method for determination of the wind velocity and direction
[NASA-TT-20233] N88-20769
WIND EFFECTS
Study of spectra of sea waves on horizontally nonuniform current in rip zone N88-20699
Circulation and exchange processes on the South Atlantic Bight Continental Shelf
[DE88-003330] N88-20781
Dynamics of the Oceanic Surface Mixed Layer
[AD-A188348] N88-20785
On the zonal momentum balance at the equator
N88-20788
The mixed layer of the western equatorial Pacific Ocean
[HIG-1861] N88-20789
Unsteady shallowing mixed layer N88-20791
Some effects of heating on the wind-driven velocity in the upper ocean N88-20792
Mixed-layer shear related to wind stress in the central equatorial Pacific N88-20793
Mixed-layer fronts in the California current
N88-20794
Horizontal scales of wind forced inertial motions
N88-20795
Wind forcing and observed oceanic wavenumber spectra N88-20797
Energy and momentum fluxes through the sea surface
N88-20798
Hamiltonian description of the interaction of surface waves with mixed-layer currents N88-20799
Monitoring ocean surface layer processes
N88-20801
WIND MEASUREMENT
A preliminary assessment of thunderstorm outflow wind measurement with airport surveillance radars
[AD-A189064] N88-20757
Mixed-layer shear related to wind stress in the central equatorial Pacific N88-20793
WIND SHEAR
Wind shear as a predictor of severe weather for the eastern United States
[PB88-157144] N88-20762
Power spectral density analysis of wind-shear turbulence for related flight simulations
[NASA-CR-182721] N88-20773
WIND TUNNEL APPARATUS
Activities report of the Large Testing Facilities Department --- aircraft/spacecraft
[ETN-88-91982] N88-20311
WIND TUNNEL MODELS
A wind tunnel model with dynamic control
[BU-352] N88-20310
Activities report of the Large Testing Facilities Department --- aircraft/spacecraft
[ETN-88-91982] N88-20311
WIND TUNNEL STABILITY TESTS
A wind tunnel model with dynamic control
[BU-352] N88-20310
WIND TUNNEL TESTS
A review of technologies applicable to low-speed flight of high-performance aircraft investigated in the Langley 14- x 22-foot subsonic tunnel
[NASA-TP-2796] N88-20264
Tests on the AFWAL 65 deg delta wing at NLR: A study of vortex flow development between Mach = 0.4 and 4
[NLR-MP-86058-U] N88-20266
The international vortex flow experiment: A test case for compressible Euler codes
[NLR-MP-86076-U] N88-20267
The construction of a three-dimensional finite volume grid generator for a wing in a wind tunnel with application to Navier-Stokes flow solvers
[FFA-TN-1987-58] N88-20277
Engine flow simulation for wind tunnel testing at NLR
[NLR-MP-87011-U] N88-20305
Activities report of the Large Testing Facilities Department --- aircraft/spacecraft
[ETN-88-91982] N88-20311
WIND TUNNELS
Activities report of the Large Testing Facilities Department --- aircraft/spacecraft
[ETN-88-91982] N88-20311
WIND TURBINES
Fatigue load measurements and evaluation of the 25m Horizontal Axis Wind Turbine (HAWT) at Petten, The Netherlands
[NLR-MP-86054-U] N88-20660
WIND VELOCITY
Determining Langmuir circulation parameters on basis of similarity theory N88-20680
Wind velocity measurement data. Zimbabwe, 4 measuring stations
[R-845-D] N88-20770
WIND VELOCITY MEASUREMENT
Method for determination of the wind velocity and direction
[NASA-TT-20233] N88-20769
Wind velocity measurement data. Zimbabwe, 4 measuring stations
[R-845-D] N88-20770
WINDOWS (APERTURES)
A high field launch for electron cyclotron heating using an external window
[DE88-005350] N88-21000
WINDPOWER UTILIZATION
Wind velocity measurement data. Zimbabwe, 4 measuring stations
[R-845-D] N88-20770
WING OSCILLATIONS
ARSPNSC: A method to calculate subsonic steady and unsteady potential flow about complex configurations
[NLR-TR-86122-U] N88-20265
WINGS
Crack distribution and growth rates for critical fastener holes in Mirage wing RH79
[AD-A189080] N88-20293
WINTER
Estimates of ocean-atmosphere thermal interaction in Gulf Stream energy-active test range in winter of 1984
N88-20679
WIRING
Gridless routing for generalized cell assemblies: Report and user manual
[EUT-87-E-180] N88-20549
Locality, communication and interconnect length in multicomputers
[CWI-CS-R8708] N88-20890

WORKLOADS (PSYCHOPHYSIOLOGY)
Identification of visual evoked response parameters sensitive to pilot mental state
[NASA-CR-4140] N88-20822
Proceedings of the Workshop on the Assessment of Crew Workload Measurements Methods, Techniques and Procedures. Volume 1: Preliminary Selection of Measures
[AD-A189004] N88-20827
A comparison of two chord keyboard coding systems for alphanumeric data entry
[AD-A189230] N88-20834
WORKSTATIONS
GM: A gate matrix layout generator
[EUT-87-E-179] N88-20875

X

X RAY ABSORPTION
Variable spectra of active galaxies
[NASA-CR-182694] N88-21091
X RAY ANALYSIS
Advances in X-ray line profile analysis to determine microstructure information about ceramics
[DE88-003938] N88-20465
The effects of normal and therapeutic baths on the central vascular organs of persons with healthy hearts, as measured by X-ray
[NASA-TT-20252] N88-20818
X RAY DIFFRACTION
The synthesis, characterization and structural studies of In(C5H4Me) by X-ray diffraction and electron diffraction techniques and a reinvestigation of the crystalline state of In(C5H5) by X-ray diffraction studies
[AD-A189110] N88-21038
X-ray diffraction study of a thin GaAs film on Si(100)
[DE88-005290] N88-21055
X RAY INSPECTION
Nondestructive testings of HTGR graphites
N88-20448
X RAY IRRADIATION
Practical constraints on sources for pulsed beam lithographies
[DE88-006594] N88-20623
X RAY LASERS
Wavelength scaling of lithium-like recombination scheme for X-UV gain production --- X-ray lasers
[ETN-88-92002] N88-20634
X RAY SCATTERING
Tungsten-carbon multilayer system studied with X-ray scattering
[DE88-005749] N88-20373
X RAY SOURCES
Variable spectra of active galaxies
[NASA-CR-182694] N88-21091
X RAY SPECTRA
Variable spectra of active galaxies
[NASA-CR-182694] N88-21091
X-29 AIRCRAFT
A correlation study of X-29A aircraft and associated analytical development
[NASA-TM-89735] N88-20296
XENON
Electron stimulated desorption and coherent electron scattering
[AD-A189091] N88-20978
XENON CHLORIDE LASERS
Direct solar-pumped iodine laser amplifier
[NASA-CR-182674] N88-20630

Y

YIELD POINT
Database of average-power damage thresholds at 1064 nm
[DE88-004352] N88-20626
YIELD STRENGTH
A direct correlation of strength with impact velocity
[AD-A189251] N88-20409

Z

ZIMBABWE
Wind velocity measurement data. Zimbabwe, 4 measuring stations
[R-845-D] N88-20770
ZINC
Technology base research on zinc/air battery systems
[DE88-004893] N88-20546
ZINC SULFIDES
Laser fluorescence spectroscopy of zinc neutrals originating from laser-irradiated and ion-bombarded zinc sulfide and zinc surfaces
[DE88-006033] N88-20620
ZINC TELLURIDES
CdZnTe as a wide-band-gap absorber for a tandem, thin-film solar cell
[DE88-001114] N88-20724
ZINC-OXYGEN BATTERIES
A new concept in an electrically rechargeable zinc-air alkaline battery
[DE88-003858] N88-20539
ZIRCONIUM
A case study of the development of a military specification - zirconium powder for thermal batteries
[AD-A188751] N88-20717

Typical Personal Author Index Listing

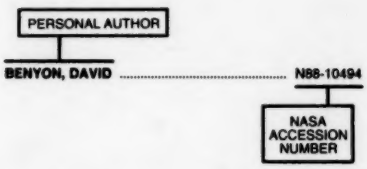

Listings in this index are arranged alphabetically by personal author. The NASA accession number denotes the number by which the citation is identified.

A

ABDEL-GAWAD, MONEM N88-20744
ABERZHAL, A. N88-20316
ABRAHAM, WARREN O. N88-20616
ACKERMAN, J. L. N88-20473
ACOSTA, ALLAN J. N88-20557
ADAIR, R. N88-21009
ADAMS, J. B. N88-20852
ADAMS, J. W. N88-20519
ADELBERGER, E. G. N88-20959
ADELMAN, HOWARD M. N88-20665
ADKINS, D. R. N88-20731
AGARWAL, ARVIND K. N88-20896
AGRAWAL, AMIT PRAKASH N88-20520
AHMADI, ALI N88-20296
AIKENS, D. M. N88-20619
AINSWORTH, N. R. G. N88-21000
AKHMETSHIN, I. K. N88-20319
AKITA, KAZUO N88-20476
AKMAN, VAROL N88-20870
N88-20903
ALBRITTON, J. N88-20662
ALENICHEVA, T. V. N88-20404
ALLENDER, D. W. N88-20981
ALLEY, THOMAS G. N88-21045
ALLISON, S. W. N88-20628
ALTES, RICHARD A. N88-20514
ALTOBELLI, S. A. N88-20589
AMANO, RYOICHI S. N88-20667
AMAZIGO, JOHN C. N88-20412
AMELL, JOHN R. N88-20834
AMERICA, PIERRE N88-20872
N88-20956
ANDERSON, A. N88-20310
ANDERSON, BRIAN JAY N88-21097
ANDERSON, KRISTIN K. N88-20611
ANDREYCHIKOV, B. M. N88-20319
N88-20320
ANGEL, S. M. N88-21013
ANGELL, C. A. N88-20452
ANTAL, M. J., JR. N88-20730
ANTOLOVICH, STEPHEN D. N88-20414
ANTONI, V. N88-21027
ANTONIEWICZ, ROBERT F. N88-20896
APT, K. R. N88-20874
ARAI, T. N88-20441
ARCHER, D. G. N88-21065
ARCHINAL, BRENT ALLEN N88-20713
ARCONE, STEVEN A. N88-20779
ARDANUY, PHILIP E. N88-20714
ARIYAWANSA, K. A. N88-20650
ARLINGHAUS, H. F. N88-20620
ARMENTROUT, PETER B. N88-20405
ARMSTRONG, CARTER A. N88-20602
ARMSTRONG, GRAHAM M. N88-20515
ARMSTRONG, LAWRENCE E. N88-20810
ARNOLD, FRED E. N88-20449
ARNOLDOV, M. N. N88-20402
ARNOLDUS, HENK F. N88-20975
ARSENAULT, RICHARD J. N88-20364
ARTEMYEV, A. O. N88-20687
ARVIZU, D. E. N88-20734
ATKINSON, DAVID J. N88-20905
ATTMANNSPRACHER, W. N88-20771
AUCIELLO, O. N88-21064
AUGUSTOGOMESPEREIRA, EDUARDO N88-20554
AVERY, P. N88-20994
AWAJI, H. N88-20442
N88-20445
AWERBUCH, BARUCH N88-20862
AYRESDECAMPOS, N. N88-20432

B

BADEN, S. B. N88-20587
BAETEN, J. C. M. N88-20918
N88-20919
BAETZ N88-20332
BAINTON, K. F. N88-20649
BAKER, ROBERT N88-20895
BALDWIN, DOUG N88-20531
N88-20841
BANERJEA, AMITAVA N88-20417
BANKS, DANIEL W. N88-20264
BANON, GERALD JEAN FRANCIS N88-20712
BAO, JINJUN N88-21109
BARBER, JACOB L. N88-21075
BARNER, J. O. N88-21002
BARNHILL, R. E. N88-20854
BARNWELL, RICHARD W. N88-20592
BARRON, M. H. N88-20997
BARTLETT, R. W. N88-21020
BATES, J. L. N88-20462
BATINA, JOHN T. N88-20269
BAUCH, R. N88-20740
BAUSER, E. N88-21061
BEACHLEY, O. T., JR. N88-21038
BECKER, R. N88-20437
BECKETT, MARCIE B. N88-20808
BEIDLER, C. D. N88-21031
BELL, J. A. N88-21057
BENGELSDORF, I. N88-20741
BENNETT, ROBERT M. N88-20269
BENNETT, W. R. N88-21057
BENNING, STEVE N88-20303
BENSLAY, R. M. N88-20484
BERGMANN, J. W. N88-20300
BERGSTRA, J. A. N88-20869
N88-20920
BERK, H. L. N88-20951
BERNDT, MICHAEL EUGENE N88-20784
BERNSTEIN, G. M. N88-20775
BERRIER, BOBBY L. N88-20280
BERTO, ZH. L. N88-20316
BEZEM, MARC N88-20950
BHASIN, KUL B. N88-20555
BHATTACHARYYA, S. K. N88-21002
BIBRING, J. P. N88-20325
BIFERNO, MICHAEL A. N88-20827
BILINSKIY, A. I. N88-20701
BILLET, M. L. N88-20558
BINASIEWICZ, E. J. N88-20540
BINGEL, BRADFORD D. N88-20273
BIRKBECK, J. C. N88-20458
BIRKHOFF, GARRETT N88-20968
BIRKMIRE, R. W. N88-20726
BIRTCHER, R. C. N88-20429
BISHOP, ALEXANDER W. N88-20515
BISOGNANO, J. J. N88-20996
BISSOT, DAVID M. N88-20408
BIWER, R. N88-20544
BLACKER, T. D. N88-20914
BLAMONT, G. N88-20315
BLAND, SAMUEL R. N88-20269
BLANDER, MILTON N88-20389
BLIEM, C. J. N88-20738
BLOM, H. A. P. N88-20287
BLOM, J. G. N88-20922
BLOOM, G. N88-20418
BOCKELEE-MORVAN, D. N88-20325
BOEHM, G. N88-20818
BOERSEN, S. J. N88-20266
BOGDAN, A. R. N88-20632
BOMMANNAVAR, A. S. N88-21055
BONDAREV, V. B. N88-20318
BORELLA, H. M. N88-20628
BORREGO, J. M. N88-20725
BOSCH, W. N88-21082
BOUCEK, GEORGE P., JR. N88-20827
BOUGE, L. N88-20874
BOUWS, E. N88-20804
BOWEN, P. R. N88-20985
BOWLES, S. N88-20293
BOXMA, O. J. N88-20947
N88-20949
BOYER, S. N88-21107
BOZZOLO, GUILLERMO H. N88-20417
BRAGAGNOLO, J. N88-20723
BRANNON, P. J. N88-20622
BRAUN, R. L. N88-20460
N88-20586
BREYER, DANIEL J. N88-20294
BRINKMAN, C. R. N88-20658
BROCKENBROUGH, J. R. N88-20659
BROER, H. W. N88-20928
BROOKS, DAVID R. N88-20772
BROOKS, E. D., III N88-20855
BROVELLI, M. N88-20740
BROVERMAN, A. Y. N88-20525
BROWN, D. R. N88-20732
BROWN, PETER F. N88-20510
BROWN, W. P. N88-20536
BRUCE, KEVIN R. N88-20308
BRUMBAUGH, RANDAL W. N88-20896
BRUSSO, J. A. N88-20418
BRYLOW, S. M. N88-20775
BUBNOV, V. A. N88-20694
BUCKLES, BILL N88-20846
BUCKMASTER, J. D. N88-20382
BUDESCU, DAVID N88-20910
BUDIANSKY, BERNARD N88-20412
BUMPUS, S. N88-20902
BUNKER, B. C. N88-21052
BUNKIN, A. F. N88-20716
BURCHAM, FRANK W., JR. N88-20307
BURGESS, MARY T. N88-20717
BURNETT, A. F. N88-20727
BURNHAM, A. K. N88-20460
BUSSELL, T. N88-20490
BUTKYAVICHYUS, YU. P. N88-20403
BUTLER, RICKY W. N88-20894
BUTTLE, D. J. N88-20650
BYAKOV, YU. A. N88-20684

C

CABRAL, MARIA ROSELI N88-20743
CALAWAY, W. F. N88-20620
CALCOTE, H. F. N88-20451
CALDECOTT, R. N88-20962
CALDWELL, D. R. N88-20788
CALLAHAN, T. J. N88-20645
CAMINS, I. N88-21013
CAMPBELL, C. S. N88-20563
CAMPONESCHI, E. T., JR. N88-20365
CANRIGHT, DAVID RALPH N88-20581
CAPE, J. A. N88-20721
CARILLON, A. N88-20634
N88-21033
CARISSIMO, BERTRAND CHARLES N88-20763
CARLSTEIN, EDWARD N88-20910
CARRERAS, B. A. N88-20848
N88-21023
CARTAXOMODESTODESOUZA, RICARDO N88-20715
CARTWRIGHT, DAVID E. N88-20780
CARY, J. R. N88-21025
CASCIO, M. N88-20333
CASSELL, CHRISTOPHER R. N88-20285
CASSIDY, R. T. N88-20458
CATES, M. R. N88-20628
CAVOLOWSKY, JOHN ARTHUR N88-21030
CEDERQUIST, JACK N. N88-20939
CERJAN, C. N88-20990
CERVELLI, D. M. N88-20586
CHAI, JOHN C. N88-20667

CHALMERS, H. N88-20332
CHAMPNEY, P. D'A. N88-20965
CHANG, D. N88-20423
CHANG, H. S. N88-20477
CHAR, J. M. N88-20483
CHARLTON, L. A. N88-21023
CHASE, L. L. N88-20620
N88-21009
CHAYKOVSKY, M. N88-20482
CHEN, G. N88-20560
CHEN, W. S. N88-20727
CHERESKIN, T. K. N88-20788
CHESS, E. K. N88-20394
CHESTNUT, GARY L. N88-20655
CHEVASSUS, P. N88-20479
CHIAN, JIH-CHEN N88-21034
CHILES, HARRY R. N88-20304
CHING, HARRY L. N88-21075
CHING, WAI-YIM N88-21049
CHIRICO, R. D. N88-21065
CHOI, J. H. N88-20477
CHOI, JEONG YEOL N88-21063
CHORN, TREVOR A. N88-20385
CHOU, PAUL B. N88-20840
CHRISTEN, D. K. N88-21046
CHRISTIANSON, C. C. N88-20544
CHU, T. L. N88-21050
CHURCHILL, MELVYN R. N88-21038
CHYI, J. I. N88-21053
CISNEROS, J. N88-20771
CLAPP, N. E., JR. N88-21079
CLARK, ARCHIE B., III N88-20292
CLARK, G. A. N88-21032
CLARKE, J. T. N88-21107
CLAUDE, H. N88-20771
CLAYTON, CURTIS DAVID N88-20360
CLERMONT, PH. N88-20874
COHEN, J. D. N88-21051
COHEN, MARVIN S. N88-20820
COHEN, R. N88-21029
COLEMAN, JOHN R. N88-20378
COLLINS, CARL B. N88-20613
COMBES, M. N88-20325
N88-20326
COMPERINI, ROBERT N88-20344
COMPTON, R. N. N88-20627
CONN, R. W. N88-21021
CONNELL, J. R. N88-20761
CONNELLY, STEPHEN F. N88-20514
COOK, KEM HOLLAND N88-21098
COPLEY, D. C. N88-20453
CORCORAN, CHRISTOPHER J. N88-20611
CORRIGAN, D. A. N88-20411
COSTA, MARIA HELENA N88-20708
COTA, STEPHEN ANDREW N88-21111
COURTNEY, T. H. N88-20416
COWAN, C. E. N88-21068
COWAN, C. L. N88-21002
CRAWFORD, ERIC E. N88-20834
CREWS, J. H., JR. N88-20372
CRIFO, J. F. N88-20325
CRIMMINS, THOMAS R. N88-20939
CROVISIER, J. N88-20325
N88-20326
CROWL, LAWRENCE A. N88-20844
CRUICKSHANK, ALEXANDER N88-20435
CUCOLO, A. N88-21058
CUNNINGHAM, HERBERT J. N88-20269
CUNNINGHAM, L. M. N88-20606
CURRO, J. G. N88-20470
N88-20471
CUSHMAN-ROISIN, BENOIT N88-20796

D

DAGLEY, IAN J. N88-20399
N88-20489
DAHLIN, GOESTA JOHAN N88-20769
N88-20972
DANIELS, D. H. W. N88-20571
DANILKIN, N. P. N88-20703
DANILKIN, S. A. N88-20404
DARMOHRAY, G. A. N88-20855
DAS, ARABINDO N88-20268
DASARO, ERIC A. N88-20795
DASH, S. M. N88-20256
DASILVA, JOAO EDUARDO OLIVEIRA N88-20929
DATLOWE, DAYTON W. N88-21094
DATTA, S. K. N88-20366
DAVIDSON, ARNOLD W. N88-20601
DAVIS, JEFFREY A. N88-21006
DEBAKKER, C. N88-20771
DEBAKKER, JACO W. N88-20872
DEBOER, FRANK S. N88-20891
DECHA-UMPHAI, KAMOLPHAN N88-20663
DEGEORGE, C. L. N88-20306
DEJONGE, J. B. N88-20300
DEKKER, J. W. M. N88-20660
DELIL, A. A. M. N88-20347
N88-20569
DELLIS, A. N. N88-21000
DELUCA, JANE P. N88-20810
DEMIN, YU. L. N88-20700
DEMUER, D. N88-20771
DENLINGER, J. D. N88-20373
DEOLIVEIRA, ISMAEL E., JR. N88-20554
DERYUGIN, V. A. N88-20313
DESILVESTRO, J. N88-20411
DESWART, H. E. N88-20748
DEUCHAMPHAI, PRAMOTE N88-20666
DEVAN, LEROY N88-20259
DEVANEY, W. E. N88-20727
DEVYATKIN, S. I. N88-20315
DEWEY, DANIEL N88-20878
DEWEY, GERALD I. N88-20710
DEWOLF, W. B. N88-20305
DHERE, A. N88-21055
DIAMOND, W. I. N88-20996
DIANOV-KLOKOV, V. I. N88-20706
DIAS, LUIZ ALBERTO VIEIRA N88-20877
DIASVELASCO, FLAVIO ROBERTO N88-20708
N88-20882
N88-21015
DIBBERN, J. S. N88-20494
DICKEY, D. W. N88-20645
DICKINSON, MARK N88-20284
DILLON, T. M. N88-20788
DIPP, THOMAS M. N88-20911
DIRESKENELI, HALDUN N88-20521
DIRKS, J. A. N88-20732
DIVER, R. B. N88-20729
DOBROLYUBOV, S. A. N88-20675
DOBSON, J. C. N88-20735
DOIRON, SCOTT D. N88-20714
DOLGOPOLOV, V. P. N88-20313
N88-20314
DOMINEK, A. N88-20397
N88-20962
DONATH, M. N88-20945
DONELSON, TERY L. N88-20286
DONOVAN, D. N88-20428
DOSS, HANI N88-20937
DOSS, K. G. R. N88-20991
DOUGHTY, D. H. N88-21052
DOVI, AUGUSTINE R. N88-20830
DOWELL, L. J. N88-20628
DOWLER, MICHAEL G. N88-20811
DOWLING, KEVIN N88-20283
DOWNER, JAMES R. N88-20491
DOYLE, RICHARD J. N88-20905
DRAKE, J. B. N88-20848
DREICER, J. N88-20944
DRESNER, L. N88-20933
DRESS, W. B. N88-20900
DROST, M. K. N88-20732
DRUMMOND, T. J. N88-21062
DRYER, FREDERICK L. N88-20381
DRYLIE, MICHAEL E. N88-20812
DUBOWSKY, S. N88-20646
DUBRAVIN, V. F. N88-20686
DUDIN, A. D. N88-20322
DUKE, EUGENE L. N88-20896
DUNCHENKO, A. G. N88-20323
DUNN, J. C. N88-20719
DURAND, A. N88-21041
DUROV, V. A. N88-20681
DURRANCE, SAMUEL T. N88-21107
DVORYASHIN, S. V. N88-20706
DYACHKOV, A. V. N88-20318
DZENIS, V. V. N88-20813

E

EASTMAN, J. A. N88-20475
EATHERLY, W. P. N88-20440
EAVES, B. C. N88-20912
EDWARDS, G. R. N88-20423
EDWARDS, R. E. N88-20824
EIDE, SHARON A. N88-20346
EIROLA, TIMO N88-20932
EKERT, FR. N88-20818
EKONOMOV, A. P. N88-20316
N88-20317
EL-HADY, NABIL M. N88-20574
ELIAS, LUIS R. N88-20614
ELKERTON, JAY N88-20842
ELLINGSON, W. A. N88-20473
N88-20474
ELLZY, MICHAEL W. N88-20385
ELSENAAR, A. N88-20266
N88-20267
EMERICH, C. N88-20326
ENCRENAZ, T. N88-20325
N88-20326
ENG, ANTHONY T. N88-20450
ERES, D. N88-21054
ERIKSEN, CHARLES C. N88-20797
ERIKSON, ROBERT N88-20284
ERKELENS, L. J. J. N88-20288
ERSKINE, F. T. N88-20775
ESOUZA, MARCELO LOPES DEOLIVEIRA N88-20350
ESTES, ROBERT D. N88-20529
ETO, M. N88-20443
N88-20444
ETTERS, R. D. N88-20391
EUCKER, P. N88-20456
EVANS, JEAN N88-20284
EYKHOFF, PIETER N88-20926
EYLER, R. L. N88-20584

F

FAGIN, P. N. N88-20458
FAIRALL, C. W. N88-20802
FALCO, C. M. N88-21057
N88-21058
FANTY, MARK A. N88-20886
FARMER, J. W. N88-21047
FARRELL, K. J. N88-20558
FARRINGTON, G. C. N88-20547
FAWLEY, W. M. N88-20618
FAY, JOHN W. N88-20965
FAZIO, GIOVANNI G. N88-21092
FEAK, GLEN ANTHONY BEER N88-20631
FEDER, MEIR N88-20511
FEDOROV, K. N. N88-20678
FELDMAN, JEROME A. N88-20886
FENN, JOHN B. N88-20982
FENN, MARTA A. N88-20772
FERIA-KAISER, VICENTE ALFONSO N88-20641
FERRANTE, JOHN N88-20417
FERRARESI, VALTAIR ANTONIO N88-20349
FERRY, D. K. N88-21037
FETTINGER, JAMES C. N88-21038
FETZER, K. N88-20332
FIELD, R. N88-20994
FIENUP, JAMES R. N88-20939
FILYUSHKIN, B. N. N88-20680
FINE, H. A. N88-21096
FINK, W. N88-20332
FINLAYSON, PAUL ALEXANDER N88-20358
FINLAYSON, T. R. N88-20428
FINLEY, CLARENCE W. N88-20417
FIRING, ERIC N88-20793
FIRSOV, K. M. N88-20705
FISCHER, JOHANNES N88-20974
FISCHER, PAUL N88-20878
FISHER, R. J. N88-20760
FITZER, E. N88-20374
FLAMENT, PIERRE N88-20794
FLEGER, STEPHEN A. N88-20825
FLINN, J. E. N88-20424
FOISTER, JAMES W., III N88-21106
FOLLSTAEDT, D. M. N88-21066
FONG, E. N. N88-21080
FONG, I. K. N88-20902
FONSECA, LEILA MARIA GARCIA N88-20712
FORTIN, PAUL N88-20296
FORWARD, ROBERT L. N88-20355
FOSTER, PAULO ROBERTO N88-20743
FOX, G. C. N88-20835
FRAAS, L. M. N88-20721
FRANCESCONI, RALPH P. N88-20810
FRANKS, L. A. N88-20628
FRANSSON, TORSTEN H. N88-20260
FRIEFELD, JERRY M. N88-20361
FRISCH, ALAN M. N88-20899
FRITZ, I. J. N88-21062
FROST, V. N88-20534
FRYE, G. C. N88-20970
FUJII, M. N88-20448
FUJIWARA, SYUZO N88-20590
FUKASAWA, T. N88-20446
FUKUSHIMA, EIICHI N88-20589
FURMANSKI, W. N88-20835

G

GADI, F. N88-20634
GAINES, EDWARD E. N88-21094
GALIMORE, REGINALD N. N88-20714
GALLAGHER, T. O. N88-20997
GALUMYAN, A. S. N88-20716
GAMARANETO, GILBERTO N88-20715
GARDNER, JOHN F. N88-20642

GARDNER, T. J. N88-20541
GARWOOD, ROLAND W., JR. N88-20791
GATLIN, GREGORY M. N88-20264
GAUSS, R. C. N88-20775
GAUTHE, B. N88-20634
GAUTHIER, A. N88-21041
GAUTIER, CATHERINE N88-20800
GAVER, D. P. N88-20907
GELMAN, B. G. N88-20318
GEOHEGAN, D. B. N88-21054
GEORGE, THOMAS F. N88-20387
N88-20975
GEORGES, T. M. N88-20783
GERAETS, W. J. H. N88-20884
GERHARZ, J. J. N88-20300
GERSTING, J. N88-21080
GHANDHI, S. K. N88-20725
GHANDHI, SORAB K. N88-21039
GILBERT, JOHN A. N88-20603
GILL, P. E. N88-20860
GILL, RICHARD D. N88-20941
GILLIES, G. T. N88-20628
GILLIOM, L. R. N88-20467
GILLIS, PETER P. N88-20409
GILMOUR, J. D. N88-20824
GINN, W. C. N88-20729
GINNEKEN, LUKAS P. P. P. N88-20549
GINZBURG, A. I. N88-20678
GIVLER, R. C. N88-20589
GLASS, I. I. N88-20575
GLASSMAN, IRVIN N88-20381
GLASSMAN, T. E. N88-21038
GLAZOV, V. N. N88-20323
GNEDYKH, V. I. N88-20316
N88-20317
GOATES, S. R. N88-20392
GODBOLE, R. M. N88-20987
GODDARD, NIGEL N88-20886
GOEBEL, D. M. N88-21021
GOERZ, D. A. N88-20985
GOLDE, MICHAEL F. N88-20386
GOLDSTEIN, C. I. N88-20913
GOLDSTEIN, DAVID N88-21074
GOOD, I. J. N88-20936
GOREE, J. G. N88-20662
GOULDING, C. A. N88-20997
GOW, ANTHONY J. N88-20779
GRANOFF, B. N88-20390
GRASMAN, J. N88-20940
GRASSOTTI, CHRISTOPHER N88-20745
GRAY, S. D. N88-20518
GRAY, S. K. N88-20466
GREATRIX, D. R. N88-20357
GRECHKO, YE. I. N88-20706
GREDEL, J. N88-21082
GREEN, M. A. N88-20963
GREGG, M. C. N88-20786
GREGG, MICHAEL C. N88-20787
GRIFFIE, TERESA M. N88-20380
GRIGORYEV, A. I. N88-20813
GRIGORYEV, A. V. N88-20316
N88-20325
N88-20326
N88-20327
GRIMARD, M. N88-20330
GRISHIN, S. D. N88-20328
GROENENDIJK, W. P. N88-20949
GRONEMEYER, S. N88-20473
GROSS, R. J. N88-20621
GRUEN, D. M. N88-20620
GRUNDER, H. A. N88-20996
GU, WENJIN N88-20503
GUELMAN, M. N88-20639
GUENNOU, H. N88-20634
GUESS, FRANK M. N88-20653
GUNTHER, S. O. N88-20606
GUO, JING N88-20749
GUPTA, KAJAL N88-20296
GURWELL, W. E. N88-21003
GUSTAFSSON, H. A. N88-20991
GUTBROD, H. N88-20991
GUZLKOWSKI, ROB N88-20283
GWINN, K. W. N88-20657
GYAMFI, MAX A. N88-20351
N88-20352

H

HABENSCHUSS, A. N88-21055
HADLEY, G. R. N88-20622
HAEGERT, D. N88-20534
HAHN, H. N88-20475
HAIDINGER, FRANK A. N88-20276
HALCOMB, D. L. N88-20468
HALPERN, JULES P. N88-21091
HAMILTON, D. S. N88-21012
HAMMOND, E. C., JR. N88-20606
N88-20608
HAN, KWANG S. N88-20630
HANNAH, P. N88-20310
HANSEN, W. L. N88-21061
HANSON, K. M. N88-20853
HARPER-SLABOSZEWICZ, VICTOR JOZEF N88-21017
HARRIGAN, R. W. N88-20638
HARRIS, J. W. N88-20991
HARRIS, REGINA N88-21074
HARROLD, R. T. N88-20538
HARTLINE, B. K. N88-20996
HARTMANNSGRUBER, R. N88-20771
HARTSUIKER, L. N88-20660
HASHIDA, T. N88-20446
HASHIOKA, MAURO HISSAO N88-20350
HAUENSTEIN, R. J. N88-21044
HAUGEN, G. R. N88-20604
HAYEK, S. I. N88-20969
HEDGES, R. O. N88-20997
HEDRICK, C. L. N88-21025
HEGARTY, MARY N88-20493
N88-20823
HEGEDUS, CHARLES R. N88-20450
HELDT, L. A. N88-20419
HELSDON, JOHN H., JR. N88-20758
HENAGER, C. H., JR. N88-20461
N88-20462
HENDERSON, DIANE N88-20785
HENDRIKS, P. R. H. N88-20921
HENEIN, HANI N88-20367
HENIG, E. T. N88-20434
HENNEKE, K. M. N88-20997
HENNEMAN, RICHARD L. N88-20826
HENNING, J. A. N88-20430
HENRICH, VICTOR E. N88-20393
HENYEY, FRANK S. N88-20799
HERMAN, I. P. N88-21059
HESKETH, G. B. N88-20648
HESSELINK, WIM H. N88-20876
HEWETT, MARLE D. N88-20896
HICKS, H. R. N88-20848
HIEFTJE, GARY M. N88-21018
HILDUM, E. A. N88-20626
HILLIER, M. J. N88-20649
HINCHLIFFE, I. N88-20986
HIPPSLEY, C. A. N88-20650
HIROOKA, Y. N88-21021
HITCHON, W. N. G. N88-20852
HJALMARSON, H. P. N88-21047
HODGDON, JAMES A. N88-20808
HODGIN, R. L. N88-20985
HODGSON, THOM J. N88-20653
HOELD, R. N88-20596
HOENLINGER, H. N88-20298
HOFFMAN, D. A. N88-20953
HOFFMAN, ROSS N. N88-20745
HOGREFE, R. L. N88-20544
HOKENSON, GUSTAVE J. N88-20556
HOLLAND, D. F. N88-21024
HOLLIS, MICHELLE S. N88-20273
HOLMES, J. A. N88-21023
HOLNICKISZULC, JAN N88-20640
HOLTZWORTH, J. D. N88-20584
HOLZAPFEL, CHRISTIAN N88-20756
HORNSBY, M. E. N88-20824
HOSSENLOPP, A. N88-21065
HOUNJET, M. H. L. N88-20265
HSING, W. W. N88-20623
HSU, C. T. N88-21022
HSU, H. Y. N88-20969
HU, HSUN N88-20410
HUBBARD, C. R. N88-20465
HUESSLER, W. N88-20671
HUFFER, FRED W. N88-20906
HUFNAGEL, H. N88-20332
HUIJSER, R. H. N88-21016
HUITEMA, G. B. N88-20928
HUNDSDORFER, WILLEM H. N88-20924
HUNJAN, M. N88-20730
HUSSAINI, M. Y. N88-20591
HUTSON, F. L. N88-20379
HUTTER, D. J. N88-21090
HWANG, IN HEON N88-20630

I

ICE, G. E. N88-21055
IGNATOVA, S. P. N88-20315
IHM, Y. E. N88-21053
IMAI, H. N88-20444
IMBO, D. N88-20321
IMHOF, WILLIAM L. N88-21094
IOKA, I. N88-20441
IRENE, E. A. N88-20377
ISAACS, RONALD G. N88-20745
ISHIHARA, M. N88-20441
ISHIYAMA, S. N88-20446
IVANOV, V. M. N88-20807
IVANOV, YU. A. N88-20688
IVANOVA, V. F. N88-20321
IVANOVSKIY, M. N. N88-20402
IVASHKEVICH, V. F. N88-20691
IZRAEL, G. N88-20321

J

JACAK, B. V. N88-20991
JACKSON, DAVID M. N88-20291
JACOBS, P. A. N88-20907
JAEGER, H. N88-20374
JAEGER, RAYMOND E. N88-20492
JAEGLE, P. N88-20634
N88-21033
JAIN, ROMESH KUMAR N88-20572
JAMEL, G. N88-20634
JAMELOT, G. N88-21033
JANKOWSKI, A. F. N88-21060
JANSEN, R. W. T. L. N88-20821
JANSSEN, P. H. M. N88-20925
JANSSEN, PETER H. M. N88-20926
N88-20927
JEA, K. C. N88-20849
JEFFRESS, GARY ALAN N88-20345
JELSKI, DANIEL A. N88-20387
JENSEN, S. M. N88-20536
JIANG, TSUNG LEO N88-20359
JOHNSON, BRUCE G. N88-20491
JOHNSON, C. A. N88-20484
JOHNSON, E. K. N88-20584
JOHNSON, GERALD K. N88-20463
JOHNSON, J. A. N88-20971
JOHNSON, J. BLAIR N88-20598
JOHNSON, M. R. N88-20901
JOHNSON, P. C. N88-21000
JONES, C. D. N88-20536
JONES, E. D. N88-21062
JONES, GUILFORD, II N88-20963
JONES, R. H. N88-20461
N88-20462
JONES, R. M. N88-20783
JONES, ROBERT E., JR. N88-21075
JONES, S. E. N88-20409
JONG, R. A. N88-20618
JOOSSE, P. A. N88-20670
JOSHI, A. N88-20413
JUHASZ, ARPAD A. N88-20380
JUST, MARCEL A. N88-20493
N88-20823

K

KALINOSKI, H. T. N88-20394
KALMAN, RUDOLF E. N88-20908
KAMMASH, T. N88-21026
KAMPERT, K. H. N88-20991
KANDIL, OSAMA A. N88-20271
N88-20574
KANT, TARUN N88-20370
KARYAGIN, V. P. N88-20313
N88-20314
KASATKIN, B. A. N88-20698
KASHER, J. C. N88-20859
KASHUBA, R. J. N88-20951
KATHONG, M. N88-20573
KATHONG, MONCHAI N88-20934
KAWAKAMI, HARAO N88-20447
KAWAMATA, K. N88-20445
KAWAMURA, YOSHIRO N88-20398
KAWANO, SANDY N88-21081
KAWASATA, K. N88-20442
KAZARYAN, V. V. N88-20676
KEHOE, MICHAEL W. N88-20301
KEIL, R. G. N88-20384
KELLERMEIER, H. N88-20332
KELLY, J. M. N88-20568
KEMELMAN, V. A. N88-20684
KEMMERLY, GUY T. N88-20264
KENNEDY, C. R. N88-20440
KERSTEN, MARTIN L. N88-20863
KERZHANOVICH, V. V. N88-20315
KESTIN, J. N88-21067
KETOJA, J. A. N88-20961
KEVORKYAN, YU. R. N88-20433
KHAN, K. K. N88-20430
KHARYUKOVA, V. P. N88-20322
KHURI, A. I. N88-20936
KHURI, ANDRE I. N88-20943

KIKUCHI, KAZUO N88-20272
KIM, J. U. N88-20483
KIM, JEE S. N88-20938
KIM, KHONG HON N88-20630
KIM, KYEKYOON (KEVIN) N88-20334
KIMBALL, K. M. N88-20540
N88-21052
KINDERVATER, G. A. P. N88-20689
KING, JAMES W. N88-20385
KING, R. B. N88-21042
KINSLEY, K. N88-21080
KIRNOZOV, F. F. N88-20323
KIROUSIS, LEFTERIS M. N88-20662
N88-20917
KLEINAU N88-20332
KLEINMANN, SUSAN G. N88-21089
KLEM, J. N88-21053
KLEMM, WILHELM N88-20401
KLISNICK, A. N88-20634
KLOMPSTRA, MARTIN H. N88-20348
KLOP, J. W. N88-20669
N88-20920
KNAPP, J. A. N88-21066
KNEUBUEHL, B. N88-20336
KNISLEY, J. R. N88-20900
KO, WILLIAM L. N88-20375
KOBZOVA, V. M. N88-20701
KOCH, D. J. N88-20852
KOCKS, U. F. N88-21056
KOERBER, WILFRIED N88-20526
KOFAL, ALLEN E. N88-20339
KOK, JOOST N. N88-20893
KOLAWA, E. N88-20976
KOLB, B. N88-20991
KOLB, G. J. N88-20737
KOLOTILIN, B. I. N88-20321
KOMEN, G. J. N88-20804
KOMEN, GERBRAND N88-20798
KONDO, Y. N88-21090
KONG, J. A. N88-20711
KONG, Y. K. N88-20477
KONING, J. N88-20883
KONISHI, T. N88-20443
KONOVALOV, E. YE. N88-20402
KOORNWINDER, TOM H. N88-20954
KOPPES, W. M. N88-20482
KORCHUGANOV, B. N. N88-20319
KORON, N. N88-20325
KOROTENKO, K. A. N88-20693
KOROVIN, V. P. N88-20676
KORT, V. G. N88-20688
KORTH, G. E. N88-20424
KORTRIGHT, J. B. N88-20373
KOSEL, T. H. N88-20421
KOSHLYAKOV, M. N. N88-20686
N88-20689
KOSSEN, L. N88-20873
KOSTYANOY, A. G. N88-20678
KOTECKI, D. E. N88-21059
KOTYUKH, A. A. N88-20707
KOVTUNENKO, V. M. N88-20313
N88-20314
KOWALENKO, V. N88-21032
KOZLOV, V. F. N88-20696
KRAEMER, WILLIAM J. N88-20810
KRAMER, D. P. N88-20468
KRANAKIS, EVANGELOS N88-20662
KRANTZ, S. G. N88-20560
KRASITSKIY, V. P. N88-20680
KRAUSE, SONJA N88-20960
KRAUSS, A. R. N88-21064
KREMNEV, R. S. N88-20313
N88-20314
KRENZIN, K. T. N88-21063
KREUTZ, EMAR N88-20526
KRIKORIAN, S. E. N88-20385
KRIZ, R. J. N88-20473
KROLL, NORBERT N88-20572
KRUEGER, ARLIN J. N88-20714
KRUGER, J. N88-20413
N88-20422
KRUSEMAN, P. N88-20804
KUDLINSKI, ROBERT A. N88-20833
KULANDER, K. C. N88-20990
KULCINSKI, F. L. N88-20356
KULL, H. J. N88-20951
KULP, T. J. N88-21013
KUNATH, RICHARD R. N88-20555
KUNERTH, D. N88-20459
KUO, HUNG-CHI N88-20750
KUO, K. K. N88-20483
KURTZ, R. L. N88-20980
KURUMADA, A. N88-20445
KURUSADA, A. N88-20442
KUSAKABE, MASAO N88-20590
KUSHNER, A. S. N88-20654
KUZMINA, N. P. N88-20694

L

LABOMBARD, B. N88-21021
LADD, JIM N88-20283
LAHAYE, R. N88-21027
LAIRD, JOHN E. N88-20898
LAITURI, TONY R. N88-20773
LAKE, RENEE C. N88-20656
LAMARRE, J. M. N88-20326
LAMB, R. G. N88-21095
LAMPPA, D. L. N88-21052
LANZANO, PAOLO N88-20845
LARESE, J. Z. N88-20428
LARGE, W. G. N88-20801
LARKO, DAVID E. N88-20714
LASKEY, KATHRYN B. N88-20820
LAUCHLE, G. C. N88-20966
LAUFFER, J. P. N88-20657
LAWDER, TIMOTHY J. N88-20746
LAWKINS, W. F. N88-20648
LEAVITT, J. A. N88-21058
LEDBETTER, H. M. N88-20366
LEE, C. K. N88-20477
LEE, J. N88-20544
N88-20551
LEE, J. K. N88-20416
LEE, M. L. N88-20392
LEE, MARIO J. N88-20562
LEE, P. C. N88-20532
LEE, R. S. N88-20418
LEE, RICHARD L. N88-21006
LEE, T. N. N88-20781
LEEMANN, C. W. N88-20996
LEIDER, H. R. N88-20464
LEININGER, M. N88-20881
LEMAIRE, P. N88-21033
LENSTRA, J. K. N88-20889
LENSTRA, JAN KAREL N88-20861
LEONARD, SUSAN R. N88-20463
LEONE, STEPHEN R. N88-20989
LERNER, JEFFREY DANIEL N88-20577
LESPANOL, ZH. N88-20321
LESTER, WILLIAM A. N88-20977
LEUNG, P. T. N88-20387
LEUNG, W. K. N88-21021
LEVA, NATALIE N88-20810
LEVIN, STEVEN MARK N88-21112
LEVINE, HOWARD A. N88-20909
LEWIS, D. A. N88-21095
LEYKIN, I. A. N88-20699
LI, CHUNYI N88-20496
LI, M. F. N88-21061
LIEW, SO KUEN N88-20611
LIGHT, R. W. N88-20623
LIN, YULIAN N88-20502
LINDEBERG, TONY N88-20277
LINDSTROM, ERIC N88-20789
LING, GILBERT N. N88-20805
LINKIN, V. M. N88-20315
LIOU, FUE-WEN N88-20643
LIPATOV, A. N. N88-20315
LIPSITT, HARRY A. N88-20435
LISOWSKI, MICHAEL N88-20754
LITTELL, RAMON C. N88-20943
LIU, A. S. N88-20429
LIU, DONG C. N88-20851
LIU, DUN CHARLES N88-20579
LIU, H. N88-20514
LIU, K. C. N88-20658
LIU, WU-MING N88-21011
LOCKWOOD, RICHARD P. N88-20368
LOCKWOOD, S. J. N88-20541
LONDON, B. N88-20420
LONG, G. G. N88-20413
LORENZZETTI, JOAO ANTONIO N88-20774
LOVISA, A. N88-20771
LOWDEN, R. A. N88-20369
LOWNDES, D. H. N88-21054
LU, MONG-MING N88-20751
LU, S. C. N88-20902
LUCAS, STEPHEN H. N88-20669
LUGTEN, JOHN BUTTERFIELD N88-21099
LUKAS, H. L. N88-20434
LUKAS, ROGER N88-20789
LUKASHEV, YU. F. N88-20688
LUKIN, D. S. N88-20703
LUND, DAVID J. N88-20809
LUNDIN, C. D. N88-20430
LUST, ROBERT V. N88-20290
LUTZ, W. N. N88-20628
LYNCH, V. E. N88-20648
N88-21023
LYNNE, KENTON N88-20686
LYON, R. E. N88-21024
LYTLE, F. W. N88-20727
LYUBIMOV, B. YA. N88-21071

M

MA, C. N88-20753
MA, D. W. N88-20560
MACDONALD, KENNETH N88-20843
MACFARLANE, J. N88-20945
MACKENZIE, FRED T. N88-20803
MADEY, T. E. N88-20980
MAEDA, CHIKAYOSHI N88-20454
MAH, C. S. N88-20585
MAHAJAN, S. M. N88-21019
MAI, TSUN-ZEE N88-20849
MAILHE, C. C. N88-20545
MAJESWKI, S. N88-20994
MAJORS, P. D. N88-20589
MAJUMDAR, A. N88-20880
MAKAR, G. L. N88-20413
MAKOUS, J. L. N88-21057
N88-21058
MAKOWIECKI, D. M. N88-21060
MAKOWITZ, H. N88-20880
MALIK, K. N88-20315
MALLON, R. G. N88-20586
MALONE, JACQUELINE C. N88-20506
MALONE, THOMAS B. N88-20825
MALTSEV, D. V. N88-20716
MANGUM, SCOTT N88-20895
MANVELYAN, O. S. N88-20322
MARCHE, P. N88-20771
MARINOPOULOS, STERGIOS N88-20291
MARION, J. N88-21010
MARITATO, L. N88-21058
MARR, J. J. N88-20544
MARSH, O. J. N88-21044
MARTIN, CARL J. N88-20669
MARTIN, R. L. N88-20824
MARTIN, S. J. N88-20970
MARTINELLI, LUIGI N88-20580
MARTINI, S. N88-21027
MARUYAMA, T. N88-20448
MASCARENHAS, NELSON DELFINO DAVILA
N88-20712
MASHBURN, D. N. N88-21054
MASINSKAS, J. J. N88-20595
MASON, MARY L. N88-20290
MASON, R. E. N88-21004
MASSEY, R. T. N88-20468
MASUO, RYUICHI N88-20454
MATAYA, M. C. N88-20423
MATHESON, N. N88-20258
MATLOCK, D. K. N88-20423
MATSUI, HIROYUKI N88-20398
MATSUO, H. N88-20444
MATTHEWS, R. B. N88-21004
MATVEEV, L. V. N88-21071
MAUERSBERGER, GARY N88-20303
MAZUREK, W. N88-20478
MCBRIDE, M. W. N88-20558
MCCURDY, ALAN H. N88-20602
MCEVILY, A. J. N88-20431
MCGREW, SETH G. N88-20779
MCINTOSH, GORDON CAMPBELL N88-21113
MCINTYRE, L. C., JR. N88-21058
MCKEAGUE, IAN W. N88-20906
MCKERNAN, M. A. N88-21060
MCLEOD, P. S. N88-20721
MCLIN, M. N88-20452
MCMACKIN, I. A. N88-20633
MCSHEA, J. C. N88-20632
MCVAY, L. N88-20490
MEANS, K. H. N88-20584
MEDLEY, H. W. N88-20519
MEEKS, W. H., III N88-20953
MEGIE, G. N88-20771
MEHROTRA, KISHAN G. N88-20514
MELIKYAN, R. A. N88-20509
MELNGAILIS, JOHN N88-21040
MENDES, CELSO LUIZ N88-20715
MENON, R. N88-20430
METCALF, JAMES I. N88-20515
METZGER, GISELE N88-20553
MEUSER, WILFRIED N88-20973
N88-20974
MEZH, B. N88-20316
MICHAELS, A. I. N88-20637
MICHELSEN, C. N88-20944
MICKELSEN, R. A. N88-20727
MIKADO, TUNEO N88-20476
MIKKOLA, D. E. N88-20418
MILAM, D. N88-20626
MILES, JOHN L., JR. N88-21075

MILLER, A. K. N88-20657
MILLER, J. F. N88-20544
MILLER, JAMES R. N88-20514
MILOVIDOVA, A. V. N88-20402
MINDEN, M. L. N88-20536
MINES, G. L. N88-20736
MISTREE, FARROKH N88-20291
MITCHINER, J. L. N88-20914
MITSEL, A. A. N88-20705
MITSUOII, FERNANDO AUGUSTA N88-20708
MIYAHARA, YOSHINORI N88-20480
MIYOSHI, KAZUHISA N88-20454
MOBILIA, JOSEPH N88-21094
MODDEMAN, W. E. N88-20458
MOELLER, C. N88-20634
MOELLER, C. P. N88-21000
MOGI, H. N88-20441
MOHR, P. B. N88-20464
MOIN, PARVIZ N88-20583
MOK, W. S. N88-20730
MOLCHANY, JEROME W. N88-20809
MONIN, A. S. N88-20685
MOORE, ARCHIE L. N88-20506
MOORE, H. F. N88-20484
MOORE, TIMOTHY S. N88-20887
MOORE, WAYNE A. N88-20709
MORGESON, D. N88-20944
MORKOC, H. N88-21053
N88-21055
MOROSIN, B. N88-20465
MOROZ, I. P. N88-20701
MOROZ, V. I. N88-20316
N88-20317
N88-20325
N88-20326
MOROZOV, YE. G. N88-20688
MORRISON, IAN R. N88-20823
MORUKOV, B. V. N88-20807
MOSER, WILLIAM R. N88-20757
MOSHKIN, B. YE. N88-20316
N88-20317
MOSKALEVA, L. P. N88-20322
MOSS, A. C. N88-20371
MOSS, C. E. N88-20997
MOSS, H. W. N88-21107
MOSS, R. W. N88-21003
MOTE, J. D. N88-20456
MOUGEY, J. N88-20996
MOUM, J. N. N88-20788
MUELLER, W. N88-20332
MUFSON, S. L. N88-21090
MUKHIN, L. M. N88-20318
N88-20319
MULCAHEY, T. P. N88-20544
MULLER, PETER N88-20785
MUNZERT, K. N88-20771
MURA, JOSE CLAUDIO N88-20715
MURATA, SHIGEO N88-20590
MURDMAA, I. O. N88-20683
MURDOCH, SCOTT N88-20488
MURDOCK, WILLIAM P., JR N88-20516
MURRAY, W. N88-20860
MUSTAFA, ERROL N88-21100

N

NABATOV, V. N. N88-20697
NAGY, DALE A. N88-20415
NAIK, R. A. N88-20372
NAIK, VIJAY K. N88-20831
NANUT, VICTOR N88-20399
N88-20486
N88-20489
NASH, J. G. N88-20530
NATION, J. A. N88-20998
NAUMENKO, YE. K. N88-20682
NAVROTSKAYA, S. YE. N88-20686
NEELIN, JAMES DAVID N88-20764
NELSON, D. N88-20420
NELSON, L. S. N88-20395
NENAROKOV, D. F. N88-20318
NEUHOFF, DAVID L N88-20939
NEVANLINNA, OLAVI N88-20932
NEWBERRY, MICHAEL VAN N88-21101
NEWBOLD, W. T. N88-20775
NEWCOMB, A. W. N88-20274
NEWELL, ALLEN N88-20898
NEWNAM, B. E. N88-20625
NGUYEN, A. N88-21065
NGUYEN, P. D. N88-20546
NICHOLS, F. A. N88-20637
NICHOLSON, M. M. N88-21036
NICOLET, M.-A. N88-20976
N88-21035
NIELSEN, C. N88-20469
NIKOLSKIY, YU. V. N88-20326
NIMIS, J. N88-20483
NING, CARLOS HO SHIH N88-20743
NIXON, MARK W. N88-20656
NOACK, W. N88-21082
NOBACK, R. N88-20295
NOCEDAL, JORGE N88-20851
NOEL, B. W. N88-20628
NOGUEIRA, CELSO FIGUEIREDO N88-20930
NOID, D. W. N88-20466
NOLTHENIUS, H. J. N88-20995
NOMURA, S N88-20444
NOVAK, JOSEPH T. N88-20561
NUTT, S. R. N88-21060
NYGREN, R. N88-21021
NYYSSONEN, D. N88-20838

O

OBERLE, WILLIAM F. N88-20380
OGALLAGHER, J. N88-20718
OGANOV, V. S. N88-20813
OGLESBY, PAUL HARVEY N88-21110
OGORODNIKOV, B. I. N88-20319
OHANLAN, JOSEPH T., JR. N88-20710
OHARA, G. P. N88-20333
OKU, T. N88-20441
N88-20442
N88-20443
N88-20444
N88-20446
N88-20448
OLDHAM, W. G. N88-20533
OLSON, D. B. N88-20451
ONDREJKA, A. R. N88-20519
OOKA, K. N88-20448
ORLOV, L. I. N88-20702
ORLOV, O. I. N88-20807
ORTOLANI, S. N88-21027
OSHKORN, A. N88-20316
OSTGAARD, JOHN N88-20303
OTSUKA, N. N88-21053
OVCHINNIKOV, I. M. N88-20688
OWYOUNG, A. N88-20622
OZMIDOV, R. V. N88-20697

P

PABALAN, R. T. N88-21069
PAKA, V. T. N88-20688
PALETS, B. L. N88-20817
PALMER, D. R. N88-20783
PALMER, R. S. N88-21002
PANCHENKO, V. S. N88-20817
PANDA, BINAYAK N88-20635
PANGELS, HENNING N88-20283
PANTELEYEV, G. G. N88-20679
PAPKOV, O. V. N88-20314
PAREKH, D. E. N88-20562
PARENT, J. O. N88-20367
PARENTEAU, L N88-20978
PARIS, MICHEL N88-20553
PARK, A. N88-20397
N88-20962
PARK, CHUNG KYU N88-20765
PARK, STEPHEN K. N88-20833
PARTAIN, L. D. N88-20721
PARTER, S. V. N88-20913
PASDELOUP, MAURICE N88-20553
PATERA, ANTHONY T. N88-20878
PATRICK, MERRELL L. N88-20831
PAULSON, JOHN W., JR. N88-20264
PAVLOV, A. M. N88-20678
PAVLOVA, G. D. N88-20402
PAXMAN, RICHARD G. N88-20939
PAYNE, S. A. N88-21009
PAYS, MICHEL N88-20553
PAZIK, J. C. N88-21038
PEL, L. N88-20275
PELLIN, M. J. N88-20620
PENN, LANNING M. N88-20714
PENNOCK, S. T. N88-20859
PENNYCOOK, S. J. N88-21054
PEREKHVATOV, V. V. N88-20684
PERMENTER, KATHRYN E. N88-20825
PESETSKAYA, N. N. N88-20278
PETERS, HARTMUT N88-20787
PETERS, K. A. N88-20606
PETERS, KEVIN N88-20608
PETERS, L., JR. N88-20397
PETHERAM, J. C. N88-20632
PETRYANOV, I. V. N88-20319
PHILLIPS, J. E. N88-20726
PHILLIPS, L. R. N88-20914
PHILLIPS, ROBERT M. N88-21043
PICHKHADZE, K. M. N88-20313
N88-20314
PICRAUX, S. T. N88-20623
PIEHLER, HENRY R. N88-20367
PIERINI, P. N88-20469
PILCHOWSKI, HANS-ULRICH N88-20331
PILGER, J. P. N88-21003
PINKEL, R. N88-20790
PINOLI, A. A. N88-20546
PINTODEGARRIDO, JUAN CARLOS N88-20715
PISTEK, P. N88-20777
PITZER, K. S. N88-21069
PLESHIVTSEV, A. D. N88-20402
PODYMOV, I. S. N88-20694
POE, C. C., JR. N88-20363
POHJOLAINEN, S. N88-21108
POKHUNKOV, S. A. N88-20704
POMMERO, ZH. P. N88-20316
PONOMAREV, YU. N. N88-20705
POPE, DAVID P. N88-20435
POPOV, A. A. N88-20817
PORSHNEV, N. V. N88-20318
POSKANZER, A. M. N88-20991
POTTER, R. T. N88-20300
POUKEY, J. W. N88-20335
POWELL, D. C. N88-20761
POWERS, SHERYLL GOECKE N88-20279
PRATER, R. N88-21000
PRELL, W. L. N88-20759
PRESTWICH, K. R. N88-20999
PRICE, DAVID L. N88-20463
PRICE, JAMES F. N88-20792
PRITCHARD, JOCELYN I. N88-20665
PROK, GEORGE M. N88-20455
PROKOPCHIK, A. YU. N88-20403
PROSCHAN, FRANK N88-20938
PUDOV, A. N. N88-20321
PURDY, KARL N88-20303

Q

QUINN, M. C. N88-20967
QUINTO, P. FRANK N88-20264

R

RACK, H. J. N88-20662
RADZEWICZ, C. N88-20633
RAGONIDEMORAESCORREA, VIRGINIA N88-20708
RAINER, F. N88-20626
RAJIYAH, HARINDRA N88-20664
RAKHMANOV, A. S. N88-20813
RAMAKER, DAVID E. N88-20379
N88-20978
N88-20979
N88-20980
RAMAN, RAJEEV N88-20640
RAMOND, P. N88-20994
RAMSEY, LAWRENCE W. N88-21088
RAMSTAD, T. N88-20376
RAPP, RICHARD H. N88-20752
RAQUET, CHARLES A. N88-20555
RATNARPARKHI, P. N88-20662
RAYMER, M. G. N88-20633
RAYMOND, F. N88-21041
RAZUMOV, A. V. N88-20957
N88-21072
N88-21073
REDIKER, ROBERT H. N88-20611
REDMAN, LANCE D. N88-20489
REDNER, ALEX S. N88-20673
REECE, CHARLES E. N88-20600
REIF, JOHN H. N88-20837
REIFENBERGER, R. G. N88-20624
REIGBER, C. N88-21082
REKERS, JAN N88-20864
RENNIE, MICHAEL W. N88-20847
RENSHAW, A. W. N88-21079
REYNOLDS, W. C. N88-20562
REYNOLDS, WILLIAM C. N88-20583
RHEA, DONALD C. N88-20344
N88-20832
RICCI, WILLIAM S. N88-20406
RICCO, A. J. N88-20970
RICE, C. K. N88-20588
RICHARDSON, J. M. N88-21029
RIEDL, GUENTHER N88-20528
RIEDLINGER, SHELLEY H. N88-20776
RIEFFE, H. CH. N88-20660
RIFF, R. N88-20668
RILEY, J. P. N88-20783
RINALDI, STEVEN M. N88-20615
RINNOOYKAN, A. H. G. N88-20689

RITTER, H. G. N88-20991
RIVIERE, A. C. N88-21000
ROBERTS, R. A. N88-20473
ROBERTSON, N. N88-20649
ROBINSON, M. L. N88-20423
ROBL, EUGENE ANTHONY N88-20766
RODENBURG, P. H. N88-20916
ROERDINK, J. B. T. M. N88-20940
ROGOVSKIY, G. N. N88-20313
N88-20314
ROKAR, F. N88-20326
RONQUIST, EINAR M. N88-20678
ROONEY, M. N88-20453
ROSEN, A. N88-20632
ROSENBERG, A. N88-20632
ROSENBLOOM, PAUL S. N88-20696
ROSS, M. N88-20958
ROSS, P. N. N88-20539
ROTHBLUM, U. G. N88-20912
ROTIN, V. A. N88-20318
ROTTA, JULIUS N88-20594
ROTTLER, J. S. N88-20856
N88-20857
N88-20858
ROUSE, WILLIAM B. N88-20826
ROY, T. N. N88-20513
ROYER, M. N88-21041
ROZOVA, YE. V. N88-20816
RUIJSENAARS, S. N. M. N88-20955
RUMMEL, REINER N88-20752
RUTTEN, JAN J. M. M. N88-20956
RYAN, J. W. N88-20753
RYAN, T. W., III N88-20645
RZHEVSKIY, N. N. N88-20692

S

SAAD, Y. N88-20888
SABOUNGI, MARIE LOUISE N88-20380
N88-20463
SACHS, ALEXANDER N88-20651
SADJADI, FIROOZ N88-21005
SAFONOV, M. P. N88-20321
SAGDEYEV, R. Z. N88-20313
N88-20314
SAILORS, D. B. N88-20513
SAKASHITA, T. N88-20448
SAMARA, G. A. N88-21047
SAMDE, HIDEO N88-20978
N88-20979
N88-20980
SANCHE, L. N88-20978
SANCHEZ, BRAULIO V. N88-20780
SANKO, N. F. N88-20325
N88-20326
SANOKAWA, KONOMO N88-20439
SANOTSKIY, YA. V. N88-20315
SANTANNABINS, LEONARDO N88-20708
SANTARIUS, J. F. N88-20356
SANTIAGO-MANDUJANO, FERNANDO N88-20793
SANZ-SERNA, J. M. N88-20922
SARGENT, G. N88-20534
SARKISYAN, A. S. N88-20700
SARPKAYA, T. N88-20567
SARYCHEV, V. A. N88-20324
SATO, S. N88-20442
N88-20445
SAUBER, JEANNE M. N88-20754
SAUNDERS, M. A. N88-20660
SAVCHENKO, V. V. N88-20324
SAVELSBERGH, MARTIN W. P. N88-20948
SAWICKA, B. D. N88-20473
SAZONOV, V. V. N88-20324
SCALES, DOMINIC R. N88-21093
SCARPETTI, R. D. N88-20985
SCHAFFER, M. N88-21027
SCHARLEMANN, E. T. N88-20618
SCHEPER, CHARLOTTE N88-20895
SCHIESS, JAMES R. N88-20309
SCHILLING, C. H. N88-20461
N88-20462
SCHIRBER, J. E. N88-21062
SCHMIDT, H. R. N88-20991
SCHMIT, LUCIEN A. N88-20290
SCHOENLEIN, L. H. N88-20461
N88-20462
SCHOR, A. L. N88-20568
SCHOUTEN, H. J. N88-20867
SCHRA, L. N88-20426
SCHREIER, G. N88-21082
SCHROETER, H. N88-21082
SCHUDLICH, REBECCA R. N88-20792
SCHUETZ, D. N88-20300
SCHUTTE, W. C. N88-21020
SCHWEIZER, K. S. N88-20470
N88-20471
SCOTTI, STEPHEN J. N88-20669
SCRUBY, C. B. N88-20650
SEATON, C. T. N88-21057
SECHRIST, FRANK S. N88-20714
SEFER, N. R. N88-20645
SEGAL, E. N88-20474
SEIDEL, DAVID A. N88-20269
SELEZNEV, G. F. N88-20684
SELLERS, SUZANNE M. N88-20905
SEMENOV, YE. V. N88-20679
SEMENOV, YU. N88-20329
SENONER N88-20828
SENSBURG, O. N88-20298
SEREDENKO, M. M. N88-20816
SETHURAMAN, JAYARAM N88-20937
N88-20938
SEYLER, C. E. N88-20998
SHADRIN, I. F. N88-20688
SHAFFER, STEVEN N88-21074
SHAH, A. H. N88-20366
SHAHMIRIAN, VARAZ N88-20522
SHAN, W. N88-21061
SHANMUGAN, K. N88-20534
SHAPIRO, G. I. N88-20695
SHAPIRO, JEFFREY H. N88-20612
SHAPIRO, L. H. N88-20782
SHARPE, DAVID L. N88-20257
SHAUB, YU. B. N88-20677
SHAW, C. B., JR. N88-20636
SHELNUTT, J. A. N88-20390
SHERETOV, E. P. N88-20321
SHIINO, KAZAUO N88-20590
SHINDO, Y. N88-20366
SHIPILOV, S. D. N88-20278
SHIZGAL, IRVIN N88-20892
SHLANCHYAUSKAS, A. A. N88-20690
SHLYAZHAS, R. B. N88-20690
SHMATKO, B. A. N88-20402
SHMOYS, DAVID B. N88-20861
SHROUF, K. C. N88-20997
SHULL, C. L. N88-20636
SHUPE, JON A. N88-20291
SIBUL, L. H. N88-20512
SIDDONS, D. P. N88-21011
SIEBECKER, HANS N88-20297
SIEBES, ARNO N88-20863
SIEFRING, CARL LEWIS N88-20767
SIEGEL, R. W. N88-20475
SIERRAALCAZAR, H. B. N88-20546
SIGGIA, E. D. N88-20565
SIGMAR, D. J. N88-21022
SIKIVIE, P. N88-20994
SILK, M. G. N88-20649
SILVA, CARLOS ALBERTO BOMFIM N88-20607
SILVA, V. M. N88-20478
SIMITSES, G. J. N88-20668
SIMMONS, G. J. N88-20952
SIMONI, PAULO OUVERA N88-20897
SIMPSON, J. W. N88-21029
SINGH, JEFF N88-20283
SINGH, T. N88-20383
SINHA, N. N88-20256
SINHA, SHYAMA P. N88-20384
SKITOVICH, B. I. N88-20319
SKRUTSKIE, MICHAEL F. N88-21102
SLENTZ, G. E. N88-20997
SMAGA, J. A. N88-20544
SMEDINGA, REIN N88-20904
SMEDLEY, J. N88-20483
SMIRNOV, G. G. N88-20322
SMIT, DIRK-JAN N88-21070
SMITH, H. G. N88-20428
SMITH, J. N88-20987
SMITH, J. A. N88-20790
SMITH, JEFFREY H. N88-20351
N88-20352
SMITH, M. C. N88-21062
SMITH, R. D. N88-20394
SMITH, WAYNE ALLEN N88-20582
SMULDERS, P. N88-20770
SNYDER, AARON N88-20262
SNYDER, C. E. N88-21079
SNYDER, S. C. N88-20636
SO, F. C. N88-20976
SOBIESZCZANSKI-SOBIESKI, JAROSLAW N88-20830
SOBIESZCZANSKISOBIESKI, JAROSLAW N88-20829
SODA, NORIMUNE N88-20480
SODERSTROM, TORSTEN N88-20926
SOLOMON, SEAN C. N88-20754
SOLOSKI, EDWARD J. N88-20449
SOLOVEV, L. D. N88-21072
N88-21073
SOMORJAI, G. A. N88-21046
SPANBURG, CRAIG S. N88-20537
SPANNER, G. E. N88-20732
SPARKS, C. J. N88-21055
SPEAR, ROBERT J. N88-20399
N88-20486
N88-20489
SPECTOR, ALFRED Z. N88-20885
SPECTOR, SCOTT J. N88-20388
SPENCER, GERALD L. N88-20407
SPIJKERVET, A. L. N88-20946
SPOHN, R. N88-20534
SPRUCK, J. N88-20953
STADNYK, B. I. N88-20315
STAMPER, DAVID A. N88-20809
STAMPS, D. W. N88-20395
STANBERY, B. J. N88-20727
STASEVICH, V. I. N88-20703
STEBBINS, ALBERT JOSEPH, III N88-21103
STECH, JOSE LUIZ N88-20774
STEELE, W. A. N88-20464
STEELE, W. V. N88-21065
STEFANOV, B. N88-21028
STEGEMAN, G. I. N88-21057
STEPHENS, MICHAEL A. N88-20935
STEWART, J. M. N88-20465
N88-20727
STEWART, JAMES J. N88-20362
STINE, W. B. N88-20736
STINTON, D. P. N88-20369
STOBER, AL N88-20608
STOCK, LARRY V. N88-20630
STOHL, F. V. N88-20390
STOICA, PETRE N88-20926
N88-20927
STOKES, JAMES N88-21074
STOLYARCHUK, P. G. N88-20315
STONE, H. M. N88-20762
STONE, J. L. N88-20733
STRUBE, M. M. N88-21065
SUENKEL, HANS N88-20752
SUGAMA, TOSHIFUMI N88-20457
SUIT, WILLIAM T. N88-20309
SUKHANOV, K. G. N88-20314
SULLIVAN, N. N88-20994
SUN, FUCHUN N88-20503
SUNDELIN, R. M. N88-20996
SUREAU, A. N88-20634
SUREK, T. N88-20728
SURESH, S. N88-20659
SURKOV, YU. A. N88-20321
N88-20322
N88-20323
SUTTON, W. A. N88-20484
SUZUKI, H. N88-20448
SZKODY, RON N88-20303
SZUMILIN, KRYSTYNA N88-20960

T

TABOR, J. N88-20879
TAGUE, J. A. N88-20512
TAKACS, P. Z. N88-21011
TAKAHASHI, H. N88-20446
TAKANO, YOSHIHIDE N88-20768
TAKENS, F. N88-20928
TAMANO, T. N88-21027
TAN, A. N88-21105
TAN, LOON-SENG N88-20449
TANAKA, D. K. N88-20413
TANNER, D. N88-20994
TARDOS, EVA N88-20861
TARNOPOLSKIY, V. I. N88-20324
TARTT, DAVID M. N88-20896
TATARINOV, A. M. N88-20813
TATSIY, L. P. N88-20323
TAYLOR, I. N. N88-21002
TAYLOR, J. R. N88-20609
N88-20619
TAYLOR, P. N88-21027
TELSCHOW, K. N88-20459
TENHAGEN, P. J. W. N88-20836
N88-20866
N88-20867
N88-20868
TENHAGEN, PAUL J. W. N88-20865
TENHAVE, A. A. N88-20660
N88-20661
TERAESRANTA, H. N88-21108
TEZAKI, ATSUMU N88-20398
THART, W. G. J. N88-20371
THOMPSON, A. W. N88-20367
THOMPSON, S. L. N88-20856
N88-20857
N88-20858
THORN, C. N88-20994
THORNTON, EARL A. N88-20666
THORPE, GLEN C. N88-20517
TIKHOMIROV, A. N. N88-20322

TIKHONOV, M. A. N88-20817
TIMCHENKO, V. N88-20329
TIMOFEEV, I. YA. N88-20278
TITTMANN, B. R. N88-20744
TIWARI, S. N. N88-20573
TIWARI, SURENDRA N. N88-20934
TKACHEV, L. G. N88-20593
TODD, M. J. N88-20819
TOLCOTT, MARTIN A. N88-20820
TOLLIVER, J. S. N88-21025
TOMA, R. N88-20321
TOMIYAMA, T. N88-20868
TOMIYAMA, TETSUO N88-20865
TORCZYNSKI, J. R. N88-20621
TRAXLER, JOHN M. N88-20261
TREGUBOV, V. S. N88-20691
TROITZSCH, J. N88-20400
TRUKHCHEV, D. I. N88-20700
TSAKANOV, V. M. N88-20507
N88-20508
TSANG, F. N88-20469
TSAO, J. Y. N88-20623
TSCHERNING, C. CHRISTIAN N88-20752
TSYBANEVA, T. B. N88-20688
TUMMILLO, A. F. N88-20544
TUOMELA, J. N88-20931
TURCOTTE, DONALD L. N88-20742
TURNER, M. S. N88-21096
TUTTLE, B. A. N88-20540
TYNER, C. E. N88-20737

U

UGACHI, H. N88-20445
UN, SUN N88-20806
URAGAKI, H. N88-20448
URBANOWICZ, J. T. N88-20576
URLINGS, P. J. M. N88-20946
UROP, S. N88-21108
USHER, JOHN S. N88-20653

V

VACHA, LUBOS J. N88-20492
VAGLIO, R. N88-21058
VAIDYANATHAN, S. N88-21002
VANBREUKELEN, G. J. P. N88-20821
VANBUGGENUM, R. I. J. N88-20571
VANDENASSEM, D. N88-21016
VANDENBERG, B. N88-20570
VANDENBERG, J. L. N88-20947
VANDERGEEST, P. J. N88-20288
VANDERHOEK, H. N88-20275
VANDERHOUWEN, P. J. N88-20923
VANDERLINDEN, H. H. N88-20660
VANGINNEKEN, L. P. P. P. N88-20875
VANGLABBEEK, R. J. N88-20918
N88-20919
VANGOOL, M. F. C. N88-20281
VANHOVE, M. A. N88-21048
VANLEEUWEN, E. H. N88-20595
VANLEEUWEN, H. P. N88-20426
VANLIERE, R. N88-20836
N88-20866
VANLIESHOUT, G. J. P. N88-20875
VANLONDEN, A. N88-20610
VANMOERKERKEN, R. A. N88-20804
VANNEERVEN, W. L. N88-20987
VANNIER, M. W. N88-20473
N88-20474
VANSICLEN, C. D. N88-20425
N88-21020
VARACALLE, D. J., JR. N88-21020
VASILAKIS, J. D. N88-20338
VASSILIOU, M. S. N88-20744
VEEFKIND, A. N88-21028
VERMASEREN, J. A. M. N88-20987
VERWER, J. G. N88-20922
VETH, B. N88-20871
VIEIRAMONTEIRO, ANTONIO MIGUEL N88-21015
VIJAYAKAR, SANDEEP M. N88-20644
VINYARD, S. N88-20645
VISSER, A. HUIBERT N88-20527
VITANYI, PAUL M. B. N88-20862
N88-20890
VLASOV, M. N. N88-20704
VOIGT, J. A. N88-20540
N88-21052
VOLKMER, KENT N88-20351
N88-20352
VOLOSHIN, ARKADY S. N88-20673
VONHOLLE, W. N88-20418
VOSS, HENRY D. N88-21094

W

WAGNER, FRED E. N88-20337
WAHL, KURT N88-20401
WAHLS, RICHARD A. N88-20592
WALKER, J. N88-20994
WALLIN, WAYNE E. N88-20361
WALTER, J. N88-20459
WALTON, CHRISTINA N. N88-21008
WALTON, JAMES T. N88-20307
WALTON, O. R. N88-20586
WAN, DER-SHEN N88-21014
WANDZURA, S. M. N88-20536
WANG, JOHN D. N88-20774
WANG, LI N88-20498
WANG, S. H. N88-20902
WANHILL, R. J. H. N88-20427
WARN-VARNAS, ALEX N88-20778
WARNER-SELPH, M. A. N88-20645
WATKINS, DANIEL M. N88-20367
WAY, T. C. N88-20824
WAYNE, C. E. N88-20560
WEAVER, DAVID P. N88-20383
WEAVER, M. J. N88-20376
N88-20411
WEBB, J. N. N88-20300
WEBB, T., III N88-20759
WEBER, E. R. N88-21061
WEBER, MARK E. N88-20757
WEBER, W. J. N88-20461
N88-20462
WEBSTER, C. E. N88-20544
WEHBEH, ELIAS GEORGE N88-20578
WEIJLAND, W. P. N88-20873
WEIRICK, L. J. N88-20739
WEIS, M. J. N88-20423
WEISGERBER, P. N88-20740
WELCH, J. M. N88-21085
WELLER, ROBERT A. N88-20792
WELLS, ANN L. N88-20617
WESSENDORF, K. O. N88-20550
WEST, H. H. N88-20560
WHIFFEN, B. W. N88-20487
WHITE, ALAN R. N88-20992
WHITE, C. L. N88-20419
WHITE, D. H. N88-20984
WHITE, G. D. N88-21003
WHITE, R. C. N88-20915
WHITELAW, J. H. N88-20559
WHITLOW, WOODROW, JR. N88-20263
WHITMORE, STEPHEN A. N88-20302
WIETING, ALLAN R. N88-20666
WIGMANS, RICHARD N88-20605
N88-20968
WILLIAMS, FORMAN A. N88-20381
WILLIAMS, JEFFERY THOMAS N88-20523
WILLIAMS, T. A. N88-20732
WILSON, ERMA L. N88-20273
WILSON, K. L. N88-21021
WILSON, LONNIE A. N88-20535
WILSON, WILLIAM S. N88-20399
WINSTON, R. N88-20718
WISNIEWSKI, W. Z. N88-21090
WISSER, THOMAS N88-20284
WITT, T. N88-20735
WOLF, D. E. N88-20256
WOLF, EMIL N88-21007
WOLSTENCROFT, K. N. N88-20299
WOLTERS, G. F. N88-21001
WONG, C. C. N88-20395
WONG, K. C. N88-20985
WOOD, A. E. J. N88-20299
WORLEY, B. A. N88-20942
WORTHAM, MARTIN N88-20284
WRENN, GREGORY A. N88-20830
WRIGHT, D. D. N88-20606
WRIGHT, GEORGE B. N88-21081
WRIGHT, JON N88-20799
WRIGHT, M. H. N88-20880
WRIGHT, R. N. N88-20424
N88-20425
WU, J. J. N88-20338
WU, J. Z. Y. N88-20647
WUNSCH, CARL N88-20778

X

XIA, YIFEI N88-20500
XING, SHOUWEI N88-20502
XING, SHUCHEN N88-20496
XU, QIFENG N88-20499

Y

YAMAZAKI, YOSHIHIRO N88-20743
YAN, YAN N88-20497
YANAGIZAWA, MITSUNORI N88-20272
YANSON, KH. A. N88-20613
YAROSHCHUK, YE. V. N88-20696
YEAGER, D. M. N88-20966
YEE, K. S. N88-20659
YEFIMOV, S. S. N88-20679
YEGORIKHIN, V. D. N88-20688
YEN, W. M. N88-20993
YERGENSEN, STEPHEN N88-20832
YOKOTA, JEFFREY WAYNE N88-20270
YORK, R. C. N88-20996
YOUNG, C. E. N88-20620
YOUNG, D. M. N88-20849
YOUNGBLOOD, WALLACE W. N88-20353
YU, P. Y. N88-21061
YUCE, H. N88-20420

Z

ZABAL, X. A. N88-20839
ZABEL, H. N88-21055
ZACHARIAS, G. L. N88-20822
ZACHARY, ANDREW LEE N88-21104
ZANG, THOMAS A. N88-20591
ZANINO, R. N88-21022
ZANIO, K. R. N88-20724
ZANONI, R. N88-21057
ZARKOVA, L. N88-21028
ZASOVA, L. V. N88-20317
ZAYCHIK, V. YE. N88-20807
ZAYTSEVA, S. YE. N88-20322
ZERGOUG, M. N88-20552
ZHANG, D. L. N88-20575
ZHANG, Y. N88-20465
ZHANG, Y. Z. N88-21019
ZHAO, BORAO N88-20496
ZHAO, X.-A. N88-20976
ZHU, ZUMING N88-20456
ZHUMANOV, KH. A. N88-20716
ZIMMERMAN, WAYNE F. N88-20351
N88-20352
ZIPPERIAN, T. E. N88-20970
N88-21062
ZITTEL, WERNER N88-20629
ZUND, JOSEPH D. N88-20709
ZWICK, RAMI N88-20910

Typical Corporate Source Index Listing

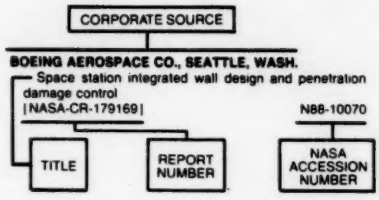

Listings in this index are arranged alphabetically by corporate source. The title of the document provides the user with a brief description of the subject matter. The report number helps to indicate the type of document cited (e.g., NASA report, translation, NASA contractor report). The NASA accession number denotes the number by which the citation is identified. The titles are arranged under each corporate source in ascending accession number order.

A

ACADEMY OF SCIENCES OF THE ARMENIAN SSR, ERIVAN.
Transformation coefficient in wave-field acceleration scheme
[DE88-700158] N88-20507
Slow waves in waveguide with elliptical cross section
[DE88-700159] N88-20508
Polarization of electrons in an electromagnetic wave field in the presence of magnetic field
[DE88-700169] N88-20509

ADMIRALTY RESEARCH ESTABLISHMENT, TEDDINGTON (ENGLAND).
Flow/acoustic interaction in duct inflow
[AD-A189264] N88-20967

AEROCHEM RESEARCH LABS., INC., PRINCETON, N. J.
A new process for synthesis of silicon nitride powders for advanced ceramics
[AD-A189354] N88-20451

AEROJET ENERGY CONVERSION CO., SACRAMENTO, CALIF.
Innovative, counterflow gas/fine solids, direct contact heat exchanger
[DE88-004744] N88-20585

AERONAUTICAL RESEARCH INST. OF SWEDEN, STOCKHOLM.
The construction of a three-dimensional finite volume grid generator for a wing in a wind tunnel with application to Navier-Stokes flow solvers
[FFA-TN-1987-58] N88-20277

AERONAUTICAL RESEARCH LABS., MELBOURNE (AUSTRALIA).
Australian aerodynamic design codes for aerial tow bodies
[AD-A189048] N88-20258
Crack distribution and growth rates for critical fastener holes in Mirage wing RH79
[AD-A189080] N88-20293

AERONAUTICAL SYSTEMS DIV., WRIGHT-PATTERSON AFB, OHIO.
A comparison of two chord keyboard coding systems for alphanumeric data entry
[AD-A189230] N88-20834

AIR FORCE ACADEMY, COLO.
MOPAC manual: A general molecular orbital package, fourth edition
[AD-A188623] N88-20362

AIR FORCE ASTRONAUTICS LAB., EDWARDS AFB, CALIF.
Kinetic mechanisms for ionization and afterburning suppression
[AD-A189219] N88-20383

AIR FORCE GEOPHYSICS LAB., HANSCOM AFB, MASS.
Laser gyro attitude control system feasibility
[AD-A189368] N88-20285
A polarization diversity meteorological radar system
[AD-A189291] N88-20515

AIR FORCE INST. OF TECH., WRIGHT-PATTERSON AFB, OHIO.
Interaction between two-dimensional sonic jets and supersonic flow to model heat addition in a supersonic combustor
[AD-A189572] N88-20261
The evaluation and selection of a 5th ground antenna site for the global positioning system
[AD-A189495] N88-20286
Expected value analysis for an unmanned expendable launch vehicle payload escape system
[AD-A189494] N88-20337
Optimal thrust vector control of coplanar orbital evasive maneuvers
[AD-A189544] N88-20346
Viscoelastic behavior of a polyetheretherketone (PEEK) composite
[AD-A189545] N88-20388
Threshold fatigue crack growth in Ti-6Al-2Sn-4Zr-6Mo
[AD-A189560] N88-20415
Alternative force structuring strategies for military satellite communication systems
[AD-A189492] N88-20516
Modification of parabolic dish antenna pattern using two symmetrically placed circular flat plates
[AD-A189543] N88-20517
Laser programming integrated circuits
[AD-A189590] N88-20537
Investigation of heat transfer to a flat plate in a shock tube
[AD-A189538] N88-20561
Semiclassical theory of injected lasers with arbitrary stable and unstable resonators
[AD-A189514] N88-20615
Resonator coupling of two ring cavity, argon-ion lasers
[AD-A189558] N88-20616
Theory of laser cooling and spectroscopy of harmonically trapped single atoms
[AD-A189576] N88-20617
Cyclic crack growth emanating at a round notch considering viscoplasticity
[AD-A189577] N88-20655
Specification for an infrared satellite surveillance system for the detection of aircraft
[AD-A189592] N88-20748
Retinotopic mapping of the human visual system with magnetoencephalography
[AD-A189557] N88-20811
An analysis of physiological data related to motion sickness for use in a real-time motion sickness indicator
[AD-A189589] N88-20812
A simulation study of a parallel processor with unbalanced loads
[AD-A189573] N88-20887
Predicting oscillatory finite difference solutions to the heat equation: A comparative study of the coefficient and matrix methods
[AD-A189591] N88-20911
Aberrations: Their effect on off-axis beam steering
[AD-A189601] N88-21008
Optical study of germanium, germanium plus arsenic, and germanium plus gallium implants in gallium arsenide
[AD-A189600] N88-21045
Frozen orbit analysis in the Martian system
[AD-A189574] N88-21106

AIR FORCE WRIGHT AERONAUTICAL LABS., WRIGHT-PATTERSON AFB, OHIO.
An investigation of classical dynamic scaling techniques applied to an oleo-pneumatic landing gear strut
[AD-A187664] N88-20292
Architecture specification for PAVE PILLAR avionics
[AD-A188722] N88-20303
High-temperature thermosets derived from the Diels-Alder polymerization of bisbenzocyclobutenes and bimaleimides
[AD-A188800] N88-20449

ALABAMA A & M UNIV., NORMAL.
Model of Jovian F region ionosphere
[NASA-CR-182587] N88-21105

ALABAMA UNIV., HUNTSVILLE.
Development of fiber optic systems for recording and transmitting holographic information
[AD-A189406] N88-20603
Magnetohydrodynamic (MHD) simulation of solar prominence formation N88-21109

ALABAMA UNIV., TUSCALOOSA.
A direct correlation of strength with impact velocity
[AD-A189251] N88-20409

ALASKA UNIV., FAIRBANKS.
Mechanical properties of sea ice and sea ice deformation in the near-shore zone
[PB88-147889] N88-20782

ALLEN CORP. OF AMERICA, ALEXANDRIA, VA.
MANPRINT handbook for RFP (Request For Proposal) development
[AD-A188321] N88-21075

APPLIED RESEARCH LAB., STATE COLLEGE, PA.
Measurement and analysis of the noise radiated by low Mach numbers centrifugal blowers
[AD-A189226] N88-20966

ARGONNE NATIONAL LAB., ILL.
The coordination cluster theory for metallic solutions
[DE88-005934] N88-20389
Temperature dependence of Kr precipitation in Ni
[DE88-005953] N88-20429
Liquid alloys: New perspectives and challenges
[DE88-005935] N88-20463
Recent developments in nondestructive evaluation for structural ceramics
[DE88-005889] N88-20473
X-ray computed tomography for structural ceramic applications: Beam hardening corrections
[DE88-005891] N88-20474
Processing of nanophase ceramics
[DE88-005985] N88-20475
Sodium-sulfur technology evaluation at Argonne National Laboratory
[DE88-002852] N88-20544
Testing and development of electric vehicle batteries for EPRI Electric Transportation Program
[DE88-005894] N88-20551
Laser fluorescence spectroscopy of zinc neutrals originating from laser-irradiated and ion-bombarded zinc sulfide and zinc surfaces
[DE88-006033] N88-20620
Overview of the DOE-ECUT Tribology Program
[DE88-002878] N88-20637
Algorithms with conic termination for nonlinear optimization
[DE88-005893] N88-20851
Diffraction theory in QCD and beyond
[DE88-005958] N88-20992
Cermet-fueled reactors for advanced space applications
[DE88-005528] N88-21002
A novel method for sputter-deposition of high T(sub c) superconductor films via a computer-controlled mass analyzed ton beam
[DE88-006001] N88-21064

ARIZONA STATE UNIV., TEMPE.
Computer aided surface representation
[DE88-005408] N88-20854
Modeling and transport in semiconductor devices
[AD-A188760] N88-21037

ARIZONA UNIV., TUCSON.
Electromagnetic scattering from and natural resonances of the circular strip N88-20523
Optics for large telescope N88-21014
Competing interactions in metallic superlattices
[DE88-005344] N88-21057
Superconducting superlattice structures
[DE88-005346] N88-21058
Asymptotic giant branch populations in composite stellar systems N88-21098
Global solar oscillations observed in the visible to near infrared continuum N88-21110

ARMY ARMAMENT RESEARCH, DEVELOPMENT AND ENGINEERING CENTER, WATERVLIET, N.Y.
Hydrogen embrittlement of gun steel
[AD-A188972] N88-20407

ARMY ARMAMENT RESEARCH AND DEVELOPMENT COMMAND, WATERVLIET, N. Y.
Structural integrity of metallic armature rail guns
[AD-A188735] N88-20333
Effect of rotation on the lateral stability of a free-flying column subjected to an axial thrust with directional control
[AD-A188690] N88-20338

ARMY AVIATION RESEARCH AND DEVELOPMENT COMMAND, MOFFETT FIELD, CALIF.
An experimental investigation of the flap-lag-torsion aeroelastic stability of a small-scale hingeless helicopter rotor in hover
[NASA-TP-2546] N88-20257

ARMY AVIATION SYSTEMS COMMAND, ST. LOUIS, MO.
AVSCOM'S modifications to Teledyne Systems Company's air-to-air fire control system simulation model
[AD-A189136] N88-20294

ARMY COLD REGIONS RESEARCH AND ENGINEERING LAB., HANOVER, N.H.
Microwave and structural properties of saline ice
[AD-A189307] N88-20779

ARMY FOREIGN SCIENCE AND TECHNOLOGY CENTER, CHARLOTTESVILLE, VA.
Feasibility report: Operation of light air cushion vehicle at McMurdo Sound, Antarctica
[AD-A189057] N88-20494

ARMY LAB. COMMAND, WATERTOWN, MASS.
Hydrogen induced cracks in armor steel weldments fabricated with austenitic filler alloys
[AD-A188733] N88-20406
A case study of the development of a military specification - zirconium powder for thermal batteries
[AD-A188751] N88-20717

ARMY RESEARCH INST. FOR THE BEHAVIORAL AND SOCIAL SCIENCES, ALEXANDRIA, VA.
A comparison of terrain association and resection as methods of position location
[AD-A189480] N88-20710

ARMY RESEARCH INST. OF ENVIRONMENTAL MEDICINE, NATICK, MASS.
Plasma cortisol, renin and aldosterone during an intense heat acclimation program
[AD-A189387] N88-20810

ASHLAND PETROLEUM CO., KY.
Aviation turbine fuels from tar sands bitumen and heavy oils. Part 3: Laboratory sample production
[AD-A189278] N88-20484

ATMOSPHERIC AND ENVIRONMENTAL RESEARCH, INC., CAMBRIDGE, MASS.
A study of satellite emission computed tomography
[AD-A189567] N88-20745

ATOMIC ENERGY RESEARCH ESTABLISHMENT, HARWELL (ENGLAND).
Ultrasonic inspection of irregular surfaces
[AERE-R-12465] N88-20648
Investigation of the use of horizontally polarised shear waves for TOFD studies on austenitic steel
[AERE-R-12145] N88-20649
A study of the dynamics of high temperature brittle intergranular fracture by acoustic emission
[AERE-R-12479] N88-20650

B

BALLISTIC RESEARCH LABS., ABERDEEN PROVING GROUND, MD.
A simplified computer code for reduction to burning rates of closed bomb pressure-time data (MINICB)
[AD-A189112] N88-20380

BATTELLE COLUMBUS LABS., RESEARCH TRIANGLE PARK, N.C.
Determination of the partition coefficients of organophosphorus compounds using high-performance liquid chromatography
[AD-A189276] N88-20385
Texture profile in thermomechanically processed 2-inch-thick 5 Ni-steel armor plate
[AD-A189275] N88-20410

BATTELLE COLUMBUS LABS., OHIO.
Proceedings of the 1987 International Symposium on Condensing Heat Exchangers
[DE88-005230] N88-20564

BATTELLE PACIFIC NORTHWEST LABS., RICHLAND, WASH.
Review of selenium thermodynamic data
[DE88-006194] N88-21068

BOEING AEROSPACE CO., SEATTLE, WASH.
Application of expert systems in project management decision aiding
[NASA-CR-180762] N88-21074

BOEING CO., SEATTLE, WASH.
Cadmium sulfide/copper ternary heterojunction cell research
[DE88-001122] N88-20727

BOEING COMMERCIAL AIRPLANE CO., SEATTLE, WASH.
Integrated autopilot/autothrottle based on a total energy control concept: Design and evaluation of additional autopilot modes
[NASA-CR-4131] N88-20308

BOEING MILITARY AIRPLANE DEVELOPMENT, SEATTLE, WASH.
Multi-crew pictorial format display evaluation
[AD-A189349] N88-20824

BOSTON UNIV., MASS.
Mechaniams of photoinduced electron transfer
[DE88-004917] N88-20983

BRIGHAM YOUNG UNIV., PROVO, UTAH.
Supercritical fluid chromatography/supersonic jet spectroscopy
[DE88-004438] N88-20392

BRISTOL UNIV. (ENGLAND).
Air-jet spoiler
[BU-364] N88-20299
A wind tunnel model with dynamic control
[BU-352] N88-20310

BROOKHAVEN NATIONAL LAB., UPTON, N. Y.
Studies of transverse phonon modes in premartensitic indium-thallium alloys
[DE88-003481] N88-20428
The effect of Ca(OH)2-treated ceramic microspheres on the mechanical properties of high-temperature lightweight cement composites
[DE88-004590] N88-20457
Proceedings of the 19th International Symposium on Condensing Heat Exchangers
[DE88-005230] N88-20564
On the norm equivalence of singularly perturbed elliptic difference operators
[DE88-006353] N88-20913
Applications of the lateral shearing interferometer in measurement of synchrotron radiation optical elements
[DE88-005184] N88-21011

BROWN UNIV., PROVIDENCE, R. I.
Materials Research Laboratory at Brown University
[AD-A188006] N88-20396
Ductile failure
[AD-A189429] N88-20654
Theory and experiments of fracture in cyclic compression: Single phase ceramics, transforming ceramics and ceramic composites
[DE88-005792] N88-20659
Model validation research: Comparison of simulated and observed climate patterns for the past 18,000 years
[DE88-004945] N88-20759
Exploring the relation between interface structure and mechanical properties in multilayer structures
[DE88-005428] N88-21060
Two studies of nonlinear processes in irreversible thermodynamics
[DE88-005794] N88-21067

C

CALIFORNIA INST. OF TECH., PASADENA.
Cavitation inception
[AD-A189220] N88-20557
The physical structure of concurrent problems and concurrent computers
[DE88-005812] N88-20835
Properties of reactively sputtered WNx films Zhao, X. -A.
[AD-A188711] N88-20976
Thin-film diffusion barriers for metal-semiconductor contacts
[AD-A188712] N88-21035

CALIFORNIA UNIV., BERKELEY.
High-temperature metal matrix composites
[AD-A189516] N88-20367
Transition metal cluster chemistry
[AD-A188731] N88-20405
Joint services electronics program
[AD-A189262] N88-20533
Transport and stability properties of free shear flows N88-20577
A finite-amplitude analysis of the buoyant instability of a highly viscous film over a less viscous half-space N88-20581
Quantum Monte Carlo study of the MIES associated with H2 (X 1 sigma sub g (+)) and H2 (B 1 sigma sub u (+))
[AD-A189063] N88-20977
On the structure of pulsed plasma jets N88-21030
MOSFET performance degradation due to hot carriers N88-21063
Velocity resolved far-infrared spectroscopy of galactic sources N88-21099
Early reheating and cosmic strings N88-21103
Resonant Alfven wave instabilities driven by streaming fast particles N88-21104
A low-frequency measurement of the spectrum of the cosmic microwave background radiation N88-21112

CALIFORNIA UNIV., BERKELEY. LAWRENCE BERKELEY LAB.
Tungsten-carbon multilayer system studied with X-ray scattering
[DE88-005749] N88-20373
A new concept in an electrically rechargeable zinc-air alkaline battery
[DE88-003858] N88-20539
A novel class of positive electrodes for rechargeable batteries
[DE88-004559] N88-20545
Very large vortex calculations in two dimensions
[DE88-005748] N88-20587
Improved methods for high resolution electron microscopy
[DE88-005731] N88-20609
Biophysical applications of solid state and tritium NMR
[DE88-005328] N88-20806
Modeling the behavior of oriented permanent magnet material using current double theory
[DE88-004446] N88-20963
Physics at large transverse momenta
[DE88-005758] N88-20986
Fragmentation and flow in central collisions
[DE88-005386] N88-20991
Recent progress in structure determination by LEED (Low-Energy Electron Diffraction) measure the properties of the deep donors (DX-cent)
[DE88-003851] N88-21048
Prediction of high-temperature thermodynamic properties of mixed electrolyte solutions including solubility equilibria, vapor pressure depression and boiling point elevation
[DE88-006344] N88-21069

CALIFORNIA UNIV., DAVIS.
Robust decentralized control of large flexible structures
[DE88-005416] N88-20902
Experimental studies of plasma heating due to the parametric decay of a large amplitude pump into lower hybrid waves N88-21017

CALIFORNIA UNIV., LOS ANGELES.
Control augmented structural synthesis
[NASA-CR-4132] N88-20290
Seasonal variations and excitation mechanisms of the equatorially trapped waves N88-20751
Hydrogen pumping and release by graphite under high flux plasma bombardment
[DE88-005880] N88-21021

CALIFORNIA UNIV., SANTA BARBARA.
Development of electrostatic-accelerator free-electron lasers
[AD-A189507] N88-20614

CARLOW ASSOCIATES, INC., FAIRFAX, VA.
Advanced human factors engineering tool technologies
[AD-A189390] N88-20825

CARNEGIE-MELLON UNIV., PITTSBURGH, PA.
NAVLAB: An autonomous navigation testbed
[AD-A189049] N88-20283
High-temperature metal matrix composites
[AD-A189516] N88-20367
Understanding machines from text and diagrams
[AD-A189034] N88-20493
The acoustic-modeling problem in automatic speech recognition
[AD-A188529] N88-20510
Mental models of mechanical systems: Individual differences in qualitative and quantitative reasoning
[AD-A189035] N88-20823
Distributed transaction processing and the Camelot system
[AD-A188614] N88-20885
Soar: An architecture for general intelligence
[AD-A188742] N88-20898

CARPENTER TECHNOLOGY CORP., READING, PA.
Grain refinement during primary breakdown of alloy 718
[DE88-005193] N88-20423

CD METROLOGY, INC., GERMANTOWN, MD.
Computer software for the computation of the scattered field and the optical microscope image of line objects patterned in thick layers
[PB88-153705] N88-20838

CENTER FOR MATHEMATICS AND COMPUTER SCIENCE, AMSTERDAM (NETHERLANDS).
Low-order spectral models of atmospheric circulation: A survey
[CWI-AM-R8705] N88-20748
Logical input devices and interaction
[CWI-CS-R8738] N88-20836
Approximation algorithms for scheduling unrelated parallel machines
[CWI-OS-R8714] N88-20861
On proving register atomicity
[CWI-CS-R8707] N88-20862
Using design axioms and topology to model database semantics
[CWI-CS-R8711] N88-20863
A parser generator for finitely ambiguous context-free grammars
[CWI-CS-R8712] N88-20864
The concept of intelligent integrated interactive CAD systems
[CWI-CS-R8717] N88-20865
A model for graphical interaction
[CWI-CS-R8718] N88-20866
Parallel graphical output from dialogue cells
[CWI-CS-R8719] N88-20867
Organization of design knowledge in an intelligent CAD environment
[CWI-CS-R8720] N88-20868
Algebra of Communicating Processes (ACP)tau: A universal axiom system for process specification
[CWI-CS-R8725] N88-20869
Steps into a geometer's workbench
[CWI-CS-R8726] N88-20870
An integrated data description language for coding design knowledge
[CWI-CS-R8731] N88-20871
Designing equivalent semantic models for process creation
[CWI-CS-R8732] N88-20872
Verification of a systolic algorithm for string comparison
[CWI-CS-R8734] N88-20873
Two normal form theorems for Communicating Sequential Processes (CSP) program
[CWI-CS-R8735] N88-20874
Perspectives on parallel computing
[CWI-OS-R8709] N88-20889
Locality, communication and interconnect length in multicomputers
[CWI-CS-R8708] N88-20890
A proof rule process creation
[CWI-CS-R8710] N88-20891
An amoeba replicated service organisation
[CWI-CS-R8723] N88-20892
A fully abstract semantics for data flow nets
[CWI-CS-R8724] N88-20893
Geometry and graphics applied to robotics
[CWI-CS-R8727] N88-20903
Algebraic specifications for parameterized data types: The case of minimal computable algebras and parameters with equality
[CWI-CS-R8714] N88-20916
On effectively labeling planar projections of polyhedra
[CWI-CS-R8715] N88-20917
Merge and termination in process algebra
[CWI-CS-R8716] N88-20918
Abstraction and empty process in process algebra
[CWI-CS-R8721] N88-20919
A convergence theorem in process algebra
[CWI-CS-R8733] N88-20920
Type-checking Mini-ML: An algebraic specification with user-defined syntax
[CWI-CS-R8737] N88-20921
A Lagrangian moving grid scheme for one-dimensional evolutionary partial differential equations
[CWI-NM-R8713] N88-20922
Stabilization of explicit difference schemes by smoothing techniques
[CWI-NM-R8714] N88-20923
Convergence of Runge-Kutta methods on classes of stiff initial value problems
[CWI-NM-R8717] N88-20924
Stochastic and chaotic oscillations
[CWI-AM-R8704] N88-20940
Non- and semi-parametric maximum likelihood estimators and the von Misis Method, part 1
[CWI-MS-R8709] N88-20941
Sojourn times in feedback queues
[CWI-OS-R8710] N88-20947
Local search for constrained routing problems
[CWI-OS-R8711] N88-20948
Two queues with alternating service and switching times
[CWI-OS-R8712] N88-20949
Consistency of rule-based expert systems
[CWI-CS-R8736] N88-20950
Group theoretic interpretations of Askey's scheme of hypergeometric orthogonal polynomials
[CWI-PM-R8703] N88-20954
Action-angle maps and scattering theory for some finite-dimensional integrable systems. The pure solution case
[CWI-PM-R8704] N88-20955
Solving reflexive domain equations in a category of complete metric spaces
[CWI-CS-R8709] N88-20956
String theory and algebraic geometry of moduli spaces
[CWI-PM-R8705] N88-21070

CHARLES RIVER ANALYTICS, INC., CAMBRIDGE, MASS.
Identification of visual evoked response parameters sensitive to pilot mental state
[NASA-CR-4140] N88-20822

CHEVRON RESEARCH CO., RICHMOND, CALIF.
Research on multibandgap solar cells
[DE87-012261] N88-20721

CHICAGO UNIV., ILL.
Performance and cost benefits associated with nonimaging secondary concentrators used in point-focus dish solar thermal applications
[DE88-001104] N88-20718
Particle physics and cosmology
[DE88-004944] N88-21096

CINCINNATI UNIV., OHIO.
Silicon-germanium heterostructures N88-21034

CLEMSON UNIV., S.C.
High-temperature metal matrix composites
[AD-A189516] N88-20367
Fracture criteria for discontinuously reinforced metal matrix composites
[NASA-CR-182665] N88-20662

COLORADO SCHOOL OF MINES, GOLDEN.
Grain refinement during primary breakdown of alloy 718
[DE88-005193] N88-20423

COLORADO STATE UNIV., FORT COLLINS.
Properties of molecular solids and fluids at high pressure and temperature
[DE88-004195] N88-20391

COLORADO UNIV., BOULDER.
Phase velocity and attenuation of plane elastic waves in a particle-reinforced composite medium
[AD-A189414] N88-20366
Dynamical modeling of marine boundary layer convection N88-20750
Excimer laser photolysis studies of T-V (Translation-to-Vibration) energy transfer
[AD-A189613] N88-20989
Comparison of analytic and full guiding center behavior at a trapped-passing interface in stellarators
[DE88-004174] N88-21025

COLUMBIA UNIV., NEW YORK, N.Y.
Initial stages of silicon growth on the (100) surface of silicon by localized laser CVD
[DE88-005420] N88-21059
Variable spectra of active galaxies
[NASA-CR-182694] N88-21091

COMMISSION OF THE EUROPEAN COMMUNITIES, ISPRA (ITALY).
A five year weathering experiment with solar collectors
[DE88-900369] N88-20740

COMPUTER SCIENCES CORP., HAMPTON, VA.
CODAC (Cockpit Oriented Display of Aircraft Configurations) version 1.4 user's guide
[NASA-CR-181650] N88-20273

COMPUTER SOFTWARE MANAGEMENT AND INFORMATION CENTER, ATHENS, GA.
Sixteenth NASTRAN (trademark) Users' Colloquium
[NASA-CP-2505] N88-20652

CONNECTICUT UNIV., STORRS.
The fatigue behavior of ferritic and austenitic steels at elevated temperatures
[DE88-006304] N88-20431
Energy transfer and non-linear optical properties at near ultraviolet wavelengths: Rare earth 4f yields 5d transitions in crystals and glasses
[DE88-005403] N88-21012

CONSIGLIO NAZIONALE DELLE RICERCHE, PADUA (ITALY).
Reversed field pinch operation with a thin shell
[DE88-005521] N88-21027

CONSTRUCCIONES AERONAUTICAS S.A., MADRID (SPAIN).
Development of isostatic mounts and associated guidelines
[CASA-IM-WP-301] N88-20354

CONTINUOUS ELECTRON BEAM ACCELERATOR FACILITY, NEWPORT NEW, VA.
Progress in diagnostic techniques for SC cavities
[CEBAF-PR-88-003] N88-20600
The continuous electron beam accelerator facility
[CEBAF-PR-87-017] N88-20996

CORNELL UNIV., ITHACA, N.Y.
An L-U implicit multigrid algorithm to solve the Euler equations for transonic flow in rotating turbomachinery passages N88-20270
Combustion theory and related questions
[AD-A189160] N88-20382
Systems near the onset and in the well-developed regimes of turbulence
[DE88-005365] N88-20565
An adaptive grid technique for solution of the Euler equations N88-20579
Multigrid solution of the Euler equations N88-20582
Low threshold ridge waveguide single quantum well lasers N88-20631
An analysis of large deformation axisymmetric inelastic problems by finite element and boundary element methods N88-20664
Correlation of data on strain accumulation adjacent to the San Andreas Fault with available models
[NASA-CR-180757] N88-20742
Upward propagating electric fields from thunderstorms and VLF transmitters N88-20767
Collective acceleration of electrons and ions in a high relativistic electron beam
[DE88-005261] N88-20998
Infrared constraints on the nature of dark matter N88-21102

D

DAVID SARNOFF RESEARCH CENTER, PRINCETON, N.J.
High power, high efficiency, 2D laser diode arrays for pumping solid state lasers
[DE88-004042] N88-20632

DAYTON UNIV., OHIO.
An electrochemical and spectroscopic study of electrode systems
[AD-A189274] N88-20384

DECISION SCIENCE CONSORTIUM, INC., FALLS CHURCH, VA.
A personalized and prescriptive decision aid for choice from a database of options
[AD-A188726] N88-20820

DEFENCE RESEARCH ESTABLISHMENT, OTTAWA. (ONTARIO).
Observations on electrostatic effects in a filter test system
[AD-A188797] N88-20378

DEFENCE TECHNOLOGY AND PROCUREMENT GROUP, THUN (SWITZERLAND).
What is the maximum length of a spin stabilized projectile
[PB88-130919] N88-20336

DELAWARE UNIV., NEWARK.
Stable, high-efficiency, CuInSe2-based, polycrystalline, thin-film tandem solar cells
[DE88-001116] N88-20726

DENVER UNIV., COLO.
Characterization and fundamental studies on CuO sorbent materials to determine attrition mechanisms on substrate gamma alumina
[DE88-003674] N88-20456

DEPARTMENT OF DEFENSE, WASHINGTON, D. C.
Soviet military power, 1987 N88-21114

DEPARTMENT OF ENERGY, WASHINGTON, D. C.
Technology '87: Research and Development Laboratory Technology Transfer Program
[DE88-003142] N88-21084

DEUTSCHE FORSCHUNGS- UND VERSUCHSANSTALT FUER LUFT- UND RAUMFAHRT, BRUNSWICK (WEST GERMANY).
On the Kutta condition for flows around lifting airfoils and wings
[DFVLR-FB-87-40] N88-20268
Solution of two-dimensional Euler equations: Experience with a finite volume code
[DFVLR-FB-87-41] N88-20572

DEUTSCHE FORSCHUNGS- UND VERSUCHSANSTALT FUER LUFT- UND RAUMFAHRT, COLOGNE (WEST GERMANY).
The German processing and archiving facility for ERS-1
[ESA-CR(P)-2531] N88-21082

DEUTSCHE FORSCHUNGS- UND VERSUCHSANSTALT FUER LUFT- UND RAUMFAHRT, STUTTGART (WEST GERMANY).
Design studies for a solar pumped laser device
[DFVLR-FB-87-39] N88-20629

DOUGLAS AIRCRAFT CO., INC., LONG BEACH, CALIF.
Proceedings of the Workshop on the Assessment of Crew Workload Measurements Methods, Techniques and Procedures. Volume 1: Preliminary Selection of Measures
[AD-A189004] N88-20827
DOW CHEMICAL CO., WALNUT CREEK, CALIF.
Improve the lifetime of the hollow fiber sodium sulfur cell
[DE88-004881] N88-20469
DRAPER (CHARLES STARK) LAB., INC., CAMBRIDGE, MASS.
Modelling and control of an annular momentum control device
[NASA-CR-4138] N88-20491
DREXEL UNIV., PHILADELPHIA, PA.
Detection and angle estimation of coherent plane waves N88-20522
Stratospheric trace gas distributions from fair infrared thermal emission spectroscopy N88-20749
DUKE UNIV., DURHAM, N. C.
Data traffic reduction schemes for sparse Cholesky factorizations
[NASA-CR-181626] N88-20831

E

EDGERTON, GERMESHAUSEN AND GRIER, INC., IDAHO FALLS, IDAHO.
Creep behavior of consolidated rapidly solidified Type 304 stainless steel powder containing helium
[DE88-005536] N88-20424
Experimental and theoretical methods for investigating helium effects in rapidly solidified metals
[DE88-005542] N88-20425
Ultrasonic characterization of non-uniform porosity distributions in SiC ceramic
[DE88-004814] N88-20459
Mission directed goals for electric vehicle battery research and development: The Task Force on electric vehicle battery goals
[DE88-005601] N88-20548
An experimental method for species concentration measurements in a welding arc using laser-induced fluorescence
[DE88-005638] N88-20636
Overview of recent activities in the Heat Cycle Research Program
[DE88-005544] N88-20738
A report on the study of algorithms to enhance vector computer performance for the discretized one-dimensional time-dependent heat conduction equation: EPIC research, phase 1
[DE88-005642] N88-20880
Quality enhancement with machine intelligence
[DE88-005639] N88-20901
Modeling of laser ultrasound generation in a weld pool
[DE88-005546] N88-20971
Analytically modeling the carbothermic reduction of alumina in a thermal plasma
[DE88-005535] N88-21020
Potential off-normal events and associated radiological source terms for the compact ignition tokamak: Fusion Safety Program
[DE88-004112] N88-21024
Spin off businesses as mechanisms for transferring technologies
[DE88-005640] N88-21085
EG AND G ENERGY MEASUREMENTS, INC., GOLETA, CALIF.
Noncontact thermometry via laser pumped, thermographic phosphors: Characterization of systematic errors and industrial applications
[DE88-005599] N88-20628
ELTECH SYSTEMS, INC., FAIRPORT HARBOR, OHIO.
Aluminum-air battery development
[DE88-006617] N88-20542
Aluminum-air battery development
[DE88-006618] N88-20543
ENVIRONMENTAL RESEARCH INST. OF MICHIGAN, ANN ARBOR.
Reduced tolerance imaging 2, volume 2
[AD-A189604] N88-20939
EUROPEAN SPACE AGENCY. EUROPEAN SPACE RESEARCH AND TECHNOLOGY CENTER, ESTEC, NOORDWIJK (NETHERLANDS).
The preparation, assembly and mounting of RF coaxial cables
[ESA-PSS-01-718-ISS-1] N88-20504
EXECUTIVE OFFICE OF THE PRESIDENT, WASHINGTON, D. C.
Aeronautics and space report of the President: 1986 activities N88-21067

F

FEDERAL AVIATION ADMINISTRATION, ATLANTIC CITY, N.J.
Alaska Loran C probe test results
[AD-A189131] N88-20284
FERMI NATIONAL ACCELERATOR LAB., BATAVIA, ILL.
Finite State Tables for general computer programming applications
[DE88-006254] N88-20881
FLORIDA STATE UNIV., TALLAHASSEE.
Subduction N88-20796
Bias reduction when there is no unbiased estimate
[AD-A189407] N88-20937
Stochastic comparisons of order statistics, with applications in reliability
[AD-A189408] N88-20938
FLORIDA UNIV., GAINESVILLE.
Research in applied mathematics related to identification of noisy systems
[AD-A189355] N88-20908
The parameterization of orthogonal matrices: A review mainly for statisticians
[AD-A189144] N88-20936
Regional Conference on the Analysis of the Unbalanced Mixed Model
[AD-A188747] N88-20943
Research in high energy elementary particle physics
[DE88-006065] N88-20994
FORD AEROSPACE AND COMMUNICATIONS CORP., NEWPORT BEACH, CALIF.
CdZnTe as a wide-band-gap absorber for a tandem, thin-film solar cell
[DE88-001114] N88-20724
FRAUNHOFER-INST. FUER BETRIEBSFESTIGKEIT, DARMSTADT (WEST GERMANY).
Standardized environmental fatigue sequence for the evaluation of composite components in combat aircraft (ENSTAFF = ENvironmental faISTAFF)
[LBF-FB-179] N88-20300
FUJI ELECTRIC CO. LTD., YOKOSUKA (JAPAN).
Notch sensitivity of graphite materials for VHTR N88-20447

G

GA TECHNOLOGIES, INC., SAN DIEGO, CALIF.
A high field launch for electron cyclotron heating using an external window
[DE88-005350] N88-21000
Reversed field pinch operation with a thin shell
[DE88-005521] N88-21027
GENERAL ACCOUNTING OFFICE, WASHINGTON, D. C.
Aquila remotely piloted vehicle: Its potential battlefield contribution still in doubt
[PB88-120241] N88-20289
Alternative fuels: Information on DOE's (Department of Energy's) methanol vehicle demonstration program
[PB88-118203] N88-20481
GENERAL DYNAMICS CORP., HUNTSVILLE, ALA.
Turnaround operations analysis for OTV. Volume 1: Executive summary
[NASA-CR-179316] N88-20340
Turnaround operations analysis for OTV. Volume 2: Detailed technical report
[NASA-CR-179317] N88-20341
Turnaround operations analysis for OTV. Volume 3: Technology development plan
[NASA-CR-179318] N88-20342
Turnaround operations analysis for OTV. Volume 4: WBS and dictionary and cost methodology
[NASA-CR-179319] N88-20343
GENERAL ELECTRIC CO., CINCINNATI, OHIO.
Nondestructive evaluation of carbon-carbon coatings
[AD-A189524] N88-20453
GENERAL ELECTRIC CO., PRINCETON, N.J.
High power, high efficiency, 2D laser diode arrays for pumping solid state lasers
[DE88-004042] N88-20632
GENERAL ELECTRIC CO., SAN JOSE, CALIF.
Cermet-fueled reactors for advanced space applications
[DE88-005528] N88-21002
GEOLOGICAL SURVEY, MENLO PARK, CALIF.
Geodetic measurement of deformation east of the San Andreas fault in Central California
[NASA-CR-182709] N88-20754
GEORGE WASHINGTON UNIV., WASHINGTON, D.C.
An interpretation of the ethylenic, carbidic, and graphite auger lineshapes of chemisorbed carbon species
[AD-A189092] N88-20379
Electron stimulated desorption and coherent electron scattering
[AD-A189091] N88-20978
Image charge, coherent scattering, and symmetry effects in electron stimulated desorption: O(-) from O sub 2 condensed on metals
[AD-A189093] N88-20979
The magnitude of secondary electron contributions in photon stimulated desorption
[AD-A189094] N88-20980
GEORGIA INST. OF TECH., ATLANTA.
The effect of microstructure on the fatigue crack growth resistance of nickel base superalloys
[AD-A189526] N88-20414
Analysis of shell-type structures subjected to time-dependent mechanical and thermal loading
[NASA-CR-182705] N88-20668
Human problem solving in dynamic environments. Understanding and supporting operators in large-scale, complex systems
[AD-A189539] N88-20826
GEORGIA UNIV., ATHENS.
Optical studies of dynamical processes in disordered system
[DE88-005965] N88-20993
The relationship of the chemical bonding topology of high critical temperature copper oxide superconductors to that of the chevrel phases and the ternary lanthanide rhodium borides
[AD-A189255] N88-21042
GESELLSCHAFT FUER SCHWERIONENFORSCHUNG M.B.H., DARMSTADT (WEST GERMANY).
Fragmentation and flow in central collisions
[DE88-005386] N88-20991
GESELLSCHAFT FUER STRAHLEN- UND UMWELTFORSCHUNG M.B.H., MUNICH (WEST GERMANY).
Ozone sonde and Dobson spectrometer data obtained during the MAP/GLOBUS 1983 campaign over Western Europe
[BPT-5/87] N88-20771
GOSUDARSTVENNYI KOMITET PO ISPOLZOVANIYU ATOMNOI ENERGII, MOSCOW (USSR).
Study of activationless reactions of point defects with impurities and impurity-defect complexes in alpha-iron
[TI88-701028] N88-20433
Chronometrically invariant formulation of electrodynamics equation
[TI88-701030] N88-21071
GOSUDARSTVENNYI KOMITET PO ISPOLZOVANIYU ATOMNOI ENERGII, OBNINSK (USSR).
Vibration spectra of oxygen and vanadium atoms in vanadium-oxygen disordered interstitial alloys
[DE87-703166] N88-20404
GOSUDARSTVENNYJ KOMITET PO ISPOLZOVANIYU ATOMNOI ENERGII, SERPUKHOV (USSR).
Introduction to classical mechanics of systems with constraints, part 1
[TI88-701055] N88-20957
Introduction to classical mechanics of systems with constraints, part 2
[TI88-701056] N88-21072
Introduction to classical mechanics of systems with constraints, part 3
[TI88-701057] N88-21073
GRONINGEN RIJKSUNIVERSITEIT (NETHERLANDS).
SIMSAT: Simulation package for flexible systems. Beams in space
[TW-278] N88-20348
Predicate-transformer semantics of general recursion
[CS-8709] N88-20876
Using trace theory to model discrete events
[CS-8708] N88-20904
Unfoldings of quasi-periodic tori
[ZW-8706] N88-20928

H

HAMILTON STANDARD, WINDSOR LOCKS, CONN.
Large-Scale Advanced Prop-Fan (LAP)
[NASA-CR-182112] N88-20306
HAMPTON INST., VA.
Direct solar-pumped iodine laser amplifier
[NASA-CR-182674] N88-20630
HARVARD UNIV., CAMBRIDGE, MASS.
Interaction of particulate and transformation toughening
[AD-A189321] N88-20412
Mathematical models of sound waves in fluids
[AD-A189270] N88-20968
HAUT COMMISSARIAT A LA RECHERCHE, ALGIERS (ALGERIA).
Simplified physical approach of the control by eddy current
[TI88-701076] N88-20552

HAWAII UNIV., HONOLULU.
Photolytic formation of free radicals and their effect on hydrocarbon pyrolysis chemistry in a concentrated solar environment
[DE88-004129] N88-20730
Dynamics of the Oceanic Surface Mixed Layer
[AD-A188348] N88-20785
The mixed layer of the western equatorial Pacific Ocean
[HIG-1861] N88-20789
Mixed-layer shear related to wind stress in the central equatorial Pacific N88-20793
Global mixed-layer natural and anthropogenic fluxes N88-20803

HELSINKI UNIV. OF TECHNOLOGY, ESPOO (FINLAND).
New way to solve Volterra equations of the second kind
[PB88-148820] N88-20931
What do multistep methods approximate
[PB88-148838] N88-20932
Period-doubling universality in multidimensional dissipative and conservative systems
[PB88-148812] N88-20961

HELSINKI UNIV. OF TECHNOLOGY, KYLMAELAE (FINLAND).
Solar microwave radiation maps measured at Metsaehovi Radio Research Station in 1978-1979
[PB88-127543] N88-21108

HOKENSON (GUSTAVE J.), LOS ANGELES, CALIF.
Coherent structure-reflective turbulent viscous flow modeling
[AD-A188339] N88-20556

HONEYWELL SYSTEMS AND RESEARCH CENTER, MINNEAPOLIS, MINN.
Passive autonomous infrared sensor technology
[AD-A188698] N88-21005

HOUSTON UNIV., TEX.
The design of aircraft using the decision support problem technique
[NASA-CR-4134] N88-20291

HUGHES RESEARCH LABS., MALIBU, CALIF.
Advanced space propulsion study - antiproton and beamed power propulsion
[AD-A189218] N88-20355
Intergrated circuit design, phase 2
[AD-A189060] N88-20530
Phase preservation cleanup in a double-pass Raman amplifier SBS (Stimulated Brillouin Scattering) conjugator
[AD-A189428] N88-20536
Development of Si/SiGe heterostructures
[AD-A189527] N88-21044

I

IBARAKI UNIV., HITACHI (JAPAN).
Fracture criterion of reactor graphite under multiaxial stresses N88-20442
Degradations of thermal shock resistance and the fracture toughness of reactor graphite subjected to neutron irradiation N88-20445

IDAHO STATE UNIV., POCATELLO.
A report on the study of algorithms to enhance vector computer performance for the discretized one-dimensional time-dependent heat conduction equation: EPIC research, phase 1
[DE88-005642] N88-20880

IIT RESEARCH INST., BARTLESVILLE, OKLA.
The thermodynamic properties of organic oxygen compounds
[DE88-001208] N88-21065

IIT RESEARCH INST., CHICAGO, ILL.
Corrosion-wear process under rolling-sliding motion
[AD-A189603] N88-20635

ILLINOIS UNIV., CHICAGO.
Bipropellant combustion in a liquid rocket combustion chamber N88-20359
A polarimetric rain backscatter model developed for coherent polarization diversity radar applications N88-20520

ILLINOIS UNIV., URBANA.
Application of railgun principle to high-velocity hydrogen pellet injection for magnetic fusion reactor refueling
[DE88-005830] N88-20334
Processing of nanophase ceramics
[DE88-005985] N88-20475
On the design of parallel numerical methods in message passing and shared memory environments
[DE88-003566] N88-20888
Electrical characteristics of MBE (Molecular Beam Epitaxyl)-grown GaAs/sub 1-x/Sb/sub x on InP and correlation with film microstructure
[DE88-003841] N88-21053
X-ray diffraction study of a thin GaAs film on Si(100)
[DE88-005290] N88-21055

IMPERIAL COLL. OF SCIENCE AND TECHNOLOGY, LONDON (ENGLAND).
Two-phase flows in the wake of in-cylinder projectiles
[AD-A189422] N88-20559
Comparison between computed and measured swirl and turbulence in reciprocating engines
[PDR/IC-CFDU/32] N88-20647

INDIAN INST. OF TECH., BOMBAY.
Transient dynamics of fibre reinforced composite plates
[IIT-B/CE/RR/87-1] N88-20370

INDIANA UNIV., BLOOMINGTON.
Development and evaluation of instrumentation and methods for multi-element analysis
[AD-A189345] N88-21018

INFRARED LABS., INC., TUCSON, ARIZ.
Advanced components for spaceborne infrared astronomy
[NASA-CR-177470] N88-20601

INSTITUTO DE PESQUISAS ESPACIAIS, SAO JOSE DOS CAMPOS (BRAZIL).
Orbit correction strategy for an Earth observation satellite
[INPE-4287-PRE/1159] N88-20331
Utilization of strapdown inertial and non-inertial sensors in determination of satellite attitude by Kalman filters
[INPE-4313-TDL/280] N88-20349
Gas consumption estimation of an attitude control system of an artificial satellite (utilizing DRF) in limit cycle phase
[INPE-4336-RPE/553] N88-20350
Numerical methods in the resolution of control electrovalve model
[INPE-4154-RPE/540] N88-20554
Synthesis method applied to the design of an electron gun for a gyrotron
[INPE-4357-TDL/298] N88-20607
A procedure for automatic classification of crop areas
[INPE-4467-PRE/1240] N88-20708
Restoration techniques for redisplay of LANDSAT-5 satellite imagery
[INPE-4189-PRE/1076] N88-20712
Analysis for architecture for image processing
[INPE-4294-PRE/1165] N88-20715
Roys and radiosondes in the region
[INPE-4362-PRE/1188] N88-20743
The use of a barotropic finite element model for the study of circulation on the continental shelf of the southeast coast of Brazil
[INPE-4401-PRE/1218] N88-20774
Interpolation algorithms for digital terrain models
[INPE-4373-PRE/1196] N88-20877
An implementation of the OPS5 language for computers compatible with IBM-PC
[INPE-4291-PRE/1162] N88-20882
Mathematic modeling of visual perception problems
[INPE-4355-PRE/1186] N88-20897
A study of data compactation using numerical methods
[INPE-4317-TDL/284] N88-20929
Local refinement of stress field by finite element method
[INPE-4321-TDL/288] N88-20930
Aspects and applications of primary processing of visual information
[INPE-4290-PRE/1161] N88-21015

INTERNATIONAL ATOMIC ENERGY AGENCY, VIENNA (AUSTRIA).
Study of defects in metals by positron annihilation
[DE88-701042] N88-20432

INTERNATIONAL BUSINESS MACHINES CORP., POUGHKEEPSIE, N.Y.
Measurement and analysis of the noise radiated by low Mach numbers centrifugal blowers
[AD-A189226] N88-20966

INTERNATIONAL METEOROLOGICAL INST., STOCKHOLM (SWEDEN).
Activities report in meteorology
[AR-86-87] N88-20755

IOWA STATE UNIV. OF SCIENCE AND TECHNOLOGY, AMES.
Numerical solution of ill posed problems in partial differential equations
[AD-A189383] N88-20909
Very high energy gamma ray astrophysics
[DE88-005821] N88-21095

ISTITUTO NAZIONALE DI FISICA NUCLEARE, FRASCATI (ITALY).
Superconducting superlattice structures
[DE88-005346] N88-21058

J

JAPAN ATOMIC ENERGY RESEARCH INST., TOKAI.
IAEA Specialists' Meeting on Graphite Component Structural Design
[DE88-780006] N88-20439
Statistical considerations of graphite strength for assessing design allowable stresses N88-20441
High temperature Young's modulus of IG-110 graphite N88-20443
Effects of high temperature neutron irradiation on the physical, chemical and mechanical properties of fine-grained isotropic graphite N88-20444

JET PROPULSION LAB., CALIFORNIA INST. OF TECH., PASADENA.
The space station assembly phase: Flight telerobotic servicer feasibility, volume 1
[NASA-CR-182689] N88-20351
The space station assembly phase: Flight telerobotic servicer feasibility. Volume 2: Methodology and case study
[NASA-CR-182690] N88-20352
The Deep Space Network
[NASA-CR-182700] N88-20524
Bragg-cell receiver study
[NASA-CR-182684] N88-20535
Environmental projects. Volume 5, part 1: Study of subsurface contamination. Part 2: Guide to implement environmental compliance programs
[NASA-CR-182691] N88-20741
Passive DF: A tutorial, part 1
[NASA-CR-182669] N88-20846
Two dimensional uncorrelated bias in fix algorithms
[NASA-CR-182683] N88-20847
Predictive monitoring research: Summary of the PREMON system
[NASA-CR-182687] N88-20905

JOHNS HOPKINS UNIV., BALTIMORE, MD.
A fundamental understanding of the effect of alloying elements on the corrosion resistance of rapidly solidified Mg alloys
[AD-A189385] N88-20413
Corrosion, passivity and breakdown of alloys used in high energy density batteries
[DE88-004891] N88-20422
IUE program SUGSD: Varability time scale of H Ly-alpha from Uranus
[NASA-CR-182706] N88-21107

JOINT PUBLICATIONS RESEARCH SERVICE, ARLINGTON, VA.
JPRS report: Science and technology. USSR: Space
[JPRS-USP-88-002] N88-20312
Vega-1 and Vega-2 automatic stations: Functioning of landing modules in Venusian atmosphere N88-20313
Vega-1 and Vega-2 automatic stations: Functioning of flyby vehicles during encounter with Halley's comet N88-20314
Thermal structure of Venusian Atmosphere determined from results of measurements from Vega-2 landing module N88-20315
Research on absorption of UV radiation in Venusian atmosphere from Vega-1 and Vega-2 landing modules N88-20316
Vertical structure of Venusian cloud layer at landing sites of Vega-1 and Vega-2 vehicles N88-20317
Gas-chromatographic analysis of products of thermal reactions of aerosol in Venusian cloud layer on Vega-1 and Vega-2 automatic interplanetary stations N88-20318
Roentgenoradiometric analysis of aerosol in Venusian clouds by Vega-1 and Vega-2 automatic interplanetary stations N88-20319
Chemical composition and structure of Venusian clouds determined from results of roentgenoradiometric experiments carried out by landing modules of Vega-1 and Vega-2 automatic interplanetary stations N88-20320
Determining chemical composition of aerosol in Venusian cloud layer on Vega-1 automatic interplanetary station using Malakhit mass spectrum analyzer N88-20321
Elemental composition of Venusian rocks in northeastern part of Terra Aphrodite (determined using data from Vega-2 landing module) N88-20322
Content of natural radioactive elements in Venusian rocks determined using data from Vega-1 and Vega-2 stations N88-20323
Some periodicities in motion of Halley's Comet relative to center of mass N88-20324
Results of infrared spectrometer experiment. 1: Infrared radiation of parent molecules in Halley's Comet N88-20325
Results of infrared spectrometer experiment. 2: Infrared radiometry of nucleus of Halley's Comet N88-20326

Analysis of hydrocarbon band 3.35 in spectrum of Halley's Comet using data from infrared spectrometer on Vega-1 spacecraft N88-20327
Soviet space transport systems N88-20328
Features of Soyuz TM spacecraft N88-20329
JPRS report: Science and technology. China [JPRS-CST-88-003] N88-20495
Simulation of effect of anti-radar stealth principle N88-20496
Adaptive control of scientific balloon-borne gondola attitude N88-20497
Analysis of spectral reflectance characteristics of targets under satellites and automatic cloud recognition N88-20498
Orbit accuracy requirement of GPS for precise positioning and orbit determination within local area N88-20499
On error equations for determining Earth rotation parameters with VLBI network N88-20500
JPRS report: Science and technology. China [JPRS-CST-87-030] N88-20501
Recommendations on developing polycrystalline alumina fiber N88-20502
Computer-aided transformation of descriptive mode of mathematical models of a control system N88-20503
JPRS report: Science and technology. USSR: Earth sciences [JPRS-UES-88-001] N88-20674
Determination of mean thermohaline characteristics of the ocean N88-20675
Spectral reflective characteristics of sea surface N88-20676
Anisotropy of microstructural eddy motion in surface layer during calm N88-20677
Mushroom-shaped currents (eddy dipoles) under rotation and stratification conditions N88-20678
Estimates of ocean-atmosphere thermal interaction in Gulf Stream energy-active test range in winter of 1984 N88-20679
Determining Langmuir circulation parameters on basis of similarity theory N88-20680
Thermodynamic theory of fluctuations and Rayleigh light scattering in solutions N88-20681
Research on influence of individual sea water components on spectral brightness coefficient of outgoing radiation N88-20682
Relationship between oceanic geological formations and tectonic structures N88-20683
Numerical modeling of wave migration of seismic data N88-20684
Negative viscosity in global circulations N88-20685
Propagation of subsurface salinity maximum in tropical Atlantic N88-20686
Space-time analysis of oceanographic fields by modified empirical orthogonal functions method N88-20687
Intrathermocline lens of Mediterranean water in tropical North Atlantic N88-20688
Dynamics of synoptic ocean eddies N88-20689
Turbulent transfer of momentum and heat in boundary layer of fluid beyond an obstacle. 1: Hydrodynamic characteristics N88-20690
Generalized expression for radio navigation parameter error N88-20691
Experience with and ways to upgrade accuracy of hydromagnetic surveys in ocean N88-20692
Vertical turbulent transfer of matter in thin ocean surface layer during daytime heating N88-20693
Phenomenological description of eddy registered in Gulf Stream N88-20694
Contribution to theory of quasigeostrophic motions of finite amplitude in viscous stratified ocean N88-20695
Numerical model of Rayleigh instability and spin-off eddies on fronts N88-20696
Research on turbulence in bottom boundary layer in ocean N88-20697
Invariant characteristics of acoustic field in stratified ocean N88-20698
Study of spectra of sea waves on horizontally nonuniform current in rip zone N88-20699
Model of hydrodynamic adjustment of temperature, salinity and current fields N88-20700
Resolution of the magnetotelluric method for determining local inhomogeneities in the sedimentary cover N88-20701
Interactive automated system for testing analog units of digital seismic stations N88-20702
Trajectory synthesis of ionograms in presence of artificial ionospheric inhomogeneities N88-20703
Effect of nitrogen dioxide release on thermosphere N88-20704
Influence of nonlinear spectroscopic effects on atmospheric propagation of intense laser radiation at 10.6 microns wavelength N88-20705
Synchronous measurements of effective photon path length in visible and near-IR spectral regions in real cloud systems N88-20706
Influence of hydrometeorological factors on visibility of objects detected by radar N88-20707
JPRS report: Science and technology. USSR: Life sciences [JPRS-ULS-88-004] N88-20815
Increase in influence of oxygen on the body in the presence of helium N88-20816
Regulation of hemodynamics upon imitation of the transition to weightlessness (mathematical modeling) N88-20817

K

KANSAS UNIV. CENTER FOR RESEARCH, INC., LAWRENCE.
Adaptive algorithms for HF antenna arrays [AD-A189329] N88-20534
KATHOLIEKE UNIVERSITEIT, NIJMEGEN (NETHERLANDS).
Distraction and inhibition in continuous CRT performance: A replication and some new findings [PB88-150941] N88-20821
KENT STATE UNIV., OHIO.
Large momentum pairing in one-dimensional systems [AD-A189226] N88-20981
KENTUCKY UNIV., LEXINGTON.
A direct correlation of strength with impact velocity [AD-A189251] N88-20409
Applicability of aerospace thermal insulation technologies to the civilian sector [DE88-003717] N88-21086
KERNFORSCHUNGSANLAGE, JUELICH (WEST GERMANY).
Computer simulation of tropospheric chemistry [JUEL-2144] N88-20756

L

LA JOLLA INST., CALIF.
Hamiltonian description of the interaction of surface waves with mixed-layer currents N88-20799
LAWRENCE LIVERMORE NATIONAL LAB., CALIF.
Use of the LLNL 40 kV electric gun to study the shock response of 21-6-9 stainless steel [DE87-014550] N88-20418
Kinetics of polymer decomposition [DE88-005500] N88-20460
Abrasion and impact resistant coatings [DE88-003562] N88-20464
Particle-dynamics calculations of gravity flow of inelastic, frictional spheres [DE88-005224] N88-20586
Remote fiber fluorimetry techniques for pressure measurements [DE88-004486] N88-20604
Wiggler taper optimization for free-electron-laser amplifiers with moderate space-charge effects [DE88-003758] N88-20618
Causes of damage in multilayer dielectric coatings exposed to high average power visible laser radiation [DE88-005363] N88-20619
Laser fluorescence spectroscopy of zinc neutrals originating from laser-irradiated and ion-bombarded zinc sulfide and zinc surfaces [DE88-006033] N88-20620
Database of average-power damage thresholds at 1064 nm [DE88-004352] N88-20626
Gaussian techniques on shared memory multiprocessor computers [DE88-005426] N88-20855
Experimental verification of a finite-difference time-domain thin slot algorithm [DE88-005572] N88-20859
Robust decentralized control of large flexible structures [DE88-005416] N88-20902
Stochasticity in nonlinear Hamiltonian systems [DE88-005499] N88-20915
The automated symbolic derivation of state equations for dynamic systems [DE88-000968] N88-20945
Physics of condensed matter at extreme conditions [DE88-006232] N88-20958
Electron emission from conductors subjected to intense, short-pulse electric fields [DE88-005412] N88-20985
Numerical simulations of multiphoton processes in many electron atoms [DE88-003293] N88-20990
Nonlinear refractive index measurements of glasses and crystals [DE88-005673] N88-21009
Guidelines for estimation and characterization of the thermo-mechanical properties of new optical materials [DE88-004359] N88-21010
Enzyme-based fiber optic sensors [DE88-005674] N88-21013
Initial stages of silicon growth on the (100) surface of silicon by localized laser CVD [DE88-005420] N88-21059
Exploring the relation between interface structure and mechanical properties in multilayer structures [DE88-005428] N88-21060
Lattice relaxation of the DX centers in Ga/sub 1-x/Al/sub x/As and of the pressure-induced deep donors in GaAs [DE88-005452] N88-21061
LETTERMAN ARMY INST. OF RESEARCH, SAN FRANCISCO, CALIF.
Pursuit tracking performance decrements associated with decreasing ambient illumination [AD-A189336] N88-20809
LOCKHEED MISSILES AND SPACE CO., PALO ALTO, CALIF.
Stimulated Emission of Energetic Particles (SEEP) [AD-A188724] N88-21094
LOS ALAMOS NATIONAL LAB., N. MEX.
Interfacial chemistry-structure and fracture of ceramic composites [DE88-005516] N88-20461
Projected performance of RF-linac-driven free-electron lasers in the VUV and soft X-ray regions [DE88-004294] N88-20625
Noncontact thermometry via laser pumped, thermographic phosphors: Characterization of systematic errors and industrial applications [DE88-005599] N88-20628
Method to evaluate image-recovery algorithms based on task performance [DE88-005382] N88-20853
Dynamic run-time graphics [DE87-008997] N88-20879
SEAT: A strategic engagement analysis tool [DE88-000498] N88-20944
Intermediate energy neutrino physics [DE88-005378] N88-20984
Fragmentation and flow in central collisions [DE88-005386] N88-20991
A segmented calorimeter for low-energy particle beams in space [DE88-001806] N88-20997
Compatibility in space reactor fuel systems [DE88-005698] N88-21004
A symmetric set of Euler angles and oblique orientation space sections [DE88-005317] N88-21056
LOUISIANA STATE UNIV., BATON ROUGE.
Boundary effects on the drag of a cylinder in axial motion at low Reynolds number N88-20578
LOVELACE FOUNDATION FOR MEDICAL EDUCATION AND RESEARCH, ALBUQUERQUE, N. MEX.
Velocity and concentration measurements in flowing suspensions by nuclear magnetic resonance [DE88-006225] N88-20589

M

MARTIN MARIETTA CORP., DENVER, COLO.
Orbital transfer vehicle concept definition and system analysis study. Volume 2: OTV concept definition and evaluation. Book 1: Mission and system requirements [NASA-CR-179321] N88-20339
MARYLAND UNIV., BALTIMORE.
Determination of the partition coefficients of organophosphorus compounds using high-performance liquid chromatography [AD-A189276] N88-20385
MARYLAND UNIV., COLLEGE PARK.
Composites strengthening [AD-A189258] N88-20364
Advances in X-ray line profile analysis to determine microstructure information about ceramics [DE88-003936] N88-20465
MASSACHUSETTS INST. OF TECH., CAMBRIDGE.
Statistical signal processing using a class of iterative estimation algorithms [AD-A189050] N88-20511
Heat pipe transient analysis: Vapor dynamics [DE88-005132] N88-20568
Fiber-coupled external-cavity semiconductor high power laser [AD-A188454] N88-20611
Coherent laser radar system theory [AD-A188759] N88-20612
The dynamic control of robotic manipulators in space [NASA-CR-182710] N88-20646

Remote sensing of earth terrain
[NASA-CR-182677] N88-20711
Geodetic measurement of deformation east of the San Andreas fault in Central California
[NASA-CR-182709] N88-20754
A preliminary assessment of thunderstorm outflow wind measurement with airport surveillance radars
[AD-A189064] N88-20757
Studies toward observing and modelling large energetic ocean regions
[AD-A189267] N88-20778
Spectral element methods: Algorithms and architectures
[NASA-CR-182701] N88-20878
Evolution of poloidal variation of impurity density and ambipolar potential in rotating tokamak plasma, part 1
[DE88-006263] N88-21022
Focused ion beam fabrication of graded channel FET's in GaAs and Si
[AD-A189166] N88-21040

MASSACHUSETTS UNIV., AMHERST.
Mixing of viscous fluids: Behavior of microstructures and chaos
[DE88-006287] N88-20566
Computation and graphics in mathematical research
[DE88-005796] N88-20953
Analysis of deep sky sources found by the infrared astronomy satellite
[AD-A189605] N88-21089
Polarization properties of SiO masers N88-21113

MATERIALS RESEARCH LABS., MELBOURNE (AUSTRALIA).
Anomalous shock sensitivity/density relationship for RDX-polyethylene wax and related formulations from MRL Small Scale Gap Test (SSGT) measurements
[MRL-R-1099] N88-20399
Examination of polysulfide sealants by scanning electron microscopy
[MRL-R-1096] N88-20478
A comparative assessment of US and UK explosives qualified as replacements for tetryl
[MRL-R-1094] N88-20486
A pyrotechnic delay ignition system for a submarine launched marine signal
[MRL-R-1079] N88-20487
A defect investigation of Thunderflash MK N5 (Navy)
[MRL-TN-522] N88-20488
Recommended replacements for tetryl in Australian production fuzes and related ordnance
[MRL-R-1089] N88-20489
Some properties of Australian produced explosive composition H-6
[MRL-TN-525] N88-20490
Theoretical investigation of the wave shaping process in a section of ladder fracture tape
[MRL-R-1081] N88-20595
Temperature estimates for a free flowing railgun plasma
[MRL-R-1054] N88-21032

MAX-PLANCK-INST. FUER FESTKOERPERFORSCHUNG, STUTTGART (WEST GERMANY).
Lattice relaxation of the DX centers in Ga/sub 1-x/Al/sub x/As and of the pressure-induced deep donors in GaAs
[DE88-005452] N88-21061

MEGA ENGINEERING, SILVER SPRING, MD.
Use of reinforced inorganic cement materials for spark wire and drift chamber wire frames
[NASA-CR-180759] N88-20438

MERIDIAN CORP., FALLS CHURCH, VA.
Federal Ocean Energy Technology
[DE87-012279] N88-20722

MESSERSCHMITT-BOELKOW-BLOHM G.M.B.H., OTTOBRUNN (WEST GERMANY).
Documentation and installation of the hypersonic arbitrary-body computer program (Mark 3 version) of A.E. Gentry on the IBM computer system
[MBB/LKE-127/S/PUB/256] N88-20276
Aeroelastic models in aircraft design
[MBB/LKE-294/S/PUB/249] N88-20298
Study of the optimization of satellite system design for transfer orbit
[MBB-URV-135] N88-20332
General fuselage coordinates for the calculation of three-dimensional boundary layers
[MBB/LKE-122/S/PUB/244] N88-20596
Buckling and breakdown problems in structural mechanics. Failure of prestressed double-walled containers or rings
[MBB-UR-E-956/87] N88-20671
Pressurizing systems and air conditioning systems
[MBB/LKE-312/S/PUB/246] N88-20828

MIAMI UNIV., CORAL GABLES, FLA.
Circulation and exchange processes on the South Atlantic Bight Continental Shelf
[DE88-003330] N88-20781

MICHIGAN TECHNOLOGICAL UNIV., HOUGHTON.
Processing, structure and properties of heavily deformed in situ composites
[AD-A189611] N88-20416
Use of the LLNL 40 kV electric gun to study the shock response of 21-6-9 stainless steel
[DE87-014550] N88-20418
Stress corrosion cracking and metal-induced embrittlement: Comparative studies of local chemistries
[DE88-003235] N88-20419
Power spectral density analysis of wind-shear turbulence for related flight simulations
[NASA-CR-182721] N88-20773

MICHIGAN UNIV., ANN ARBOR.
Micromechanical and microstructural studies of ceramic superplasticity
[DE88-005793] N88-20472
Online aiding for human-computer interfaces
[AD-A189239] N88-20842
The Magnetically Insulated Inertial Confinement Fusion (MICF): A novel approach
[DE88-005460] N88-21026
Galaxy evolution in dense clusters N88-21101

MIDWEST RESEARCH INST., GOLDEN, COLO.
Performance and cost benefits associated with nonimaging secondary concentrators used in point-focus dish solar thermal applications
[DE88-001104] N88-20718
Research on multibandgap solar cells
[DE87-012261] N88-20721
SERI's Photovoltaic R and D Project: Recent progress and future directions
[DE88-001129] N88-20728
Progress of amorphous silicon based solar cells and modules
[DE88-004686] N88-20733
Power from the sun: Principles of high temperature solar thermal technology
[DE87-001104] N88-20736

MINNESOTA UNIV., MINNEAPOLIS.
Dynamics of high-speed mechanisms with elastic members N88-20643
Experimental and theoretical constraints on the origin of mid-ocean ridge geothermal fluids N88-20784
The automated symbolic derivation of state equations for dynamic systems
[DE88-000968] N88-20945
A mass spectrometer evolved gas analysis experiment for in-situ analysis of cometary dust volatiles N88-21097

MISSOURI UNIV., COLUMBIA.
Northern Hemisphere circulation and the principal components of subsequent summer patterns in North America and West Africa N88-20765
Pressure-dependent DLTS (Deep Level Transient Spectroscopy) experiments on Si-doped AlGaAs
[DE88-003842] N88-21047

MISSOURI UNIV., KANSAS CITY.
Theoretical studies on the electronic structure and properties of complex ceramic crystals and glasses
[DE88-005837] N88-21049

MONASH UNIV., CLAYTON (AUSTRALIA).
Studies of transverse phonon modes in premartensitic indium-thallium alloys
[DE88-003481] N88-20428

MORGAN STATE UNIV., BALTIMORE, MD.
The calibration of photographic and spectroscopic films: Reciprocity failure and thermal responses of IIaO film at liquid nitrogen temperatures
[NASA-CR-181094] N88-20606
The calibration of photographic and spectroscopic films: The response of 2aO film to small dosages of alpha particles from 3/10th's rad to 8 rads at energy levels 153 MeV, 79 MeV and 47 MeV
[NASA-CR-177830] N88-20608

MOUND LAB., MIAMISBURG, OHIO.
Improved glass-ceramic to metal seals in actuator and detonator applications with an aluminum-containing austenitic stainless steel
[DE88-004691] N88-20456
Processing of glass to aluminum (low melting metals) seals via an injection molding technique
[DE88-004689] N88-20468

MUELLER ASSOCIATES, INC., BALTIMORE, MD.
Status of alcohol fuels utilization technology for highway transportation: A 1986 perspective. Volume 2: Compression ignition engines
[DE88-006059] N88-20485

N

NATIONAAL INST. VOOR KERNFYSICA EN HOGE ENERGIEFYSICA, AMSTERDAM (NETHERLANDS).
High resolution hadron calorimetry
[NIKHEF-H/87-8] N88-20605
Proton/antiproton yields W(+/-)boson gamma X as a test of the quark charges
[NIKHEF-H/87-11] N88-20987
Energy loss of particles in dense matter-calorimetry
[NIKHEF-H/87-12] N88-20988
Hadronic overlap and total multiplicity distributions in high energy physics collisions
[NIKHEF-H/87-10] N88-21001

NATIONAL ACADEMY OF SCIENCES - NATIONAL RESEARCH COUNCIL, WASHINGTON, D. C.
Activities and objectives of the Polar Research Board
[DE88-004543] N88-20747
Outlook for the fusion hybrid and tritium-breeding fusion reactors
[PB88-149281] N88-21029

NATIONAL AERONAUTICS AND SPACE ADMINISTRATION, WASHINGTON, D.C.
Aeronautical engineering: A continuing bibliography with indexes (supplement 224)
[NASA-SP-7037(224)] N88-20254
Finite element calculations for aerodynamic coefficients of a 3-dimensional body in subsonic flow using Green's function method
[NASA-TT-20208] N88-20272
Calculation of the distributed loads on the blades of individual multiblade propellers in axial flow using linear and nonlinear lifting surface theories
[NASA-TT-20173] N88-20278
Procedure for detection and identification of a helicopter
[NASA-TT-20234] N88-20297
Reinforcing of thermoplastic polycarbonate and polysulfone with carbon fibers: Production and characteristics of UD-compound objects
[NASA-TT-20158] N88-20374
Measurement of detonation temperature of hydrogen-oxygen mixture by CARS (Coherent Anti-Stokes Raman Spectroscopy)
[NASA-TT-20227] N88-20398
Flame retardants
[NASA-TT-20250] N88-20400
Potassium cuprate (3)
[NASA-TT-20246] N88-20401
Quantitative determination of a hydrogen impurity in a sodium coolant by hydride thermal dissociation
[NASA-TT-20239] N88-20402
Decomposition of hypochlorite in the presence of copper in a homogeneous medium
[NASA-TT-20199] N88-20403
A calorimetric determination of the enthalpy of formation and a description of the defect structure of the ordered beta-phase /Ni, Cu/ /1-x/ Al/x/
[NASA-TT-20157] N88-20434
Formation of nuclei during precipitation in metallic mixed crystals
[NASA-TT-20248] N88-20437
Evaluation of flammability for cable-like polymers
[NASA-TT-20225] N88-20476
Safety research of insulating materials of cable for nuclear power generating station
[NASA-TT-20202] N88-20477
Aging properties of cable polmers (2)
[NASA-TT-20228] N88-20479
Lubricating properties of molybdenum disulfide. Part 3: Performance of molybdenum disulfide-containing oils in fluid lubrication
[NASA-TT-20156] N88-20480
Method for set-up for researching signal curve development
[NASA-TT-20235] N88-20526
System for detecting objects that represent a threat
[NASA-TT-20244] N88-20528
EDF's studies and first choices regarding the design of electrical equipment
[NASA-TT-20222] N88-20553
Detonation velocity of the hydrazinum nitrate-hydrazine water system
[NASA-TT-20213] N88-20590
Some problems of the theory of bubble growth and condensation in bubble chambers
[NASA-TT-20232] N88-20593
The influence of Mach number and heat transfer on the turbulent flow wall law
[NASA-TT-20230] N88-20594
The use of four-photon Raman spectroscopy for the remote sensing of natural objects
[NASA-TT-20257] N88-20716

Method for determination of the wind velocity and direction
[NASA-TT-20233] N88-20769

Use of diphosphonates to correct disorders in calcium metabolism and mineral composition of bone tissue with 60-day hypokinesia in rats
[NASA-TT-20220] N88-20807

Changes in the status of the human tibia during antiorthostatic hypokinesia
[NASA-TT-20221] N88-20813

Aerospace medicine and biology: A continuing bibliography with indexes (supplement 309)
[NASA-SP-7011(309)] N88-20814

The effects of normal and therapeutic baths on the central vascular organs of persons with healthy hearts, as measured by X-ray
[NASA-TT-20252] N88-20818

Method for determining the coordinates of sound sources by means of a sound measurement system
[NASA-TT-20242] N88-20972

Method for determining artillery position
[NASA-TT-20238] N88-20973

Method for determining artillery position
[NASA-TT-20237] N88-20974

NATIONAL AERONAUTICS AND SPACE ADMINISTRATION. AMES RESEARCH CENTER, MOFFETT FIELD, CALIF.

An experimental investigation of the flap-lag-torsion aeroelastic stability of a small-scale hingeless helicopter rotor in hover
[NASA-TP-2546] N88-20257

A correlation study of X-29A aircraft and associated analytical development
[NASA-TM-89735] N88-20296

NATIONAL AERONAUTICS AND SPACE ADMINISTRATION. GODDARD SPACE FLIGHT CENTER, GREENBELT, MD.

The 1987 Airborne Antarctic Ozone Experiment: The Nimbus-7 TOMS data atlas
[NASA-RP-1201] N88-20714

Crustal dynamics project data analysis, 1987. Volume 2: Mobile VLBI geodetic results 1982-1986
[NASA-TM-100689-VOL-2] N88-20753

Tidal estimation in the Pacific with application to SEASAT altimetry
[NASA-TM-100694] N88-20780

Relativistic jet models for the BL Lacertae object Mrk 421 during three epochs of observation
[NASA-TM-89727] N88-21090

NATIONAL AERONAUTICS AND SPACE ADMINISTRATION. HUGH L. DRYDEN FLIGHT RESEARCH CENTER, EDWARDS, CALIF.

Flight tests of external modifications used to reduce blunt base drag
[NASA-TM-100433] N88-20279

Aircraft flight flutter testing at the NASA Ames-Dryden Flight Research Facility
[NASA-TM-100417] N88-20301

The design and use of a temperature-compensated hot-film anemometer system for boundary-layer flow transition detection on supersonic aircraft
[NASA-TM-100421] N88-20304

Configuration management issues and objectives for a real-time research flight test support facility
[NASA-TM-100437] N88-20832

The use of an automated flight test management system in the development of a rapid-prototyping flight research facility
[NASA-TM-100435] N88-20896

NATIONAL AERONAUTICS AND SPACE ADMINISTRATION. HUGH L. DRYDEN FLIGHT RESEARCH FACILITY, EDWARDS, CALIF.

Formulation of a general technique for predicting pneumatic attenuation errors in airborne pressure sensing devices
[NASA-TM-100430] N88-20302

Exhaust-gas pressure and temperature survey of F404-GE-400 turbofan engine
[NASA-TM-88273] N88-20307

Development of an interactive real-time graphics system for the display of vehicle space positioning
[NASA-TM-100429] N88-20344

Delamination stresses in semicircular laminated composite bars
[NASA-TM-4026] N88-20375

Western aeronautical test range real-time graphics software package MAGIC
[NASA-TM-100425] N88-20506

Preliminary in-flight boundary layer transition measurements on a 45 deg swept wing at Mach Numbers between 0.9 and 1.8
[NASA-TM-100412] N88-20598

NATIONAL AERONAUTICS AND SPACE ADMINISTRATION. LYNDON B. JOHNSON SPACE CENTER, HOUSTON, TEX.

Johnson Space Center's strategic game plan: Charting a course to the year 2000 and beyond
[NASA-TM-89733] N88-21076

NATIONAL AERONAUTICS AND SPACE ADMINISTRATION. LANGLEY RESEARCH CENTER, HAMPTON, VA.

Application of a nonisentropic full potential method to AGARD standard airfoils
[NASA-TM-100560] N88-20263

A review of technologies applicable to low-speed flight of high-performance aircraft investigated in the Langley 14- x 22-foot subsonic tunnel
[NASA-TP-2796] N88-20264

Steady and unsteady transonic small disturbance analysis of realistic aircraft configurations
[NASA-TM-100557] N88-20269

Static performance of an axisymmetric nozzle with post-exit vanes for multiaxis thrust vectoring
[NASA-TP-2800] N88-20280

Lateral and longitudinal stability and control parameters for the space shuttle discovery as determined from flight test data
[NASA-TM-100555] N88-20309

Simulated impact damage in a thick graphite/epoxy laminate using spherical indenters
[NASA-TM-100539] N88-20363

Ply-level failure analysis of a graphite/epoxy laminate under bearing-bypass loading
[NASA-TM-100578] N88-20372

Numerical experiments on the stability of controlled boundary layers
[NASA-CR-181649] N88-20591

Slip velocity method for three-dimensional compressible turbulent boundary layers
[NASA-TM-100586] N88-20592

A preliminary investigation of finite-element modeling for composite rotor blades
[NASA-TM-100559] N88-20656

Optimal placement of tuning masses for vibration reduction in helicopter rotor blades
[NASA-TM-100562] N88-20665

Fluid-thermal-structural study of aerodynamically heated leading edges
[NASA-TM-100579] N88-20666

Active cooling design for scramjet engines using optimization methods
[NASA-TM-100581] N88-20669

Summary of along-track data from the Earth radiation budget satellite for several major desert regions
[NASA-RP-1197] N88-20772

On the sensitivity of complex, internally coupled systems
[NASA-TM-100537] N88-20829

A new algorithm for general multiobjective optimization
[NASA-TM-100536] N88-20830

Data traffic reduction schemes for sparse Cholesky factorizations
[NASA-CR-181626] N88-20831

Digital enhancement of flow field images
[NASA-TP-2770] N88-20833

A survey of provably correct fault-tolerant clock synchronization techniques
[NASA-TM-100553] N88-20894

NATIONAL AERONAUTICS AND SPACE ADMINISTRATION. LEWIS RESEARCH CENTER, CLEVELAND, OHIO.

Numerical simulation of subsonic and transonic propeller flow
[NASA-TM-100163] N88-20262

Interfacial adhesion: Theory and experiment
[NASA-TM-100830] N88-20417

Development of a torsion balance for adhesion measurements
[NASA-TM-100799] N88-20454

Availability and cost estimate of a high naphthene, modified aviation turbine fuel
[NASA-TM-100823] N88-20455

Optical RF distribution links for MMIC phased array antennas
[NASA-TM-100841] N88-20555

Cryogenic Fluid Management Technology Workshop. Volume 2: Roundtable Discussion of Technology Requirements
[NASA-CP-10009] N88-20599

NATIONAL AEROSPACE LAB., AMSTERDAM (NETHERLANDS).

ARSPNSC: A method to calculate subsonic steady and unsteady potential flow about complex configurations
[NLR-TR-86122-U] N88-20265

Tests on the AFWAL 65 deg delta wing at NLR: A study of vortex flow development between Mach = 0.4 and 4
[NLR-MP-86058-U] N88-20266

The international vortex flow experiment: A test case for compressible Euler codes
[NLR-MP-86076-U] N88-20267

Flight simulator experiments concerning take-off visibility minima
[NLR-TR-86050-U] N88-20281

A method and measures to evaluate trackers for air traffic control
[NLR-TR-86072-U] N88-20287

Flight simulations of MLS interception procedures applicable to laterally segmented approach paths
[NLR-MP-86037-U] N88-20288

How to generate equal probability design load conditions
[NLR-TR-86060-U] N88-20295

Engine flow simulation for wind tunnel testing at NLR
[NLR-MP-87011-U] N88-20305

Moveable thermal joints for deployable or steerable spacecraft radiator systems
[NLR-MP-87016-U] N88-20347

Fracture characteristics of carbon and aramid unidirectional composites in interlaminar shear and open hole tensile tests
[NLR-TR-86083-U] N88-20371

Fracture mechanics and creep crack growth of 1 percent Cr 1/2 percent Mo steel with and without prior exposure to creep conditions
[NLR-TR-86051-U] N88-20426

Aircraft corrosion problems and research in the Netherlands
[NLR-MP-86066-U] N88-20427

Feasibility demonstration of a sensor for high-quality two-phase flow
[NLR-TR-87009-U] N88-20569

Three-dimensional shear layer experiments and their use as test cases for calculation methods
[NLR-MP-86036-U] N88-20570

Development, manufacturing and testing of a gas-loaded variable conductance methanol heat pipe
[NLR-MP-87010-U] N88-20571

Modelling and simulation of a rate controlled manipulator arm
[NLR-TR-87010-U] N88-20639

Fatigue load measurements and evaluation of the 25m Horizontal Axis Wind Turbine (HAWT) at Petten, The Netherlands
[NLR-MP-86054-U] N88-20660

European approaches in standard spectrum development
[NLR-MP-87007-U] N88-20661

Expert systems for decision support in military aircraft mission preparation
[NLR-MP-87013-U] N88-20946

Development of an optical diagnostic instrument. Part 2: Instrument development
[NLR-TR-87079-L-PT-2] N88-21016

Activities report in aeronautics and astronautics
[ETN-88-91332] N88-21115

NATIONAL BUREAU OF STANDARDS, BOULDER, COLO.

Time-domain system for identification of the natural resonant frequencies of aircraft relevant to electromagnetic compatibility testing
[PB88-164520] N88-20519

NATIONAL BUREAU OF STANDARDS, GAITHERSBURG, MD.

Reference model for DBMS (database management system) user facility
[PB88-169446] N88-21080

NATIONAL BUREAU OF STANDARDS, WASHINGTON, D.C.

Advances in X-ray line profile analysis to determine microstructure information about ceramics
[DE88-003938] N88-20465

NATIONAL CENTER FOR ATMOSPHERIC RESEARCH, BOULDER, COLO.

Monitoring ocean surface layer processes
N88-20801

NATIONAL OCEANIC AND ATMOSPHERIC ADMINISTRATION, BOULDER, COLO.

Survey of acoustic techniques for monitoring El Nino
[PB88-157615] N88-20783

NATIONAL TRANSPORTATION SAFETY BOARD, WASHINGTON, D. C.

Aircraft accident report: Midair collision of Cessna-340A, N8716K, and North American SNJ-4N, N711SQ, Orlando, Florida, May 1, 1987
[PB88-910402] N88-20282

NATIONAL WEATHER SERVICE, GARDEN CITY, N.Y.

Wind shear as a predictor of severe weather for the eastern United States
[PB88-157144] N88-20782

NAVAL AIR DEVELOPMENT CENTER, WARMINSTER, PA.

Optimization of binary pigment coatings
[AD-A189103] N88-20450

NAVAL HEALTH RESEARCH CENTER, SAN DIEGO, CALIF.
Lifting and carrying capacities relative to physical fitness measures
[AD-A189305] N88-20808
NAVAL OCEAN RESEARCH AND DEVELOPMENT ACTIVITY, BAY ST. LOUIS, MISS.
Predictions and studies with a one-dimensional ice/ocean model
[AD-A189158] N88-20776
NAVAL OCEAN SYSTEMS CENTER, SAN DIEGO, CALIF.
HF (High Frequency) Maximum Usable Frequency (MUF) model uncertainty assessment
[AD-A189132] N88-20513
NAVAL POSTGRADUATE SCHOOL, MONTEREY, CALIF.
Application of a flux vector splitting methodology towards the solution of unsteady transonic flows, with future emphasis on the blade flutter problem
[AD-A189500] N88-20260
Development of a constitutive equation for HSLA (High-Strength Low-Alloy)-100 at cryogenic temperatures
[AD-A189243] N88-20408
An experimental investigation of decelerating flow about two-dimensional cambered plates
[DE88-006598] N88-20567
Unsteady shallowing mixed layer N88-20791
MacCAD (Macintosh Computer Aided Design), computer aided design tool for system analysis
[AD-A189241] N88-20843
Robustifying the Kalman filter
[AD-A189240] N88-20907
NAVAL RESEARCH LAB., WASHINGTON, D.C.
Mode priming in an overmoded gyrotron oscillator
[AD-A189151] N88-20602
Bathymetric hazard survey test
[AD-A189150] N88-20775
Inversion algorithms for geophysical problems
[AD-A189252] N88-20845
NAVAL SHIP RESEARCH AND DEVELOPMENT CENTER, BETHESDA, MD.
Compression of composite materials: A review
[AD-A189272] N88-20365
NAVAL SURFACE WEAPONS CENTER, DAHLGREN, VA.
Nonaxisymmetric body supersonic, aerodynamic prediction
[AD-A189338] N88-20259
NAVAL SURFACE WEAPONS CENTER, SILVER SPRING, MD.
Synthesis of energetic materials
[AD-A189115] N88-20482
NAVAL UNDERWATER SYSTEMS CENTER, NEW LONDON, CONN.
Optimal and conventional space-time processing in flow noise
[AD-A189104] N88-20965
NETHERLANDS ENERGY RESEARCH FOUNDATION, PETTEN.
Computer programs for calculating group cross-section covariances from uncertainty parameters in the ENDF/B-V format. UNC 32/33
[ECN-202] N88-20995
NEW HAMPSHIRE UNIV., DURHAM.
Body tensor formalism in finite deformation elasticity and application to the torsion of a circular cylinder N88-20651
NEW MEXICO STATE UNIV., LAS CRUCES.
Conformal geometry, Hotine's conjecture, and differential geodesy
[AD-A189265] N88-20709
NEW SOUTH WALES UNIV., KENSINGTON (AUSTRALIA).
An investigation of Doppler satellite positioning multi-station adjustment software N88-20345
Computerised measurement of human horizontal smooth pursuit eye movements N88-20819
NORTH CAROLINA STATE UNIV., RALEIGH.
A novel method for sputter-deposition of high T(sub c) superconductor films via a computer-controlled mass analyzed ion beam
[DE88-006001] N88-21064
NORTH CAROLINA UNIV., CHAPEL HILL.
Thermal oxide growth on silicon: Intrinsic stress and silicon cleaning effects
[AD-A188790] N88-20377
Measures of similarity between fuzzy concepts: A comparative analysis
[AD-A189430] N88-20910
NOTRE DAME UNIV., IND.
Erosion in dual-phase microstructures
[DE88-004507] N88-20421

O

OAK RIDGE GASEOUS DIFFUSION PLANT, TENN.
Noncontact thermometry via laser pumped, thermographic phosphors: Characterization of systematic errors and industrial applications
[DE88-005599] N88-20628
OAK RIDGE NATIONAL LAB., TENN.
The influence of the fiber-matrix bond on the mechanical behavior of NICALON/SiC composites
[DE88-006155] N88-20389
Studies of transverse phonon modes in premartensitic indium-thallium alloys
[DE88-003481] N88-20428
The statistical characterization of tensile strengths for a nuclear-type graphite N88-20440
Molecular dynamics of laser ablation of a polymer coating
[DE88-004337] N88-20466
Optimum transformer design for a pulsed power system
[DE88-006054] N88-20525
Efficiency characteristics of speed modulated drives at predicted torque conditions for air-to-air heat pumps
[DE88-005846] N88-20588
Studies of compound states of negative ions using laser beams
[DE88-004708] N88-20627
Dynamic tensile cyclic fatigue of Si3N4
[DE88-003919] N88-20658
Implementation of a 3-D nonlinear MHD (magnetohydrodynamics) calculation on the Intel hypercube
[DE88-000625] N88-20848
A Darwinian approach to artificial neural systems
[DE87-013184] N88-20900
Nonlinear differential equations
[DE88-006047] N88-20933
Deterministic uncertainty analysis
[DE88-006139] N88-20942
Fully implicit three-dimensional MHD (magnetohydrodynamics) stability and evolution in toroidal geometry
[DE88-000624] N88-21023
Comparison of analytic and full guiding center behavior at a trapped-passing interface in stellarators
[DE88-004174] N88-21025
Discussion of radiation effects and high-temperature oxide superconductors
[DE88-001427] N88-21046
Photon-controlled growth of multilayered structures
[DE88-005061] N88-21054
X-ray diffraction study of a thin GaAs film on Si(100)
[DE88-005290] N88-21055
A menu-driven knowledge retrieval system accessing ASCII data
[DE88-001742] N88-21079
OFFICE NATIONAL D'ETUDES ET DE RECHERCHES AEROSPATIALES, PARIS (FRANCE).
Activities report of the Large Testing Facilities Department
[ETN-88-91982] N88-20311
Activities report of the Materials Department
[ETN-88-91984] N88-20436
Activities report of the Systems Department
[ETN-88-91987] N88-20505
Activities report of the Lille Institute of Fluid Mechanics
[ETN-88-91983] N88-20597
Activities report of the Structures Department
[ETN-88-91986] N88-20672
Activities report of the Physics Department
[ETN-88-91985] N88-20964
Activities report of the Toulouse Research Center
[ETN-88-91988] N88-21077
OFFICE OF NAVAL RESEARCH LIASON OFFICE, FAR EAST, APO, SAN FRANCISCO, CALIF.
ONR Far East Scientific Bulletin, volume 12, number 3, July-September 1987
[AD-A188554] N88-21081
OFFICE OF THE UNDER SECRETARY OF DEFENSE (ACQUISITIONS), WASHINGTON, D.C.
Report of the Defense Science Board Summer Study on Technology Base Management
[AD-A188560] N88-21078
OHIO STATE UNIV., COLUMBUS.
Material parameter measurements at high temperatures
[NASA-CR-182707] N88-20397
Applications of the differential reflectivity radar technique: Focus on estimation of rainfall parameters and microwave attenuation prediction N88-20521
Force distribution and trajectory control for closed kinematic chains with applications to walking machines N88-20642
Finite element methods for quasi-prismatic bodies with application to gears N88-20644
Determination of Earth rotation by the combination of data from different space geodetic systems
[NASA-CR-181388] N88-20713
Comparisons of global topographic/isostatic models to the Earth's observed gravity field
[NASA-CR-182696] N88-20752
Measurement of the properties of lossy materials inside a finite conducting cylinder
[NASA-CR-182664] N88-20962
The astrophysics of nebulae and active galactic nuclear emission-line regions: New methods and applications N88-21111
OLD DOMINION UNIV., NORFOLK, VA.
Computational technique for compressible vortex flows using the integral equation solution
[NASA-CR-182695] N88-20271
Graphics and flow visualization of computer generated flow fields
[NASA-CR-182679] N88-20573
Development of disturbances in swept wing flows
[NASA-CR-182675] N88-20574
Finite element methodology for nonlinear free and harmonic forced vibrations of beam and plate structures N88-20663
Conservative finite volume solutions of a linear hyperbolic transport equation in two and three dimensions using multiple grids
[NASA-CR-182715] N88-20934
OREGON STATE UNIV., CORVALLIS.
On the zonal momentum balance at the equator N88-20788
OREGON UNIV., EUGENE.
Investigations of the origins of metastable, light-induced changes in hydrogenated amorphous silicon
[DE88-001117] N88-21051
ORINCON CORP., LA JOLLA, CALIF.
Signal-filter design and system performance for polarimetric radar
[AD-A189257] N88-20514

P

PACIFIC NORTHWEST LABS., RICHLAND, WASH.
Development and evaluation of supercritical fluid chromatography-mass spectrometry
[DE88-005122] N88-20394
Interfacial chemistry-structure and fracture of ceramic composites
[DE88-005516] N88-20461
PNL-1 improved ceramic composites through controlled fiber matrix interaction
[DE88-005680] N88-20462
Heat pipe transient analysis: Vapor dynamics
[DE88-005132] N88-20568
An assessment methodology for thermal energy storage evaluation
[DE88-004642] N88-20732
Simulating high-resolution vertical plane array wind characteristics using lower-spatial-resolution wind measurements
[DE88-005626] N88-20761
Cermet-fueled reactors for advanced space applications
[DE88-005528] N88-21002
Molybdenum-base cermet fuel development
[DE88-005529] N88-21003
PARIS-SUD UNIV., ORSAY (FRANCE).
Wavelength scaling of lithium-like recombination scheme for X-UV gain production
[ETN-88-92002] N88-20634
Experimental study of the role of plasma polarization on line shape in dense laboratory plasmas
[ETN-88-92001] N88-21033
PENNSYLVANIA HOSPITAL, PHILADELPHIA.
Molecular and electronic mechanism in the control of Na+ and K+ permeability of excitable cell membrane by ligand binding on receptor sites
[AD-A188725] N88-20805
PENNSYLVANIA STATE UNIV., UNIVERSITY PARK.
Studies of transverse phonon modes in premartensitic indium-thallium alloys
[DE88-003481] N88-20428
Laser ignition of nitramine composite propellants and crack propagation and branching in burning solid propellants
[AD-A189260] N88-20483
Estimation-correlation, modeling, and identification in adaptive array processors
[AD-A189130] N88-20512
High Reynolds number pump facility for cavitation research
[AD-A189310] N88-20558

The Euler-Bernoulli beam equation with boundary energy dissipation
[AD-A189517] N88-20560
Similarity theories and microturbulence in the atmospheric mixed layer N88-20802
Acoustic radiation from line- and point-loaded plates: Uniformly asymptotic solutions
[AD-A189367] N88-20969
Development of high stability fiber optic spectrophotometric systems for study of solar/stellar magnetic activity
[AD-A189327] N88-21088

PENNSYLVANIA UNIV., PHILADELPHIA.
Polymeric electrolytes for ambient temperature lithium batteries
[DE88-004896] N88-20547
Topics in curved and flat space electromagnetism N88-21100

PHILIPS INTERNATIONAL B.V., EINDHOVEN (NETHERLANDS).
Consistency of rule-based expert systems
[CWI-CS-R8736] N88-20950

PINNACLE RESEARCH INST., CUPERTINO, CALIF.
Technology base research on zinc/air battery systems
[DE88-004893] N88-20546

PITTSBURGH UNIV., PA.
Measurement of rate constants of elementary gas reactions of importance to upper atmosphere and combustion systems
[AD-A189432] N88-20386
Texture profile in thermomechanically processed 2-inch-thick 5 Ni-steel armor plate
[AD-A189275] N88-20410

PLANNING RESEARCH CORP., HAMPTON, VA.
Summary of along-track data from the Earth radiation budget satellite for several major desert regions
[NASA-RP-1197] N88-20772

POLISH ACADEMY OF SCIENCES, WARSAW.
Structural clearances and internal friction: Simulation by Eigen distortions
[ISSN-0208-5658] N88-20640

PRINCETON UNIV., N. J.
Fuels combustion research
[AD-A189114] N88-20381
Parametric study of acceleration-induced stresses and frequency changes in doubly-rotated crystal resonators
[AD-A189261] N88-20532
Calculations of viscous flows with a multigrid method N88-20580
The pressure drag and momentum flux during a cold frontal passage over the Alps N88-20763
Sample models of steady and low frequency circulations in the tropical atmosphere, with application to tropical air-sea interactions N88-20764

PULSE SCIENCES, INC., SAN LEANDRO, CALIF.
Electron emission from conductors subjected to intense, short-pulse electric fields
[DE88-005412] N88-20985

PURDUE UNIV., WEST LAFAYETTE, IND.
Electrosorptive detection of simple organic compounds in liquid chromatography
[AD-A188757] N88-20376
Characterization of redox states of nickel hydroxide film electrodes by in-situ Raman spectroscopy
[AD-A189288] N88-20411
Contrasting conductance/viscosity relations in liquid states of vitreous and polymer solid electrolytes
[AD-A189378] N88-20452
A study of the interaction of light with sub-micron metallic surfaces
[DE88-003138] N88-20624
Electrical characteristics of MBE (Molecular Beam Epitaxyl)-grown GaAs/sub 1-x/Sb/sub x on InP and correlation with film microstructure
[DE88-003841] N88-21053

R

RASOR ASSOCIATES, INC., SUNNYVALE, CALIF.
Thermionic Technology Program. A: Insulator test and evaluation
[DE88-004707] N88-20735

RENSSELAER POLYTECHNIC INST., TROY, N.Y.
Research on single-crystal CdTe solar cells
[DE88-001115] N88-20725
Research on mercury cadmium telluride
[AD-A189155] N88-21039

RESEARCH TRIANGLE INST., RESEARCH TRIANGLE PARK, N.C.
A fault injection experiment using the AIRLAB Diagnostic Emulation Facility
[NASA-CR-178390] N88-20895

RHODE ISLAND UNIV., KINGSTON.
Gordon Conference on Intermetallic Compounds held at Tilton, New Hampshire on 20-24 July 1987
[AD-A188502] N88-20435

RIJKSLUCHTVAARTDIENST, THE HAGUE (NETHERLANDS).
Activities report in civil aeronautics
[ETN-88-91344] N88-20255

ROCHESTER UNIV., N. Y.
Describing constraints on a digital circuit's behavior
[AD-A189200] N88-20531
Doubly periodic output from a dye laser pumped by a free-running argon laser
[DE88-005027] N88-20633
On relaxation algorithms based on Markov random fields
[AD-A189043] N88-20840
Design of the CONSUL programming language
[AD-A189202] N88-20841
An interface between object-oriented systems
[AD-A189245] N88-20844
Computing with structured connections networks
[AD-A189244] N88-20886
Knowledge retrieval as specialized inference
[AD-A189042] N88-20899
Coherence effects in optical physics with special reference to spectroscopy
[AD-A189520] N88-21007

ROCKWELL INTERNATIONAL CORP., CANOGA PARK, CALIF.
Solar dynamic power system definition study
[NASA-CR-180877] N88-20361

ROCKWELL INTERNATIONAL CORP., GOLDEN, COLO.
Grain refinement during primary breakdown of alloy 718
[DE88-005193] N88-20423

ROCKWELL INTERNATIONAL CORP., THOUSAND OAKS, CALIF.
Ultrasonic physical modeling of seismic wave propagation from graben-like structures
[AD-A189066] N88-20744

ROCKWELL INTERNATIONAL SCIENCE CENTER, ANAHEIM, CALIF.
Solid-state electrochemical processes in dye films
[AD-A188756] N88-21036

ROYAL NETHERLANDS METEOROLOGICAL INST., DE BILT.
The evaluation of automatic barometers, illustrated by the Nakaasa barometer
[KNMI-TR-95] N88-20610
Energy and momentum fluxes through the sea surface N88-20798
Evaluation of wave calculations using GONO in the period October 1985 - April 1986
[KNMI-TR-96] N88-20804

RSIC ASSOCIATES, BELMONT, MASS.
Parallel image compression
[NASA-CR-180758] N88-20837

S

SACLANT ASW RESEARCH CENTER, LA SPEZIA (ITALY).
Deep water mass circulation in the Alboran Basin. Measurements - January to April 1982: ALBORAN 2
[AD-A189205] N88-20777

SALERNO UNIV. (ITALY).
Superconducting superlattice structures
[DE88-005346] N88-21058

SAN DIEGO STATE UNIV., CALIF.
Study of photochromic materials for use in optical signal processing
[AD-A189068] N88-21006

SANDIA NATIONAL LABS., ALBUQUERQUE, N. MEX.
Trajectory code studies, 1987
[DE88-006218] N88-20335
Novel catalysts for methane activation
[DE88-003637] N88-20390
Uncertainties in hydrogen combustion
[DE88-005354] N88-20395
Advances in X-ray line profile analysis to determine microstructure information about ceramics
[DE88-003938] N88-20465
A new polymer-based hydrogen getter
[DE88-004538] N88-20467
Integral equation theory of homopolymer melts
[DE88-005304] N88-20470
Integral equation theory of polymer blends
[DE88-005305] N88-20471
A hybrid transform/DPCM encoder for data compression
[DE87-014852] N88-20518
Electrical properties of medium field, chem-prep varistors
[DE88-006147] N88-20540
Scale-up of a batch-type chemical powder preparation process for high field varistor fabrication
[DE88-006801] N88-20541
Quartz oscillator analysis
[DE88-005886] N88-20550
Velocity and concentration measurements in flowing suspensions by nuclear magnetic resonance
[DE88-006225] N88-20589
Refractive index gradients in nuclear-reactor-pumped lasers: Gasdynamic effects
[DE88-006099] N88-20621
Multimode-waveguide laser beam deflector
[DE88-006222] N88-20622
Practical constraints on sources for pulsed beam lithographies
[DE88-006594] N88-20623
Intelligent control of robot manipulators in hazardous environments
[DE88-003305] N88-20638
Component mode synthesis using experimental modes enhanced by mass loading
[DE88-006097] N88-20657
Status of the Magma Energy Project
[DE88-002413] N88-20719
Design of the Sandia-Israel 20-kW reflux heat-pipe solar receiver/reactor
[DE88-001312] N88-20729
Control strategies and hardware used in solar thermal applications
[DE88-004631] N88-20731
Crystalline photovoltaic cell technology: Present and future
[DE88-004684] N88-20734
Direct absorption receiver control studies
[DE87-013653] N88-20737
Oxidation/sulfidation of materials in an SO3/SO2/O2 thermochemical-transport, distributed-receiver, solar-energy system
[DE88-005875] N88-20739
Characteristics of the positive lighting flash
[DE88-005854] N88-20760
MASPLT: A one-dimensional graphics post processor for wave propagation codes
[DE88-005506] N88-20856
HISPLT: A history graphics post processor for wave propagation codes
[DE88-005507] N88-20857
CSQPLT: A graphics post processor for multidimensional wave propagation codes
[DE88-005508] N88-20858
A knowledge system for automatic finite element mesh generation: AMEKS
[DE87-014894] N88-20914
Campaign graphs
[DE88-005336] N88-20952
Measuring thin film properties using SAW (Surface Acoustic Wave) devices: Diffusivity and surface area
[DE88-002216] N88-20970
Design of electron beam accelerator for microwave application
[DE88-005252] N88-20999
Hydrogen pumping and release by graphite under high flux plasma bombardment
[DE88-005880] N88-21021
Pressure-dependent DLTS (Deep Level Transient Spectroscopy) experiments on Si-doped AlGaAs
[DE88-003842] N88-21047
A hydroxycarbonate route to superconductor precursor powders
[DE88-003638] N88-21052
Electrical characteristics of MBE (Molecular Beam Epitaxyl)-grown GaAs/sub 1-x/Sb/sub x on InP and correlation with film microstructure
[DE88-003841] N88-21053
Energy loss rates for light holes in InGaAs/GaAs strained layer single quantum wells
[DE88-005744] N88-21062
Rapid e-beam heating for measuring thermodynamics of metastable materials
[DE88-003565] N88-21066

SATCON TECHNOLOGY CORP., CAMBRIDGE, MASS.
Modelling and control of an annular momentum control device
[NASA-CR-4138] N88-20491

SCIENCE APPLICATIONS INTERNATIONAL CORP., MCLEAN, VA.
Federal Ocean Energy Technology
[DE87-012279] N88-20722
Broadband correlation analysis
[AD-A188732] N88-20839

SCIENCE APPLICATIONS INTERNATIONAL CORP., PRINCETON, N.J.
Fully-coupled analysis of jet mixing problems. Three-dimensional PNS model, SCIP3D
[NASA-CR-4139] N88-20256

SCRIPPS INSTITUTION OF OCEANOGRAPHY, LA JOLLA, CALIF.
Observations of waves and Langmuir circulation with Doppler sonars N88-20790
Radiative processes affecting ocean mixed-layer heat content and their monitoring from satellite N88-20800
SMITHSONIAN ASTROPHYSICAL OBSERVATORY, CAMBRIDGE, MASS.
Theoretical investigation of EM wave generation and radiation in the ULF, ELF and VLF bands by the electrodynamic orbiting tether
[NASA-CR-182720] N88-20529
Space infrared telescope facility wide field and diffraction limited array camera (IRAC)
[NASA-CR-182704] N88-21092
SOCIETE ANONYME DE TELECOMMUNICATIONS, PARIS (FRANCE).
Study for the determination of general and specific properties of wide energy-band gap HgHdTe in the 1-2 micrometer wavelength range
[AD-A189177] N88-21041
SOCIETE NATIONALE INDUSTRIELLE AEROSPATIALE, LES MUREAUX (FRANCE).
Study on long term evolution Towards European Autonomous Manned Spaceflight (STEAMS)
[SNIAS-SE/LS/AP-35-073] N88-20330
SOLAR KINETICS, INC., DALLAS, TEX.
Point-focus concentrator reflector assembly, phase 1
[DE88-003616] N88-20720
SOUTH CAROLINA UNIV., COLUMBIA.
Estimating system and component reliabilities under partial information on cause of failure
[AD-A189107] N88-20653
SOUTH DAKOTA SCHOOL OF MINES AND TECHNOLOGY, RAPID CITY.
Atmospheric electrical modeling in support of the NASA F-106 storm hazards project
[NASA-CR-181639] N88-20758
SOUTHERN METHODIST UNIV., DALLAS, TEX.
Thin-film cadmium telluride solar cells
[DE88-001107] N88-21050
SOUTHERN RESEARCH INST., BIRMINGHAM, ALA.
Nondestructive evaluation of carbon-carbon coatings
[AD-A189524] N88-20453
SOUTHWEST RESEARCH INST., SAN ANTONIO, TEX.
Engine testing for synfuel operation
[DE88-006044] N88-20645
SPECTRAN CORP., STURBRIDGE, MASS.
SBIR-Long fluoride fiber
[AD-A188595] N88-20492
SPIRE CORP., BEDFORD, MASS.
Research on high-efficiency, stacked, multijunction, amorphous silicon alloy thin-film solar cells
[DE88-001108] N88-20723
STANFORD UNIV., CALIF.
Non-destructive evaluation techniques applied to the study of fatigue microcrack growth in steel alloys
[DE88-004090] N88-20420
Control of structure in turbulent flows: Bifurcating and blooming jets
[AD-A189607] N88-20562
Center for Turbulence Research 1987 activities
[NASA-CR-182693] N88-20583
Constrained nonlinear programming
[DE88-005695] N88-20860
Survival analysis using additive risk models
[AD-A189053] N88-20906
Elimination of quantifiers of linear variables and corresponding transfer principles
[DE88-005692] N88-20912
Tests for uniformity arising from a series of events
[AD-A189069] N88-20935
On the role of complete reducibility in general competitive equilibrium models
[DE88-005693] N88-21083
STAR MICROWAVE, CAMPBELL, CALIF.
Modulatable thin film field emission space gun
[AD-A189279] N88-21043
STATE UNIV. OF NEW YORK, BUFFALO.
Photochemistry at structured surfaces: A classical electromagnetic approach
[AD-A189519] N88-20387
Spontaneous decay and atomic fluorescence near a metal surface of an absorbing dielectric
[AD-A187508] N88-20975
The synthesis, characterization and structural studies of In(C5H4Me) by X-ray diffraction and electron diffraction techniques and a reinvestigation of the crystalline state of In(C5H5) by X-ray diffraction studies
[AD-A189110] N88-21038
STRAINOPTIC TECHNOLOGIES, INC., NORRISTOWN, PA.
Spectral contents readout of birefringent sensors
[NASA-CR-179430] N88-20673

T

TECHNISCHE HOGESCHOOL, DELFT (NETHERLANDS).
Design graphs for the first two bending Eigenvibration forms of rotating beams consisting of two beam points
[IW-86006R] N88-20670
TECHNISCHE HOGESCHOOL, EINDHOVEN (NETHERLANDS).
Verification of the momemtum theory for rotors using measurements on a model helicopter
[R-840-S] N88-20275
Gridless routing for generalized cell assemblies: Report and user manual
[EUT-87-E-180] N88-20549
Wind velocity measurement data. Zimbabwe, 4 measuring stations
[R-845-D] N88-20770
GM: A gate matrix layout generator
[EUT-87-E-179] N88-20875
Simulation of measuring points for three dimensional measurements
[WPB-0115] N88-20883
Further results on the McMillan degree and the Kronecker indices of ARMA models
[EUT-87-E-175] N88-20925
Model structure selection for multivariable systems by cross-validation methods
[EUT-87-E-176] N88-20926
On the expectation of the product of four matrix-valued Gaussian random variables
[EUT-87-E-178] N88-20927
Arcs in cesium seeded noble gases resulting from a magnetically induced electric field
[EUT-87-E-177] N88-21028
TENNESSEE UNIV., KNOXVILLE.
Transformation, metallurgical response and behavior of the weld fusion zone and heat affected zone in Cr-Mo steels for fossil energy application
[DE88-006037] N88-20430
Studies of compound states of negative ions using laser beams
[DE88-004708] N88-20627
TEXAS UNIV., AUSTIN.
Preconditioned conjugate gradient algorithms and software for solving large sparse linear systems
[DE88-002180] N88-20849
WKB theory of wave tunneling for Hermitian vector systems of integral equations
[DE88-005332] N88-20951
Observations on energy transport in tokamaks: A new formula for turbulent transport
[DE88-005309] N88-21019
TEXAS UNIV., DALLAS.
Proof of the feasibility of coherent and incoherent schemes for pumping a gamma-ray laser
[AD-A189238] N88-20613
TOHOKU UNIV., SENDAI (JAPAN).
Application of ISRM testing methods to fracture toughness testing of graphite N88-20446
TOKYO INST. OF TECH. (JAPAN).
Nondestructive testings of HTGR graphites N88-20448
TORONTO UNIV., DOWNSVIEW (ONTARIO).
A study of combustion and flow behaviour in solid-propellant rocket motors
[UTIAS-280] N88-20357
An interferometric investigation of the diffraction of planar shock waves over a half-diamond cylinder in air
[UTIAS-322] N88-20575
Pseudo-stationary oblique-shock-wave reflections in low gamma gases: Isobutane and sulphur hexafluoride
[UTIAS-TN-267] N88-20576
TUEBINGEN UNIV. (WEST GERMANY).
Preparation of photometric measurements on a million stars in the framework of the satellite project HIPPARCOS/TYCHO
[ETN-88-91502] N88-21093

U

UNITED KINGDOM ATOMIC ENERGY AUTHORITY, ABINGDON (ENGLAND).
A high field launch for electron cyclotron heating using an external window
[DE88-005350] N88-21000
UNIVERSITY OF NORTHERN ILLINOIS, DE KALB.
Molecular dynamics of laser ablation of a polymer coating
[DE88-004337] N88-20466
UNIVERSITY OF SOUTHERN CALIFORNIA, LOS ANGELES.
Fluidization mechanisms in slurry flows
[DE88-005191] N88-20563

UNIVERSITY OF SOUTHERN ILLINOIS, CARBONDALE.
Material instabilities in solids
[AD-A189525] N88-20388
UTAH UNIV., SALT LAKE CITY.
The effect of combustion gas flow on the rotational dynamics of a spinning solid fuel rocket N88-20358
Numerical model of the time independent mean flow in a rotating rocket motor N88-20360
Planetary scale barotropic spectral model N88-20766
Multiple scattering of polarized light in cirrus clouds N88-20768

V

VIGYAN RESEARCH ASSOCIATES, INC., HAMPTON, VA.
The effect of sting interference at low speeds on the drag coefficient of an ellipsoidal body using a magnetic suspension and balance system
[NASA-CR-181611] N88-20274
VIRGINIA UNIV., CHARLOTTESVILLE.
Noncontact thermometry via laser pumped, thermographic phosphors: Characterization of systematic errors and industrial applications
[DE88-005599] N88-20628

W

WAGENINGEN AGRICULTURAL UNIV. (NETHERLANDS).
The radar scattering coefficient as a function of forest stand parameters and viewing angle. An empirical study of the Pinus sylvestris L. in the Kootwijk forest (The Netherlands), extended with observations in the Speulder and Sprielder forest (The Netherlands)
[ETN-88-91348] N88-20527
Expert system techniques and decision support system: A case study (Dec. 1985 - Jun. 1986)
[ETN-88-91347] N88-20884
WARSAW TECHNICAL UNIV. (POLAND).
Double layer polarization of nonconducting spheroidal particles and its application to Kerr effect
[ISSN-0208-05658] N88-20960
WASHINGTON STATE UNIV., PULLMAN.
Conic algorithms for unconstrained minimization with special consideration of problems with large sparse Hessians: A summary of research performed
[DE88-002549] N88-20850
WASHINGTON UNIV., SEATTLE.
Structures and fluxes in a deep convecting mixed layer N88-20786
Equatorial turbulence: Mixed layer and thermocline N88-20787
Horizontal scales of wind forced inertial motions N88-20795
Wind forcing and observed oceanic wavenumber spectra N88-20797
Searches for forces weaker than gravity
[DE88-003579] N88-20959
WEST VIRGINIA UNIV., MORGANTOWN.
Reduction of erosion in elbows due to flow modifications, phase 1
[DE88-001028] N88-20584
WESTINGHOUSE RESEARCH AND DEVELOPMENT CENTER, PITTSBURGH, PA.
Vapor-mist for lightweight high voltage space insulation systems
[DE87-011704] N88-20538
WISCONSIN UNIV., MADISON.
SOAR: Space orbiting advanced fusion power reactor
[AD-A189234] N88-20356
Propagator solutions of partial differential equations applied to plasma transport
[DE88-006432] N88-20852
Helical ripple transport in stellarators at low collision frequency
[DE88-006431] N88-21031
WISCONSIN UNIV., MILWAUKEE.
Dynamic modelling of flexible rotor shafts mounted on hydrodynamic bearings N88-20641
Improvement of the Reynolds-stress model by a new pressure-strain correlation
[NASA-CR-182699] N88-20667
WOODS HOLE OCEANOGRAPHIC INSTITUTION, MASS.
Some effects of heating on the wind-driven velocity in the upper ocean N88-20792
Mixed-layer fronts in the California current N88-20794
WYLE LABS., INC., HUNTSVILLE, ALA.
Spacecraft fire-safety experiments for space station: Technology development mission
[NASA-CR-182114] N88-20353

Y

YALE UNIV., NEW HAVEN, CONN.
Model catalyst studies of SMSI (Strong Metal/Support Interactions) and the role of D-electrons in chemisorption and catalysis
[DE88-004518] N88-20393
Molecular collision processes in gases and at surfaces
[AD-A189518] N88-20982

Typical Contract Number Index Listing

Listings in this index are arranged alphanumerically by contract number. Under each contract number the NASA accession numbers denoting documents that have been produced as a result of research done under that contract are arranged in ascending order. The NASA accession number denotes the number by which the citation is identified.

ACE-PRF-17371-AC2 ..... N88-20803
AERO/RD-134/100/10/83-84/362 ..... N88-20370
AF PROJ. 2307 ..... N88-20562
AF PROJ. 4976 ..... N88-20898
AF-AFOSR-0049-86 ..... N88-20802
AF-AFOSR-0057-85 ..... N88-21089
AF-AFOSR-0078-86 ..... N88-20861
N88-20862
AF-AFOSR-0101-84 ..... N88-20414
AF-AFOSR-0124-87 ..... N88-20575
N88-20576
AF-AFOSR-0156-84 ..... N88-20653
AF-AFOSR-0166-85 ..... N88-20386
AF-AFOSR-0184-86 ..... N88-20388
AF-AFOSR-0185-86 ..... N88-20981
AF-AFOSR-0195-87 ..... N88-20435
AF-AFOSR-0240-86 ..... N88-20381
AF-AFOSR-0252-84 ..... N88-20909
AF-AFOSR-0253-85 ..... N88-20560
CNRS PROJ. C3 ..... N88-20874
DA PROJ. RR0-24 ..... N88-20482
DA PROJ. RR0-4206 ..... N88-20493
N88-20823
DA PROJ. RR0-4209 ..... N88-20842
DA PROJ. 1L1-61101-A-71-A N88-20385
DA PROJ. 1L1-61102-BH-57 ..... N88-20559
DA PROJ. 2O1-61102-B-74-F N88-20826
DA PROJ. 2Q6-1102-B-74-F N88-20910
DAAA15-86-C-0064 ..... N88-20825
DAAG29-81-D-0100 ..... N88-20385
N88-20410
DAAG29-84-C-0023 ..... N88-20451
DAAG29-84-K-0058 ..... N88-20862
N88-20890
DAAG29-84-K-0089 ..... N88-20416
DAAG29-84-K-0095 ..... N88-20612
DAAG29-84-K-0133 ..... N88-20532
DAAG29-84-K-0146 ..... N88-21037
DAAG29-85-K-0022 ..... N88-20382
DAAG29-85-K-0033 ..... N88-20989
DAAG29-85-K-0099 ..... N88-20908
DAAG29-85-K-0181 ..... N88-20405
DAAG29-85-K-0192 ..... N88-21035
DAAG29-85-K-1092 ..... N88-20976
DAAL02-85-C-0134 ..... N88-21005
DAAL03-86-K-0014 ..... N88-20603
DAAL03-86-K-0094 ..... N88-20937
N88-20938
DACA76-85-C-0001 ..... N88-20531
N88-20840
N88-20841
N88-20844
DACA76-86-C-0019 ..... N88-20283
DAJA45-84-C-0032 ..... N88-20559
DAJA45-87-C-0020 ..... N88-21041
DARPA ORDER 5205 ..... N88-20939
DARPA ORDER 5307 ..... N88-20744
DARPA ORDER 6065 ..... N88-20412
DARPA ORDER 6140 ..... N88-21044
DE-AC01-85CE-90232 ..... N88-20585
DE-AC01-86CE-30844 ..... N88-20722
DE-AC02-76CH-00016 ..... N88-20428
N88-20457
N88-20564
N88-20913
N88-21011
DE-AC02-76CH-03000 ..... N88-20881
DE-AC02-77ER-04380 ..... N88-20983
DE-AC02-78ET-51013 ..... N88-21022
DE-AC02-80ER-10569 ..... N88-20998
DE-AC02-80ER-10587 ..... N88-21096
DE-AC02-80ER-10774 ..... N88-21095
DE-AC02-81ER-10830 ..... N88-20393
DE-AC02-82ER-12046 ..... N88-20854
DE-AC02-83CH-10093 ..... N88-20718
N88-20721
N88-20723
N88-20724
N88-20725
N88-20726
N88-20727
N88-20728
N88-20733
N88-20736
N88-21050
N88-21051
DE-AC02-83CH10093 ..... N88-20722
DE-AC02-83ER-13044 ..... N88-20565
DE-AC03-76SF-00098 ..... N88-20373
N88-20422
N88-20469
N88-20539
N88-20545
N88-20546
N88-20547
N88-20587
N88-20609
N88-20806
N88-20963
N88-20986
N88-21048
N88-21061
N88-21069
DE-AC03-84ER-51044 ..... N88-21000
DE-AC03-84SF-12221 ..... N88-20730
DE-AC03-85SF-15933 ..... N88-20538
DE-AC03-86SF-15954 ..... N88-20735
DE-AC04-76DP-00053 ..... N88-20458
N88-20468
DE-AC04-76DP-00789 ..... N88-20335
N88-20390
N88-20395
N88-20465
N88-20467
N88-20470
N88-20471
N88-20518
N88-20540
N88-20541
N88-20550
N88-20567
N88-20589
N88-20621
N88-20622
N88-20623
N88-20638
N88-20657
N88-20719
N88-20720
N88-20729
N88-20731
N88-20734
N88-20737
N88-20739
N88-20760
N88-20835
N88-20856
N88-20857
N88-20858
N88-20914
N88-20952
N88-20970
N88-20999
N88-21047
N88-21052
N88-21053
N88-21062
N88-21066
DE-AC04-76DP-03533 ..... N88-20423
DE-AC05-84ER-40150 ..... N88-20600
N88-20996
DE-AC05-84OR-21400 ..... N88-20369
N88-20421
N88-20428
N88-20430
N88-20466
N88-20485
N88-20525
N88-20588
N88-20627
N88-20658
N88-20848
N88-20900
N88-20933
N88-20942
N88-21023
N88-21025
N88-21046
N88-21054
N88-21055
N88-21079
N88-21086
DE-AC05-84OT-21400 ..... N88-20628
DE-AC06-76RL-01830 ..... N88-20394
N88-20461
N88-20462
N88-20568
N88-20732
N88-20761
N88-21002
N88-21003
N88-21068
DE-AC06-81ER-40048 ..... N88-20959
DE-AC07-76ID-01570 ..... N88-20424
N88-20425
N88-20459
N88-20548
N88-20636
N88-20738
N88-20880
N88-20901
N88-20971
N88-21020
N88-21024
N88-21065
DE-AC21-84MC-21349 ..... N88-20584
DE-AC22-86PC-91024 ..... N88-20456
DE-AS03-82ER-12092 ..... N88-20420
DE-AS03-84ER-52104 ..... N88-21021
DE-AS05-81ER-10954 ..... N88-20849
DE-FC22-83FE-60149 ..... N88-21065
DE-FG01-81ER-60013 ..... N88-20747
DE-FG02-84ER-45056 ..... N88-21012
DE-FG02-84ER-45109 ..... N88-20431
DE-FG02-84ER-45162 ..... N88-20624
DE-FG02-84ER-45167 ..... N88-20659
DE-FG02-84ER-45170 ..... N88-21049
DE-FG02-84ER-52111 ..... N88-20334
DE-FG02-85ER-13333 ..... N88-20566
DE-FG02-85ER-25001 ..... N88-20888
DE-FG02-85ER-53201 ..... N88-20852
N88-21031
DE-FG02-85ER-60304 ..... N88-20759
DE-FG02-86ER-25015 ..... N88-20953
DE-FG02-86ER-45238 ..... N88-20391
DE-FG02-86ER-45255 ..... N88-20419
DE-FG02-86ER-53216 ..... N88-21031
DE-FG02-87ER-13687 ..... N88-21067
DE-FG02-87ER-13723 ..... N88-21026
DE-FG02-87ER-13761 ..... N88-20633
DE-FG02-87ER-25047 ..... N88-20851
DE-FG02-87ER-45297 ..... N88-21057
N88-21058
DE-FG02-87ER-45302 ..... N88-20472
DE-FG03-85ER-25009 ..... N88-20835
DE-FG03-86ER-53228 ..... N88-21027
DE-FG03-87ER-25028 ..... N88-20912

DE-FG03-87ER-25030 ..... N88-21083
DE-FG05-80ET-53088 ..... N88-20860
N88-20951
N88-21019
DE-FG05-85ER-52121 ..... N88-21029
DE-FG05-85ER-60355 ..... N88-20781
DE-FG05-86ER-40272 ..... N88-20994
DE-FG06-85ER-25007 ..... N88-20850
DE-FG09-87ER-45291 ..... N88-20993
DE-FG22-86PC-90534 ..... N88-20392
DE-FG22-88PC-90957 ..... N88-20563
DNA-001-85-C-0368 ..... N88-20575
N88-20578
EPRI PROJ. 2020-3 ..... N88-21068
ESA-5188/82/NL-HP(SC) N88-21016
ESA-5245/82-NL-PB(SC) N88-20354
ESA-6292/85-HGE-I(SC) N88-21082
ESA-6533/85-NL-IW(SC) N88-21016
ESPIRIT PROJ. 999 ..... N88-20549
ESPRIT PROJ. 432 ..... N88-20869
N88-20892
N88-20919
ESTEC-4906/81-NL-PP(SC) N88-20332
ESTEC-6668/86-NL-PP N88-20330
FOM-EEL-PROJ-33.0417 ..... N88-20549
F04611-86-C-0039 ..... N88-20355
F08635-87-C-0125 ..... N88-20409
F19628-83-K-0038 ..... N88-21086
F19628-85-C-0002 ..... N88-20757
F19628-85-C-0034 ..... N88-20744
F19628-85-C-0088 ..... N88-21043
F19628-85-K-0005 ..... N88-21007
F19628-86-C-0084 ..... N88-20745
F19628-86-C-0124 ..... N88-20492
F19628-86-K-0026 ..... N88-20709
F30602-81-C-0205 ..... N88-20534
F30602-84-C-0017 ..... N88-20514
F33615-83-C-1046 ..... N88-20939
F33615-83-C-2301 ..... N88-20484
F33615-83-C-3618 ..... N88-20824
F33615-84-C-5007 ..... N88-20453
F33615-84-K-1520 ..... N88-20510
N88-20885
N88-20898
F33615-86-C-2620 ..... N88-20384
F33615-86-C-2705 ..... N88-20356
F33615-86-C-3600 ..... N88-20827
F49620-84-C-0057 ..... N88-20533
F49620-84-K-0005 ..... N88-20562
F49620-85-C-0007 ..... N88-20937
N88-20938
F49620-85-C-0065 ..... N88-20982
F49620-85-C-0075 ..... N88-20556
F49620-86-C-0009 ..... N88-20387
F49620-86-C-0014 ..... N88-20413
F49620-87-C-0017 ..... N88-20367
F49620-87-C-0104 ..... N88-21044
MDA903-82-C-0145 ..... N88-20826
MDA903-83-K-0347 ..... N88-20910
MDA903-85-C-0215 ..... N88-21040
NAGW-1067 ..... N88-21105
NAG1-441 ..... N88-20630
NAG1-463 ..... N88-20758
NAG1-574 ..... N88-20878
NAG1-591 ..... N88-20271
NAG1-717 ..... N88-20773
NAG1-724 ..... N88-20662
NAG1-729 ..... N88-20574
NAG1-801 ..... N88-20646
NAG2-316 ..... N88-21092
NAG3-534 ..... N88-20668
NAG3-784 ..... N88-20397
N88-20962
NAG5-198 ..... N88-21090
NAG5-270 ..... N88-20711
NAG5-435 ..... N88-21107
NAG5-814 ..... N88-20754
NAG8-570 ..... N88-21091
NAG8-617 ..... N88-20867
NAG9-636 ..... N88-20529
NASW-3047 ..... N88-20434
NASW-4307 ..... N88-20272
N88-20276
N88-20297
N88-20374
N88-20398
N88-20400
N88-20401
N88-20402
N88-20403
N88-20437
N88-20476
N88-20477
N88-20479
N88-20480
N88-20526
NAS1-16300 ..... N88-20528
NAS1-16535 ..... N88-20553
NAS1-17816 ..... N88-20590
NAS1-17919 ..... N88-20593
NAS1-17964 ..... N88-20594
NAS1-17999 ..... N88-20716
NAS1-18107 ..... N88-20769
N88-20807
NAS1-18117 ..... N88-20813
NAS2-12154 ..... N88-20818
NAS2-12351 ..... N88-20972
NAS2-12591 ..... N88-20973
NAS3-23051 ..... N88-20974
NAS3-24864 ..... N88-20308
NAS3-25067 ..... N88-20256
NAS5-27340 ..... N88-20822
NAS5-30040 ..... N88-20274
NAS5-30051 ..... N88-20895
NAS5-30056 ..... N88-20273
NAS7-918 ..... N88-20591
N88-20831
N88-20291
N88-20601
N88-20673
N88-20344
N88-20306
N88-20361
N88-20353
N88-20742
N88-21074
N88-20438
N88-20837
N88-20351
N88-20352
N88-20535
N88-20741
N88-20846
N88-20847
N88-20905
NAS8-36108 ..... N88-20339
NAS8-36924 ..... N88-20340
N88-20341
N88-20342
N88-20343
NAS9-16023 ..... N88-20491
NAS9-17560 ..... N88-20491
NATO-523/85 ..... N88-20798
NA81RA-C-00046 ..... N88-20782
NCC1-68 ..... N88-20573
N88-20934
NCC2-313 ..... N88-20296
NCC2-460 ..... N88-20583
NGR-36-008-161 ..... N88-20752
NGT5-0103 ..... N88-20754
NIVR-423-020405N N88-21016
NIVR-1995 ..... N88-20295
NIVR-2502-N N88-20569
NIVR-02801-N N88-20571
NR PROJ. 395066 ..... N88-20611
NR 083-400 ..... N88-20792
N88-20792
NSERC-A1647 ..... N88-20575
NSF CHE-86-20274 ..... N88-20387
NSF DCR-83-02391 ..... N88-20862
N88-20890
NSF DCR-83-20136 ..... N88-20844
N88-20886
NSF DCR-86-02071 ..... N88-20851
NSF DMC-86-13489 ..... N88-20531
NSF DMR-83-16893 ..... N88-20396
NSF DMS-84-01297 ..... N88-20560
NSF DMS-84-03664 ..... N88-20560
NSF DMS-85-01306 ..... N88-20560
NSF ECS-85-01988 ..... N88-20861
NSF MCS-81-20790 ..... N88-20861
NSF MCS-83-11422 ..... N88-20861
NSF OCE-82-14639 ..... N88-20788
NSF OCE-82-14791 ..... N88-20800
NSF OCE-83-14486 ..... N88-20793
NSF-DCR-83-51665 ..... N88-20899
NSG-1490 ..... N88-20290
NSG-5074 ..... N88-20606
N88-20608
NSG-5265 ..... N88-20713
N00014-76-C-0197 ..... N88-20792
N00014-76-C-0838 ..... N88-21018
N00014-77-C-0636 ..... N88-21036
N00014-79-C-0472 ..... N88-20790
N00014-79-C-0762 ..... N88-20483
N00014-79-C-0824 ..... N88-21094
N00014-80-C-0197 ..... N88-20899
N00014-80-C-0308 ..... N88-20614
N00014-80-C-0941 ..... N88-20611
N00014-80-K-0852 ..... N88-20379
N88-20978
N88-20979
N88-20980
N00014-81-K-0742 ..... N88-20511
N00014-82-K-0193 ..... N88-20840
N88-20886
N00014-83-C-0485 ..... N88-20820
N00014-83-K-056 ..... N88-20557
N00014-83-K-0125 ..... N88-20862
N88-20890
N00014-84-C-0111 ..... N88-20795
N00014-84-C-0134 ..... N88-20792
N00014-84-C-0218 ..... N88-20788
N00014-84-K-0289 ..... N88-20452
N00014-84-K-0365 ..... N88-21042
N00014-84-K-0655 ..... N88-20886
N00014-85-C-0466 ..... N88-20968
N00014-85-C-0639 ..... N88-20536
N00014-85-G-0241 ..... N88-20778
N00014-85-K-0007 ..... N88-20364
N00014-85-K-0151 ..... N88-21039
N00014-85-K-0168 ..... N88-20862
N88-20890
N00014-85-K-0250 ..... N88-20802
N00014-85-K-0556 ..... N88-20411
N00014-85-K-0573 ..... N88-20805
N00014-85-K-0584 ..... N88-20493
N88-20823
N00014-86-C-2488 ..... N88-20613
N00014-86-D-0701 ..... N88-20839
N00014-86-K-0043 ..... N88-20387
N88-20975
N00014-86-K-0059 ..... N88-20936
N00014-86-K-0156 ..... N88-20906
N88-20935
N00014-86-K-0262 ..... N88-20654
N00014-86-K-0280 ..... N88-20366
N00014-86-K-0305 ..... N88-20377
N00014-86-K-0556 ..... N88-20376
N00014-86-K-0688 ..... N88-20802
N00014-86-K-0752 ..... N88-20800
N00014-86-K-0753 ..... N88-20412
N00014-87-G-0090 ..... N88-20943
N00014-87-G-0091 ..... N88-20785
N00014-87-K-0266 ..... N88-21038
N00014-87-K-0740 ..... N88-20842
N00024-85-C-6041 ..... N88-20512
N88-20966
N88-20969
N62269-85-C-0265 ..... N88-20635
N66001-84-C-0104 ..... N88-20530
OPM-85-75 ..... N88-21075
PROJ. F66-701 ..... N88-20820
PROJ. RR0-1308 ..... N88-20379
N88-20978
N88-20979
N88-20980
PROJ. RR0-4108 ..... N88-20805
W-31-109-ENG-38 ..... N88-20389
N88-20429
N88-20463
N88-20473
N88-20474
N88-20475
N88-20544
N88-20551
N88-20620
N88-20637
N88-20851
N88-20992
N88-21064
W-7405-ENG-36 ..... N88-20625
N88-20853
N88-20879
N88-20944
N88-20984
N88-20991
N88-20997
N88-21004
N88-21056
W-7405-ENG-48 ..... N88-20418
N88-20480
N88-20484
N88-20542
N88-20543
N88-20586
N88-20604
N88-20618
N88-20619
N88-20620
N88-20626
N88-20632
N88-20855
N88-20859
N88-20902
N88-20915
N88-20945
N88-20958

	N88-20985
	N88-20990
	N88-21009
	N88-21010
	N88-21013
	N88-21059
	N88-21060
ZWO-10-70-10	N88-20928
ZWO-125-20-04	N88-20893
314-40-32	N88-20741
324-02-16	N88-20601
476-30-20-11	N88-20351
	N88-20352
480-52-02	N88-20353
505-43-11	N88-20454
505-43-81-01	N88-20669
505-45-33-04	N88-20308
505-60-01-01	N88-20833
505-61-01-02	N88-20274
505-61-71-02	N88-20264
505-62-21	N88-20262
505-62-71-01	N88-20256
505-63-01-05	N88-20372
505-63-11	N88-20829
	N88-20830
505-63-11-01	N88-20290
	N88-20291
505-63-21	N88-20301
505-63-21-01	N88-20263
	N88-20269
505-63-31	N88-20673
505-63-51-01	N88-20656
505-63-51-10	N88-20665
505-66-11	N88-20896
505-66-21-01	N88-20894
	N88-20895
505-67-11-01	N88-20822
505-68-01-01	N88-20758
505-68-31	N88-20302
505-68-71-03	N88-20273
505-68-91-06	N88-20280
505-90-01	N88-20417
505-90-21-01	N88-20591
	N88-20831
506-41-31	N88-20361
506-43-11-04	N88-20363
506-43-31-03	N88-20666
506-44-2A	N88-20555
506-46-11-03	N88-20491
506-46-21-01	N88-20309
532-09-01	N88-20375
533-02-08	N88-20307
533-02-11	N88-20279
533-02-21	N88-20598
549-01-00-05-59	N88-20905
665-45-30-01	N88-20772
763-01-21-10	N88-20592

Typical Report Number Index Listing

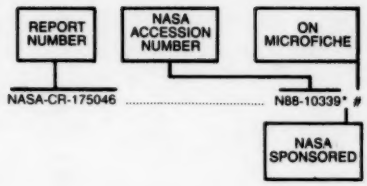

Listings in this index are arranged alphanumerically by report number. The NASA accession number denotes the number by which the citation is identified. An asterisk (*) indicates that the item is a NASA report. A pound sign (#) indicates that the item is available on microfiche.

AAMU-NAG-88-1 ..... N88-21105* #

AD-A187508 ..... N88-20975 #
AD-A187664 ..... N88-20292 #
AD-A188006 ..... N88-20396 #
AD-A188321 ..... N88-21075 #
AD-A188339 ..... N88-20556 #
AD-A188348 ..... N88-20785 #
AD-A188454 ..... N88-20611 #
AD-A188502 ..... N88-20435 #
AD-A188529 ..... N88-20510 #
AD-A188554 ..... N88-21081 #
AD-A188560 ..... N88-21078 #
AD-A188595 ..... N88-20492 #
AD-A188614 ..... N88-20885 #
AD-A188623 ..... N88-20362 #
AD-A188690 ..... N88-20338 #
AD-A188698 ..... N88-21005 #
AD-A188711 ..... N88-20976 #
AD-A188712 ..... N88-21035 #
AD-A188722 ..... N88-20303 #
AD-A188724 ..... N88-21094 #
AD-A188725 ..... N88-20805 #
AD-A188726 ..... N88-20820 #
AD-A188731 ..... N88-20405 #
AD-A188732 ..... N88-20839 #
AD-A188733 ..... N88-20406 #
AD-A188735 ..... N88-20333 #
AD-A188742 ..... N88-20898 #
AD-A188747 ..... N88-20943 #
AD-A188751 ..... N88-20717 #
AD-A188756 ..... N88-21036 #
AD-A188757 ..... N88-20376 #
AD-A188759 ..... N88-20612 #
AD-A188760 ..... N88-21037 #
AD-A188790 ..... N88-20377 #
AD-A188797 ..... N88-20378 #
AD-A188800 ..... N88-20449 #
AD-A188972 ..... N88-20407 #
AD-A189004 ..... N88-20827 #
AD-A189034 ..... N88-20493 #
AD-A189035 ..... N88-20823 #
AD-A189042 ..... N88-20899 #
AD-A189043 ..... N88-20840 #
AD-A189048 ..... N88-20258 #
AD-A189049 ..... N88-20283 #
AD-A189050 ..... N88-20511 #
AD-A189053 ..... N88-20906 #
AD-A189057 ..... N88-20494 #
AD-A189060 ..... N88-20530 #
AD-A189063 ..... N88-20977 #
AD-A189064 ..... N88-20757 #
AD-A189066 ..... N88-20744 #
AD-A189068 ..... N88-21006 #
AD-A189069 ..... N88-20935 #
AD-A189080 ..... N88-20293 #
AD-A189091 ..... N88-20978 #
AD-A189092 ..... N88-20379 #
AD-A189093 ..... N88-20979 #
AD-A189094 ..... N88-20980 #
AD-A189103 ..... N88-20450 #
AD-A189104 ..... N88-20965 #
AD-A189107 ..... N88-20653 #
AD-A189110 ..... N88-21038 #
AD-A189112 ..... N88-20380 #
AD-A189114 ..... N88-20381 #
AD-A189115 ..... N88-20482 #
AD-A189130 ..... N88-20512 #
AD-A189131 ..... N88-20284 #
AD-A189132 ..... N88-20513 #
AD-A189136 ..... N88-20294 #
AD-A189144 ..... N88-20936 #
AD-A189150 ..... N88-20775 #
AD-A189151 ..... N88-20602 #
AD-A189155 ..... N88-21039 #
AD-A189158 ..... N88-20776 #
AD-A189160 ..... N88-20382 #
AD-A189166 ..... N88-21040 #
AD-A189177 ..... N88-21041 #
AD-A189200 ..... N88-20531 #
AD-A189202 ..... N88-20841 #
AD-A189205 ..... N88-20777 #
AD-A189216 ..... N88-20355 #
AD-A189219 ..... N88-20383 #
AD-A189220 ..... N88-20557 #
AD-A189226 ..... N88-20966 #
AD-A189228 ..... N88-20981 #
AD-A189230 ..... N88-20834 #
AD-A189234 ..... N88-20356 #
AD-A189238 ..... N88-20613 #
AD-A189239 ..... N88-20842 #
AD-A189240 ..... N88-20907 #
AD-A189241 ..... N88-20843 #
AD-A189243 ..... N88-20408 #
AD-A189244 ..... N88-20886 #
AD-A189245 ..... N88-20844 #
AD-A189251 ..... N88-20409 #
AD-A189252 ..... N88-20845 #
AD-A189255 ..... N88-21042 #
AD-A189257 ..... N88-20514 #
AD-A189258 ..... N88-20364 #
AD-A189260 ..... N88-20483 #
AD-A189261 ..... N88-20532 #
AD-A189262 ..... N88-20533 #
AD-A189264 ..... N88-20967 #
AD-A189265 ..... N88-20709 #
AD-A189267 ..... N88-20778 #
AD-A189270 ..... N88-20968 #
AD-A189272 ..... N88-20365 #
AD-A189274 ..... N88-20384 #
AD-A189275 ..... N88-20410 #
AD-A189276 ..... N88-20385 #
AD-A189278 ..... N88-20484 #
AD-A189279 ..... N88-21043 #
AD-A189288 ..... N88-20411 #
AD-A189291 ..... N88-20515 #
AD-A189305 ..... N88-20808 #
AD-A189307 ..... N88-20779 #
AD-A189310 ..... N88-20558 #
AD-A189321 ..... N88-20412 #
AD-A189327 ..... N88-21088 #
AD-A189329 ..... N88-20534 #
AD-A189336 ..... N88-20809 #
AD-A189338 ..... N88-20259 #
AD-A189345 ..... N88-21018 #
AD-A189349 ..... N88-20824 #
AD-A189354 ..... N88-20451 #
AD-A189355 ..... N88-20908 #
AD-A189361 ..... N88-20535* #
AD-A189367 ..... N88-20969 #
AD-A189368 ..... N88-20285 #
AD-A189378 ..... N88-20452 #
AD-A189383 ..... N88-20909 #
AD-A189385 ..... N88-20413 #
AD-A189387 ..... N88-20810 #
AD-A189390 ..... N88-20825 #
AD-A189408 ..... N88-20603 #
AD-A189407 ..... N88-20937 #
AD-A189408 ..... N88-20938 #
AD-A189414 ..... N88-20366 #
AD-A189422 ..... N88-20559 #
AD-A189428 ..... N88-20536 #
AD-A189429 ..... N88-20654 #
AD-A189430 ..... N88-20910 #
AD-A189432 ..... N88-20386 #
AD-A189447 ..... N88-20846* #
AD-A189473 ..... N88-20847* #
AD-A189480 ..... N88-20710 #
AD-A189492 ..... N88-20516 #
AD-A189494 ..... N88-20337 #
AD-A189495 ..... N88-20286 #
AD-A189500 ..... N88-20260 #
AD-A189507 ..... N88-20614 #
AD-A189514 ..... N88-20615 #
AD-A189516 ..... N88-20367 #
AD-A189517 ..... N88-20560 #
AD-A189518 ..... N88-20982 #
AD-A189519 ..... N88-20387 #
AD-A189520 ..... N88-21007 #
AD-A189524 ..... N88-20453 #
AD-A189525 ..... N88-20388 #
AD-A189526 ..... N88-20414 #
AD-A189527 ..... N88-21044 #
AD-A189538 ..... N88-20561 #
AD-A189539 ..... N88-20826 #
AD-A189543 ..... N88-20517 #
AD-A189544 ..... N88-20346 #
AD-A189545 ..... N88-20368 #
AD-A189557 ..... N88-20811 #
AD-A189558 ..... N88-20616 #
AD-A189560 ..... N88-20415 #
AD-A189567 ..... N88-20745 #
AD-A189572 ..... N88-20261 #
AD-A189573 ..... N88-20887 #
AD-A189574 ..... N88-21106 #
AD-A189576 ..... N88-20617 #
AD-A189577 ..... N88-20655 #
AD-A189589 ..... N88-20812 #
AD-A189590 ..... N88-20537 #
AD-A189591 ..... N88-20911 #
AD-A189592 ..... N88-20746 #
AD-A189600 ..... N88-21045 #
AD-A189601 ..... N88-21008 #
AD-A189603 ..... N88-20635 #
AD-A189604 ..... N88-20939 #
AD-A189605 ..... N88-21089 #
AD-A189607 ..... N88-20562 #
AD-A189611 ..... N88-20416 #
AD-A189613 ..... N88-20989 #

AECC-86-JAA-001-F ..... N88-20585 #

AERE-R-12145 ..... N88-20649 #
AERE-R-12465 ..... N88-20648 #
AERE-R-12479 ..... N88-20650 #

AEROCHEM-TP-469 ..... N88-20451 #

AFAL-TR-87-049 ..... N88-20383 #
AFAL-TR-87-070 ..... N88-20355 #
AFAL-TR-87-075 ..... N88-20977 #

AFATL-TR-87-74 ..... N88-20409 #

AFGL-ERP-974 ..... N88-20285 #

AFGL-TR-87-0105 ..... N88-20515 #
AFGL-TR-87-0137 ..... N88-20285 #
AFGL-TR-87-0218 ..... N88-21088 #
AFGL-TR-87-0233 ..... N88-20709 #
AFGL-TR-87-0256 ..... N88-20744 #
AFGL-TR-87-0321 ..... N88-20745 #
AFGL-TR-88-0006 ..... N88-21007 #

AFIT/DS/PH/76-3 ..... N88-20615 #
AFIT/DS/PH/87-5 ..... N88-20617 #

AFIT/GA/AA/87D-2 ..... N88-20346 #
AFIT/GA/AA/87D-5 ..... N88-20561 #
AFIT/GA/AA/87D-07 ..... N88-20261 #

AFIT/GAE/AA/87D-3 ..... N88-20655 #
AFIT/GAE/AA/87D-10 ..... N88-20368 #
AFIT/GAE/AA/87D-13 ..... N88-20415 #

AFIT/GCS/ENG/87D-20 ..... N88-20887 #

AFIT/GE/ENG/87D-16 ..... N88-20612 #
AFIT/GE/ENG/87D-62 ..... N88-20537 #
AFIT/GE/ENG/87D-67 ..... N88-20517 #

AFIT/GEO/ENP/87D-1 ..... N88-20618 #

AFIT/GEP/ENP/87D-1 ..... N88-21045 #
AFIT/GEP/ENP/87D-5 ..... N88-20911 #
AFIT/GEP/ENP/87D-6 ..... N88-20611 #
AFIT/GEP/ENP/87D-10 ..... N88-21008 #

AFIT/GSO/AA/87D-2 ..... N88-21106 #

AFIT/GSO/ENP/87D-1 ..... N88-20746 #

AFIT/GSO/ENS/87D-4 ..... N88-20286 #
AFIT/GSO/ENS/87D-8 ..... N88-20516 #
AFIT/GSO/ENS/87D-13 ..... N88-20337 #

AFOSR-87-0217TR ..... N88-20938 #
AFOSR-87-0219TR ..... N88-20937 #
AFOSR-87-1155TR ..... N88-20533 #
AFOSR-87-1660TR ..... N88-20556 #
AFOSR-87-1724TR ..... N88-20981 #
AFOSR-87-1725TR ..... N88-20386 #
AFOSR-87-1749TR ..... N88-20435 #
AFOSR-87-1864TR ..... N88-20653 #
AFOSR-87-1892TR ..... N88-20413 #
AFOSR-87-1894TR ..... N88-20381 #
AFOSR-87-1917TR ..... N88-20909 #
AFOSR-88-0036TR ..... N88-20562 #
AFOSR-88-0038TR ..... N88-21089 #
AFOSR-88-0089TR ..... N88-20367 #
AFOSR-88-0093TR ..... N88-21044 #
AFOSR-88-0125TR ..... N88-20388 #
AFOSR-88-0132TR ..... N88-20982 #
AFOSR-88-0147TR ..... N88-20560 #
AFOSR-88-0176TR ..... N88-20414 #

AFWAL-TR-84-2070-PT-3 ..... N88-20484 #
AFWAL-TR-86-3056 ..... N88-20292 #
AFWAL-TR-87-1114 ..... N88-20303 #
AFWAL-TR-87-1148-VOL-2 ..... N88-20639 #
AFWAL-TR-87-1161 ..... N88-20510 #
AFWAL-TR-87-1163 ..... N88-20885 #
AFWAL-TR-87-1177 ..... N88-20898 #
AFWAL-TR-87-2047 ..... N88-20384 #
AFWAL-TR-87-2048 ..... N88-20356 #
AFWAL-TR-87-3047 ..... N88-20624 #
AFWAL-TR-87-4073 ..... N88-20449 #
AFWAL-TR-87-4086 ..... N88-20453 #
AFWAL-TR-3043-VOL-1 ..... N88-20627 #

AIAA-88-0710 ..... N88-20263* #
AIAA-88-2167 ..... N88-20344* #
AIAA-88-2378 ..... N88-20629* #
AIAA-88-2434 ..... N88-20630* #
AIAA-88-2553 ..... N88-20279* #

ALGO-PUB-0033 ..... N88-20535* #
ALGO-PUB-0098-PT-1 ..... N88-20848* #

ALSO-PUB-0045 ..... N88-20847* #

ANL-HEP-CP-87-120 ..... N88-20992 #

ANL-87-24 ..... N88-20474 #
ANL-87-44 ..... N88-20551 #

ANL/FE-87-2 ..... N88-20473 #

ANL/MCS-TM-104 ..... N88-20851 #

AR-88-87 ..... N88-20755 #
AR-005-132 ..... N88-21032 #
AR-005-164 ..... N88-20488 #
AR-005-170 ..... N88-20487 #
AR-005-172 ..... N88-20595 #
AR-005-184 ..... N88-20489 #
AR-005-189 ..... N88-20490 #
AR-005-190 ..... N88-20486 #
AR-005-193 ..... N88-20478 #
AR-005-197 ..... N88-20399 #

ARCCB-TR-87027 ..... N88-20338 #
ARCCB-TR-87030 ..... N88-20407 #
ARCCB-TR-87031 ..... N88-20333 #

ARE-TM-(UHA)-87511 ..... N88-20967 #

ARI-RN-87-51 ..... N88-20826 #
ARI-RN-87-68 ..... N88-20910 #

ARI-TR-756 ..... N88-20710 #

ARL-AERO-TM-389 ..... N88-20258 #

ARL-MAT-TM-398 ..... N88-20293 #

ARL/PSU/TR-87-005 ..... N88-20512 #
ARL/PSU/TR-87-009 ..... N88-20966 #
ARL/PSU/TR-87-010 ..... N88-20969 #

ARO-21057.5-EL ..... N88-21037 #
ARO-21192.6-PH ..... N88-20612 #
ARO-21308.14-MA ..... N88-20382 #
ARO-21353.7-EG ..... N88-20532 #
ARO-21450.6-MS ..... N88-20416 #
ARO-21828.1-MS-S ..... N88-20451 #
ARO-21970.2-PH ..... N88-20989 #
ARO-22291.9-MS ..... N88-21035 #
ARO-22291.11-MS ..... N88-20976 #
ARO-22356.12-MA ..... N88-20908 #
ARO-22736.4-CH ..... N88-20405 #
ARO-23573.18-EG ..... N88-20603 #
ARO-23699.16-MA ..... N88-20938 #
ARO-23699.17-MA ..... N88-20937 #

ASD-TR-87-5006 ..... N88-20634 #

ATC-140 ..... N88-20757 #

AVSCOM-TM-88-B-001 ..... N88-20656* #
AVSCOM-TM-88-B-003 ..... N88-20665* #

AVSCOM-TR-85-A-9 ..... N88-20257* #

B-205804 ..... N88-20289 #
B-226783 ..... N88-20481 #

BNL-40419 ..... N88-20457 #
BNL-40534 ..... N88-20428 #
BNL-40626 ..... N88-21011 #
BNL-40740 ..... N88-20913 #
BNL-52066-VOL-2 ..... N88-20564 #

BPT-5/87 ..... N88-20771 #

BRL-TR-2941 ..... N88-20380 #

BU-362 ..... N88-20310 #
BU-364 ..... N88-20299 #

B8711193 ..... N88-20890 #
B8711194 ..... N88-20956 #
B8711195 ..... N88-20891 #
B8711196 ..... N88-20863 #
B8711197 ..... N88-20864 #
B8713958 ..... N88-20810 #
B8715224 ..... N88-20804 #
B8717219 ..... N88-20916 #
B8717220 ..... N88-20917 #
B8717221 ..... N88-20918 #
B8717222 ..... N88-20865 #
B8717223 ..... N88-20866 #
B8717224 ..... N88-20867 #
B8719780 ..... N88-20670 #
B8723354 ..... N88-20889 #
B8723355 ..... N88-20947 #
B8723356 ..... N88-20948 #
B8723612 ..... N88-21001 #
B8723613 ..... N88-20605 #
B8723762 ..... N88-20923 #
B8723958 ..... N88-20954 #
B8723959 ..... N88-20955 #
B8723960 ..... N88-21070 #
B8723961 ..... N88-20922 #
B8723965 ..... N88-20940 #
B8723966 ..... N88-20748 #
B8723967 ..... N88-20862 #
B8723969 ..... N88-20919 #
B8723971 ..... N88-20892 #
B8723972 ..... N88-20893 #
B8723973 ..... N88-20869 #
B8723974 ..... N88-20870 #
B8723975 ..... N88-20903 #
B8725236 ..... N88-20570 #
B8725238 ..... N88-20266 #
B8725239 ..... N88-20427 #
B8725240 ..... N88-20267 #
B8725241 ..... N88-20347 #
B8729110 ..... N88-20987 #
B8729208 ..... N88-20426 #
B8729209 ..... N88-20948 #
B8729553 ..... N88-20966 #
B8729597 ..... N88-20295 #
B8729598 ..... N88-20371 #
B8729599 ..... N88-20569 #
B8729600 ..... N88-20639 #
B8729608 ..... N88-20995 #
B8729620 ..... N88-20571 #
B8729621 ..... N88-20660 #
B8729622 ..... N88-20661 #

B8729623 ..... N88-20305 #
B8729624 ..... N88-20288 #
B8729648 ..... N88-20924 #
B8729650 ..... N88-20871 #
B8729651 ..... N88-20872 #
B8729652 ..... N88-20920 #
B8729653 ..... N88-20873 #
B8729654 ..... N88-20874 #
B8729655 ..... N88-20950 #
B8729656 ..... N88-20921 #
B8729657 ..... N88-20836 #
B8731189 ..... N88-20941 #
B8731192 ..... N88-20949 #
B8731194 ..... N88-20861 #
B8731945 ..... N88-20928 #
B87239968 ..... N88-20668 #

CAL-1683 ..... N88-21091* #

CASA-IM-WP-301 ..... N88-20354 #

CEBAF-PR-87-017 ..... N88-20996 #
CEBAF-PR-88-003 ..... N88-20600 #

CMU-CS-86-171 ..... N88-20898 #
CMU-CS-87-100 ..... N88-20685 #
CMU-CS-87-125 ..... N88-20510 #

CMU-RI-TR-87-24 ..... N88-20263 #

CNA-207 ..... N88-20849 #

CONF-870294-2 ..... N88-20688 #
CONF-870438-39 ..... N88-20636 #
CONF-870488-2 ..... N88-20633 #
CONF-870629-14 ..... N88-21027 #
CONF-870656-49 ..... N88-20985 #
CONF-870691-9 ..... N88-20971 #
CONF-870691-10 ..... N88-20459 #
CONF-870739-15 ..... N88-20998 #
CONF-870753-72 ..... N88-20418 #
CONF-870762-1 ..... N88-20637 #
CONF-870784-4 ..... N88-20990 #
CONF-870901-28 ..... N88-20963 #
CONF-870947-9 ..... N88-20848 #
CONF-870947-10 ..... N88-21023 #
CONF-871006-5 ..... N88-20997 #
CONF-871041-6 ..... N88-20394 #
CONF-871101-81 ..... N88-20880 #
CONF-871105-2 ..... N88-21025 #
CONF-871112-3 ..... N88-20733 #
CONF-871121-2 ..... N88-20544 #
CONF-871121-4 ..... N88-20539 #
CONF-871124-26 ..... N88-20467 #
CONF-871124-27 ..... N88-21047 #
CONF-871124-35 ..... N88-21052 #
CONF-871124-36 ..... N88-21010 #
CONF-871124-47 ..... N88-21066 #
CONF-871124-62 ..... N88-21055 #
CONF-871124-63 ..... N88-21060 #
CONF-871124-64 ..... N88-21058 #
CONF-871124-66 ..... N88-21061 #
CONF-871124-72 ..... N88-21062 #
CONF-871124-74 ..... N88-20429 #
CONF-871124-76 ..... N88-20373 #
CONF-871125-21 ..... N88-21064 #
CONF-871147-4 ..... N88-20466 #
CONF-871190-2 ..... N88-20471 #
CONF-871190-3 ..... N88-20470 #
CONF-871234-8 ..... N88-20458 #
CONF-871234-10 ..... N88-20468 #
CONF-871243-5 ..... N88-20991 #
CONF-871249-1 ..... N88-20390 #
CONF-871250-1 ..... N88-20457 #
CONF-871251-3 ..... N88-20855 #
CONF-871254-3 ..... N88-20621 #
CONF-880103-3 ..... N88-20719 #
CONF-880110-19 ..... N88-21013 #
CONF-880110-20 ..... N88-20958 #
CONF-880118-1 ..... N88-20461 #
CONF-880122-6 ..... N88-20568 #
CONF-880122-7 ..... N88-21003 #
CONF-880122-8 ..... N88-21002 #
CONF-880128-5 ..... N88-20588 #
CONF-880132-6 ..... N88-20761 #
CONF-880141-1 ..... N88-21053 #
CONF-880149-1 ..... N88-20999 #
CONF-880153-1 ..... N88-20853 #
CONF-880212-2 ..... N88-20734 #
CONF-880220-15 ..... N88-20657 #
CONF-880236-1 ..... N88-20638 #
CONF-880236-1 ..... N88-20952 #
CONF-880315-1 ..... N88-20914 #
CONF-880315-2 ..... N88-20944 #
CONF-880315-3 ..... N88-20945 #
CONF-880318-1 ..... N88-20625 #

CONF-880320-1 ..... N88-20737 #
CONF-880327-1 ..... N88-21079 #
CONF-880345-1 ..... N88-20901 #
CONF-880402-8 ..... N88-20632 #
CONF-880424-1 ..... N88-20518 #
CONF-8608206-1-DRAFT ..... N88-20849 #
CONF-8609133-SUMM ..... N88-20439 #
CONF-8704110-15 ..... N88-20738 #
CONF-8704165-3 ..... N88-20879 #
CONF-8704247-VOL-2 ..... N88-20564 #
CONF-8705168-7 ..... N88-21057 #
CONF-8705256-1 ..... N88-20587 #
CONF-8706103-5 ..... N88-20389 #
CONF-8706103-6 ..... N88-20463 #
CONF-8707125-1 ..... N88-21046 #
CONF-8707141-3 ..... N88-20984 #
CONF-8708178-2 ..... N88-21069 #
CONF-8708199-1 ..... N88-20428 #
CONF-8709110-15 ..... N88-20618 #
CONF-8709157-3 ..... N88-21000 #
CONF-8709172-4 ..... N88-21056 #
CONF-8709212-1 ..... N88-21048 #
CONF-8710110-1 ..... N88-20424 #
CONF-8710111-28 ..... N88-20395 #
CONF-8710116-2 ..... N88-20658 #
CONF-8710124-4 ..... N88-20800 #
CONF-8710165-4 ..... N88-20626 #
CONF-8710165-6 ..... N88-20619 #
CONF-8710201-1 ..... N88-20970 #
CONF-8710254-3 ..... N88-20620 #
CONF-8710262-1 ..... N88-20586 #
CONF-8710264-1 ..... N88-20423 #
CONF-8710273-1 ..... N88-21009 #
CONF-8710274-1 ..... N88-20992 #
CONF-8711115-1 ..... N88-20465 #
CONF-8711115-5 ..... N88-20475 #
CONF-8711118-2 ..... N88-20628 #
CONF-8711127-1 ..... N88-20728 #
CONF-8711143-1 ..... N88-21054 #
CONF-8711147-1 ..... N88-21059 #
CONF-8711148-1 ..... N88-21020 #
CONF-8711153-1 ..... N88-21085 #

CRDEC-CR-88015 ..... N88-20385 #

CRREL-87-20 ..... N88-20779 #

CS-8708 ..... N88-20904 #
CS-8709 ..... N88-20876 #

CSRD-614 ..... N88-20888 #

CUMER-87-3 ..... N88-20366 #

CWI-AM-R8704 ..... N88-20940 #
CWI-AM-R8705 ..... N88-20748 #

CWI-CS-R8707 ..... N88-20862 #
CWI-CS-R8708 ..... N88-20890 #
CWI-CS-R8709 ..... N88-20956 #
CWI-CS-R8710 ..... N88-20891 #
CWI-CS-R8711 ..... N88-20863 #
CWI-CS-R8712 ..... N88-20864 #
CWI-CS-R8714 ..... N88-20916 #
CWI-CS-R8715 ..... N88-20917 #
CWI-CS-R8716 ..... N88-20918 #
CWI-CS-R8717 ..... N88-20865 #
CWI-CS-R8718 ..... N88-20866 #
CWI-CS-R8719 ..... N88-20867 #
CWI-CS-R8720 ..... N88-20868 #
CWI-CS-R8721 ..... N88-20919 #
CWI-CS-R8723 ..... N88-20892 #
CWI-CS-R8724 ..... N88-20893 #
CWI-CS-R8725 ..... N88-20869 #
CWI-CS-R8726 ..... N88-20870 #
CWI-CS-R8727 ..... N88-20903 #
CWI-CS-R8731 ..... N88-20871 #
CWI-CS-R8732 ..... N88-20872 #
CWI-CS-R8733 ..... N88-20920 #
CWI-CS-R8734 ..... N88-20873 #
CWI-CS-R8735 ..... N88-20874 #
CWI-CS-R8736 ..... N88-20950 #
CWI-CS-R8737 ..... N88-20921 #
CWI-CS-R8738 ..... N88-20836 #

CWI-MS-R8709 ..... N88-20941 #

CWI-NM-R8713 ..... N88-20922 #
CWI-NM-R8714 ..... N88-20923 #
CWI-NM-R8717 ..... N88-20924 #

CWI-OS-R8709 ..... N88-20889 #
CWI-OS-R8710 ..... N88-20947 #
CWI-OS-R8711 ..... N88-20948 #
CWI-OS-R8712 ..... N88-20949 #
CWI-OS-R8714 ..... N88-20861 #

CWI-PM-R8703 ..... N88-20954 #
CWI-PM-R8704 ..... N88-20955 #
CWI-PM-R8705 ..... N88-21070 #

C4E-ONR-1 ..... N88-20842 #

DE87-001104 ..... N88-20736 #
DE87-008997 ..... N88-20879 #
DE87-011704 ..... N88-20538 #
DE87-012261 ..... N88-20721 #
DE87-012279 ..... N88-20722 #
DE87-013184 ..... N88-20900 #
DE87-013653 ..... N88-20737 #
DE87-014550 ..... N88-20418 #
DE87-014852 ..... N88-20518 #
DE87-014894 ..... N88-20914 #
DE87-703166 ..... N88-20404 #
DE88-000498 ..... N88-20944 #
DE88-000624 ..... N88-21023 #
DE88-000625 ..... N88-20848 #
DE88-000968 ..... N88-20945 #
DE88-001028 ..... N88-20584 #
DE88-001104 ..... N88-20718 #
DE88-001107 ..... N88-21050 #
DE88-001108 ..... N88-20723 #
DE88-001114 ..... N88-20724 #
DE88-001115 ..... N88-20725 #
DE88-001116 ..... N88-20726 #
DE88-001117 ..... N88-21051 #
DE88-001122 ..... N88-20727 #
DE88-001129 ..... N88-20728 #
DE88-001208 ..... N88-21065 #
DE88-001312 ..... N88-20729 #
DE88-001427 ..... N88-21046 #
DE88-001742 ..... N88-21079 #
DE88-001806 ..... N88-20997 #
DE88-002180 ..... N88-20849 #
DE88-002216 ..... N88-20970 #
DE88-002413 ..... N88-20719 #
DE88-002549 ..... N88-20850 #
DE88-002852 ..... N88-20544 #
DE88-002878 ..... N88-20637 #
DE88-003138 ..... N88-20624 #
DE88-003142 ..... N88-21084 #
DE88-003235 ..... N88-20419 #
DE88-003293 ..... N88-20990 #
DE88-003305 ..... N88-20638 #
DE88-003330 ..... N88-20781 #
DE88-003481 ..... N88-20428 #
DE88-003562 ..... N88-20464 #
DE88-003565 ..... N88-21066 #
DE88-003566 ..... N88-20888 #
DE88-003579 ..... N88-20959 #
DE88-003616 ..... N88-20720 #
DE88-003637 ..... N88-20390 #
DE88-003638 ..... N88-21052 #
DE88-003674 ..... N88-20456 #
DE88-003717 ..... N88-21086 #
DE88-003758 ..... N88-20618 #
DE88-003841 ..... N88-21053 #
DE88-003842 ..... N88-21047 #
DE88-003851 ..... N88-21048 #
DE88-003858 ..... N88-20539 #
DE88-003919 ..... N88-20658 #
DE88-003938 ..... N88-20465 #
DE88-004042 ..... N88-20632 #
DE88-004090 ..... N88-20420 #
DE88-004112 ..... N88-21024 #
DE88-004129 ..... N88-20730 #
DE88-004174 ..... N88-21025 #
DE88-004195 ..... N88-20391 #
DE88-004294 ..... N88-20625 #
DE88-004337 ..... N88-20466 #
DE88-004352 ..... N88-20626 #
DE88-004359 ..... N88-21010 #
DE88-004438 ..... N88-20392 #
DE88-004446 ..... N88-20963 #
DE88-004486 ..... N88-20604 #
DE88-004507 ..... N88-20421 #
DE88-004518 ..... N88-20393 #
DE88-004538 ..... N88-20467 #
DE88-004543 ..... N88-20747 #
DE88-004559 ..... N88-20545 #
DE88-004590 ..... N88-20457 #
DE88-004631 ..... N88-20731 #
DE88-004642 ..... N88-20732 #
DE88-004666 ..... N88-20733 #
DE88-004684 ..... N88-20734 #
DE88-004689 ..... N88-20468 #
DE88-004691 ..... N88-20458 #
DE88-004707 ..... N88-20735 #
DE88-004708 ..... N88-20627 #
DE88-004744 ..... N88-20585 #
DE88-004814 ..... N88-20459 #
DE88-004881 ..... N88-20469 #
DE88-004891 ..... N88-20422 #

DE88-004893 ..... N88-20548 #
DE88-004896 ..... N88-20547 #
DE88-004917 ..... N88-20983 #
DE88-004944 ..... N88-21096 #
DE88-004945 ..... N88-20759 #
DE88-005027 ..... N88-20633 #
DE88-005061 ..... N88-21054 #
DE88-005122 ..... N88-20394 #
DE88-005132 ..... N88-20568 #
DE88-005184 ..... N88-21011 #
DE88-005191 ..... N88-20563 #
DE88-005193 ..... N88-20423 #
DE88-005224 ..... N88-20586 #
DE88-005230 ..... N88-20584 #
DE88-005252 ..... N88-20999 #
DE88-005261 ..... N88-20998 #
DE88-005290 ..... N88-21055 #
DE88-005304 ..... N88-20470 #
DE88-005305 ..... N88-20471 #
DE88-005309 ..... N88-21019 #
DE88-005317 ..... N88-21056 #
DE88-005328 ..... N88-20806 #
DE88-005332 ..... N88-20951 #
DE88-005336 ..... N88-20952 #
DE88-005344 ..... N88-21057 #
DE88-005346 ..... N88-21058 #
DE88-005350 ..... N88-21000 #
DE88-005354 ..... N88-20395 #
DE88-005363 ..... N88-20619 #
DE88-005365 ..... N88-20585 #
DE88-005378 ..... N88-20984 #
DE88-005382 ..... N88-20853 #
DE88-005386 ..... N88-20991 #
DE88-005403 ..... N88-21012 #
DE88-005408 ..... N88-20854 #
DE88-005412 ..... N88-20985 #
DE88-005416 ..... N88-20902 #
DE88-005420 ..... N88-21059 #
DE88-005426 ..... N88-20855 #
DE88-005428 ..... N88-21060 #
DE88-005452 ..... N88-21061 #
DE88-005460 ..... N88-21026 #
DE88-005499 ..... N88-20915 #
DE88-005500 ..... N88-20460 #
DE88-005506 ..... N88-20856 #
DE88-005507 ..... N88-20857 #
DE88-005508 ..... N88-20858 #
DE88-005516 ..... N88-20461 #
DE88-005521 ..... N88-21027 #
DE88-005528 ..... N88-21002 #
DE88-005529 ..... N88-21003 #
DE88-005535 ..... N88-21020 #
DE88-005536 ..... N88-20424 #
DE88-005542 ..... N88-20425 #
DE88-005544 ..... N88-20738 #
DE88-005546 ..... N88-20971 #
DE88-005572 ..... N88-20859 #
DE88-005599 ..... N88-20628 #
DE88-005601 ..... N88-20548 #
DE88-005626 ..... N88-20761 #
DE88-005638 ..... N88-20636 #
DE88-005639 ..... N88-20901 #
DE88-005640 ..... N88-21085 #
DE88-005642 ..... N88-20880 #
DE88-005673 ..... N88-21009 #
DE88-005674 ..... N88-21013 #
DE88-005680 ..... N88-20462 #
DE88-005692 ..... N88-20912 #
DE88-005693 ..... N88-21083 #
DE88-005695 ..... N88-20860 #
DE88-005698 ..... N88-21004 #
DE88-005731 ..... N88-20609 #
DE88-005744 ..... N88-21062 #
DE88-005748 ..... N88-20587 #
DE88-005749 ..... N88-20373 #
DE88-005758 ..... N88-20986 #
DE88-005792 ..... N88-20659 #
DE88-005793 ..... N88-20472 #
DE88-005794 ..... N88-21067 #
DE88-005796 ..... N88-20953 #
DE88-005812 ..... N88-20835 #
DE88-005821 ..... N88-21095 #
DE88-005830 ..... N88-20334 #
DE88-005837 ..... N88-21049 #
DE88-005846 ..... N88-20588 #
DE88-005854 ..... N88-20760 #
DE88-005875 ..... N88-20739 #
DE88-005880 ..... N88-21021 #
DE88-005886 ..... N88-20550 #
DE88-005889 ..... N88-20473 #
DE88-005891 ..... N88-20474 #
DE88-005893 ..... N88-20851 #
DE88-005894 ..... N88-20551 #
DE88-005934 ..... N88-20389 #
DE88-005935 ..... N88-20463 #
DE88-005953 ..... N88-20429 #

DE88-005958 ..... N88-20992 #
DE88-005965 ..... N88-20993 #
DE88-005985 ..... N88-20475 #
DE88-006001 ..... N88-21064 #
DE88-006033 ..... N88-20620 #
DE88-006037 ..... N88-20430 #
DE88-006044 ..... N88-20645 #
DE88-006047 ..... N88-20933 #
DE88-006054 ..... N88-20525 #
DE88-006059 ..... N88-20485 #
DE88-006065 ..... N88-20994 #
DE88-006097 ..... N88-20657 #
DE88-006099 ..... N88-20621 #
DE88-006139 ..... N88-20942 #
DE88-006147 ..... N88-20540 #
DE88-006155 ..... N88-20369 #
DE88-006194 ..... N88-21068 #
DE88-006216 ..... N88-20335 #
DE88-006222 ..... N88-20622 #
DE88-006225 ..... N88-20589 #
DE88-006232 ..... N88-20958 #
DE88-006254 ..... N88-20881 #
DE88-006263 ..... N88-21022 #
DE88-006287 ..... N88-20566 #
DE88-006304 ..... N88-20431 #
DE88-006344 ..... N88-21069 #
DE88-006353 ..... N88-20913 #
DE88-006431 ..... N88-21031 #
DE88-006432 ..... N88-20852 #
DE88-006594 ..... N88-20623 #
DE88-006598 ..... N88-20567 #
DE88-006601 ..... N88-20541 #
DE88-006617 ..... N88-20542 #
DE88-006618 ..... N88-20543 #
DE88-700158 ..... N88-20507 #
DE88-700159 ..... N88-20508 #
DE88-700169 ..... N88-20509 #
DE88-701042 ..... N88-20432 #
DE88-780006 ..... N88-20439 #
DE88-900369 ..... N88-20740 #

DFVLR-FB-87-39 ..... N88-20629 #
DFVLR-FB-87-40 ..... N88-20268 #
DFVLR-FB-87-41 ..... N88-20572 #

DO-TM-87/5 ..... N88-20987 #

DODA-AR-004-553 ..... N88-20258 #
DODA-AR-004-560 ..... N88-20293 #

DOE/CE-0148-REV-1 ..... N88-20548 #

DOE/CH-10093/14 ..... N88-20722 #

DOE/ER-0355 ..... N88-21084 #
DOE/ER-04380/8 ..... N88-20983 #
DOE/ER-10569/5 ..... N88-20998 #
DOE/ER-10587/T6 ..... N88-21096 #
DOE/ER-10774/8 ..... N88-21095 #
DOE/ER-10830/6 ..... N88-20393 #
DOE/ER-12046/T4 ..... N88-20854 #
DOE/ER-12092/T1 ..... N88-20420 #
DOE/ER-13044/T2 ..... N88-20565 #
DOE/ER-13333/1 ..... N88-20566 #
DOE/ER-13687/1 ..... N88-21067 #
DOE/ER-13723/1 ..... N88-21026 #
DOE/ER-13761/2 ..... N88-20633 #
DOE/ER-25001/58 ..... N88-20886 #
DOE/ER-25007/T1 ..... N88-20850 #
DOE/ER-25009/493 ..... N88-20835 #
DOE/ER-25015/12 ..... N88-20953 #
DOE/ER-40048/200-L7 ..... N88-20959 #
DOE/ER-40272/49 ..... N88-20994 #
DOE/ER-45056/7 ..... N88-21012 #
DOE/ER-45109/T1 ..... N88-20431 #
DOE/ER-45162/3 ..... N88-20624 #
DOE/ER-45167/7 ..... N88-20659 #
DOE/ER-45170/4 ..... N88-21049 #
DOE/ER-45238/T2 ..... N88-20391 #
DOE/ER-45255/2 ..... N88-20419 #
DOE/ER-45291/T1 ..... N88-20993 #
DOE/ER-45297/4 ..... N88-21057 #
DOE/ER-45297/7 ..... N88-21058 #
DOE/ER-45302/1 ..... N88-20472 #
DOE/ER-52111/T2 ..... N88-20334 #
DOE/ER-53201/T3 ..... N88-21031 #
DOE/ER-53201/T4 ..... N88-20852 #
DOE/ER-60013/T1 ..... N88-20747 #
DOE/ER-60304/3 ..... N88-20759 #
DOE/ER-60355/3 ..... N88-20781 #

DOE/ET-51013/225-PT-1 ..... N88-21022 #
DOE/ET-53088/304 ..... N88-21019 #
DOE/ET-53088/307 ..... N88-20951 #

DOE/MC-21349/2531 ..... N88-20584 #

DOE/PC-90534/8 ..... N88-20392 #
DOE/PC-90957/T5 ..... N88-20563 #
DOE/PC-91024/T4 ..... N88-20456 #

DOE/SF-12221/T8 ..... N88-20730 #
DOE/SF-15933/T1 ..... N88-20538 #
DOE/SF-15954/T2 ..... N88-20735 #

DOT/FAA/CT-TN87/23 ..... N88-20284 #

DOT/FAA/PM-86-38 ..... N88-20757 #

DREO-TN-87-18 ..... N88-20378 #

DRIC-BR-103850 ..... N88-20967 #

DSCI-87-18 ..... N88-20820 #

DTRC-87/050 ..... N88-20365 #

E-3725 ..... N88-20262* #
E-3977 ..... N88-20454* #
E-3987 ..... N88-20599* #
E-4011 ..... N88-20455* #
E-4019 ..... N88-20417* #
E-4031 ..... N88-20555* #

ECN-202 ..... N88-20995 #

EFI-893(44)-88 ..... N88-20507 #
EFI-894(45)-88 ..... N88-20508 #
EFI-914(65)-88 ..... N88-20509 #

EGG-FSP-7872 ..... N88-21024 #

EGG-M-05687 ..... N88-20424 #
EGG-M-08887 ..... N88-20971 #
EGG-M-10887 ..... N88-20738 #
EGG-M-11187 ..... N88-20459 #
EGG-M-11787 ..... N88-21020 #
EGG-M-36386 ..... N88-20636 #
EGG-M-38987 ..... N88-20880 #
EGG-M-39887 ..... N88-21085 #
EGG-M-40187 ..... N88-20901 #

EGG-MS-7734 ..... N88-20425 #

EPRI-EA-5655 ..... N88-21068 #

ERIM-167400-101-F-VOL-2 ..... N88-20939 #

ESA-CR(P)-2502 ..... N88-20354 #
ESA-CR(P)-2509-PT-2 ..... N88-21016 #
ESA-CR(P)-2518 ..... N88-20332 #
ESA-CR(P)-2520 ..... N88-20330 #
ESA-CR(P)-2531 ..... N88-21082 #

ESA-PSS-01-718-ISS-1 ..... N88-20504 #

ESL-719300-1 ..... N88-20962* #

ETN-88-91315 ..... N88-20275 #
ETN-88-91316 ..... N88-20770 #
ETN-88-91319 ..... N88-20683 #
ETN-88-91332 ..... N88-21115 #
ETN-88-91338 ..... N88-20610 #
ETN-88-91339 ..... N88-20804 #
ETN-88-91340 ..... N88-20670 #
ETN-88-91344 ..... N88-20255 #
ETN-88-91347 ..... N88-20884 #
ETN-88-91348 ..... N88-20527 #
ETN-88-91382 ..... N88-20671 #
ETN-88-91436 ..... N88-20596 #
ETN-88-91437 ..... N88-20276 #
ETN-88-91439 ..... N88-20298 #
ETN-88-91440 ..... N88-20828 #
ETN-88-91502 ..... N88-21093 #
ETN-88-91718 ..... N88-20995 #
ETN-88-91719 ..... N88-20281 #
ETN-88-91720 ..... N88-20295 #
ETN-88-91721 ..... N88-20287 #
ETN-88-91722 ..... N88-20371 #
ETN-88-91723 ..... N88-20265 #
ETN-88-91724 ..... N88-20569 #
ETN-88-91725 ..... N88-20639 #
ETN-88-91727 ..... N88-20570 #
ETN-88-91728 ..... N88-20288 #
ETN-88-91729 ..... N88-20426 #
ETN-88-91730 ..... N88-20660 #
ETN-88-91731 ..... N88-20266 #
ETN-88-91732 ..... N88-20427 #
ETN-88-91733 ..... N88-20267 #
ETN-88-91735 ..... N88-20661 #
ETN-88-91736 ..... N88-20571 #
ETN-88-91737 ..... N88-20305 #
ETN-88-91738 ..... N88-20946 #

ETN-88-91739 ..... N88-20347 #
ETN-88-91740 ..... N88-20605 #
ETN-88-91741 ..... N88-21001 #
ETN-88-91742 ..... N88-20987 #
ETN-88-91743 ..... N88-20988 #
ETN-88-91745 ..... N88-20954 #
ETN-88-91746 ..... N88-20955 #
ETN-88-91747 ..... N88-21070 #
ETN-88-91748 ..... N88-20889 #
ETN-88-91749 ..... N88-20947 #
ETN-88-91750 ..... N88-20948 #
ETN-88-91751 ..... N88-20949 #
ETN-88-91752 ..... N88-20861 #
ETN-88-91753 ..... N88-20862 #
ETN-88-91754 ..... N88-20890 #
ETN-88-91755 ..... N88-20956 #
ETN-88-91756 ..... N88-20891 #
ETN-88-91757 ..... N88-20863 #
ETN-88-91758 ..... N88-20864 #
ETN-88-91759 ..... N88-20916 #
ETN-88-91760 ..... N88-20917 #
ETN-88-91761 ..... N88-20918 #
ETN-88-91762 ..... N88-20865 #
ETN-88-91763 ..... N88-20866 #
ETN-88-91764 ..... N88-20867 #
ETN-88-91765 ..... N88-20868 #
ETN-88-91766 ..... N88-20919 #
ETN-88-91768 ..... N88-20892 #
ETN-88-91769 ..... N88-20893 #
ETN-88-91770 ..... N88-20869 #
ETN-88-91771 ..... N88-20870 #
ETN-88-91772 ..... N88-20903 #
ETN-88-91776 ..... N88-20871 #
ETN-88-91777 ..... N88-20872 #
ETN-88-91778 ..... N88-20920 #
ETN-88-91779 ..... N88-20873 #
ETN-88-91780 ..... N88-20874 #
ETN-88-91782 ..... N88-20950 #
ETN-88-91783 ..... N88-20921 #
ETN-88-91784 ..... N88-20836 #
ETN-88-91785 ..... N88-20922 #
ETN-88-91786 ..... N88-20923 #
ETN-88-91789 ..... N88-20924 #
ETN-88-91790 ..... N88-20940 #
ETN-88-91791 ..... N88-20748 #
ETN-88-91796 ..... N88-20504 #
ETN-88-91798 ..... N88-20941 #
ETN-88-91822 ..... N88-20925 #
ETN-88-91823 ..... N88-20926 #
ETN-88-91824 ..... N88-21028 #
ETN-88-91825 ..... N88-20927 #
ETN-88-91826 ..... N88-20875 #
ETN-88-91827 ..... N88-20549 #
ETN-88-91866 ..... N88-20904 #
ETN-88-91867 ..... N88-20876 #
ETN-88-91868 ..... N88-20348 #
ETN-88-91869 ..... N88-20928 #
ETN-88-91879 ..... N88-20277 #
ETN-88-91880 ..... N88-20755 #
ETN-88-91892 ..... N88-20310 #
ETN-88-91903 ..... N88-20299 #
ETN-88-91916 ..... N88-20647 #
ETN-88-91922 ..... N88-20629 #
ETN-88-91923 ..... N88-20268 #
ETN-88-91924 ..... N88-20572 #
ETN-88-91931 ..... N88-20756 #
ETN-88-91935 ..... N88-20771 #
ETN-88-91936 ..... N88-20300 #
ETN-88-91955 ..... N88-20354 #
ETN-88-91956 ..... N88-21016 #
ETN-88-91960 ..... N88-20332 #
ETN-88-91962 ..... N88-20330 #
ETN-88-91967 ..... N88-21082 #
ETN-88-91982 ..... N88-20311 #
ETN-88-91983 ..... N88-20597 #
ETN-88-91984 ..... N88-20436 #
ETN-88-91985 ..... N88-20964 #
ETN-88-91986 ..... N88-20672 #
ETN-88-91987 ..... N88-20505 #
ETN-88-91988 ..... N88-21077 #
ETN-88-92001 ..... N88-21033 #
ETN-88-92002 ..... N88-20634 #

EUR-10906 ..... N88-20740 #

EUT-87-E-175 ..... N88-20925 #
EUT-87-E-176 ..... N88-20926 #
EUT-87-E-177 ..... N88-21028 #
EUT-87-E-178 ..... N88-20927 #
EUT-87-E-179 ..... N88-20675 #
EUT-87-E-180 ..... N88-20549 #

E290.1 ..... N88-20557 #

FEI-1782 ..... N88-20404 #

FFA-TN-1987-58 ..... N88-20277 #

FJSRL-TR-87-0006 ..... N88-20362 #

FNAL-TM-1508 ..... N88-20681 #

FSU-TR-M773 ..... N88-20938 #
FSU-TR-M777 ..... N88-20937 #

GA-A-18834 ..... N88-21027 #
GA-A-19056 ..... N88-21000 #

GAO/NSIAD-88-19 ..... N88-20289 #

GAO/RCED-88-38BR ..... N88-20481 #

GDSS-SP-87-018-VOL-1 ..... N88-20340* #
GDSS-SP-87-018-VOL-2 ..... N88-20341* #
GDSS-SP-87-018-VOL-3 ..... N88-20342* #
GDSS-SP-87-018-VOL-4 ..... N88-20343* #

GRI-87/0091-2 ..... N88-20564 #

H-1375 ..... N88-20307* #
H-1417 ..... N88-20375* #
H-1436 ..... N88-20598* #
H-1444 ..... N88-20673* #
H-1445 ..... N88-20301* #
H-1451 ..... N88-20304* #
H-1455 ..... N88-20508* #
H-1460 ..... N88-20344* #
H-1462 ..... N88-20302* #
H-1463 ..... N88-20832* #
H-1472 ..... N88-20279* #
H-1477 ..... N88-20696* #

HAC-REF-G0031 ..... N88-20536 #
HAC-REF-G3810 ..... N88-21044 #

HIG-1861 ..... N88-20789 #

HL86/1146 ..... N88-20649 #
HL87/1057(C14) ..... N88-20648 #
HL87/1113 ..... N88-20650 #

HOKE-87-AF-01 ..... N88-20556 #

HTKK-MAT-A250 ..... N88-20931 #

HTKKK-MAT-A251 ..... N88-20932 #

IABG-B-TF-2194 ..... N88-20300 #

IAE-4331/11 ..... N88-20433 #
IAE-4347/1 ..... N88-21071 #

IAEA-R-3650-F ..... N88-20432 #

ICASE-88-14 ..... N88-20831* #
ICASE-88-20 ..... N88-20591* #

IFSR-304 ..... N88-21019 #
IFSR-307 ..... N88-20951 #

IFVE-OTF-86-212-PT-1 ..... N88-20957 #
IFVE-OTF-86-213-PT-2 ..... N88-21072 #
IFVE-OTF-86-214-PT-3 ..... N88-21073 #

IIT-B/CE/RR/87-1 ..... N88-20370 #

IITRI-M06140-6 ..... N88-20635 #

IMA-87-0132 ..... N88-20789 #

INIS-MF-11057 ..... N88-20552 #

INPE-4154-RPE/540 ..... N88-20554 #
INPE-4189-PRE/1076 ..... N88-20712 #
INPE-4287-PRE/1159 ..... N88-20331 #
INPE-4290-PRE/1161 ..... N88-21015 #
INPE-4291-PRE/1162 ..... N88-20882 #
INPE-4294-PRE/1165 ..... N88-20715 #
INPE-4313-TDL/260 ..... N88-20349 #
INPE-4317-TDL/264 ..... N88-20929 #
INPE-4321-TDL/268 ..... N88-20930 #
INPE-4338-RPE/553 ..... N88-20350 #
INPE-4355-PRE/1186 ..... N88-20897 #
INPE-4357-TDL/298 ..... N88-20607 #
INPE-4362-PRE/1188 ..... N88-20743 #
INPE-4373-PRE/1196 ..... N88-20677 #
INPE-4401-PRE/1218 ..... N88-20774 #
INPE-4467-PRE/1240 ..... N88-20708 #

IR-1 ..... N88-21041 #

ISBN-9-06-144175-7 ..... N88-20925 #

ISBN-9-06-144176-5 ..... N88-20926 #
ISBN-9-06-144177-3 ..... N88-21026 #
ISBN-90-6144-178-1 ..... N88-20927 #
ISBN-90-6144-179-X ..... N88-20875 #
ISBN-90-6144-180-3 ..... N88-20549 #
ISBN-951-754-201-1 ..... N88-21108 #
ISBN-951-754-247-X ..... N88-20931 #
ISBN-951-754-252-6 ..... N88-20932 #
ISBN-951-754-256-9 ..... N88-20961 #

ISSN-0082-5255 ..... N88-20357 #
ISSN-0082-5255 ..... N88-20575 #
ISSN-0082-5263 ..... N88-20576 #
ISSN-0167-9708 ..... N88-20549 #
ISSN-0167-9708 ..... N88-20875 #
ISSN-0167-9708 ..... N88-20925 #
ISSN-0167-9708 ..... N88-20926 #
ISSN-0167-9708 ..... N88-20927 #
ISSN-0167-9708 ..... N88-21026 #
ISSN-0169-1708 ..... N88-20610 #
ISSN-0169-1708 ..... N88-20804 #
ISSN-0171-1342 ..... N88-20268 #
ISSN-0171-1342 ..... N88-20572 #
ISSN-0171-1342 ..... N88-20629 #
ISSN-0176-0777 ..... N88-20771 #
ISSN-0208-5658 ..... N88-20640 #
ISSN-0208-05658 ..... N88-20960 #
ISSN-0321-3429 ..... N88-20278* #
ISSN-0349-0068 ..... N88-20755 #
ISSN-0366-0885 ..... N88-20756 #
ISSN-0379-4059 ..... N88-20504 #
ISSN-0721-5320 ..... N88-20300 #
ISSN-0784-3143 ..... N88-20932 #

ITP-SB-87-28 ..... N88-20987 #

IW-86006R ..... N88-20670 #

IWGGCR-11 ..... N88-20439 #

JAERI-M-86-192 ..... N88-20439 #

JINR-P-13-3726 ..... N88-20593* #

JPL-D-4307 ..... N88-20535* #
JPL-D-4492 ..... N88-20647* #
JPL-D-4825 ..... N88-20848* #

JPL-PUB-87-4-VOL-5-PT-1-PT-2 ..... N88-20741* #
JPL-PUB-87-40 ..... N88-20905* #
JPL-PUB-87-42-VOL-1 ..... N88-20351* #
JPL-PUB-87-42-VOL-2 ..... N88-20352* #

JPL-400-333 ..... N88-20524* #

JPRS-CST-87-030 ..... N88-20501 #
JPRS-CST-88-003 ..... N88-20495 #

JPRS-UES-88-001 ..... N88-20674 #

JPRS-ULS-88-004 ..... N88-20815

JPRS-USP-88-002 ..... N88-20312 #

JUEL-2144 ..... N88-20756 #

K/ETAC-32 ..... N88-20628 #

KAERI/RR-325/81 ..... N88-20477* #

KNMI-TR-95 ..... N88-20610 #
KNMI-TR-96 ..... N88-20804 #

L-16318 ..... N88-20833* #
L-16364 ..... N88-20264* #
L-16371 ..... N88-20280* #
L-16401 ..... N88-20772* #

LA-UR-87-1270 ..... N88-20879 #
LA-UR-87-3131 ..... N88-20944 #
LA-UR-87-3575 ..... N88-20997 #
LA-UR-87-4245 ..... N88-20625 #
LA-UR-88-5 ..... N88-21056 #
LA-UR-88-97 ..... N88-20984 #
LA-UR-88-111 ..... N88-20853 #
LA-UR-88-153 ..... N88-20991 #

LA-11071-MS ..... N88-21004 #

LAIR-243 ..... N88-20809 #

LBF-FB-179 ..... N88-20300 #

LBL-21343 ..... N88-20469 #
LBL-23927 ..... N88-21048 #
LBL-23959 ..... N88-20547 #

LBL-23960 ..... N88-20546 #
LBL-23972 ..... N88-20963 #
LBL-24177 ..... N88-20422 #
LBL-24181 ..... N88-20539 #
LBL-24244 ..... N88-20545 #
LBL-24334 ..... N88-20587 #
LBL-24356 ..... N88-20373 #
LBL-24375 ..... N88-20986 #
LBL-24384 ..... N88-20606 #
LBL-24477 ..... N88-20609 #
LBL-24523 ..... N88-21061 #
LBL-24627 ..... N88-21069 #

LMSC/D068456 ..... N88-21094 #

MBB-UR-E-956/87 ..... N88-20671 #

MBB-URV-135 ..... N88-20332 #

MBB/LKE-122/S/PUB/244 ..... N88-20596 #
MBB/LKE-127/S/PUB/256 ..... N88-20276 #
MBB/LKE-294/S/PUB/249 ..... N88-20298 #
MBB/LKE-312/S/PUB/246 ..... N88-20628 #

MCR-86-2601-VOL-2-BK-1 ..... N88-20339* #

MECH-112 ..... N88-20412 #

MLM-3476(OP) ..... N88-20468 #
MLM-3478(OP) ..... N88-20458 #

MML-1987-1 ..... N88-20364 #

MRL-R-1054 ..... N88-21032 #
MRL-R-1079 ..... N88-20467 #
MRL-R-1081 ..... N88-20595 #
MRL-R-1089 ..... N88-20469 #
MRL-R-1094 ..... N88-20466 #
MRL-R-1096 ..... N88-20478 #
MRL-R-1099 ..... N88-20399 #

MRL-TN-522 ..... N88-20458 #
MRL-TN-525 ..... N88-20490 #

MTL-TR-87-50 ..... N88-20406 #
MTL-TR-87-55 ..... N88-20717 #
MTL-TR-87-59 ..... N88-20410 #

NADC-87008-60 ..... N88-20450 #
NADC-87151-60 ..... N88-20635 #

NAS 1.15:4026 ..... N88-20375* #
NAS 1.15:88273 ..... N88-20307* #
NAS 1.15:89727 ..... N88-21090* #
NAS 1.15:89733 ..... N88-21076* #
NAS 1.15:89735 ..... N88-20296* #
NAS 1.15:100163 ..... N88-20262* #
NAS 1.15:100412 ..... N88-20598* #
NAS 1.15:100417 ..... N88-20301* #
NAS 1.15:100421 ..... N88-20304* #
NAS 1.15:100425 ..... N88-20506* #
NAS 1.15:100429 ..... N88-20344* #
NAS 1.15:100430 ..... N88-20302* #
NAS 1.15:100433 ..... N88-20279* #
NAS 1.15:100435 ..... N88-20696* #
NAS 1.15:100437 ..... N88-20832* #
NAS 1.15:100536 ..... N88-20830* #
NAS 1.15:100537 ..... N88-20829* #
NAS 1.15:100539 ..... N88-20363* #
NAS 1.15:100553 ..... N88-20894* #
NAS 1.15:100555 ..... N88-20309* #
NAS 1.15:100557 ..... N88-20269* #
NAS 1.15:100559 ..... N88-20656* #
NAS 1.15:100560 ..... N88-20263* #
NAS 1.15:100562 ..... N88-20665* #
NAS 1.15:100578 ..... N88-20372* #
NAS 1.15:100579 ..... N88-20666* #
NAS 1.15:100581 ..... N88-20669* #
NAS 1.15:100586 ..... N88-20592* #
NAS 1.15:100689-VOL-2 ..... N88-20753* #
NAS 1.15:100694 ..... N88-20780* #
NAS 1.15:100799 ..... N88-20454* #
NAS 1.15:100823 ..... N88-20455* #
NAS 1.15:100830 ..... N88-20417* #
NAS 1.15:100841 ..... N88-20555* #
NAS 1.21:7011(309) N88-20814*
NAS 1.21:7037(224) N88-20254*
NAS 1.26:4131 ..... N88-20308* #
NAS 1.26:4132 ..... N88-20290* #
NAS 1.26:4134 ..... N88-20291* #
NAS 1.26:4138 ..... N88-20491* #
NAS 1.26:4139 ..... N88-20256* #
NAS 1.26:4140 ..... N88-20822* #
NAS 1.26:177470 ..... N88-20601* #
NAS 1.26:177830 ..... N88-20608* #
NAS 1.26:178390 ..... N88-20695* #

NAS 1.26:179316 ..... N88-20340* #
NAS 1.26:179317 ..... N88-20341* #
NAS 1.26:179318 ..... N88-20342* #
NAS 1.26:179319 ..... N88-20343* #
NAS 1.26:179321 ..... N88-20339* #
NAS 1.26:179430 ..... N88-20673* #
NAS 1.26:180757 ..... N88-20742* #
NAS 1.26:180758 ..... N88-20837* #
NAS 1.26:180759 ..... N88-20438* #
NAS 1.26:180762 ..... N88-21074* #
NAS 1.26:180877 ..... N88-20361* #
NAS 1.26:181094 ..... N88-20606* #
NAS 1.26:181388 ..... N88-20713* #
NAS 1.26:181611 ..... N88-20274* #
NAS 1.26:181626 ..... N88-20831* #
NAS 1.26:181639 ..... N88-20758* #
NAS 1.26:181649 ..... N88-20591* #
NAS 1.26:181650 ..... N88-20273* #
NAS 1.26:182112 ..... N88-20306* #
NAS 1.26:182114 ..... N88-20353* #
NAS 1.26:182587 ..... N88-21105* #
NAS 1.26:182664 ..... N88-20962* #
NAS 1.26:182665 ..... N88-20662* #
NAS 1.26:182669 ..... N88-20846* #
NAS 1.26:182674 ..... N88-20630* #
NAS 1.26:182675 ..... N88-20574* #
NAS 1.26:182677 ..... N88-20711* #
NAS 1.26:182679 ..... N88-20573* #
NAS 1.26:182683 ..... N88-20847* #
NAS 1.26:182684 ..... N88-20535* #
NAS 1.26:182687 ..... N88-20905* #
NAS 1.26:182689 ..... N88-20351* #
NAS 1.26:182690 ..... N88-20352* #
NAS 1.26:182691 ..... N88-20741* #
NAS 1.26:182693 ..... N88-20583* #
NAS 1.26:182694 ..... N88-21091* #
NAS 1.26:182695 ..... N88-20271* #
NAS 1.26:182696 ..... N88-20752* #
NAS 1.26:182699 ..... N88-20667* #
NAS 1.26:182700 ..... N88-20524* #
NAS 1.26:182701 ..... N88-20878* #
NAS 1.26:182704 ..... N88-21092* #
NAS 1.26:182705 ..... N88-20668* #
NAS 1.26:182706 ..... N88-21107* #
NAS 1.26:182707 ..... N88-20397* #
NAS 1.26:182709 ..... N88-20754* #
NAS 1.26:182710 ..... N88-20646* #
NAS 1.26:182715 ..... N88-20934* #
NAS 1.26:182720 ..... N88-20529* #
NAS 1.26:182721 ..... N88-20773* #
NAS 1.55:2505 ..... N88-20652* #
NAS 1.55:10009 ..... N88-20599* #
NAS 1.60:2546 ..... N88-20257* #
NAS 1.60:2770 ..... N88-20833* #
NAS 1.60:2796 ..... N88-20264* #
NAS 1.60:2800 ..... N88-20280* #
NAS 1.61:1197 ..... N88-20772* #
NAS 1.61:1201 ..... N88-20714* #
NAS 1.77:20156 ..... N88-20480* #
NAS 1.77:20157 ..... N88-20434* #
NAS 1.77:20158 ..... N88-20374* #
NAS 1.77:20173 ..... N88-20278* #
NAS 1.77:20199 ..... N88-20403* #
NAS 1.77:20202 ..... N88-20477* #
NAS 1.77:20208 ..... N88-20272* #
NAS 1.77:20213 ..... N88-20590* #
NAS 1.77:20220 ..... N88-20607* #
NAS 1.77:20221 ..... N88-20813* #
NAS 1.77:20222 ..... N88-20553* #
NAS 1.77:20225 ..... N88-20476* #
NAS 1.77:20227 ..... N88-20398* #
NAS 1.77:20228 ..... N88-20479* #
NAS 1.77:20230 ..... N88-20594* #
NAS 1.77:20232 ..... N88-20593* #
NAS 1.77:20233 ..... N88-20769* #
NAS 1.77:20234 ..... N88-20297* #
NAS 1.77:20235 ..... N88-20526* #
NAS 1.77:20237 ..... N88-20974* #
NAS 1.77:20238 ..... N88-20973* #
NAS 1.77:20239 ..... N88-20402* #
NAS 1.77:20242 ..... N88-20972* #
NAS 1.77:20244 ..... N88-20528* #
NAS 1.77:20246 ..... N88-20401* #
NAS 1.77:20248 ..... N88-20437* #
NAS 1.77:20250 ..... N88-20400* #
NAS 1.77:20252 ..... N88-20818* #
NAS 1.77:20257 ..... N88-20716* #

NASA-CP-2505 ..... N88-20652* #
NASA-CP-10009 ..... N88-20599* #

NASA-CR-4131 ..... N88-20308* #
NASA-CR-4132 ..... N88-20290* #
NASA-CR-4134 ..... N88-20291* #
NASA-CR-4138 ..... N88-20491* #
NASA-CR-4139 ..... N88-20256* #
NASA-CR-4140 ..... N88-20822* #
NASA-CR-177470 ..... N88-20601* #
NASA-CR-177830 ..... N88-20608* #
NASA-CR-178390 ..... N88-20895* #
NASA-CR-179316 ..... N88-20340* #
NASA-CR-179317 ..... N88-20341* #
NASA-CR-179318 ..... N88-20342* #
NASA-CR-179319 ..... N88-20343* #
NASA-CR-179321 ..... N88-20339* #
NASA-CR-179430 ..... N88-20673* #
NASA-CR-180757 ..... N88-20742* #
NASA-CR-180758 ..... N88-20837* #
NASA-CR-180759 ..... N88-20438* #
NASA-CR-180762 ..... N88-21074* #
NASA-CR-180877 ..... N88-20361* #
NASA-CR-181094 ..... N88-20606* #
NASA-CR-181388 ..... N88-20713* #
NASA-CR-181611 ..... N88-20274* #
NASA-CR-181626 ..... N88-20831* #
NASA-CR-181639 ..... N88-20758* #
NASA-CR-181649 ..... N88-20591* #
NASA-CR-181650 ..... N88-20273* #
NASA-CR-182112 ..... N88-20306* #
NASA-CR-182114 ..... N88-20353* #
NASA-CR-182587 ..... N88-21105* #
NASA-CR-182664 ..... N88-20962* #
NASA-CR-182665 ..... N88-20662* #
NASA-CR-182669 ..... N88-20846* #
NASA-CR-182674 ..... N88-20630* #
NASA-CR-182675 ..... N88-20574* #
NASA-CR-182677 ..... N88-20711* #
NASA-CR-182679 ..... N88-20573* #
NASA-CR-182683 ..... N88-20847* #
NASA-CR-182684 ..... N88-20535* #
NASA-CR-182687 ..... N88-20905* #
NASA-CR-182689 ..... N88-20351* #
NASA-CR-182690 ..... N88-20352* #
NASA-CR-182691 ..... N88-20741* #
NASA-CR-182693 ..... N88-20583* #
NASA-CR-182694 ..... N88-21091* #
NASA-CR-182695 ..... N88-20271* #
NASA-CR-182696 ..... N88-20752* #
NASA-CR-182699 ..... N88-20667* #
NASA-CR-182700 ..... N88-20524* #
NASA-CR-182701 ..... N88-20878* #
NASA-CR-182704 ..... N88-21092* #
NASA-CR-182705 ..... N88-20668* #
NASA-CR-182706 ..... N88-21107* #
NASA-CR-182707 ..... N88-20397* #
NASA-CR-182709 ..... N88-20754* #
NASA-CR-182710 ..... N88-20646* #
NASA-CR-182715 ..... N88-20934* #
NASA-CR-182720 ..... N88-20529* #
NASA-CR-182721 ..... N88-20773* #

NASA-RP-1197 ..... N88-20772* #
NASA-RP-1201 ..... N88-20714* #

NASA-SP-7011(309) N88-20814*
NASA-SP-7037(224) N88-20254*

NASA-TM-4026 ..... N88-20375* #
NASA-TM-88273 ..... N88-20307* #
NASA-TM-89727 ..... N88-21090* #
NASA-TM-89733 ..... N88-21076* #
NASA-TM-89735 ..... N88-20296* #
NASA-TM-100163 ..... N88-20262* #
NASA-TM-100412 ..... N88-20598* #
NASA-TM-100417 ..... N88-20301* #
NASA-TM-100421 ..... N88-20304* #
NASA-TM-100425 ..... N88-20506* #
NASA-TM-100429 ..... N88-20344* #
NASA-TM-100430 ..... N88-20302* #
NASA-TM-100433 ..... N88-20279* #
NASA-TM-100435 ..... N88-20896* #
NASA-TM-100437 ..... N88-20632* #
NASA-TM-100536 ..... N88-20830* #
NASA-TM-100537 ..... N88-20829* #
NASA-TM-100539 ..... N88-20363* #
NASA-TM-100553 ..... N88-20894* #
NASA-TM-100555 ..... N88-20309* #
NASA-TM-100557 ..... N88-20269* #
NASA-TM-100559 ..... N88-20656* #
NASA-TM-100560 ..... N88-20263* #
NASA-TM-100562 ..... N88-20665* #
NASA-TM-100578 ..... N88-20372* #
NASA-TM-100579 ..... N88-20666* #
NASA-TM-100581 ..... N88-20669* #
NASA-TM-100586 ..... N88-20592* #
NASA-TM-100689-VOL-2 ..... N88-20753* #
NASA-TM-100694 ..... N88-20780* #
NASA-TM-100799 ..... N88-20454* #
NASA-TM-100823 ..... N88-20455* #
NASA-TM-100830 ..... N88-20417* #
NASA-TM-100841 ..... N88-20555* #
NASA-TP-2546 ..... N88-20257* #
NASA-TP-2770 ..... N88-20833* #
NASA-TP-2796 ..... N88-20264* #
NASA-TP-2800 ..... N88-20280* #

NASA-TT-20156 ..... N88-20480* #
NASA-TT-20157 ..... N88-20434* #
NASA-TT-20158 ..... N88-20374* #
NASA-TT-20173 ..... N88-20278* #
NASA-TT-20199 ..... N88-20403* #
NASA-TT-20202 ..... N88-20477* #
NASA-TT-20208 ..... N88-20272* #
NASA-TT-20213 ..... N88-20590* #
NASA-TT-20220 ..... N88-20807* #
NASA-TT-20221 ..... N88-20813* #
NASA-TT-20222 ..... N88-20553* #
NASA-TT-20225 ..... N88-20476* #
NASA-TT-20227 ..... N88-20398* #
NASA-TT-20228 ..... N88-20479* #
NASA-TT-20230 ..... N88-20594* #
NASA-TT-20232 ..... N88-20593* #
NASA-TT-20233 ..... N88-20769* #
NASA-TT-20234 ..... N88-20297* #
NASA-TT-20235 ..... N88-20526* #
NASA-TT-20237 ..... N88-20974* #
NASA-TT-20238 ..... N88-20973* #
NASA-TT-20239 ..... N88-20402* #
NASA-TT-20242 ..... N88-20972* #
NASA-TT-20244 ..... N88-20528* #
NASA-TT-20246 ..... N88-20401* #
NASA-TT-20248 ..... N88-20437* #
NASA-TT-20250 ..... N88-20400* #
NASA-TT-20252 ..... N88-20818* #
NASA-TT-20257 ..... N88-20716* #

NBSIR-87/3077 ..... N88-20519 #
NBSIR-87/3618 ..... N88-20838 #
NBSIR-88/3709 ..... N88-21080 #

NHRC-87-26 ..... N88-20808 #

NIKHEF-H/87-8 ..... N88-20605 #
NIKHEF-H/87-10 ..... N88-21001 #
NIKHEF-H/87-11 ..... N88-20987 #
NIKHEF-H/87-12 ..... N88-20988 #

NIPER-271 ..... N88-21065 #

NLR-MP-86036-U ..... N88-20570 #
NLR-MP-86037-U ..... N88-20288 #
NLR-MP-86054-U ..... N88-20660 #
NLR-MP-86058-U ..... N88-20266 #
NLR-MP-86066-U ..... N88-20427 #
NLR-MP-86076-U ..... N88-20267 #
NLR-MP-87007-U ..... N88-20661 #
NLR-MP-87010-U ..... N88-20571 #
NLR-MP-87011-U ..... N88-20305 #
NLR-MP-87013-U ..... N88-20946 #
NLR-MP-87016-U ..... N88-20347 #

NLR-TR-86050-U ..... N88-20281 #
NLR-TR-86051-U ..... N88-20426 #
NLR-TR-86060-U ..... N88-20295 #
NLR-TR-86072-U ..... N88-20287 #
NLR-TR-86083-U ..... N88-20371 #
NLR-TR-86122-U ..... N88-20265 #
NLR-TR-87009-U ..... N88-20569 #
NLR-TR-87010-U ..... N88-20639 #
NLR-TR-87053-U ..... N88-20300 #
NLR-TR-87079-L-PT-2 ..... N88-21016 #

NOAA-TM-ERL-WPL-149 ..... N88-20783 #

NOAA-TM-NWS-ER-75 ..... N88-20762 #

NORDA-195 ..... N88-20776 #

NOSC-TD-1140 ..... N88-20530 #

NOSC/TR-1184 ..... N88-20513 #

NPS55-87-014 ..... N88-20907 #
NPS67-87-006 ..... N88-20260 #

NRL-MR-6102 ..... N88-20602 #
NRL-MR-6138 ..... N88-20845 #

NRL-9048 ..... N88-20775 #

NSR-25-15 ..... N88-20735 #

NSWC/TR-86-253 ..... N88-20259 #

NTSB/AAR-88/02 ..... N88-20282 #

NUSC-TR-7997 ..... N88-20965 #

OCR-84-184041-A002 ..... N88-20514 #

ORNL-6428 ..... N88-20942 #

ORNL/M-455 ..... N88-20627 #

ORNL/SUB-81-07685/02-77 ..... N88-20430 #
ORNL/SUB-83-43336/01 ..... N88-20421 #
ORNL/SUB-85-22007/3-VOL-2 ..... N88-20485 #
ORNL/SUB-85-28609/1 ..... N88-20645 #
ORNL/SUB-86-55951/1 ..... N88-21086 #

ORNL/TM-10620 ..... N88-20525 #
ORNL/TM-10655 ..... N88-20933 #
ORNL/TM-10667 ..... N88-20369 #

OS-TR-719300-2 ..... N88-20397* #

OSU-388 ..... N88-20752* #

PB88-118203 ..... N88-20481 #
PB88-120241 ..... N88-20289 #
PB88-127543 ..... N88-21108 #
PB88-130919 ..... N88-20336 #
PB88-147889 ..... N88-20782 #
PB88-148812 ..... N88-20961 #
PB88-148820 ..... N88-20931 #
PB88-148838 ..... N88-20932 #
PB88-149281 ..... N88-21029 #
PB88-150941 ..... N88-20821 #
PB88-153705 ..... N88-20838 #
PB88-157144 ..... N88-20762 #
PB88-157615 ..... N88-20783 #
PB88-164520 ..... N88-20519 #
PB88-169448 ..... N88-21080 #
PB88-910402 ..... N88-20282 #

PDR/IC-CFDU/32 ..... N88-20647 #

PFC/RR-87-8-PT-1 ..... N88-21022 #

PNL-SA-15107 ..... N88-21003 #
PNL-SA-15224 ..... N88-21002 #
PNL-SA-15269 ..... N88-20461 #
PNL-SA-15272 ..... N88-20394 #
PNL-SA-15370 ..... N88-20761 #
PNL-SA-15374 ..... N88-20568 #
PNL-SA-15419 ..... N88-20462 #

PNL-6372 ..... N88-20732 #

PSU/ARL-TR-87-011 ..... N88-20558 #

R-293 ..... N88-20936 #
R-840-S ..... N88-20275 #
R-845-D ..... N88-20770 #

R/D-4352-R-AN ..... N88-20559 #

RADC-TR-86-159 ..... N88-20534 #
RADC-TR-87-3 ..... N88-20514 #
RADC-TR-87-41 ..... N88-21043 #
RADC-TR-87-84 ..... N88-20492 #
RADC-TR-87-206 ..... N88-21006 #

RAE-TR-87048 ..... N88-20300 #

REPT-87-MA-01 ..... N88-20821 #
REPT-87-8-ONR ..... N88-20823 #
REPT-87-9-ONR ..... N88-20493 #
REPT-87SRC17 ..... N88-21005 #
REPT-88B0042 ..... N88-20753* #
REPT-88B0061 ..... N88-20780* #
REPT-88B0107 ..... N88-20714* #
REPT-375 ..... N88-20713* #
REPT-85142 ..... N88-20257* #

RFP-4123 ..... N88-20423 #

RI/RD87-250 ..... N88-20361* #

R8701 ..... N88-20822* #

SACLANTCEN-SM-195 ..... N88-20777 #

SAIC-87/1873 ..... N88-20839 #

SAIC/PR-TR-87 ..... N88-20256* #

SAND-86-1943 ..... N88-20731 #
SAND-87-0311 ..... N88-20550 #
SAND-87-0652 ..... N88-20856 #
SAND-87-0653 ..... N88-20857 #
SAND-87-1252C ..... N88-20621 #
SAND-87-1424C ..... N88-20737 #
SAND-87-1518C ..... N88-20657 #

SAND-87-1533 ..... N88-20729 #
SAND-87-1577C ..... N88-21066 #
SAND-87-1591C ..... N88-21047 #
SAND-87-1592C ..... N88-21062 #
SAND-87-1606 ..... N88-20623 #
SAND-87-1621C ..... N88-20467 #
SAND-87-1753 ..... N88-20739 #
SAND-87-1824 ..... N88-20540 #
SAND-87-2018 ..... N88-20858 #
SAND-87-2194 ..... N88-20541 #
SAND-87-2242C ..... N88-20914 #
SAND-87-2255C ..... N88-20518 #
SAND-87-2277C ..... N88-20395 #
SAND-87-2333C ..... N88-20470 #
SAND-87-2334C ..... N88-20471 #
SAND-87-2539C ..... N88-20970 #
SAND-87-2560C ..... N88-20719 #
SAND-87-2590C ..... N88-21053 #
SAND-87-2615 ..... N88-20760 #
SAND-87-2780C ..... N88-20638 #
SAND-87-2836C ..... N88-20390 #
SAND-87-2922C ..... N88-21052 #
SAND-87-3036C ..... N88-20485 #
SAND-87-3068 ..... N88-20335 #
SAND-87-3086C ..... N88-20734 #
SAND-87-7014 ..... N88-20720 #
SAND-87-7159 ..... N88-20567 #
SAND-88-0091C ..... N88-20999 #
SAND-88-0096 ..... N88-20622 #
SAND-88-0113C ..... N88-20952 #
SAND-88-7011 ..... N88-20589 #

SAR-1 ..... N88-20529* #
SAR-1 ..... N88-20646* #

SC5384.FR ..... N88-21036 #
SC5420.FR ..... N88-20744 #

SDSMT/IAS/R-87/02 ..... N88-20758* #

SER-A-1 ..... N88-21108 #

SERI/SP-273-3054 ..... N88-20736 #

SERI/STR-211-3189 ..... N88-20721 #
SERI/STR-211-3217 ..... N88-20724 #
SERI/STR-211-3224 ..... N88-20725 #
SERI/STR-211-3229 ..... N88-21050 #
SERI/STR-211-3230 ..... N88-20727 #
SERI/STR-211-3231 ..... N88-20723 #
SERI/STR-211-3249 ..... N88-20726 #
SERI/STR-211-3256 ..... N88-21051 #
SERI/STR-253-3113 ..... N88-20718 #

SERI/TP-211-3272 ..... N88-20728 #

SNIAS-SE/LS/AP-35-073 ..... N88-20330 #

SOL-87-13 ..... N88-20860 #

SR-1 ..... N88-20709 #

SU-SOL-87-17 ..... N88-20912 #
SU-SOL-88-1 ..... N88-21083 #

SU-TR-396 ..... N88-20906 #

TISL-5481 ..... N88-20534 #

TI88-701028 ..... N88-20433 #
TI88-701030 ..... N88-21071 #
TI88-701055 ..... N88-20957 #
TI88-701056 ..... N88-21072 #
TI88-701057 ..... N88-21073 #
TI88-701076 ..... N88-20552 #

TKK-F-B109 ..... N88-20961 #

TM-19 ..... N88-20535* #

TPR-3 ..... N88-20456 #

TR-14 ..... N88-20452 #
TR-18 ..... N88-21038 #
TR-19 ..... N88-20377 #
TR-36 ..... N88-20980 #
TR-38 ..... N88-20979 #
TR-39 ..... N88-20379 #
TR-40 ..... N88-20978 #
TR-56 ..... N88-21042 #
TR-65 ..... N88-20411 #
TR-136 ..... N88-20653 #
TR-208 ..... N88-20841 #
TR-211 ..... N88-20844 #
TR-212 ..... N88-20840 #
TR-213 ..... N88-20886 #

TR-214 ..... N88-20899 #
TR-222 ..... N88-20531 #
TR-400 ..... N88-20935 #
TR-532 ..... N88-20511 #

TSL-87-4 ..... N88-20852 #
TSL-87-7 ..... N88-21031 #

TW-278 ..... N88-20348 #

UBUFFALO/DC/87/TR-54 ..... N88-20975 #
UBUFFALO/DC/88/TR-65 ..... N88-20387 #

UCB/ERL-87/1 ..... N88-20533 #

UCID-20839-87-3 ..... N88-20464 #
UCID-21284 ..... N88-20604 #
UCID-21293 ..... N88-20480 #
UCID-21327 ..... N88-20859 #

UCLA/PPG-1123 ..... N88-21021 #

UCRL-15980 ..... N88-20902 #
UCRL-15982 ..... N88-20832 #
UCRL-21018-VOL-3 ..... N88-20542 #
UCRL-21018-VOL-4 ..... N88-20543 #
UCRL-53838 ..... N88-20915 #
UCRL-96104 ..... N88-21009 #
UCRL-96204 ..... N88-20985 #
UCRL-96473 ..... N88-20418 #
UCRL-96735 ..... N88-20618 #
UCRL-97418 ..... N88-20945 #
UCRL-97493 ..... N88-20990 #
UCRL-97573 ..... N88-20619 #
UCRL-97680 ..... N88-20586 #
UCRL-97761 ..... N88-21060 #
UCRL-97801 ..... N88-20626 #
UCRL-97813 ..... N88-21010 #
UCRL-97894 ..... N88-21059 #
UCRL-97907 ..... N88-21013 #
UCRL-97939 ..... N88-20855 #
UCRL-98170 ..... N88-20958 #

USAAVSCOM-TM-87-F-3 ..... N88-20294 #

UTD-GRL-8702 ..... N88-20613 #

UTIAS-TN-267 ..... N88-20576 #

UTIAS-280 ..... N88-20357 #
UTIAS-322 ..... N88-20575 #

WPB-0115 ..... N88-20883 #

WYLE-68300-1 ..... N88-20353* #

ZW-8706 ..... N88-20928 #

FEDERAL REGIONAL DEPOSITORY LIBRARIES

ALABAMA

AUBURN UNIV. AT MONTGOMERY LIBRARY
Documents Department
Montgomery, AL 36193
(205) 271-9650

UNIV. OF ALABAMA LIBRARY
Documents Dept.-Box S
University, AL 35486
(205) 348-6046

ARIZONA

DEPT. OF LIBRARY, ARCHIVES AND PUBLIC RECORDS
Third Floor—State Cap.
1700 West Washington
Phoenix, AZ 85007
(602) 255-4121

UNIVERSITY OF ARIZONA LIB.
Government Documents Dept.
Tucson, AZ 85721
(602) 621-6433

ARKANSAS

ARKANSAS STATE LIBRARY
One Capitol Mall
Little Rock, AR 72201
(501) 371-2326

CALIFORNIA

CALIFORNIA STATE LIBRARY
Govt. Publications Section
P.O. Box 2037
Sacramento, CA 95809
(916) 324-4863

COLORADO

UNIV OF COLORADO LIB.
Government Pub. Division
Campus Box 184
Boulder, CO 80309
(303) 492-8834

DENVER PUBLIC LIBRARY
Govt. Pub. Department
1357 Broadway
Denver, CO 80203
(303) 571-2131

CONNECTICUT

CONNECTICUT STATE LIBRARY
Government Documents Unit
231 Capitol Avenue
Hartford, CT 06106
(203) 566-7029

FLORIDA

UNIV. OF FLORIDA LIBRARIES
Library West
Documents Department
Gainesville, FL 32611
(904) 392-0367

GEORGIA

UNIV. OF GEORGIA LIBRARIES
Government Reference Dept.
Athens, GA 30602
(404) 542-8949

HAWAII

UNIV. OF HAWAII LIBRARY
Govt. Documents Collection
2550 The Mall
Honolulu, HI 96822
(808) 948-8230

IDAHO

UNIV. OF IDAHO LIBRARY
Documents Section
Moscow, ID 83843
(208) 885-6344

ILLINOIS

ILLINOIS STATE LIBRARY
Information Services Branch
Centennial Building
Springfield, IL 62756
(217) 782-5185

INDIANA

INDIANA STATE LIBRARY
Serials Documents Section
140 North Senate Avenue
Indianapolis, IN 46204
(317) 232-3686

IOWA

UNIV. OF IOWA LIBRARIES
Govt. Documents Department
Iowa City, IA 52242
(319) 353-3318

KANSAS

UNIVERSITY OF KANSAS
Doc. Collect—Spencer Lib.
Lawrence, KS 66045-2800
(913) 864-4662

KENTUCKY

UNIV. OF KENTUCKY LIBRARIES
Govt. Pub. Department
Lexington, KY 40506-0039
(606) 257-3139

LOUISIANA

LOUISIANA STATE UNIVERSITY
Middleton Library
Govt. Docs. Dept.
Baton Rouge, LA 70803
(504) 388-2570

LOUISIANA TECHNICAL UNIV. LIBRARY
Documents Department
Ruston, LA 71272-0046
(318) 257-4962

MAINE

UNIVERSITY OF MAINE
Raymond H. Fogler Library
Tri-State Regional Documents Depository
Orono, ME 04469
(207) 581-1680

MARYLAND

UNIVERSITY OF MARYLAND
McKeldin Lib.—Doc. Div.
College Park, MD 20742
(301) 454-3034

MASSACHUSETTS

BOSTON PUBLIC LIBRARY
Government Docs. Dept.
Boston, MA 02117
(617) 536-5400 ext.226

MICHIGAN

DETROIT PUBLIC LIBRARY
Sociology Department
5201 Woodward Avenue
Detroit, MI 48202-4093
(313) 833-1409

MICHIGAN STATE LIBRARY
P.O. Box 30007
Lansing, MI 48909
(517) 373-1593

MINNESOTA

UNIVERSITY OF MINNESOTA
Government Pubs. Division
409 Wilson Library
309 19th Avenue South
Minneapolis, MN 55455
(612) 373-7870

MISSISSIPPI

UNIV. OF MISSISSIPPI LIB.
Documents Department
University, MS 38677
(601) 232-5857

MONTANA

UNIV. OF MONTANA
Mansfield Library
Documents Division
Missoula, MT 59812
(406) 243-6700

NEBRASKA

UNIVERSITY OF NEBRASKA - LINCOLN
Love Library
Documents Department
Lincoln, NE 68588-0410
(402) 472-2562

NEVADA

UNIVERSITY OF NEVADA LIB.
Govt. Pub. Department
Reno, NV 89557-0044
(702) 784-6579

NEW JERSEY

NEWARK PUBLIC LIBRARY
5 Washington Street
Newark, NJ 07101-0630
(201) 733-7812

NEW MEXICO

UNIVERSITY OF NEW MEXICO
Zimmerman Library
Government Pub. Dept.
Albuquerque, NM 87131
(505) 277-5441

NEW MEXICO STATE LIBRARY
Reference Department
325 Don Gaspar Avenue
Santa Fe, NM 87503
(505) 827-3826

NEW YORK

NEW YORK STATE LIBRARY
Empire State Plaza
Albany, NY 12230
(518) 474-5563

NORTH CAROLINA

UNIVERSITY OF NORTH CAROLINA AT CHAPEL HILL
Davis Library
BA/SS Documents Division
Chapel Hill, NC 27515
(919) 962-1151

NORTH DAKOTA

UNIVERSITY OF NORTH DAKOTA
Chester Fritz Library
Documents Department
Grand Forks, ND 58202
(701) 777-4629
In cooperation with North Dakota State Univ. Library

OHIO

STATE LIBRARY OF OHIO
Documents Department
65 South Front Street
Columbus, OH 43266-0334
(614) 462-7051

OKLAHOMA

OKLAHOMA DEPT. OF LIB.
Government Documents
200 NE 18th Street
Oklahoma City, OK 73105
(405) 521-2502, ext. 252

OKLAHOMA STATE UNIV. LIB.
Documents Department
Stillwater, OK 74078
(405) 624-6546

OREGON

PORTLAND STATE UNIV. LIB.
Documents Department
P.O. Box 1151
Portland, OR 97207
(503) 229-3673

PENNSYLVANIA

STATE LIBRARY OF PENN.
Government Pub. Section
P.O. Box 1601
Harrisburg, PA 17105
(717) 787-3752

TEXAS

TEXAS STATE LIBRARY
Public Services Department
P.O. Box 12927—Cap. Sta.
Austin, TX 78711
(512) 475-2996

TEXAS TECH. UNIV. LIBRARY
Govt. Documents Department
Lubbock, TX 79409
(806) 742-2268

UTAH

UTAH STATE UNIVERSITY
Merrill Library, U.M.C. 30
Logan, UT 84322
(801) 750-2682

VIRGINIA

UNIVERSITY OF VIRGINIA
Alderman Lib.—Public Doc.
Charlottesville, VA 22903-2498
(804) 924-3133

WASHINGTON

WASHINGTON STATE LIBRARY
Documents Section
Olympia, WA 98504
(206) 753-4027

WEST VIRGINIA

WEST VIRGINIA UNIV. LIB.
Documents Department
Morgantown, WV 26506-6069
(304) 293-3640

WISCONSIN

MILWAUKEE PUBLIC LIBRARY
814 West Wisconsin Avenue
Milwaukee, WI 53233
(414) 278-3065

ST. HIST LIB. OF WISCONSIN
Government Pub. Section
816 State Street
Madison, WI 53706
(608) 262-4347

WYOMING

WYOMING STATE LIBRARY
Supreme Ct. & Library Bld.
Cheyenne, WY 82002
(307) 777-5919

National Aeronautics and
Space Administration
Code NTT-4
Washington, D.C.
20546

Official Business

Penalty for Private Use, $300

SPECIAL FOURTH-CLASS RATE
POSTAGE & FEES PAID
NASA
PERMIT No. G 27

NASA

POSTMASTER: If Undeliverable (Section 158
Postal Manual) Do Not Return